

Sheet Pile Design by Pile Buck

Notice

The information, including technical and engineering data, figures, tables, designs, drawings, details, procedures and specifications, presented in this publication has been prepared in accordance with recognized engineering principles, and are for general information only. While every effort has been made to insure its accuracy, this information should not be used or relied upon for any specific application without independent competent professional examination and verification of its accuracy, suitability and applicability, by a licensed professional engineer acting within his or her area of competency. This manual is provided without warranty of any kind. Pile Buck®, Inc. and/or its editors disclaim any and all express or implied warranties of merchantability, fitness for any general or particular purpose or freedom from infringement of any patent, trademark, or copyright in regard to information or products contained or referred to herein. Nothing herein contained shall be construed as granting a license, express or implied, under any patents. Anyone making use of this material does so at his or her own risk and assumes any and all liability resulting from such use. The entire risk as to quality or usability of the material contained

within is with the reader. In no event will Pile Buck®, Inc. and/or its editors be held liable for any damages including lost profits, lost savings or other incidental or consequential damages arising from the use or inability to use the information contained within. Pile Buck®, Inc. and/or its editors do not insure anyone utilizing this manual against liability arising from the use of the same and hereby cannot be held liable for “consequential damages,” resulting from such use.

All advertising contained within is the exclusive representation of those registered herein. Pile Buck®, Inc. and/or its editors make no representation as to the accuracy, performance, design, specifications and/or any such “claims” made by advertisers, contained within. Anyone making use of these products does so at his or her own risk and assumes any and all liability resulting from such use. In no event will Pile Buck®, Inc. and/or its editors be held liable for any damages including lost profits, lost savings or other incidental or consequential damages arising from the use or inability to use the products advertised within. Pile Buck®, Inc. and/or its editors do not insure anyone from liability arising from the use of these products and hereby, cannot be held liable for “consequential damages,” resulting from such use.

Introduction

Books, like any other enterprise, have stories behind them, even supposedly “dry” technical books such as this one. This one’s story is a little more interesting than most.

When it was first published in 1986, the *Pile Buck Steel Sheet Piling Design Manual* quickly became the standard manual for sheet piling design. It came at a time when the manufacturers’ published manuals on the subject were rapidly becoming a thing of the past, in the U.S. at least. The changes that were taking place at the time—and certainly since then—have only reinforced the need for a book on this subject published by an entity other than a manufacturer of sheet piling.

Harry A. Lindahl, PE., who was the chief applications engineer for U.S. Steel for many years, did the vast majority of the work on the original book. Both Mr. Lindahl and Christopher Smoot, publisher of Pile Buck, recognized that even a classic such as the *Steel Sheet Piling Design Manual* needed updates and additions. The writing of the new edition began almost immediately after the publication of the original. Mr. Lindahl was in the process of writing the new book when his work was interrupted by his sudden and untimely death in 1992, and this book is dedicated to his memory.

In the intervening years, the introduction of sheeting such as aluminium, vinyl and pultruded fibreglass sheeting only made a new book even more necessary, and so Chris Smoot turned to me to finish this work. It has been an interesting task because sheet piling is unique in many ways. There are few design elements of geotechnical engineering where the geotechnical and structural aspects of the design are so closely intertwined. Moreover, from an aesthetic standpoint, one cannot look at the various types of sheet pile structures, especially cofferdams, without being impressed as to the visual impact of the structure. Sheet piling does in fact have a sort of “structural art” all of its own, especially when properly installed, something that most geotechnical design elements sorely lack.

This book contains many additions and revisions from the previous work; some of these are as follows:

- ❖ Inclusion of non-ferrous sheet piles, which led to the book’s name change to the *Sheet Piling Design by Pile Buck*
- ❖ Addition of extensive information on the seismic design of sheet pile walls.
- ❖ An expanded treatment of lateral earth pressures and . . . other loads on sheet pile walls.

- ❖ Addition of information on “non-classical” methods of sheet pile wall design, and an overview of LRFD with sheet piling.
- ❖ Information on transverse bending, which is a relatively new phenomenon recognised in sheet piling.
- ❖ A section on corrosion and corrosion protection.

There are two other items that need to be noted.

The first concerns the use of public domain publications. Pile Buck has a long tradition of making available many of the public domain publications that are put out by the U.S. Government. In this work we have incorporated many of these; however, our practice is to integrate these into the text rather than present them as separate works. We have listed in the back those publications that we have used; however, we should make a special note of two that have been especially used:

- ❖ Ebeling, R.M., and Morrison, E.E. *The Seismic Design Of Waterfront Retaining Structures*. NCEL Technical Report R-939. Port Hueneme, California: Naval Civil Engineering Laboratory, 1993.
- ❖ Department of the Army, U.S. Army Corps of Engineers. *Design Of Sheet Pile Cellular Structures Cofferdams And Retaining Structures*. EM 1110-2-2503. Washington, DC, 1989.

The second concerns the worked examples. The calculational capacity available to design engineers has grown significantly since the original work was published. We have added many new problems and reworked ones from the original work as well. We have also employed computer software for the analysis of sheet pile walls. The most important one is *SPW 911 v. 2*, the sheet pile analysis software available from Pile Buck. We have also used other software packages, including CFRAME, the structural analysis program from the U.S. Army Corps of Engineers, and the academic version of two other programs: Maple V Release 4 for the Macintosh from Waterloo Maple, Inc., and SEEP-W, which is part of the GeoSlope Office from Geo-Slope International, Ltd.

So now we commend this work to our readers, hoping that its use will result in many successful sheet pile designs.

Don C. Warrington, P.E.
<http://www.vulcanhammer.net>

Table of Contents

NOTICE **I**

INTRODUCTION **II**

TABLE OF CONTENTS **III**

TABLE OF FIGURES **X**

TABLE OF TABLES **XVI**

TABLE OF EXAMPLES **XVII**

CHAPTER 1. OVERVIEW OF SHEET PILING ... **1**

1.1. TYPES OF SHEET PILING **1**

1.1.1. WOOD 1

1.1.2. STEEL SHEET PILING 1

1.1.2.1. Larssen Shapes 2

1.1.2.2. Z-Type Shapes 2

1.1.2.3. Straight Web Sections 3

1.1.2.4. Cold Finished Piling 3

1.1.2.5. High Modulus Sections 3

1.1.2.6. Interlocks for Steel Piling 3

1.1.2.6.1. History 3

1.1.2.6.2. Ball and Socket Interlocks 5

1.1.2.6.3. Jaw Type Interlocks 5

1.1.2.7. Sheet Piling Nomenclature and Identification ... 6

1.1.2.8. Ordering Sheet Piling 6

1.1.2.9. Steel Sheet Piling Today 6

1.1.3. CONCRETE 6

1.1.4. LIGHT-GAUGE ALUMINIUM 6

1.1.5. VINYL SHEET PILING 7

1.1.6. PULTRUDED FIBREGLASS SHEET PILING 7

1.2. APPLICATIONS **7**

1.2.1. TEMPORARY APPLICATIONS 7

1.2.1.1. Temporary Box Cofferdams 7

1.2.1.2. Land Cofferdams 7

1.2.1.3. Trench Excavations 9

1.2.1.4. Cellular Cofferdams 9

1.2.1.4.1. Circular Type Cells 9

1.2.1.4.2. Diaphragm Type Cells 10

1.2.1.4.3. Cloverleaf Cells 10

1.2.1.4.4. Modified Types 10

1.2.1.4.5. Components of Cellular Cofferdams 10

1.2.2. PERMANENT APPLICATIONS 11

1.2.2.1. Marine Bulkheads 11

1.2.2.2. Cellular Bulkheads 11

1.2.2.3. Barge Docks 11

1.2.2.4. Coastal Construction 11

1.2.2.4.1. Bulkheading 11

1.2.2.4.2. Protective Structures 13

1.2.2.5. Other Permanent Applications 13

1.2.2.5.1. Water Control Structures; Weirs and Dams ... 13

1.2.2.5.2. Flood Control Structures 13

1.2.2.5.3. Navigation Structures 13

1.2.2.5.4. Graving Docks and Dry-docks 13

1.2.2.5.5. Artificial Islands 13

1.2.2.6. Highway Applications 13

1.2.2.6.1. Retaining Walls and Abutments 13

1.2.2.6.2. Bridge Protection Cells 14

1.2.2.7. Marinas and Boat Launching Facilities 14

1.2.2.7.1. Bulkheading 14

1.2.2.7.2. Breakwaters 14

1.2.2.7.3. Other Applications 14

1.3. BACKFILL MATERIALS FOR SHEET PILE WALLS **14**

1.3.1. OVERVIEW OF BACKFILL TYPES 14

1.3.2. LIGHTWEIGHT BACKFILL 15

1.3.3. SAND DIKES 15

1.3.4. DREDGED BULKHEADS 15

1.3.5. COMPACTION OF FILL 15

1.3.6. PLACING BACKFILL 15

1.4. FAILURE MODES AND LOADS OF SHEET PILE WALLS **15**

1.4.1. GENERAL CONSIDERATIONS 15

1.4.2. FAILURE MODES FOR SHEET PILING 17

1.4.2.1. Deep-seated failure 17

1.4.2.2. Rotational failure due to inadequate pile penetration 17

1.4.2.3. Flexural Failure of Sheet Piling 17

1.4.2.4. Anchorage Failure 17

1.4.2.5. Special Failures due to Earthquake Motion ... 17

1.5. APPLICATION OF ENGINEERING PRINCIPLES TO SHEET PILING DESIGN **17**

CHAPTER 2. STRUCTURAL DESIGN OF SHEET PILE WALLS **19**

2.1. MATERIALS USED IN SHEET PILING **19**

2.1.1. GRADES OF SHEET PILING STEEL 19

2.1.1.1. Basic Grade: ASTM A-328 19

2.1.1.2. Higher Strength Grade: ASTM A-572 19

2.1.1.3. Corrosion Resisting Grade: ASTM A-690 19

2.1.1.4. Structural Factors of Safety for Steel Sheet Piling..19

2.1.2. OTHER MATERIALS 19

2.2. BENDING OF SHEET PILING **19**

2.2.1. THEORY OF PURE BENDING OF SHEETING ... 19

2.2.2. APPLICATION OF BENDING TO SPECIFIC SHEET PILE SECTIONS 21

2.2.3. COMBINED AXIAL AND FLEXURAL STRESSES 21

2.2.4. SECTION MODULUS OF U- SHAPED SHEETING 21

2.2.5. TRANSVERSE BENDING FAILURE 22

2.2.6. SHEAR FAILURE 23

2.3. INTERLOCK STRENGTH FOR FLAT SHEETING ... **23**

CHAPTER 3. OVERVIEW OF SOIL MECHANICS **25**

3.1. INTRODUCTION **25**

3.2. SOILS **25**

3.2.1. OVERVIEW OF SOIL TYPES 25

3.2.2. UNIFIED SOIL CLASSIFICATION SYSTEM (USCS) 25

3.2.2.1. Coarse-Grained (Cohesionless or Granular) Soils 27

3.2.2.2. Fine-Grained (Cohesive or Organic) Soils 27

3.2.2.3. Examples of Sample Descriptions	31	3.5.13. RESILIENT MODULUS TEST (DYNAMIC)	46
3.2.3. MODIFIED UNIFIED SYSTEM (MUD)	31	3.6. FIELD EXPLORATION, TESTING, AND	
3.2.3.1. Definition of Terms	31	INSTRUMENTATION	46
3.2.3.2. Visual - Manual Identification	33	3.6.1. REVIEW OF PROJECT REQUIREMENTS	47
3.2.3.3. Soil Sample Identification Procedure	33	3.6.2. OFFICE REVIEW OF AVAILABLE DATA	47
3.2.3.4. Other Information for Describing Soils	35	3.6.2.1. Topographic Maps	47
3.2.3.5. Preparing the Word Picture	35	3.6.2.2. Aerial Photographs	47
3.2.3.6. Examples Of Complete Soil Descriptions	35	3.6.2.3. Geological Maps and Reports	47
3.3. LOGGING	35	3.6.2.4. Soils Conservation Service Surveys	47
3.4. SPECIAL MATERIALS AND DIFFICULT SOILS .35		3.6.2.5. Potentiometric Surface Map	47
3.4.1. PERMAFROST AND FROST PENETRATION	35	3.6.2.6. Adjacent Projects	47
3.4.1.1. Characteristics	35	3.6.3. FIELD RECONNAISSANCE	47
3.4.1.2. Classification	35	3.6.4. SOIL BORINGS AND TEST PITS	49
3.4.2. LIMESTONE AND RELATED MATERIALS	37	3.6.4.1. Soil Borings	49
3.4.2.1. Karst Topography	37	3.6.4.1.1. Auger Borings	49
3.4.2.2. Calcareous Soils	37	3.6.4.1.2. Hollow-Stem Auger Borings	49
3.4.3. QUICK CLAYS	41	3.6.4.1.3. Wash Borings	49
3.4.4. OTHER MATERIALS AND CONSIDERATIONS	41	3.6.4.1.4. Percussion Drilling	49
3.4.4.1. Man-Made and Hydraulic Fills	41	3.6.4.1.5. Rotary Drilling	49
3.4.4.2. Chemically Reactive Soils	41	3.6.4.2. Test Pits	49
3.4.4.3. Lateritic Soils	41	3.6.4.3. Test Trenches	49
3.5. LABORATORY TESTING	41	3.6.5. SAMPLING	49
3.5.1. GRAIN-SIZE ANALYSIS	41	3.6.5.1. Disturbed and Undisturbed Sampling	49
3.5.1.1. Sieve Analysis	42	3.6.5.2. Types of Soil Sampling	49
3.5.1.2. Hydrometer	42	3.6.5.2.1. Bag Bulk Samples	49
3.5.2. MOISTURE CONTENT	42	3.6.5.2.2. Split-Barrel	49
3.5.3. ATTERBERG LIMITS	42	3.6.5.2.3. Shelby Tube	50
3.5.3.1. Liquid Limit	42	3.6.5.2.4. Piston Samplers	50
3.5.3.2. Plastic Limit	42	3.6.6. PENETRATION RESISTANCE TESTS	50
3.5.4. SPECIFIC GRAVITY OF SOILS	42	3.6.6.1. Standard Penetration Test (SPT)	50
3.5.5. STRENGTH TESTS	43	3.6.6.1.1. Procedure	50
3.5.5.1. Unconfined Compression Tests	43	3.6.6.2. Corrections	50
3.5.5.2. Triaxial Compression Tests	43	3.6.6.3. Correlations	51
3.5.5.2.1. Unconsolidated-Undrained (UU), or Q Test	43	3.6.6.3.1. Compactness and Consistency	51
3.5.5.2.2. Consolidated-Undrained (CU), or R Test	43	3.6.6.3.2. Relative Density of Granular (but fine grained)	
3.5.5.2.3. Consolidated-Drained (CD), or S Test	43	Deposits	51
3.5.5.3. Direct Shear	43	3.6.6.3.3. Undrained Shear Strength	53
3.5.5.4. Miniature Vane Shear (Torvane) and Pocket		3.6.6.3.4. Drained Friction Angle f'	53
Penetrometer	45	3.6.6.4. Cone Penetrometer Test (CPT)	53
3.5.6. CONSOLIDATION TEST	45	3.6.6.4.1. Test Description	53
3.5.6.1. One-Dimensional Test	45	3.6.6.4.2. Correlations	55
3.5.6.2. Constant Rate of Strain Test	45	3.6.6.5. Dynamic Cone Penetrometer Test	57
3.5.7. ORGANIC CONTENT	45	3.6.6.6. Dilatometer Test (DMT)	57
3.5.8. SHRINKAGE AND SWELL	45	3.6.6.7. Pressuremeter Test (PMT)	58
3.5.8.1. Shrinkage	45	3.6.7. FIELD VANE TEST	59
3.5.8.2. Swell	45	3.6.8. POCKET PENETROMETER	59
3.5.9. PERMEABILITY	45	3.6.9. TORVANE SHEAR DEVICE	59
3.5.9.1. Constant-Head Test	46	3.6.10. INFILTRATION TEST	59
3.5.9.2. Falling-Head Test	46	3.6.11. PERMEABILITY TESTS	61
3.5.9.3. Flexible Wall Permeability	46	3.6.12. SEEPAGE TEST	62
3.5.10. ENVIRONMENTAL CORROSION TESTS	46	3.6.12.1. Constant Head Test	62
3.5.11. COMPACTION TESTS	46	3.6.12.2. Rising Head Test	62
3.5.11.1. Standard Proctor	46	3.6.12.3. Falling Head Test	62
3.5.11.2. Modified Proctor	46	3.6.12.4. Open-End Borehole Test	62
3.5.12. RELATIVE DENSITY TESTS	46	3.6.12.5. Exfiltration Test	62
3.5.12.1. Maximum Index Density	46	3.6.12.6. Pumping Test	62
3.5.12.2. Minimum Index Density	46	3.6.12.7. Gravity and Pressure Tests	63

3.6.13. ENVIRONMENTAL CORROSION TESTS	63
3.6.14. GROUT PLUG PULL-OUT TEST	63
3.6.15. GROUNDWATER MEASUREMENTS AND PIEZOMETERS	65
3.7. MEASUREMENT OF SOIL PROPERTIES IN SITU	65
3.7.1. IN-PLACE DENSITY	65
3.7.2. DETECTION OF COMBUSTIBLE GASES	65

CHAPTER 4.

BASIC EARTH PRESSURE CONCEPTS	66
4.1. LATERAL EARTH PRESSURE COEFFICIENT	66
4.2. TOTAL AND EFFECTIVE STRESSES	66
4.2.1. TOTAL STRESS	66
4.2.2. EFFECTIVE STRESS	66
4.3. MOHR-COULOMB SHEAR STRENGTH	66
4.4. EARTH PRESSURE AND WALL MOVEMENT	67
4.4.1. AT-REST PRESSURES	67
4.4.2. WALL MOVEMENTS	69
4.4.3. ACTIVE PRESSURES	69
4.4.4. PASSIVE PRESSURES	70
4.4.5. WALL FRICTION AND ADHESION	70
4.4.6. COHESIVE SOILS	70

CHAPTER 5.

STATIC EARTH PRESSURES	71
5.1. RANKINE THEORY	71
5.1.1. ACTIVE EARTH PRESSURES	73
5.1.2. PASSIVE EARTH PRESSURES	74
5.2. COULOMB THEORY	77
5.2.1. ACTIVE EARTH PRESSURES	77
5.2.2. PASSIVE EARTH PRESSURES	78
5.3. LOG-SPIRAL THEORY	79
5.4. EARTH PRESSURES COMPUTED USING THE TRIAL WEDGE PROCEDURE	79
5.4.1. HYDROSTATIC WATER PRESSURES	85

CHAPTER 6.

DYNAMIC EARTH PRESSURES	87
6.1. OVERVIEW OF EARTHQUAKE LOADS	87
6.1.1. LIMIT STATES	87
6.1.2. KEY ROLE OF LIQUEFACTION HAZARD ASSESSMENT	87
6.1.3. CHOICE OF DESIGN GROUND MOTIONS	87
6.1.3.1. Design Seismic Event	87
6.1.3.2. Local soil conditions	89
6.1.3.3. Seismic Coefficients	89
6.1.3.4. Vertical Ground Accelerations	90
6.2. INTRODUCTION TO DYNAMIC EARTH PRESSURES	90
6.3. DYNAMIC ACTIVE EARTH PRESSURE FORCE.	93
6.3.1. VERTICAL POSITION OF PAE ALONG BACK OF WALL	95
6.3.2. SIMPLIFIED PROCEDURE FOR DYNAMIC ACTIVE	

EARTH PRESSURES	97
6.3.3. LIMITING VALUE FOR HORIZONTAL ACCELERATION	98
6.4. EFFECT OF SUBMERGENCE OF THE BACKFILL ON THE MONONOBE-OKABE METHOD OF ANALYSIS	101
6.4.1. SUBMERGED BACKFILL WITH NO EXCESS PORE PRESSURES	101
6.4.1.1. Restrained water case	101
6.4.1.2. Free water case	102
6.4.2. SUBMERGED BACKFILL WITH EXCESS PORE PRESSURE	102
6.4.2.1. Restrained water case	102
6.4.2.2. Alternate Procedure	102
6.4.2.3. Free water case	103
6.4.3. PARTIAL SUBMERGENCE	103
6.5. DYNAMIC PASSIVE EARTH PRESSURES	103
6.5.1. SIMPLIFIED PROCEDURE FOR DYNAMIC PASSIVE EARTH PRESSURES	109
6.5.2. EXAMPLE	109
6.6. EFFECT OF VERTICAL ACCELERATIONS ON THE VALUES FOR THE DYNAMIC ACTIVE AND PASSIVE EARTH PRESSURES	109
6.7. CASES WITH SURFACE LOADINGS	110

CHAPTER 7.

WATER AND WATER FLOW IN SOIL	114
7.1. HYDROSTATIC WATER AND SURCHARGE	114
7.2. STEADY STATE SEEPAGE	114
7.2.1. THEORY OF GROUNDWATER FLOW	115
7.3. ANALYSIS OF GROUNDWATER FLOW	118
7.3.1. EFFECT OF GROUNDWATER ON EFFECTIVE UNIT WEIGHT	118
7.3.2. SIMPLIFIED METHOD OF ANALYSIS	119
7.3.3. FLOW NET TECHNIQUE	119
7.3.4. FINITE ELEMENT ANALYSIS	122
7.4. SEEPAGE FORCES	122
7.4.1. SEEPAGE THROUGH INTERLOCKS	123
7.5. WAVE ACTION	123

CHAPTER 8.

OTHER LOADS ON SHEET PILE WALLS	126
8.1. EFFECT OF SURFACE LOADINGS	126
8.1.1. ELASTIC SOLUTIONS	126
8.1.1.1. Uniform surcharge	126
8.1.1.2. Line loads	126
8.1.1.3. Strip loads	126
8.1.1.4. Ramp load	126
8.1.1.5. Triangular Load	126
8.1.1.6. Area loads	126
8.1.1.7. Point loads	126
8.1.2. TRIAL WEDGE ANALYSIS	126
8.1.3. FINITE ELEMENT METHODS	127
8.2. ADDITIONAL APPLIED LOADS	127
8.2.1. BOAT IMPACT	129
8.2.2. MOORING PULLS	129

8.2.3. ICE FORCES	130
8.2.4. WIND FORCES	130

CHAPTER 9.

DESIGN OF CANTILEVERED AND ANCHORED WALLS USING CLASSICAL METHODS131

9.1. DEFINITION OF CLASSICAL METHODS ...131

9.1.1. USE OF COMPUTER SOFTWARE FOR CLASSICAL METHODS	131
---	-----

9.2. DATA REQUIRED FOR ANALYSIS131

9.2.1. MINIMUM INFORMATION REQUIRED FOR DESIGN	131
--	-----

9.2.1.1. Soil Weight	133
----------------------------	-----

9.2.1.2. Angle of Internal Friction ϕ	133
--	-----

9.2.1.3. Angle of Friction between Soil and Wall δ	133
---	-----

9.2.1.4. Adhesion	133
-------------------------	-----

9.2.1.5. Cohesion	133
-------------------------	-----

9.2.1.6. Ground Slopes β	133
--------------------------------------	-----

9.2.1.7. Surcharges	133
---------------------------	-----

9.2.1.8. External Loads	133
-------------------------------	-----

9.2.1.9. Water	133
----------------------	-----

9.2.1.10. Project Data	134
------------------------------	-----

9.2.2. LOAD CASES	134
-------------------------	-----

9.3. CANTILEVER WALLS134

9.3.1. OVERVIEW	134
-----------------------	-----

9.3.2. CANTILEVER SHEET PILING IN 125 GRANULAR SOILS	135
--	-----

9.3.2.1. Conventional Method	135
------------------------------------	-----

9.3.2.2. Simplified Method	137
----------------------------------	-----

9.3.2.3. Chart Solutions	137
--------------------------------	-----

9.3.2.4. Factors of Safety and Rules of Thumb	137
---	-----

9.3.3. CANTILEVER SHEET PILING IN COHESIVE SOILS	142
--	-----

9.3.3.1. Wall Entirely in Cohesive Soil	142
---	-----

9.3.3.2. Wall in Cohesive Soil with Granular Backfill Above Dredge line	146
---	-----

9.4. ANCHORED WALLS147

9.4.1. GENERAL	147
----------------------	-----

9.4.2. FREE EARTH SUPPORT METHOD	150
--	-----

9.4.2.1. Design in Granular Soil	150
--	-----

9.4.2.2. Design in Cohesive Soils	155
---	-----

9.4.2.3. Rowe's Moment Reduction Theory	162
---	-----

9.4.2.3.1. Cohesionless Soils	163
-------------------------------------	-----

9.4.2.3.2. Cohesive Soils	166
---------------------------------	-----

9.4.3. FIXED EARTH SUPPORT METHOD (EQUIVALENT BEAM METHOD)	166
--	-----

9.4.3.1. Overview of Blum's Method	166
--	-----

9.4.3.2. Implementation of Fixed Earth Support	167
--	-----

9.4.4. GRAPHICAL METHODS	178
--------------------------------	-----

9.4.5. DANISH RULES	178
---------------------------	-----

9.4.6. HIGH SHEET PILE WALLS (TWO ANCHOR SYSTEM)	179
--	-----

9.5. LOAD AND RESISTANCE FACTOR DESIGN (LRFD)179

CHAPTER 10.

SHEET PILING DESIGN BY SOIL-STRUCTURE INTERACTION ANALYSIS182

10.1. INTRODUCTION	182
--------------------------	-----

10.2. SOIL-STRUCTURE INTERACTION METHOD	182
---	-----

10.3. PRELIMINARY INFORMATION	182
-------------------------------------	-----

10.4. SSI MODEL	182
-----------------------	-----

10.5. NONLINEAR SOIL SPRINGS	183
------------------------------------	-----

10.6. NONLINEAR ANCHOR SPRINGS	183
--------------------------------------	-----

10.7. APPLICATION OF SSI ANALYSIS	185
---	-----

10.8. COMPARISON OF SSI ANALYSIS TO CLASSICAL RESULTS	185
---	-----

CHAPTER 11.

ANCHOR SYSTEMS AND TIEBACKS187

11.1. GENERAL CONSIDERATIONS	187
------------------------------------	-----

11.2. TRADITIONAL ANCHOR SYSTEMS	187
--	-----

11.2.1. TIE RODS	187
------------------------	-----

11.2.2. WALES	189
---------------------	-----

11.2.3. ANCHORS	190
-----------------------	-----

11.2.3.1. Anchor Blocks (Deadmen Anchors)	191
---	-----

11.2.3.2. Continuous Deadmen near Ground Surface	193
--	-----

11.2.3.3. Short Deadmen near Ground Surface	193
---	-----

11.2.4. ANCHOR SLAB DESIGN BASED ON MODEL TESTS	194
---	-----

11.2.4.1. General Case in Granular Soils	194
--	-----

11.2.4.2. Anchor Slab in Cohesive Soils	206
---	-----

11.2.5. REACTION PILES	206
------------------------------	-----

11.2.6. TENSION PILES	206
-----------------------------	-----

11.3. TIEBACKS206	
-------------------------	--

11.3.1. PRINCIPLES OF TIEBACK SYSTEMS	207
---	-----

11.3.2. TEMPORARY AND PERMANENT TIEBACKS	207
--	-----

11.3.3. DEFINITIONS	207
---------------------------	-----

11.3.4. TYPES OF TIEBACKS	210
---------------------------------	-----

11.3.5. NOMENCLATURE FOR TIEBACK SYSTEMS	210
--	-----

11.3.6. CAPACITY OF TIEBACK ANCHORS	211
---	-----

11.3.6.1. Overview	211
--------------------------	-----

11.3.6.2. Cohesionless Soils—Low Pressure Grouting (FHWA Formula)	211
---	-----

11.3.6.3. Cohesionless Soils—Small Diameter Anchors	213
---	-----

11.3.6.3.1. No grout penetration in anchor zones	213
--	-----

11.3.6.3.2. Grout penetration in anchor zone (very pervious soils)	214
--	-----

11.3.6.3.3. Empirical Relationships	214
---	-----

11.3.6.4. Cohesive Soils—Large Diameter Anchors	214
---	-----

11.3.6.4.1. Straight-shafted Anchor	214
---	-----

11.3.6.4.2. Belled Anchor	214
---------------------------------	-----

11.3.6.4.3. Multi-belled Anchor	215
---------------------------------------	-----

11.3.6.5. Reduction Factors for Clay	215
--	-----

11.3.6.6. Gravel Packed Anchors	215
---------------------------------------	-----

11.3.7. FORCES ON THE VERTICAL MEMBERS	217
--	-----

11.3.8. OVERALL (GLOBAL) SYSTEM STABILITY	217
---	-----

11.3.9. TESTING TIEBACK ANCHORS	217
---------------------------------------	-----

11.3.9.1. Overview	217
--------------------------	-----

11.3.9.2. Proof Testing	217
11.3.9.3. Evaluation of Creep Movement	218
11.3.9.4. Performance Testing	219
11.3.9.5. Lock-Off Force	221
11.3.10. WALL MOVEMENT AND SETTLEMENT	221
11.3.11. STEPS FOR CHECKING TIEBACK SHORING SUBMITTAL	221
11.3.12. TIEBACK DESIGN AND TESTING EXAMPLES	221
11.3.13. ROCK ANCHORS	229
11.3.13.1. Failure of Steel Tendon	229
11.3.13.2. Failure of Grout Steel Bond	229
11.3.13.3. Failure of Grout-rock Bond	229
11.3.13.4. Failure of Rock Mass	229
11.3.13.5. Factor of Safety and Testing	229

CHAPTER 12.

ANALYSIS AND DESIGN OF ANCHORED WALLS AND ANCHOR SYSTEMS FOR EARTHQUAKE LOADS

12.1. INTRODUCTION	231
12.2. BACKGROUND	231
12.2.1. SUMMARY OF THE JAPANESE CODE FOR DESIGN OF ANCHORED SHEET PILE WALLS	233
12.2.2. DISPLACEMENTS OF ANCHORED SHEET PILES DURING EARTHQUAKES	234
12.3. DESIGN OF ANCHORED SHEET PILE WALLS FOR EARTHQUAKE LOADINGS	234
12.3.1. CONSIDERATIONS FROM STATIC ANALYSIS	234
12.3.2. INCLUSION OF EARTHQUAKE LOADS	235
12.3.3. FLEXURE OF THE SHEET PILE WALL BELOW THE DREDGE LEVEL	238
12.3.4. DESIGN OF ANCHORED SHEET PILE WALLS - NO EXCESS PORE WATER PRESSURES	239
12.3.5. DESIGN OF ANCHORED SHEET PILE WALLS - EXCESS PORE WATER PRESSURES	247
12.4. USE OF FINITE ELEMENT ANALYSES	250
12.5. EXAMPLE PROBLEM	250

CHAPTER 13.

SHEET PILING COFFERDAMS

13.1. GENERAL	266
13.2. GEOTECHNICAL DESIGN OF SHEET PILE COFFERDAMS	266
13.2.1. LATERAL PRESSURE DISTRIBUTION	266
13.2.2. PRESSURE DISTRIBUTIONS IN BRACED CUTS	266
13.2.2.1. Braced Cuts in Sand	269
13.2.2.2. Braced Cuts in Clay	269
13.2.2.3. Mixed Soils	269
13.2.2.4. Surcharge Loads Against Braced Cuts	269
13.2.3. BASE STABILITY	269
13.2.3.1. Granular Soils	270
13.2.3.2. Cohesive Soils	270
13.2.3.3. Piping	271
13.2.4. WATER COFFERDAMS	271

13.3. STRUCTURAL DESIGN OF COFFERDAM

COMPONENTS	273
13.3.1. BEAM LOADS ON WALES AND SPANS	273
13.3.2. COLUMN LOADING OF STRUTS AND WALES	274
13.3.3. CIRCULAR BRACING	274
13.3.4. RAKING BRACES	275
13.4. EXAMPLES OF BRACED EXCAVATIONS	277
13.5. PRESSURISED TIEBACKS	305
13.6. DEEP OPEN CUT EXCAVATIONS	309
13.7. NOTES REGARDING BRACED COFFERDAMS	310

CHAPTER 14.

HIGH MODULUS WALLS

14.1. PILES REINFORCED WITH COVER PLATES	311
14.2. MASTER PILES, KING PILES AND BOX PILES	311
14.2.1. MASTER PILES	311
14.2.2. ARC BUCKSTAY WALLS	311
14.2.3. Z-TYPE MASTER OR KING PILE WALLS	313
14.2.4. BOX PILES	313
14.2.5. PIPE SECTIONS	313
14.3. HZ WALL SYSTEMS	314
14.3.1. DESIGN	314
14.3.2. ANCHOR SYSTEMS FOR HZ WALLS	314
14.3.3. DESIGN PROCEDURES FOR HZ AND KING PILE SYSTEMS	314

CHAPTER 15.

CELLULAR COFFERDAMS

15.1. PLANNING, LAYOUT AND ELEMENTS OF COFFERDAMS	319
15.1.1. AREAS OF CONSIDERATION	319
15.1.1.1. Height of Protection	319
15.1.1.2. Area of Enclosure	319
15.1.1.3. Staging	321
15.1.1.4. Hydraulic Model Studies	321
15.1.2. ELEMENTS OF COFFERDAMS	321
15.1.2.1. Scour Protection	321
15.1.2.2. Berms	321
15.1.2.3. Flooding Facilities	321
15.1.2.4. Tie-ins	322
15.1.2.4.1. Tie-in to Land	322
15.1.2.4.2. Tie-in to Existing Structures	322
15.1.2.5. Cell Layout and Geometry	323
15.1.2.6. Protection and Safety Features	323
15.2. DESIGN PARAMETERS	323
15.2.1. FORCES	325
15.2.1.1. Applied External Forces	325
15.2.1.2. Reactive Berm Force	325
15.2.2. SATURATION LINE AND SEEPAGE CONTROL	325
15.2.2.1. Seepage through Cell	325
15.2.2.2. Foundation Underseepage	326

15.2.3. LOADING CONDITIONS	326	15.3.8.4. Vertical Shear Resistance	362
15.2.3.1. Maximum Pool Condition	326	15.3.8.4.1. Terzaghi's Method	362
15.2.3.2. Initial Filling Condition	326	15.3.8.4.2. Schroeder-Maitland Method	363
15.2.3.3. Drawdown Condition	326	15.3.8.5. Horizontal Shear Resistance	365
15.2.4. SITE CONDITIONS	327	15.3.8.6. Pullout of Outboard Sheets	366
15.2.5. EQUIVALENT WIDTH	327	15.3.8.7. Penetration of Inboard Sheets	367
15.2.6. SOIL FILL MATERIALS	327	15.3.8.8. Slipping Between Sheeting and Cell Fill	367
15.2.6.1. Selection of Cell Fill	327	15.3.9. EXAMPLES OF CELLULAR COFFERDAM DESIGN USING CLASSICAL METHODS	367
15.2.6.2. Borrow Area	329	15.3.10. RECOMMENDED PRACTICES FOR DESIGN AND INSTALLATION OF CELLULAR COFFERDAMS	399
15.2.6.3. Location	329	15.4. FINITE ELEMENT METHODS	399
15.2.7. FACTORS OF SAFETY	329	15.4.1. BACKGROUND	399
15.3. CLASSICAL DESIGN METHODS	330	15.4.2. FINITE ELEMENT COFFERDAM MODELS	401
15.3.1. HISTORICAL OVERVIEW	330	15.4.2.1. Vertical Slice Analysis	401
15.3.2. DESIGN PROCESS	330	15.4.2.2. Axisymmetric Cell Analysis	402
15.3.3. EXTERNAL CELL STABILITY	331	15.4.2.3. Horizontal Slice Analysis	402
15.3.3.1. Sliding Analysis by Trial Wedge Method	331	15.4.2.4. General Modelling Techniques	406
15.3.3.1.1. Method of Analysis	331	15.4.3. ESTIMATES OF CELL DEFORMATIONS	406
15.3.3.1.2. Multiwedge System Analysis	331	15.4.3.1. Cell Bulging during Filling	406
15.3.3.1.3. Design Considerations	338	15.4.3.2. Deflections Produced by Berm Placement	406
15.3.3.1.4. Seismic Sliding Stability	339	15.4.3.3. Cofferdam Unwatering and Exterior Flood	406
15.3.3.2. Overturning	341	15.4.3.4. Construction Excavation	406
15.3.3.3. Rotation (Hansen's Method)	341	15.4.4. STRUCTURAL CONTINUITY BETWEEN CELLS AND ARCS	406
15.3.4. DEEP-SEATED SLIDING ANALYSIS	342	15.4.5. STRUCTURE—FOUNDATION INTERACTION	407
15.3.4.1. Introduction	342	15.4.5.1. Foundation Stress at Cofferdam Base	407
15.3.4.2. Study of Subsurface Conditions	343	15.4.5.2. Investigation of Foundation Problems	407
15.3.4.3. Methods of Sliding Stability Analysis	345	15.4.6. FILL INTERACTION BETWEEN CELLS AND ARC	407
15.3.4.3.1. Wedge Method	346	15.4.7. SPECIAL COFFERDAM CONFIGURATIONS	407
15.3.4.3.2. Approximate Method	346	15.4.7.1. Cloverleaf Cells	407
15.3.4.3.3. Culmann's Method	346	15.4.7.2. Diaphragm Cells	407
15.3.4.4. Prevention of Sliding Failure	346	15.5. FOUNDATION TREATMENT	407
15.3.5. BEARING CAPACITY ANALYSIS	346	15.5.1. PROBLEM FOUNDATIONS AND TREATMENT	407
15.3.5.1. Bearing Capacity of Soils	347	15.5.2. GROUTING	409
15.3.5.1.1. Terzaghi Method	347	15.5.2.1. Correctional Methods	409
15.3.5.1.2. Hansen Method	349	15.5.2.2. Problems Related to Strength	409
15.3.5.1.3. Limit-equilibrium Method	349	15.5.2.3. Problems Related to Permeability	409
15.3.5.2. Bearing Capacity of Rock	349	15.5.2.4. Selection of Treatment	409
15.3.6. SETTLEMENT OF SHEET PILE COFFERDAM	351	15.5.2.5. Selection of Location	410
15.3.6.1. Settlement of Cofferdam on Clay	353	15.5.2.6. Selection of Grout	410
15.3.6.2. Settlement of Cofferdam on Sand	354	15.5.2.7. Selection of Type of Grouting	410
15.3.6.2.1. Settlement Due to Dewatering of Cofferdam Area	354	15.5.2.8. Special Instructions	410
15.3.7. SEEPAGE ANALYSIS	354	15.6. DEWATERING AND PRESSURE RELIEF	411
15.3.7.1. Seepage through Cell Fill	354	15.6.1. PURPOSE OF DESIGN	411
15.3.7.2. Foundation Underseepage	355	15.6.2. DEWATERING AND PRESSURE RELIEF	411
15.3.7.3. Control of Seepage	357	15.6.2.1. Initial Dewatering	411
15.3.7.3.1. Penetration of Sheet Piles to Deeper Levels	357	15.6.2.2. Foundation Dewatering	413
15.3.7.3.2. Providing Berm on the Downstream Surface	357	15.6.2.3. Pressure Relief	413
15.3.7.3.3. Increasing the Width of Cofferdam	357	15.6.3. SURFACE WATER CONTROL	413
15.3.7.3.4. Installation of Pressure Relief Systems	357	15.6.4. EMERGENCY FLOODING	413
15.3.8. INTERNAL CELL STABILITY	357	15.7. INSTRUMENTATION OF CELLULAR COFFERDAMS	414
15.3.8.1. Basic Concepts	357	15.7.1. SYSTEMATIC MONITORING	414
15.3.8.1.1. Maximum Internal Cell Pressure	357	15.7.2. PROPER PLANNING	414
15.3.8.1.2. Point of Fixity	359		
15.3.8.2. Pile Interlock Tension	359		
15.3.8.2.1. Dealing with Interlock Tension	361		
15.3.8.3. Shear Failure within the Cell (Resistance to Tilting)	362		

15.7.3. PURPOSE OF INSTRUMENTATION	414	17.3.3.1. Fresh Water	437
15.7.4. TYPES OF INSTRUMENTS	415	17.3.3.2. Salt Water	439
15.7.4.1. Observation Wells	415	17.3.4. IMMERSED AND SEMI-IMMERSED ZONE	439
15.7.4.2. Piezometers	415	17.3.4.1. Fresh Water	439
15.7.4.3. Inclinometers	415	17.3.4.2. Salt Water	439
15.7.4.4. Earth Pressure Measuring Devices	417	17.3.4.2.1. Splash Zone	439
15.7.4.5. Strain Gages	417	17.3.4.2.2. Tidal Zone	441
15.7.4.6. Precise Measurement Systems	418	17.3.4.2.3. Continuously Submerged Zone	441
15.7.5. ACCURACY OF REQUIRED MEASUREMENTS	418	17.3.5. BURIED ZONE	441
15.7.6. COLLECTION, PROCESSING, AND EVALUATION OF DATA	419	17.3.5.1. Disturbed Soil	441
15.7.7. EXAMPLE OF INSTRUMENTATION	419	17.3.5.2. Salt Water	441
CHAPTER 16.		17.4. DESIGN FOR PROTECTION OF STEEL PILING IN MARINE ENVIRONMENTS	442
CELLULAR SHEET PILING STRUCTURES, MOORING CELLS AND DOLPHINS	421	17.4.1. METHODS FOR PROTECTING STEEL PILING	442
16.1. GENERAL	421	17.4.2. SACRIFICIAL METAL	442
16.2. LOADS	421	17.4.3. ENCASMENT	445
16.2.1. LATERAL LOADS	421	17.4.4. SPECIAL STEELS	445
16.2.2. IMPACT	422	17.4.4.1. ASTM A-690 Grade	446
16.2.3. WAVE ACTION	423	17.4.5. COATINGS	446
16.2.4. EARTHQUAKE FORCE	423	17.4.5.1. Metallic Coatings	446
16.2.5. VERTICAL LOADS	423	17.4.5.1.1. Galvanizing	446
16.3. STABILITY OF DOLPHINS	423	17.4.5.1.2. Flame Spraying	451
16.3.1. IN SAND	425	17.4.5.2. Non-Metallic Coatings	453
16.3.2. IN CLAY	425	17.4.5.3. Cathodic Protection	454
16.3.3. FRICTIONAL FORCES	425	17.5. PROTECTION OF WALES, TIE RODS, AND ACCESSORIES	455
16.4. BEARING CAPACITY	426	17.6. CORROSION CONSIDERATIONS IN DESIGN OF TIEBACKS	457
16.5. SKELETAL SHEET PILE CELL DOCKS	426	17.6.1. CORROSION OF PRESTRESSING STEEL	457
CHAPTER 17.		17.6.2. ANCHOR PROTECTION AGAINST CORROSION	458
CORROSION AND PROTECTION	431	17.6.2.1. Protection of the Bond Zone	459
17.1. OVERVIEW OF CORROSION	431	17.6.2.2. Protection of Unbonded Length	459
17.2. TYPES OF CORROSION IN STEEL SHEET PILING	431	17.6.2.3. Protection at the Anchor Head	461
17.2.1. PITTING CORROSION	431	CHAPTER 18.	
17.2.2. UNIFORM CORROSION	433	LATERAL EARTH PRESSURE TABLES AND CHARTS	463
17.2.3. GALVANIC ACTION	433	18.1. RANKINE THEORY	463
17.2.4. STRAY CURRENT CORROSION	434	18.2. COULOMB THEORY	465
17.2.5. FATIGUE CORROSION	434	18.3. LOG-SPIRAL THEORY	473
17.2.6. BACTERIA AND FOULING	434	CHAPTER 19.	
17.3. CORROSION ENVIRONMENTS	434	REFERENCES, NOTATION AND GLOSSARY.	474
17.3.1. NON-MARINE ENVIRONMENTS	434	19.1. REFERENCES AND BIBLIOGRAPHY	474
17.3.2. COASTAL AND MARINE ENVIRONMENTS	435	19.2. NOTATION	490
17.3.2.1. Corrosion Rates by Zone	435	19.2.1. GREEK LETTER SYMBOLS	490
17.3.2.2. pH Value	435	19.2.2. ROMAN LETTER SYMBOLS	491
17.3.2.3. Salinity	435	19.2.3. VARIABLES FOR CELLULAR COFFERDAMS	494
17.3.2.4. Pollution	437	19.3. GLOSSARY	496
17.3.2.5. Wind	437		
17.3.2.6. Rain	437		
17.3.3. ATMOSPHERIC ZONE	437		

Table of Figures

Figure 1-1 Typical Wood Sheet Pile Sections	1
Figure 1-2 Freistadt Sheet Piling	2
Figure 1-3 Historical Sheet Pile Sections	2
Figure 1-4 Typical Hot-Rolled Steel Sheet Piling	2
Figure 1-5 Typical Cold-Rolled Sheet Piling Sections	3
Figure 1-6 Types of Interlocks Used in Sheet Piling	5
Figure 1-7 Typical Concrete Sheet Piling	6
Figure 1-8 Typical Aluminium Sheet Pile Sections	6
Figure 1-9 Typical Cellular Cofferdam Arrangement	9
Figure 1-10 Circular Cells	9
Figure 1-11 Diaphragm Cell	10
Figure 1-12 Cloverleaf Cells	10
Figure 1-13 Modified Cellular Cofferdams	10
Figure 1-14 Steel Sheet Piling for Cellular Cofferdams	11
Figure 1-15 Deep-Seated Failure	17
Figure 1-16 Rotational Failure Due to Inadequate Penetration	17
Figure 1-17 Flexural Failure of Sheet Piling	17
Figure 1-18 Anchorage Failure	18
Figure 1-19 Potential Failure Modes for Anchored Sheet Pile Walls due to Earthquake Activity	18
Figure 2-1 Distribution of Transverse Bending in a PZ-27 Section (after Hartman)	22
Figure 3-1 Principal Soil Deposits	25
Figure 3-2 Correlations of Strength Characteristics for Granular Soils	27
Figure 3-3 Friction Angle of Granular Backfills	30
Figure 3-4 Plasticity Chart for Unified Classification System	31
Figure 3-5 Typical Boring Log	37
Figure 3-6 Empirical Correlation Between Friction Angle and Plasticity Index from Triaxial Tests on Normally Consolidated Clays	42
Figure 3-7 Undrained Strength Ratio versus Overconsolidation Ratio	43
Figure 3-8 Correlation Between C_N and Effective Overburden Pressure	51
Figure 3-9 Correlations between Relative Density and Standard Penetration Resistance in Accordance with Gibbs and Holtz	54
Figure 3-10 Correlations of Standard Penetration Resistance with Unconfined Strength of Clay	54
Figure 3-11 ϕ' vs. N' for Granular Materials	54
Figure 3-12 Typical Log from Mechanical Friction-Cone	55
Figure 3-13 q_c/N versus D_{50}	57
Figure 3-14 Soil classification from cone penetrometer	57
Figure 3-15 Schematic of the Marchetti Flat Dilatometer	58
Figure 3-16 Dilatometer	58
Figure 3-17 Dilatometer (Continued)	59
Figure 3-18 Menard Pressuremeter Equipment	61
Figure 3-19 Vane Shear Test Equipment	62
Figure 3-20 Open-end Borehole Test	63
Figure 4-1 Shear strength parameters	67
Figure 4-2 Definition and development of at rest, active and passive earth pressures	67
Figure 4-3 Variations of earth pressure force with wall movement calculated by finite element analyses	69
Figure 5-1 Three Earth Pressure Theories for Active and Passive Earth Pressures	71
Figure 5-2 Computation of Rankine active and passive earth pressures for level backfills	73
Figure 5-3 Rankine active and passive earth pressures for inclined backfills	75
Figure 5-4 Coulomb active and passive earth pressures for inclined backfills and inclined walls	77
Figure 5-5 Coulomb and log-spiral passive earth pressure coefficients with $\delta = f/2$ -vertical wall and level backfill	81
Figure 5-6 Coulomb and log-spiral passive earth pressure coefficients with $d = f$ -vertical wall and level backfill	81
Figure 5-7 Comparison of Active Earth Pressure Coefficients	82
Figure 5-8 Comparison of Passive Earth Pressure Coefficients	82
Figure 5-9 Example of trial wedge procedure	83
Figure 5-10 Example of trial wedge procedure, hydrostatic water table	85

Figure 5-11 Equilibrium of horizontal hydrostatic water pressure forces acting on backfill wedge	86
Figure 6-1 Static and Dynamic Horizontal Pressure Components and Anchor Force Settings on a Sheet Pile Wall	91
Figure 6-2 Driving and resisting Mononobe-Okabe active seismic wedge, no saturation	91
Figure 6-3 Driving and resisting Mononobe-Okabe passive seismic wedge, no saturation	91
Figure 6-4: Variation in K_{AE} and $K_{AE} \cdot \cos \delta$ with k_h	93
Figure 6-5 Variation in $K_{AE} \cdot \cos \delta$ with k_h , ϕ , and β	94
Figure 6-6 Equivalent static formulation of the Mononobe-Okabe active dynamic earth pressure problem	94
Figure 6-7 Variation in α_{PE} with Ψ for δ equal to f vertical wall and level backfill	95
Figure 6-8 Variation in α_{AE} with Ψ for δ equal to zero degrees, vertical wall and level backfill	95
Figure 6-9 Variation in dynamic active horizontal earth pressure coefficient with peak horizontal acceleration	97
Figure 6-10 Values of factor F_{AE} for determination of K_{AE}	97
Figure 6-11 Point of action of P_{AE}	98
Figure 6-12 Static active earth pressure force and incremental dynamic active earth pressure force for dry backfill	98
Figure 6-13 Limiting values for horizontal acceleration equals $k_h^* \cdot g$	99
Figure 6-14 Modified effective friction angle	103
Figure 6-15 Effective unit weight for partially submerged backfills	105
Figure 6-16 Variation α_{PE} with Ψ for δ equal to $\phi/2$, vertical wall and level backfill	105
Figure 6-17 Variation in α_{PE} with Ψ for δ equal to zero degrees, vertical wall and level backfill	106
Figure 6-18 Equivalent static formulation of the Mononobe- Okabe passive dynamic earth pressure problem	106
Figure 6-19 Values of factor F_{PE}	106
Figure 6-20 Example of Passive Dynamic Earth Pressure Computation	107
Figure 6-21 Example of Simplified Computation of Dynamic Passive Earth Pressures	109
Figure 6-22 Mononobe-Okabe active wedge relationships including surcharge loading the pseudo-static analysis	110
Figure 6-23 Static active earth pressure force including surcharge (Continued)	111
Figure 6-24 Static active earth pressure force including surcharge (Concluded)	113
Figure 6-25 Static active earth pressure force and incremental dynamic active earth pressure force including surcharge	113
Figure 7-1 Coulomb active earth pressures for a partially submerged backfill and a uniform surcharge	115
Figure 7-2 Permeability of Sand and Sand-Gravel Mixtures	115
Figure 7-3 Coulomb active earth pressures for a backfill subjected to steady state flow	118
Figure 7-4 Two distributions for unbalanced water pressures	121
Figure 7-5 Flow Net Construction and Seepage Analysis	122
Figure 7-6 Depth of Sheet Piling to Prevent Piping in a Braced Cofferdam	123
Figure 7-7 Depth of Sheet Piling in Stratified Sand to Prevent Piping in a Braced Cofferdam	125
Figure 8-1 Theory of elasticity equations for pressures on wall due to surcharge loads	127
Figure 8-2 Point load	129
Figure 8-3 Dynamic active wedge analysis including a surcharge loading	130
Figure 9-1 Typical Cantilever Walls	135
Figure 9-2 Design Pressure Distribution for a Cantilever Wall	135
Figure 9-3 Resultant Earth-Pressure Diagram	137
Figure 9-4 Simplified Method	138
Figure 9-5 Chart for Determining Wall Depth for Uniform Cohesive Soil	138
Figure 9-6 SPW 911 Example for Cantilevered Sheet Piling Wall in Cohesionless Soils	142
Figure 9-7 Initial Earth Pressure for Design of Cantilever Sheet Piling Entirely in Cohesive Soil, Conventional Method	143
Figure 9-8 Initial Earth Pressure for Design of Cantilever Sheet Piling Entirely in Cohesive Soil, Simplified Method	143
Figure 9-9 SPW 911 Example for Cantilevered Sheet Piling Wall in Cohesive Soils	146
Figure 9-10 Cantilever Steel Sheet Pile Wall in Cohesive Soil with Granular Backfill	147
Figure 9-11 SPW 911 Results for Example 10	149
Figure 9-12 Effect of Depth of Penetration on Pressure Distribution and Deflected Shape	149
Figure 9-13 Anchored Sheet Pile Walls, Free Earth Support Method, Granular Soil	150
Figure 9-14 Anchored Steel Sheet Pile Wall in Homogeneous Granular Soil	151
Figure 9-15 SPW 911 Solution for Example 11, Full Passive Earth Pressure Coefficient Method	155
Figure 9-16 SPW 911 Solution for Example 11, Reduced Passive Earth Pressure Coefficient Method	157
Figure 9-17 Free Earth Support Method of Anchored Bulkhead Design in Clay with Granular Backfill	157
Figure 9-18 Anchored Steel Sheet Pile Wall in Cohesive Soil with Granular Backfill	158

Figure 9-19 SPW 911 Solution for Example 12, Full Passive Earth Pressure Coefficient Method	161
Figure 9-20 SPW 911 Solution for Example 12, Reduced Passive Earth Pressure Coefficient Method	162
Figure 9-21 Rowe's Moment Reduction Curves for Cohesionless and Cohesive Soils	163
Figure 9-22 SPW911 Results for Example 13	165
Figure 9-23 Anchored Sheet Pile Wall to Illustrate Blum's Method	166
Figure 9-24 SPW 911 Solution for Example 14	170
Figure 9-25 Finite Element Model for Fixed Earth Support Method	171
Figure 9-26 Loads for CFRAME Model for Fixed Earth Support Example	171
Figure 9-27 CFRAME Deflection Diagram for Example 14	175
Figure 9-28 CFRAME Moment Diagram for Example 14	175
Figure 9-29 CFRAME Shear Diagram for Example 14	175
Figure 9-30 Variation in Toe Moment for Fixed Earth Support Method	177
Figure 9-31 Danish Method of Sheet Pile Wall Design	178
Figure 9-32 Typical Anchorage for Two Tie Rods	179
Figure 10-1 System for SSI Analysis	182
Figure 10-2 Distributed Soil Springs	183
Figure 10-3 Anchor Spring	185
Figure 10-4 Wall/soil system	185
Figure 11-1 Typical Anchored Walls	187
Figure 11-2 Anchor Force Components for Inclined Anchors	189
Figure 11-3 Typical Wale Details	190
Figure 11-4 Analysis of Anchor Blocks and Continuous Anchor Wall	191
Figure 11-5 Effects of Depth and Spacing of Anchor Blocks	193
Figure 11-6 Continuous Deadman Anchor near Ground Surface	193
Figure 11-7 Short Deadman near Ground Surface	194
Figure 11-8 Geometrical Parameters for an Anchor Slab	194
Figure 11-9 Geometrical Parameters for Anchor Slabs with Limited Height and Length	194
Figure 11-10 Earth Pressure Coefficients for the Normal Earth Pressure in Front of an Anchor Slab	197
Figure 11-11 Dimensionless Resistance Factor Ratio for Continuous Anchor Slab, $l/L = 1$	198
Figure 11-12 Dimensionless Resistance Factor Ratio for Anchor Slab Spacing $l/L = 0.75$	199
Figure 11-13 Dimensionless Resistance Factor Ratio for Anchor Slab Spacing $l/L = 0.50$	199
Figure 11-14 Dimensionless Resistance Factor Ratio for Anchor Slab Spacing $l/L = 0.25$	201
Figure 11-15 Location of Line of Action of Anchor Force_	201
Figure 11-16 Relative Distance from Base of Slab to Resultant of Earth Pressure in Front of Anchor Slab	201
Figure 11-17 SPW911 Solution for Example 15	203
Figure 11-18 Layout of Location of Anchor Wall for Example 15	203
Figure 11-19 Pressure Diagram on Sheet Pile Anchor	205
Figure 11-20 Slab Layout for Ovesen's Method Example	205
Figure 11-21 Geometrical Parameters for Anchor Slab in Clay	206
Figure 11-22 Resistance of Anchor Slabs in Plastic Clay	206
Figure 11-23 Components of Tieback Systems	209
Figure 11-24 Tieback Types	210
Figure 11-25 Single Tier Tieback System	210
Figure 11-26 Multi-Tier Tieback System	211
Figure 11-27 Anchor Capacities in Cohesionless Soils	215
Figure 11-28 Reduction Factors for Clay	217
Figure 11-29 Potential Failure Plane	217
Figure 11-30 Dial Indicator Setup for Proof Testing	219
Figure 11-31 Wall Configuration for Example 17	222
Figure 11-32 SPW 911 Solution for Example 17	223
Figure 11-33 Wall Configuration for Example 18	226
Figure 11-34 SPW 911 Solution for Example 18	227
Figure 11-35 Pullout Capacity of Shallow Anchors in Rock	230
Figure 12-1 Decrease in failure surface slope of the active and passive sliding wedges with increasing lateral accelerations	235

Figure 12-2 Measured distributions of bending moment in three model tests on anchored bulkhead	237
Figure 12-3 Anchored sheet pile walls retaining backfills which undergo movements during earthquakes	238
Figure 12-4 Anchored sheet pile wall with no excess pore water pressure due to earthquake shaking (Case 1)	239
Figure 12-5 Static and inertial horizontal force components of the Mononobe-Okabe earth pressure forces	242
Figure 12-6 Static and inertial horizontal force components of the Mononobe-Okabe earth pressure forces	245
Figure 12-7 Distributions of horizontal stress corresponding to ΔP_{AE}	245
Figure 12-8 Horizontal pressure components and anchor force acting on sheet pile wall	245
Figure 12-9 Dynamic forces acting on an anchor block (for $\delta = 0^\circ$)	246
Figure 12-10 Anchored sheet pile wall with excess pore water pressures generated during earthquake shaking (Case 2)	247
Figure 12-11 Anchored sheet pile wall design problem	250
Figure 12-12 Horizontal earth pressure components in free earth support design	251
Figure 12-13 Horizontal active and passive earth pressure components acting on a continuous slender anchor	255
Figure 12-14 Five Horizontal Active Earth Pressure Force Components of P_{AE} with $D = 20.24'$	257
Figure 12-15 Distributions of horizontal stresses corresponding to ΔP_{AE}	259
Figure 12-16 Required Geometry of Tie Rod	262
Figure 12-17 Seismic design problem for a continuous anchor block	262
Figure 12-18 Simplified procedure for siting a continuous anchor wall	265
Figure 13-1 Deformation of Sheet Piling in Braced Cofferdams	266
Figure 13-2 Pressure Distributions for Brace Loads in Internally Braced Cuts	267
Figure 13-3 Diagram Illustrating Assumed Mechanism for Failure by Heave of the Bottom of a Wide Excavation	270
Figure 13-4 Diagram for the Determination of Bearing Pressure Coefficient N_c	271
Figure 13-5 Pressure from Water Distribution	271
Figure 13-6 Assumptions Used in the Hinge Method	273
Figure 13-7 Typical Strut Arrangement for a Braced Excavation	274
Figure 13-8 Sketch of Circular Ring Wale System	277
Figure 13-9 Diagram Illustrating the Use of Raking Braces in Construction of a Deep Cut	275
Figure 13-10 Braced Excavation for Example 20	277
Figure 13-11 SPW 911 Results for Example 20	279
Figure 13-12 CFRAME Model for Example 20, No Toe Configuration	279
Figure 13-13 CFRAME Moment Diagram for Example 20, No Toe Configuration	279
Figure 13-14 Loading of CFRAME Model for Example 20, Configuration with Toe	282
Figure 13-15 CFRAME Deflection Plot for Example 20, Configuration with Toe	286
Figure 13-16 CFRAME Moment Diagram for Example 20, Configuration with Toe	286
Figure 13-17 Braced Excavation for Example 21	289
Figure 13-18 SPW Results for Example 21	290
Figure 13-19 CFRAME Model for Example 21	291
Figure 13-20 CFRAME Loads for Example 21	291
Figure 13-21 CFRAME Shear Diagram for Example 21	295
Figure 13-22 CFRAME Moment Diagram for Example 21	297
Figure 13-23 CFRAME Deflection Diagram for Example 21	297
Figure 13-24 SPW 911 Results for Example 22	299
Figure 13-25 SEEP-W Finite Element Model	299
Figure 13-26 SEEP-W Results: Total Head	301
Figure 13-27 SEEP-W Results: Gradient	302
Figure 13-28 Flow Net for Seepage Example	303
Figure 13-29 Bridge Pier Cofferdam for Example 23	305
Figure 13-30 SPW 911 Solution for Example 23	306
Figure 13-31 Typical Cross-Section of Tieback System	307
Figure 13-32 Pressure Distribution for Tied Back Walls	307
Figure 13-33 Lateral Pressure Distribution for Deep Cut-and-Cover Tunnelling	309
Figure 14-1 HZ Wall System	313
Figure 14-2 HZ Wall For Example 24	315
Figure 14-3 SPW 911 Results for Example 24	317
Figure 15-1 Schematic Deflector Layout	321

Figure 15-2 Typical Floodgate Arrangement	322
Figure 15-3 Typical Tie-in Details	323
Figure 15-4 Arrangements of Connecting Wyes and Tees	325
Figure 15-5 Estimate of Free Water Location in Fill	325
Figure 15-6 Maximum Pool Condition	326
Figure 15-7 Initial Filling Condition	326
Figure 15-8 Drawdown Condition	327
Figure 15-9 Typical Cellular Cofferdam Geometry for Equivalent Width	329
Figure 15-10 Sign convention for geometry	333
Figure 15-11 Geometry of the Typical i th Wedge and Adjacent Wedges	333
Figure 15-12 Distribution of Pressures and Resultant Forces Acting on a Typical Wedge	334
Figure 15-13 Free Body Diagram of the P^{th} Wedge	335
Figure 15-14 Derivation of the General Wedge Equation	337
Figure 15-15 Overturning Stability, Typical Loading and Nomenclature	339
Figure 15-16 Rotation -- Hansen's method, cell founded on rock	341
Figure 15-17 Rotation – Hansen's Method, Cell Founded on Soil, Rupture Surface into the Cell Fill	342
Figure 15-18 Rotation – Hansen's Method, Cell Founded on Soil, Rupture Surface into the Foundation	343
Figure 15-19 Deep-seated sliding failure	343
Figure 15-20 Sliding along Weak Seam Near Bottom Of Cell (approximate method)	345
Figure 15-21 Bearing capacity failure	347
Figure 15-22 Base soil pressure diagram	350
Figure 15-23 Cellular cofferdam on compressible soils	353
Figure 15-24 Influence value I for vertical stress P at depth z below the centre of a rectangular loaded area on a uniformly thick layer resting on a rigid base	354
Figure 15-25 Partial flow net beneath a cell on sand	355
Figure 15-26 Resultant Interlock Pressure and Point of Maximum Horizontal Pressure	358
Figure 15-27 Interlock Stress at Connection	361
Figure 15-28 Vertical shear resistance, Terzaghi method	362
Figure 15-29 Vertical Shear Resistance, Schroeder-Maitland Method	365
Figure 15-30 Horizontal Shear Resistance, Cummings Method	365
Figure 15-31 Schematic drawing, vertical slice model	401
Figure 15-32 Vertical Slice Analysis, Finite Element Method	402
Figure 15-33 Schematic drawing, axisymmetric model	403
Figure 15-34 Finite Element Mesh for Axisymmetric Analyses of Main Cell Filling	403
Figure 15-35 Schematic Drawing, Horizontal Slice Analysis	405
Figure 15-36 Finite Element Mesh for Horizontal Slice Analysis of Cell Filling	405
Figure 16-1 Cellular Sheet-Pile Dolphin (Isolated Single Cell)	421
Figure 16-2 Load and Energy-Deflection Curves for Cylindrical Rubber Fenders, Side Loaded	
•(a) Approximate Load-Deflection Curves	422
•(b) Approximate Energy-Deflection Curves	422
Figure 16-3 Load and Energy-Deflection Curves for Rectangular Rubber Fenders, Side Loaded	
•(a) Approximate Load-Deflection Curves	423
•(b) Approximate Energy-Deflection Curves	423
Figure 16-4 Determination of Embedment Depth D for Vertical Shaft Subject to a Horizontal Force in Sand	425
Figure 16-5 Determination of Embedment Depth D for Vertical Shaft Subject to a Horizontal Force in Clay	425
Figure 16-6 Frictional Forces Contributing to Stability of Sheet-Pile Dolphin in Sand	426
Figure 16-7 Skeletal Barge Dock Sheet Pile Cells	426
Figure 16-8 Elevation View for Example 28	427
Figure 16-9 Plot of D vs. c for Example 28	429
Figure 16-10 Force Diagram for Overturning Moment	429
Figure 17-1 Corrosion Rate Profile of Steel Sheet Piling	435
Figure 17-2 Variation in Corrosion of Iron as a Function of Salinity	437
Figure 17-3 Time-corrosion Curves for Industrial and Marine Atmospheres	438
Figure 17-4 Comparative Corrosion of Two Types of Steel in a Marine Environment	439

Figure 17-5 Time-Corrosion Curves for Soils	442
Figure 17-6 Encased Sheet Pile Wall	445
Figure 17-7 Cathodic Protection Systems	454
Figure 17-8 Repairing Tie Rods	455
Figure 17-9 Simple Corrosion Protected Tendon	458
Figure 17-10 Encapsulated Double Corrosion Protected Tendons	459
Figure 17-11 Bonded Tendon	461
Figure 17-12 Anchor Head Details	462
Figure 18-1 Rankine Active Earth Pressure Coefficients K_a	463
Figure 18-2 Rankine Passive Earth Pressure Coefficients K_p	463
Figure 18-3 Coulomb Active Earth Pressure Coefficients K_a , $\delta = 0^\circ$	465
Figure 18-4 Coulomb Active Earth Pressure Coefficients K_a , $\delta = 5^\circ$	465
Figure 18-5 Coulomb Active Earth Pressure Coefficients K_a , $\delta = 10^\circ$	466
Figure 18-6 Coulomb Active Earth Pressure Coefficients K_a , $\delta = 15^\circ$	466
Figure 18-7 Coulomb Active Earth Pressure Coefficients K_a , $\delta = 20^\circ$	467
Figure 18-8 Coulomb Active Earth Pressure Coefficients K_a , $\delta = 25^\circ$	467
Figure 18-9 Coulomb Active Earth Pressure Coefficients K_a , $\delta = 30^\circ$	469
Figure 18-10 Coulomb Active Earth Pressure Coefficients K_a , $\delta = 35^\circ$	469
Figure 18-11 Coulomb Passive Earth Pressure Coefficients K_a , $\delta = 0^\circ$	470
Figure 18-12 Coulomb Passive Earth Pressure Coefficients K_a , $\delta = 5^\circ$	470
Figure 18-13 Coulomb Passive Earth Pressure Coefficients K_a , $\delta = 10^\circ$	471
Figure 18-14 Coulomb Passive Earth Pressure Coefficients K_a , $\delta = 15^\circ$	471
Figure 18-15 Coulomb Passive Earth Pressure Coefficients K_a , $\delta = 20^\circ$	471
Figure 18-16 Active and passive earth pressure coefficients with wall friction-sloping backfill	473

Table of Tables

Table 2-1 Section Properties and Allowable Bending Stresses for Selected Steel Sheet Sections	21
Table 3-1 Unified Soil Classification System for Coarse-Grained Soils	29
Table 3-2 Unified Soil Classification for Fine-Grained Soils	30
Table 3-3 Visual Identification of Samples	34
Table 3-4 Problem Soils and Conditions	38
Table 3-5 Hammer Efficiencies for Various Types and Origins of SPT Hammers	51
Table 3-6 Relative Density or Consistency of Soils as a Function of SPT N Values	53
Table 4-1 Approximate Magnitudes of Movements Required to Reach Minimum Active and Maximum Passive Earth Pressure Conditions	70
Table 5-1 Ultimate Friction Factors for Dissimilar Materials	81
Table 6-1 Values of kh based on Whitman and Liao Relationships	90
Table 9-1 Forces and Moment Arms for Maximum Moment in Example 11	155
Table 9-2 Results of Rowe's Moment Reduction Method for Example 11 for Different Sections	166
Table 9-3 Forces and Moment Arms for Maximum Moment in Example 14	170
Table 9-4 Results of CFRAME Program for Example 14	173
Table 9-5 Tabulated Results for Fixed Earth Support Example	177
Table 10-1 System Parameters	185
Table 11-1 Nomenclature for Figure 11-25 and Figure 11-26	213
Table 11-2 Tieback Proof Test Criteria	218
Table 11-3 Support Results for Example 18	227
Table 11-4 Typical Values of Bond Stress for Selected Rock Types	229
Table 12-1 Qualitative and Quantitative Description of the Reported Degrees of Damage	234
Table 12-2 Ten Stages of the Analyses in the Design of Anchored Walls for Seismic Loadings	241
Table 12-3 Horizontal Force Components	251
Table 12-4 Moments About Tie Rod Due to Active Earth Pressures Table	253
Table 12-5 Moments About Tie Rod Due to Passive Earth Pressures	253
Table 12-6 Moment Internal to the Sheet Pile at $y = 12.79$ Feet Below the Water Table and About the Elevation of the Tie Rod	254
Table 12-7 Design Moment for Sheet Pile Wall in Dense Sand	254
Table 12-8 Summary of Depth of Penetration Calculations	258
Table 12-9 Tie Rod Force T_{FES}	259
Table 12-10 Moment of Forces Acting Above the Point $y = 15.32$ feet Below the Water Table and About the Tie Rod	261
Table 12-11 Design Moment for Sheet Pile Wall in Dense Sand	262
Table 13-1 CFRAME Results for Example 20, No Toe Configuration	281
Table 13-2 CFRAME Results for Example 20, Configuration with Toe	283
Table 13-3 Summary of Results for Example 20	287
Table 13-4 CFRAME Results for Example 21	293
Table 13-5 Summary of Results for Example 21	298
Table 13-6 Results of Transverse Bending Analysis	306
Table 15-1 Design Criteria--Factors of Safety	330
Table 15-2 Terzaghi Bearing Capacity Factors (after EM 1110-1-1905)	349
Table 15-3 Allowable Bearing Pressures for Fresh Rock of Various Types	351
Table 15-4 Coefficients of Internal Pressure	359
Table 15-5 Wall Friction	367
Table 15-6 Advantages and Disadvantages of Various Types of Surface-Mounted Strain Gages	418
Table 17-1 Galvanic Series for Seawater	433
Table 17-2 Relative Corrodibility of Atmospheres at 20 Locations throughout the World	438
Table 17-3 Corrosion Rate of Sheet Piling at Various Locations	439
Table 17-4 Description of Coating Systems on Steel Piles Exposed to the Atlantic Ocean at Dam Neck, VA	446
Table 17-5 Aluminium vs. Zinc Flame Sprayed Coatings	453

Table of Examples

Example 1 Rankine Active Coefficients and Wall Pressures	74
Example 2 Rankine Passive Coefficients and Wall Pressures	75
Example 3 Coulomb Active Coefficients and Wall Pressures	78
Example 4 Coulomb Passive Coefficients and Wall Pressures	79
Example 5 Computation of Active Dynamic Earth Pressures	99
Example 6 Computation of Passive Dynamic Earth Pressures	107
Example 7 Computation of K_{PE} , P_{PE} , and α_{PE}	109
Example 8 Design of Cantilevered Sheet Pile Wall (Granular Soil)	138
Example 9 Design of Cantilever Sheet Pile Wall (Purely Cohesive Soils)	145
Example 10 Design of Cantilevered Sheet Pile Walls (Cohesive soils with Cohesionless Backfill)	147
Example 11 Anchored Sheet Pile Wall in Cohesionless Soil, Free Earth Support Method	153
Example 12 Anchored Wall in Cohesive Soil with Cohesionless Backfill	158
Example 13 Rowe's Moment Reduction Method, Cohesionless Soils	165
Example 14 Fixed Earth Support Method	169
Example 15 Design of Wales and Anchors for Sheet Pile Wall in Cohesionless Soils	203
Example 16 Tieback Testing	221
Example 17 Single Tier Tieback Shoring Wall	222
Example 18 Multiple Tier Tiebacks	226
Example 19 Design Example For Earthquake Loading of an Anchored Sheet Pile Wall	250
Example 20 Braced Excavation in Granular Soil	277
Example 21 Braced Excavation in Cohesive Soil	289
Example 22 Design of Braced Cofferdam for Seepage	298
Example 23 Water Cofferdam with Transverse Bending	303
Example 24 HZ Wall Design	315
Example 25 Cellular Cofferdam on Rock	367
Example 26 Cellular Retaining Wall on Sand	378
Example 27 Cellular Retaining Wall on Clay	390
Example 28 Design of a Mooring Dolphin – Granular Soil	427
Example 29: Sacrificial Metal Requirements	443

Chapter One: Overview of Sheet Piling

The term *sheet piling* refers to any retaining wall type that is a) installed into the ground by driving or pushing, rather than pouring or injection, and b) is of relatively thin crosssection and low weight so that the weight of the wall does not assist in the wall's stability.

The modern sheet piling industry is a little more than 100 years old with perhaps the most important changes in type and selection of products occurring since the early 1970's.

Sheet piling have been used in a wide variety of applications, especially marine bulkheads and retaining walls where space is limited. In addition to these, a special type of retaining wall is the cellular cofferdam, which are used extensively for both temporary and permanent structures.

1.1. Types of Sheet Piling¹

Sheet piling are made in a number of materials. The material chosen depends upon a number of factors including both strength and environmental requirements. The designer must consider the possibility of material deterioration and its effect on the structural integrity of the system. Concrete is capable of providing a long service life under normal circumstances but has relatively high initial costs when compared to steel sheet piling. They are more difficult to install than steel piling. Long-term field observations indicate that steel sheet piling provides a long service life when properly designed. Permanent installations should allow for subsequent installation of cathodic protection before excessive corrosion occurs.

1.1.1. Wood

Thousands of years ago, timber logs were placed or pounded into the earth to act as retaining walls or crude dams. Rows of logs were sometimes paralleled and the centre filled with earth to make a stronger wall. Logs were probably lashed together with rope, and a strong back added to combine the logs into a wall. Eventually, it was found that sawn, shaped logs fit together better with less loss of fill through the joints. This led to the first manufactured sheet pilings having a positive interlocking mechanism between each sheet. Timber sheet piles called "Wakefield" piles were fabricated of three flat wooden pieces. The centre section was offset from the outer sections thus forming a groove and a tongue for joining adjacent piles. A variation of this system was a single timber section in which the groove and tongue were cut to shape. Wakefield type sheet piling is still being used today (see *Figure 1-1*.) Many wood sheet pile walls follow the "Navy Wall" design concept, where loads are transferred to round timber master piles and standard dimensional lumber is used for the sheeting.

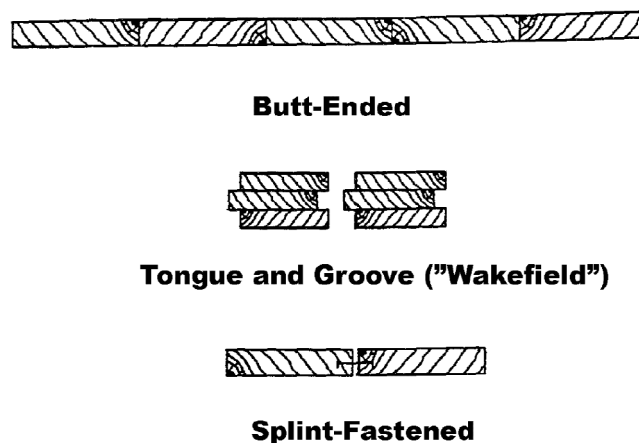


Figure 1-1: Typical Wood Sheet Pile Sections

The interlocking systems devised for timber or concrete sheet piling have been based on the tongue and groove concept. This method serves to keep the wall aligned while providing a longer path against infiltration with more potential contact points than a simple butt joint. The efficiency of such joints depends on good installation practice but the long-term effectiveness is often in jeopardy due to impact from waves or from settlement. The development of filter cloth membrane material for the lining the backside of these walls has reduced the need for more positive interlocks on walls made of these products. As a consequence, many shallow timber bulkheads are built with regular dimension lumber. Timber sheet piling continues to enjoy an important position, in the industry providing relatively inexpensive bulkheads for homes, commercial property and marinas. Timber sheeting is also used extensively in retainment work for shallow trenches and land cofferdams where water intrusion is not a factor.

1.1.2. Steel Sheet Piling

Metal sheet piling was a natural advancement in the evolution of this product as we entered the "Iron Age" in the mid-1800's. Cast iron was used to make some crude sections, but these were not successful due to lack of ductility. Toward the end of the century, Bessemer steel was developed and mills began hot-rolling I-beams, channels and angles, among other structural shapes. Freistadt-type piling appeared about 1890, fabricated from a rolled channel section as shown in *Figure 1-2*. Z-bars riveted to the web provided a groove into which the flange of a channel could slide, thus forming a crude but innovative interlock. A "Universal" type sheet piling introduced in Great Britain about 1895 utilized hot-rolled I-beams and special clips to join the flanges of the I-beams together. The efficiency of this wall was low because the I-beams were aligned in the weak structural direction.

¹ For a more detailed description of the various types of sheet piling and their installation, see *Pile Driving by Pile Buck*, available from Pile Buck.

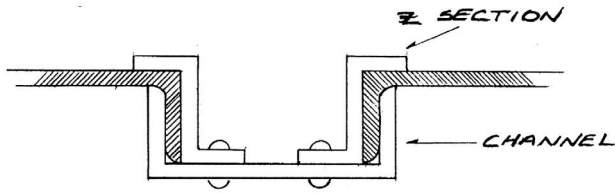


Figure 1-2: Freistadt Sheet Piling

1.1.2.1. Larssen Shapes

Inventors were striving to develop a sheet piling that would contain interlocks rolled into the beam during the manufacturing process, rather than attached afterwards by riveting. Gregson (USA) patented a bulb and jaw interlock in 1899, however this still resulted in production of a flat section with relatively small section modulus. Trygve Larssen obtained a German patent in 1904 for a deep, hot rolled section that greatly increased the strength and efficiency of steel walls and represented a major advancement. Larssen's piling wall assumed a "wave shape" when assembled and all subsequent developments for efficient sheet pile walls are based on this concept. Larssen's section still contained a partially fabricated interlock and it was not until 1914, that a rivetless Larssen interlock appeared in Germany.

In the United States, Lackawanna Steel Co. (later acquired by Bethlehem Steel Corp.) was a flat sheet piling shape and several arched types with rolled, integral interlocks as early as 1910. Carnegie Steel Co. (U.S. Steel Corp.) offered three flat sections with rolled-on interlocks and one fabricated section. By 1929, Carnegie's catalogue illustrated four deep-arch, two shallow-arch and two straight sections. Some of these and other historical sections of sheet piling are shown in Figure 1-3.

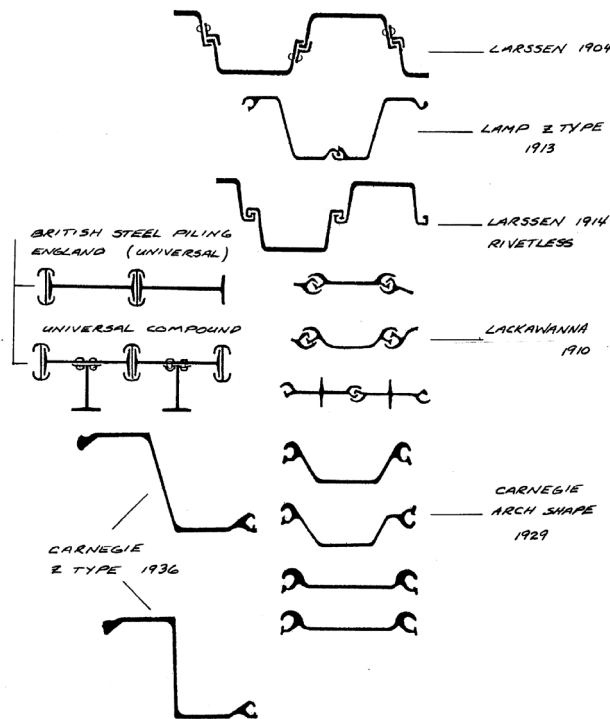


Figure 1-3: Historical Sheet Pile Sections

1.1.2.2. Z-Type Shapes

Z-shaped piles followed the Larssen concept for a wave-shaped profile but with the added advantage that the interlocks are formed on the outer elements of the section. The extra metal is put to best use, since it is well out from the neutral axis of the wall. Larssen interlocks are located on the neutral axis. Surprisingly, Z-shaped piles were produced in Europe as early as 1911. The Ransome profile looked very much like some of today's lightweight Z-shapes. The deeper Lamp Z-pile introduced about 1913, resembles a modern ball and socket Z-type pile.

In Europe, Z-type shapes fell from favour when the Larssen U-types were developed. Two Z-shapes were introduced in the United States in the 1930's and became quite popular. PZ-38 and PZ-32 offered wider and deeper sections than any of the arch shaped shapes then available. Z-shaped piles obtained some impetus in the U.S. from the longstanding controversy regarding the actual moment-resisting properties of U and Arch shaped sections.

Z-shaped piles interlock on the wall extremities and provide a solid web connecting the two flanges. When the PZ-27 section was introduced in the 1940's, its section modulus of 30.2 in³/ft was almost three times that published for the arch section with the identical weight per square foot of wall. This section subsequently became the all-time most popular sheet piling section in history. Z-type shapes are now produced with section moduli ranging from 8.6 to about 85 in³/foot of wall.

The Z-type piling is predominantly used in retaining and floodwall applications where bending strength governs the design and no deflection (swing) between sheets is required.

Most producers do not guarantee any swing although some can generally be attained or area can be built by providing some bent pieces in the run. Turns in the wall alignment can be made with standard bent or fabricated corners. Typical configurations are shown in Figure 1-4.

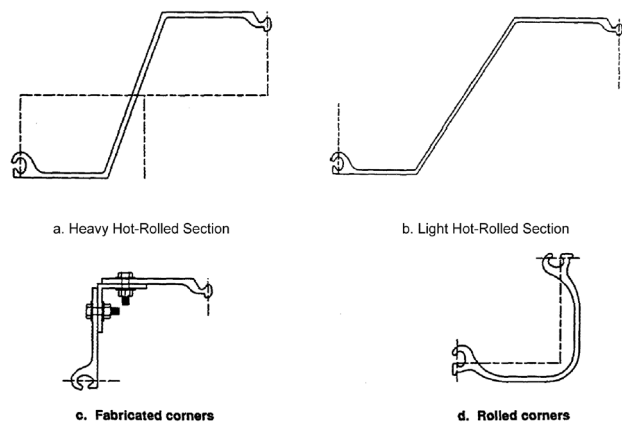


Figure 1-4: Typical Hot-Rolled Steel Sheet Piling

Z-piles are not used in applications when interlock strength is required such as filled cells. These sheets would tend to stretch and flatten in these cases. No minimum interlock strength is offered for this reason. When interlock tension is the primary consideration for design, an arched or straight web piling should be used.

1.1.2.3. Straight Web Sections

Flat profile sections were originally produced only because of mill rolling limitations. Competition and customer demand prompted the expansion into structurally efficient sheet piling. It was discovered that these flat profiles had strength in tension that was advantageous for building circular, filled structures from sheet piling. About 1908 a large cellular cofferdam was built on the Black Rock River in Buffalo N.Y. in order to de-water the site for a new lock. This concept was progressively expanded to include circular and diaphragm-shaped cells for piers and breakwaters that might have formerly been built of timber cribs or masonry.

The use of large diameter, cellular cofferdams was given a special impetus in the 1930's when the Tennessee Valley Authority²⁰⁴ began a series of hydro dams and navigation locks on that river system in the south-eastern United States. Not only did TVA engineers develop new design methods for designing these large structures, they developed better ways of installing and maintaining them.

Flat sheets have little strength to resist bending, but do have very strong interlocks to resist "hoop" stress. These piles are used almost exclusively for building large, filled cellular structures. Flat sheets must provide some ability to "swing" between sheets so that a circle can be closed. Most manufacturers will guarantee a minimum swing of 8 to 10 degrees between adjacent sheets for standard lengths of piling. For overly long pieces, these warranties must generally be negotiated.

Available interlock strengths must be known in advance in order to design a structure that will be safe against bursting. Most manufacturers will guarantee a "minimum" interlock strength based on tension tests conducted on a number of representative production samples. It has been determined from experience that interlock dimensional tolerances that fall within certain limitations will provide tension values characteristic of the entire production run.²

Flat sheet piling is available only as a hot rolled product, since the cold-finishing process does not provide an interlock with sufficient strength in tension. Interlock strengths have been gradually increased due to the demand to build larger cells for deeper cofferdams.

Most flat sheet piling has been used to construct temporary cellular cofferdams. After the initial use, the sheets are pulled and used in other portions of the project or perhaps sold for another project elsewhere. Other flat sheets are used in permanent structures such as breakwaters, earth containment sites, piers and other applications. Cellular cofferdams are discussed in more detail in 1.2.1.4.

1.1.2.4. Cold Finished Piling

Since the early 1970's another method of producing steel sheet piling has greatly expanded the availability and the selection of sections. This new method uses hot-rolled sheets in coil form, fed through a series of cold-rolling stands to form "Z" or "arch" shapes complete with a simple, hook-type interlock. This involves a relatively inexpensive capital expenditure com-

pared to the hot-rolled product and has attracted a number of new producers.

These steel pilings are shallow-depth sections, cold formed to a constant thickness of less than 0.25 inch and manufactured in accordance with ASTM A 857. Yield strength is dependent on the gauge thickness and varies between 25 and 36 kips per square inch (ksi). These sections have low-section moduli and very low moments of inertia in comparison to heavy-gauge Z-sections. Specialized coatings such as hot dip galvanized, zinc plated, and aluminized steel are available for improved corrosion resistance. Light-gauge piling should be considered for temporary or minor structures. Light-gauge piling can be considered for permanent construction when accompanied by a detailed corrosion investigation. Field tests should minimally include pH and resistivity measurements. See Figure 1-5 for typical light-gauge sections.

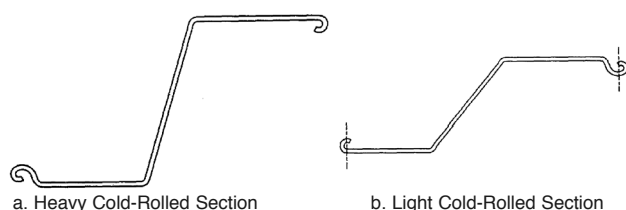


Figure 1-5: Typical Cold-Rolled Sheet Piling Sections

1.1.2.5. High Modulus Sections

There is a limited but regular demand for sheet piling with strength properties that exceed those available from standard products. These may be required for deep excavations, poor soil conditions, deeper dredge lines and other special conditions. These are discussed in detail in Chapter 14.

1.1.2.6. Interlocks for Steel Piling

There are no established industry standards for interlocks found on steel sheet piling. All manufacturers have the same objectives for the interlocks:

- (1) Provide permanent connection of individual sheets in order to form a continuous, relatively water or earth tight wall
- (2) Permit reasonably free sliding to grade during installation
- (3) Meet the strength requirements for the application.

Various types of interlocks are shown in Figure 1-6.

1.1.2.6.1. History

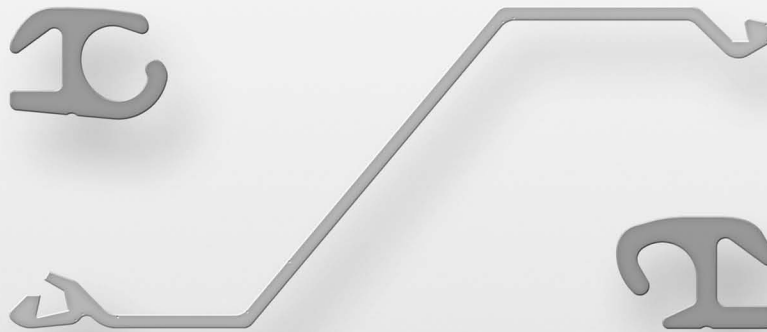
The original interlocks devised for steel pilings were rather crude, riveted additions to a basic structural shape. When the Larssen U-shaped sheet piling section was introduced in 1903, the interlocks were still attached in this manner. Within a few years however, Larssen shapes with hot-formed, integral interlocks were developed which revolutionized the industry both as to the quality of the product and the cost. The Larssen development was and still is a rather simple shaped "hook" formed on the leading edge of each channel section. In the United

² It would of course be impractical to take test samples from each pile.

800.848.6249 www.fosterpiling.com

Z SHEET PILING

- Preferred Sheet Pile Shape
- High Strength to Weight Ratio
- Cost Effective Walls
- Wide Range of Connectors Available



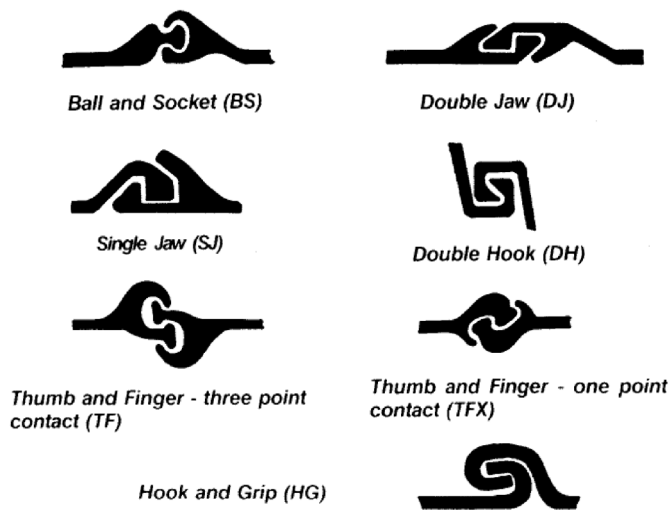


Figure 1-6: Types of Interlocks Used in Sheet Piling

States the 1910 Lackawanna Steel sections utilized a “thumb and finger” design. These types were utilized in the cellular cofferdam built on the Black Rock Canal and were developed as much for their strength in tension as their general application to other uses. We are not aware that any U.S. manufacturer ever produced or considered producing Larssen type sheets and interlocks.

As late as 1923, Carnegie Steel Co. utilized a “ball and socket” interlock. By 1929 this company had abandoned this design and switched to a modern line of arch type sheets with smoothly contoured thumb and finger interlocks.

The thumb and finger design was promoted as having desirable threading characteristics while providing a circuitous path for potential leakage. This interlock very seldom gave any problems from an installation or withdrawal standpoint and the sections with these interlocks were popular with contractors long after the introduction of the Z-type shapes despite the shortfall on strength. These designs are no longer produced.

The thumb and finger design provides three points of contact between the elements of the interlock when stressed. This not only accounts for the high strength of these connections, but also provides a double seal against water intrusion or soil leakage. The strength developed is controlled at the mill by close attention to predetermined dimensional tolerances of the thumb and the slot opening between the finger and the thumb. The dimensions of the finger are also important since this element must not yield or it would allow the thumb to rotate and slip out of lock. The formulation of the steel is a major factor and higher interlock strengths are obtained by utilizing steels of higher minimum yield strength. Tension tests conducted in the mill laboratory are based on a straight, direct pull. When these sections are stressed in the field, they are angled to one another. However, experience has shown that production interlocks when proven by sample testing, have been completely satisfactory. There are very few instances of cell failure from interlock deficiencies where dimensional tolerances were met.

The thumb and finger type interlock is also designed to allow a degree of angularity or swing between interlocks.

Traditionally, designers could count on at least 10 degrees swing per joint. From this, the minimum diameter circle or arc that could be built using that particular sheet piling section could be determined.

Some producers offer a smaller swing and/or restrict the lengths for which swing guarantees are made. It is important that manufacturers' catalogues be consulted for this information, particularly where smaller radii are to be utilized for connecting arcs of cofferdams.

Another interlock design utilized for flat sheets is based on a single contact point between elements. This type is sometimes referred to as a “power hook” interlock. At the present time, there is only one producer of utilizing this style interlock. While popular in Europe, it has not been extensively used in the United States.

1.1.2.6.2. Ball and Socket Interlocks

Ball and Socket interlocks are found on U.S. and some imported Z-type sheet piles. The basic design goes back to the Lampe or Ransome design earlier in the century. The modern ball and socket interlock was designed to “present a smooth, clean wall face, to locate metal where it would do the most good strengthwise, to present an efficient seal against leakage, to permit easy threading and to take punishment during driving.” Of course this is the objective of all manufacturers. If the ball of this interlock is driven leading, then it clears a path for the socket to follow.

1.1.2.6.3. Jaw Type Interlocks

The Single Jaw interlock found on some European Z-shapes is similar to the ball and socket but with angular contours rather than oval. By exercising rigid control over dimensions and product straightness, these closer fitting interlocks seem to offer few problems in installation while providing a tight fit against water intrusion.

The Double Jaw design found on certain European and Japanese Z-type sheet piling is a unique design, with perhaps some additional advantages all wall corners. When ball and socket Z-pile walls intersect, a special fabricated corner section must generally be provided. Producers of the double jaw type are able to offer a simple, hot-rolled structural bar connector that is basically an elbow with two thumbs.

Hook and Grip Interlocks is the type utilized on all cold-finished sheet piles, both Z and arch types. This interlock is formed by bending the edges of the section during one of the last passes through the cold-forming rolls. Some have questioned the long-term suitability of this interlock for repetitive temporary applications.

Except for cellular cofferdams, most sheet piling is used for straight wall construction. Accordingly, there is generally no need for swing guarantees between sheets. From a practical standpoint, some swing can be obtained. This is because the interlocks must have sufficient clearance for sliding. Some large, internally braced circular cofferdams have been built with Z-type sheet piles.

Since manufacturers only warrant the performance of their

own products, it is wise not to interlock the sheet piling of different manufacture together. This would apply particularly to cellular cofferdams. Where interlocks must be mixed, it should be done with a fabricated section at one location.

1.1.2.7. Sheet Piling Nomenclature and Identification

U.S. producers of sheet piling standardized the identification of sheet piling sections so they could be specified without reference to a particular manufacturers product. The identification included a "P" (piling) "Z" (type or shape) and "27" the weight, or PZ-27. Arch and flat shapes were similarly described. Non-U.S. and cold-finishing producers have their own "in house" identification systems. There is now no universal nomenclature system. It is common practice recently to specify the bending moment to be satisfied which then allows the contractor considerable flexibility in his selection of a section and a supplier. This bending moment specification should not be used blindly, however, as many sheet pile designs (especially those using vinyl or pultruded fibreglass sheeting) are principally governed by deflection.

1.1.2.8. Ordering Sheet Piling

Like other steel products, steel sheet piling may be ordered by reference to a standard specification. In the United States this standard is published by the American Society of Testing Materials (ASTM) 1916 Race Street, Philadelphia, PA 19103-1187. The basic ASTM Specification A-328 and others listed may be obtained by writing to the Society or visiting their website <http://www.astm.org>.

This specification covers the steel making process, the chemistry requirements, the minimum yield and ultimate strength. Delivery is referenced in ASTM Specification A-6. The ASTM Specification does not cover interlock tolerances, straightness, interlock strength, nor does it cover rental or second hand material. These are between buyer and seller.

Other Specifications include:

- Canadian Specification CSA 44 W, CAST 44W/70
- British Specification BS4360 – Various Grades
- European Specification: ST SP 37; ST SP 45; ST SP 5.

1.1.2.9. Steel Sheet Piling Today

While the annual consumption of sheet piling in this country rarely exceeds 250,000 U.S. tons, the number of producers and the availability of sections has increased dramatically in the last ten years. In 1960 there were two U.S. producers, each offering nine sheet piling sections. Today there are at least 14 U.S. and non-U.S. producers offering over 200 sections in this country. Competitive factors have generated development of new, wider, more-efficient sections. Large Z-shapes are now available for deep construction with section modulus of almost twice that previously available. A wall system has been developed using large H-sections combined with light Z-shapes that greatly increases the section modulus. Light weight "gauge" material is produced on the cold forming mills for economical shallow bulkheading and trench work.

Higher strength steels up to 60 ksi yield point have also been effectively used in sheet piling design. These grades offer the opportunity to save weight or to extend bending or interlock strengths beyond those of conventional grades. For those applications that require it, corrosion resistant steel can also be specified as well.

1.1.3. Concrete

These piles are precast sheets 6 to 12 inches deep, 30 to 48 inches wide, and provided with tongue-and-groove or grouted joints. The grouted-type joint is cleaned and grouted after driving to provide a reasonably watertight wall. A bevel across the pile bottom, in the direction of pile progress, forces one pile against the other during installation. Concrete sheet piles are usually prestressed to facilitate handling and driving. Special corner and angle sections are typically made from reinforced concrete due to the limited number required. Concrete sheet piling can be advantageous for marine environments, streambeds with high abrasion, and where the sheet pile must support significant axial load. Past experience indicates this pile can induce settlement (due to its own weight) in soft foundation materials. In this case the watertightness of the wall will probably be lost. Typical concrete sections are shown in *Figure 1-7*. This type of piling may not be readily available in all localities.

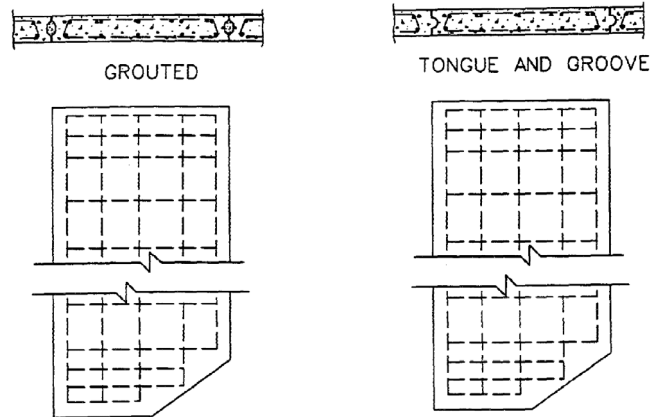


Figure 1-7: Typical Concrete Sheet Piling

1.1.4. Light-gauge aluminium

Aluminium sheet piling is available as interlocking corrugated sheets made from aluminium alloy 5052 or 6061. These sections have a relatively low-section modulus and moment of inertia necessitating tiebacks for most situations. A Z-type section is also available in a depth of 6 inches and a thickness of up to 0.25 inch. See *Figure 1-8* for typical sections.³

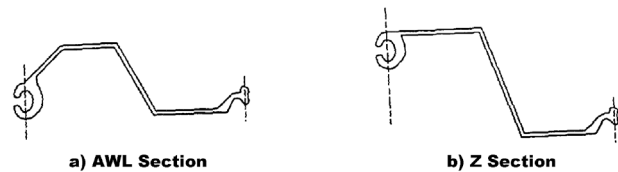


Figure 1-8: Typical Aluminium Sheet Pile Sections

³ Aluminum sheet piling configurations (and their resistance to corrosion) are discussed more fully in *Pile Driving by Pile Buck*.

1.1.5. Vinyl Sheet Piling

Vinyl sheet piling is a relatively new type of sheeting which can be applied in a wide variety of ways for seawalls and other applications of sheet piling. It is generally manufactured by continuous extrusion. The raw material, plastic resin compound, is melted and pushed through a die. This die shapes the plastic into the computer aided design cross section. The sheet is then cooled and cut to length. The sheets can be extruded to the length required for different retaining wall applications.

Vinyl sheeting comes in a number of configurations. The most common configuration is a Z-sheet type of configuration similar to those shown in *Figure 1-4*. Others are similar to aluminium sheeting shown in *Figure 1-8*. The individual sheets have interlocking male and female edges. The interlocking edges are extruded as part of the sheet to insure consistent strength throughout the retaining wall. As is the case with other sheeting, vinyl sheeting requires transition pieces such as corners and intersections. These are designed to interface properly with the other sheeting the manufacturer makes.

Vinyl sheeting is made of a modified polyvinyl chloride (PVC), which makes it suitable for most marine environments and not subject to leaching, corrosion or similar deterioration mechanisms. The technology that has brought us vinyl siding for homes, plastic automotive parts such as bumpers and dashboards, and durable home appliances, is now being utilized to produce a sheet piling for marine retaining walls, sea walls or bulkheads. The vinyl also includes a UV stabilizer to reduce deterioration due to sunlight.

Because vinyl sheet piling generally has a low modulus of elasticity and strength relative to metal sheet piling, deflection frequently becomes the governing factor in the design of the wall, and should be determined in the design process.

1.1.6. Pultruded Fibreglass Sheet Piling

Pultruded sheet piling is a section of piling that is manufactured by the continuous processing of raw materials by pulling resin-rich reinforcements through a heated steel die to form profiles of constant cross section of continuous length. The first reinforcement utilized in the profile are long continuous glass fibres referred to as "roving". Glass roving runs the length of the pultruded profile and gives the shape its "longitudinal strength". To add multidirectional reinforcement, continuous glass "matting" is added. The roving and matting is now pulled through a resin bath where the glass fibres are saturated with a liquid thermosetting resin. This process is typically referred to as the "wet-out" process.

The coated fibres are now assembled to the proper shape by a forming guide and finally drawn through a heated (curing) die. Once exiting the die, the pultruded shape is cooled and the resulting high strength, reinforced composite sheet piling is cut to length.

Pultruded sheet piling is suitable for a wide variety of applications for light bulkheads. As is the case with vinyl sheeting, deflection is frequently the controlling factor in design, although the strength of the material is several times higher than vinyl.

1.2. Applications

Sheet piling has a potential application anywhere a retaining or membrane type wall is needed. The application may be either temporary or permanent. This chapter will review traditional ways in which this product has been applied and describe a number of innovative additional uses.

1.2.1. Temporary Applications

If sheet piling had never been developed as a method for building permanent walls, it would have been invented as a tool for contractors. While no statistics are kept, it is estimated that at least half of the annual production of sheet piling is utilized for temporary applications. Steel sheet piling, particularly, has the inherent strength to allow it to be driven, pulled, and reused a number of times before its value as a tool is lost.

There is a large rental business in sheet piling and many contractors prefer to rent this material rather than maintain their own stock. When sheet piling used for temporary applications has been trimmed to the point where lengths no longer have a ready application, the material can be used for a final, permanent project.

1.2.1.1. Temporary Box Cofferdams

Single-wall box cofferdams are the means by which bridge piers and other heavy foundations with relatively small area are constructed under dry conditions. Sheet piling sections form a structural wall that is generally braced internally against the soil or water pressure outside. The sheet pile membrane excludes earth and water from the site while the permanent work is being constructed. Since these piling sections are subject to bending stresses, "Z", arch or "U" type sheet piling sections are utilized.

When a series of piers requiring cofferdams are to be built, contractors generally purchase or rent enough sheet piling to build several cofferdams, then pull and re-use the piling a number of times at the other pier locations. The owner may specify that the cofferdam be left in place where tremie seals are required, or to protect against streambed scour.

1.2.1.2. Land Cofferdams

Steel sheet piling may be considered for retainment walls of any temporary excavation. While other methods for retaining soil such as soldier beams and lagging, slurry walls, soil nailing etc. have evolved, sheet piling is advantageous where high ground water or flowing soil loss threatens not only the new excavation but also adjacent existing foundations. Sheet piling can be driven below the proposed excavation level in order to cut off flow into the bottom of the hole. Cross-lot or raker beam bracing were traditional means of supporting large sheeted excavations. This is now accomplished mainly with external tiebacks into soil or rock.

A variation of the rectangular or square box cofferdam is the circular type. This design employs circular compression ring walers rather than cross bracing and frees the inside to allow more efficient digging and placement. If the diameter is sufficiently large, the circle may be closed by the natural swing



**IS YOUR JOB
DRIVING
YOU TO
THE WALL?**

**TRY OUR
NEW CLAMP.**

**PUT THE
SHEETS
AGAINST
THE WALL!**

When a pile driver talks... we listen™. Please call or write:



APE Corporate Offices
7032 South 196th
Kent, Washington 98032
800-248-8498 or
253-872-0141
Fax: 253-872-8710

APE CANADA
1965 Ramey Road
Port Colburn, ON
L2G 7MG
905-328-0850
Fax: 905-834-8486

APE Mid-Atlantic Regional Ofc.
500 Newton Rd. Suite 200
Virginia Beach, VA 23462
866-399-7500
Fax: 757-518-9741
Cell: 757-373-9328

APE Northeast Regional Ofc.
Route 15 North & Taylor Rd.
Wharton, NJ 07885
973-989-1909
Fax: 973-989-1923
888-217-7524

APE Southeast Regional Ofc.
1023 Snively Avenue
Winter Haven, FL 33880
863-324-0378
Fax: 863-318-9409

APE S. Central Regional Ofc.
11128 FM Hwy. 1488
Conroe, TX 77384
936-271-1044
Fax: 936-271-1046
800-596-2877

APE Western Regional Office
160 River Road
Rio Vista, CA 94571
707-374-3266
Fax: 707-374-3270
888-245-4401

Alessi Equipment, Inc.
35 Rosslyn Place
Mt. Vernon, NY 10550
914-699-6300
Fax: 914-699-5300

Imeco-Austria
431-368-2513
Fax: 431-369-8104

between sheet piling sections, otherwise, a number of pre-bent sheets must be provided for in the design.

Sheet piling used in temporary excavations is often left in place since the cost of removal may offset the salvage value. Some building codes or specifications require this action, particularly where the piling has been installed to protect sensitive underground utilities.

1.2.1.3. Trench Excavations

It has become almost mandatory that major trench excavations be sheeted and shored.

This is done for the following reasons:

- To meet OSHA rules;
- To protect the workmen;
- To protect adjacent structures; and
- To keep the hole free of earth and water.

The engineer often specifies sheet piling. Because most trenches are relatively shallow excavations, lighter-weight sheets may be satisfactory and there are a large number of shapes and sections from which to choose for this purpose.

Trench excavations require bracing consisting of one or several rows of horizontal walers with cross bracing, spaced to permit machine-excavation and installation of the permanent construction. Some bracing may be pre-fabricated and also serves as a guide template for aligning the piling.

Other temporary applications for straight walls include:

- Temporary support of embankments or existing foundations on highway or subway construction projects.
- Construction of temporary bin walls for separating materials in bulk storage yards at job-sites.
- Temporary marine facilities such as a receiving dock to allow off-loading of heavy equipment.

1.2.1.4. Cellular Cofferdams

When large areas in relatively deep water are to be de-watered and excavated, a single-wall braced cofferdam may be impractical. Builders have used earth dikes, timber cribbing or double-wall sheet piling structures for such cofferdams. However the most successful development, and one that has utilized hundreds of thousands of tons of flat type sheet piling is the cellular cofferdam. This structure consists of a series of interconnected, cellular units filled with select soil.

A cellular cofferdam is a gravity retaining structure formed from a series of interconnected cells filled with select soil. Because the fill imparts hoop tension to the walls, flat or shallow arched sheet piling sections with specially designed interlocks are utilized for building the cells. Cellular cofferdams can be used for temporarily excluding water from deep, large excavations such as for locks, dams, and hydraulic structures, and also for permanent docks or walls where single wall bulkheads cannot be used. A typical cellular cofferdam arrangement is shown in *Figure 1-9*.

A great deal of practical experience has been obtained in the design, construction, and operation of cellular cofferdams beginning in the 1930's with the TVA construction of large

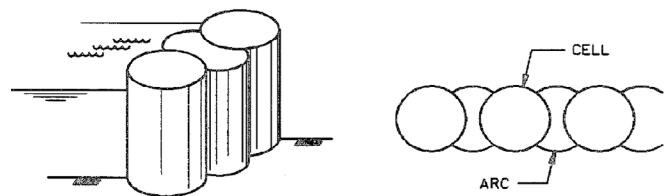


Figure 1-9: Typical Cellular Cofferdam Arrangement

hydro-dam projects on the Tennessee River and extending to the 1980's with lock and dam construction sponsored by the U.S. Army Corps of Engineers.

1.2.1.4.1. Circular Type Cells

This type consists of individual large diameter circles connected together by arcs of small diameter, as shown in *Figure 1-10*. These arcs generally intercept the circles at a point making an angle of 30 to 45 degrees with the longitudinal axis of the cofferdam. The prime feature of the circular type cofferdam is that each cell is self-supporting and independent of the next.

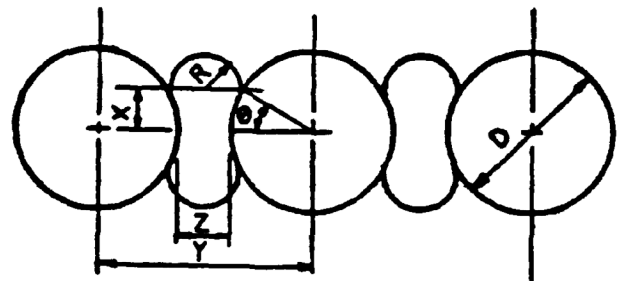


Figure 1-10: Circular Cells

The circular type requires fewer piles per linear foot of cofferdam as compared with a diaphragm type of equal design,

Straight-type (flat) sheet piling sections are assembled around a circular template at the site and driven into place. Granular fill is added to make the cell self-supporting. Similar units are built adjacent and extending around the perimeter of the proposed excavation. All cells are interconnected and the space between filled, producing a freestanding wall.

The stability of this wall is dependent upon shear resistance developed in the fill and friction in the interlocks of the sheet piling. It has been found that there is roughly a 1.25 to 1 ratio between the required diameter of the cells and the water depth, so that a 50 ft. head of water would require about a 62.5 ft. diameter cell. The sheet piling in the cell walls is subjected to hoop tension and must develop very high strength in the interlocks between sheets.

Cells require less space than a dike. They offer less restriction to stream flow and less vulnerable to scouring during flood. Cells are often combined with earth dikes, the cells being used parallel to the stream flow and dikes used on the downstream arms.

Circular cells are limited to dimensions which can be safely satisfied using interlock strengths available from manufacturers, since interlock stresses from fill and water pressure are a function of diameter.

1.2.1.4.2. Diaphragm Type Cells

A variation of the circular cell is the diaphragm cell. This type of cell consists of two series of circular arcs connected together by diaphragms perpendicular to the axis of the cofferdam. It is common practice to make the radii of the arcs equal to the distances between the diaphragms. At the intersection point the two arcs and the diaphragm make angles of 120 degrees with each other. A diaphragm cell is shown in *Figure 1-11*.

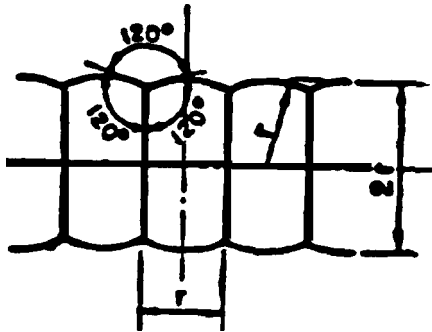


Figure 1-11: Diaphragm Cell

This design utilizes curved front and rear walls, but straight interior walls. The radius of the curved walls is based on the spacing of the interior walls and thus hoop tension can be managed. This cofferdam type can be designed to utilize the lightest flat-type sheets (i.e. PSA-23) that have lower interlock strengths. The design has also been utilized for high head cofferdams prior to the development of higher-strength interlocks. Increasing the length of the diaphragms can easily widen the diaphragm type cofferdam. This increase will not raise the interlock stress, which is a function of the radius of the arc portion of the cell. At any given level, there is a uniform interlock stress throughout the section. The stress is smaller than that at the point of a circular cell of an equal design.

The diaphragm cell will distort excessively unless the various units are filled essentially simultaneously with not over 5 feet of differential soil height in adjacent cells.

Diaphragm cells are not independently stable and failure of one cell could lead to failure of the entire cofferdam.

The diaphragm type has some disadvantages:

- (1) It must be constructed and filled in stages and requires more templates; and,
- (2) It may be more vulnerable to failure since the rupture of one cell will cause distress in adjacent cells. (The circular type is a series of independent units.)

1.2.1.4.3. Cloverleaf Cells

The cloverleaf design is a variation of the circular unit. This type of cell consists of four arc walls, within each of the four quadrants, formed by two straight diaphragm walls normal to each other, and intersecting at the center of the cell. Adjacent cells are connected by short arc walls and are proportioned so that the intersection of arcs and diaphragms forms three angles of 120 degrees. A typical layout is shown in *Figure 1-12*. The cloverleaf is used when a large cell width is required for stabil-

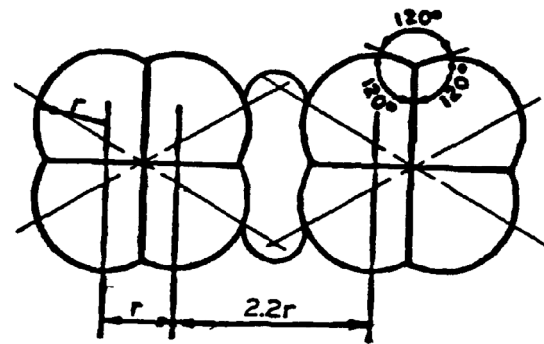


Figure 1-12: Cloverleaf Cells

ity against a high head of water. This type has the advantage of stability over the individual cells, but has the disadvantage of being difficult to form by means of templates. An additional drawback is the requirement that the separate compartments be filled so that differential soil height does not exceed 5 feet.

It is used where a very large unit is required and where the hoop tension in a circle would be excessive. The cloverleaf utilizes cross walls curved sections. Radii are kept small enough to produce manageable interlock tension. The cloverleaf cell uses more steel than circular or diaphragm type cells, and is adaptable to greater heights, however this style construction is rarely used and will not be discussed further.

1.2.1.4.4. Modified Types

It may be possible to eliminate or change certain arcs in the circular or diaphragm arrangements, as shown in *Figure 1-13*. However, the remaining portions of the cells must be adequately anchored before this is practical. This style has been adapted to permanent cellular type piers and wharves rather than temporary water – excluding cofferdams.

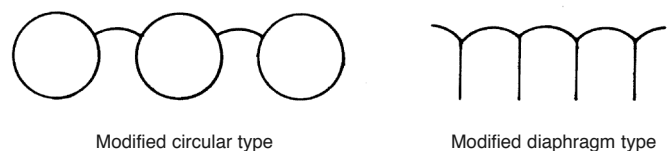


Figure 1-13: Modified Cellular Cofferdams

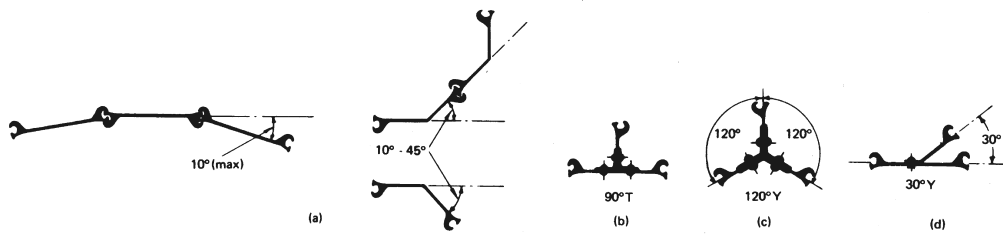
1.2.1.4.5. Components of Cellular Cofferdams

The major components of cellular cofferdams are the steel sheet piling for the cells, the cell fill, and the earth berms that are often used to increase stability.

As mentioned earlier, most straight sheet pile sections permit a maximum deflection angle of 10 degrees per pair. When larger deflection angles are required for small diameter cells, bent piles must be provided as shown in *Figure 1-14*. Junction points in cellular cofferdams required special prefabricated pieces, commonly 90 degree T's or 30 and 120 degree Y's. Some of these connections are shown in *Figure 1-14*.

Sheet pile manufacturers should be contacted in advance regarding their available interlock strengths, practical saving between sheets and fabricated specialties.

More detail on the design and construction of cellular cofferdams will be found in Chapter 14.



For deflection angles up to 10°, use straight pile sections. For deflection angles beyond 10°, bend web of pile to an angle equal to required deflection angle.

Figure 1-14: Steel Sheet Piling for Cellular Cofferdams

1.2.2. Permanent Applications

The advantage of sheet piling is as a pre-manufactured product with known properties, which can be shipped to a project site and assembled, under diversified conditions, into a permanent wall. In North America, it has been used mostly for bulkheads at marine terminal facilities, marinas, and commercial and residential waterfront properties. It has also been extensively used for navigation structures, water control, floodwalls and land walls.

1.2.2.1. Marine Bulkheads

Sheet piling can be used a number of ways in the design and construction of a port operating facility. An anchored sheet pile bulkhead provides a vertical wall, behind which useable land area may be created and in front of which shipping may tie up for loading and unloading.

Anchored bulkheads obtain their stability from the support provided by penetration into the soil below the dredged bottom combined with an anchorage support system installed near the top of the wall. The sheet piling is then designed as a beam on two supports under load from soil pressure and surcharges. The bending moment in the beam must be countered by the shape and tensile strength of the sheet pile “beam”. For most deep applications, anchored bulkheads will utilize Z, U, or HZ type sheet piling. Anchored bulkheads may be located parallel to shore (marginal wall) or perpendicular to shore (finger pier).

Anchored bulkheads may be built for planned dredged depths of up to about 50 feet of water by utilizing the strongest sections currently available, combined with high strength grades of steel.

Sheet pile walls are also utilized in the construction of deck-type marginal wharves, as a screen wall between the rear of the deck and the land area.

Special high modulus sheet pile wall systems have become a factor in deep-water marine facilities construction. This method utilizes large “master piles” as the main strength units of the wall. Wall strengths several times that available with conventional sheet piling are possible.

1.2.2.2. Cellular Bulkheads

Bulkheads for special situations can be created from sheet pile cellular structures. These applications include sites where high rock prohibits the required penetration for support of a single wall, where deep water and heavy loads make a single

wall unfeasible, where tidal fluctuations are extreme, where site development is to take place over an extended period of time or combinations of these situations.

Cellular structures are extremely useful for land creation and development projects. The cells are self-supporting and can be built in advance of landfill materials. They provide a curtain to prevent water pollution and, as vertical structures, take up much less space than a dike. A notable use of a cellular cofferdam to replace an existing dam took place in 2000-1, when the Main Street and Hennepin Island dams were replaced with circular cellular cofferdams in Minneapolis, MN. Cellular cofferdams were chosen both for economic reasons and because they met the aesthetic, historical and environmental requirements of the project.⁴

Cellular bulkheads may be of either circular or diaphragm construction. Circular cells are more popular for stability reasons, although the diaphragm type can utilize a lighterweight pile and provides a somewhat flatter face for breasting vessels.

1.2.2.3. Barge Docks

Self-supporting cells are utilized for other port operations such as mooring and turning dolphins. Single, circular cells in series have been used along the inland rivers for mooring fleets of barges. The cells diameter varies between about 15 and 30 feet. These are built sufficiently high to accommodate fluctuations in water levels. Some facilities have as many as 50 or 60 cells spread over a mile of shoreline to accommodate barge fleets.

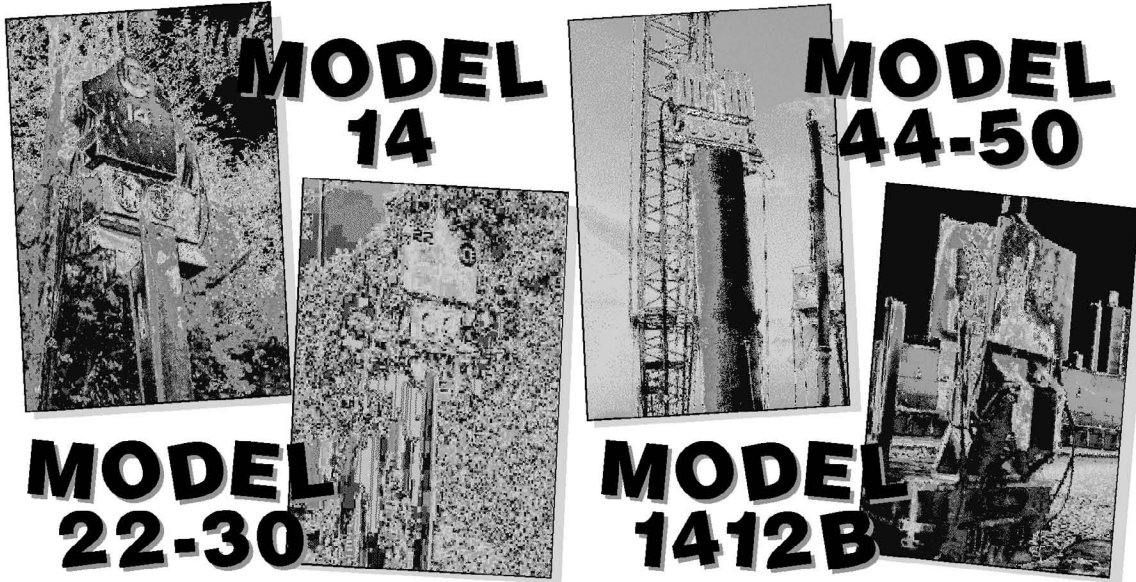
1.2.2.4. Coastal Construction

There is always a need for permanent wall construction around rivers, lakes and seashore. This requirement ranges from bulkheads to protect private property to jetties, breakwaters and seawalls built by governmental agencies for the general public welfare.

1.2.2.4.1. Bulkheading

Relatively shallow anchored or cantilevered bulkheads are used to create or protect private property along the waterfront. The “Navy-type” timber wall is a basic means of building relatively inexpensive bulkheads for private homes or commercial operations such as marinas, particularly along the salt-water coastal areas. This design consists of round, timber piles installed about five feet apart, supporting a curtain wall of sawn timbers. A filter cloth membrane is sometimes added.

⁴ Zawaki, W., Rudolph, R., Winberg, T., and Quist, J. (2001) “A Dam for a Dam” *Civil Engineering*, February, pp. 56-61.



A VIBRO FOR EVERY JOB

Whether you're driving or extracting sheets, H-piles, timber, pipe or casings, ICE has a vibratory driver/extractor to meet the challenges of your job situations.

We also offer the largest selection of clamps and accessories including bias weights, suppressors, power units, extensions, lead guides and more to add leverage to your vibro investment.

Our problem-solving expertise, supported by our nationwide network of sales and service locations, are important reasons why you see more bright green and yellow ICE logos on more jobsites.



Model	Freq. (VPM)	Eccentric Moment	Amplitude (In.)	Engine (H.P.)	Max. Pull Extract (Tons)	Susp. Weight Lbs. (wo/Clamp)
23-40	1600	230	.58	40	13	1180
11-23	1900	1100	.92	220	40	4300
216	1600	1100	.94	200	40	4230
14-23	1900	1400	1.10	220	40	4450
22-23V	1400-1600	2200	.89	220	40	7900
22-30	1600	2200	.89	335	40	7900
416L	1600	2200	.91	335	40	7900
28-35	1600	2800	1.06	350	40	8400
44-30V	1200-1600	4400	1.17	335	80	12100
44-50	1600	4400	1.17	575	80	12100
44-70	1650	4400	1.17	740	80	12100
66-70	1300	6600	1.23	740	80	15250
66-80	1600	6600	1.23	800	80	15250
1412-B	1250	10000	1.3	800	150	25750
V360	1500	11300	1.46	1050	225	25900
125	1500	12500	1.25	1320	300	36100
1412BT	1250	20000	2	2x800	300	25750
V360T	1500	22600	1.46	2x1050	450	69850
EXCAVATOR-MOUNTED						
30 Ton Sup.		1100-1267	1.02	N/A	-	3628
45 Ton Sup.		1100-1267	1.01	N/A	-	4178



INTERNATIONAL CONSTRUCTION EQUIPMENT, INC.
www.iceusa.com

301 Warehouse Drive • Matthews, NC 28104
 Phones: 888 ICEUSA1 & 704 821-8200
 Fax: 704 821-8201 • e-mail: info@iceusa.com



Matthews NC • Lakeland FL • Metairie LA • Seattle WA • New Town Square PA • Sayreville NJ • Houston TX
 Fort Wayne IN • Virginia Beach VA • Boston MA • Montreal Quebec • Singapore • Kuala Lumpur • Shanghai

Lightweight steel sheet piling is also extensively utilized for shallow applications. The strength and corrosion resisting qualities of aluminium sheet piling have also attracted owners and contractors to this material.

1.2.2.4.2. Protective Structures

Breakwaters are built by private or governmental agencies to protect the facilities and marine traffic in their harbours. Large cellular cofferdam structures have been built to create artificial harbours, particularly on the Great Lakes. These cells are generally filled with crushed stone and topped with armour stone or concrete. Stone berms may be added on both sides for further stability. Some designs have employed a sloped face in order to intercept breaking waves at a more favourable angle and reduce the reflection.

Single-wall wave deflectors have been used in some less exposed applications. These have generally been braced in some fashion, with structural piling or short stiffener walls of sheet piling.

Jetties are structures projecting from harbour entrance channels to assist in the maintenance of channel depths. While stone is the most common method of building jetties, sheet piling has also been employed for these devices.

Groins are shallow walls constructed more or less perpendicular to the shoreline and extending into the water. Their purpose is to trap sand being moved parallel to the beach by wind or water currents, thereby building a beach. Groins have become quite controversial because of their questionable value to the overall beach environment. Historically, large groins have been built of sheet pile cells, and small groins of cantilevered or braced walls. They have had a relatively short life on the sea-coast because of abrasion and salt-water corrosion. However, those built along the Great Lakes have been in use for many years.

Seawalls are structures built parallel to the shore for the purpose of protecting onshore properties from storm activated wave action. Since these structures are designed to trap and break waves, the vertical faces offered by sheet pile walls by themselves does not provide a completely satisfactory service. Most sheet pilings used in these applications are employed as cut-off walls in and under stone or concrete walls to prevent underscour. However in non-ocean applications, such as inlets or lakes, sheet pile seawalls have provided protection for many private structures.

1.2.2.5. Other Permanent Applications

1.2.2.5.1. Water Control Structures; Weirs and Dams

The U.S. Army Corps of Engineers and a number of regional water authorities in the Southern United States utilize Z-type or arch sheet piling in standard designs for box-type check dams. Many of these have been built in relatively remote locations. Sheet piling can be taken into the sites by truckload and assembled into the designed configuration on the spot.

1.2.2.5.2. Flood Control Structures

Sheet piling has been frequently utilized in construction of permanent structures for water storage and flood control. Sheet

piling also is employed in the core of dikes, levees and dams to prevent undermining by burrowing animals as well as to control seepage. Concrete floodwalls generally utilize a sheet pile core or toe wall.

Some very large dams have utilized sheet piling in the core to assist in reducing seepage through and under the structure. The Oahe Dam on the Missouri River is a large earth fill dam that utilized this method. Most flood control pumping plants will utilize large quantities of sheet piling in controlling ground water around and under the facility.

1.2.2.5.3. Navigation Structures

The U.S. Army Corps of Engineers has built many large navigation structures on the inland waterways of the United States. The large water control dams and navigation locks are concrete structures generally built with the help of temporary cellular cofferdams. Guide walls extend upstream and downstream from the locks and it was found feasible to build these large non-critical structures on circular sheet pile cells which support the weight of the walls and also serve to control the water movement in these channels.

An entire navigation lock was built on the Ohio River using large diameter sheet pile cells for the walls rather than masonry. This election was made to save time and until a permanent structure could be funded.

Sheet piling bulkhead walls are common along navigation canals around the world. One of the first applications for ASTM A-690 grade corrosion-resisting sheet piling was for a replacement wall along the Old Erie Canal in New York State. While corrosion was not a factor here, the owners were attracted to the rich, brown appearance of the steel, having used a similar type in bare steel applications previously for bridges.

1.2.2.5.4. Graving Docks and Dry-docks

A number of these large structures have been built for both commercial and military purposes utilizing large-diameter steel sheet piling cells to form the walls. In some cases, the diaphragm type of construction was selected. A dry-dock is essentially a permanent cofferdam that must be dewatered in order to carry out repairs on vessels in the dry.

1.2.2.5.5. Artificial Islands

Large-diameter artificial islands can be created from filled sheet pile cells for locating transmission towers in bodies of deep water, for oil drilling platforms, etc. The retained soil takes up less space than sloped fill, is protected from scour and the steel cells offer some protection from ship collision.

1.2.2.6. Highway Applications

1.2.2.6.1. Retaining Walls and Abutments

In Europe, sheet piling is regularly employed for fill retention on highway ramps and underpasses and along cuts and embankments. In the United States, sheet piling has not been widely accepted for highway structures because of appearance. Under the right circumstances, steel will develop a tight rusting effect that blends into natural surroundings better than concrete. In urban areas steel sheet piling walls have been cov-

ered with fascia panels for appearance sake.

Sheet piling abutments and wing walls have been utilized to some extent for Forest Service and rural county bridge construction. This system takes advantage of the ability of steel shapes to carry vertical loads as well as horizontal loads. With this system, cofferdams and formwork at these relatively remote sites is eliminated.

1.2.2.6.2. Bridge Protection Cells

The practice of locating large sheet pile cells around critical main piers of major bridges to protect them from ship collision is a growing one. The cells are sacrificial and are designed to stop or divert the ship so that any impact will not affect the stability of the main structure. An example of a structure to be fitted with these devices is the Sunshine Skyway Bridge across the Tampa Bay ship channel near St. Petersburg, Florida. Its predecessor had suffered a fatal collision from a ship.

1.2.2.7. Marinas and Boat Launching Facilities

1.2.2.7.1. Bulkheading

Lighter weight steel and aluminium sheet piling find many applications around small boat harbours. Marinas generally require bulkheading of the shoreline to create land for parking and services. Launching ramps cut into the shoreline require sheet piling for cofferdams as well as embankment retention. While boat slips are generally created from floating or pile supported finger piers, there are occasions where filled piers formed from parallel lines of sheet piling may be practical.

1.2.2.7.2. Breakwaters

Permanent breakwaters at marinas or small boat harbours have used sheet piling in the form of filled cells, single-wall, braced construction, or as a cantilever wall supported by a rubble-mound dike.

1.2.2.7.3. Other Applications

Sheet piling should be considered for any application where a vertically faced wall is required. Some of the innovative uses that have been made are:

- Curtain wall surrounding shallow water oil well drilling and production sites, to retain spillage and protect the environment.
- A similar application around large, circular petroleum storage tanks at a refinery.
- Bulkheading of tees and greens of water holes at golf courses⁵.
- A large permanent cellular cofferdam at the Aswan Dam in Egypt protects some of the important ancient sites from the impounded waters of the dam.
- Scrap pits built in metal working mills utilizing a box-type structure built of sheet piling. Concrete deteriorates quickly from abrasion and impact of the heavy scrap.
- Separator walls for bulk material storage.

What other applications? There may be many which have not come to the attention of the authors. Certainly any idea the

reader might have for a possible use is worthy of discussion with the producers of sheet piling.

1.3. Backfill Materials for Sheet Pile Walls

The term “backfill” is a general term applying to all soil that is near enough to a newly constructed retaining structure to affect its design and performance. It includes material that remains in place as well as material brought to the site for placement during construction. It includes material in front of the wall that will provide resistance as well as material behind the wall that supports surcharge loads and itself generates active loads against the wall.

1.3.1. Overview of Backfill Types

The ideal wall would contain an idealized soil: lightweight, free draining, well graded, homogeneous with optimum engineering properties. This combination is rarely found insitu and often prohibitively expensive to create. The advantages of certain soil types for backfill are well established and these materials should be utilized if at all possible.

Terzaghi listed five general classes of backfill that might be encountered in retaining wall work:

1. Coarse-grained soils without an admixture of fines – very permeable, typically clean sand and gravel. This is the most desirable backfill, either as an in-situ material or as an import into the site. The engineering properties of this soil are well established or can be readily determined. They drain freely and remain stable over the long term. The amount of laboratory testing required for design is a minimum for these soils.
2. Same as 1, but of low permeability due to presence of silt. This is more typical of fill which might be obtained from dredging operations or which might exist in many marine locations. While not having the desirable free-draining characteristics, this fill is often all that is available at reasonable cost. It is best used in conjunction with select material placed against the wall for better drainage.
3. Residual soil with stones, fine silty sand, and granular mixtures with conspicuous clay content. This type of soil is typically found inland -- a non-homogeneous mixture of ordinary fill materials that is used primarily because of ready availability and cost. This fill is more likely to be found in-situ at land-sited walls. Its properties are more difficult to determine.
4. Very soft or soft clay, organic silts or silty clays. This type of backfill is the type that should be excavated and disposed of as quickly as possible since it has none of the characteristics for permanent retaining structures. Quite often however, this material is encountered in building temporary cofferdams in which case it is acting as a load rather than part of an engineered structure. In other cases it might be found at the site of a permanent bulkhead and may be impractical to remove. In this case, special methods for improving the quality of this fill may have to be planned as part of the design.

⁵ An example of this is the Medinah Country Club near Chicago, site of the 1990 United States Open.

5. Medium or stiff clay. These are generally undesirable. Their long-term strength is difficult to access and then generally produces active earth pressure much higher than granular materials. They have poor drainage characteristics.

Terzaghi recommended that “if a wall is designed before the backfill is selected, design for the worst condition, otherwise specify the characteristics of the backfill and design accordingly.”

1.3.2. Lightweight Backfill

Where they can be obtained, certain materials might be used for backfills to reduce active pressure. These include oyster shells, “pop-corn” slag, wood fibre products etc. Oyster shells for example weigh only about half what moist sand does and exhibit an equivalent friction angle. Soil pressures would be about half those created by sand backfill. Lightweight blast furnace slag has been used for some Great Lakes area bulkheads.

1.3.3. Sand Dikes

Tchebotarioff proposed the use of sand dikes adjacent to bulkhead walls that would provide the desirable characteristics of granular materials while permitting the use of poorer quality dredged material up-land from the wall. This method is commonly used.

1.3.4. Dredged Bulkheads

Marine bulkheads are often constructed by driving sheet piling into existing soil at or above the low water line. The area in front of the wall is then excavated to the desired depth to create the facility. In other cases, the line of sheet piling is driven into relatively deep water and then backfilled with soil to create land. The method used may affect the stresses which the parts of the wall may be subjected to during construction as well as having an effect on the progression of wall pressure from at-rest conditions to the lower active state.

1.3.5. Compaction of Fill

Compaction of dumped backfill may be desirable to reduce the materials compressibility, increase its strength, control expansion and reduce the possible effect from frost. However, compaction will reduce the permeability and overcompaction can greatly increase lateral pressure near the top of the wall and unfavourably for the anchorage. Increasing the density of soil in the passive area is desirable if it can be accomplished.

However, compaction on the active side should be carefully specified both in the degree of densification and the method of attainment. Heavy compaction equipment should be kept well back from newly constructed bulkheads.

If specified, densification can be accounted for in assigning engineering values to the soil for design. Hydraulic fill cannot be compacted during placement. Hydraulic fill should be accounted for in design as a temporary, increased load against a possibly unstabilised wall⁶.

1.3.6. Placing Backfill

Backfilling of sheet pile walls may be initiated as soon as a

significant length of wall has been constructed. Generally speaking, all backfill should be clean and free draining unless approved by the design engineer.

All backfill should be placed in horizontal lifts. For clean sands and gravels, the uncompacted lift thickness can be up to 12”; for silts, clays, and silty clay mixtures, the maximum thickness should be 9”.

If the backfill is compacted, it should be mechanically compacted to 92 to 93 percent of the maximum dry density obtained by the Standard Proctor Test, ASTM D 698 (AASHTO T 99). For moisture sensitive soils, the water content should be controlled in the range of ± 2 percent of optimum as determined by ASTM D 698 (AASHTO T 99).

Compaction within 5 feet of the back of the wall shall be accomplished with lightweight hand operated compaction equipment.

1.4. Failure Modes and Loads of Sheet Pile Walls

Up to now we have discussed the various types and applications of sheet piling. The rest of this manual will be spent in the actual design procedures necessary for successful sheet pile walls and cofferdams.

1.4.1. General Considerations

The design of sheet pile retaining walls requires several successive operations:

- (a) Evaluation of the forces and lateral pressures that act on the wall;
- (b) Determination of the required depth of piling penetration;
- (c) Computation of the maximum bending moments in the piling;
- (d) Computation of the stresses in the wall and selection of the appropriate piling section; and
- (e) The design of the waling and anchoring system.

Before these operations can be initiated, however, certain preliminary information must be obtained. In particular, the controlling dimensions must be set. These include the elevation of the top of the wall, the elevation of the ground surface in front of the wall (commonly called the dredge line), the maximum water level, the mean tide level or normal pool elevation and the low water level. A topographical survey of the area is also helpful.

Earth pressure theories have developed to the point where it is possible to obtain reliable estimates of the forces on sheet pile walls exerted by homogeneous layers of soil with known physical constants. The uncertainties involved in the design of sheet pile structures no longer result from an inadequate knowledge of the fundamentals involved. They are caused by the fact that the structure of natural soil deposits is usually quite complex, whereas the theories of bulkhead design inevitably presuppose homogeneous materials. Because of these conditions, it is essential that a subsurface investigation be performed with exploratory borings and laboratory tests of representative samples. On this basis, a soil profile can be drawn and the engineering prop-

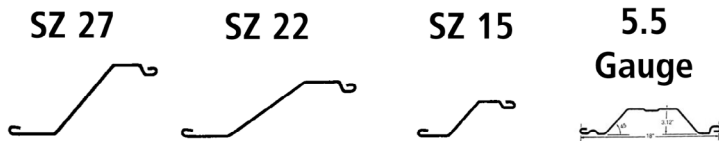
⁶ In general however, hydraulic fills should not be placed directly against a new wall.

SHORELINE STEEL, INC.

P.O. Box 480519, 58201 Main Street • New Haven, MI 48048
(800) 522-9550 • (586) 749-9559 • Fax (586) 749-6653

www.shorelinesteel.com

We are a leading producer of domestic cold formed steel sheet piling in sections ranging from 10 gauge to 3/8" thick. For any sheet piling requirement we can satisfy your needs with a top quality product and prompt delivery.



	Thickness (Nominal)	Weight (Sq. Ft.)	Weight (Lin. Ft.)	Sec. Mod (Ft. Wall)	Moment of Inertia in ⁴ (Ft. Wall)	Laying Width	Wall Depth
10-10 ga.	.134	7.2	10.8	2.2	3.5	18.00	3.12
8-8 ga.	.164	8.8	13.2	2.62	4.2	18.00	3.12
7-7 ga.	.179	9.6	14.4	2.8	4.4	18.00	3.12
6-6 ga.	.194	10.5	15.8	3.0	4.9	18.00	3.12
5-5 ga.	.209	11.3	16.9	3.4	5.4	18.00	3.12
LZ 8	.164	8.3	17.2	3.6	8.1	25.00	4.50
LZ 7	.179	9.1	18.8	3.9	8.9	25.00	4.50
LZ 5	.209	10.6	21.9	4.6	10.4	25.00	4.50
LZ 3	.239	11.9	24.6	5.2	11.8	25.00	4.50
LZ 250	.250	12.3	25.6	5.4	12.4	25.00	4.50
SZ-10	.164	9.4	17.2	7.3	27.4	22.00	7.50
SZ-11	.179	10.3	18.8	7.9	29.8	22.00	7.50
SZ-12	.209	12.0	21.9	9.2	34.8	22.00	7.50
SZ-14	.239	13.5	24.6	10.4	39.9	22.00	7.50
SZ-15	.250	14.0	25.6	10.9	41.8	22.00	7.50
SZ-14.5	.250	14.5	32.4	13.0	61.49	26.75	9.46
SZ-14.5	.270	15.8	35.1	14.0	86.40	26.75	9.46
SZ 18	.312	18.1	40.4	16.2	76.83	26.75	9.46
SZ 20	.340	19.8	44.1	17.5	83.37	26.75	9.46
SZ 21	.350	20.3	45.3	18.1	86.00	26.75	9.46
SZ 22	.375	21.8	48.6	19.3	91.92	26.75	9.46
SZ 222	.312	22.1	40.4	26.7	163.09	22.00	12.25
SZ-250	.250	15.9	32.4	16.6	89.42	24.46	10.75
SZ-313	.312	19.9	40.4	20.6	111.53	24.46	10.75
SZ-340	.340	21.5	44.1	22.4	121.45	24.46	10.75
SZ-350	.350	22.1	45.3	22.9	124.62	24.46	10.75
SZ-375	.375	23.7	48.6	24.5	133.55	24.46	10.75
SZ-24	.340	24.1	44.1	29.0	177.52	22.00	12.25
SZ-25	.350	24.8	45.3	29.7	181.91	22.00	12.25
SZ 27	.375	26.6	48.6	32.0	195.18	22.00	12.25

- All sections available in bare or galvanized steel.
- All Zee sections available in doubles.
- All sections produced exactly to customer specified length(s).
- All steel fully melted and manufactured in the USA.

DOMESTIC STEEL SHEET PILING



For more information, please call toll free
(800) 522-9550

or visit our website at: www.shorelinesteel.com

Also Available:

- Corners
- Tees and Crosses
- Capping
- Coatings

SHORELINE  STEEL, INC.

erties of the different soil strata can be accurately determined. These properties should reflect the field conditions under which the wall is expected to operate. Only after these preliminary steps are taken should the final design be undertaken.

1.4.2. Failure Modes for Sheet Piling

The object of sheet pile wall design is to prevent failure of the wall in service. The loads exerted on wall/soil system tend to produce a variety of potential failure modes. The following is an overview of these failure modes.

1.4.2.1. Deep-seated failure

A potential rotational failure of an entire soil mass containing an anchored or cantilever wall is illustrated in Figure 1-15. This potential failure is independent of the structural characteristics of the wall and/or anchor. The adequacy of the system (i.e. factor of safety) against this mode of failure should be assessed by the geotechnical engineer through conventional analyses for slope stability.

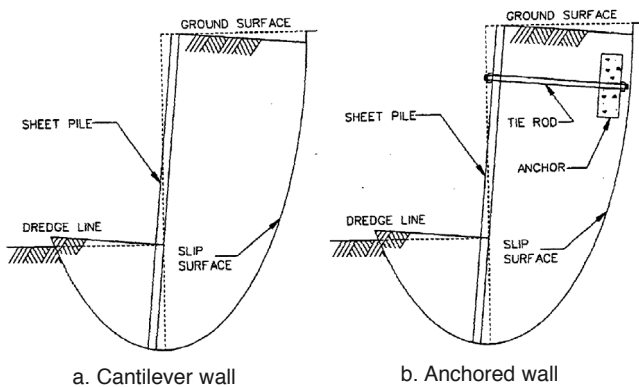


Figure 1-15: Deep-Seated Failure

This type of failure neither can be remedied by increasing the depth of penetration nor by repositioning the anchor. The only recourse when this type of failure is anticipated is to change the geometry of retained material or improve the soil strengths.

1.4.2.2. Rotational failure due to inadequate pile penetration

Lateral soil and/or water pressures exerted on the wall tend to cause rigid body rotation of a cantilever or anchored wall as illustrated in Figure 1-16. This type of failure is prevented by adequate penetration of the piling in a cantilever wall or by a proper combination of penetration and anchor position for an anchored wall.

1.4.2.3. Flexural Failure of Sheet Piling

For basic design analysis, sheet pile walls are treated like a beam in pure bending for structural purposes. Flexural failure involves exceeding the maximum allowable bending moment at a point in the sheeting. Such a failure is shown in Figure 1-17.

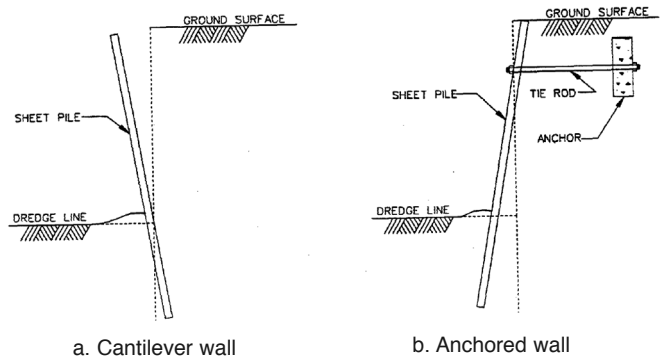


Figure 1-16: Rotational Failure Due to Inadequate Penetration

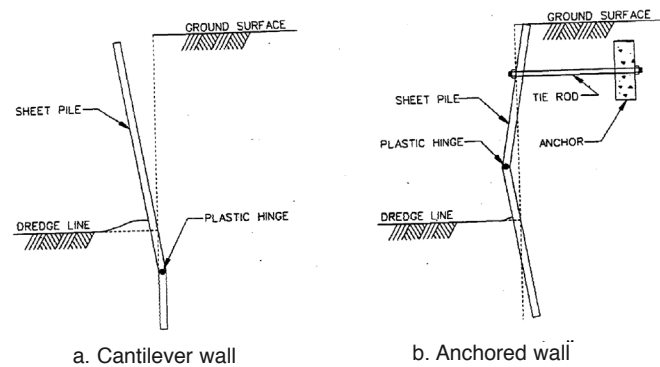


Figure 1-17: Flexural Failure of Sheet Piling

1.4.2.4. Anchorage Failure

Failure of the system may be initiated by overstressing the anchor components as illustrated and Figure 1-18. This is discussed in detail in Chapter 11.

1.4.2.5. Special Failures due to Earthquake Motion

Anchored sheet pile walls show the most varied modes of failure of most waterfront retaining structures. These modes are summarised in Figure 1-19. Most of these are similar to static failure but their possibility is of course increased with seismic activity.

1.5. Application of Engineering Principles to Sheet Piling Design

The design of most geotechnical elements, such as spread footings, driven piles and the like, is primarily driven by the strength of the surrounding soil first and the structural integrity of the element second. Sheet piling, however, should be considered a structure that happens to be in the ground; therefore, we will consider the structural design aspects first. Following that we will look at the loads applied to the piling, first the applied loads and second the earth pressure loads and failure modes. The order these are in are as follows:

- Chapter 2 discusses the structural design of sheet pile

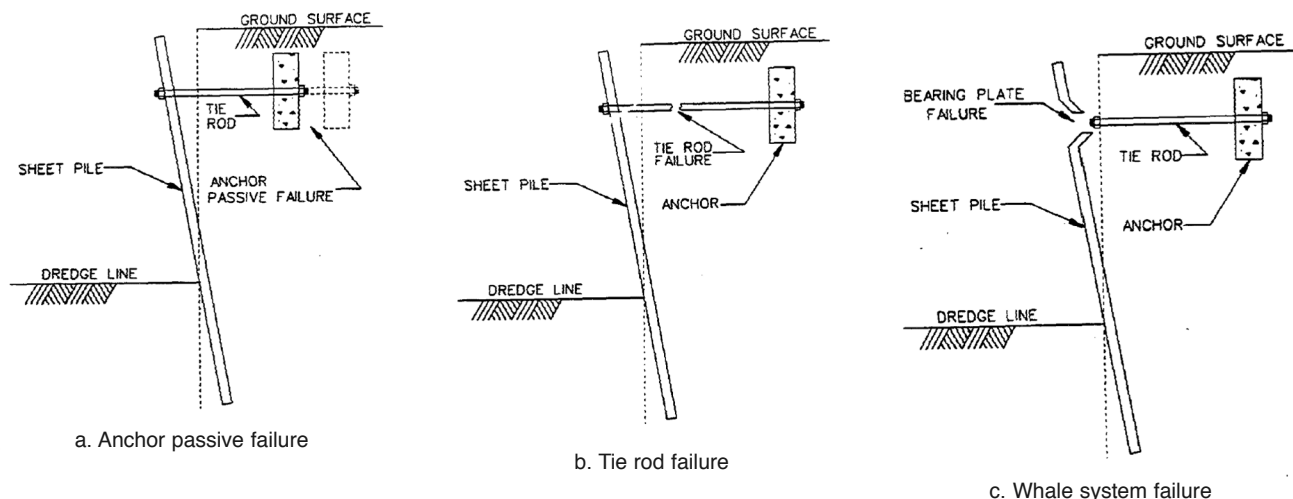


Figure 1-18 Anchorage Failure

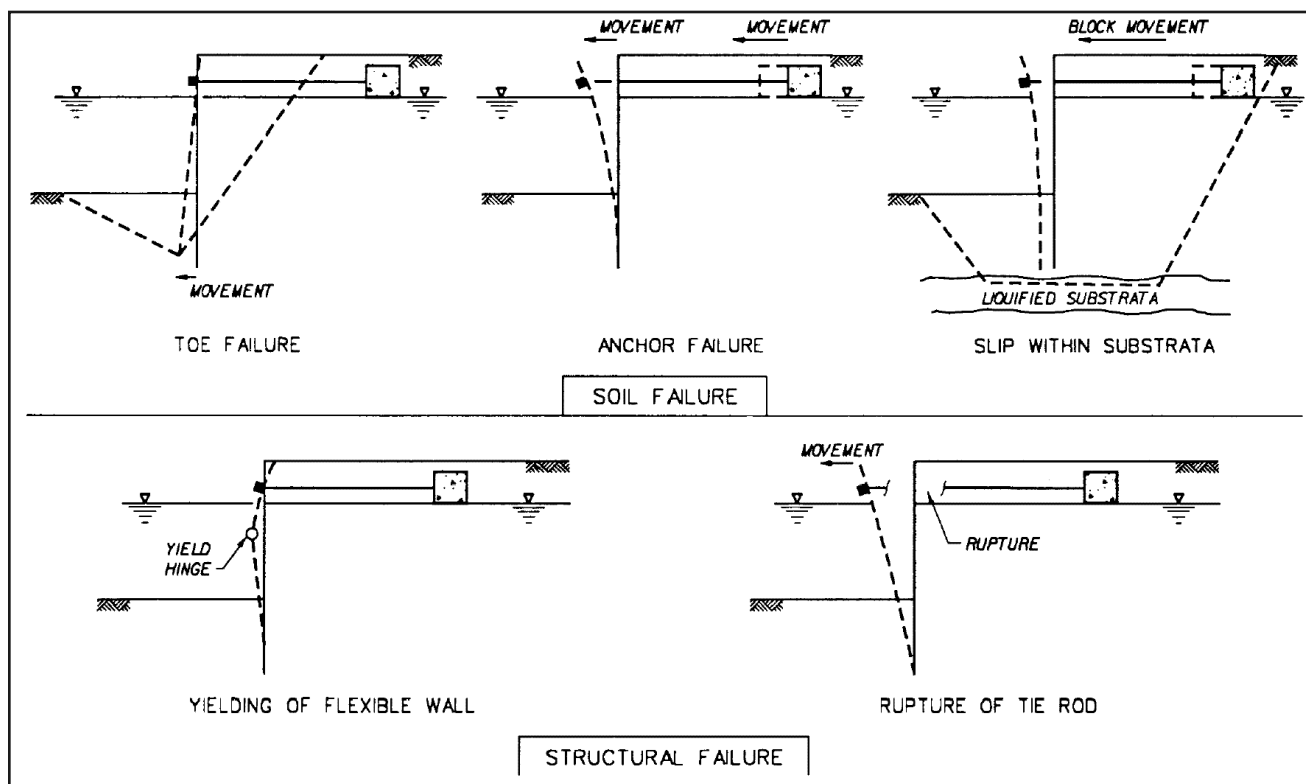


Figure 1-19: Potential Failure Modes for Anchored Sheet Pile Walls due to Earthquake Activity

- walls, including the strengths in various failure modes.
- Chapter 3 is an overview of the basic principles of soil mechanics as they apply to sheet pile walls, including laboratory and field soil testing.
 - Chapter 4 gives an overview of basic lateral earth pressure concepts that apply to sheet piles.
 - Chapter 5 is a detailed look at static earth pressure loads on sheet pile walls.
 - Chapter 6 is a detailed look at dynamic earth pressure

- loads, which start out as an applied load but end up becoming an earth pressure load.
 - Chapter 7 reviews the effect of water on sheet piling, including hydrostatic effects, groundwater flow and soil boiling.
 - Chapter 8 summarises other loads that sheet piles experience, such as surface loads.
- We can then proceed to show design methods for the various configurations of sheet pile walls.

Chapter Two:

Structural Design of Sheet Pile Walls

2.1. Materials Used in Sheet Piling

2.1.1. Grades Of Sheet Piling Steel

2.1.1.1. Basic Grade: ASTM A-328

The basic specification for steel sheet piling in the United States has been ASTM A-328 published by the American Society of Testing Materials. This grade has been satisfactory for most applications in that it provided a relatively high yield point for design and a high ultimate strength for driveability. The formulation is not well respected for weldability, although procedures for welding this grade have been published or are available from the manufacturers. The steel is not particularly tough and fractures originating at notches have been noted, particularly in cold environments. This steel has a minimum yield point of 39 ksi and a minimum tensile strength of 70 ksi.

2.1.1.2. Higher Strength Grade: ASTM A-572

Higher strength steels for structural applications are available for sheet piling such as the ASTM A-572 series. All strengths may not be available from every manufacturer, however Grade 50 is almost always offered. High strength grades find application (1) to substitute a lighter section of higher strength for a heavier section of regular strength, (2) to maintain safety factors against yield where it cannot be accomplished with section modulus. High strength grades can maintain some safety factor against yield where corrosion might reduce section properties. High strength steels, are generally more weldable than higher carbon grades.

ASTM A-572 Grade 50 has a minimum yield point of 50 ksi and a minimum tensile strength of 70 ksi. Safety factors for the high strength steels are similar to lower strength grades. It is now available as silicon killed, fine-grain formulation with greatly improved Charpy V-Notch impact properties. This steel might be considered for fracture critical applications, (for example, construction in arctic regions) and structures subject to impact. This is a premium priced formulation.

2.1.1.3. Corrosion Resisting Grade: ASTM A-690

ASTM-A-690 Grade was developed to recognize specially formulated steel for sheet and H-piles for use in salt-water applications. This grade has shown advantages over regular carbon steels for resisting corrosion in the salt-water splash zone that is an area of concern. The steel also provides a minimum yield point of 50 ksi and therefore can be designed along the lines of A-572 steels. In some cases weight can be reduced, thus providing a saving which will pay some of the additional cost of the grade. More discussion of this material is provided in 17.4.4.1.

2.1.1.4. Structural Factors of Safety for Steel Sheet Piling

Most steel sheet piling is still designed using allowable stress design methods; thus, a factor of safety is usually specified that reduces the allowable stress in the pile from the yield stress. The allowable stress is thus

$$\text{Equation 2-1: } \sigma_{allow} = F_{reduction} \sigma_y$$

where

- σ_{allow} = Allowable Stress of the Material
- $F_{reduction}$ = Reduction factor of safety
- σ_y = Yield Stress of the Material, psi or kPa

With steel piling in pure bending (see below), there are two reduction factors used:

For static loads, for permanent works the reduction factor is generally 0.65, or the allowable stress is 65% of the yield stress. For the grades listed above:

$$\text{ASTM A328: } \sigma_{allow} = (0.65)(39) \approx 25 \text{ ksi}$$

$$\text{ASTM A572, ASTM A690: } \sigma_{allow} = (0.65)(50) \approx 32.5 \text{ ksi}$$

For earthquake loads, the reduction factor is generally $(1.33)(0.65) \approx 0.87$, or the allowable stress is 87% of the yield stress. Using this increased value for earthquake loads presupposes a static analysis to insure that the static case is not in fact the governing case for a particular situation (see Example 19). For the grades listed above:

$$\text{ASTM A328: } \sigma_{allow} = (0.87)(39) \approx 34 \text{ ksi}$$

$$\text{ASTM A572, ASTM A690: } \sigma_{allow} = (0.87)(50) \approx 43.5 \text{ ksi}$$

2.1.2. Other materials

Aluminium used in sheet piling is generally the same as other extruded aluminium shapes. Material properties can be obtained from the manufacturers and is also discussed extensively in *Pile Driving by Pile Buck*. Also discussed more extensively in the same book is wood; greenheart wood, for example, has excellent material properties.

Vinyl and pultruded fibreglass piles are made of materials whose properties vary widely from manufacturer to manufacturer. Thus, it is critical in the specification of these sections to verify both the mechanical properties and the method in which these mechanical properties were obtained. It is also important to note that, with both of these materials, application of these material properties are subject many factors, such as creep (in the case of vinyl sections) and transverse bending and localised buckling (with both of these materials.)

2.2. Bending of Sheet Piling

2.2.1. Theory of Pure Bending of Sheeting

For the structural analysis of sheet piling, the primary

**They say,
“everybody
puts their pants
on the same
way in the
morning...”**



**...but it's what
happens after
that which
counts!**

IHC IHC
Hydrohammer®

PO Box 26
6, Smitweg
2960 AA Kinderdijk, The Netherlands
Phone 011 31 78 6910302
Fax 011 31 78 691 0304
Email sales@ihchh.com
Web site <http://www.ihchh.com>

**North American distributor:
VULCAN FOUNDATION EQUIPMENT**

2501 Riverside Drive
P.O. Box 5413
Chattanooga, TN 37406
Phone (423) 698-1581
Fax (423) 698-1587
Toll Free (800) 742-6637
Email sales@vulcanhammer.com

Web site <http://www.vulcanhammer.com>



Member of the IHC Caland Group

object is to analyse failure due to excess bending moment and stresses. Most of the analysis of cantilever and anchored walls involve the computation of pure bending. For the case of pure bending, the maximum allowable bending moment is given by the equation

Equation 2-2: $M_{allow} = S_{min} \sigma_{allow}$

where

- M_{allow} = Allowable bending moment
- S_{min} = Minimum Section Modulus

Both the allowable bending moment and the section modulus are specified as per lineal foot or meter of wall. The strength of sheet piling to resist bending is a combination of the shape of the section and the material out of which it is made. The allowable stress of the material is a function of the material itself.

2.2.2. Application of Bending to Specific Sheet Pile Sections

The century long development of sheet piling has led to a proliferation of sections of all kinds. These are constantly changing; a table of these is beyond the scope of this book, although they are available in both printed and online form from Pile Buck. For the purposes of the example problems in this book, however, we will use several commonly used sections that have been manufactured in steel for many years. These are shown in Table 2-1.

2.2.3. Combined Axial and Flexural Stresses

Additionally, sheet piling can experience axial loading as

well from sources such as concrete pile caps at the top, axial forces due to the vertical component of an inclined anchor, and the friction of the soil. Especially with the pile caps, these can induce buckling in the sheet piling. This can be computed by modifying Equation 2-2 and solving for the maximum (or allowable) stress:

Equation 2-3:

$$\sigma_{max} = \frac{P_{axial}}{A_{axial}} + \frac{M_{max} + P_{axial} (\delta_{max} + e_p)}{S_{wall}} < \sigma_{allow}$$

Where

- M_{max} = maximum moment of the sheeting
- P_{axial} = axial load on sheeting
- A_{axial} = area of the sheeting subject to axial loads
- δ_{max} = maximum deflection of the sheeting
- e_p = eccentricity of the load from the centreline of the sheeting

This type of loading on sheet piles is especially important for HZ walls, and is demonstrated in Example 24.

It is recommended that unless it can be shown that buckling of the piling is unlikely,

Equation 2-4: $\frac{M_{max}}{10} > P_{axial} (\delta_{max} + e_p)$

2.2.4. Section Modulus of U- Shaped Sheeting

As noted above, the section modulus is strictly a function of the physical shape of the material; however, with steel sheeting, Larssen and Z-shapes have been involved in a long running difference between European and American practice.

Larssen and other U-shaped piles remain popular in

Table 2-1 Section Properties and Allowable Bending Stresses for Selected Steel Sheet Sections

Section Designation	Moment of Inertia I in ⁴ per foot of wali	Section Modulus S in ³ per ft of wall	M _{allowable} ft-kips per linear ft of wall ASTM A328 Grade Steel Sheet Piling Static Loading (σ _{allow} = 0.65 σ _y)	M _{allowable} ft-kips per linear ft of wall ASTM A572 Grade Steel Sheet Piling Static Loading (σ _{allow} = 0.65 σ _y)	M _{allowable} ft-kips per linear ft of wall ASTM A328 Grade Steel Sheet Piling Earthquake Loading (σ _{allow} = 0.87 σ _y)	M _{allowable} ft-kips per linear ft of wall ASTM A572 Grade Steel Sheet Piling Earthquake Loading (σ _{allow} = 0.87 σ _y)
PZ22	84.4	18.1	38	49	51.3	66
PZ27	184.2	30.2	64	82	85.6	109
PZ35	361.2	48.5	102	131	137.4	176
PZ40	490.8	60.7	128	164	172.0	220

These values were developed using Equation 2-1 and the reduction factors listed previously.

Europe and the Far East but were displaced in the United States by the Z-type profile. Why? At the heart of the problem is a difference in engineering philosophy.

As we said before, sheet pile walls are considered to act as a beam. For most shapes, the neutral axis will fall midway⁷ between the two outer faces of the sheeting, in a manner similar to H-beams. With a Larssen wall, the line of the interlocks falls on the neutral axis, whereas for a Z-wall it does not. Since the inception of the Larssen type pile, which interlocks along the neutral axis of the wall, there has been concern about the ability of the interlocks to transfer horizontal shear, without which the full section strength cannot be developed.

The European philosophy has been quite liberal toward this and one will find that the section modulus published for Larssen shapes is always based on full transfer or the "combined basis" with a reduction from this state left to the engineer.

Most American engineers have taken a more conservative approach and assumed that since this transfer cannot be counted upon without welding the joints, the section modulus of a wall with interlocks on the neutral axis should be based on the properties of the single pile rather than the combined pile system. This philosophy of course fostered the development of the Z-type shapes that interlock on the faces of the wall where horizontal shear is zero.

Realistically, there is general agreement that there is always some fixity attained in the interlocks, ranging from 100 percent downward. The American approach often resulted in a

large safety factor many times and an uneconomical use of material. The European method may have produced some marginal safety factors at times but apparently few actual failures have been documented.

A series of shallow-depth arch sheet piles have been developed by the cold finishing industry. These sections, for the most part, interlock with their neighbours on one wall face, away from the neutral axis. The questions raised in the preceding paragraph do not apply to these shapes and the published section modulus may be used in a manner similar to the Z-shapes.

2.2.5. Transverse Bending Failure⁸

Transverse bending is a relatively newly recognized mode of failure in sheet piling. Although it interacts with classical bending, it is a separate failure mode of its own.

As we have seen, sheet-piling loads are primarily developed by lateral earth pressures, which in turn develop shears, moments, rotations and deflections in the beam. In addition to the flexural loading that is developed along the axis of the sheet pile, these pressures also act directly on the sheeting, producing transverse loading as shown in Figure 2-1. In essence, the lateral pressure is flattening the sheet; the plate bending at the corners is the resistance of the sheeting to this flattening. This bending is independent of classical flexure, but the combined stresses can exceed the limit of the material even when classical flexure predicts otherwise.

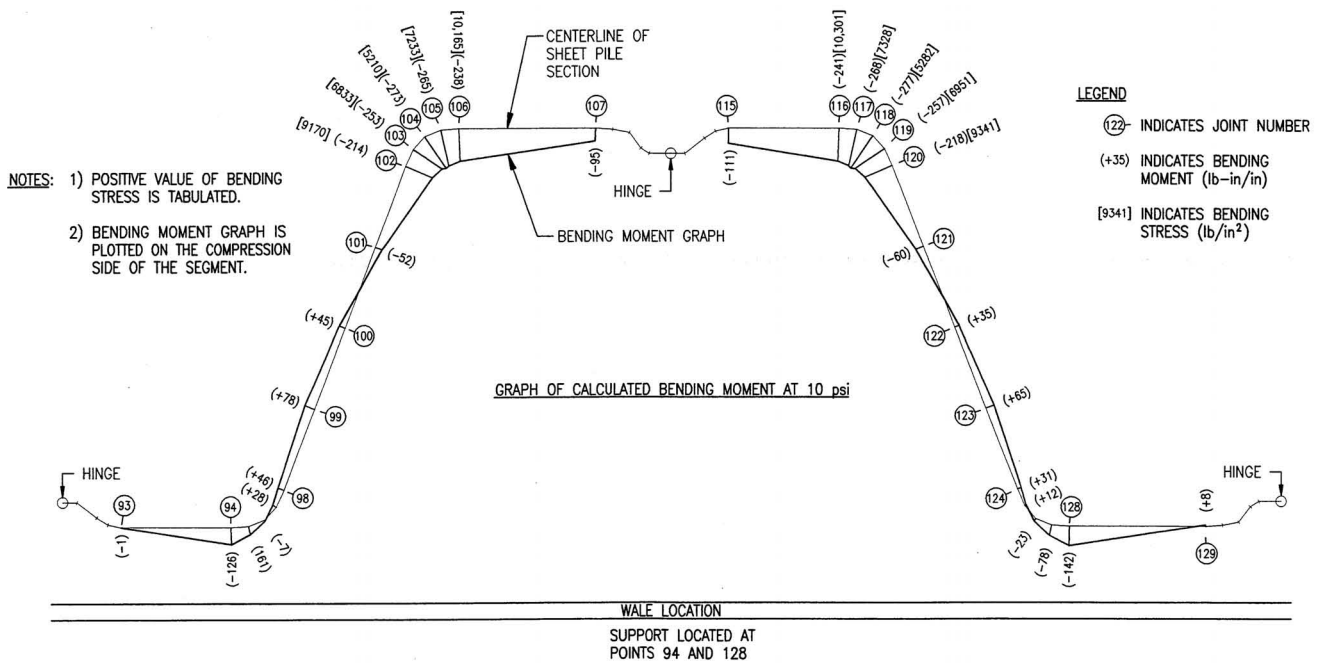


Figure 2-1: Distribution of Transverse Bending in a PZ-27 Section (after Hartman)

⁷ Technically speaking, if one were to take an exact shape of a single Z-section and determine the neutral axis in the usual direction of bending, one would find that the exact lack of symmetry with the interlocks would result in the neutral axis being shifted slightly towards the female interlock. However, the neighbouring sheet would be oriented in a reverse fashion, and thus would offset this effect. Thus, for a Z wall, the neutral axis is in fact centred between the outer faces.

⁸ All of the material in this book on the subject of transverse bending is based on Hartman, R.J., and Neal, J.A. (1997) "Report of Investigation of the Effect of Transverse Loads on the Behavior of Z-Shape Steel Sheet Piling," prepared for the L.B. Foster Company and Bethlehem Steel Corporation. This includes the figures on this subject as well; the author is grateful for their furnishing this material.

To quantify this type of failure, both finite element and laboratory studies have been performed to determine the magnitude of these stresses. These stresses have two critical points along the sheet pile wall: a) at the support(s), and b) at the point of maximum moment. Once the transverse bending stresses are determined for various values of transverse pressure and force, these are combined with classical flexural stresses to determine the maximum allowable moment in a sheet piling section. The equation for maximum allowable moment is in the form

$$\text{Equation 2-5: } M_{allow-t} = \frac{I}{c_t} (0.65 \sigma_y - \lambda_t p)$$

Where

- $M_{allow-t}$ = allowable moment on the sheeting, in-lb/ft of wall or kN-m/m of wall
- I = moment of inertia of the sections, in⁴ /ft of wall or m⁴ per m of wall
- c_t = distance from neutral axis to the point of maximum transverse stress in sheeting, in or m
- λ_t = ratio of transverse bending stresses to the lateral pressure on the sheeting, dimensionless
- p = lateral pressure on the sheeting, psi or kPa

The use of this relationship will be illustrated in Example 23. Although this phenomenon has been studied only in steel sheet piling, there is evidence that it takes place in other materials, especially vinyl and composite sheeting, where large deflections and lower transverse mechanical properties amplify the effects seen in steel.

2.2.6. Shear Failure

Although generally not considered with structures, shear failure is a possibility with sheet piling. The minimum shear area per foot or metre of wall length can be computed using the equation

$$\text{Equation 2-6: } A_{vmin} = \frac{V_{max}}{\tau_{allow}}$$

Where

- A_{vmin} = minimum shear area
- V_{max} = maximum shear on sheeting
- τ_{allow} = maximum allowable shear stress

For Z-shaped sections, the shear area can be estimated by the formula

$$\text{Equation 2-7: } A_v = \frac{t_w h}{w}$$

Where

- t_w = thickness of the sheet web and flange
- h = height of the sheeting, i.e., the distance from the outer most flats
- w = width of the section

For wood piling, the shear area can be taken to be two-thirds of the rectangular area per foot or metre of wall.

2.3. Interlock Strength for Flat Sheeting

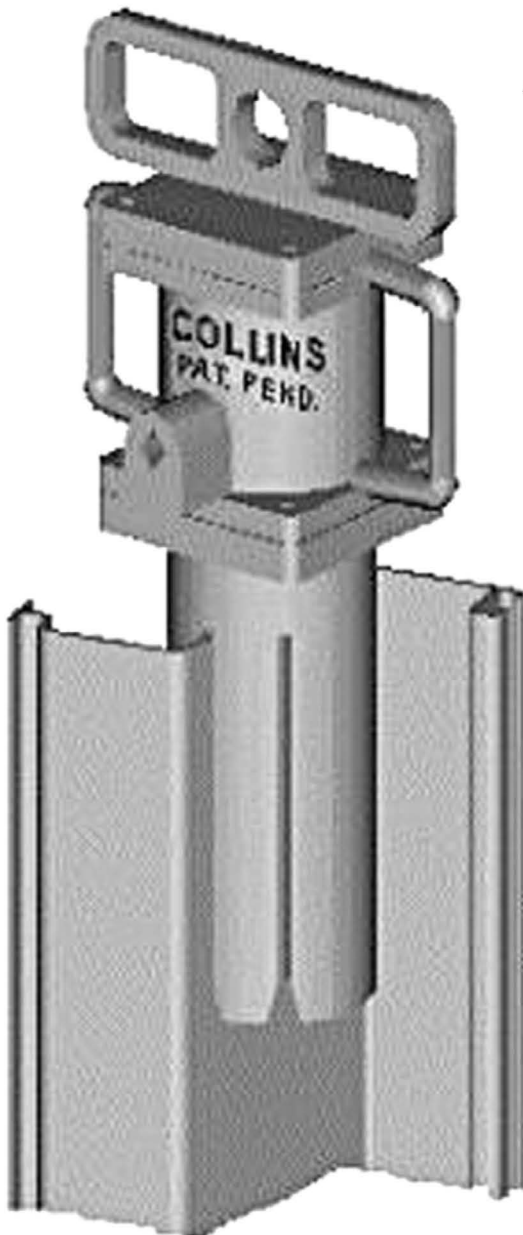
Minimum guaranteed interlock strengths required with flat type sheets used for circular cellular construction are not covered by ASTM specification. These strengths are a function of the manufacturer's design, rolling tolerances and steel strength. One lightweight flat (actually a shallow-arch) profile has a minimum strength of 12,000 pounds per inch of interlock. Because of the shallow arch, the manufacturer recommends a maximum design pull of 3,000 pounds per inch. The flat profiles offered by several producers generally provide a low value of minimums beginning at 16,000 pounds per inch and extending to 28,000 pounds per inch. It has been common practice to allow a safety factor of 2 for this type design, either permanent or temporary. The guaranteed strengths are ultimate values rather than yield.

THE COLLINS 150# AIR HAMMER

*New Patent Pending
Design. Out Drives
Heavier Hammers.
"No Leads" required.*

*Drives all brands
of VSP &
CSP+Pin Piles.*

5 day delivery, Cont. U.S.
Visa & MC.



COLLINS COMPANY

Since 1953

Toll Free 888-300-0100

Cell 360-708-5320

www.vinylsheetpiling.com

collins@whidbey.net

Chapter Three: Overview of Soil Mechanics

3.1. Introduction

This section presents an overview of basic soil mechanics, especially as they relate to retaining walls in general and sheet pile walls in particular. For engineering purposes, we shall consider the earth to be made up of rock and soil.

- Soil will be defined as naturally occurring mineral particles which are readily separated into relatively small pieces, and in which the mass may contain air, water, or organic materials (derived from decay of vegetation).
- Rock is that naturally occurring material composed of mineral particles so firmly bonded together that relatively great effort is required to separate the particles (i.e., blasting or heavy crushing forces).

The mineral particles of the soil mass are formed from decomposition of the rock by weathering (by air, ice, wind, and water) and chemical processes. Because they generally do not enter into sheet piling design, we will not discuss rocks further.

3.2. Soils

3.2.1. Overview of Soil Types

See *Figure 3-1* for principal soil deposits grouped in terms of origin (e.g., residual, colluvial, etc.) and mode of occurrence (e.g., fluvial, lacustrine, etc.).

Beyond these general geologic classifications, geotechnical engineers further classify soils to enable quantification of

their engineering properties. Two systems are discussed in this book: the Unified Soil Classification System (USCS) and the Modified Unified System (MUD). The laboratory and field tests used with both of these systems, such as tests for grain size, Atterberg limits, etc., are discussed elsewhere in this book.

3.2.2. Unified Soil Classification System (USCS)

This system is used primarily for engineering purposes and is particularly useful to the geotechnical engineer. Therefore, they should be used for all structural-related projects; such as bridges, retaining walls, buildings, etc. Precise classification requires that a grain size analysis and Atterberg Limits tests be performed on the sample. The method is discussed in detail in ASTM D 2487. The system is summarised in *Table 3-1* for granular soils and in *Table 3-2* for fine grained soils. The tables show the division between the two, which in turn determines the table to be used.

One of the main uses of soil classification systems is the determination of various soil properties based on the classification of the soil. Soils can be classified by the Unified System using visual inspection, Atterberg Limits and sieve analysis, tests which a) are relatively easy to perform and b) make greater allowance for sample disturbance than, say, consolidation or triaxial tests. Many correlations exist that enable soil properties to be estimated using the soil classification and in some cases other relatively simple tests. These correlations

Figure 3-1: Principal Soil Deposits

Major Division	Principal Soil Deposits	Pertinent Engineering Characteristics
SEDIMENTARY SOILS		
Residual Material formed by disintegration of underlying parent rock or partially indurated material.	Residual sands and fragments of gravel size formed by solution and leaching of cementing material, leaving the more resistant particles; commonly quartz.	Generally favorable foundation conditions.
	Residual clays formed by decomposition of silicate rocks, disintegration of shales, and solution of carbonates in limestone. With few exceptions becomes more compact, rockier, and less weathered with increasing depth. At intermediate stage may reflect composition, structure, and stratification of parent rock.	Variable properties requiring detailed investigation. Deposits present favourable foundation conditions except in humid and tropical climates, where depth and rate of weathering are very great.
Organic Accumulation of highly organic material formed in place by the growth and subsequent decay of plant life.	Peat. A somewhat fibrous aggregate of decayed and decaying vegetation matter having a dark colour and odour of decay.	Very compressible. Entirely unsuitable for supporting building foundations.
	Muck. Peat deposits which have advanced in stage of decomposition to such extent that the botanical character is no longer evident.	
TRANSPORTED SOILS		
Alluvial Material transported and deposited by running water.	Floodplain deposits. Deposits laid down by a stream within that portion of its valley subject to inundation by floodwaters.	

Major Division	Principal Soil Deposits	Pertinent Engineering Characteristics
TRANSPORTED SOILS		
	Point bar. Alternating deposits of arcuate ridges and swales (lows formed on the inside or convex bank of mitigating river bends.) Ridge deposits consist primarily of silt and sand, swales are clay-filled.	Generally favorable foundation conditions; however, detailed investigations are necessary to locate discontinuities. Flow slides may be a problem along riverbanks. Soils are quite pervious.
	Channel fill. Deposits laid down in abandoned meander loops isolated when rivers shorten their courses. Composed primarily of clay; however, silty and sandy soils are found at the upstream and downstream ends.	Fine-grained soils are usually compressible. Portions may be very heterogeneous. Silty soils generally present favourable foundation conditions.
	Backswamp. The prolonged accumulation of floodwater sediments in flood basins bordering a river. Materials are generally clays but tend become siltier near riverbank.	Relatively uniform in a horizontal direction. Clays are usually subjected to seasonal volume changes.
	Alluvial Terrace deposits. Relatively narrow, flat-surfaced, river-flanking remnants of floodplain deposits formed by entrenchment of rivers and associated processes.	Usually drained, oxidized. Generally favourable foundation conditions.
	Estuarine deposits. Mixed deposits of marine and alluvial origin laid down in widened channels at mouths of rivers and influenced by tide of body of water into which they are deposited.	Generally fine-grained and compressible. Many local variations in soil conditions.
	Alluvial-Lacustrine deposits. Material deposited within lakes (other than those associated with glaciation by waves, currents, and organo-chemical processes. Deposits consist of unstratified organic clay or clay in central portions of the lake and typically grade to stratified silts and sands in peripheral zones.	Usually very uniform in horizontal direction. Fine-grained soils generally compressible.
	Deltaic deposits. Deposits formed at the mouths of rivers that result in extension of the shoreline.	Generally fine-grained and compressible. Many local variations in soil condition.
	Piedmont deposits. Alluvial deposits at foot of hills or mountains. Extensive plains or alluvial fans.	Generally favorable foundation conditions.
Aeolian Material transported and deposited by wind.	Loess. A calcareous, unstratified deposit of silts or sandy or clayey silt traversed by a network of tubes formed by root fibres now decayed.	Relatively uniform deposits characterized by ability to stand in vertical cuts. Collapsible structure. Deep weathering or saturation can modify characteristics.
	Dune sands. Mounds, ridges, and hills of uniform fine sand characteristically exhibiting rounded grains.	Very uniform grain size; may exist in relatively loose condition.
Glacial Material transported and deposited by glaciers, or by meltwater from the glacier.	Glacial till. An accumulation of debris, deposited beneath, at the side (lateral moraines, or at the lower limit of a glacier (terminal moraine. Material lowered to ground surface in an irregular sheet by a melting glacier is known as a ground moraine.	Consists of material of all sizes in various proportions from boulder and gravel to clay. Deposits are unstratified. Generally present favourable foundation conditions; however, rapid changes in conditions are common.
	Glacio-Fluvial deposits. Coarse and fine-grained materials deposited by streams of melt water from glaciers. Material deposited on ground surface beyond terminal of glacier is known as an outwash plain. Gravel ridges known as kames and eskers.	Many local variations. Generally, these present favourable foundation conditions.
	Glacio-Lacustrine deposits. Materials deposited within lakes by melt water from glaciers. Consisting of clay in central portions of lake and alternate layers of silty clay or silt and clay (varved clay in peripheral zones.	Very uniform in a horizontal direction.
Marine Material transported and deposited by ocean waves and currents in shore and off-shore areas.	Shore deposits. Deposits of sands and/or gravels formed by the transporting, destructive, and sorting action of waves on the shoreline.	Relatively uniform and of moderate to high density.

and currents in shore and offshore areas.	Marine clays. Organic and inorganic deposits of fine-grained material.	Generally very uniform in composition. Compressible and usually very sensitive to remoulding.
Colluvial Material transported and deposited by gravity.	Talus. Deposits created by gradual accumulation of unsorted rock fragments and debris at base of cliffs.	Previous movement indicates possible future difficulties. Generally unstable foundation conditions.
	Hillwash. Fine colluvium consisting of clayey sand, sand silt, or clay.	
	Landslide deposits. Considerable masses of soil or rock that have slipped down, more or less as units, from their former position on steep slopes.	
Pyroclastic Material ejected from volcanoes and transported by gravity, wind and air.	Ejecta. Loose deposits of volcanic ash, lapilli, bombs, etc.	Typically shardlike particles of silt size with larger volcanic debris. Weathering and redeposition produce highly plastic, compressible clay. Unusual and difficult foundation conditions.
	Pumice. Frequently associated with lava flows and mudflows, or may be mixed with nonvolcanic sediments.	

enable the geotechnical engineer to make estimates – in some cases the only estimates possible – of soil properties for preliminary design purposes.

Many of the “typical properties” of soils are based on SPT results; these are discussed with the SPT. Those discussed in this section are derived from other tests. It should be noted that these “typical” properties and correlations are of varying quality, expressed by standard deviation, which is the range above and below the average trend, within which about two-thirds of all values occur. These relationships are useful in preliminary analyses but must not supplant careful tests of structural properties. The relationships should never be applied in final analyses without verification by tests of the particular material concerned.

3.2.2.1. Coarse-Grained (Cohesionless or Granular) Soils

Coarse-grained soils are those soils where more than half of particles finer than 3” size can be distinguished by the naked eye. The smallest particle that is large enough to be visible corresponds approximately to the size of the opening of No. 200 sieve used for laboratory identification. Sands are divided from gravels on the No. 4 sieve size, and gravels from cobbles on the 3” size. The division between fine and medium sands is at the No. 40 sieve, and between medium and coarse sand at the No. 10 sieve. Generally, the engineering properties of cohesionless or granular soils are as follows:

- Excellent foundation material for supporting structures and roads.
- The best embankment material.
- The best backfill material for retaining walls.
- Might settle under vibratory loads or blasts.
- Dewatering can be difficult due to high permeability.
- If free draining not frost susceptible.

Correlations between friction angle, relative density and Unified classifications are shown in Figure 3-2 and Figure 3-3.

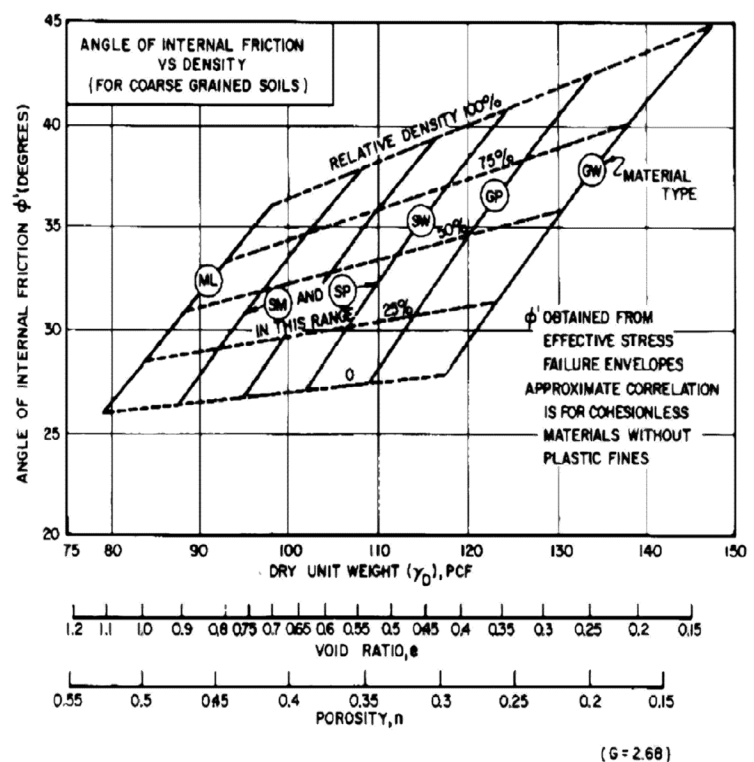


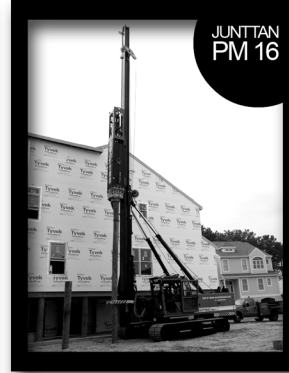
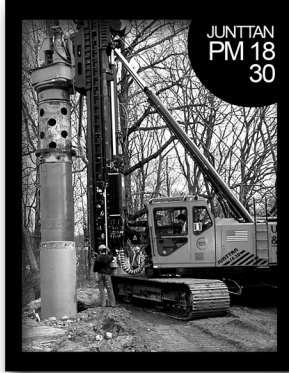
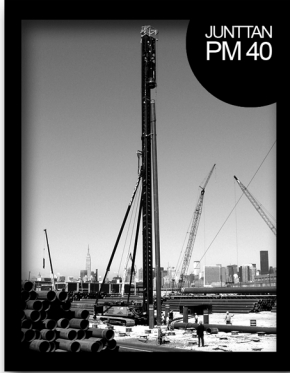
Figure 3-2: Correlations of Strength Characteristics for Granular Soils

3.2.2.2. Fine-Grained (Cohesive or Organic) Soils

Soils are identified as fine-grained when more than half of the particles are finer than No. 200 sieve (as a field guide, such particles cannot be seen by the naked eye). Fine-grained soils are classified according to plasticity characteristics determined in Atterberg limit tests. A plasticity chart for use with both coarse- and fine-grained soils is given in Figure 3-4.

In general, the engineering properties of cohesive soils are as follows:

- Very often, possess low shear strength.
- Plastic and compressible.
- Loses part of shear strength upon wetting.
- Loses part of shear strength upon disturbance.



Jackpot!*

*Junttan has been at the forefront of fully hydraulic piling machines for over 20 years. The first Junttan rigs manufactured in the early 80's, are still in everyday work. This hard won experience benefits our customers every day and on every continent: our machines have proven themselves in the most demanding conditions in over 40 countries across the world... You are interested in making money - with Junttan machines **You can do it!**

[we go the extra mile
to get **YOU** the extra feet
JUNTTAN]

Junttan | KUOPIO FINLAND
Tel: +358-17-287-4400
Fax: +358-17-287-4411
www.junttan.com | junttan@junttan.com

Ahti Knopp | USA / FINLAND
Sales manager
Tel: 1-404-514-8056
ahti.knopp@junttan.com

Simo Tanner | USA / Miami
Sales representative
Tel: 1-305-338-9793
simo.tanner@junttan.com

David Thomas | USA / Atlanta
Sales representative
Tel: 1-404-282-20263
david.thomas@is-m.net

Cleon W. Godard | USA / Pittsburgh
Agent
Tel: 1-724-554-3753
cwgodard@hotmail.com

Successful partnering* / Some of our partners already driving piles with Junttan in U.S. soil

Underpinning & Foundation SKANSKA
Tel: 1-718-786-6557
Peter.MacKenna@Underpinning.com

G. Donaldson Construction Co.
Tel: 1-401-334-2565
cdonaldson@gdonaldson.com

Norwalk Marine Contractors
Tel: 1-203-866-3344
skipgardella@norwalkmarine.com

Sun Marine Maintenance
Tel: 1-302-539-6756
sunmarine@dmv.com

Jet Drive General Marine Contracting Co.
Tel: 1-516-763-2829
jetsters@aol.com

Table 3-1: Unified Soil Classification System for Coarse-Grained Soils⁹

Primary Division for Field and Laboratory Identification		Group Symbol	Typical Names ¹⁰	Laboratory Classification Criteria		Supplementary Criteria For Visual Identification	
Coarse-grained soils. (More than half of material finer than 3" sieve is larger than No. 200 Sieve)	Gravel. (More than half of the coarse fraction is larger than No. 4 Sieve, about 1/4")	Clean gravels. (Less than 5% of material smaller than No. 200 Sieve size.)	GW	Well-graded gravels, gravel-sand mixtures, little or no fines.	$C_u = \frac{D_{60}}{D_{10}} > 4$ $1 < C_z = \frac{(D_{30})^2}{D_{10}D_{60}} < 4$		Wide range in grain size and substantial amounts of all intermediate particle size.
			GP	Poorly graded gravels, gravel-sand mixtures, little or no fines.	Not meeting both criteria for GW		Predominantly one size (uniformly graded) or a range of sizes with some sizes missing (gap graded.)
		Gravels with fines. (More than 12% of material smaller than No. 200 Sieve Size.)	GM	Silty gravels and gravel-sand-silt mixtures.	Atterberg limits below "A" line, or PI < 4.	Atterberg limits above "A" line with 4 < PI < 7 is borderline case GM-GC.	Nonplastic fines or fines or low plasticity.
			GC	Clayey gravels and gravel-sand- clay mixtures.	Atterberg limits above "A" line, and PI > 7.		Plastic fines.
	Sands. More than half of the coarse fraction is smaller than No. 4 sieve.	Clean Sands. (Less than 5% of material smaller than No. 200 sieve.)	SW	Well-graded sands, gravelly sands, little or no fines.	$C_u = \frac{D_{60}}{D_{10}} > 6$ $1 < C_z = \frac{(D_{30})^2}{D_{10}D_{60}} < 3$		Wide range in grain sizes and substantial amounts of all intermediate particle sizes.
			SP	Poorly graded sands and gravelly sands, little or no fines.	Not meeting both criteria for SW.		Predominately one size (uniformly graded) or a range of sizes with some intermediate sizes missing (gap graded.)
		Sands with fines. (More than 12% of material smaller than No. 200 sieve size.)	SM	Silty sands, sand-silt mixtures.	Atterberg limits below "A" line, or PI < 4.	Atterberg limits above "A" line with 4 <PI < 7 is borderline case SM-SC.	Nonplastic fines or fines of low plasticity.
			SC	Clayey sands, sand-clay mixtures.	Atterberg limits above "A" line with PI > 7.		Plastic fines.

- Shrinks upon drying and expands upon wetting.
- Very poor material for backfill.
- Poor material for embankments.
- Practically impervious.
- Clay slopes are prone to landslides.

- High Capillarity and frost susceptibility
- Relatively low permeability
- Difficult to compact

Compared to clay, silts exhibit the following characteristics:

- Better load sustaining qualities
- Less compressible
- More permeable
- Exhibit less volume change

Differing from clays are silts; some characteristics of silts are as follows:

Relatively low shear strength

⁹ Cohesionless materials with 5-12% smaller than No. 200 sieve are borderline cases, designated GW-GM, SW-SC, etc.

¹⁰ Materials with 5 to 12 percent smaller than No. 200 sieve are borderline cases, designated: GW-GM, SW-SC, etc.

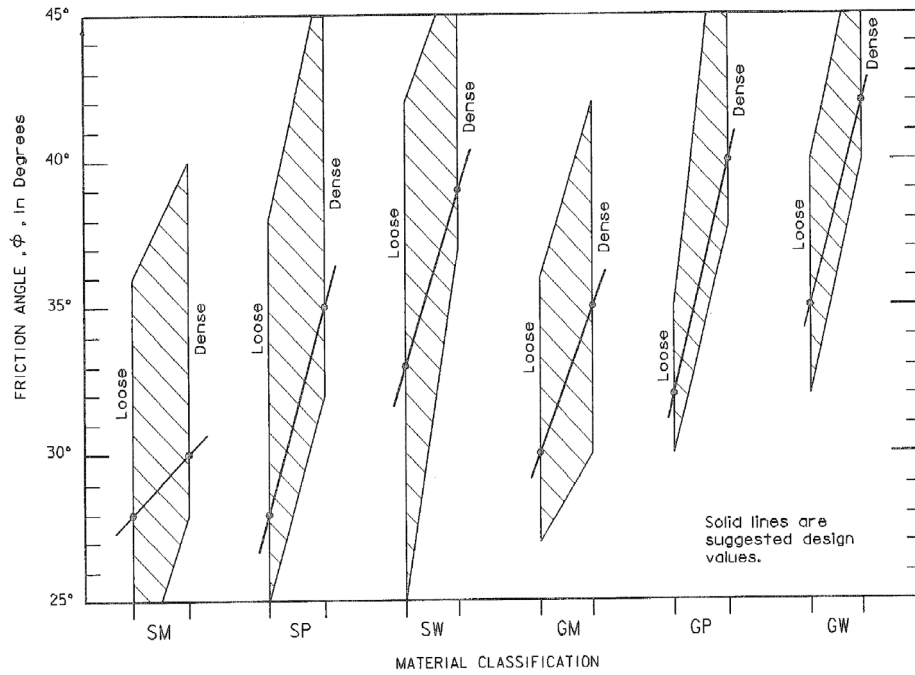


Figure 3-3: Friction Angle of Granular Backfills

Table 3-2: Unified Soil Classification for Fine-Grained Soils

Primary Division for Field and Laboratory Identification	Group Symbol	Typical Names ¹⁰	Laboratory Classification Criteria		Supplementary Criteria For Visual Identification			
					Dry Strength	Reaction to Shaking	Toughness near Plastic Limit	
Fine-grained soils. (More than half of material is smaller than No. 200 sieve size.) (Visual: more than half of particles are so fine that they cannot be seen by naked eye.)	Silts and clays. (Liquid limit < 50.)	ML	Inorganic silts, very fine sands, rock flour, silty or clayey fine sands.	Atterberg limits below "A" line, or PI < 4.	Atterberg limits above "A" line with PI between 4 and 7 is borderline case ML-CL.	None to slight.	Quick to slow.	None
		CL	Inorganic clays of low to medium plasticity; gravelly clays, silty clays, sandy clays, lean clays.	Atterberg limits above "A" line, with PI > 7.		Medium to high.	None to very slow.	Medium.
		OL	Organic silts and organic silt-clays of low plasticity.	Atterberg limits below "A" line.	Slight to medium.	Slow.	Slight.	
		MH	Inorganic silts, micaceous or diatomaceous fine sands or silts, elastic silts.	Atterberg limits below "A" line.	Slight to medium.	Slow to none.	Slight to medium.	
		CH	Inorganic silts of high plasticity, fat clays.	Atterberg limits above "A" line.	High to very high.	None.	High.	
		OH	Organic clays of medium to high plasticity.	Atterberg limits below "A" line.	Medium to high.	None to very slow.	Slight to medium.	
	Highly organic soils.	Pt	Peat, muck and other highly organic soils.	High ignition loss, LL and PI decrease after drying.	Organic color and odor, spongy feel, frequently fibrous texture.			

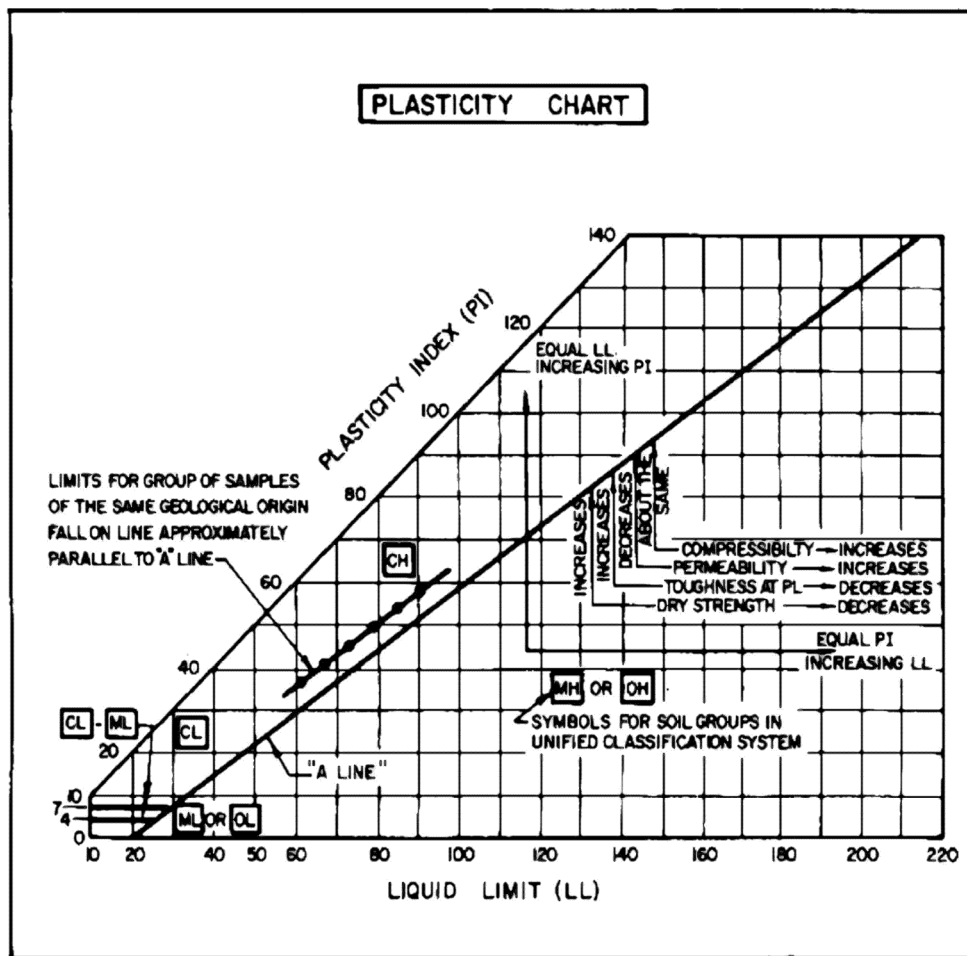


Figure 3-4: Plasticity Chart for Unified Classification System

3.2.2.3. Examples of Sample Descriptions

- Granular soils:
 - o Medium dense, grey coarse to fine SAND, trace silt, trace fine gravel (SW).
 - o Dry, dense, light brown coarse to fine SAND, some silt (SM).
- Fine grained soils:
 - o Very stiff brown silty CLAY (CL), wet
 - o Stiff brown clayey SILT (ML), moist
 - o Soft dark brown organic CLAY (OH), wet.

3.2.3. Modified Unified System (MUD)

For many years, soils engineers have successfully used the Unified Soil Classification System to categorize soil samples. The major advantage of this system is the easily understood word picture used to describe the soil samples after classification. The major disadvantage is the number of time-consuming classification tests that must be done to develop the word picture.

At present, numerous private firms and State agencies are using the nomenclature of the Unified System but without the classification testing. This process of visually identifying soil samples as known as the Modified Unified Description (MUD).

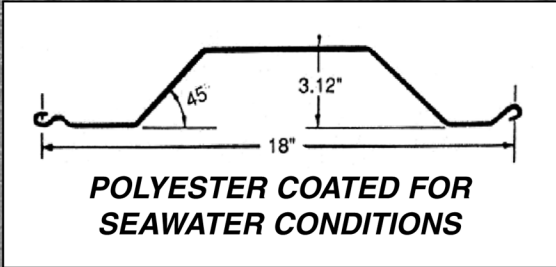
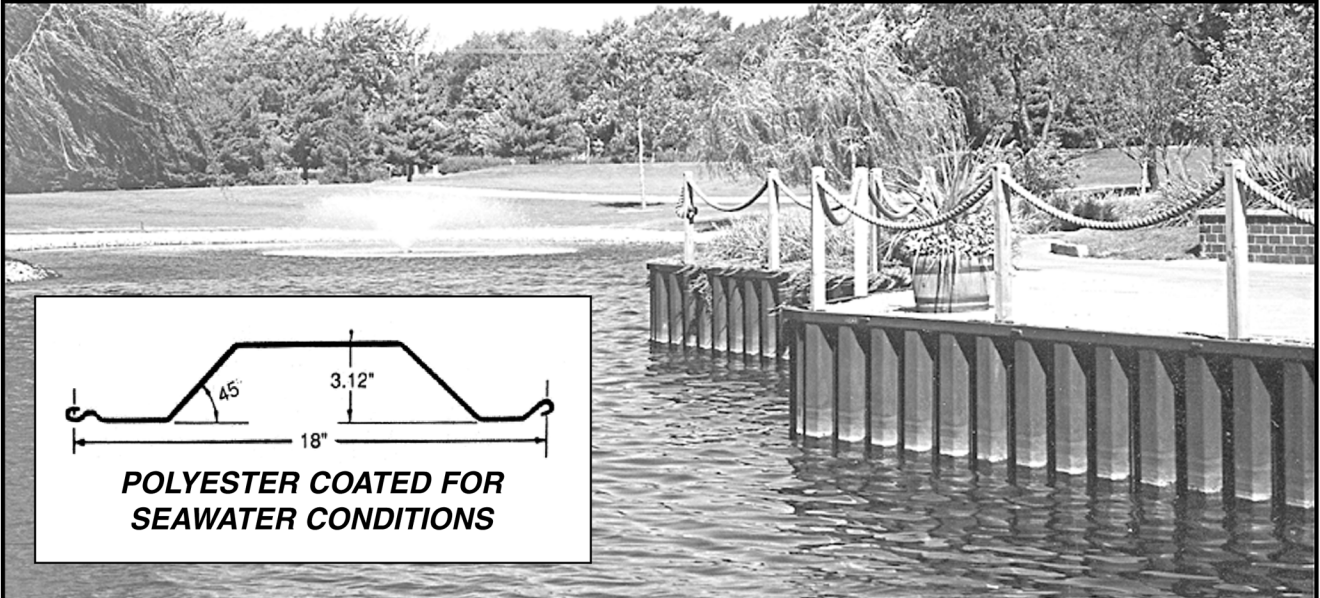
The procedure involves visually and manually examining soil samples with respect to texture, plasticity and colour. A method is presented for preparing a "word picture" of a sample for entering on a subsurface exploration log or other appropriate data sheet. The procedure applies to soil descriptions made in the field or laboratory.

It should be understood that the soil descriptions are based upon the judgment of the individual making the description. Classification tests are not intended to be used to verify the description, but to provide further information for analysis of soil design problems or for possible use of the soil as a construction material.

It is the intent of this system to describe only the constituent soil sizes that have a significant influence on the visual appearance and behaviour of the soil. This description system is intended to provide the best word description of the sample to those involved in the planning, design, construction, and maintenance processes.

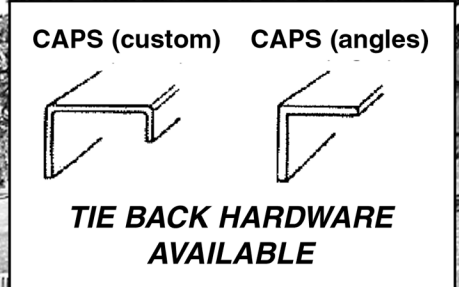
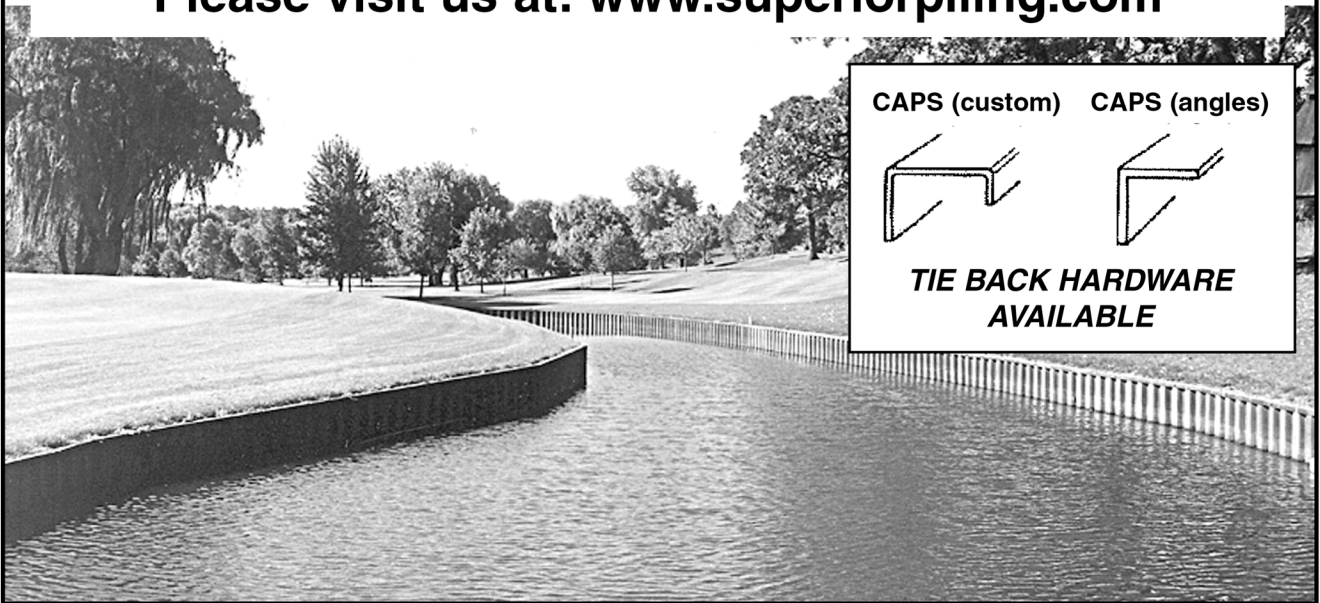
3.2.3.1. Definition of Terms

- Boulder - A rock fragment, usually rounded by weathering or abrasion, with an average dimension of 12 inches or more.
- Cobble - A rock fragment, usually rounded or subrounded,



SUPERIOR PILING, INC

7247 S. 78th AVENUE, BRIDGEVIEW, IL 60455
1-800-544-1196 • 708-496-1196 • FAX 708-496-1261
Please visit us at: www.superiorpiling.com



with an average dimension between 3 and 12 inches.

- Gravel¹¹ - Rounded, subrounded, or angular particles of rock that will pass a 3 inch square opening sieve (76.2 mm) and be retained on a Number 10 U.S. standard sieve (2.0 mm).
- Sand - Particles that will pass the Number 10 U.S. standard sieve and be retained on the Number 200 U.S. standard sieve (0.074 mm).
- Silt - Material passing the Number 200 U.S. standard sieve that is nonplastic and exhibits little or no strength when dried.¹²
- Clay - Material passing the Number 200 U.S. standard sieve that can be made to exhibit plasticity (putty like property) within a wide range of water contents and exhibits considerable dry strength.¹³
- Fines - The portion of a soil passing a Number 200 U.S. standard sieve.
- Marl - Unconsolidated white or dark grey calcium carbonate deposit.
- Muck - Finely divided organic material containing various amounts of mineral soil.
- Peat - Organic material in various stages of decomposition.
- Organic Clay - Clay containing microscopic size organic matter. May contain shells and/or fibres.
- Organic Silt - Silt containing microscopic size organic matter. May contain shells and/or fibres.
- Coarse-Grained Soil - Soil having a predominance of gravel and/or sand.
- Fine-Grained Soil - Soil having a predominance of silt and/or clay.
- Mixed-Grained Soil - Soil having significant proportions of both fine-grained and coarse-grained sizes.

3.2.3.2. Visual - Manual Identification

Constituents are identified considering grain size distribution and the results of the manual tests. In addition to the principal constituent, other constituents that may affect the engineering properties of the soil should be identified. Secondary constituents are generally indicated as modifiers to the principal constituent (i.e., sandy clay or silty gravel). Other constituents can be included in the description through the use of terms such as with, some and trace. Details of visual identification of samples can be found in *Table 3-3*.

Other terms that might be used include the following:

- Marl - A white or grey calcium carbonate paste. May contain granular spheres, shells, organic material or inorganic soils. Reacts with weak hydrochloric acid.
- Muck - Black or dark brown finely divided organic material mixed with various proportions of sand, silt, and clay. May contain minor amounts of fibrous material such as roots, leaves, and sedges.
- Peat - Black of dark brown plant remains. The visible plan remains range from coarse fibres to finely divided organic material.

- Organic Clay - Dark grey clay with microscopic size organic material dispersed throughout. May contain shells and /or fibres. Has weak structure that exhibits little resistance to kneading.
- Organic Silt - Dark grey silt with microscopic size organic material dispersed throughout. May contain shells and/or fibres. Has weak structure that exhibits little resistance to kneading.
- Fill - Man-made deposits of natural soils and/or waste materials. Document the components carefully since presence and depth of fill are important engineering considerations.

3.2.3.3. Soil Sample Identification Procedure

- First Decision -
 - Is sample coarse-grained, fine-grained, mixed-grained or organic?
 - If mixed-grained, decide whether coarse-grained or fine-grained predominates.
- 2nd Decision -
 - What is principal component?
 - Use as noun in soil description. Example: Silty Sand
- 3rd Decision -
 - What is secondary component?
 - Use as adjective in soil description. Example: Silty Sand
- 4th Decision -
 - Are there additional components?
 - Use as additional adjective. Example: Silty Sand, Gravelly
- Examples Of Descriptions Of The Soil Components
 - Sand - Describes a sample that consists of both fine and coarse sand particles.
 - Gravel - Describes a sample that consists of both fine and coarse gravel particles.
 - Silty fine Sand - Major component fine sand, with non plastic fines.
 - Sandy Gravel - Major component gravel size, with fine and coarse sand. May contain small amount of fines.
 - Gravelly Sand - Major component sand, with gravel. May contain small amount of fines.
 - Gravelly Sand, Silty - Major component sand, with gravel and nonplastic fines.
 - Gravelly Sand, Clayey - Major component sand, with gravel and plastic fines.
 - Sandy Gravel, Silty - Major component gravel size, with sand and nonplastic fines.
 - Gravelly Sand, Clayey - Major component gravel size, with sand and plastic fines.
 - Silty Gravel - Major component gravel size, with nonplastic fines. May contain sand.
 - Clayey Gravel - Major component gravel size, with plastic fines. May contain sand and silt.
 - Clayey Silt - Major component silt size, with sufficient clay to impart plasticity and considerable strength when dry.

¹¹ The term "gravel" in this system denotes a particle size range and should not be confused with "gravel" used to describe a type of geological deposit or a construction material.

¹² New York State Soil Mechanics Bureau STP-2 - Issuance No. 7.41-5/75 "Soil Description Procedure".

¹³ When applied to gradation test results, silt size is defined as that portion of the soil finer than the No. 200 U.S. standard sieve and coarser than 0.002 mm. Clay size is that portion of soil finer than 0.002 mm. For the visual-manual procedure, the identification will be based on plasticity characteristics.

Table 3-3: Visual Identification of Samples

Definitions of Soil Components and Fractions		
I. Grain Size Material Boulders Cobbles	Fraction	Sieve Size 12"+ 3" - 12"
Gravel: The particles may have an angular, rounded, or subrounded shape. Gravel size particles usually occur in varying combinations with other particle sizes.	Coarse Fine	3/4" - 3" No. 4 to 3/4"
Sand: Gritty grains that can easily be seen and felt. No plasticity or cohesion.	Coarse Medium Fine	No. 10 to No. 4 No. 40 to No. 10 No. 200 to No. 40
Fines (Silt & Clay):		Passing No. 200
Silt - Identified by behaviour. Fines that have no plasticity. May be rolled into a thread but will easily crumble. Has no cohesion. When dry, can be easily broken by hand into powdery form.		
Clay - Identified by behaviour. Fines are plastic and cohesive when in a moist or wet state. Can be rolled into a thin thread that will not crumble. When dry, forms hard lumps that cannot be readily broken by hand.		
Clay is often encountered in combination with other soil sizes. If a sample exhibits plasticity or cohesion, it contains clay. The amount of clay can be related to the degree of plasticity or cohesiveness; the higher the clay content the greater the plasticity.		
Grading of Coarse Soils ¹⁴	Well-Graded	Soil contains a good representation of all particle sizes from largest to smallest.
	Poorly-Graded	Soil contains particles about the same size. A soil of this type is sometimes described as being uniform.
	Gap-Graded	Soil does not contain one or more intermediate particles sizes. A soil consisting of gravel and fine sand would be gap graded because of the absence of medium and coarse sand sizes.
Coarse- and Fine-Grained Soils	Descriptive Adjective	Percentage Requirement
	Trace	1 - 10%
	Little	10 - 20%
	Some	20 - 35%
	And	35 - 50%
Fine-Grained Soils. Identify in accordance with plasticity characteristics, dry strength, and toughness.		
Stratified Soils	Descriptive Term	Thickness
	Alternating	
	Thick	
	Thin With	
	Parting	0 to 1/16" thickness
	Seam	1/16 to 1/2" thickness
	Layer	1/2 to 12" thickness
Stratum	Greater than 12" thickness	
Varved Clay	Alternating seams or layers of sand, silt and clay	
Pocket	Small, erratic deposit, usually less than 1 foot	
Lens	Lenticular deposit	
Occasional	One or less per foot of thickness	
Frequent	More than one per foot of thickness	

¹⁴ Descriptions of fine-grained soils should not include a grading.

- o Silty Clay - Major component clay, with silt size. Higher degree of plasticity and higher dry strength than clayey silt.

The above system may be expanded where necessary to provide meaningful descriptions of the sample. Examples: Shale fragments - Cobble and gravel size, silty. Decomposed rock - Gravel size

3.2.3.4. Other Information for Describing Soils

- Colour Of The Sample - Brown, Grey Red, Black, etc. The colour description is restricted to two colours. If more than two colours exist, the soil should be described as multi-coloured or mottled and the two predominant colours given.
- Moisture condition. Judge by appearance of sample before manipulating. The in-situ moisture content of a soil should be described as dry, moist, or wet.
- Plasticity - Plastic, Low Plastic, Nonplastic. Note: Sample must be in moist or wet condition for plasticity determination. For dry samples requiring wetting make note in description. Example - "plastic (low or nonplastic) when wet." Plasticity not required for marl, muck and peat.
- Structure - Fissured, Blocky, Varved, Layered. (Indicate approximate thickness of layers). The description of layering for coarse-grained soils must be made from field observations before sample is removed from sampler.
- Particle shape. Coarse-grained soils are described as \ angular, sub-angular, sub-rounded, or rounded. Gravel, cobbles, and boulders can be described as flat, elongated, or flat and elongated. Descriptions of fine-grained soils will not include a particle angularity or shape.

Any additional descriptive terms considered helpful in identifying the soil should be included. Examples of such terms include calcareous, cemented, and gritty. Material origins or local names should be included in parentheses (i.e., fill, iron rock)

3.2.3.5. Preparing the Word Picture

The word-picture is the description of the soil sample as determined by the visual-manual procedure. Where applicable, the following are to be included in the word-picture (*a sample of this appears also*):

- Colour of the sample: *Brown*
- Description of Soil Components: *Silty Gravel*
- Moisture Condition: *moist*
- Plasticity: *nonplastic*
- Structure
- Particle shape: *angular*
- Other: *cemented*

The written description for the given example is: Brown Silty angular Gravel, moist, nonplastic, cemented.

3.2.3.6. Examples Of Complete Soil Descriptions

- Light Grey Silty Clay, moist, plastic, with 1/2 inch layers of wet, grey Silt, nonplastic
- Red brown Clayey Silt with 1/4 inch layers of Silty Clay, moist, plastic

- Brown Silty fine Sand, wet, nonplastic
- Grey Sandy rounded Gravel, dry, nonplastic
- Grey Sandy angular Gravel, Clayey, moist, low plastic
- Dark Brown Silty Sand, wet, nonplastic
- Red Brown Sand, dry, nonplastic, with roots
- Fill - Brown Sandy subrounded Gravel, with pieces of brick and cinders, wet, nonplastic
- Fill containing cinders, paper, garbage, and glass, wet
- Dark Grey Organic Clay, with shells and roots, moist, plastic If SPT data is not available, consistency can be estimated based on visual-manual examination of the material. Refer to ASTM D 2488 for consistency criteria.

3.3. Logging

The boring log shown in *Figure 3-5* is typical for borings and test pits. The majority of information to be included on this form is self-explanatory.

3.4 Special Materials and Difficult Soils

Many types of soils create special problems in design and construction, especially those that experience large changes in volume. Types of special materials are shown in *Table 3-4*.

3.4.1. Permafrost and Frost Penetration

3.4.1.1. Characteristics

In non-frost susceptible soil, volume increase is typically 4% (porosity 40%, water volume increase in turning to ice = 10%, total heave = 40% x 10% = 4%). In susceptible soil heave is much greater as water flows to colder zones (forming ice lenses). The associated loss of support upon thaw can be more detrimental to structure than the heave itself.

3.4.1.2. Classification

Silts are the most susceptible to frost heave. Soils of types SM, ML, GM, SC, GC, and CL are classified as having frost heave potential.

3.4.2. Limestone and Related Materials

Limestone, dolomite, gypsum and anhydrite are characterized by their solubility and thus the potential for cavity presence and cavity development. Limestones are defined as those rocks composed of more than 50% carbonate minerals of which 50% or more consist of calcite and/or aragonite. Some near shore carbonate sediments (also called limestone, marl, chalk) could fit this description. Such sediments are noted for erratic degrees of induration, and thus variability in load supporting capacity and uncertainty in their long-term performance under sustained loads. The most significant limestone feature is its solubility. An extremely soluble one can be riddled with solution caves, channels, or other open, water, or clay filled features.

Geological reconnaissance, drilling, and other forms of bedrock verification may check presence of solution features. Geophysical techniques, including shallow seismic refraction, resistivity and gravimetry are often found to be valuable supplements.

Available The Only Full Line

American-Made PZ Sheet Piles with Ball & Socket Interlocks

Petersburg, Virginia



CHAPARRAL STEEL
www.chaparralsteel.com



Distributed Exclusively by L.B. Foster Company • 1-800-255-4500 • www.sheetpiling.com

STATE OF FLORIDA DEPARTMENT OF TRANSPORTATION
FIELD BORING LOG

FORM 675-020-13
MATERIALS - 0594

SHEET 1 OF 5

PROJECT NO. <u>79100-1523</u>		NAME <u>S.R. 40 / Tomoka River</u>		COUNTY <u>Volusia</u>		DISTRICT <u>5</u>		
LOCATION <u>STA 14+80, 27.5 m RT CL Survey</u>				TOWNSHIP <u>14S</u>		RANGE <u>31E</u>		
ROAD NUMBER <u>State Road # 40</u>				SURFACE ELEVATION <u>+0.68 m, NGVD</u>				
EQUIPMENT TYPE <u>CME 45</u>		RIG NO. <u>7476</u>		BORING NO. <u>4</u>				
DATE STARTED <u>8/27/90</u>		COMPLETED <u>8/28/90</u>		DRILLED BY <u>Jenkins</u>				
LOGGED BY <u>Dawson</u>		BORING TYPE: <u>AUGER, WASHED, PERCUSSION, ROTARY</u>		<u>Rotary</u>				
WATER TABLE: <u>0 HR. 0.46 m</u> <u>24 HRS. 0.46 m</u> HRS. _____				CASED, UNCASED, DRILLING MUD. <u>Cased/Uncased</u>				
SAMPLE CONDITIONS: <input checked="" type="checkbox"/> DISTURBED <input type="checkbox"/> GOOD <input type="checkbox"/> LOST <input type="checkbox"/> CORE SAMPLE SAMPLE TYPES: A: AUGER SB: SPLIT BARREL S: SHELBY TUBE RC: ROCK CORE TESTS: W.C.: WATER CONTENT (%) T: TORVANE (kPa) V: IN-SITU VANE TEST (kPa)								
ELEV. (M)	DEPTH (M)	S. P. T. BLOWS	MATERIAL DESCRIPTION	SAMPLES			TESTS	REMARKS
				CON.	NO. TYPE	REC. (%)		
		2	Dark brown fine SAND, trace peat (SP)					
		4		G	S-1	100		
		4						
		2		G	S-2	20		
		3	Light grey to dark brown fine SAND (SP)					
		2		G	S-3	50	WC = 20 -200 = 3	
		2						
		2		G	S-4	100		
		3						
		3		G	S-5	100		
		4	Greenish-grey silty fine SAND, few shell fragments (SM)					
		3		G	S-6	100	WC = 20 -200 = 3	
		4						
		3		G	S-7	100		
		5						
		5		G	S-8	100		
		7						
		5		G	S-9	100	WC = 29 -200 = 18	
		6						
		9		G	S-10	100		
		4	Light to dark grey fine SAND with silt, trace to few shell (SP-SM)					
		7						
		8						
		11		G	S-11	75		
		7						
		2						

RECYCLED PAPER

Figure 3-5: Typical Boring Log

3.4.2.1. Karst Topography

In places such as Kentucky, Virginia, Pennsylvania, Tennessee, Indiana, California, Texas, and New Mexico, limestone is prone to being cavernous. Such leads to the following:

- Uneven underground erosion leads to erratic depth and quality of “bedrock”.
- Erosion also leads to underground caverns and water flows.
- Expansion of underground voids can lead to sinkholes.

3.4.2.2. Calcareous Soils

Calcareous soils are some of the most challenging types of soils for the design and installation of piling. Because they frequently appear in areas where offshore oil is found (i.e., southeast Asia, the Persian Gulf, Australia, etc.), a great deal of research has been done on these soils. Because of the complex nature of these soils and the variable way in which they are formulated, their properties are complex and not as well quantified as other types of soils.

Table 3-4: Problem Soils and Conditions¹⁵

Problem Soils	
Soil	Description
Organic	Colloids or fibrous materials such as peats, organic silts, and clays of many estuarine, lacustrine, or fluvial environments are generally weak and will deform excessively under load. These soils are usually not satisfactory for supporting even very light structures because of excessive settlements.
Normally consolidated clays	Additional loads imposed on soil consolidated only under the weight of the existing environment will cause significant long-term settlements, particularly in soft and organic clays. These clays can be penetrated several centimetres by the thumb. The magnitude and approximate rate of settlement should be determined, in order to determine acceptability of settlements for the function and characteristics of the structure. Bottoms of excavations may heave and adjoining areas settle unless precautions are taken to prevent such movement.
Sensitive clays	The ratio of undisturbed to remoulded strength is the sensitivity of clay. Clays having remoulded strengths 25% or less of the undisturbed strength are considered sensitive and subject to excessive settlement and possible catastrophic failure. Such clays preconsolidated by partial desiccation or erosion of overlying soil may support shear stresses caused by foundation loads if these loads are well within the shear strength of the clay.
Swelling and shrinking clays and shales	Clays, especially those containing montmorillonite or smectite, expand or contract from changes in water content and are widely distributed throughout the United States and the world. Clay shales may swell significantly following stress relief as in a cut or excavation and following exposure to air. Foundations in these soils may have excessive movements unless the foundation soil is treated or provisions are made in the design to account for these movements or swell pressures developed in the soil on contact with moisture.
Collapsible soils	The open, porous structure of loosely deposited soil such as silty clays and sands with particles bonded with soluble salts may collapse following saturation. These soils are often strong and stable when dry. Undisturbed samples should be taken to accurately determine the in situ density.
Loose granular soils	All granular soils are subject to some densification from vibration, which may cause significant settlement and liquefaction of soil below the water table; however, minor vibration, pile driving, blasting, and earthquake motion in loose to very loose sands may induce significant settlement. Limits to potential settlement and applicable densification techniques should be determined.
Glacial tills	Till is usually a good foundation soil except boulders and soft layers may cause problems if undetected during the field investigation.
Fills	Unspecified fills placed randomly with poor compaction control can settle significantly and provide unsuitable foundation soil. Fills should usually be engineered granular, cohesive materials of low plasticity index < 12 and liquid limit < 35. Suitable materials of the Unified Soil Classification System include GW, GM, GC, GP, SW, SP, SM, SC, and CL soils. Compaction beneath structures to " 92% of optimum density for cohesive fill or 95% for cohesionless fill using ASTM Standard Test Methods D 1557 has provided highly successful constructability and in-service performance.

Problem Conditions

Condition	Description
Meander loops	Soils that fill abandoned waterways are usually weak and cut-offs highly compressible. The depth of these soils should be determined and estimates made of potential settlement early in design to allow time for development of suitable measures for treating the soil or accommodating settlement.
Landslides	Potential landslides are not easily detected, but evidence of displacement such as bowed trees and tilted or warped strata should be noted. Sensitive clays and cutting action of eroding rivers significantly increase the risk of landslides. Slopes and excavations should be minimized, seasonal variations in the local water table considered in the design, and suitable arrangements for drainage

¹⁵Based on information from the Canadian Foundation Engineering Manual, 2nd edition.

Problem Conditions Continued

Kettle holes

provided at the top and toe of slopes.

The retreating continental ice sheet left large blocks of ice that melted and left depressions, which eventually filled with peat or with soft organic soils. Lateral dimensions can vary from a few to several hundred feet. Depths of kettle holes usually do not exceed 40% of lateral dimensions and can sometimes be identified as shallow surface depressions.

Mined areas and sinkholes

Voids beneath the surface soil may lead to severe ground movements and differential settlement from subsidence or caving. Sinkholes are deep depressions formed by the collapse of the roofs of underground caverns such as in limestone. Maps of previous mined areas are helpful when available. Published geological data, nondestructive in situ tests and past experience help indicate the existence of subsurface cavities. Investigations should be thorough to accurately determine the existence and location of any subsurface voids.

Lateral soil distortions

Lateral distortions are usually not significant, but can occur in highly plastic soils near the edge of surface loads. These distortions can adversely affect the performance of foundations of structures and embankments. Driven piles can cause large lateral displacements and excessive pressures on retaining walls.

Downdrag

Compression of fills or consolidation of soft soil adjacent to wall footings or piles cause downdrag on the footing or pile. This leads to substantial loads at the base of the foundation that can exceed the bearing capacity of the underlying soil supporting the footing or pile. Failure of the foundation can occur with gross distortion.

Vibrations

Cohesionless soil, especially loose sands and gravels, can densify and settle when subject to machine vibration, blasts, and earthquakes. Distortion with negligible volume change can occur in loose, saturated sands due to liquefaction. Low-level sustained vibration can densify saturated sands.

Living coral and coralline debris is generally found in tropical regions where the water temperature exceeds 20° C. Coral is a term commonly used for the group of animals which secrete an outer skeleton composed of calcium carbonate, and which generally grow in colonies. The term "coral reef" is often applied to large concentrations of such colonies that form extensive submerged tracts around tropical coasts and islands. In general, coralline soils deposited after the breakdown of the reef, typically by wave action, are thin (a few meters thick) and form a veneer upon cemented materials (limestones, sandstones, etc.). Calcareous soils are those that are composed of primarily sand size particles of calcium carbonate, which may be indurated to varying degrees. They can originate from biological processes such as sedimentation of skeletal debris and coral reef formation. They can also occur because of chemical precipitation of particles such as oolites. Because of their association with coral reefs, these soils appear mostly between the latitudes of 30°N and 30°S.

Because the granular coralline and algal materials are derived from organisms which vary in size from microscopic shells to large coralheads several meters in diameter, the fragments are broadly graded and range in size from boulders to fine-grained muds. Similarly, the shape of these materials varies from sharp, irregular fragments to well-rounded particles. Geologists generally refer to coralline deposits as "biogenic materials". When cemented, they may be termed "reefrock," or "beachrock," or other names that imply an origin through cementation of particles into a hard, coherent material.

Coralline deposits are generally poor foundation materials in their natural state because of their variability and suscepti-

bility to solution by percolating waters, and their generally brittle nature. Coralline materials are often used for compacted fill for roads and light structures. Under loads, compaction occurs as the brittle carbonate grains fracture and consolidate. They can provide a firm support for mats or spread footings bearing light loads, but it is necessary to thoroughly compact the material before using it as a supporting surface. Heavy structures in coral areas are generally supported on pile foundations because of the erratic induration. Predrilling frequently is required. The brittle, crushable nature of calcareous sands complicates the site investigation. This makes both the site investigation itself and a meaningful correlation of test data to actual soil properties difficult. However, there are some important soil properties to watch for.

By definition, these soils have higher than average carbonate content. The calcareous soils most prone to difficulties have a carbonate content by weight above 50 percent. Problems are especially pronounced above 80 percent, where many pile driven into these soils have abnormally low capacities.

The grain structure of these soils is highly variable due to the diverse nature of the soils. This variability is one of the most important factors in the unpredictability of these soils. This variability can manifest itself in the angularity, size, or void structure of the grains or other factors. Light cementation can lead to both low shaft friction and toe capacity.

Bulk Density. Void ratios for calcareous sands can vary from 0.8 to 1.4 as opposed to 0.4 to 0.9 for noncarbonated sands. The tendency to voids of all sizes is one of the most difficult problems encountered with calcareous sands.

Specific Gravity normally varies from 2.75 to 2.85 with these soils. Friction Angle is generally greater than 35 degrees

HPSI Vibros



from a
"Little Guy"

to a
"BIG Guy"



Whether it's an excavator mounted vibratory for driving lightweight vinyl or aluminum sheet piling on up to a 20,000 in. lb. machine for driving large diameter caisson, we have a vibro suitable for your job.

SALES & RENTALS

(Distributors throughout North America)

From "The Engineers of Pile Driving Equipment"™

HYDRAULIC POWER SYSTEMS, INC.

Kansas City Offices and Plant
1203 Ozark
N. Kansas City, MO 64116
Phone (816) 221-4774
Fax (816) 221-4591
E-mail info@hpsi-worldwide.com
<http://www.hpsi-worldwide.com>



International & Domestic Sales
745 U.S. Hwy 1
N. Palm Beach, FL 33408
Phone (561) 687-5525
Fax (561) 841-3479
E-mail info@hpsi-worldwide.com
<http://www.hpsi-worldwide.com>

*Vibratory Pile Hammers • Hydraulic Augers • Winch Systems
Custom Manufacturing • Hydraulic Impact Hammers • Lead Systems*

and can be greater than 50 degrees. This may decline with increased confining pressure, and the surface friction angle may decrease with surface roughness.

Because of extreme variability in engineering properties of natural coral formation, it is not prudent to make preliminary engineering decisions based on "typical properties." Unconfined compression strengths of intact specimens may range from 100nst to 600nst, and porosity may range from less than 40% to over 50%.¹⁶

Other characteristics include:

- Solution cavities.
- Extreme variations in porosity.
- Void ratios in coral up to two.
- Chimney-like sinkholes and collapse structures.
- Slump failures, ravelling.
- Rock settlement and consolidation.
- Piles or bridging often required.

Calcareous soils are highly compressible under pressure loading and are subject to softening under cyclic loading.

3.4.3. Quick Clays

Quick clays are characterized by their great sensitivity or strength reduction upon disturbance. All quick clays are of marine origin. Because of their brittle nature, collapse occurs at relatively small strains. Slopes in quick clays can fail without large movements¹⁷. Other characteristics include:

- Severe loss of strength when disturbed by construction activities of seismicground shaking.
- Replacement of formation water containing dissolved salt with fresh water results in strength loss.
- Produces landslide prone areas (such as Anchorage, Alaska).

Quick clays are generally confined to far north areas such as Eastern Canada, Alaska and Scandinavia. They are readily recognized by measured sensitivities greater than about 15 and by the distinctive, strain-softening shape of their stress-strain curves from strength or compressibility tests.

3.4.4. Other Materials and Considerations

3.4.4.1. Man-Made and Hydraulic Fills

Composition and density are the main concerns. Unless these can be shown to be non-detrimental to the performance of the foundation, bypassing with deep foundations, or removal and replacement are in order. Other characteristics include:

- Found in coastal facilities, levees, dikes and tailings dams.
- High void ratio.
- Uniform gradation but variable grain size within same fill.
- High liquefaction potential
- Lateral spreading.
- Easily eroded.

3.4.4.2. Chemically Reactive Soils

For foundation construction, the main concerns usually are corrosion and gas generation. Corrosion potential is determined in terms of pH, resistivity, stray current activity, groundwater position, chemical analysis, etc; and a compatible foundation treatment, e.g., sulphate resistant concrete, lacquers, creosote, cathodic protection, etc., is prescribed. For gas concentration, organic matter content and field-testing for gas are usually performed. If gas generation is expected, some form of venting system is designed. The potential presence of noxious or explosive gases should be considered during the construction excavations and tunnelling.

3.4.4.3. Lateritic Soils

Lateritic soils are found in tropical climates throughout the world. Typical characteristics are as follows:¹⁸

- Found where tropical rain forest and savannas are located.
- Deep residual soil profile.
- Shield and sedimentary cover outside shield in Central and South America, Central and West Africa, southeast Asia, and other parts of the world.
- Loss of soil strength with time.
- High void ratio and permeability.
- Aggregate deterioration.
- Variable moisture content.
- Shrinkage cracks.
- Easily compacts.
- Shear Characteristics somewhere between sand and silt.
- Landslide prone.
- Depth of wetting affects slope stability.
- Varied foundation conditions.

3.5. Laboratory Testing

As with other phases of a subsurface investigation program, the laboratory testing must be intelligently planned in advance but flexible enough to be modified based on test results. The ideal laboratory program will provide the engineer with sufficient data to complete an economical design, yet not tie up laboratory personnel and equipment with superfluous testing. The cost for laboratory testing is insignificant compared to the cost of an over-conservative design. This article is limited to a brief description of the tests, their purpose and the uses of the resulting data.

Not every test outlined below is applicable to every project. Engineering judgment must be exercised in setting up a testing program that will produce the information required on each specific project.

3.5.1. Grain-Size Analysis

This test is performed in two stages: sieve analysis for coarse-grained soils (sands, gravels) and hydrometer analysis

¹⁶ For more information see Sowers, F.G., Failure in Limestone in Humid Subtropics, Journal of the geotechnical engineering Division, ASCE, Vol. 101, No. GR8, 1975, and Way, S.D., Terrain Analysis - A Guide to Site Selection Using Aerial Photographic Interpretation, Dowden, Hutchinson & Ross, Inc., Stroudsburg, PA., 1973.

¹⁷ For further information see Anne, Q.A., Quick Clays and California: No Quick Solutions, Focus on Environmental Geology, Ronald Rark, ed., pp 140-145, 1973.

¹⁸ For further information see Gidigas, M.D., Laterite Soil Engineering, Elsevier Scientific Publishing Co., 1976; Persons, S.B., Laterite Genesis, Location, Use, Plenum Press, 1970; U.S. Agency for International Development, Engineering Study of Laterite and Lateritic Soils in Connection With Construction of Roads, Highways and Airfields, Southeast Asia, 1969; U.S. Agency for International Development, Laterite, Lateritic Soils and Other Problem Soils of Africa, 1971; U.S. Agency for International Development, Laterite and Lateritic Soils and Other Problem Soils of the Tropics, 1975.

for fine-grained soils (clays, silts). Soils containing both types are tested in sequence, with the material passing the No. 200 sieve (0.075 mm or smaller) analysed by hydrometer.

3.5.1.1. Sieve Analysis

This test provides a direct measurement of the particle size distribution of a soil by causing the sample to pass through a series of wire screens with progressively smaller openings of known size. The amount of material retained on each sieve is weighed. See ASTM C 136.

3.5.1.2. Hydrometer

This test is based on Stokes Law. The diameter of a soil particle is defined as the diameter of a sphere which has the same unit mass and which falls at the same velocity as the particle. Thus, a particle size distribution is obtained by using a hydrometer to measure the change in specific gravity of a soil-water suspension as soil particles settle out over time.

Results are reported on a combined grain size distribution plot as the percentage of sample smaller than, by weight, versus the log of the particle diameter. These data are necessary for a complete classification of the soil. The curve also provides other parameters, such as effective diameter (D^{10}) and coefficient of uniformity (C_u). Tests shall be performed in accordance with ASTM D 422 (AASHTO T 88).

3.5.2. Moisture Content

The moisture content, is defined as the ratio of the weight of water in a sample to the weight of solids. The wet sample is weighed, and then oven-dried to a constant weight at a temperature of about 230° F (110° C). The weight after drying is the weight of solids. The change in weight, which has occurred during drying, is equivalent to the weight of water. For organic soils, a reduced drying temperature of approximately 140° F (60° C) is sometimes recommended. Tests shall be performed in accordance with ASTM D 2216 (AASHTO T 265).

The moisture content is valuable in determining the properties of soils and can be correlated with other parameters. A good technique is to plot the moisture content from SPT samples as a function of depth.

3.5.3. Atterberg Limits

The liquid limit, plastic limit and shrinkage limit are all Atterberg Limits. However, for classification purposes, the term Atterberg Limits generally refers to the liquid and plastic limits only. The tests for these two are described here; the shrinkage limit test is described below.

The liquid limit (LL) is the moisture content of a soil at the boundary between the liquid and plastic states. The plastic limit (PL) is the moisture content at the boundary between the plastic and semi-solid states. The plasticity index (PI) is

the difference between the LL and PL. The results are generally reported as LL vs. PI values and can be plotted on the same graph as the moisture content above. These values are useful in soil classification and have been correlated with other parameters. For example, the drained shear strength of normally consolidated clays is similar to that of loose sands ($c' = 0$), except that ϕ is generally lower. An empirical correlation of the effective angle of internal friction, ϕ' , with plasticity index for normally consolidated clays is shown in Figure 3-6. The drained shear strength of over-consolidated clays is similar to that of dense sands (again with lower ϕ'), where there is a peak strength ($c' \neq 0$) and a "residual" shear strength ($c' = 0$).

3.5.3.1. Liquid Limit

The liquid limit is determined by ascertaining the moisture content at which two halves of a soil cake will flow together for a distance of 0.5 inch (13 mm) along the bottom of the groove separating the halves, when the bowl they are in is dropped 25 times for a distance of 0.4 inches (10 mm) at the rate of 2 drops/second. Tests shall be performed in accordance with ASTM D 4318 (AASHTO T 89).

3.5.3.2. Plastic Limit

The plastic limit is determined by ascertaining the lowest moisture content at which the material can be rolled into

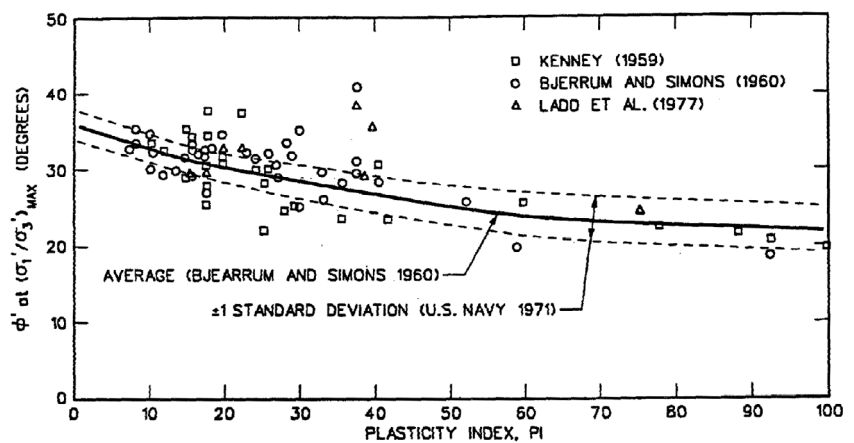


Figure 3-6: Empirical Correlation Between Friction Angle and Plasticity Index from Triaxial Tests on Normally Consolidated Clays

threads 0.125 inches (3.2 mm) in diameter without crumbling. Tests shall be performed in accordance with ASTM D 4318 (AASHTO T 90).

3.5.4. Specific Gravity of Soils

The specific gravity of soil, G_s , is defined as the ratio of the mass in air of a given volume of soil particles to the mass in air of an equal volume of gas free distilled water at a stated temperature (typically 68° F (20° C)). The specific gravity is determined by means of a calibrated pycnometer, by which the mass and temperature of a deaired soil/distilled water

sample is measured. Tests shall be performed in accordance with ASTM D 854 (AASHTO T 100). This method is used for soil samples composed of particles less than the No. 4 sieve (4.75 mm). For particles larger than this sieve, use the procedures for Specific Gravity and Absorption of Coarse Aggregate (ASTM C 127 or AASHTO T 85).

The specific gravity of soils is needed to relate a weight of soil to its volume, and it is used in the computations of other laboratory tests.

3.5.5. Strength Tests

The shear strength of a soil is the maximum shearing stress the soil structure can resist before failure. Soils generally derive their strength from friction between particles (expressed as the angle of internal friction, ϕ), or cohesion between particles (expressed as the cohesion, c in units of force/unit area), or both. These parameters are expressed in the form of total stress (c, ϕ) or effective stress (c, ϕ). The total stress on any subsurface element is produced by the overburden pressure plus any applied loads. The effective stress equals the total stress minus the pore water pressure.

The common methods of ascertaining these parameters in the laboratory are discussed below. All of these tests should be performed only on undisturbed samples.

3.5.5.1. Unconfined Compression Tests

While under no confining pressure, a cylindrical sample is subjected to an axial load until failure. This test is only performed on cohesive soils. Total stress parameters are obtained. The cohesion is taken as one-half the unconfined compressive strength, q_u . This test is a fast and economical means of approximating the shear strength at shallow depths, but the reliability is poor with increasing depth. Tests shall be performed in accordance with ASTM D 2166 (AASHTO T 208).

One common relationship that is used in connection with unconfined compressive strength is the " s_u/p " relationship, or the ratio of the unconfined compressive strength to the vertical effective stress at a given point (would be q_u/σ_3 in our notation.) A correlation with the overconsolidation ratio is shown in Figure 3-7.

3.5.5.2. Triaxial Compression Tests

In this test a cylindrical sample is subjected to an axial load until failure while also being subjected to confining pressure approximating the in-situ stress conditions. Various types of tests are possible with the triaxial apparatus as summarized below.

3.5.5.2.1. Unconsolidated-Undrained (UU), or Q Test

In this test the specimen is not permitted to change its initial water content before or during shear. The results are total

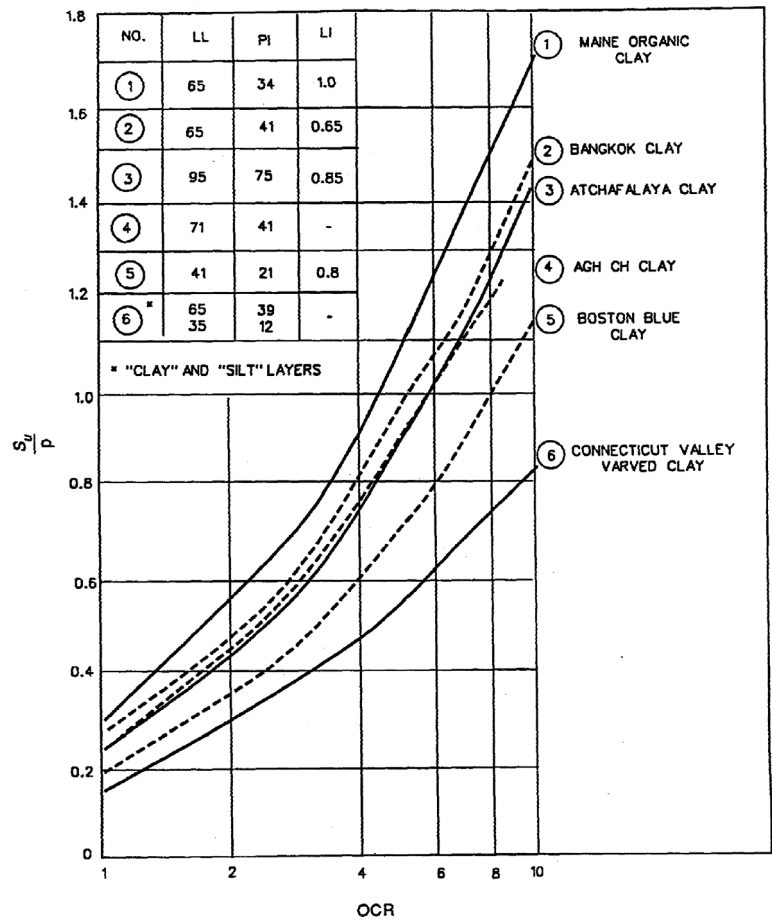


Figure 3-7: Undrained Strength Ratio versus Overconsolidation Ratio

stress parameters. This test is used primarily in the calculation of immediate embankment stability during quick-loading conditions. Refer to ASTM D 2850 (AASHTO T 296).

3.5.5.2.2. Consolidated-Undrained (CU), or R Test

In this test the specimen is allowed to consolidate under the confining pressure prior to shear, but no drainage is permitted during shear. A minimum of three tests at different confining pressures is required to derive the total stress parameters. If pore pressure measurements are taken during testing, the effective stress parameters can also be derived. Refer to ASTM D 4767 (AASHTO T 297).

3.5.5.2.3. Consolidated-Drained (CD), or S Test

This test is similar to the CU test (above) except that drainage is permitted during shear and the rate of shear is very slow. Thus, the build-up of excess pore pressure is prevented. As with the CU test, a minimum of three tests is required. Effective stress parameters are obtained. This test is used to determine parameters for calculating long-term stability of embankments.

3.5.5.3. Direct Shear

In this test a thin soil sample is placed in a shear box consisting of two parallel blocks and a normal force is applied. One block remains fixed while the other block is moved par-

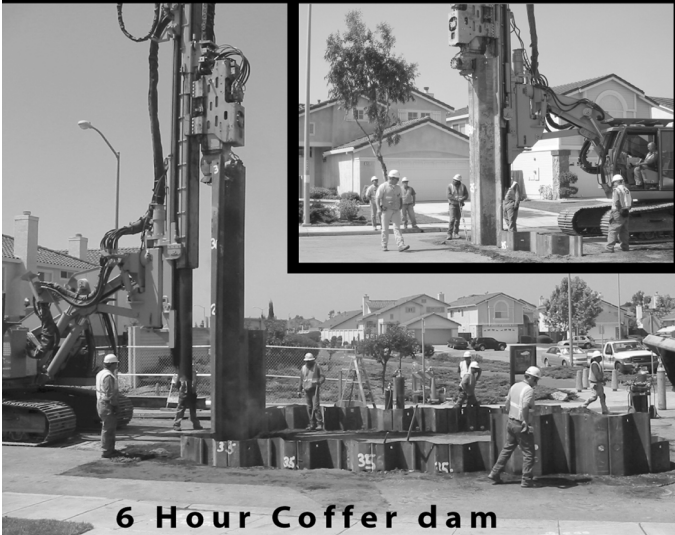
ABI'S VARIABLE MOMENT HAMMER



Does not vibrate on startup or shut down
 Can run in 10% increments of force
 Can push the pile with 40,000 lbs of crowd



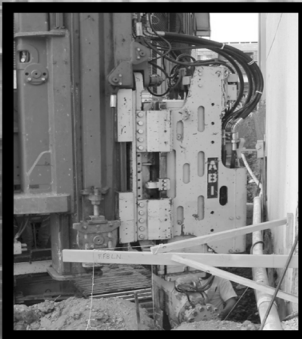
DO YOU DARE VIBRATE THIS CLOSE?



WE DO, ALL THE TIME!



ASK FOR OUR VIDEO



HAMMER & STEEL, INC
 (WEST COAST)
 TOLL FREE: 877-224-3356
 www.abi-delmag.com

CALL FOR SALES & RENTALS

HAMMER & STEEL, INC
 (MID-WEST & EAST COAST)
 TOLL FREE: 800-325-7453
 www.hammersteel.com

allel to it in a horizontal direction. The soil fails by shearing along a plane that is forced to be horizontal. A series of at least three tests with varying normal forces is required to define the shear strength parameters for a particular soil. This test is typically run as a consolidated-drained test on cohesionless materials. Tests shall be performed in accordance with ASTM D 3080 (AASHTO T 236).

3.5.5.4. Miniature Vane Shear (Torvane) and Pocket Penetrometer

These tests are used only as an index of the undrained shear strength (S_u) of clay samples and should not be used in place of a laboratory test program. Both tests consist of hand-held devices that are pushed into the sample and either a torque resistance (torvane) or a tip resistance (pocket penetrometer) is measured. They can be performed in the lab or in the field, typically on the ends of undisturbed thin-walled tube samples, as well as along the sides of test pits. Miniature vane shear tests shall be performed in accordance with ASTM D 4648.

3.5.6. Consolidation Test

When large loads such as embankments are applied to the surface, cohesive subsoils will consolidate, i.e., settle over time, through a combination of the rearrangement of the individual particles and the squeezing out of water. The amount and rate of settlement is of great importance in construction. For example, an embankment may settle until a gap exists between an approach and a bridge abutment. The calculation of settlement involves many factors, including the magnitude of the load, the effect of the load at the depth at which compressible soils exist, the water table, and characteristics of the soil itself. Consolidation testing is performed to ascertain the nature of these characteristics.

3.5.6.1. One-Dimensional Test

The most often used method of consolidation testing is the one-dimensional test. In this test, a specimen is placed in a consolidometer (oedometer) between two porous stones, which permit drainage. Specimen size can vary depending on the equipment used. Various loading procedures can be used during a one-dimensional test with incremental loading being the most common. With this procedure the specimen is subjected to increasing loads, usually beginning at approximately 1/8 ksf (5 kPa) and doubling each increment up to 32 ksf (1600 kPa). After each load application the change in sample height is monitored incrementally for, generally, 24 hours. To evaluate the recompression parameters of the sample, an unload/reload cycle can be performed during the loading schedule. To better evaluate the recompression parameters for over consolidated clays, the unload/reload cycle may be performed after the preconsolidation pressure has been defined. After the maximum loading has been reached, the loading is removed in decrements. Tests shall be performed in accordance with ASTM D 2435 (AASHTO T 216). The data from a

consolidation test is usually presented on an e-log p curve, which plots void ratio (e) as a function of the log of pressure (p), or an e-log p curve where e equals % strain. The parameters necessary for settlement calculation can be derived from these curves: compression index (C_c), recompression index (C_r), preconsolidation pressure (p_o or P_c) and initial void ratio (e_o). A separate plot is prepared of change in sample height versus log time for each load increment; from this, the coefficient of consolidation (c_v) and coefficient of secondary compression (C_{α}) can be derived. These parameters are used to predict the rate of primary settlement and amount of secondary compression.

3.5.6.2. Constant Rate of Strain Test

Other loading methods include the Constant Rate of Strain Test (ASTM D 4186) in which the sample is subjected to a constantly changing load while maintaining a constant rate of strain; and the single-increment test, sometimes used for organic soils, in which the sample is subjected only to the load expected in the field. A direct analogy is drawn between laboratory consolidation and field settlement amounts and rates.

3.5.7. Organic Content

Organic soils demonstrate very poor engineering characteristics, most notably low strength and high compressibility. In the field these soils can usually be identified by their dark colour, musty odour and low unit weight. The most used laboratory test for design purposes is the Ignition Loss test, which measures how much of a sample's mass burns off when placed in a muffle furnace. The results are presented as a percentage of the total sample mass. Tests shall be performed in accordance with ASTM D 2974 (AASHTO T 267).

3.5.8. Shrinkage and Swell

3.5.8.1. Shrinkage

These tests are performed to determine the limits of a soil's tendency to lose volume during decreases in moisture content. The shrinkage limit (SL) is defined as the maximum water content at which a reduction in water content will not cause a decrease in volume of the soil mass. Tests shall be performed in accordance with ASTM D 427 (AASHTO T 92).

3.5.8.2. Swell

Some soils, particularly those containing montmorillonite clay, tend to increase their volume when their moisture content increases. These soils are unsuitable for roadway construction. The swell potential can be estimated from the test methods shown in ASTM D 4546 (AASHTO T 258).

3.5.9. Permeability

The laboratory determination of soil permeability can be performed by one of the following test methods. Permeability can also be determined either directly or indirectly from a consolidation test.

3.5.9.1. Constant-Head Test

This test uses a permeameter into which the sample is placed and compacted to the desired relative density. Water (preferably de-aired) is introduced via an inlet valve until the sample is saturated. Water is then allowed to flow through the sample while a constant head is maintained. The permeability is measured by the quantity of flow of discharge over a specified time. This method is generally used only with coarse-grained soils. Tests shall be performed in accordance with ASTM D 2434 (AASHTO T 215).

3.5.9.2. Falling-Head Test

This test uses an apparatus and procedure similar to the constant-head test (above), but the head is not kept constant. The permeability is measured by the decrease in head over a specified time. This method is generally used for fine-grained soils. Tests shall be performed in accordance with FM 5-513.

3.5.9.3. Flexible Wall Permeability

For fine-grained soils, tests performed using a triaxial cell are generally preferred. In-situ conditions can be modelled by application of an appropriate confining pressure. The sample can be saturated using back pressuring techniques. Water is then allowed to flow through the sample and measurements are taken until steady-state conditions occur. Tests shall be performed in accordance with ASTM D 5084.

3.5.10. Environmental Corrosion Tests

These tests are performed to determine the corrosion classification of soil and water. A series of tests includes pH, resistivity, chloride content, and sulphate content testing. The testing can be done either in the laboratory or in the field.

3.5.11. Compaction Tests

These tests are used to determine the optimum water content and maximum dry density, which can be achieved for a particular soil using a designated compactive effort. Results are used to determine appropriate methods of field compaction and to provide a standard by which to judge the acceptability of field compaction. Compacting a sample in a test mould of known volume using a specified compactive effort performs the test. The water content and the weight of the sample required to fill the mould are determined. Results are plotted as density versus water content. By varying the water content of the sample, several points on the moisture-density curve shall be obtained in accordance with the standard procedures specified.

The compactive effort used is dependent upon the proposed purpose of the site and the loading to which it will be subjected. The most commonly used laboratory test compactive efforts are described below.

3.5.11.1. Standard Proctor

This test method uses a 5.5-pound (2.5 kg) rammer dropped from a height of 12 inches (305 mm). The sample is compacted in three layers. Tests shall be performed in accordance with ASTM D 698 (AASHTO T 99).

3.5.11.2. Modified Proctor

This test method uses a 10-pound (4.54 kg) rammer dropped from a height of 18 inches (457 mm). The sample is compacted in five layers. Tests shall be performed in accordance with ASTM D 1557 (AASHTO T 180).

3.5.12. Relative Density Tests

Proctor tests often do not produce a well-defined moisture-density curve for cohesionless, free-draining soils. Additionally, maximum densities from Proctor tests may be less than those obtained in the field or by vibratory methods. For these soils, it may be preferable to perform tests, which determine standard maximum and minimum densities of the soil. The density of the in-situ soil can then be compared with these maximum and minimum densities and its relative density and/or percent compaction can be calculated.

3.5.12.1. Maximum Index Density

This test requires that either oven-dried or wet soil be placed in a mould of known volume, and that a 2-psi (14 kPa) surcharge load is applied. The mould is then vertically vibrated at a specified frequency for a specified time. The weight and volume of the sample after vibrating are used to calculate the maximum index density. Tests shall be performed in accordance with ASTM D 4253.

3.5.12.2. Minimum Index Density

This test is performed to establish the loosest condition, which can be attained by standard laboratory procedures. Several methods can be used, but the preferred method is to carefully pour a steady stream of oven-dried soil into a mould of known volume through a funnel. Funnel height should be adjusted continuously to maintain a free fall of the soil of approximately 0.5 inches (13 mm). Tests shall be performed in accordance with ASTM D 4254.

3.5.13. Resilient Modulus Test (Dynamic)

This test is used to determine the dynamic elastic modulus of a base or subgrade soil under conditions that represent a reasonable simulation of the physical conditions and stress states of such materials under flexible pavements subjected to wheel loads. A prepared cylindrical sample is placed in a triaxial chamber and conditioned under static or dynamic stresses. A repeated axial stress is then applied at a fixed magnitude, duration, and frequency. The resilient modulus, M_r , is calculated by dividing the deviator stress by the resilient axial strain. This value is used in the design and evaluation of pavement systems. Tests shall be performed in accordance with AASHTO T 294.

3.6. Field Exploration, Testing, and Instrumentation

Subsurface investigations are essential for the successful geotechnical construction project. Because of the varying complexity of projects and soil conditions, it is impossible to establish a rigid format to be followed in conducting subsur-

face investigations; however, there are basic steps that should be considered for any project. By outlining and describing these steps, it will be possible to standardize procedures and considerably reduce time and expense often required to go back and obtain information not supplied by the initial investigation.

3.6.1. Review of Project Requirements

The first step in performing a subsurface investigation is a thorough review of the project requirements. It is necessary that the information available to the geotechnical engineer include the project location, alignment, structure locations, structure loads, approximate bridge span lengths and pier locations, and cut and fill area locations. The geotechnical engineer should have access to typical section, plan and profile sheets, and cross sections with a template for the proposed roadway showing cuts and fills. This information aids the geotechnical engineer in planning the investigation and minimizes expensive and time-consuming backtracking.

3.6.2. Office Review of Available Data

Following review of the existing data, the geotechnical engineer should visit the project site. After gaining a thorough understanding of the project requirements, the geotechnical engineer should collect all relevant available information on the project site. Review of this information can aid the engineer in understanding the geology, geography and topography of the area and assist him in laying out the field explorations and locating potential problems. Existing data may be available from the following sources:

3.6.2.1. Topographic Maps

These maps are prepared by the U.S. Geological Survey (USGS) and the U.S. Coast and Geodetic Survey (USCGS) and are readily available. They are sometimes also prepared on a larger scale by the Department during early planning phases of a project. These maps portray physical features, configuration and elevation of the ground surface, and surface water features. This data is valuable in determining accessibility for field equipment and possible problem areas.

3.6.2.2. Aerial Photographs

They are valuable in that they can provide the basis for reconnaissance and, depending on the age of the photographs, show manmade structures, excavations, or fills that affect accessibility and the planned depth of exploration. Historical photographs can also help determine the reasons and/or potential of general scour and sinkhole activity.

3.6.2.3. Geological Maps and Reports

Considerable information on the geological conditions of an area can often be obtained from geological maps and reports. These reports and maps often show the location and relative position of the different geological strata and present information on the characteristics of the different strata. This

data can be used directly to evaluate the rock conditions to be expected and indirectly to estimate possible soil conditions since the parent material is one of the factors controlling soil types. Geological maps and reports can be obtained from the USGS, state geological surveys, university libraries, and other sources.

3.6.2.4. Soils Conservation Service Surveys

These surveys are compiled by the U.S. Department of Agriculture usually in the form of county soils maps. These surveys can provide valuable data on surface soils including mineralogical composition, grain size distribution, and the depth to rock, water table information, drainage characteristics, geologic origin, and the presence of organic deposits.

3.6.2.5. Potentiometric Surface Map

The potentiometric surface elevation shown on the map can supplement and be correlated with what was found in the field by the drillers.

3.6.2.6. Adjacent Projects

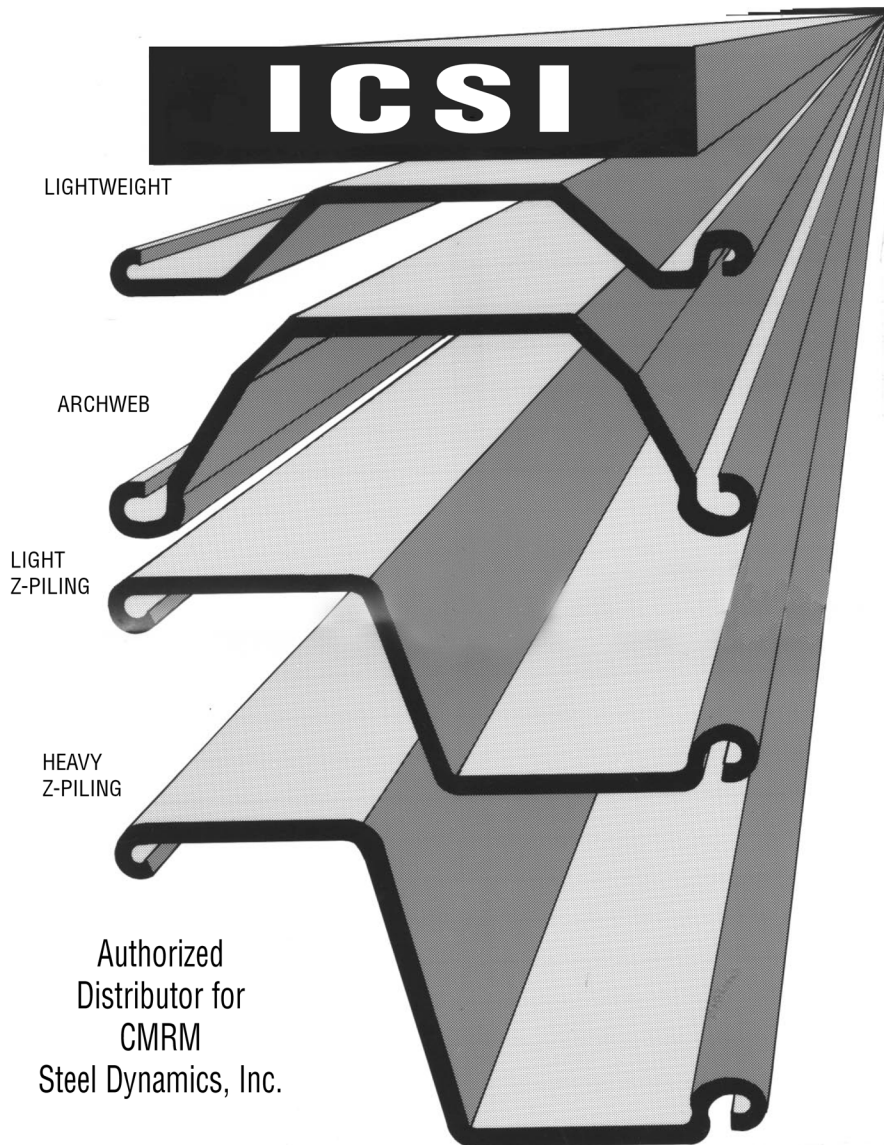
Data may be available on nearby projects. This data is extremely useful in setting preliminary boring locations and depths and in predicting problem areas. Maintenance records for existing nearby roadways and structures may provide additional insight into the subsurface conditions. For example, indications of differential settlement or slope stability problems may provide the engineer with valuable information on the long-term characteristics of the site.

3.6.3. Field Reconnaissance

Site visitation is vital to enable the engineer to gain first-hand knowledge of field conditions and correlate this information with previous data. In particular, the following should be noted during the field reconnaissance:

- Nearby structures should be inspected to ascertain their foundation performance and potential to damage from vibration or settlement from foundation installation.
- Also, the structure's usages must be looked at to check the impact the foundation installation may have (i.e. a surgical unit, printing company, etc.).
- On water crossings, banks should be inspected for scour and the streambed inspected for evidence of soil deposits not previously indicated.
- Note any feature that may affect the boring program, such as accessibility, structures, overhead utilities, signs of buried utilities, or property restrictions.
- Note any feature that may assist in the engineering analysis, such as the angle of any existing slopes and the stability of any open excavations or trenches.
- Any drainage features, including signs of seasonal water tables.
- Any features that may need additional borings or probing such as muck pockets.

INTERNATIONAL CONSTRUCTION SERVICES, INC.



**We have
PZ-22,
PZ-27,
PZ-35
and
PZ-40
Equivalents!!**

**NEW AND USED
FOR SALE
FOR RENT**

ALSO
Lightweight Piling
Waterloo Sheet Piling
H-bearing Pile
Structural Sections
Piling Accessories
Coatings

Authorized
Distributor for
CMRM
Steel Dynamics, Inc.

Call Now!

**International Construction Services, Inc.
Corporate Headquarters**

P.O. Box 15598

Pittsburgh, PA 15244-0598

Ph: (888) 593-1600 or (412) 788-6430

Fax: (412) 788-9180 • E-mail: icsi@nb.net

**New York Area
888-593-1600**

**Chicago, IL
815-609-9527**

**Sacramento, CA
916-989-6720**

3.6.4. Soil Borings and Test Pits

3.6.4.1. Soil Borings

Soil borings are probably the most common method of subsurface exploration in the field.

3.6.4.1.1. Auger Borings

Rotating an auger while simultaneously advancing it into the ground either hydraulically or mechanically advances auger borings. The auger is advanced to the desired depth and then withdrawn. Samples of cuttings can be removed from the auger; however, the depth of the sample can only be approximated. These samples are disturbed and should be used only for material identification. This method is used to establish soil strata and water table elevations, or to advance to the desired stratum before Standard Penetration Testing (SPT) or undisturbed sampling is performed. However, it cannot be used effectively in soft or loose soils below the water table without casing or drilling mud to hold the hole open. See ASTM D 1452 (AASHTO T 203).

3.6.4.1.2. Hollow-Stem Auger Borings

A hollow-stem auger consists of a continuous flight auger surrounding a hollow drill stem. The hollow-stem auger is advanced similar to other augers; however, removal of the hollow stem auger is not necessary for sampling. SPT and undisturbed samples are obtained through the hollow drill stem, which acts like a casing to hold the hole open. This increases usage of hollow-stem augers in soft and loose soils. See ASTM D 6151 (AASHTO T 251).

3.6.4.1.3. Wash Borings

In this method, the boring is advanced by a combination of the chopping action of a light bit and the jetting action of water flowing through the bit. This method of advancing the borehole is used only when precise soil information is not required between sample intervals.

3.6.4.1.4. Percussion Drilling

In this method, the drill bit advances by power chopping with a limited amount of water in the borehole. Slurry must be periodically removed. The method is not recommended for general exploration because of the difficulty in determining stratum changes and in obtaining undisturbed samples. However, it is useful in penetrating materials not easily penetrated by other methods, such as those containing boulders.

3.6.4.1.5. Rotary Drilling

A downward pressure applied during rapid rotation advances hollow drill rods with a cutting bit attached to the bottom. The drill bit cuts the material and drilling fluid washes the cuttings from the borehole. This is, in most cases, the fastest method of advancing the borehole and can be used in any type of soil except those containing considerable amounts of large gravel or boulders. Drilling mud or casing can be used to keep the borehole open in soft or loose soils, although the former makes identifying strata change by examining the cuttings difficult.

3.6.4.2. Test Pits

These are the simplest methods of inspecting subsurface soils. Test pits are used to examine and sample soils *in situ*, to determine the depth to groundwater, and to determine the thickness of topsoil. They consist of excavations performed by hand, backhoe, or dozer, and range from shallow manual or machine excavations to deep, sheeted, and braced pits. Hand excavations are often performed with posthole diggers or hand augers. They offer the advantages of speed and ready access for sampling. They are severely hampered by limitations of depth and by the fact they cannot be used in soft or loose soils or below the water table. Hand-cut samples are frequently necessary for highly sensitive, cohesive soils, brittle and weathered rock, and soil formation with honeycomb structure.

3.6.4.3. Test Trenches

Test trenches are particularly useful for exploration in very heterogeneous deposits such as rubble fills, where borings are either meaningless or not feasible. They are also useful for detection of fault traces in seismicity investigations.

3.6.5. Sampling

3.6.5.1. Disturbed and Undisturbed Sampling

Disturbed samples are primarily used for classification tests and must contain all of the constituents of the soil even though the structure is disturbed.

Undisturbed samples are taken primarily for laboratory strength and compressibility tests and in those cases where the in-place properties of the soil must be studied.

3.6.5.2. Types of Soil Sampling

Common methods of sampling during field explorations include those listed below. All samples should be properly preserved and carefully transported to the laboratory such that sample integrity is maintained. See ASTM D 4220.

3.6.5.2.1. Bag Bulk Samples

These are disturbed samples obtained from auger cuttings or test pits. The quantity of the sample depends on the type of testing to be performed, but can range up to 50 lb (25 kg) or more. Testing performed on these samples includes classification, moisture-density, Limerock Bearing Ratio (LBR), and corrosivity tests. A portion of each sample should be placed in a sealed container for moisture content determination.

3.6.5.2.2. Split-Barrel

Also known as a split-spoon sample, this method is used in conjunction with the Standard Penetration Test. The sampler is a 2" (50.8 mm) (O.D.) split barrel that is driven into the soil with a 140-pound (63.5 kg) hammer dropped 30 inches (760 mm). After it has been driven 18 inches (450 mm), it is withdrawn and the sample removed. The sample should be immediately examined, logged and placed in sample jar for storage. These are disturbed samples and are not suitable for strength or consolidation testing. They are adequate for mois-

ture content, gradation, and Atterberg Limits tests, and valuable for visual identification. See ASTM D 1586.

3.6.5.2.3. *Shelby Tube*

This is thin-walled steel tube, usually 3 inches (76.2 mm) (O.D.) by 30 inches (910 mm) in length. It is pushed into the soil with a relatively rapid, smooth stroke and then retracted. This produces a relatively undisturbed sample provided the Shelby tube ends are sealed immediately upon withdrawal. Refer to ASTM D 1587 (AASHTO T 207). This sample is suitable for strength and consolidation tests. This sampling method is unsuitable for hard materials. Good samples must have sufficient cohesion to remain in the tube during withdrawal. Refer to ASTM D 1587 (AASHTO T 207).

3.6.5.2.4. *Piston Samplers*

3.6.5.2.4.1. *Stationary*

This sampler has the same standard dimensions as the Shelby Tube, above. A piston is positioned at the bottom of the thin-wall tube while the sampler is lowered to the bottom of the hole, thus preventing disturbed materials from entering the tube. The piston is locked in place on top of the soil to be sampled. A sample is obtained by pressing the tube into the soil with a continuous, steady thrust. The stationary piston is held fixed on top of the soil while the sampling tube is advanced. This creates suction while the sampling tube is retrieved thus aiding in retention of the sample. This sampler is suitable for soft to firm clays and silts. Samples are generally less disturbed and have a better recovery ratio than those from the Shelby Tube method.

3.6.5.2.4.2. *Floating*

This sampler is similar to the stationary method above, except that the piston is not fixed in position but is free to ride on the top of the sample. The soils being sampled must have adequate strength to cause the piston to remain at a fixed depth as the sampling tube is pushed downward. If the soil is too weak, the piston will tend to move downward with the tube and a sample will not be obtained. This method should therefore be limited to stiff or hard cohesive materials.

3.6.5.2.4.3. *Retractable*

This sampler is similar to the stationary sampler, however, after lowering the sampler into position the piston is retracted and locked in place at the top of the sampling tube. A sample is then obtained by pushing the entire assembly downward. This sampler is used for loose or soft soils.

3.6.5.2.4.4. *Hydraulic (Osterberg)*

In this sampler, a movable piston is attached to the top of a thin-wall tube. Sampling is accomplished as hydraulic pressure pushes the movable piston downward until it contacts a stationary piston positioned at the top of the soil sample. The distance over which the sampler is pushed is fixed; it cannot be over-pushed. This sampler is used for very soft to firm cohesive soils.

3.6.6. *Penetration Resistance Tests*

The most common test is the Standard Penetration Test (SPT), which measures resistance to the penetration of a standard sampler in borings. The method is rapid, and when tests are properly conducted in the field, they yield useful data, although there are many factors that can affect the results. A more controlled test is the cone penetrometer test in which a cone shaped tip is jacked from the surface of the ground to provide a continuous resistance record.

3.6.6.1. *Standard Penetration Test (SPT)*

This test is probably the most widely used field test in the United States. It has the advantages of simplicity, the availability of a wide variety of correlations for its data, and the fact that a sample is obtainable with each test.

3.6.6.1.1. *Procedure*

- The test is covered under ASTM Standard D1586, which requires the use of a standard 2" (O.D.) split barrel sampler, driven by a 140-pound (63.6 kg) hammer dropping 30" (760 mm) in free fall. The procedure is generalized as follows:
- Clean the boring of all loose material, and material disturbed by drilling.
- Insert sampler, verifying the sampler reaches the same depth as was drilled.
- Obtain a consistent 30" free-fall drop of the hammer with two wraps of a rope around the cathead on the drill rig. (Cables attached to the hoisting drum should not be used because it is difficult to obtain free fall.)
- The sampler is advanced a total of 18 inches (450 mm).
- The number of blows required to advance the sampler for each of three 6" (150 mm) increments is recorded. The sum of the number of blows for the second and third increments is called the Standard Penetration Value, or more commonly, N-value (blows per foot {300 mm}).

The SPT values should not be used indiscriminately. They are sensitive to the fluctuations in individual drilling practices and equipment. Studies have also indicated that the results are more reliable in sands than clays. Although extensive use of this test in subsurface exploration is recommended, it should always be augmented by other field and laboratory tests, particularly when dealing with clays. The type of hammer (safety or automatic) shall be noted on the boring logs, since this will affect the actual input driving energy.

A method to measure the energy during the SPT has been developed (ASTM D 4633). Since there is a wide variability of performance in SPT hammers, this method is useful to evaluate an individual hammer's performance. The SPT installation procedure is similar to pile driving because it is governed by stress wave propagation. As a result, if force and velocity measurements are obtained during a test, the energy transmitted can be determined.

3.6.6.2. *Corrections*

SPT values should be corrected for at least two factors: the

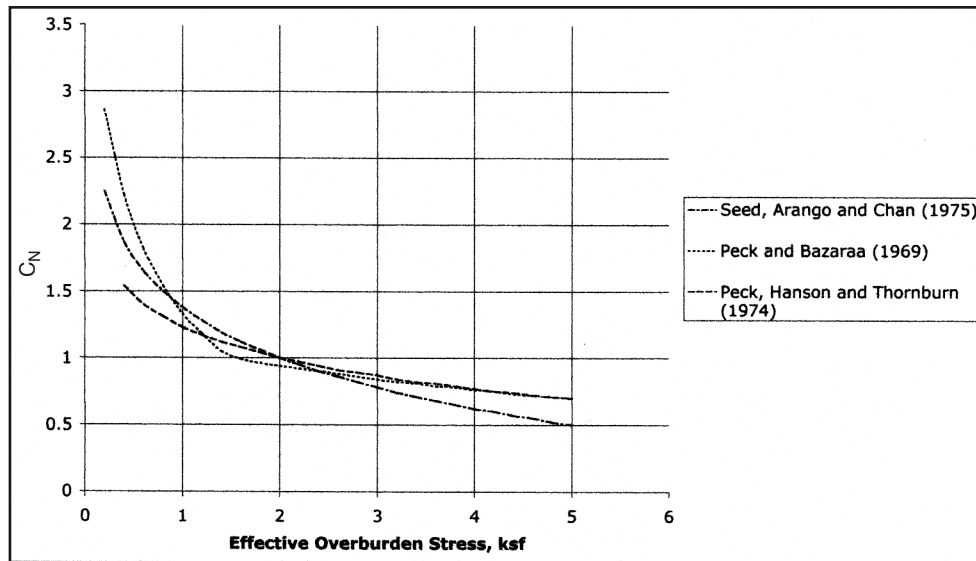


Figure 3-8: Correlation Between C_N and Effective Overburden Pressure

overburden pressure and the efficiency of the hammer.

Figure 3-8 shows the correction factor C_N , which is function of the effective overburden stress. Using this correction results in a value of N that would have been measured if the effective overburden stress had been 2 ksf.

Turning to hammer efficiency, prior to 1980, this was not well recognized as influencing the blow count and was usually not considered in analysis. Historically, SPT tests in the U.S. have been performed with machines with a mechanical efficiency of around 60%. Other types of testing equipment

(especially the newer automatic hammers) have different efficiencies. Table 3-5 shows hammer efficiencies for various types of hammers.

The corrected SPT blow count can be computed by the equation

$$\text{Equation 3-1: } N_{60} = C_N N \frac{e_{\text{hammer}}}{60}$$

Where

- N_{60} = corrected N value for overburden and efficiency, blows/foot

Table 3-5 Hammer Efficiencies for Various Types and Origins of SPT Hammers

Country	Type of Ram	Type of Ram Lifting and Release Mechanism	Efficiency e_{hammers} Percent
Japan	Donut	Free-fall	78
	Donut	Rope & Pulley with special release	67
U.S.A.	Safety	Rope & Pulley	60
	Donut	Rope & Pulley	45
	Automatic	Automatic hoisting mechanism	90
Argentina	Donut	Rope & Pulley	45
China	Donut	Free-fall	60
	Donut	Rope and Pulley	50

- C_N = correction factor for overburden pressure
- e_{hammer} = efficiency of the SPT hammer used, percent
- N = SPT blow count obtained in the field

3.6.6.3. Correlations

Because the Standard Penetration Test is relatively simple to run, it has given rise to many correlations with many different soil properties. These are especially useful in situations where undisturbed samples are unavailable, which is frequently the case with deep foundations. Some of these correlations are discussed below.

3.6.6.3.1. Compactness and Consistency

Table 3-6 shows the basic relationship of SPT results results with compactness for granular soils and consistency for cohesive soils. Although this type of table is usual for rough estimates of soil properties, when possible more accurate correlations should be used; some of these are shown in the following sections.

3.6.6.3.2. Relative Density of Granular (but fine grained) Deposits

If the test is a true standard test, the “ N ” value is influenced



**Test the latest
in Pile Driving
Technology!**

**Immediate
Availability for
Rent, Lease or
Sale!**

**BAUER Equipment USA
205 Wilcox
McKinney, TX 75069**

**Contact: Mr. Robert Kaindl
Toll Free: 1-866-DRILL RIG
Phone: 1-972-540 6361
Fax: 1-972-540 1411
E-Mail: BMABranchUSA@aol.com
Homepage: www.bauer.de**



**Leader in
Advanced Foundation Technology**

Table 3-6: Relative Density or Consistency of Soils as a Function of SPT N Values

Nomenclature	Relative Density, Percent	Internal Friction Angle ϕ, degrees	Moist Unit Weight, pcf	Safety Hammer SPT N_{60} Value (Blow/Foot {300 mm})
Cohesionless Soils				
Very Loose	0-15%	< 28	<100	Less than 4
Loose	15-35%	28-30	95-125	4 – 10
Medium Dense	35-65%	30-36	110-130	10 – 30
Dense	65-85%	36-41	110-140	30 – 50
Very Dense	85-100%	> 41	> 130	> 50
Nomenclature	Hand Manipulation Characteristics	Estimated Unconfined Compression Strength q_u, ksf	Moist Unit Weight, pcf	Safety Hammer SPT N_{60} Value (Blow/Foot {300 mm})
Cohesionless Soils				
Very Soft	<i>Extruded between fingers when squeezed</i>	< 0.50	100-120	< 2
Soft	<i>Moulded by light finger pressure</i>	0.5 - 1	100-120	2 – 4
Firm or Medium	<i>Moulded by strong finger pressure</i>	1 - 2	110-130	4 – 8
Stiff	<i>Readily indented by thumb but penetrated with great effort</i>	2 - 4	120-140	8 – 15
Very Stiff	<i>Readily indented by thumbnail</i>	4 - 8	120-140	15 – 30
Hard	<i>Indented with difficulty by thumbnail</i>	> 8	> 130	> 30

by the effective vertical stress at the level where “N” is measured, density of the soil, stress history, gradation and other factors.¹⁹ The Gibbs & Holtz correlation of Figure 3-9 is commonly used to estimate the relative density from SPT.

3.6.6.3.3. Undrained Shear Strength

A crude estimate for the undrained shear strength can be made using Figure 3-10. Correlations are not meaningful for medium to soft clays where effects of disturbance are excessive.

3.6.6.3.4. Drained Friction Angle ϕ'

The drained friction angle ϕ' can be estimated from N'

using Figure 3-11. This is used mostly with retaining walls where the drained friction angle is significant for long-term behaviour of the wall.

3.6.6.4. Cone Penetrometer Test (CPT)

3.6.6.4.1. Test Description

The Cone Penetrometer Test is a quasi-static penetration test in which a cylindrical rod with a conical point is advanced through the soil at a constant rate and the resistance to penetration is measured. A series of tests performed at varying depths at one location is commonly called a sounding.

Several types of penetrometers are in use, including

¹⁹ Marcuson, W.F. III, and Bieganouski, W.A., SPT and Relative Density in Coarse Sands, Journal of geotechnical engineering Division, ASCE, Vol. 103, No. GT 11, 1977.

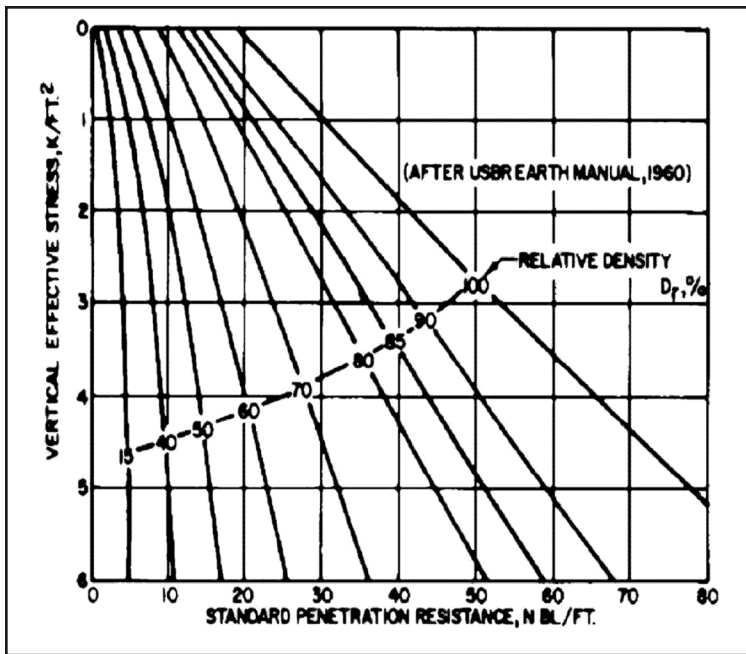


Figure 3-9: Correlations between Relative Density and Standard Penetration Resistance in Accordance with Gibbs and Holtz²⁰

Figure 3-10: Correlations of Standard Penetration Resistance with Unconfined Strength of Clay

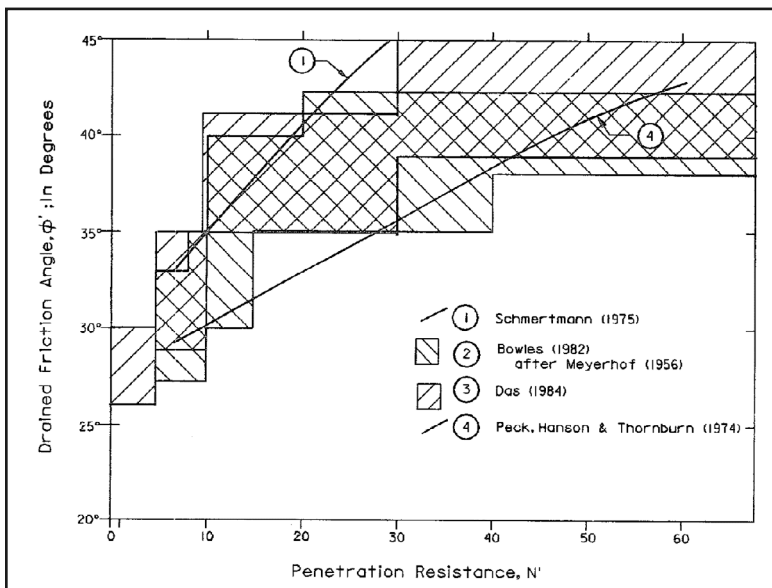
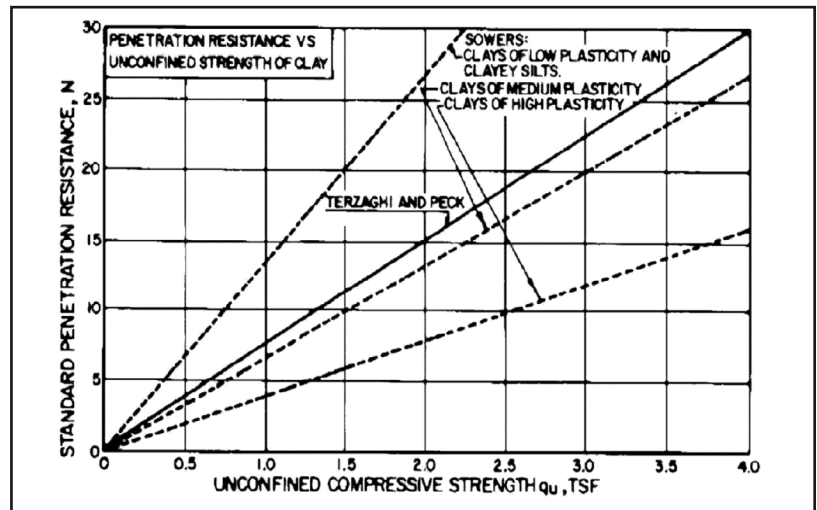


Figure 3-11 ϕ' vs. N' for Granular Materials

²⁰ Lacroix, Y. and Horn, H.M., Direct Determination and Indirect Evaluation of Relative Density and Earthwork Construction Projects, ASTM STP 523, 1973.

mechanical (mantle) cone, mechanical friction-cone, electric cone, electric friction-cone, and piezocone penetrometers. Cone penetrometers measure the resistance to penetration at the tip of the penetrometer, or the end-bearing component of resistance. Friction-cone penetrometers are equipped with a friction sleeve, which provides the added capability of measuring the side friction component of resistance. Mechanical penetrometers have telescoping tips allowing measurements to be taken incrementally, generally at intervals of 8 inches (200 mm) or less. Electric (or electronic) penetrometers use electric force transducers to obtain continuous measurements with depth. Piezocone penetrometers are electric penetrometers, which are also capable of measuring pore water pressures during penetration.

For all types of penetrometers, cone dimensions of a 60-degree tip angle and a 1.55 in² (10 cm²) projected end area are standard. Friction sleeve outside diameter is the same as the base of the cone. Penetration rates should be between 0.4 to 0.8 in/sec (10 to 20 mm/sec). Tests shall be performed in

accordance with ASTM D 3441 (which includes mechanical cones) and ASTM D 5778 (which includes piezocones).

The penetrometer data is plotted showing the end-bearing resistance, the friction resistance and the friction ratio (friction resistance divided by end bearing resistance) as functions of depth. Pore pressures, if measured, can also be plotted with depth. The results should also be presented in tabular form indicating the interpreted results of the raw data. A sample log is shown in Figure 3-12.²¹

The friction ratio plot can be analysed to determine soil type. Many correlations of the cone test results to other soil parameters have been made, and design methods are available for spread footings and piles. The penetrometer can be used in sands or clays, but not in rock or other extremely dense soils. Generally, soil samples are not obtained with soundings, so penetrometer exploration should always be augmented by SPT borings or other borings with soil samples taken.

The piezocone penetrometer can also be used to measure

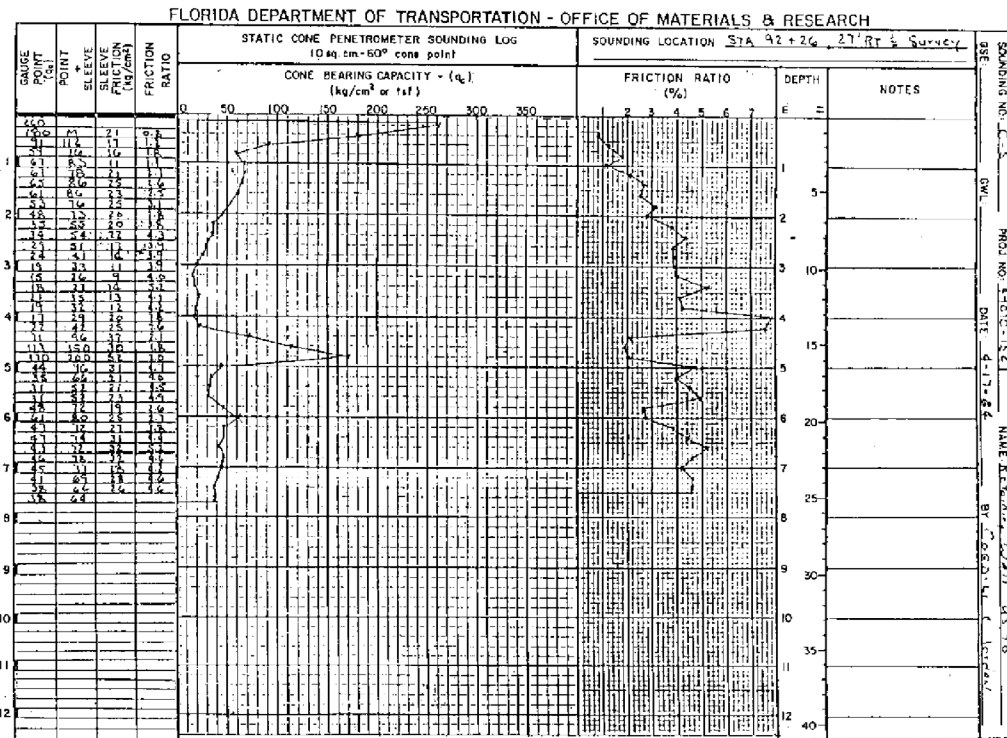


Figure 3-12: Typical Log from Mechanical Friction-Cone

the dissipation rate of the excessive pore water pressure. This type of test is useful for subsoils, such as fibrous peat or muck that are very sensitive to sampling techniques. The cone should be equipped with a pressure transducer that is capable of measuring the induced water pressure. To perform this test, the cone will be advanced into the subsoil at a standard rate of 0.8 inch/sec (20 mm/sec). Pore water pressures will be measured immediately and at several time intervals thereafter.

Use the recorded data to plot a pore pressure versus log-time graph. Using this graph one can directly calculate the pore water pressure dissipation rate or rate of settlement of the soil.

3.6.6.4.2. Correlations

The ratio (q_c/N) is typically in the range of 2 to 6 and is related to median grain size (see Figure 3-13). If static cone

²¹ The log for a standard cone penetration test would only include the first three plots: tip resistance, local friction, and friction ratio.

American Construction Material Exchange, Inc.

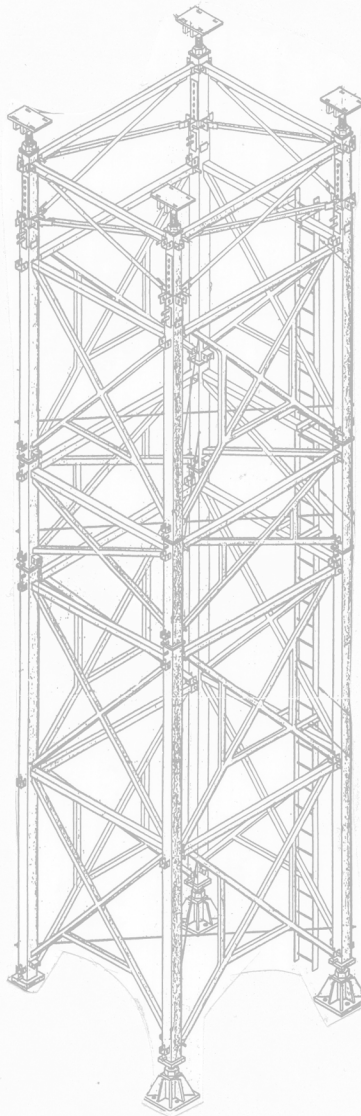
USED PIPE

10-3/4" O.D. X .250
 12.75" O.D. X .312
 14" O.D. X .500
 18" O.D. X .375
 18" O.D. X .500
 22.75 O.D. X .375
 24" O.D. X .375
 24" O.D. X .500
 36" O.D. X .750 NEW
 42" O.D. X 1.000 NEW

USED/SURPLUS STEEL BEAMS

W40x149#
 W36x300#, W36x260#, W36x245#
 W36x230#, W36x210#, W36x194#
 W36x182#, W36x170#, W36x160#
 W36x150#, W36x135#
 W33x291#, W33x241#, W33x221#
 W33x201#
 W30x211#, W30x191#, W30x173#, 116#
 W27x94#, W27x84#
 W24x146#, W24x131#, W24x117#
 W24x104#, W24x94#
 W21x122#, W21x111#, W21x101#
 W18x119#, W18x97#, W18x96#
 W18x86#, W18x76#, W18x55#
 W16x100#, W16x89#, W16x57#
 W14x159#, W14x145#, W14x132#, W14x120#
 W14x109#, W14x99#, W14x90#, W14x82#
 W14x74#, W14x68#, W14x61#
 W12x120#, W12x79#, W12x72#, W12x65#
 W12x53#, W12x45#, W12x35#, W12x26#
 W10x112#, W10x100#, W10x68#, W10x49#,
 W8x48#, W8x40#

MOST STOCK LOCATED ON THE WEST COAST



WANTED:

We are looking for:
**Used Flat Sheet Piles
 & AZ18 Sheets**

USED MISC. AVAILABLE

HP12x53#, HP12x74#,
 HP12x84#, HP14x89#
 HP14x102#, HP14x117#
 STEEL PLATES
 CHANNELS - 8", 12" & 15"
 18" DOUBLE CHANNELS
 CREOSOTE TIMBERS
 180 Pcs. 14"x14'x23'-28'
 120 Pcs. 8"x24'x30'

SHORE TOWER SYSTEM

100 KIP PER LEG
 LARGE QUANTITY AVAILABLE
 WILL RENT OR SELL

NEW, PRIME W/MTR'S

W14 x 90, W14 x 109
 W14 x 120
 HP14x89#

E-Mail Address: rogerkadel@comcast.net

"ACME" P.O. Box 2600 TUALATIN, OR. 97062

PHONE: (503) 590-5100 FAX: (503) 590-5200 MOBILE: (503) 705-1190

penetration resistance q_c and N values are measured during the field exploration, an actual q_c - N correlation could be made.

The undrained strength of fine-grained soils may be estimated by using a modification of bearing capacity theory:

$$\text{Equation 3-2: } q_u = \frac{q_c - p_o}{N_k}$$

Where

- q_c = unit point resistance of cone penetrometer
- p_o = the in situ total overburden pressure
- N_k = empirical cone factor typically in the range of 10 to 20. The N_k value should be based on local experience and correlation to laboratory tests.

Cone penetration tests also may be used to infer soil classification to supplement physical sampling. Figure 3-14 indicates probable soil type as a function of cone resistance and friction ratio. Cone penetration tests may produce erratic results in gravelly soils.

3.6.6.5. Dynamic Cone Penetrometer Test

This test is similar to the cone penetrometer test except, instead of being pushed at a constant rate, the cone is driven into the soil. The number of blows required to advance the cone in 6" (150 mm) increments is recorded. A single test generally consists of two increments. Tests can be performed continuously to the depth desired with an expendable cone, which is left in the ground upon drill rod withdrawal, or they can be performed at specified intervals by using a retractable cone and advancing the hole by auger or other means between tests. Samples are not obtained.

Blow counts can generally be used to identify material type and relative density. In granular soils, blow counts from the second 6" (150 mm) increment tend to be larger than for the first increment. In cohesive soils, the blow counts from the two increments tend to be about the same. While correlations between blow counts and engineering properties of the soil exist, they are not as widely accepted as those for the SPT.

3.6.6.6. Dilatometer Test (DMT)

The dilatometer is a 3.75" (95 mm) wide and 0.55" (14 mm) thick stainless steel blade with a thin 2.4" (60 mm) diameter expandable metal membrane on one side. While the membrane is flush with the blade surface, the blade is either pushed or driven into the soil using a penetrometer or drilling rig. Rods carry pneumatic and electrical lines from the membrane to the surface. At depth intervals of 8 inch (200 mm), the pressurized gas expands the membrane and both the pressure required to begin membrane movement and that required to expand the membrane into the soil 0.04 inches (1.1 mm) are measured.

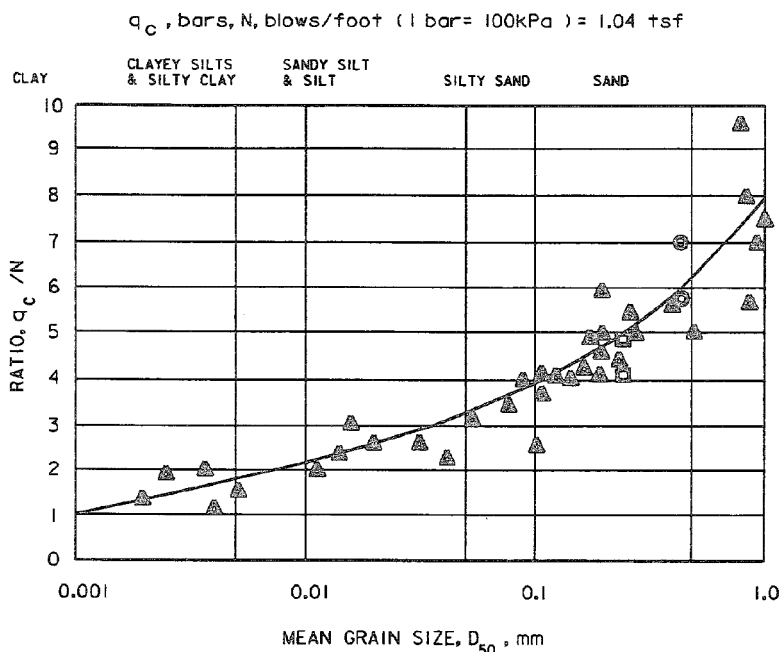


Figure 3-13: q_c/N versus D_{50} ²²

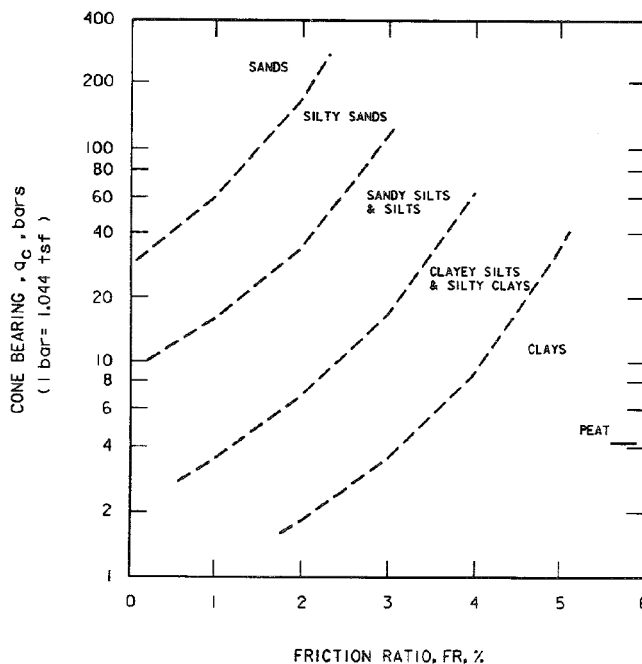


Figure 3-14: Soil classification from cone penetrometer

Additionally, upon venting the pressure corresponding to the return of the membrane to its original position may be recorded (see Figure 3-15, Figure 3-16 and Figure 3-17).

Through developed correlations, information can be deduced concerning material type, pore water pressure, in-situ horizontal and vertical stresses, void ratio or relative density, modulus, shear strength parameters, and consolidation parameters. Compared to the pressuremeter, the flat

²²Robertson, P. K., and Campanella, R. G. 1983. "Interpretation of Cone Penetration Tests; Parts I and II," Canadian Geotechnical Journal, Vol 20, No. 4, pp 718-745.

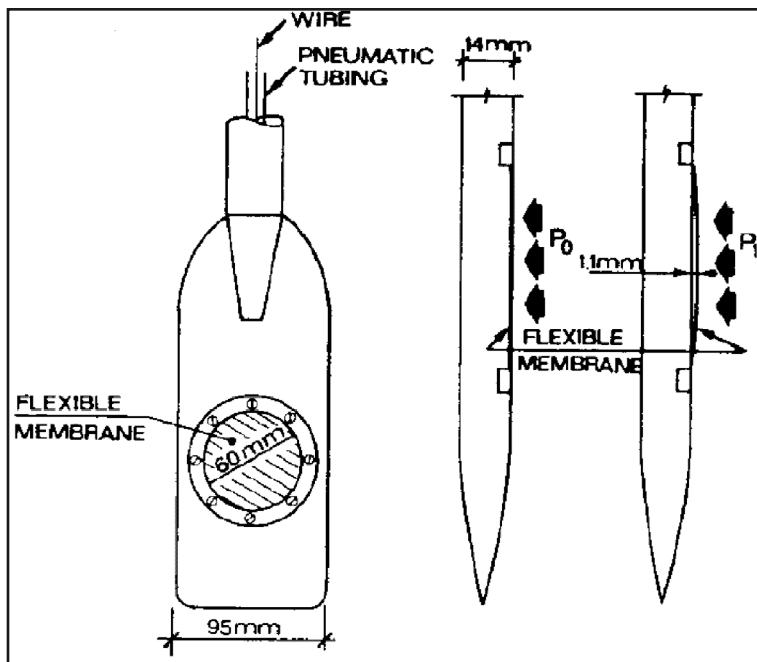
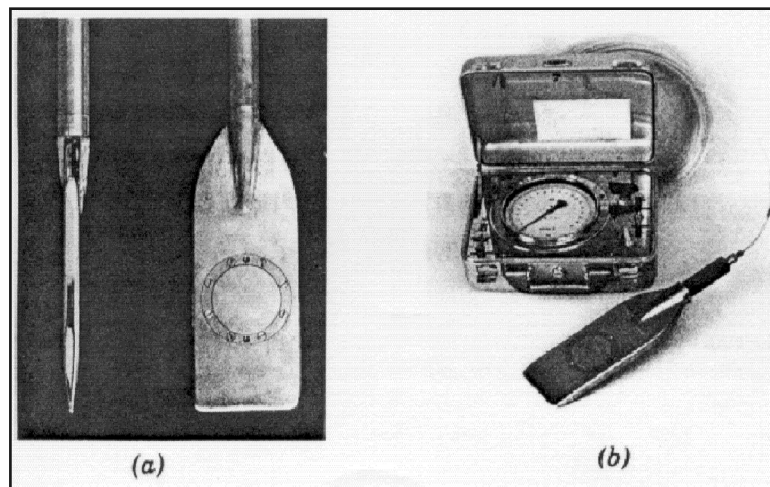


Figure 3-15: Schematic of the Marchetti Flat Dilatometer²³

Figure 3-16: Dilatometer²⁴



dilatometer has the advantage of reduced soil disturbance during penetration.

3.6.6.7. Pressuremeter Test (PMT)

This test is performed with a cylindrical probe placed at the desired depth in a borehole. The Menard type pressuremeter requires pre-drilling of the borehole; the self-boring type pressuremeter advances the hole itself, thus reducing soil disturbance. The Menard probe contains three flexible rubber membranes (see Figure 3-18). The middle membrane provides measurements, while the outer two are guard cells to reduce the influence of end effects on the measurements. When in place, the guard cell membranes are inflated by pressurized gas while the middle membrane is inflated with

water by means of pressurized gas. The pressure in all the cells is incremented and decremented by the same amount. The measured volume change of the middle membrane is plotted against applied pressure. Tests shall be performed in accordance with ASTM D 4719. Studies have shown that the guard cells can be eliminated without sacrificing the accuracy of the test data provided the probe is sufficiently long.

Furthermore, pumped air can be substituted for the pressurized gas used to inflate the membrane with water. The TAXAM pressuremeter is an example of this type.

Test results are normally used to directly calculate bearing capacity and settlements, but the test can be used to estimate strength parameters. The undrained strength of fine-grained materials is given by:

²³ Baldi, G., Bellotti R., Ghionna, V., Jamiolkowski, M., Marchetti, S. and Pasqualini, E. Flat Dilatometer Tests in Calibration Chambers, Use of Insitu Tests in geotechnical engineering, ASCE Specialty Conference, Geotechnical Special Publication No. 6, 1986.

²⁴ Marchetti, Silvano, In-Situ Tests by Flat Dilatometer, Journal of the geotechnical engineering Division, ASCE, Vol. 106, No. GT3, March 1980.

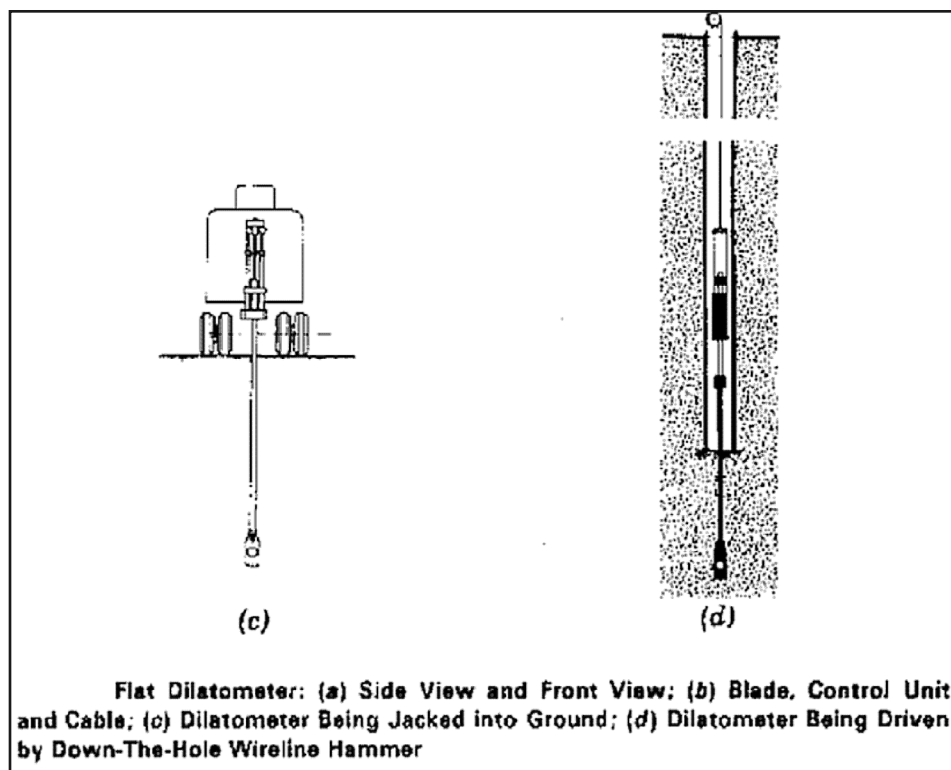


Figure 3-17: Dilatometer (Continued)

$$\text{Equation 3-3: } q_u = \frac{p_l - p'_{ho}}{2K_b}$$

Where

- p_l = limit pressure
- p'_{ho} = effective at-rest horizontal pressure
- K_b = a coefficient typically in the range of 2.5 to 3.5 for most clays.

Correlation with laboratory tests and local experience is recommended. The pressuremeter test is very sensitive to borehole disturbance and the data may be difficult to interpret for some soils.

3.6.7. Field Vane Test

This test consists of advancing a four-bladed vane into cohesive soil to the desired depth and applying a measured torque at a constant rate until the soil fails in shear along a cylindrical surface. (See Figure 3-19) The torque measured at failure provides the undrained shear strength of the soil. A second test run immediately after remoulding at the same depth provides the remoulded strength of the soil and thus information on soil sensitivity. Tests shall be performed in accordance with ASTM D 2573.

This method is commonly used for measuring shear strength in soft clays and organic deposits. It should not be used in stiff and hard clays. Results can be affected by the presence of gravel, shells, roots, or sand layers. Shear strength

may be overestimated in highly plastic clays and a correction factor should be applied.

3.6.8. Pocket Penetrometer

Used for obtaining the shear strength of cohesive, non-gravelly soils on field exploration or construction sites. Commercial penetrometers are available which read unconfined compressive strength directly. The tool is used as an aid to obtaining uniform classification of soils. It does not replace other field tests or laboratory tests.

3.6.9. Torvane Shear Device

Used for obtaining rapid approximations of shear strength of cohesive, non-gravelly soils on field exploration. Can be used on ends of Shelby tubes, penetration samples, block samples from test pits or sides of test pits. The device is used in uniform soils and does not replace laboratory tests.

3.6.10. Infiltration Test

The infiltration rate of a soil is the maximum rate at which water can enter the soil from the surface under specified conditions. The most common test uses a double-ring infiltrometer. Two open cylinders, approximately 20 inch (500 mm) high and 12 to 24 inch (300 to 600 mm) in diameter, are driven concentrically into the ground. The outer ring is driven to a depth of about 6 inch (150 mm), the inner ring to a depth of 2 to 4 inch (50 and 100 mm). Both are partially filled with water. As the water filtrates into the soil, measured

The Discovery Channel goes APE!!



John White, President, APE being filmed by Discovery Channel for upcoming show about pile hammers.

APE was featured on the **Discovery Channel** recently. It is a great bit of Deep Foundation News. You can view the show right on your computer by clicking on this link: www.apevibro.com/asp/video.asp. Just select the "APE on Discovery" and enjoy the show. It shows the APE quad driving 40 foot diameter piles.



Jack Xu, Managing Director for APE China, stands on Caisson beam of Quad Kong System, Dec. 2001.



Wendy Setlege, wife of Randy Setlege, President of Agra Group and John and Teresa White stand in front of the "Quad Kong" which is four APE Model 400 vibratory driver/extractors mounted together to install 40 foot diameter concrete pipe piles in China.

When a pile driver talks... we listen™. Please call or write:



APE Corporate Offices
7032 South 196th
Kent, Washington 98032
800-248-8498 or
253-872-0141
Fax: 253-872-8710

APE CANADA
1965 Ramey Road
Port Colburn, ON
LZG 7M6
905-328-0850
Fax: 905-834-8486

APE Mid-Atlantic Regional Ofc.
500 Newton Rd. Suite 200
Virginia Beach, VA 23462
866-399-7500
Fax: 757-518-9741
Cell: 757-373-9328

APE Northeast Regional Ofc.
Route 15 North & Taylor Rd.
Wharton, NJ 07885
973-989-1909
Fax: 973-989-1923
888-217-7524

APE Southeast Regional Ofc.
1023 Snively Avenue
Winter Haven, FL 33880
863-324-0378
Fax: 863-318-9409

APE S. Central Regional Ofc.
11128 FM Hwy. 1488
Conroe, TX 77384
936-271-1044
Fax: 936-271-1046
800-596-2877

APE Western Regional Office
160 River Road
Rio Vista, CA 94571
707-374-3266
Fax: 707-374-3270
888-245-4401

Alessi Equipment, Inc.
35 Rosslyn Place
Mt. Vernon, NY 10550
914-699-6300
Fax: 914-699-5300
Imeco-Austria
431-368-2513
Fax: 431-369-8104

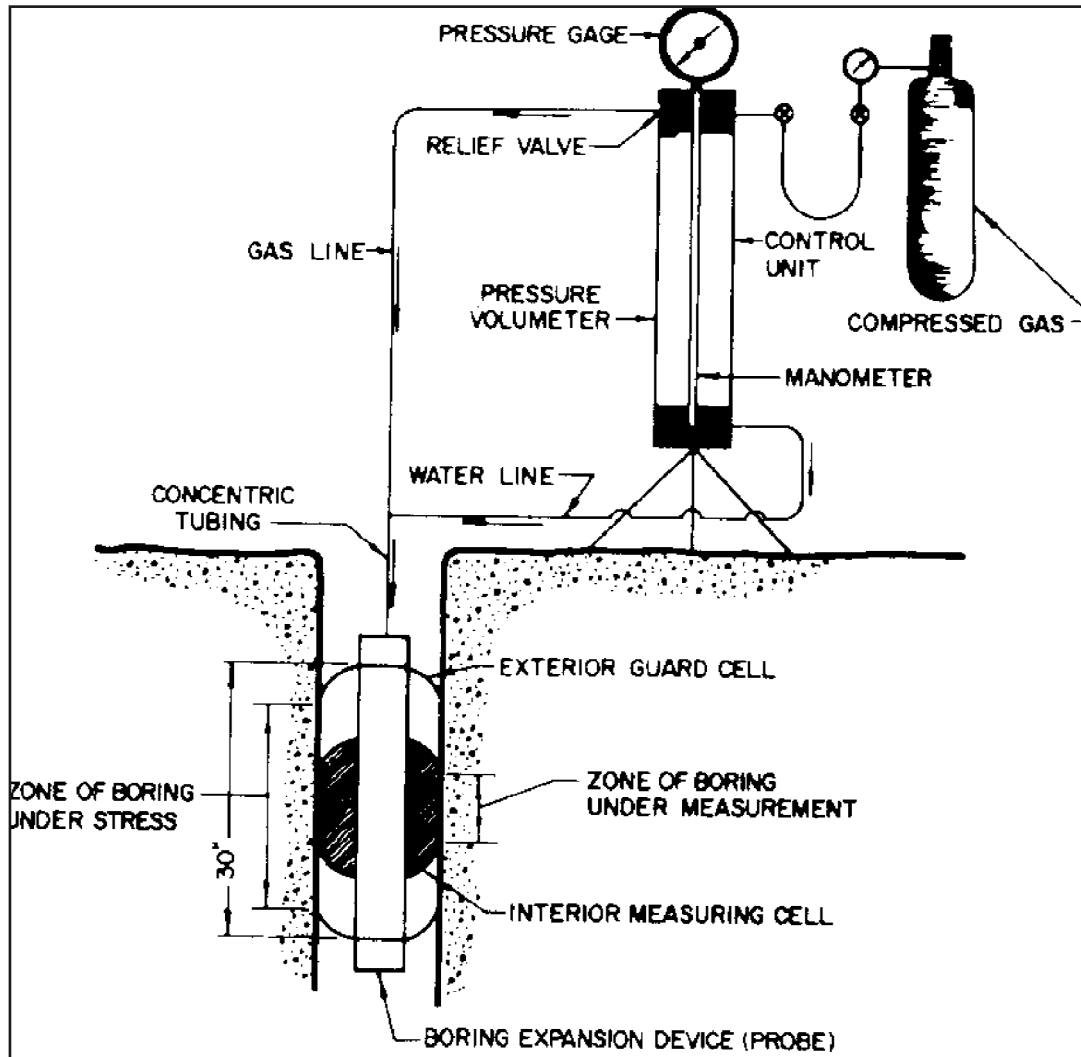


Figure 3-18: Menard Pressuremeter Equipment

volumes are added to keep the water levels constant. The volumes of water added to the inner ring and to the annular space during a specific time interval, equivalent to the amounts, which have infiltrated the soil. These are converted into infiltration rates, expressed in units of length per unit time, usually inches (millimetres) per hour. The infiltration rate is taken as the maximum infiltration velocity occurring over a period of several hours. In the case of differing velocities for the inner ring and the annular space, the maximum velocity from the inner ring should be used. The time required to run the test is dependent upon soil type. Tests shall be performed in accordance with ASTM D 3385. Drainage engineers in evaluating runoff, ditch or swale infiltration use information from this test.

3.6.11. Permeability Tests

Permeability, also known as hydraulic conductivity, is the measure of the rate of flow of water through soils, usually

measured when the soil is saturated. Field permeability tests measure the coefficient of permeability (hydraulic conductivity) of in-place materials. The area and length factors are often combined in a "shape factor" or "conductivity coefficient." Measurement of permeability is highly sensitive to both natural and test conditions. The difficulties inherent in field permeability testing require that great care be taken to minimize sources of error and to correctly interpret, and compensate for, deviations from ideal test conditions.

Permeability differs from infiltration or percolation rates in that permeability values are corrected for the hydraulic boundary conditions, including the hydraulic gradient, and thus is representative of a specific soil property.

Many types of field permeability tests can be performed. In geotechnical exploration, equilibrium tests are the most common. These include constant and variable head gravity tests and pressure (Packer) tests conducted in single borings. In a few geotechnical investigations, and commonly in water

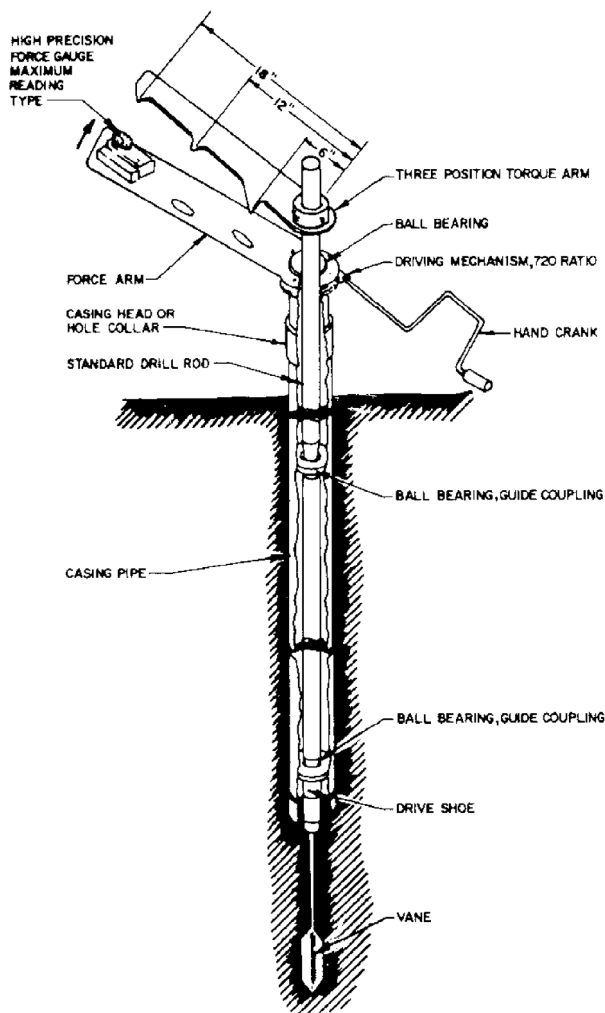


Figure 3-19: Vane Shear Test Equipment

resource or environmental studies, non-equilibrium “aquifer” or “pump” tests are conducted (a well is pumped at a constant rate for an extended period of time).

3.6.12. Seepage Test

These tests can be constant head, falling head, or rising head tests. The constant head test is the most generally applicable and, in areas of unknown permeability, should be performed first. The falling head and rising head methods are used in areas where the permeability is low enough to permit accurate measurement of the change in water level. Results are used in the design of exfiltration systems. The more commonly performed tests include:

3.6.12.1. Constant Head Test

This is the most generally applicable permeability test. It may be difficult to perform in materials of either very high or very low permeability since the flow of water may be difficult to maintain or to measure.

3.6.12.2. Rising Head Test

In a saturated zone with sufficiently permeable materials, this test is more accurate than a constant or a falling head test. Plugging of the pores by fines or by air bubbles is less apt to occur in a rising head test. In an unsaturated zone, the rising head test is inapplicable.

3.6.12.3. Falling Head Test

In zones where the flow rates are very high or very low, this test may be more accurate than a constant head test. In an area of unknown permeability, the constant head test should be attempted before a falling head test.

3.6.12.4. Open-End Borehole Test

This test can be conducted as either a constant head or a variable head test. An open-end pipe or casing is installed to the desired depth within a uniform soil. The pipe/casing is then cleaned out flush with the bottom of the pipe/casing while the hole is kept filled with water. Clear water is added through a metering system to maintain gravity flow at a constant head until measurements indicate a steady-state flow is achieved. The permeability is calculated from the rate of steady-state flow, height of head and radius of pipe (see Figure 3-20).

3.6.12.5. Exfiltration Test

This test is performed as a constant head test. A 7” (175 mm) diameter (or larger) hole is augered to a standard depth of 10 feet (3 meters). Approximately 0.125 ft³ (0.0035 m³) of 0.5” (13 mm) diameter gravel is poured to the bottom of the hole to prevent scour. A 6” (150 mm) diameter (or larger), 9-foot (2.75 meter) long casing which is perforated with 0.5-inch (12.7 mm) holes on 2” (51 mm) centres over the bottom 6.0 feet (1.8 m) is then lowered into the hole. Water is added and the amount required to maintain a constant water level over specified time intervals is recorded.

3.6.12.6. Pumping Test

Pumping tests are used in large-scale investigations to more accurately measure the permeability of an area. The results are used in the design of dewatering systems and other situations where the effects of a change in the water table are to be analysed. Pumping tests require a test hole and at least one observation well, although several observation wells at varying distances from the test hole are preferable. As water is pumped from the test hole, water level changes within each observation well and corresponding times is recorded. Pumping is continued at a constant rate until the water level within each observation well remains constant. Permeability calculations are made based on the rate of pumping, the measured draw down, and the configuration of the test hole and observation wells. Refer to ASTM D 4050.

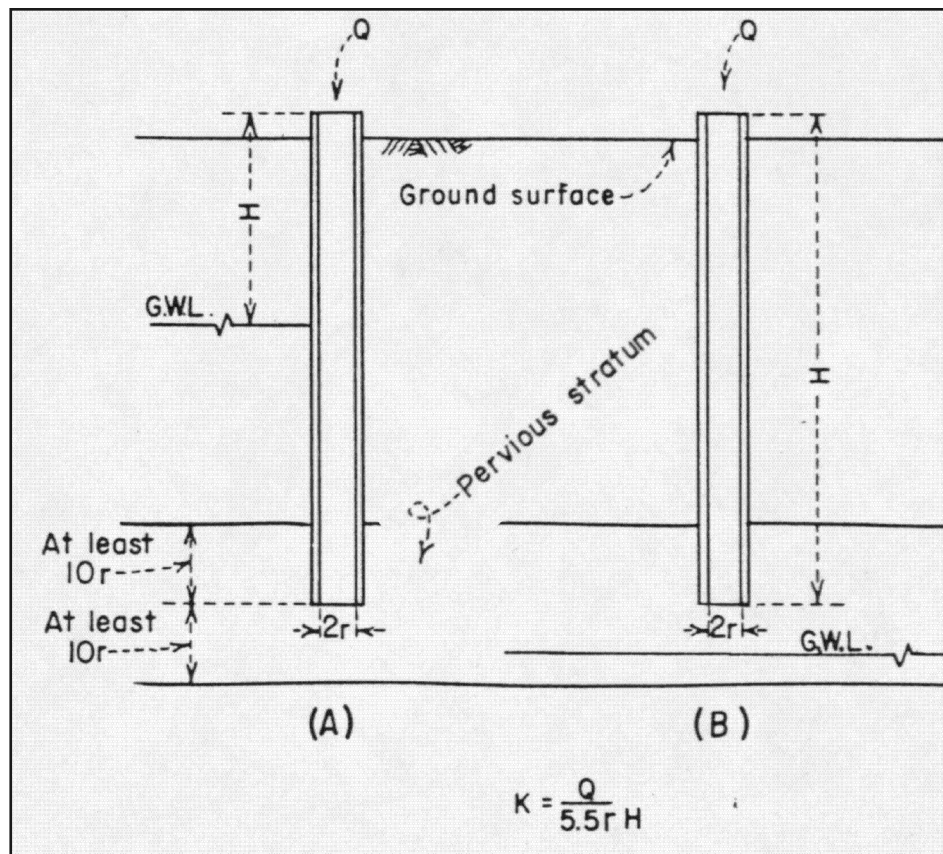


Figure 3-20: Open-end Borehole Test²⁵

3.6.12.7. Gravity and Pressure Tests

In a boring, gravity and pressure tests are appropriate. The segment of the boring tested is usually 5 to 10 feet, but may be larger. A large number of tests must be conducted to achieve an overall view of the seepage characteristics of the materials. The zone of influence of each test is small, usually a few feet or perhaps a few inches. These methods can detect changes in permeability over relatively short distances in a boring, which conventional pump or aquifer tests cannot. Exploration boring (as opposed to “well”) methods are therefore useful in geotechnical investigations where inhomogeneity and anisotropy may be of critical importance. Results from pressure tests using packers in fractured rock may provide an indication of static heads, inflow capacities, and fracture deformation characteristics, but conventional interpretation methods do not give a true permeability in the sense that it is measured in porous media.

3.6.13. Environmental Corrosion Tests

These tests are carried out on soil and water at structure locations, on structural backfill materials and on subsurface materials along drainage alignments to determine the corrosion classification to be considered during design. For structures, materials are classified as slightly, moderately, or extremely aggressive, depending on their pH, resistivity, chlo-

ride content, and sulphate content. For roadway drainage systems, test results for each stratum are presented for use in determining alternate culvert materials. Testing shall be performed in the field and/or the laboratory according to the standard procedures.

3.6.14. Grout Plug Pull-out Test

This test is performed when the design of drilled shafts in rock is anticipated. However, the values obtained from this test should be used carefully. Research has indicated that the results are overly conservative.

A 4” (100 mm) diameter (minimum) by 30” (760 mm) long core hole is made to the desired depth in rock. A high strength steel bar with a bottom plate and a reinforcing cage over the length to be grouted is lowered to the bottom of the hole. Sufficient grout is poured into the hole to form a grout plug approximately 2 feet (600 mm) long. After curing, a centre hole jack is used to incrementally apply a tension load to the plug with the intent of inducing a shear failure at the grout - limestone interface. The plug is extracted, the failure surface examined, and the actual plug dimensions measured.

The ultimate shear strength of the grout-limestone interface is determined by dividing the failure load by the plug perimeter area. This value can be used to estimate the skin friction of the rock-socketed portion of the drilled shaft.

vulcanhammer.net

Your complete online resource for information on geotechnical engineering and deep foundations:

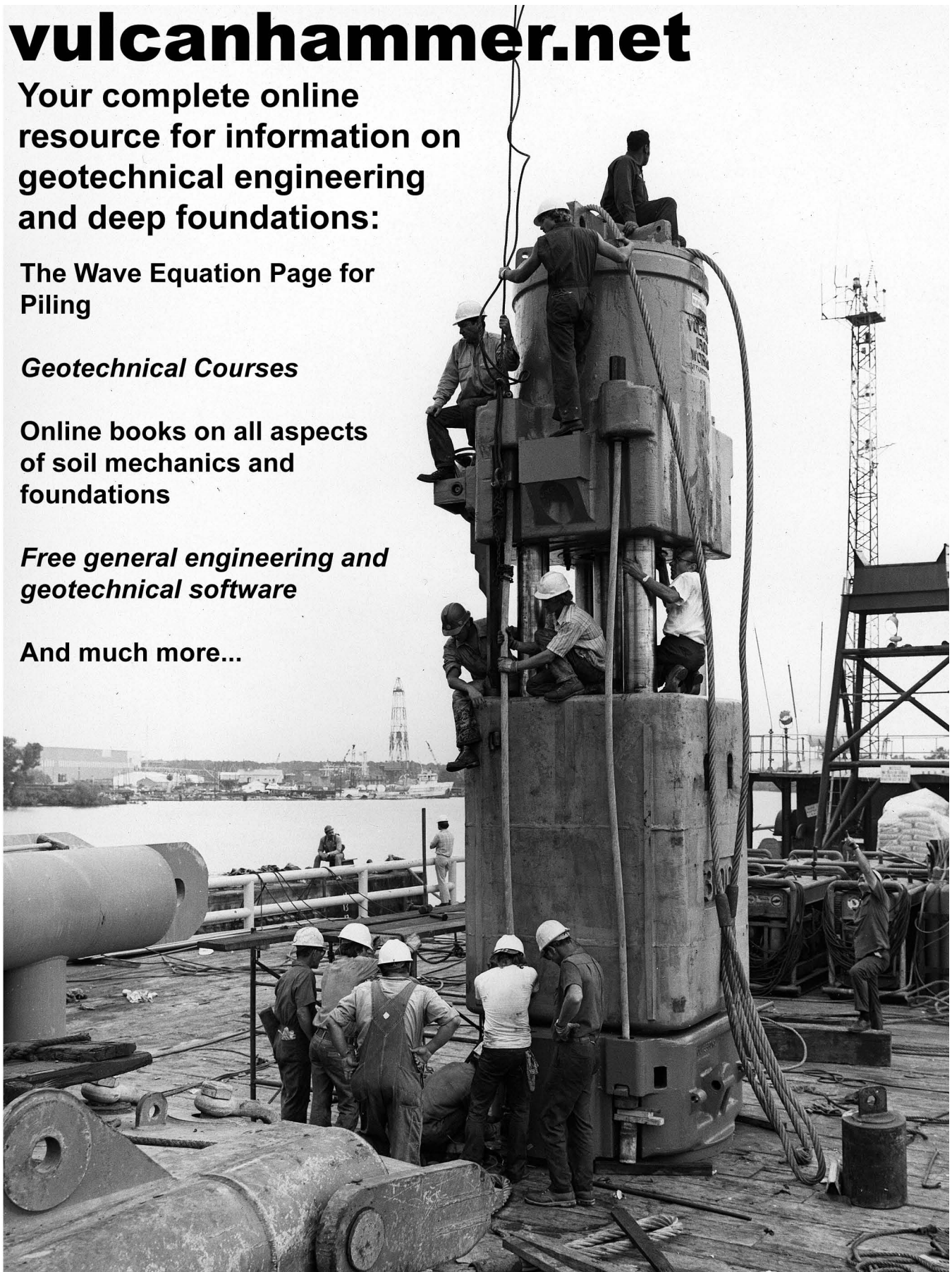
The Wave Equation Page for Piling

Geotechnical Courses

Online books on all aspects of soil mechanics and foundations

Free general engineering and geotechnical software

And much more...



3.6.15. Groundwater Measurements and Piezometers

The groundwater level should be measured at the depth at which water is first encountered as well as at the level at which it stabilizes after drilling. If necessary, the boring should be kept open with perforated casing until stabilization occurs. On many projects, seasonal groundwater fluctuation is of importance and converting the borings to standpipe piezometers can make long-term measurements.

The pore water pressure should be checked often during embankment construction. After the fill is in place, it can be monitored at a decreasing frequency. The data should be plotted (as pressure or feet (meters) of head) as a function of time. A good practice is to plot pore water pressure, settlement, and embankment elevation on the same time-scale plot for comparison.

3.7. Measurement of Soil Properties *in situ*

A great number of tools and methods have been devised for measuring *in situ* engineering properties of soil and rock. The most common tools, the split spoon sampler and the cone penetrometer, have been previously discussed. This section describes other methods commonly used in exploration programs or during construction control.

3.7.1. In-Place Density

In-place soil density can be measured on the surface by displacement methods to obtain volume and weight, and by nuclear density meters. Density at depth can be measured only in certain soils by the drive cylinder (sampling tube) method.

- Displacement Methods. Direct methods of measuring include sand displacement and water balloon methods.²⁶ The sand displacement and water balloon methods are the most widely used methods because of their applicability to a wide range of material types and good performance. The sand displacement method (ASTM Standard D1556, Density of Soil in Place by the Sand Cone Method) is the most frequently used surface test and is the reference test for all other methods. A procedure for the water or rubber balloon method is given in ASTM Standard D2167, Density of Soil in Place by the Rubber Balloon Method.
- Drive-Cylinder Method. The drive cylinder (ASTM Standard D2937, Density of Soil in Place by the Drive-

Cylinder Method) is useful for obtaining subsurface samples from which the density can be ascertained, but it is limited to moist, cohesive soils containing little or no gravel and moist, fine sands that exhibit apparent cohesion.

- Nuclear Moisture-Density Method. Use ASTM Standard D2922, Density of Soil and Soil-Aggregate in Place by Nuclear Methods (Shallow Depth). Before nuclear density methods are used on the job, results must be compared with density and water contents determined by displacement methods. Based on this comparison, correlations may be required to the factory calibration curves or a new calibration curve may have to be developed.²⁷

3.7.2. Detection of Combustible Gases

Methane and other combustible gases may be present in areas near sanitary landfills, or at sites near or over peat bogs, marshes and swamp deposits. Commercially available indicators are used to detect combustible gases or vapours and sample air in borings above the water table. The detector indicates the concentration of gases as a percentage of the lower explosive limit from 0 to 100 on the gage. The lower explosive limit represents the leanest mixture that will explode when ignited. The gage scale between 60% and 100% is coloured red to indicate very dangerous concentrations. If concentrations are judged serious, all possibilities of spark generation (e.g., pile driving, especially mandrel driven shells) should be precluded, and a venting system or vented crawl space should be considered. The system could be constructed as follows:

- Place a 6" layer of crushed stone (3/4" size) below the floor slab; a polyethylene vapour barrier should overlie the crushed stone.
- Install 4" diameter perforated pipe in the stone layer below the slab; the top of the pipe should be immediately below the bottom of the slab.
- The pipes should be located such that gas rising vertically to the underside of the floor slab does not have to travel more than 25 feet laterally through the stone to reach a pipe.
- The pipes can be connected to a single, non-perforated pipe of 6" diameter, and vented to the atmosphere at roof level²⁸.

²⁶ ASTM STP 523, Evaluation of Relative Density and Its Role in Geotechnical Projects Involving Cohesionless Soils, 1972

²⁷ Safety regulations pertaining to the use of nuclear gages are contained in U.S. Corps of Engineers, Radiological Safety, ER385-1-80.

²⁸ Further details on gas detection and venting can be found in Noble, G., Sanitary Landfill Design Handbook, Technomic Publishing Co., Westport, CT., 1976, and United States Environmental Protection Agency (EPA), Process Design Manual, Municipal Sludge Landfills, EPA-625 11-78-010, SW 705, 1978.

Chapter Four: Basic Earth Pressure Concepts

The loads governing the design of a sheet pile wall arise primarily from the soil and water surrounding the wall and from other influences such as surface surcharges and external loads applied directly to the piling. Competent application of these theories requires a complete understanding of basic soil mechanics, the makeup and engineering properties of soils, and testing methods, both field and laboratory.

The loading of sheet pile walls by the soil specifically requires understanding of lateral earth pressure theory. Since this is frequently not covered completely in soils textbooks, this chapter will discuss this in detail. Current methodologies for evaluating these loads are discussed in the following paragraphs.²⁹

4.1. Lateral Earth Pressure Coefficient

Earth pressures reflect the state of stress in the soil mass. The concept of an earth pressure coefficient, K , is often used to describe this state of stress. The lateral earth pressure coefficient is defined as the ratio of horizontal stresses to the vertical stresses at any depth below the soil surface:

$$\text{Equation 4-1: } K = \frac{\sigma_h}{\sigma_v}$$

Where

- K = lateral earth pressure coefficient
- σ_h = horizontal earth pressure
- σ_v = vertical earth pressure

The magnitude of the earth pressure exerted on the wall depends, among other effects, on the physical and strength properties of the soil, the interaction at the soil-structure interface, the ground-water conditions, and the deformations of the soil-structure system.

4.2. Total and Effective Stresses

These limit states are determined by the shear strength of the soil. This is determined by one of two methods: a) total stress method, or b) effective stress method. Earth pressure is also influenced by the time-dependent nature of soil strength, which varies due to creep effects and chemical changes in the soil.

4.2.1. Total Stress

Soil consists of a skeletal framework of solid particles interspersed with void spaces. Above the ground water table, the voids may contain both moisture and air. When the soil is submerged, the void spaces are completely filled with water. In either case, the total vertical stress of the soil is given by the equation

$$\text{Equation 4-2: } \sigma = \gamma_t z$$

Where

- σ = Total stress of the soil
- γ_t = effective unit weight of the soil
- z = Distance of the soil from the surface

Equation 4-2 assumes the soil has a uniform unit weight. If the unit weight varies, Equation 4-2 can be applied layer by layer and summed.

4.2.2. Effective Stress

Inspection of Equation 4-2 will show that the total stress is similar for soils as the hydrostatic pressure for water, which is given by Equation 7-5. Below the phreatic surface, water in the soil voids acts very much as it does as a body of water; however, it does not add anything to the shear resistance of a cohesionless soil. Thus, hydrostatic stresses are referred to as neutral stresses. Only the actual soil grains are effective in developing shear resistance and the pressure due to the soil particles alone is referred to as effective stress. The effective stress, σ' , is equal to the difference between the total stress, σ , and the pore water pressure, u .

$$\text{Equation 4-3: } \sigma' = \sigma - u$$

Where

- σ' = Effective stress of the soil

Obviously, the most common source of pore water pressure is static groundwater; however, seepage, capillary action, and consolidation of poor draining soils are also possible sources.

The practical meaning of this for the sheet pile designer is that effective stresses should generally be used in all calculations. Water pressure should then be treated as a separate force. This is accomplished by using the moist or dry unit weight of the soil above the water table and the buoyant weight below as effective unit weights to calculate the effective pressure.

4.3. Mohr-Coulomb Shear Strength

In an effective stress analysis the Mohr-Coulomb shear strength relationship defines the ultimate shearing resistance of the backfill as

$$\text{Equation 4-4: } \tau_f = c + \sigma'_n \tan \phi$$

Where

- τ_f = ultimate shearing resistance of the backfill
- c = effective cohesion
- σ'_n = effective normal stress on the failure plane,
- ϕ = effective angle of internal friction.

²⁹ Some of the material may show views that do not reflect sheet pile walls, but the basic earth pressure concepts for sheet pile walls and other types of retaining walls is the same.

These quantities are illustrated in Figure 4-1.

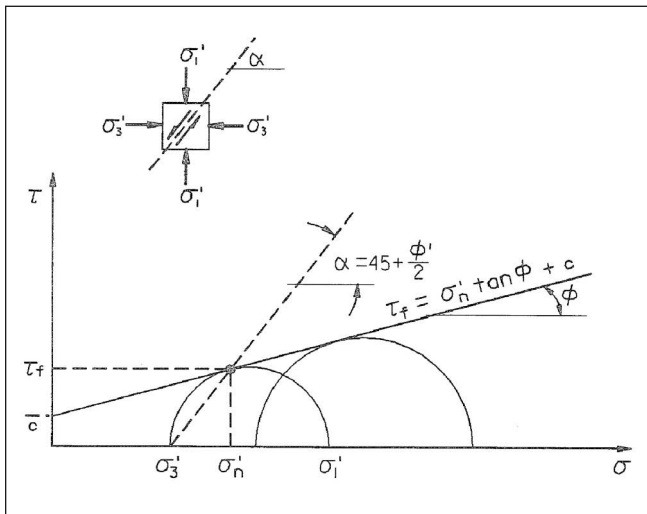


Figure 4-1: Shear strength parameters

The two principal stresses can be related by:

$$\text{Equation 4-5: } \sigma_1' = \sigma_3' \frac{1 + \sin \phi}{1 - \sin \phi} + 2c \sqrt{\frac{1 + \sin \phi}{1 - \sin \phi}}$$

If we use the trigonometric relationship

$$\text{Equation 4-6: } \frac{1 + \sin \phi}{1 - \sin \phi} = \tan^2 \left(45^\circ + \frac{\phi}{2} \right)$$

Equation 4-5 reduces to

$$\text{Equation 4-7: } \sigma_1' = \sigma_3' \tan^2 \left(45^\circ + \frac{\phi}{2} \right) + 2c \tan \left(45^\circ + \frac{\phi}{2} \right)$$

If we then define

$$\text{Equation 4-8: } N_\phi = \tan^2 \left(45^\circ + \frac{\phi}{2} \right)$$

Equation 4-7 reduces further to

$$\text{Equation 4-9: } \sigma_1' = \sigma_3' N_\phi + 2c \sqrt{N_\phi}$$

If we take Equation 4-5 and solve for σ_3' , we have

$$\text{Equation 4-10: } \sigma_3' = \sigma_1' \frac{1 - \sin \phi}{1 + \sin \phi} - 2c \sqrt{\frac{1 - \sin \phi}{1 + \sin \phi}}$$

Noting the trigonometric identity

$$\text{Equation 4-11: } \frac{1 - \sin \phi}{1 + \sin \phi} = \cot^2 \left(45^\circ + \frac{\phi}{2} \right)$$

Equation 4-10 reduces to

$$\text{Equation 4-12: } \sigma_3' = \sigma_1' \cot^2 \left(45^\circ + \frac{\phi}{2} \right) - 2c \cot \left(45^\circ + \frac{\phi}{2} \right)$$

4.4. Earth Pressure and Wall Movement

The results of the previous section can be observed in tri-axial compression tests, where soil stress and movement are induced by the testing apparatus. In actual conditions, soil stress and movement are induced by the retaining wall itself; how the soil is actually stressed depends on that movement. The various types of earth pressures described are shown in Figure 4-2 on the circle where σ_h , σ_a , $\sigma_p = \sigma_3$ on the Mohr diagram.

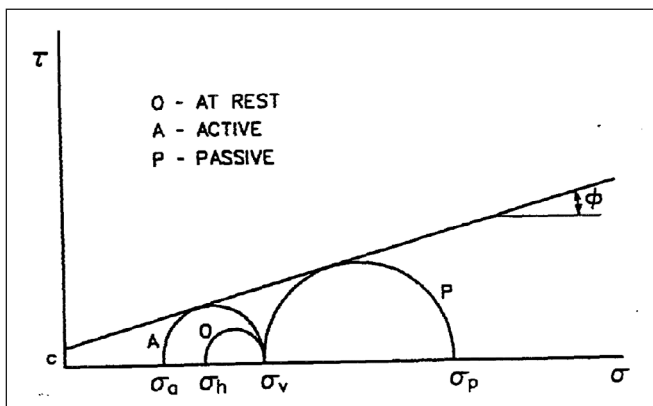


Figure 4-2: Definition and development of at rest, active and passive earth pressures

4.4.1. At-rest pressures

At-rest pressure refers to a state of stress where there is no lateral movement or strain in the soil mass. In this case, the lateral earth pressures are the pressures that existed in the ground prior to installation of a wall. For the special case of a horizontal backfill surface and a normally consolidated backfill (no compaction or other prestress effects) the at-rest pressure coefficient K_o can be estimated from Jaky's Equation³⁰

$$\text{Equation 4-13: } K_o = 1 - \sin \phi'$$

and the lateral earth pressure computed by

$$\text{Equation 4-14: } \sigma_o = \gamma' z K_o$$

where

- γ' = effective unit weight (moist or saturated above water table, submerged or buoyant below water table)
- z = depth below surface of backfill along a vertical plane

³⁰ Jaky, J. 1944. "The Coefficient of Earth Pressure At-Rest," Journal, Society of Hungarian Architects and Engineers, Budapest, Hungary, pp 355-358.

"Skyline is all you need"

SKYLINE

Skyline Steel, LLC

Best of ALL Worlds

"There's one near you"

- General Catalog
- HZ Steel Wall System
- Product Datasheets
- Anchorage Systems
- Installation of Steel Sheet Piles
- Impervious Wall: Part 1 Design
- Impervious Wall: Part 2 Practical Aspects
- Impervious Wall: Movie
- Project Planning
- Prosheet Design Software
- Sheet Piling Durability Analysis
- HZ / AZ Stresses
- Autocad Sections
- Contact Us

Best Product Range



Best Manufacturing

Best Stocking



Best Sales Team

Best Engineering Support



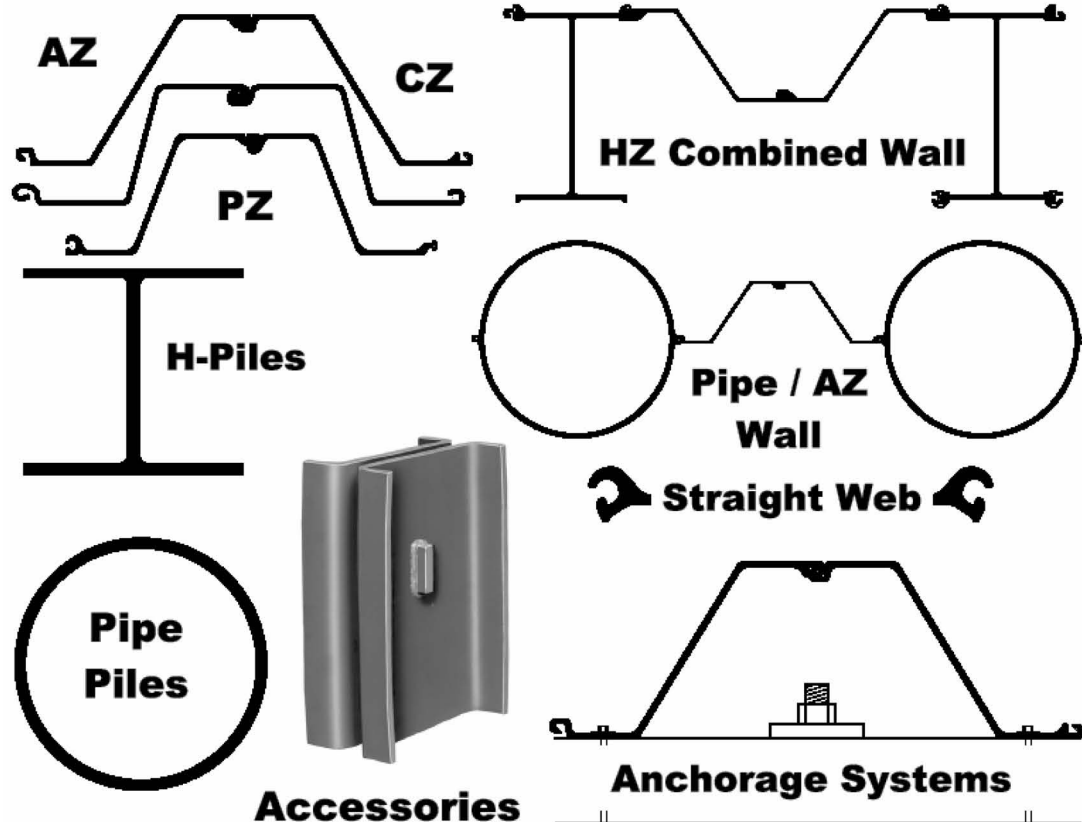
Best Customer Service

Technical Hotline
1-866-8Skyline
1-866-878-9546

Corporate
(973) 428-6100

Call for an office near you.

1-866-8Skyline www.skylinesteel.com



For preconsolidated soils, Jaky's equation can be expanded to³¹

Equation 4-15: $K_o = (1 - \sin \phi') OCR^{\sin \phi'}$

Where

- OCR = overconsolidation ratio

Most engineering materials quantify their lateral stress characteristics in terms of Poisson's Ratio. Poisson's ratio can be roughly approximated to the lateral earth pressure coefficient by the equation³²

Equation 4-16: $K_o = \frac{\nu}{1 - \nu}$

Using Equation 4-13, Poisson's ratio for soils can be related to the internal friction angle by the relationships

Equation 4-17: $\phi = \frac{2\nu - 1}{\nu - 1}$

and

Equation 4-18: $\nu = \frac{\tan \phi - 1}{\tan \phi + 2}$

It is interesting to note that, for purely cohesive soils ($\phi = 0$), $\nu = 1/2$, which is a very "typical" value given. For overconsolidated soils, these relationships are much more complicated.

4.4.2. Wall movements

Implicit in "at-rest" earth pressures is one of two states: a) the state where there is no wall, only a "semi-infinite" mass of

earth with increasing effective stress with depth, and b) the state where the wall does not move at all. Condition (a) is of no interest in retaining wall design of any kind and b) is exceptional with flexible sheet pile walls. Walls can move either towards or away from the soil, depending upon how they are loaded and how they interface with the soil. Walls that move towards the soil will obviously generate higher lateral earth pressures than those that move away from the soil.

The extent of the wall movement required to effect a change in the lateral earth pressure coefficient varies for differing kinds of soils. For stiff soils like dense sands or heavily overconsolidated clays, the required movement is relatively small. An example is shown in Figure 4-3. In this example, a movement of a wall away from the fill by 0.3% of the wall height is sufficient to develop minimum pressure, while a movement of 2% of the wall height toward the fill is sufficient to develop the maximum pressure. A summary of approximate wall movements necessary to mobilise active or passive earth pressures for different types of soils is given in Table 4-1.

Earth pressure against excavation sheeting, which is restrained by tiers of non-yielding struts or pre-tensioned anchors, may never attain the full active state. These walls should be destined for pressures somewhere between active and at-rest or fully at-rest.

4.4.3. Active pressures

When the walls move or rotate away from the soil, allowing the soil the opportunity to expand laterally, full shear resistance is mobilised and the active state of stress is entered, as shown in Figure 4-2 when $\sigma_3 = \sigma_a$. This state represents the lower limit of K in Equation 4-1. Modifying this equation using this figure, the active earth pressure coefficient is

Equation 4-19: $K_a = \frac{\sigma_a}{\sigma_v} = \frac{\sigma_3}{\sigma_1}$

If we consider purely cohesionless soils ($c = 0$), Equation 4-12 can be easily substituted into Equation 4-19 and the active earth pressure coefficient becomes

Equation 4-20:

$K_a = \cot^2 \left(45^\circ + \frac{\phi}{2} \right) = \tan^2 \left(45^\circ - \frac{\phi}{2} \right)$

This expression of active earth pressure coefficient is applied directly in Rankine theory (see 5.1) where other considerations (wall-soil friction, log-spiral failure surfaces, etc.) are not considered. Keep in mind that this expression is only valid for level backfill.

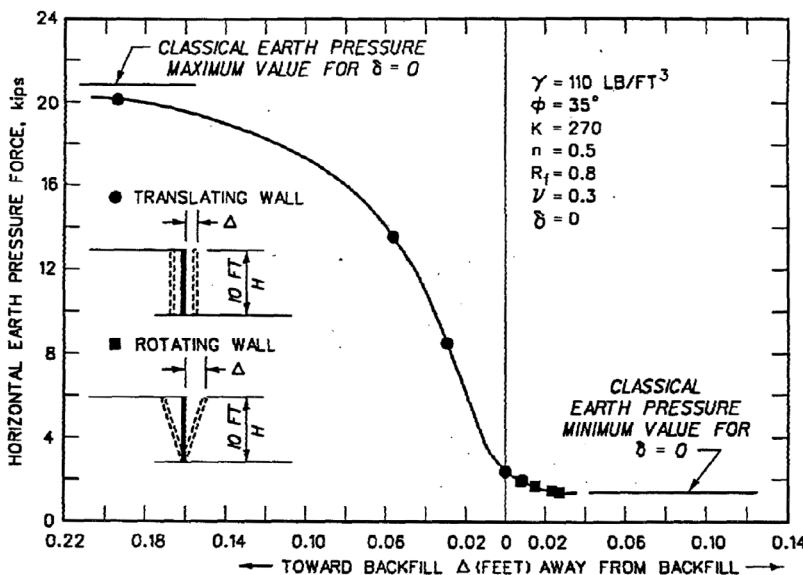


Figure 4-3: Variations of earth pressure force with wall movement calculated by finite element analyses³³

³¹ Coduto, Donald P., Foundation Design: Principles and Practices. Upper Saddle River, NJ: Prentice Hall, 2001, p. 751.
³² Tschebotarioff, G.P., Soil Mechanics, Foundations and Earth Structures. New York: McGraw-Hill Book Company, 1951, p. 248. A derivation of this equation is given in Verruijt, A., Soil Mechanics. Delft, the Netherlands: Delft University of Technology, 2001. Text available at <http://www.vulcanhammer.net>.
³³ Clough, G. W., and Duncan, J. M. 1971. "Finite Element Analyses of Retaining Wall Behavior," Journal of the Soil Mechanics and Foundations Division, American Society of Civil Engineers, Vol 97, No. SM12, Proceedings Paper No. 8583, pp 1657-1673.

Table 4-1 Approximate Magnitudes of Movements Required to Reach Minimum Active and Maximum Passive Earth Pressure Conditions³⁴

Type of Backfill	Δ/H , Active Condition, Percent	Δ/H , Passive Condition, Percent
Dense Sand	0.1%	1%
Medium-Dense Sand	0.2%	2%
Loose Sand	0.4%	4%

4.4.4. Passive pressures

The passive state of stress is activated when a retaining wall moves toward the soil rather than away from it. The passive state represents the upper limit of K in Equation 4-1. In a similar manner with active pressures (see Figure 4-2,) the passive pressure is given by the equation

$$\text{Equation 4-21: } K_p = \frac{\sigma_p}{\sigma_v} = \frac{\sigma_1}{\sigma_3}$$

Again if we consider purely cohesionless soils, Equation 4-7 can be substituted into Equation 4-21 to obtain the result (for level backfill)

$$\text{Equation 4-22: } K_p = \tan^2\left(45^\circ + \frac{\phi}{2}\right)$$

As with active pressures, the effects of wall-soil friction are not considered.

Another way of looking at passive vs. active and at rest pressures is to consider the mechanism by which lateral earth pressure takes place. With at rest and active earth pressures, the Poisson effect of the vertical stress results in a horizontal stress. With passive pressures, the Poisson effect of the horizontal stress results in vertical one up to the value of effective stress.

4.4.5. Wall friction and adhesion

The equations for active and passive earth pressure coefficients do not take into account friction between soil and wall, which reduces active pressure and increases passive pressure. These considerations are the basis for Coulomb and Log-Spiral theory, and will be discussed further below.

4.4.6. Cohesive Soils

The forgoing discussion of active and passive states has assumed purely cohesionless soil. While these are the most desirable for backfill, it is not always possible to work with these for every wall. If we assume a purely cohesive soil ($\phi = 0$), both Equation 4-7 and Equation 4-12 reduce to

$$\text{Equation 4-23: } \sigma'_3 = \sigma'_1 - 2c$$

For the active pressure, assuming that the soil is uniform, i.e., $\sigma_1 = \gamma z$, and that there is no surcharge, i.e., $\sigma_3 = 0$, this equation reduces to

$$\text{Equation 4-24 } \gamma z - 2c = 0$$

This can be solved for the depth as

$$\text{Equation 4-25: } H_c = z = \frac{2c}{\gamma}$$

Where H_c = critical height. This concept is illustrated in Figure 5-2 (b). For areas above the critical height, active pressures are negative and thus do not develop at all.

In slope stability work, this concept has been generalised through the stability number. For a given slope height, cohesion and unit weight, this is defined as

$$\text{Equation 4-26: } N_o = \frac{\gamma H}{c}$$

Where N_o = stability number. Comparison with Equation 4-25 reveals that, at the critical height, $N_o = 2$. One way of applying a factor of safety is to raise the stability number above this number by the required amount.

Equation 4-23 can be rearranged to illustrate the passive pressures to yield

$$\text{Equation 4-27: } \sigma'_1 = \sigma'_3 + 2c$$

This is illustrated in Figure 5-2 (e).

The long-term ability of fine-grained, cohesive silts to maintain the conditions described in these equations is doubtful. For long-term analyses, the results of consolidated-drained (S or C-D) tests should be used. These will include both internal friction and cohesion of the soil in the assumed properties.

³⁴ Clough, G. W. and Duncan, J. M. 1991. Chapter 6: Earth Pressures, in Foundation Engineering Handbook, Second Edition, edited by H. Y. Fang, Van Nostrand Reinhold, NY, pp. 223-235.

Chapter Five: Static Earth Pressures

Failure within a semi-infinite mass of soil occurs along inclined planes when gravitational forces exceed the shearing resistance of the soil. A retaining wall is inserted into this process to prevent a failure and its consequences or to provide a vertical working face for private or commercial purposes.

Earth pressure study and the theories developed from it were originally directed toward advancement of the design of rigid retaining structures. Physicists such as Coulomb³⁵ and Rankine³⁶ have had the most influence on practical design through their application of earth pressure theory to reliable standard procedures. Additionally, the log-spiral failure surface theory has advanced the design of sheet pile walls. These are the three theories we plan to discuss for “classical” methods of sheet piling wall design. The three failure mechanisms are illustrated in Figure 5-1.

Rankine's theory, Coulomb's wedge theory, and the logarithmic spiral procedure result in similar values for active and passive thrust when the interface friction between the wall and the backfill is equal to zero. For interface friction angles greater than zero, the wedge method and the logarithmic spiral procedure result in nearly the same values for active thrust. The logarithmic spiral procedure results in accurate values for passive thrust for all values of interface friction between the wall and the backfill. The accuracy of the passive

thrust values computed using the wedge method diminishes with increasing values of interface friction because the boundary of the failure block becomes increasingly curved.

5.1. Rankine Theory

In 1857, William Rankine of Scotland offered a simplification of Coulomb's general theory that was widely accepted and is still utilized because of its simplicity and conservatism. Rankine's methods are based on the following assumptions:

- (1) The soil is homogeneous and isotropic, possesses internal friction, and is in a state of plastic equilibrium.
- (2) The failure surface is a plane surface. The surface is level or uniformly sloped.
- (3) The shear strength is mobilized uniformly on all potential failure planes throughout the backfill.
- (4) The presence of the wall does not influence the state of stress in the backfill (there are no vertical stresses between the wall and the adjacent fill and no friction is developed.)
- (5) The failure is a two-dimensional problem.

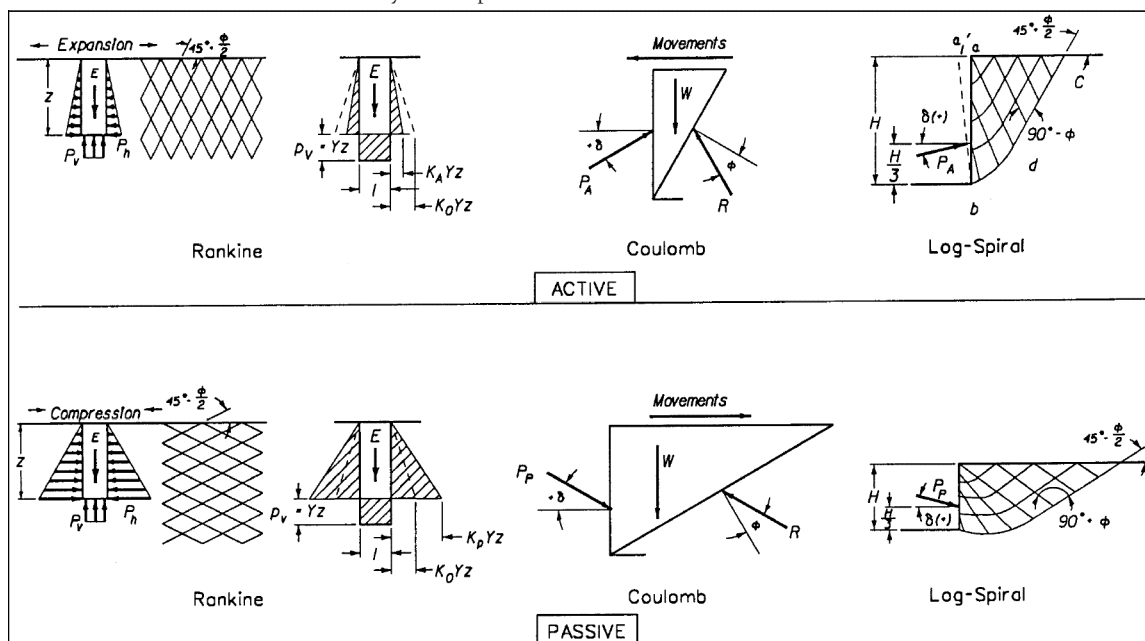


Figure 5-1: Three Earth Pressure Theories for Active and Passive Earth Pressures

³⁵Coulomb, C. A. 1776. Essai sur une application des règles des maximis et minimis à quelques problèmes de statique relatifs à l'architecture, Mém. acad. roy. près divers savants, Vol. 7, Paris. It is interesting to note that the Rankine theory, although the simpler, was not the first to be published. As is the case with many soil mechanics theories of the eighteenth and nineteenth centuries, it took many years for the theory to be actually put into practice.

³⁶Rankine, W. (1857). "On the Stability of Loose Earth", Phil. Trans. Roy. Soc. London, Vol. 147.

LBT. ENTERPRISES, LTD.

PRIME® PILE CUTTER



Feature (1)

2-part cradle to support the cut off for easier and safer disposal.



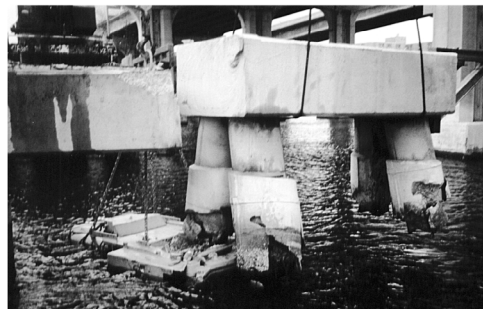
Aurora, Illinois

43" Steel casing filled with concrete and 16 pcs - 1 1/2" Rebar. A slice above it all.



Product (8) 16" P.C.P.C.

Exposing Rebar on a 18" Round Pile



Feature (2). 30" P.C.P.C. Easily attaches to most crane hooks. Here we see the 30" model cutting off a huge Pile Cap.



Feature (5). Crushers: for the Prime Concrete Pile Cutter. They are available in different shapes and sizes.

CONSISTENCY, SIMPLICITY, SPEED;

3 REASONS TO MAKE ANYONE SMILE

FOR MORE INFORMATION CALL LBT TOLL FREE AT 1-800-665-7396 OR 1-204-254-6424

VISIT OUR WEBSITE www.pilecutter.com OR EMAIL US AT prime@pilecutter.com

LBT ENTERPRISES LTD. 245 MELNICK RD. WINNIPEG, MANITOBA CANADA

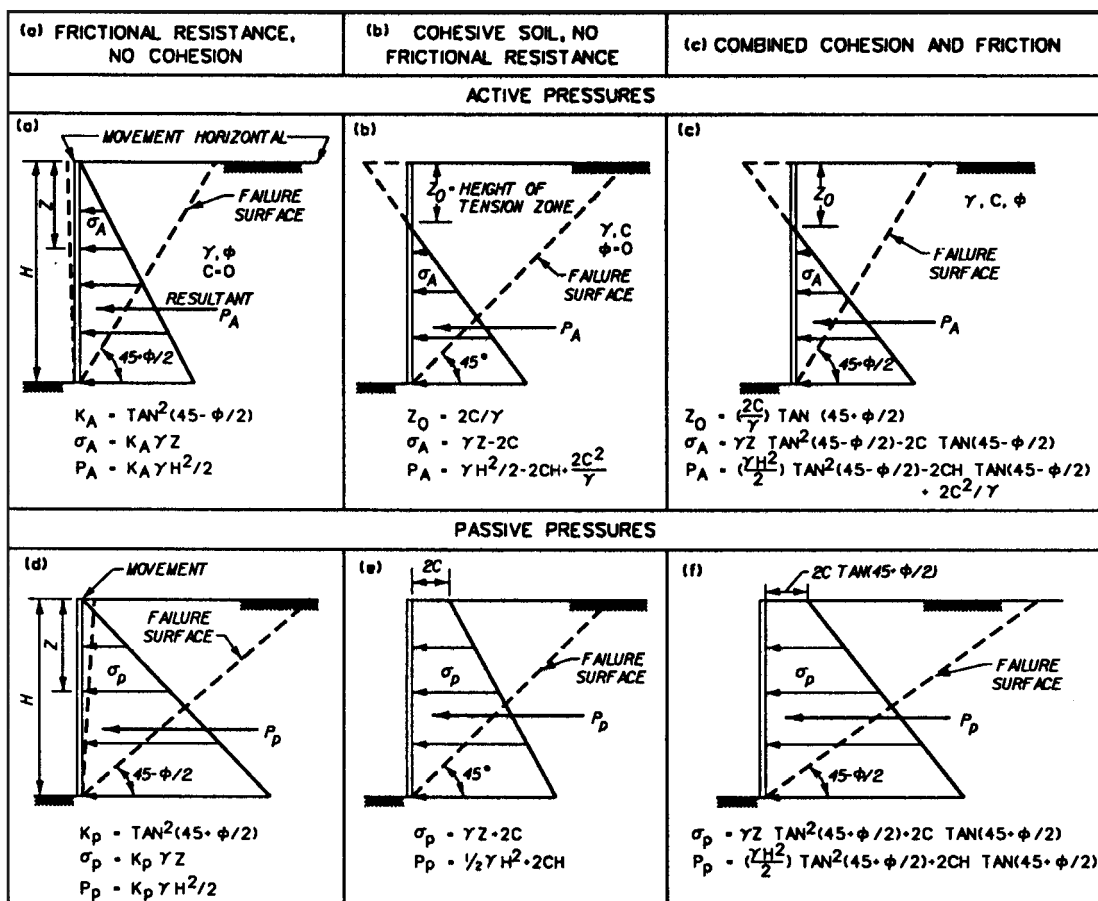


Figure 5-2: Computation of Rankine active and passive earth pressures for level backfills

When a state of failure has been reached, active and passive failure zones will develop as shown in Figure 5-2. With a level backfill, the failure planes rise at an angle of $45^\circ + \phi/2$ with the horizontal for the active case and $45^\circ - \phi/2$ for the passive case.

Rankine's work applied to cohesionless, granular soil exhibiting internal friction. Rankine developed coefficients K_a and K_p as functions of the angle of internal friction of the soil and the slope of the backfill. In 1910, Rankine's equations were expanded by Resal to include the cohesion value for soils that exhibit dual properties. These equations are illustrated in Figure 5-2. It is thus possible to analyse three types of soil, according to the strength parameters assigned for the soil:

1. Frictional ($c = 0, \phi \gg 0$);
2. Cohesive ($c = S_u, \phi = 0$); or
3. A combination of the two ($c \gg 0, \phi \gg 0$).

The Rankine method is generally a conservative approach³⁷ since it tends to underestimate passive pressure and overestimate active pressure. Rankine procedures are often utilized where soil properties have been estimated. Cohesion is generally an insignificant value in Rankine equations and is often ignored. The effects of surcharge and groundwater pressures

may be incorporated into theory. Rankine lateral earth pressure coefficients are tabulated in 18.1.

5.1.1. Active Earth Pressures

Let us begin by considering Equation 4-12. We can use this equation because Assumption 4 for Rankine theory states that the wall does not influence the state of stress in the backfill. From Equation 4-20, which also is based on the same assumption, the Rankine active earth pressure coefficient can be computed as

$$\text{Equation 5-1: } K_a = \tan^2\left(45^\circ - \frac{\phi}{2}\right)$$

This equation can also be written as

$$\text{Equation 5-2: } K_a = \frac{1 - \sin \phi}{1 + \sin \phi}$$

We can then substitute the value of K_a from Equation 5-1 into Equation 4-12 to obtain

$$\text{Equation 5-3: } \sigma_a = \gamma_t z K_a - 2c\sqrt{K_a} \quad (\text{see Equation 4-12})$$

If we define the quantity

$$\text{Equation 5-4: } K_{ac} = 2\sqrt{K_a}$$

³⁷ This is not always the case; see Figure 5-7 for comparisons with Coulomb and log-spiral theory for the active case and Figure 5-8 for the passive case.

Equation 5-3 reduces to

$$\text{Equation 5-5: } \sigma_a = \gamma_t z K_a - c K_{ac}$$

Considering first the case of a purely cohesionless and frictional soil, the second term of Equation 5-3 drops out to yield

$$\text{Equation 5-6: } \sigma_a = \gamma_t z K_a$$

The variation in the active earth pressure is linear with z , as shown in Figure 5-2(a). A planar slip surface extends upwards from the heel of the wall through the backfill, inclined at an angle α_A from horizontal. For frictional backfills, α_A is equal to

$$\text{Equation 5-7: } \alpha_A = 45^\circ + \frac{\phi}{2}$$

P_A is the resultant force of the σ_a distribution and is equal to

$$\text{Equation 5-8: } P_A = \frac{K_A \gamma_t H^2}{2}$$

acting normal to the back of the wall at one-third H above the heel of wall. In these expressions, γ is the dry unit weight.

Equation 5-6 assumes a dry, homogeneous soil. For soils that are layered and have the effects of the water table, a more general way of stating the active earth pressure is

$$\text{Equation 5-9: } \sigma_a = K_a \sigma'$$

It is important in any calculation for sheet piling to include all variations of soil unit weight and the effect of buoyancy at various depths. Equation 5-1 assumes a level backfill. For a dry frictional backfill inclined at an angle β from horizontal, the Rankine active earth pressure coefficient is determined by computing the resultant forces acting on vertical planes within an infinite slope verging on instability³⁸. K_A is equal to

$$\text{Equation 5-10: } K_A = \cos \beta \frac{\cos \beta - \sqrt{\cos^2 \beta - \cos^2 \phi}}{\cos \beta + \sqrt{\cos^2 \beta - \cos^2 \phi}}$$

with the limitation that β is less than or equal to ϕ . Equation 5-9 still applies but is inclined at the backfill slope angle β , as shown in Figure 5-3. The distribution of s_a is linear with depth along the back of the wall. Thus, there are shear stresses on vertical (and hence horizontal) planes. P_A is computed using Equation 5-8. It is inclined at an angle β from the normal to the back of the wall, and acts at one-third H above the heel of the wall.

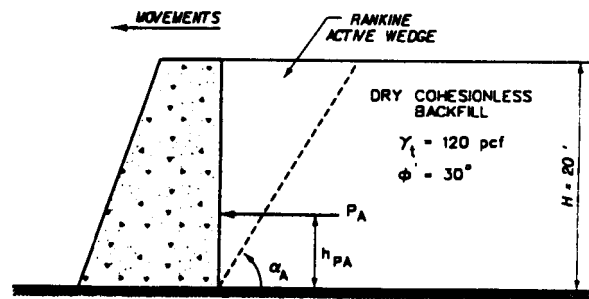
For purely cohesive soils, Equation 5-3 reduces to

$$\text{Equation 5-11: } \sigma_a = \gamma_t z - 2c$$

This equation shows that tensile stresses develop to a depth Z_0 at the top of the backfill to wall interface in a backfill whose shear strength is either fully or partially attributed to the cohesion or undrained strength. A gap may form within this region

over time. During rainstorms, these gaps will fill with water, resulting in hydrostatic water pressures along the back of the wall to depth Z_0 . Tensile stresses are set equal to zero over the depth Z_0 when applying this theory to long term wall designs because c' goes to zero with time for clayey soils due to changes in water content. For clayey backfills, retaining walls are designed using equivalent fluid pressure values³⁹ rather than active earth pressures because earth pressure theories do not account for the effects of creep in clayey backfills⁴⁰.

The P_A and α_A relationships for backfills whose strengths are defined using S_u or an effective cohesion and effective angle of internal friction are given in Figure 5-2. We will discuss the application of these concepts in more detail when dealing with wall design.



Example 1 Rankine Active Coefficients and Wall Pressures

For a wall of height $H = 20$ ft retaining a dry level cohesionless backfill with $\phi' = 30$ degrees and $\delta = 0$ degrees, compute K_A , α_A , and P_A .

$$\text{Equation 5-12: } K_A = \tan^2 (45^\circ - 30^\circ/2) \text{ (Equation 5-1)}$$

$$K_A = 1/3$$

$$\text{Equation 5-13: } P_A = \frac{1}{3} \cdot \frac{1}{2} (120 \text{ pcf}) (20 \text{ ft})^2 \text{ (Equation 5-8)}$$

$$P_A = 8,000 \text{ lb per ft of wall}$$

$$\text{Equation 5-14: } \alpha_A = 45^\circ + 30^\circ/2 \text{ (Equation 5-7)}$$

$$\alpha_A = 60^\circ \text{ from the horizontal}$$

$$h_{PA} = H/3 = 6.67 \text{ ft}$$

5.1.2. Passive Earth Pressures

The derivation of the Rankine theory of passive earth pressures follows the same steps as were used in the derivation of the active earth pressure relationships. The forces and stresses corresponding to this limiting state are shown in Figure 5-2 (d), (e), and (f) for a vertical wall retaining the three types of soil backfill. The effects of surcharge and groundwater pressures are not included in this figure. To develop passive earth pressures, the wall moves towards the backfill, with the resulting displacements sufficient to fully mobilize the shear resistance within the soil mass. The passive earth pressure, σ_p , normal to the back of the wall at depth z is equal to

³⁸This is described by Terzaghi, K. 1943, *Theoretical Soil Mechanics*, John Wiley & Sons, New York, and Taylor, D. 1948. *Fundamentals of Soil Mechanics*, John Wiley & Sons, Inc., New York, pp. 488-491.

³⁹Terzaghi, K., and Peck, R. 1967. *Soil Mechanics in Engineering Practice*, Second Edition, John Wiley & Sons, Inc., New York.

⁴⁰Clough, G. W. and Duncan, J. M. 1991. Chapter 6: Earth Pressures, in *Foundation Engineering Handbook*, Second Edition, edited by H. Y. Fang, Van Nostrand Reinhold, NY, pp. 223-235.

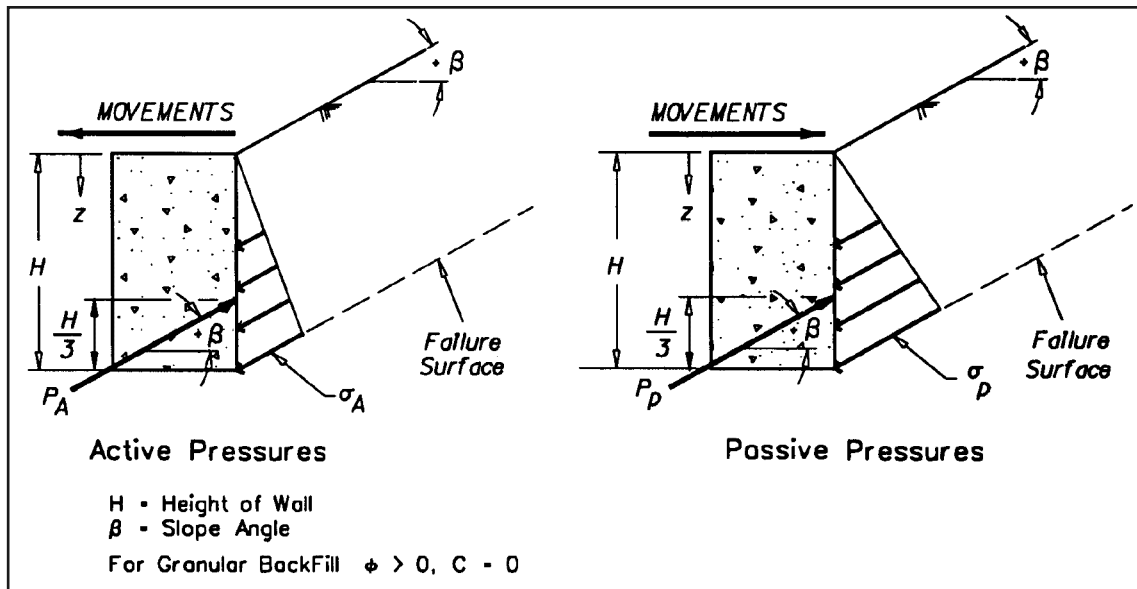


Figure 5-3: Rankine active and passive earth pressures for inclined backfills

Equation 5-15: $\sigma_p = \gamma_t z K_p + 2c\sqrt{K_p} = \sigma'_1$ (see Equation 4-9)

and the Rankine passive earth pressure coefficient, K_p , for level backfill is equal to

Equation 5-16: $K_p = \tan^2\left(45^\circ + \frac{\phi}{2}\right) = N_\phi$ (see Equation 4-9)

The passive earth pressure coefficient can also be written as

Equation 5-17: $K_p = \frac{1 + \sin \phi}{1 - \sin \phi}$

As with the active case, if we define the quantity

Equation 5-18: $K_{pc} = 2\sqrt{K_p}$

Equation 5-15 reduces to

Equation 5-19: $\sigma_p = \gamma_t z K_p + cK_{pc}$

A planar slip surface extends upwards from the heel of the wall through the backfill and is inclined at an angle α_p from horizontal, where α_p is equal to

Equation 5-20: $\alpha_p = 45^\circ + \frac{\phi}{2}$

P_p is the resultant force of the σ_p distribution and is equal to

Equation 5-21: $P_p = \frac{K_p \gamma H^2}{2}$

for dry frictional backfills and is normal to the back of the wall at one-third H above the heel of the wall. The P_p and α_p relationships for backfills whose strengths are defined using S_u or an effective cohesion and effective angle of internal friction are given in Figure 5-2. K_p for a frictional backfill inclined at an angle β from horizontal is equal to

Equation 5-22:

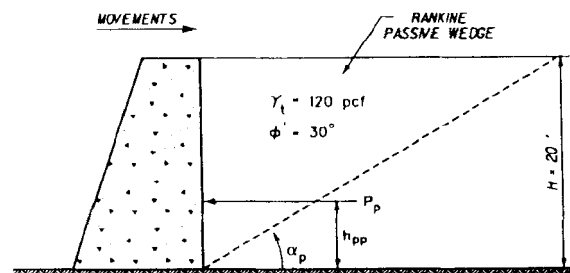
$$K_p = \cos \beta \frac{\cos \beta + \sqrt{\cos^2 \beta - \cos^2 \phi}}{\cos \beta - \sqrt{\cos^2 \beta - \cos^2 \phi}}$$

with the limitation that b is less than or equal to f. P_p is computed using Equation 5-21. It is inclined at an angle β from the normal to the back of the vertical wall, and acts at one-third H above the back of the wall. With $c = 0$, σ_p from Equation 5-15 becomes

Equation 5-23: $\sigma = \gamma_t z K_p$

The distribution of σ_p is linear with depth along the back of the wall and is inclined at the backfill slope angle β , as shown in Figure 5-3.

Passive pressures with cohesive soils will be dealt with in conjunction with the design of cantilever and anchored



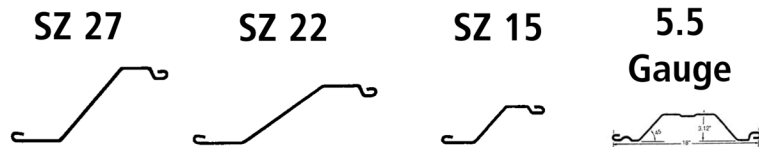
Example 2: Rankine Passive Coefficients and Wall Pressures

SHORELINE STEEL, INC.

P.O. Box 480519, 58201 Main Street • New Haven, MI 48048
(800) 522-9550 • (586) 749-9559 • Fax (586) 749-6653

www.shorelinesteel.com

We are a leading producer of domestic cold formed steel sheet piling in sections ranging from 10 gauge to 3/8" thick. For any sheet piling requirement we can satisfy your needs with a top quality product and prompt delivery.



	Thickness (Nominal)	Weight (Sq. ft.)	Weight (Lin. Ft.)	Sec. Mod in ⁴ (Ft. Wall)	Moment of Inertia in ⁴ (Ft. Wall)	Laying Width	Wall Depth
10-10 ga.	.134	7.2	10.8	2.2	3.5	18.00	3.12
8-8 ga.	.164	8.8	13.2	2.62	4.2	18.00	3.12
7-7 ga.	.179	9.6	14.4	2.8	4.4	18.00	3.12
6-6 ga.	.194	10.5	15.8	3.0	4.9	18.00	3.12
5-5 ga.	.209	11.3	16.9	3.4	5.4	18.00	3.12
LZ 8	.164	8.3	17.2	3.6	8.1	25.00	4.50
LZ 7	.179	9.1	18.8	3.9	8.9	25.00	4.50
LZ 5	.209	10.6	21.9	4.6	10.4	25.00	4.50
LZ 3	.239	11.9	24.6	5.2	11.8	25.00	4.50
LZ 250	.250	12.3	25.6	5.4	12.4	25.00	4.50
SZ-10	.164	9.4	17.2	7.3	27.4	22.00	7.50
SZ-11	.179	10.3	18.8	7.9	29.8	22.00	7.50
SZ-12	.209	12.0	21.9	9.2	34.8	22.00	7.50
SZ-14	.239	13.5	24.6	10.4	39.9	22.00	7.50
SZ-15	.250	14.0	25.6	10.9	41.8	22.00	7.50
SZ-14.5	.250	14.5	32.4	13.0	61.49	26.75	9.46
SZ-14.5	.270	15.8	35.1	14.0	86.40	26.75	9.46
SZ-18	.312	18.1	40.4	16.2	76.83	26.75	9.46
SZ-20	.340	19.8	44.1	17.5	83.37	26.75	9.46
SZ-21	.350	20.3	45.3	18.1	86.00	26.75	9.46
SZ-22	.375	21.8	48.6	19.3	91.92	26.75	9.46
SZ-222	.312	22.1	40.4	26.7	163.09	22.00	12.25
SZ-250	.250	15.9	32.4	16.6	89.42	24.46	10.75
SZ-313	.312	19.9	40.4	20.6	111.53	24.46	10.75
SZ-340	.340	21.5	44.1	22.4	121.45	24.46	10.75
SZ-350	.350	22.1	45.3	22.9	124.62	24.46	10.75
SZ-375	.375	23.7	48.6	24.5	133.55	24.46	10.75
SZ-24	.340	24.1	44.1	29.0	177.52	22.00	12.25
SZ-25	.350	24.8	45.3	29.7	181.91	22.00	12.25
SZ-27	.375	26.6	48.6	32.0	195.18	22.00	12.25

- All sections available in bare or galvanized steel.
- All Zee sections available in doubles.
- All sections produced exactly to customer specified length(s).
- All steel fully melted and manufactured in the USA.

Also Available:

- Corners
- Tees and Crosses
- Capping
- Coatings

DOMESTIC STEEL SHEET PILING



For more information, please call toll free
(800) 522-9550
 or visit our website at: www.shorelinesteel.com

SHORELINE STEEL, INC.

walls. For a wall of height $H = 20$ ft retaining a dry level cohesionless backfill with $\phi' = 30$ degrees and $\delta = 0$ degrees, compute K_p , α_p , and P_p .

Equation 5-24:

$$K_p = \tan^2 (45^\circ + 30^\circ/2) \text{ (Equation 5-16)}$$

$$K_p = 3.0$$

Equation 5-25:

$$P_p = 3.0 \cdot \frac{1}{2} (120 \text{ pcf}) (20')^2 \text{ (Equation 5-21)}$$

$$P_p = 72,000 \text{ lb per ft of wall}$$

Equation 5-26:

$$\alpha_p = 45^\circ - 30^\circ/2 \text{ (Equation 5-20)}$$

$$\alpha_p = 30^\circ \text{ from the horizontal}$$

$$h_{pp} = H/3 = 6.67 \text{ ft}$$

5.2. Coulomb Theory

Coulomb's work preceded Rankine's by over 50 years and was the basis for Rankine's and other subsequent research into soil pressures. Coulomb analyzed the equilibrium of wedge-shaped soil masses. The mass is assumed to be a rigid body sliding along a plane surface due to its own weight and uniform surcharge. The shear strength is mobilized uniformly along the failure plane, and includes cohesion and friction if both are present.

As the wall yields, the failure wedge tends to move downward for the active case. For the passive case, where the wall is forced against the soil, the wedge slides upward along the failure plane. These differential movements involve vertical displacements between the wall and backfill and create tangential stresses on the back of the wall due to soil friction and adhesion. The resulting force on the wall is, therefore, inclined at an angle normal to the wall. This angle is known as the angle of wall friction, δ . For the active case, when the active wedge slides downward relative to the wall, δ is taken as positive (+). For the passive case, when the passive wedge slides upward relative to the wall, δ is taken as negative.

The Coulomb equations have the advantage of providing a direct solution where the following conditions hold:

- There is only one soil material (material properties are constant). There can be more than one soil layer if all the soil layers are horizontal.
- The backfill surface is planar (it may be inclined).
- The backfill is completely above or completely below the water table, unless the top surface is horizontal, in which case the water table may be anywhere within the backfill.
- Any surcharge is uniform and covers the entire surface of the driving wedge.
- The backfill is cohesionless, unless the top surface is horizontal, in which case the backfill may be either cohesionless or cohesive.

The Coulomb theory of active and passive earth pressures looks at the equilibrium of the forces acting on a soil wedge, assuming that the wall movements are sufficient to fully mobilize the shear resistance along a planar surface that extends from the heel of the wall into the backfill as shown in Figure 5-4. Coulomb's wedge theory allows for shear stresses along the wall to backfill interface. The forces corresponding to the active and passive states of stress are shown in Figure 5-4 for a wall with a face inclined at angle $+\theta$ from vertical, retaining a frictional backfill inclined at angle $+\beta$. The effects of surcharge and groundwater pressures are not included in this figure. For virtually any sheet pile wall, $\theta = 0$.

Although Coulomb's equation solves only for forces, it is commonly expressed as the product of a constant horizontal pressure coefficient K and the area under a vertical effective stress diagram. Horizontal earth pressures can be calculated as the product of K times the effective vertical stress. Lateral earth pressure coefficients for Coulomb theory are tabulated in 18.2.

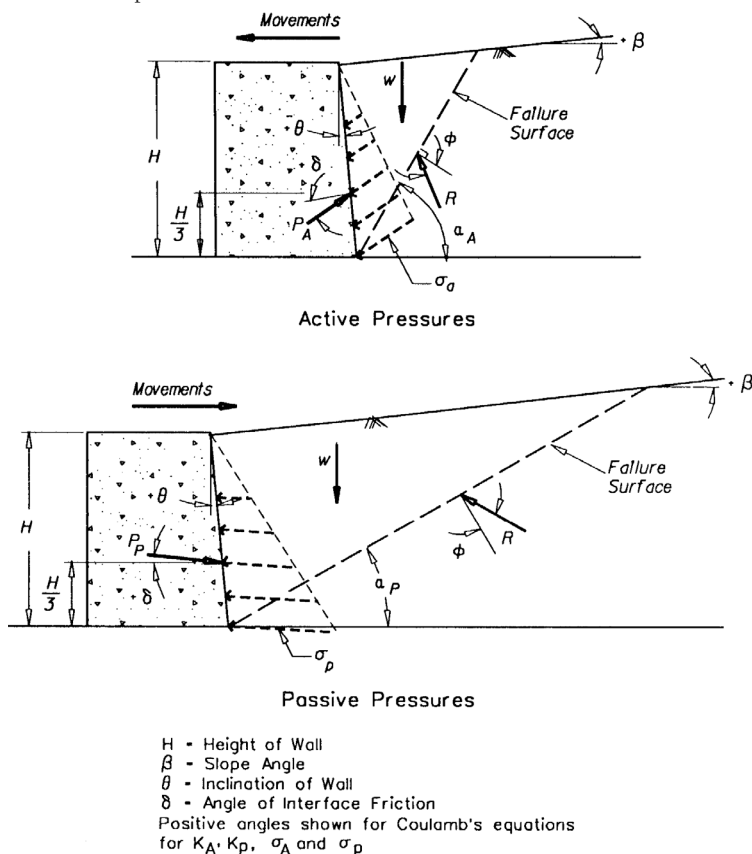


Figure 5-4: Coulomb active and passive earth pressures for inclined backfills and inclined walls

5.2.1. Active Earth Pressures

In the active case the wall movements away from the backfill are sufficient to fully mobilize the shear resistance within a soil wedge. Coulomb's theory assumes that the presence of the wall introduces shearing stress along the interface, due to the downward movement of

the backfill along the back of the wall as the wall moves away from the backfill. The active earth pressure force P_A is computed using Equation 5-8 and is oriented at an angle δ to the normal along the back of the wall at a height equal to $H/3$ above the heel, as shown in Figure 5-4. The shear component of P_A acts upward on the soil wedge due to the downward movement of the soil wedge along the face of the wall. K_A is equal to

Equation 5-27:

$$K_A = \frac{\cos^2(\phi - \theta)}{\cos^2\theta \cos(\theta + \delta) \left[1 + \sqrt{\frac{\sin(\phi + \delta) \sin(\phi - \beta)}{\cos(\delta + \theta) \cos(\beta - \theta)}} \right]^2}$$

for frictional backfills. For a level backfill and no wall inclination ($\beta = \theta = 0$), this equation reduces to

Equation 5-28:

$$K_a = \frac{\cos(\phi)^2}{\left(\sqrt{\sin(\phi) \sin(\phi + \delta)} + \sqrt{\cos(\delta)} \right)^2}$$

The active earth pressure, σ_a , along the back of the wall at depth z can be then computed and oriented at an angle d to the normal along the back of the wall. The variation in σ_a is assumed linear with depth for a dry backfill, as shown in Figure 5-4.

The planar slip surface extends upwards from the heel of the wall through the backfill and is inclined at an angle α_A from horizontal. α_A is equal to

Equation 5-29:

$$\alpha_A = \phi + \tan^{-1} \left[\frac{-\tan(\phi - \beta) + c_1}{c_2} \right]$$

$$c_1 = \sqrt{[\tan(\phi - \beta)][\tan(\phi - \beta) + \cot(\phi - \theta)][1 + \tan(\delta + \theta)\cot(\phi - \theta)]}$$

$$c_2 = 1 + [[\tan(\delta + \theta)] \cdot [\tan(\phi - \beta) + \cot(\phi - \theta)]]$$

One widely quoted reference for effective angles of friction along interfaces between various types of materials, δ , is Table 5-1⁴¹.

For a wall of height $H = 20'$ retaining a dry cohesionless backfill with $\phi' = 30$ degrees, $\delta = 3$ degrees, $\beta = 6$ degrees, and $\theta = 0$ degrees, compute K_A , α_A , and P_A .

Equation 5-30:

$$K_A = \frac{\cos^2(30-0)}{\cos^2(0) \cos(0+3) \left[1 + \sqrt{\frac{\sin(30+3) \sin(30-6)}{\cos(3+0) \cos(6-0)}} \right]^2}$$

(Equation 5-27)

$$K_A = 0.3465$$

$$\text{Equation 5-31: } P_A = 0.3465 \cdot \frac{1}{2} (120 \text{ pcF}) (20')^2 \quad (\text{Equation 5-8})$$

$$P_A = 8316 \text{ lb per ft of wall}$$

$$\text{Equation 5-32: } c_1 = \sqrt{[\tan(30-6)][\tan(30-6) + \cot(30)][1 + \tan(3)\cot(30)]}$$

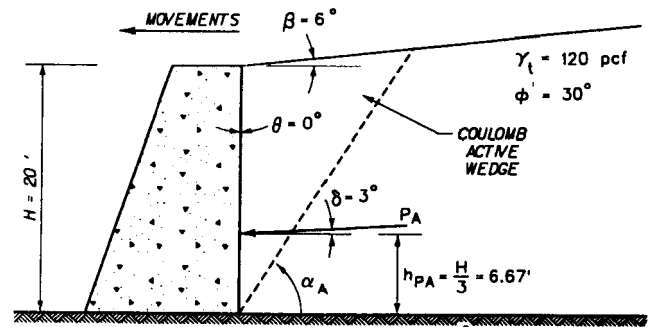
$$c_1 = 1.0283$$

$$c_2 = 1 + [[\tan(3)] \cdot [\tan(30-6) + \cot(30)]]$$

$$c_2 = 1.11411$$

$$\alpha_A = 30 + \tan^{-1} \left[\frac{-\tan(30-6) + 1.0283}{1.11411} \right] \quad (\text{Equation 5-29})$$

$$\alpha_A = 57.6^\circ \text{ from the horizontal}$$



Example 3: Coulomb Active Coefficients and Wall Pressures

5.2.2. Passive Earth Pressures

The forces and stresses corresponding to the passive states of stress are shown in Figure 5-4 for a wall with a face inclined at angle $+\theta$ from vertical, and retaining a frictional backfill inclined at angle $+\beta$. The effects of surcharge and groundwater pressures are not included in this figure. To develop passive earth pressures, the wall moves towards the backfill, with the resulting displacements sufficient to mobilize fully the shear resistance along the linear slip plane. Coulomb's theory allows for a shear force along the back of the walls that is due to the upward movement of the backfill as the wall moves towards the backfill. The passive earth pressure force P_p is computed using Equation 5-21 and oriented at an angle δ to the normal along the back of the wall at a height equal to $H/3$ above the heel of the wall, as shown in Figure 5-4. The shear component of P_p acts downward on the soil wedge due to the upward movement of the soil wedge along the face of the wall. This is the reverse of the situation for the shear component of P_A . K_p is equal to

Equation 5-33:

$$K_p = \frac{\cos^2(\phi + \theta)}{\cos^2\theta \cos(\delta - \theta) \left[1 - \sqrt{\frac{\sin(\phi + \delta) \sin(\phi + \beta)}{\cos(\delta - \theta) \cos(\beta - \theta)}} \right]^2}$$

for frictional backfills. For level backfill and no wall inclination ($\beta = \theta = 0$), this reduces to

Equation 5-34:

$$K_p = \frac{\cos(\phi)^2}{\left(\sqrt{\sin(\phi) \sin(\phi + \delta)} - \sqrt{\cos(\delta)} \right)^2}$$

⁴¹Potyondy, J. C. 1961 (Dec). "Skin Friction Between Various Soils and Construction Materials," *Geotechnique*, Vol II, No. 4, pp 339-353, and Peterson, M. S., Kulhawy, F. H., Nucci, L. R., and Wasil, B. A. 1976, "Stress-Deformation Behavior of Soil-Concrete Interfaces," Contract Report B-49, Department of Civil Engineering, Syracuse University, Syracuse, NY, also provide recommendations for d values from static direct shear test results.

The passive earth pressure, σ_p , along the back of the wall at depth z is computed using Equation 5-23 and oriented at an angle δ to the normal along the back of the wall. The variation in σ_p is assumed linear with depth for a dry backfill, as shown in Figure 5-4.

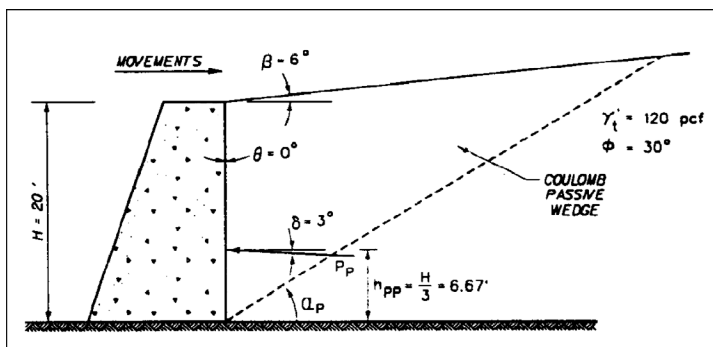
The planar slip surface extends upwards from the heel of the wall through the backfill and is inclined at an angle α_p from horizontal. α_p equal to

Equation 5-35:
$$\alpha_p = -\phi + \tan^{-1} \left[\frac{\tan(\phi + \beta) + c_3}{c_4} \right]$$

where

$$c_3 = \sqrt{[\tan(\phi + \beta)][\tan(\phi + \beta) + \cot(\phi + \theta)][1 + \tan(\delta - \theta)\cot(\phi + \theta)]}$$

$$c_4 = 1 + \{[\tan(\delta - \theta)] \cdot [\tan(\phi + \beta) + \cot(\phi + \theta)]\}$$



Example 4: Coulomb Passive Coefficients and Wall Pressures

Coulomb passive earth pressure coefficients must be used with *great care*; see the following section on the log-spiral theory for details.

Equation 5-36:
$$K_p = \frac{\cos^2(30+0)}{\cos^2(0) \cos(3-0) \left[1 - \sqrt{\frac{\sin(30+3) \sin(30+6)}{\cos(3-0) \cos(6-0)}} \right]^2}$$
 (Equation 5-33)

$$K_p = 4.0196$$

Equation 5-37:
$$P_p = 4.0196 \cdot \frac{1}{2} (120 \text{ pcf}) (20')^2$$
 (Equation 5-21)

$$PP = 96,470 \text{ lb per ft of wall}$$

Equation 5-38:
$$c_3 = \sqrt{[\tan(30+6)] [\tan(30+6) + \cot(30)] [1 + \tan(3)\cot(30)]}$$

$$c_3 = 1.3959$$

$$c_4 = 1 + \{[\tan(3)] \cdot [\tan(30+6) + \cot(30)]\}$$

$$c_4 = 1.1288$$

$$\alpha_p = -30 + \tan^{-1} \left[\frac{\tan(30+6) + 1.3959}{1.1288} \right]$$
 (Equation 5-35)

$$\alpha_p = 32.0^\circ \text{ from the horizontal}$$

For wall of height $H = 20$ ft retaining a dry cohesionless backfill with $\phi' = 30$ degrees, $\delta = 3$ degrees, $\beta = 6$ degrees, and $\theta = 0$ degrees, compute K_p , α_p , and P_p .

5.3. Log-Spiral Theory

Equation 5-33 and Equation 5-35 provide reasonable estimates for K_p and the orientation of the slip plane, α_p , so long as δ is restricted to values that are less than $\phi/2$. Coulomb's relationship overestimates the value for K_p when δ is greater than $\phi/2$. The large shear component of P_p introduces significant curvature in the failure surface. The Coulomb procedure, however, restricts the theoretical slip surface to a plane. Figure 5-5 and Figure 5-6 show the variation in the values for K_p with friction angle, computed using Coulomb's equation for K_p based on a plane failure surface versus a curved log spiral failure surface analysis. When δ is greater than $\phi/2$, the value for K_p must be computed using a method of analysis which uses a curved failure surface to obtained valid values.

Values for the active and passive earth pressure coefficients are presented in Figure 18-16, which provides values for K_A and K_p for walls with vertical faces (as is typical with sheet piling) retaining horizontal or inclined backfills⁴². The sign convention for the angles is shown in the insert figures in Figure 18-16. Note that the sign convention for δ is determined by the orientation of the shear stress acting on the wedge of the soil. δ is positive when the shear is acting upward on the soil wedge, the usual case for active pressures, and negative if the shear acts downward on the soil mass, the usual case for passive pressures. The values for K_A and K_p from these figures and this table are accurate for all values of d less than or equal to ϕ . A comparison between the active log-spiral coefficients and those from Rankine and Coulomb theories is shown in Figure 5-7; the passive coefficients are compared in Figure 5-8.

5.4. Earth Pressures Computed Using the Trial Wedge Procedure

The trial wedge procedure of analysis is used to calculate the earth pressure forces acting on walls when the backfill supports point loads or loads of finite width or when there is seepage within the backfill. The procedure involves the solution of the equations of equilibrium for a series of trial wedges within the backfill for the resulting earth

⁴² In Figure 18-16, if the backfill slopes upward from the wall, the ratio of δ/ϕ is considered to be negative, and this ratio becomes positive if the backfill slopes downward from the wall.



ABI'S TELESCOPIC, 180 DEGREE ROTATING MAST

Work in tight spaces and still get high production
Keep the rigs busy with 5 different attachments
Vibrate, drill, impact & press piles and shoring

HIGH PRODUCTION, REQUIRES LITTLE SPACE



beam on the left

ABI
300 trench feet/day



rig on the same spot

plate on the right



Drive sheet pile on both sides, track forward

ASK FOR OUR VIDEO



Press sheet pile in limited space

HAMMER & STEEL, INC
(WEST COAST)
TOLL FREE: 877-224-3356
www.abi-delmag.com

CALL FOR SALES & RENTALS

HAMMER & STEEL, INC
(MID-WEST & EAST COAST)
TOLL FREE: 800-325-7453
www.hammersteel.com

Table 5-1: Ultimate Friction Factors for Dissimilar Materials

Interface Materials	Friction Factor, $\tan \delta$	Friction angle, δ degrees
Mass concrete on the following foundation materials:		
Clean sound rock.....	0.70	35
Clean gravel, gravel-sand mixtures, coarse sand...	0.55 to 0.60	29 to 31
Clean fine to medium sand, silty medium to coarse sand, silty or clayey gravel.....	0.45 to 0.55	24 to 29
Clean fine sand, silty or clayey fine to medium sand.....	0.35 to 0.45	19 to 24
Fine sandy silt, nonplastic silt.....	0.30 to 0.35	17 to 19
Very stiff and hard residual or preconsolidated clay.....	0.40 to 0.50	22 to 26
Medium stiff and stiff clay and silty clay.....	0.30 to 0.35	17 to 19
(Masonry on foundation materials has same friction factors.)		
Steel sheet piles against the following soils:		
Clean gravel, gravel-sand mixtures, well-graded rock fill with spalls.....	0.40	22
Clean sand, silty sand-gravel mixture, single size hard rock fill.....	0.30	17
Silty sand, gravel or sand mixed with silt or clay	0.25	14
Fine sandy silt, nonplastic silt.....	0.20	11
Formed concrete or concrete sheet piling against the following soils:		
Clean gravel, gravel-sand mixture, well-graded rock fill with spalls.....	0.40 to 0.50	22 to 26
Clean sand, silty sand-gravel mixture, single size hard rock fill.....	0.30 to 0.40	17 to 22
Silty sand, gravel or sand mixed with silt or clay	0.30	17
Fine sandy silt, nonplastic silt.....	0.25	14
Various structural materials:		
Masonry on masonry, igneous and metamorphic rocks:		
Dressed soft rock on dressed soft rock.....	0.70	35
Dressed hard rock on dressed soft rock.....	0.65	33
Dressed hard rock on dressed hard rock.....	0.55	29
Masonry on wood (cross grain).....	0.50	26
Steel on steel at sheet pile interlocks.....	0.30	17

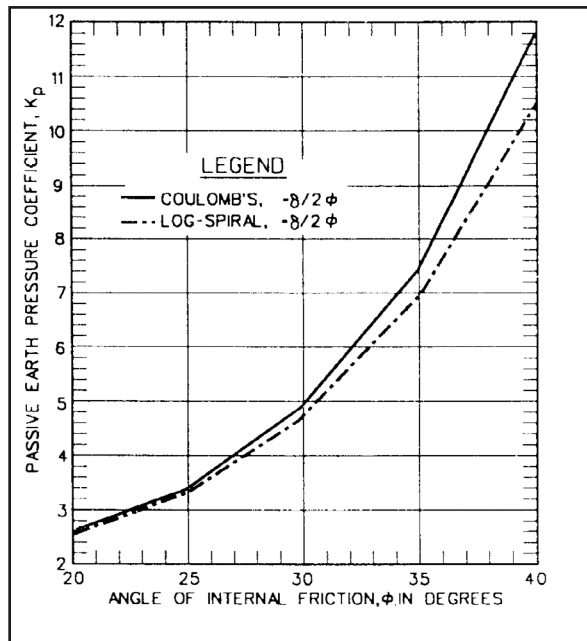


Figure 5-5: Coulomb and log-spiral passive earth pressure coefficients with $\delta = \phi/2$ -vertical wall and level backfill

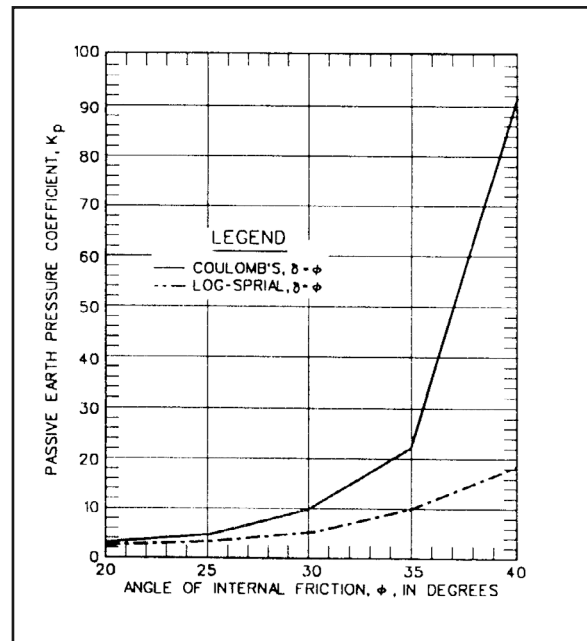


Figure 5-6: Coulomb and log-spiral passive earth pressure coefficients with $\delta = \phi$ -vertical wall and level backfill

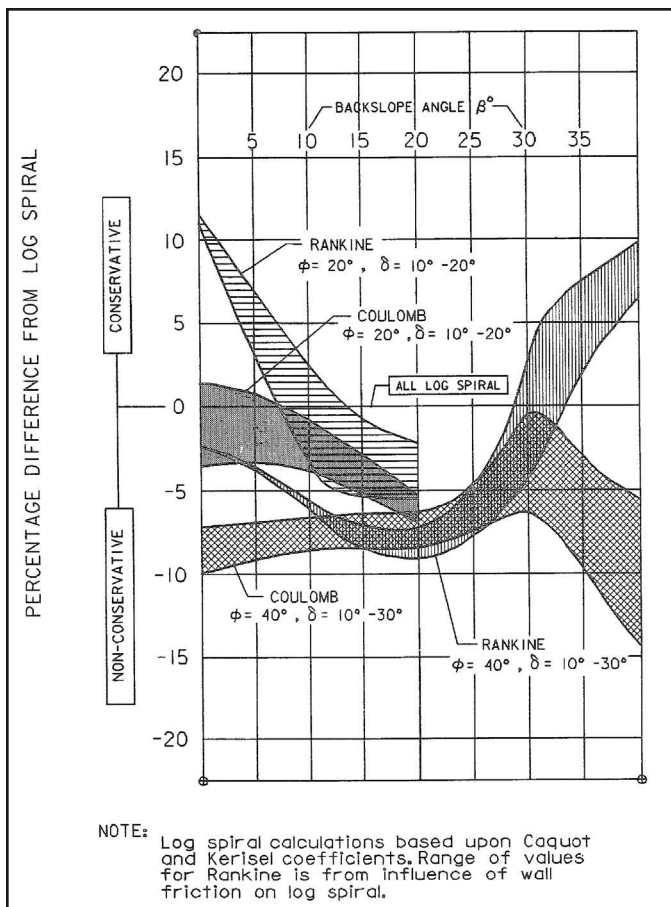


Figure 5-7: Comparison of Active Earth Pressure Coefficients⁴³

pressure force on the back of the wall. When applying this procedure to active earth pressure problems, the shear strength along the trial slip plane is assumed to be fully mobilized. The active earth pressure force is equal to the largest value for the earth pressure force acting on the wall obtained from the series of trial wedge solutions. The steps involved in the trial wedge procedure are described using the retaining wall problem shown in Figure 5-9⁴⁴.

A 20 feet high wall retains a saturated sand backfill with ϕ equal to 30 degrees and δ equal to 30 degrees. The backfill is drained by a vertical gravel drain along the back of the wall, with weep holes along its base. In this problem, a heavy rainfall is presumed to have resulted in steady state seepage within the backfill. The solution for the active earth pressure force on the back of the wall using the trial wedge procedure is outlined in the following eight steps.

1) Determine the variation in pore water pressures within the backfill. In this example the flow net for steady state seepage is constructed graphically and is shown in Figure 5-9.

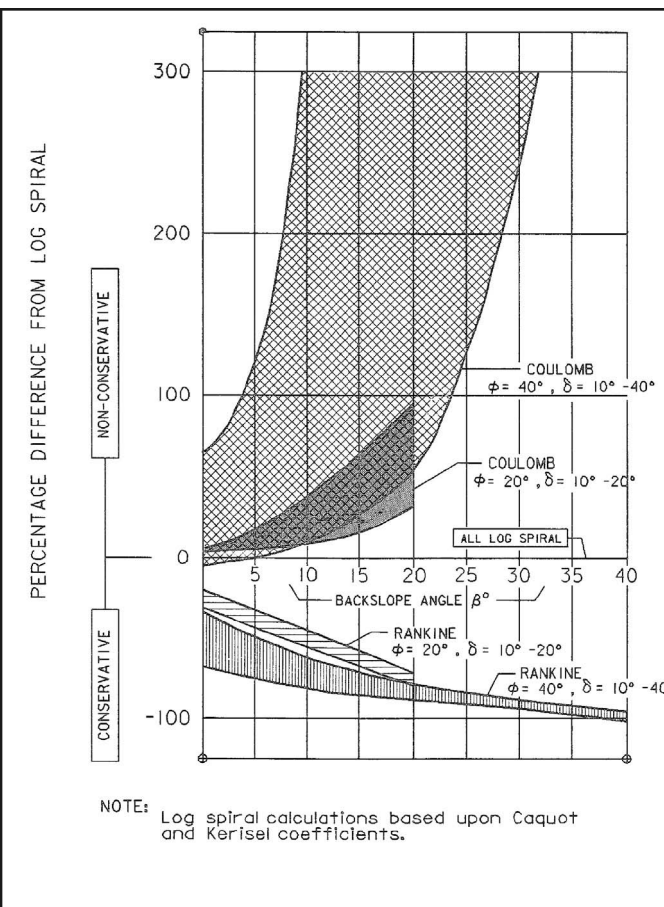


Figure 5-8: Comparison of Passive Earth Pressure Coefficients⁴³

2) Assume an inclination for the trial slip surface, α , defining the soil wedge to be analysed.

3) Assume sufficient displacement so the shear strength of the sand is fully mobilized along the plane of slip, resulting in active earth pressures. For this condition, the shear force, T , required for equilibrium along the base of the soil wedge is equal to the ultimate shear strength force along the slip surface.

Equation 5-39: $T = N \tan\phi$

4) Calculate the total weight of the soil within the trial wedge, W .

5) Calculate the variation in pore water pressure along the trial slip surface. Using the flow net, the pore water pressure is computed at a point by first solving for h_p , using Equation 7-10, and then computing u using Equation 7-11. An example of the distribution in u along the trial slip surface for $\alpha = 45$ degrees is shown in Figure 5-9.

6) Calculate the pore water pressure force. $U_{static} - \alpha$, acting

⁴³Driscoll, D. D. 1979 (Dec). Retaining Wall Design Guide, Foundation Services, Inc., Portland, OR, Prepared for USDA Forest Service. Available from: USDA Forest Service Region 6, 319 S.W. Pine St., Portland, OR 97208 or a more detailed description of the various types of sheet piling and their installation, see *Pile Driving by Pile Buck*, available from Pile Buck.

⁴⁴This problem was originally solved by Terzaghi, K. 1943, *Theoretical Soil Mechanics*, John Wiley & Sons, New York.) and described by Lambe, T. and Whitman, R. 1969, *Soil Mechanics*, John Wiley & Sons, Inc., New York, Chapters 13 and 23.

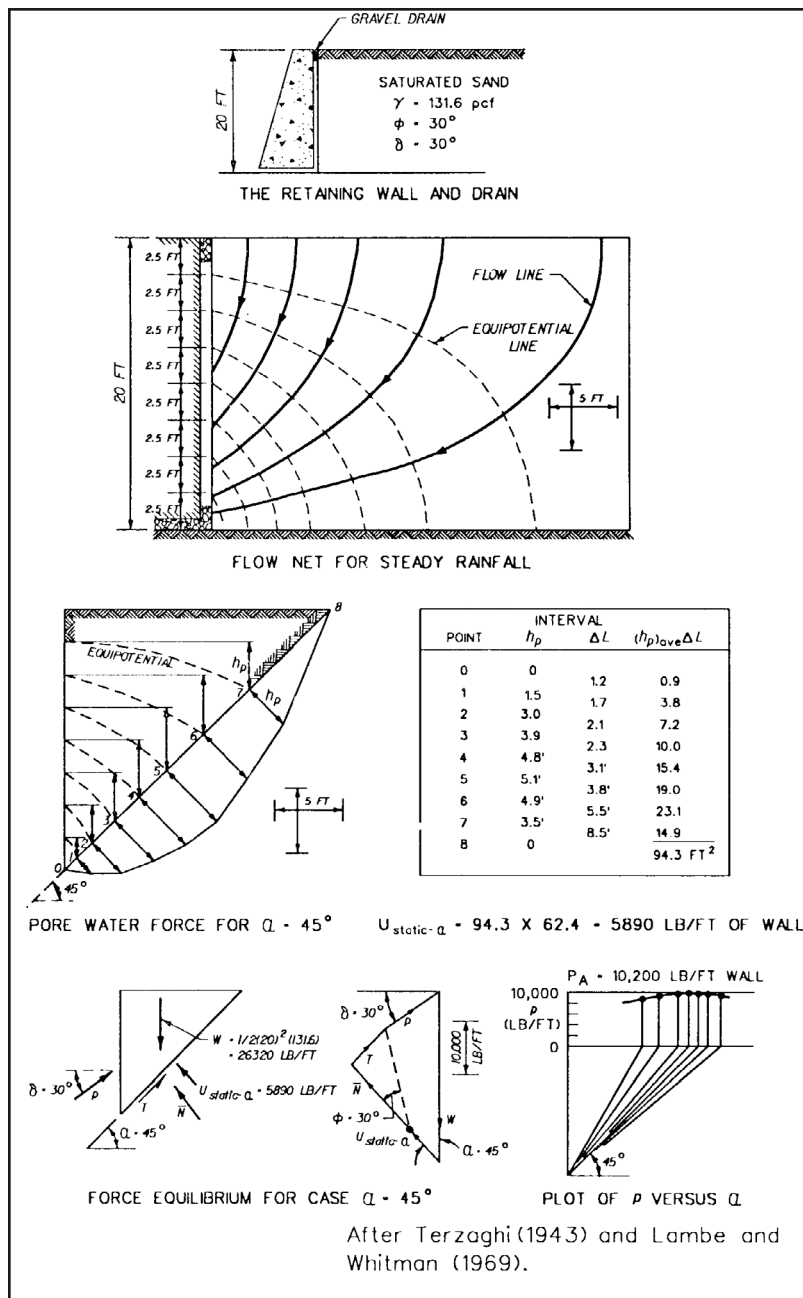


Figure 5-9 Example of trial wedge procedure

normal to the trial slip surface, inclined at angle α to the horizontal. $U_{static-\alpha}$ is the resultant of the pore water pressures calculated in step (5).

7) Analyse the trial wedge for the corresponding effective earth pressure force, P , acting at an angle $\delta = 30$ degrees to the normal to the back of the wall. Using the equations of equilibrium ($\sum F_x = 0$ and $\sum F_y = 0$), the resulting equation for the unknown force P is equal to

Equation 5-40:

$$P = \frac{(W - U_{static-\alpha} \cos \alpha) \tan(\alpha - \phi) + U_{static-\alpha} \sin \alpha}{\sin \delta \tan(\alpha - \phi) + \cos \delta}$$

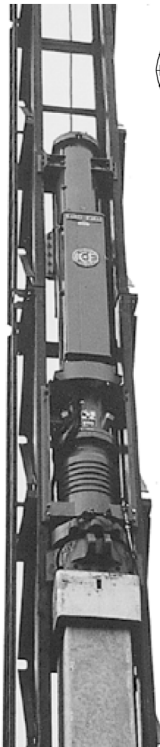
Note that because of the presence of the free flowing drain along the back of the wall in which the total head equals the elevation head, the pore water pressures are equal to zero along the back of the wall.

8) Repeat steps 2 through 7 for other trial slip surfaces until the largest value for P is computed, as shown in Figure 5-9. The slip surface that maximizes the value for P corresponds to the critical slip surface, $\alpha_A = \alpha$ and $P_A = P$. In this case, $\alpha_A = 45$ degrees, and $P_A = 10,300$ pounds per foot of wall and acts at $\delta = 30$ degrees from the normal to the back of the wall.

2 COMPLETE LINES OF DIESEL HAMMERS . . .

1 SOURCE!

Now you can select from two complete lines of diesel hammers - the fuel-injected S-Series or the legendary design of the I-Series - from one solid source — ICE. Contact your ICE rep today to determine which type of diesel hammer will help make your jobs the most profitable.



FUEL-INJECTED DIESELS

- Compression-timed fuel injection.
- Fast starts, even in cold weather.
- Optimum combustion.
- Redesigned components.
- Special coatings for durability.
- Seven models.
- Ram weights from 3000 to 20,000 lbs.
- Fully backed by ICE service & support.

MODEL	RAM WEIGHT	RATED ENERGY
325	3,000 lbs. (1361 kg)	26,000 ft.-lbs. (35.3 kJ)
425	4,088 lbs. (1854 kg)	42,000 ft.-lbs. (57 kJ)
605	7,000 lbs. (3175 kg)	60,000 ft.-lbs. (81.3 kJ)
805	8,000 lbs. (3629 kg)	80,000 ft.-lbs. (108.5 kJ)
1005	10,000 lbs. (4536 kg)	100,000 ft.-lbs. (135.6 kJ)
1205	12,000 lbs. (5443 kg)	120,000 ft.-lbs. (162.7 kJ)
2055	20,000 lbs. (9072 kg)	170,000 ft.-lbs. (203.5 kJ)



I-SERIES DIESELS

- Based on the legendary design.
- Simple splash fuel system.
- More bpm in more varied soils.
- 9 models.
- Ram weights from 1,760 to 22,100 lbs.
- Most rated energy in their class.
- Low maintenance.
- Competitively priced.
- Fully backed by ICE service & support.

MODEL	RAM WEIGHT	RATED ENERGY
I-8	1,760 lbs. (803 kg)	20,100 ft.-lbs. (27,252 Nm)
I-12	2,822 lbs. (1280 kg)	30,200 ft.-lbs. (40,960 Nm)
I-19	4,015 lbs. (1820 kg)	43,225 ft.-lbs. (58,605 Nm)
I-30	6,615 lbs. (3000 kg)	71,700 ft.-lbs. (97,212 Nm)
I-36	7,940 lbs. (3600 kg)	90,540 ft.-lbs. (122,756 Nm)
I-46	10,145 lbs. (4602 kg)	107,700 ft.-lbs. (146,022 Nm)
I-62	14,600 lbs. (6623 kg)	165,000 ft.-lbs. (223,710 Nm)
I-80	17,700 lbs. (8030 kg)	212,400 ft.-lbs. (287,976 Nm)
I-100	22,100 lbs. (10,024kg)	265,500 ft.-lbs. (359,970 Nm)



INTERNATIONAL CONSTRUCTION EQUIPMENT, INC.
www.iceusa.com

301 Warehouse Drive • Matthews, NC 28104
 Phones: 888 ICEUSA1 & 704 821-8200
 Fax: 704 821-8201 • e-mail: info@iceusa.com



Matthews NC • Lakeland FL • Metairie LA • Seattle WA • New Town Square PA • Sayreville NJ • Houston TX
 Fort Wayne IN • Virginia Beach VA • Boston MA • Montreal Quebec • Singapore • Kuala Lumpur • Shanghai

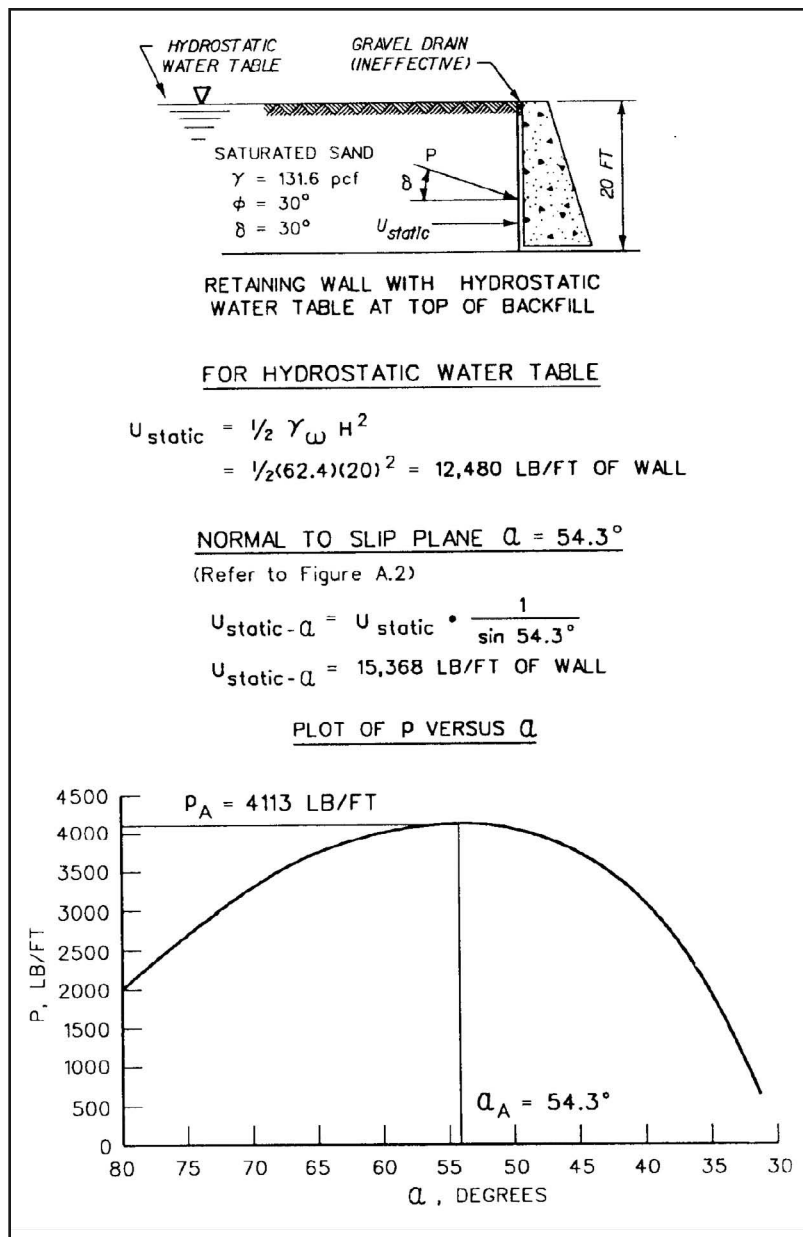


Figure 5-10: Example of trial wedge procedure, hydrostatic water table

5.4.1. Hydrostatic Water Pressures⁴⁵

Consider the possibility is that the drain shown in Figure 5-9 does not function as intended and hydrostatic pore water pressures develop along the back of the wall as shown in Figure 5-10.

For each slip surface analysed using the trial wedge method the effective force P, acting at angle δ to the normal for the wall, is given as

Equation 5-41:

$$P = \frac{[W - U_{static-\alpha} \cos \alpha] \tan(\alpha - \phi')}{\cos \delta + \sin \delta \tan(\alpha - \phi')}$$

The hydrostatic water pressure forces acting normal to the slip surface and normal to the back of the wall are $U_{static-\alpha}$

and U_{static} , respectively, and are computed as follows: The pore water pressure at the ground water table (Figure 5-11) is

Equation 5-42: $u_{static}^{top} = 0$

For a hydrostatic water table the pore water pressure distribution is linear with depth, and at the bottom of the wedge is computed as

Equation 5-43: $u_{static}^{bot} = \gamma_w H_w$

The static pore pressure distribution immediately behind the wall is triangular and the resultant force may be calculated as

⁴⁵ More information on hydrostatic pressures can be found in 7.1. Not all hydrostatic pressure problems require solution using the trial wedge method.

Equation 5-44: $U_{static} = \frac{1}{2} \gamma_w H_w^2$

The static pore pressure force acting along the planar slip surface is also triangular and the resultant force may be computed as

Equation 5-45: $U_{static-\alpha} = \frac{1}{2} \gamma_w H_w^2 \frac{1}{\sin \alpha}$

Other than this consideration, the solution of the trial wedge analysis to compute the active earth pressure force follows the same eight steps described previously.

Using the trial wedge procedure for the problem shown in Figure 5-10, the wedge that maximizes the value for P corresponds to the critical slip surface, $\alpha_A = 54.34$ degrees, and $P_A = 4,113$ pounds per foot of wall which acts at $d = 30$ degrees from the normal to the back of the wall. Although P_A for the ineffective drain case (Figure 5-10) is 6,087 pounds per foot less than for the effective drain case (Figure 5-9), the total horizontal design load for the ineffective drain is larger by 7,208 pounds per foot of wall compared to the effective drain case due to the contribution of the water pressure force ($U_{static} = 12,480$ pounds per foot of wall).

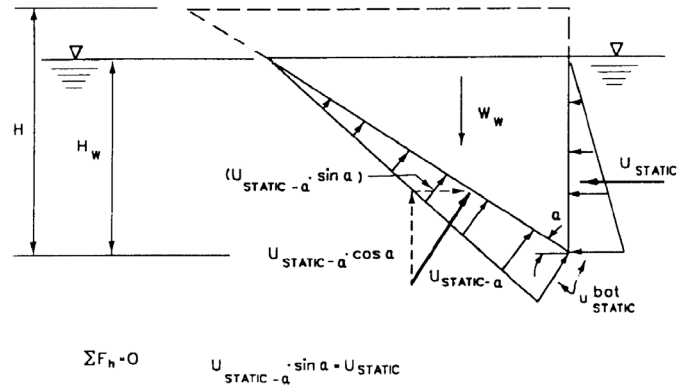


Figure 5-11: Equilibrium of horizontal hydrostatic water pressure forces acting on backfill wedge

A closed form solution exists for this example, as P_A may be calculated using Equation 5-8, with K_A computed using the Coulomb Equation 5-27. The corresponding critical slip surface α_A is given in Equation 5-29.

Chapter Six:

Dynamic Earth Pressures

6.1. Overview of Earthquake Loads

6.1.1. Limit States

A broad look at the problem of seismic safety of waterfront structures involves the three general limit states shown which should be considered in design.

1. Gross site instability: This limit state involves lateral earth movements exceeding several feet. Such instability would be the result of liquefaction of a site, together with failure of an edge retaining structure to hold the liquefied soil mass in place. Liquefaction of backfill is a problem associated with the site, mostly independent of the type of retaining structure. Failure of the retaining structure might result from overturning, sliding, or a failure surface passing beneath the structure. Any of these modes might be triggered by liquefaction of soil beneath or behind the retaining structure. There might also be a structural failure, such as failure of an anchorage that is a common problem if there is liquefaction of the backfill.

2. Unacceptable movement of retaining structure: Even if a retaining structure along the waterfront edge of a site remains essentially in place, too much permanent movement of the structure may be the cause of damage to facilities immediately adjacent to the quay. Facilities of potential concern include cranes and crane rails, piping systems, warehouses, or other buildings. Tilting and/or sliding of massive walls or excessive deformations of anchored bulkheads may cause permanent outward movement of retaining structures. Partial liquefaction of backfill will make such movements more likely, but this limit state is of concern even if there are no problems with liquefaction.

3. Local instabilities and settlements: If a site experiences liquefaction and yet is contained against major lateral flow, buildings and other structures founded at the site may still experience unacceptable damage. Possible modes of failure include bearing capacity failure, excessive settlements, and tearing apart via local lateral spreading. Just the occurrence of sand boils in buildings can seriously interrupt operations and lead to costly clean-up operations.

6.1.2. Key Role of Liquefaction Hazard Assessment

The foregoing discussion of general limit states has emphasized problems due to soil liquefaction. Backfills behind waterfront retaining structures often are cohesionless soils, and by their location have relatively high water tables. Cohesionless soils may also exist beneath the base or on the

waterside of such structures. Waterfront sites are often developed by hydraulic filling using cohesionless soils, resulting in low-density fills that are susceptible to liquefaction. Thus, liquefaction may be a problem for buildings or other structures located well away from the actual waterfront. Hence, evaluation of potential liquefaction should be the first step in analysis of any existing or new site, and the first step in establishing criteria for control of newly placed fill. The word “liquefaction” has been applied to different but related phenomena. To some, it implies a flow failure of an earthen mass in the form of slope failure or lateral spreading, bearing capacity failure, etc. Others use the word to connote a number of phenomena related to the build-up of pore pressures within soil, including the appearance of sand boils and excessive movements of buildings, structures, or slopes. Situations in which there is a loss of shearing resistance, resulting in flow slides or bearing capacity failures clearly are unacceptable. However, some shaking-induced increase in pore pressure may be acceptable, provided it does not lead to excessive movements or settlements.

Application of the procedures set forth in this book may require evaluation of: (a) residual strength for use in analyzing for flow or bearing capacity failure; or (b) build-up of excess pore pressure during shaking. As a general design principle, the predicted build-up of excess pore pressure should not exceed 30 to 40 percent of the initial vertical effective stress, except in cases where massive walls have been designed to resist larger pore pressures and where there are no nearby buildings or other structures that would be damaged by excessive settlements or bearing capacity failures. With very loose and contractive cohesionless soils, flow failures occur when the residual excess pore pressure ratio reaches about 40 percent⁴⁶. Even with soils less susceptible to flow failures, the actual level of pore pressure build-up becomes uncertain and difficult to predict with confidence when the excess pore pressure ratio reaches this level.

6.1.3. Choice of Design Ground Motions

A key requirement for any analysis for purposes of seismic design is a quantitative specification of the design ground motion. In this connection, it is important to distinguish between the level of ground shaking that a structure or facility is to resist safely and a parameter, generally called a seismic coefficient that is used as input to a simplified, pseudo-static analysis.

6.1.3.1. Design Seismic Event

Most often a design seismic event is specified by peak acceleration. However, more information concerning the

⁴⁶The word “contractive” reflects the tendency of a soil specimen to decrease in volume during a drained shear test. During undrained shearing of a contractive soil specimen, the pore water pressure increases, in excess of the pre-sheared pore water pressure value. “Dilative” soil specimens exhibit the opposite behavior; an increase in volume during drained shear testing and negative excess pore water pressures during undrained shear testing. Loose sands and dense sands are commonly used as examples of soils exhibiting contractive and dilative behavior, respectively, during shear.



LARGE DIAMETER DRILL SHAFT EQUIPMENT



SALES / RENTALS / ENGINEERING

Crane Mounted Drills, Pile Top Drills, Circulation Drill Strings, Kelly Bars, Circulation Swivels, Flat Bottom DC/RC Bits, Dual Wall Core Barrels, Core Breaker/Retrievers, Drill Pipe, Augers, Drill Buckets, Core Barrels, Cleanout Buckets, Belling Tools, Drop Chisels, Special Tooling

713 E. WALNUT STREET GARLAND, TEXAS 75040

U.S.A. TOLL FREE 1-800-527-1315

PHONE (972) 272-6461 FAX (972) 272-9194

WWW.SMHAINCO.COM

ground motion often is necessary. Duration of shaking is an important parameter for analysis of liquefaction. Magnitude is used as an indirect measure of duration. For estimating permanent displacements, specification of either peak ground velocity or predominant period of the ground motion is essential. Both duration and predominant periods are influenced strongly by the magnitude of the causative earthquake, and hence magnitude sometimes is used as a parameter in analyses.

Unless the design event is prescribed for the site in question, peak accelerations and peak velocities may be selected using one of the following approaches:

1. By using available maps for the contiguous 48 states. Such maps are available for several different levels of risk, expressed as probability of non-exceedance in a stated time interval or mean recurrence interval. A probability of non-exceedance of 90 percent in 50 years (mean recurrence interval of 475 years) is considered normal for ordinary buildings.
2. By using attenuation relations giving ground motion as a function of magnitude and distance. This approach requires a specific choice of a magnitude of the causative earthquake, requiring expertise in engineering seismology. Once this choice is made, the procedure is essentially deterministic. Generally it is necessary to consider various combinations of magnitude and distance.
3. By a site-specific probabilistic seismic hazard assessment. Seismic source zones must be identified and characterized, and attenuation relations must be chosen. Satisfactory accomplishment of such an analysis requires considerable expertise and experience with input from both experienced engineers and seismologists. This approach requires selection of a level of risk.

It is of greatest importance to recognize that, for a given site, the ground motion description suitable for design of a building may not be appropriate for analysis of liquefaction.

6.1.3.2. Local soil conditions

The soil conditions at a site should be considered when selecting the design ground motion. Attenuation relations are available for several different types of ground conditions, and hence the analyses in items (2) and (3) might be made for any of these particular site conditions. However, attenuation relations applicable to the soft ground conditions often found at waterfront sites are the least reliable. The maps referred to under item (1) apply for a specific type of ground condition: soft rock. More recent maps will apply for deep, firm alluvium, after revision of the document referenced in item (1). Hence, it generally is necessary to make a special analysis to establish the effects of local soil conditions.

A site-specific site response study is made using one-dimensional analyses that model the vertical propagation of shear waves through a column of soil. For any site-specific response study, it first will be necessary to define the ground

motion at the base of the soil column. This will require an establishment of peak acceleration for firm ground using one of the three methods enumerated above, and the selection of several representative time histories of motion scaled to the selected peak acceleration. These time histories must be selected with considerable care, taking into account the magnitude of the causative earthquake and the distance from the epicentre.

If a site response analysis is made, the peak ground motions will in general vary vertically along the soil column. Depending upon the type of analysis being made, it may be desirable to average the motions over depth to provide a single input value. At each depth, the largest motion computed in any of the several analyses using different time histories should be used.

If finite element analyses are made, it will again be necessary to select several time histories to use as input at the base of the grid, or a time history corresponding to a target spectrum.

6.1.3.3. Seismic Coefficients

A seismic coefficient (typical symbols are k_h and k_v) is a dimensionless number that, when multiplied times the weight of some body, gives a pseudo-static inertia force for use in analysis and design. The coefficients k_h and k_v are, in effect, decimal fractions of the acceleration of gravity (g). For some analyses, it is appropriate to use values of k_{hg} or k_{vg} smaller than the peak accelerations anticipated during the design earthquake event.

For analysis of liquefaction, it is conventional to use 0.65 times the peak acceleration. The reason is that liquefaction is controlled by the amplitude of a succession of cycles of motion, rather than just by the single largest peak.

In design of buildings, it is common practice to base design upon a seismic coefficient corresponding to a ground motion smaller than the design ground motion. It is recognized that a building designed on this basis may likely yield and even experience some non-life-threatening damage if the design ground motion actually occurs. The permitted reduction depends upon the ductility of the structural system; that is, the ability of the structure to undergo yielding and yet remain intact so as to continue to support safely the normal dead and live loads. This approach represents a compromise between desirable performance and cost of earthquake resistance.

The same principle applies to earth structures, once it has been established that site instability caused by liquefaction is not a problem. If a retaining wall system yields, some permanent outward displacement will occur, which often is an acceptable alternative to significantly increased cost of construction. However, there is no generally accepted set of rules for selecting an appropriate seismic coefficient. The displacement-controlled approach to design is in effect a systematic and rational method for evaluating a seismic coefficient based upon allowable permanent displacement. The AASHTO seismic design for highway bridges⁴⁷ is an example of design

guidance using the seismic coefficient method for earth retaining structures. AASHTO recommends that a value of $k_h = 0.5A$ be used for most cases if the wall is designed to move up to 10A (in.) where A is peak ground acceleration coefficient for a site (acceleration = Ag). However, use of $k_h = 0.5A$ is not necessarily conservative for areas of high seismicity. Various relationships have been proposed for estimating permanent displacements, as a function of the ratio k_h/A and parameters describing the ground motion. These are well documented in the literature. Based upon simplified assumptions and using the Whitman and Liao⁴⁸ relationship for earthquakes to magnitude 7, k_h values can be computed as follows:

Table 6-1: Values of k_h based on Whitman and Liao Relationships

	A = 0.2	A = 0.4
Displacement < 1 in.	$k_h = 0.13$	$k_h = 0.30$
Displacement < 4 in.	$k_h = 0.10$	$k_h = 0.25$

These numbers are based upon $V/Ag = 50 \text{ in/sec/g}^{49}$, which applies to deep stiff soil sites (geologic condition); smaller k_h would be appropriate for hard (e.g. rock) sites. The Whitman and Liao study did not directly address the special case of sites located within epicentral regions.

The value assigned to k_h is to be established by the seismic design team for the project considering the seismotectonic structures within the region, or as specified by the design agency.

6.1.3.4. Vertical Ground Accelerations

The effect of vertical ground accelerations upon response of waterfront structures is quite complex. Peak vertical accelerations can equal or exceed peak horizontal accelerations, especially in epicentral regions. However, the predominant frequencies generally differ in the vertical and horizontal components, and phasing relationships are very complicated. Where retaining structures support dry backfills, Whitman and Liao have shown that vertical motions have little overall influences. However, they did not directly address the special case of sites located within epicentral regions. For cases where water is present within soils or against walls, the possible influence of vertical motions have received little study. It is very difficult to represent adequately the effect of vertical motions in pseudo-static analyses, such as those set forth in this book.

The value assigned to k_v is to be established by the seismic design team for the project considering the seismotectonic structures within the region, or as specified by the design agency. However, pending the results of further studies and in the absence of specific guidance for the choice of k_v for waterfront structures the following guidance has been expressed in literature: A vertical seismic coefficient be used in situations where the horizontal seismic coefficient is 0.05 or greater for anchored sheet pile walls. This rough guidance excludes the special case of structures located within epicentral regions for the reasons discussed previously. It is recommended that three solutions should be made: one assuming the acceleration upward, one assuming it downward, and the other assuming zero vertical acceleration. If the vertical seismic coefficient is found to have a major effect and the use of the most conservative assumption has a major cost implication, more sophisticated dynamic analyses should probably be considered.

6.2. Introduction to Dynamic Earth Pressures

When considering earthquake loads, traditionally anchored sheet pile walls are designed using a “pseudostatic” method, i.e., a method that treats the dynamic loads caused by seismic events as additional static loads. This is illustrated in *Figure 6-1*.

In the 1920’s, Okabe, Mononobe and Matsuo⁵⁰ extended Coulomb’s theory of static active and passive earth pressures to include the effects of dynamic earth pressures on retaining walls. The Mononobe-Okabe theory incorporates the effect of earthquakes through the use of a constant horizontal acceleration in units of g, $a_h = k_h \cdot g$, and a constant vertical acceleration in units of g, $a_v = k_v \cdot g$, acting on the soil mass comprising Coulomb’s active wedge (or passive wedge) within the backfill, as shown in *Figure 6-2* and *Figure 6-3*. The term k_h is the fraction of horizontal acceleration, k_v is the fraction of vertical acceleration, and g is the acceleration of gravity⁵¹. In *Figure 6-2* and *Figure 6-3*, positive a_v values act downward, and positive a_h values act to the left. The acceleration of the mass in the directions of positive horizontal and positive vertical accelerations results in the inertial forces $k_h \cdot W$ and $k_v \cdot W$, as shown in *Figure 6-2* and *Figure 6-3*, where W is the weight of the soil wedge. These inertial forces act opposite to the direction in which the mass is accelerating. This type of analysis is described as a pseudostatic method of analysis, where the effect of the earthquake is modelled by an additional set of static forces, $k_h \cdot W$ and $k_v \cdot W$.

The Mononobe-Okabe theory assumes that the wall movements are sufficient to fully mobilize the shear resistance along the backfill wedge, as is the case for Coulomb’s active

⁴⁷ American Association of State Highway and Transportation Officials. (1983). “Guide Specifications for Seismic Design of Highway Bridges,” AASHTO, Washington, DC. The map in AASHTO (1983) is not accepted widely as being representative of the ground shaking hazard.
⁴⁸ Whitman, R., and Liao, S. (1985). “Seismic Design of Retaining Walls,” Miscellaneous Paper CL-85-1, US Army Engineer Waterways Experiment Station, Vicksburg, MS.
⁴⁹ Sadigh, K. (1983). “Considerations in the development of site-specific spectra,” in proceedings of Conference XXII, site-specific effects of soil and rock on ground motion and the implications for earthquake resistant design: U.S. Geological Survey Open File Report 83-845.
⁵⁰ Okabe, S. 1926. “General Theory of Earth Pressures,” Journal Japan Society of Civil Engineering, Vol. 12, No. 1, and Mononobe, N., and Matsuo, H. 1929. “On the Determination of Earth Pressures During Earthquakes,” Proceedings, World Engineering Congress, 9.
⁵¹ $1.0 \text{ g} = 32.174 \text{ ft/sec}^2 = 980.665 \text{ cm/sec}^2$.

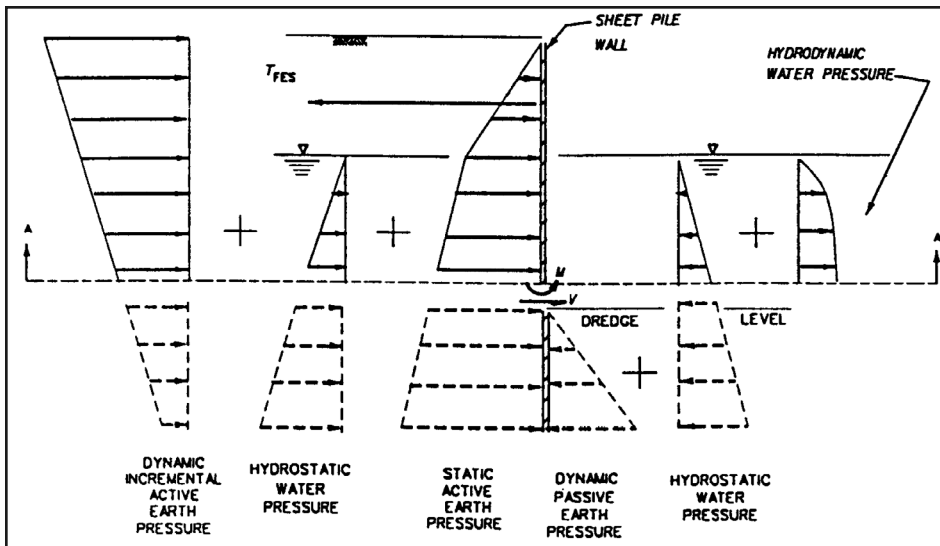


Figure 6-1: Static and Dynamic Horizontal Pressure Components and Anchor Force Settings on a Sheet Pile Wall.

Figure 6-2: Driving and resisting Mononobe-Okabe active seismic wedge, no saturation

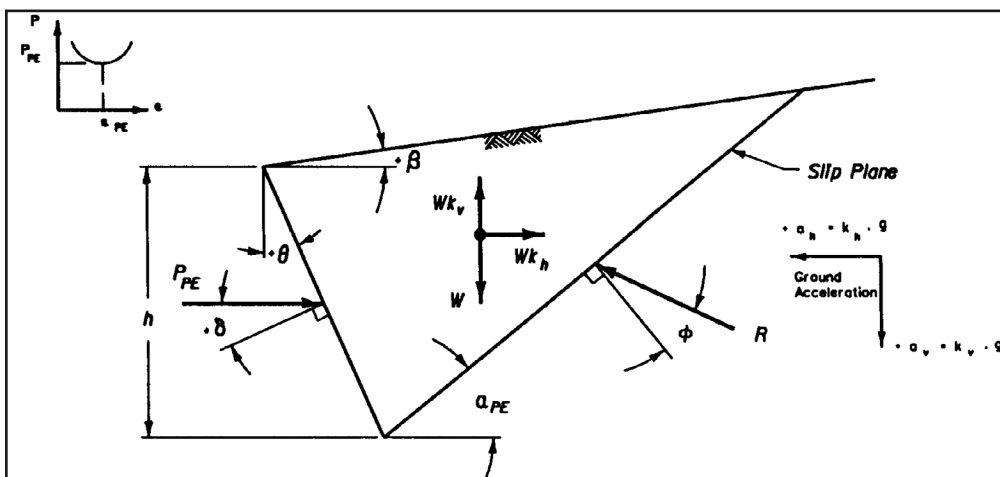
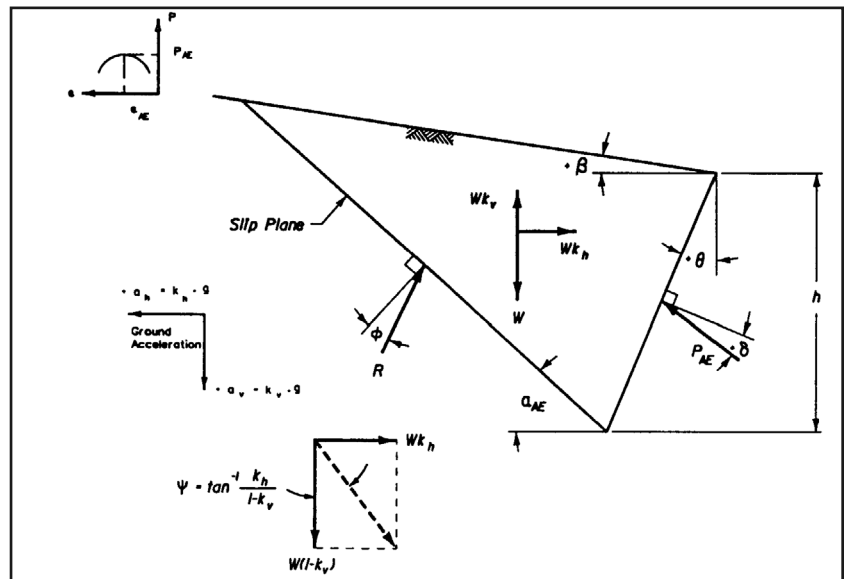


Figure 6-3: Driving and resisting Mononobe-Okabe passive seismic wedge, no saturation

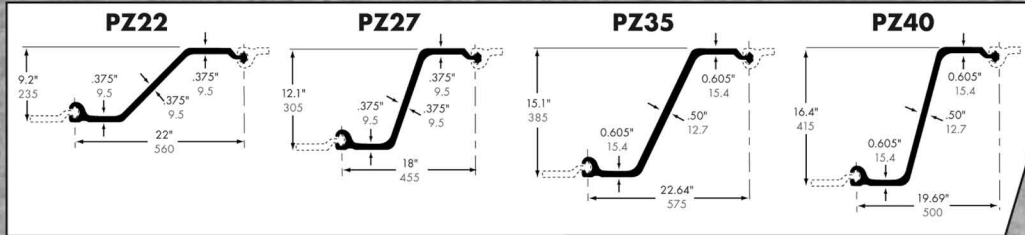
SHEET PILING

DIMENSIONS AND PROPERTIES

GRADES:
 ASTM A328
 ASTM A572 Gr. 50 & 60
 ASTM A588
 ASTM A690

U.S. Standard
 Metric (mm)

Z-PILING

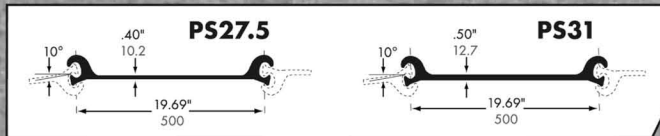


U.S. STANDARD									
Section Designation	Area in. ²	Nominal Width, in.	Weight In Pounds		Moment of Inertia in. ⁴	Section Modulus, in. ³		Surface Area sq ft per lin. ft of bar	
			Per lin. ft of bar	Per ft ² of Wall		Single Section	Per lin. ft of wall	Total Area	Nominal Coating Area *
PZ22	11.9	22	40.3	22.0	155.3	33.8	18.4	4.94	4.48
PZ27	11.9	18	40.5	27.0	281.2	46.5	31.0	4.94	4.48
PZ35	19.4	22.64	66.0	35.0	697.0	92.3	48.9	5.83	5.37
PZ40	19.3	19.69	65.6	40.0	824.8	100.6	61.3	5.83	5.37

METRIC									
Section Designation	Area cm ²	Nominal Width, mm	Weight In Kilograms		Moment of Inertia cm ⁴	Section Modulus, cm ³		Surface Area sq m per lin. m of bar	
			Per lin. m of bar	Per m ² of Wall		Single Section	Per lin. m of wall	Total Area	Nominal Coating Area *
PZ22	76.5	560	60.0	107.3	6,460	552	988	1.51	1.37
PZ27	76.8	455	60.3	131.9	11,700	760	1,663	1.51	1.37
PZ35	125.2	575	98.2	170.9	29,010	1,510	2,628	1.78	1.64
PZ40	124.4	500	97.6	195.3	34,330	1,650	3,301	1.78	1.64

PRODUCED BY TXI CHAPARRAL STEEL

FLAT SHEET PILING



U.S. STANDARD									
Section Designation	Area in. ²	Nominal Width, in.	Weight in Pounds		Moment of Inertia in. ⁴	Section Modulus, in. ³		Surface Area sq ft per lin. ft of bar	
			Per lin. ft of bar	Per ft ² of wall		Single Section	Per lin. ft of wall	Total Area	Nominal Coating Area *
PS27.5	13.27	19.69	45.1	27.5	5.3	3.3	2.0	4.48	3.65
PS31	14.96	19.69	50.9	31.0	5.3	3.3	2.0	4.48	3.65

METRIC									
Section Designation	Area cm ²	Nominal Width, mm	Weight in Kilograms		Moment of Inertia cm ⁴	Section Modulus, cm ³		Surface Area sq m per lin. m of bar	
			Per lin. m of bar	Per m ² of wall		Single Section	Per lin. m of wall	Total Area	Nominal Coating Area *
PS27.5	85.6	500	67.1	134.3	221	54	108	1.37	1.11
PS31	96.5	500	75.7	151.4	221	54	108	1.37	1.11

PRODUCED BY TXI CHAPARRAL STEEL

Notes:

All dimensions given are nominal.
 PS27.5 and PS31 interlock only with each other.
 All Z-sections interlock with one another.
 * Excludes socket interior and ball of interlock.

Interlock Strength:

PS27.5 and PS31, when properly interlocked, develop a minimum ultimate interlock strength of 16 kips/in (2800KN/m). Higher interlock strengths are available upon inquiry.

Version 3.0 • January 2003



1-800-255-4500 • www.fosterpiling.com

and passive earth pressure theories. To develop the dynamic active earth pressure force, P_{AE} , the wall movements are away from the backfill, and for the passive dynamic earth pressure force, P_{PE} , the wall movements are towards the backfill. Dynamic tests on model retaining walls indicate that the required movements to develop the dynamic active earth pressure force are on the order of those movements required to develop the static active earth pressure force.

The Mononobe-Okabe theory gives the net static and dynamic force. For positive $k_h > 0$, P_{AE} is larger than the static P_A , and P_{PE} is less than the static P_p .

6.3. Dynamic Active Earth Pressure Force

The Mononobe-Okabe relationship for P_{AE} for dry backfills⁵² is equal to

$$\text{Equation 6-1: } P_{AE} = K_{AE} \cdot \frac{1}{2} [\gamma_t (1 - k_v)] H^2$$

and acts at an angle δ from the normal to the back of the wall of height H . The dynamic active earth pressure coefficient, K_{AE} , is equal to

Equation 6-2:

$$K_{AE} = \frac{\cos^2(\phi - \psi - \theta)}{\cos\psi \cos^2\theta \cos(\psi + \theta + \delta)} \left[1 + \frac{\sin(\phi + \delta) \sin(\phi - \psi - \beta)}{\cos(\delta + \psi + \theta) \cos(\beta - \theta)} \right]^2$$

and the seismic inertia angle, Ψ , is equal to

$$\text{Equation 6-3: } \psi = \tan^{-1} \left[\frac{k_h}{(1 - k_v)} \right]$$

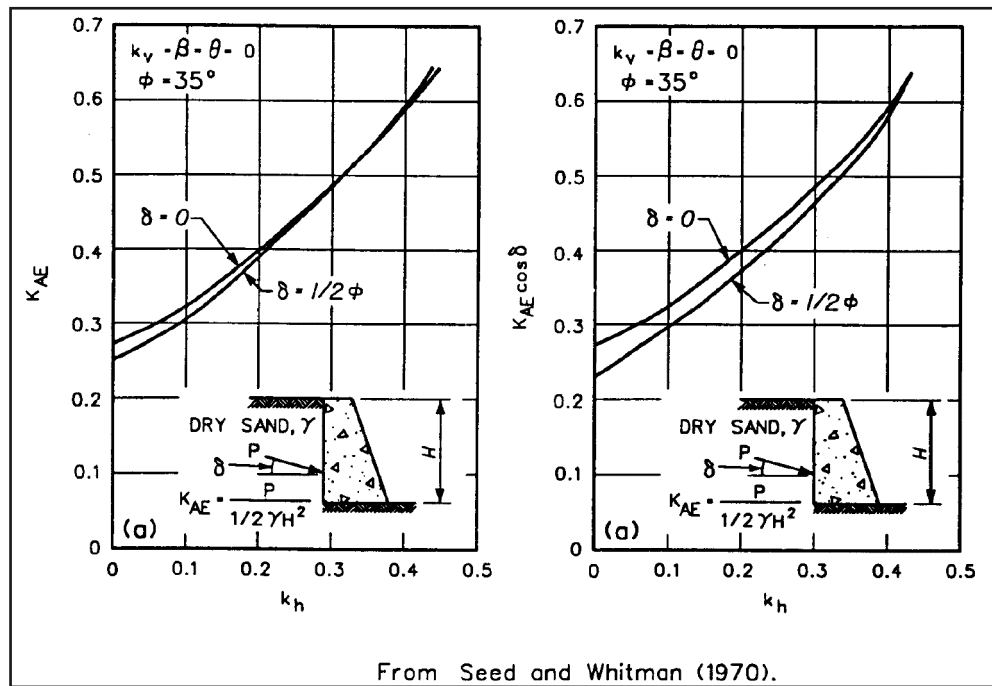
The seismic inertia angle represents the angle through which the resultant of the gravity force and the inertial forces is rotated from vertical. In the case of a vertical wall ($\theta = 0$) retaining a horizontal backfill ($\beta = 0$), Equation 6-2 simplifies to

Equation 6-4:

$$K_{AE} = \frac{\cos^2(\phi - \psi)}{\cos\psi \cos(\psi + \delta)} \left[1 + \frac{\sin(\phi + \delta) \sin(\phi - \psi)}{\cos(\delta + \psi)} \right]^2$$

Figure 6-4 and Figure 6-5 give charts from which values of K_{AE} may be read for certain combinations of parameters.

The planar slip surface extends upwards from the heel of the wall through the backfill and is inclined at an angle α_{AE} from horizontal. α_{AE} is equal to⁵³



From Seed and Whitman (1970).
 Figure 6-4: Variation in K_{AE} and $K_{AE} \cdot \cos \delta$ with k_h

⁵² Whitman, J. and Christian, J. (1990) "Seismic Response of Retaining Structures," Symposium on Seismic Design for World Port 2020, Port of Los Angeles, Los Angeles, CA.
⁵³ Zarrabi, K. 1973. "Sliding of Gravity Retaining Wall During Earthquakes Considering Vertical Acceleration and Changing Inclination of Failure Surface, SM Thesis, Department of Civil Engineering, MIT, Cambridge, MA, pp. 140.

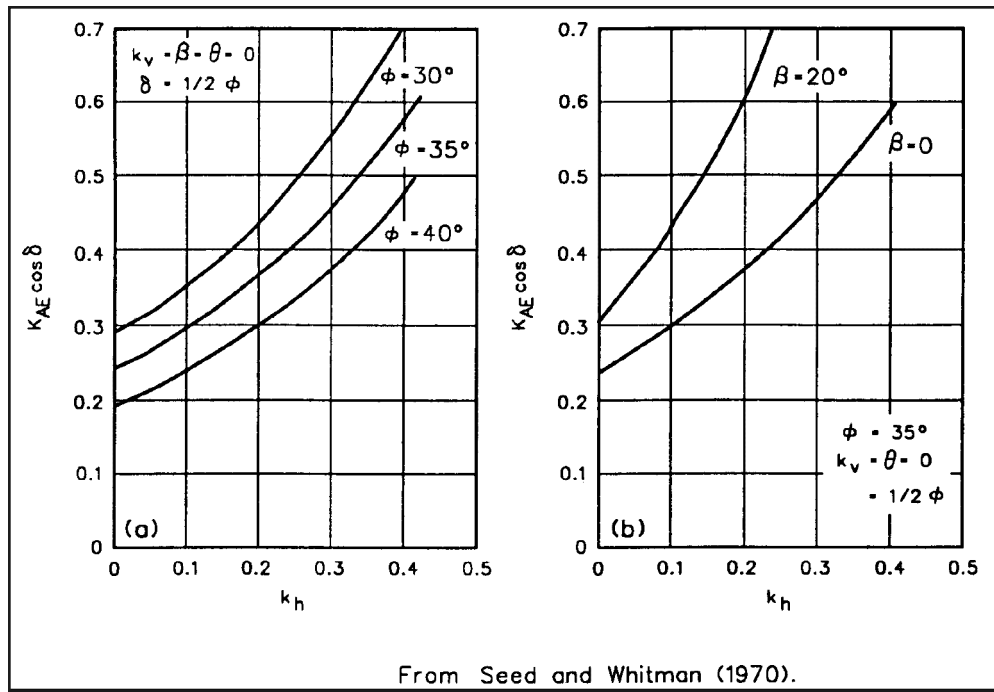


Figure 6-5: Variation in $K_{AE} \cdot \cos \delta$ with k_h , ϕ , and β

Equation 6-5:

$$\alpha_{AE} = \phi - \psi + \tan^{-1} \left[\frac{-\tan(\phi - \psi - \beta) + c_{1AE}}{c_{2AE}} \right]$$

where

Equation 6-6:

$$c_{1AE} = \frac{\sqrt{[\tan(\phi - \psi - \beta)][\tan(\phi - \psi - \beta) + \cot(\phi - \psi - \theta)]}}{[1 + \tan(\delta + \psi + \theta)\cot(\phi - \psi - \theta)]}$$

and

Equation 6-7:

$$c_{2AE} = 1 + \frac{[\tan(\delta + \psi + \theta)] \cdot [\tan(\phi - \psi - \beta) + \cot(\phi - \psi - \theta)]}{1}$$

Figure 6-7 and Figure 6-8 give α_{AE} as a function of Ψ for several values of ϕ for vertical walls retaining level backfills.

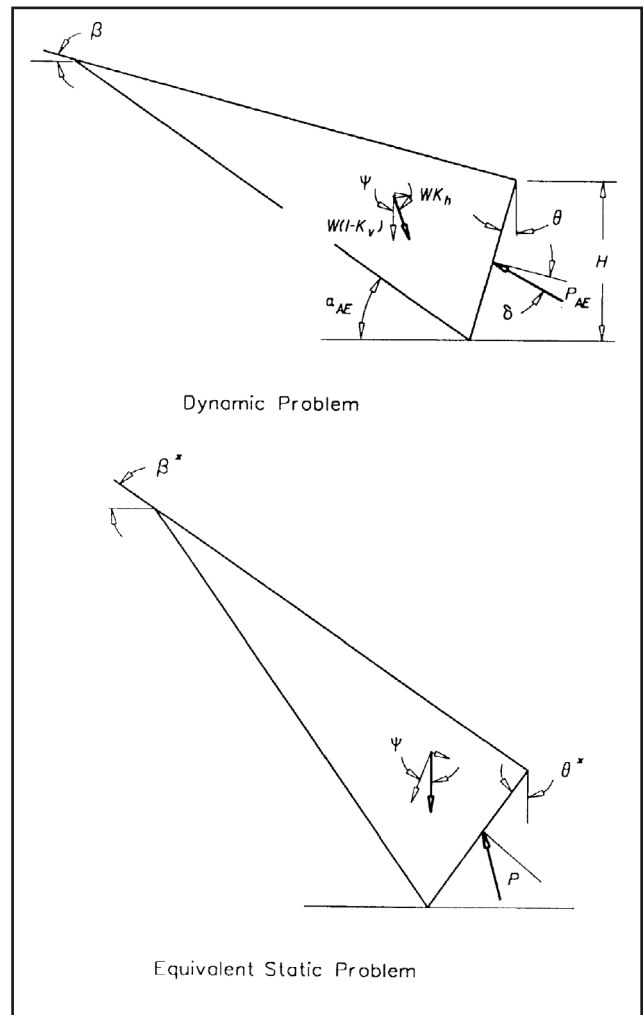


Figure 6-6: Equivalent static formulation of the Mononobe-Okabe active dynamic earth pressure problem

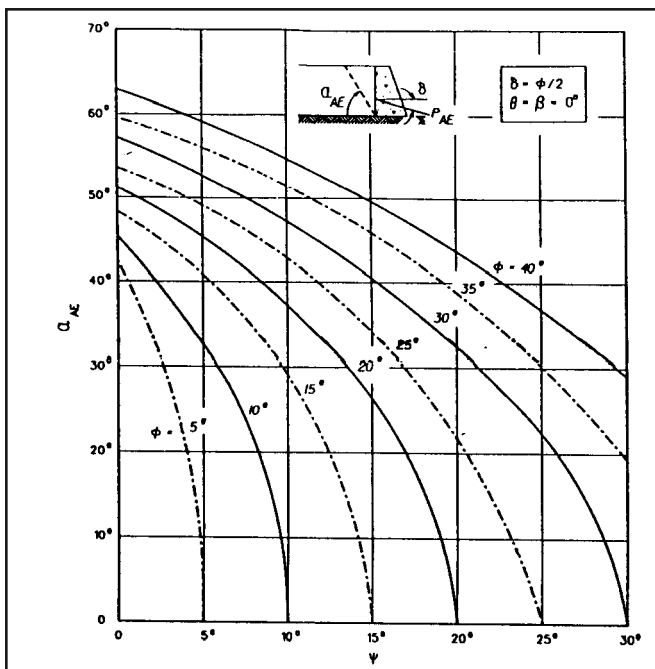


Figure 6-7: Variation in α_{PE} with Ψ for δ equal to ϕ vertical wall and level backfill.

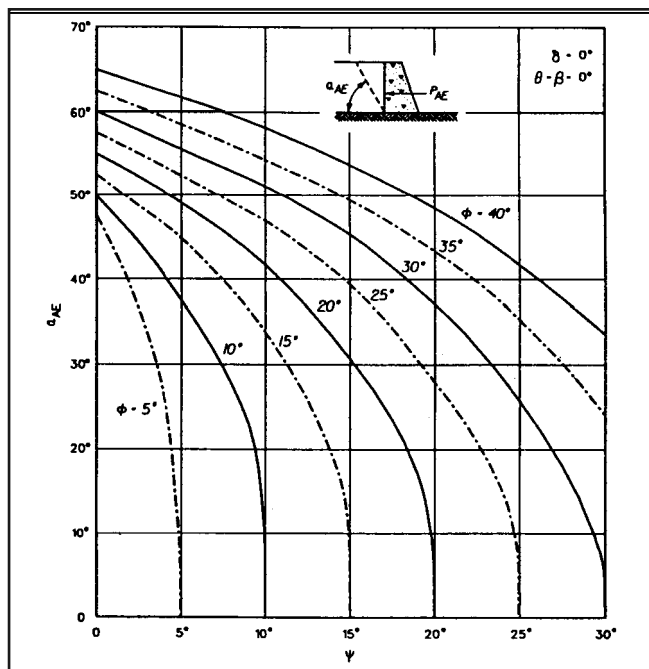


Figure 6-8: Variation in α_{PE} with Ψ for δ equal to zero degrees, vertical wall and level backfill.

A limited number of dynamic model retaining wall tests⁵⁴ on dry sands show δ to range from $\phi/2$ to $2\phi/3$, depending upon the magnitude of acceleration.

The validity of the Mononobe-Okabe theory has been demonstrated by the shaking table tests. These tests were conducted at frequencies much less than the fundamental frequency of the backfill, so that accelerations were essentially constant throughout the backfill. Figure 6-9 gives a comparison between predicted and measured values of the seismic active pressure coefficient K_{AE} .

An alternative method for determining the value of K_{AE} using tabulated earth pressures was developed by Dr. I. Arango⁵⁵, who recognized that by rotating a soil wedge with a planar slip surface through the seismic inertia angle, the resultant vector, representing vectorial sums of W , $k_h \bullet W$ and $k_v \bullet W$, becomes vertical, and the dynamic problem becomes equivalent to the static problem, as shown in Figure 6-6.

The seismic active pressure force is given by

Equation 6-8:

$$P_{AE} = [K_A(\beta^*, \theta^*) \cdot F_{AE}] \cdot \frac{1}{2} [\gamma_t (1 - k_v)] H^2$$

where

- H = actual height of the wall
- $\beta^* = \beta + \Psi$
- $\theta^* = \theta + \Psi$

and

Equation 6-9:
$$F_{AE} = \frac{\cos^2(\theta + \psi)}{\cos\psi \cos^2\theta}$$

Ψ is computed using Equation 6-3. Values of F_{AE} are also given as a function of Ψ and θ in Figure 6-10. $K_A(\beta^*, \theta^*)$ is determined from the Coulomb static K_A values by Equation 16. An alternative procedure is to approximate $K_A(\beta^*, \theta^*)$ by using the static K_A values. The product of $K_A(\beta^*, \theta^*)$ times F_{AE} is equal to K_{AE} .

6.3.1. Vertical Position of P_{AE} along Back of Wall

The Mononobe-Okabe analysis procedure does not provide a means for calculating the point of action of the resulting force. Analytical studies⁵⁶ and tests on model walls retaining dry sands⁵⁷ have shown that the position of P_{AE} along the back of the retaining wall depends upon the amount of wall movement and the mode in which the movements occur. These limited test result indicate that the vertical position of P_{AE} ranges from 0.4 to 0.55 times the height of the wall, as measured from the base of the wall. P_{AE} acts at a higher position along the back of the wall than the static active earth pressure force due to the concentration of soil mass comprising the sliding wedge above mid-wall height (Figure 6-2 and Figure 6-3). With the static force component of P_{AE} acting

⁵⁴Sherif, M., and Fang, Y. 1983 (Nov). "Dynamic Earth Pressures Against Rotating and Non-Yielding Retaining Walls," Soil Engineering Research Report No. 23, Department of Civil Engineering, University of Washington, Seattle, WA, pp. 45-47, and Ichihara, M., and Matsuzawa, H. 1973 (Dec). "Earth Pressure During Earthquake," Soils and Foundations, Vol. 13, No. 4, pp. 75-86.

⁵⁵Personal communication, as described by Seed, H., and Whitman, R. 1970. "Design of Earth Retaining Structures for Dynamic Loads," ASCE Specialty Conference on Lateral Stresses in the Ground and Design of Earth Retaining Structures, pp. 103-147.

⁵⁶Prakash, S., and Basavanna, B. 1969. "Earth Pressure Distribution Behind Retaining Wall During Earthquake," Proceeding, 4th World Conference on Earthquake Engineering, Santiago, Chile.

PZ27.COM

**“YOUR FIRST SOURCE OF INFORMATION
ON SHEET PILING”**



For more than a century, sheet piling has been a successful and economic form of retaining walls and, in some cases, a foundation bearing member. The purpose of this site is to give you, the engineer, owner, contractor or other the information you need to design, build and maintain successful sheet piling walls.

There's so much information on PZ27.com, it's hard to know where to begin!

There are several broad categories of information:

Overview of Sheet Piling, which includes: • History • Interlocks • Legal Aspects

Design Information on Sheet Piling, which includes: • Loads and stresses on sheeting • Anchor Systems
• Specifications for sheet piling, pile points and splices • Design methods and software • Seepage under and through sheet pile walls • Photo Gallery of Sheet Piling • Sample Specifications for Sheet Piling

Installation and Equipment, which includes the following: • Installation of sheet piling • Driving equipment
• Driving Tips • Sales and rentals of sheeting and equipment • Reconditioning of Sheet Piling • Inspection and Installation of Sheet Pile Cofferdams • Photo Gallery of Installation • Special types of sheeting • Cellular cofferdams, a very important topic (including photo gallery) • High modulus walls, including HZ wall systems
• Maintenance • Corrosion and Cathodic Systems • Coating Specifications • Reconditioning of Sheet Piling
• Repair and Maintenance of Sheet Piling

Glossary, so you'll know what the salesman is actually talking about!

There are also links throughout the site to more resources to help you with your sheeting requirements. So come visit www.PZ27.com NOW!

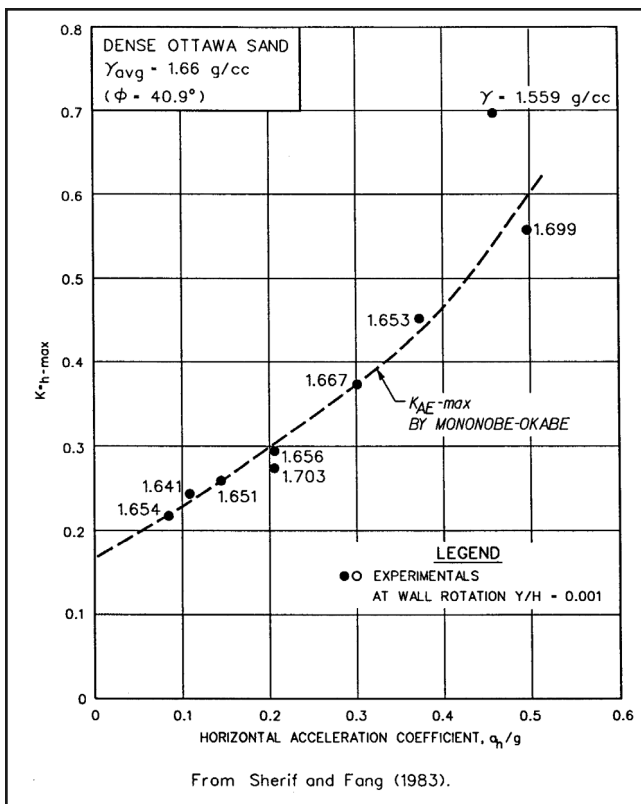


Figure 6-9: Variation in dynamic active horizontal earth pressure coefficient with peak horizontal acceleration.

below mid-wall height and the inertia force component of P_{AE} acting above mid-wall height, the vertical position of the resultant force, P_{AE} , will depend upon the magnitude of the accelerations applied to the mass comprising soil wedge.

This was shown to be the case⁵⁶ in the evaluation of the moment equilibrium of a Mononobe-Okabe wedge. The results of their analyses are summarized in Figure 6-11.

6.3.2. Simplified Procedure for Dynamic Active Earth Pressures

Seed and Whitman⁵⁸ presented a simplified procedure for computing the dynamic active earth pressure on a vertical wall retaining dry backfill. They considered the group of structures consisting of a vertical wall ($\theta = 0$) retaining a granular horizontal backfill ($\beta = 0$) with ϕ equal to 35 degrees, $\delta = \phi/2$ and k_v equal to zero. P_{AE} is defined as the sum of the initial static active earth pressure force (Equation 5-8) and the dynamic active earth pressure force increment,

$$\text{Equation 6-10: } P_{AE} = P_A + \Delta P_{AE}$$

Where

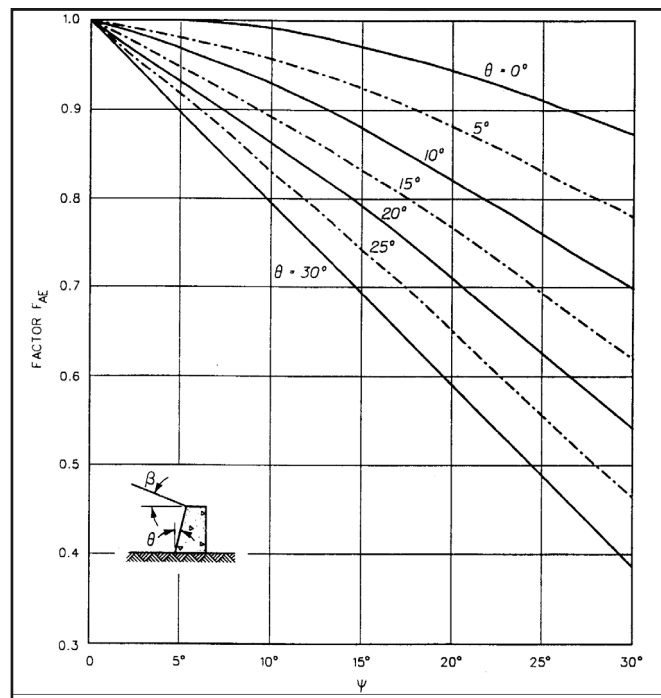


Figure 6-10: Values of factor F_{AE} for determination of K_{AE}

$$\text{Equation 6-11: } \Delta P_{AE} = \Delta K_{AE} \cdot \frac{1}{2} \gamma_t H^2.$$

The dynamic active earth pressure coefficient is equal to

$$\text{Equation 6-12: } K_{AE} = K_A + \Delta K_{AE}$$

And

$$\text{Equation 6-13: } \Delta K_{AE} = \frac{3}{4} k_h$$

Using this simplified procedure, K_A is computed using Equation 5-27, and ΔK_{AE} is computed using Equation 6-13. All forces act at an angle δ from the normal to the back of a wall, as shown in Figure 10. P_A acts at a height equal to $H/3$ above the heel of the wall, and ΔP_{AE} acts at a height equal to $0.6 \cdot H$. P_{AE} acts at a height, Y , which ranges from $H/3$ to $0.6 \cdot H$, depending upon the value of k_h .

$$\text{Equation 6-14: } Y = \frac{P_A \cdot \left(\frac{H}{3}\right) + \Delta P_{AE} \cdot (0.6H)}{P_{AE}}$$

⁵⁷ Sherif, M., Ishibashi, I., and Lee, C. 1982. "Earth Pressure Against Rigid Retaining Walls," ASCE, Journal of the Geotechnical Engineering Division, Vol. 108, No. GT5, pp. 679-695; Sherif, M., and Fang, Y. 1984a. "Dynamic Earth Pressures on Rigid Walls Rotating About the Base," Proceedings, Eighth World Conference on Earthquake Engineering, Vol. 6, San Francisco, CA, pp. 993-100; Sherif, M., and Fang, Y. 1984b. "Dynamic Earth Pressures on Walls Rotating About the Top," Soils and Foundations, Vol. 24, No. 4, pp. 109-117; Ishibashi, I., and Fang, Y. 1987 (Dec). "Dynamic Earth Pressures with Different Wall Modes," Soils and Foundations, Vol. 27, No. 4, pp. 11-22.
⁵⁸ Seed, H., and Whitman, R. 1970. "Design of Earth Retaining Structures for Dynamic Loads," ASCE Specialty Conference on Lateral Stresses in the Ground and Design of Earth Retaining Structures, pp. 103-147.

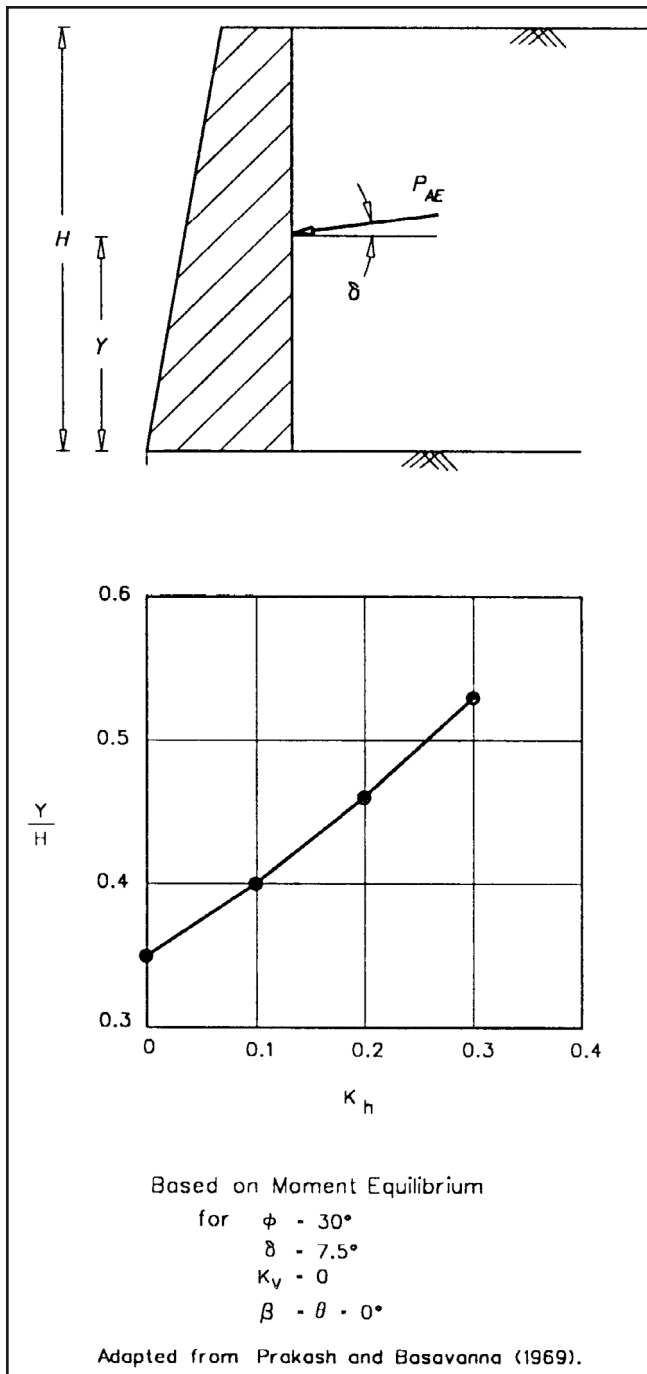


Figure 6-11: Point of action of P_{AE} .

The results of instrumented shake table tests conducted on model walls retaining dense sands show ΔP_{AE} acts at a height of between 0.43H and 0.58H, depending upon the mode of wall movement that occurs during shaking. The heights of the model walls used in the shake table tests⁵⁹ were 2.5 and 4 feet.

Seed and Whitman approximate the value for α_{AE} as equal to ϕ , where ϕ equals 35 degrees. Thus, for a wall retaining a dry granular backfill of height H, the theoretical active failure wedge would intersect the top of the backfill at a distance equal to 1.5 times H, as measured from the top of the wall ($\tan 35^\circ \approx 1/1.5$).

6.3.3. Limiting Value for Horizontal Acceleration

Richards and Elms⁶⁰ show that Equation 6-2 and Equation 6-4 are limited to cases where $(\phi - \beta)$ is greater than or equal to Y. Substituting $(\phi - \beta)$ equal to Y into Equation 6-5 results in a AE equal to the slope of the backfill (β), which is the stability problem for an infinite slope. Zarrabi⁶¹ shows that this limiting value for Y corresponds to a limiting value for k_h , which is equal to

Equation 6-15: $k_h^* = (1 - k_v) \tan(\phi - \beta)$

When k_h is equal to k_h^* , the shear strength along the failure surface is fully mobilized, and the backfill wedge verges on instability. Values of k_h^* are also shown in Figure 6-12 Static active earth pressure force and incremental dynamic active earth pressure force for dry backfill.

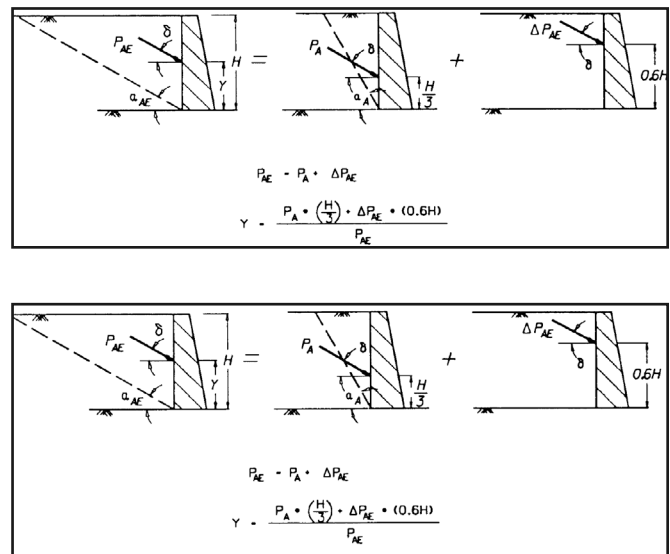


Figure 6-12: Static active earth pressure force and incremental dynamic active earth pressure force for dry backfill.

For a wall of height H = 20 ft retaining a dry cohesionless backfill with $\phi' = 30$ degrees, $\delta = 3$ degrees, $\beta = 6$ degrees, $\theta = 0$ degrees, $k_h = 0.1$ (acceleration $k_h \cdot g$ away from the wall and inertia force $k_h \cdot W$ towards the wall) and $k_v = 0.067$ (acceleration $k_v \cdot g$ acting downward and inertia force $k_v \cdot W$ acting upward), compute K_{AE} , P_{AE} , and α_{AE} .

⁵⁹Matsuzawa, H., Ishibashi, I., and Kawamura, M. 1985 (Oct). "Dynamic Soil and Water Pressures of Submerged Soils," ASCE, Journal of Geotechnical Engineering, Vol. 111, No. 10, pp. 1161-1176.
⁶⁰Richards, R., and Elms, D. 1979 (April). "Seismic Behavior of Gravity Retaining Walls," ASCE, Journal of the Geotechnical Engineering Division, Vol. 105, No. CT4, pp. 449-464.
⁶¹Zarrabi, K. 1973. "Sliding of Gravity Retaining Wall During Earthquakes Considering Vertical Acceleration and Changing Inclination of Failure Surface, SM Thesis, Department of Civil Engineering, MIT, Cambridge, MA, pp. 140.

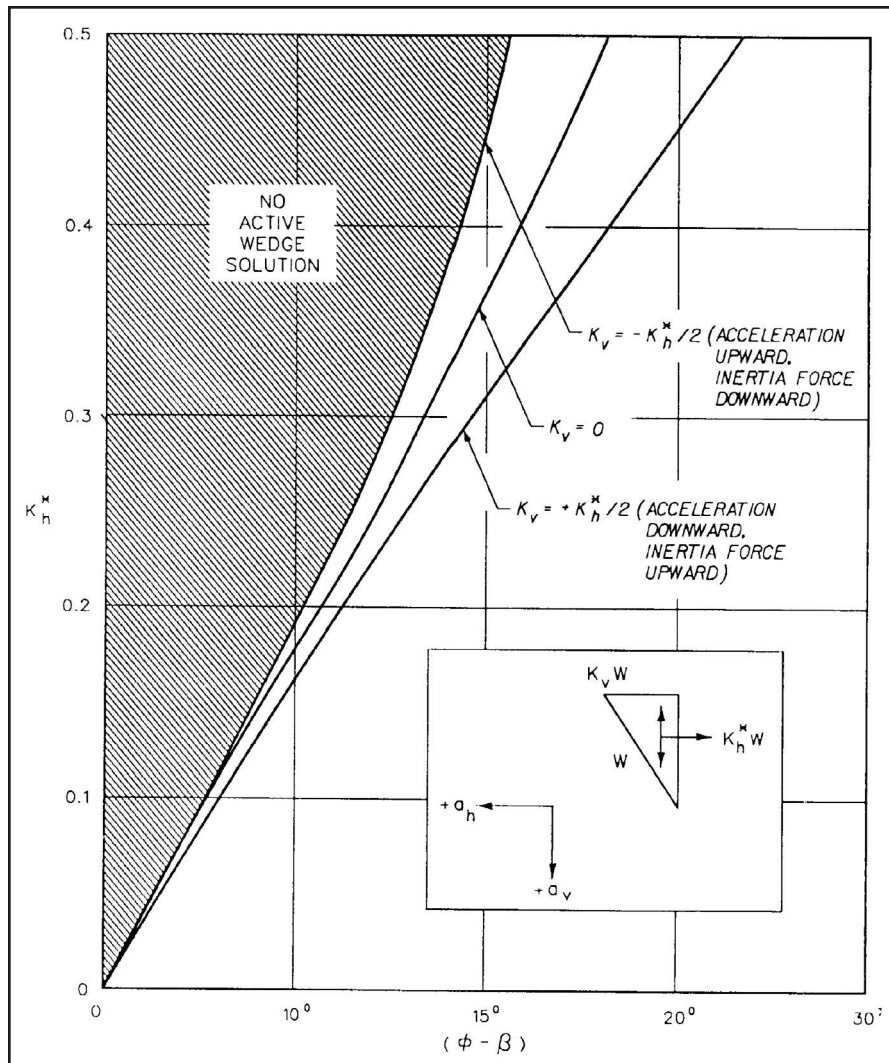
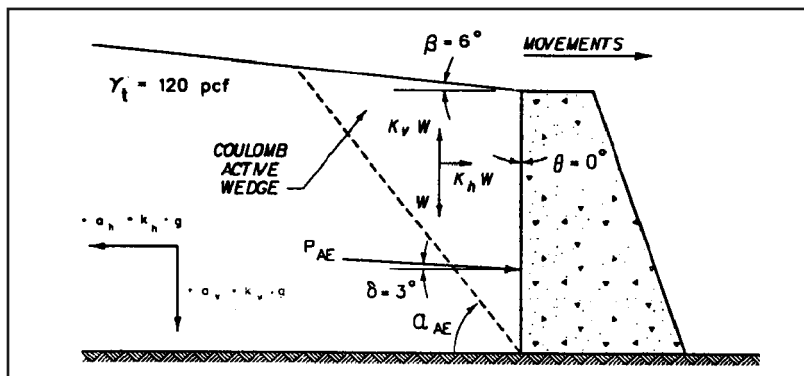


Figure 6-13: Limiting values for horizontal acceleration equals $k_h \cdot g$



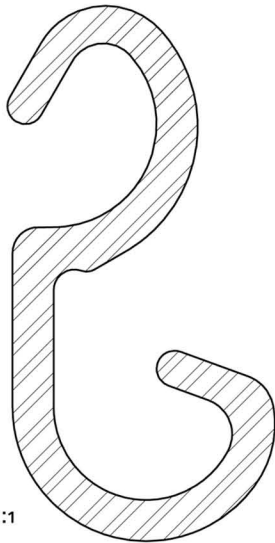
Example 5: Computation of Active Dynamic Earth Pressures⁶²

⁶² Due to space limitations, only the most basic examples for earthquake loads are included. More examples that are detailed can be found on the *Marine Construction CD-ROM, Volume 2*, available from Pile Buck. These are also available with SPW 911.

AZ 90

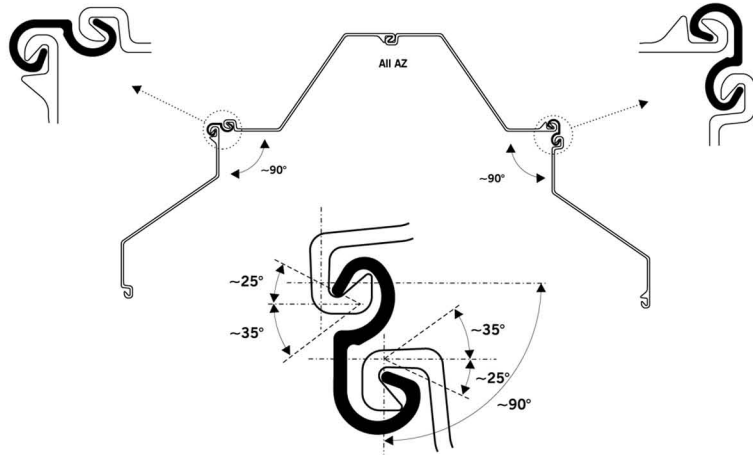
Available for immediate delivery, nation-wide

Applications: 90° corner (~25° to ~155°)



Weight: 8.9 lbs/ft (13.2 kg/m)

Steel grade: Astm A572 Grade 50 (S 355 GP)



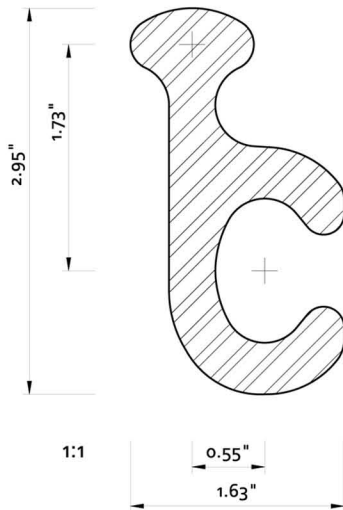
Installation Guidelines:

1. Thread the connector into the interlock while the sheet pile is out of the ground.
2. Adjust the connector to the appropriate position.
3. Tack or spot-weld the connector in place (typically a 10" weld attaching the connector to the sheet pile at the top is sufficient.)
4. Drive/extract the sheet (with the connector attached) as you would normally.

PZ 90

Priced delivered to the job site

Applications: 90° corner (~54° to ~126°)

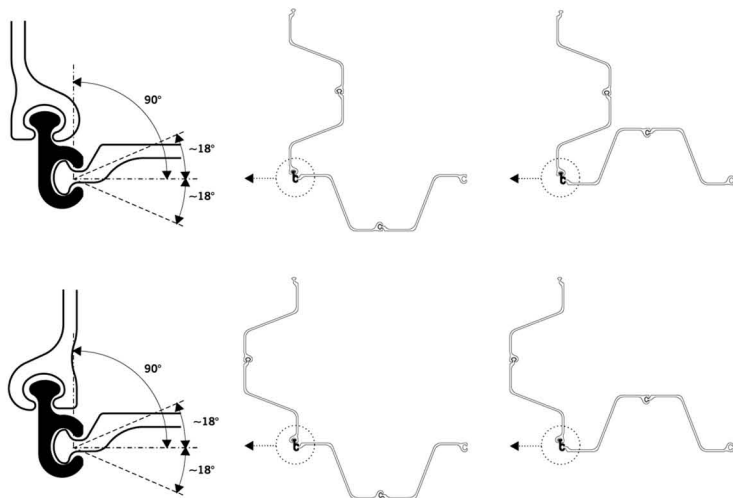


Weight: 7.1 lbs/ft (10.5 kg/m)

Steel grade: Astm A572 Grade 50 (S 355 GP)

Proper Interlocking Examples

Each interlock has a typical degree swing of 18° (+/- 5°) so that the probable swivel range is 36° (+/- 10°) when interlocking two PZ sheets via the connector.



Equation 6-16:
$$\psi = \tan^{-1} \left[\frac{0.1}{(1 - 0.067)} \right] = 6.12^\circ \text{ (by Equation 6-3)}$$

Equation 6-17:

$$K_{AE} = \frac{\cos^2(30 - 6.12)}{\cos(6.12)\cos^2(0)\cos(6.12+3) \left[1 + \frac{\sin(30+3)\sin(30-6.12-6)}{\cos(3+6.12)\cos(6)} \right]^2} = 0.4268 \text{ (by Equation 6-2)}$$

Equation 6-18:
$$P_{AE} = 0.4268 \cdot \frac{1}{2} [120 \text{ pcF} (1 - 0.067)] (20')^2 = 9557 \text{ lb per ft of wall (by Equation 6-1)}$$

Equation 6-19:

$$C_{1AE} = \left[\frac{\sqrt{[\tan(30-6.12-6)] [\tan(30-6.12-6) + \cot(30-6.12)]}}{[1 + \tan(3+6.12) \cot(30-6.12)]} \right] = 1.0652$$

$$C_{2AE} = 1 + \left[\frac{[\tan(3+6.12)] \cdot [\tan(30-6.12-6) + \cot(30-6.12)]}{1.14144} \right] = 1.14144$$

$$\alpha_{AE} = 30 - 6.12 + \tan^{-1} \left[\frac{[\tan(30-6.12-6) + 1.0652]}{1.14144} \right] = 51.58^\circ \text{ (by Equation 6-5)}$$

6.4. Effect of Submergence of the Backfill on the Mononobe-Okabe Method of Analysis

The Mononobe-Okabe relationships for P_{AE} , K_{AE} , and Ψ will differ from those expressed in Equation 6-1, Equation 6-2 and Equation 6-3, respectively, when water is present in the backfill. Spatial variations in pore water pressure with constant elevation in the backfill will alter the location of the critical slip surface and thus the value of P_{AE} . In addition, the pore water pressures may increase above their steady state values in response to the shear strains induced within the saturated portion of the backfill during earthquake shaking, as discussed in Tokimatsu and Yoshimi⁶³, Tokimatsu and Seed⁶⁴, Seed and Harder⁶⁵, and Marcuson, Hynes, and Franklin⁶⁶. In some situations, such as the case of a hydrostatic water table within the backfill or the case of excess pore water pressures equal to a constant fraction of the pre-earthquake effective overburden pressures throughout the backfill ($r_u = \text{constant}$), modified Mononobe-Okabe relationships may be used to compute P_{AE} .

6.4.1. Submerged Backfill with No Excess Pore Pressures

In this section it is assumed that shaking causes no associated build-up of excess pore pressure. The most complete study of this case appears in Matsuzawa, Ishibashi, and

Kawamura⁶⁷, Ishibashi, Matsuzawa, and Kawamura⁶⁸, and Ishibashi and Madi⁶⁹. They suggest two limiting conditions for design: (a) soils of low permeability - say $k < 1 \times 10^{-3}$ cm/sec where pore water moves with the mineral skeleton; and (b) soils of high permeability - say $k > 1$ cm/sec, where pore water can move independently of the mineral skeleton. Matsuzawa, Ishibashi, and Kawamura also suggest a parameter that can be used to interpolate between these limiting cases. However, understanding of case (b) and the interpolation parameter is still very incomplete.

6.4.1.1. Restrained water case

Here Matsuzawa, Ishibashi, and Kawamura make the assumption that pore pressures do not change as a result of horizontal accelerations. Considering a Coulomb wedge and subtracting the static pore pressures, there is a horizontal inertia force proportional to $\gamma_t \cdot k_h$ and a vertical force proportional to γ_b . Thus, in the absence of vertical accelerations, the equivalent seismic angle is:

Equation 6-20:
$$\psi_{e1} = \tan^{-1} \frac{\gamma_t \cdot k_h}{\gamma_b}$$

and the equivalent horizontal seismic coefficient is:

Equation 6-21:
$$k_{he1} = \frac{\gamma_t k_h}{\gamma_b}$$

Using k_{he1} in the Mononobe-Okabe theory together with a unit weight $g b$ will give P_{AE} , to which the static water pressures must be added.

If vertical accelerations are present, Matsuzawa, Ishibashi, and Kawamura recommend using:

Equation 6-22:
$$\psi_{e1} = \tan^{-1} \left[\frac{\gamma_t k_h}{\gamma_b (1 - k_v)} \right]$$

This is equivalent to assuming that vertical accelerations do affect pore pressures, and then it is not strictly correct to use the Mononobe-Okabe theory. However, the error in evaluating total thrust is small.

⁶³Tokimatsu, K., and Yoshimi, Y. 1983. "Empirical Correlation of Soil Liquefaction Based on SPT N-Value and Fines Content," Soils and Foundations, Vol. 23, No. 4, pp 56-74.
⁶⁴Tokimatsu, A. M., and Seed, H. B. 1987 (Aug). "Evaluation of Settlements In Sands Due to Earthquake Shaking," ASCE, Journal of the Geotechnical Division, Vol. 113, No. 8, pp. 861-878.
⁶⁵Seed, R. B. and Harder, L. F. (1990). "SPT-Based Analysis of Cyclic Pore Pressure Generation and Undrained Strength," Proceedings of the H. B. Seed Memorial Symposium, Bi Tech Publishing, Vol. II, pp. 351-376.
⁶⁶Marcuson, W., Hynes, M., and Franklin, A. 1990 (Aug). "Evaluation and Use of Residual Strength in Seismic Safety Analysis of Embankments," Earthquake Spectra, pp. 529-572.
⁶⁷Matsuzawa, H., Ishibashi, I., and Kawamura, M. 1985 (Oct). "Dynamic Soil and Water Pressures of Submerged Soils," ASCE, Journal of Geotechnical Engineering, Vol. 111, No. 10, pp. 1161-1176.
⁶⁸Ishibashi, I., Matsuzawa, H., and Kawamura, M. 1985. "Generalized Apparent Seismic Coefficient for Dynamic Lateral Earth Pressure Determination," Proceeding of 2nd International Conference on Soil Dynamics and Earthquake Engineering, edited by C. Brebbia, A. Cakmak, and A. Chaffer, QE2, pp. 6-33 to 6-42.
⁶⁹Ishibashi, I., and Madi, L. 1990 (May). "Case Studies On Quaywall's Stability With Liquefied Backfills," Proceeding of 4th U.S. Conference on Earthquake Engineering, EERI, Vol. 3, Palm Springs, CA, pp. 725-734.

6.4.1.2. Free water case

It is difficult to come up with a completely logical set of assumptions for this case. Matsuzawa, Ishibashi, and Kawamura suggest that the total active thrust is made up of:

- 1) A thrust from the mineral skeleton, computed using:

$$\text{Equation 6-23: } k_{he2} = \frac{\gamma_d}{\gamma_b} k_h = \frac{G_s}{G_s - 1} k_h$$

and

$$\text{Equation 6-24: } \psi_{e2} = \tan^{-1} \left[\frac{k_{he2}}{(1 - k_v)} \right]$$

where G_s is the specific gravity of the solids. A unit weight of γ_b is used in the equation for P_{AE} .

- 2) The hydrodynamic water pressure force for the free water within the backfill, P_{wd} , is given by the Westergaard⁷⁰ relationship

$$\text{Equation 6-25: } P_{wd} = \frac{7}{12} \cdot k_h \cdot \gamma_w H^2$$

and acts at 0.4 H above the base of the wall.

The total force behind the wall would also include the hydrostatic water pressure. This procedure is not very consistent, since the effect of the increased pore pressures is ignored in the computation of the thrust from the mineral skeleton, as is the effect of vertical acceleration upon pore pressure.

6.4.2. Submerged Backfill with Excess Pore Pressure

Excess pore pressures generated by cyclic shaking can be represented by $r_u = \Delta u / \sigma_v'$, where Δu is the excess pore pressure and σ_v' is the initial vertical stress. While there is no rigorous approach for adapting the Mononobe-Okabe solution, the following approaches are suggested.

6.4.2.1. Restrained water case

Ignoring vertical accelerations, the effective unit weight of soil becomes:

$$\text{Equation 6-26: } \gamma_{e3} = \gamma_b (1 - r_u)$$

while the effective unit weight of water is

$$\text{Equation 6-27: } \gamma_{w3} = \gamma_w + \gamma_b r_u$$

The thrust from the soil skeleton, P_{AE} is computed using

$$\text{Equation 6-28: } k_{he3} = \frac{\gamma_t}{\gamma_{e3}} k_h$$

and

$$\text{Equation 6-29: } \Psi_{e3} = \tan^{-1}[k_{he3}]$$

together with a unit weight from Equation 6-26. The effective unit weight of water, Equation 6-27, is used to compute the “static” pore pressure. The effect of vertical acceleration may be accounted for by inserting $(1 - k_v)$ in the denominator of Equation 6-29.

As r_u approaches unity, $\gamma_{e3} \rightarrow 0$ and $\gamma_{w3} = \gamma_t$, so that the fully liquefied soil is a heavy fluid. It would now be logical to add a dynamic pore pressure computed using Equation 6-25 and Equation 6-27.

6.4.2.2. Alternate Procedure

An alternative approach is to use a reduced effective stress friction angle in which the effects of the excess pore water pressures are approximated within the analysis using a simplified shear strength relationship. In an effective stress analysis, the shear resistance on a potential failure surface is reduced by reducing the effective normal stress on this plane by the amount of excess residual pore water pressure, assuming the effective friction angle is unaffected by the cyclic loading. This is equivalent to using the initial, static effective normal stress and a modified effective friction angle, ϕ_{eq} , where

$$\text{Equation 6-30: } \tan \phi'_{eq} = (1 - r_u) \tan \phi'$$

as shown in *Figure 6-14*. In the case of r_u equal to a constant within the fully submerged backfill, the use of ϕ_{eq} in Equation 6-2 and Equation 6-8 for K_{AE} and $K_A(\beta^*, \theta^*)$ approximates the effects of these excess pore water pressures within the analysis. Using k_{he1} , Ψ_{he1} (Equation 6-21 and Equation 6-20) and ϕ_{eq} in the Mononobe-Okabe theory together with a unit weight γ_b will give P_{AE} .

Calculations showed that reducing the effective stress friction angle of the soil to account for the excess pore water pressures when computing a value for P_{AE} is not exact. Comparisons between the exact values of P_{AE} , computed using γ_{e3} , k_{he3} , Ψ_{he3} in the Mononobe-Okabe theory, and the values computed using the ϕ_{eq} procedure shows this approximation to overpredict the value of P_{AE} . The magnitude error in the computed value of P_{AE} increases with increasing values of r_u and increases with decreasing values of k_h . The error is largest for the k_h equal to 0 case.

⁷⁰Westergaard, H. 1931. “Water Pressure on Dams During Earthquakes,” Transactions of ASCE, Paper No. 1835, pp. 418-433.

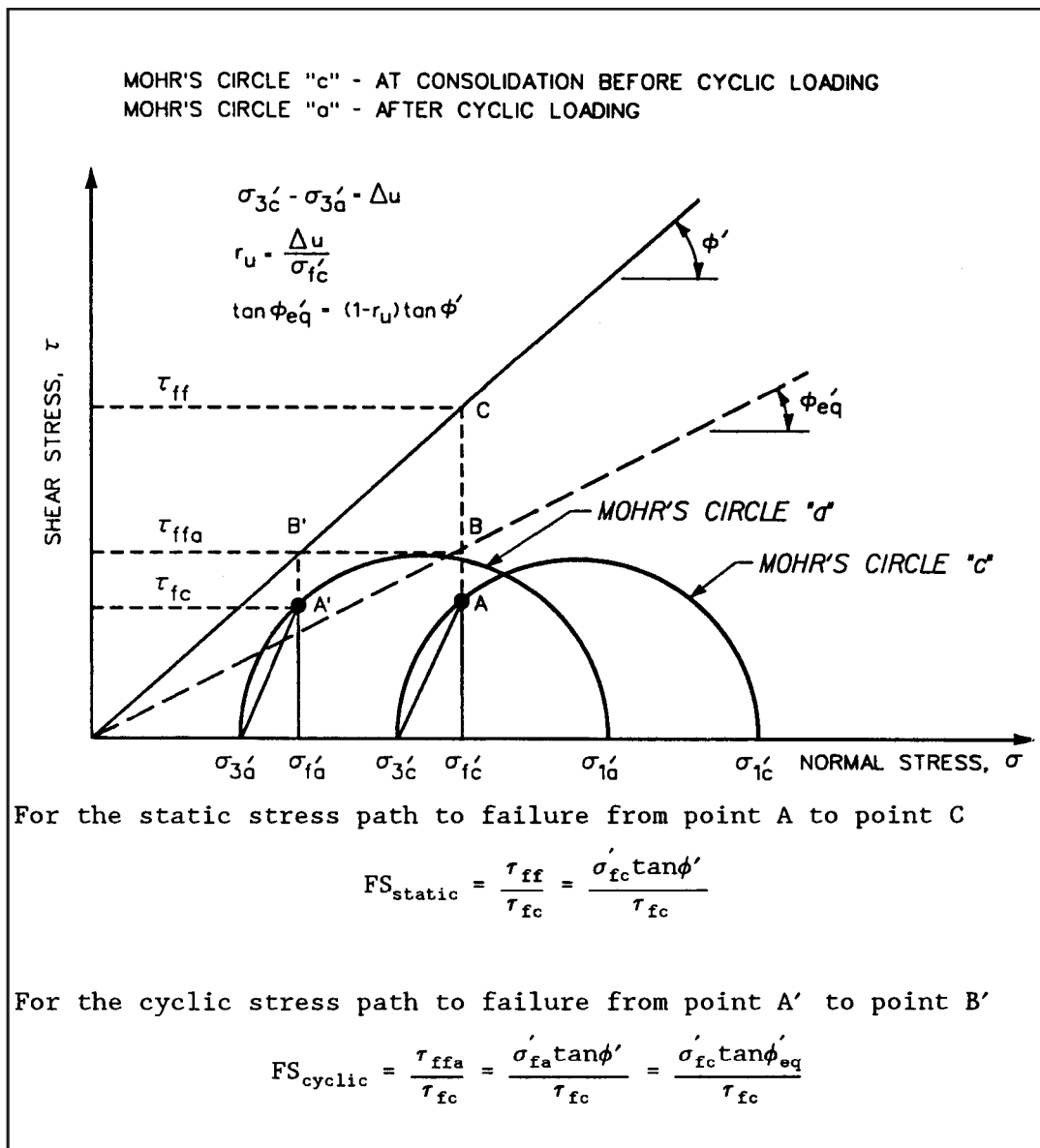


Figure 6-14: Modified effective friction angle

6.4.2.3. Free water case

The thrust from the mineral skeleton may be estimated using:

Equation 6-31: $P_{PE} = K_{PE} \cdot \frac{1}{2} [\gamma_t (1 - k_v)] H^2$

Where

$$\gamma_d = \frac{\gamma_t}{1 + w}$$

To this thrust are added the dynamic Westergaard water pressure (computed using γ_w) and a "static" water pressure computed using γ_{w3} from Equation 6-27.

6.4.3. Partial Submergence

Situations with partial submergence may be handled by weighing unit weights based on the volume of soil in the failure wedge above and below the phreatic surface, as shown in Figure 6-15.

6.5. Dynamic Passive Earth Pressures

The trial wedge procedure of analysis may be used to find the orientation of the critical slip surface that minimizes the value of the earth pressure force acting on the wall for the passive earth pressure problem shown in Figure 6-3. This minimum earth pressure force corresponds to the dynamic passive earth pressure force, P_{PE} . The orientation of the inertial forces $k_h \cdot W$ and $k_v \cdot W$ that minimize the value of P_{PE} is

The Discovery Channel goes APE!!



John White, President, APE being filmed by Discovery Channel for upcoming show about pile hammers.

APE was featured on the **Discovery Channel** recently. It is a great bit of Deep Foundation News. You can view the show right on your computer by clicking on this link: www.apevibro.com/asp/video.asp. Just select the "APE on Discovery" and enjoy the show. It shows the APE quad driving 40 foot diameter piles.



Jack Xu, Managing Director for APE China, stands on Caisson beam of Quad Kong System, Dec. 2001.



Wendy Setlege, wife of Randy Setlege, President of Agra Group and John and Teresa White stand in front of the "Quad Kong" which is four APE Model 400 vibratory driver/extractors mounted together to install 40 foot diameter concrete pipe piles in China.

When a pile driver talks... we listen™. Please call or write:



APE Corporate Offices
7032 South 196th
Kent, Washington 98032
800-248-8498 or
253-872-0141
Fax: 253-872-8710

APE CANADA
1965 Ramey Road
Port Colburn, ON
LZG 7MG
905-328-0850
Fax: 905-834-8486

APE Mid-Atlantic Regional Ofc.
500 Newton Rd. Suite 200
Virginia Beach, VA 23462
866-399-7500
Fax: 757-518-9741
Cell: 757-373-9328

APE Northeast Regional Ofc.
Route 15 North & Taylor Rd.
Wharton, NJ 07885
973-989-1909
Fax: 973-989-1923
888-217-7524

APE Southeast Regional Ofc.
1023 Snively Avenue
Winter Haven, FL 33880
863-324-0378
Fax: 863-318-9409

APE S. Central Regional Ofc.
11128 FM Hwy. 1488
Conroe, TX 77384
936-271-1044
Fax: 936-271-1046
800-596-2877

APE Western Regional Office
160 River Road
Rio Vista, CA 94571
707-374-3266
Fax: 707-374-3270
888-245-4401

Alessi Equipment, Inc.
35 Rosslyn Place
Mt. Vernon, NY 10550
914-699-6300
Fax: 914-699-5300
Imeco-Austria
431-368-2513
Fax: 431-369-8104

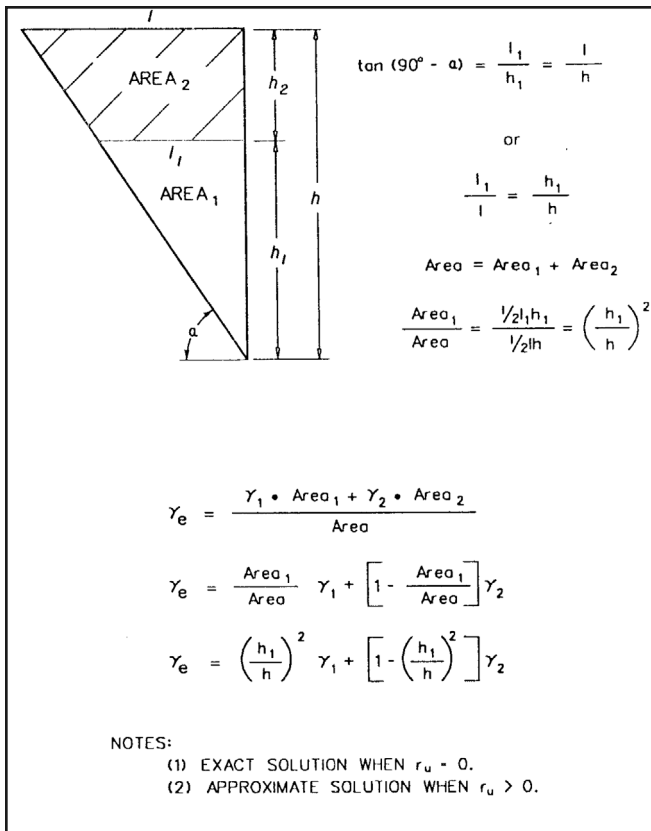


Figure 6-15: Effective unit weight for partially submerged backfills

directed away from the wall and upwards. This corresponds to the case where the soil wedge is accelerating towards the wall (positive a_h values) and downwards (positive a_v values).

The Mononobe-Okabe relationship for P_{PE} for dry backfill, given by Whitman and Christian⁷¹, is equal to

$$\text{Equation 6-32: } P_{PE} = K_{PE} \cdot \frac{1}{2} [\gamma_t (1 - k_v)] H^2$$

and acts at an angle δ from the normal to the back of the wall of height H . The dynamic passive earth pressure coefficient, K_{PE} , is equal to

$$\text{Equation 6-33:}$$

$$K_{PE} = \frac{\cos^2(\phi - \psi + \theta)}{\cos \psi \cos^2 \theta \cos(\psi - \theta + \delta) \left[1 - \sqrt{\frac{\sin(\phi + \delta) \sin(\phi - \psi + \beta)}{\cos(\delta + \psi - \theta) \cos(\beta - \theta)}} \right]^2}$$

In the case of a vertical wall ($\theta = 0$) retaining a horizontal backfill ($\beta = 0$), Equation 6-33 simplifies to

$$\text{Equation 6-34:}$$

$$K_{PE} = \frac{\cos^2(\phi - \psi)}{\cos \psi \cos(\psi + \delta) \left[1 - \sqrt{\frac{\sin(\phi + \delta) \sin(\phi - \psi)}{\cos(\delta + \psi)}} \right]^2}$$

The planar slip surface extends upwards from the heel of the wall through the backfill and is inclined at an angle α_{PE} from the horizontal. α_{PE} is equal to

$$\text{Equation 6-35:}$$

$$\alpha_{PE} = \psi - \phi + \tan^{-1} \left[\frac{\tan(\phi + \beta - \psi) + c_{3PE}}{c_{4PE}} \right]$$

where

$$\text{Equation 6-36:}$$

$$c_{3PE} = \left[\sqrt{[\tan(\phi + \beta - \psi)] [\tan(\phi + \beta - \psi) + \cot(\phi + \theta - \psi)] \cdot [1 + \tan(\delta - \theta + \psi) \cot(\phi + \theta - \psi)]} \right]$$

and

$$\text{Equation 6-37:}$$

$$c_{4PE} = 1 + \left[[\tan(\delta - \theta + \psi)] \cdot [\tan(\phi + \beta - \psi) + \cot(\phi + \theta - \psi)] \right]$$

Figure 6-16 and Figure 6-17 give α_{PE} as a function of Ψ for several values of ϕ .

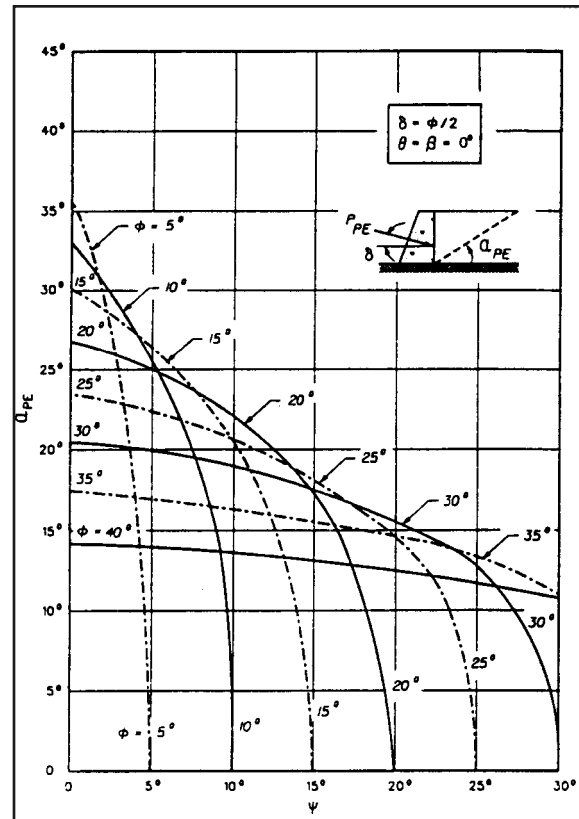


Figure 6-16: Variation α_{PE} with Ψ for δ equal to $\phi/2$, vertical wall and level backfill

The Mononobe-Okabe equation assumes a planar failure surface, which only approximates the actual curved slip surface. Mononobe-Okabe's relationship overpredicts the values for K_{PE} and the error increases with increasing values for δ and Ψ .

Rotating the passive soil wedge with a planar slip surface

⁷¹ Whitman, J., and Christian, J. 1990. "Seismic Response of Retaining Structures," Symposium Seismic Design for World Port 2020, Port of Los Angeles, Los Angeles, CA.

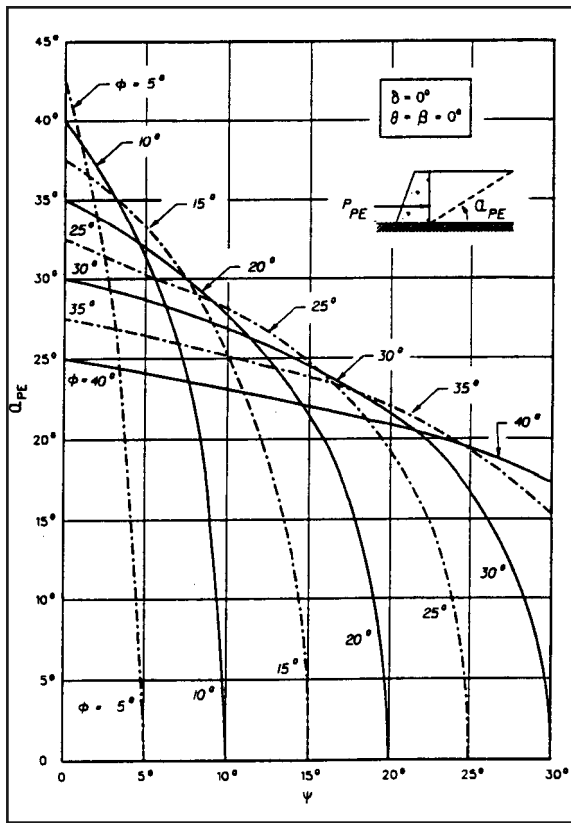


Figure 6-17: Variation in α_{PE} with Ψ for δ equal to zero degrees, vertical wall and level backfill

through the seismic inertia angle, the resultant vector, representing vectorial sums of W , $k_h \cdot W$, and $k_v \cdot W$, becomes vertical, and the dynamic passive earth pressure force problem becomes equivalent to the static problem, as shown in Figure 6-18.

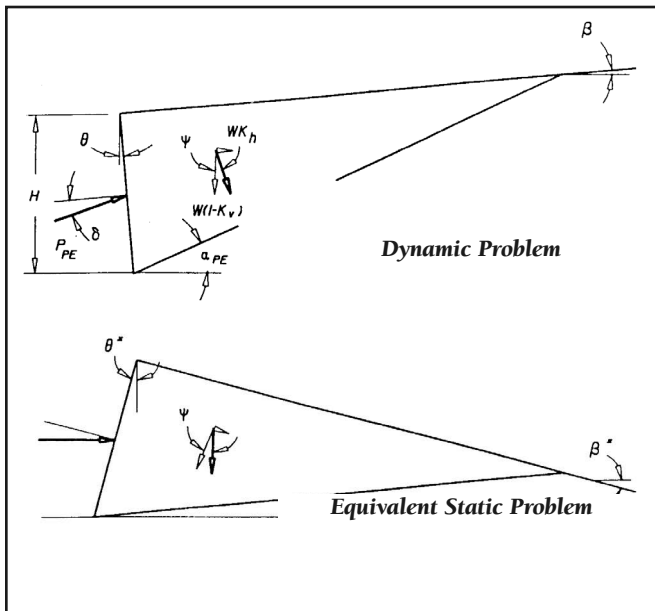


Figure 6-18: Equivalent static formulation of the Mononobe-Okabe passive dynamic earth pressure problem

The seismic passive resistance is given by

Equation 6-38:

$$P_{PE} = [K_P(\beta^*, \theta^*) \cdot F_{PE}] \cdot \frac{1}{2} [\gamma_t (1 - k_v)] H^2$$

where

$$\beta^* = \beta - \Psi$$

$$\theta^* = \theta - \Psi$$

and

Equation 6-39:
$$F_{PE} = \frac{\cos^2(\theta - \psi)}{\cos\psi \cos^2\theta}$$

Ψ is computed using Equation 6-3. Values of F_{PE} are also given as a function of Ψ and θ in Figure 6-19. $K_P(\beta^*, \theta^*)$ is determined from the Coulomb static K_P values by Equation 5-33. The Coulomb formulation assumes a planar failure surface that approximates the actual curved failure surface. The planar failure surface assumption introduces errors in determination of K_P and the error increases with increasing values of δ . The error in slip surface results in an overprediction of K_P . Thus the equivalent static formulation will be in error since the product of $K_P(\beta^*, \theta^*)$ times F_{PE} is equal to K_{PE} . An alternate procedure is to approximate $K_P(\beta^*, \theta^*)$ by using the static K_P values shown in Figure 5-5 and Figure 5-6. Calculations show K_{PE} values by the alternate procedure are smaller than K_{PE} values by Mononobe-Okabe. This procedure

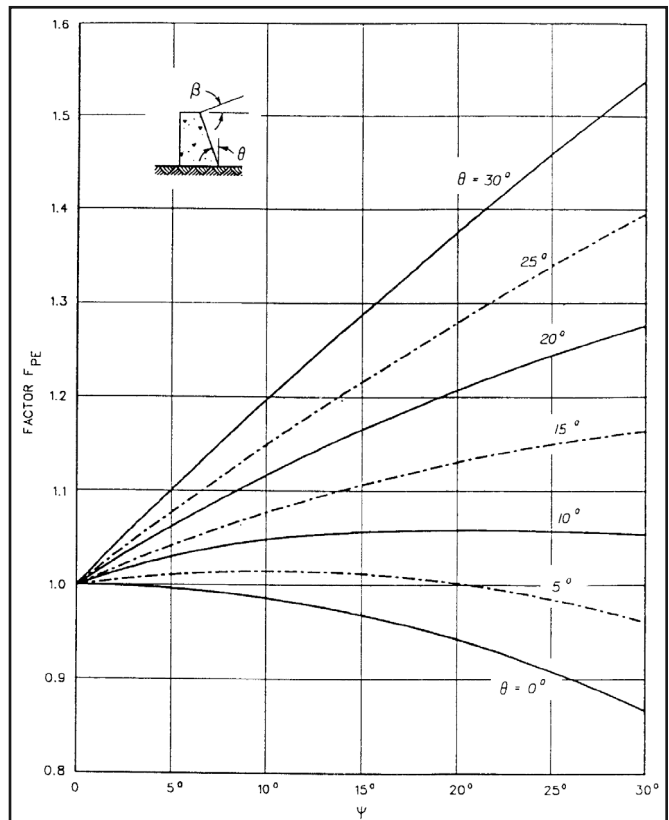


Figure 6-19: Values of factor F_{PE}

is illustrated in the procedures outlined earlier. The procedures are used to account for the effect of submergence of the backfill in computing the value of P_{PE} . For example, in the restrained water case of a fully submerged backfill, an effective unit equal to γ_b is assigned to the backfill for the case of $r_u = 0$ or Equation 6-26 with $r_u > 0$.

K_{PE} or $K_p(\beta^*, \theta^*)$ and F_{PE} are computed using an equivalent seismic inertia angle using Equation 6-22 for the case of $r_u = 0$ or Equation 6-29 with $r_u > 0$.

Example 6 Computation of Passive Dynamic Earth Pressures

For a wall (Figure 6-20) of height $H = 20$ ft retaining a dry cohesionless backfill with $\phi' = 30$ degrees, $\delta = 3$ degrees, $\beta = 6$ degrees, $\theta = 0$ degrees, $k_h = 0.1$ (acceleration $k_h \cdot g$ towards the wall and inertia force $k_h \cdot W$ away from the wall), and $k_v = 0.067$ (acceleration $k_v \cdot g$ acting downward and inertia force $k_v \cdot W$ acting upward), compute K_{PE} , P_{PE} , and α_{PE} .

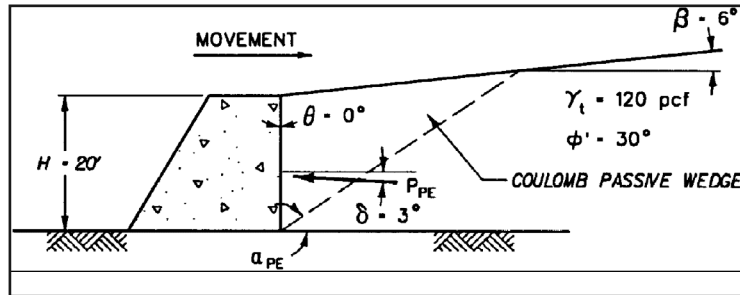


Figure 6-20: Example of Passive Dynamic Earth Pressure Computation

Equation 6-40:

$$\psi = \tan^{-1} \left[\frac{0.1}{(1 - 0.067)} \right]$$

$$= 6.118^\circ \text{ (by Equation 6-3)}$$

Equation 6-41:

$$K_{PE} = \frac{\cos^2 (30 - 6.12 + 0)}{\cos (6.12) \cos^2 (0) \cos (6.12 - 0 + 3) \left[1 - \sqrt{\frac{\sin (30 + 3) \sin (30 - 6.12 + 6)}{\cos (3 + 6.12 - 0) \cos (6 - 0)}} \right]^2}$$

$$= 3.785 \text{ (by Equation 6-34)}$$

Equation 6-42: $P_{PE} = 3.785 (1/2) [(120 \text{ pcf}) (1 - 0.067)] (20')^2 = 84,754 \text{ lb per ft of wall}$
(by Equation 6-32)

Equation 6-43:

$$c_{3PE} = \left[\sqrt{[\tan(30 + 6 - 6.12)] [\tan(30 + 6 - 6.12) + \cot(30 + 0 - 6.12)]} \cdot \right.$$

$$\left. \frac{[1 + \tan(3 - 0 + 6.12) \cot(30 + 0 - 6.12)]}{1.4547} \right] =$$

$$= 1.4893$$

Equation 6-44:

$$c_{4PE} = 1 + \left[[\tan(3 - 0 + 6.12)] \cdot [\tan(30 + 6 - 6.12) + \cot(30 + 0 - 6.12)] \right]$$

$$= 1.4547$$

Equation 6-45:

$$\alpha_{PE} = 6.12 - 30 + \tan^{-1} \left[\frac{\tan(30 + 6 - 6.12) + 1.4893}{1.4547} \right]$$

$$= 30.9^\circ \text{ (by Equation 6-35)}$$

#1 in Marine Dock Products...

Dock Fenders ♦ Dock Boxes ♦ Line Hangers
Power Pedestals ♦ Fish Tables ♦ Piling Caps
Cleats ♦ Hose Holders ♦ Trash Receptacles
Vertical Lift Ladders ♦ Standard Ladders
Floating Docks, Hardware & Floats

Manufacturer & Distributor for:

**FEND-ALL® Family
of Dock Fenders**
(Patent #6,289,836)

**FEND-OFF® Family
of Dock Fenders**

PerfectLine® Dock Boxes

The Leader in Quality and Service

Service is the #1 priority at Marina & Dock Equipment, as you, our customer, are our best and most important salespeople. Regardless of the size of your needs, you will receive the benefit of our twenty plus years of experience, expertise and integrity in the marine industry.

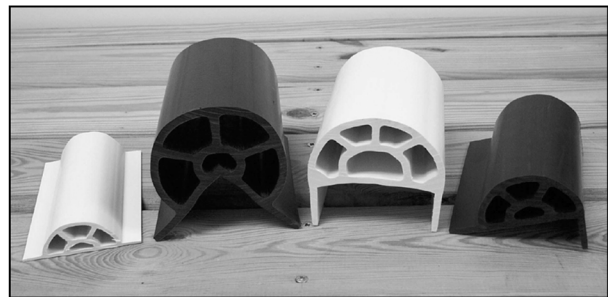
...Because Our Products are the Best!

PerfectLine® Dock Boxes



- ♦ All Resins and Gelcoats are Pure, Marine Grade Isophthalics
- ♦ UV Gelcoat for Long-lasting Protection
- ♦ Molded Non-skid Surface on Lids
- ♦ Lids have Foam Core for added Strength
- ♦ Continuous Heavy Duty Hinge and Fasteners
- ♦ Locking Hasp and Lid Retainer Cable

FEND-ALL® Dock Fenders



- ♦ Only Continuously Supported, Double-wall Fender Available
- ♦ 300% Elongation Before Breakage
- ♦ Internal Highenergy Absorption Web
- ♦ Life Expectancy of Fender Material is 10+ Years
- ♦ Contains UV and Mildew Inhibitors
- ♦ Available in Black, White or Gray

**New Style
Trash Receptacle &
Dock Boxes
Available Now!**



Marina & Dock Equipment

*A division of Alltel Industries
of South Florida, Inc.*

**1 (877) ALL-DOCK
(255-3625)**

(561) 540-2520

Fax (561) 540-2522

www.dockequipment.com or

www.marina-dock.com

e-mail: info@marina-dock.com

425 Industrial Street ♦ #4 ♦ Lake Worth, FL 33461

6.5.1. Simplified Procedure for Dynamic Passive Earth Pressures

Towhata and Islam⁷² recommended a simplified approach for computing the dynamic passive earth pressure force that is similar to the Seed and Whitman procedure for the dynamic active earth pressure force. They also considered the group of structures consisting of a vertical wall ($\theta = 0$) retaining a granular horizontal backfill ($\beta = 0$) with ϕ equal to 35 degrees, δ equal to zero, and k_v equal to zero. Equation 6-47 is presented as developed by Towhata and Islam, while Equation 6-46, Equation 6-48 and Equation 6-49 have been modified by the authors of this report. P_{PE} is defined as

Equation 6-46: $P_{PE} = P_P - \Delta P_{PE}$

where the reduction in the static passive earth pressure value P_P due to earthquake shaking is given by

Equation 6-47: $\Delta P_{PE} = \frac{1}{2} \gamma_t H^2 \cdot \Delta K_{PE}$

for a dry granular backfill. The dynamic passive earth pressure coefficient is equal to

Equation 6-48: $K_{PE} = K_P - \Delta K_{PE}$

And

Equation 6-49: $\Delta K_{PE} = \frac{17}{8} \cdot k_h \cdot$

Using this simplified procedure, K_P is computed using Equation 5-16 (Rankine), and ΔK_{PE} is computed using Equation 6-49. The incremental dynamic force ΔP_{PE} acts counter to the direction of P_P , reducing the contribution of the static passive pressure force to P_{PE} . The resulting forces P_P (Equation 5-21) and ΔP_{PE} (Equation 6-47) act normal to the back of a wall.

The simplified procedure was developed for vertical walls retaining horizontal backfills with $\delta = 0$. This simplified procedure should not be applied to dynamic passive earth pressure problems involving values of $\delta > 0$, due to the magnitude of the error involved.

6.5.2. Example

Example 7 Computation of K_{PE} , P_{PE} , and α_{PE}

For a wall (Figure 6-21) of height $H = 20$ ft retaining a dry cohesionless backfill with $\phi' = 30$ degrees, $\delta = 3$ degrees, $\beta = 6$ degrees, $\theta = 0$ degrees, $k_h = 0.1$ (acceleration $k_h \cdot g$ towards the wall and inertia force $k_h \cdot W$ away from the wall), and $k_v = 0.067$ (acceleration $k_v \cdot g$ acting downward and inertia force $k_v \cdot W$ acting upward), compute K_{PE} , P_{PE} , and α_{PE} .

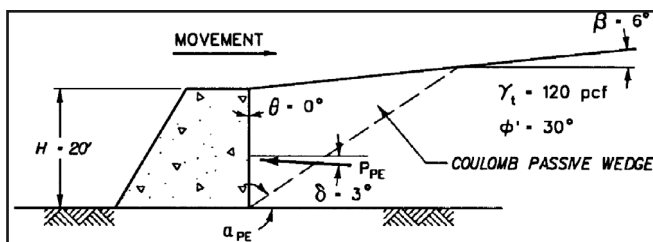


Figure 6-21: Example of Simplified Computation of Dynamic Passive Earth Pressures

Equation 6-50: $\psi = \tan^{-1} \left[\frac{0.1}{(1 - 0.067)} \right]$ (by Equation 6-3)
 $\Psi = 6.118^\circ$

Equation 6-51:

$$K_{PE} = \frac{\cos^2 (30 - 6.12 + 0)}{\cos (6.12) \cos^2 (0) \cos (6.12 - 0 + 3)} \left[1 - \frac{\sin (30 + 3) \sin (30 - 6.12 + 6)}{\cos (3 + 6.12 - 0) \cos (6 - 0)} \right]^2$$

6.6. Effect of Vertical Accelerations on the Values for the Dynamic Active and Passive Earth Pressures

In a pseudo-static analysis the horizontal and vertical accelerations of the soil mass during an earthquake are accounted for by applying equivalent inertial forces $k_h \cdot W$ and $k_v \cdot W$ to the soil wedge, which act counter to the direction of the accelerating soil wedges, as shown in Figure 6-2 and Figure 6-3. A positive horizontal acceleration value increases the value of P_{AE} and decreases the value of P_{PE} . The vertical component of acceleration impacts the computed values of both P_{AE} and P_{PE} and K_{AE} and K_{PE} .

Upward accelerations ($-k_v \cdot g$) result in smaller values of K_{AE} and larger values of P_{AE} as compared to the K_{AE} and P_{AE} values when k_v is set equal to zero. Upward accelerations ($-k_v \cdot g$) increase the value of P_{AE} due to the contribution of the term $(1 - k_v)$ in Figure 6-1. This trend is reversed when the vertical acceleration acts downward ($+k_v \cdot g$). Seed and Whitman and Chang and Chen⁷³ showed that the change in the KAE value varied with both the value of k_v and k_h .

Calculations with k_v ranging from 1/2 to 2/3 of the k_h value show that the difference between the computed values of K_{AE} with a nonzero k_v value and k_v equal to zero is less than 10 percent. Seed and Whitman⁵⁸ concluded that for typical gravity retaining wall design problems, vertical accelerations can be ignored when computing K_{AE} . The k_v value has a greater impact on the computed value of P_{PE} than on the value of P_{AE} .

Chang and Chen⁷³ show that the change in the KPE value varies with both the value of k_v and k_h . The difference between the values of K_{PE} with a nonzero k_v value and k_v set

⁷²Towhata, I., and Islam, S. 1987 (Dec.). "Prediction of Lateral Movement of Anchored Bulkheads Induced by Seismic Liquefaction," Soils and Foundations, Vol. 27, No. 4, pp. 137-147.

⁷³Chang, M., and Chen, W. 1982. "Lateral Earth Pressures on Rigid Retaining Walls Subjected to Earthquake Forces," Solid Mechanics Archives, Vol. 7, No. 4, pp. 315-362.

(by Equation 6-32)

$$K_{PE} = 3.785$$

Equation 6-52: $P_{PE} = 3.785 (1/2) [(120 \text{ pcf}) (1 - 0.067)] (20')^2$

$P_{PE} = 84,754 \text{ lb per ft of wall (by Equation 6-3)}$

Equation 6-53:

$$c_{3PE} = \left[\sqrt{[\tan(30 + 6 - 6.12)] [\tan(30 + 6 - 6.12) + \cot(30 + 0 - 6.12)]} \cdot \right.$$

$$\left. \frac{[1 + \tan(3 - 0 + 6.12) \cot(30 + 0 - 6.12)]}{c_{3PE} = 1.4893} \right]$$

$$c_{4PE} = 1 + \left[[\tan(3 - 0 + 6.12)] \cdot [\tan(30 + 6 - 6.12) + \cot(30 + 0 - 6.12)] \right]$$

$$c_{4PE} = 1.4547$$

$$\alpha_{PE} = 6.12 - 30 + \tan^{-1} \left[\frac{\tan(30 + 6 - 6.12) + 1.4893}{1.4547} \right] \text{ (by Equation 6-35)}$$

$$\alpha_{PE} = 30.9^\circ$$

equal to zero increases with increasing magnitudes of both k_v and k_h . This difference can easily be greater than 10 percent. In general, vertical accelerations acting downward ($+k_v \cdot g$) will decrease the K_{PE} and P_{PE} values from the corresponding K_{PE} and P_{PE} values for which k_v is set equal to zero. The trend is reversed when the vertical acceleration acts upward ($-k_v \cdot g$). When P_{PE} acts as a stabilizing force for a structure, vertical accelerations should be considered in the computations of the value for P_{PE} . An example is the soil region below the dredge level and in front of an anchored sheet pile wall.

6.7. Cases with Surface Loadings

There are two approaches used to approximate the additional lateral earth pressures on walls due to surface loadings; (1) the wedge method of analysis and (2) finite element analyses.

In the case of uniform surcharge q_s , the value of the dynamic active earth pressure force is computed using the modified Mononobe-Okabe relationships listed in Figure 6-22 and Equation 6-2 (or Equation 6-4 for a vertical wall retaining a horizontal backfill) for K_{AE} . The point of application of P_{AE} along the back of the wall is computed using the procedure outlined in Figure 6-22 through Figure 6-25. In this approximate procedure, the surcharge q_s is

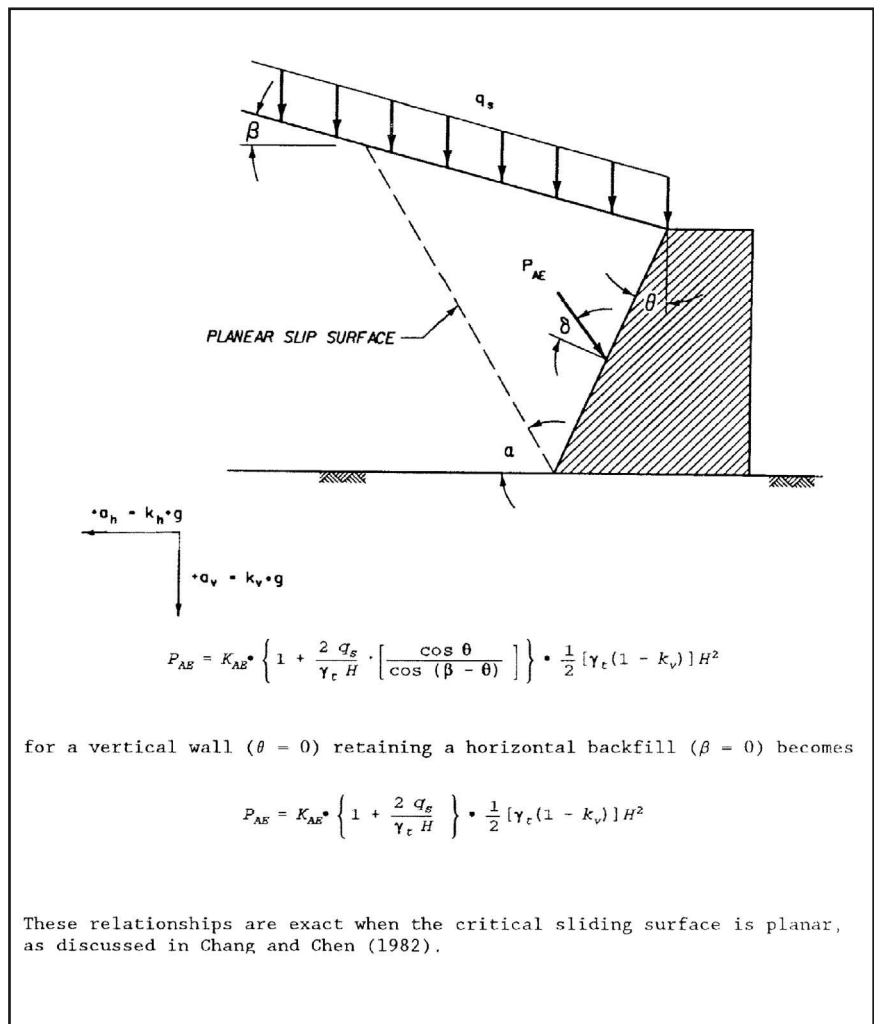


Figure 6-22: Mononobe-Okabe active wedge relationships including surcharge loading the pseudo-static analysis

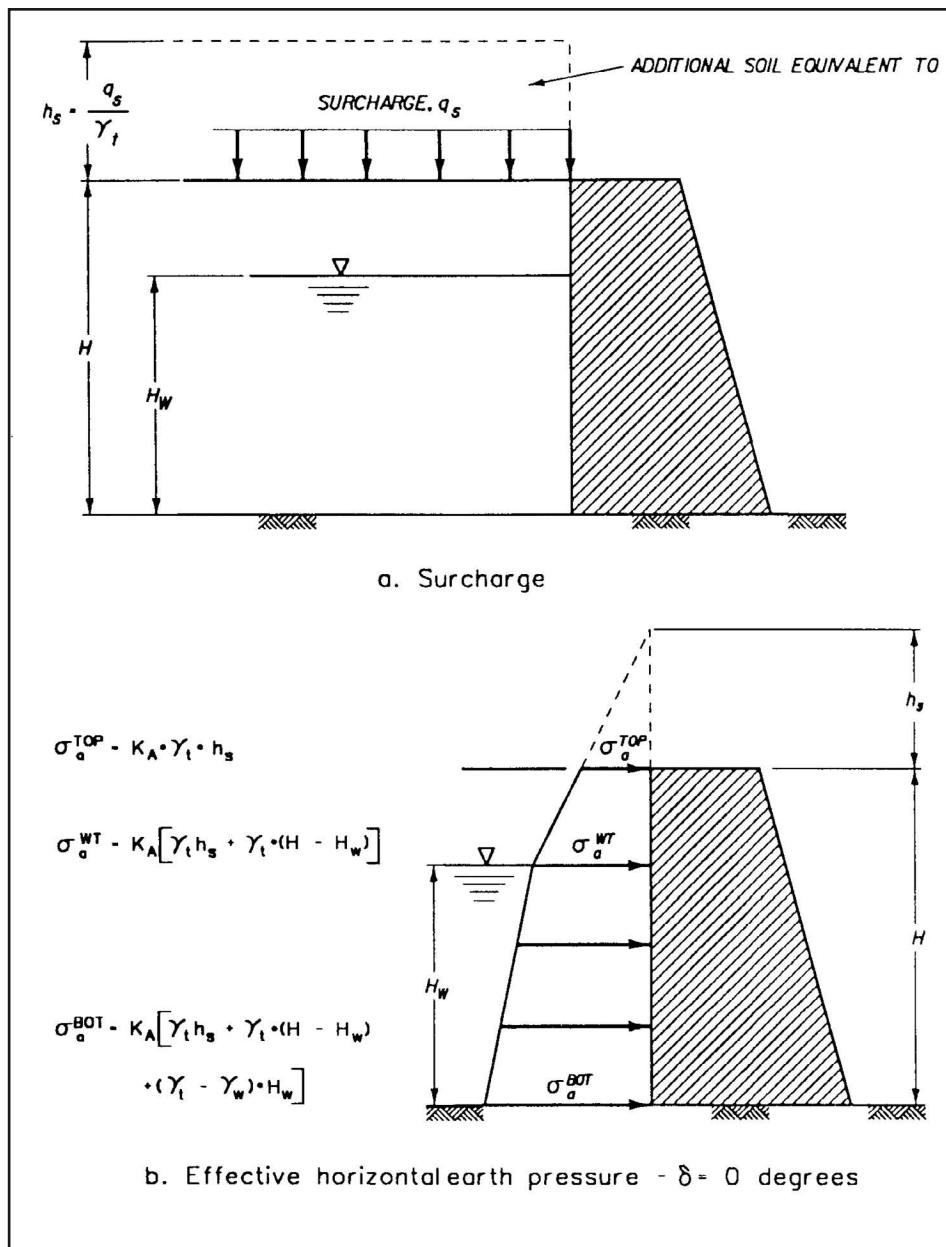


Figure 6-23: Static active earth pressure force including surcharge (Continued)

replaced by the addition of a layer of soil of height h_s equal to q_s/γ_t . The resulting problem is analysed by adapting the Seed and Whitman's simplified procedure to the problem of a uniform surcharge loading as outlined in Figure 6-25.

Pseudo-static trial wedge analyses may be performed to account approximately for both uniformly and non-uniformly distributed surface loadings. These analyses may be performed on walls whose movements satisfy the criteria listed in Table 4-1. Such analyses will give the total thrust against a wall. The effects of surface loading is included within the wedge analysis by including that portion of the surface loading between the back of the wall and the intersection of the slip surface and the backfill surface in the force equilibrium

calculation for each wedge analysed, as described in Section 3.6 for the static problem. The effect of the earthquake is modelled in the pseudo-static trial wedge analysis by an additional set of static forces, $k_h \cdot W$, $k_v \cdot W$, $k_h \cdot W_s$, and $k_v \cdot W_s$, where W is equal to the weight of the soil contained within the trial wedge and W_s is equal to the weight of surcharge contained within the region located above the trial wedge as shown in Figure 8-3 for the active earth pressure problem. The difficult part of is to determine the point of action of this force along the back of the wall.

Two-dimensional finite element analyses may be used to estimate the dynamic forces against walls because of surface loadings.



A Whole Lot of Hammer

Introducing the new line of 12 affordable and dependable hammers from Pileco, Inc.

These hammers redefine the name you've come to trust for all of your pile driving needs.

Tipping the scales
in your favor with quality equipment & world class support.



PILECO, INC.

111 Berry Rd. P.O. Box 16099 Houston, TX 77222
TEL 1-800-474-5326 • 713-691-3000 FAX 713-691-0089
www.pileco.com

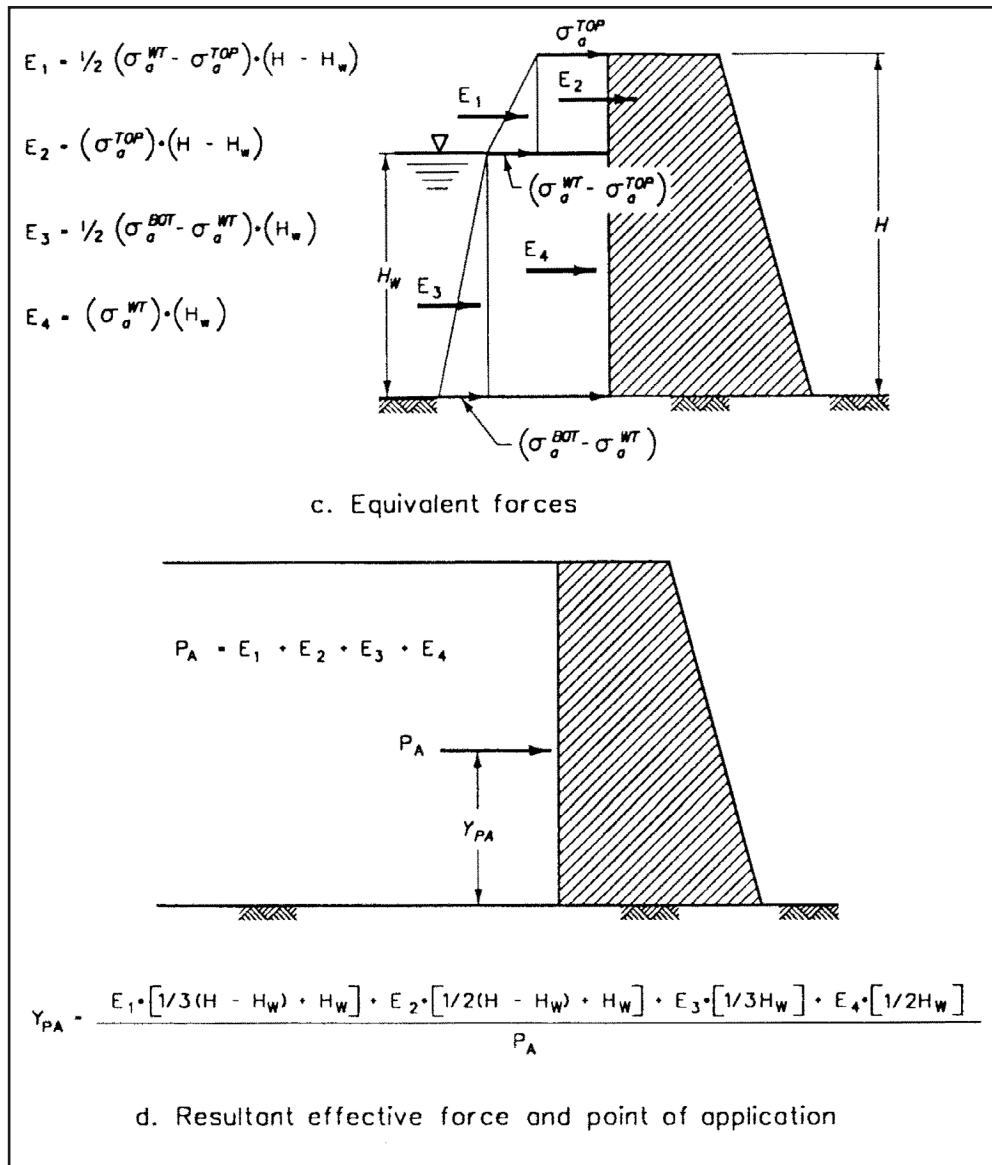


Figure 6-24: Static active earth pressure force including surcharge (Concluded)

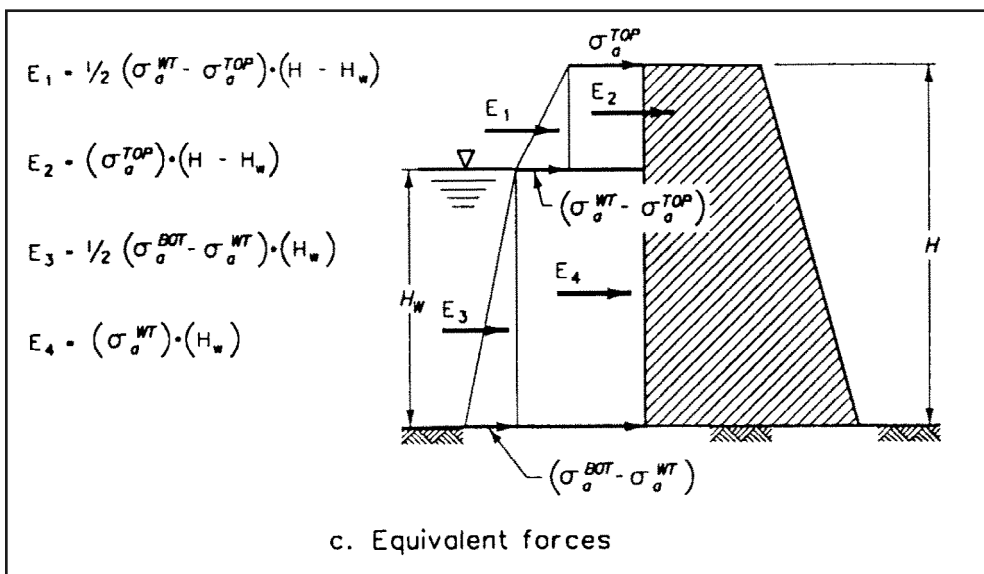


Figure 6-25: Static active earth pressure force and incremental dynamic active earth pressure force including surcharge

Chapter Seven: Water and Water Flow in Soil

Sheet pile structures almost inevitably involve water, either because they are in a marine application or because of groundwater conditions. Excluding corrosion, which is covered elsewhere, the effects of water on sheet pile walls are twofold: the effects of the hydrostatic action of water, and the effects of groundwater flow on the surrounding soil.

7.1. Hydrostatic Water and Surcharge

Sheet pile structures built today in connection with waterfront facilities are subjected to maximum earth pressure when the tide or river level is at its lowest stage. A receding tide, receding high water, or heavy rainstorm may cause a higher water level behind a sheet pile wall than in front of it, depending upon the type of backfill used. If the backfill is fine or silty sand, the height of the water behind the sheet pile wall may be several feet. If the soil behind the wall is silt or clay, full hydrostatic pressure behind the wall should be assumed up to the highest position of the previous water level.

The difference in water level on either side of the wall introduces

1. Additional pressure on the back of the wall due to hydrostatic load, and
2. Reduction in the unit weight of the soil in front of the piling (thus, a reduction of passive resistance.)

The distribution of Coulomb active earth pressures for a partially submerged wall retaining a frictional backfill and supporting a uniform surcharge, q , is shown in *Figure 7-1*. With a hydrostatic water table at height H_w above the base of the wall, the resulting pressures acting along the back of the wall are equal to the sum of:

- (1) The thrust of the soil skeleton as a result of its unit weight,
- (2) The thrust of the soil skeleton as a result of the surcharge, q , and
- (3) The thrust of the pore water.

The effective weight of the backfill, σ'_{wt} , above the water table is equal to

$$\text{Equation 7-1: } \sigma'_{wt} = \gamma_t \cdot z$$

and below the water table, σ'_{wt} is equal to

$$\text{Equation 7-2: } \sigma'_{wt} = \gamma_t \cdot (H - H_w) + \gamma' \cdot [z - (H - H_w)]$$

Where

- σ'_{wt} = effective weight of the backfill
- γ_t = total unit weight
- γ'_t = effective unit weight at depth z
- H = height of the wall
- H_w = distance from water table to bottom of wall

The buoyant unit weight, γ_b , is equal to

$$\text{Equation 7-3: } \gamma_b = \gamma_t - \gamma_w$$

Where

- γ_b = buoyant unit weight of the soil
- γ_w = unit weight of the water

For hydrostatic pore water pressures, γ' is equal to the buoyant unit weight, γ_b . σ_a is equal to the sum of the thrust of the soil skeleton because of its unit weight and the thrust of the soil skeleton because of the surcharge,

$$\text{Equation 7-4: } \sigma_a = (\sigma'_{wt} + q) \cdot K_A$$

and is inclined at an angle δ from the normal to the back of the wall. In this case, K_A is computed for a level backfill ($\beta = 0$) and a vertical wall face ($\theta = 0$). The hydrostatic water pressures are equal to

$$\text{Equation 7-5: } u = \gamma_w \cdot [z - (H - H_w)]$$

Where

- q = uniform surcharge load on the wall

and is normal to the back of the wall. The total thrust on the wall, P , is equal to the sum of the equivalent forces for the three pressure distributions. Due to the shape of the three pressure distributions, its point of action is higher up the back of the wall than one-third H above the heel.

The orientation of the failure surface is not affected by the hydrostatic water pressures and is calculated using Equation 5-29.

The equation for σ_a of a soil whose shear strength is defined in terms of the effective strength parameters c and ϕ would be equal to

$$\text{Equation 7-6: } \sigma_a = (\sigma'_{wt} + q) \cdot K_A - 2c\sqrt{K_A}$$

and inclined at an angle δ from the normal to the back of the wall.

7.2. Steady State Seepage

If the level of the water on the excavation side of the wall is always the same as the phreatic surface on the soil side, there will be no water flow and hydrostatic conditions (without unbalanced hydrostatic forces on the wall) will take place.

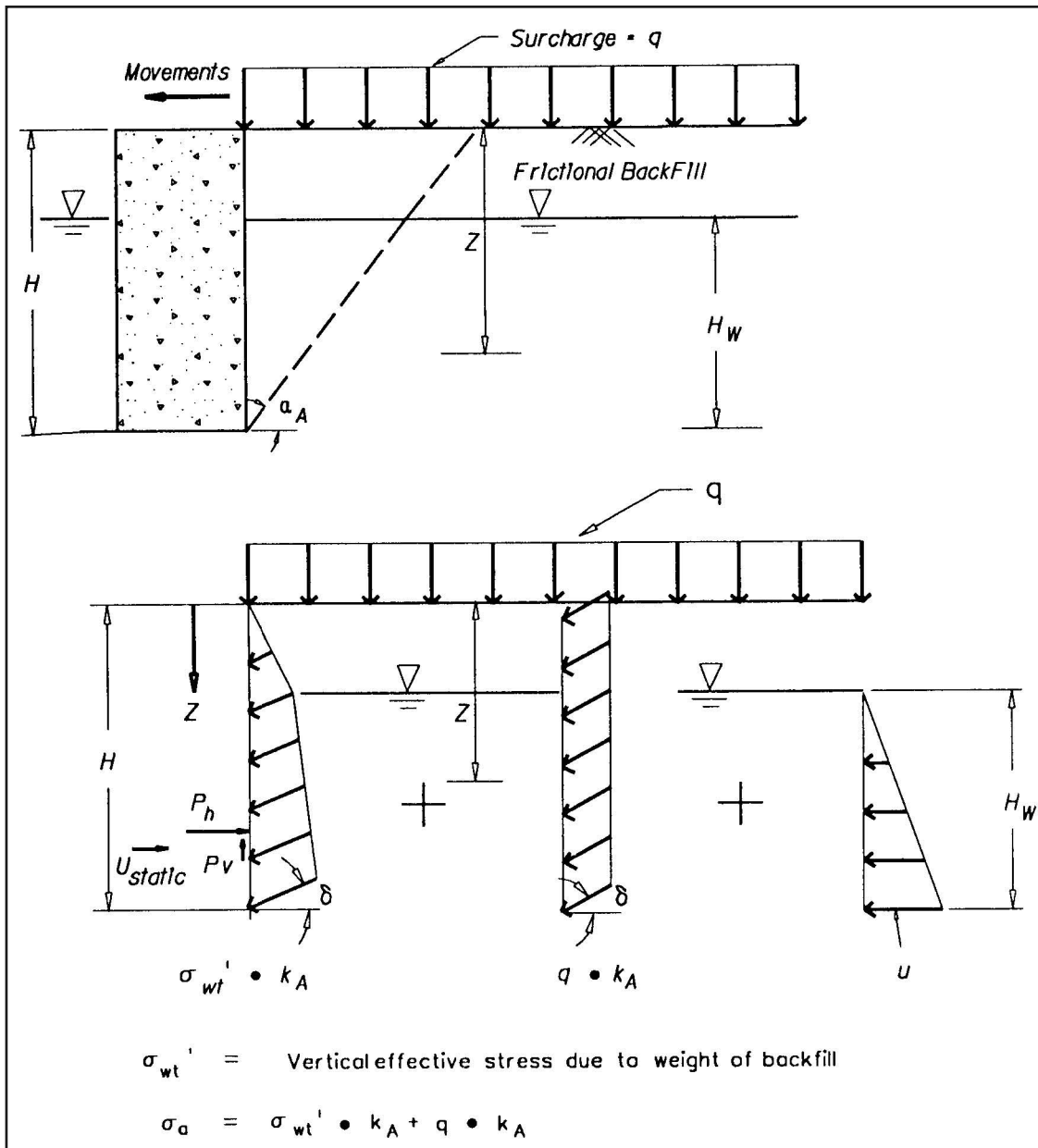


Figure 7-1 Coulomb active earth pressures for a partially submerged backfill and a uniform surcharge

However, there are many conditions that make this impossible, including tidal variations and pumping braced excavations dry below the prevailing water table. In cases such as these, water movements in the soil will take place and these will have a variety of effects on soil and wall alike.

7.2.1. Theory of Groundwater Flow

The flow of water through a soil medium is assumed to follow Darcy's law:

Equation 7-7: $q = k \frac{\Delta h}{L} A$

Where

- q = discharge (volume/time)
- A = cross-sectional area

- Δh = height of water drop, length
- L = length of water flow
- $\Delta h/L$ = the hydraulic gradient (dimensionless; use of this as the hydraulic gradient is based on Bernoulli's equation)
- k = coefficient of permeability, expressed in length per unit time

The hydraulic seepage gradient, i, at any point in the backfill is equal to

Equation 7-8: $i = \Delta h / \Delta l$

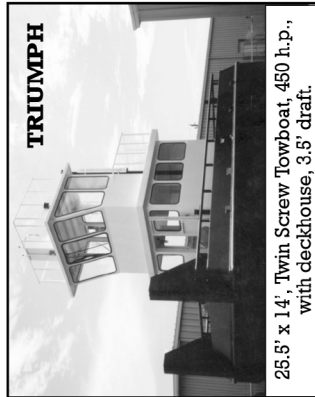
Where

- Δh = the change in total head
- Δl = the length of the flow path over which the incremental head drop occurs.

TRUCKABLE TOWBOATS AND BARGES

10 Reasons Why Quality Saves You Time and Money.

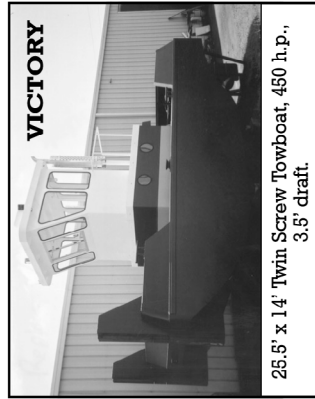
1. Improved coating system includes inorganic zinc undercoater on exterior, blasted and coated with two-part epoxies inside and out, providing superior rust prevention for the long haul.
2. Full-length engine stringers with six-point vibration isolation mounts prevent misalignment, mount failures, and eliminates excessive vibration and noise.
3. Increased capacity closed cooling system prevents overheating in warmer climates and freeze-ups in colder regions.
4. Superior hull form and hydrodynamics creates more thrust per horsepower at the propeller for superior control in close quarters.
5. PYI Packless shaft seal creates an absolutely dry bilge, preventing rust and accidental oil spills.
6. Oversized 2.5" stainless steel propeller shaft, AQUAMETT 21, prevents flexing, corrosion and premature failure.
7. Overbuilt underwater running gear withstands repeated groundings without damage to prop or rudders.
8. No "angle iron" framing. All framing is .375 and .500 flat bar, which increases strength and allows all areas to be painted, avoiding hidden corrosion.
9. Enclosed push knee structures with Johnson weld on rubber pads protects boat and barge by eliminating metal-to-metal contact. This also helps to keep boat stuck to barge.
10. Full 360-degree visibility with lower extending windows creates excellent visibility and eliminates dangerous blind spots close to boat. Quality should also mean safety.



TRIUMPH
25.5' x 14' Twin Screw Towboat, 450 h.p., with deckhouse, 3.5' draft.

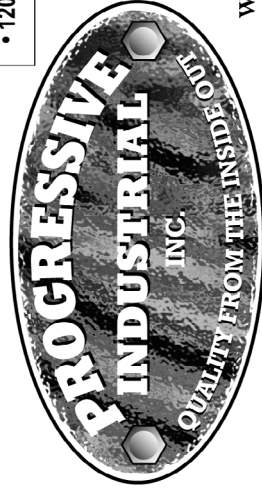


CONQUEST
25.5' x 12' Single Screw Towboat, 225 h.p., flanking rudders.



VICTORY
25.5' x 14' Twin Screw Towboat, 450 h.p., 3.5' draft.

- Just Turn the Key. Everything is Included.**
- Towing Bitt and Four Cleats
 - Running Lights
 - Lockable Pilot House and Engine Room
 - Non-skid Deck
 - Engine Room and Pilot House Lights
 - Opening Front Window in Pilot House
 - Coolant Tanks with Level Indicators
 - Large-Capacity Fuel Tank
 - Full Instrumentation
 - 1200 G.P.M Bilge Pump



Palmetto, Florida
(941) 723-0201
www.pushboats-barges.com

SECTIONAL BARGES



8' x 20' to 15' x 60' per section pin together to form as large a platform as needed.

Fast Delivery!
Call Now for a Same-Day Quote!

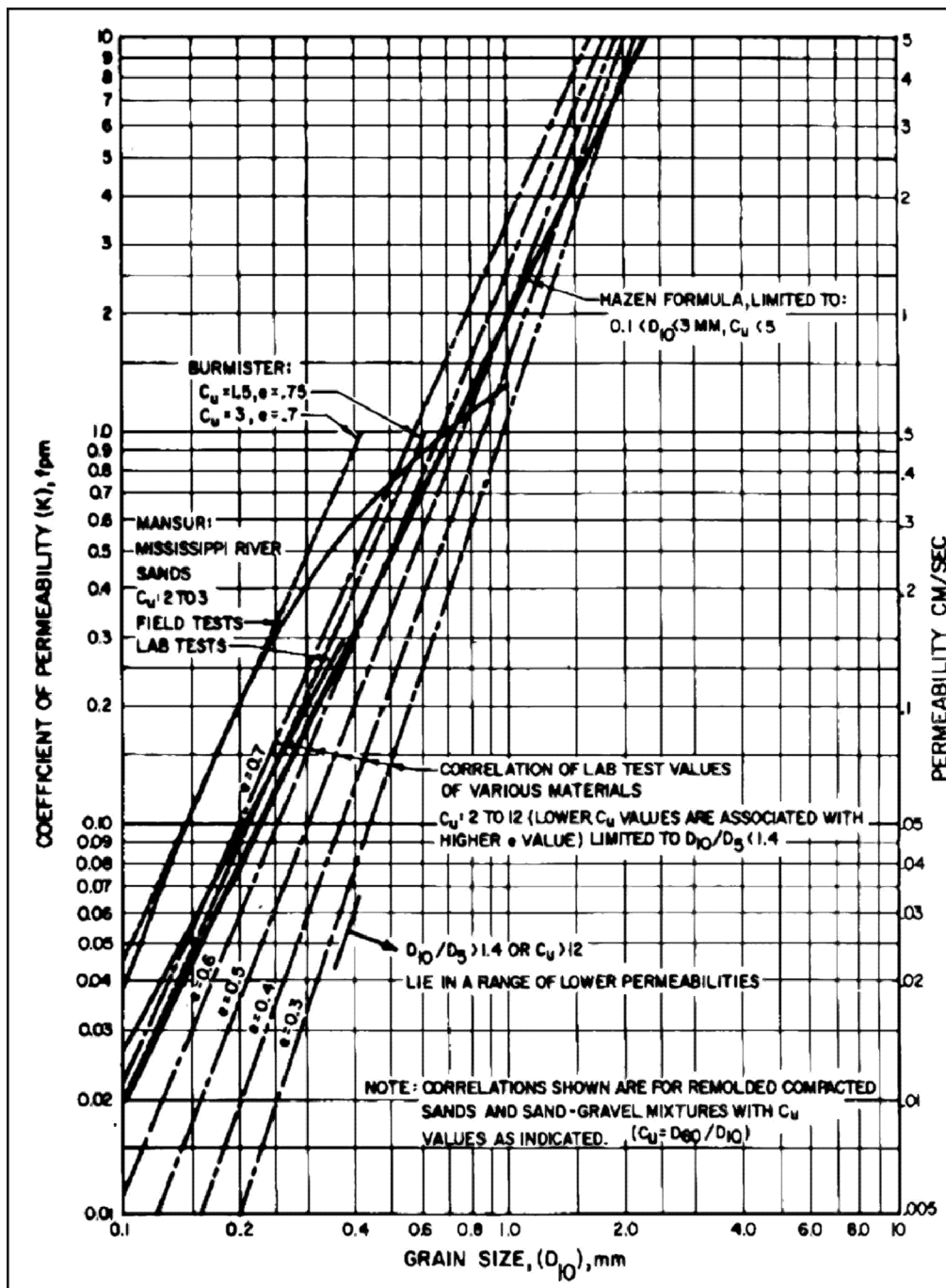


Figure 7-2: Permeability of Sand and Sand-Gravel Mixtures

This is equivalent to the length of water flow. With this, Equation 7-7 reduces to

Equation 7-9: $q = kiA$

The coefficient of permeability, k , is defined as the rate of discharge of water at a temperature of 20° C under conditions of laminar flow through a unit cross-sectional area of a soil medium under a unit hydraulic gradient. The coefficient of permeability has the dimensions of velocity and is usually

expressed in centimetres/second. The permeability of a soil depends primarily on the size and shape of the soil grains, the void ratio of the soil, the shape and arrangement of the voids, and the degree of saturation. *Permeability computed based on Darcy's law is limited to the conditions of laminar flow and complete saturation of the voids.*

Permeability is the most variable of all the material properties commonly used in geotechnical analysis. A permeability spread of ten or more orders of magnitude has been reported for a number of different types of tests and materials.

⁷⁴For typical values of permeability for a variety of soil types, see McCarthy, David, *Essentials of Soil Mechanics and Foundations*, 6th Edition. Upper Saddle River, NJ: Prentice-Hall, 2001.

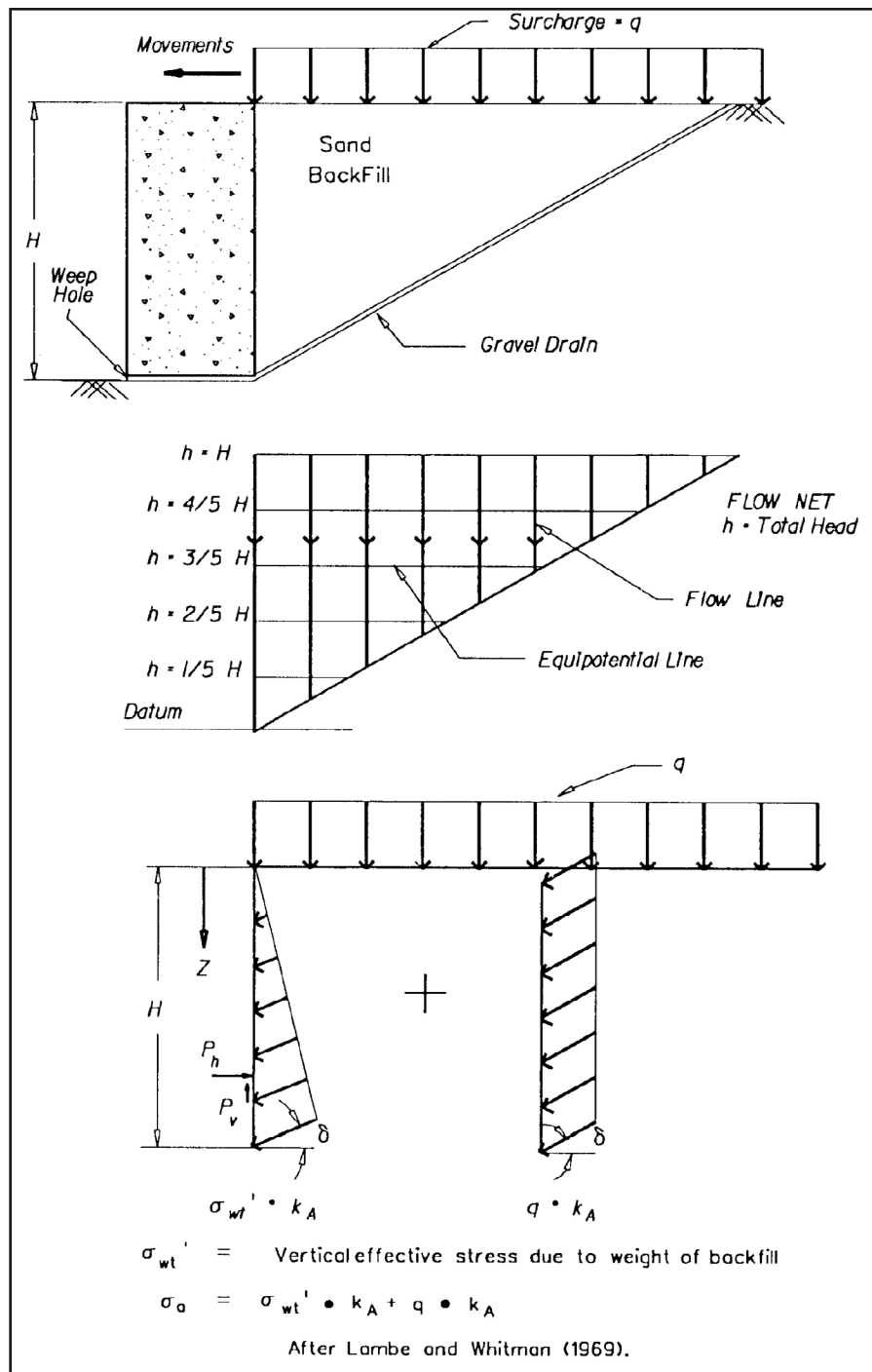


Figure 7-3: Coulomb active earth pressures for a backfill subjected to steady state flow

Coefficient of permeability is a property highly sensitive to sample disturbance, and shows a wide range of variation due to differences in structural characteristics.⁷⁴ Permeability of clean, coarse-grained samples is related to D_{10} size as shown in Figure 7-2.

7.3. Analysis of Groundwater Flow

7.3.1. Effect of Groundwater on Effective Unit Weight

Figure 7-3 shows a wall with a vertical face retaining a level

backfill, supporting a uniform surcharge load, q , and subjected to a constant water infiltration. The wall has a drainage system consisting of a gravel drain below the sand backfill, with weep holes through the wall. Steady state flow may develop during a rainstorm of sufficient intensity and duration. The resulting flow net is shown in Figure 7-3, consisting of vertical flow lines and horizontal equipotential lines, assuming the drain has sufficient permeability and thickness to be free draining (i.e. with zero pressure head within the drain). Adjacent to the back of the wall, the flow net has five

head drops. With the datum at the base of the wall, the total head at the top of the backfill is equal to the height of the wall, H, and a total head is equal to zero at the weep holes. The drop in total head between each of the five equipotential lines is equal to H/5.

The resulting pressures acting along the back of the wall are equal to the sum of (1) the thrust of the soil skeleton because of its unit weight and (2) the thrust of the soil skeleton because of the surcharge. The pore water pressure acting on the wall is equal to zero, with horizontal equipotential lines and the total head equal to the elevation head within the drained backfill. In this case, the effective weight is equal to the total weight. s_a is computed using Equation 7-4, inclined at an angle δ from the normal to the back of the wall and equal to the sum of the pressures shown in Figure 7-3. K_A is computed using Equation 5-27, and α_A is computed using Equation 5-29. Downward vertical steady state seepage in a backfill results in nearly the same earth pressures as are computed in the case of a dry backfill.

In backfills where there is a lateral component to the seepage force or the gradients vary throughout the backfill, the trial wedge procedure, in conjunction with a flow net, must be used to compute P_A and α_A . Spatial variations in u with constant elevation will alter the location of the critical slip surface from the value given in Equation 5-29. The trial wedge procedure is also required to find the values for P_A and α_A when point loads or loads of finite width are placed on top of the backfill. An example using the trial wedge procedure for a retaining wall similar to that shown in Figure 7-3 but with a vertical drain along the back of the wall is described in 5.4.

Neglecting the velocity head, the total head, h , is equal to

Equation 7-10: $h = h_e + h_p$

where h_e is the elevation head, and h_p is the pressure head equal to

Equation 7-11: $h_p = u/g_w$

With the total head equal to the elevation head for each of the equipotential lines, h_p and the pore water pressure, u , are equal to zero. With horizontal equipotential lines, the flow is vertical and directed downward ($i_y = +i$). For steady state seepage condition, the effective unit weight is equal to

Equation 7-12: $\gamma' = \gamma_b \pm \gamma_w \cdot i_y$

The seepage force is added to the buoyant unit weight when flow is downward and subtracted with upward flow. Substituting this equation into Equation 7-2 yields

Equation 7-13:

$$\gamma'_{wt} = \gamma_t \cdot (H - H_w) + (\gamma_b \pm \gamma_w \cdot i_y) \cdot [z - (H - H_w)]$$

For the example shown in Figure 7-3 with $i = +1$ and directed downward, $\gamma' = \gamma_b + (\gamma_w)(1) = \gamma_t$. Equation 7-13 thus reduces in this case to

Equation 7-14:

$$\gamma'_{wt} = \gamma' \cdot z = (\gamma_b + \gamma_w) \cdot z = \gamma_t \cdot z$$

An alternative procedure for calculating γ'_{wt} is using the total overburden pressure, σ_{wt} , and pore water pressures, u . We see that with the pore water pressure equal to zero, this procedure also results in the Equation 7-14 relationship ($\gamma' = \gamma_t$).

7.3.2. Simplified Method of Analysis

For those anchored walls in which the water table within the backfill differs from the elevation of the pool, the differences in the water pressures must be incorporated in the analysis. Terzaghi⁷⁵ describes a simplified procedure used to analyze the case of unbalanced water pressures and steady state seepage in a homogeneous granular soil. The distributions for the unbalanced water pressures along the sheet pile for the case of no seepage and for the case of steady state seepage are shown in Figure 7-4. The effective stresses computed are used to compute the active and passive earth pressures along the sheet pile wall.

The seepage force acts downward behind the sheet pile, increasing the effective unit weight and the active earth pressures, and acts upward in front of the sheet pile, decreasing the effective unit weight with steady state seepage, and the passive earth pressures. For the case of no flow, the buoyant unit weights are assigned to the frictional soils below the water table to compute the active and passive earth pressures.

For soil conditions described in Figure 7-4b, a “rule of thumb” can be applied and the gradient can be computed as

Equation 7-15: $i_y = \frac{H_u}{3D}$

Where H_u , D are defined in Figure 7-4.

7.3.3. Flow Net Technique

In the case of more complex situations than described above, a flow net may be necessary.

Figure 7-5 shows an example of flow net construction. Use this procedure to estimate seepage quantity and distribution of pore water pressures in two-dimensional flow. Flow nets are applicable for the study of cut-off walls and wellpoints, or shallow drainage installations placed in a rectangular layout whose length in plan is several times its width. Flow nets can also be used to evaluate concentration of flow lines.

Rules for flow net construction

1. When materials are isotropic with respect to permeability, the pattern of flow lines and equipotentials intersect at right

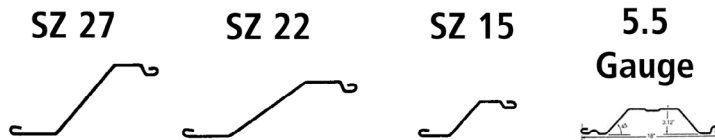
⁷⁵ Terzaghi, K. (1954). “Anchored Bulkheads,” *Transactions of the American Society of Civil Engineers*, Vol. 119, pp. 1243-1324.

SHORELINE STEEL, INC.

P.O. Box 480519, 58201 Main Street • New Haven, MI 48048
(800) 522-9550 • (586) 749-9559 • Fax (586) 749-6653

www.shorelinesteel.com

We are a leading producer of domestic cold formed steel sheet piling in sections ranging from 10 gauge to 3/8" thick. For any sheet piling requirement we can satisfy your needs with a top quality product and prompt delivery.



	Thickness (Nominal)	Weight (Sq. Ft.)	Weight (Lin. Ft.)	Sec. Mod in ³ (Ft. Wall)	Moment of Inertia in ⁴ (Ft. Wall)	Laying Width	Wall Depth
10-10 ga.	.134	7.2	10.8	2.2	3.5	18.00	3.12
8-8 ga.	.164	8.8	13.2	2.62	4.2	18.00	3.12
7-7 ga.	.179	9.6	14.4	2.8	4.4	18.00	3.12
6-6 ga.	.194	10.5	15.8	3.0	4.9	18.00	3.12
5-5 ga.	.209	11.3	16.9	3.4	5.4	18.00	3.12
LZ 8	.164	8.3	17.2	3.6	8.1	25.00	4.50
LZ 7	.179	9.1	18.8	3.9	9.9	25.00	4.50
LZ 5	.209	10.6	21.9	4.6	10.4	25.00	4.50
LZ 3	.239	11.9	24.6	5.2	11.8	25.00	4.50
LZ 250	.250	12.3	25.6	5.4	12.4	25.00	4.50
SZ-10	.164	9.4	17.2	7.3	27.4	22.00	7.50
SZ-11	.179	10.3	18.8	7.9	29.8	22.00	7.50
SZ-12	.209	12.0	21.9	9.2	34.8	22.00	7.50
SZ-14	.239	13.5	24.6	10.4	39.9	22.00	7.50
SZ-15	.250	14.0	25.6	10.9	41.8	22.00	7.50
SZ-14.5	.250	14.5	32.4	13.0	61.49	26.75	9.46
SZ-14.5	.270	15.8	35.1	14.0	86.40	26.75	9.46
SZ 18	.312	18.1	40.4	16.2	76.83	26.75	9.46
SZ-20	.340	19.8	44.1	17.5	83.37	26.75	9.46
SZ-21	.350	20.3	45.3	18.1	86.00	26.75	9.46
SZ-22	.375	21.8	48.6	19.3	91.92	26.75	9.46
SZ 222	.312	22.1	40.4	26.7	163.09	22.00	12.25
SZ-250	.250	15.9	32.4	16.6	89.42	24.46	10.75
SZ-313	.312	19.9	40.4	20.6	111.53	24.46	10.75
SZ-340	.340	21.5	44.1	22.4	121.45	24.46	10.75
SZ-350	.350	22.1	45.3	22.0	124.62	24.46	10.75
SZ-375	.375	23.7	48.6	24.5	133.55	24.46	10.75
SZ-24	.340	24.1	44.1	29.0	177.52	22.00	12.25
SZ-25	.350	24.8	45.3	29.7	181.91	22.00	12.25
SZ-27	.375	26.6	48.6	32.0	195.18	22.00	12.25

- All sections available in bare or galvanized steel.
- All Zee sections available in doubles.
- All sections produced exactly to customer specified length(s).
- All steel fully melted and manufactured in the USA.

Also Available:

- Corners
- Tees and Crosses
- Capping
- Coatings

DOMESTIC STEEL SHEET PILING



For more information, please call toll free
(800) 522-9550
 or visit our website at: www.shorelinesteel.com

SHORELINE  STEEL, INC.

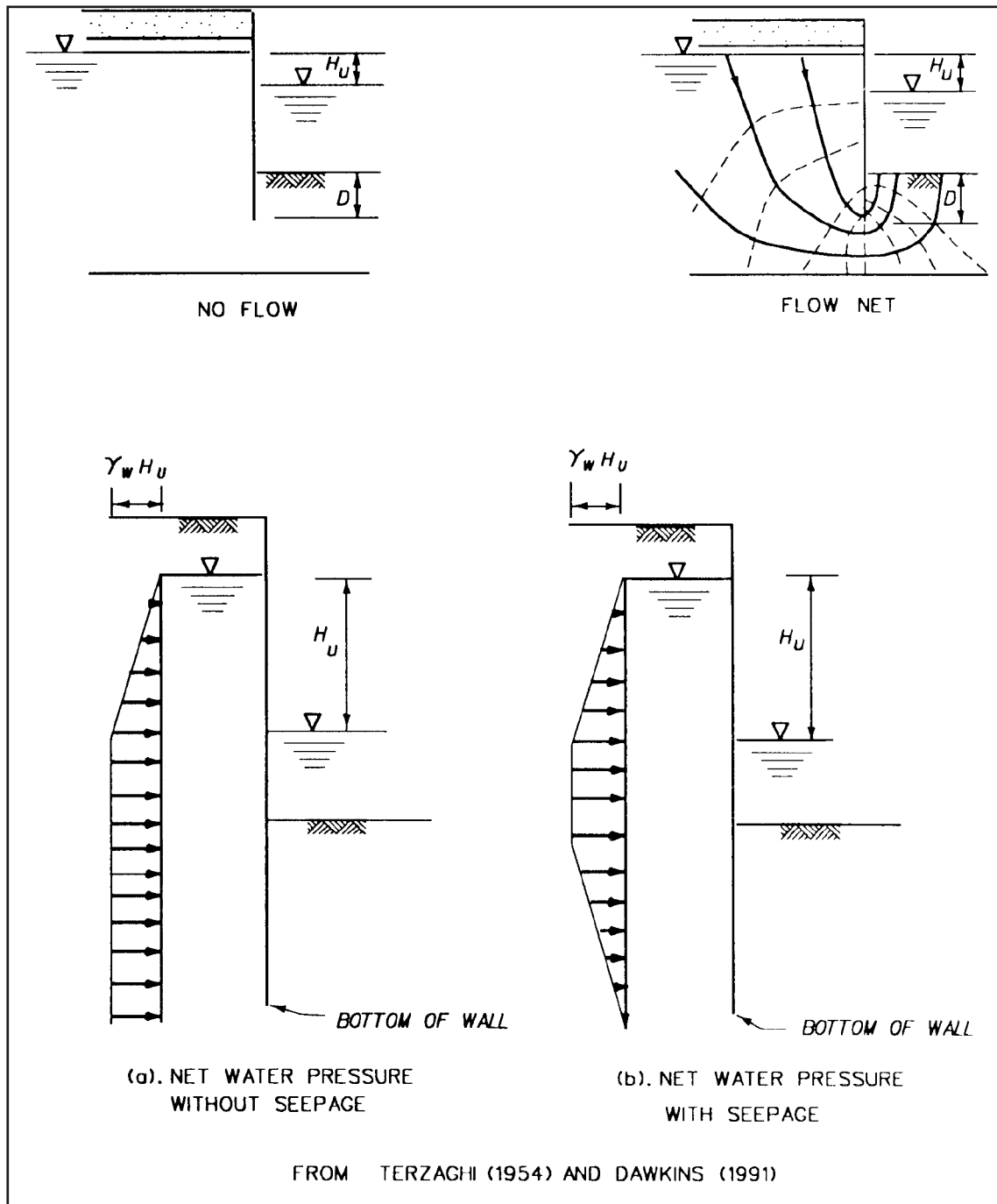


Figure 7-4: Two distributions for unbalanced water pressures

angles. Draw a pattern in which square figures are formed between flow lines and equipotentials.

2. Usually it is expedient to start with an integer number of equipotential drops, dividing total head by a whole number, and drawing flow lines to conform to these equipotentials. In the general case, the outer flow path will form rectangular rather than square figures. The shape of these rectangles (ratio b/l) must be constant.

3. The upper boundary of a flow net that is at atmospheric

pressure is a “free water surface”. Integer equipotentials intersect the free water surface at points spaced at equal vertical intervals.

4. A discharge face through which seepage passes is an equipotential line if the discharge is submerged, or a free water surface if the discharge is not submerged. If it is a free water surface, the flow net figures adjoining the discharge face will not be squares.

5. In a stratified soil profile where ratio of permeability of lay-

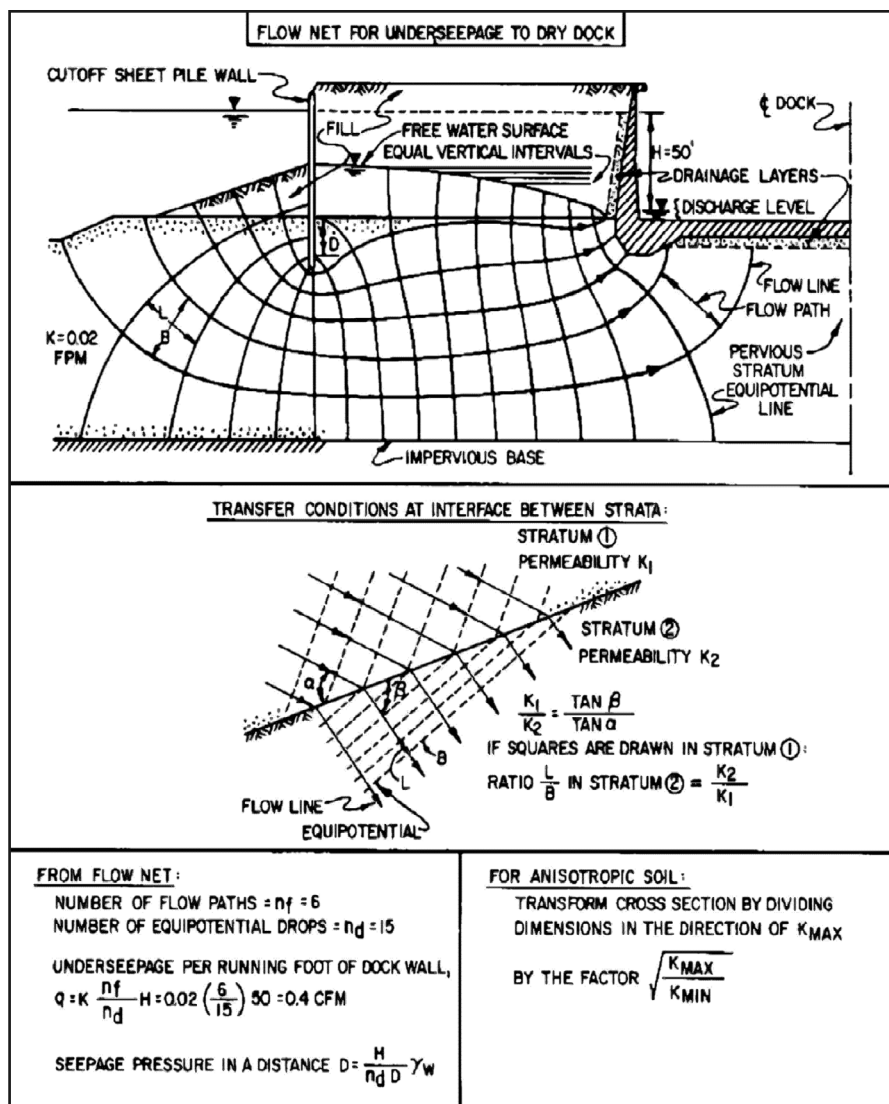


Figure 7-5: Flow Net Construction and Seepage Analysis

ers exceeds 10, the flow in the more permeable layer controls. That is, the flow net may be drawn for more permeable layer assuming the less permeable layer to be impervious. The head on the interface thus obtained is imposed on the less pervious layer for construction of the flow net within it.

6. In a stratified soil profile where ratio of permeability of layers is less than 10, flow is deflected at the interface in accordance with the diagram shown above.

7. When materials are anisotropic with respect to permeability, the cross section may be transformed by changing scale as shown above and flow net drawn as for isotropic materials. In computing quantity of seepage, the differential head is not altered for the transformation.

8. Where only the quantity of seepage is to be determined, an approximate flow net suffices. If pore pressures are to be determined, the flow net must be accurate.

The actual computations associated with flow netting are shown in Example 22.

7.3.4. Finite Element Analysis

For special cases, the flow regime can be analysed by the finite element method. Mathematical expressions for the flow are written for each of the elements, considering boundary conditions. A computer solves the resulting system of equations to obtain the flow pattern.

7.4. Seepage Forces

We have seen from the previous discussion that groundwater flow is able to alter the effective unit weight of a soil. We now turn to examining the actual affects of this phenomenon.

If we consider Equation 7-12, we can see that, if both the flow and the gradient act in an upward direction, we will reach the point where the actual buoyant weight of the soil will be zero. The gradient at which this takes place is referred to as the critical gradient, and can be found from Equation 7-

12 by the relationship

Equation 7-16: $i_{critical} = \frac{\gamma_b}{\gamma_w}$

Obviously, the uncertainties inherent in geotechnical analysis dictate the application of a factor of safety, which is computed (and given a lower bound) using the equation

Equation 7-17: $FS_{piping} = \frac{i_{critical}}{i_{max}} \geq 1.5$

The result of exceeding the critical gradient is piping or “sand boiling.” When piping takes place, the upward seepage pressure reduces the effective weight of the soil, thereby reducing the ability of the soil to offer lateral support to the sheeting. In extreme cases, the sand “boils” in the bottom of the excavation. That is, a “quick” condition is produced.

The critical gradient is a function of the unit weight properties of the soil itself. The maximum gradient can be determined by any of the methods shown above, and compared with the critical gradient and the factor of safety computed using Equation 7-17.

An alternate method of analysing piping is through a chart solution. Figure 7-6 shows the factor of safety against heaving in either loose or dense sand depending upon the geometry of the excavation, the penetration of the sheeting and the elevation of the impervious layer.

This chart assumes that $\gamma = 75_{pcf}$; if the submerged unit weight is not equal to that, the factor of safety that is actually present is modified by the equation

Equation 7-18: $FS_{actual} = \frac{\gamma}{75_{pcf}} FS_{chart}$

Also, research by Marsland⁷⁶ incorporating a safety factor of 1.5 is published in chart form.

Piping is controlled by dewatering (lowering the water table) outside the cofferdam or by driving the sheet piling deeper. The purpose of both corrective measures is to reduce the upward hydraulic gradient in the soil below the bottom of the piling. The design of sheeting penetration to control piping for various subsurface conditions is presented in Figure 7-7.

7.4.1. Seepage Through Interlocks

Some seepage will occur through the interlocks of sheet piling. As an approximation, the seepage should be assumed to be at least 1.5 gal/hr/sq. ft. of wall/ft. of net head across the wall for installations in moderately to highly permeable soils.

7.5. Wave action

The lateral forces produced by wave action are dependent on many factors, such as length, height, breaking point, frequency and depth at structure.⁷⁷

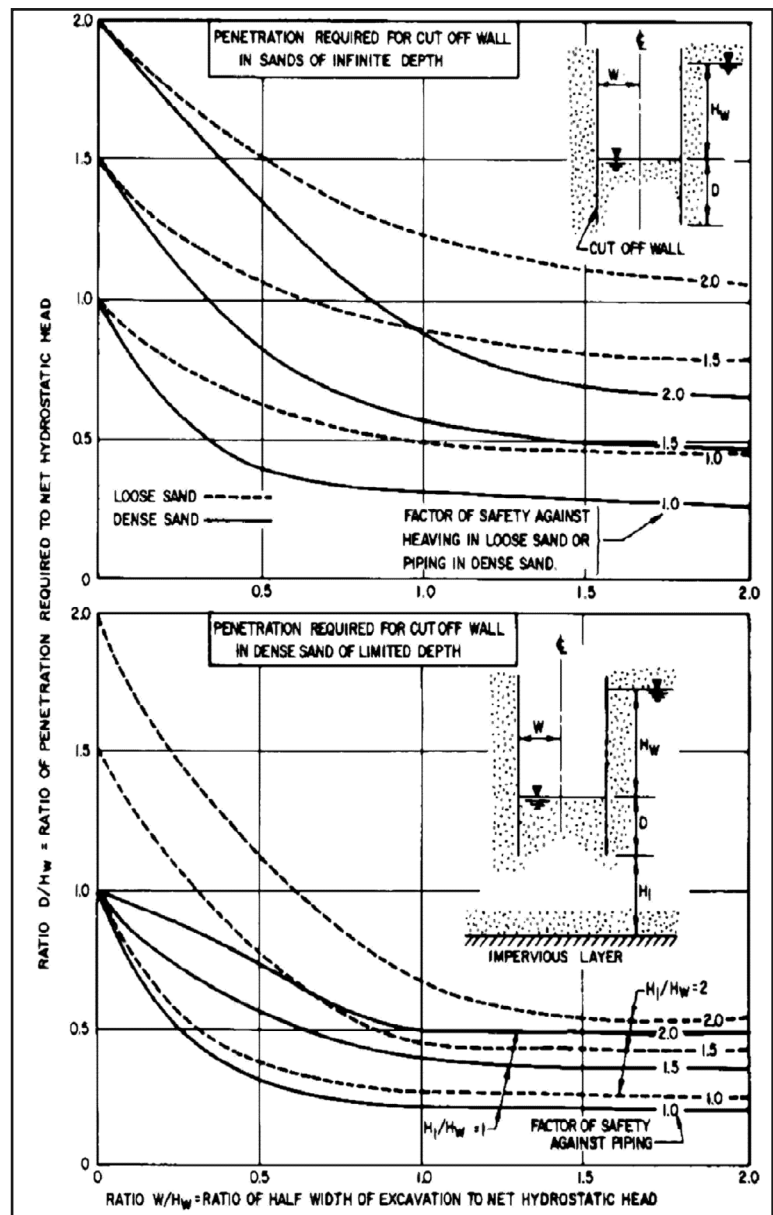


Figure 7-6: Depth of Sheet Piling to Prevent Piping in a Braced Cofferdam

⁷⁶Marsland, A. (1953) “Model Experiments to Study the Influence of Seepage on the Stability of a Sheeted Excavation in Sand.”, Vol. 3.

⁷⁷Information on wave forces can be found in the “Shore Protection Manual,” available on the Marine Construction Volume 1 CD-ROM, available from Pile Buck.



DAWSON

INNOVATIVE PILING EQUIPMENT

DAWSON CONSTRUCTION PLANT LTD
 Chesney Wold, Bleak Hall
 Milton Keynes MK6 1NE, England
 Tel: 011 44 1908 240300
 Fax: 011 44 1908 240222
 Email: mark@dcpuk.com
 Website: www.dcpuk.com

Excavator Mounted Vibrators

- Pick & Place Sheet Piles
- Drive or Extract
- Min Height = Max Pile Length
- Control Pile Line
- Compact & Robust
- Quick & Simple Attachment
- High Power to Weight Ratio
- All Hydraulic – No Electronics
- Automatic Clamp Operation
- Built In Flow Regulation
- Comprehensive Range



American Equipment & Fabricating Corp. 100 Water Street East Providence Rhode Island 02914 U.S.A. Contact: John Sheerin Tel: 401 438 2626 or 1-800-368-7453 Fax: 401 438 0764	Bay Machinery Corp. PO Box 70430 Richmond CA 94807 U.S.A. Contact: Bob Knop Tel: 510 236 9000 Fax: 510 236 7212	Equipment Corporation of America PO Box 387 Aidan PA 19018 U.S.A. Contact: Ben Dutton Tel: 610 626 2200 Fax: 610 626 2245	Hammer & Steel Inc. 11912 Missouri Bottom Rd. St. Louis Missouri 63042-2313 U.S.A. Contact: Bob Laurence Tel: 314 895 4600 or 1-800-325-7453 Fax: 314 895 4070	Mabey Bridge & Shore Inc. * 6770 Dorsey Road Baltimore MD 21227 U.S.A. Contact: Joe Atkinson Tel: 410 379 2800 or 1-800-42-MABEY Fax: 410 379 2801	Mississippi River Equipment Co. PO Box 249 520 Good Hope St. Norco, LA 70079 U.S.A. Contact: J J Waguespack Tel: 985 764 1194 Fax: 985 764 1196	Pacific American Commercial Co. 7400 Second Avenue S. P.O. Box 3742 Seattle, WA 98124 U.S.A. Contact: Ted Obermeit Tel: 206 762 3550 or 1-800-678-6379 Fax: 206 763 4232	Pile Equipment Inc. 1058 Roland Avenue Green Cove Springs Florida 32043-8361 U.S.A. Contact: Mike Elliott Tel: 904 284 1779 or 1-800-367-9416 Fax: 904 284 2588	Special Construction Machines 166 Bentworth Avenue Toronto Ontario M6A 1P7 Canada Contact: Steve Calow Tel: 416 787 4259 or 1-800-760-0925 Fax: 416 787 4362
--	---	---	---	---	---	---	--	---

*Do not supply HPH Hydraulic Hammers

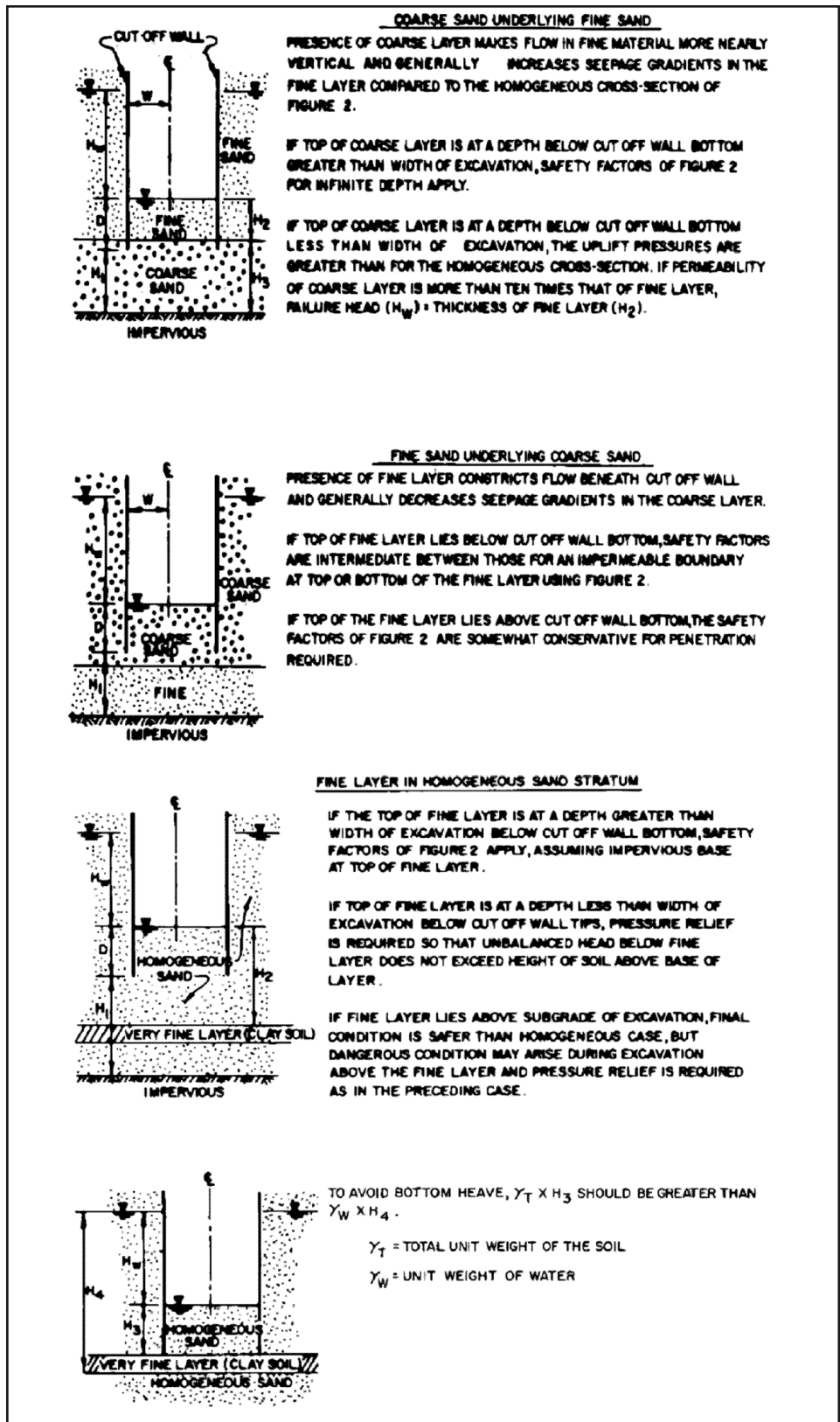


Figure 7-7: Depth of Sheet Piling in Stratified Sand to Prevent Piping in a Braced Cofferdam

The analysis of hydraulic flow around sheeting is demonstrated in Example 22.

Chapter Eight: Other Loads on Sheet Pile Walls

This chapter describes loads on sheet pile walls other than those directly induced by the soil (lateral earth pressure loads) or water (hydrostatic loads, perhaps modified by groundwater movement.)

8.1. Effect of Surface Loadings

Unlike shallow foundations and gravity walls, sheet pile walls do not induce a significant vertical compressive load on the soil. Sheet pile walls are, however, affected by these kinds of loads due to stockpiled material, machinery, roadways, and other influences resting on the soil surface near the wall. These loads increase the lateral pressures on the wall. There are three approaches used to approximate the additional lateral earth pressures on walls due to surface loadings; (1) elastic solutions, (2) the wedge method of analysis, and (3) finite element analyses.

8.1.1. Elastic Solutions

Elastic solutions of the type shown in *Figure 8-1* can be used to calculate the increase in the horizontal earth pressure σ_x , using either a solution for a point load, a line load or a strip load acting on the surface of an elastic mass, i.e. the soil backfill.

8.1.1.1. Uniform surcharge

A uniform surcharge is assumed to be applied at all points on the soil surface. The effect of the uniform surcharge is to increase the effective vertical soil pressure in Equation 5-3 and Equation 5-15 by an amount equal to the magnitude of the surcharge.

8.1.1.2. Line loads

A continuous load parallel to the wall but of narrow dimension perpendicular to the wall may be treated as a line load as shown in *Figure 8-1 (a)*. The lateral pressure on the wall is given by the equation in *Figure 8-1 (a)*.

8.1.1.3. Strip loads

A strip load is continuous parallel to the longitudinal axis of the wall but is of finite extent perpendicular to the wall as illustrated in *Figure 8-1 (b)*. The additional pressure on the wall is given by the equations in *Figure 8-1 (b)*. Any negative pressures calculated for strips loads are to be ignored.

8.1.1.4. Ramp load

A ramp load, *Figure 8-1 (c)*, increases linearly from zero to a maximum that subsequently remains uniform away from the wall. The ramp load is assumed to be continuous parallel

to the wall. The equation for lateral pressure is given by the equation in *Figure 8-1 (c)*.

8.1.1.5. Triangular Load

A triangular load, *Figure 8-1 (d)*, first increases linearly from zero to a maximum then decreases in the same manner back to zero. The triangular load is considered continuous parallel to the wall. The equation for later pressure is given by the equation in *Figure 8-1 (d)*.

8.1.1.6. Area loads

A surcharge distributed over a limited area, both parallel and perpendicular to the wall, should be treated as an area load. The lateral pressures induced by area loads may be calculated using Newmark's Influence Charts⁷⁸ (Newmark 1942). The lateral pressures due to area loads vary with depth below the ground surface and with horizontal distance parallel to the wall. Because the design procedures discussed in this book are based on a typical unit slice of the wall/soil system, it may be necessary to consider several slices in the vicinity of the area load.

8.1.1.7. Point loads

A surcharge load distributed over a small area may be treated as a point load. The equations for evaluating lateral pressures are given in *Figure 8-2*. Because the pressures vary horizontally parallel to the wall; it may be necessary to consider several unit slices of the wall/soil system for design.

8.1.2. Trial Wedge Analysis

Trial wedge analyses, as described in 5.4, may be performed to account for uniform and irregular surface load distributions for those walls whose movements satisfy the criteria listed in *Table 4-1*. The wedge analysis described in 5.4 is modified by including that portion of the surface loading between the back of the wall and the intersection of the trial slip surface and the backfill surface in the force equilibrium calculation for each wedge analysed. The resulting relationship for a vertical wall retaining a partially submerged backfill (for a hydrostatic water table) is given as

Equation 8-1:

$$P = \frac{[W - U_{\text{static}} \cos \alpha] \tan(\alpha - \phi')}{\cos \delta + \sin \delta \tan(\alpha - \phi')}$$

with a restricted to values of $\alpha > \phi$, since $P > 0$.

$P_A = P$ and $\alpha_A = \alpha$ for the static critical wedge as well. For a

⁷⁸Newmark, N. M. 1942. "Influence Charts for Computation of Stresses in Elastic Foundations," University of Illinois Engineering Experiment Station Bulletin, Series No. 338, Vol 61, No. 92, Urbana, IL, reprinted 1964, pp 28.

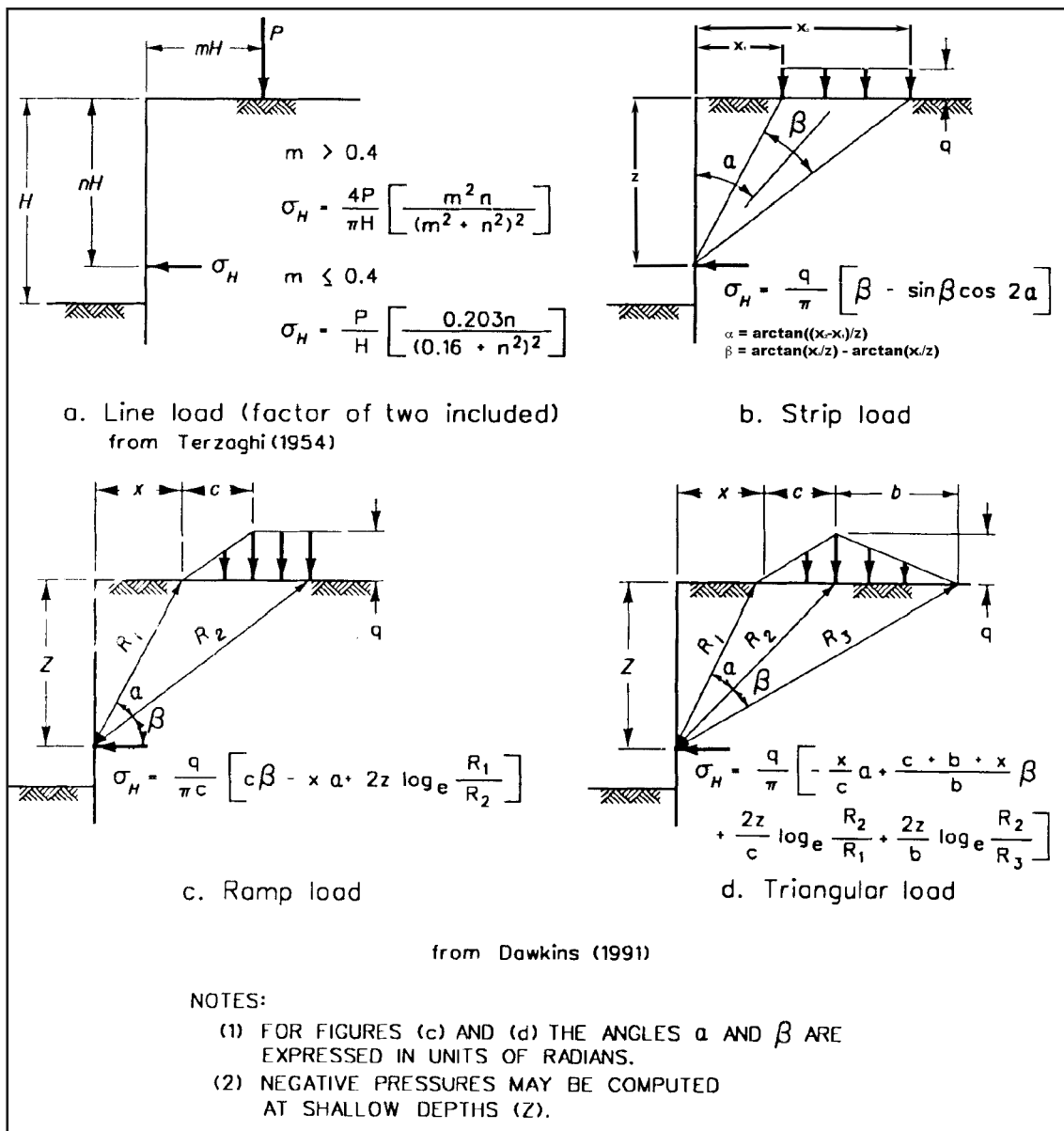


Figure 8-1: Theory of elasticity equations for pressures on wall due to surcharge loads

surcharge loading, Equation 8-1 simplifies to

Equation 8-2:

$$p = \frac{[W + W_s - U_{static} - \alpha \cos \alpha] \tan(\alpha - \phi')}{\cos \delta + \sin \delta \tan(\alpha - \phi')}$$

where W_s is computed using

Equation 8-3: $W_s = q_s l_c$

Where $l_c = l = (H/\tan \alpha) - x$ for $l_q > 1$ (refer to Figure 8-3), otherwise $l_c = l_q$.

The difficult part of the problem is to determine the point of action of this force along the back of the wall. The point of

action of the resulting earth pressure force for an infinitely long line load parallel to the wall may be computed using the simplified procedure⁷⁹.

8.1.3. Finite Element Methods

The finite element method of analysis has been applied to a variety of earth retaining structures and used to calculate stresses and movements for problems involving a wide variety of boundary and loading conditions⁸¹.

8.2. Additional Applied Loads

Sheet pile walls are widely used in many applications and can be subjected to a number of additional loads, other than lateral pressure exerted by soil and water.

⁷⁹Terzaghi, K., and Peck, R. 1967. *Soil Mechanics in Engineering Practice*, Second Edition, John Wiley & Sons, Inc., New York, Article 31.

Another Tool In The Toolshed



TECHNO DRILL HYDRAULIC PILING/DRILLING RIGS

VIBRATORY DRIVERS/EXTRACTORS

HYDRAULIC DRILLING & PILING RIGS

FUEL INJECTED S-SERIES DIESEL HAMMERS

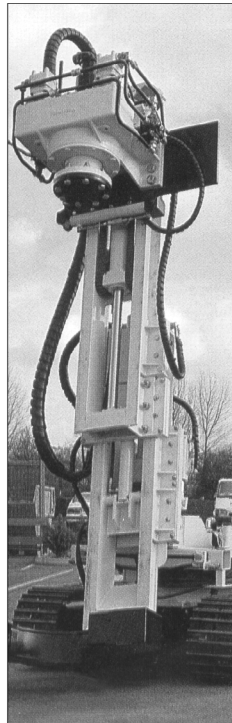
IMPACT ATOMIZATION I-SERIES DIESEL HAMMERS

EXCAVATOR-MOUNTED ATTACHMENTS

HYDRAULIC IMPACT HAMMERS

TOP-DRIVE AUGERS

LEADS & SPOTTERS



**INTERNATIONAL
CONSTRUCTION
EQUIPMENT, INC.**
www.iceusa.com

301 Warehouse Drive • Matthews, NC 28104

Phones: 888 ICEUSA1

& 704 821-8200

Fax: 704 821-8201 • e-mail: info@iceusa.com



Matthews NC • Lakeland FL • Metairie LA • Seattle WA • New Town Square PA • Sayreville NJ • Houston TX
Fort Wayne IN • Virginia Beach VA • Boston MA • Montreal Quebec • Singapore • Kuala Lumpur • Shanghai

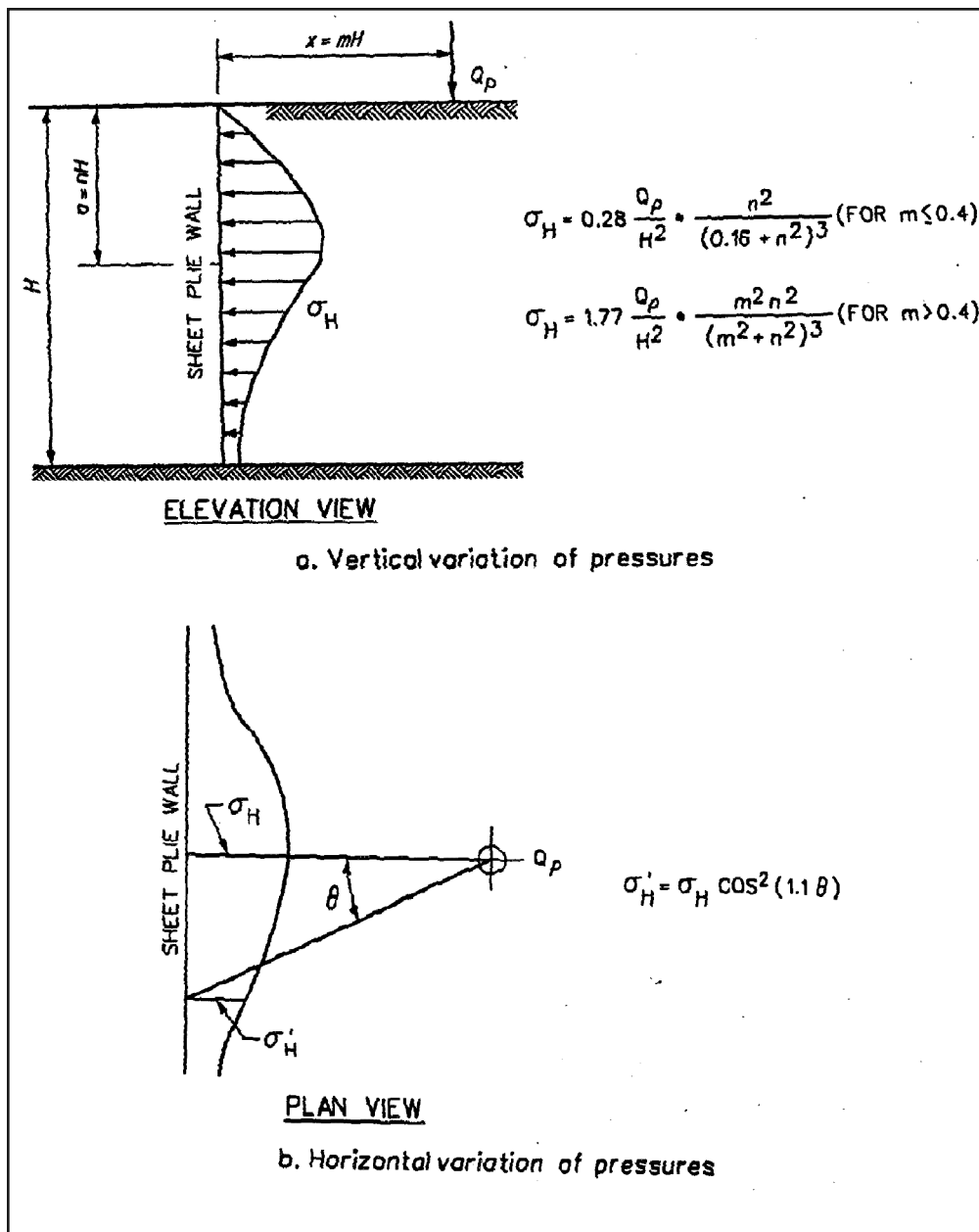


Figure 8-2: Point load⁸⁰

8.2.1. Boat impact

Although it becomes impractical to design a sheet pile wall for impact by large vessels, waterfront structures can be struck by loose barges or smaller vessels propelled by winds or currents. Construction of a submerged berm that would ground a vessel will greatly reduce this possibility of impact. When the sheet pile structure is subject to docking impact, a fender system should be provided to absorb and spread the reaction. The designer should weigh the risk of impact and resulting damage as it applies to his situation. If conditions

require the inclusion of either of these boat impact forces in the design, they should be evaluated based on the energy to be absorbed by the wall. The magnitude and location of the force transmitted to the wall will depend on the vessel's mass, approach velocity, and approach angle⁸².

8.2.2. Mooring pulls

Lateral loads applied by a moored ship are dependent on the shape and orientation of the vessel, the wind pressure, and currents applied. Due to the use of strong synthetic lines,

⁸⁰Terzaghi, K. 1954. "Anchored Bulkheads," Transactions, American Society of Civil Engineers, Vol 119.

⁸¹Some key aspects of the application of the finite element method in the analysis of U-frame locks, gravity walls, and basement walls are summarized in Ebeling, R. 1990 (Dec). "Review Of Finite Element Procedures for Earth Retaining Structures," Miscellaneous Paper ITL-90-5, Information Technology Laboratory, US Army Engineer Waterways Experiment Station, Vicksburg, MS.

⁸²Information on such loads can be found in "Piers and Wharves," found on the Marine Construction Volume 2 CD-ROM, available from Pile Buck.

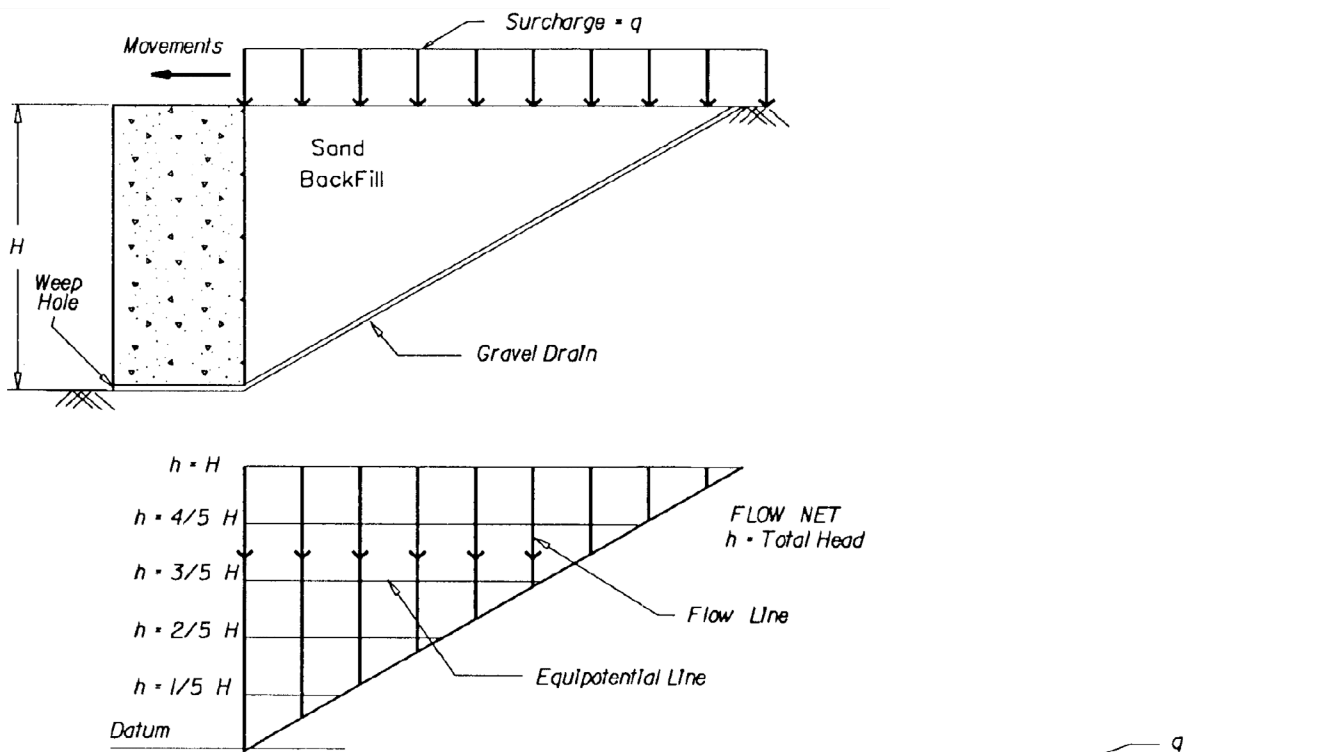
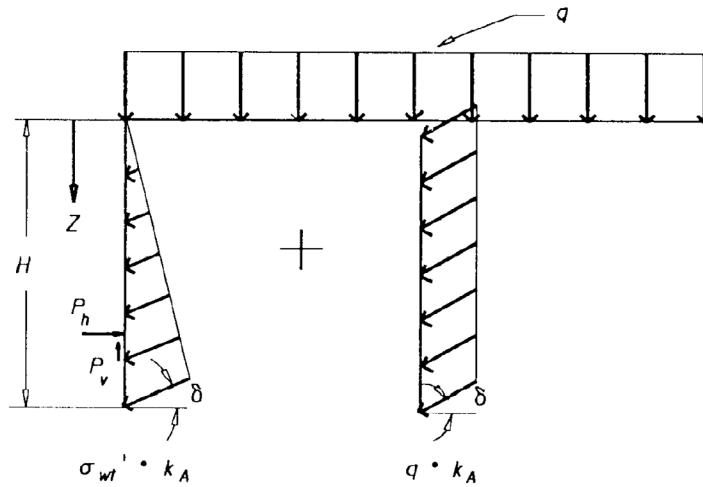


Figure 8-3: Coulomb active earth pressures for a backfill subjected to steady state flow



$$\sigma_{wt}' = \text{Verticaleffective stress due to weight of backfill}$$

$$\sigma_o = \sigma_{wt}' \cdot k_A + q \cdot k_A$$

After Lambe and Whitman (1969).

large forces can be developed. Therefore, it is recommended that mooring devices be designed independent of the sheet pile wall.

8.2.3. Ice forces

Ice can affect marine-type structures in many ways. Typically, lateral pressures are caused by impact of large floating ice masses or by expansion upon freezing. Expansive lateral pressures induced by water freezing in the backfill can be avoided by backfilling with a clean free-draining sand or gravel or installation of a drainage collector system⁸³.

8.2.4. Wind forces

When sheet pile walls are constructed in exposed areas, wind forces should be considered during construction and throughout the life of the structure. For sheet pile walls with up to 20 feet of exposure and subjected to hurricanes or cyclones with basic winds speeds of up to 100 mph, a 50-psf design load is adequate. Under normal circumstances, for the same height of wall exposure, a 30-psf design load should be sufficient⁸⁴.

⁸³Information on such loads can be found in "Ice Engineering," found on the *Marine Construction* Volume 2 CD-ROM, available from Pile Buck.

⁸⁴For more severe conditions, wind load should be computed in accordance with American National Standards Institute (ANSI) A58.1 (ANSI 1982).

Chapter Nine:

Design of Cantilevered and Anchored Walls Using Classical Methods

9.1 Definition of Classical Methods

Up to this point, we have been discussing basic soil mechanics and lateral earth pressure theory. Now we turn to the application of these theories to the practical design of sheet pile walls. Broadly speaking, there are three methods that can be used for the design of sheet pile walls:

- 1) Classical methods;
- 2) Methods that enhance classical methods by include soil-pile interaction; and
- 3) Discrete methods such as finite element analysis.

This chapter will deal with classical methods. “Classical” methods have the following characteristics:

- Sheet pile wall assumed to be a vertical beam. The balancing of forces determines the values at the reaction locations from which the depth of penetration and the anchor force are derived. Shears and moments are then computed providing the data for selection of the sheet piling “beam” section. After this, the anchor or bracing system is designed using input data from these previous determinations. Cantilevered walls generally never consider the flexibility of the sheeting; anchored walls use Rowe’s moment reduction methods to consider wall flexibility.
- Soil forces are assumed to follow Rankine, Coulomb or log-spiral distribution and failure. A sheet pile wall supports vertical earth fill, which attempts to fail along inclined planes, influenced by gravity. The soil resists this attempted failure by its inherent shearing strength, which is motivated by friction or by cohesion between the soil particles. In the case of driving forces, the lateral pressure is reduced from vertical pressure by a coefficient K_o or K_a , and increased in the case of resisting forces by a coefficient K_p . Earth pressures can be estimated by utilizing equations (Rankine or Coulomb) or by graphical means. Additional influential factors include surcharge loads, ground water, seepage, external horizontal loads and earthquake.
- End fixity of the sheet pile wall assumed to be completely free or fixed, depending upon the theory being used. Although other methods have been developed to analyse sheet-piling walls, classical methods have been successfully

used to design many successful sheet pile walls.

One of the appeals of classical methods for sheet pile design is that the calculations can be done by hand. For many years, this was the only option. However, even classical methods can present computational complexities that invite the use of computer assistance.

One computer software package that can be used for this purpose is SPW 911 v. 2, which is available from Pile Buck. This analyzes both cantilevered and anchored sheet pile walls using classical methods described in this book. In the example problems included below, we will include solutions for these problems using SPW 911.

9.2. Data Required for Analysis

This book has discussed the traditional application of soil properties toward estimating driving and resisting forces against flexible retaining walls.

Having determined these forces, the structural analysis of the retaining system can be accomplished.

9.2.1. Minimum Information Required for Design

- The ground surface profile extending to a minimum distance of 10 times the exposed height of the wall on either side.
- The soil profile on each side of the wall including:
 - Location and slope of subsurface layer boundaries
 - Strength parameters for each layer to a depth below the dredge line not less than five times the exposed height of the wall on each side. Parameters include:
 - Soil weights γ - Dry, moist, saturated, submerged.
 - Angle of Internal Friction for all layers - ϕ
 - Cohesion $c = 1/2 q_u$ (unconfined compressive strength)
- Angle of Friction between soil and wall - δ
- Coefficients K_o (at rest), K_a (active), K_p (passive)
- Magnitudes and locations of surface surcharge loads.
- Slopes of fill above and below surface
- Magnitudes and locations of external loads—ice, wind, impact, mooring, earthquake, waves.
- Safety factors.
- Groundwater elevation on each side of the wall and seepage characteristics; Tidal elevations.
- Wall Height, Dredge Depth
- Proposed Construction Sequence

S T O M P P E R

FOR DRIVING

SHEET PILE

M A N D R E L S



The Stompper Mandrel Sheet has been developed and patented since 1996. The Stompper Mandrel for Sheetpile is like nothing else. The Stompper, method, apparatus and Lifting Apparatus is the **ONLY** patented mandrel and lifting device for driving sheetpile. It is protected under one or more of U.S. Patent Numbers, 5,503,503 and 5,803,672 and 6,231,271. The Stompper has a built in lubrication gallery for high blow count soils. Stab Cat, Inc. has Stompper Sheets available at this time for the installation of sheetpile, i.e. Vinyl, etc. The lifting apparatus (shackles) used in conjunction with the Stompper allows for easier handling of heavier sheetpile and for a faster driving cycle.

For more information visit www.stabcat.com



9.2.1.1. Soil Weight

Estimate weight from field density determinations or from laboratory measurements. Use saturated weight for active pressures above the water level and submerged weight below. Use moist or dry weight for passive side above any water level and submerged weight below.

9.2.1.2. Angle of Internal Friction ϕ

For all layers of soil in-situ or proposed as fill, estimate from field density (SPT) tests, indexing and classification tests, or determine from laboratory shear tests and Mohr circle diagrams. ϕ angle selected for design should approximate that expected long term, in the structure.

9.2.1.3. Angle of Friction between Soil and Wall δ

For conservative designs, ignore the affect of friction between soil and wall for both active and passive cases. This generally means that Rankine theory should be applied. For non-conservative designs, assume δ as a fraction of ϕ , or use the values given in *Table 5-1*. When $\delta/\phi > -1/2$ for the passive case, Coulomb coefficients may be unrealistically high unless a log spiral analysis is used.

9.2.1.4. Adhesion

Adhesion between wall and soil is a phenomenon equivalent to friction between the two. Adhesion cannot be counted on for the longer term and is generally ignored.

9.2.1.5. Cohesion

- Estimate from field tests such as either the SPT, Dutch cone, vane shear or from observations.
- Measure from unconfined compression test ($c = 1/2 q_u$)
- Obtain from triaxial test data and Mohr Circle.

9.2.1.6. Ground Slopes β

For dredged bulkheads, (soil left in place) the profile of the in-situ layers should be examined since sloping layers may affect the analytical approach to be used.

Sloping ground behind or in front of the wall will have an effect on the slope of the failure surface and ultimately the pressure coefficients K_a and K_p . Working bulkheads supporting parking facilities, marinas, marine terminal and similar operations are planned for a level backfill and the angle $\beta = 0$.

Land sited walls in conjunction with highways, railroads, private and commercial properties may exhibit sloped conditions on both active and passive sides. These slopes and most often positive slopes but could occasionally be negative. If slopes are plane, Coulomb or Rankine equations can be used. If irregular, wedge analysis will produce more accurate pressure determinations.

9.2.1.7. Surcharges

It is common practice to include as a minimum, a uni-

form live load of 200-300 psf to account for materials storage and construction machinery near to the wall. SPW 911 has as a default a uniform live load of 200 psf.

Generally, heavy surcharge loads from raw material piles should be kept well back from either the wall or the anchor system so as not to influence wall pressures. If this is not possible, the load should be supported on a deck and bearing piles.

Heavy track-mounted cranes should be supported on piles so that possible settlement will not affect their operation. Marine handling equipment and trucking operating on rigid paving within the failure wedge can be accounted for as a uniform live load, however in the case of unpaved or light flexible pavement, heavy wheel loads may have to be separately treated as point loads.

Loads from long footers, rectangular spread footings, roadways and railroads that would influence total pressure on the wall should be examined as line or strip loads using methods outlined in the section on surcharge loads. In general, surcharges should be discounted when calculating passive resistance. Horizontal loads from irregular surcharges are best analyzed by the wedge method. Formulas for estimating lateral pressures from surcharges are found in 8.1.1.

9.2.1.8. External Loads

Ice is usually not a factor with solid bulkheads, however the pressure exerted by freezing water and floating ice should be considered in designing free standing walls such as cofferdams and shear walls. Frost in clay fill materials can produce significant temporary pressure increases. Clay fill should be avoided if possible. Waves and wave impact should be considered when designing cofferdams and other freestanding sheet pile structures. Mooring forces from vessel impact should be absorbed and distributed through fender piles or fendering material rather than taken into the backfill through the wall.

Wind forces can be potentially damaging during installation, but can be accounted for with temporary bracing. Earthquakes have the potential to increase active pressure and decrease passive resistance resulting in damage or destruction of retaining structures.

Steel structures exhibit inherent ductility that allows those structures to deform without necessarily failing. However, a destructive earthquake changes the shearing properties of the soil. The need to consider these forces will depend on location and importance of the structure.

9.2.1.9. Water

Bulkheads should be designed for low water conditions since this will produce maximum active pressures. Any tidal effects should be included as an unbalanced head of water. Heavy rainfall, melting snow and flooding can also add significant loads on the active side of a wall. Sheet pile interlocks eventually fill with soil and corrosion products and

water does not drain freely. Design anchorage and penetration for these conditions.

As with all structures, safety factors are applied in design to account for loading and construction uncertainties and to provide a protective cushion against failure. When safety factors are set too high, costs go up. When set too low, the safety of the public or the service life of the structure may be in jeopardy.

Bulkheads and land walls ordinarily are not critical structures that will endanger life if they fail. There have been few cases reported where sheet piling failed due to overstressing. Most bulkhead failures can be traced to failure of the anchor, displacement of the base of the wall, rotational failure of a large block of soil, or failure due to corrosion deterioration. Most of these problems can be traced to events such as overdredging, overloading, undetected weak underlying strata, poor connection details, or poor installation practice.

With this in mind, generous safety factors should be applied to passive pressures or to penetration depths and to anchorage design.

Failures of land and water cofferdams have usually been due to internal bracing failures or failure of cantilevered sections of the sheet piling often soil failure at the base. These are areas where larger safety factors should be applied.

9.2.1.10. Project Data

The elevations of significant parts of the wall must be determined for purposes of design.

These include:

- 1) Elevation of the top of fill behind the wall.
- 2) Elevation of high and low water levels.
- 3) Elevation of the planned dredge depth in front of the wall.

9.2.2. Load cases

The loads applied to a wall fluctuate during its service life. Consequently, several loading conditions must be defined within the context of the primary function of the wall. As a minimum, a cooperative effort among structural, geotechnical, and hydraulic engineers should identify the load cases outlined to be considered in the design.

(1) Usual conditions. The loads associated with this condition are those most frequently experienced by the system in performing its primary function throughout its service life. The loads may be of a long-term sustained nature or of an intermittent, but repetitive, nature. The fundamental design of the system should be optimized for these loads. Conservative factors of safety should be employed for this condition.

(2) Unusual conditions. Construction and/or maintenance operations may produce loads of infrequent occurrence and are short duration, which exceed those of the usual condition. Wherever possible, the sequence of operations should be specified to limit the magnitudes and duration of loading, and the performance of the wall should be carefully monitored to prevent permanent damage. Lower factors of safety or higher material stresses may be used for these conditions with the intent that the system should experience no more than cosmetic damage.

(3) Extreme conditions. A worst-case scenario representing the widest deviation from the usual loading condition should be used to assess the loads for this case. The design should allow the system to sustain these loads without experiencing catastrophic collapse but with the acceptance of possible major damage that requires rehabilitation or replacement. To contrast usual and extreme conditions, the effects of a hurricane on a hurricane protection wall would be the "usual" condition governing the design, while the loads of the same hurricane on an embankment retaining wall would be "extreme."

9.3. Cantilever Walls

9.3.1. Overview

A cantilevered sheet pile wall performs somewhat like a cantilevered beam. The sheet piling is driven to a sufficient depth into the ground to become fixed as a vertical cantilever resisting a load from active earth pressure. Walls designed as cantilevers usually undergo large lateral deflections and are readily affected by scour and erosion in front of the wall. Since the lateral support for a cantilevered wall comes from passive pressure exerted on the embedded portion, penetration depths can be quite large, resulting in large moments and deflections. This is especially pronounced in non-ferrous sheeting such as aluminum, vinyl and fiberglass; cantilevered walls are generally not recommended for these types of sheeting. Cantilevered walls are usually limited to a maximum freestanding height of about 15 feet.

Cantilever walls are usually used as floodwall or as earth retaining walls with low wall heights (10 to 15 feet or less). Because cantilever walls derive their support solely from the foundation soils, they may be installed in relatively close proximity (but not less than 1.5 times the overall length of the piling) to existing structures. Typical cantilever wall configurations are shown in *Figure 9-1*.

The effect of the application of an external load against a cantilever is illustrated in *Figure 1-16a*. When the active pressure of the soil towards the top of the wall is applied above the dredge line, the cantilever rotates above a transition point below the dredge line. This rotation is resisted by the combination of active and passive pressures below the dredge line. Since passive pressures are greater than active pressure, even with the effective stress advantage on the

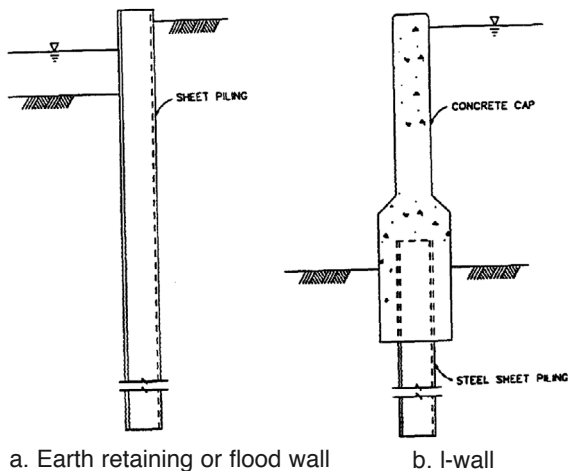


Figure 9-1: Typical Cantilever Walls

active side, stability is possible with sufficient penetration of the sheet piling into the soil. The pressure distribution is illustrated in *Figure 9-2*.

Equilibrium of the wall requires that the sum of horizontal forces and the sum of moments about any point must both be equal to zero. The two equilibrium equations may be solved for the location of the transition point (i.e. the distance z in *Figure 9-2*) and the required depth of penetration (distance d in *Figure 9-2*). Because the simultaneous equations are usually cubic in z and d , either a trial and error or a cubic equation solution is required.

With cantilever walls, the depth of penetration of the piling governs rotational stability by a combination of penetration and anchor position for an anchored wall. Because of the complexity of behavior of the wall/soil system, a number of simplifying assumptions are employed in the classical design techniques. Foremost of these assumptions is that the deformations of the system are sufficient to produce limiting active and passive earth pressures at any point on the wall/soil interface. Other assumptions are discussed in the following paragraphs.

The distribution of earth pressure is different for sheet piling in granular soils and sheet piling in cohesive soils. In addition, the pressure distribution in clays is likely to change with time. Therefore, the design procedures for steel sheet piling in both types of soils are discussed separately.

9.3.2. Cantilever Sheet Piling in Granular Soils

In designing cantilever sheet piling walls in purely granular soils, there are two methods that are generally used: the conventional method and the simplified method. We will also look at a chart method for preliminary analysis. Finally, we will show Example 8, which will show how these methods are done in more detail.

9.3.2.1. Conventional Method

The conventional method is the complete application of

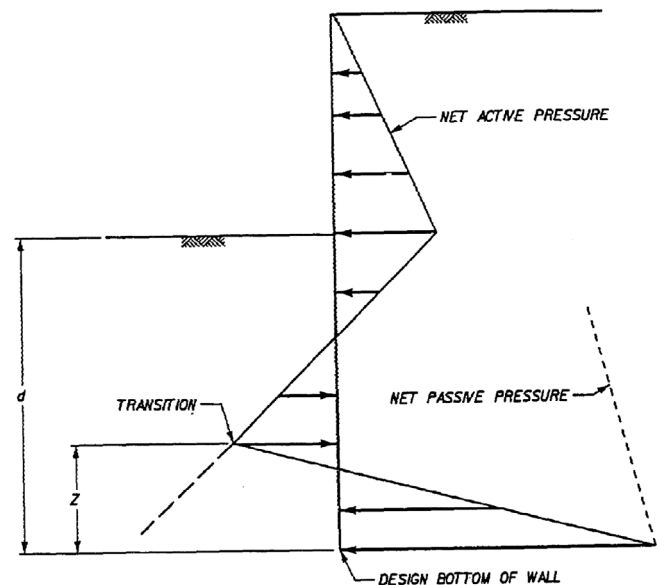
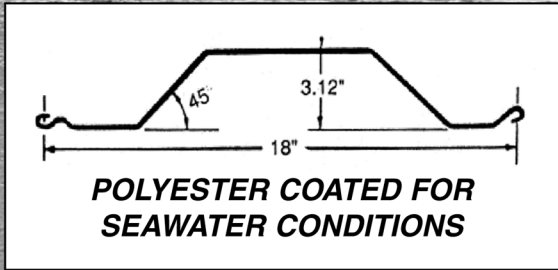
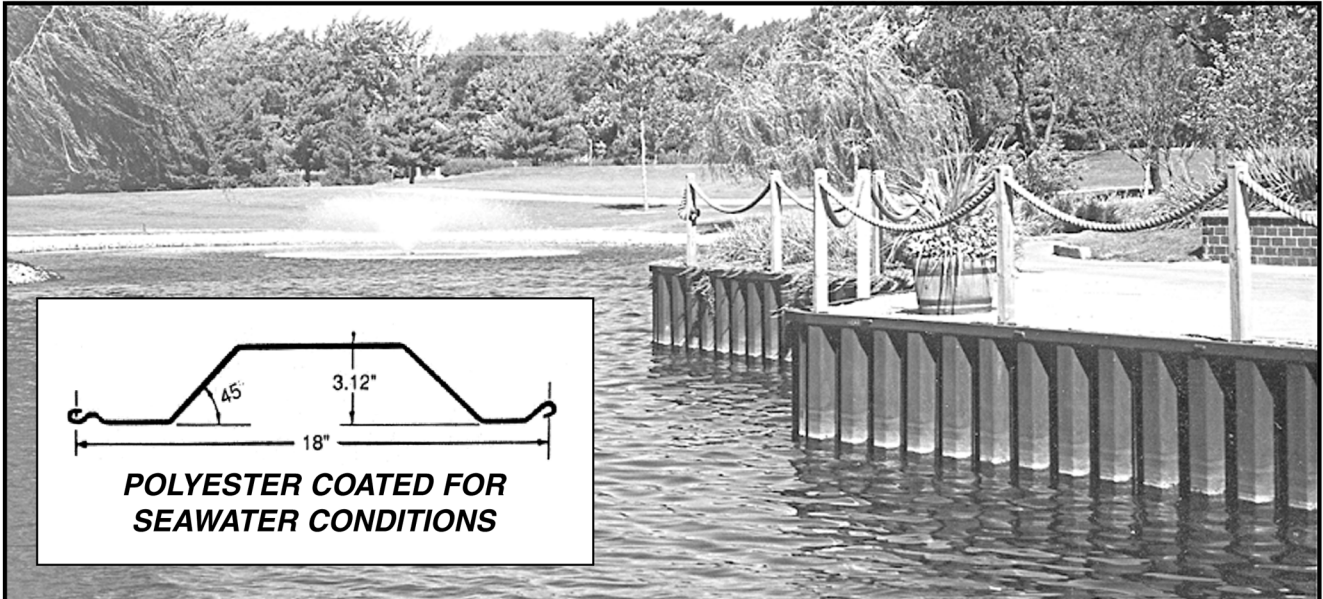


Figure 9-2: Design Pressure Distribution for a Cantilever Wall

the principles and assumptions shown in *Figure 9-2*. For clarity, we will set forth this method for the case where the soil is homogenous and without water on either side of the sheeting. For cases of layered soil and water, the method is the same, although the pressure distributions would be somewhat different due to the variable soil properties. For cases of two or more layers of soil, the earth pressure distributions would be somewhat different due to the variable soil properties.

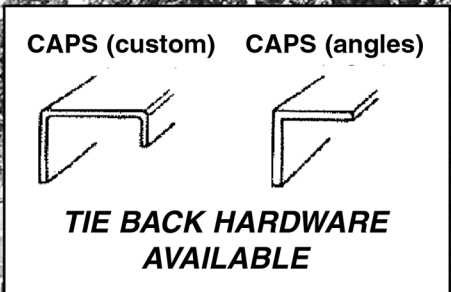
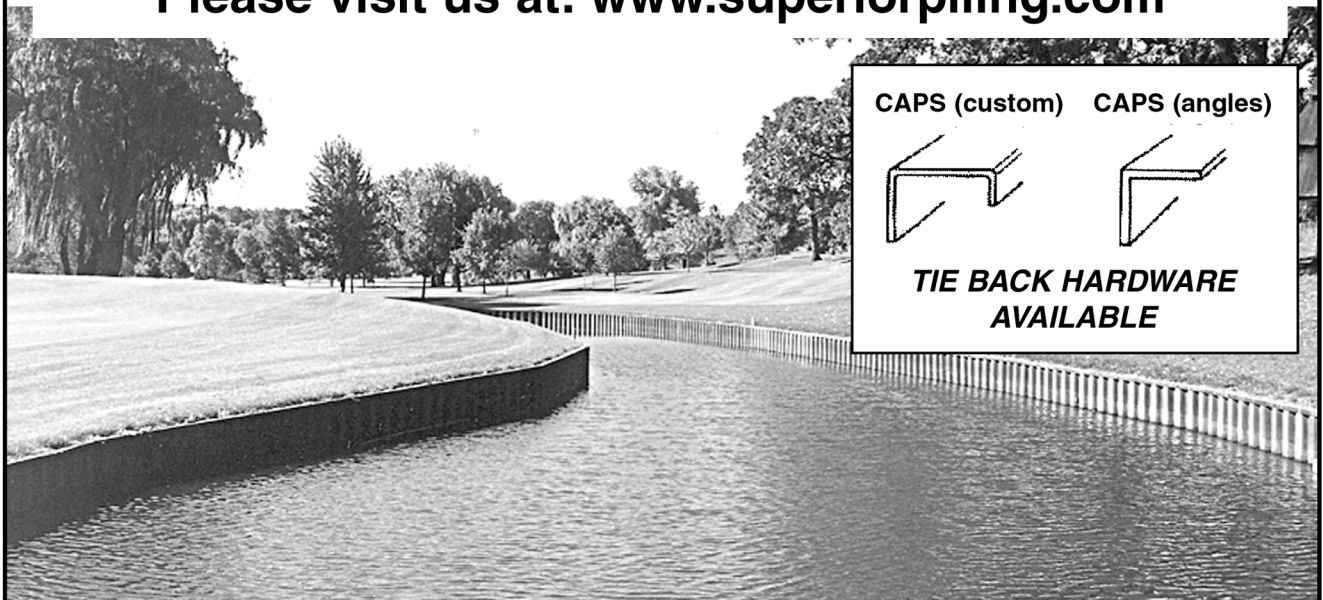
The conventional design procedure for granular soils is as follows:

1. Determine the active and passive lateral pressures using appropriate coefficients of lateral earth pressure. Rankine coefficients are the most conservative; they can be used with any type of sheeting, especially non-ferrous materials. If Coulomb coefficients are used, it should be used conservatively for the passive case, i.e., lateral pressures should be calculated using the curved failure surface (log spiral) method as shown in *Figure 18-16*. The resulting earth pressure diagram for a homogeneous granular soil is shown in *Figure 9-3*. All calculations must be based on a unit length of wall, one foot or metre.
2. Determine both the factor of safety and the method (reduced passive coefficient or sheet extension method.) Reducing the passive earth pressure coefficient is a more consistent way to apply the factor of safety. These methods are discussed in 9.3.2.4.
3. Satisfy the requirements of static equilibrium: the sum of the forces in the horizontal direction must be zero and the sum of the moments about any point must be zero. The sum of the horizontal forces may be written in terms of pressure



SUPERIOR PILING, INC

7247 S. 78th AVENUE, BRIDGEVIEW, IL 60455
1-800-544-1196 • 708-496-1196 • FAX 708-496-1261
Please visit us at: www.superiorpiling.com



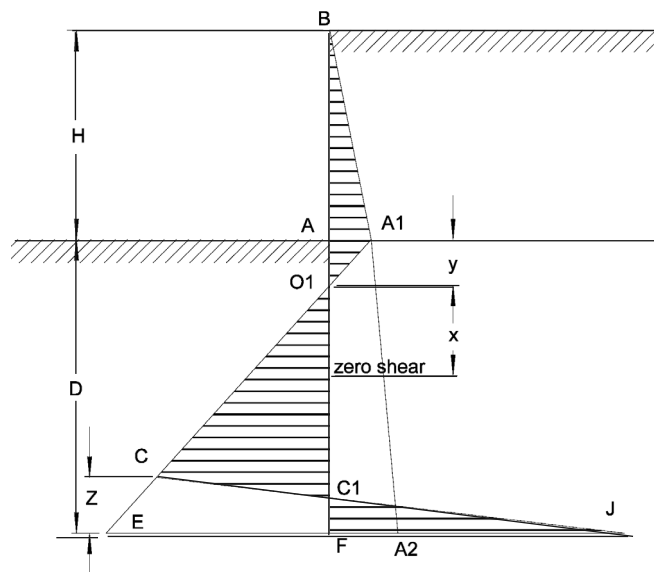


Figure 9-3: Resultant Earth-Pressure Diagram

areas:

Equation 9-1:

$$\text{Area}(BAA_1) + \text{Area}(AA_1A_2F) + \text{Area}(ECJ) - \text{Area}(EA_1A_2) = 0$$

Solve the above equation for the distance, Z. For a uniform granular soil,

Equation 9-2:

$$Z = \frac{K_p D^2 - K_a (H + D)^2}{(K_p - K_a)(H + 2D)}$$

4. Take moments about the point F and solve the equation for D. This can be done either by solving the high (fourth or fifth) order equation directly or through an iterative process.

5. Apply a factor of safety to extend the pile toe, if the reduced earth pressure coefficient is not being used.

6. Compute the maximum bending moment, which occurs at the point of zero shear. This is done first by determining the point y, from which the forces generated from the most active pressures above this point can be determined. The point where these forces equal the forces below the point O1 is the point of zero shear and maximum moment. Once this is determined, the moment at this point can be determined using the forces already computed.

7. Compute the required section modulus, which occurs at the point of zero shear, by solving Equation 2-2 for the section modulus:

Equation 9-3:
$$S_{\min} = \frac{M_{\max}}{\sigma_{\text{allow}}}$$

Although one can make rough estimates of displacements with formulae, the best way to estimate wall displacement is by using a computer program such as SPW 911.

9.3.2.2. Simplified Method

In view of the uncertainties involved with the soil, modelling theoretical pressure distribution may not produce results any better than some simplified approaches. Several shortcuts have been developed for cantilever wall designs that yield satisfactory results. Probably the most widely used of these methods is the one presented below⁸⁵. This method is the method used by SPW 911.

The simplified method is based on the assumptions shown in Figure 9-4.

The simplified method varies from the conventional method in several important respects:

- Eliminates the “bottom triangle” where the earth pressures reverse themselves again; F₃ replaces the forces at the toe.
- Uses the force triangles for resultant forces “F1” and “F2”;
- Computes the distance x’ that satisfies the conditions of equilibrium, i.e., moments about point C=0; and,
- Increases the penetration by 0.2x’ to compensate for simplification⁸⁶.

9.3.2.3. Chart Solutions

Figure 9-5 gives a useful method to design cantilever sheet piling in homogeneous granular soil, analysed by the conventional method. This chart allows the designer to obtain directly the depth ratio, D/H, and the maximum moment ratio, M_{max} / γK_aH³ as a function of the ratio of passive to active pressure coefficients, K_p/K_a, for various positions of water level. It is, therefore, independent of the method of obtaining K_p or K_a. The chart was developed for a wet unit weight, γ, equal to twice the submerged unit weight, γ’. To use Figure 9-5, one may determine ϕ and γ from soil data, δ from Table 5-1 and K_p or K_a and K_a from Equation 5-27 and Equation 5-33. A design example is given at the end of Example 8.

9.3.2.4. Factors of Safety and Rules of Thumb

All of the methods above require a factor of safety to be applied for successful sheet pile wall design. There are two main methods of applying a factor of safety:

1. Add 20-40% of the calculated depth of penetration, AF for the conventional method and AC1 for the simplified one. This will yield an approximate factor of safety of 1.5 (20%) to 2.0 (40%).

⁸⁵This method is shown in the *British Steel Corporation Piling Handbook* (1984) Fourth Edition. Scunthorpe, South Humberside, England: British Steel Corporation.

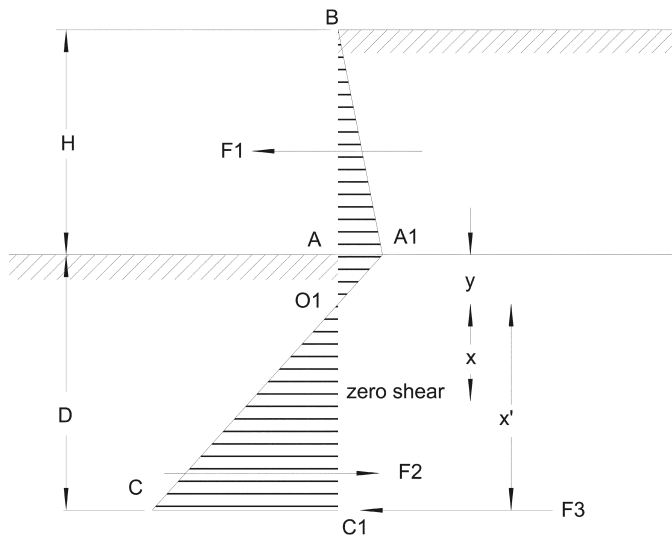


Figure 9-4: Simplified Method

2. Reduce the passive earth pressure coefficient by dividing it by 1.5—2.0⁸¹. This is probably the better of the two methods, because it can be done at the beginning of the problem, and is more consistent to apply amongst the three

design methods.

It is important to note that neither of these is a “direct” application of a factor of safety, such as we see in most structural and geotechnical analysis. This is one of the most difficult concepts we have in sheet piling design.

As a practical matter, cantilever sheet pile walls should be designed for a free height H of no more than 12’ for steel sheet piling. The penetration D should be at least half of the free height H. Cantilever walls should *never* be used with non-metallic sections (vinyl, pultruded fibreglass) and sparingly with aluminium.

Example 8: Design of Cantilevered Sheet Pile Wall (Granular Soil)

❖ Given:

■ Medium Sand

• $\gamma = 115$ pcf

• $\gamma' = 115 - 62.4 = 52.6$ pcf; groundwater table at dredge line on both sides of the wall

• $\phi = 35^\circ$

• Level backfill, $\beta = 0$

■ Steel Sheet Piling

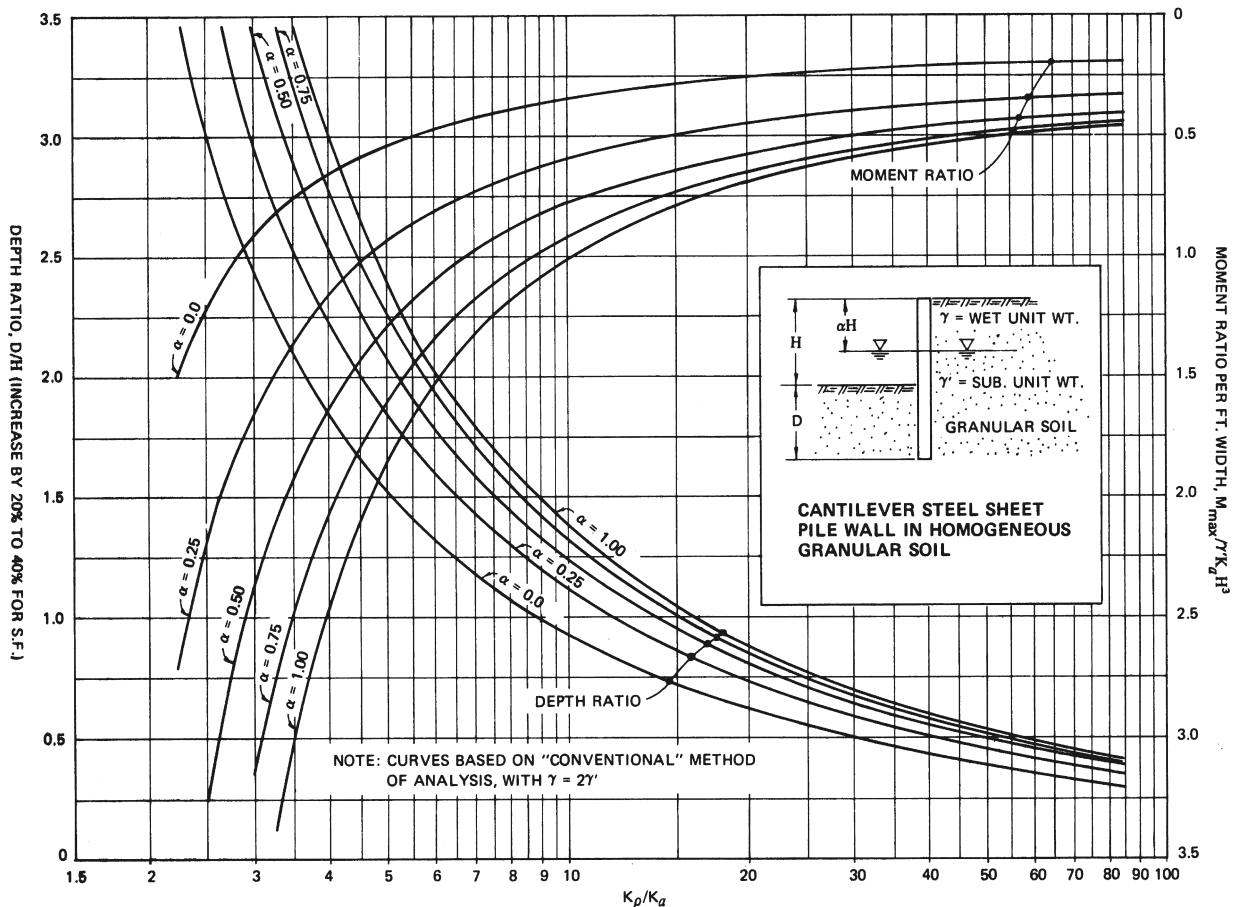


Figure 9-5: Chart for Determining Wall Depth for Uniform Cohesive Soil

⁸⁶This is not a factor of safety, but a factor necessitated by the elimination of the pressures below the point C. Once this is done, factors of safety are then applied.

⁸⁷We used Maple V Release 4 to assist in the hand calculations. This enabled us to carry significant figures which would otherwise be inappropriate in strictly “hand” calculations. This leads in some cases to minor variations in the results.

- $\delta = 22^\circ$ (from Table 5-1)
- $\delta/\phi = -0.63$
- $\theta = 0$
- $H = 14'$

■ Divide passive earth pressure coefficient by 1.5 for factor of safety.

❖ Find

- Depth of penetration D of sheeting
- Sheeting section for maximum moment

❖ Solution⁸⁷

■ Earth Pressure Coefficients

- Rankine
 - Active: 0.27 (Equation 5-1)
 - Passive: 3.68 (Equation 5-16)
- Coulomb
 - Active: 0.24 (Equation 5-27)
 - Passive: 9.25 (Equation 5-33)
- Log-Spiral
 - Active: 0.27 (Figure 18-16, nearly identical to Rankine case)
 - Passive: 7.92. From Figure 18-16, for level backfill ($\beta/\phi = 0$) without reduction for wall friction, $K_p = 10.2$. Since $\delta/\phi = -0.63$ and $\phi = 35^\circ$, per table in upper left hand corner $K_p = (10.2)(.776) = 7.92$.

- Selection of Earth Pressure Coefficients
- Use Log-Spiral coefficients, applying the reduction factor to the passive coefficient as a factor of safety
- ◆ $K_a = 0.27$
- ◆ $K_p = 7.92/1.5 = 5.28$

■ Conventional Method: Determination of Depth of Sheet Penetration

- Compute earth pressures along the wall (refer to Figure 9-3)
 - $p_{A1} = \gamma H K_a = 436.3$ psf
 - $p_{A2} = p_{A1} + \gamma' D K_a = 436.3 + 14.3 D$ psf
 - $p_E = \gamma' D (K_p - K_a) - p_{A1} = 263.3 D - 436.3$ psf
 - $p_J = p_E + p_{A1} + \gamma H K_p = 263.3 D + 8495.6$ psf

- Compute value of Z using summation of forces

Static equilibrium along the wall requires that the sum of the forces along the wall equal zero. This can be used to compute the value of Z. This summation of forces is given by Equation 9-1; however, the solution given in Equation 9-2 cannot be directly applied here because of the water table. Equation 9-1 can be expressed in terms of the earth pressures as

Equation 9-4:

$$\frac{Hp_{A1}}{2} + \frac{(p_{A1} + p_{A2})D}{2} + \frac{(p_E + p_J)Z}{2} - \frac{(p_E + p_{A2})D}{2} = 0$$

Substituting the values for the pressure and solving for Z yields

Equation 9-5:

$$Z = \frac{249D^2 - 872.6D - 6108.1}{526.6D + 8059.3} \text{ ft.}$$

- Compute value of D using summation of moments

The second requirement of static equilibrium is that the moments at any point equal zero.

Equation 9-5 is an equation in two unknowns. To solve for Z and D, we need another equation. The summation of moments equation will give us the equation we need. We will sum moments about point F as follows:

Equation 9-6:

$$M_F = \frac{Hp_{A1}}{2} \left(D + \frac{H}{3} \right) + p_{A1} \frac{D^2}{2} + (p_E + p_J) \frac{Z^2}{6} - (p_E + p_{A2}) \frac{D^2}{6} + (p_{A2} - p_{A1}) \frac{D^2}{6} = 0$$

Again substituting both the earth pressures computed and the value for Z given in Equation 9-5, we have

Equation 9-7:

$$43.9D^3 - 218.1D^2 - 3054.1D - 14252.3 - \frac{(249D^2 - 872.6D - 6108.1)^2}{526.6D + 8059.3} = 0$$

The only real, positive root for this fifth order equation is $D = 13.1'$, which is the penetration of the sheeting below the dredge line. Substituting this into Equation 9-5 yields $Z = 1.69'$.

■ Simplified Method: Determination of Depth of Sheet Penetration (see Figure 9-4)

- Compute distance y from A to O_1 . The equation for this distance is

Equation 9-8:

$$y = \frac{p_{A1}}{\gamma'(K_p - K_a)}$$

Substituting the variables, for this case $y = 1.66'$.

- Compute the forces acting on the sheet pile wall. These can be divided up into three areas:
 - Area AA₁B: $p_1 = p_{A1} H / 2 = 3054.1$ lbs.
 - Area AA₁O₁: $p_2 = p_{A1} y / 2 = 361.5$ lbs.
 - Area O₁CC₁: $p'_3 = \gamma' (K_p - K_a) x^2 / 2 = 131.7 x^2$ lbs.

- Sum the moments about point C₁. The summation is

vulcanhammer.net

Your complete
online resource
for information on
geotechnical
engineering and
deep foundations

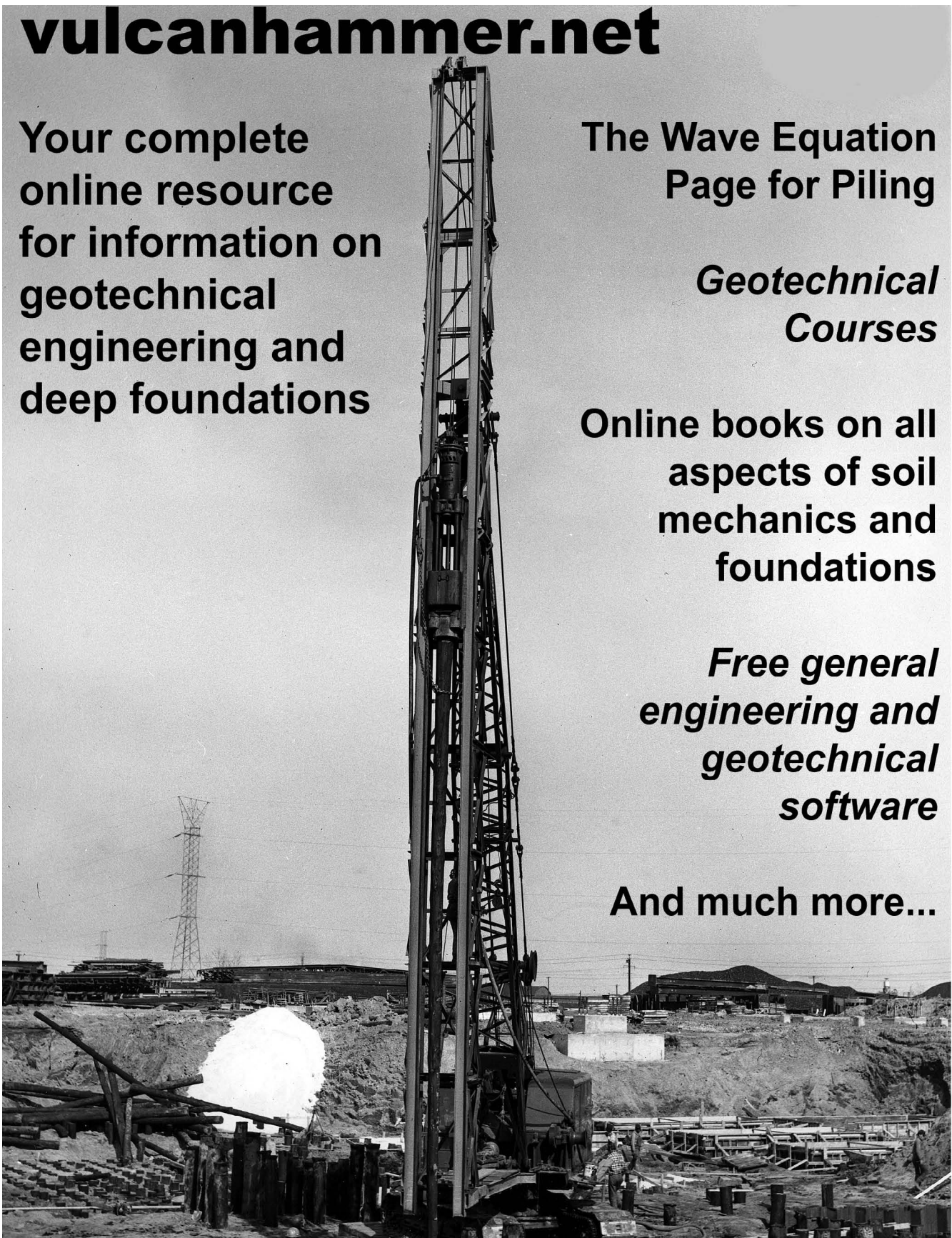
The Wave Equation
Page for Piling

*Geotechnical
Courses*

Online books on all
aspects of soil
mechanics and
foundations

*Free general
engineering and
geotechnical
software*

And much more...



<http://www.vulcanhammer.net>

<http://www.vulcanhammer.org>
email me@vulcanhammer.net

<http://www.chet-aero.com>

Equation 9-9:

$$p_1 \left(\frac{H}{3} + y + x' \right) + p_2 \left(\frac{2y}{3} + x' \right) - p_3 \frac{x'}{3} = 0$$

Substituting the forces and value for y into this equation yields

Equation 9-10:

$$43.9x'^3 - 3415.5x - 19172.1 = 0$$

The one real root of this equation is $x' = 10.9$.

- Add the simplified method factor to x' and solve for the total penetration D. The penetration is given by the equation

Equation 9-11: $D = y + 1.2x'$

Substituting the variables into this equation yields $D = 14.7'$, which includes the factor of safety.

■ Determination of value of maximum moment.

- The maximum moment for the sheeting is the same in both cases. It takes place at the point of zero shear, i.e.,

Equation 9-12: $p_1 + p_2 = p_3$

Where $p_3 = \gamma (K_p - K_a) x^2 / 2 = 131.7 x^2$ lbs. The computation of the point of maximum moment is thus very similar to the computation of the penetration of the sheeting in the simplified method; it is yet another simplification of the calculations.

Substituting values of p_1 , p_2 and p_3 in to Equation 9-12 and solving for x yields $x = 5.1'$.

- Compute the maximum moment at point x. This computation is similar to Equation 9-9 and is given by the equation

Equation 9-13:

$$M_{\max} = p_1 \left(\frac{H}{3} + y + x \right) + p_2 \left(\frac{2y}{3} + x \right) - p_3 \frac{x}{3}$$

Direct substitution of the variables into this equation will yield $M_{\max} = 31,310$ ft-lbs/ft of wall length.

- Select sheet piling section. Most sheet piling specifications will give a maximum allowable moment for a given section. In the cases of those that do not, the maximum allowable section modulus can be computed using Equation 9-3. For example, for a 25 ksi allowable stress steel, the section modulus would be $(31.310 \text{ ft-kips/ft})(12 \text{ in/ft})/(25 \text{ ksi}) = 15.0 \text{ in}^3/\text{ft}$

of wall. Thus any of the sections shown in *Table 2-1* can be used in this case.

■ Simplified Method using SPW 911

- SPW 911 uses the simplified method for cantilever walls. Detailed input instructions for the program are given in the program help, but the input is divided up into six sections:
- Job data, which contains general information about the client and the job.
- Excavation data, which includes information about the depth of the dredge line, the location of the water table (it can be different on the two sides of the wall), and the slope of the ground on either side of the wall.
- Soils data, which include soil unit weights, active and passive earth pressure coefficients, pressure models (Rankine, Coulomb, etc.), and other data. Soils can be layered in the program, as they usually appear this way in the field. Although the program does compute earth pressure coefficients for the various earth pressure theories, it is recommended that the user compute these independently as a check. Also, the user can reduce the passive earth pressure coefficients by a factor of safety, which means that the program results will be the final results for the wall. (The program already includes the factor for the simplified method.)
- Wall data, which includes data for the structural analysis of the sheeting such as modulus of elasticity, section modulus, etc. The program has a user-editable database for various sections of sheet piling.
- Data on the supports, which are used with anchored walls.
- Setup data, which include data on the designer and the ability to change units.

The results of the SPW 911 run for this example are shown in *Figure 9-6*.

On the left are the maximum values (top to bottom) of active wall pressure, moment, wall shear, and deflection. These are shown graphically superimposed onto the sheeting. The program also shows the results in tabular form. The deflection assumes the use of PZ 27 sheeting. The results are the same as the simplified method. The program itself allows the user to input the passive earth pressure reduction factor directly.

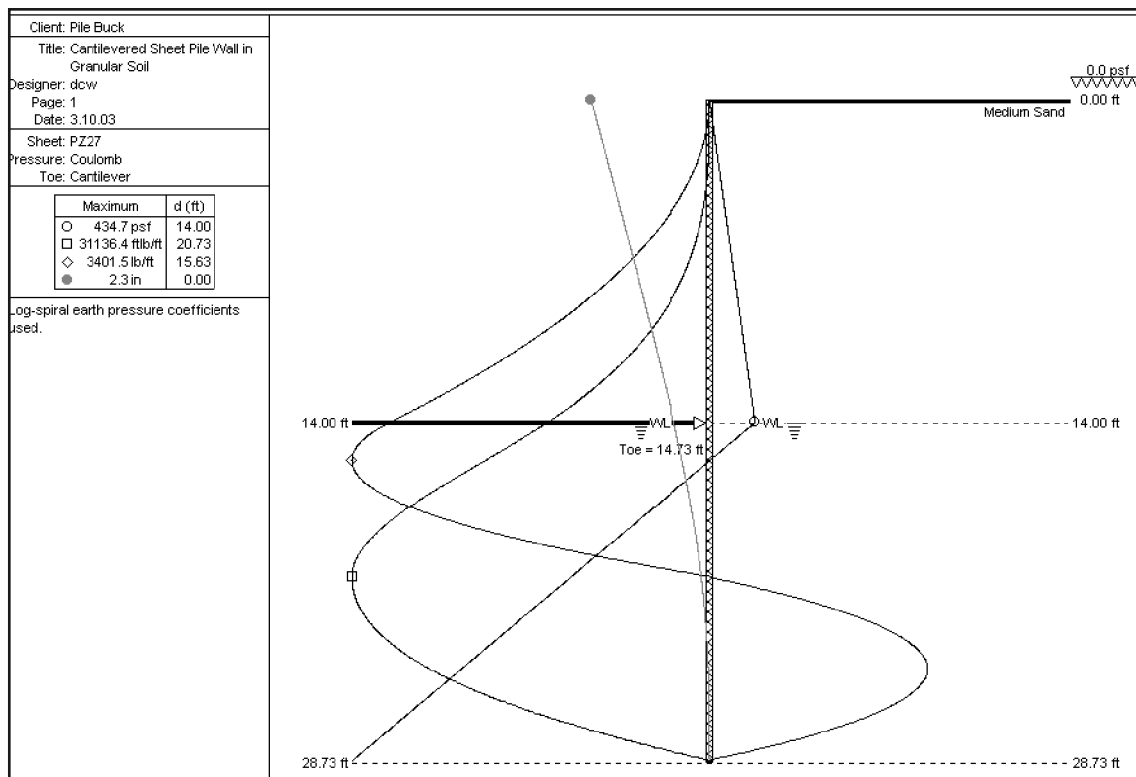


Figure 9-6: SPW 911 Example for Cantilevered Sheet Piling Wall in Cohesionless Soils

■ Chart Solution

- To use *Figure 9-5*, we need to know first the ratio of passive to active earth pressure coefficients, K_p/K_a and the distance of the water table to the surface to the distance from the surface to the dredge line α . These ratios are $5.28/0.27 = 19.5$ and 1 respectively. The earth pressure ratio used allows us to include the factor of safety without adding the depth beyond the chart solution.
- Applying these values to the chart, the depth ratio is 0.9, which translates into a depth of 12.6'. The maximum moment ratio is 0.7, which translates into a maximum moment of 29.93 ft-kips/ft of wall length.
- Although this chart was computed using the conventional method, the results vary from that method because the chart assumes the submerged unit weight to be half the unit weight, which was not done in the calculations.
- The chart solution is a good check to the other methods of sheet piling wall design, but caution should be used in using the chart data for design.

9.3.3. Cantilever Sheet Piling in Cohesive Soils

Clay soils provide special problems to the designer of retaining walls primarily because:

- 1) Their shear strength changes with water content;
- 2) Their ability to maintain cohesion over an extended period is doubtful;
- 3) Their lack of permeability allows the possibility of increased active pressure from pore water or frost that was not foreseen.

Generally, it is desirable to replace clay backfill with granular, even if the base material into which the sheets are driven for support consists of plastic materials. Two cases are presented here:

- (1) a wall entirely in clay that might reflect a short-term operation and
- (2) a wall driven into clay but with a granular backfill.

Different lateral earth pressures develop for each case; however, the earth pressure theory for each is essentially the same.

9.3.3.1. Wall Entirely in Cohesive Soil

Design of sheet piling in cohesive soils is complicated by the fact that the strength of clay changes with time and, accordingly, the lateral earth pressures also change with time. The depth of penetration and the size of piling must

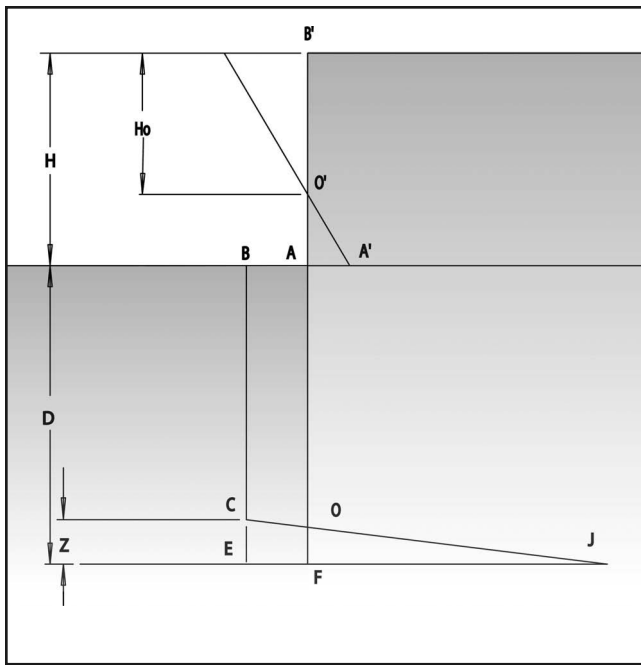


Figure 9-7: Initial Earth Pressure for Design of Cantilever Sheet Piling Entirely in Cohesive Soil, Conventional Method

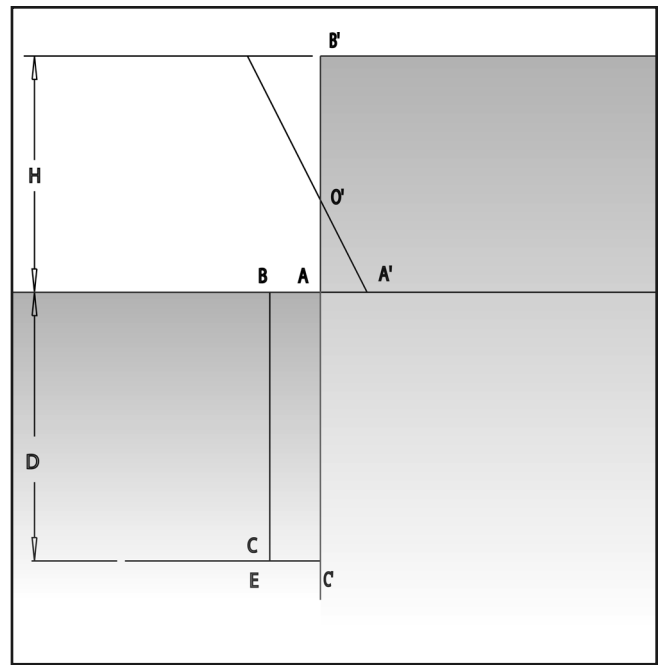


Figure 9-8: Initial Earth Pressure for Design of Cantilever Sheet Piling Entirely in Cohesive Soil, Simplified Method

satisfy the pressure conditions that exist immediately after installation and the long-term conditions after the strength of the clay has changed. Immediately after the sheet piling is installed, earth pressure may be calculated on the assumption that undrained strength of the clay prevails. That is, it is assumed that the clay derives all its strength from cohesion and no strength from internal friction. The analysis is usually carried out in terms of total stress using a cohesion value, c , equal to one-half the unconfined compressive strength, q_u . The method is usually referred to as a “ $\phi = 0$ ” analysis.

As is the case with cohesionless soils, the conventional method can be used for cohesive soils as well. Figure 9-7 illustrates the initial pressure conditions for sheet piling embedded in cohesive soil for its entire depth for the conventional method.

When $\phi = 0$, $K_a = K_p = 1$ and $K_{ac} = K_{pc} = 2$. For the passive earth pressure on the left side of the piling, Equation 5-19 reduces again to

$$\text{Equation 9-14: } p_p = \gamma_t (z - H) + 2c$$

and the active pressure on the right side of the piling is given by:

$$\text{Equation 9-15: } p_a = \gamma_t z - 2c$$

The negative earth pressure or tension zone, as shown by the line above H_0 , is ignored because the soil may develop tension cracks in the upper portion. Since the slopes of the active and passive pressure lines are equal ($K_a = K_p$), the net

resistance on the left side of the wall is constant below the dredge line and is given by:

$$\text{Equation 9-16: } p_p - p_a = 4c - \gamma_t H$$

Note that, theoretically, there will be no net pressure and the wall will fail if

$$\text{Equation 9-17: } \gamma_t H > 4c$$

From this we define the critical wall height as

$$\text{Equation 9-18: } H_{cw} = \frac{4c}{\gamma_t} = 2H_c$$

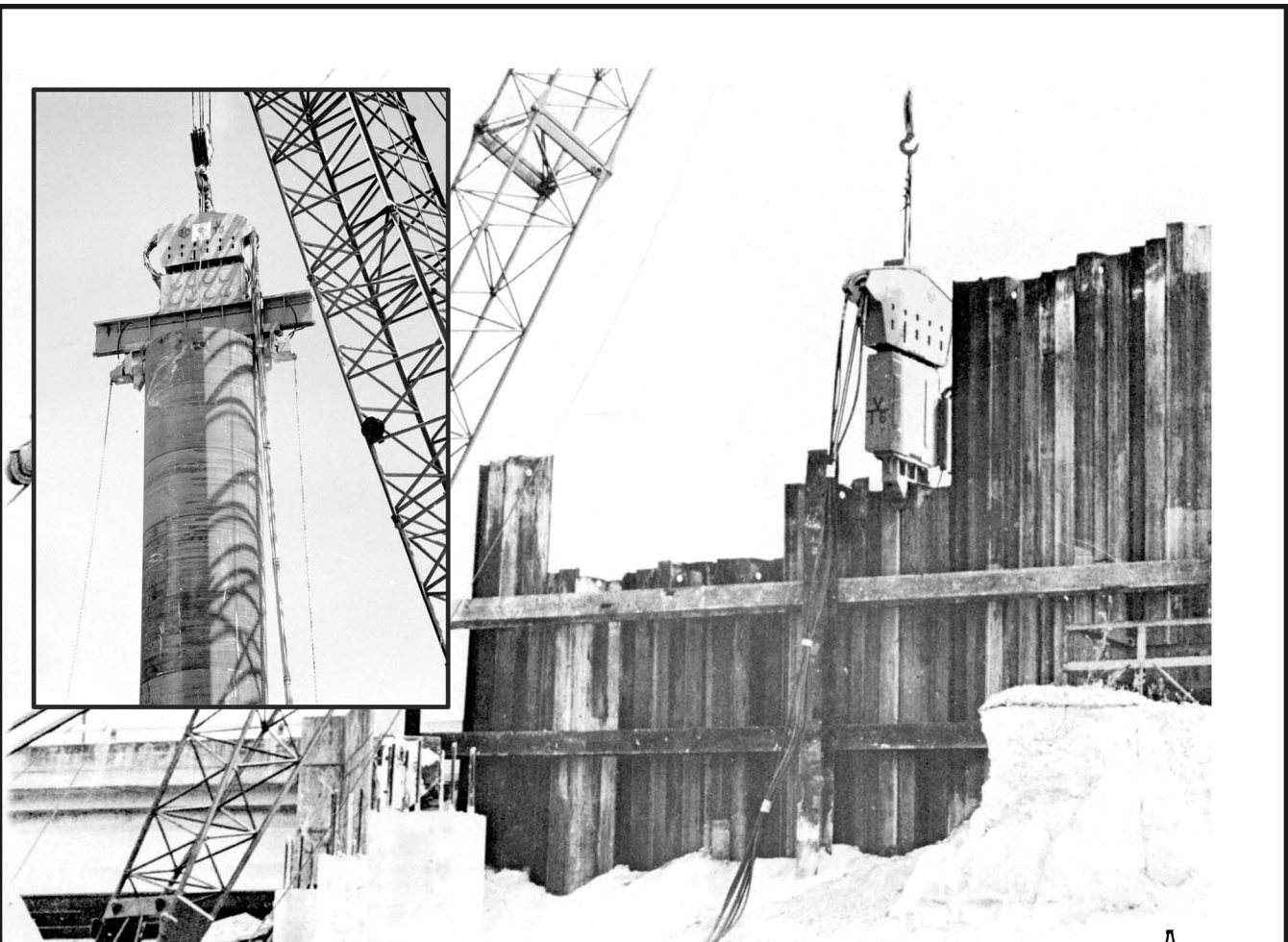
This should not be confused with the critical height H_c , which is the point at which the active pressure becomes greater than zero.

For the lower portion, where the piling moves to the right, the net resistance is given by:

$$\text{Equation 9-19: } p_p - p_a = 4c + \gamma_t H$$

The method of solution is the same as that presented for the design of cantilevered sheet pile walls in granular soils. The point d and the depth of penetration D are chosen so as to satisfy the conditions of static equilibrium; i.e., the sum of the horizontal forces equal to zero and the sum of the moments about any point equal to zero.

Similar to the simplified method for granular soils, the design may be made using the pressure diagram, i.e., by assuming the passive pressure on the right of the piling is

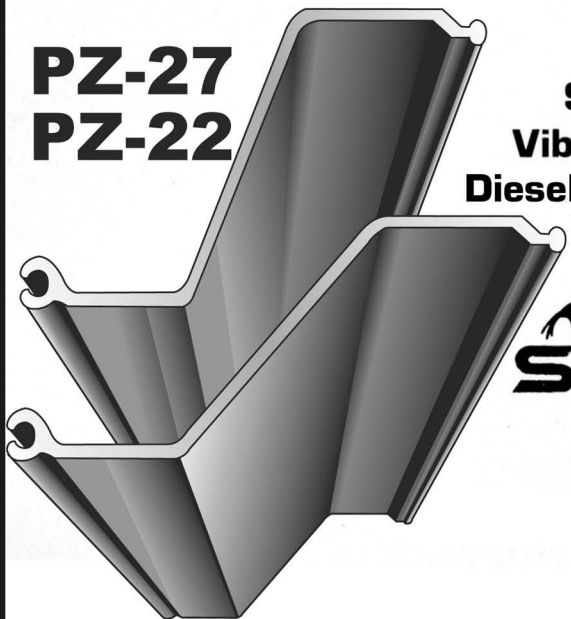


Seaboard Steel Corp.

Sales / Rentals

PZ-27
PZ-22

Steel Sheet Piling
Steel HP Bearing Piles
Vibratory Driver/Extractors
Diesel and Hydraulic Pile Hammers
Vertical Earth Augers



Seaboard Steel Corp.
3912 Goodrich Ave.
Sarasota, FL 34234

941-355-9773
1-800-533-2736
Fax: 941-351-7064



replaced by the concentrated reaction, C. The depth D_0 should be increased by 20 to 40 percent to obtain the total design depth of penetration using this method. The pressure diagram for the simplified method is shown in Figure 9-8.

The most straightforward way to apply a factor of safety is to reduce the soil cohesion in a manner similar to reducing the passive earth pressure coefficient for granular soils, i.e., divide it by 1.5-2.

Example 9: Design of Cantilever Sheet Pile Wall (Purely Cohesive Soils)

❖ Given:

- Medium Soft Clay
 - $\gamma = 120$ pcf
 - $\gamma' = 120 - 62.4 = 57.6$ pcf; groundwater table at dredge line on both sides of the wall
 - $\phi = 0$ (for the long term case, $\phi = 27^\circ$)
 - Level backfill, $\beta = 0$
 - $q_u = 1500$ psf
 - To apply factor of safety, $q_{u1} = 1500/1.5 = 1000$ psf
 - $c = 500$ psf
- Sheet Piling
 - $\theta = 0$
 - $H = 14'$

❖ Find

- Depth of penetration D of sheeting
- Sheeting section for maximum moment
- It should be emphasised that the analysis below is valid for the short-term case.

❖ Solution

- Conventional Method: Determination of Depth of Sheet Penetration (see Figure 9-7):
 - Check the critical wall height. This is done using Equation 9-18. For this wall, $H_{cw} = (4)(500)/(120) = 16.7' > H = 14'$.
 - Compute the point of zero pressure (critical height) using Equation 4-25. In this case, $H_c = H_o = 16.7/2 = 8.3'$
 - We need to note the pressures at the various points are as follows:

Equation 9-20: $p_A' = \gamma H - 2c$

Equation 9-21: $p_E = 4c - \gamma H$

Equation 9-22: $p_j = 4c + \gamma H$

Substituting and solving:

- $p_A' = 680$ psf
- $p_E = 320$ psf
- $p_j = 3680$ psf
- Compute Z by summing the forces for static equilibrium. For this case,

Equation 9-23:

$$\frac{(H - H_o)p_{A1}}{2} + \frac{(p_E + p_J)Z}{2} - p_E D = 0$$

Making the appropriate substitutions,

Equation 9-24: $Z = .16D - .963$

- Compute D by summing moments about point F. The summation is expressed by the equation

Equation 9-25:

$$\sum M_F = \frac{p_A'(H - H_o)}{2} \left(D + \frac{H - H_o}{3} \right) + \frac{p_E Z}{2} \frac{Z}{3} - p_E D \frac{D}{2} = 0$$

Making the appropriate substitutions, the expression in D is

Equation 9-26: $134.4D^2 - 1618.4D - 4567.3 = 0$

The positive root for this is $D = 14.4'$; thus, $Z = 1.34'$.

- Simplified Method: Determination of Depth of Sheet Penetration (see Figure 9-8)

- Compute the forces acting on the sheet pile wall.

These can be divided up into three areas:

Area AO'A: $p_1 = p_A' (H - H_o) / 2 = 1926.7$ lbs.

Area BACC₁: $p_2 = p_C D' = p_E D' = 320 D'$ lbs.

Where D' = distance from dredge line to sheeting toe without correction for simplified method.

- Sum the moments about point C₁. The summation is

Equation 9-27:

$$\sum M_{C_1} = p_1 \left(\frac{(H - H_o)}{3} + D' \right) - p_2 \left(\frac{D'}{2} \right) = 0$$

Substituting the variables into this equation yields

Equation 9-28: $160D'^2 - 1936.7D' - 3639.3 = 0$

The one real root of this equation is $D' = 13.7'$.

- Add the simplified method factor to x' and solve for the total penetration D .

The penetration is given by the equation

Equation 9-29: $D = 1.2D'$

Substituting the variables into this equation yields $D = 16.4'$, which includes the factor of safety.

- Determination of value of maximum moment.

- The maximum moment for the sheeting is the same in both cases. It takes place at the point of zero shear, i.e.,

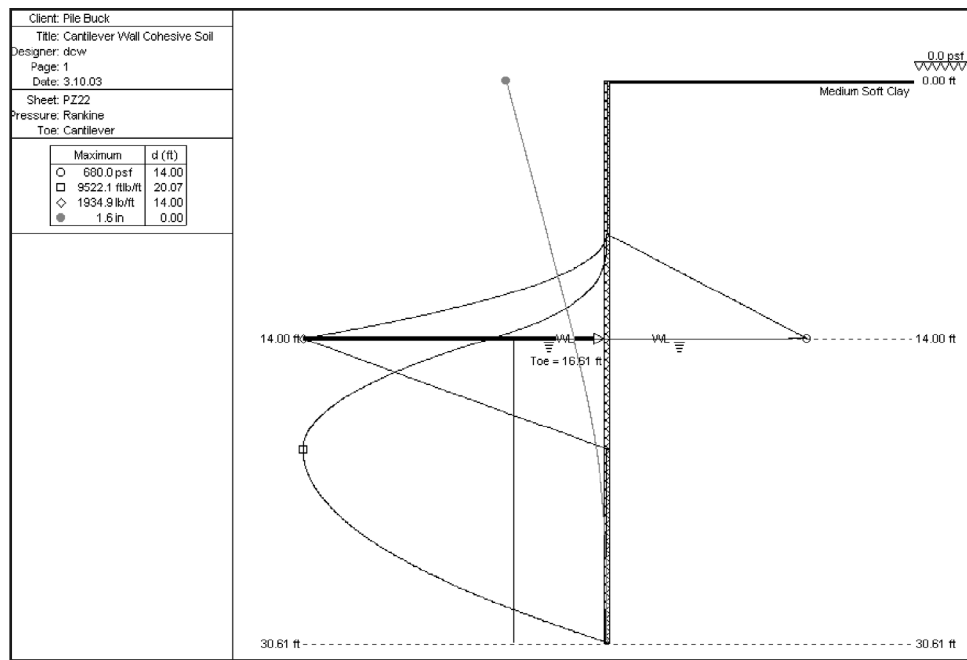


Figure 9-9: SPW 911 Example for Cantilevered Sheet Piling Wall in Cohesive Soils

Equation 9-30: $p_1 = p_2 (x)$

Where x is the distance from the dredge line to the point of zero shear, and substitutes directly in p_2 for D' . The computation of the point of maximum moment is thus very similar to the computation of the penetration of the sheeting in the simplified method; it is yet another simplification of the calculations. Substituting values of p_1 and p_2 and p_3 in to Equation 9-30 and solving for x yields $x = 6'$.

- Compute the maximum moment at point x . This computation is similar to Equation 9-9 and is given by the equation

Equation 9-31:

$$M_{\max} = p_1 \left(\frac{(H - H_o)}{3} + x \right) - p_2 (x) \left(\frac{x}{2} \right)$$

Direct substitution of the variables into this equation will yield $M_{\max} = 9,439$ ft-lbs/ft of wall length. Again any of the sheet piling shown in Table 2-1 will be acceptable for bending moment.

- Select sheet piling section. Same method as given in Example 8.
- Simplified Method using SPW 911
 - The results of SPW 911 are shown in Figure 9-9. The input is essentially the same as in Example 8, except that it is necessary to input both the regular earth pressure coefficients K_a and K_p and the ones related to cohesive soil K_{ac} and K_{pc} . It should also be noted that, since this wall is a temporary structure, the minimum fluid pressure for this case is set to zero.

9.3.3.2. Wall in Cohesive Soil with Granular Backfill Above Dredge line

The above methods may also be extended to the case where sheet piling is driven in clay and backfilled with granular soil. The only difference is the active pressure coefficient above the dredge line is equal to K_a for a granular backfill. The methods of design are exactly the same as discussed previously.

The long-term condition for sheet piling in clays must also be considered, as mentioned previously, due to time dependent changes in ϕ and c . The analysis should be carried out using effective stress parameters c' and ϕ' obtained from consolidated-drained tests, or from consolidated-undrained tests in which pore pressure measurements are made. Limited experimental data indicates that the long-term value of c is quite small, and that for design purposes c may be conservatively taken as zero. The final value of ϕ is usually between 20 and 30 degrees. The lateral pressures in the clay over a long period of time approach those for a granular soil. Therefore, the long-term condition is analyzed as described in the preceding section for granular soils.

Figure 9-10 provides design curves for cantilever sheet piling in cohesive soil with granular soil backfill based upon the simplified method of analysis. This chart allows the designer to obtain directly the depth ratio, D/H , and the maximum moment ratio, $M_{\max}/\gamma K_a H^3$, as a function of the net passive resistance, $2q_u - p_v$, divided by the expression $\gamma K_a H$. The chart is, therefore, independent of the method of obtaining K_a and was developed for a wet unit weight, γ , equal to twice the submerged unit weight, γ' .

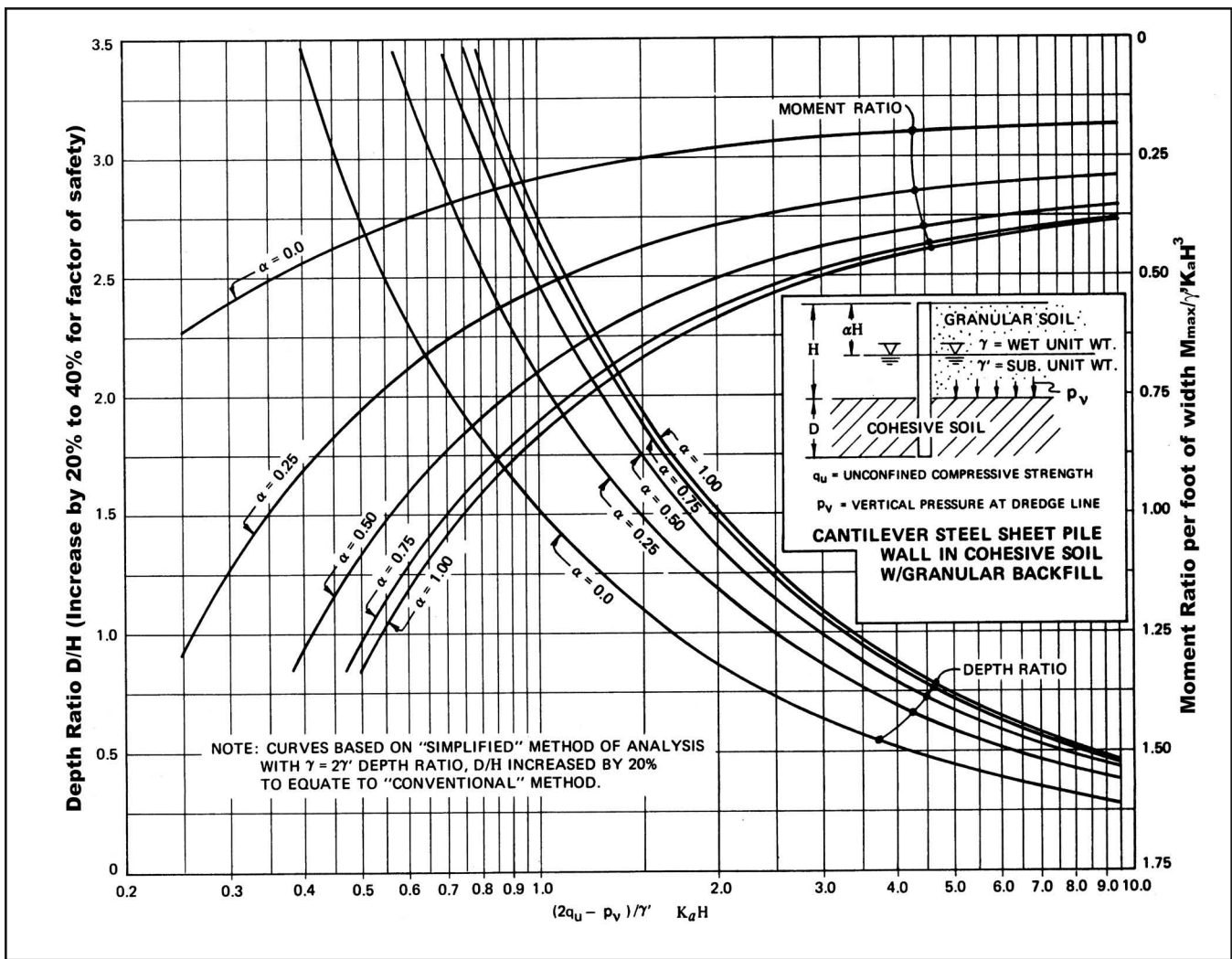


Figure 9-10: Cantilever Steel Sheet Pile Wall in Cohesive Soil with Granular Backfill

Example 10: Design of Cantilevered Sheet Pile Walls (Cohesive soils with Cohesionless Backfill)

❖ Given

- Sheet pile wall, 14' elevation to dredge line
- Soil Profile
 - Above dredge line, same soil as Example 8. Use same earth pressure coefficients.
 - Below dredge line, same soil as Example 9. Use same soil properties, including reduced cohesion.
 - Water table at 7' below the surface on both sides of the wall.

❖ Find

- Penetration of toe
- Maximum moment for selection of sheeting profile.

❖ Solution

- Chart Solution (see Figure 9-10)
 - Compute vertical pressure at the dredge line, which is the effective stress, or $p_v = (7)(115) + (7)(52.6) = 1173.2$ psf
 - Compute $(2q_u - p_v) / (\gamma K_a H) = ((2)(1000) - 1173.2) / ((52.6)(0.27)(14)) = 4.2$.

- Since the depth ratio $a = 7/14 = 0.5$, $D/H = 0.75$ and $M_{max} / \gamma K_a H^3 = 0.4$. From this, $D = (0.75)(14) = 10.5'$ and $M_{max} = 15,588$ ft-lbs/ft of wall length.
- Chart was actually developed using $\gamma' = \gamma/2$. If this is assumed, then $\gamma' = 115/2 = 57.5$ pcf, $p_v = 1207.5$, $(2q_u - p_v) / (\gamma' K_a H) = 3.6$, $D/H = 0.85$, $M_{max} / \gamma' K_a H^3 = 0.42$, $D = 11.9'$ and $M_{max} = 17,892$ ft-lbs/ft of wall. Looking at Table 2-1, any of the sections would be acceptable.

■ Simplified Method with SPW 911

- The results for this are shown in Figure 9-11. The results fall between the two different figures given above, due in large measure to the differences resulting from using the original γ in the SPW 911 solution.

9.4. Anchored Walls

9.4.1. General

Anchored sheet pile walls derive their support by two means: passive pressure on the front of the embedded portion against wall and an anchorage system located near the top of

HPSI Vibros



from a
"Little Guy"

to a
"BIG Guy"



Whether it's an excavator mounted vibratory for driving lightweight vinyl or aluminum sheet piling on up to a 20,000 in. lb. machine for driving large diameter caisson, we have a vibro suitable for your job.

SALES & RENTALS

(Distributors throughout North America)

From "The Engineers of Pile Driving Equipment"™

HYDRAULIC POWER SYSTEMS, INC.

Kansas City Offices and Plant
1203 Ozark
N. Kansas City, MO 64116
Phone (816) 221-4774
Fax (816) 221-4591
E-mail info@hpsi-worldwide.com
<http://www.hpsi-worldwide.com>



International & Domestic Sales
745 U.S. Hwy 1
N. Palm Beach, FL 33408
Phone (561) 687-5525
Fax (561) 841-3479
E-mail info@hpsi-worldwide.com
<http://www.hpsi-worldwide.com>

*Vibratory Pile Hammers • Hydraulic Augers • Winch Systems
Custom Manufacturing • Hydraulic Impact Hammers • Lead Systems*

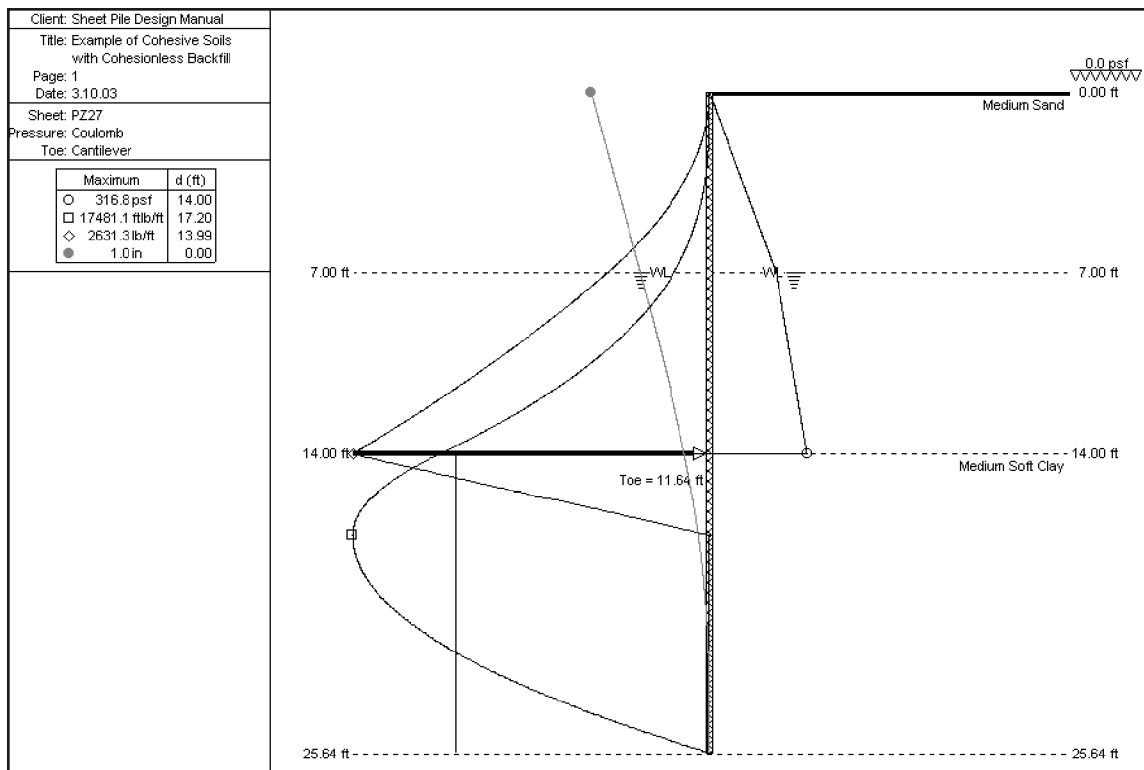


Figure 9-11: SPW 911 Results for Example 10

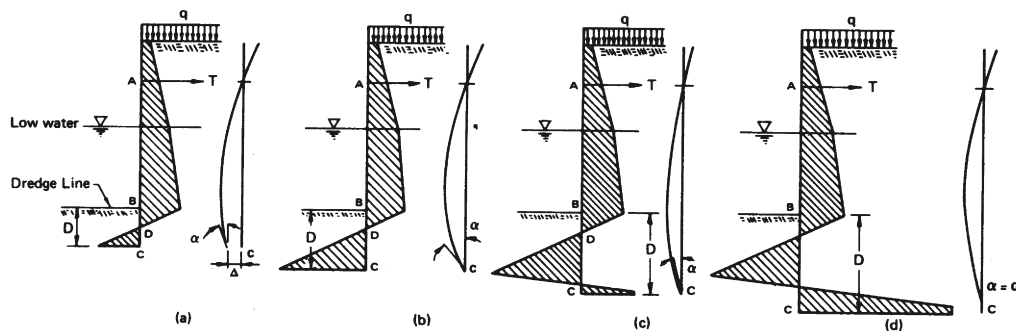


Figure 9-12: Effect of Depth of Penetration on Pressure Distribution and Deflected Shape

the piling. Design of the anchorage system will be discussed in chapter 11; this section will focus on the design of the wall itself. The overall stability of anchored sheet pile walls and the stresses in the members depends on the interaction of a number of factors, including the relative stiffness of the piling, the depth of piling penetration, the relative compressibility and strength of the soil, the amount of anchor yield, etc. As a general rule, the greater the depth of penetration, the lower the resultant flexural stresses. However, Rowe's experiments, described in this section, make a strong case that in most cases active earth pressures are reduced after wall flexure.

Figure 9-12 shows the historically accepted relationship between depth of penetration, lateral pressure distribution and elastic line or deflection shape.

Case (a) is commonly called the free earth support method. The passive pressures in front of the wall are insufficient to prevent lateral deflection and rotations at point C. Cases (b), (c)

and (d) show the effect of increasing the depth of penetration. In cases (b) and (c) the passive pressure has increased enough to prevent lateral deflection at C; however, rotation still occurs. In case (d) passive pressures have sufficiently developed on both sides of the wall to prevent both lateral deflection and rotation at C. This case is commonly called the fixed earth support method because point C is essentially fixed. Cases (a) and (d) represent the two extremes in design.

The principal methods in current usage for the design of anchored sheet pile walls are grouped and discussed in the following order:

- Free Earth Support Method
- Free Earth Support with Rowe's Moment Reduction Method
- Fixed Earth Support Method
- Equivalent Beam
- Equal Moments

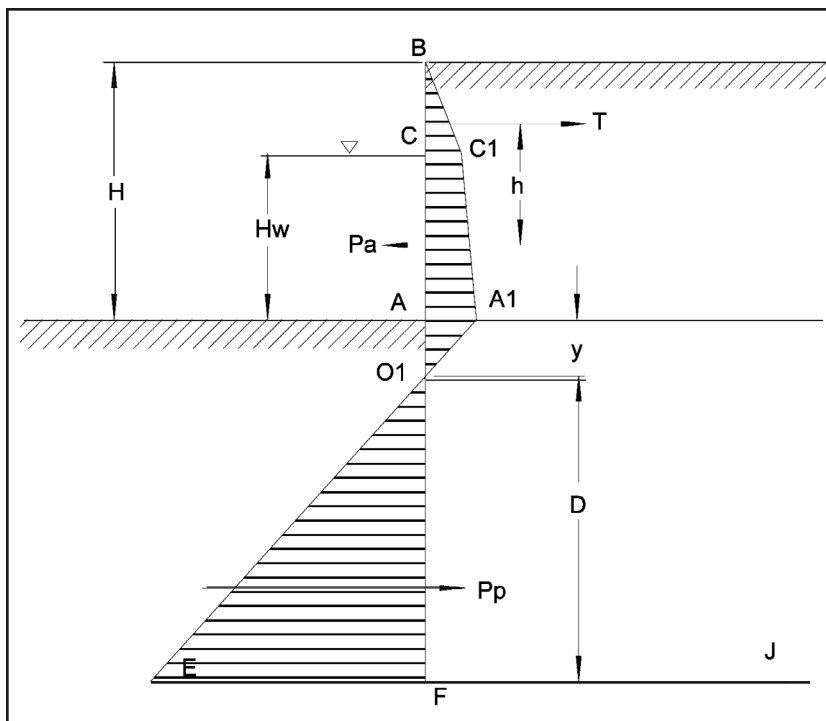


Figure 9-13: Anchored Sheet Pile Walls, Free Earth Support Method, Granular Soil

- Terzaghi
- Tschebotarioff
- Danish Rules

The Free Earth Support (FES) method generally produces much higher bending moments than other methods. If the factor of safety is applied, the actual pressure distribution and shape of the elastic curve probably approaches the fixed condition. In this case, the section modulus required by free earth support is larger than needed, and the wall is uneconomical. However by not increasing the penetration sufficiently, the wall becomes vulnerable to overdredging or changing soil properties.

The free earth support method was the principal system used by designers in the United States for many years. It is a simple approach and produces a very conservative if not economical design. In Europe, Fixed Earth Support and a number of semi-empirical procedures have been employed for at least 50 years. These procedures produce smaller bending moments while still providing adequate safety factors against toe or anchorage failure.

There has always been some controversy concerning the actual character of earth pressure on both sides of the wall and the influence of wall flexibility on these elements of design. Sheet piling, produced from steel, aluminium and timber, is quite flexible causing earth pressures to redistribute or differ from assumed classical distribution. In particular, it has been observed that the bending moments in sheet piling generally decreases with increasing flexibility of the wall material. This is

due to the interdependence between the type of deflection or yield of the buried portion of the sheet piling and the corresponding distribution of passive earth pressure. With increasing flexibility the yield of the buried part assumes the character of a rotation about the lower edge of the bulkhead causing the centre of the passive pressure to move closer to the dredge line. This in turn decreases the bending moment. It would appear then that there is an opportunity to reduce bending moments produced by Free Earth Support methods and attain more economical designs. Peter Rowe, a British investigator, published a series of reports beginning in 1951 concerning these relationships that have changed the historical approach to free earth support design.

9.4.2. Free Earth Support Method

In this classical method, the piling is designed to penetrate just deep enough to satisfy minimum stability requirements, assuming that the maximum possible passive resistance is fully mobilized. The sheet piling is assumed to be inflexible below the dredge line and that no pivot point exists below this point, (no passive resistance develops on the backside of the piling). Earth pressures may be computed by the methods discussed earlier. With these assumptions, the design becomes a problem in simple statics. Procedures for the design of anchored sheet discussed separately below.

9.4.2.1. Design in Granular Soil

Figure 9-13 shows the general pressure distributions for an anchored sheet pile wall in granular soil. It assumes that the soil is homogeneous. The same soil parameters used with cantilever walls are required with anchored ones as well. The possible reduction of K_p for a factor of safety is discussed below.

The procedure is as follows:

1. Compute the unit active pressure p_{C1} at the elevation CC_1 .
2. Compute the unit active pressure p_{A1} at the elevation AA_1 .
3. Compute the slope of the line A_1E , which equal to $K_p - K_a$.
4. Locate the point of zero pressure O_1^{88} , which is y below the dredge line. The distance y is computed by the equation

Equation 9-32:
$$y = \frac{P_{A1}}{\gamma'(K_p - K_a)}$$

5. Find the resultant active pressure P_a , which is the sum of the

⁸⁸Equation 9-32 assumes that the soil properties do not change at the dredge line. If this is the case, the lateral earth pressure will have a discontinuity, and the numerator will then be the lateral earth pressure for the soil below the dredge line.

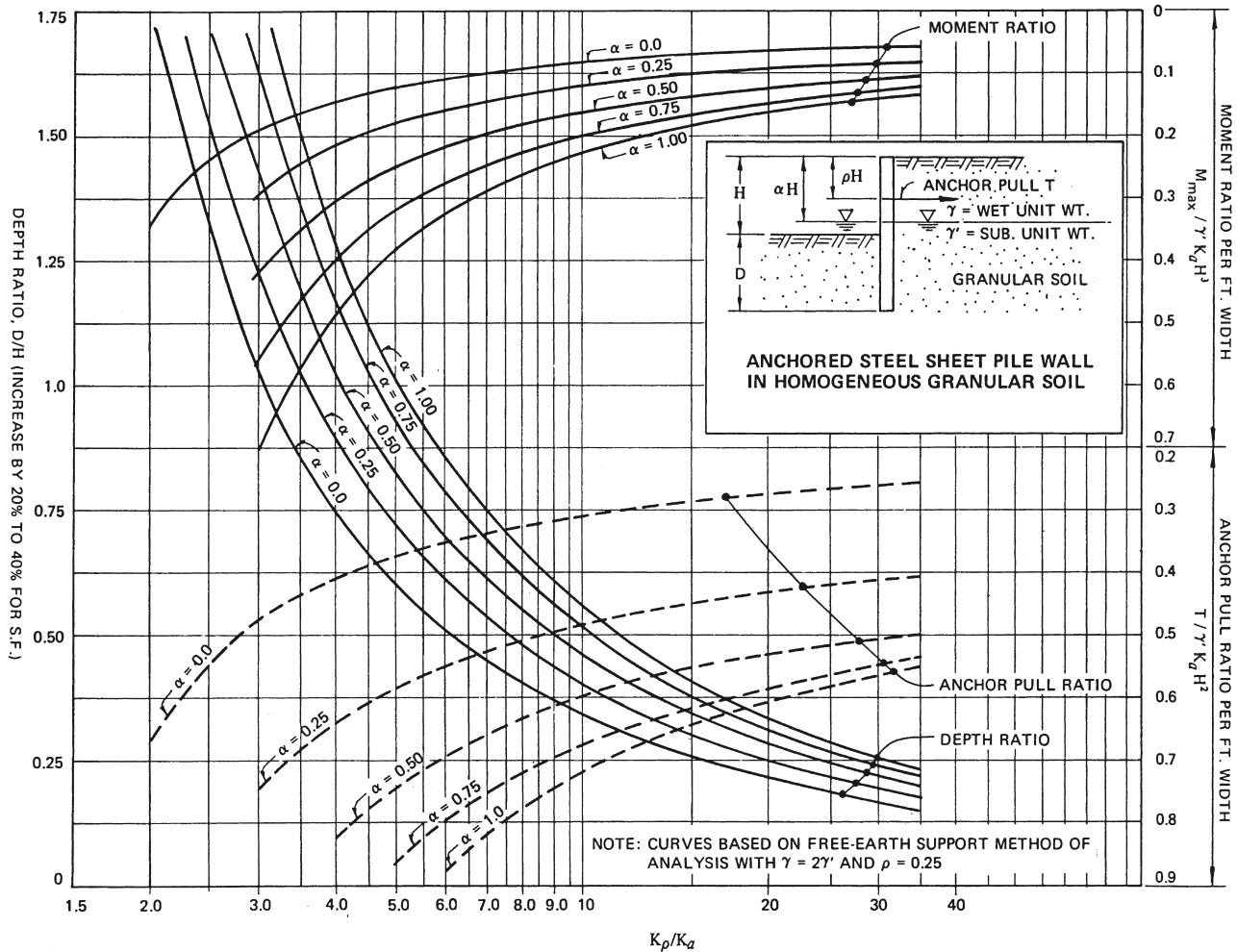


Figure 9-14: Anchored Steel Sheet Pile Wall in Homogeneous Granular Soil

active pressure areas BCC_1 , CC_1A_1A and AA_1O_1 . Find the location of P_a by summing moments of the individual resultants about the anchor.

6. Find the resultant passive pressure P_p , which is the combined active and passive pressure O_1FE , given by the equation

$$\text{Equation 9-33: } P_p = \frac{\gamma'(K_p - K_a)D^2}{2}$$

7. Solve for depth D by summing moments about the anchor. How this is done depends upon the factor of safety method used. For the free earth support method, there are three methods used:

a. Increase the moment about the anchor caused by the active pressure P_a by a factor of safety. This forces an increase in D . This is the method used by SPW 911. Typically, a factor of safety of 2 is applied. The moment equation to be solved would be in this case

Equation 9-34:

$$\sum M = P_a hFS - P_p \left(\frac{2D}{3} + y + H_t \right) = 0$$

b. Divide the passive earth pressure coefficient by 1.5 – 2. As with cantilever walls, doing this applies the factor of safety up front. This method can be used with SPW 911 with the “Defined FOS” option. The equation is then

Equation 9-35:

$$\sum M = P_a h - P_p \left(\frac{2D}{3} + y + H_t \right) = 0$$

c. Do not decrease the passive earth pressure coefficient and increase the depth below the dredge line $y+D$ computed by Equation 9-35 by 20 – 40%.

8. Obtain the anchor force by summing horizontal forces,

SHEET PILING CONSULTING

**HARTMAN ENGINEERING
BUFFALO, NY
716-759-2800**



**Bridge Pier Cofferdam
Brunswick, GA**



**Water Intake Cofferdam
Kenton County, KY**

The firm has provided professional engineering services related to cofferdams and retaining structures for more than 35 years. Services include design, consultation, assistance with problems, investigations and reports.

Services are available in the United States and Internationally. Professional Licenses are held for thirty six states. International projects include designs in Egypt, Marshall Islands, Panama and Puerto Rico.



**Circular Cofferdam Around
Collapsed Rectangular Cofferdam
Mayaguez, Puerto Rico**

See our other page in this publication for information on testing, research, and educational services.

Equation 9-36: $T = P_p - P_a$.

9. Locate the point of zero shear. Don't forget to include the anchor force.

10. Compute the maximum moment at this point by summing moments. As with the shear, include the anchor force.

Design charts have also been developed for anchored walls in homogeneous granular soil for the free earth support method as shown in Figure 9-14.

These curves give the depth ratio, D/H, the maximum moment ratio, $M_{max}/\gamma K_a H^3$, and the tie rod ratio, $T/\gamma K_a H^2$, as a function of the ratio of the passive to active earth pressure coefficient, K_p/K_a . The curves are independent of the method of obtaining K_p or K_a . The curves in Figure 9-14 were developed for a wet unit soil weight, γ , equal to twice the submerged unit weight, γ' , and a depth of anchor equal to 0.25H as shown. Resulting moments and tie rod tension are force per unit length of wall.

Example 11: Anchored Sheet Pile Wall in Cohesionless Soil, Free Earth Support Method

- ❖ Given
 - Sheet pile wall, 10' elevation to dredge line
 - Anchor located 2' below the surface
 - Soil Profile
 - Granular Soil
 - $\gamma = 100$ pcf
 - $\gamma' = 60$ pcf
 - $\phi = 30^\circ$
 - $c = 0$
 - Water table 4' below the surface on both sides of the wall (no unbalanced hydrostatic forces)
 - Uniform surcharge loading of 200 psf at the surface
- ❖ Find
 - Depth of penetration of sheeting
 - Maximum moment of sheeting; select suitable sheeting profile
 - Determine anchor load per linear foot of wall
- ❖ Solution
 - Determine lateral earth pressure coefficients
 - In this case, we will use Rankine coefficients for simplicity.
 - $K_a = 0.33$ (Equation 5-1)
 - $K_p = 3$ (full), or $K_p = 3/2 = 1.5$ (reduced, divided by a factor of safety of 2) (Equation 5-16). In the case of the full passive earth pressure method, a factor of safety of 2 is applied.
 - Compute the unit active pressure p_{C1} at the elevation CC_1 . Although theoretically the surcharge pressure should be included here, from a conceptual and a computational standpoint it is easier to consider the

- effects of the surcharge separately. $p_{C1} = (4)(100)(0.33) = 133$ psf
- Compute the unit active pressure p_{A1} at the elevation AA_1 . $P_{A1} = 133 + (6)(60)(0.33) = 253$ psf
- Compute the lateral pressure from the surcharge p_C . $p_C = p_{surcharge} K_a = (200)(0.33) = 67$ psf.
- Compute the slope of the line A_1E , which equal to $K_p - K_a$. For full K_p , $K_p - K_a = 3 - 0.33 = 2.67$. For reduced K_p , $K_p - K_a = 1.5 - 0.33 = 1.167$.
- Locate the point of zero pressure O_1 ⁸⁹, which is y below the dredge line. The distance y is computed by Equation 9-32. For the full passive pressure, $y = (253)/((60)(2.67)) = 1.58'$. For reduced passive pressure, $y = (253)/((60)(1.167)) = 3.62'$.
- Find the magnitude and location of the resultant active pressure P_a , which is the sum of the active pressure areas BCC_1 , CC_1A_1A and AA_1O_1 .
 - Surcharge loadings. The active force due to surcharge loading is generally split into forces above the dredge line and those below.
 - Above the dredge line: $P_{C+} = (67)(10) = 666.67$ lb/ft

Below the dredge line:

- ◆ Full passive earth pressure coefficient: $P_{C-} = 66.67 D + (67)(1.58') = 66.67 D + 105.56$ lb/ft.
- ◆ Reduced passive earth pressure coefficient: $P_{C-} = 66.67 D + (67)(3.62') = 66.67 D + 241.27$ lb/ft.
- BCC_1
 - Force: $(133)(4)/2 = 267$ lb/ft
 - Location from anchor: $(2)(4)/(3) - 2 = 0.667' = 8"$
- CC_1A_1A
 - Force: $(133 + 253)(6)/2 = 1,160$ lb/ft.
 - Location from anchor: For a "trapezoidal" load such as this, the location of the resultant from "point 1" is given by the equation

Equation 9-37:
$$z = \frac{p_1 + 2p_2}{3(p_1 + p_2)} L$$

Where z = distance from point 1 of resultant, p_1 and p_2 are the lateral pressures at points 1 and 2 respectively, and L is the distance from point 1 to point 2. In this case, $z = (133 + (2)(253))/(3(133+253))(6) = 3.31'$ from "point 1," or $3.31 + 4 - 2 = 5.31'$ from the anchor.

- AA_1O_1
 - Full passive earth pressure coefficient
 - ◆ Force: $(253)(1.58)/2 = 201$ lb/ft
 - ◆ Location from anchor = $(1.58)/(3) + 6 + 4 - 2 = 8.52'$
 - Reduced passive earth pressure coefficient
 - ◆ Force: $(253)(3.62)/2 = 458.4$ lb/ft
 - ◆ Location from anchor: = $(3.62)/(3) + 6 + 4 - 2 = 9.21'$
- Compute resultant active pressure P_a
 - Full passive earth pressure coefficient: $P_a = 267 +$

⁸⁹Equation 9-32 assumes that the soil properties do not change at the dredge line. If this is the case, the lateral earth pressure will have a discontinuity, and the numerator will then be the lateral earth pressure for the soil below the dredge line.

$$1160 + 201 + 667 + 66.67 D + 106 = 2399 + 66.67 D \text{ lb/ft}$$

- Reduce passive earth pressure coefficient: $P_a = 267 + 1160 + 458 + 667 + 66.67D + 242 = 2793 + 66.67 D \text{ lb/ft}$
- Determine location of resultant from anchor
Full passive earth pressure coefficient: $h = (10048 + 66.66(D + 1.58)(0.5D + 8.79))/(66.67D + 2399)$
Reduced passive earth pressure coefficient: $h = (12558 + 66.67(D+3.61)(0.5D + 9.81))/(66.67D + 2793)$
- Find the resultant passive pressure P_p , which is the combined active and passive pressure O_1FE , given by Equation 9-33.
 - Full passive earth pressure coefficient: $P_p = 80 D^2$.
 - Reduced passive earth pressure coefficient: $P_p = 35 D^2$.
- Solve for depth D by summing moments about the anchor.
- Full passive earth pressure coefficient: Substituting the variables into Equation 9-34, $53.3 D^3 + 700 D^2 - 1278 D - 21952 = 0$. The only positive solution of this equation is $D = 5.4'$. The total penetration of the toe is $5.4' + 1.58' = 6.99'$.
- Reduced passive earth pressure coefficient.
Substituting the variables into Equation 9-35, $23.3 D^3 + 373 D^2 - 774.6 D - 14924 = 0$. The only positive solution to this equation is $D = 6.17'$. The total penetration of the toe is $6.17' + 3.62' = 9.8'$.
- Obtain the anchor force by summing horizontal forces.
 - Full passive earth pressure coefficient: $P_a = 2760 \text{ lb/ft}$. For the passive pressure, substituting $D = 5.4'$ into $P_p = 80 D^2$ yields $P_p = 2336 \text{ lb/ft}$. Substituting this into Equation 9-36 with this value of P_p will yield an anchor force that is too low, as the wall was extended – and thus the passive pressure increased – to provide a factor of safety against over-turning. To properly compute the anchor load, we must compute a distance D' from O_1 to the point where the moment generated by the active pressure and that of the passive pressure are the same. In other words, using a full passive earth pressure coefficient,

Equation 9-38:

$$\sum M = P_a h - \frac{\gamma'(K_p - K_a) D'^2}{2} \left(\frac{2D'}{3} + y + H_t \right) = 0$$

Substituting the variables into this equation yields $53.3 D^3 + 733 D^2 - 639 - 10976 = 0$. The only positive root of this equation is $D' = 3.78'$. This yields a $P_p' = 1146 \text{ lb/ft}$, and substituting this into Equation 9-36 yields $T = 1146 - 2760 = -1506 \text{ lb/ft}^{90}$. Because no factors of safety are applied to this load, this load should be increased by about 30%, or $T = (1506)(1.3) = 1958 \text{ lb/ft}$ for designing the anchor system

(see Equation 11-2.)

- Reduced passive earth pressure coefficient: $P_a = 3204$, $P_p = 1333 \text{ lb/ft}$. These values can be directly substituted into Equation 9-36, so $T = 1333 - 3204 = -1871 \text{ lb/ft}$. The load used for anchor design is thus $(1871)(1.3) = 2433 \text{ lb/ft}$.
 - The design of the anchor system is discussed in Chapter 11.
 - Determine the maximum moment and sheeting profile. The point of zero shear (maximum moment) is usually near the dredge line, and not below O_1 as is the case with cantilever walls.
 - Full passive earth pressure coefficient: Let us assume that the point of zero shear is between the water table and the dredge line. There are two constant forces completely above the water table: the anchor force, $T = -1506 \text{ lb/ft}$, and the soil above the water table, $P_1 = 267 \text{ lb/ft}$. There are two forces that are left; both of these are dependent upon the location of the point of zero shear. These are the surcharge force, $P_C' = 67 (4 + x_{\text{remain}})$, and the force between the water table and the point of zero shear, $P_2' = x_{\text{remain}}(133 + p_{\text{xr}})/2$. For these equations, x_{remain} = distance from water table to the point of zero shear, and p_{xr} = lateral earth pressure at the point of zero shear without the surcharge. At the point of zero shear, $P_1 + T + P_2' + P_C' = 0$. Substituting, this yields $10 x_{\text{remain}}^2 + 200 x_{\text{remain}} - 973 = 0$. The positive solution to this equation is $x_{\text{remain}} = 4.04'$, which means that the point of zero shear is $8.04'$ below the top of the sheeting. The lateral earth pressure at this point is $p_{\text{zs}} = 214 \text{ psf}$.
- Once the point of zero shear is determined, the maximum moment is determined by summing the moments of the forces about the point of zero shear. The forces and moment arms are shown in *Table 9-1*. The resultant moment, and the maximum moment on the sheeting, is 4200 ft-lb/ft of wall length.
- Reduced passive earth pressure coefficient: Let us again assume that the point of zero shear is between the water table and the dredge line. There are two constant forces completely above the water table: the anchor force, $T = -1871 \text{ lb/ft}$, and the soil above the water table, $P_1 = 267 \text{ lb/ft}$. There are two forces that are left; both of these are dependent upon the location of the point of zero shear. These are the surcharge force, $P_C' = 67 (4 + x_{\text{remain}})$, and the force between the water table and the point of zero shear, $P_2' = x_{\text{remain}}(133 + p_{\text{xr}})/2$. At the point of zero shear, $P_1 + T + P_2' + P_C' = 0$. Substituting, this yields $10 x_{\text{remain}}^2 + 200 x_{\text{remain}} - 1338 = 0$. The positive solution to this equation is $x_{\text{remain}} = 5.29'$, which means that the point of zero shear is $9.29'$ below the top of the sheeting. The lateral earth pressure at this point is

⁹⁰The negative sign indicates that the load is away from the excavation side of the wall, which is what we would expect.

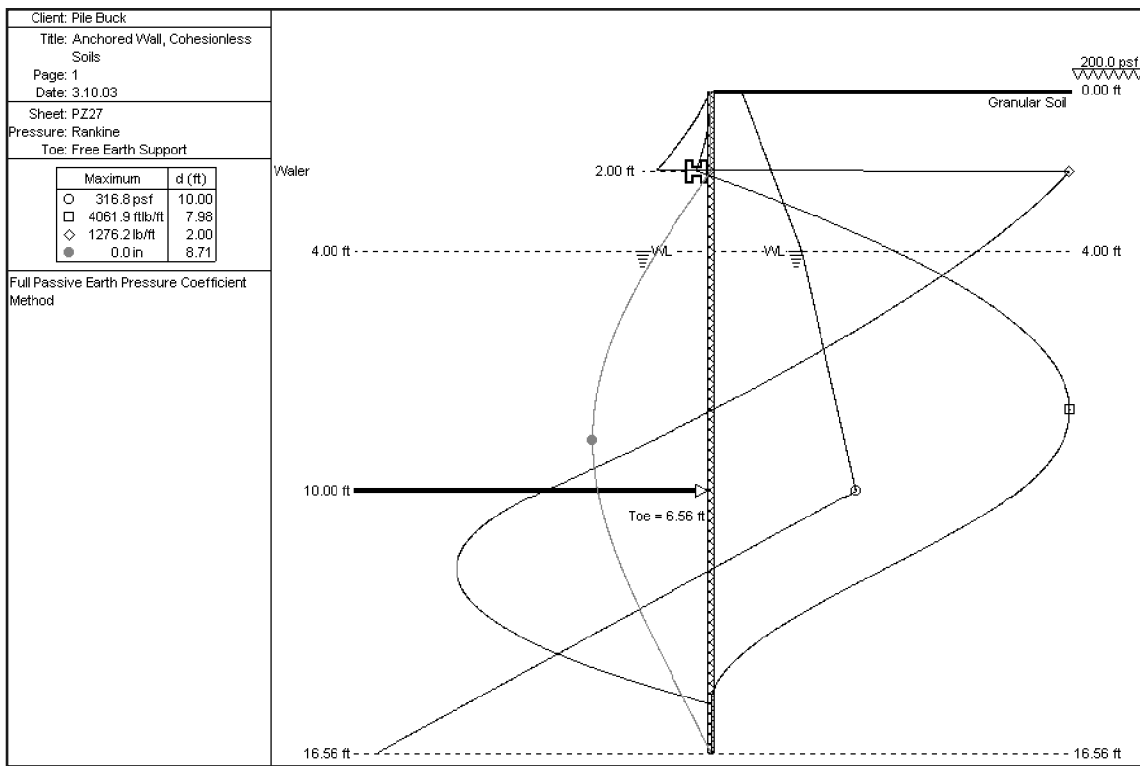


Figure 9-15: SPW 911 Solution for Example 11, Full Passive Earth Pressure Coefficient Method

Table 9-1: Forces and Moment Arms for Maximum Moment in Example 11

Force	Magnitude, Full Passive Earth Pressure Coefficient, lb/ft	Distance from Point of Zero Shear, Full Passive Earth Pressure Coefficient, ft.	Magnitude, Reduced Passive Earth Pressure Coefficient, lb/ft	Distance from Point of Zero Shear, Reduced Passive Earth Pressure Coefficient, ft.
P_1	267	5.38	267	6.62
T	-1506	6.04	-1871	7.29
P_C'	536	4.02	619	4.65
P_2'	703	1.87	985	2.39
		(Equation 9-37)		(Equation 9-37)

$p_{zs} = 239 \text{ psf.}$

Once the point of zero shear is determined, the maximum moment is determined by summing the moments of the forces about the point of zero shear. The forces and moment arms are shown in Table 9-1. The resultant moment, and the maximum moment on the sheeting, is 6640 ft-lb/ft of wall β

- Referring to Table 2-1, any of the sheeting profiles are suitable for use in this case.

■ Solution using SPW 911

- The solution for both the full and reduced passive earth pressure coefficient methods are shown in Figure 9-15 and Figure 9-16, respectively. The solu-

tions are close to those computed above. The results in Figure 9-15 are the “default” options for the program. The results in Figure 9-16 are obtained by defining the “factor of safety” as unity, then using a reduction factor for the passive earth pressure coefficient. Since this coefficient has been reduced, the factor of safety has been in reality already applied.

9.4.2.2. Design in Cohesive Soils

Use of permanent sheet pile walls with cohesive soils for both backfill and soils below the dredge line is unadvisable. However, if a cohesionless backfill is used, anchored sheet pile walls can be used. Figure 9-17 shows the resulting pressure distribution and application of the free earth support method for an anchored sheet pile wall in cohesive soil with sand backfill.

The following design procedure may be used:

- Determine the immediate and long-term strength of the soil by undrained tests ($\phi = 0$) and drained tests ($c \geq 0, \phi > 0$), respectively.
- Determine method of factor of safety inclusion.
- Calculate the total active pressure due to the sand backfill above the dredge line using methods similar to those in Example 11.



INTERNATIONAL

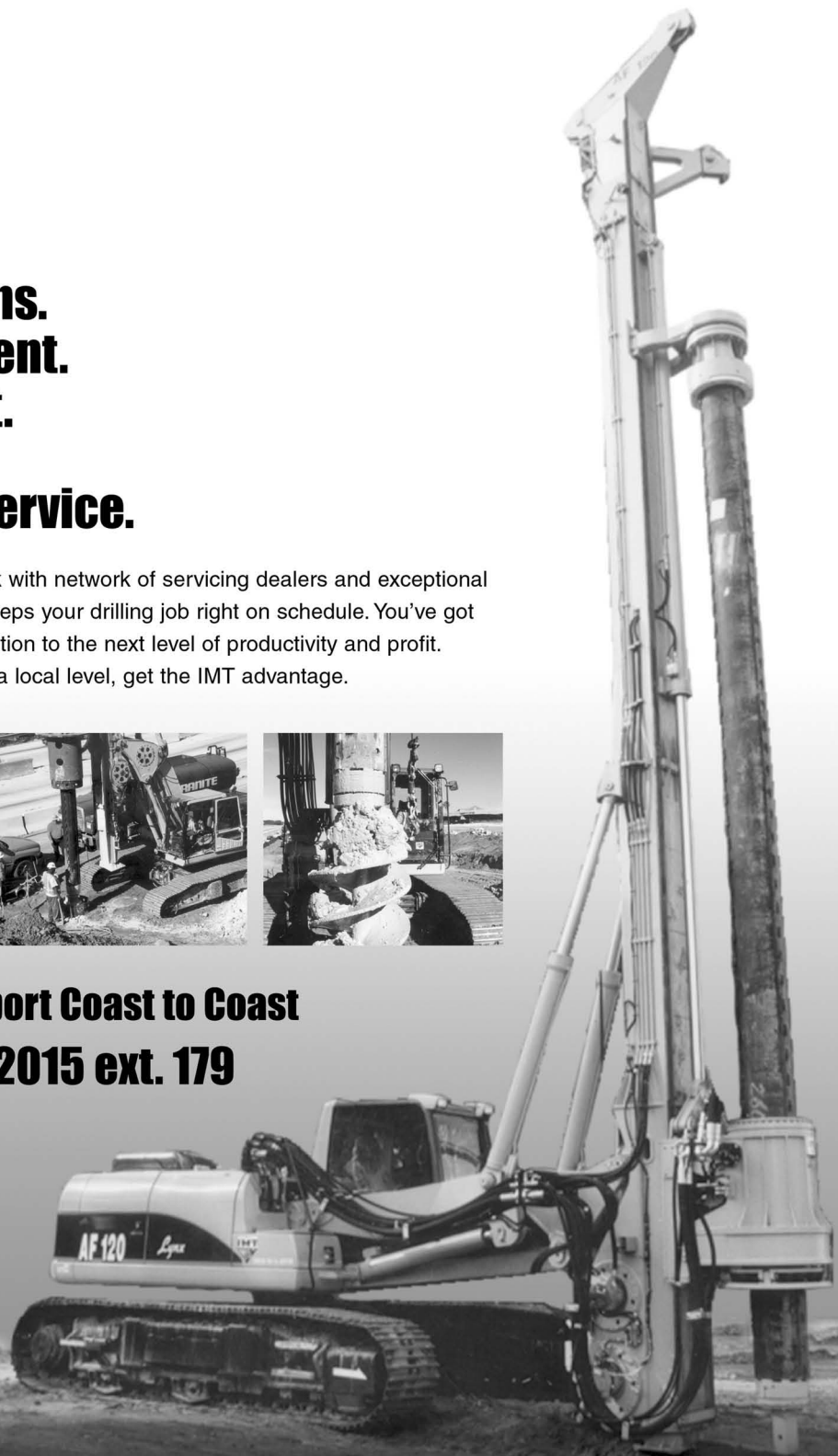
**More Locations.
More Equipment.
More Support.**

Same Local Service.

Our expanding, easy-to-work with network of servicing dealers and exceptional parts and service support keeps your drilling job right on schedule. You've got the power to take your operation to the next level of productivity and profit. For unstoppable support on a local level, get the IMT advantage.



**For Product Support Coast to Coast
Call (561) 683-2015 ext. 179**



KELLY TRACTOR



**ATLANTIC &
SOUTHERN**
EQUIPMENT, LLC

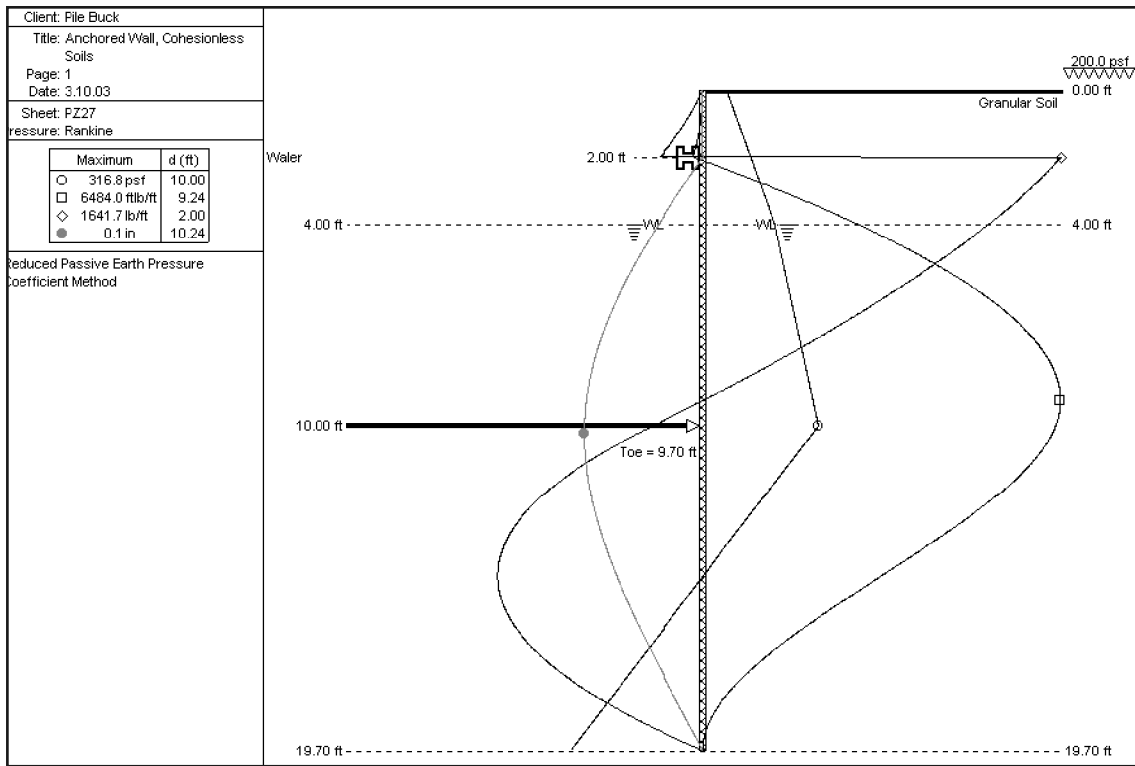


Figure 9-16: SPW 911 Solution for Example 11, Reduced Passive Earth Pressure Coefficient Method

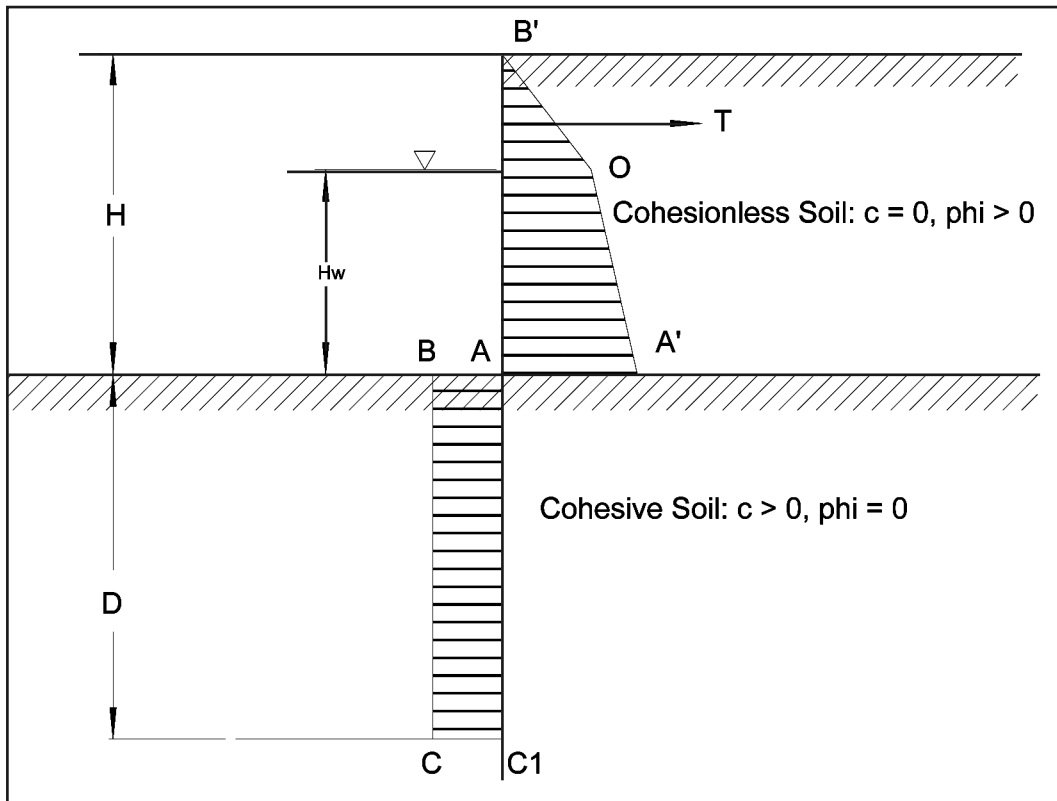


Figure 9-17 Free Earth Support Method of Anchored Bulkhead Design in Clay with Granular Backfill

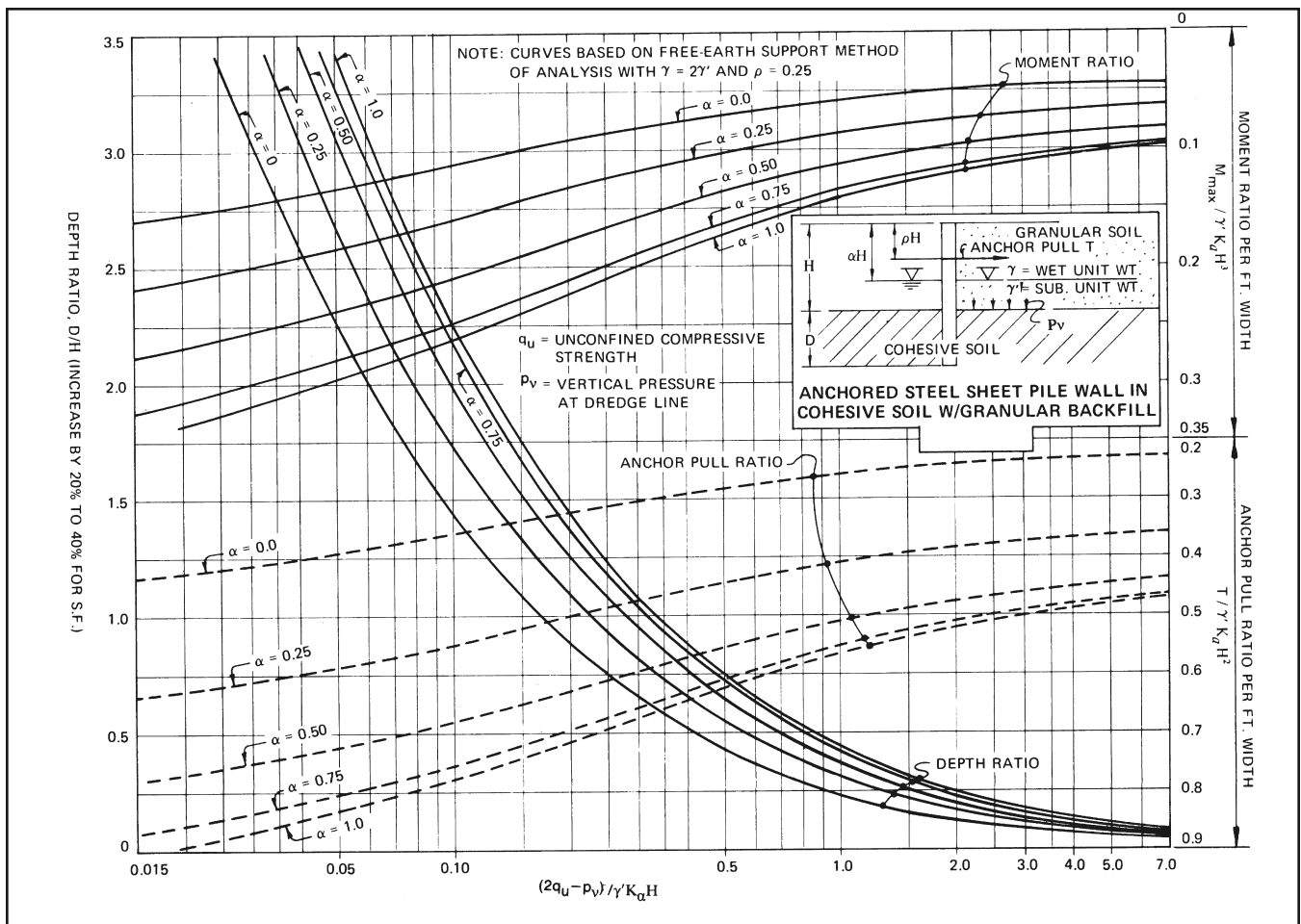


Figure 9-18: Anchored Steel Sheet Pile Wall in Cohesive Soil with Granular Backfill

4. Satisfy equilibrium by summing moments about the anchor level. Solve for depth D as in the previous case.
5. Compute the tie rod loads.
6. Determine the point of zero shear and calculate the maximum bending moment.

As is the case with cohesionless soils, a chart is available to determine the penetration and maximum bending moment for cohesive soils with cohesionless backfill. Figure 9-18 presents design curves for anchored steel sheet pile walls in cohesive soil with granular backfill. These curves give the depth ratio D/H , the maximum moment ratio, $M_{max}/\gamma K_a H^3$, and the anchor pull ratio, $\gamma K_a H^2$, as a function of the “Net Passive Pressure Coefficient” $(2q_u - p_v)/\gamma K_a H$. The term $(2q_u - p_v)$ is the net passive pressure on the left side of the wall below the dredge line where p_v is the vertical pressure at the dredge line $= \gamma H$. The term $\gamma K_a H$ will normally vary from about 300 to 500; therefore, practical values of the net passive pressure coefficient can be quite small for low strength soils. For this reason the curves have been extended to include this lower range. The curves in Figure 9-18 were developed for a wet

unit soil weight, γ , equal to twice the submerged unit weight, γ' , and for a depth of anchor rod below the top of the wall equal to $0.25H$.

Example 12: Anchored Wall in Cohesive Soil with Cohesionless Backfill

- ❖ Given (see Figure 9-17 for this problem)
 - Sheet pile wall, 4 m elevation to dredge line
 - Use pultruded fibreglass sheet piling
 - Anchor located 1 m below the top of the sheet piling wall
 - Soil Profile
 - Dense Fine Sand above dredge line
 - $\gamma = 18.6 \text{ kN/m}^3$
 - $\gamma' = 18.6 - 9.8 = 8.8 \text{ kN/m}^3$
 - $\phi = 35^\circ$
 - $c = 0$
 - Water table 2 m below the surface on both sides of the wall (no unbalanced hydrostatic forces)
 - Uniform surcharge load of 10 kPa at the surface
 - $K_a = 0.27$
 - Medium Clay below the dredge line
 - $\gamma' = 7.4 \text{ kN/m}^3$

- $\phi = 0$
- $c = 30$ kPa

❖ Find

- Depth of penetration of sheeting
- Maximum moment of sheeting; select suitable sheeting profile
- Determine anchor load per linear foot of wall

❖ Solution

■ Factors of Safety

- We will consider two methods of applying the factor of safety:
- Full passive cohesion. Increase the moment of active pressures by a factor of safety. The factor we will use is 2. This is the default option for SPW 911. It should be noted, however, that, to properly solve for the anchor load, the problem must be solved again with $FS = 1$.
- Reduced passive cohesion. We will divide the passive earth pressure coefficient by 1.5. This can range from 1.5 – 2, depending upon the application and the nature of the soil data. For this problem, the reduced cohesion is $30/1.5 = 20$ kPa.

■ Determine total active pressure of the sand backfill above the dredge line. This is the same for both factors of safety. Keep in mind that *Figure 9-17* assumes no surcharge loading; this needs to be added.

- Effective stress at point B' = 10 kPa. Active earth pressure at this point = $(0.27)(10) = 2.7$ kPa.
- Effective stress at point O = $10 + (2)(18.6) = 47.2$ kPa. Active earth pressure at this point = $(0.27)(47.2) = 12.7$ kPa.
- Effective stress at point A' = $p_v = 47.2 + (2)(8.8) = 64.8$ kPa. Active earth pressure at this point = $(0.27)(64.8) = 17.5$ kPa.
- Force $OB' = 2((2.7 + 12.7) / 2) = 15.4$ kN/m of wall length. The resultant of this force is 1.22 m below the surface, or 0.22 m below the anchor.⁹¹
- Force $OA' = 2((12.7 + 17.5) / 2) = 30.2$ kN/m of wall length. The resultant of this force is 3.05 m below the surface, or 2.05 m below the anchor.
- Total active force = $15.4 + 30.2 = 45.6$ kN/m of wall length.

■ Determine the passive pressure and sum moments about the anchor load to determine the depth of the sheeting.

- The net passive pressure can be determined by generalising Equation 9-16 to

$$\text{Equation 9-39: } p_B = p_p - p_a = 2q_u - p_v = 4c - p_v$$

For the full passive cohesion, $p_B = (4)(30) - 64.8 = 55.2$ kPa. The passive force $BC = 55.2D$. The distance of the resultant force is $3 + D/2$ from the anchor or $4 + D/2$ from the top of the wall.

For the reduced passive cohesion, $p_B = (4)(20) - 64.8 = 15.2$ kPa. The passive force $BC = 15.2D$. The distance of the resultant force is $3 + D/2$ from the anchor or $4 + D/2$ from the top of the wall.

- Moments can now be summed about the anchor.

For full passive cohesion, with a factor of safety of 2, $(2)((15.4)(0.22) + (30.2)(2.05)) - (55.2D)(3 + D/2) = 0$. The positive solution of this equation is $D = 0.71$ m, and the net passive force is $(55.2)(0.71) = 39$ kN/m of wall length.

For reduced passive cohesion, $(15.4)(0.22) + (30.2)(2.05) - (15.2D)(3 + D/2) = 0$. The positive solution of this equation is $D = 1.19$ m, and the net passive force is $(15.2)(1.19) = 18.2$ kN/m of wall length.

■ Compute the tie rod loads.

- For full passive cohesion, the net passive force cannot be used to compute the tie rod load as it has a factor of safety applied to it. It is necessary to compute the toe length D with full cohesion and a factor of safety of unity. In this case, $((15.4)(0.22) + (30.2)(2.05)) - (55.2D)(3 + D/2) = 0$, and $D = 0.37$ m (of course this is not to be used for toe design!) The net passive force is thus $(55.2)(0.37) = 20.5$ kN/m. The tie rod force is thus $T = 20.5 - 15.4 - 30.2 = -25.2$ kN/m of wall length.
- For the reduced passive cohesion, the net passive force of 18.2 kN/m can be used. The tie rod force is thus $T = 18.2 - 15.4 - 30.2 = -27.5$ kN/m of wall length.

■ Determine the point of zero shear and compute the maximum moment on the sheeting.

- We will begin by assuming the point of zero shear falls somewhere between the water table and the dredge line. This means that the force OB' will apply in its entirety and the force OA' only partially. Using a similar approach to that in Example 11, let us refer to the distance from the water table to the point of zero shear as x' . The active force from the water table to the point of zero shear is thus $F' = (x')(p_O + x' K_a \gamma')/2$, and thus summing forces, $T + F_{OB'} + F' = 0 = T + F_{OB'} + (x')(p_O + x' K_a \gamma')/2$. The value of T is different depending upon the factor of safety method used and thus the value of x' and F' will be different.

Full passive cohesion: $T = -25.2$ kN/m, so substituting this and the values for p_O , K_a and γ' , the summation of forces becomes $-9.7 + (x')(25.5 + 2.4 x')/2 = 0$, and the positive root of this is $x' = 0.71$ m. This

⁹¹See methods given in Example 11 for determining this distance with "trapezoidal" loads.



HOT ROLLED SHEET PILE SECTIONS FROM

CORUS

ONLY AVAILABLE THROUGH

**— JD —
FIELDS
& Company, Inc.**

FRODINGHAM Z-PILING

Section	Centres	Height	Web	Flange	Section Area	Mass		Combined Moment of Inertia	Section Modulus
						lbs/ft	lbs/ft ²		
1N-RU3	19.00	6.72	0.38	0.38	6.35	34.22	21.61	47.28	14.08
1N	19.00	6.69	0.35	0.35	5.98	32.22	20.35	44.46	13.29
1N-RD3	19.00	6.66	0.32	0.32	5.49	29.56	18.67	40.78	12.25
2N-RU3	19.00	9.28	0.38	0.41	7.32	39.42	24.90	108.65	22.68
2N	19.00	9.25	0.33	0.38	6.84	36.84	23.27	99.89	21.60
2N-RD3	19.00	9.22	0.30	0.35	6.36	34.25	21.63	93.11	20.20
3NA	19.00	12.00	0.37	0.38	7.82	42.14	26.61	188.27	31.38
4N-RU3	19.00	13.03	0.44	0.58	10.87	56.58	37.00	306.44	47.04
4N	19.00	13.00	0.41	0.55	10.31	55.57	35.10	291.96	44.92
4N-RD3	19.00	12.97	0.38	0.52	9.76	52.57	33.20	277.50	42.79
5	16.75	12.25	0.47	0.67	14.29	67.66	48.62	381.23	58.88

LARSEN SECTIONS

Section	Driving width per pile	depth	Flat of Pan			Thickness		Weight		Combined Section Modulus per ft of wall	Combined Moment of Inertia per ft of wall
			in. (b)	in. (h)	in. (f)	in. (d)	in. (t)	per lin ft of pile	per sq. ft. of wall		
Frodingham	in. (b)	in. (h)	in. (f)	in. (d)	in. (t)	lbs	lbs	in ² /ft	in ⁴ /ft		
6W	20.67	8.35	13.03	0.31	0.25	30.04	17.48	11.35	47.66		
LX 8	23.62	12.2	9.84	0.32	0.31	36.66	18.62	15.44	94.19		
LX 12	23.62	12.2	15.2	0.38	0.32	42.89	21.79	22.47	137.14		
LX 12d	23.62	12.2	15.2	0.39	0.32	43.85	22.28	23.06	140.73		
LX 12d10	23.62	12.2	15.2	0.39	0.39	48.91	24.85	23.84	145.48		
LX 16	23.62	14.96	14.37	0.41	0.35	49.79	25.28	30.53	228.35		
LX 20	23.62	16.93	12.99	0.49	0.35	55.84	28.37	37.62	318.43		
LX 20d	23.62	17.72	12.99	0.44	0.39	56.6	28.76	37.36	330.97		
20Wd	20.67	15.75	13.11	0.44	0.39	54.18	31.45	37.73	297.12		
LX 25	23.62	18.11	13.82	0.53	0.39	63.78	32.4	46.63	422.21		
LX 25d	23.62	17.72	12.83	0.61	0.43	67.11	34.09	47.32	419.21		
LX 32	23.62	18.11	13.39	0.75	0.43	76.78	39.01	59.68	540.44		
LX 32d	23.62	17.72	12.6	0.85	0.51	84.92	43.14	62.27	551.59		
LX 38	23.62	18.11	13.27	0.89	0.57	94.28	47.9	70.77	640.83		
GSP2	15.75	7.87	10.43	0.41	0.34	33.13	25.24	16.29	64.12		
GSP3	15.75	9.84	10.67	0.51	0.34	40.36	30.75	24.28	119.48		
GSP4	15.75	13.39	10.2	0.61	0.38	51.13	39.93	42.39	283.7		
6-42	19.69	17.72	12.99	0.81	0.55	89.27	54.41	78.33	693.33		
6 (122)	16.54	17.32	9.76	0.87	0.55	82.23	59.66	77.88	674.54		
6 (131)	16.54	17.32	9.88	1	0.55	87.73	63.65	85.9	743.99		
6 (138)	16.54	17.32	9.88	1.13	0.55	92.84	67.36	93.09	806.31		

SALES & RENTALS

-ALSO-

- H-BEAMS 8", 10", 12" & 14"
- STEEL PIPE 1/2" - 48" O.D.
- USED SHEET PILING

J.D. FIELDS & CO. INC. CORPORATE HEADQUARTERS
 15995 North Barkers Landing, Suite 230, Houston, TX 77079
 (281) 558-7199 F (281) 558-9918
 www.jdfields.com

ADDITIONAL OFFICES THROUGHOUT THE U.S.

Dallas, TX -	(972) 869-3794	Chicago, IL	(708)333-5511
New Orleans, LA	(504) 832-7294	Tulsa, OK	(918)459-4638
Philadelphia, PA	(610) 317-6308	Denver, CO	(303)331-6190
Antioch, CA	(925)778-9740	Los Angeles, CA	(714)257-2005

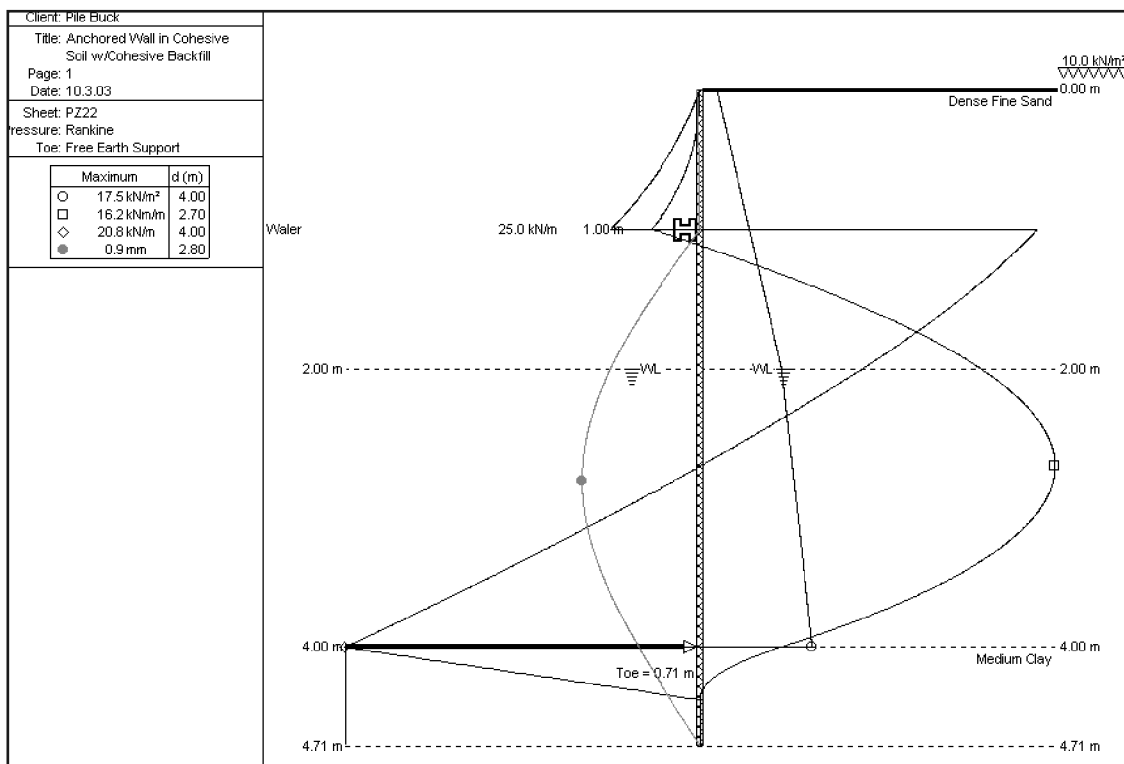


Figure 9-19: SPW 911 Solution for Example 12, Full Passive Earth Pressure Coefficient Method

means that the point of zero shear is 1.71 m below the anchor and 2.71 below the top of the wall.

Reduced passive cohesion: $T = -27.5 \text{ kN/m}$, so substituting this and the values for p_O , K_a and γ , the summation of forces becomes $-12.1 + (x')(25.5 + 2.4 x')/2 = 0$, and the positive root of this is $x' = 0.87 \text{ m}$. This means that the point of zero shear is 1.87 m below the anchor and 2.87 below the top of the wall.

- Determine the maximum moment at the point of zero shear. This involves both computing the magnitude of F' and the location of the resultant of this force. Both of these are in turn dependent upon the lateral earth pressure at the point x' , which we will refer to as $p' = p_O + x' \gamma K_a$.

Full passive cohesion: We first compute $p' = 12.7 + (0.71)(8.8)(0.27) = 14.4 \text{ kPa}$. The resultant force $F' = (0.71)(12.7 + 14.4)/2 = 9.7 \text{ kN/m}$ of wall length. Using Equation 9-37, the resultant is located 0.36 m below the water table or 2.36 m from the top of the wall. Summing moments about the top of the wall, the maximum moment $M_{\text{max}} = (15.4)(1.22) + (-25.2)(1) + (9.7)(2.36) = 16.6 \text{ kN-m/m}$ of wall length.

Reduced passive cohesion: We first compute $p' = 12.7 + (0.87)(8.8)(0.27) = 14.8 \text{ kPa}$. The resultant force $F' = (0.87)(12.7 + 14.8)/2 = 12.1 \text{ kN/m}$ of wall

length. Using Equation 9-37, the resultant is located 0.44 m below the water table or 2.44 m from the top of the wall. Summing moments about the top of the wall, the maximum moment $M_{\text{max}} = (15.4)(1.22) + (-25.2)(1) + (12.1)(2.44) = 20.8 \text{ kN-m/m}$ of wall length.

Since the maximum bending moment for the smallest sheet pile shown in Table 2-1 (PZ22) is 167.6 kN-m/m of wall length, any of these sections is suitable.

- Analyse the wall using SPW 911. The results for the full passive cohesion method are shown in Figure 9-19 and the reduced passive cohesion method in Figure 9-20. The results shown are similar to those computed above.
- Chart solution. Figure 9-18 is the applicable chart. Since the anchor distance from the top of the wall is 25% of the distance from the top to the dredge line, this chart is applicable. We will use the reduced passive cohesion factor of safety method, so $c = 20 \text{ kPa}$ and $q_{\text{u}} = 40 \text{ kPa}$. The water table ratio $a = 0.5$. The value for the x-axis $(2q_{\text{u}} - p_v)/(\gamma K_a H) = ((2)(40) - 64.8)/((8.8)(0.27)(4)) = 1.6$. From this, the following ratios can be determined and the respective values computed:
 - Depth ratio = 0.25. The depth is thus $0.25H = (0.25)(4) = 1 \text{ m}$.
 - Moment ratio = $0.1 = M_{\text{max}}/(\gamma K_a H^3)$. From this, $M_{\text{max}} = 15.2 \text{ kN-m/m}$.

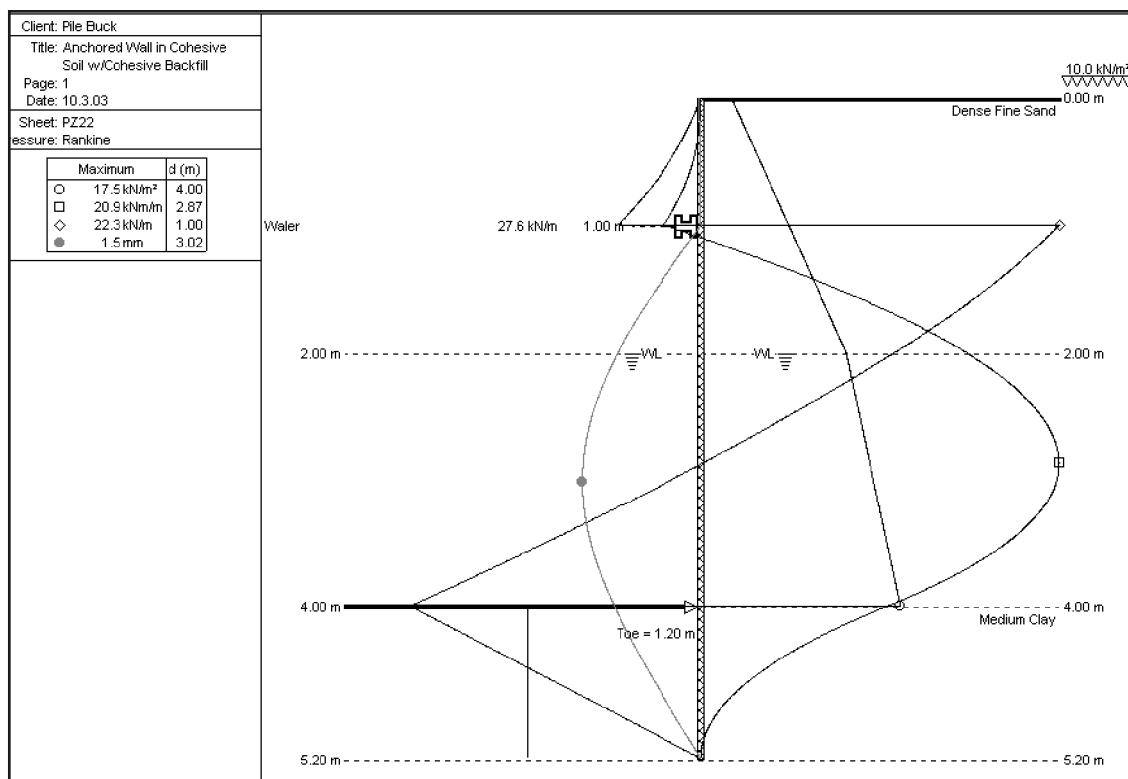


Figure 9-20: SPW 911 Solution for Example 12, Reduced Passive Earth Pressure Coefficient Method

- Anchor pull ratio = $0.48 = T_{\max}/(\gamma' K_a H^2)$. From this, $T_{\max} = 18.24$ kN/m. The differences are largely due to the differences in the way in which the saturated weight of the soil are handled. The low value of D also makes for large variations in the result for changes in the value of D . In reality, for all of the methods described, D is too small to be practical; it should be increased to take into considerations construction variations and uncertainties in the soil properties.

9.4.2.3. Rowe's Moment Reduction Theory

Steel sheet piling is quite flexible, causing earth pressures to redistribute or differ from the classical hydrostatic distribution. In particular, it has been observed that the bending moment in sheet piling generally decreases with increasing flexibility of the piling. This is due to the interdependence between the type of deflection or yield of the buried portion of the sheet piling and the corresponding distribution of passive earth pressure. With increasing flexibility, the yield of the buried part assumes the character of a rotation about the lower edge of the bulkhead causing the centre of the passive pressure to move closer to the dredge line. This in turn

decreases the maximum bending moment. Consequently, if a reduction in the maximum bending moment calculated by the free earth support method is neglected, an uneconomical and wasteful design will result. However, if the moment reduction is considered, a lower section modulus will be required introducing the possibility of using a lighter piling section.

Realising this, European engineers developed a semi-empirical method for analysis of flexible walls. These became known as the "Danish Rules." These rules assume that arching of the sheeting redistributes active pressure, thereby reducing bending moments.

Beginning in 1952, Peter Rowe⁹² published a series of reports describing model tests. These linked pile flexibility with reduced bending moments when the model bulkheads met the criteria for free earth support. Rowe found that, with increasing flexibility, the buried portion tends to rotate about the lower edge of the bulkhead, causing the centre of passive pressure to move upward and closer to the dredge line. This reduces the free span and the moment. Rowe's early work was conducted with loose sand, but his later work with denser materials indicated an even more pronounced effect.

Rowe's method can generally be safely utilized where base

⁹²Rowe, P. W., *Anchored Sheet Pile Walls*, Proceedings Institution of Civil Engineers, Part I, Vol. 1, London, England, 1952; Rowe, P. W., *A Theoretical and Experimental Analysis of Sheet Pile Walls*, Proceedings, Institution of Civil Engineers, Part I, Vol. 1, London, England, 1955; Rowe, P. W., *Sheet Pile Walls Encastred at Anchorage*, Proceedings, Institution of Civil Engineers, Part I, Vol. 1, London England, 1955; Rowe, P. W., *Sheet Pile Walls in Clay*, Proceedings, Institution of Civil Engineers, Part I, Vol. 1, London, England, 1957.

⁹³It is interesting to note that Karl Terzaghi recommended that moment reduction be limited to 50% of the design moment, and to use moment reduction only in clean sands. See Terzaghi, K. (1954) "Anchored Bulkheads." *Transactions of the American Society of Civil Engineers*, Vol. 119, Paper 2720.

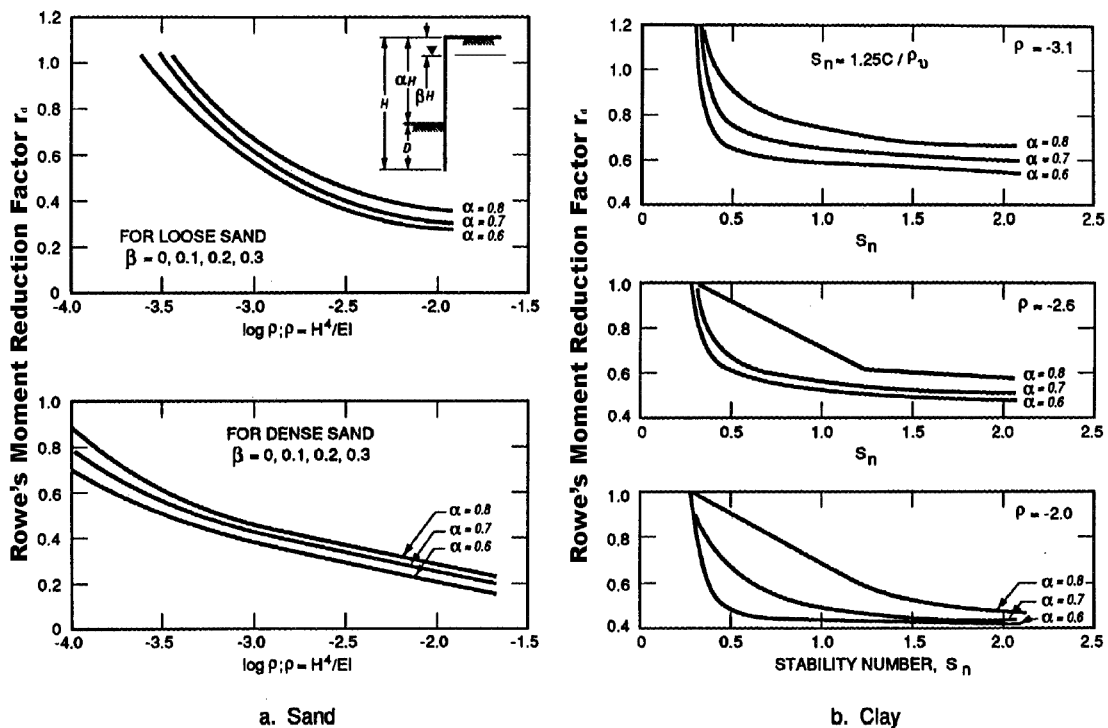


Figure 9-21 Rowe's Moment Reduction Curves for Cohesionless and Cohesive Soils

materials consist of medium compact to very compact coarse-grained materials or stiff clay. The moment reduction aspects for loose granular or undrained fine-grained materials should be examined cautiously although Kulhawy reports that Rowe moment reduction methods are also reliable for designing walls in loose granular soils. Since the reduction factors depend upon penetration, the method should not be used to reduce moments from free earth support analysis of walls that obtain their toe support from short penetration into shale or rock⁹³. Flexibility numbers for sections that have interlocks located on the neutral axis of the wall should be based on the assumption of lubricated interlocks unless welded. Also, in the absence of supporting information, the method is not recommended for walls containing mixed sections, i.e. master pile type walls.

9.4.2.3.1. Cohesionless Soils

To use Rowe's moment reduction method with cohesionless soils, the following procedure should be used:

1. Compute the maximum moment in the sheeting using the Free Earth Support method as described in 9.4.2.1. Appropriate safety factors should be applied irrespective of how this is done.
2. Compute Rowe's moment reduction coefficient using the equation

Equation 9-40:
$$\rho = \frac{H^4}{EI}$$

Where

- ρ = Rowe's moment reduction coefficient. It is important to use the U.S. units described below for proper results with Rowe's moment reduction curves.
- H = total wall height, ft. (see Figure 9-21a.) Note that the nomenclature in this figure is somewhat different from that used with both cantilever wall design and the free earth support method for anchored walls.
- E = modulus of elasticity of sheet piling material, psi
- I = section modulus of sheet piling, in⁴/ft of wall

3. Determine the geometrical coefficients a and b which are shown in Figure 9-21a.
4. Take the common logarithm of ρ . If the value of β is less than or equal to 0.3, the value of Rowe's moment reduction factor r_d can be determined. This is defined as

Equation 9-41:
$$r_d = \frac{M_{design}}{M_{FES}}$$

Where

- r_d = moment reduction ratio
- M_{design} = reduced moment due to flexibility of sheet pile wall.
- M_{FES} = maximum moment in the sheeting from free earth support method.



HIGHLY PRODUCTIVE SHEET PILE PRESSING



THE ABI PRESS CAN PRESS A PANEL OF 4 x 40ft SHEETS IN AS LITTLE AS 20 MINUTES



NO VIBRATION

SHORING CLOSE TO STRUCTURES



ASK FOR THE VIDEO



WORK IN LIMITED SPACE



IN A CHICAGO STREET

HAMMER & STEEL, INC (WEST COAST)
TOLL FREE: 877-224-3356
www.abi-delmag.com

CALL FOR SALES & RENTALS

HAMMER & STEEL, INC (MID-WEST & EAST COAST)
TOLL FREE: 800-325-7453
www.hammersteel.com

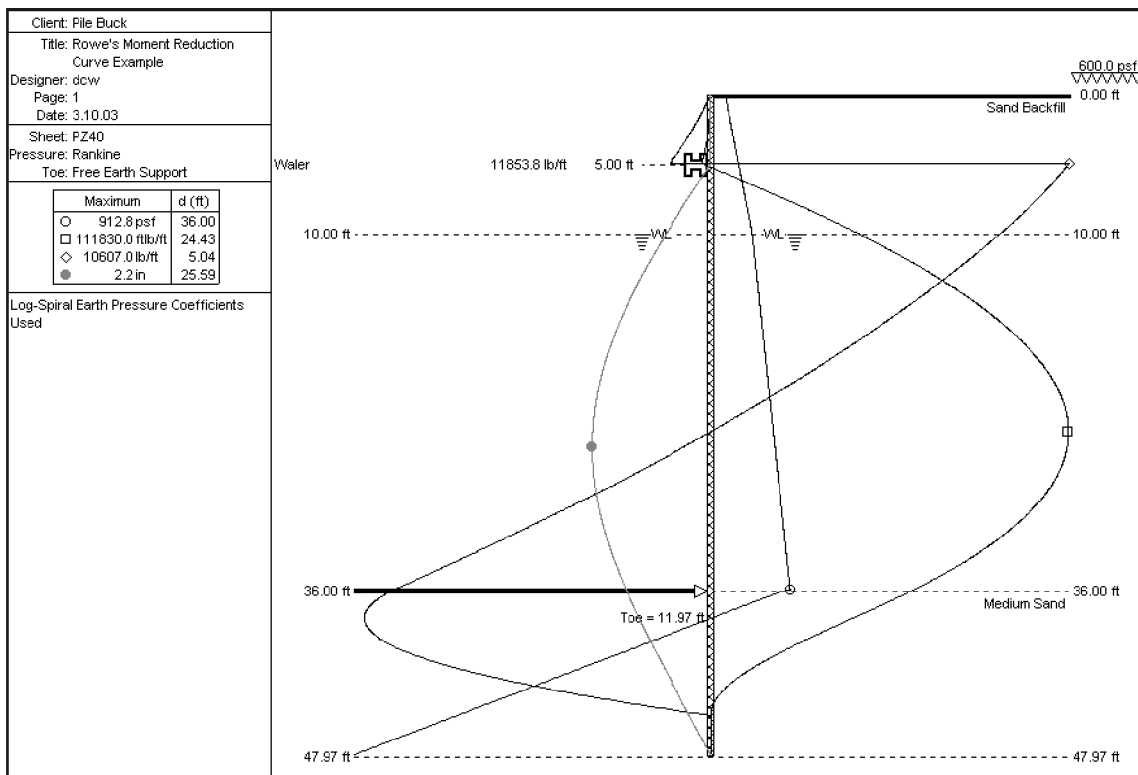


Figure 9-22: SPW911 Results for Example 13

5. Determine the reduced moment due to wall flexibility by solving Equation 9-41 for M_{design} , or

Equation 9-42: $M_{design} = r_d M_{FES}$

6. The tie rod load is unaffected by Rowe's moment reduction method.

Example 13: Rowe's Moment Reduction Method, Cohesionless Soils

❖ Given

- Anchored Sheet Pile Wall
 - Excavation Depth = 36'
 - Water level on both sides of the wall = 10'
 - Uniform surcharge of 600 psf
 - Soil Layer 1: Sand Backfill
 - $\gamma = 110$ pcf
 - $\gamma' = 60$ pcf
 - $\phi = 34^\circ$
 - $\delta = 0^\circ$
 - $K_a = 0.28$
 - Soil layer extends to excavation depth.
 - Soil Layer 2: Medium Sand
 - $g' = 65$ pcf
 - $f = 34.5^\circ$
 - $d/f = -0.4$
 - $K_a = 0.26$
 - $K_p = 6.63$

❖ Find

- Required sheeting section for maximum flexural stress using Rowe's Moment Reduction Curves

❖ Solution

■ Since our object is to demonstrate the use of Rowe's Moment Reduction Curves, we will dispense with the hand calculations and simply present the SPW911 results in Figure 9-22. This also serves as the figure that illustrates our problem. The SPW911 analysis in this case used the free earth pressure method with the full passive earth pressure coefficient.

■ The maximum moment from this analysis is 111.8 ft-kips/ft of wall. Using Table 2-1, only the PZ40 sheeting is capable of this flexural load using ASTM A328; PZ35 could be used with ASTM A572 or ASTM A690.

■ The properties for Rowe's method common to all of the sheet piling sections are as follows:

- Modulus of elasticity $E = 30,000,000$ psi
- Wall height = 48' (rounded up very slightly from SPW 911.)
- $\alpha = 36/48 = 0.75$
- $\beta = 10/48 = 0.208$

■ The results of applying Rowe's Moment Reduction method are shown in Table 9-2. As we would expect, the reduction in moment increased with the reduction in moment of inertia⁹⁴. Using this, PZ35 becomes a possibility in ASTM A328, as does PZ27 for ASTM A572 or ASTM A690.

⁹⁴Bulkheads constructed by front dredging from an established surface might be considered for a greater reduction of moment.

Table 9-2: Results of Rowe’s Moment Reduction Method for Example 11 for Different Sections

Section	PZ22	PZ27	PZ35	PZ40
Moment of Inertia, in ⁴ /ft	84.4	184.2	361.2	490.8
ρ (Equation 9-40)	0.002097	0.000961	0.00049	0.000361
log ρ	-2.68	-3.01	-3.31	-3.44
r _d	0.5	0.7	0.9	1.0
M _{design} , ft-kip/ft (Equation 9-42)	55.9	78.3	100.6	111.8

9.4.2.3.2. Cohesive Soils

Rowe⁹⁵ also extended the moment reduction theory to cohesive soils by introducing the stability number concept. The stability number is the ratio of the cohesion below the dredge line to pn at the dredge line and is a measure of the net passive resistance, i.e., to account for adhesion. This stability number is given by the equation

$$\text{Equation 9-43: } S_n = \frac{5c}{4p_v}$$

The relationship between the stability numbers and the moment reduction for cohesive soils is shown in Figure 9-21b.

Curves for three wall flexibility numbers are given. The designer, knowing the stability number, S_n, and the depth to height ratio, a, can determine the moment reduction and, therefore, size the piling for a particular flexibility ρ. Values of ρ between those given can be interpolated.

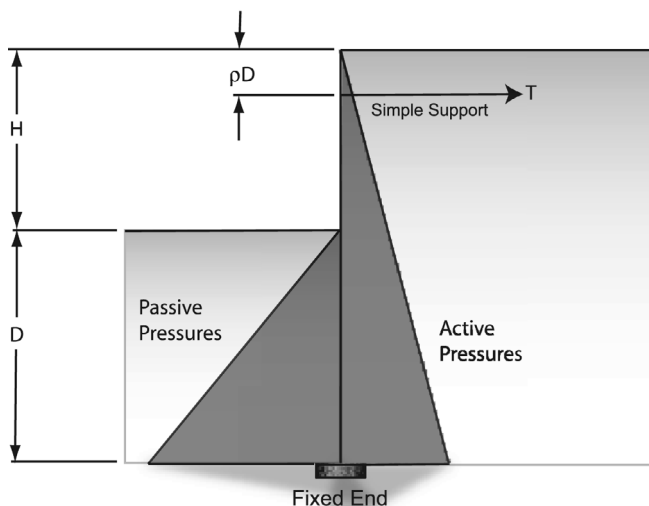


Figure 9-23: Anchored Sheet Pile Wall to Illustrate Blum’s Method

9.4.3. Fixed Earth Support Method (Equivalent Beam Method)

9.4.3.1. Overview of Blum’s Method

An alternative to the free earth support method – and one that is more popular in Europe than in the U.S. – is the fixed earth support method. The method was originally developed by Dr. Hermann Blum⁹⁶. To illustrate the concept, we present a “simple” example.

Consider an anchored sheet pile wall with a single support, uniform granular soil and no water as shown in Figure 9-23.

Let us assume that the toe of the sheet is a fixed end for structural purposes; this is Blum’s first condition, and this sets Blum’s method apart from the free earth support method. If we neglect the anchor, the system will be a simple cantilever with two distributed forces, the active pressure

$$\text{Equation 9-44: } p_a = -K_a \gamma x$$

and the passive pressure

$$\text{Equation 9-45: } p_p = K_p \gamma (x - H)$$

where x is the distance from the top of the sheet pile wall. The moment at any point due to the active pressure is

$$\text{Equation 9-46: } M_a = -\frac{K_a \gamma x^3}{6}$$

and the passive pressure

$$\text{Equation 9-47: } M_p = \frac{K_p \gamma (x - H)^3}{6}, \quad x \geq H$$

Now let us add a simple support at the point of the support. The moment due to this force at any point in the beam is given by the equation

$$\text{Equation 9-48: } M_T = T(x - \rho H), \quad x \geq \rho H$$

With the addition of the support, the system is statically indeterminate. The moment equations, however, can be solved if we treat each of the three forces acting on the beam (active pressure, passive pressure and support) separately and then sum the resulting deflections they produce at the support. We will use the dummy unit load method to determine these deflections.⁹⁷ This method states that the deflection at a point can be determined by applying a unit load at the desired point and the deflection determined by the equation

⁹⁵Rowe, P. (1957) “Sheet Pile Walls in Clay.” *Proceedings, Institution of Civil Engineers*, Part I, Vol. 1. London, England.
⁹⁶A summary in English of Dr. Blum’s work is found in the article “Bending Moment Acting on Anchored Steel Sheet Piling Walls,” founding in U.S. Steel publication *Design Extracts from Former Publications*. 1963. Pittsburgh, PA: United States Steel Corporation. Blum’s method is also summarised in Verruijt, A. (2001) *Soil Mechanics*, available at <http://www.vulcanhammer.net>. Most of what follows is based on his summary.
⁹⁷For information on this I am indebted to Dr. Edwin P. Foster of the University of Tennessee at Chattanooga, and his graduate class notes. This method is also dealt with in detail in Harker, R.J. (1986) *Elastic Energy Methods of Design Analysis*. New York: Elsevier.

$$\text{Equation 9-49: } \delta = \int_0^{H+D} \frac{mM}{EI} dx$$

where

m = moment due to the dummy unit load

M = moment due an actual moment

E = modulus of elasticity of the material

I = moment of inertia of the sheeting

For the active pressure and the anchor force, one must integrate from the support ($x = \rho H$) to the end of the beam ($x = H + D$). For the passive force, one must integrate from the excavation line ($x = H$) to the end of the beam. If we integrate the deflection at the anchor caused by each of these forces, sum the three resulting deflections, set them equal to zero, and solve for the anchor force, we have

Equation 9-50:

$$T = \frac{\gamma}{40((1-\rho)H+D)^3} \left(\begin{aligned} &4(K_a - K_p)D^5 + 5(\rho(K_p - K_a) - K_p + 4K_a)HD^4 + 20K_a(2-\rho)H^2D^3 \\ &+ 10K_a(4-3\rho)H^3D^2 + 20K_a(1-\rho)H^4D + K_a(4-5\rho+\rho^5)H^5 \end{aligned} \right)$$

We now note that we still have two unknowns: the anchor force T and the depth of penetration D. It is at this point that we introduce Blum's other condition: the moments about the toe equal zero, even though the toe is fixed. There is a reaction at the toe, which represents the residual of the net force on the wall. It is generally accounted for in design by increasing the penetration D of the wall beyond the excavation line by 20%.

The moments at the end can be obtained by substituting $x = H + D$ in to Equation 9-46, Equation 9-47 and Equation 9-48. If we then sum these moments, set the summation equal to zero, and as before solve them for the anchor force, we obtain

Equation 9-51:

$$T = \frac{\gamma(D^3(K_a - K_p) + K_a(3HD^2 + 3H^2D + H^3))}{6(H(1-\rho) + D)}$$

Obviously we can solve this equation and the previous one together and determine the result for T and D; however, from a practical standpoint only a numerical solution is possible. If we add the water table, as we did for the charts, the complexity increases.

Blum's assumption of a fixed end has been widely criticised (especially in the U.S.), but it should be kept in mind that Blum's assumption is more of a design objective than an assumption of actual conditions. If the sheet were to be

lengthened, the maximum moment—which can also be obtained from the above equations—would be lowered with the increased penetration of the sheet. A longer sheet would also be more resistant to overturing failure.

This concept, although applied first to steel sheeting, has potential with non-metallic sections, where maximum allowable moments tend to be lower.

9.4.3.2. Implementation of Fixed Earth Support

An examination of the previous section indicates that the method is deceptively simple; actual implementation becomes computationally complex very quickly. As a result, this method has had several simplifications, including that of Gregory Tschebotarioff⁹⁸. The hand solution method we will use here is as presented in the British Steel Corporation *Piling Handbook*⁹⁹. SPW 911 also uses this method.

For this simplification, the lateral earth pressures are computed in the usual manner. Formally speaking, towards the toe of the sheet-piling wall, the lateral earth pressures reverse themselves; however, we can simplify these in the same way we did for the cantilever walls, i.e., by applying a force F_3 at point F that replaces these forces. In doing so, we must add a toe length of 20% of the distance O_1F (distance D) to account for this simplification.

The procedure for fixed earth support on anchored walls is as follows:

1. Compute the lateral earth pressures and forces in the same way as was done for the free earth support method. This includes the forces P_a and P_p and the location of the point O_1 (distance y).
2. Ignoring the beam below the point O_1 , compute the moments of the beam about the point O_1 . This will include the moment due to P_a and the anchor force T. Since P_a and the locations of the resultants are known, the force T can be computed.
3. Sum moments about point F. Include moments from forces P_a , P_p and T. Since P_p is a function of D, D can be computed from this summation.
4. Compute the magnitude of the maximum moment by locating the point of zero shear and summing moments.

⁹⁸Tschebotarioff, G.P. (1973) *Soil Mechanics, Foundations and Earth Structures*. Second Edition. New York: McGraw-Hill Book Company.

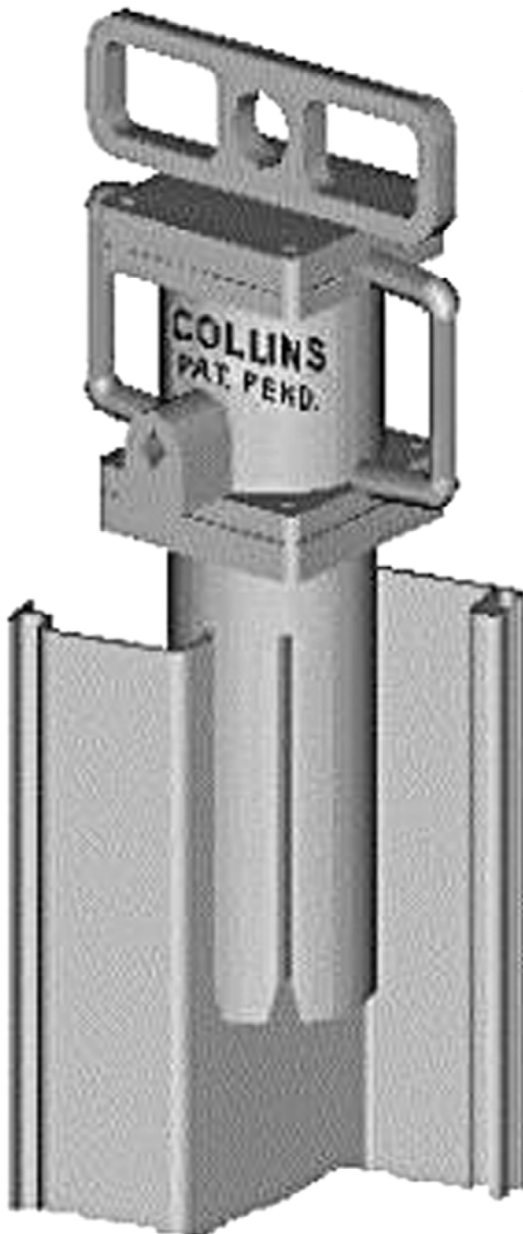
⁹⁹British Steel Corporation *Piling Handbook*. (1984) Fourth Edition. Scunthorpe, England: British Steel Corporation.

THE COLLINS 150# AIR HAMMER

*New Patent Pending
Design. Out Drives
Heavier Hammers.*

"No Leads" required.

*Drives all brands
of VSP &
CSP+Pin Piles.*



5 day delivery, Cont. U.S.
Visa & MC.

COLLINS COMPANY

Since 1953

Toll Free 888-300-0100

Cell 360-708-5320

www.vinylsheetpiling.com

collins@whidbey.net

5. There are two factors of safeties to consider: the ratio of the restoring (primarily passive) moments to the disturbing (primarily active) moments about point T, and the factor of safety against rotational failure about point F. The former is a result of the computations and can be checked at the end of the calculations. The latter can be dealt with (if desired) by reducing the passive earth pressure coefficient as we have done before.

In addition to the simplifications, this method can be implemented using most any direct stiffness (finite element) structural analysis program. We will illustrate this in the following example.

Example 14: Fixed Earth Support Method

❖ Given

- Problem as outlined in Example 11.

❖ Find

- Depth of penetration of sheeting.
- Maximum moment of sheeting; select suitable sheeting profile.
- Determine anchor load per linear foot of wall.
- Use fixed earth support method.
- Use actual active and passive earth pressure coefficients. The method is the same if reduced coefficients are used.

❖ Solution

- Determine lateral earth pressure coefficients

- $K_a = 0.33$ (Equation 5-1)
- $K_p = 3$ (Equation 5-16)

■ Compute the unit active pressure p_{C1} at the elevation CC_1 . Although theoretically the surcharge pressure should be included here, as before we will consider the effects of the surcharge separately. $p_{C1} = (4)(100)(0.33) = 133$ psf

■ Compute the unit active pressure p_{A1} at the elevation AA_1 . $P_{A1} = 133 + (6)(60)(0.33) = 253$ psf

■ Compute the lateral pressure from the surcharge p_C . $p_C = p_{\text{surcharge}} K_a = (200)(0.33) = 67$ psf.

■ Compute the slope of the line A_1E , which equals to $K_p - K_a = 3 - 0.33 = 2.67$.

■ Locate the point of zero pressure O_1^{100} , which is y below the dredge line. The distance y is computed by Equation 9-32, thus $y = (253)/((60)(2.67)) = 1.58'$.

■ Find the magnitude and location of the resultant active pressure P_a , which is the sum of the active pressure areas BCC_1 , CC_1A_1A and AA_1O_1 . This should include the surcharge loading above point y .

- Surcharge loadings.
 - Above the dredge line
 - ◆ Force: $P_{C+} = (67)(10') = 666.67$ lb/ft
 - ◆ Location from point $O_1 = 5 + 1.58 = 6.58'$
 - Between the dredge line and point O_1
 - ◆ Force: $P_{C-} = (67)(1.58) = 105.6$ lb/ft

◆ Location from point $O_1 = 1.58/2 = 0.79'$

- BCC_1
 - Force: $(133)(4)/2 = 267$ lb/ft
 - Location from point $O_1: 10 - (2)(4)/(3) + 1.58 = 8.92'$
- CC_1A_1A
 - Force: $(133 + 253)(6)/2 = 1,160$ lb/ft.
 - Location from point O_1 : In this case, $z = (133 + (2)(253))/(3(133+253))(6) = 3.31'$ from point C or $10 - 4 - 3.31 + 1.58 = 4.27'$.
- AA_1O_1
 - Force: $(253)(1.58)/2 = 201$ lb/ft
 - Location from point $O_1 = (2)(1.58)/(3) = 1.06'$
- Compute resultant active pressure P_a
 - $P_a = 666.67 + 105.6 + 267 + 1160 + 201 = 2399$ lb/ft
- Determine location of resultant from anchor
 - Full passive earth pressure coefficient: $h = ((666.67)(6.58) + (105.6)(0.79) + (267)(8.92) + (1160)(4.27) + (201)(1.06))/2399 = 5.0'$

- Compute the anchor force by summing moments about point O_1 .

- The anchor is $8' + 1.58' = 9.58'$ from point O_1 . The summation of moments is $(2399)(5) = 9.58T$, and so $T = 1254$ lb/ft of wall length.

- Find the resultant passive pressure P_p , which is the combined active and passive pressure O_1FE , given by Equation 9-33.

- $P_p = 80 D^2$. This moment arm about the point F is $D/3$.
- The surcharge load acts in an opposite manner and so $P_{\text{sur}} = -66.7 D$. The moment arm for this point about the point F is $D/2$.
- The moment arm for the active force P_a (including the surcharge load) is $5 + D$.
- The moment arm for the anchor is $9.58 + D$.

- Solve for depth D by summing moments about point F.

- Including all of the forces and moment arms, the summation of moments results in the equation $26.7 D^3 - 33.3 D^2 - 1145.3 D = 0$. The largest positive solution for this is $D = 7.2'$. The distance from the dredge line to the toe is thus $1.58 + (1.2)(7.2) = 10.2'$

- Determine the maximum moment and sheeting profile. The point of zero shear (maximum moment) is usually near the dredge line, and not below O_1 as is the case with cantilever walls.

- Let us assume that the point of zero shear is between the water table and the dredge line. There are two constant forces completely above the water table: the anchor force, $T = -1254$ lb/ft, and the soil above the water table, $P_1 = 267$ lb/ft. There are two forces that are left; both of these are dependent upon the location of the point of zero shear. These are the surcharge force, $P_C' = 67 (4 + x_{\text{remain}})$, and the force between the water table and the point of zero shear,

¹⁰⁰Equation 9-32 assumes that the soil properties do not change at the dredge line. If this is the case, the lateral earth pressure will have a discontinuity, and the numerator will then be the lateral earth pressure for the soil below the dredge line.

Table 9-3: Forces and Moment Arms for Maximum Moment in Example 14

Force	Magnitude, lb/ft	Distance from Point of Zero Shear, ft.
P_1	267	4.45
T	-1254	5.11
P_C'	474	3.56
P_2'	513	1.46 (Equation 9-37)

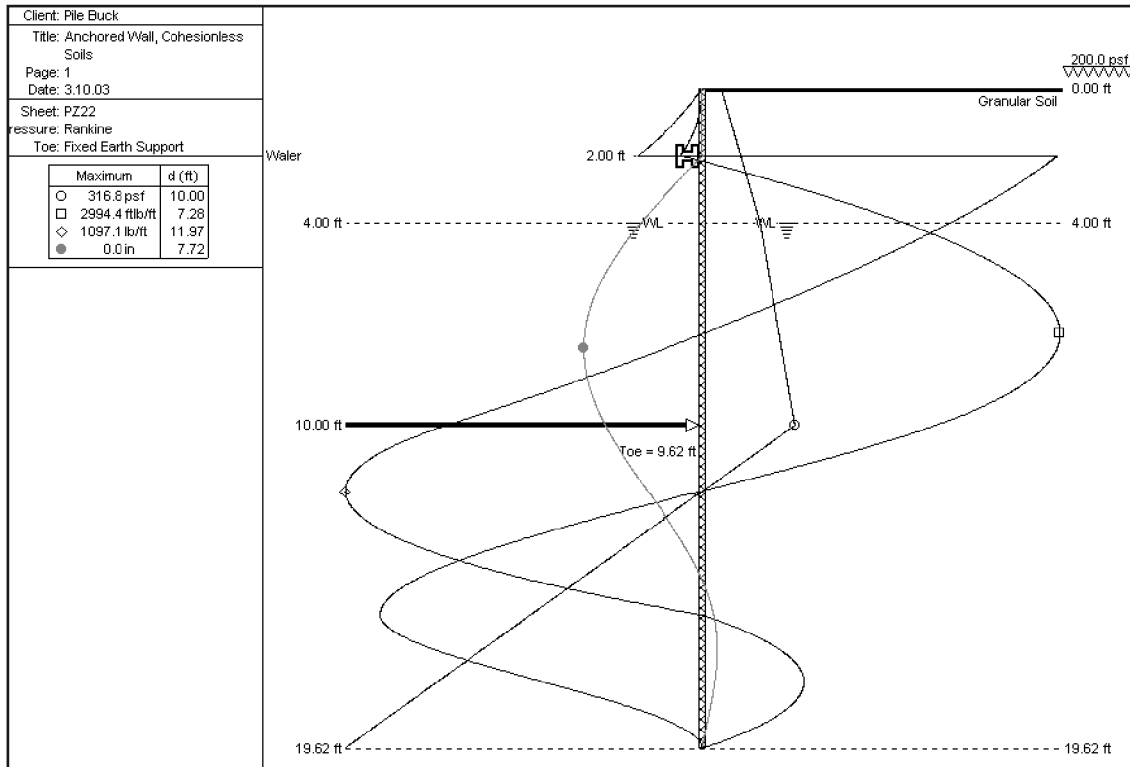


Figure 9-24: SPW 911 Solution for Example 14

$P_2' = x_{\text{remain}}(133 + p_{xr})/2$. For these equations, x_{remain} = distance from water table to the point of zero shear, and p_{xr} = lateral earth pressure at the point of zero shear without the surcharge. At the point of zero shear, $P_1 + T + P_2' + P_C' = 0$. Substituting, this yields $10 x_{\text{remain}}^2 + 200 x_{\text{remain}} - 721 = 0$. The positive solution to this equation is $x_{\text{remain}} = 3.11'$, which means that the point of zero shear is 7.11' below the top of the sheeting. The lateral earth pressure at this point is $p_{zs} = 196$ psf.

Once the point of zero shear is determined, the maximum moment is determined by summing the moments of the forces about the point of zero shear. The forces and moment arms are shown in Table 9-3. The resultant moment, and the maximum moment on the sheeting, is 2793 ft-lb/ft of wall length. As before, this is well below the moments of any of

the sheets listed in Table 2-1.

■ Solution using SPW 911

- The solution is shown in Figure 9-24.
- There are several important observations from the SPW 911 result that need to be noted.

The results shown here are similar to those obtained in hand calculations but not identical. The reason for this concerns the way in which the surcharge loading was handled. SPW 911 integrates the surcharge loading into the earth pressure profile while it was handled separately in the hand calculations. Integrating the surcharge increases the distance y and decreases the distance D . This in turn decreases the total toe, since more of the toe distance is in y and thus the cor

FIXED EARTH SUPPORT METHOD

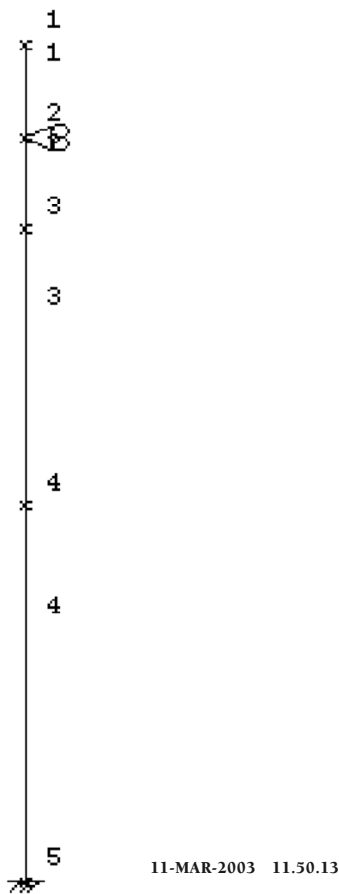


Figure 9-25:
Finite Element Model for Fixed Earth Support Method

rection factor for the simplified method will increase the total toe distance less than when the surcharge is considered separately. This is an example of how a legitimate decision of problem solving can lead to different results.

The SPW result in Figure 9-24 shows the “point of contraflexure,” i.e., the point where the curvature of the beam changes from convex towards the excavation (left side) to convex towards the active pressure (right side). Identifying this point is important in many variations of the fixed earth support method, although not critical here. For uniform cohesionless soils, the distance D can be computed directly by the equation

Equation 9-52:
$$D = \sqrt{\frac{6R}{\gamma'(K_p - K_a)}}$$

Where R is the horizontal reaction at the point of

FIXED EARTH SUPPORT METHOD

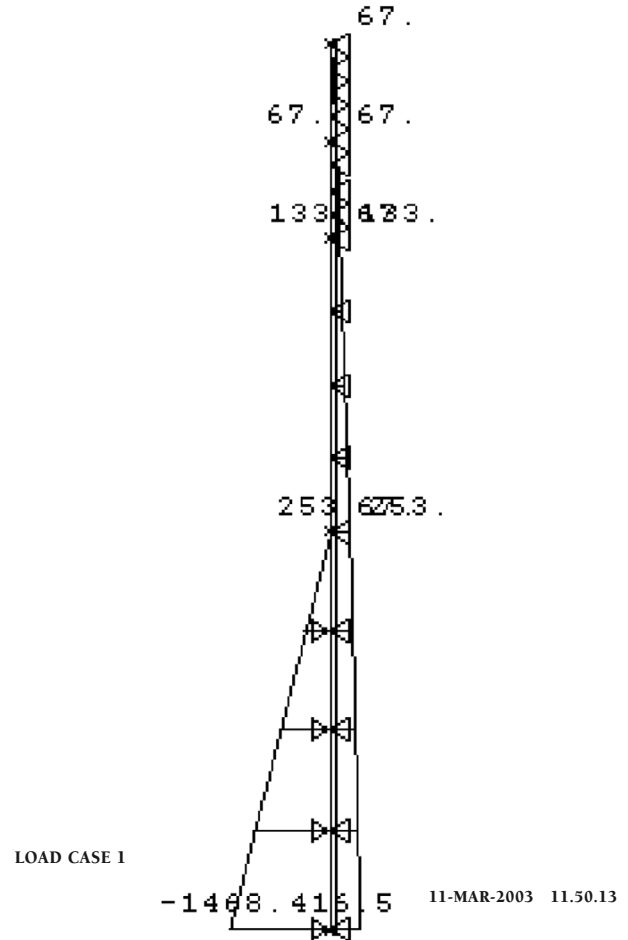


Figure 9-26:
Loads for CFRAME Model for Fixed Earth Support Example

contraflexure (frequently assumed the same as O_1 , and very close to this in the SPW911 analysis) if the beam were simply supported there.

- Solution using Structural Analysis Program
 - As noted, we can solve problems such as this using a structural analysis program. The program we will use here is CFRAME¹⁰¹, although any structural analysis program that can handle “ramped” loads (and that includes most of them) can be used.

We started by dividing the beam into four elements and five nodes. The nodes are located at the top of the beam, the anchor, the water table, the dredge line and the toe of the wall. The anchor is simply supported and the toe of the beam is rigidly supported. This is illustrated in Figure 9-25.

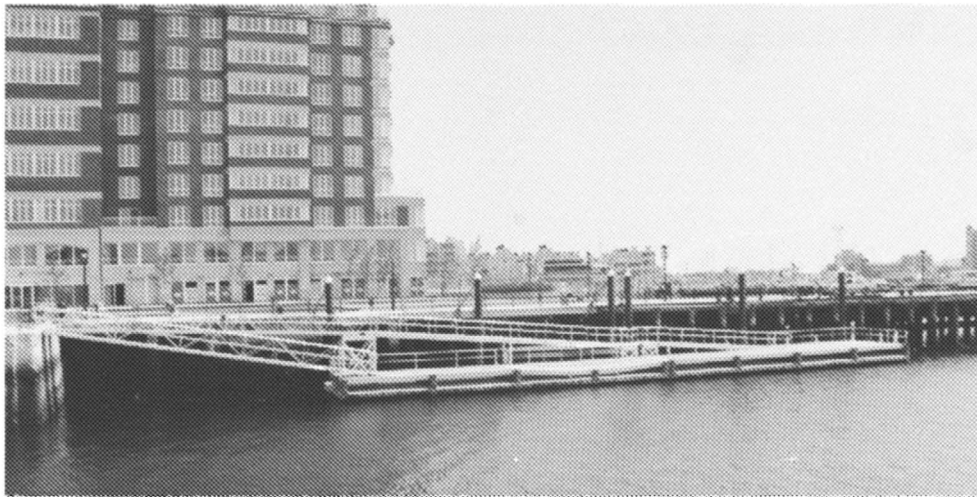
We apply the earth pressures to each element. There are two ways of doing this in CFRAME:

¹⁰¹This program was produced by the U.S. Army Corps of Engineers. The documentation for it is found in Hartman, J.P., and Jobst, J.J. (1983) *User's Guide: Computer Program with Interactive Graphics for Analysis of Plane Frame Structures (CFRAME)*. Instruction Report K-83-1. St. Louis, MO: U.S. Army Engineer District, 1983.

RAVENS MARINE

WE MANUFACTURE THE COMPLETE PICTURE

Aluminum Gangways, Floating Docks and Walkways, Fixed Piers, Aluminum Retaining Wall Systems, Accommodation Ladders with Fixed and Adjustable Steps, Pre-stressed Concrete Floating Docks and Breakwater Systems.



Ravens Marine

3295 Old Dixie Highway • Kissimmee, FL 34744

PH: 407-935-9799 • FAX: 407-935-9436

Website: www.ravensmarine.com E-Mail: ravens@ravensmarine.com

Table 9-4: Results of CFRAME Program for Example 14

RUN DATE = 11-MAR-2003
 RUN TIME = 11.46.14

FIXED EARTH SUPPORT METHOD

*** JOINT DATA ***

JOINT	X Y		-----FIXITY-----					
	--- FT ---		X	Y	R	KX ---LB / IN---	KY ---	KR IN-LB /RAD
1	.00	.00						
2	.00	-2.00	*					
3	.00	-4.00						
4	.00	-10.00						
5	.00	-18.16	*	*	*			

*** MEMBER DATA ***

MEMBER	END END		LENGTH FT	I IN**4	A IN**2	AS IN**2	E PSI	G PSI
	A	B						
1	1	2	2.00	.8470E+02	.6460E+01	.6460E+01	.3000E+08	.1154E+08
2	2	3	2.00	.8470E+02	.6460E+01	.6460E+01	.3000E+08	.1154E+08
3	3	4	6.00	.8470E+02	.6460E+01	.6460E+01	.3000E+08	.1154E+08
4	4	5	8.16	.8470E+02	.6460E+01	.6460E+01	.3000E+08	.1154E+08

*** LOAD CASE 1

MEMBER	LA	PA	LB	PB	ANGLE
	FT	LB / FT	FT	LB / FT	DEG
1	.00	.6700E+02	2.00	.6700E+02	.00
1	.00	.0000E+00	2.00	.6700E+02	.00
2	.00	.6700E+02	2.00	.6700E+02	.00
2	.00	.6700E+02	2.00	.1330E+03	.00
3	.00	.6700E+02	6.00	.6700E+02	.00
3	.00	.1330E+03	6.00	.2530E+03	.00
4	.00	.6700E+02	8.16	.6700E+02	.00
4	.00	.2530E+03	8.16	.4165E+03	.00
4	.00	.0000E+00	8.16	-.1468E+04	.00

1 LOAD CASE 1

JOINT	JOINT DISPLACEMENTS		
	DX	DY	DR
	IN	IN	RAD
1	.1767E-01	.0000E+00	-.7357E-03

Table 9-4 continued

2	.0000E+00	.0000E+00	-.7421E-03
3	-.1740E-01	.0000E+00	-.6443E-03
4	-.3043E-01	.0000E+00	.3188E-03
5	.0000E+00	.0000E+00	.0000E+00

MEMBER END FORCES						
MEMBER	JOINT	AXIAL LB	SHEAR LB	MOMENT IN-LB	MOMENT EXTREMA IN-LB	LOCATION IN
1	1	.0000E+00	.0000E+00	.0000E+00	.0000E+00	.00
	2	.0000E+00	.2010E+03	-.2144E+04	-.2144E+04	24.00
2	2	.0000E+00	.1141E+04	-.2144E+04	.2150E+05	24.00
	3	.0000E+00	-.8071E+03	.2150E+05	-.2144E+04	.00
3	3	.0000E+00	.8071E+03	.2150E+05	.3898E+05	41.76
	4	.0000E+00	.7529E+03	.2777E+05	.2150E+05	.00
4	4	.0000E+00	-.7529E+03	.2777E+05	.2777E+05	.00
	5	.0000E+00	-.1959E+04	-.5526E+02	-.2689E+05	68.54

STRUCTURE REACTIONS			
JOINT	FORCE X LB	FORCE Y LB	MOMENT IN-LB
2	.1342E+04	.0000E+00	.0000E+00
5	-.1959E+04	.0000E+00	-.5526E+02

TOTAL	-.6170E+03	.0000E+00	

1							
MEMBER END FORCES							
MEMBER	LOAD CASE	JOINT	AXIAL LB	SHEAR LB	MOMENT IN-LB	MOMENT EXTREMA IN-LB	LOCATION IN
1	1	1	.0000E+00	.0000E+00	.0000E+00	.0000E+00	.00
		2	.0000E+00	.2010E+03	-.2144E+04	-.2144E+04	24.00
2	1	2	.0000E+00	.1141E+04	-.2144E+04	.2150E+05	24.00
		3	.0000E+00	-.8071E+03	.2150E+05	-.2144E+04	.00
3	1	3	.0000E+00	.8071E+03	.2150E+05	.3898E+05	41.76
		4	.0000E+00	.7529E+03	.2777E+05	.2150E+05	.00
4	1	4	.0000E+00	-.7529E+03	.2777E+05	.2777E+05	.00
		5	.0000E+00	-.1959E+04	-.5526E+02	-.2689E+05	68.54

FIXED EARTH SUPPORT METHOD

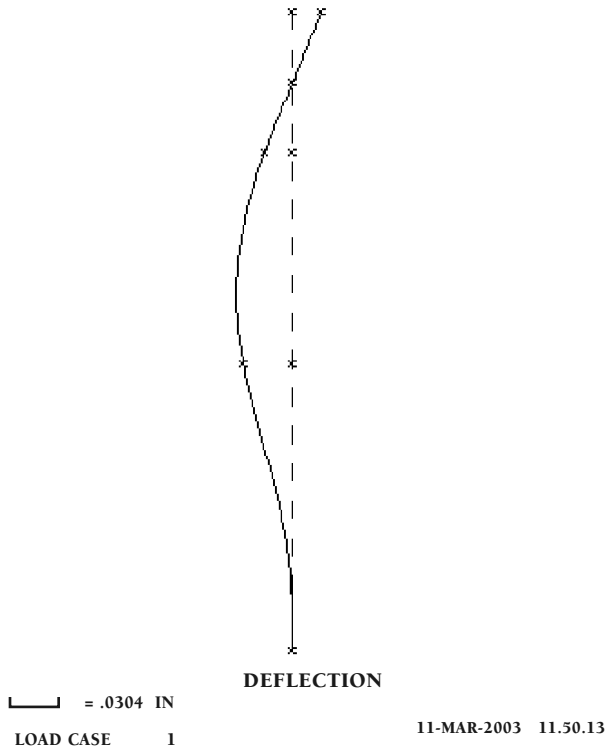


Figure 9-27: CFRAME Deflection Diagram for Example 14

FIXED EARTH SUPPORT METHOD

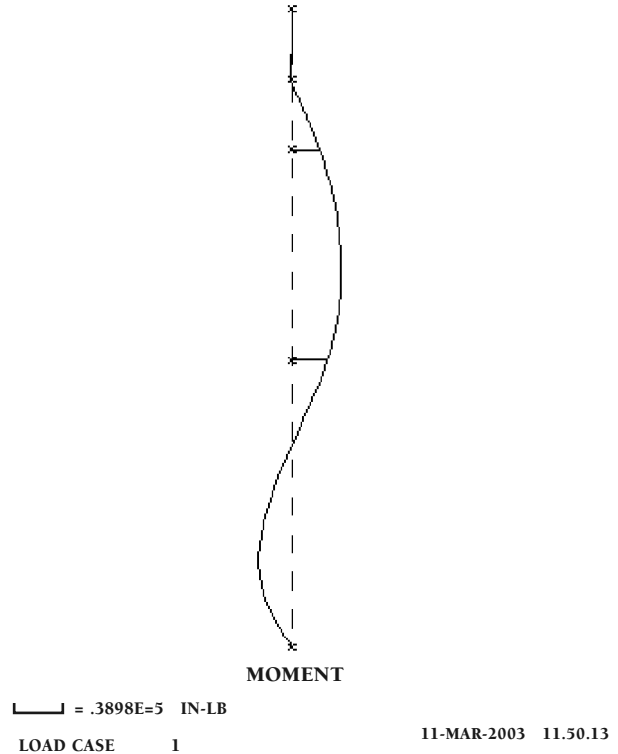


Figure 9-28: CFRAME Moment Diagram for Example 14

FIXED EARTH SUPPORT METHOD

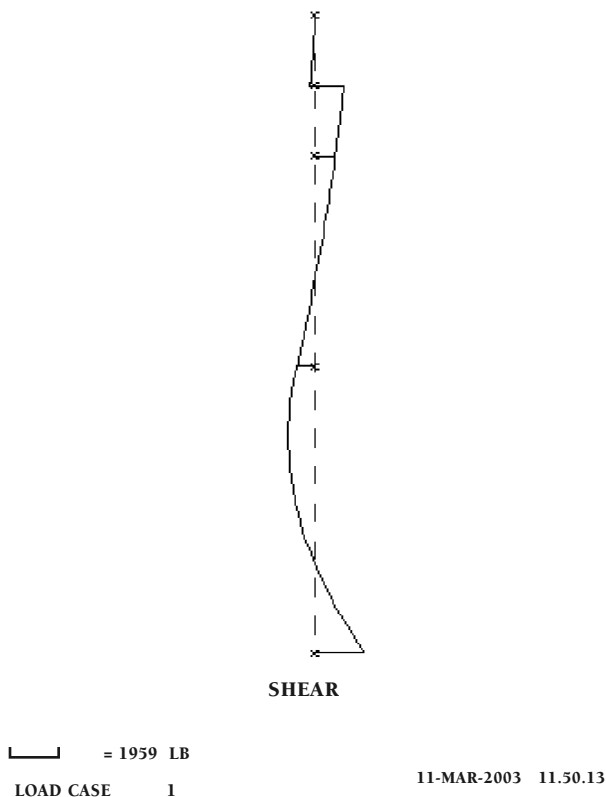


Figure 9-29: CFRAME Shear Diagram for Example 14

- ◆ Consolidating the various earth pressures into one profile and entering it into CFRAME element by element. This is similar to the method used in SPW911. Since we must vary the location of node 5 by trial and error to determine the point at which the moments at node 5 are zero, we need to construct a table of earth pressures for various possible locations of node 5. Consolidating the pressures makes this job simpler; however, for illustrative purposes we will opt to—
- ◆ Enter each type of earth pressure separately, as shown in Figure 9-26. We assume a sheeting section, in this case PZ22.
- The tabular results are shown in Table 9-4. Graphical output for deflection, moment and shear along the entire sheeting wall are shown in Figure 9-27, Figure 9-28 and Figure 9-29, respectively. Shear and moment diagrams for the individual elements are also available.

The results just presented are for a total pile length of 18.16'. To arrive at this toe length, CFRAME was run for several values between 17' and 19'. The earth pressures – both active and passive – at the toe were varied with the length. The object was to determine the point at which the toe moment was zero. The variation in toe moment with pile length is shown in Figure 9-30. Linear interpolation gives a pile length for zero toe moment of 18.16'. The results from this length show an actual toe moment of 553 in-lb/ft = 46 ft-lb/ft, which is very small indeed.

PTC 50HD Vibrodriever

JOB REPORT

A 50HD installing moorings in Buzzards Bay in New England, U.S.A.

1.2 m (48") diameter casings have to be driven in 12 m (40') deep water near Buzzards bridge. Casings are vertical and also 20° raked.

Average length of the casings 24 m (80'). Max length 40 m (130').

Wall thickness : 11 mm (7/16").

To drive these casings customer has chosen a **PTC 50HD** Vibrodriever of 4,400 in-lbs eccentric moment.

A Linkbelt 100 t crawler crane is utilized mounted on a pontoon.

Soil : silty sand with S.P.T ≤ 20

TECHNICAL DATA AND EQUIPMENT:

One **PTC** Vibrodriever **50HD** with 2x 85 t Duplex caissons clamps.

PTC Hydraulic Power pack Type **450**



Casing guide

20° Raked Piles



- 20 °C



International Headquarters

158, rue Diderot, F-93698 PANTIN CEDEX - FRANCE
 Tel: + 33 1 49 42 72 95 Fax: + 33 1 48 44 00 02
 website: www.ptc.fr E-Mail Vibrofonneur@ptc.fr

PTC branch in the US
 P.O. BOX 396
 Marylhurst, OR, USA 97096
 Andy Schroeder
 Phone: (503) 656-0422
 fax: (503) 656-2652
 e-mail andrew.schroeder@comcast.net

U.S. Distributors:
American Equipment & Fabricating Co.
 100 Water Street
 E. Providence, RI, USA 02914
 Phone: (401) 438-2626
 Fax: (401) 438-0764
 e-mail: WIN@AMERICAN-EQUIPMENT.COM

Foundation Equipment & Supply, Inc.
 P.O. Box 1226
 Newberg, OR, USA 97132
 Phone: (503) 537-9994
 Fax: (503) 554-9322
 Mobile: (503) 860-2207
 e-mail: mcolby@teleport.com

Conmaco Inc.
 1602 Engineers Road
 Belle Chasse, LA, USA 70037-3137
 Phone: (504) 394-7330
 Fax: (504) 393-8715
 e-mail: mfavaloro@comaco.com

Conmaco Inc.
 3036 Yadkin Road
 Chesapeake, VA, USA 23323
 Phone: (757) 485-5010
 Fax: (757) 485-0856

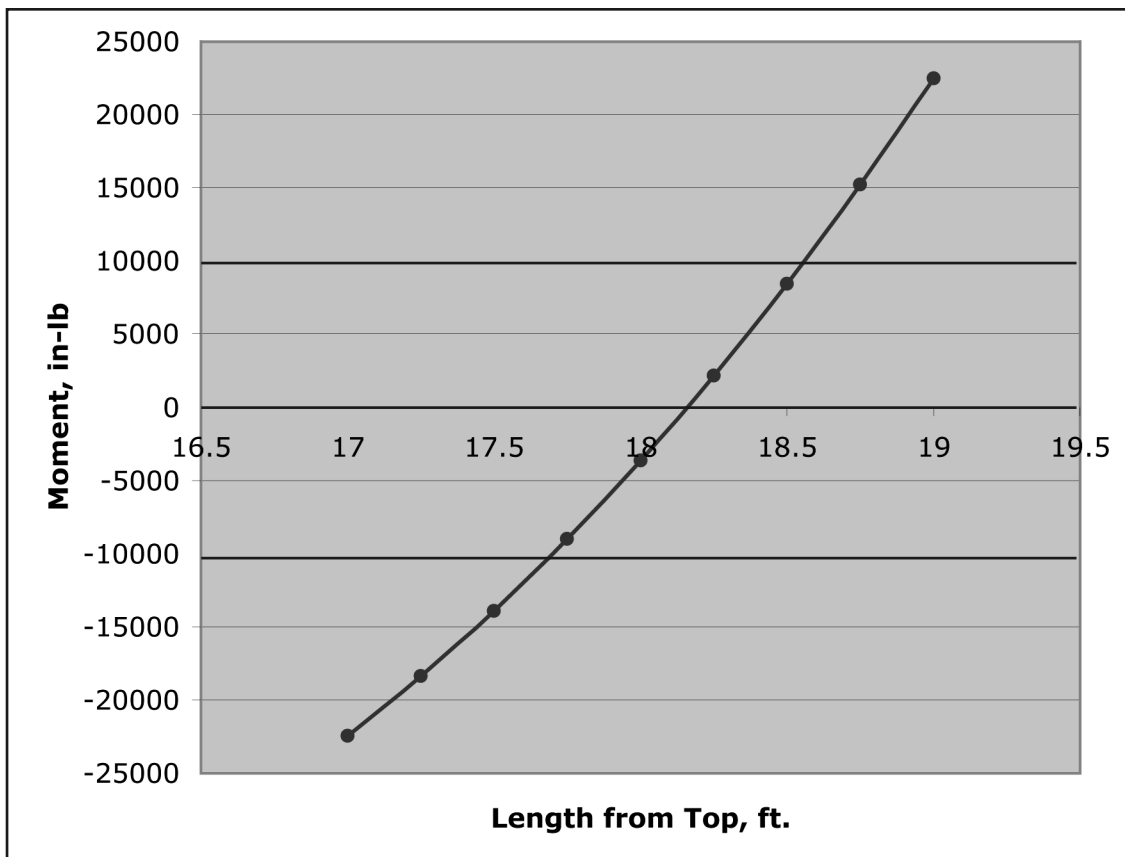


Figure 9-30: Variation in Toe Moment for Fixed Earth Support Method

Table 9-5: Tabulated Results for Fixed Earth Support Example

Method	Sheeting Length, ft.	Maximum Moment, ft-lb-ft of wall	Maximum Shear, lb/ft of wall	Deflection, in.	Anchor load, lb/ft of wall
Hand Calculations	20.2	2793	-	-	1254
SPW911	19.62	2994	1097	0.0	1289
CFRAME	19.79	3248	1073 ¹⁰²	0.03	1342

With a direct implementation of Blum’s method such as this, we can add the factor for the fixed end reaction to the entire length D. Thus the actual length of the sheeting below the dredge line should be $(1.2)(8.16) = 9.79'$. The other results are shown in Table 9-5.

The variation the results amongst these methods shown needs some explanation.

- ◆ The difference between the hand calculations and SPW911 has already been noted. Since the toe length

computation is different, the rest of the results will be different also.

- ◆ The difference between the CFRAME results and the other methods are due to variations in the fixed earth support method. In its basic form, the fixed earth support method involves the analysis of a statically indeterminate structure with ramped, distributed loads. Use of Terzaghi’s simplification (assume the toe to be simply supported and require the rotation to be zero there 103) does produce a statically determinate structure (for a

¹⁰²The maximum shear for the entire wall (1959 lb/ft of wall length) is shown to take place at the toe of the wall; this is in reality the F₃ force. Element output shows that the maximum shear (which takes place just below the dredge line) is 1073 lb/ft.

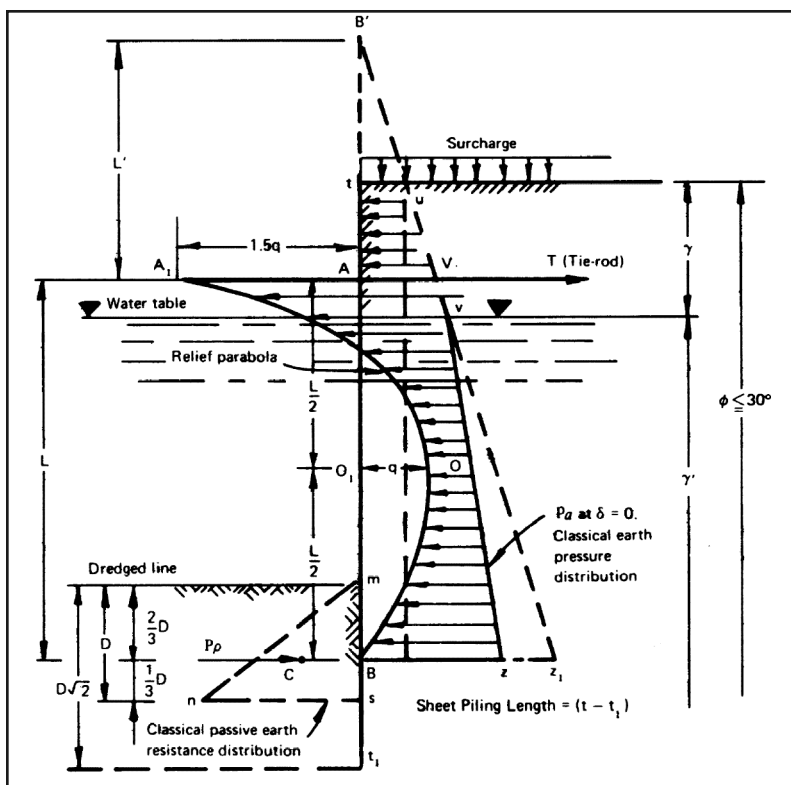


Figure 9-31:
Danish Method of Sheet Pile Wall Design

single support) but still requires the use of methods such as slope deflection or the dummy unit load method for proper analysis. This has led to simplifications such as the one shown in the hand calculations and SPW911, but it is too much to expect perfect matches in the results.

- ◆ The use of a direct stiffness program such as CFRAME allows us to eliminate the simplifications, although the iterative process can be a little tedious.
 - The use of a structural program such as CFRAME to analyse anchored sheet piling walls also provides us with an independent check without having to resort to hand calculations. It is also a good transition to finite element methods of analysis for sheet pile walls.

9.4.4. Graphical Methods

Traditionally, graphical methods have been used to analyse the shear, moment and deflection characteristics of sheet pile walls with complex or irregular loading. Although modern CAD systems can make graphical solutions precise to a higher degree than previously possible, the use of other computerised methods, such as SPW 911 or the application of programs such as Maple and Matlab to hand calculations have rendered graphical methods obsolete in practice.¹⁰⁴

9.4.5. Danish Rules

The Danish Rules, published by the Danish Society of Civil

Engineers, are based on studies of a number of existing sheet pile structures and are purely empirical. They apply to single anchored sheet pile walls in cohesionless material and represent the least conservative approach to design. Although the Danish Rules have been subject to considerable criticism, especially with respect to the assumed pressure distribution, they have formed the design basis for many very economical sheet pile structures in use today.

Figure 9-31 shows the assumed pressure distribution on a sheet pile wall. The wall is assumed to be simply supported at points A and B, where B is located at the centre of the passive resistance. The active earth pressure distribution is obtained by Coulomb's theory (with no wall friction) and modified by a parabola to decrease the lateral pressure in the middle region of AB by an amount q, and increase the pressure by 1.5q at A. The quantity q may be considered a reduction factor due to the arching effect of the soil, thereby causing concentration near the top and bottom of the wall.

The magnitude of q, the parabolic stress relief ordinate, is expressed by

$$\text{Equation 9-53: } q = k \frac{10L' + 4L}{10L' + 5L} p_m$$

Where

- L' = height of soil above point A, including the equivalent height of surcharge converted in terms of γ of the backfill

¹⁰³This method is identical in results to Blum's original method and the one we used with CFRAME, which fixed the end (thus guaranteeing no rotation) but required a zero moment.

¹⁰⁴An excellent treatment of graphical methods for sheet piling design can be found in the book *Practical Design of Sheet Pile Bulkheads*, Second Edition (1986), published by TradeArbed, New York, NY.

- L = length AB
- p_m = the equivalent uniformly distributed pressure on the wall between the simple supports A and B that will give the same bending moment, M_1 , as the trapezoidal Coulomb active pressure distribution AVZB, i.e., $p_m = 8M_1/L^2$

and k is defined by the equation

Equation 9-54:
$$k = \frac{1}{1 + \frac{1}{100 \sin \phi} \sqrt{\frac{aE(n+1)}{F_b L}}}$$

Where

- ϕ = average angle of internal friction between points A and B
 - n = ratio of the negative bending moment at the anchor level to the maximum positive bending moment of the span, L , below the tie rod
 - E = modulus of elasticity of steel = 29×10^6 psi
 - a = distance between extreme fibres of sheet piling
 - F_b = allowable steel bending stress in sheet piling, psi
- The value of k varies from about 0.80 to 0.90 for steel and may be assumed equal to 0.9 for design purposes.

The bending moments and anchor pull can be determined from the pressure distribution established between A and B. The following approximate relationships may be used. The tension, T , in the tie rod at point A is

Equation 9-55:
$$T = A_L + A_o + \frac{M_o}{L} + \frac{qL}{12}$$

Where

- A_L = reaction at A corresponding to the earth pressure diagram AVZB
- A_o = resultant of the pressure above the tie rod
- M_o = cantilever moment at A due to the pressure above the tie rod

The soil reaction at B is

Equation 9-56:
$$B = B_L - \frac{M_o}{L} - \frac{qL}{3}$$

Where B_L = reaction at B corresponding to the earth pressure diagram AVZB

The maximum positive bending moment to be used for design of the sheet piling is

Equation 9-57:
$$M = M_L - \frac{M_o}{2} - \frac{17qL^2}{192}$$

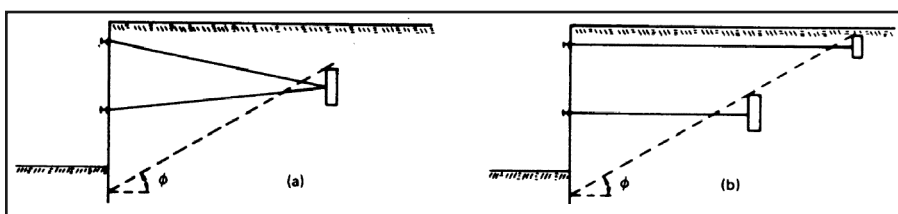


Figure 9-32: Typical Anchorage for Two Tie Rods

Where M_L = the maximum bending moment corresponding to the earth pressure diagram AVZB.

The required depth, D , is determined by the condition that the total passive earth pressure, calculated according to Coulomb's theory (with $\delta = 1/2\phi$), should equal the reaction B. This necessitates a trial and error approach. The driving depth should be increased to $\sqrt{2D}$ to provide a margin of safety of approximately 2.

9.4.6. High Sheet Pile Walls (Two Anchor System)

When the height between the dredge line and the anchor is greater than about 35 feet, it may prove economical to utilize a second tie rod at a lower level. This will reduce both the moment in the wall and the required depth of penetration. Figure 9-32 shows two arrangements for a sheet pile wall having two tie rods. Method (a) is preferred because the different tie rod lengths and separate anchors used in method (b) tend to cause different horizontal deflections at the two wales.

The analysis of walls with multiple supports is discussed in Chapter 12.

9.5. Load and Resistance Factor Design (LRFD)

Load and Resistance Factor Design (LRFD) methods involve the use of statistical methods to determine the actual combined effect of various types of loads on a structure. The various loads (dead, live, earthquake, etc.) are combined using factors, then compared with a load capacity which itself is factored. Fortunately all of the factors have been determined for a given code or structure type in advance so the designer does not have to deal with the statistical calculations directly.

To begin, the factored load is given by the equation

Equation 9-58:
$$P_u = \sum_{m=1}^n \gamma_m P_m$$

Where

- P_u = factored normal load or moment
- γ_m = load factor for a particular type of load m
- P_m = load or moment for a particular type of load or moment

The factored load is then compared with the load capacity by the equation

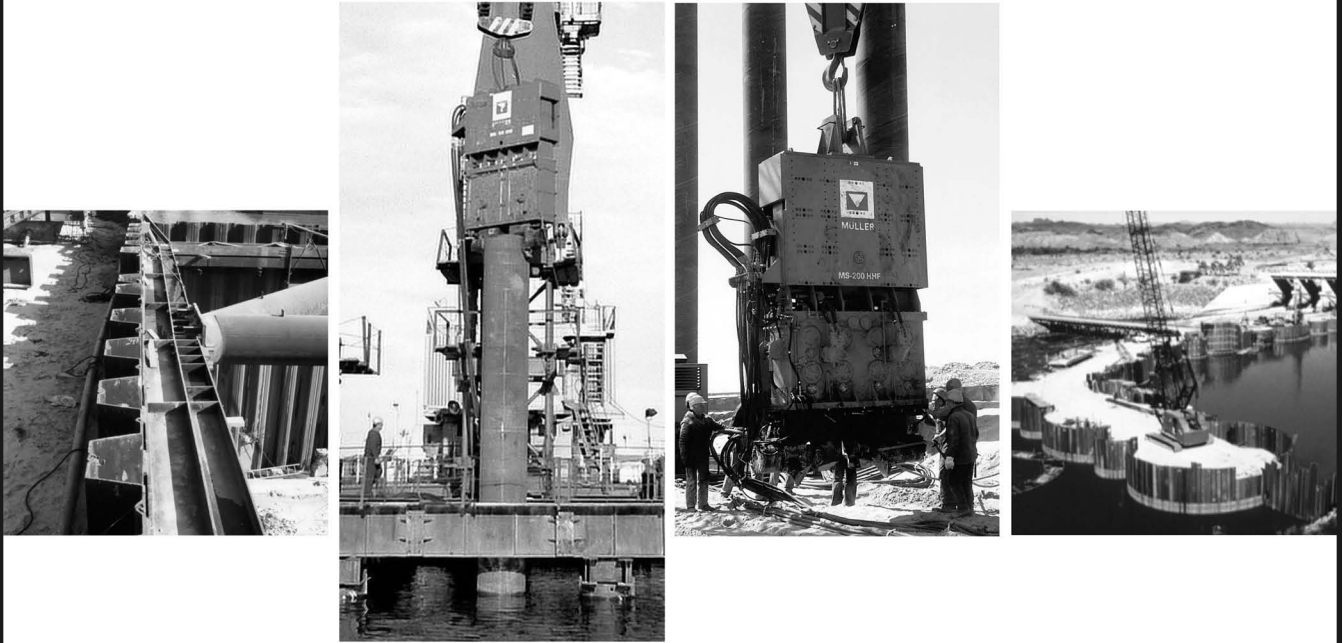
Equation 9-59:
$$P_u \leq \Phi P_n$$

Where

- Φ = resistance factor
- P_n = nominal normal load capacity, either from force or moment

It should be emphasized that these loads can either be force or moment loads.

Leading supplier of systems for port and special construction works.



For individual solutions we present tailor-made system offers for

- **Driven sections**

Steel Sheet Piles System LARSEN and HOESCH, UNION Straight Web Sections, Light Weight Sections, Trench Sheets, Wall-Sections, LARSEN Box-Piles, UNION-Box Piles, Peine Steel Bearing Piles PSt, Peine Steel Sheet Piling PSp including special services i.e. Coating, Welding, Interlock Sealing, Water Tightness etc.

- **Driving and extracting technology**

Vibrators, Excavator-mounted Vibrators, Ramming Hammers, Drilling Equipment, Leaders and Carriers, Power-packs

- **Anchor technology**

- **Trenching technology**

- **Flood protection**

ThyssenKrupp GfT Bautechnik GmbH

P.O. Box 10 22 53, D-45022 Essen

Altendorfer Str. 120, D-45143 Essen

Phone: +49 (2 01) 188-39 77

Fax: +49 (2 01) 188-37 72

export-bautechnik@tkx-gft.thyssenkrupp.com

www.tkgftbautechnik.com

ThyssenKrupp GfT Bautechnik

A company of ThyssenKrupp Services



ThyssenKrupp

Both the load factors γ and the resistance factors Φ are generally specified by the applicable code, be it ASCE, ACI or AASHTO. Normally the codes give several sets of factors for Equation 9-58 and the designer applies the equation for all of the load factor combinations to see which combination yields the highest factored load. The resistance factors for Equation 9-59 are usually a function of the application.

At this point the use of LRFD in sheet piling design is in a state of transition. Sheet pile walls are generally analysed for either failure by overturning or failure by overstressing the structure in bending. As is the case with conventional, allowable stress design (ASD) techniques, both of these need to be considered separately.

With overturning and wall length calculations, most codes and specifications currently continue to use factor of safety methods as are described in this book. As with other types of retaining walls and geotechnical structures, LRFD has been first applied to structural analysis, and so the use of LRFD for purely geotechnical design has lagged behind.

With the analysis of moment failure, for a sheet-piling wall with only static earth pressure loading, one possible procedure to analyse the wall is as follows:

1. Compute the normal moment P for the sheet-piling wall using the yield or other maximum strength of the material without the application of a factor of safety.
2. Compute the maximum moment using design techniques shown earlier and apply the applicable load factor to arrive at the factored load P_u using Equation 9-58.
3. Compare this with the normal moment multiplied by the resistance factor using Equation 9-59.

In the case of multiple loads (earth pressure, surcharge, seismic), the load factors for each of these are usually different; therefore, their influence on the structure will be differently accounted for than is the case with classical methods. One possible method of dealing with this problem is with superposition; however, keep in mind that different load distributions will result in differing locations for the maximum moment, and also combinations of moments may result in a maximum factored moment whose location is not the same as any of the maximum moments for each of the load types.

Chapter Ten:

Sheet Piling Design

By Soil-Structure Interaction Analysis

Introduction

The classical design procedures discussed in Chapter 7 rely on several simplifying and often contradictory assumptions regarding the behaviour of the wall/soil system. Some of the anomalies contained in the classical procedures are:

- *Incompatible pressures and displacements.* In both cantilever and anchored wall design, the soil pressures are assumed to be either the limiting active or passive pressure at every point without regard to the magnitude or direction of wall/soil displacements. In the case of an anchored wall, the tendency of wall motion to produce a passive condition above the anchor is ignored. The effects of wall and anchor flexibilities on soil pressures are ignored, and the displacements are calculated based on hypothetical, and perhaps, unrealistic supports.

- *Variations due to handling of surcharge.* We have seen that changes in the way surcharges are handled can affect the results in a substantial way (Example 14). Superposition is a well-established engineering practice but the “rules of thumb” used with classical methods can sometimes defeat the application of this principle.

- *Multiple anchors.* Approximate methods of design have been proposed for walls with multiple anchors, however these methods introduce further simplifying assumptions regarding system behaviour and suffer from the same limitations as those for single anchored walls. We will look at this in detail in Example 20.

10.2. Soil-Structure Interaction Method

The soil-structure interaction (SSI) method of analysis described in this chapter enforces compatibility of deflections, soil pressures, and anchor forces while accounting for wall and anchor flexibilities. The SSI method is based on a one-dimensional (1-D) finite element model of the wall/soil system consisting of linearly elastic beam-column elements for the wall, distributed nonlinear Winkler springs to represent the soil and nonlinear concentrated springs to represent any anchors.

10.3. Preliminary Information

Required preliminary information for application of the SSI method includes the system characteristics needed with classical methods as well as the penetration of the sheet piling, sheet piling material and cross-sectional properties (area,

moment of inertia, and modulus of elasticity), and anchor properties (tie rod area, modulus of elasticity, and flexible length). These data will be available for analysis of an existing wall/soil system. For use of the SSI method as a supplemental tool in design of a new system, an initial design using one of the classical methods may be performed and the SSI analysis used to refine the design.

10.4. SSI Model

The one-dimensional model of a typical 1-foot slice of the wall/soil system is shown in *Figure 10-1*. Nodes in the model are defined at the top and bottom of the wall, at soil layer boundaries on each side, at the groundwater elevation on each side, at the anchor elevations and at other intermediate locations to assure that the length of each beam element is no more than 6 inches.

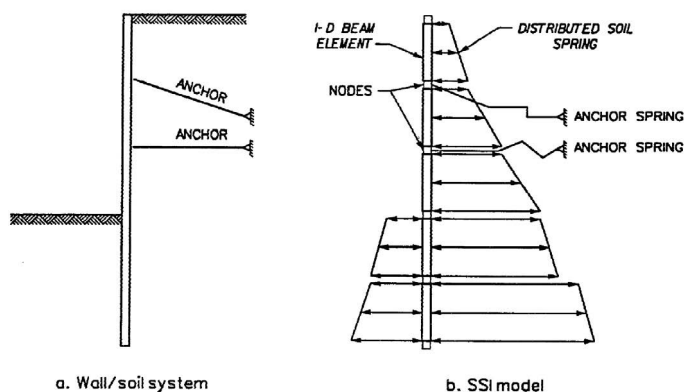


Figure 10-1: System for SSI Analysis

Lateral support is provided by the distributed soil springs and concentrated anchor springs. At present, there is no acceptable procedure to account for the effects of wall friction or adhesion in resisting vertical motions of the wall. The effects of these factors are included in the assessment of the lateral resistance of the soil. When an inclined anchor produces axial force in the piling, the bottom of the wall is assumed to be fixed against vertical translation. Conventional matrix structural analysis is used to relate the deformations of the system (defined by the horizontal and vertical translations and the

rotations of the nodes) to the applied external forces. This results in a system of $3N$ (for a model with N nodes) nonlinear simultaneous equations that must be solved by iteration.

10.5. Nonlinear Soil Springs

The forces exerted by the distributed soil springs vary with lateral wall displacement between the active and passive limits as shown in Figure 10-2. Active and passive soil pressures are calculated for a factor of safety of 1 by the procedures described in 1.5, including wall/soil friction and adhesion. The at-rest pressure p_o , corresponding to zero wall displacement, is obtained by solving Equation 4-1 for the horizontal stress for at-rest earth pressures, or

$$\text{Equation 10-1: } p_o = K_o \sigma'$$

The at-rest coefficient should be ascertained by the geotechnical engineer during soil exploration. In the absence of test data, K_o may be estimated by Equation 4-13. Although the variation of soil pressure between limits follows a curved path, the simplified bilinear representation shown in Figure 10-2 is used. The displacements at which limiting active or passive pressure are reached depend on the type of soil and the flexibility of the wall.

These influences are characterised by soil stiffness values and an estimate of the distance from the wall to which the soil

is significantly stressed (the interaction distance)¹⁰⁵. With known values of soil stiffness, the transition displacements, p_a and p_p in Figure 10-2, for any node in the model are obtained for sand as

$$\text{Equation 10-2: } \Delta_a = \gamma d \frac{p_o - p_a}{s_a p_v}$$

$$\text{Equation 10-3: } \Delta_p = \gamma d \frac{p_p - p_o}{s_p p_v}$$

and for clay as

$$\text{Equation 10-4: } \Delta_a = d \frac{p_o - p_a}{s_a}$$

$$\text{Equation 10-5: } \Delta_p = d \frac{p_p - p_o}{s_p}$$

Where

- $p_a, p_o,$ and p_p = active, at-rest, and passive pressures
- s_a and s_p = active and passive soil stiffnesses, respectively
- p_v = effective vertical soil pressure
- g = effective soil unit weight
- d = interaction distance, all at the node of interest

10.6. Nonlinear Anchor Springs

Anchors are represented as concentrated nonlinear springs in which the force varies with wall displacement as shown in Figure 10-3. The limiting tension force is given by

$$\text{Equation 10-6: } F_t = A_r f_y$$

Where

- A_r = the effective area of the tie rod
- f_y = yield stress of the material

The limiting force in compression F_c depends on the manner in which the tie rod is connected to the wales and the compressive axial load capacity of the tie rod (rod buckling) and may vary from zero to the yield value given in Equation 10-6. The displacements at which the linear variation of force ceases are given by

$$\text{Equation 10-7: } \Delta_t = \frac{F_t L_{tie}}{E_{tie} A_{tie}}$$

$$\text{Equation 10-8: } \Delta_c = \frac{F_c L_{tie}}{E_{tie} A_{tie}}$$

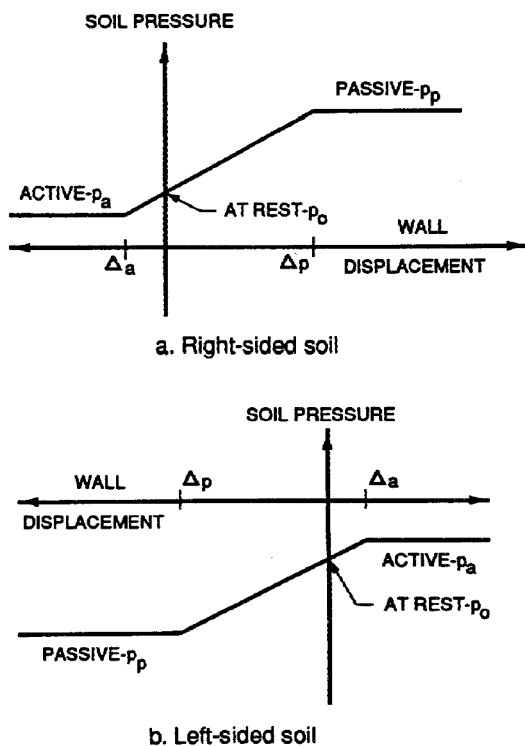
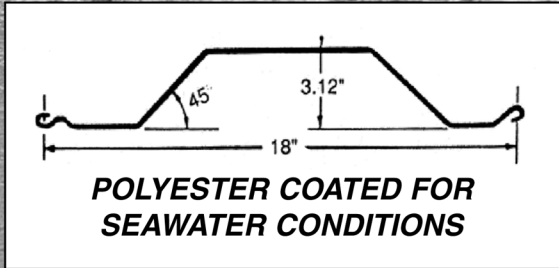
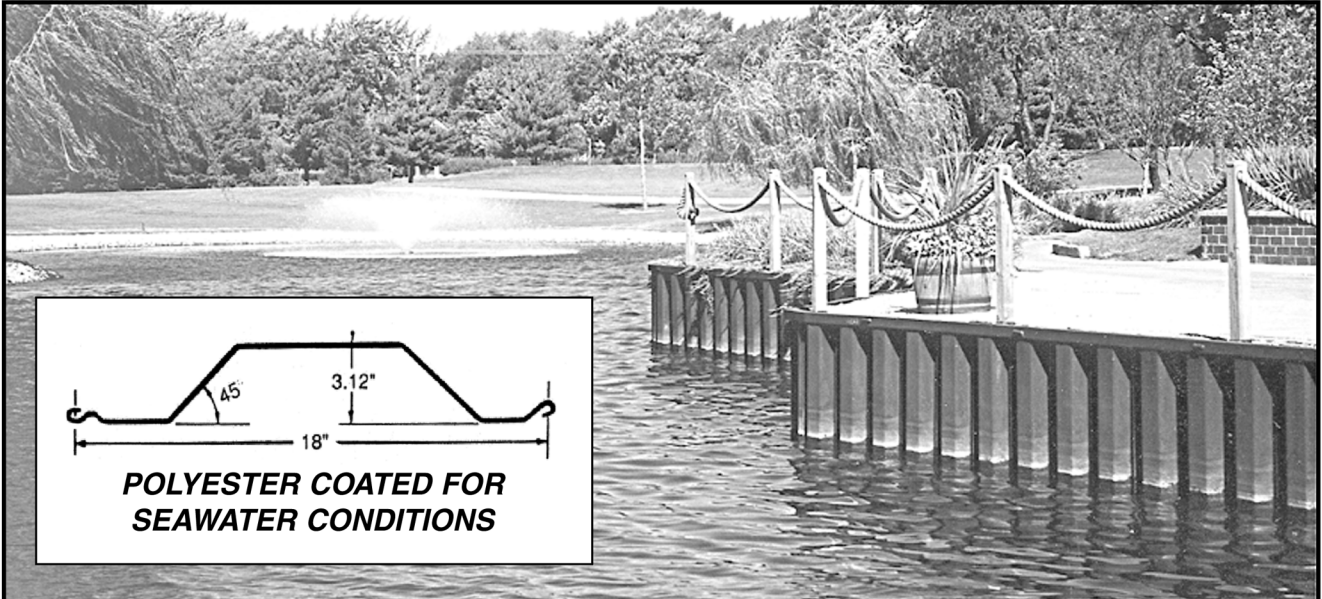


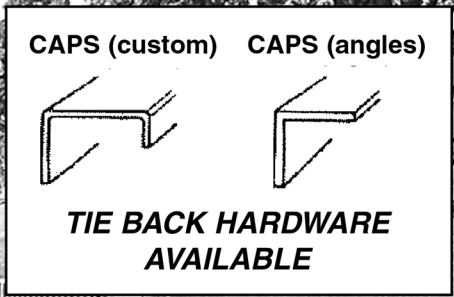
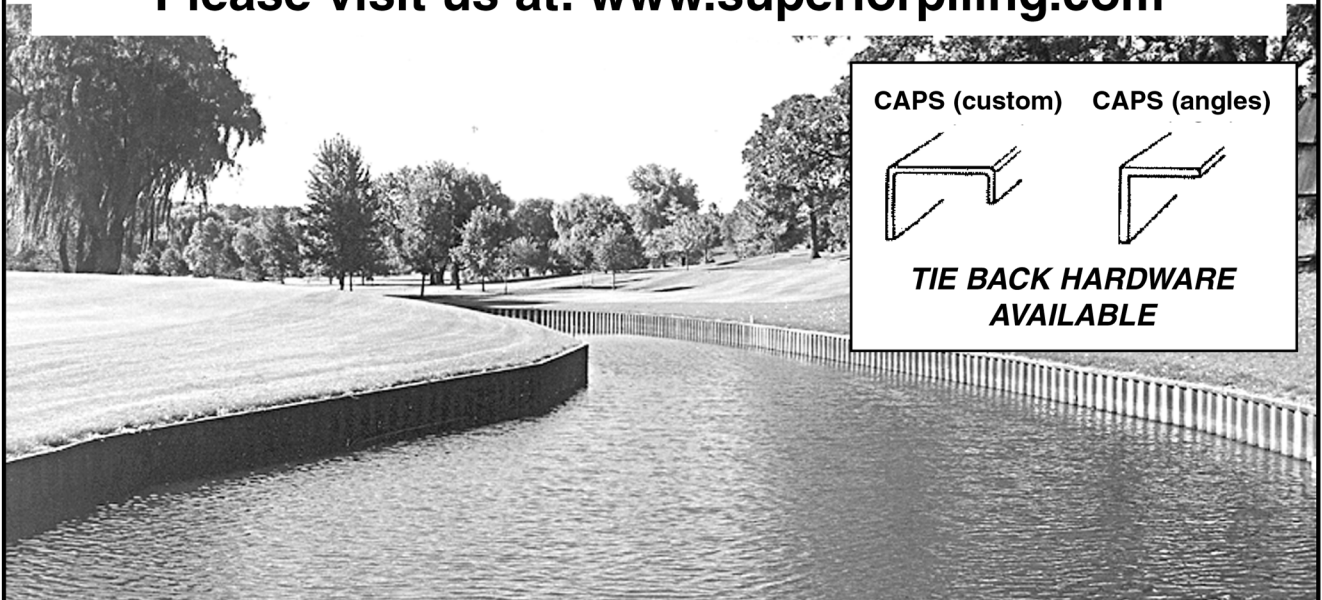
Figure 10-2: Distributed Soil Springs

¹⁰⁵Rules of thumb for estimating the interaction distance are provided by Dawkins, William P. (1992), "User's Guide: Computer Program for Winkler Soil-Structure Interaction Analysis of Sheet Pile Walls (CWALSSD)," U.S. Army Engineer Waterways Experiment Station, Vicksburg, MS. Representative soil stiffnesses are given by Terzaghi, K. 1955. "Evaluation of Coefficients of Subgrade Reaction," *Geotechnique*, Vol 5, pp 297-326.



SUPERIOR PILING, INC

7247 S. 78th AVENUE, BRIDGEVIEW, IL 60455
1-800-544-1196 • 708-496-1196 • FAX 708-496-1261
Please visit us at: www.superiorpiling.com



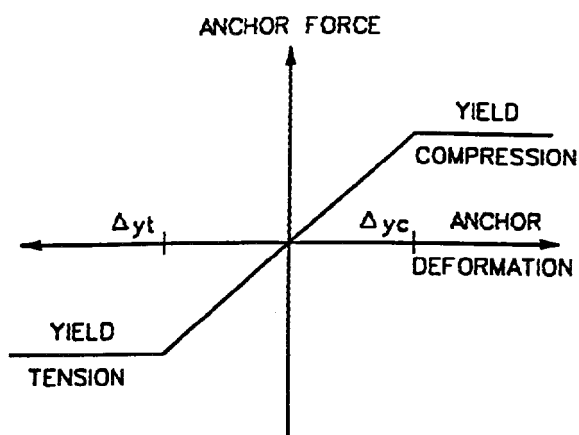


Figure 10-3: Anchor Spring

Where

- L_{tie} = length of tie rods attached to discrete anchors or the unbonded length of grouted anchors
- E_{tie} = modulus of elasticity of the rod
- A_{tie} = cross-sectional area of the rod

The force-deformation characteristic for cable tendons should be obtained from manufacturer's specifications.

10.7. Application of SSI Analysis

The SSI procedure provides solutions in which forces (bending moments, shears, anchor force, and soil pressures) are compatible with wall displacements at all points. In addition, solutions may be obtained by this method for stages intermediate to the final configuration as well as allowing for multiple anchors. However, it must be emphasized that the procedure is a "gravity turn-on" and does not take into account the cumulative effects of the construction sequence. The greatest uncertainty in the method is in selecting the soil stiffness parameters; consequently, the method should be used to evaluate the sensitivity of the solution to variations in soil stiffness. Terzaghi has indicated that the forces in the system are relatively insensitive to large variations in soil stiffness, although calculated displacements are significantly affected. Although the forces and displacements are compatible in the solution, it must be recognized that the calculated deflections are only representative of the deformation of the wall and do not include displacements of the entire wall/soil mass.

10.8. Comparison of SSI Analysis to Classical Results

The use of SSI analysis for sheet pile walls is a recent event, and comparison of classical methods with SSI analysis is only now beginning to be made. This section is a brief summary of one such study¹⁰⁶. The intent of the portion of the study sum-

marised here was to investigate the influence of the angle of wall friction on the results of classical design and 1-D SSI analyses of anchored retaining walls.

Data for the system to be considered for this study is shown in Figure 10-4 and Table 10-1. The effects of several permutations of wall friction angle and factors of safety were analyzed using the classical sheet pile analysis program CWALSHT¹⁰⁷. Coulomb coefficients were used for most of the analyses except for some of the passive coefficients, in which case log-spiral ones were used. Steel sheet piling, with an elastic modulus of 29,000 ksi and an allowable stress of 25 ksi was used.

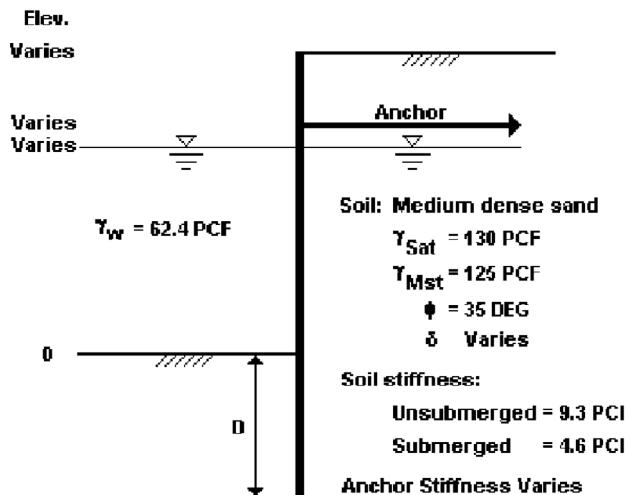


Figure 10-4: Wall/soil system

Table 10-1: System Parameters

Elevations, ft				
System	Wall Top	Anchor	Water	Anchor Stiffness, lb/in.
40-ft Wall	40	31.50	29.00	24x10 ³
30-ft Wall	30	23.50	21.75	18x10 ³
20-ft Wall	20	15.75	14.50	10x10 ³

SSI analyses using the computer program CWALSSI¹⁰⁸ (Dawkins 1994) were performed for the wall/soil system with depths of penetration from the classical design. Unfactored soil (i.e., active and passive factors of safety equal to 1) and wall friction values from the Coulomb and log-spiral theories were used. Both rigid and flexible anchors were considered. The flexible anchor stiffnesses were based on a steel rod with cross section area producing an anchor stress of approximately 25 ksi, based on the computed anchor forces and an effective length of 50 ft.

The maximum bending moments predicted by the classical Free Earth Method and the two SSI variations are nearly the same. The slight differences in shapes of the moment dia-

¹⁰⁶The study summarised here is Dawkins, W.P. (2001) Investigation of Wall Friction, Surcharge Loads and Moment Reduction Curves for Anchored Sheet-Pile Walls. Report ERDC/ITL TR-01-4. Vicksburg, MS: U.S. Army Corps of Engineers, Waterways Experiment Station, Engineer Research and Development Centre, Information Technology Laboratory.

¹⁰⁷Dawkins, W.P. (1991) "User's Guide: Computer Program for Design and Analysis of Sheet-Pile Walls by Classical Methods (CWALSHT) including Rowe's Moment Reduction." Instruction Report IITL-91-1, Vicksburg, MS: U.S. Army Engineer Waterways Experiment Station.

grams are a result of: the higher (passive) pressures above the anchor in the SSI analyses; the location of the resultant of the passive pressure distribution on the left side of the wall below the dredge line; and, the differences in penetration for the classical and SSI systems. Soil pressures below the anchor are full active values in all cases.

The following conclusions were based on the results of this limited study:

a. The relationships between depth of penetration, maximum bending moment, and anchor force with increasing wall friction angle are nearly linear.

b. An initial item of interest was whether the angle of wall friction could be adjusted to produce SSI moments that would more closely approximate the moments resulting from application of Rowe's moment reduction to the classical Free Earth moments. The results suggested the desired effect cannot be achieved for very flexible walls. For stiffer walls, there is little

or no reduction permitted, and both Classical and SSI analyses yield essentially the same maximum moments.

c. The anchor force predicted by the classical Free Earth Method is significantly lower than that indicated by the SSI analysis. Rowe gave reduction factors for anchor forces similar to his moment reduction curves. The effect of application of anchor force reduction factors has not been investigated. However, the results of this study suggest that reduction of the Free Earth anchor force would be unconservative. In all cases, the Free Earth Method significantly underestimates the anchor force as compared to the SSI method.

d. The SSI analysis cannot represent the behaviour of the system observed by Rowe. The Winkler model of the nonlinear soil cannot reproduce the conditions (which have been suggested to be the result of soil arching between the anchor and the passive zone below the dredge line) observed in Rowe's experiments.

¹⁰⁸Dawkins, W.P. (1994) "User's Guide: Computer Program for 1-D SSI Analysis of Sheet Pile Walls (CWALSSI)." Instruction Report ITL-94-6. Vicksburg, MS: U.S. Army Engineer Waterways Experiment Station.

Chapter Eleven: Anchor Systems and Tiebacks

11.1. General Considerations

Anchors provide permanent support to bulkheads and land walls, and are extensively used to support temporary walls at land excavation sites. The proper design of anchorage systems is vital to the safety of these structures. Virtually every failure of a retaining structure can be traced directly to failure of the support medium rather than failure of the wall itself. This section will describe both traditional methods of providing single anchorages utilizing tie rods and the relatively new soil or rock anchors.

11.2. Traditional Anchor Systems

In bulkhead design, three important results must be obtained:

1. The depth of penetration required for support of the wall at the base
2. The maximum bending moment in the wall which must be satisfied by an adequate section
3. The reaction at the upper support or anchor that must be transferred to the rear of the wall.

The purpose of anchorage systems is to take care of the reaction load (3). To accomplish this, anchorage systems generally have three components:

- (1) The anchor itself, which distributes the load from the sheet piling system to the soil;
- (2) The wale, which transfers the distributed load from the sheet pile wall to the “point loads” of the anchors and tie rods; and
- (3) The tie rod, which connects the wale and anchor and transfers the load from one to another.

Figure 11-1 shows some various configurations of anchorage systems. In the case of H-pile anchorages, the H-pile acts as both anchor and tie rod in a manner similar to uplift piles.

11.2.1. Tie Rods

The design methods we have considered report the load on each support as a “continuous” load along the wall, in units of force per unit length. In theory, we can use this load directly for the design of the tie rods:

$$\text{Equation 11-1: } T_{FES} = T$$

Where

- T_{FES} = tie rod load without factor of safety applied, lb/ft or kN/m

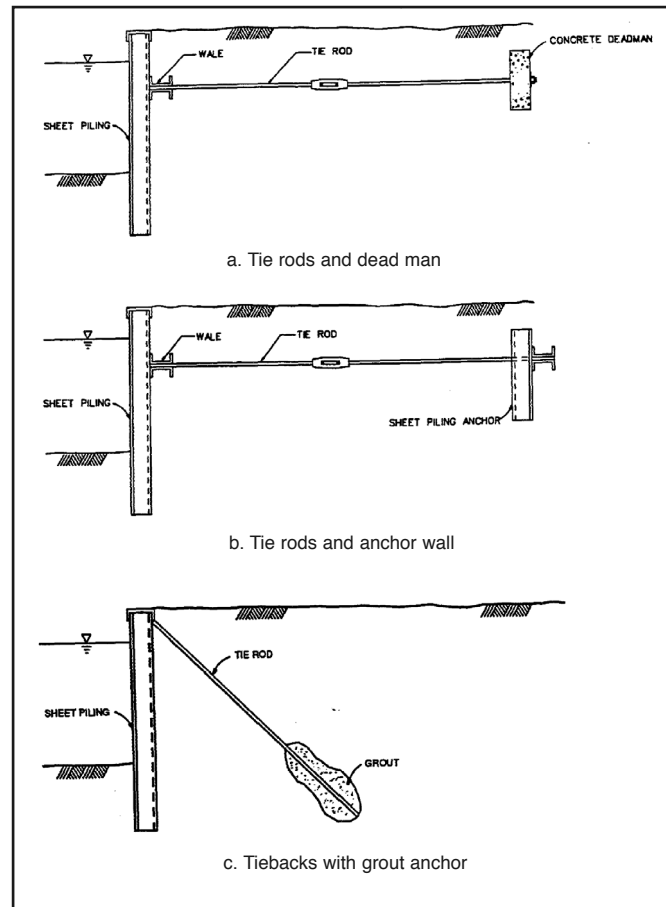


Figure 11-1: Typical Anchored Walls

- T = load at a support computed using the methods described previously, lb/ft or kN/m

In reality, however, the tie rod load is increased by a number of factors:

- The real distribution may be somewhat different and the corresponding anchor tension may be greater than that computed.
- The anchor pull may also increase because of repeated application and removal of heavy surcharges or an unequal yield of adjacent anchorages that causes over loading.
- The inclination of the tie rod-anchor system from the horizontal, which is common in anchorage systems (see Figure 11-2.)

Because of these possibilities, Equation 11-1 should be modified to be

$$\text{Equation 11-2: } T_{design} = \frac{T_{FES} F_{tr}}{\cos \alpha_{tie}}$$

EXtremely Versatile

ICE'S EX-SERIES
of excavator-mounted augers is punching holes in the idea that you need a separate drilling rig to get the job done.



- No gears or gear boxes
- Uses existing hydraulics
- 2-speed (optional)
- 80,000 lb maximum crowd force
- Seven models to match your excavator
- Available in HEX or API connector
- One-year warranty

MODEL	MAX TORQUE	POWER hp	CROWD FORCE	SPEED rpm	WEIGHT
EX-5	5,000 ft-lb	44	80,000 lbs	186	995
EX-8	8,300 ft-lb	88	80,000 lbs	111	1,495
EX-12	12,000 ft-lb	131	80,000 lbs	78	1,522
EX-17	17,000 ft-lb	146	80,000 lbs	56	1,914
EX-25	25,000 ft-lb	184	80,000 lbs	39	2,392
EX-40	40,000 ft-lb	184	80,000 lbs	23	2,697
EX-50	50,000 ft-lb	184	80,000 lbs	20	3,250

Call ICE to see why the new **EX-SERIES** is an **EXcellent** addition to your tool box.



INTERNATIONAL CONSTRUCTION EQUIPMENT, INC.
www.iceusa.com

301 Warehouse Drive • Matthews, NC 28104
Phones: 888 ICEUSA1
& 704 821-8200
Fax: 704 821-8201 • e-mail: info@iceusa.com



Matthews NC • Lakeland FL • Metairie LA • Seattle WA • New Town Square PA • Sayreville NJ • Houston TX
Fort Wayne IN • Virginia Beach VA • Boston MA • Montreal Quebec • Singapore • Kuala Lumpur • Shanghai

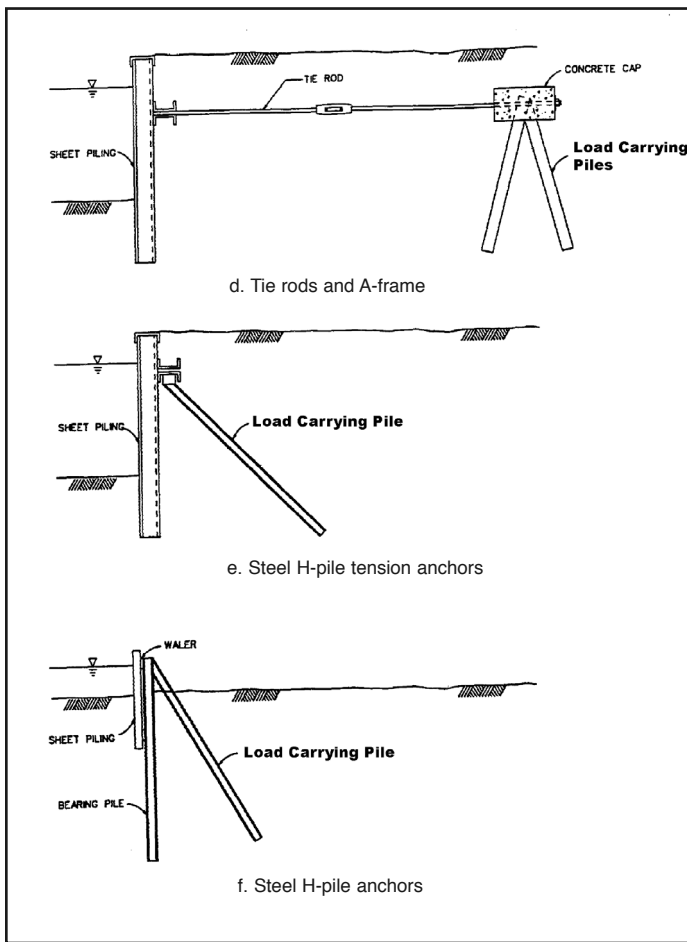


Figure 11-1: Typical Anchored Walls (continued)

Where

- T_{design} = design load on the tie rod, lb/ft or kN/m
- F_{tr} = factor to account for variations in the loading
 $\phi = 1.3$ for both static and earthquake loading conditions
 $\phi = 1.5 - 2$ at splices and connections where stress concentration can develop
- α_{tie} = Inclination of tie rod with the horizontal, degrees

From this, the cross-sectional area of the tie rod is computed by the equation

Equation 11-3:
$$A_{tie} = \frac{T_{design} L}{\sigma_{allow}}$$

Where

- A_{tie} = cross-sectional area of the tie rod, in² or m²
- σ_{allow} = allowable stress of the tie rod material, psi or kPa = 60% of the yield strength of the material. This is recommended for both static and earthquake loading (the latter by the Japanese code). For ASTM A-36, this is $(0.6)(36) = 21.6$ ksi. In some cases, the allowable stress is only 40% of the yield.
- L = distance between tie rods, ft or m. This should generally be no greater than 12' (3.6 m).

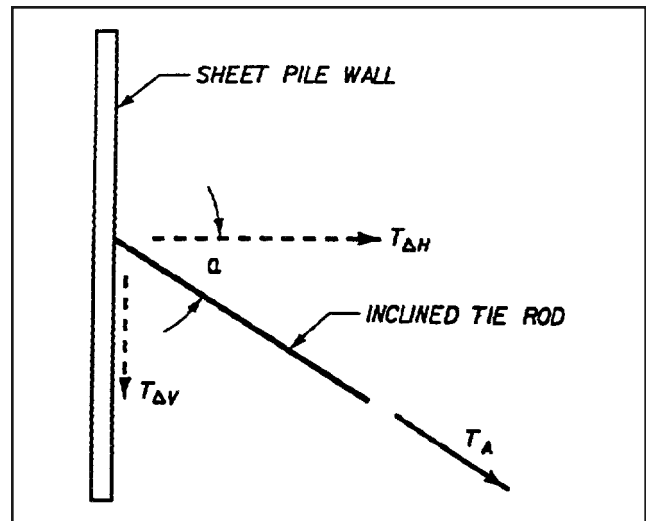


Figure 11-2: Anchor Force Components for Inclined Anchors

Any soft soil below the tie rods, even at great depth, may consolidate under the weight of recent backfill, causing the ground to settle. A small settlement will cause the tie rods to sag under the weight of the soil above them. This sagging will result in an increase in tensile stress in the tie rod as it tends to pull the sheeting. In order to eliminate this condition, one of the following methods may be used:

1. Support the tie rods with light vertical piles at 20 to 30 foot intervals
2. Encase the anchor rods in large conduits

Tie rods are usually round structural steel bars with upset threaded ends to avoid a reduction in the net area due to the threads. In order to take up slack, turnbuckles are usually provided in every tie rod.

11.2.2. Wales

The horizontal reaction from an anchored sheet pile wall is transferred to the tie rods by a flexural member known as a wale. It normally consists of two spaced structural steel channels placed with their webs back to back in the horizontal position. Figure 11-3 shows common arrangements of wales and tie rods located on both the inside and outside of a sheet pile wall. The channels are spaced with a sufficient distance between their webs to clear the upset end of the tie rods. Pipe segments or other types of separators are used to maintain the required spacing when the channels are connected together. If wales are constructed on the inside face of the sheet piling, every section of sheet piling is bolted to the wale to transfer the reaction of the piling. While the best location for the wales is on the outside face of the wall, where the piling will bear against the wales, they are generally placed inside the wall to provide a clear outside face.

For sizing purposes, the response of a wale may be assumed to be somewhere between that of a continuous beam

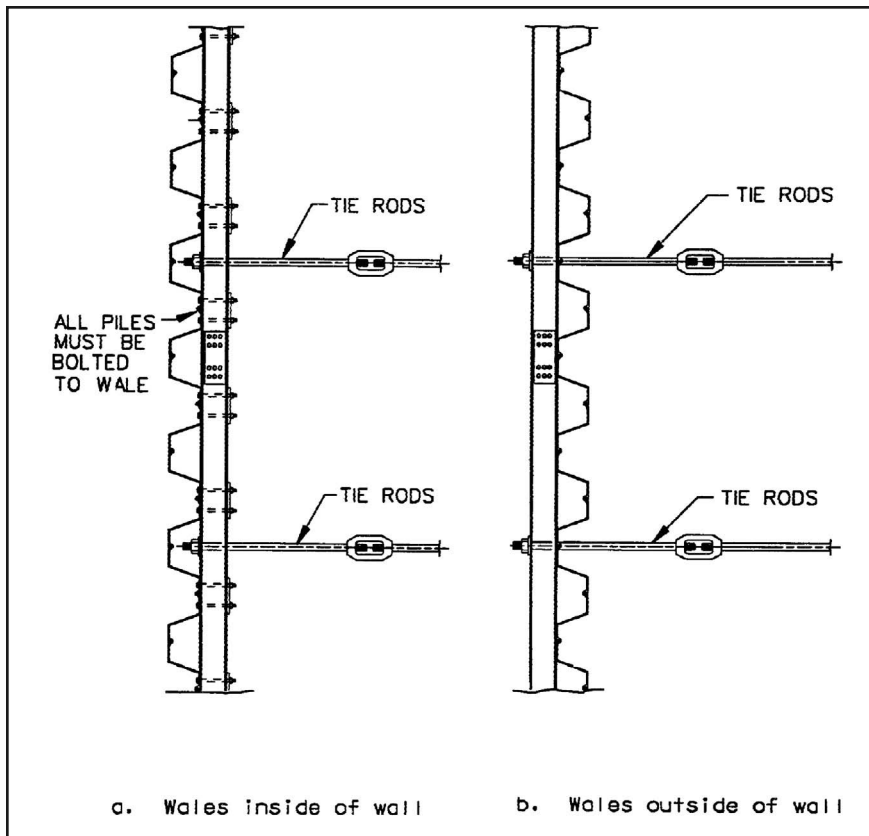


Figure 11-3 Typical Wale Details

on several supports (the tie rods) and a single span on simple supports. Therefore, the maximum bending moment for design will be somewhere between

$$\text{Equation 11-4: } \frac{T_{FES} L^2}{10} < M_{\max} < \frac{T_{FES} L^2}{8}$$

The above expressions are only approximations. An exact analysis would have to take into account the elasticity of the tie rods, the rigidity of the wale and the residual stresses induced during bolting operations.

The required section modulus of the wale is

$$\text{Equation 11-5: } S = \frac{M_{\max}}{\sigma_{\text{allow}}}$$

Where

- S = the section modulus of the wale for both channels
- σ_{allow} = allowable steel bending stress

If we combine Equation 11-4 and Equation 11-5, the section modulus is given by

$$\text{Equation 11-6: } S = \frac{T_{FES} L^2}{10\sigma_{\text{allow}}}$$

Wales are connected to the sheet piling by means of fixing plates and bolts. Each bolt transmits a pull proportional to the width, ℓ' , of a single sheet pile, and equal to

$$\text{Equation 11-7: } R_b = T_{FES} \ell' (FS)$$

Where

- R_b = pull in pounds per bolt
- ℓ' = The driving distance of a single sheet pile (if each section is bolted)
- FS = a desired safety factor to cover stresses induced during bolting (between 1.2 and 1.5)

The fixing plate may be designed as a beam simply supported at two points (the longitudinal webs of the wale) and bearing a single load, R_b , in the centre.

The wales are field bolted at joints known as fishplates or splices. It is preferable to splice both channels at the same point and place the joint at a recess in the double piling element. Splices should be designed for the transmission of the bending moment.

11.2.3. Anchors

There are several types of anchors in use; however, there are two design parameters that are common to both:

- The location of the anchor relative to the failure surface of the sheet pile wall. In order for an anchorage system to be effective, it must be located outside of the potential active failure zone developed behind a sheet pile wall.

Figure 1-15(b) and Figure 1-18(a) show examples of installations that will not provide the full anchorage capacity required because of failure to recognize the above considerations. Its capacity is also impaired if it is located in unstable ground or if the active failure zone prevents the development of full passive resistance of the system. This is discussed more fully for the various types

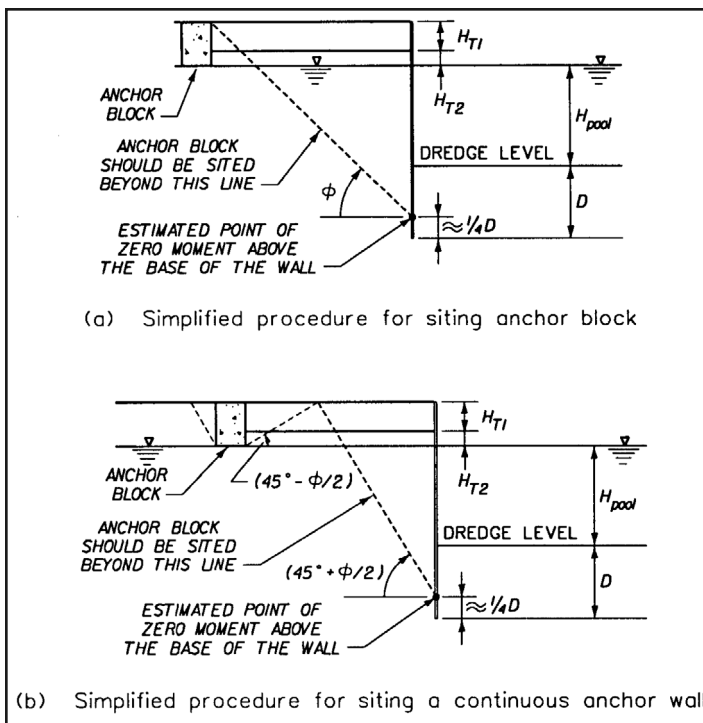


Figure 11-4:

Analysis of Anchor Blocks and Continuous Anchor Wall

of anchors. There are two criteria for determining the proper location of an anchor:

- o Anchor blocks, where each tie rod is attached to an individual block not connected to another. These should be set back from the wall as shown in Figure 11-4(a). The full resistance of the anchor block is developed if the anchorage is outside of the broken line. If the anchorage is within this area, only partial resistance is developed due to the intersection of the active and passive failure wedges. However, the theoretical reduction in anchor capacity may be analytically determined¹⁰⁹.
- o Continuous walls, either concrete or steel sheeting, where the tie rods are connected to a wall that is parallel to the sheet pile wall. These should be set back from the wall as shown in Figure 11-4(b); if this is done, the full passive pressure of the anchor wall is developed. If the wall is closer than this, the continuous wall capacity is reduced. As is the case with anchor blocks, partial resistance can be developed if the failure zone of the anchor is within the failure zone of the wall.¹¹⁰
- o A more conservative approach for either type of anchor is to combine the two criteria. We will illustrate this in Example 15.

The design of the active and passive pressures that give the anchor the resistance it requires. There are three methods used to do this:

- o The “classical” method, based on active and passive pressures. In essence the anchor is assumed to be a very short retaining wall; the net capacity is thus the difference

between the passive pressure on the side with the tie rod and the active pressure on the opposite side. For continuous walls, this is expressed as

$$\text{Equation 11-8: } T_{ult-a} < P_p - P_a$$

If the wall is set back as shown in Figure 11-4, for a homogeneous cohesionless soil, the active and passive soil forces are

$$\text{Equation 11-9: } P_a = \frac{\gamma(H_{T1} + H_{T2})^2}{2} K_a$$

and

$$\text{Equation 11-10: } P_p = \frac{\gamma(H_{T1} + H_{T2})^2}{2} K_p$$

The value of K_p is computed either using Rankine conditions or Figure 18-16 and $\delta/\phi = -0.5$. If the anchorage wall penetrates below the water table and/or a soil layer, the equations should be modified accordingly.

This force acts at a distance of $2(H_{T1} + H_{T2})/3$ from the surface, and this is the optimum point to locate the tie rod. In the case where the soils are not homogeneous around the anchor or the water table intervenes, the tie rod connection to the anchorage should be ideally located at the point of the resultant earth pressures acting on the anchorage. For design in cohesive soils, both the immediate and the long-term pressure conditions should be checked to determine the critical case. If the soil has both internal friction and cohesion, a trial wedge method should be employed.

- o The method of Ovesen, based on model tests. This is discussed in 11.2.4. The underlying principle is the same as the first method but empirical data is included to improve the results.
- o The method specific to short deadmen anchors near the ground surface, discussed in 11.2.3.3.

The active and passive pressure distributions for granular and cohesive soils are also shown in Figure 11-6. A safety factor of 2 – 2.5 against failure is recommended; i.e.,

$$\text{Equation 11-11: } T_{ult-a} > 2T_{FES} \text{ or } T_{ult-a} > 2.5T_{FES}$$

For seismic loadings (see Example 19 for design details)

$$\text{Equation 11-12: } T_{ult-a} = T_{FES}$$

11.2.3.1. Anchor Blocks (Deadmen Anchors)

Care must be exercised to see that the anchor block or deadman does not settle after construction. This is generally not a problem in undisturbed soils, however, where the

¹⁰⁹ Terzaghi, K., Theoretical Soil Mechanics, p. 232.

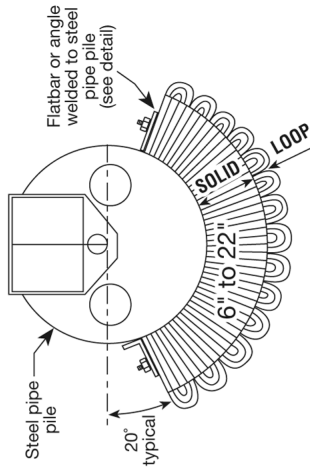
¹¹⁰ NAVFAC DM 7.02, Foundations and Earth Structures

MARINE FENDERS OFFSHORE OR DOCKSIDE

MODEL 153



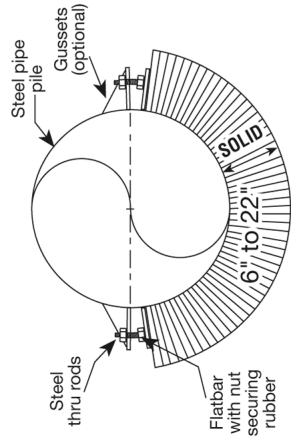
153 TYPE "A" WELD-ON



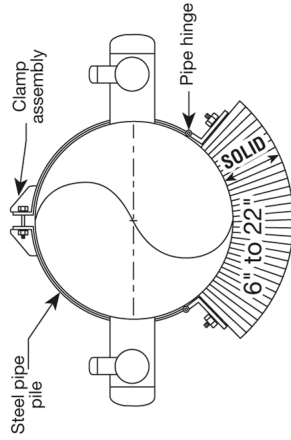
MODEL 153 PIPE PILE/DOLPHIN FENDERS

Weld-On, Bolt-On, Strap-On
Applications: Ferry Landings, Barge Facilities, Mooring Dolphins, Bridge Foundations

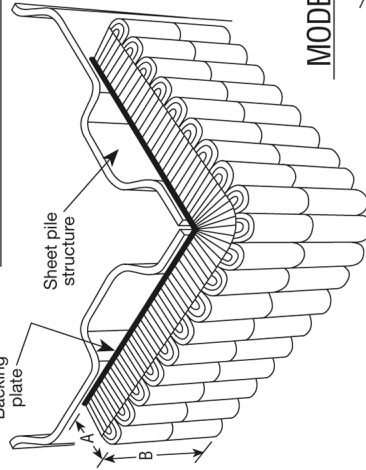
153 TYPE "B" BOLT-ON



153 TYPE "C" STRAP-ON



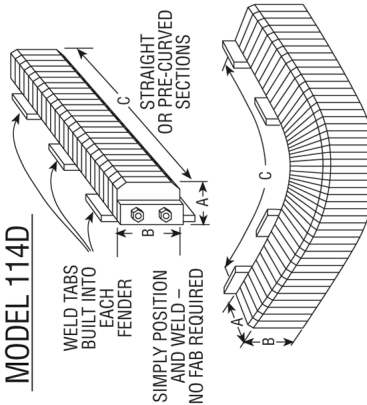
MODEL 114 SHEET PILE FENDERS



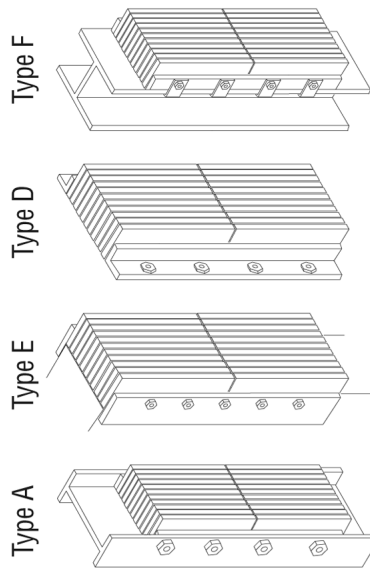
Weld-On or Bolt-On Applications
Designed and Engineered to Your Specifications

WELD-ON D-GUARD FENDERS

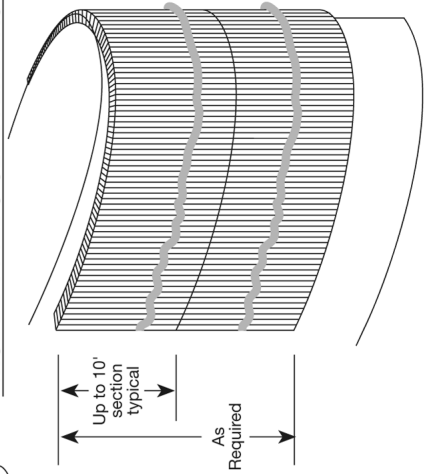
MODEL 114D



MODEL 115 I-BEAM/STRUCTURAL FENDERS



MODEL 114LDC CELL FENDERS



1-800-426-3917

Email: sales@schuytterrubber.com
Website: www.schuytterrubber.com

16901 Wood-Red Rd.
Woodinville, WA 98072
425-488-2255 Fax: 425-488-2424



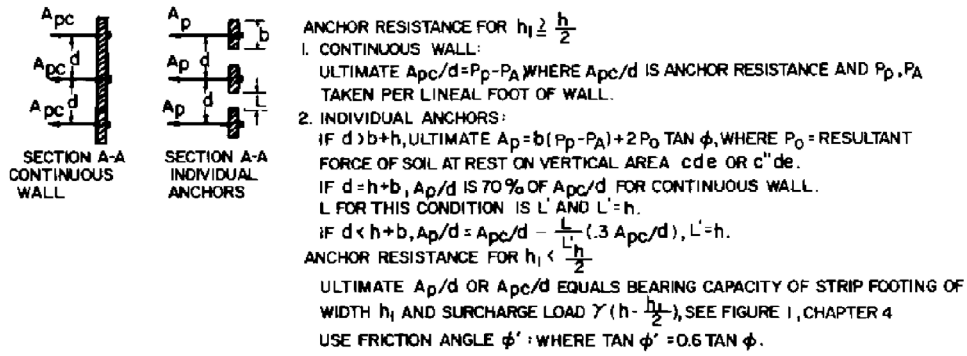


Figure 11-5: Effects of Depth and Spacing of Anchor Blocks

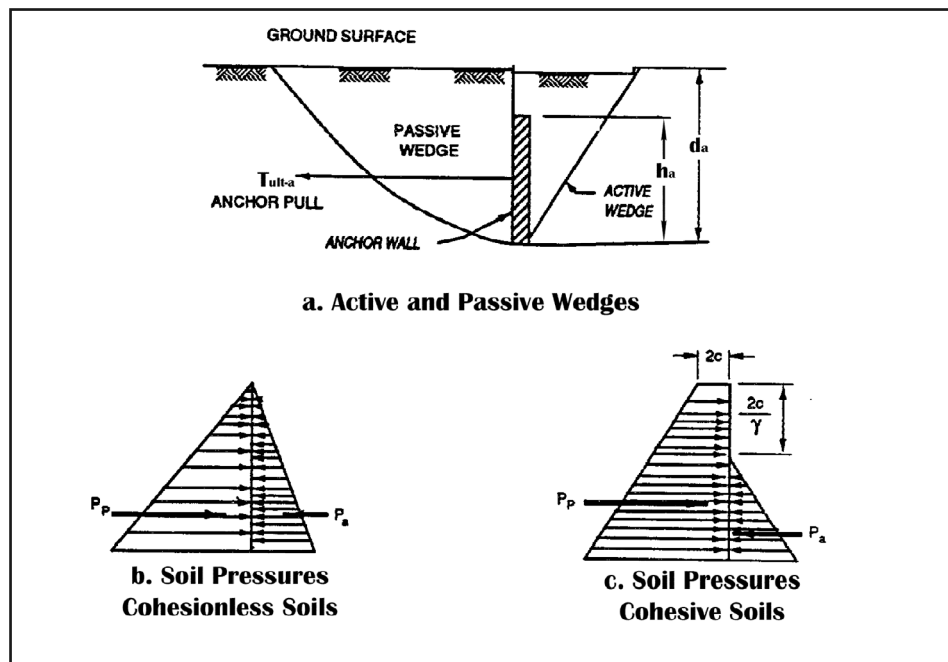


Figure 11-6: Continuous Deadman Anchor near Ground Surface

anchorage must be located in unconsolidated fill, piles may be needed to support the blocks. In addition, the soil within the passive wedge of the anchorage should be compacted to at least 90 percent of the maximum density unless the deadman is forced against firm natural soil. Figure 11-5 shows other important criteria for the design of both continuous and individual deadmen.

11.2.3.2. Continuous Deadmen near Ground Surface

Short steel sheet piles driven in the form of a continuous wall may be used to anchor tie rods. The tie rods are connected with a waling system similar to that for the “parent” wall, and resistance is derived from passive pressure developed as the tie rod pulls against the anchor wall. To provide some sta-

bility during installation of the piling and the wales, pairs of the piling should be driven to a greater depth at frequent intervals. A continuous deadman is shown in Figure 11-6.

For the case of

Equation 11-13: $h_a > 0.6 \cdot d_a$

one can assume the deadman extends to ground surface and compute the ultimate capacity of the deadman according to Equation 11-8.

11.2.3.3. Short Deadmen near Ground Surface

Figure 11-7 shows a deadman of length, L, located near the ground surface, subjected to an anchor pull, T. Experiments have indicated that at the time of failure, due to edge effects,

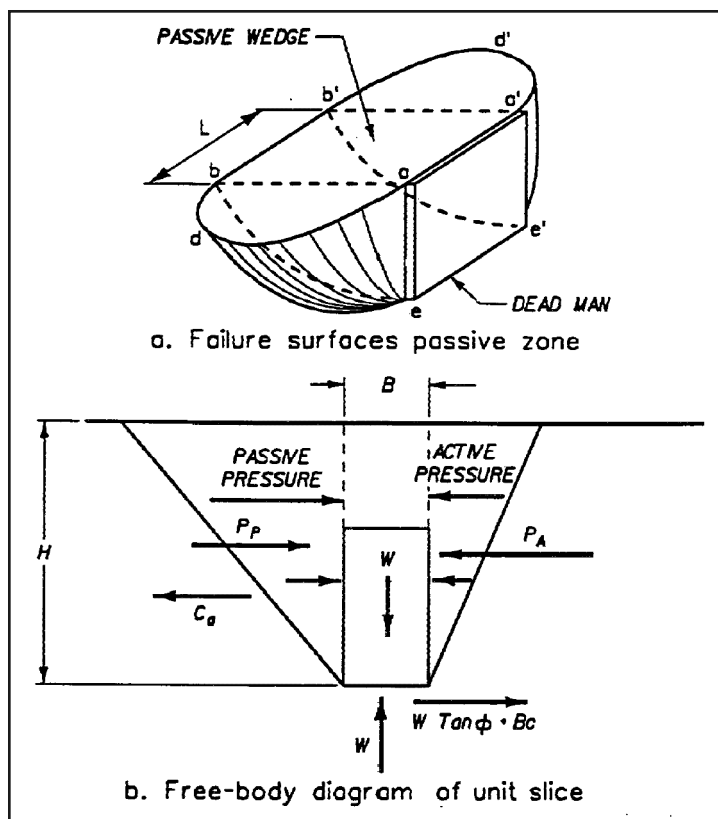


Figure 11-7: Short Deadman near Ground Surface

the heave of the ground surfaces takes place in an area as shown. The surface of sliding at both ends is curved.

Integration of the resistance along these curved sliding surfaces results in the following expression for the ultimate capacity of short deadmen in granular soils

$$A_{ult} \leq \ell(P_p - P_a) + \frac{\gamma K_o H_d^3}{3} (\sqrt{K_p} + \sqrt{K_a}) \tan \phi$$

Equation 11-14:

where

- A_{ult} = ultimate capacity of the deadman, pounds
- ℓ = length of the deadman, feet
- P_p, P_a = total passive and active pressure, pounds per lineal foot
- K_o = coefficient of earth pressure at rest = 0.4 for design of deadman
- γ = unit weight of soil, pounds per cubic foot
- K_p, K_a = coefficients of passive and active earth pressure
- H_d = height of deadman, feet
- ϕ = angle of internal friction

For cohesive soils, the cohesive resistance should replace the second term in the above expression, thus

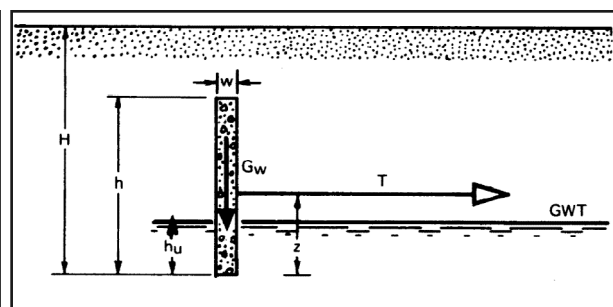


Figure 11-8: Geometrical Parameters for an Anchor Slab

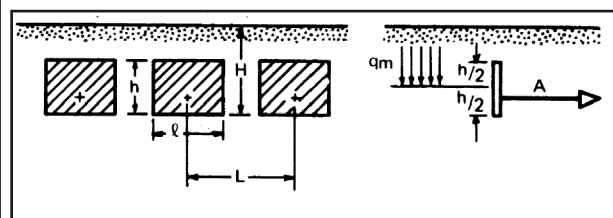


Figure 11-9 Geometrical Parameters for Anchor Slabs with Limited Height and Length

$$\text{Equation 11-15: } A_{ult} \leq L(P_p - P_a) + 2cH^2$$

Where c = the cohesion of the soil, pounds per square foot

11.2.4. Anchor Slab Design Based on Model Tests

11.2.4.1. General Case in Granular Soils

N. K. Ovesen¹¹¹ conducted 32 different model tests in granular soil and developed a procedure for designing anchor slabs located in a zone where the anchor resistance can be fully mobilized. The proposed method considers that the earth pressure in front of the slab is calculated based on a rupture surface corresponding to a translation of the slab.

This method can be used to solve the general case in Figure 11-8 for rectangular anchors of limited height and length located at any depth as shown in Figure 11-9. Surface loads behind the anchor slab are not included in this publication since their influence is small on the anchor resistance for granular soils with an angle of internal friction equal to or greater than 30 degrees.

Nomenclature:

- A = resultant anchor force per slab, lbs.
- GWT=ground water table
- G_w = weight per foot of wall of the anchor plus the soil on top of the slab, lbs. per foot
- H = distance from base of slab to ground surface, ft.
- L = distance between centres of two consecutive slabs, ft.

¹¹¹Ovesen, N., and Krebs (1964) Anchor Slabs Calculations and Model Tests. The Danish Geotechnical Institute, Bulletin No. 16.

- T = resultant anchor force, lbs. per foot
- W = thickness of anchor slab, ft.
- Z = distance from base of slab to resultant anchor force, ft.
- h_u = distance from base of slab to ground water table, ft.
- h = actual height to anchor slab, ft.
- ℓ = actual length of anchor slab, ft.
- q_m = vertical effective stress in earth at midpoint of actual height of anchor slab, lbs. per square foot
- γ = Unit weight of soil, lbs. per cubic foot
- γ' = Submerged unit weight of soil, lbs. per cubic foot

Ovesen suggests that a two-step procedure be used to find the ultimate resistance of the anchor per slab:

1. The dimensionless anchor resistance factor, R_o , is determined for the “basic case”. The basic case is a continuous strip, $\ell = L$, extending the full height, $h = H$, of the anchor.
2. The dimensionless anchor resistance factor, R, which is dependent upon R_o is calculated for the actual anchor dimensions under consideration. Knowing R, the ultimate resistance of the anchor slab A_{ult} can be calculated.

A similar two-step procedure is used to find Z, the location of the line of the action of the anchor tie-rod force. The application of Ovesen’s method is described below.

- A. Determine the dimensionless anchor resistance factor, R_o , for the “basic case”. For a given angle of internal friction, ϕ , and angle of wall friction, δ calculate $\tan \delta$, and use *Figure 11-10* to obtain the earth pressure coefficient, K_g . Calculate the Rankine active earth pressure coefficient K_a using Equation 5-1 and then solve for R_o ,

$$\text{Equation 11-16: } R_o = K_\gamma - K_a$$

For those cases where the tangent of the angle of wall friction, $\tan \delta$ is not known, first calculate the normal and tangential active earth pressure per foot of wall on the back of the slab,

$$\text{Equation 11-17: } P_A = P_H K_a$$

$$\text{Equation 11-18: } F_A = - P_A \tan \phi$$

Calculate G_w , which is the weight per foot of wall of the anchor plus the soil on

$$\text{Equation 11-19: } K_\gamma \tan \phi = \frac{G_w - F_A}{P_H}$$

Use *Figure 11-10* to obtain K_γ .

- B. Calculate the hydrostatic earth pressure per foot of wall,

$$\text{Equation 11-20: } P_H = \frac{\gamma H^2}{2} - \frac{\gamma_w h_u^2}{2}$$

In the case where the anchor slab does not penetrate the water table, $h_u = 0$ and the second term is ignored.

- C. Calculate, T_o , the ultimate anchor resistance per foot of wall for the “basic case”,

$$\text{Equation 11-21: } T_o = P_H R_o$$

- D. Calculate the dimensionless resistance factor, R, for the actual anchor slab dimensions is then calculated by the formula³⁹ below or by the use of *Figure 11-11* through *Figure 11-14*, which is Equation 11-22 plotted for various values of ℓ/L , ℓ/h , and h/H .

Equation 11-22:

$$\frac{R}{R_o} = 1 + R_o^{\frac{2}{3}} \left(1.1E^4 + \frac{1.6B}{1 + \frac{5\ell}{h}} + \frac{0.4R_o E^3 B^2}{1 + \frac{\ell}{20h}} \right)$$

Where

$$\text{Equation 11-23: } E = 1 - \frac{h}{H}$$

And

$$\text{Equation 11-24: } B = 1 - \left(\frac{\ell}{L} \right)^2$$

- E. The ultimate anchor resistance per slab, A_{ult} is computed using

$$\text{Equation 11-25: } A_{ult} = q_m h \ell R$$

Where

$$\text{Equation 11-26: } q_m = \gamma \left(H - \frac{h}{2} \right)$$

The ultimate anchor resistance per foot of wall T_{ult} is equal to,

$$\text{Equation 11-27: } T_{ult} = \frac{A_{ult}}{L}$$

- F. The location of Z shown in *Figure 11-8*, which is the line of action of the anchor tie-rod force, can be obtained directly from *Figure 11-15* when the ground water table is at or below the anchor slab base ($h_u = 0$). The main purpose of this location is to place the location of the tieback in the same place as the resultant force.

Use the following method to find Z when the ground water table is above the anchor slab base ($h_u > 0$). Calculate M_H , the hydrostatic earth pressure moment, about the base of the anchor *Figure 11-8*.

$$\text{Equation 11-28: } M_H = \frac{\gamma H^3}{6} \left(1 - \left(1 - \frac{\gamma'}{\gamma} \right) \left(\frac{h_u}{H} \right)^3 \right)$$

HPSI Vibros



from a
"Little Guy"

to a
"BIG Guy"



Whether it's an excavator mounted vibratory for driving lightweight vinyl or aluminum sheet piling on up to a 20,000 in. lb. machine for driving large diameter caisson, we have a vibro suitable for your job.

SALES & RENTALS

(Distributors throughout North America)

From "The Engineers of Pile Driving Equipment"™

HYDRAULIC POWER SYSTEMS, INC.

Kansas City Offices and Plant
1203 Ozark
N. Kansas City, MO 64116
Phone (816) 221-4774
Fax (816) 221-4591
E-mail info@hpsi-worldwide.com
<http://www.hpsi-worldwide.com>



International & Domestic Sales
745 U.S. Hwy 1
N. Palm Beach, FL 33408
Phone (561) 687-5525
Fax (561) 841-3479
E-mail info@hpsi-worldwide.com
<http://www.hpsi-worldwide.com>

*Vibratory Pile Hammers • Hydraulic Augers • Winch Systems
Custom Manufacturing • Hydraulic Impact Hammers • Lead Systems*

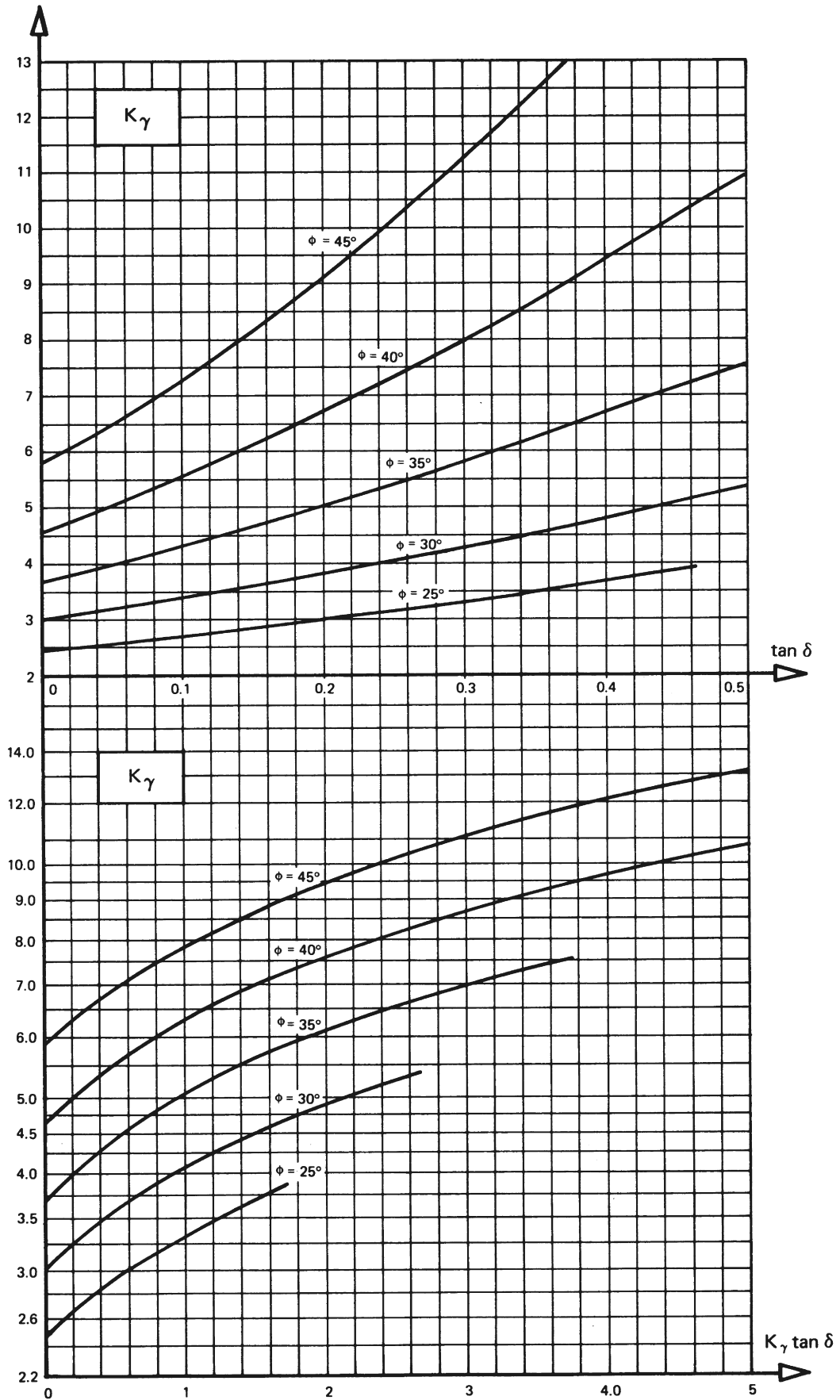


Figure 11-10: Earth Pressure Coefficients for the Normal Earth Pressure in Front of an Anchor Slab

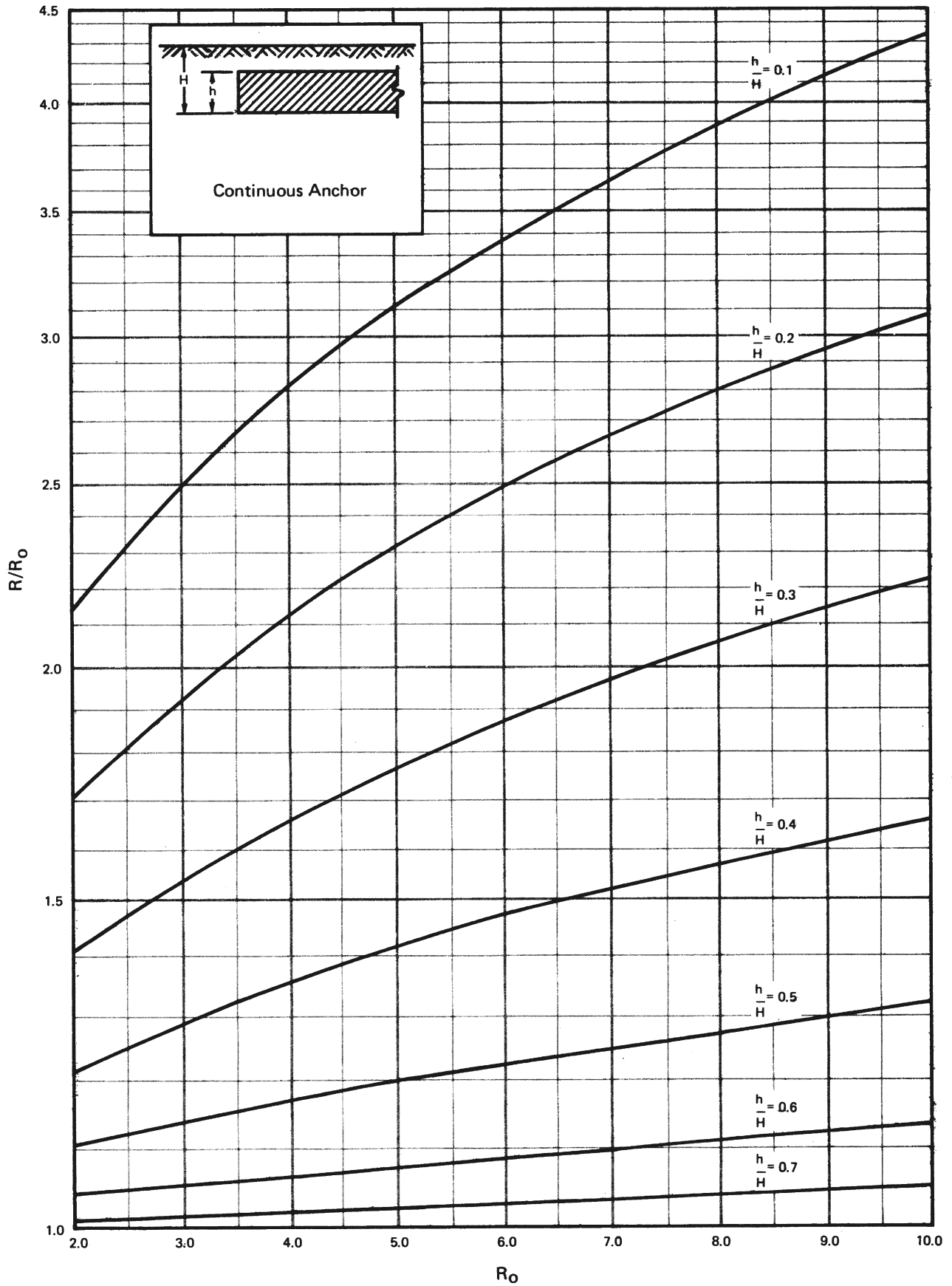


Figure 11-11: Dimensionless Resistance Factor Ratio for Continuous Anchor Slab, $l/L = 1$

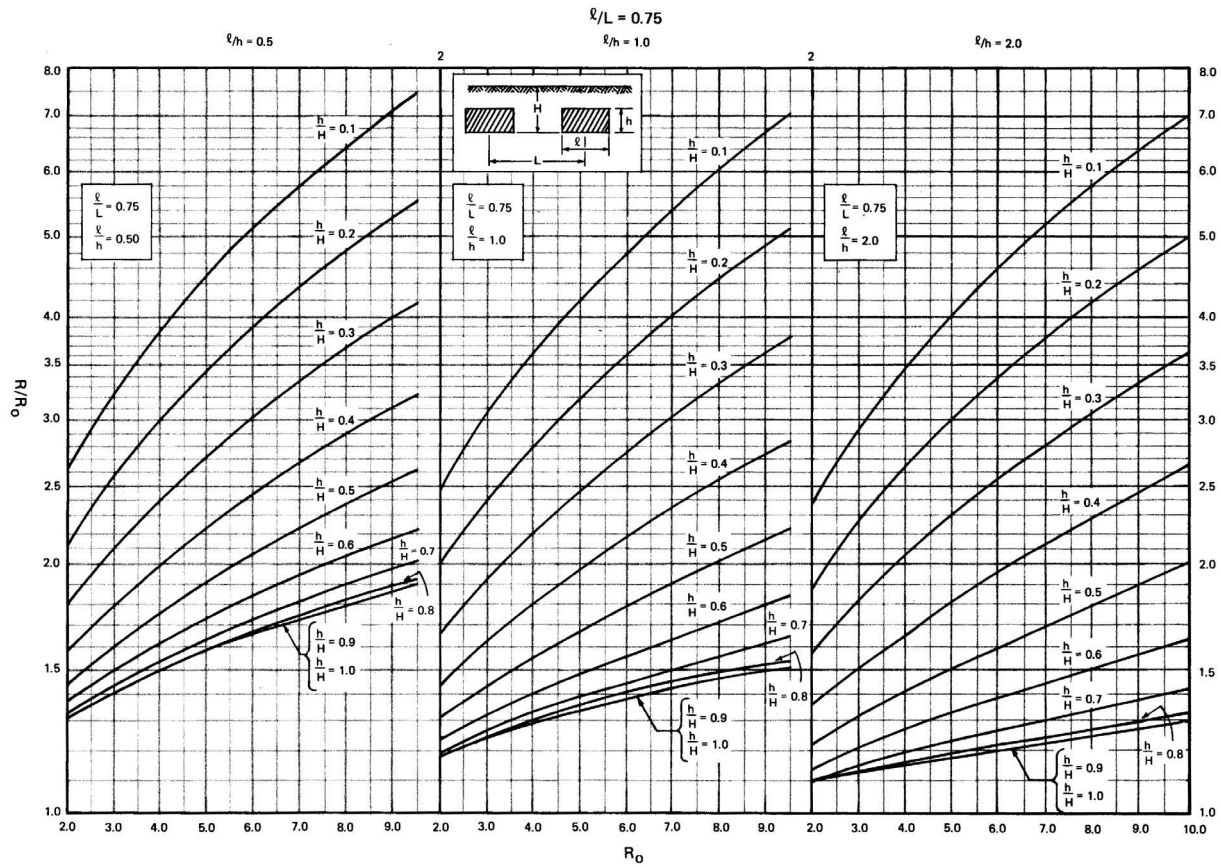


Figure 11-12: Dimensionless Resistance Factor Ratio for Anchor Slab Spacing $l/L = 0.75$

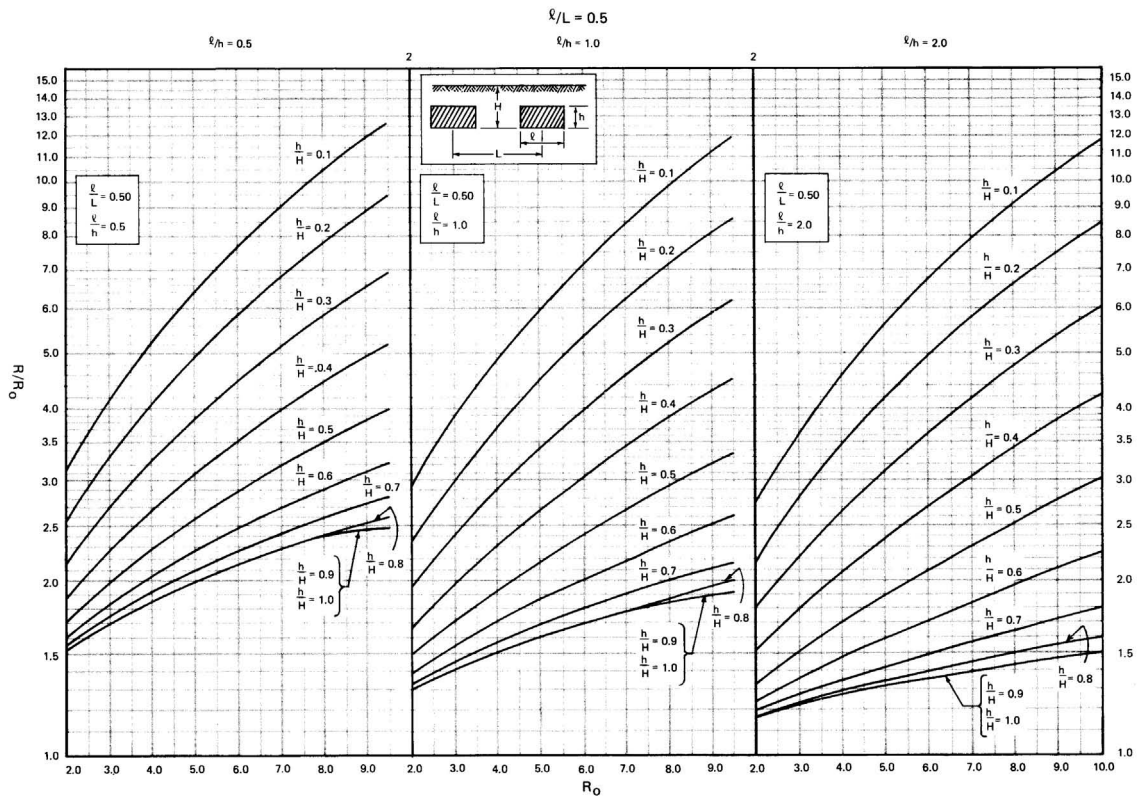
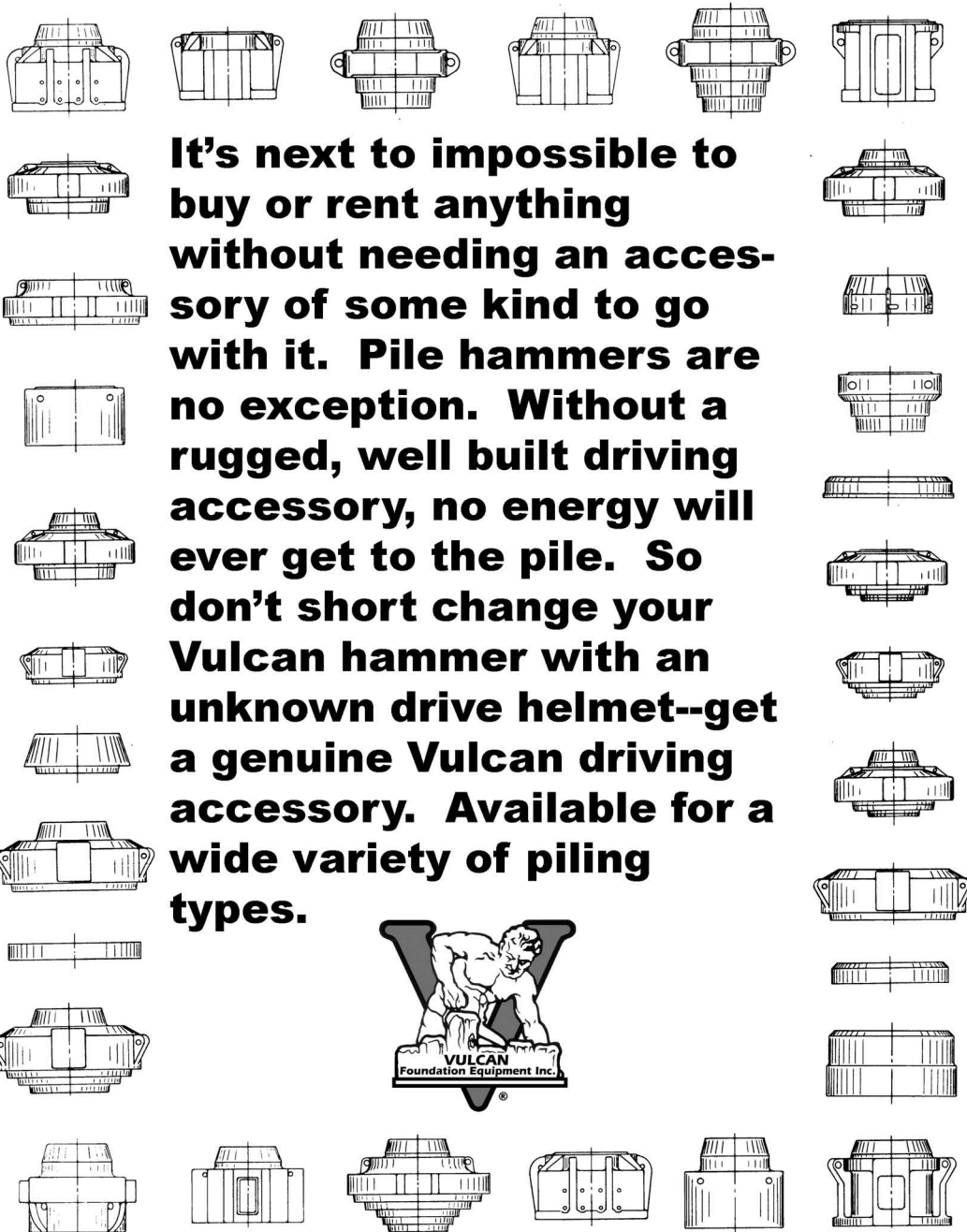


Figure 11-13: Dimensionless Resistance Factor Ratio for Anchor Slab Spacing $l/L = 0.50$

Everything Needs an Accessory



It's next to impossible to buy or rent anything without needing an accessory of some kind to go with it. Pile hammers are no exception. Without a rugged, well built driving accessory, no energy will ever get to the pile. So don't short change your Vulcan hammer with an unknown drive helmet--get a genuine Vulcan driving accessory. Available for a wide variety of piling types.



- ✍ **Vulcan Air/Steam Pile Hammers**
- ✍ **IHC Hydrohammers**
- ✍ **IHC Fundex Equipment**
- ✍ **Genuine Factory Parts**
- ✍ **Service and Technical Support**
- ✍ **Extensive Dealer Network**

VULCAN FOUNDATION EQUIPMENT

111 Berry Road
 P.O. Box 16099
 Houston, TX 77222
 Phone (713) 691 3000
 Fax (713) 691 0089
 Toll Free (800) 742-6637
 Email sales@vulcanhammer.com
 Web site <http://www.vulcanhammer.com>

Member of the IHC Caland Group

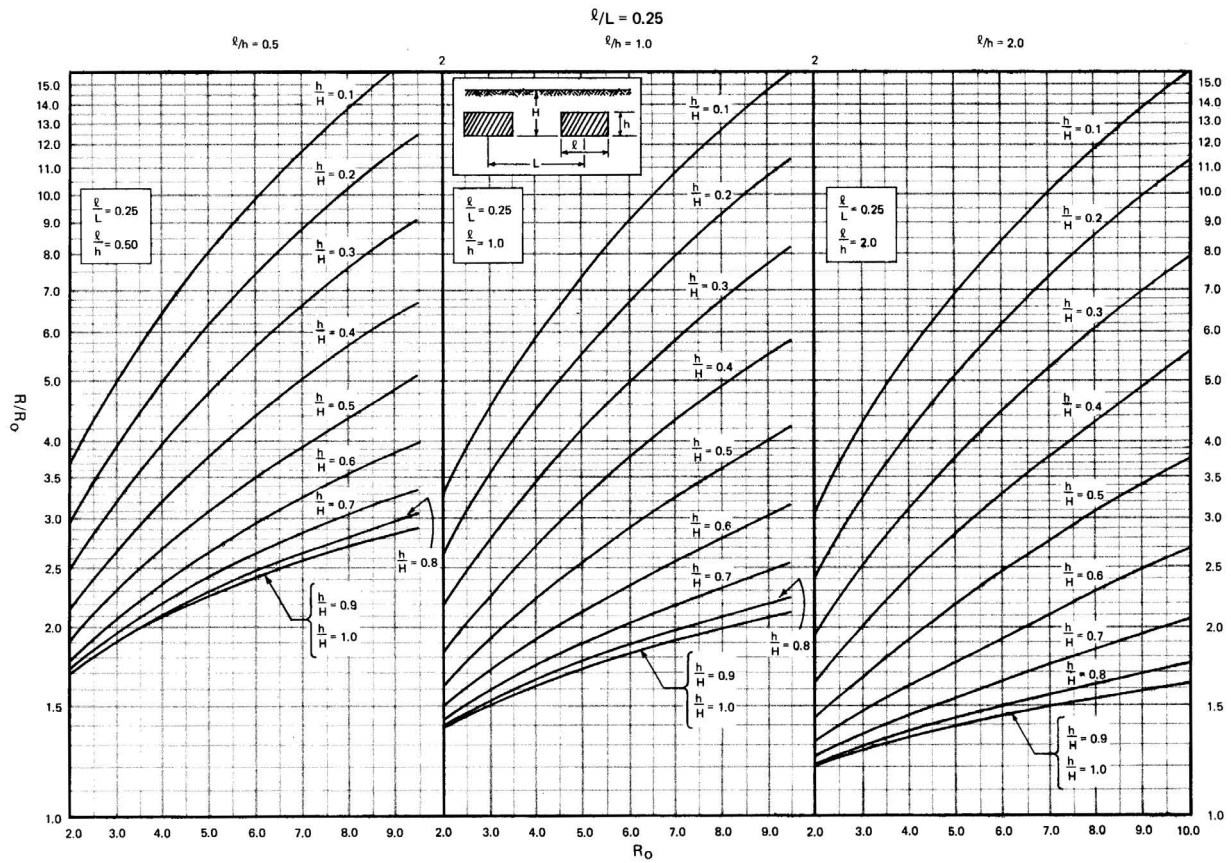


Figure 11-14: Dimensionless Resistance Factor Ratio for Anchor Slab Spacing $l/L = 0.25$

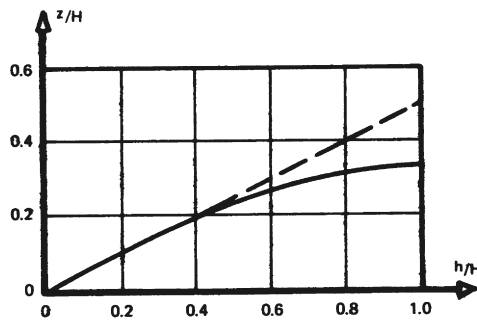


Figure 11-15: Location of Line of Action of Anchor Force

If we assume the submerged unit weight to be one half of the wet unit weight, Equation 11-28 reduces to

$$\text{Equation 11-29: } M_H = \frac{\gamma H^3}{6} \left(1 - \frac{1}{2} \left(\frac{h_u}{H} \right)^3 \right)$$

Calculate P_H , T_O , F_A , G_w , K_a , K_γ as defined in the anchor resistance calculations previously outlined. For $K_\gamma \tan \delta$, use Figure 11-16 to obtain the dimensionless relative distance factor ζ . Then for the basic case, Z_o , the distance from the base of the anchor slab to the line of action of the anchor force is

Equation 11-30:

$$Z_o = \frac{M_H}{T_o} \left(3\zeta K_\gamma - K_a - \frac{W}{M_H} \left(\frac{G_w}{2} - F_A \right) \right)$$

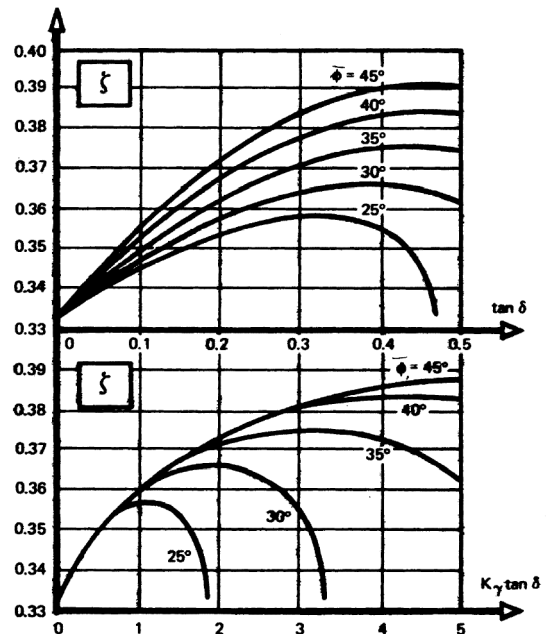


Figure 11-16: Relative Distance from Base of Slab to Resultant of Earth Pressure in Front of Anchor Slab

For the actual anchor slab dimensions, the distance, Z , from the base of the anchor to the anchor tie force is calculated using the following formula:

$$\text{Equation 11-31: } \frac{Z}{H} = \frac{h}{2H} - \left(\frac{1}{2} - \frac{Z_0}{H} \right) \left(\frac{h}{H} \right)^{\left(\frac{1}{1 - \frac{2Z_0}{H}} \right)}$$

G. An estimate of the horizontal movement, D , of the anchor slab may be obtained by solving the equation:

$$\text{Equation 11-32: } \log_{10} \left(\frac{\Delta}{H} \right) = 2.5 \left(\frac{T_{act}}{T_{ult}} \right) - 2 \sin \phi - 2.6$$

Where

$$0.30 \leq \frac{T_{act}}{T_{ult}} \leq 0.90$$

$$32^\circ \leq \phi \leq 41^\circ$$

$$0.25 \leq \frac{h}{H} \leq 1.0$$

And either $H = L$ in combination with:

$$0.25 \leq \frac{l}{L} \leq 1.0$$

Or $h = \ell$ in combination with:

$$0 \leq \frac{l}{L} \leq 1.0$$

We present an example of anchored wall design below.

Example 15: Design of Wales and Anchors for Sheet Pile Wall in Cohesionless Soils

❖ Given

➤ Anchored Sheet Piling Wall

- Excavation depth = 26'
- Depth of the water table on both sides = 6'
- Depth of anchor = 5'
- Soil Layers

Sand Backfill to excavation depth

- ◆ $\phi = 34^\circ$
- ◆ $K_a = 0.28$ (Rankine)
- ◆ $K_p = 3.54$ (Rankine)
- ◆ $\gamma = 110$ pcf
- ◆ $\gamma' = 60$ pcf
- ◆ $\delta = 0$ (for Rankine condition)

Medium sand below excavation depth

- ◆ $\phi = 36^\circ$
- ◆ $\delta = 14.4^\circ$
- ◆ $K_a = 0.26$ (Log-Spiral)

- ◆ $K_p = 6.63$ (Log-Spiral)

- ◆ $\gamma' = 65$ pcf

❖ Find

- Beam necessary for wale.
- Tie rod size and spacing.
- Design of anchor wall.
- Design of anchor slab, using Ovesen's method

❖ Solution

➤ We will simply solve this problem using SPW 911.

The solution is shown in *Figure 11-17*. This also serves as the diagram to illustrate the example. The problem is solved using the fixed earth support solution.

➤ Let us assume that we will be using PZ22 sheeting throughout.

- Let us also assume that we will have a tie rod every six piles, for a distance between the tie rods of 11'.
- The SPW 911 shows that the anchor load is 5,575 lbs.

➤ For the wale design, we use Equation 11-6. Since we are using ASTM A36 material in the wale, the allowable stress $f_s = 22$ ksi. Substituting, $S = (5575 \text{ lb/ft})(12 \text{ in/ft})(11 \text{ ft})^2 / ((10)(22,000 \text{ psi})) = 36.8 \text{ in}^3$. This condition can be satisfied by two 2-C12 X 20.7 channels. For the two channels, the total section modulus is 43 in^3 .

➤ To design the tie rod, we use Equation 11-2. Since the tie rod will be level, the cosine term is ignored and $T_{design} = (1.3)(5575) = 7248 \text{ lb/ft}$. The minimum area is then computed by Equation 11-3, thus $A_{tie} = (7248)(11') / (22,000 \text{ psi}) = 3.62 \text{ in}^2$, and thus the diameter is 2.15 in. Thus, we can use a 2 1/4" diameter rod, upsetting the ends to preserve the diameter inside the threads. For a Unified National Coarse thread, a 2 3/4"-4 thread, with a minor diameter of 2.4433", would be more than suitable.¹¹²

➤ The basic layout of the anchor wall is shown in *Figure 11-18*, with all dimensions in feet.

The objective of the location of the anchor wall is twofold: 1) to keep the anchor wall out of both the active failure zone and the internal friction zone of the wall, 2) keep the failure zones of the two walls separate. *Figure 11-18* shows this being done. In this case, it is necessary for the anchor wall to be 40.55' (actually we should use 41') behind the main sheet-piling wall. Although this distance can be determined analytically, in this case we used CAD software and laid the wall out to scale. In addition to giving us the distances we need, it also helps us to visualize the design.

The drawing also shows that, to meet both of the above conditions, the wall can be up to 13.828' in length. Obviously, it is advantageous for us to make it shorter, as we will see.

➤ For an anchored sheet pile wall, the design procedure is similar to a sheet-piling wall below the dredge line. The net soil forces are the sum of the active and passive resist

¹¹²Information on both U.S. unit thread series (UNC, UNF and other) and SI series can be found in Oberg, E., and Jones, F.D. (1974) *Machinery's Handbook*, Nineteenth Edition. New York: Industrial Press. Most fastener manufacturers also publish information on thread configuration and material strength for both UN and SI threads.

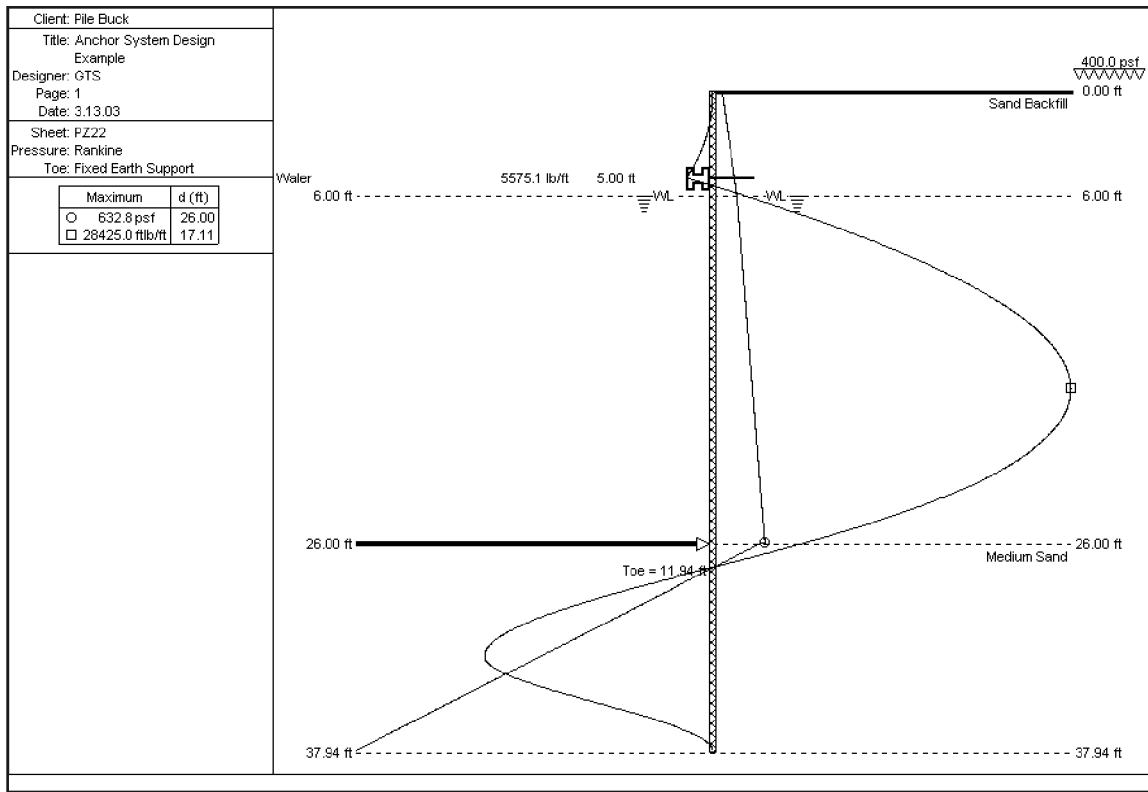


Figure 11-17: SPW911 Solution for Example 15

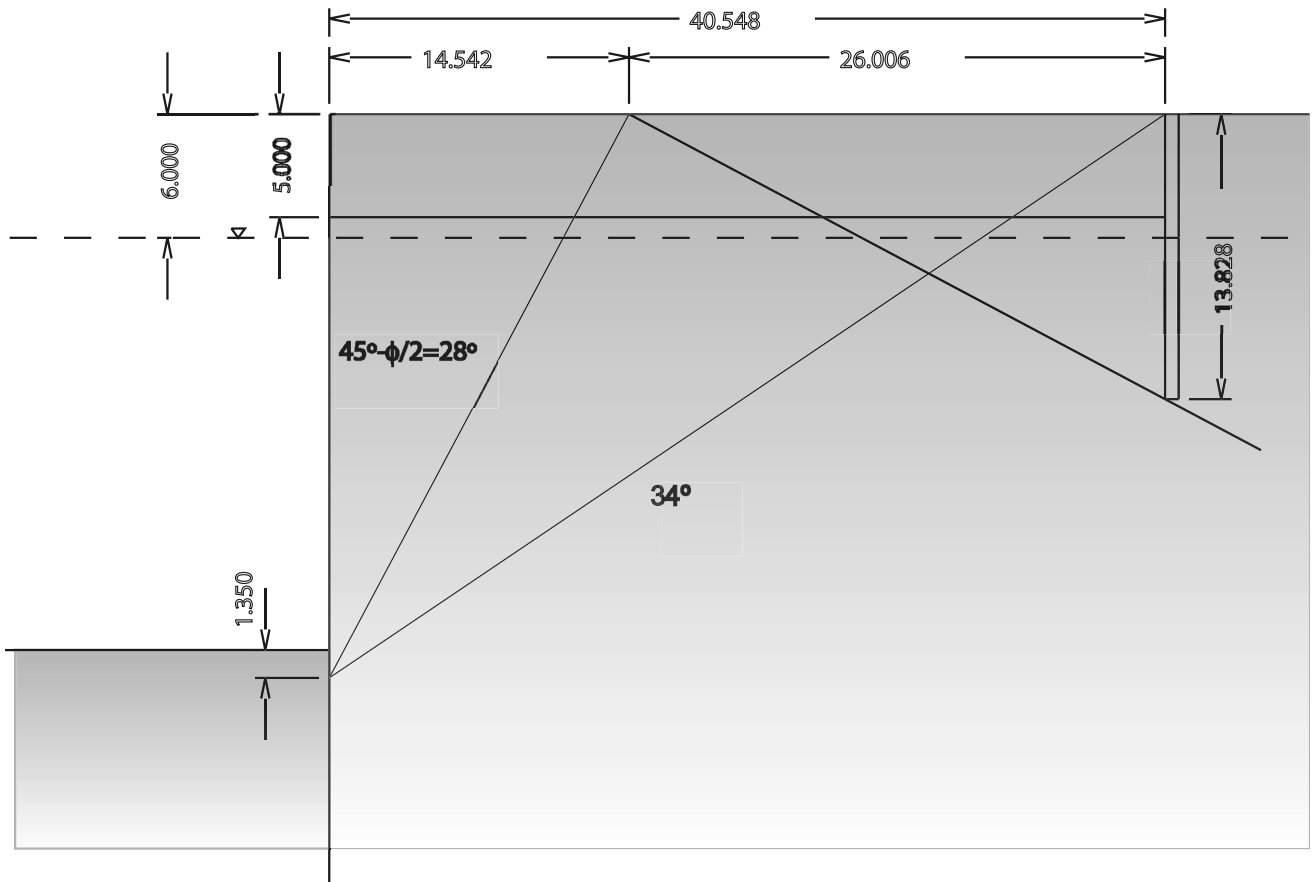
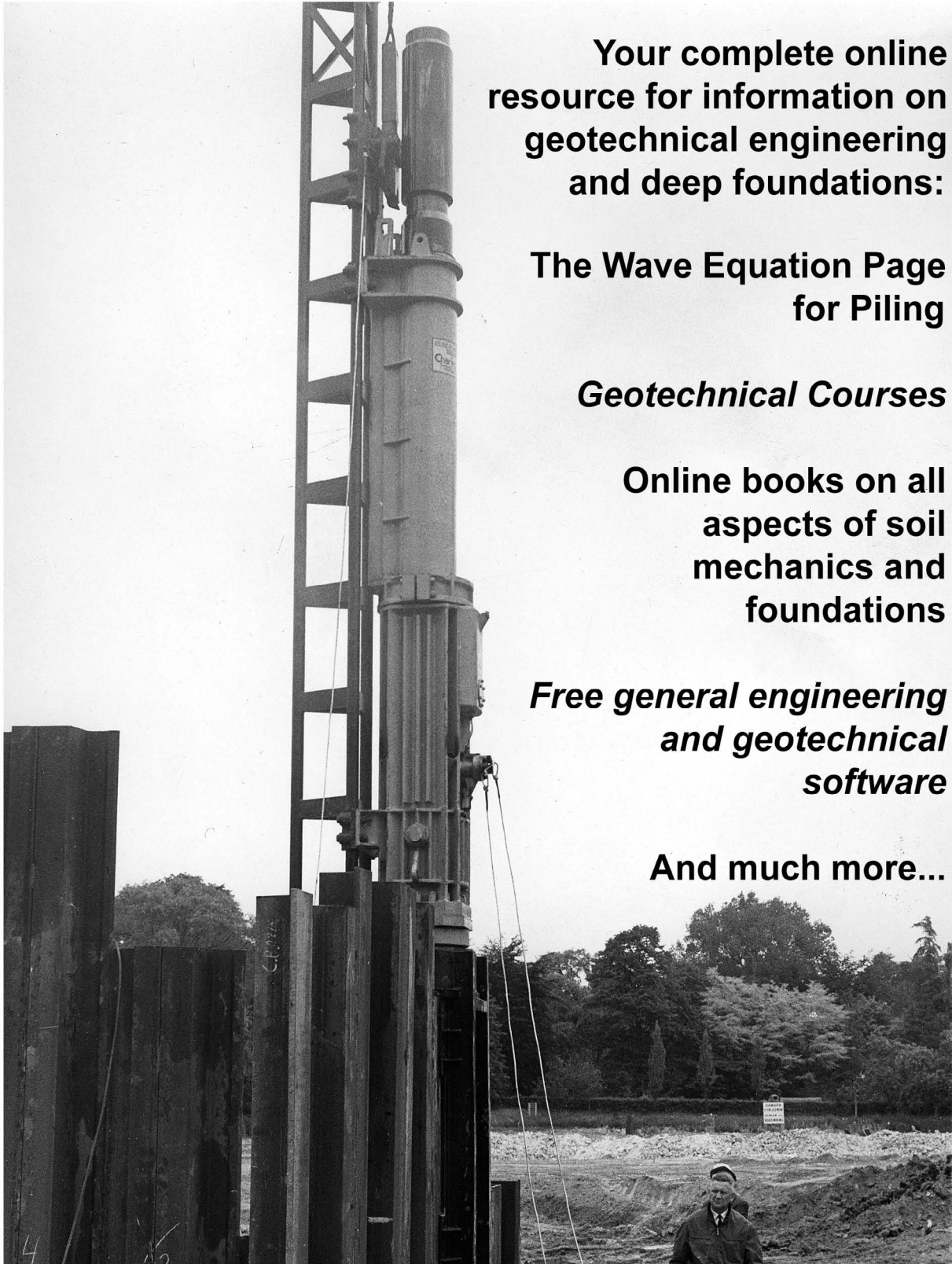


Figure 11-18: Layout of Location of Anchor Wall for Example 15

vulcanhammer.net



**Your complete online
resource for information on
geotechnical engineering
and deep foundations:**

**The Wave Equation Page
for Piling**

Geotechnical Courses

**Online books on all
aspects of soil
mechanics and
foundations**

***Free general engineering
and geotechnical
software***

And much more...

<http://www.vulcanhammer.net>

<http://www.vulcanhammer.org>
email me@vulcanhammer.net

<http://www.chet-aero.com>

ances; the total load on the wall is that of the anchor. The length affects the equations for these forces, specifically if the wall extends to below the water line. Let us assume to start with that the wall will extend below the water table, as shown in Figure 11-19.

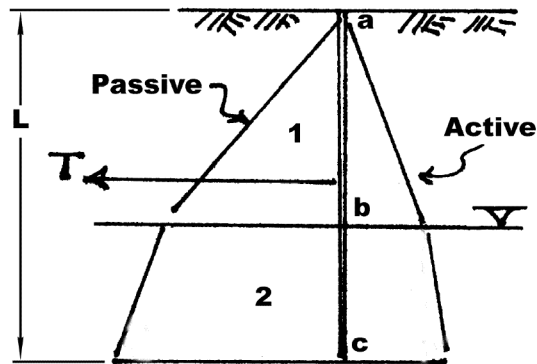


Figure 11-19: Pressure Diagram on Sheet Pile Anchor

The net force is divided into two parts; the part above the water line (1) and the part below the water line (2). We will assume Rankine conditions in this case, because the full angle of interface friction, d , used in computing K_p can only be mobilized if the anchor has sufficient dead weight or, in general, is restrained against upward movement. The summation of forces on the wall (including the anchor pull plus a factor of safety of 2.5) is

Equation 11-33:

$$\frac{5}{2}T = \frac{K_p - K_a}{2} \left(\gamma H_w^2 + (2\gamma H_w + \gamma'(L - H_w))(L - H_w) \right)$$

Locating the resultants of each force and summing moments about the top of the wall (again including the anchor pull factor of safety) yields

Equation 11-34:

$$\frac{5}{2}TH_w = \left(K_p - K_a \right) \left(\frac{\gamma H_w}{3} + \left(\begin{array}{l} \gamma H_w^2 + \\ (2\gamma H_w + \gamma'(L - H_w))(L - H_w) \\ \left(H_w + \frac{(L - H_w)(3\gamma H_w + 2\gamma'(L - H_w))}{6\gamma H_w + 3\gamma'(L - H_w)} \right) \end{array} \right) \right)$$

Substitution of the variables yields two equations: for the force, $97.63(L + 12.42)(L - 2.42) = 13937.5$, and for the moment, $11715.9(L + 16)(L - 2.94)(L^2 + 10.44L + 30.65) / (2880 + 180L) = 69687.5$. The solution of these two equations yields two values for H , 9.06' and 8.51' respectively. We should pick the larger of the two, and in practical terms, the height of the wall should be 9.5'.

➤With Ovesen's method, the first thing that needs to be considered is the maximum possible depth of the slab in view of Figure 11-15. Given the proximity of the tie rod to the water table, it is reasonable to assume that the anchor slab will in fact extend into the water table.

- Since we are using Rankine assumptions, from Figure 11-10 $K_\gamma = 5$. From this $R_0 = 5 - 0.28 = 4.72$.
- From Equation 11-20, $P_H = 3037.5$ lb/ft. The ultimate anchor resistance per foot of wall for the basic case (from Equation 11-21) is $T_o = (3037.5)(4.72) = 14329$ lb/ft of wall.

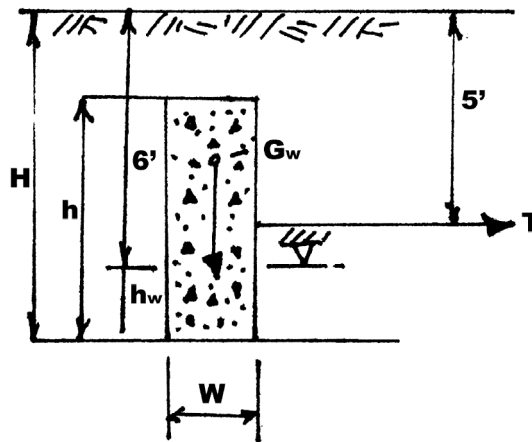


Figure 11-20: Slab Layout for Ovesen's Method Example

- Let us assume a slab configuration such as is shown in Figure 11-20 with $H = 7.5'$ and $h = 5.5'$. We will use for a slab thickness $W = 2'$. In specifying a slab thickness, a separate structural analysis should be considered. Keep in mind that, if reinforcement is used, most spread footings require that the minimum reinforcement for the cover is 3" in all directions.
- Using Equation 11-22 and substituting the parameters determined, the results for various spacings of anchors are as follows:

$$l/L = 0.25, R = 10.87, R/R_0 = 2.31, A_{ult} = 85,966 \text{ lb}, T_{ult} = 7815 \text{ lb/ft}, FS = 1.4.$$

$$l/L = 0.5, R = 7.7, R/R_0 = 1.63, A_{ult} = 121,583 \text{ lb}, T_{ult} = 11,053 \text{ lb/ft}, FS = 1.98.$$

$$l/L = 0.75, R = 5.96, R/R_0 = 1.26, A_{ult} = 141,340 \text{ lb}, T_{ult} = 12,849 \text{ lb/ft}, FS = 2.3.$$

$$l/L = 1, R = 4.78, R/R_0 = 1.01, A_{ult} = 151,240 \text{ lb}, T_{ult} = 13,749 \text{ lb/ft}.$$

- We generally prefer to have a factor of safety greater than 2; therefore, the case of $l/L = 0.5$ is just below being acceptable. Using linear interpolation with the factors of safety, we should specify an $l/L = 0.55$. Dewatering may be necessary, especially for an anchor

that requires excavation. This is also true for anchors that are placed below the wales with the tie rods extending up at an angle (see *Figure 11-2*).

- We need to check the actual location of the tie rod force (as opposed to where the tie rod is actually at.) We first compute Z_0 using Equation 11-30. $\zeta = 0.365$ from *Figure 11-16*, and the values of the various parameters are as follows:

$$M_H = 7706.25 \text{ ft-lbs}$$

$$T_o = 14,329 \text{ lbs}$$

$$G_w = 3,095 \text{ lb/ft}$$

$$F_A = -579 \text{ lb/ft}$$

- From the above $Z_0 = 3.09'$. Using Equation 11-31, $Z = 2.63'$. This is the distance of the actual centre of the anchor resistance from the bottom of the slab. Since the actual location of the tie rod is 2.5' from the bottom of the slab, this checks out well.
- An estimate of the movement of the slab is given by Equation 11-32. $T_{act} = 5575 \text{ lb/ft}$. For each of the anchor slab spacings, the estimated displacement is as follows:

$$l/L = 0.25, \Delta = 1.04''.$$

$$l/L = 0.5, \Delta = 0.31''.$$

$$l/L = 0.75, \Delta = 0.21''.$$

$$l/L = 1, \Delta = 0.18''.$$

11.2.4.2. Anchor Slab in Cohesive Soils

Mackenzie¹¹³ performed model tests in plastic clay based upon the full resistance of the wedge in front of the anchor block being mobilized. The geometric parameters shown in *Figure 11-21* used in conjunction with the experimental curve shown in *Figure 11-22* give a dimensionless factor R that is dependent upon the ratio H/h . Knowing R , the ultimate capacity of the anchor slab, T_{ult} , per unit of slab width can be determined as follows:

$$\text{Equation 11-35: } T_{ult} = Rch$$

Where

- $R \leq 8.5$
- c = cohesion of the soil

This experimental curve can be used for design purposed providing consideration is given to a proper factor of safety for a specific application.

11.2.5. Reaction Piles

Brace piles forming A-frames can sometimes be used effectively to anchor sheet pile walls, as shown in *Figure 11-1 (d)*. If only two piles form each frame, it is necessary to connect the frames with a continuous reinforced concrete cap. The anchor rods can then be attached to the concrete cap. However, if three piles are used, each frame can support a tie rod through the centre pile and act independently. The pile

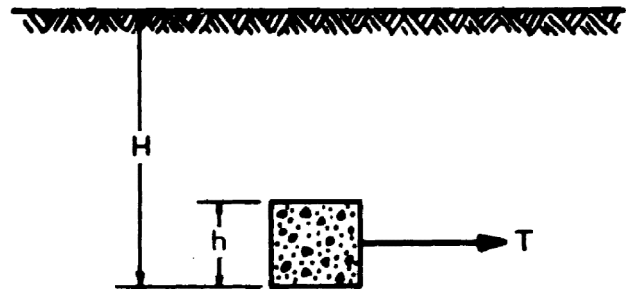


Figure 11-21: Geometrical Parameters for Anchor Slab in Clay

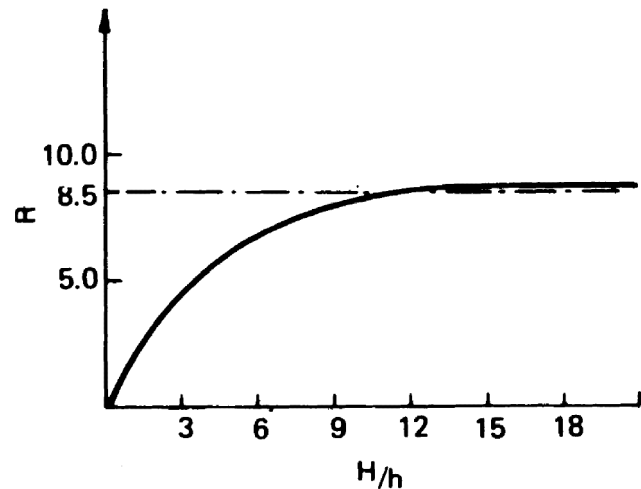


Figure 11-22: Resistance of Anchor Slabs in Plastic Clay

angled toward the wall will be in compression while the pile or piles angled away from the wall will be in tension. The resulting forces are easily determined from a force polygon. This method of support can be used effectively only if the brace piles can be adequately seated in underlying stratum of soil or, preferably, rock.

11.2.6. Tension Piles

Battered steel pile tension ties (generally H-piles) connected directly to a sheet pile wall through wales may also be used as anchors. An illustration of this type of anchor system is shown in *Figure 11-1 (e) and (f)*. The reaction is developed through friction and/or adhesion between the pile and the soil behind the wall.

Only the length of pile outside the active failure zone should be considered effective in mobilizing resistance. The actual capacity of the piles should be checked by pull out tests in the field. Particular attention should be given to the connection details at the wale since this may be subject to rotational stresses from backfill loading on the tension pile or vertical force components.

11.3. Tiebacks

Flexible sheet pile walls usually require one or more points of support in addition to toe support in order to be stable and

¹¹³MacKenzie, T.R. (1955) Strength of Deadman Anchors in Clay. Master's Thesis, Princeton University.

economical. Drilled-in ties that utilize the shear strength of the soil or rock behind the wall and at some depth below the surface comprise a system that was developed in Europe in the 1930's.

Interest in this method developed in the United States in the 1950's as a means of clearing large excavations of the mass of cross-lot structural bracing required for support. The ties were relatively expensive but saved enough construction time to more than make up the cost differential. Since then, experience and reliability have improved and costs have been reduced. Tieback support systems have virtually replaced structural bracing for most large, temporary excavations. In addition, the method is being used extensively to support permanent walls¹¹⁴.

The material in this manual on tiebacks is a general overview. Many aspects of tiebacks are specific to the method by which they are installed and the structural configuration of the tieback itself; many of these methods are proprietary. Any application of tiebacks should be done with a complete understanding of the method and configuration actually being used or specified.

11.3.1. Principles of Tieback Systems

A tieback consists of 3 major components:

1. An anchor zone which acts as a reaction to resist the earth and water pressures;
2. A support member which transfers load from the wall reaction to the anchor zone; and
3. A point of support or reaction at the wall.

These are illustrated in *Figure 11-23*.

The anchors are installed using specially designed drilling equipment operating from the face of the wall. Anchors are inclined from 15° to 45° from the horizontal that produces both vertical and horizontal force components.

The anchors must bypass potential failure zones behind the wall and penetrate into adequate soil beyond. The ties, or tendons as they are called, are usually high strength steel bars or strands. Cement grout is generally the transfer medium between tendon and soil or rock.

After installation of each tie, it is post-tensioned to some percentage of the design load as a pre-test. The design of tiebacks is based on principles of soil mechanics along with empirical rules.

❖ Advantages of Tiebacks

- For excavations:
 - Provide a clear work area inside temporary excavation walls.
 - Reduce the settlement behind walls by controlling the deformation of the wall.

- Avoid problems associated with moving structural bracing as construction proceeds.
- For permanent land walls and marine bulkheads:
 - Allows anchor system to be installed without disturbing existing facilities behind the wall.
 - Anchors will be located away from proposed near-surface facilities and from potential damage from surface loads.
 - High capacity can reduce size and number of anchors.
 - Flexible walls instead of formed concrete walls save space and expense.
- ❖ Disadvantages of Tiebacks
 - Provision must be made for the vertical force component.
 - Since connections are made on the face of the wall, this represents a possible encumbrance that is not a problem with conventional wale and tie rod systems.
 - Conventional systems can be excavated and inspected, which is impossible with tiebacks.
 - In the case of land walls, permission must be obtained from the surface owner of the land in which the anchors are founded.

11.3.2. Temporary and Permanent Tiebacks

There are only a few differences in approach between tiebacks for permanent use and those for temporary support.

- ❖ Permanent ties must be protected against long term corrosion attack while most temporary tiebacks are for short-term use and can be installed bare.
- ❖ Permanent tiebacks supporting bulkheads generally consist of a single row of ties installed through the top of the wall above water. These may be very high capacity anchors. However, most temporary installations consist of multiple rows of lower capacity ties and therefore, shorter lengths¹¹⁵.
- ❖ Post-tensioning procedures may differ, since temporary ties are often prestressed to control ground movement.

11.3.3. Definitions

- ❖ A *tieback* system is a structural system that uses an anchor in the ground to secure a tendon that applies a force to a structure. Tiebacks are also referred to as ground anchors.
- ❖ Vertical or near vertical tiebacks are called *tiedowns*.
- ❖ The *tendon* is made up of prestressing steel with sheathing, and anchorage. The anchor transmits the tensile force in the prestressing steel to the ground. Cement grout, or polyester resin, or mechanical anchors are used to anchor the steel in the ground. The anchorage is made up of an anchor head or nut, and a bearing plate.
- ❖ The *anchor head* or *nut* is attached to the prestressing steel, and transfers the tieback force to a *bearing plate* that evenly distributes the force to the structure.

Anchor heads can be restressable or non-restressable.

A *restressable anchor head* is one where the tieback force

¹¹⁴Probably the best-known application of tiebacks—albeit not a sheet piling wall—was during the construction of the original World Trade Centre towers in New York City; the tied back walls were exposed again and reinforced after the towers were destroyed on 11 September 2001.

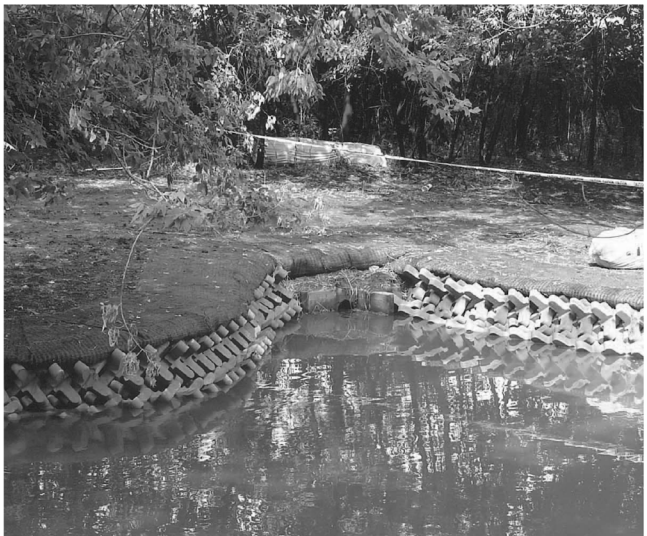
¹¹⁵Permanent land walls can also utilize the multiple tier approach.

Marine Solutions

Solutions for Breakwaters, Shore Protection and Marina Docks

Economy, durability, and versatility

CONTECH® Marine Products provide economical and effective solutions for various marine applications, including shore protection, primary and secondary breakwaters, jetties and marina docks.



For more information, call Toll Free: 800-338-1122.
Or, visit our web site at www.contech-cpi.com

CONTECH
CONSTRUCTION PRODUCTS INC.

INNOVATIVE CIVIL ENGINEERING SITE SOLUTIONS

 American
Owned and Operated

©2003 CONTECH Construction Products Inc. All Rights Reserved

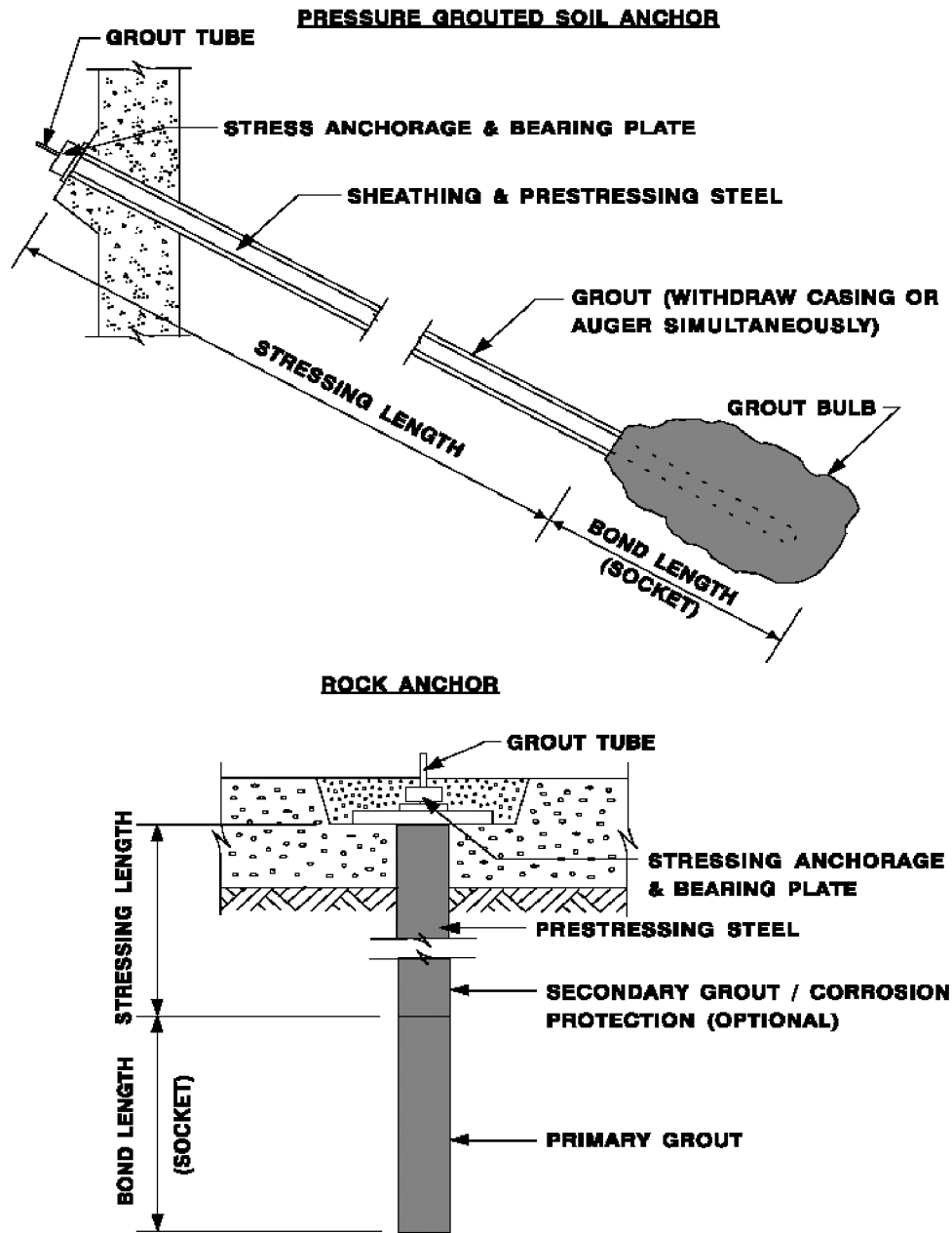


Figure 11-23: Components of Tieback Systems

can be measured or increased any time during the life of the structure.

The load cannot be adjusted when a *non-restressable anchor head* is used.

- ❖ A *coupling* can be used to transmit the anchor force from one length of prestressing steel to another.
- ❖ The *anchor length* is the designed length of the tieback where the tieback force is transmitted to the ground.
- ❖ The *tendon bond length* is the length of the tendon, which is bonded to the anchor grout. Normally the tendon bond length is equal to the anchor length.
- ❖ The *unbonded length* of the tendon is the length, which is

free to elongate elastically.

- ❖ The *jacking length* is that portion which is required for testing and stressing of the tieback.
- ❖ The *unbonded testing length* is the sum of the unbonded length and the jacking length.
- ❖ A *sheath* or *bond breaker* is installed over the unbonded length to prevent the prestressing steel from bonding to surrounding grout.
- ❖ The *anchor diameter* is the design diameter of the anchor.
- ❖ *Anchor grout* is used to transmit the tieback force to the ground.

The anchor grout is also called the *primary grout*.

Secondary grout is injected into the drill hole after stressing to provide corrosion protection for unsheathed tendons.

- ❖ Tiebacks carry various loads during their lifetimes.
 - The *design load* is the maximum anticipated load that will be applied to the tieback.
 - The *test load* is the maximum load applied during testing.
 - The *lock-off load* or transfer load is the load transferred to the tieback upon completion of stressing.
 - The *alignment load* is the load transferred to the tieback upon completion of stressing.
 - The *alignment load* is a nominal load maintained on a tieback during testing to keep the testing equipment in position.
 - The *lift-off load* is the load required to lift the anchor head or nut from the bearing plate.
 - The *residual load* is the load carried by the tieback at any time.
 - The *load transfer rate* is the tieback capacity per unit length of anchor.

11.3.4. Types of Tiebacks

The basic types of tiebacks are: pressure-injected; low-pressure-grouted, straight-shafted; single-underreamed; multiunderreamed; and postgrouted. These tiebacks are shown in Figure 11-24.

Pressure-injected tiebacks are used in sandy or gravelly soils. Grout pressures in excess of 150 psi (1034 kPa) are used to achieve high load transfer rates.

Low-pressure-grouted, straight-shafted tiebacks are installed in rock, cohesive soils, and sandy or gravelly soils. They can be made using a variety of drilling and grouting techniques. The grout pressure is less than 150 psi (1034 kPa).

Single-underreamed tiebacks are installed primarily in the United States using large uncased drill holes in cohesive soils. Sand-cement grout or concrete is used in grouting the tieback and the grout or concrete is not placed under pressure.

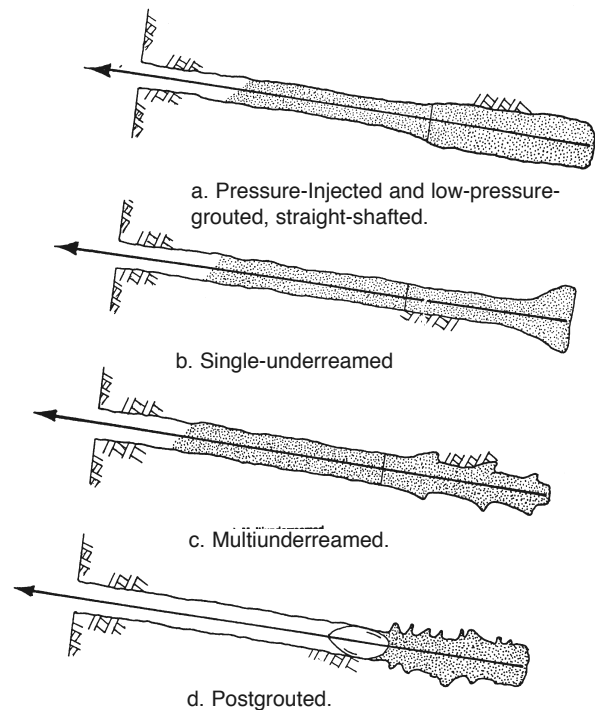


Figure 11-24: Tieback Types

Multiunderreamed tiebacks are used in stiff cohesive soils and weak rocks. The spacing of the underreams is selected in order to induce a shear failure along the cylinder determined by the tips of the underreams.

Postgrouted tiebacks are primarily used in cohesive soils. In granular soils and rock, postgrouting is used to increase the rate of load transfer.

Mechanical type tiebacks are helical auger systems that use methods developed for the electrical industry. These have been used since Roman times. The Manta Ray anchors fall into this category.

11.3.5. Nomenclature for Tieback Systems

The embedded portion of the piling below level of excava-

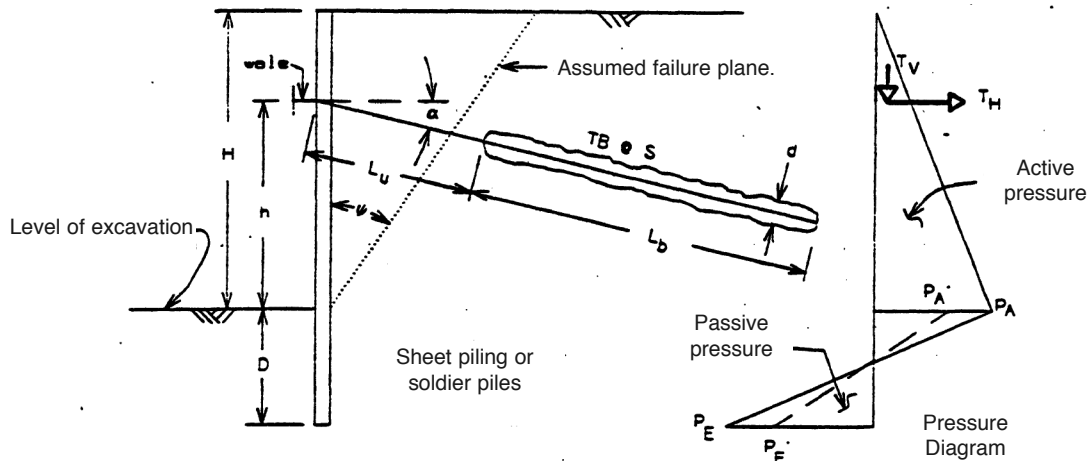


Figure 11-25: Single Tier Tieback System

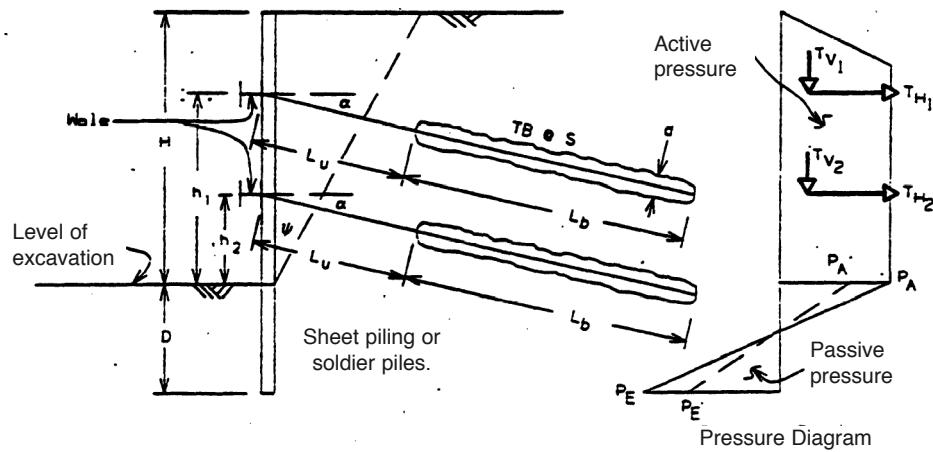


Figure 11-26: Multi-Tier Tieback System

tion. The embedment depth and the horizontal component of the tieback design force required are determined by analyzing the active, passive, and surcharge pressures acting on the piling. A factor of safety is achieved by increasing the calculated embedment depth an additional 20% to 40%. The higher percentage should be used when soil properties are derived from log of test borings or other soil information and not determined from laboratory or in-situ tests used specifically to determine soil strength.

11.3.6. Capacity of Tieback anchors

11.3.6.1. Overview

There are several different types of tieback anchors. Their capacity depends on a number of interrelated factors:

- Location - amount of overburden above the tieback
- Drilling method and drilled hole configuration
- Strength and type of the soil
- Relative density of the soil
- Grouting method
- Tendon type, size, and shape

The presence of water either introduced during drilling or existing ground water can cause significant reduction in anchor capacity when using a rotary drilling method in some cohesive soils (generally the softer clays).

High pressure grouting of 150 psi or greater in granular soils can result in significantly greater tieback capacity than by tremie or low pressure grouting methods. High pressure grouting is seldom used for temporary tieback systems.

Regrouting of tieback anchors has been used successfully to increase the capacity of an anchor. This method involves the placing of high-pressure grout in a previously formed anchor. Regrouting breaks up the previously placed anchor grout and disperses new grout into the anchor zone; compressing the soil and forming an enlarged bulb of grout thereby increasing the anchor capacity. Regrouting is done through a separate grout tube installed with the anchor tendon. The

separate grout tube will generally have sealed ports uniformly spaced along its length that open under pressure allowing the grout to exit into the previously formed anchor.

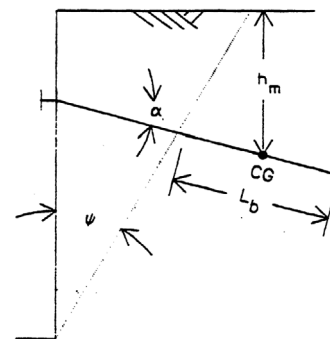
Due to the many factors involved, the determination of anchor capacity can vary quite widely. Proof tests or performance tests of the tiebacks are needed to confirm the anchor capacity.

Bond capacity is the resistance to pull out of the tieback that is developed by the interaction of the anchor grout (or concrete) surface with the soil along the bonded length. Determining or estimating the bond (resisting) capacity is a prime element in the design of a tieback anchor.

Included with some shoring designs there may be a soils laboratory report that will contain recommended value for the bond capacity to be used for tieback anchor design. The appropriateness of the value of the bond capacity will only be proven during tieback testing.

11.3.6.2. Cohesionless Soils—Low Pressure Grouting (FHWA Formula)

For most of the temporary shoring work normally encountered, the tieback anchors will be straight shafted with low-pressure grout placement. For these conditions the following equation can generally be used for estimating the tieback anchor capacity:



Equation 11-36:

$$P_{ult} = \pi d L_b \gamma h_m \tan \phi$$

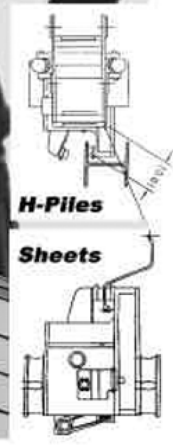
Features:

MAN TO MACHINE

- Eccentrics Located In Side Arm*
- Centerline of Dynamic Force is Closer to Gripping Jaws*
- Off Center Loading (moment) Recuced by 56%*
- 22% More Amplitude Than Nearest Competition*
- Increase Distance Between Jaws resists Off Center Loading by 62%*
- Individual Actuating Cylinder for Side Grip and Bottom Clamp*
- Side Grip Actuation Cylinders Are rigidly Mounted To Prevent Failure*
- Increased Tilting Capability For Greater Left/Right Reach*
- Rectangular Clamp Jaws Provide More Clamping Area*
- Built In USA, Not Finland*
- Nationwide Service*

Finally, A Robot Vibro That Works

ROBOTIC VIBRO



When a pile driver talks... we listen™. Please call or write:



APE Corporate Offices
 7032 South 196th
 Kent, Washington 98032
 800-248-8498 or
 253-872-0141
 Fax: 253-872-8710

APE CANADA
 1965 Ramey Road
 Port Colburn, ON
 LZG 7MG
 905-328-0850
 Fax: 905-834-8486

APE Mid-Atlantic Regional Ofc.
 500 Newton Rd. Suite 200
 Virginia Beach, VA 23462
 866-399-7500
 Fax: 757-518-9741
 Cell: 757-373-9328

APE Northeast Regional Ofc.
 Route 15 North & Taylor Rd.
 Wharton, NJ 07885
 973-989-1909
 Fax: 973-989-1923
 888-217-7524

APE Southeast Regional Ofc.
 1023 Snively Avenue
 Winter Haven, FL 33880
 863-324-0378
 Fax: 863-318-9409

APE S. Central Regional Ofc.
 11128 FM Hwy. 1488
 Conroe, TX 77384
 936-271-1044
 Fax: 936-271-1046
 800-596-2877

APE Western Regional Office
 160 River Road
 Rio Vista, CA 94571
 707-374-3266
 Fax: 707-374-3270
 888-245-4401

Alessi Equipment, Inc.
 35 Rosslyn Place
 Mt. Vernon, NY 10550
 914-699-6300
 Fax: 914-699-5300

Imeco-Austria
 431-368-2513
 Fax: 431-369-8104

Table 11-1: Nomenclature for Figure 11-25 and Figure 11-26

Variable	Explanation
H	Depth of excavation
D	Embedment depth of Piling
h	Height of tieback above level of excavation, generally about $3H/4$
T_H	Horizontal component of the tieback design force
TV	Vertical component of the tieback design force
s	Horizontal spacing of the tieback
d	Diameter of the drill hole for the tieback
ψ	Angle between assumed failure plane and vertical, generally $45^\circ - f/2$ for a level surface. Values of ψ commonly vary between 20° and 35° depending upon the type of soil. For design of temporary shoring systems, it is normally acceptable to consider the failure plane to start at the elevation of the bottom of the excavation and extend upward at an angle ψ from the vertical. For sloping or irregular surfaces, a wedge failure or similar type analysis may be necessary to predict the location of the failure plane.
α	Angle of inclination from horizontal of tieback. Normally, 10° to 15° is used for the angle α to facilitate the placement of grout or concrete. Angles up to 45° may be used to reduce the tieback length, reach stronger soil layers, or to avoid obstacles, but larger angles induce larger vertical forces so care must be taken with these as well.
L_b	Bonded length of tieback, which is also referred to as the anchor length of the tieback. The required bonded length depends on the soil or rock properties, the anchor type, and the required anchor capacity.
L_u	Unbonded length of tieback. Unbonded length is normally specified to start at some minimum distance past the failure plane to ensure that no portion of the bonded length falls within the failure wedge. Accurate determination of this length depends on how well known the soil properties are and how accurately the location of the failure plane can be predicted. To ensure that the bonded length falls beyond the failure-plane it is common practice to extend the unbonded length about 5 feet beyond the assumed failure plane. The minimum recommended unbonded length is 15 feet.

Where

d = diameter of drill hole

L_b = bonded length of the tieback

γ = unit weight of the soil

ϕ = angle of internal friction of the soil

CG = centre of $L_b = L_b/2$

h_m = vertical distance from the ground line to the centre of L_b

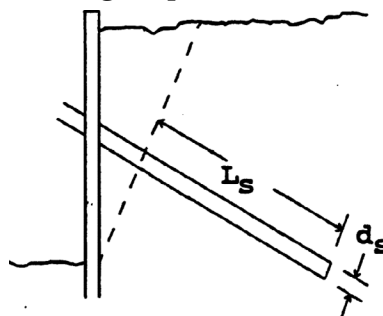
ψ = angle between assumed failure plane and vertical.

11.3.6.3. Cohesionless Soils—Small Diameter Anchors

Small diameter anchors are generally installed in granular soils with grouting taking place under high pressure (usually greater than 150 psi (1035 kPa).) The anchor capacity will depend upon the soil type, grouting pressure, anchor length, and anchor diameter. The way in which these factors com-

bine to determine anchor loads is not clear; therefore, the load predicting techniques are often quite crude. The theoretical relationships in combination with the empirical data can be used to estimate ultimate anchor load.

11.3.6.3.1. No grout penetration in anchor zones



Equation 11-31: $P_u = p_i \pi d_s L_s \tan \phi_e$

Where

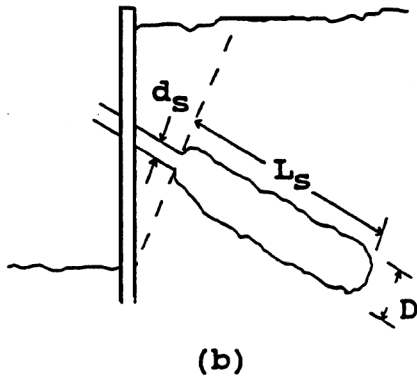
- d_s = diameter of anchor shaft
- L_s = length of anchor shaft
- ϕ_e = effective friction angle between soil and grout
- p_i = grout pressure

or

Equation 11-38: $P_u = L_s n_1 \tan \phi_e$

Where $n_1 = 8.7 - 11.1$ k/ft (127 - 162 kN/m).

11.3.6.3.2. Grout penetration in anchor zone (very pervious soils)



(b)

Equation 11-39:

$$P_u = A \bar{\sigma}_v \pi D L_s \tan \phi_e + B \bar{\sigma}_{v@end} \pi / 4 (D^2 - d_s^2)$$

Where

- d_s, D, L_s , and ϕ_e are as before
- $\bar{\sigma}_v$ = average vertical effective stress at anchor entire anchor length
- $\bar{\sigma}_{v@end}$ = vertical effective stress at anchor end closest to wall

$A = (\text{Contact pressure at anchor soil interface}) / (\text{effective vertical stress, } \bar{\sigma}_v)$

Littlejohn reports typical values of A ranging between 1 and 2

$B = \text{bearing A value capacity factor similar to } N_q \text{ but smaller in magnitude. of } B = N_q / (1.3 - 1.4) \text{ is recommended provided } \geq 25D$; where h is the depth to anchor.

Since the values of D, A and B are difficult to predict, Littlejohn also suggests:

Equation 11-40: $P_u = L_s n_2 \tan \phi_e$

Where

- $n_2 = 26 - 40$ kips/ft or (380 - 580 kN/m)
- $L_s = 3 - 12$ ft or (0.9 - 3.7 m)
- $D = 15 - 24$ inches or (400 - 610 m)
- depth to anchor = 40 - 50 ft or (12.2 - 15.1 m)

11.3.6.3.3. Empirical Relationships

Figure 11-27 presents an empirical plot of the load capacity of anchors founded in cohesionless soils. This figure was developed by Ostermayer and represents the range of anchor capacities that may develop in soils of varying densities and gradations. The chart was developed for anchor diameters of 4" - 6" and a depth of overburden of 13'.

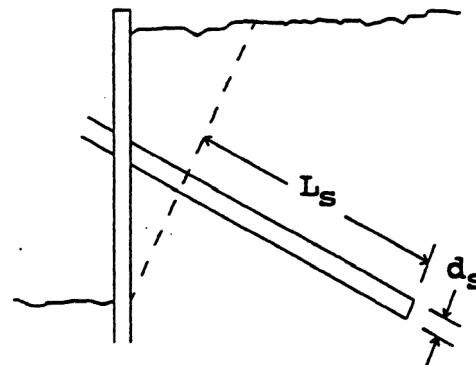
11.3.6.4. Cohesive Soils—Large Diameter Anchors

Large diameter anchors can be either straight shafted, single-belled, or multi-belled.

These anchors are most commonly used in stiff to hard cohesive soils that are capable of remaining open when unsupported: however, hollow flight augers can be used to install straight-shafted anchors in less competent soils.

The methods used to estimate the ultimate pullout capacity of large diameter anchors are largely based on the observed performance of anchors and are, therefore, empirical in nature. The following equations can be used to estimate anchor load capacity; field-testing of anchors is required to determine true anchor capacity.

11.3.6.4.1. Straight-shafted Anchor

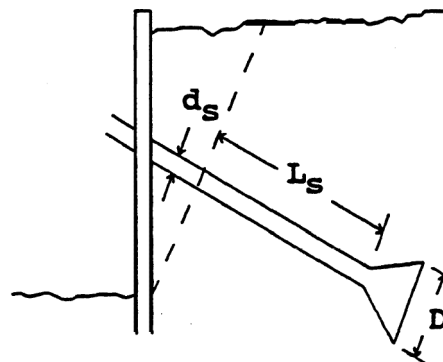


Equation 11-41: $P_u = \alpha s_u \pi d_s L_s$

Where

- d_s = diameter of anchor shaft
- L_s = length of anchor shaft
- s_u = undrained shear strength of soil
- α = Reduction factor in due to disturbance, etc. = 0.3 - 0.5.

11.3.6.4.2. Belled Anchor



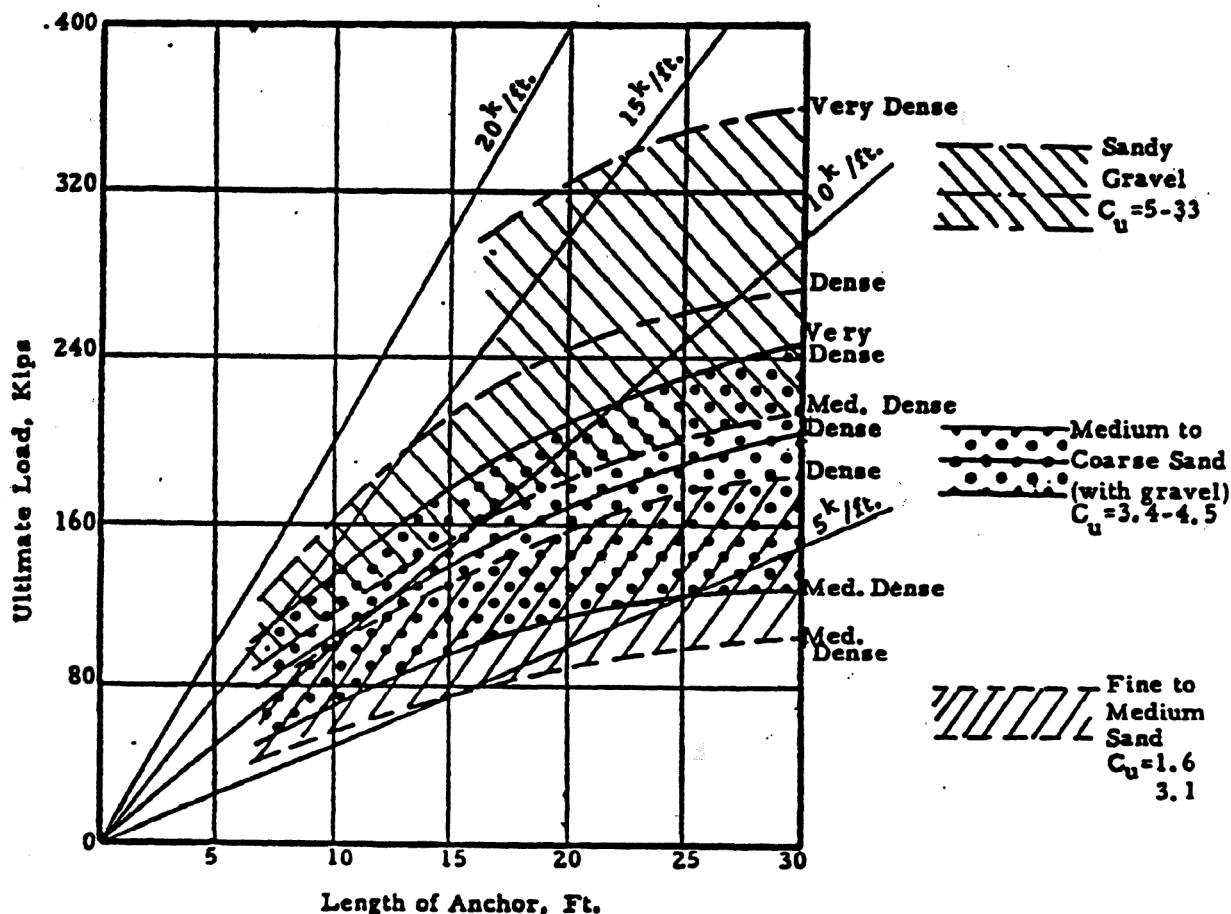


Figure 11-27: Anchor Capacities in Cohesionless Soils

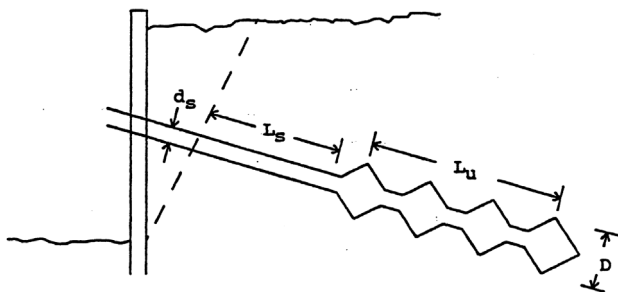
Equation 11-42:
$$P_u = \alpha s_u \pi d_s L_s + \frac{\pi(D^2 - d_s^2)}{4} N_c s_u$$

Where

D = diameter of anchor bell

N_c = bearing capacity factor = 9

11.3.6.4.3. Multi-belled Anchor



Equation 11-43:

$$P_u = \alpha s_u \pi d_s L_s + \pi/4 (D^2 - d_s^2) N_c s_u + \beta s_u \pi D L_u$$

Where

L_u = length of underreamed portion of anchor

β = reduction factor in S_u for soil between underream tips = 0.75 - 1.0

In order for failure to occur between the underream tips, the tips must be spaced at 1.5 - 2.0 times the belled diameter with the bell diameter equal to 2.0 to 3.0 times the shaft diameter.

11.3.6.5. Reduction Factors for Clay

Reduction factors for anchors in clay are shown in Figure 11-28.

11.3.6.6. Gravel Packed Anchors

A gravel packed anchor is used on cohesive soils primarily to increase the value of the undrained shear strength coefficient, α. The original anchor hole is filled with angular gravel. A small closed-end casing is then driven into the hole displacing the gravel into the surrounding clay. Grout is then injected as the casing is withdrawn.

The grout penetrates the gravel and increases the effective anchor diameter. The irregular surface also improves the strength along the grout-soil interface.

PZ27.COM

“YOUR FIRST SOURCE OF INFORMATION ON SHEET PILING”



For more than a century, sheet piling has been a successful and economic form of retaining walls and, in some cases, a foundation bearing member. The purpose of this site is to give you, the engineer, owner, contractor or other the information you need to design, build and maintain succesful sheet piling walls.

There's so much information on PZ27.com, it's hard to know where to begin!

There are several broad categories of information:

Overview of Sheet Piling, which includes: • History • Interlocks • Legal Aspects

Design Information on Sheet Piling, which includes: • Loads and stresses on sheeting • Anchor Systems
• Specifications for sheet piling, pile points and splices • Design methods and software • Seepage under and through sheet pile walls • Photo Gallery of Sheet Piling • Sample Specifications for Sheet Piling

Installation and Equipment, which includes the following: • Installation of sheet piling • Driving equipment
• Driving Tips • Sales and rentals of sheeting and equipment • Reconditioning of Sheeting • Inspection and Installation of Sheet Pile Cofferdams • Photo Gallery of Installation • Special types of sheeting • Cellular cofferdams, a very important topic (including photo gallery) • High modulus walls, including HZ wall systems
• Maintenance • Corrosion and Cathodic Systems • Coating Specifications • Reconditioning of Sheet Piling
• Repair and Maintenance of Sheet Piling

Glossary, so you'll know what the salesman is actually talking about!

There are also links throughout the site to more resources to help you with your sheeting requirements. So come visit www.PZ27.com NOW!

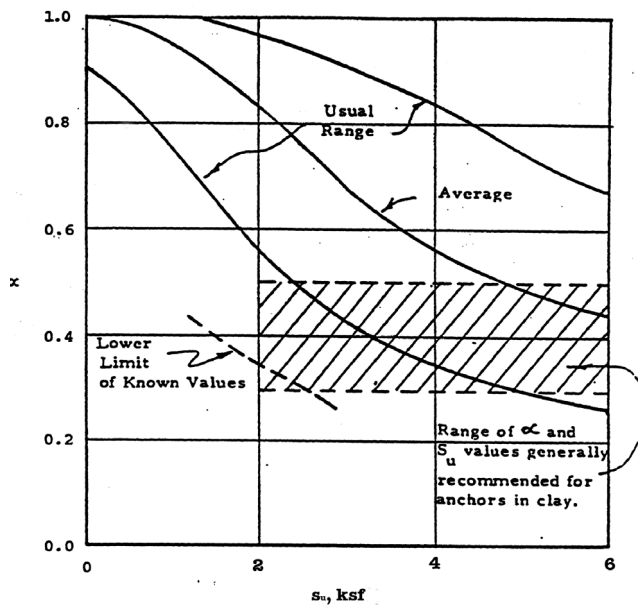
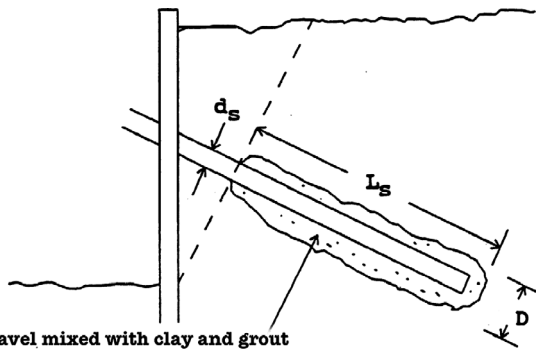


Figure 11-28: Reduction Factors for Clay

Littlejohn proposed that the following equation be used for determining the ultimate load of a gravel packed anchor. There are terms for both frictional resistance and end bearing. A substantial increase in the value of the undrained shear strength coefficient is recommended, and the anchor diameter is larger.



Angular gravel mixed with clay and grout

$$\text{Equation 11-44: } P_u = \alpha s_u \pi D L_s + \frac{\pi (D^2 - d_s^2)}{4} N_c s_u$$

Where

$$N_c = 9$$

$\alpha = 0.6 - 0.75 =$ undrained shear strength coefficient

11.3.7. Forces On The Vertical Members

Tiebacks are generally inclined, therefore the vertical component of the tieback force must be resisted by the vertical member through skin friction on the embedded length of the piling in contact with the soil and by end bearing. Problems with tied back walls have occurred because of excessive downward wall movement. The pile capacity should always be checked to ensure that it can resist the vertical component of the tieback force. The sheet pile sample problem demonstrates one method to account for the vertical load on the piling.

Ultimate values (without safety factors) for friction and end bearing of piling follow:

Driven Piling

Skin Friction

$$= N/25 \text{ ksf for concrete piles}$$

$= N/50 \text{ ksf for WF sections (based on a rectangular perimeter equal to two times the width of the flange added to two times the depth of the section).}$

End Bearing:

$$\text{Cohesionless Soil: } = 8N \text{ ksf}$$

$\text{Cohesive Soil: } = 9s_u \text{ or } = 4.5q_u \text{ (based on a rectangular perimeter equal to two times the width of the flange added to two times the depth of the section).}$

Special Note: For sheet piling use $N/50$ for skin friction for depth D on both faces, but do not use end bearing.

Drilled Piling

Skin Friction $= N/50 \text{ ksf}$

End Bearing

$$\text{Cohesionless Soil: } = 4N \text{ ksf}$$

$$\text{Cohesive Soil: } = 9s_u \text{ or } = 4.5q_u \text{ (based on the gross area).}$$

$N =$ SPT (Standard Penetration Test) value

11.3.8. Overall (Global) System Stability

To ensure overall stability of an anchored system slope stability analysis may be required in addition to the general (local) system analysis except when the horizontal component of the anchor is greater than total height of the vertical member. Figure 11-29 depicts the foregoing.

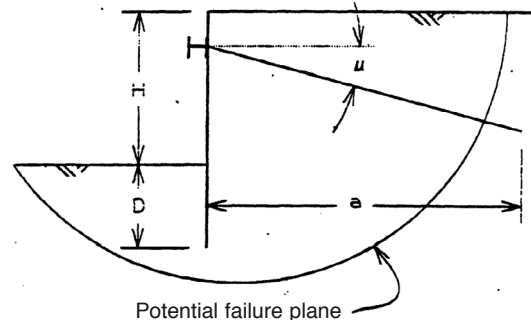


Figure 11-29: Potential Failure Plane

$$\text{Equation 11-45: } a/(H + D) > 1.0$$

Where:

$a =$ The horizontal component of the tieback anchor length

$H + D =$ the vertical member's total length.

11.3.9. Testing Tieback Anchors

11.3.9.1. Overview

The contractor is responsible for providing a reasonable test method for verifying the capacity of the tieback anchors after installation. Anchors are tested to assure that they can sustain the design load over time without excessive movement. The need to test anchors is more important when the

Table 11-2: Tieback Proof Test Criteria

Test Load	Load Hold Duration	Percentage of tiebacks to be load tested
<u>Cohesionless Soils</u>		
Normal Risk		
1.2 to 1.3 Design Load	10 Minutes	10% for each soil type encountered
High Risk		
1.3 Design Load	10 Minutes	20% to 100%
<u>Cohesive Soils</u>		
Normal Risk		
1.2 to 1.3 Design Load	30 Minutes	10%
High Risk		
1.3 Design Load	60 minutes	30% to 100%*
*Use 100% when in soft clay or when ground water is encountered. Use load hold of 60 minutes for 10% and load hold of 10 minutes for remaining 90% of tiebacks.		

system will support, or be adjacent to existing structures, and when the system will be in place for an extended period of time.

The number of tiebacks tested; the duration of the test, and the allowable movement, or load loss, specified in the contractor's test methods should take into account the degree of risk to the adjacent surroundings. High-risk situations would be cases where settlement or other damage would be experienced by adjacent facilities. See *Table 11-2* for a list of minimum recommended criteria for testing temporary tieback anchors.

Generally the shoring plans should include tieback load testing criteria which should minimally consist of proof load test values; frequency of testing (number of anchors to be tested), test load duration, and allowable movement or loss of load permissible during the testing time frame and the anticipated life of the shoring system. The shoring plans should also include the measures that are to be taken when, or if, test anchors fail to meet the specified criteria.

Pressure gages or load cells used for determining test loads should have been recently calibrated by a certified lab, they should be clean and not abused, and they should be in good working order. The calibration dates should be determined and recorded.

Tiebacks that do not satisfy the testing criteria may still have some value. Often an auxiliary tieback may make up for the reduced value of adjacent tiebacks; or additional reduced value tiebacks may be installed to supplement the initial low value tiebacks.

11.3.9.2. Proof Testing

Proof testing of tiebacks anchors is normally accomplished by applying a sustained proof load to a tieback anchor and measuring anchor movement over a specified period of time. Proof testing may begin after the grout has achieved the desired strength. A specified number of the tieback anchors will be proof tested by the method specified on the Contractor's approved plans (see *Table 11-2*).

Generally, the unbonded length of a tieback is left ungrouted prior to and during testing. This ensures that only the bonded length is carrying the proof load during testing. It is not desirable to have loads transferred to the soil through grout (or concrete) in the unbonded region since this length is considered to be within the zone of the failure wedge.

As an alternative, for small diameter drilled holes (6 inches or less) a plastic sheathing may be used over the unbonded length of the tendon to separate the tendon from the grout (see *Figure 9-3*). The sheathing permits the tendon to be grouted full length before proof testing. A void must be left between the top of the grout and the soldier pile to allow for movement of the grout column during testing.

Research has shown that small diameter tiebacks develop most of their capacity in the bonded length despite the additional grout in the unbonded length zone. This phenomenon is not true for larger diameter tieback anchors.

Generally the contractor will specify an alignment load of 5 to 10% of the design load that is initially applied to the tendon to secure the jack against the anchor head and stabilize the setup. The load is then increased until the proof load is achieved. Generally a maximum amount of time is specified

to reach proof load. Once the proof load is attained, the load hold period begins. Movement of the tieback anchor is normally measured by using a dial indicator gage mounted on a tripod independent of the tieback and shoring and positioned in a manner similar to that shown in Figure 11-30.

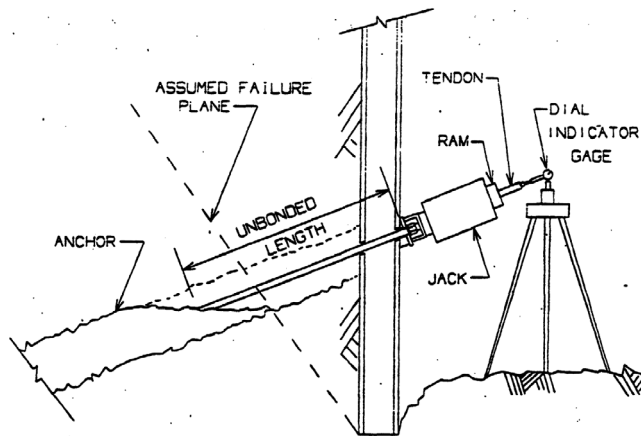


Figure 11-30: Dial Indicator Setup for Proof Testing

The tip of the dial indicator gage is positioned against a flat surface perpendicular to the centreline of the tendon (This can be a plate secured to the tendon). The piston of the jack may be used in lieu of a plate if the jack is not going to have to be cycled during the test. As long as the dial indicator gage is mounted independently of the shoring system, only movement of the anchor due to the proof load will be measured. Continuous jacking to maintain the specified proof load during the load hold period is essential to offset losses resulting from anchor creep or movement of the shoring into the supporting soil.

Measurements from the dial indicator gage are taken periodically during the load hold period. The total movement measured during the load hold period of time is compared to the allowable value indicated on the approved shoring plans to determine the acceptability of the anchor.

It is important that the proof load be reached quickly. When excessive time is taken to reach the proof load, or the proof load is held for an excessive amount of time before beginning. The measurement of creep movement, the creep rate indicated will not be representative. For the proof test to be accurate, the starting time must begin when the proof load is first reached.

As an alternative to measuring movement with a dial indicator gage, the contractor may propose a "lift-off test". A "lift-off test" compares the force on the tieback at seating to the force required to lift the anchor head off of the bearing plate. The comparison should be made over a specified period of time. The lost force can be converted into creep movement to provide an estimate of the amount of creep over-the life of the shoring system.

Use of the "lift-off test" may not accurately predict overall anchor movement. During the time period between lock-off

and lift-off, the tieback may creep and the wall may move into the soil. These two components cannot be separated. If the test is done accurately, results are likely to be a conservative measure of anchor movement. Use of dial indicator gage to monitor creep rather than lift-off tests.

11.3.9.3. Evaluation of Creep Movement

Long-term tieback creep can be estimated from measurements taken during initial short term proof testing: In effect, measurements made at the time of proof testing can be extrapolated to determine anticipated total creep over the period the shoring system is in use if it is assumed that the anchor creep is roughly modelled by a curve described by the "log" of time.

The general formula listed below for the determination of the anticipated long-term creep is only an estimate of the potential anchor creep and should be used in conjunction with periodic monitoring of the wall movement. This formula will not accurately predict anchor creep for soft cohesive soils.

Based on the assumed creep behaviour, the following general formula can be utilized to evaluate the long-term effects of creep:

$$\text{Equation 11-46: } \Delta_{2-3} = C \log_{10} \left(\frac{T_3}{T_2} \right)$$

Where

D = creep movement specified on the plans for times T_1 , T_2 or T_3 (or measured in the field)

T_1 = time of first movement measurement during load hold period (usually one minute after proof load is applied)

T_2 = time of last movement measurement during load hold period

T_3 = time the shoring system will be in use

And

$$\text{Equation 11-47: } C = \frac{\Delta_{1-2}}{\log_{10} \left(\frac{T_2}{T_1} \right)}$$

If using a "lift-off test" to estimate the creep movement, the following approximation needs to be made for substitution into Equation 11-47:

$$\text{Equation 11-48: } \Delta_{1-2} \approx \frac{(P_1 - P_2)L}{AE}$$

Where

P_1 = force at seating

P_2 = force at lift-off

$L = L_u + 0$ to 5 feet of the bonded length necessary to develop the tendon

A = area of the strand or bar in the anchor

E = modulus of elasticity of the strand or bar in the anchor

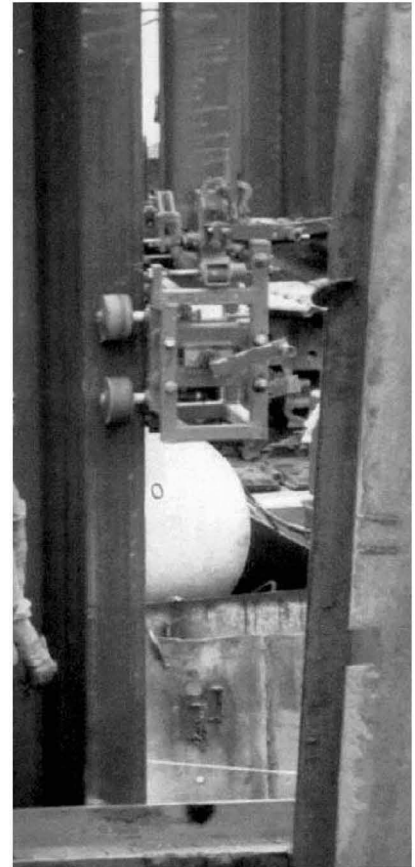
STAB CAT

FOR

THREADING

SHEET PILE

THREADER



The **Stab Cat Threader** has been developed since 1995. The **Stab Cat** is protected by U.S. patents 5,407,304 and 5,618,135. The **Stab Cat** has been proven time and again in strong winds (35 mph @ Port of Beaumont TX with one hundred foot sheets) the only damage sustained was a couple of bent wheel shafts. These were handily replaced with some "old" one-inch bolts from the Contractor's tool shack while new wheel shafts were "overnighted" to the Contractor. The Stab Cat set a double-walled cofferdam in 12-foot of water to excavate the Belle, a 45-ton barque longue (Ship for La Salle – French explorer, circa 1686) in Matagorda Bay in Texas. (SEE NATIONAL GEOGRAPHIC VOL.191, NO.5 MAY 1997). **Stab Cat** is not designed and built by some CAD operator in an office in cyber time that has never had a pair of work gloves on. It is designed, built and patented by real Pile drivers in real time.

For more information visit www.stabcat.com



11.3.9.4. Performance Testing

Performance testing is similar to, but more extensive, than proof testing. Performance testing is used to establish the movement behaviour for a tieback anchor at a particular site.

Performance testing is not normally specified for temporary shoring, but it can be utilized to identify the causes of anchor movement. Performance testing consists of incremental loading and unloading of a tieback anchor in conjunction with measuring movement.

11.3.9.5. Lock-Off Force

The lock-off force is the percentage of the required design force that the anchor wedges or anchor nut is seated at after seating losses. A value of $0.8T_{DESIGN}$ is typically recommended as the lock-off force but lower or higher values are used to achieve specific design needs.

One method for obtaining the proper lock-off force for strand systems is to insert a shim plate under the anchor head equal to the elastic elongation of the tendon produced by a force equal to the proof load minus the lock-off load. A correction for seating of the wedges in the anchor head is often subtracted from the shim plate thickness. To determine the thickness of the shim plate use the following equation:

$$t_{shim} = \frac{(P_{Proof} - P_{lockoff})L}{AE} - \Delta L$$

where:

t_{shim} = thickness of shim

P_{Proof} = Proof load

$P_{lockoff}$ = Lock-off load

A = Area of tendon steel (bar or strands)

E = Modulus of Elasticity of strand or bar

ΔL = seating loss

$L \approx$ Elastic length of tendon (usually the unbonded length + 3 to 5 feet of the bonded length necessary to develop the tendon)

11.3.10. Wall Movement and Settlement

As a rule of thumb, the settlement of the soil behind a tied back wall, where the tiebacks are locked-off at a high percentage of the design force, can be approximated as equal to the movement at the top of the wall caused by anchor creep and deflection of the piling.

If a shoring system is to be in close proximity to an existing structure where settlement might be detrimental, significant deflection and creep of the shoring system would not be acceptable: If a shoring system will not affect permanent structures; or when the shoring might support something like a haul road, reasonable lateral movement and settlement can be tolerated.

Seating loss can vary between 3/8" to 5/8" for strand systems. The seating loss should be determined by the designer of the system and verified during installation. Often times, wedges are mechanically seated minimizing seating loss resulting in the use of a lesser value for the seating loss. For thread bar systems, seating loss is much less than that for strand systems and can vary between 0" to 1/16".

After seating the wedges in the anchor head at the proof load, the tendon is loaded, the shim is removed and the whole anchor head assembly is seated against the bearing plate.

11.3.11. Steps For Checking Tieback Shoring Submittal

1. Review plan submittal for completeness.
2. Determine K_a and K_p .
3. Develop pressure diagrams.
4. Determine forces.
5. Determine the moments around the top of the pile (or some other convenient location).
6. Solve for depth (D), for both lateral and vertical loads, and tieback force (T_H).
7. Check pile section.
8. Check anchor capacity.
9. Check miscellaneous details.
10. Check adequacy of tieback test procedure.
11. Review corrosion proposal.
12. Consider effects of wall deflection, and subsequent soil settlement on any surface feature behind the shoring wall.

11.3.12. Tieback Design and Testing Examples

Example 16: Tieback Testing

Measurement and time method:

Given:

The shoring plans indicate that a proof load shall be applied in 2 minutes or less then the load shall be held for ten minutes. The test begins immediately upon reaching the proof load value. Measurements of movement are to be taken at 1, 4, 6, 8 and 10 minutes. The proof load is to be 133% of the design load. The maximum permissible movement between 1 and 10 minutes of time will not exceed 0.1 inches. All tiebacks are to be tested. The system is anticipated to be in place for 1 year.

Find:

Determine the long-term effects of creep.

Solution:

$A = 0.1$ inches

$T_1 = 1$ minute

$T_2 = 10$ minutes

$T_3 = (1 Y) (365 D/Y) (24 H/D) (60 M/H) = 525,600$ minutes

$$C = \frac{\Delta_{1-2}}{\log_{10}\left(\frac{T_2}{T_1}\right)} = \frac{1}{10\log_{10}\left(\frac{10}{1}\right)} = 0.1$$

Long Term

$$\Delta_{2-3} = C \log_{10}\left(\frac{T_2}{T_3}\right) = 0.1\log_{10}\left(\frac{525,600}{10}\right) = 0.47" \approx \frac{1}{2}"$$

The proof load, and duration of test are reasonable and exceed the minimums shown in Table 11-2. Applying the

proof load in. a short period of time and beginning the test immediately upon reaching that load ensure the test results will be meaningful and can be compared to the calculated long-term creep movement for the anchor.

If the shoring system were in close proximity to an existing structure that could not tolerate a 1/2 inch of settlement the design would not be acceptable. If the shoring would not affect permanent structures or when the shoring might support something like a haul road, the anticipated movement would be tolerable.

Lift off load method:

Given:

Lift off test will be performed 24 hours after wedges are seated (1 minute). The force at seating the wedges will be 83,000 pounds and the lift off force will be no less than 67,000 pounds.

Solution

$L = 20'$, which is the unbonded length of $15' + 5'$

$A = 0.647 \text{ in}^2$

$E = 28,000,000 \text{ psi}$

$T_2 = 1 \text{ minute}$, this is the time the wedges are seated

$$\Delta_{1-2} \approx ((P_1 - P_2)L)/AE$$

$$\approx ((83,000 - 67,900)(20)(12))/((0.647)(28 \times 10^6))$$

$$\approx 0.2 \text{ in}$$

$$C \approx 0.2 / [\log_{10}(1440/1)]$$

$$\approx 0.06$$

$$\text{Long term } \Delta_{1-3} \approx (C) \log_{10}(T_3/T_2) = (0.06) \log_{10}(525,600/1)$$

$$\approx 0.34 \text{ inches} \approx 5/16 \text{ inch}$$

Example 17: Single Tier Tieback Shoring Wall

This example problem illustrates the analysis for a single tier tieback sheet pile wall next to a haul road and demonstrates the following principles:

The use of the "Free Earth Support Method" of sheet pile analysis with Rowe's "Moment Reduction Theory" to

determine the required depth of embedment (D), the required sheet pile section modulus ($S_{REQUIRED}$), and the design tieback force(T).

Low pressure grouted anchor tieback analysis.

Review of proof loading and lock-off loading.

The Contractor's shoring submittal outlined below is to be reviewed for adequacy.

Anchor Details: 5/8" Dywidag bars at 10' 0" centre spacing centred in 6" diameter (d) drilled holes that are to be grouted with low-pressure grout. $T_{DESIGN} = 25 \text{ Kips}$.

$$T_{proof} = (1.3)T_{DESIGN}$$

Proof Testing of Tiebacks: (Notes on the shoring plans)

Alternate anchors will be proof tested to T_{PROOF} after the anchor grout has obtained adequate strength.

The exposed end of the anchor rod shall not show movement of more that 2 inches while jacking up to the proof load value.

The proof load (T_{PROOF}) shall be attained and held for 15 minutes. Anchor movement shall not exceed 0.1 inches between 1 and 15 minute, Readings shall be taken at 1, 5, 10 and 15 minutes. The system will be in place approximately 6 months.

Anchors failing the -test criteria shall be replaced.

Analysis:

$$\text{Top failure wedge width} = 15' \tan(45^\circ - \phi/2) = 7.0' < 10' + 2'$$

Since light haul road traffic is to be beyond the active failure wedge limits, the use of minimal friction on the sheet piling for the active condition may be permitted.

For simplified analysis, use the alternate loading of 100 psf for traffic surcharge.

Solution:

SPW 911 was used to determine the actual tieback and wall loads. The result is shown in Figure 11-32. SPW 911 reports a factor of safety of 3.3.

Compute Tieback Forces:

Tieback force per lineal foot of wall = 2268.1 lb/ft

$$\text{Tieback force per tieback} = (2268.1)(10) = 22,681 \text{ lb}$$

$$\text{Actual tension in tieback} = 22,681 / \cos 15^\circ = 23,481 \text{ lb} < 25\text{K per plans}$$

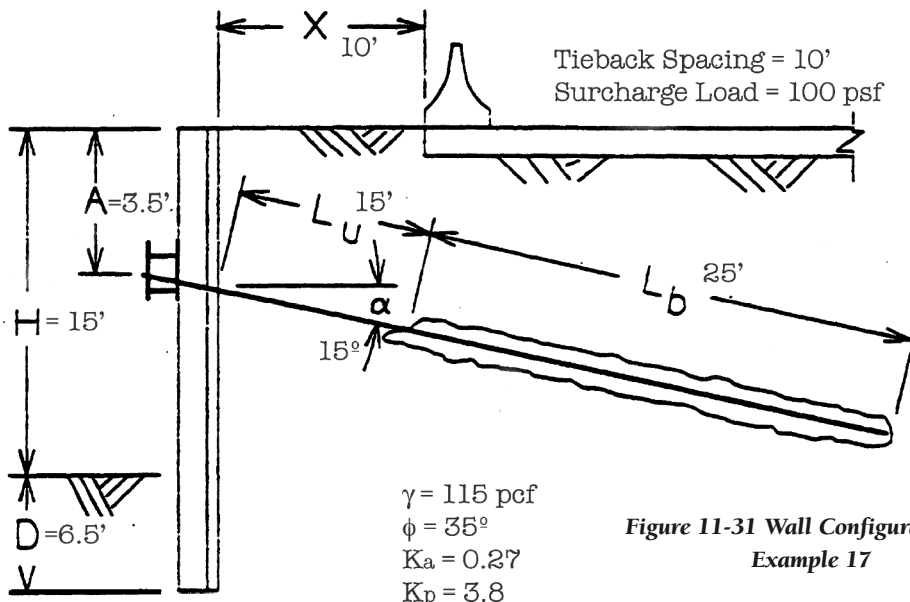


Figure 11-31 Wall Configuration for Example 17

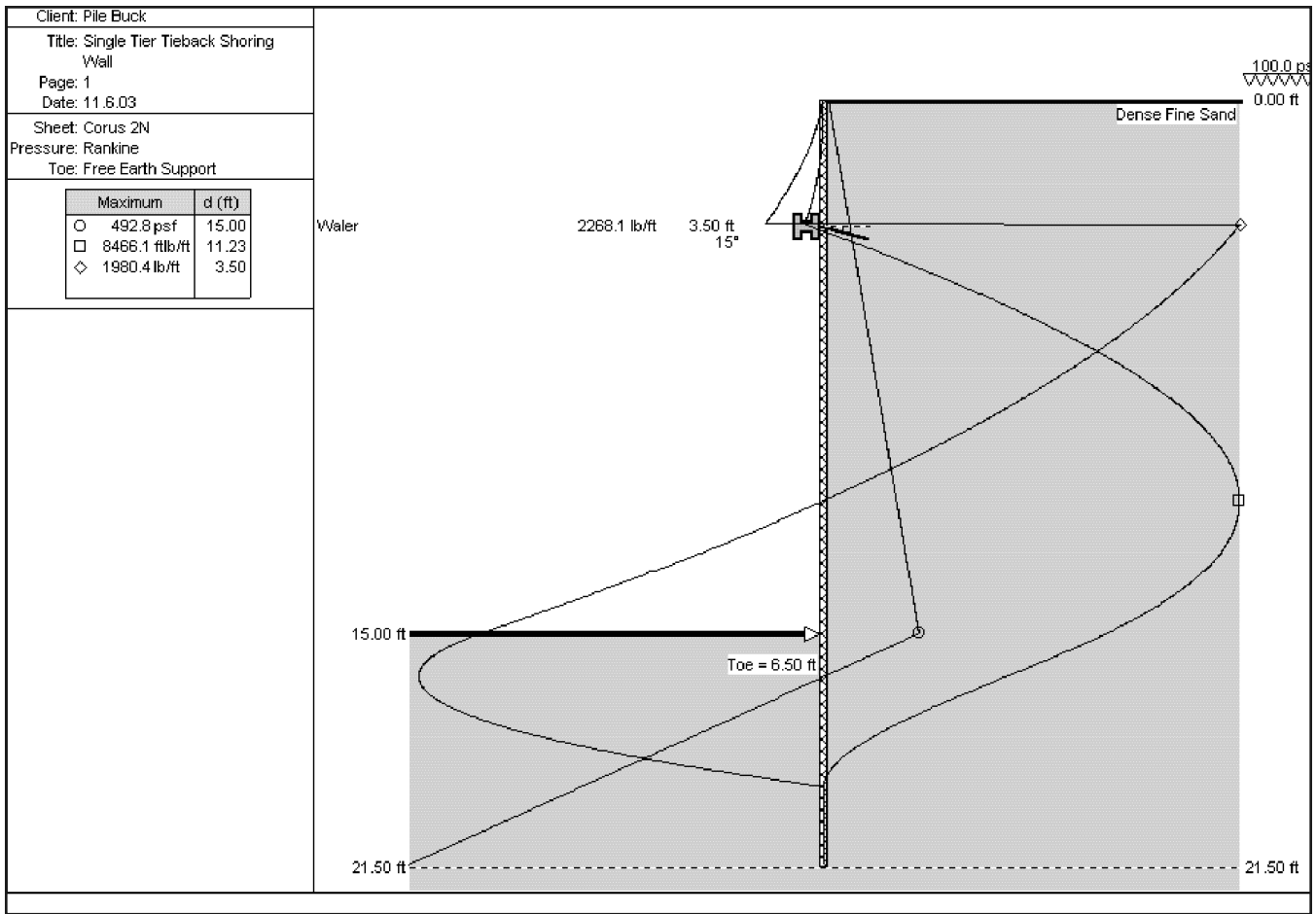
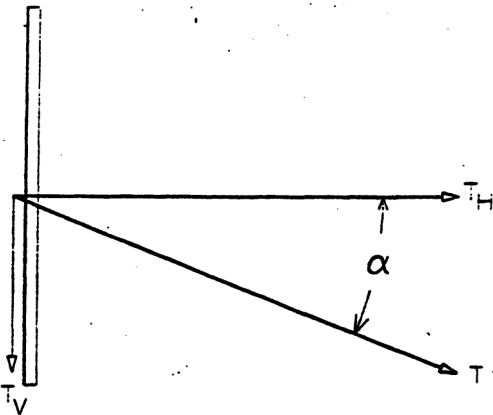


Figure 11-32: SPW 911 Solution for Example 17

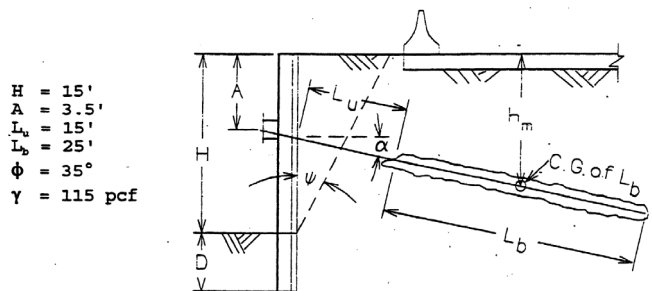
Design horizontal force per lineal foot of wall = $(25,000)(\cos 15^\circ)/10 = 2,419 \text{ lb/ft}$
 Design vertical force per lineal foot of wall = $(25,000)(\sin 15^\circ)/10 = 647 \text{ lb/ft}$



Total frictional resistance below excavation line = $(0.54)(6.5)(2 \text{ sides}) = 7.02 \text{ kips/ft}$
 Using safety factor of two, design frictional resistance = $7.02/2 = 3.51 \text{ kips/ft} = 3,510 \text{ lb/ft}$
 Resistance = $3,510 \text{ lb/ft} > 647 \text{ lb/ft}$ OK

Check Anchor Tendon Capacity:
 Plan calls for 5/8" Dywidag bars spaced at 10' 0" centres.
 $F_{ult} = 157 \text{ ksi}$
 $A_{bar} = 0.28 \text{ in}^2$
 $T_{design} < 0.6 F_{ult} A_{bar} = (0.6)(157)(0.28) = 26.4 \text{ kips} > 25 \text{ kips}$ OK
 $T_{proof} < 0.8 F_{ult} A_{bar} = (0.8)(157)(0.28) = 35.4 \text{ kips} > (1.3)(25) = 32.5 \text{ kips}$ OK

Check downward force due to prestressing:
 Resistance to downward force is furnished by the skin friction on both sides of the embedded sheet piling.
 For a soil with $\phi = 35^\circ$, assume an SPT value of $N = 27$
 Frictional resistance = $N/50 \text{ ksf} = 27/50 = 0.54 \text{ ksf}$



COMPOSITE Z™



Composite Z sheet profile

FEATURES

Corrosion resistant
 High strength reinforced composite
 No coating required
 Lightweight for easy installation
 Non-conductive
 Easy to cut
 Easy to thread
 Domestic "Ball & Socket" interlock

Products

Z-100 sheet pile
 Z-200 sheet pile
 Z-90 Corner
 Z-100 Cap system
 Z-200 Cap system
 Z-Beam wale system
 EZ-Deck composite decking

Equipment

Vibratory Hammers
 Model 10
 Model 20



"the sheet pile of tomorrow available today"

Contact us:

Voice: 561-848-2050
 Fax: 561-842-7209
 Z@compositeZ.com

Composite Components, Inc.

P.O. Box 14295
 North Palm Beach, FL 33408
 www.CompositeZ.com

Assumed

failure wedge angle $\psi = 45^\circ - \phi/2 = 27.5^\circ$ $\alpha = 15^\circ$

Check L_u minimum:

$$\begin{aligned} L_u \text{ minimum} &= (H - 3.5') (\sin \psi) / \sin [180^\circ - (90^\circ - \alpha) - \psi] \\ &= (15' - 3.5') \sin 27.5^\circ / \sin 77.5^\circ \\ &= 5.4' < 15' \text{ OK} \end{aligned}$$

Determine h_m :

$$\begin{aligned} h_m &= 3.5 + (L_u + L_b/2) \sin \alpha \\ &= 3.5 + (15' + L_b/2) \sin 15^\circ \\ &= 7.4' + 0.13L_b \end{aligned}$$

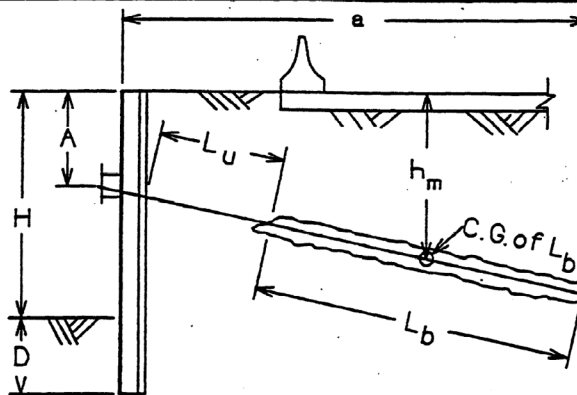
Determine L_b using FHWA formula:

$$\begin{aligned} P_{ult} &= \pi (d) (L_b) (\gamma) (h_m) \tan \phi \\ &= \pi (0.5) (L_b) (115) (7.4 + 0.13L_b) \tan 35^\circ \\ &= 936L_b + 16.4 (L_b)^2 = 33,650 \text{ Lb} \end{aligned}$$

$$P_{ult} = 33,650 \text{ Lb} > T_{\text{PROOF}} = 32,500 \text{ Lb} \quad \text{OK}$$

Proof testing will verify actual anchor capacities.

Simplified Wall Stability Check For Single Tier Tieback:



If $a/(H + D) > 1$, The wall may be considered stable.

$$\begin{aligned} \text{where: } a &= \text{horizontal component of the tie.} \\ &= (L_u + L_b) \cos \alpha \\ &= (15' + 25') \cos 15^\circ = 38.6 \text{ feet} \end{aligned}$$

$$a/(H + D) = 38.6' / (15' + 6.5') = 1.8 > 1 \quad \text{OK}$$

Lock-Off Force

A value of $0.8T_{DESIGN}$ is typically recommended as a minimum value for low to normal risk conditions. The use of $0.8T_{DESIGN}$ would be satisfactory for this case provided small settlements behind the wall will not be detrimental.

Check Proof Loading

$$C = \Delta_{1-2} / [\log_{10}(T_2/T_1)] = 0.1 / [\log_{10}(15/1)] = 0.085$$

$$\begin{aligned} \text{Long term } \Delta &= (C) \log_{10}(T_3/T_2) \\ &= (0.085) \log_{10}(262,800/15) \\ &= 0.36 \text{ in.} \end{aligned}$$

A long-term movement of the wall can be approximated but if neither wall movement nor settlement behind the wall will be detrimental then 0.36 inch would be acceptable.

the support loads. Using the topmost load as an example, these are as follows:

- Distributed support load = 10,856 lb/ft (from SPW 911)
- Distributed axial load on tiebacks = $10,856 \text{ lb/ft} / \cos 20^\circ = 11,553 \text{ lb/ft}$
- Distributed vertical load of tiebacks on wall = $(10,856) (\tan 20^\circ) = 3,951 \text{ lb/ft}$
- Frictional resistance generated by support = $(10,856) (0.4) = 4,342 \text{ lb/ft}$
- Axial load per support = $(11,553)(7.5) = 86,645 \text{ lb}$
- Test load per support = $(86,645)/(0.8) = 108,307 \text{ lb}$

These are tabulated for all of the supports in Table 11-3.

The frictional resistance is greater than the vertical load, $13,424 \text{ lb/ft} > 12,215 \text{ lb/ft}$, so the wall should be capable of resisting the vertical load. It is interesting to note that the maximum possible tieback inclination for this particular coefficient of friction is $\arctan(0.4) = 21.8^\circ$.

We now design the topmost tieback itself.

Example 18: Multiple Tier Tiebacks

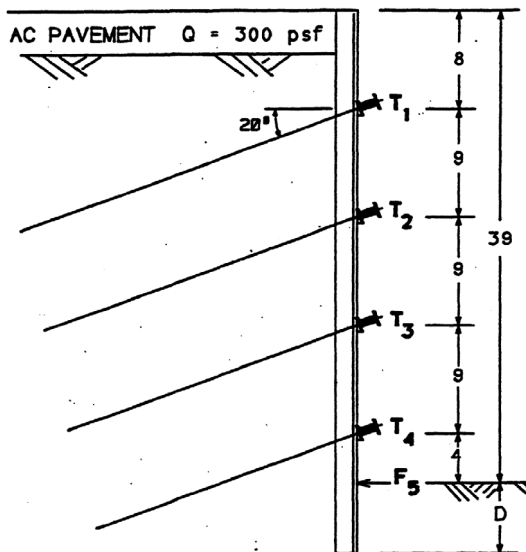


Figure 11-33: Wall Configuration for Example 18

Given

- Wall as shown above
- Soils: Cohesionless, $\gamma = 115 \text{ pcf}$, $\phi = 35^\circ$, $c = 0$, $K_a = 0.27$, $K_p = 2.6$
- Tiebacks spaced at 7' 6" along the walls, drilled with 8" drill

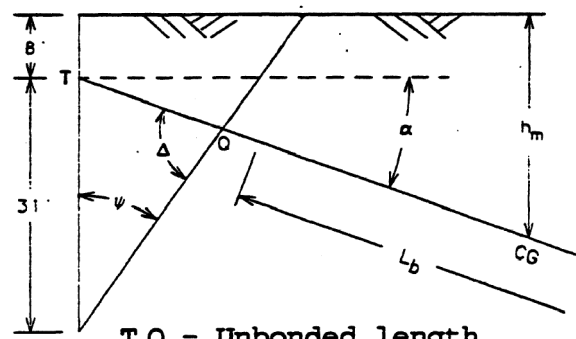
Find

- Tieback loads
- Design of tiebacks

Solution

We use SPW 911 to solve the problem. The solution is shown in Figure 11-34. A detailed discussion of earth pressure distribution for multiply supported excavations is given elsewhere. In this case we used the area distribution method.

All of the support loads are shown in the SPW 911 solution. There are several results that can be computed from



$T_1Q = \text{Unbonded length}$

$L_b = \text{Bonded Length}$

$P = 86,645 \text{ lb.}$

$P_{ult} = 108,307 \text{ lb. (proof)}$

$\psi = 35^\circ$

Compute Unbonded Length:

$$T_1Q = 31 (\sin \psi) / \sin \Delta = 31 (0.5736) / 0.9659 = 18.4' > 15'$$

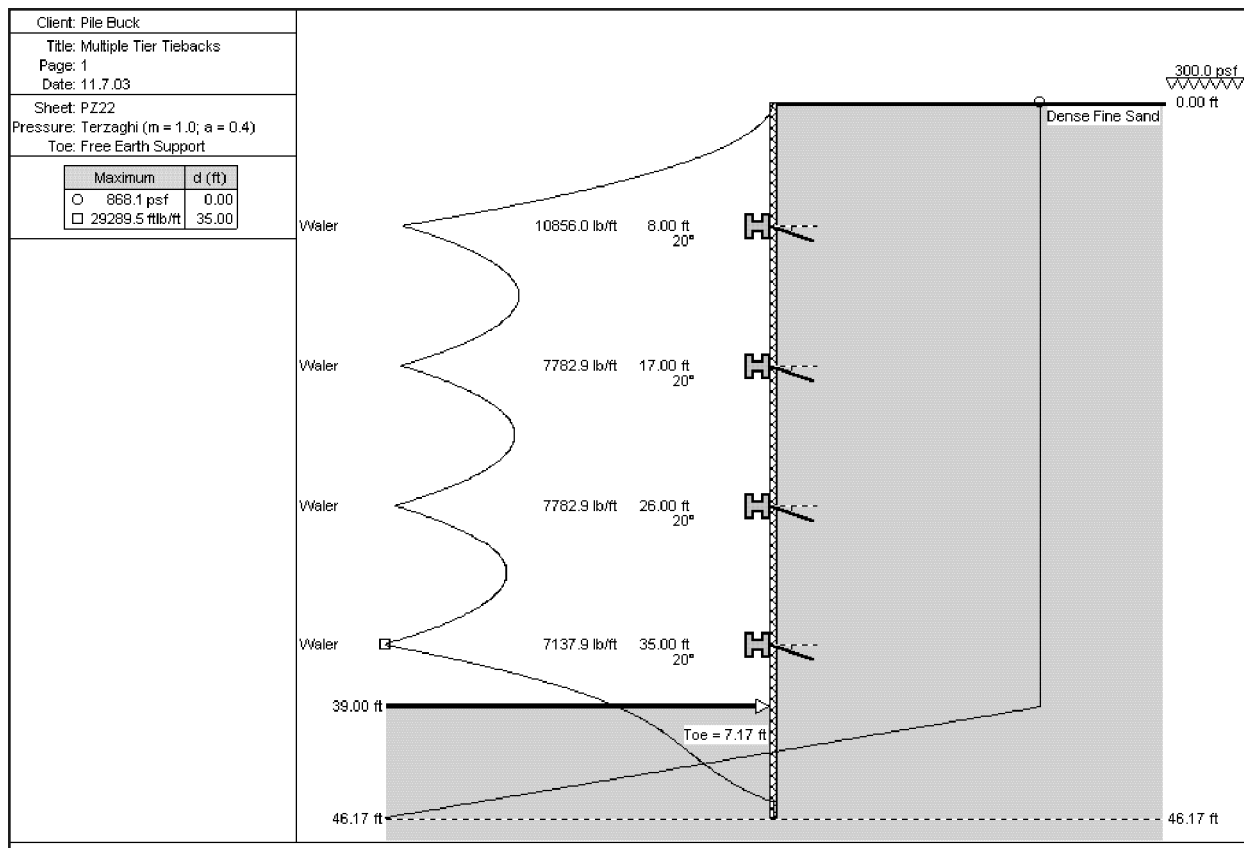


Figure 11-34: SPW 911 Solution for Example 18

Table 11-3: Support Results for Example 18

Tieback	Support Load, lb/ft	Axial Load, lb/ft	Vertical Load, lb/ft	Frictional resistance, lb/ft	Axial Load per lb.	Load Support, Test Load per Support, lb.
1	10,856	11553	3,951	4,342	86,645	108,307
2	7,783	8,282	2,833	3,113	62,118	77,647
3	7,783	8,282	2,833	3,113	62,118	77,647
4	7,138	7,596	2,598	2,855	56,970	71,212
Total	33,560	35,713	12,215	13,424	267,851	334,814

Compute distance h_m from ground surface to centre of length L_b , thus $h_m = 8 + (T_1Q + L_b/2) \sin \alpha = 8 + (18.4 + L_b/2)(0.342) = 14.29 + 0.171L_b$

To solve for L_b , use Equation 11-36:

$$108,307 = \pi (8/12)(115)(14.29 + 0.171L_b)(\tan 35^\circ)L_b$$

$$108,307 = 2.411.6L_b + 28.85L_b^2$$

$$L_b^2 + 83.58L_b - 3,754.1$$

$$L_b = 32.4', \text{ or use } 32' 6''$$

Other tiebacks can be designed in the same way.

Multiple tieback systems approximate a multiple strutted

system. The soil pressure diagram for either system should more appropriately approximate a trapezoid rather than a triangle. This would be especially true for soft to medium clays.

A long bond length is required at the elevation of the upper tier primarily because of the low h_m value. The tiebacks of the upper tier would have been better designed by reducing the centre-to-centre tie spacing to achieve a shorter required bond length. Another way to reduce the bonded length would be to locate the upper ties tie-centre with respect to the second tier ties and to increase the tie slope angle in order to increase the h_m value. The most practical way to decrease the length requirement of the upper tier tie would be to

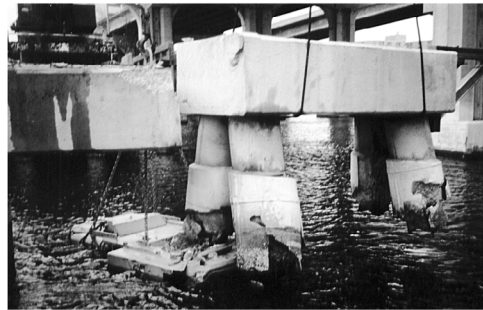
LBT. ENTERPRISES, LTD.

PRIME® PILE CUTTER



Feature (1)

2-part cradle to support the cut off for easier and safer disposal.



Feature (2). 30" P.C.P.C. Easily attaches to most crane hooks. Here we see the 30" model cutting off a huge Pile Cap.



Aurora, Illinois

43" Steel casing filled with concrete and 16 pcs - 1 1/2" Rebar. A slice above it all.



Product (8) 16" P.C.P.C.

Exposing Rebar on a 18" Round Pile



Feature (5). Crushers: for the Prime Concrete Pile Cutter. They are available in different shapes and sizes.

CONSISTENCY, SIMPLICITY, SPEED;

3 REASONS TO MAKE ANYONE SMILE

FOR MORE INFORMATION CALL LBT TOLL FREE AT 1-800-665-7396 OR 1-204-254-6424

VISIT OUR WEBSITE www.pilecutter.com OR EMAIL US AT prime@pilecutter.com

LBT ENTERPRISES LTD. 245 MELNICK RD. WINNIPEG, MANITOBA CANADA

Table 11-4: Typical Values of Bond Stress for Selected Rock Types

Rock Type (Sound, Non-Decayed)	Ultimate Bond Stresses Between Rock and Anchor Plus (δ_{skin}), psi
Granite & Basalt	250 - 450
Limestone (competent)	300 - 400
Dolomitic Limestone	200 - 300
Soft Limestone	150 - 220
Slates and Hard Shales	120 - 200
Soft Shales	30 - 120
Sandstone	120 - 150
Chalk (variable properties)	30 - 150
Marl (stiff, friable, fissured)	25 - 36

Note: It is not generally recommended that design bond stresses exceed 200 psi even in the most competent rocks.

increase the diameter of the drilled hole to 16" or to 18". This would substantially increase the effective bond per linear foot of tie.

Three tiers of tiebacks properly spaced should have been adequate for the soil conditions and design parameters used in this case.

11.3.13. Rock Anchors

Anchor design must consider the following failure modes:

11.3.13.1. Failure of Steel Tendon

Design stress within the steel is usually limited to 50 to 60% of the ultimate stress (50% for permanent installations).

11.3.13.2. Failure of Grout Steel Bond

The bond capacity depends on the number and length of tendons, or steel bars (plain or deformed) and other factors¹¹⁶.

11.3.13.3. Failure of Grout-rock Bond

The bonding capacity between the rock and the grout may be determined from the following formula:

$$\text{Equation 11-49: } P_u = \pi d_s L_o \delta_{skin}$$

Where:

P_u = load capacity of anchor

d_s = diameter of drilled shaft

L_o = length of grout-anchor bond

δ_{skin} = grout-rock bond strength

Typical grout-rock stresses for various rock types are presented in Table 11-4.

11.3.13.4. Failure of Rock Mass

The criterion for failure in rock mass is based on the weight of rock contained within a cone emanating from the bonded zone. Figure 11-35 shows design criteria. Actual failure of anchor in this mode would be controlled by discontinuity patterns and weathering of the rock.

11.3.13.5. Factor of Safety and Testing

Anchors in soil should be designed using a minimum factor of safety of 2.0; a higher factor of safety is used for permanent or critical structures. All production anchors should be proof loaded to 115% to 150% of the design load. Additional testing to higher capacities and to determine creep characteristics may be justified for permanent installations or where the design conditions warrant. Guidelines for testing are

¹¹⁶Littlejohn, G.S., and Bruce, D.A., Rock Anchors, State of the Art, Foundation Publications, Ltd., 1977. (Originally published in Ground Engineering magazine between May 1975 and May 1976).

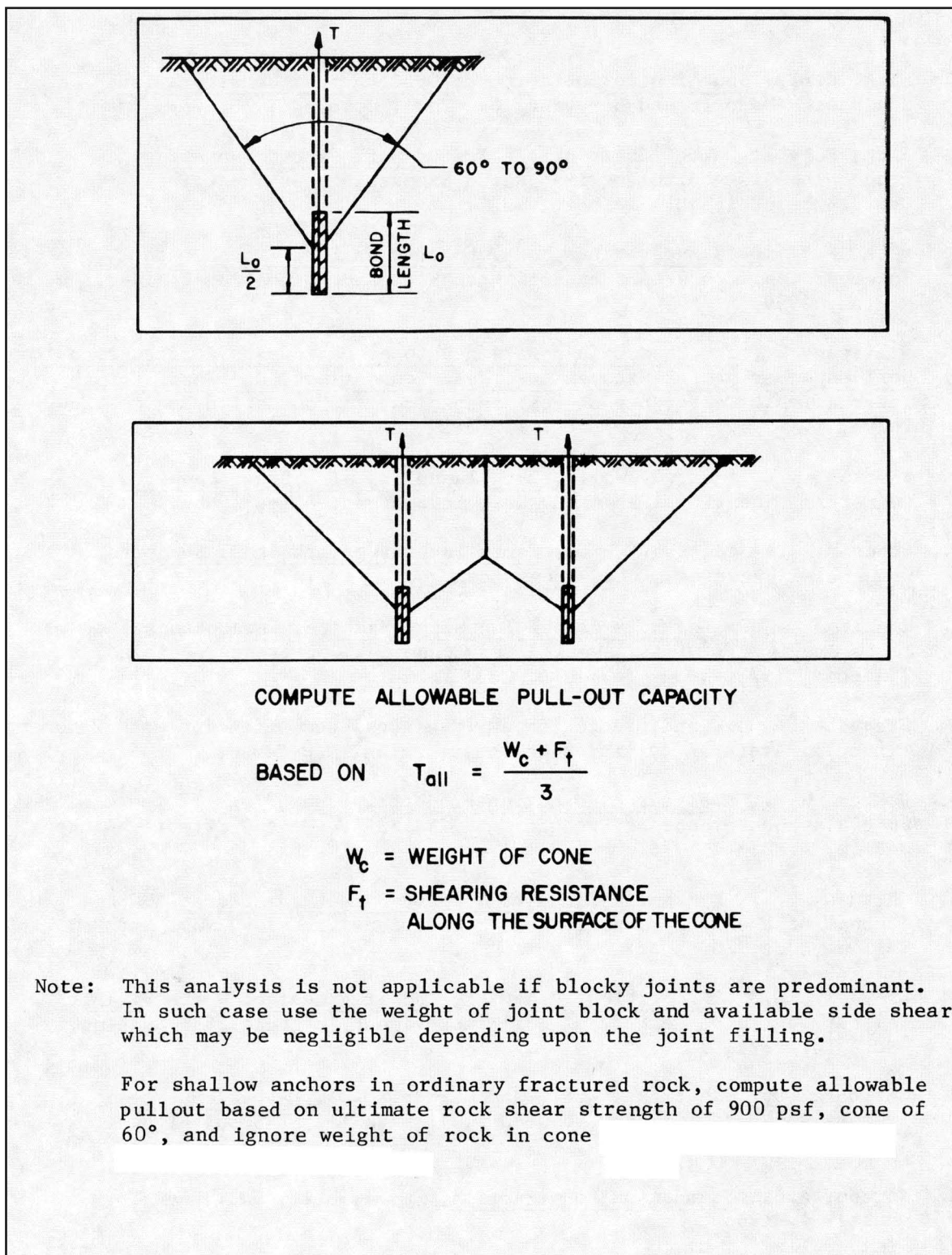


Figure 11-35: Pullout Capacity of Shallow Anchors in Rock

Chapter Twelve:

Analysis and Design of Anchored Walls and Anchor Systems for Earthquake Loads

This section describes the procedures for evaluating the stability and safety of anchored sheet pile walls during earthquakes. Although these can be evaluated using the classical methods described earlier, the implementation of these has many unique features, and so is treated separately.

12.1. Introduction

For earthquake analysis, the free earth support method is used to determine the required depth of sheet pile penetration below the dredge level and the force the anchor must resist so that excessive sheet pile wall movements do not occur during earthquake shaking. The forces acting on both the sheet pile wall and anchor during the earthquake include the static and dynamic earth pressure forces, the static and hydrodynamic pool water pressure forces and the steady state and residual excess pore water pressure forces within the submerged backfill and foundation soils. Because anchored walls are flexible and because it is difficult to prevent some permanent displacement during a major seismic event, it is appropriate to use active and passive earth pressure theories to evaluate dynamic as well as static earth pressures. The Mononobe-Okabe theory is used to evaluate the dynamic earth pressures.

There have been very few documented cases of waterfront anchored walls that have survived earthquakes or of walls that have failed for reasons other than liquefaction.

Hence uncertainty remains concerning the procedures outlined in this chapter and the difficulty of ensuring adequacy of anchored sheet pile walls during strong earthquake shaking (e.g. one rough index is seismic coefficients above 0.2).

One of the few seismic design procedures for anchored sheet pile walls is the Japanese Code. Using the observations regarding the performance of anchored sheet pile walls during earthquake shaking, the following improvements over past practice are recommended:

- (1) Anchors must be placed further away from the wall.
- (2) Larger seismic coefficients are required. They are to be assigned with consideration of the seismotectonic structures as well as the characteristics of soil and structural features comprising the wall, the anchorage and its foundation.
- (3) There is a limitation upon the build-up of excess pore pressures in backfill.

The procedures outlined in this chapter are to be viewed as interim guidance, an improvement over past practice. An

anchored sheet pile wall is a complex structure and its performance (e.g. displacements) during earthquake shaking depends upon the interactions between the many components of the structural system (e.g. sheet pile wall, backfill, soil below dredge level, foundation, and anchorage), which impact overall wall performance. The seismic design of anchored sheet pile walls using the procedures described in this chapter requires considerable judgement during the course of design by an earthquake engineer experienced in the problems associated with the seismic design of anchored sheet pile walls.

As a general design principle, anchored sheet pile walls sited in seismic environments should be founded in dense and dilative cohesionless soils with no silt or clay size particles. The proposed design procedure presumes this to be the case. Strength parameters are to be assigned in accordance with the criteria described earlier.

Additionally, the design procedure is limited to the case where excess pore water pressures are less than 30 percent of the initial vertical effective stress.

12.2. Background

Agbabian Associates¹¹⁷ summarize the performance of anchored sheet pile walls at 26 harbours during earthquakes in Japan, the United States, and South America. Their survey indicates that the catastrophic failures of sheet pile walls are due to the large-scale liquefaction of the backfill and/or the foundation, including the foundation soil located in front of the sheet pile wall and below the dredge level. For those structures that underwent excessive movements but did not suffer a catastrophic failure, there was little or no evidence of damage due to the vibrations of structures themselves. For those walls whose backfill and foundation soils did not liquefy but did exhibit excessive wall moments during the earthquake, the survey identified the source of these excessive sheet pile wall movements as:

- (1) the soil in front of the sheet pile wall and below the dredge level moved outward (toe failure),
- (2) the anchor block moved towards the pool (anchor failure), or
- (3) the entire soil mass comprising the sheet pile structure and the anchor block moved as one towards the pool (block movement).

The report identified a number of factors that may con-

SPW911 v.2

Sheet Piling Design Software

Do you, as a professional engineer or contractor, know of ANY sheet piling design software that has all of these features?

- Completely graphical, easy to use interface
- Windows 95, 98, 2000, Me and NT 4.0
- Customizable database for soils, sheet piles and clients
- Analyzes steel, vinyl or aluminum sheet piling
- Assists design of both cantilever and anchored walls using free earth and fixed earth support methods
- Uses accepted methodology of classical sheet pile wall design
- Rankine, Coulomb and Terzaghi pressure models available
- Passive softening may be switched on or off
- Alternative methods of modeling cohesive soils, including tension cracks
- Water table may be defined above ground level
- Sloping ground allowed
- Multiple soil layers may be entered
- Supports may be placed above ground level
- Frame loads analyzed by the area distribution or hinge methods
- Can be used with single and multiple wale designs
- Graphical or tabular display of pressure, shear force, bending moment or deflection. Graphs may be superimposed on the main design diagram or shown with axes
- Point and click editing of designs
- Prints out in attractive format you can customize with your firm's name and stamp
- Checks and reports for designs not conforming to safety factors, or stress or load requirements
- Rules of thumb feature offers additional safety option
- Metric or imperial units; work in metric and produce imperial output, or vice versa
- Complete context-sensitive and searchable help for all aspects of program operation

**New Windows
2000, NT, XP
Version Now
Available!**

**At Just
\$299.95,
no other
software program
available today
can match the
features of
SPW911 v.2!**

Details Inside



Go to: www.pilingsoftware.com

tribute to the excessive wall movements, including:

- (1) a reduction in soil strength due to the generation of excess pore water pressures within the submerged soils during the earthquake shaking,
- (2) the action of the inertial forces due to the acceleration of the soil masses in front and behind the sheet pile wall and the anchor block, and
- (3) the hydrodynamic water pressures along the front of the wall during the earthquake.

The Japanese Ports and Harbours commissioned a study by Kitajima and Uwabe¹¹⁸ to summarize the performance of 110 quay walls during various earthquakes that occurred in Japan during the past several decades. This survey included a tally of both damaged and undamaged waterfront structures and the dates on which the earthquakes occurred. Most of these waterfront structures were anchored bulkheads, according to Gazetas, Dakoulas, and Dennehy¹¹⁹. In their survey, Kitajima and Uwabe were able to identify the design procedure that was used for 45 of the bulkheads. This is identified as the Japanese code. Their survey showed that (1) the percentage of damaged bulkheads was greater than 50 percent, including those designed using the Japanese design procedure and (2) the percentage of bulkhead failures did not diminish with time. These two observations indicate that even the more recently enacted Japanese code is not adequate. To understand the poor performance of anchored sheet pile walls during earthquakes, it is useful to review the Japanese code that was used in the design of the most recent sheet pile walls that were included in the Kitajima and Uwabe survey.

12.2.1. Summary of the Japanese Code for Design of Anchored Sheet Pile Walls

Most of the case histories regarding the performance of anchored sheet pile walls during earthquakes that were included in the Agabian Associates and the Kitajima and Uwabe surveys are for Japanese waterfront structures. To understand the performance of these Japanese waterfront structures, it is useful to review the Japanese design procedures that were used for the most recently constructed waterfront structures included in the surveys. The Japanese code for the design of anchored sheet pile walls as described by Gazetas, Dakoulas, and Dennehy consists of the following five steps:

- (1) Estimate the required sheet pile embedment depth using the free earth support method, with the factor of safety that is

applied to the shear strength of the soil reduced from 1.5 for static loadings to 1.2 for dynamic loadings. The effect of the earthquake is incorporated in the analysis through the inertial forces acting on the active and passive soil wedges by using the Mononobe-Okabe method to compute P_{AE} and P_{PE} .

- (2) The horizontal seismic coefficient, k_h , used in the Mononobe-Okabe relationships for P_{AE} and P_{PE} is a product of three factors: a regional seismicity factor (0.10 ± 0.05), a factor reflecting the subsoil conditions (1 ± 0.2), and a factor reflecting the importance of the structure (1 ± 0.5).

- (3) Design the tie rod using a tension force value computed on the assumption that the sheet pile is a simple beam supported at the dredge line and by the tie rod connection. Allowable stress in the tie rod steel is increased from 40 percent of the yield stress in a design for static loadings to 60 percent of the yield stress in the design for dynamic loadings.

- (4) Design the sheet pile section. Compute the maximum bending moment, referred to as the free earth support moment, in the sheet pile using the simple beam of Step 3. In granular soils Rowe's procedure is used to account for flexure of the sheet pile below the dredge level. A reduction of 40 to 50 percent in the free earth support moment value is not unusual. Allowable stress in the sheet pile steel is increased from 60 percent of the yield stress in a design for static loadings to 90 percent of the yield stress in the design for dynamic loadings.

- (5) Design the anchor using the tie rod force of step 2 increased by a factor equal to 2.5 in the design for both static and dynamic loadings and assume the slip plane for the active wedge starts at the dredge line.

From the modes of failure observed in the Kitajima and Uwabe study of anchored sheet pile walls that were designed using the Japanese code, Gazetas, Dakoulas and Dennehy identified the following as the primary deficiencies in the Japanese code procedure:

- (1) The values for the seismic coefficients, k_v and k_h , used in the Mononobe-Okabe relationships for P_{AE} and P_{PE} are not determined from a site response analysis but are specified within the Japanese code ($k_v = 0$, and k_h is within a narrow range of values for most of the waterfront structures involved in the study).

- (2) The resistance provided by the anchor is over estimated because the code allows the anchor to be placed too close to the sheet pile wall such that the passive wedge that develops

¹¹⁷Agabian Associates. (1980). "Seismic Response of Port and Harbor Facilities," Report P80-109-499, El Segundo, CA.

¹¹⁸Kitajima, S., and Uwabe, T. (1979) (Mar). "Analysis on Seismic Damage in Anchored Sheet-Piling Bulkheads," Report of the Japanese Port and Harbor Research Institute, Vol. 18, No. 1, pp. 67-130. (in Japanese).

¹¹⁹Gazetas, C., Dakoulas, P., and Dennehy, K. (1990). "Empirical Seismic Design Method for Waterfront Anchored Sheetpile Walls," Proceedings of ASCE Specialty Conference on Design and Performance of Earth Retaining Structures, Geotechnical Special Publication No. 25, pp. 232-250.

in front of the anchor interferes with the active wedge developing within the backfill behind the sheet pile wall.

(3) The code does not account for the earthquake induced excess pore water pressures within the submerged soils and the corresponding reduction in the shear strength for the submerged soil regions, nor the excess water pressure forces and hydrodynamic forces acting on the sheet pile structure.

Gazetas, Dakoulas, and Dennehy listed only one of the failures of the sheet pile walls designed using the Japanese Code as a general flexural failure. In this case, the structural failure was attributed to corrosion of the steel at the dredge level.

Each of these deficiencies is addressed in the steps used in the design of anchored sheet pile walls using the free earth support method of analysis.

12.2.2. Displacements of Anchored Sheet Piles during Earthquakes

In the Kitajima and Uwabe survey of damage to anchored sheet pile walls during earthquakes, the level of damage to the waterfront structure was shown to be a function of the movement of the top of the sheet pile during the earthquake. The damage can be categorized as one of five levels as given in Table 12-1. Their survey shows that for sheet pile wall displacements of 10 cm (4 inches) or less, there was little or no damage to the Japanese waterfront structures as a result of the earthquake shaking. Conversely, the level of damage to the waterfront structure increased in proportion to the magnitude of the displacements above 10 cm (4 inches). Using the information on the anchored sheet pile walls survey reported in Kitajima and Uwabe and using simplified theories and the free earth support method of analysis, Gazetas, Dakoulas, and Dennehy showed that the post-earthquake displacements at the top of the sheet pile wall correlated to (1) the depth of sheet pile embedment below the dredge level and (2) the distance between the anchor and the sheet pile.

Two anchored bulkheads were in place in the harbour of San Antonio, Chile, during the very large earthquake of 1985. A peak horizontal acceleration of about 0.6g was recorded within 2 km of the site. One experienced a permanent displacement of nearly a meter, and use of the quay was severely restricted. There was evidence of liquefaction or at least poor compaction of the backfill, and tie rods may not have been preloaded. The second bulkhead developed a permanent displacement of 15 cm, but the quay remained functional after the earthquake. This bulkhead had been designed using the Japanese procedure with a seismic coefficient of 0.15, but details concerning compaction of the backfill are unknown.

Table 12-1: Qualitative and Quantitative Description of the Reported Degrees of Damage

Degree of Damage	Description of Damage	Permanent Displacement at the Top of Sheet Pile	
		(Inches)	(Cm)
0	No damage	<1	<2
1	Negligible damage to the wall itself; noticeable damage to related structures (concrete apron)	4	10
2	Noticeable damage to walls	12	30
3	General shape of anchored sheet pile preserved, but significantly damaged	24	60
4	Complete destruction, no recognizable shapes of wall	48	120

12.3. Design of Anchored Sheet Pile Walls for Earthquake Loadings

12.3.1. Considerations from Static Analysis

In the design of anchored sheet pile walls for static earth pressure and water pressure loads, the free earth support method or any other suitable method may be used to determine the required depth of sheet pile embedment below the dredge level and the magnitude of the design anchor force required to restrict the wall movements to acceptable levels. The interrelationship between the changes in earth pressures, the corresponding changes in the sheet pile displacements, and the changes in the distribution of bending moments along the sheet pile make the free earth support method of analysis an attractive design tool. Rowe's¹²⁰ free earth support method of analysis assumes that the sheet pile wall moves away from the backfill and displaces the foundation soils that are below the dredge level and in front of the wall, as shown in *Figure 12-1*. These assumed displacements are sufficient to fully mobilize the shear resistance within the backfill and foundation, resulting in active earth pressures along the back of the sheet pile wall and passive earth pressures within the foundation in front of the sheet pile wall, as shown in *Figure 12-1*.

The free earth support method is described in 9.4.2. Rowe's moment reduction curves can also be used as well.

Various important load and material factors in common practice are as follows: The allowable stress in the sheet pile is usually restricted to between 50 percent and 65 percent of

¹⁰⁶The study summarised here is Dawkins, W.P. (2001) Investigation of Wall Friction, Surcharge Loads and Moment Reduction Curves for Anchored Sheet-Pile Walls. Report ERDC/ITL TR-01-4. Vicksburg, MS: U.S. Army Corps of Engineers, Waterways Experiment Station, Engineer Research and Development Centre, Information Technology Laboratory.

¹²⁰Rowe, P. W. 1952. "Anchored Sheet Pile Walls," *Proceedings of Institution of Civil Engineers*, Vol 1, Part 1, pp 27-70.

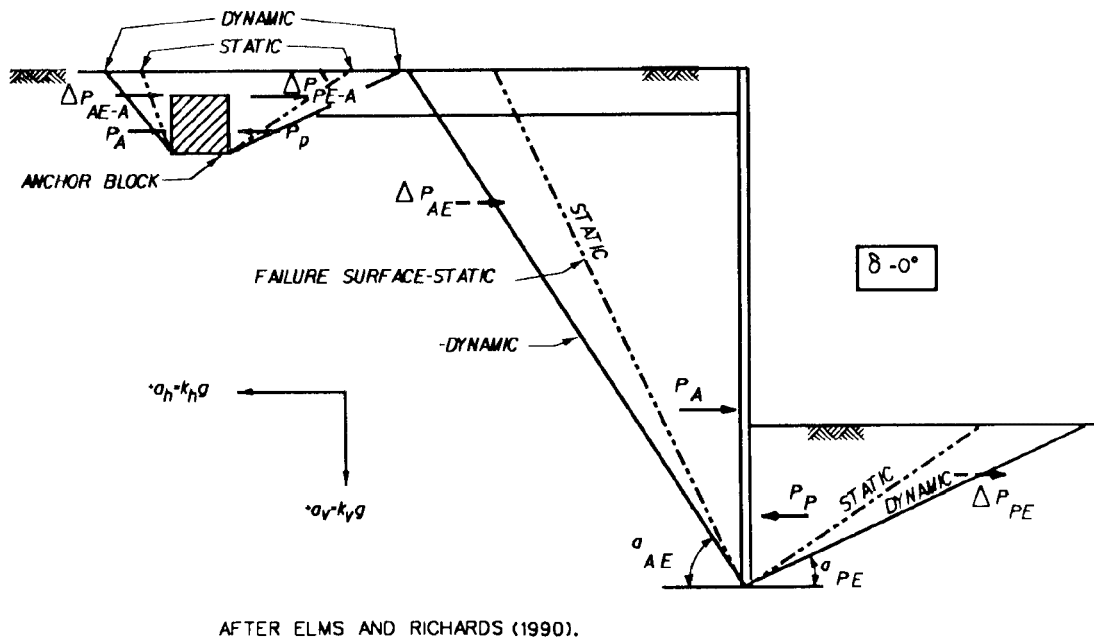


Figure 12-1: Decrease in failure surface slope of the active and passive sliding wedges with increasing lateral accelerations

the yield stress of the steel (60 percent in the Japanese Code). The allowable stress (gross area) in the tie rod steel is usually between 40 and 60 percent of the yield stress, and the tie rod force is designed using the equilibrium anchor force increased by a factor equal to 1.3. The anchor is designed using the equilibrium anchor force increased by a factor equal to between 2.0 and 2.5.

This design procedure for static loadings is extended to dynamic problems in the following sections.

12.3.2. Inclusion of Earthquake Loads

The first step is to check for the possibility of excess pore pressures or liquefaction (see Seed and Harder¹²¹ or Marcuson, Hynes, and Franklin¹²²). The presence or absence of these phenomena will have a major influence on design. The potential for excessive deformations is to be considered¹²³.

The proposed design procedure quantifies the effect of earthquake shaking in the free earth support analysis of anchored sheet pile walls through the use of inertial forces within the backfill, the soil below the dredge level in front of the sheet pile wall and the hydrodynamic water pressure force in the pool in front of the wall. These inertial forces are superimposed on the static forces along the sheet pile wall. Certain adjustments are made to the load and material factors, as is detailed in the following sections, when earthquake

loads are included in the analysis.

An important design consideration is the placement of the anchor. It should be located far enough from the wall such that the active wedge from the wall (starting at the bottom of the wall) and the passive wedge from the anchor do not intersect. The inertial forces due to the acceleration of the soil mass have the effect of decreasing the slope of the active and passive soil wedge failure surfaces, as shown in Figure 12-1. The slope angles α_{AE} and α_{PE} for the slip planes decrease (the slip planes become flatter) as the acceleration levels increase in value.

When the horizontal accelerations are directed towards the backfill ($+k_h \cdot g$), the incremental increases in the earth pressure forces above the static earth pressure forces, denoted as ΔP_{AE} and ΔP_{PE} in Figure 12-1, are directed away from the backfill. This has the effect of increasing the driving force behind the sheet pile wall and decreasing the stabilizing force in front of the sheet pile wall. The effect of increased accelerations on the distribution of moments are twofold, (1) increased values for the maximum moment within the sheet pile and (2) a lowering of the elevation of the point of contraflexure along the sheet pile. The anchored sheet pile wall model tests in dry sands by Kurata, Arai, and Yokoi, Steedman and Zeng and Kitajima and Uwabe¹²⁴ have confirmed this interrelationship, as shown in Figure 12-2. This

¹²¹Seed, R. B. and Harder, L. F. (1990). "SPT-Based Analysis of Cyclic Pore Pressure Generation and Undrained Strength," Proceedings of the H. B. Seed Memorial Symposium, Bi Tech Publishing, Vol. II, pp. 351-376.
¹²²National Research Council (1985). *Liquefaction of Soils During Earthquakes*: National Academy Press, Washington, DC, 240 p.
¹²³Kurata, S., Arai, H. and Yokoi, T. (1965). "On the Earthquake Resistance of Anchored Sheet Pile Bulkheads," Proceedings, 3rd World Conference On Earthquake Engineering, New Zealand; Steedman, R., and Zeng, X. 1988. "Flexible Anchored Walls Subject to Base Shaking," Report CUED/D-soils TR 217, Engineering Department Cambridge University, UK.

Marine Solutions

Solutions for Breakwaters, Shore Protection and Marina Docks

Economy, durability, and versatility

CONTECH® Marine Products provide economical and effective solutions for various marine applications, including shore protection, primary and secondary breakwaters, jetties and marina docks.



For more information, call Toll Free: 800-338-1122.
Or, visit our web site at www.contech-cpi.com

CONTECH
CONSTRUCTION PRODUCTS INC.

INNOVATIVE CIVIL ENGINEERING SITE SOLUTIONS

 American
Owned and Operated

©2003 CONTECH Construction Products Inc. All Rights Reserved

type of sheet pile response shows that as the value for acceleration increases, the point of contraflexure moves down the pile, and the response of the sheet pile (described in terms of sheet pile displacements, earth pressures along the sheet pile and distribution of moments within the sheet pile) will approach those of the free earth support. This increase in the value of the maximum moment and the movement of the point of contraflexure towards the bottom of the sheet pile with increasing acceleration reflects the development of a fully active stress state within the soil that is located below the dredge level and behind the sheet pile wall. Thus, the value for Rowe's moment reduction factor that is applied to the moment distribution corresponding to the free earth support method will increase in value, approaching the value of one, with increasing values for accelerations. This effect is not taken into account directly in the design. However, it is indirectly considered if the moment equilibrium requirement of the free earth method requires a greater depth of embedment when earthquake loadings are included.

Another factor affecting the orientation of the failure planes and thus the corresponding values for the dynamic earth pressure forces is the distribution of total pore water pressures within the backfill and foundation. The total pore water pressure is a combination of the steady state seepage and any excess pore water pressures resulting from earthquake induced shear strains within the submerged soils.

The proposed procedures for the seismic stability analysis of anchored sheet pile walls that undergo movements during earthquakes are categorized as one of three types of analyses, depending upon the magnitude of excess pore water pressures generated during the earthquake (Figure 12-3). They range from the case of no excess pore water pressures (Case 1) to the extreme case corresponding to the complete liquefaction of the backfill (Case 3) and the intermediate case of residual excess pore water pressures within the backfill and/or the soil in front of the sheet pile (Case 2).

In Figure 12-3, $U_{static-b}$ corresponds to the steady state pore water pressure force along the back of the sheet pile wall, $U_{static-t}$ the steady state pore water pressure force along the front toe of the wall and U_{pool} the hydrostatic water pressure force exerted by the pool along the front of the wall. In the case of balanced water pressures, the sum of $U_{static-b}$ is equal to U_{pool} and $U_{static-t}$. $U_{inertia}$ corresponds to the hydrodynamic water pressure force along the front of the wall due to earthquake shaking of the pool. $U_{shear-b}$ and $U_{shear-t}$ correspond to the excess pore water pressure force acting along the back of the wall and along the front of the wall (Case 2). In the case of a liquefied backfill, HF_{static} and $HF_{inertia-b}$ are equal to the equivalent heavy fluid hydrostatic pressure of the liquefied backfill and the inertia force due to the acceleration of a liquefied backfill.

An anchored sheet pile wall cannot be designed to retain a

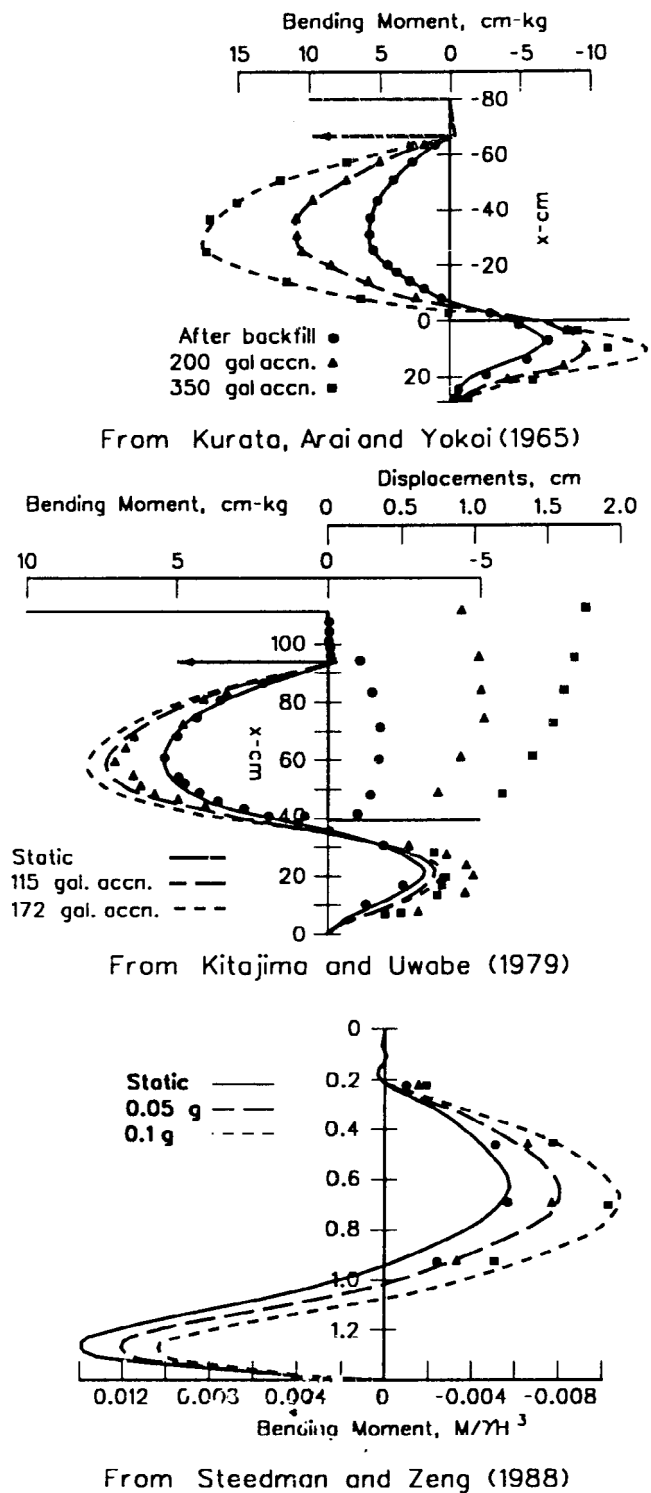
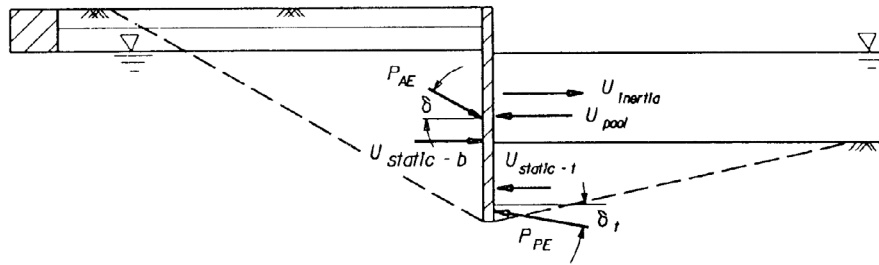


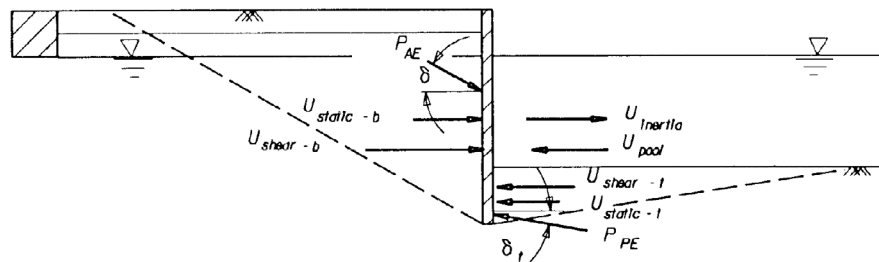
Figure 12-2 Measured distributions of bending moment in three model tests on anchored bulkhead

liquefied backfill and foundation, and hence Case 3 is only of academic interest. Site improvement techniques or the use of alternative structures should be investigated in this situation.

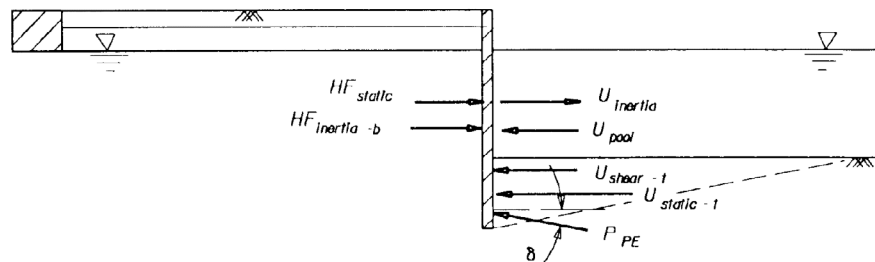
A procedure for determining the potential for liquefaction



CASE 1: Submerged Backfill, No Excess Pore Water Pressures Due to Earthquakes.



CASE 2: Submerged Backfill, Excess Pore Water Pressures Due To Earthquake.



CASE 3: Liquefied Backfill.

Figure 12-3: Anchored sheet pile walls retaining backfills which undergo movements during earthquakes

within the submerged backfill or the potential for the development of excess pore water pressures is discussed in numerous articles, including the National Research Council, Seed, Tokimatsu, Harder, and Chung, Seed and Harder or Marcuson, Hynes, and Franklin¹²⁵. The design procedure is limited to the case where excess pore water pressures are less than 30 percent of the initial vertical effective stress.

12.3.3. Flexure of the Sheet Pile Wall Below the Dredge Level

Justification of the use of Rowe's moment reduction factor values, obtained from static tests on dynamic problems, is empirical. The damage surveys of anchored sheet pile walls that failed due to earthquake shaking listed one sheet pile

wall that exhibited a general flexural failure. The structural failure of this wall, designed using the Japanese Code, was attributed to corrosion at the dredge level. The Japanese Code uses the Rowe's reduction factor values to reduce the maximum free earth support moment in the design of the sheet pile section, thus relying on flexure of the sheet pile wall below the dredge level during earthquake shaking.

Flexure of the sheet pile below the dredge level is caused by several factors, including the depth of penetration and flexural stiffness of the sheet pile wall and the strength and compressibility of the soil. In Rowe's procedure, the dependence of the value of r_d on the soil type incorporates the dependence of the level of moment reduction on the compressibility and strength of the soil as well as the magnitude

¹²⁵Seed, H. B., Tokimatsu, K., Harder, L. F., and Chung, R. M. (1985) (Dec). "Influence of SPT Procedures in Soil Liquefaction Resistance Evaluations," ASCE, Journal of the Geotechnical Engineering Division, Vol. 111, No. 12, pp. 1425-1445.

¹²⁶Seed, H. B. 1987 (Aug). "Design Problems in Soil Liquefaction," ASCE, Journal of the Geotechnical Engineering Division, Vol. 113, No. 8, pp. 827-845.

and distribution of sheet pile displacements below the dredge level.

The ability of the system to develop flexure below the dredge level during earthquake shaking must be carefully evaluated prior to application of Rowe's moment reduction factor or any portion of the reduction factor. This is especially true when analyzing the seismic stability of an existing sheet pile wall founded in a contractive soil. A sheet pile wall founded in dense granular soils is far more likely to develop flexure below the dredge level during earthquake shaking than one founded in loose soils. Dense soils that dilate during shearing are far less susceptible to large displacements during earthquake shaking than are loose soils¹²⁶. Loose soils contract during shearing and are susceptible to large displacements and even flow failures caused by earthquake shaking. As a general design principle, anchored sheet pile walls sited in seismic environments should be founded in dense and dilative cohesionless soils with no silt or clay site particles.

12.3.4. Design of Anchored Sheet Pile Walls - No Excess Pore Water Pressures

The presence of water within the backfill and in front of the sheet pile wall results in additional static and dynamic forces acting on the wall and alters the distribution of forces within the active and passive soil wedges developing behind and in front of the sheet pile wall. This section describes the first of two proposed design procedures using the free earth support method to design anchored sheet pile walls retaining submerged or partially submerged backfills and including a pool of water in front of the sheet pile wall, as shown in Figure 12-4. This analysis, described as Case 1 in Figure 12-3, assumes that no excess pore water pressures are generated within the submerged portion of the backfill or within the foundation during earthquake shaking.

The evaluation of the potential for the generation of excess pore water pressures during the shaking of the submerged soil regions is determined using the procedure described in

the National Research Council, Seed, Tokimatsu, Harder, and Chung, Seed and Harder or Marcuson, Hynes, and Franklin. Stability of the structure against block movements should also be checked during the course of the analysis. The ten stages of the analyses in the design of anchored walls for seismic loadings using the free earth support method of analysis are labelled A through J in Table 12-2.

The 13 steps in the design of the anchored sheet pile wall retaining submerged backfill as shown in Figure 12-4 are as follows:

(1) Perform a static loading design of the anchored sheet pile wall using the free earth support method of analysis or any other suitable method of analysis.

(2) Select the k_h value to be used in the analysis¹²⁷.

(3) Consider k_v .

(4) Compute P_{AE} and with the shear strength of the backfill fully mobilized. P_{AE} acts at an angle δ to the normal to the back of the wall. The pore pressure force $U_{static-b}$ is determined from the steady state flow net for the problem. By definition, only steady state pore water pressures exist within the submerged backfill and foundation of a Case 1 anchored sheet pile wall ($r_u = 0$). In the restrained water case of a fully submerged soil wedge with a hydrostatic water table, P_{AE} is computed using an effective unit weight equal to the buoyant unit weight. K_{AE} or $K_A(b^*, q^*)$ is computed using an equivalent horizontal acceleration, k_{he1} , and an equivalent seismic inertia angle, $\Psi e1$. In the case of a partially submerged backfill, this simplified procedure will provide approximate results by increasing the value assigned to the effective unit weight, g_e , based upon the proportion of the soil wedge that is above and below the water table. P_{AE} is computed with gt replaced by g_e . K_{AE} (Equation 34) or $K_A(b^*, q^*)$ is computed using an equivalent horizontal acceleration, k_{he1} , and an

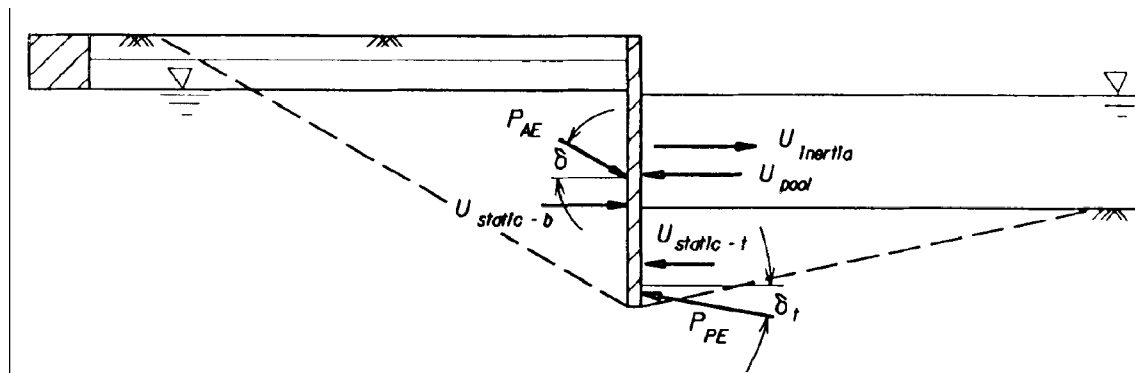


Figure 12-4 Anchored sheet pile wall with no excess pore water pressure due to earthquake shaking (Case 1).

¹²⁷The values for seismic coefficients are to be established by the seismic design team for the project considering the seismotectonic structures within the region, or as specified by the design agency. The earthquake-induced displacements for the anchored sheet pile wall are dependent upon numerous factors, including how conservatively the strengths, seismic coefficients (or accelerations), and factors of safety have been assigned, as well as the compressibility and density of the soils, and the displacement at the anchorage.



ABI'S EXCAVATOR MOUNTED VIBRATORS:

- Use existing controls on the excavator
- Fast installation: attaches to the bucket pin
- Can push and adjust the pile with excavator boom
- Several models available to suit excavator sizes

VIBRATE PILE WITH YOUR EXCAVATOR



IT'S EASY AND COST EFFECTIVE



ABI, INC
(WEST COAST)
TOLL FREE: 877-224-3356
www.abi-delmag.com

ASK FOR OUR VIDEO

HAMMER & STEEL, INC
(MID-WEST & EAST COAST)
TOLL FREE: 800-325-7453
www.hammersteel.com

Table 12-2: Ten Stages of the Analyses in the Design of Anchored Walls for Seismic Loadings

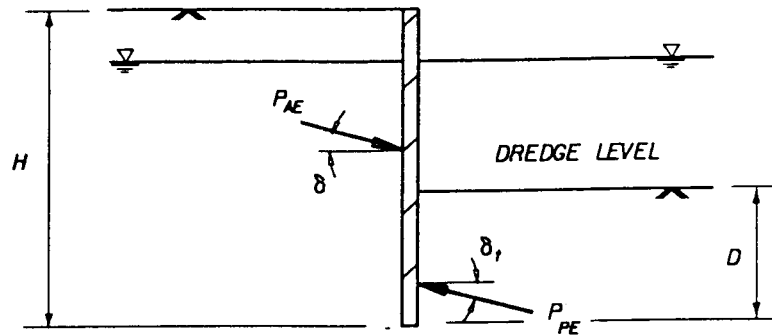
Stage of Analysis	Design Steps	Description
A		Evaluate potential for liquefaction or excessive deformations.
B	1	Static design: Provides initial depth of penetration for seismic analysis.
C	2, 3	Determine the average site specific acceleration for wall design.
D	4, 5	Compute dynamic earth pressure forces and water pressure forces.
E	6	Sum the moments due to the driving forces and the resisting forces about the tie rod elevation.
F	4-6	Alter the depth of penetration and repeat steps 4 and 6 until moment equilibrium is achieved. The minimum depth of embedment has been computed when moment equilibrium is satisfied.
G	7	Sum horizontal forces to compute the tie rod force (per foot of wall).
H	8, 9	Compute the maximum bending moment, apply Rowe's moment reduction factor and size the flexible wall (if applicable).
I	10	Size the tie rods and select their spacing.
J	11-13	Design and site the anchorage.

equivalent seismic inertia angle, Ψ_{he1} , with g_b replaced by g_e . A more refined analysis may be conducted using the trial wedge procedure for the forces shown in *Figure 12-4*. To compute the point of action of P_{AE} in the case of a partially submerged backfill, redefine P_{AE} in terms of the static force, P_A , and the dynamic active earth pressure increment, ΔP_{AE} . This procedure is demonstrated in *Figure 12-5*. First compute K_A and the static effective earth pressure distribution along the back of sheet pile wall. P_A is equal to the resultant force for this static effective stress distribution along the back of the wall, which also provides for the point of action for P_A . Solve for the force ΔP_{AE} as equal to the difference between P_{AE} and P_A . Assume that ΔP_{AE} acts at a height equal to 0.6H above the base of the sheet pile. Compute the point of action of force P_{AE} and correcting this relationship for the new locations along the back of the sheet pile for the forces P_A and ΔP_{AE} .

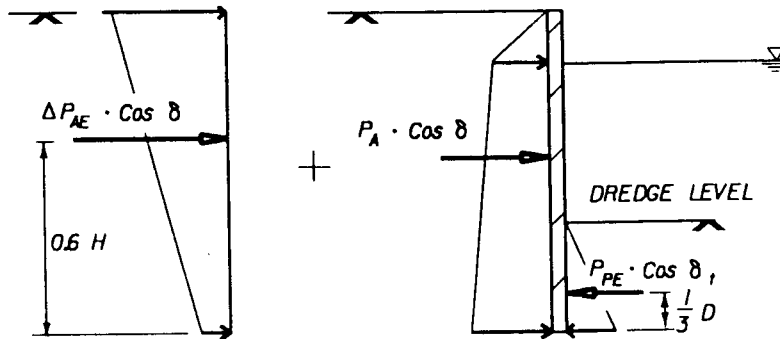
(5) Compute P_{PE} acting in front of the sheet pile and using a factor of safety, FS_p , applied to both the shear strength of the soil and the effective angle of friction along the interface. δ equal to $\phi/2$ is a reasonable value for dense frictional soils. In a static free earth support method of analysis, FS_p is set

equal to 1.5, and in a dynamic earth pressure analysis, the minimum value assigned to FS_p is 1.2. $U_{static-t}$ is determined from the steady state flow net for the problem. By definition, only steady state pore water pressures exist within the submerged backfill and foundation of a Case 1 anchored sheet pile wall ($r_u = 0$). In the restrained water case of a fully submerged soil wedge with a hydrostatic water table, P_{PE} is computed using an effective unit weight equal to the buoyant unit weight. For low to moderate levels of earthquake shaking, assume that P_{PE} acts at a height equal to approximately 1/3 of the height of the soil in front of the sheet pile wall and at an angle d to the normal to the face of the wall.¹²⁸ K_{PE} or $K_p(b^*, q^*)$ is computed using an equivalent horizontal acceleration, k_{he1} , and an equivalent seismic inertia angle, Ψ_{e1} . In the case of steady state seepage, this simplified procedure will provide approximate results by decreasing the value assigned to the effective unit weight according to the magnitude of the upward seepage gradient¹²⁹.

(6) To determine the minimum required depth of sheet pile penetration, the clockwise and counterclockwise moments of the resultant earth pressure forces and resultant water pres-



(a.) Mononobe - Okabe Earth Pressure Forces P_{AE} and P_{PE} .



(b.) Horizontal Force Components. of P_{AE} and P_{PE} .

Figure 12-5: Static and inertial horizontal force components of the Mononobe-Okabe earth pressure forces

sure forces about Figure 12-4 anchor are computed as follows:

$$\text{Equation 12-1: Counterclockwise Moment} = P_{AE} \cos \delta_b \cdot (Y_a - Y_{AE}) + U_{\text{static-b}} \cdot (Y_a - Y_{ub}) + U_{\text{inertia}} \cdot (Y_a - Y_i)$$

And

$$\text{Equation 12-2: Clockwise Moment} = - U_{\text{pool}} \cdot (Y_a - Y_{up}) - P_{PE} \cdot \cos \delta_t \cdot (Y_a - Y_{PE}) - U_{\text{static}} \cdot (Y_a - Y_{ut})$$

¹²⁸In a static design by the free earth support method of analysis, a triangular earth pressure is assumed along the front of the wall, with the resulting force P_p assigned to the lower third point. Experience has shown that reasonable static designs resulted when the appropriate strength parameters and adequate factors of safety were used in conjunction with this simplified assumption. A similar approach is used in the dynamic design. The point of application of P_{PE} may move downward from its static point of application for anchored sheet pile walls as the value for kh increases. However, no satisfactory procedure was found for computing the point of application of P_{PE} for this structure. In the interim, the assumption of P_{PE} acting at approximately 1/3 of the height of the soil in front of the wall is restricted to low to moderate levels of earthquake shaking (e.g. one rough index is $k_h < 0.1$) and with conservative assumptions regarding all parameters used in the analysis. For higher levels of shaking and less conservative assumptions for parameters, a larger value for F_{SP} than 1.2 and/or a lower point of application would be assigned.

¹²⁹Equation 6-33 for K_{PE} is restricted to cases where the value of f is greater than Ψ_{e1} . This limiting case may occur in cases of high accelerations and/or low shear strengths. One contributing factor is the submergence of the soil in front of the anchored wall, which approximately doubles the value of the equivalent seismic inertia angle over the corresponding dry soil case.

Where

- δ_b = effective angle of friction along the backfill to sheet pile wall interface
- δ_t = effective angle of friction along the toe foundation to sheet pile wall interface
- $U_{static-b}$ = resultant steady state pore water pressure force along the back of the wall
- $U_{static-t}$ = resultant steady state pore water pressure force below the dredge level along the front of the wall
- U_{pool} = resultant hydrostatic water pressure force for the pool
- $U_{inertia}$ = hydrodynamic water pressure force for the pool, directed away from the wall
- Y_a = distance from the base of sheet pile to the anchor
- Y_{AE} = distance from the base of sheet pile to P_{AE}
- Y_{ub} = distance from the base of sheet pile to $U_{static-b}$ (from a flow net)
- Y_i = distance from the base of sheet pile to $U_{inertia}$
- Y_{up} = distance from the base of sheet pile to U_{pool}
- Y_{PE} = distance from the base of sheet pile to PPE
- Y_{ut} = distance from the base of sheet pile to $U_{static-t}$ (from a flow net).

The effective friction angles are computed by the equations

Equation 12-3:
$$\tan\phi_t = \frac{\tan\phi'}{FS_p}$$

and

Equation 12-4:
$$\tan\delta_t = \frac{\tan\delta}{FS_p}$$

The value for the Clockwise Moment about *Figure 12-4* anchor is compared to the value for the Counterclockwise Moment, resulting in the following three possibilities:

- If the value of the Clockwise Moment is equal to the value of the Counterclockwise Moment, the sheet pile wall is in moment equilibrium, and the depth of penetration below the dredge level is correct for the applied forces.
- If the value of the Clockwise Moment is greater than the value of the Counterclockwise Moment, the trial sheet pile embedment depth below the dredge level is too deep and should be reduced.
- If the value of the Clockwise Moment is less than the value of the Counterclockwise Moment, the trial sheet pile embedment depth below the dredge level is shallow and should be increased.

Note that the sheet pile wall is in moment equilibrium for only one depth of sheet pile penetration within the foundation. For those trial sheet pile penetration depths in which moment equilibrium is not achieved, a new trial depth of sheet pile penetration is assumed, and steps 4 through step 6 are repeated.

(7) Once the required depth of sheet pile penetration is determined in step 6, the equilibrium anchor force per foot width of wall, T_{FES} , is computed using the equations for horizontal force equilibrium.

Equation 12-5:

$$T_{FES} = P_{PE}\cos\delta_t + U_{static-t} + U_{pool} - U_{inertia} - P_{AE}\cos\delta_b - U_{static-b}$$

In some situations the value for T_{FES} computed in a seismic analysis can be several times the value computed in the static analysis due to the effect of the inertial forces acting on both the active and passive soil wedges and the pool of water. Large anchor forces per foot width of wall will impact both the selection of the type of anchorage, anchor geometry and the number of rows and spacing of tie rods along the wall (see steps 10 through 12).

(8) The distribution of the moments within the sheet pile is computed from the external earth pressures along the front and back of the sheet pile and from the anchor force. To accomplish this, the earth pressure forces shown in *Figure 12-4* must be converted to equivalent earth pressures distributions. One approach for doing this is to separate P_{AE} into its static and incremental dynamic components and corresponding points of action, as discussed in step 4 and shown in *Figure 12-6* and *Figure 12-7*. *Figure 12-8* is used to define the variation in horizontal stress with depth for the dynamic earth pressure force increment ΔP_{AE} . At a given elevation, an imaginary section is made through the sheet pile, as shown in *Figure 12-8*, and the internal shear force V and internal bending moment M are represented. The internal shear force V is equal to the sum of earth pressures and water pressures and T_{FES} acting on the free body diagram of the sheet pile above Section A-A'. The internal bending moment M is equal to moment of the earth pressures, water pressures about Section A-A'. The maximum bending moment within the sheet pile is denoted as M_{FES} . The value for M_{FES} is determined by calculating the internal bending moment at the elevation at which the shear is equal to zero.

(9) The design moment for the sheet pile, M_{design} , is given by Equation 9-42. Using the currently available moment reduction curves, the value of correction factor will change from the static case only if the depth of penetration or the flexural stiffness, EI , of the wall changes in order to meet moment equilibrium requirements for seismic loadings. The ability of the system to develop flexure below the dredge level during earthquake shaking must be carefully evaluated prior to application of Rowe's moment reduction factor or any portion thereof.

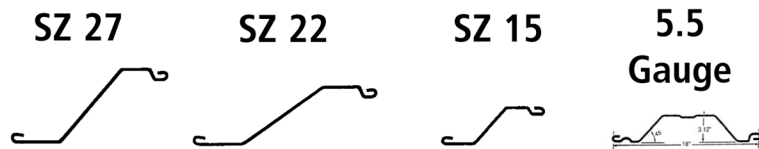
In a static design, the allowable stress in the sheet pile is usually restricted to between 50 and 65 percent of the yield

SHORELINE STEEL, INC.

P.O. Box 480519, 58201 Main Street • New Haven, MI 48048
(800) 522-9550 • (586) 749-9559 • Fax (586) 749-6653

www.shorelinesteel.com

We are a leading producer of domestic cold formed steel sheet piling in sections ranging from 10 gauge to 3/8" thick. For any sheet piling requirement we can satisfy your needs with a top quality product and prompt delivery.



	Thickness (Nominal)	Weight (Sq. ft.)	Weight (Lin. Ft.)	Sec. Mod in ⁴ (Ft. Wall)	Moment of Inertia in ⁴ (Ft. Wall)	Laying Width	Wall Depth
10-10 ga.	.134	7.2	10.8	2.2	3.5	18.00	3.12
8-8 ga.	.164	8.8	13.2	2.62	4.2	18.00	3.12
7-7 ga.	.179	9.6	14.4	2.8	4.4	18.00	3.12
6-6 ga.	.194	10.5	15.8	3.0	4.9	18.00	3.12
5-5 ga.	.209	11.3	16.9	3.4	5.4	18.00	3.12
LZ 8	.164	8.3	17.2	3.6	8.1	25.00	4.50
LZ 7	.179	9.1	18.8	3.9	8.9	25.00	4.50
LZ 5	.209	10.6	21.9	4.6	10.4	25.00	4.50
LZ 3	.239	11.9	24.6	5.2	11.8	25.00	4.50
LZ 250	.250	12.3	25.6	5.4	12.4	25.00	4.50
SZ-10	.164	9.4	17.2	7.3	27.4	22.00	7.50
SZ-11	.179	10.3	18.8	7.9	29.8	22.00	7.50
SZ-12	.209	12.0	21.9	9.2	34.8	22.00	7.50
SZ-14	.239	13.5	24.6	10.4	39.9	22.00	7.50
SZ-15	.250	14.0	25.6	10.9	41.8	22.00	7.50
SZ-14.5	.250	14.5	32.4	13.0	61.49	26.75	9.46
SZ-14.5	.270	15.8	35.1	14.0	86.40	26.75	9.46
SZ-18	.312	18.1	40.4	16.2	76.83	26.75	9.46
SZ-20	.340	19.8	44.1	17.5	83.37	26.75	9.46
SZ-21	.350	20.3	45.3	18.1	86.00	26.75	9.46
SZ-22	.375	21.8	48.6	19.3	91.92	26.75	9.46
SZ-222	.312	22.1	40.4	26.7	163.09	22.00	12.25
SZ-250	.250	15.9	32.4	16.6	89.42	24.46	10.75
SZ-313	.312	19.9	40.4	20.6	111.53	24.46	10.75
SZ-340	.340	21.5	44.1	22.4	121.45	24.46	10.75
SZ-350	.350	22.1	45.3	22.9	124.62	24.46	10.75
SZ-375	.375	23.7	48.6	24.5	133.55	24.46	10.75
SZ-24	.340	24.1	44.1	29.0	177.52	22.00	12.25
SZ-25	.350	24.8	45.3	29.7	181.91	22.00	12.25
SZ-27	.375	26.6	48.6	32.0	195.18	22.00	12.25

DOMESTIC STEEL SHEET PILING

- All sections available in bare or galvanized steel.
- All Zee sections available in doubles.
- All sections produced exactly to customer specified length(s).
- All steel fully melted and manufactured in the USA.



For more information, please call toll free
(800) 522-9550

or visit our website at: www.shorelinesteel.com

Also Available:

- Corners
- Tees and Crosses
- Capping
- Coatings

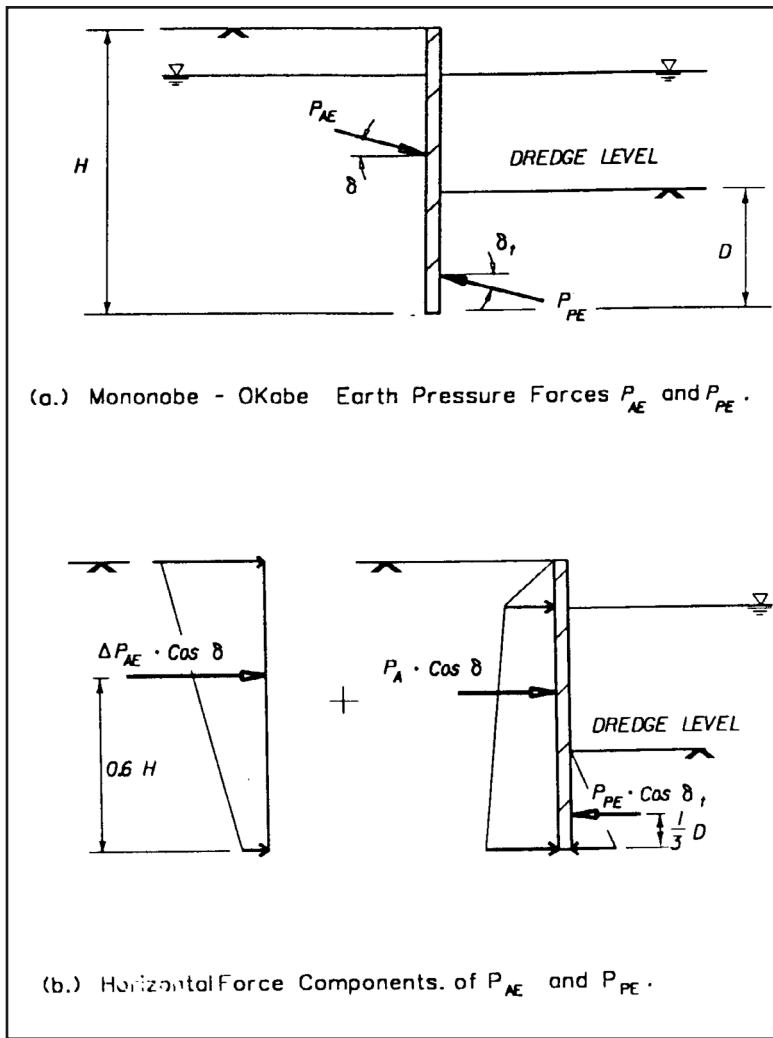


Figure 12-6: Static and inertial horizontal force components of the Mononobe-Okabe earth pressure forces

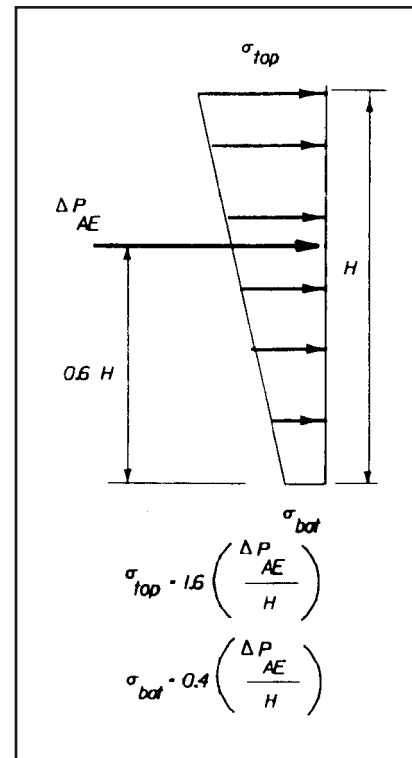


Figure 12-7: Distributions of horizontal stress corresponding to ΔP_{AE}

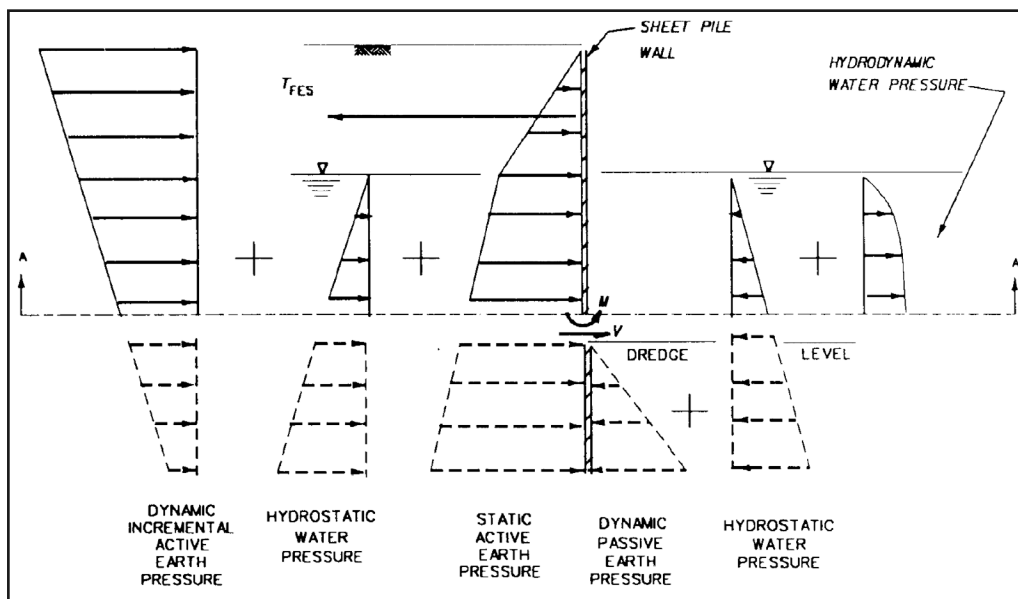
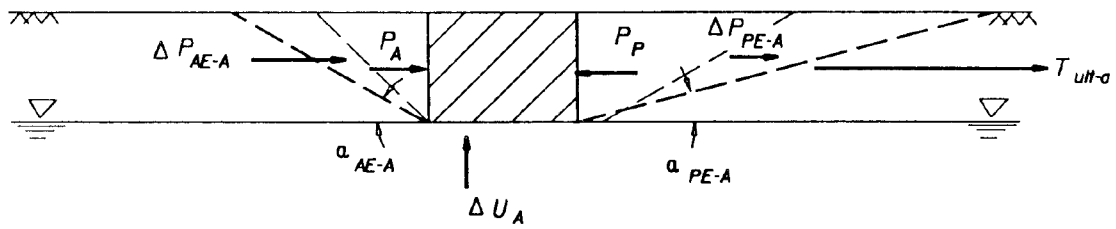
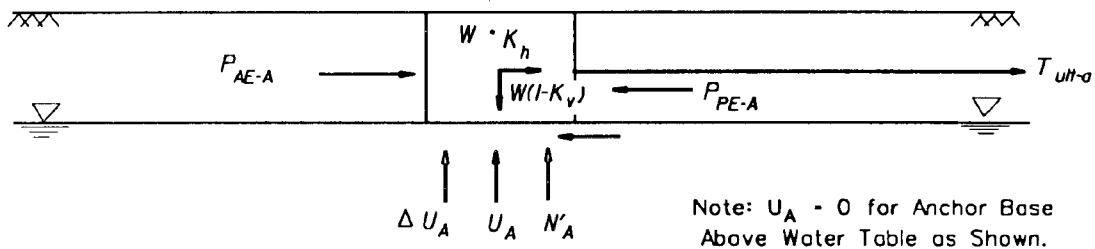


Figure 12-8: Horizontal pressure components and anchor force acting on sheet pile wall



(a) Forces On Anchor Block.



(b) Slip Plane And Dynamic Forces.

Figure 12-9: Dynamic forces acting on an anchor block (for $\delta = 0^\circ$)

strength. Higher allowable stresses may be considered for use in the design for dynamic earth pressures, given the short duration of loading during earthquakes. The allowable stresses for earthquake loading may be increased 33 percent above the value specified for static loading. This corresponds to an allowable stress in the sheet pile restricted to between 67 and 87 percent of the yield strength. The effects of corrosion should be considered during the course of wall design for static and seismic loadings.

(10) The design of tie rods is discussed in detail in 11.2.1. The effects of corrosion should be considered during the course of wall design for both static and seismic loadings.

(11) The design of the anchorage for seismic loadings follows the approach that is proposed for the design of the flexible wall and differs from the approach used when designing for static loadings. In the case of static loads, the ultimate force (per foot width of wall) which the anchor is to be designed, T_{ult-a} , is given by Equation 11-11 and the static earth pressure forces P_A and P_P on the front and back of the anchor block are computed using the ultimate shear strength with $\delta = 0^\circ$ for slender anchorage¹³⁰. The proposed design procedure for seismic loadings is described in steps 12 and 13. Seismic loads usually control the anchorage design.

(12) For those waterfront structures in which the anchor consists of a plate or a concrete block, a major contribution to the forces resisting the pulling force T_{ult-a} is provided by the for-

mation of a passive soil wedge in front of the block, as shown in Figure 12-9a. In a seismic analysis, T_{ult-a} is set equal to T_{FES} . The Mononobe-Okabe equations are used to compute the dynamic active earth pressure force, P_{AE} , and the dynamic passive earth pressure force, P_{PE} , acting on the anchor block during earthquake shaking (Figure 12-9b). P_{AE} is computed with the shear strength of the backfill fully mobilized and $\delta = 0^\circ$ for slender anchorage and $\delta \leq \phi/2$ for mass concrete anchorage. P_{PE} is computed using a factor of safety FS_P applied to the shear strength of the soil and the effective angle of friction along the interface. At a minimum FS_P is set equal to a value between 1.2 and 1.5, depending on the allowable displacement and on how conservatively the strengths and seismic coefficients have been assigned. In general and with all parameters constant, the larger the factor of safety, the smaller the anchorage displacement due to earthquake shaking.

Water pressure forces are not included along the sides of the block because most anchor blocks are constructed on or just above the water table, as idealized in this figure. If the water table extends above the base of the block, these forces are to be included in the analysis.

The size of the block is proportioned such that

Equation 12-6:

$$T_{ult-a} = P_{PE} \cdot \cos \delta_t - P_{AE} \cdot \cos \delta_b - W \cdot k_h + N' \cdot \tan \delta_A$$

Where

Equation 12-7:

$$N' = W(1 - k_v) - U_A - P_{PE} \cdot \sin \delta_t + P_{AE} \cdot \sin \delta_b$$

¹³⁰Dismuke, T. (1991). Chapter 12: Retaining Structures And Excavations, Foundation Engineering Handbook, Second Edition, edited by H. Y. Fang, Van Nostrand Reinhold, NY, pp. 447-510.

When the magnitude of computed anchor block forces prohibits the use of shallow anchor blocks, alternative anchorage systems are to be investigated. These include the use of multiple tie rods and anchorage, A-frame anchors, sheet pile anchorage, soil or rock anchors and tension H-piles.

By definition, no excess pore water pressures are generated within the backfill ($\Delta U_A = 0$) for the Case 1 anchored sheet pile walls. U_A is equal to the resultant steady state pore water pressure force along the base of the anchor. The orientation of a linear failure plane in front of the anchor block, a P_E , in Figure 12-9a is approximated using Equation 6-35.

(13) The anchor block is to be located a sufficient distance behind the sheet pile wall so that the active failure surface behind the sheet pile wall does not intersect the passive failure surface developing in front of the anchor during earthquake shaking. The required minimum distance between the back of the sheet pile and the anchor block increases with increasing values of acceleration, as shown in Figure 12-1. The orientation of the active slip surface behind the sheet pile wall, α_{AE} , is calculated in step 4, and the orientation of the passive slip surface in front of the anchor block, α_{PE} is calculated in step 12.

12.3.5. Design of Anchored Sheet Pile Walls - Excess Pore Water Pressures

This section describes the proposed procedure, using the free earth support method, to design anchored sheet pile walls retaining submerged or partially submerged backfills and including a pool of water in front of the sheet pile wall, as shown in Figure 12-10. This analysis, described as Case 2 in Figure 12-3, assumes that excess pore water pressures are generated within the submerged portion of the backfill or within the foundation during earthquake shaking. The magnitude and distribution of these excess pore water pressures depend upon several factors, including the magnitude of the earthquake, the distance from the site to the fault generating the earthquake and the properties of the submerged soils. The evaluation of the magnitude of these excess pore water pressures is estimated using the procedure described in Seed and Harder or Marcuson, Hynes, and Franklin¹³¹. This design procedure is limited to the case where excess pore water pressures are less than 30 percent of the initial vertical effective stress. Stability of the structure against block movements should also be checked during the course of the analysis.

Many of the details regarding the procedures used are common to the Case 1 analysis.

The 14 steps in the design of the anchored sheet pile wall retaining submerged backfill as shown in Figure 12-10 are as follows:

(1) Perform a static loading design of the anchored sheet pile wall using the free earth support method of analysis or any other suitable method of analysis.

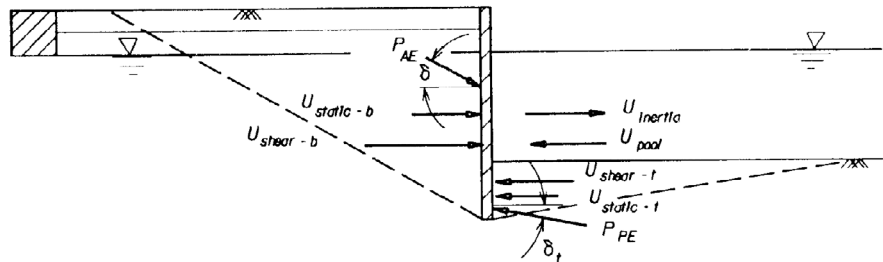


Figure 12-10: Anchored sheet pile wall with excess pore water pressures generated during earthquake shaking (Case 2)

(2) Select the k_h value to be used in the analysis¹³².

(3) Consider k_v .

(4) Compute P_{AE} and with the shear strength of the backfill fully mobilized. P_{AE} acts at an angle δ to the normal to the back of the wall. The pore pressure force $U_{static-b}$ is determined from the steady state flow net for the problem. The post-earthquake residual excess pore water pressures are identified as U_{shear} in Figure 12-10 and are determined using the procedures described in Seed and Harder or Marcuson, Hynes, and Franklin. In the restrained water case of a fully submerged soil wedge with a hydrostatic water table, P_{AE} is computed using an effective unit weight equal to the buoyant unit weight. K_{AE} or $K_A(b^*, q^*)$ is computed using an equivalent horizontal acceleration, k_{he3} , and an equivalent seismic inertia angle, Ψ_{e3} . An alternative approach is to use a modified effective friction angle, ϕ_{eq} , with r_u equal to the average value within the backfill. In the case of a partially submerged backfill, this simplified procedure will provide approximate results by increasing the value assigned to the effective unit weight, γ_e , based upon the proportion of the soil wedge that is above and below the water table. P_{AE} is computed with γ_t replaced by γ_e . The unit weight assigned to the soil below the water table is given by

$$\text{Equation 12-8: } \gamma_e = \gamma_b (1 - r_u)$$

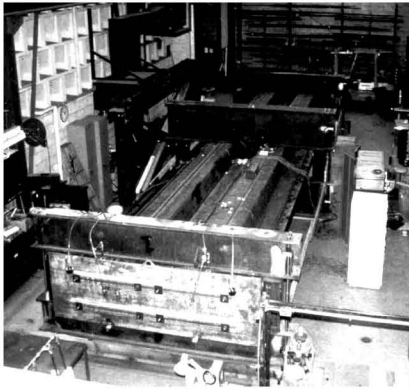
when computing the value of γ_e . K_{AE} or $K_A(b^*, q^*)$ is computed using an equivalent horizontal acceleration,

¹³¹Seed, R. B. and Harder, L. F. (1990). "SPT-Based Analysis of Cyclic Pore Pressure Generation and Undrained Strength," *Proceedings of the H. B. Seed Memorial Symposium*, Bi Tech Publishing, Vol. II, pp. 351-376; Marcuson, W., Hynes, M., and Franklin, A. 1990 (Aug). "Evaluation and Use of Residual Strength in Seismic Safety Analysis of Embankments," *Earthquake Spectra*, pp. 529-572.

¹³²The values for seismic coefficients are to be established by the seismic design team for the project considering the seismotectonic structures within the region, or as specified by the design agency. The earthquake-induced displacements for the anchored sheet pile wall are dependent upon numerous factors, including how conservatively the strengths, seismic coefficients (or accelerations), and factors of safety have been assigned, as well as the compressibility and density of the soils, and the displacement at the anchorage.

SHEET PILING CONSULTING

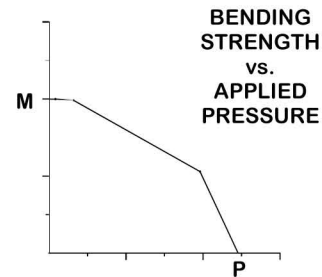
**HARTMAN ENGINEERING
BUFFALO, NY
716-759-2800**



**TESTING BENDING STRENGTH OF
Z-SHAPE SHEET PILING**
Testing showed that transverse stresses
reduce the useful strength of sheet piling

**TYPICAL DESIGN AID DEVELOPED
BY HARTMAN ENGINEERING
FOR SELECTION OF Z-SHAPE
SHEET PILING SECTION**

Provides engineers with a method to
incorporate transverse stress into
designs.



Hartman Engineering has more than 35 years experience in design of cofferdams, assisting with cofferdam problems, and providing continuing education seminars for engineers and contractors. In 1990 the firm began testing and research projects sponsored by Bethlehem Steel Corporation and L. B. Foster Company. Hartman Engineering has also worked with TXI/Chaparral Steel to design sheet piling sections which optimize resistance to transverse stress loadings.

Please contact us if you have a need for professional engineering services or continuing education seminars in our specialized area of practice.

See our other page in this publication for information on design and construction phase engineering services.

Equation 12-9: $k_{he} = \frac{\gamma_t}{\gamma_e} k_h$

and an equivalent seismic inertia angle,

Equation 12-10: $\Psi_e = \arctan(k_{he})$

For this case, the excess residual pore water pressures are superimposed upon the hydrostatic pore water pressures. To compute the point of action of P_{AE} in the case of a partially submerged backfill, redefine P_{AE} in terms of the static force, P_A , and the dynamic active earth pressure increment, ΔP_{AE} .

(5) Compute P_{PE} acting in front of the sheet pile and apply a factor of safety FS_P equal to 1.2 to both the shear strength of the soil and the effective angle of friction along the interface. Refer to step 5 above. The pore pressure force $U_{static-t}$ is determined from the steady state flow net for the problem. In the restrained water case of a fully submerged soil wedge with a hydrostatic water table, P_{PE} is computed with γ_t replaced by the effective unit weight of soil below the water table, Ψ_e . An average ru value is used within the soil in front of the wall. K_{PE} or $K_p(b^*, q^*)$ is computed using an equivalent horizontal acceleration, k_{he} , and an equivalent seismic inertia angle, Ψ_e , computed the same way as in the previous step. In the case of steady state seepage, this simplified procedure will provide approximate results by decreasing the value assigned to the effective unit weight according to the magnitude of the upward seepage gradient. For low to moderate levels of earthquake shaking, assume that P_{PE} acts at a height equal to approximately 1/3 of the height of the soil in front of the sheet pile wall and at an angle δ_t to the normal to the face of the wall.¹³³

(6) To determine the required depth of sheet pile penetration, the clockwise and counterclockwise moments of the resultant earth pressure forces and resultant water pressure forces about *Figure 12-10* anchor are computed as follows:

Equation 12-11:

$$\begin{aligned} \text{Counterclockwise Moment} = & P_{AE} \cos \delta_b \cdot (Y_a - Y_{AE}) + \\ & U_{static-b} \cdot (Y_a - Y_{ub}) \\ & + U_{shear-b} \cdot (Y_a - Y_{utaub}) + U_{inertia} \cdot (Y_a - Y_i) \end{aligned}$$

And

Equation 12-12:

$$\begin{aligned} \text{Clockwise Moment} = & - U_{pool} \cdot (Y_a - Y_{up}) - P_{PE} \cdot \cos \delta_t \cdot \\ & (Y_a - Y_{PE}) - U_{static-t} \\ & \cdot (Y_a - Y_{ut}) - U_{shear-t} \cdot (Y_a - Y_{utaut}) \end{aligned}$$

Where

- $U_{shear-b}$ = resultant excess pore water pressure force along the back of the wall
- $U_{shear-t}$ = resultant excess pore water pressure force below the dredge level along the front of the wall
- Y_{utaub} = distance from the base of sheet pile to $U_{shear-b}$
- Y_{utaut} = distance from the base of sheet pile to $U_{shear-t}$

Values for Y_{utaub} , $U_{shear-b}$, Y_{utaut} and $U_{shear-t}$ are computed using the procedure described in Seed and Harder or Marcuson, Hynes, and Franklin. The value for the Clockwise Moment is compared to the value for the Counterclockwise Moment, resulting in one of three possibilities listed in steps 6a through step 6c in the previous section. The sheet pile wall is in moment equilibrium for only one depth of sheet pile penetration within the foundation. For those trial sheet pile penetration depths in which moment equilibrium is not achieved, a new trial depth of sheet pile penetration is assumed, and step 4 through step 6 is repeated.

(7) Once the required depth of sheet pile penetration is determined in step 6, the equilibrium anchor force per foot width of wall, T_{FES} , is computed using the equations for horizontal force equilibrium.

Equation 12-13:

$$T_{FES} = P_{PE} \cos \delta_t + U_{static-t} + U_{shear-t} + U_{pool} - U_{inertia} - P_{AE} \cos \delta_b - U_{static-b} - U_{shear-b}$$

Additional commentary is provided in step 7 of Section 7.4.1.

(8) The distribution of the moments within the sheet pile, M_{FES} , is computed using the procedure described in step 8 of the previous section.

(9) The computation of the design moment for the sheet pile, M_{design} , is described in step 9 of the previous section.

(10) The design tie rod force, T_{design} , is computed using the procedure described in step 10 of the previous section.

(11) The design of the anchor block for seismic loadings differs from the approach used when designing for static loadings. The reader is referred to the discussion in step 11 of the previous section.

(12) For those waterfront structures in which the anchor consists of slender anchorage or mass concrete anchorage, a major contribution to the forces resisting the pulling force

¹³³In a static design by the free earth support method of analysis, a triangular earth pressure is assumed along the front of the wall, with the resulting force P_p assigned to the lower third point. Experience has shown that reasonable static designs resulted when the appropriate strength parameters and adequate factors of safety were used in conjunction with this simplified assumption. A similar approach is used in the dynamic design. The point of application of P_{PE} may move downward from its static point of application for anchored sheet pile walls as the value for k_h increases. However, no satisfactory procedure was found for computing the point of application of P_{PE} for this structure. In the interim, the assumption of P_{PE} acting at approximately 1/3 of the height of the soil in front of the wall is restricted to low to moderate levels of earthquake shaking (e.g. one rough index is $k_h < 0.1$) and with conservative assumptions regarding all parameters used in the analysis. For higher levels of shaking and less conservative assumptions for parameters, a larger value for FS_P than 1.2 and/or a lower point of application would be assigned.

T_{ult-a} is provided by the formation of a passive soil wedge in front of the block. The procedure described in step 12 of the previous section is used to compute P_{AE} , P_{PE} , and α_{PE} . The size of the block is proportioned using Equation 12-6 relationship, where N' is equal to

Equation 12-14:

$$N' = W(1 - k_v) - U_A - DU_A - P_{PE} \cdot \sin\delta_t + P_{AE} \cdot \sin\delta_b$$

The excess pore water pressure force along the base of the block is equal to DU_A (see Seed and Harder or Marcuson, Hynes, and Franklin). An alternative procedure for incorporating residual excess pore water pressures in the analysis is by using r_u and an equivalent angle of interface friction along the base of block, d_A .

Equation 12-15: $\tan\delta_{A\text{ eq}} = (1 - r_u)\tan\delta_A$

In this case, the value for N' in Equation 12-6 is given by

Equation 12-16:

$$N' = W(1 - k_v) - U_A - P_{PE} \cdot \sin\delta_t + P_{AE} \cdot \sin\delta_b$$

Reducing the effective stress friction angle along the soil to concrete interface so as to account for the excess pore water pressures is not an exact procedure.

(13) The required minimum distance between the back of the sheet pile and the anchor block is computed following the procedure described in step 13 of the previous section.

(14) The residual excess pore water pressures within the submerged backfill and foundation will be redistributed after earthquake shaking has ended. The post earthquake static stability (k_h and k_v equal to zero) of any earth retaining structure should be evaluated during the redistribution of the excess pore water pressures within the soil regions.

12.4. Use of Finite Element Analyses

Finite element analyses should be considered only if: (a) the cost implications of the simplified design procedures indicate that more detailed study is warranted, (b) it is necessary to evaluate permanent displacements that might result from the design seismic event, or (c) there is concern about the influence of surface loadings. It is particularly difficult to model well the various features of an anchored wall, especially when there is concern about excess pore pressures. Iai and Kameoka give one example of a detailed analysis of an actual failure¹³⁴.

12.5 Example Problem

Example 19: Design Example For Earthquake Loading of an Anchored Sheet Pile Wall

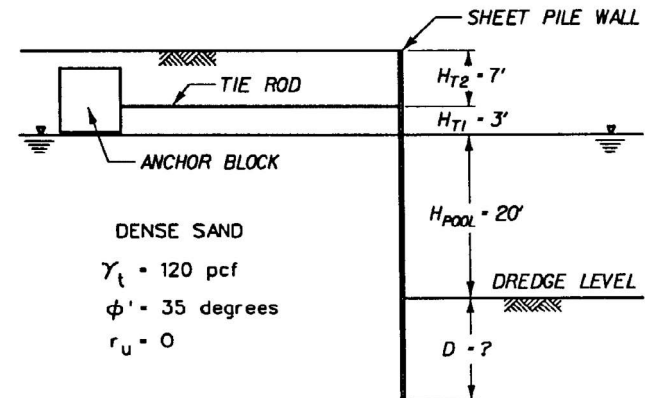


Figure 12-11: Anchored sheet pile wall design problem

Given

- o Anchored sheet pile wall shown in Figure 12-11.
- o Assume $k_h = 0.2$, $k_v = 0.1$ and no excess pore water pressures are generated during earthquake shaking ($r_u = 0$).

Find

- o Depth of penetration of wall D for both static and earthquake loading.
- o Required section modulus of sheeting for both static and earthquake loading.
- o The results of the computations shown are rounded for ease of checking calculations and not to the appropriate number of significant figures.

Solution

- o Definition of Parameters
 - Friction angle $\delta = \phi/2 = 17.5^\circ$ degrees
 - Active earth pressure coefficient $K_A = 0.246$, say $K_A = 0.25$
 $K_A \cdot \cos \delta = 0.24$
 - "Factored" Passive earth pressure coefficient K_p
Factor of Safety on shear strength = 1.5^{135}
 $\tan\phi'_L = \tan 35^\circ/1.5 = 25^\circ$
 $\tan\phi'_L = \tan 17.5^\circ/2 = 11.9^\circ$ or 12°
 $\delta_t/\phi_t = 0.5$
Using the Log-spiral solution for K_p with $\delta/\phi = -0.5$,
 $R_d = 0.808$
 - o $K_p (\delta/\phi = -1.0, f = 25 \text{ degrees}) = 4.4$
 - o $K_p (\delta/\phi = -0.5) = 0.808 \cdot 4.4 = 3.56$
 - o $K_p \cos\delta = 3.56 \cdot \cos 12^\circ = 3.48$

o Depth of Penetration

¹³⁴Iai, S., and Kameoka, T. 1991. "Effective Stress Analysis of a Sheet Pile Quaywall," *Proceeding of Second International Conference on Recent Advances in Geotechnical Earthquake Engineering and Soil Dynamics*, Paper No. 4.14, Vol. I, St. Louis, MO, pp. 649-656.

¹³⁵The passive earth pressure coefficient reduction is applied differently here than in other problems. Here, it is applied to the friction angle, elsewhere to the coefficient itself.

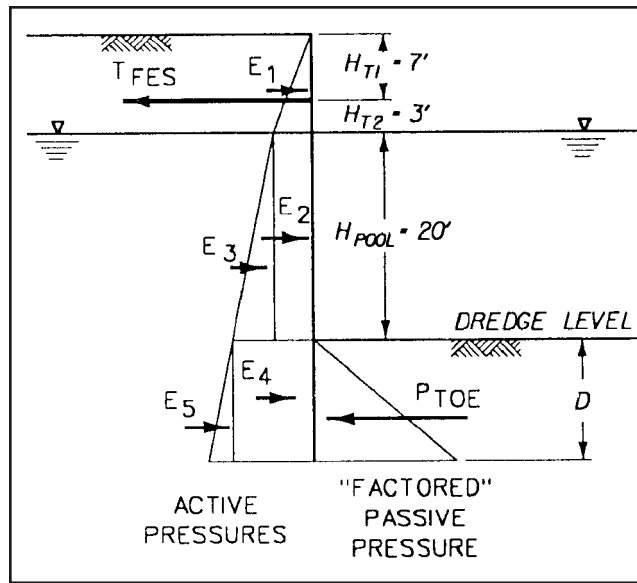


Figure 12-12: Horizontal earth pressure components in free earth support design

Table 12-3 Horizontal Force Components

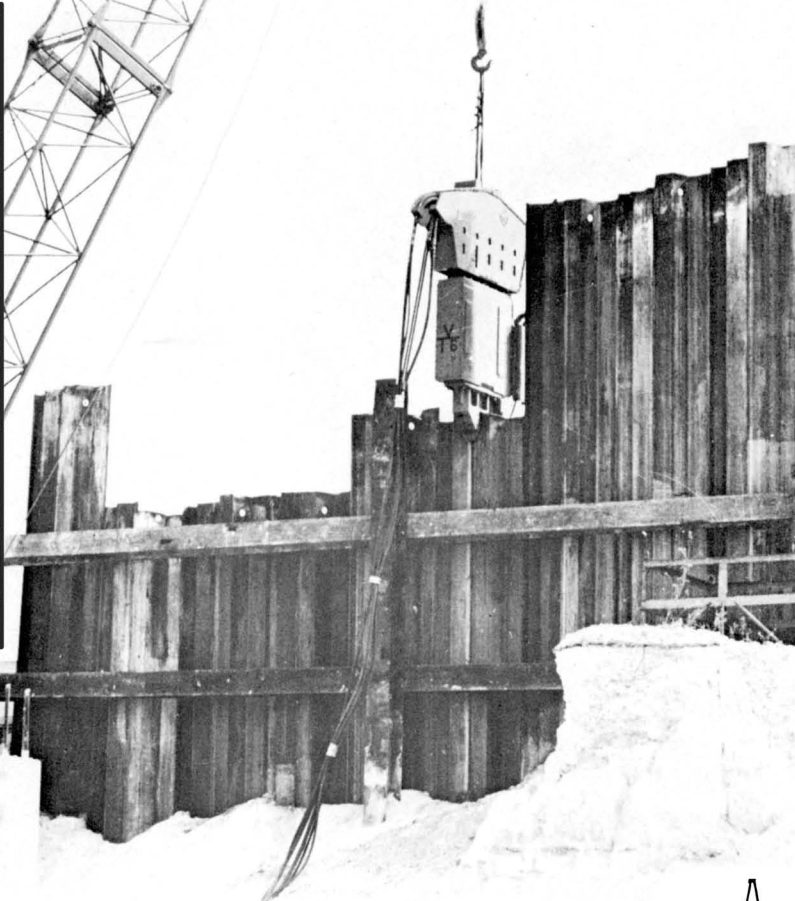
Horizontal Force Designation	Horizontal Force	Distance to Tie Rod
E ₁	$K_A \cos \delta \cdot \frac{1}{2} \gamma_t (H_{T1} + H_{T2})^2$	$\frac{1}{3}(2 H_{T2} - H_{T1})$
E ₂	$K_A \cos \delta \cdot \frac{1}{2} \gamma_t (H_{T1} + H_{T2}) H_{pool}$	$H_{T2} + \frac{1}{2} H_{pool}$
E ₃	$K_A \cos \delta \cdot \frac{1}{2} \gamma_b (H_{pool})^2$	$H_{T2} + \frac{2}{3} H_{pool}$
E ₄	$K_A \cos \delta \cdot [\gamma_t (H_{T1} + H_{T2}) + \gamma_b \cdot H_{pool}] \cdot D$	$H_{T2} + H_{pool} + \frac{1}{2} D$
E ₅	$K_A \cos \delta \cdot \frac{1}{2} \gamma_b (D)^2$	$H_{T2} + H_{pool} + \frac{2}{3} D$
P _{TOE}	$K_p \cos \delta_t \cdot \frac{1}{2} \gamma_b \cdot (D)^2$	$H_{T2} + H_{pool} + \frac{2}{3} D$

• Table 12-3 summarizes the horizontal force components acting on Figure 12-12 sheet pile wall and are expressed in terms of the generalized dimensions H_{T1} , H_{T2} , H_{pool} , and D . The horizontal force components and their moment about the elevation of the tie rod are summarized in Table 12-4 and Table 12-5. The forces and moments are expressed in terms of the unknown depth of penetration, D .

• Equilibrium of moments about the elevation of the tie rod (CCW moment +ve) requires

Equation 12-17:

$$\begin{aligned} \sum M_{tie\ rod} &= 0 \\ 0 &= M_{active} + M_{passive} \\ 0 &= -62.2 D^3 = 1,863.3 D^2 + 12,983.5 D + 119,554 \\ D &= 10.02 \text{ ft. } (D = 10' \text{ for construction}) \end{aligned}$$



Seaboard Steel Corp.
Sales / Rentals

PZ-27
PZ-22



Steel Sheet Piling
Steel HP Bearing Piles
Vibratory Driver/Extractors
Diesel and Hydraulic Pile Hammers
Vertical Earth Augers



Seaboard Steel Corp.
3912 Goodrich Ave.
Sarasota, FL 34234

941-355-9773
1-800-533-2736
Fax: 941-351-7064



Table 12-4: Moments About Tie Rod Due to Active Earth Pressures Table

Horizontal Force Designation	Horizontal Force (lb per ft wall)	Distance to Tie Rod (ft)	Moment About Tie Rod -CCW Moment + 've- (ft-lb per ft wall)
E ₁	1,440	-0.33	-475
E ₂	5,760	13	74,880
E ₃	2,765	16.33	45,149
E ₄	564.5D	23 + $\frac{1}{2}$ D	12,983.5 D + 282.3 D ²
E ₅	6.91 (D) ²	23 + $\frac{2}{3}$ D	159.0 D ² + 4.6 D ³
$M_{Active} = 4.6 D^3 + 441.3 D^2 + 12,983.5 D + 119,554$			

Table 12-5: Moments About Tie Rod Due to Passive Earth Pressures

Horizontal Force Designation	Horizontal Force (lb per ft wall)	Distance to Tie Rod (ft)	Moment About Tie Rod -CCW Moment + 've- (ft-lb per ft wall)
P _{TOE}	100.2 (D) ²	23 + $\frac{2}{3}$ D	-66.8 D ³ - 2,304.6 D ²
$M_{Passive} = -66.8 D^3 - 2,304.6 D^2$			

o Tie Rod Force T_{FES}

- Horizontal force equilibrium

Equation 12-18:

$$\sum F_h = 0$$

$$E_1 + E_2 + E_3 + E_4 + E_5 - P_{TOE} - T_{FES} = 0$$

$$1,440 + 5,760 + 2,765 + 5,656 + 694 - 10,060 - T_{FES} = 0$$

$$T_{FES} = 6,255 \text{ lb per ft of wall}$$

o Maximum Moment MFES

- The maximum value of moment, MFES, occurs at the elevation of zero shear within the sheet pile. First, determine the elevation of zero shear and then compute the moment internal to the sheet pile by computing the moments of the earth pressures and water pressures about the elevation of the tie rod (refer to Step 8 discussion in previous sections). This usually occurs at an elevation above the dredge level. By modifying the relationships given in Table 12-3, the equilibrium of horizontal forces at a depth, y, below the water table is expressed as

Equation 12-19:

$$E_1 + E_{2x} + E_{3x} - T_{FES} = 0$$

$$1,440 + 288 \cdot y + 6.912 \cdot y^2 - 6,255 = 0$$

$$6.912 \cdot y^2 + 288y - 4,815 = 0$$

$$y = 12.79 \text{ ft below the water table}$$

- From the calculations summarized in Table 12-6 the maximum moment internal to the sheet pile at y = 12.79 ft below the water table is equal to MFES = 47,165 ft-lb per ft of wall.

o Design Moment M_{design}

- The design moment, M_{design}, is obtained through application of Rowe's moment reduction procedure.

Equation 12-20:

$$H = H_{T1} + H_{T2} + H_{pool} + D$$

$$H = 7 + 3 + 20 + 10 = 40 \text{ ft (480.24 in.)}$$

$$E = 30 \times 10_6 \text{ psi}$$

$$\text{Flexibility Number } \rho = H^4 / (EI)$$

Table 12-6: Moment Internal to the Sheet Pile at y = 12.79 Feet Below the Water Table and About the Elevation of the Tie Rod

Horizontal Force Designation	Horizontal Force (lb per ft wall)	Lever Arm (ft)	Moment (ft-lb per ft wall)
E ₁	1,440	-0.33	-475
E _{2x}	3,683.5	$3 + \frac{1}{2} (12.79)$	34,607
E _{3x}	1,130.7	$3 + \frac{2}{3} (12.79)$	13,033

Table 12-7: Design Moment for Sheet Pile Wall in Dense Sand

Section Designation	I (in. ⁴ per ft of wall)	ρ (in. ² /lb per ft of wall)	r _d (Figure 7.2)	M _{design} (ft-lb per ft of wall)
PZ22	84.4	21.0	0.45	21,224
PZ27	184.2	9.62	0.68	32,072
PZ35	361.2	4.91	1.0	47,165
PZ40	490.8	3.61	1.0	47,165

$$\rho = \frac{(480.24 \text{ in.})^4}{(30 \times 10^6 \text{ psi}) \cdot I}$$

$$\rho = \frac{1,773.0}{I}$$

- T_{FES} = 6,255 lb per ft of wall
- T_{design} = 8,132 lb per ft of wall

$$\text{Minimum area of rod} = \frac{6 \text{ ft} \cdot 8,132 \text{ lb per ft of wall}}{0.4 \cdot 36,000 \text{ psi}}$$

where I = moment of inertia per ft of wall. The values of M_{design} are given in Table 12-7 for four sheet pile sections.

- Gross Area = 3.39 in²

where M_{design} = r_d · M_{FES}

$$\text{Diameter} = \sqrt{\frac{4 \cdot \text{Area}}{\pi}} = 2.08 \text{ in.}$$

o Selection of the Sheet Pile Section

• The allowable bending moment M_{allowable} is given by Table 2-1. Comparison of the design moment values to the allowable bending moments indicates that all four pile sections would be adequate. The lightest section, PZ22, would be selected for this design based upon static loading. Corrosion must also be addressed during the course of the sheet pile wall design. Additionally, the deflection of the anchored sheet pile wall would be checked, as we did in other examples.

o Design Anchorage

- T_{ult-a} = 2.5 · T_{FES} (Equation 11-11)
- T_{FES} = 6,255 lb per ft of wall
- T_{ult-a} = 15,638 lb per ft of wall
- If the overall height of the anchor, h_a, is not less than about 0.6 times the depth from the ground surface to the bottom of anchorage, designated d_a in Figure 12-13, the anchor behaves as if it extended to the ground surface (see 11.2.3.2.) Using Rankine theory as before, for a slender anchor the ultimate capacity for a continuous anchor is required to satisfy Equation 11-8 with d = 0 degrees.

o Design Tie Rod

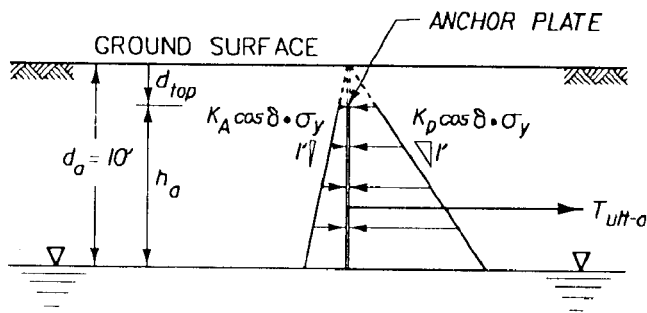
- T_{design} = 1.3 T_{FES}
- Assume:

- 6 ft spacing of anchors
- s_{yield} = 36,000 psi
- s_{allowable} = 0.4 s_{yield} (40 % of yield)

- For anchorage above the water table

Equation 12-21: $T_{ult-a} \leq \frac{1}{2} \gamma_t (h_a)^2 \cdot (K_p - K_A)$

- For $\phi' = 35$ degrees and $\delta = 0$ degrees, K_p = 3.69 and K_A = 0.27. Substituting,



Equation 12-22:

$$T_{ult-a} \leq \frac{1}{2} \gamma_t (h_a)^2 \cdot (K_P - K_A)$$

= 15,638 lb per ft of wall < 20,520 lb per ft run of continuous anchor

- \$h_a \ge 0.6 \cdot 10' = 6\$ ft.
Because the value of \$T_{ult-a}\$ is significantly less than the capacity of a continuous wall, a series of separate anchorages would be investigated.

o Site Anchorage

- To be effective, the anchorage must be located such that the potential active failure zone behind the sheet pile wall and the potential passive failure zone in front of the anchorage does not intersect. Design criteria for deadman anchorage is shown in Figure 11-4. The use of the estimated point of zero moment in the wall (at \$\approx D/4\$) accounts for the increased depth of penetration due to the use of \$FS_p = 1.5\$ used in the calculation of the passive earth pressure force provided by the soil below the dredge level¹³⁶.

o Design for Earthquake Loading

Now we can turn to the design of an anchored sheet pile wall for seismic loading, using the steps we have already defined for this procedure

1. We have already analysed the static wall. The calculated depth of penetration \$D\$ equals 10.02 ft.
2. Horizontal Seismic Coefficient, \$k_h\$. \$k_h = 0.2\$
3. Vertical Seismic Coefficient, \$k_v\$. \$k_v = +0.1, 0\$ and \$-0.1\$. For this example we will only consider the case for \$k_v = +0.1\$ due to the length of the calculations involved.

4. Depth of Penetration (steps 4 through 6.) The depth of penetration, \$D\$, equal to 10 ft was found not to be stable under earthquake loading. The required minimum depth of penetration is best determined by the trial and error procedure of first assuming a value for \$D\$ and checking if moment equilibrium of the earth and water pressure forces about the

elevation of the tie rod is satisfied. This iterative procedure results in a minimum required depth of penetration equal to 20.24 ft. The calculations involved in Steps 4 through 6 are summarized in the following paragraphs for the case of \$D\$ set equal to 20.24 ft.

a. Backfill

- i. Effective Unit Weight for the Partially Submerged Backfill.

Equation 12-23:

$$\gamma_e = \left(\frac{h_1}{h}\right)^2 \cdot (\gamma_t - \gamma_w) + \left[1 - \left(\frac{h_1}{h}\right)^2\right] \cdot \gamma_t$$

1. with \$D = 20.24\$ ft;
2. \$h_1 = 40.24\$ ft
3. \$h = 50.24\$ ft

$$\gamma_e = \left(\frac{40.24}{50.24}\right)^2 \cdot (120 \text{ pcf} - 62.4 \text{ pcf}) + \left[1 - \left(\frac{40.24}{50.24}\right)^2\right] \cdot 120$$

- ii. Equivalent Horizontal Seismic Coefficient, \$k_{he1}\$, for the backfill

- iii. For the restrained water case with \$r_u = 0\$

Equation 12-24:

$$k_{he1} = \frac{\gamma_t}{\gamma_e} \cdot k_h$$

$$k_{he1} = \frac{120 \text{ pcf}}{79.97 \text{ pcf}} \cdot 0.2 = 0.3001$$

- iv. Seismic Inertia Angle, \$\Psi_{e1}\$, for the Backfill

Equation 12-25:

$$\psi_{e1} = \tan^{-1} \left[\frac{k_{he1}}{1 - k_v} \right]$$

$$\psi_{e1} = \tan^{-1} \left[\frac{0.3001}{1 - 0.1} \right]$$

$$\Psi_{e1} = 18.44^\circ$$

- v. Dynamic Active Earth Pressure, \$P_{AE}\$

1. With \$\phi' = 35^\circ\$, \$\delta = f/2 = 17.5^\circ\$ and \$\Psi_{e1} = 18.44^\circ\$, \$K_{AE} = 0.512\$.

Equation 12-26:

$$P_{AE} = K_{AE} \cdot \frac{1}{2} [\gamma_e (1 - k_v)] H^2$$

$$P_{AE} = 0.512 \cdot \frac{1}{2} [79.97 \text{ psf} \cdot (1 - 0.1)] (50.24')^2$$

$$P_{AE} = 46,506 \text{ lb per ft of wall}$$

¹³⁶ Duncan, J. M. 1985. Lecture Notes Regarding the Design of Anchored Bulkheads.



**FINALLY
THE NEXT
GENERATION
OF SHEET PILING**

PZC™

WIDER • LIGHTER • STRONGER

**LEARN MORE:
WWW.SHEET-PILING.COM**



Horizontal Force Designation	Horizontal Force (lb per ft wall)	Distance to Pile Tip (ft)
E_1	1,410	43.57
E_2	5,640	30.24
E_3	2,707	26.91
E_4	11,187	10.12
E_5	2,772	6.75

Figure 12-14 Five Horizontal Active Earth Pressure Force Components of P_{AE} with $D = 20.24'$

2. $(P_{AE})_x = P_{AE} \cdot \cos\delta = 44,354$ lb per ft of wall

Equation 12-31:

vi. Horizontal Static Active Earth Pressure Component of P_{AE}
 1. With a hydrostatic water table and $r_u = 0$, the horizontal-static active earth pressure force components of P_{AE} are computed using the relationships in Table 12-3.

$$Y_{PAE} = \frac{(P_A)_x \cdot Y_{PA} + (\Delta P_{AE})_x \cdot Y_{\Delta PAE}}{(P_{AE})_x}$$

$$Y_{PAE} = \frac{23,716 \cdot 18.42 + 20,638 \cdot 30.14}{44,354}$$

2. With $\phi' = 35^\circ$ and $\delta = \phi/2 = 17.5^\circ$, $K_A = 0.246$, $K_A \cdot \cos\delta = 0.235$.

$Y_{PAE} = 23.87$ ft above the pile tip.

3. Above the water table $\gamma_t = 120$ pcf is used to calculate the effective overburden pressure while below the water table $\gamma' = \gamma_t - \gamma_w (= 57.6$ pcf) is used to calculate the effective overburden pressure with $r_u = 0$. The resulting values for the five horizontal static force components E_1 through E_5 of P_{AE} are given in Table C.9 (forces shown in Figure 12-12).

b. Below Dredge Level

i. Equivalent Horizontal Seismic Coefficient, k_{he1} , Used in Front of Wall. For the restrained water case with $r_u = 0$,

Equation 12-27:

$$(P_A)_x = E_1 + E_2 + E_3 + E_4 + E_5$$

$$(P_A)_{3c} = 23,716 \text{ lb per ft of wall}$$

Equation 12-32:

$$k_{he1} = \frac{\gamma_t}{\gamma_b} \cdot k_h$$

$$k_{he1} = \frac{120 \text{ pcf}}{(120 \text{ pcf} - 62.4 \text{ pcf})} \cdot 0.2$$

$k_{he1} = 0.4167$

Equation 12-28:

$$Y_{PA} = \frac{1,410 \cdot 43.57 + 5,640 \cdot 30.24 + 2,707 \cdot 26.91 + 11,187 \cdot 10.12 + 2,772 \cdot 6.75}{23,716}$$

$Y_{PA} = 18.42$ ft above the pile tip.

ii. Seismic Inertia Angle, Ψ_{e1} , Used in Front of Wall

Equation 12-33:

$$\psi_{e1} = \tan^{-1} \left[\frac{k_{he1}}{1 - k_v} \right]$$

$$\psi_{e1} = \tan^{-1} \left[\frac{0.4167}{1 - 0.1} \right]$$

$\Psi_{e1} = 24.84^\circ$

vii. Horizontal Component of the Incremental Dynamic Active Earth Pressure Force, $(\Delta P_{AE})_x$

iii. "Factored" Strengths Used in Front of Wall

Equation 12-29:

$$(\Delta P_{AE})_x = (P_{AE})_x - (P_A)_x$$

$$(\Delta P_{AE})_x = 44,354 - 23,716 = 20,638 \text{ lb per ft of wall}$$

Equation 12-30:

$Y_{\Delta PAE} = 0.6 \cdot H = 0.6 \cdot 50.24' = 30.14$ ft above the pile tip.

Equation 12-34: $\tan\phi'_t = \frac{\tan 35^\circ}{1.2} = 30.3^\circ$ (FSP = 1.2)¹³⁷

Equation 12-35: $\tan \delta_t = \frac{\tan 17.5^\circ}{1.2} = 14.7^\circ (\delta = \phi/2)$

iv. "Factored" Dynamic Passive Earth Pressure Coefficient K_{PE} Using the equivalent static formulation with K_p by Log-Spiral method.¹³⁸

Equation 12-36:
 $\beta^* = \beta - \Psi_{e1} = -24.84^\circ$
 $\theta^* = \theta - \Psi_{e1} = -24.84^\circ$

Equation 12-37:
 $K_p (\beta^* = -24.84, \theta^* = -24.84, \phi = 30.3, \delta = -\phi) = 3.56$

Equation 12-38: R = 0.746 from Caquot and Kerisel
 For $\phi = 30.3^\circ$ and $\delta = -\phi/2$,

Equation 12-39: $K_p (\beta^*, \theta^*, \phi, \delta = -\phi/2) = 3.56 \cdot 0.746 = 2.66$

Equation 12-40:

$$F_{PE} = \frac{\cos^2 (\theta - \psi_{e1})}{\cos \psi_{e1} \cos^2 \theta}$$

$$F_{PE} = \frac{\cos^2 [0 - (-24.84)]}{\cos (24.84) \cos^2 (0)} = 0.907$$

Equation 12-41:
 $K_{PE} = K_p (\beta^*, \theta^*, \phi, \delta = -\phi/2) \cdot F_{PE} = 2.66 \cdot 0.907 = 2.41$

Equation 12-42: $K_{PE} \cdot \cos \delta_t = 2.41 \cdot \cos(14.7) = 2.33$

v. "Factored" Horizontal Dynamic Passive Earth Pressure Force P_{PE}

Equation 12-43:

$$(P_{PE})_x = K_{PE} \cdot \cos \delta_t \cdot \frac{1}{2} [\gamma_b \cdot (1 - k_v)] D^2$$

$$= 2.33 \cdot \frac{1}{2} [(120 \text{ pcf} - 62.4 \text{ pcf}) \cdot (1 - 0.1)] (20.24)^2$$

$$(P_{PE})_x = 24,740 \text{ lb per ft of wall}$$

Equation 12-44:¹³⁹
 $Y_{PE} \approx \frac{1}{3} \cdot D^* = \frac{1}{3} \cdot 20.24 = 6.75 \text{ ft above the pile tip.}$

c. Pool In Front of Wall

i. Hydrodynamic Water Pressure Force P_{wd}

$$P_{wd} = \frac{7}{12} k_h \gamma_w (H_{pool})^2$$

Equation 12-45:

$$= \frac{7}{12} \cdot 0.2 \cdot 62.4 \text{ pcf} (2')^2 = 2,912 \text{ lb per ft of wall}$$

Equation 12-46:

$$Y_{P_{wd}} = 0.4 \cdot H_{pool} = 8 \text{ ft above the dredge level}$$

d. Depth of Penetration

i. Equilibrium of Moments About The Elevation of the Tie Rod

Equation 12-47:

$$\Sigma M_{CCW} = (P_{AE})_x \cdot (H_{T2} + H_{pool} + D - Y_{P_{AE}}) + P_{wd} \cdot (H_{T2} + H_{pool} - 0.4 \cdot \text{pool})$$

$$= 44,354 \cdot (3' + 20' + 20.24' - 23.87') + 2,912 \cdot (3' + 20' - 8')$$

$$= 859,137 + 43,680$$

$$= 902,817 \text{ ft} \cdot \text{lb per ft. of wall}$$

Equation 12-48:

$$\Sigma M_{CW} = -(P_{PE})_x \cdot (H_{T2} + H_{pool} + D - Y_{PE})$$

$$= -24,740 \cdot (3' + 20' + 20.24' - 6.75')$$

$$= -902,763 \text{ ft} \cdot \text{lb per ft of wall}$$

Moment Imbalance = $\Sigma M_{CCW} + \Sigma M_{CW} = 54 \text{ ft} \cdot \text{lb per ft of wall}$. Small moment imbalance value so $D = 20.24 \text{ ft}$ for the case of $k_h = 0.2$ and $k_v = +0.1$. The two additional cases of $k_v =$ and $k_v = -0.1$ are summarized in *Table C.10*. The required minimum depth of penetration is equal to 20.24 ft (20.5 ft for construction).

Case	k_h	k_v	D (ft)	$\frac{D}{D_{Static}}$
Static	0	0	10.02	1.0
Dynamic	0.2	-0.1	14.88	1.5
Dynamic	0.2	0	17.1	1.7
Dynamic	0.2	+0.1	20.24	2.0

Table 12-8: Summary of Depth of Penetration Calculations

5. Steps above.

6. Steps above.

7. Tie Rod Force T_{FES}

a. Horizontal force equilibrium for the case of $D = 20.24 \text{ ft}$ with $k_h = 0.2$ and $k_v = +0.1$, so the $\Sigma F_h = 0$ results in

Equation 12-49: $T_{FES} = (P_{AE})_x + P_{wd} - (P_{PE})_x$

for a hydrostatic water table with $ru = 0$.

Equation 12-50:
 $T_{FES} = 44,354 + 2,912 - 24,740 = 22,526 \text{ lb per ft of wall.}$

The two additional cases of $k_v = 0$ and $k_v = -0.1$ are summa-

¹³⁷ $F_{Sp} = 1.2$ for illustration purposes only. See discussion in footnote to step 5.

¹³⁸This quantity can also be solved by the method of Mononobe-Okabe, in which case the result is $K_{PE} = 2.85$. Since this is larger than the log-spiral result, we will use the log-spiral result.

¹³⁹ $Y_{PE} = 1/3 \cdot D$ for illustration purposes only. See discussion in footnote to step 5.

Case	k_h	k_v	D (ft)	T_{FES} lb per ft of wall	$\frac{T_{FES}}{(T_{FES})_{static}}$
Static	0	0	10.02	6,255	1
Dynamic	0.2	-0.1	14.88	20,819	3.3
Dynamic	0.2	0	17.1	21,368	3.4
Dynamic	0.2	+0.1	20.24	22,526	3.6

Table 12-9: Tie Rod Force T_{FES}

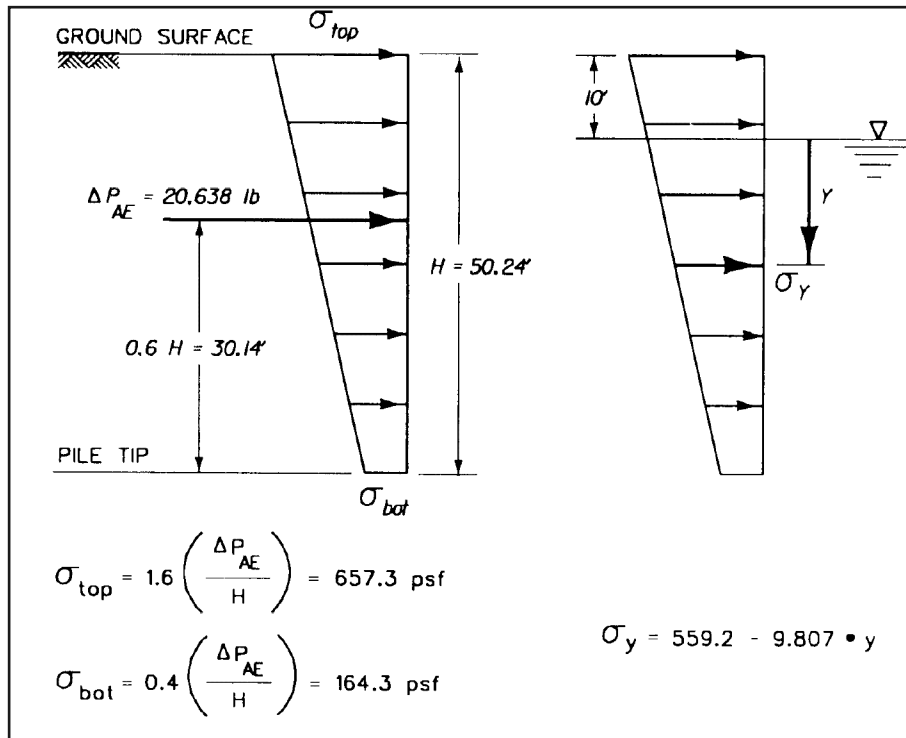


Figure 12-15: Distributions of horizontal stresses corresponding to ΔP_{AE}

rized in Table 12-9. The anchorage is designed using $T_{FES} = 22,526$ lb per ft of wall.

8. Maximum Moment M_{FES}

a. The maximum value of moment internal to the sheet pile wall, M_{FES} , occurs at the elevation of zero shear within the sheet pile. First determine the elevation of zero shear and then compute the moment of earth and water pressure forces about the tie rod. Above the dredge level, at elevation y below the hydrostatic water table

Equation 12-51: $(P_{AE})_x + P_{wd} - T_{FES} = 0$ with

Equation 12-52: $(P_{AE})_x = (P_A)_x + (\Delta P_{AE})_x$
 $(P_A)_x$ above the dredge level

Equation 12-53:
 $(P_A)_x = E_1 + E_2 y + E_3 y = 1,410 + 282 y + 6.768 y^2$

With $(\Delta P_{AE})_x$ equal to 20,638 lb per ft of wall, the equivalent stress distribution is given in Figure 12-15.

MARINE CONSTRUCTION ON CD-ROM!

46 titles on CD Rom & more than 8,300 detail-packed "pages" on dozens of MARINE CONSTRUCTION topics give you all the instruction you need to design and construct:

- HARBORS / PIERS
- RIPRAP / GROINS
- SHORE PROTECTION
- BREAKWATERS / JETTIES
- MAINTENANCE
- PILE PROTECTION
- STEEL SHEET PILING
- TIMBER PILING
- CELLULAR COFFERDAMS
- BULKHEADS / SEAWALLS
- MARINE DOCKS
- MARINAS
- DREDGING
- PILE HAMMERS
- PIPELINES / OUTFALLS
- BARGES / CRANES
- MOORINGS
- PORTS AND MORE,
- MORE, MORE!

BUY BOTH VOLUMES FOR \$159.95 TODAY.

Pile Buck® Mail/Fax Order Form

Name : _____

Company Name : _____

Address: _____

City: _____ State: _____ Zip: _____

Type Of Business: _____

Phone: _____ Fax: _____

Name On Credit Card _____ Exp. Date: _____

Credit Card Number: _____

VIN Number _____ This is the ID number on your physical credit card. On MasterCard, Visa and Discover, it is the three digit number found on the back in the signature area. On American Express, it is the four digit number found on the front of the card, on the right side.

Title	Pages	Title	Pages
q SHORE PROTECTION MANUAL VOLUME 1 Complete coverage of coastal engineering, wave motion, wave and water levels, littoral processes, planning analysis.	633	q ICE ENGINEERING Ice formation, characteristics, growth, jams, breaking, adhesion, control forces, computations and design.	129
q SHORE PROTECTION MANUAL VOLUME 2 Complete coverage of structural features, structural design, physical factors, engineering analysis, case studies.	633	q HANDBOOK FOR MARINE GEOTECHNICAL ENGINEERING Site surveys, soil properties, shallow and pile foundations, anchors, scour, slopes, stability, examples.	254
q ENVIRONMENTAL ENGINEERING FOR COASTAL SHORE PROTECTION Protection projects, environmental resources, beaches and dunes, human-made structures, environmental monitoring, models.	189	q COASTAL GEOLOGY Coastal terminology and geologic environments, coastal morphodynamics and geological investigations.	298
q DESIGN OF RIPRAP REVETMENT Coverage of revetment types, design guidelines for rock riprap, guidelines for other revetments, design examples.	172	q SEISMIC DESIGN OF WATERFRONT RETAINING STRUCTURES Seismic design considerations for waterfront sites, retaining walls, earth pressures, backfills and design examples.	323
q RIPRAP PROTECTION ON NAVIGABLE WATERWAYS Model investigation into the effects of propeller wash and riprap stability.	58	q DREDGING AND DREDGED MATERIAL DISPOSAL Design considerations, equipment and techniques, disposal alternatives.	93
q STABILITY OF ROCK RIPRAP FOR PROTECTION AT TOE ABUTMENTS LOCATED AT THE FLOODPLAIN Research into rock riprap stability, scour concerns and gravel, example problems.	122	q COASTAL SEDIMENTATION AND DREDGING Coastal sedimentation and erosion, harbor entrances, shore protection, beach preservation, dredging.	66
q STABILITY OF RIPRAP TO PROTECT BRIDGE PIERS Investigation of scour at bridge openings including piers and riprap stability.	126	q BENEFICIAL USES OF DREDGED MATERIAL Dredged material as a resource, wetland, upland, island and aquatic habitats, beaches and beach nourishment.	283
q STUDY OF PUBLIC USE OF JETTIES, GROINS AND BREAKWATERS Types of coastal and navigation structures, legal and public use of U.S. Army C.O.S. jetties, groins and breakwaters.	56	q WATER LEVELS AND WAVE HEIGHTS FOR COASTAL ENGINEERING DESIGN Tides and tidal datums, storm surges, shoreline interaction, wave and water levels, analysis for design.	269
q CONSTRUCTION MATERIALS FOR COASTAL STRUCTURES Materials for coastal structures, stone, soils, cement, wood, steel, plastics recycled materials and corrosion.	427	q STORM SURGE ANALYSIS Storm surges, historical data, boundary conditions, physical models, surge simulation and related effects.	224
q HYDRAULIC DESIGN OF SMALL BOAT HARBORS Design factors, studies of water levels, waves, currents, shoreline changes, etc.	131	q SAND BYPASSING SYSTEM SOLUTION Sand bypassing concepts, coastal processes and site investigations, bypassing systems and design considerations.	207
q LOW COST SHORE PROTECTION Available options such as bulkheads, groins, perched beaches, etc., selection and permit requirements.	111	q DESIGN OF BEACH FILLS Site characteristics, fill stabilization, design, plans and specifications, performance monitoring and maintenance.	111
q TIDAL HYDRAULICS Estuaries, tides and other long waves, hydrodynamics, sedimentation, design considerations and case histories.	153	q COASTAL PROTECTION Wave parameters, rubble-mound structures, wall design, floating breakwaters, wave forces, case histories.	352
q COASTAL PROJECT MONITORING Coastal monitoring data handling, waves, water, salinity and sediment, topographic and structural surveys, ice conditions.	121	q HYDROGRAPHIC SURVEYING Survey accuracy, visual and manual techniques, EPSs, tides, water levels, depth measurement, special surveys.	333
q ENVIRONMENTAL ENGINEERING FOR SMALL BOAT BASINS Permit processing, water body designations (salt, fresh, Great Lakes,) basin design, environmental effects of pollution, etc.	40	q DRYDOCKING FACILITIES CHARACTERISTICS Basic drydocking facilities characteristics, graving drydocks, marine railways, marine lifts, etc.	152
q COASTAL GROINS AND NEARSHORE BREAKWATERS Beach stabilization, design of groins and nearshore breakwaters, construction and postconstruction activities, examples.	91	q GRAVING DRYDOCKS Site considerations, shipyard layout, types of drydocks and structural design, flooding, dewatering and support facilities.	112
q COASTAL LITTORAL TRANSPORT Waves, littoral processes, nearshore currents, beach topography and nourishment, sediment transport processes, examples.	143	q WEIGHT HANDLING EQUIPMENT Types of equipment, traveling and non-traveling, selection, operating features, recommended capacities, design criteria.	227
q DESIGN OF COASTAL REVETMENTS, SEAWALLS, AND BULKHEADS Functional design methods covering revetments, seawalls, bulkheads and environmental impacts with sample problems.	109	q YARD CRAFT Yard craft design, maximum towing efficiency, hydrostatics and stability, components, etc.	68
q GENERAL CRITERIA FOR WATERFRONT CONSTRUCTION Piling types, deck and substructure, hardware and fittings, strength evaluation of structures, deterioration, case histories.	101	q TRACKAGE Railroad trackage, roadways, ballast and sub-ballast, ties, trackage components, yards, turnouts and crossovers.	77
q CONSTRUCTION WITH LARGE STONE Engineered stone structures, material problems, quarry evaluation, stone testing, measurement for payment.	61	q DOCKSIDE UTILITIES FOR SHIP SERVICE General utility requirements, berthing, supply and fueling piers, miscellaneous provisions.	144
q COASTAL INLET HYDRAULICS AND SEDIMENTATION Inlet geology, hydrodynamic analysis of tidal inlets, sediment and shoaling rates, design analysis.	135	q MARINE RAILWAYS Principles and types of marine railways, site selection, design loads, track or groundways, cradles, etc.	58
q COASTAL CONSTRUCTION MANUAL Coastal environment, site and structure design recommendations, construction materials, design procedures and examples.	278	q SEAWALLS, BULKHEADS AND QUAYWALLS Protective waterfront structures, such as seawalls, bulkheads, quaywalls, selection and basic design criteria.	86
q HARBORS Basic planning and design parameters, layout of facilities, turning and anchor-age basins, aids to navigation.	118	q PIERS AND WHARVES Facility planning, load requirements, structural design, tender systems, separators, and access facilities.	213
q DESIGN OF BREAKWATERS AND JETTIES Design of rubble-mound structures, jetties, vertical walls, floating structures, breakwaters, environmental impacts, with models.	185	q FERRY TERMINALS AND SMALL CRAFT BERTHING FACILITIES Planning and layout criteria, environmental factors, design criteria for berthing systems, basins, entrance channels, etc.	99

AVAILABLE ON CD-ROM ONLY

VOLUMES I & II
\$159.95

VOLUME I
\$99.95

For PC & Macintosh

VOLUME II
\$99.95

Table 12-10: Moment of Forces Acting Above the Point $y = 15.32$ feet Below the Water Table and About the Tie Rod¹⁴⁰

Horizontal Force Designation	Horizontal Force (lb per ft wall)	Lever Arm (ft)	Moment About Tie Rod -CCW +ve - (ft-lb per ft wall)
E_1	1,410	-0.33	-465
E_{2x}	4,320	$3 + \frac{1}{2} (15.32)$	46,051
E_{3x}	1,588	$3 + \frac{2}{3} (15.32)$	20,983
$(\Delta P_{AE})_x$	13,499	4.68*	63,175
P_{wd}	1,709	$3 + 0.6 \cdot (15.32)$	<u>20,836</u>
$M_{FES} = 150,580$ ft-lb per ft wall			

Equation 12-54:

$$(\Delta P_{AE})_x = \frac{1}{2} \cdot (\sigma_{top} + \sigma_y) \cdot (10' + y)$$

$$= \frac{1}{2} \cdot (657.3 + 559.2 - 9.807y) \cdot (10 + y)$$

$$\Delta P_{AE} = -4.9035 y^2 + 559.215 y + 6,082.5$$

$$P_{wd} = \frac{7}{12} \cdot k_h \gamma_w (y)^2$$

$$P_{wd} = 7.28 y^2$$

$$T_{FES} = 22,526 \text{ lb per ft of wall}$$

Above the dredge level

Equation 12-55: $(P_A)_x + (\Delta P_{AE})_x + P_{wd} - T_{FES} = 0$

becomes

Equation 12-56: $9.1445y^2 + 841.215 y - 15,033.5 = 0$

$$y = \frac{-(841.215) \pm \sqrt{(841.215)^2 - 4(9.1445)(-15,033.5)}}{2(9.1445)}$$

$y = 15.32$ ft below the water table (above dredge level \therefore ok)

The maximum moment internal to the sheet pile at $y = 15.32$ ft below the water table is equal to $M_{FES} = 150,580$ ft-lb per ft of wall.

9. Design Moment M_{design}

a. The design moment, M_{design} , is obtained through application of Rowe's moment reduction procedure. The ability of the system to develop flexure below the dredge level during earthquake shaking must be carefully evaluated prior to application

of Rowe's moment reduction factor or any portion of the reduction factor.

Equation 12-57:

$$H = H_{T1} + H_{T2} + H_{pool} + D$$

$$H = 7' + 3' + 20' + 20.24' = 50.24 \text{ ft} = (602.88 \text{ in.})$$

$$E = 30 \times 10^6 \text{ psi}$$

$$\text{Flexibility number } \rho = H^3 / (EI)$$

$$\rho = \frac{(602.88 \text{ in})^4}{(30 \times 10^6 \text{ psi}) \cdot I}$$

$$\rho = \frac{4,403.54}{I}$$

where $I =$ moment of inertia per ft of wall. The values of M_{design} are given in *Table 12-11* for four sheet pile sections.

where $M_{design} = r_d \cdot M_{FES}$ Comparison of the design moment values (M_{design} in *Table 12-11*) to the allowable bending moments ($M_{allowable}$ in *Table 2-1*) indicates that the pile section would be upgraded from PZ22 to PZ27 due to seismic considerations. Corrosion must also be addressed during the course of sheet pile wall design.

10. Design Tie Rods

a. For seismic loadings $T_{design} = 1.3 \cdot T_{FES}$; therefore, with $T_{FES} = 22,526$ lb per ft of wall, $T_{design} = 29,284$ lb per ft of wall. Assume (a) 6 ft spacing of tie rods and (b) $\sigma_{yield} = 36,000$ psi and c) $\sigma_{allowable} = 0.6 \cdot \sigma_{yield}$.

Equation 12-58:

$$\text{Minimum area of rod} = \frac{6 \text{ ft.} \cdot 29,284 \text{ lb per ft of wall}}{0.6 \cdot 36,000 \text{ psi}}$$

¹⁴⁰From Figure C.5 pressure distribution for $y = 15.32$ ft

Table 12-11: Design Moment for Sheet Pile Wall in Dense Sand

Section Designation	I (in. ⁴ per ft of wall)	ρ (in. ² /lb per ft of wall)	r_d (Figure 7.2)	M _{design} (ft-lb per ft of wall)
PZ22	84.4	52.2	0.38	57,220
PZ27	184.2	23.9	0.46	69,267
PZ35	361.2	12.2	0.58	87,336
PZ40	490.8	9.0	0.74	111,429

Case	k_h	k_v	D (ft)	$\frac{\sigma_{allowable}}{\sigma_{yield}}$	T _{design} (lb per ft of wall)	Area (in. ²)	Rod Diameter (in.)
Static	0	0	10.02	0.4	8,132	3.30	2.08
Dynamic	0.2	-0.1	14.88	0.6	27,065	7.52	3.09
Dynamic	0.2	0	17.1	0.6	27,778	7.72	3.13
Dynamic	0.2	+0.1	20.24	0.6	29,284	8.13	3.22

Figure 12-16: Required Geometry of Tie Rod¹⁴¹

Gross Area = 8.13 in.²

$$\text{Minimum Diameter} = \sqrt{\frac{4 \cdot \text{Area}}{\pi}} = 3.22 \text{ inches}$$

b. Table C.15 summarizes the required geometry of tie rod for the four load cases.

c. Comparison of the minimum diameter of tie rod required for seismic loading to the diameter required for static loading indicates that for a 6 ft spacing, the diameter of the tie rods ($\sigma_{yield} = 36,000$ psi) would be upgraded from 2.08 in. to 3.22 in.

11. Design of Anchorage

a. For seismic loadings use Equation 11-12.. In the case of $k_h = 0.2$ and $k_v = +0.1$, $T_{ult-a} = 22,526$ lb per ft of wall The dynamic forces acting on the continuous anchor wall are shown in Figure 12-17.

12. Size Anchor Wall

a. Assume that a continuous concrete wall is selected to be the anchorage. The “factored” dynamic earth pressures that develop in front of the anchor wall provide nearly all of the lateral resistance to the pull force T_{ult-a} . The anchor wall will

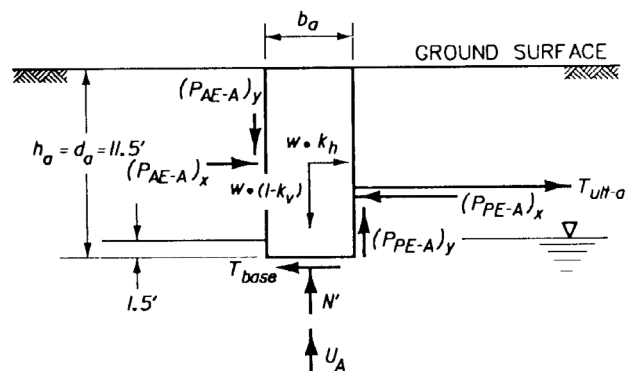


Figure 12-17: Seismic design problem for a continuous anchor block

be designed using ϕ_t and δ_t due to the magnitude of T_{ult-a} for seismic loading (equal to 3.6 times the static value). The required depth and width of anchor wall is best determined by the trial and error procedure of first assuming a value for d_a and checking if equilibrium of horizontal forces acting on the anchor is satisfied. Once the value of d_a is determined, equilibrium of the vertical forces acting on the anchor wall will dictate the minimum value of wall width b_a .

¹⁴¹Calculated for the case of (a) 6 ft spacing of tie rods (b) $\sigma_{yield} = 36,000$ psi and (c) $T_{design} = 1.3 \cdot T_{FES}$

b. This iterative procedure results in a minimum required depth of anchorage equal to 11.5 ft and a minimum width of anchor wall equal to 4.5 ft. The calculations involved in Step 12 are summarized in the following paragraphs for $d_a = 11.5$ ft and $(b_a)_{\min} = 4.5$ ft in Figure 12-17.

c. Dynamic Active Earth Pressure Force P_{AE-A}

i. For the case of $d_a = 11.5$ ft (the anchor submerged 1.5 ft below the water table), the effective unit weight is equal to $\gamma_e = 118.94$ pcf with $h_1 = 1.5$ ft and $h = 11.5$ ft.

ii. The equivalent horizontal seismic coefficient k_{he1} is equal to 0.2018 (obtained by substituting γ_e for γ_b). A value of k_{he1} equal to 0.2 is used in the subsequent calculations.

iii. For the case of $k_{he1} = 0.2$ and $k_v = +0.1$,

Equation 12-59:
$$\psi_{e1} = \tan^{-1} \left[\frac{k_{he1}}{1 - k_v} \right] = 12.529^\circ$$

With $\phi' = 35^\circ$, $\delta = 17.5^\circ$, and $Y_{e1} = 12.529^\circ$, $K_{AE} = 0.3987$, $K_{AE} \cdot \cos \delta = 0.38$ and $K_{AE} \cdot \sin \delta = 0.12$. With $d_a = 11.5$ ft,

Equation 12-60:

$$(P_{AE-A})_x = K_{AE} \cdot \cos \delta \cdot \frac{1}{2} [\gamma_e (1 - k_v)] (d_a)^2$$

$$(P_{AE-A})_x = 0.38 \cdot \frac{1}{2} [118.94 \text{ pcf} (1 - 0.1)] (11.5')^2$$

$$(P_{AE-A})_x = 2,690 \text{ lb per ft of wall}$$

by a similar calculation, $(P_{AE-A})_y = 849$ lb per ft of wall.

d. Dynamic Passive Earth Pressure Force P_{PE-A}

i. With $\phi' = 35^\circ$ and with FS_p set equal to 1.2 in this example (see step 12 discussion regarding the relationship between anchorage displacement and FS_p), $\phi'_t = 30.3^\circ$ and for $\delta = 17.5^\circ$, $\delta_t = 14.7^\circ$.

ii. For $\Psi = 12.529^\circ$ (refer to P_{AE-A} calculations), $\phi'_t = 30.3^\circ$ and $\delta_t = 14.7^\circ$. $K_{PE} = 4.06$, $K_{PE} \cdot \cos \delta_t = 3.93$ and $K_{PE} \cdot \sin \delta_t = 1.03$.

iii. With $d_a = 11.5$ ft,

Equation 12-61:

$$(P_{PE-A})_x = K_{PE} \cdot \cos \delta \cdot \frac{1}{2} [\gamma_e (1 - k_v)] (d_a)^2$$

$$(P_{PE-A})_x = 3.93 \cdot \frac{1}{2} [118.94 \text{ pcf} (1 - 0.1)] (11.5')^2$$

$$(P_{PE-A})_x = 27,818 \text{ lb per ft of wall}$$

iv. By a similar calculation $(P_{PE-A})_y = 7,291$ lb per ft of wall

e. Size Anchor

i. The depth of the continuous anchor wall is governed by the equilibrium of horizontal forces. Ignoring the contribution of the shear force along the base of the wall, $T_{ult-a} = (P_{PE-A})_x - (P_{AE-A})_x - W \cdot k_h$. For the concrete wall, the weight W per foot run of wall with $d_a = 11.5$ ft and $\gamma_{conc} = 150$ pcf is given by $W = \gamma_{conc} \cdot b_a \cdot d_a = 1,725 \cdot b_a$. Introducing this relationship for W and $k_h = 0.2$, $T_{ult-a} = 22,526$ lb per ft of wall ($k_v = +0.1$), $(P_{PE-A})_x = 27,818$ lb per ft of wall, and $(P_{AE-A})_x = 2,690$ lb per ft of wall into the modified equation of horizontal equilibrium results in a maximum value of b_a equal to 7.5 ft for $d_a = 11.5$ ft. Larger b_a values would result in excessive horizontal inertia forces acting on the concrete block, requiring revisions of the previous calculations.

ii. Mobilization of friction along interface between the front of the anchor wall and the passive wedge requires that the wall have sufficient dead weight to restrain against upward movement as it displaces the soil in front of the wall. The equation of equilibrium of vertical forces acting on the wall is used to compute the minimum width of anchor wall. With N' set equal to zero,

Equation 12-62:

$$0 = W (1 - k_v) - U_A - (P_{PE-A})_y + (P_{AE-A})_y$$

With $W = 1,725 \cdot b_a$, $k_v = 0.1$, $U_A = 62.4$ pcf $\cdot 1.5' \cdot b_a = 93.6 \cdot b_a$, $(P_{PE-A})_y = 7,291$ lb per ft of wall and $(P_{AE-A})_y = 849$ lb per ft of wall, the modified equation of vertical equilibrium results in a minimum value of b_a equal to 4.4 ft or $(b_a)_{\min} \approx 4.5$ ft.

iii. Other types of anchorages to be considered include slender anchorage, multiple tie rods and anchorage, A-frame anchors, sheet pile anchorage, soil or rock anchors and tension H-piles. Slender anchorage refers to a slender wall designed using the procedure described in this section with δ set equal to 0 degrees.

13. Site Anchorage (Step 13)

a. The anchor wall is to be located a sufficient distance behind the sheet pile wall so that the dynamic active failure surface does not intersect the passive failure developing in front of the anchor wall. Figure 12-18 outlines the minimum required distances for this design problem.

b. Dynamic Active Wedge - Sheet Pile Wall. With $\phi' = 35^\circ$, $\delta = 17.5^\circ$ and $\Psi_{e1} = 18.44^\circ$. $\alpha_{AE} = 40.695^\circ$ and

What Is Unique About This Picture?

Is it the one piece patented eccentric/gears? No, we put that to work in 1990.

Is it helical gears and spherical bearings for driving at any angle? No, that idea has always been a reality at APE.

Is it the rifle drilled top plate mounted directly to the motors to eliminate all those unwanted hoses? No, our very first machine had this feature.

How about the clamp cylinders machined from a solid block of steel to eliminate tie rods and bolt on guards? No, APE put that idea to work in 1991.

Is it the lifting bail, mounted 90 degrees from the length of the vibro to prevent cable damage during hoisting? No, that idea was incorporated years ago.

Is it the caisson clamps with built in guides? No, APE always had that too.

Could it be the anti-wear hydraulic hoses? No, the mining companies invented it and we put it to work in our industry in 1994.

The fact it runs on vegetable oil? No, we have been running on vegetable oil for over 13 years.

Is it the recessed hydraulic motors tucked in out of harm's way? No!

Is it the JIC fittings throughout? No, we put that idea to work long ago.

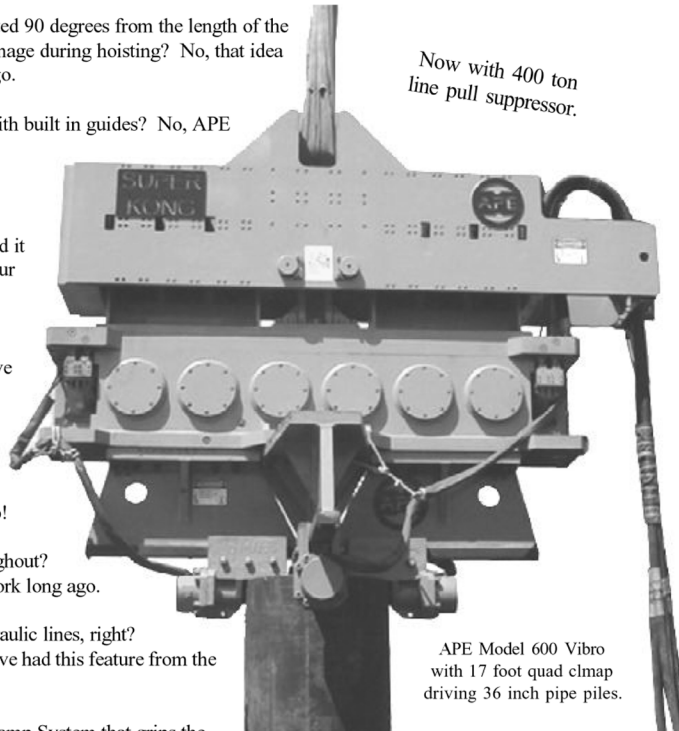
I know! The pig tail hydraulic lines, right? No, All APE machines have had this feature from the very beginning.

Is it the patented Quad Clamp System that grips the pile with four clamps 90 degrees apart for balanced energy transfer? No, but you're getting close.

Take a closer look. Notice that our 17 foot quad clamp system is driving 36 inch diameter pipe.

Today's technology requires larger caissons. We are driving and extracting piles and caissons in excess of 40 feet in diameter. However, what good is a clamping device if it can only be used on super large piles?

No other four clamp system can squeeze down to a 36 inch diameter pile. That feature is handy when you're responsible for building the new San Francisco Oakland Bay Bridge. Good ideas help make profits for you.



*Now with 400 ton
line pull suppressor.*

APE Model 600 Vibro
with 17 foot quad clamp
driving 36 inch pipe piles.

APE. We Put Good Ideas To Work

When a pile driver talks... we listen™. Please call or write:



APE Corporate Offices
7032 South 196th
Kent, Washington 98032
800-248-8498 or
253-872-0141
Fax: 253-872-8710

APE CANADA
1965 Ramey Road
Port Colburn, ON
LZG 7M6
905-328-0850
Fax: 905-834-8486

APE Mid-Atlantic Regional Ofc.
500 Newton Rd. Suite 200
Virginia Beach, VA 23462
866-399-7500
Fax: 757-518-9741
Cell: 757-373-9328

APE Northeast Regional Ofc.
Route 15 North & Taylor Rd.
Wharton, NJ 07885
973-989-1909
Fax: 973-989-1923
888-217-7524

APE Southeast Regional Ofc.
1023 Snively Avenue
Winter Haven, FL 33880
863-324-0378
Fax: 863-318-9409

APE S. Central Regional Ofc.
11128 FM Hwy. 1488
Conroe, TX 77384
936-271-1044
Fax: 936-271-1046
800-596-2877

APE Western Regional Office
160 River Road
Rio Vista, CA 94571
707-374-3266
Fax: 707-374-3270
888-245-4401

Alessi Equipment, Inc.
35 Rosslyn Place
Mt. Vernon, NY 10550
914-699-6300
Fax: 914-699-5300

Imeco-Austria
431-368-2513
Fax: 431-369-8104

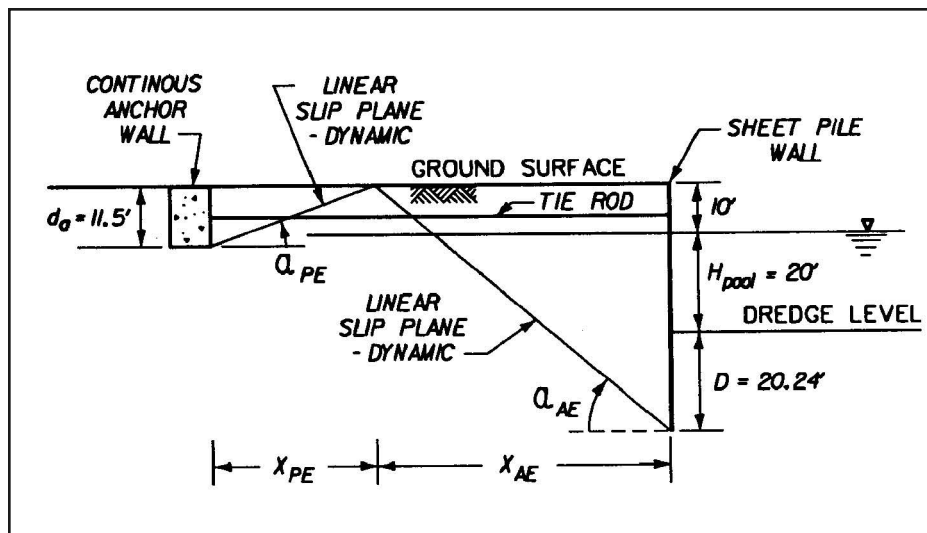


Figure 12-18: Simplified procedure for siting a continuous anchor wall

Equation 12-63:

$$x_{AE} = \frac{50.24'}{\tan \alpha_{AE}} = 58'$$

Equation 12-64:

$$x_{PE} = \frac{11.5'}{\tan \alpha_{PE}} = 35'$$

c. Dynamic Passive Wedge - Anchor Wall. With $\phi'_t = 30.3^\circ$, $\delta_t = 14.7^\circ$ and $\Psi_{e1} = 12.529^\circ$, $\alpha_{PE} = 18.27^\circ$ and

d. Site Anchorage. Site concrete anchor wall at a distance of 93 ft behind the sheet pile wall ($= x_{AE} + x_{PE}$).

Chapter Thirteen: Sheet Piling Cofferdams

13.1. General

A cofferdam is a retaining structure, usually temporary, which is utilized to keep water or earth out of an excavation site until the permanent works are constructed. Such structures usually consist of vertical sheet piling walls forming a closed perimeter and braced internally or externally by a system of structural members or ties.

The bracing system consists of horizontal members called wales, which transfer loads from the sheet piling to compression members called struts, or to external supports called tie backs or anchors.

The safe design of these temporary structures is important, since the safety of workmen or the protection of other structures is almost always involved. The participation of wales and struts in the overall stability of cofferdams must be evaluated much more closely than the support system of an anchored bulkhead. The sequence of construction regarding the excavation of soil or the pumping out of water from a cofferdam will affect the loads on all elements of the system. Maximum loading conditions may occur during the construction phase, or during the placement of permanent work due to removal or relocation of bracing, rather than after the cofferdam is completed. In addition, pressures outside the wall may contribute to instability of the floor of the cofferdams that must be evaluated and accounted for in design planning.

Types of sheet pile cofferdams include the following:

- **Water Cofferdams.** Sheet piling “box” cofferdams are virtually the only means for constructing permanent piers for bridges or other structures in water under dry conditions. Loads on these walls consist of unbalanced pressure from water and submerged earth.
- **Land Sited Cofferdams and Trench Retainment Systems.** Sheet pile cofferdams are constructed on land for any underground construction where workmen and adjacent structures must be protected against collapse of the excavation walls. If the area to be excavated is relatively small in area or the wall-to-wall distance is reasonable, internal cross bracing consisting of wales and struts is practical. If the area is large and the walls well apart, internal braces such as sloping raker struts, or external anchors behind the wall must be used. The values of earth pressure and its probable distribution against rigidly braced walls have been found to be at some variance with the pattern obtained by anchored, yielding walls.

13.2. Geotechnical Design of Sheet Pile Cofferdams

13.2.1. Lateral Pressure Distribution

At the time the first row of struts is placed the excavation is not deep enough to have appreciably altered the original

state of stress in the soil. The lateral pressure at the level of the first row of struts is, therefore, higher than the active pressure since no significant yielding of the soil mass has occurred. As the excavation continues to the level of the second set of struts, the rigidity of the first set prevents horizontal yielding of the soil near the surface. However, the external lateral pressure tends to rotate the sheeting about the upper support level so that a certain inward displacement of the sheeting will occur at the level of the second set of struts by the time these struts are in place. As the excavation continues, greater deflections occur at the lower struts mobilizing soil strength and producing an arching effect that reduces lateral pressures. At the completion of the excavation, the sheeting will have deformed to a position indicated by line *ab1* in *Figure 13-1*. Thus, the resulting lateral pressure diagram will have the maximum values occurring in the upper portion of the wall.

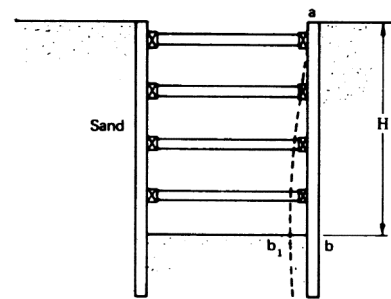


Figure 13-1: Deformation of Sheet Piling in Braced Cofferdams

In general, the deformation pattern resembles the arching, active condition and distribution of pressure is more likely to be parabolic rather than the triangular shape associated with the Rankine and Coulomb theories.

13.2.2. Pressure Distributions in Braced Cuts

The pressure distributions for braced cuts are different for sands and clays. *Figure 13-2* shows these distributions. These pressure distributions are based on the following assumptions:

- Apply to excavations greater than 20' deep.
- An artificial loading diagram is used for determining strut loads.
- Water table is below the bottom of the excavation. If it is not, the distributions must be modified as discussed below.

It should be noted that there are other possible distributions of pressure; however, this manual will use these in the sample problems. The basic solution methodology should be the same even with different distributions. These distributions are explained in more detail in the following sections.

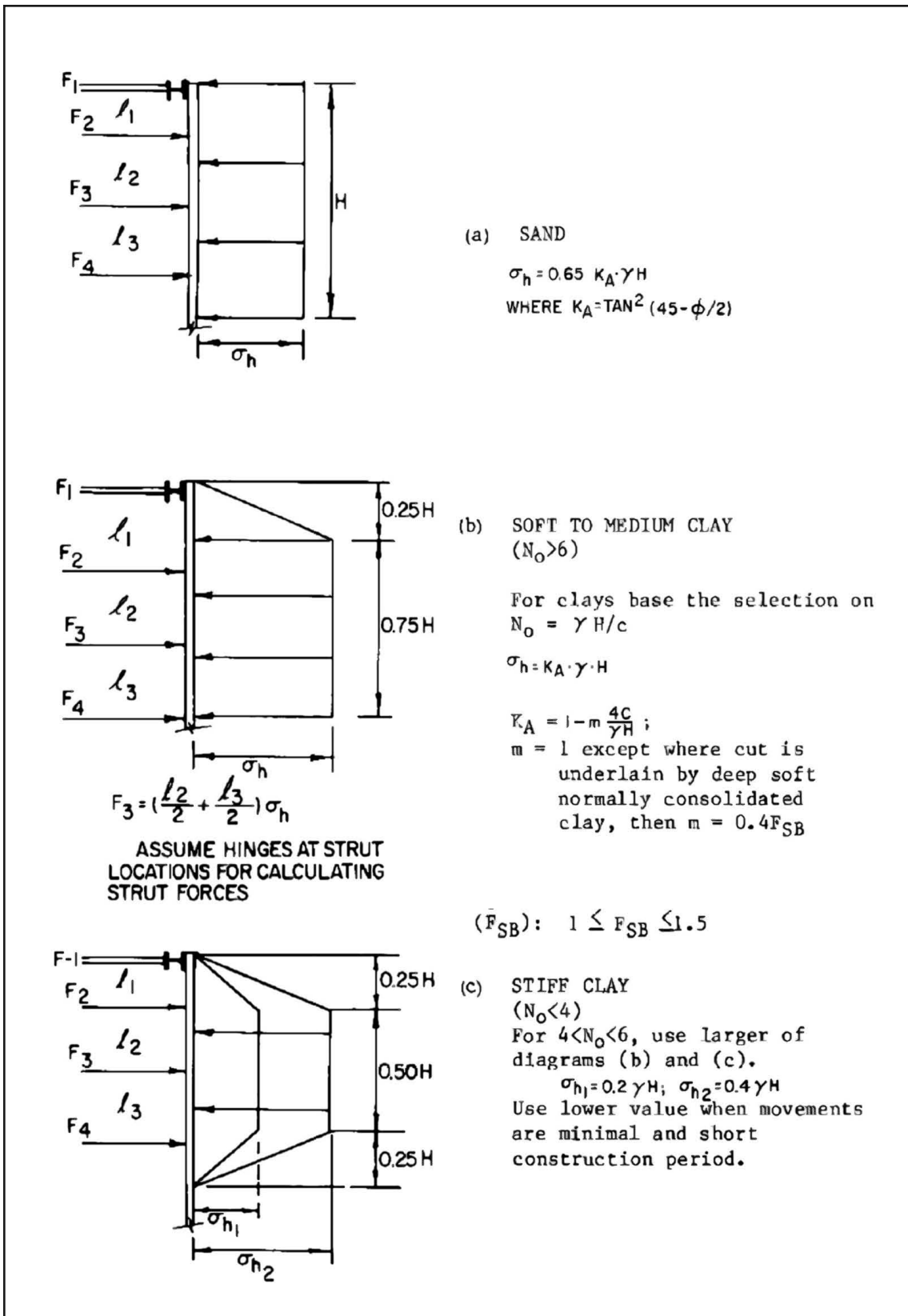


Figure 13-2: Pressure Distributions for Brace Loads in Internally Braced Cuts

vulcanhammer.net

Your complete
online resource for
information on
geotechnical
engineering and
deep foundations

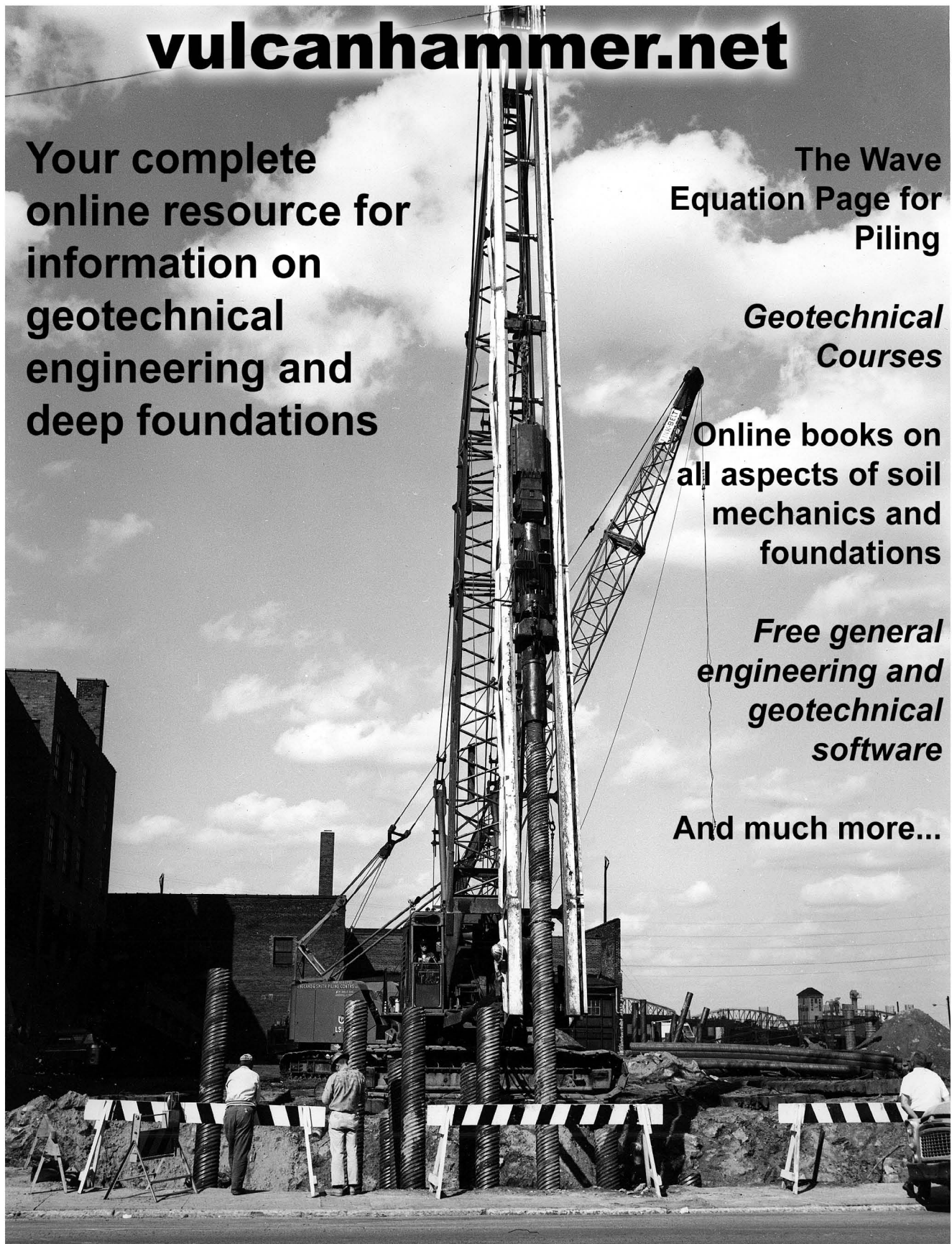
The Wave
Equation Page for
Piling

*Geotechnical
Courses*

Online books on
all aspects of soil
mechanics and
foundations

*Free general
engineering and
geotechnical
software*

And much more...



<http://www.vulcanhammer.net>

<http://www.vulcanhammer.org>
email me@vulcanhammer.net

<http://www.chet-aero.com>

13.2.2.1. Braced Cuts in Sand

For braced cuts in dry or moist sand, a rectangular pressure distribution as proposed by Peck et al.¹⁴² and others may be considered. This distribution pattern is shown in *Figure 13-2 (a)*, along with the value of p_b .

If groundwater is present, and the pilings are tight and extend to an impermeable stratum, hydrostatic conditions will develop behind the wall. For water table at the backfill surface, use the submerged (buoyant) unit weight of soil in the equation of *Figure 13-2 (a)* and add the pressures from the unbalanced groundwater level. For a water table intermediate between the top and bottom of the cut, interpolate between the diagrams using the appropriate unit weight for the soil.

If seepage takes place behind the wall, the effective weight of the soil will be greater than the buoyant weight and may be conservatively assumed as the moist condition value. Water pressures along the back of the wall and in the backfill under seepage conditions can be reasonably estimated by flow net analysis.

13.2.2.2. Braced Cuts in Clay

For braced cuts in clay, Peck and others have suggested trapezoidal pressure distribution patterns. The use of these diagrams implies the designer has a good understanding of soil mechanics and is able to distinguish between the clays by sensitivity, cohesion values etc. The pressure distribution depends upon the stability number of the clay, which is given by Equation 4-26. Soft to medium clays ($N_o > 6$) have a pressure distribution as shown in *Figure 13-2 (b)* and stiffer clays ($N_o < 4$) as shown in *Figure 13-2 (c)*.

The value of 'm' used in the determination of the ordinate for earth pressure applies to situations where the cut is underlain by a deep deposit of soft clay. Its value can only be determined by empirical means from measurements and performance of an actual excavation. Experience thus far, reported by Peck from cases in Mexico City and in Oslo, Norway, leads to the conclusion that the value of 'm' is on the order of 0.4 for sensitive clays. For insensitive clays the value of 'm' may be taken as 1.0.

Water pressure is not added to the soil pressure since it is already included in the undrained strength considerations. *Figure 13-2 (b)* and *Figure 13-2 (c)* give maximum pressure values, which result in conservative designs for some struts. However, with the passage of time, creep effects cause the lateral earth pressure to increase appreciably. This phenomenon was studied in model tests by Kirkman,¹⁴³ from which it was concluded that the design of more permanent cofferdams in clay should be based on earth pressures calculated according to the classical theories (Rankine, Coulomb or Log spiral) using a cohesion value of zero and a ϕ angle as determined by drained triaxial tests.

13.2.2.3. Mixed Soils

For a single layer of sand overlying a single layer of clay, Peck³¹ suggested substituting \bar{q} and $\bar{\gamma}$ for $2c$ and g in the equations for clay. These values are determined as follows:

$$\text{Equation 13-1: } \bar{q} = \frac{\gamma_s K_s H_s^2 \tan \phi + (H - H_s) n q_u}{H}$$

$$\bar{\gamma} = \frac{\gamma_s H_s + (H - H_s) \gamma_c}{H}$$

Where

- γ_s = saturated unit weight of sand
- K_s = hydrostatic pressure ratio for the sand layer (may be taken as 1.0 for design purposes)
- H_s = thickness of the sand layer
- ϕ = angle of internal friction of the sand
- H = total depth of excavation
- q_u = unconfined compressive strength of the clay
- γ_c = saturated unit weight of the clay
- n = coefficient of progressive failure. The value of n usually ranges from 0.5 to 1.0. This value varies with the creep characteristics of the clay, the length of time during which the excavation remains open, and the care exercised in construction. In Chicago clay, the value ranges between 0.75 and 1.0.

It should be recognized that Equation 13-1 and the diagrams in *Figure 13-2 (b)* and *Figure 13-2 (c)* are based on studies of 20- to 40-foot deep excavations above the water table with strut spacings of 6 to 20 feet. Before application to other conditions, including other depths or strut spacings and hydrostatic or seepage conditions special study may be required.

Surcharge loads from point, line or strip loads adjacent to the cofferdam must also be taken into account in final design.

13.2.2.4. Surcharge Loads Against Braced Cuts

A procedure for handling surcharge loads similar to that for bulkheads can be applied to braced cuts. A uniform surcharge load of at least 300 psf is generally assumed to account for materials storage and light equipment near the wall. When converted to an equivalent height of soil, the pressure envelope is rectangular with an intensity of K_a .

Surcharge from point and line loads near the wall are quite intensive in the upper half of the excavation, putting more stress into the upper bracing sets than the lower. Equations based on Bousinesq's work are an acceptable way of estimating these loads.

13.2.3. Base Stability

The stability of the base of cuts must be checked. Unstable situations will require supplemental procedures beyond the simple shoring of the excavation walls. These procedures may

¹⁴²Peck, R.B., Hanson, W.E., and Thornburn, T.H. (1974) *Foundation Engineering*. New York: John Wiley and Sons.

¹⁴³Kirkman, R. (1958) Discussion. *Proceedings, Brussels Conference 58 on Earth Pressure Problems*.

include additional penetration of the sheeting, well pointing, deep wells etc, and could affect the sizing of the sheeting and location of bottom supports.

13.2.3.1. Granular Soils

In the absence of seepage forces, the base stability of a braced cut in granular soil can be checked as follows:

Equation 13-2:
$$FS = 2N_{\gamma_2} \frac{\bar{\gamma}_2}{\bar{\gamma}_1} K_a \tan \phi$$

where

- FS = Factor of safety
- N_{γ_2} = bearing capacity factor for soil below excavation level, determined from Table 15-2.
- γ_2 = average effective unit weight for soil within a depth below excavation level equal to excavation width.
- γ_1 = average effective unit weight for soil above excavation level.
- $K_a = \tan^2 (45-\phi/2)$

Equation 13-2 applies when the sheeting extends only to the base of the excavation. The factor of safety can be increased if the sheeting extends deeper and is adequately designed. In this case, the soil inside the excavation above the base of the piling acts as a surcharge. Where an unbalanced water head exists across the sheeting the value of γ_2 must be determined by subtracting the upward seepage force from the weight of the soil.

13.2.3.2. Cohesive Soils

Because of the load decrease from excavation, soils in the passive zone just below the excavation will experience changes in pore water pressure accompanied by swelling of the soil. This could result in heave at the bottom of the excavation and settlement of the surrounding ground surface. When the base width is large compared to the depth of excavation, the following method of analysis developed by Terzaghi has been recommended. (See Figure 13-3).

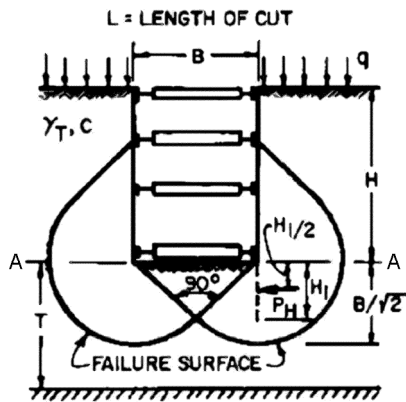


Figure 13-3: Diagram Illustrating Assumed Mechanism for Failure by Heave of the Bottom of a Wide Excavation

In this case, the vertical column of soil along the sheeting is assumed to exert a pressure on the horizontal plane A-A. When the pressure exerted by this soil column exceeds the bearing capacity of the soil beneath the sheeting a bearing type failure will occur, resulting in heave of the bottom of the excavation and settlement of the surround ground surface. Based on this failure model, the factor safety against heave can be expressed by:

Equation 13-3:
$$FS = \frac{N_c c}{\gamma H - \frac{\sqrt{2}cH}{B}}$$

where

- N_c = bearing capacity factor (see Table 15-2).
- H = height of excavation
- B = width of excavation
- γ = unit weight of soil
- c = unit cohesion of soil

Use undrained strength of soil at natural water content as determined from an unconfined compression test.

The factor of safety should be at least 1.5 or the piling should extend an additional distance below excavation. Ideally this should extend at least $\sqrt{2}B/2$, but this is usually not absolutely necessary. In this case, the force acting on the length of the sheet below the bottom of the excavation can be computed as

Equation 13-4:

$$P_H = \frac{\sqrt{2}}{2} (\gamma HB - \sqrt{2}cH - \pi cB), H_1 > \sqrt{2} \frac{B}{3}$$

$$P_H = \frac{3}{2} H_1 \left(\gamma H - \sqrt{2} \frac{cH}{B} - \pi c \right), H_1 < \sqrt{2} \frac{B}{3}$$

This force acts halfway between the excavation depth and the toe of the pile, i.e., $H_1/2$ below the excavation depth.

The foregoing applies to a general case behind a continuous wall. In cases where the cofferdam is square, rectangular or circular in geometry and the depth of excavation exceeds the width, the proximity of the four walls aids in overall resistance to heave. In such cases, a method of analysis developed by Bjerrum and Eide can be used. Their method visualizes the cofferdam as a deep “negative footing.” That is, the excavation produces shear stress in the soil similar, but of opposite direction, to those caused by a deep foundation. Using this analogy the factor safety against heaving may be expressed by:

Equation 13-5:
$$FS = \frac{N_c}{N_o} - \frac{q}{\gamma H}$$

where

- c = unit cohesion of soil
- N_c = bearing capacity factor - to be determined according to chart presented in Figure 13-4.
- γ = average unit weight of soil within depth of excavation

- q = surface surcharge loading
- H = height of excavation

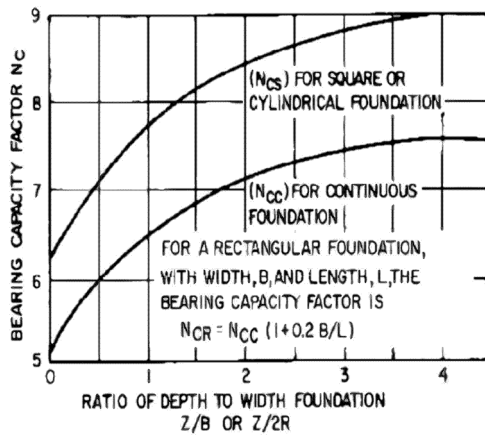


Figure 13-4: Diagram for the Determination of Bearing Pressure Coefficient N_c

Equation 13-3 and Equation 13-5 apply when the sheeting extends only to the base of the excavation. To increase the factor of safety to the desired level, the sheeting can be extended below the excavation line. In this case, the soil inside the excavation above the base of the piling acts as a surcharge and develops adhesion along the adjoining sheet piles. The depth can be computed by the equation

$$\text{Equation 13-6: } d = \frac{B}{2} \left(FS N_o + \frac{q}{c} - N_c \right)$$

Where d = depth of piling below dredge level. As stated before, the design factor of safety is usually at least 1.5.

13.2.3.3. Piping

For excavations in pervious materials, the possibility of piping or “sand boiling” must be investigated. Piping occurs when an unbalanced hydrostatic head causes large upward seepage pressures in the soil at the bottom of the excavation. This is discussed in detail in 7.4.

13.2.4. Water Cofferdams

The top elevation of the cofferdam should be based on the design high water condition. The toe of the sheets should be founded in an impervious layer or penetrate deeply enough to prevent heave, piping or boiling inside after dewatering. When the outside head is substantial, it may be necessary to pour a heavy concrete seal placed by the tremie method.

Loads from water pressure are readily evaluated, as shown in Figure 13-5. However, the process of drawdown inside the cofferdam and installation of the wales must be carefully planned so that neither the sheets nor the wales are seriously overstressed.

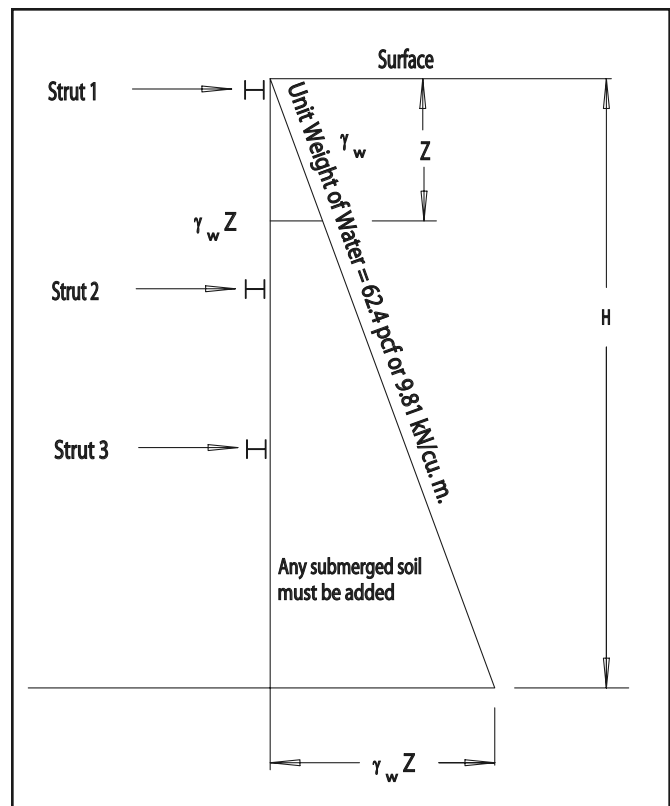


Figure 13-5: Pressure from Water Distribution

The pressure distributions from unbalanced water levels inside and outside the cofferdam are triangular. Usually, unbalanced submerged soil pressure would also be distributed triangularly; however, it has been found that the pressure diagram against rigidly braced sheeting takes a more rectangular form.

In the case of deep cofferdams, bracing frames should be in position prior to starting drawdown. Frames can be fabricated and hung from vertical spud piles, to be used as a guide template for spinning sheets and lowered into position when the box is closed.

Locating the first wale near the top of the cofferdam will provide a platform for workmen. Spacing to the next tier will be based either on the limiting strength of the sheeting for that span, or the designers decision to limit the size of wales by using more struts.

Other factors to be considered in design:

- Scour along the base that may change load or support conditions.
 - Wave action that may impact the wall but also increase the unbalanced head and total load.
 - Temperature that may increase stresses in upper bracing.
- Details of wale splices, stiffening at struts, corner connections are important to the stability of the frame and should follow good practice.

American Construction Material Exchange, Inc.

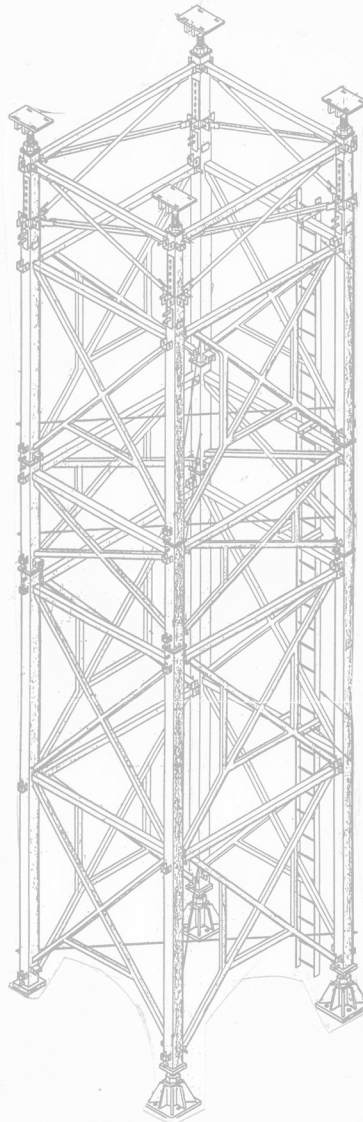
USED PIPE

10-3/4" O.D. X .250
 12.75" O.D. X .312
 14" O.D. X .500
 18" O.D. X .375
 18" O.D. X .500
 22.75 O.D. X .375
 24" O.D. X .375
 24" O.D. X .500
 36" O.D. X .750 NEW
 42" O.D. X 1.000 NEW

USED/SURPLUS STEEL BEAMS

W40x149#
 W36x300#, W36x260#, W36x245#
 W36x230#, W36x210#, W36x194#
 W36x182#, W36x170#, W36x160#
 W36x150#, W36x135#
 W33x291#, W33x241#, W33x221#
 W33x201#
 W30x211#, W30x191#, W30x173#, 116#
 W27x94#, W27x84#
 W24x146#, W24x131#, W24x117#
 W24x104#, W24x94#
 W21x122#, W21x111#, W21x101#
 W18x119#, W18x97#, W18x96#
 W18x86#, W18x76#, W18x55#
 W16x100#, W16x89#, W16x57#
 W14x159#, W14x145#, W14x132#, W14x120#
 W14x109#, W14x99#, W14x90#, W14x82#
 W14x74#, W14x68#, W14x61#
 W12x120#, W12x79#, W12x72#, W12x65#
 W12x53#, W12x45#, W12x35#, W12x26#
 W10x112#, W10x100#, W10x68#, W10x49#,
 W8x48#, W8x40#

MOST STOCK LOCATED ON THE WEST COAST



WANTED:

We are looking for:
**Used Flat Sheet Piles
 & AZ18 Sheets**

USED MISC. AVAILABLE

HP12x53#, HP12x74#,
 HP12x84#, HP14x89#
 HP14x102#, HP14x117#
 STEEL PLATES
 CHANNELS - 8", 12" & 15"
 18" DOUBLE CHANNELS
 CREOSOTE TIMBERS
 180 Pcs. 14"x14'x23'-28'
 120 Pcs. 8"x24'x30'

SHORE TOWER SYSTEM

100 KIP PER LEG
 LARGE QUANTITY AVAILABLE
 WILL RENT OR SELL

NEW, PRIME W/MTR'S

W14 x 90, W14 x 109
 W14 x 120
 HP14x89#

E-Mail Address: rogerkadel@comcast.net

"ACME" P.O. Box 2600 TUALATIN, OR. 97062

PHONE: (503) 590-5100 FAX: (503) 590-5200 MOBILE: (503) 705-1190

13.3. Structural Design of Cofferdam Components

Wales and struts are the key elements in any system of braced retaining structures. This is true whether the cofferdams be in water, soil or both. Their spacing within the cofferdam is not only governed by the requirements of the permanent construction but also by the wall movement that can be tolerated by facilities outside the cofferdam. The advantage of closely positioned tiers of bracing is to prevent excessive movement behind the wall that might affect utilities, pavement or structures. Additional bracing sets provide more redundancy to the overall system, but may be economical in that it slows construction activity. Obviously both safety and practicality must be addressed in arriving at a design.

Many of the calculations necessary for the design of sheet pile cofferdams can be done with standard structural analysis programs. These, along with the hand calculations, will be illustrated in the example problems in this chapter.

13.3.1. Beam Loads on Wales and Spans

Braced cofferdams are generally three-dimensional structures with both sides and ends; therefore, their loading is more complicated than with anchored sheet pile walls. With beam loading, which takes place from lateral pressure from soil, groundwater, and surcharge loading against the sheet piling membrane, many of the principles are the same, but their implementation has key differences.

As with anchored walls, the horizontal wales are assumed to be uniformly loaded beams over multiple supports. Between each support, the beam stresses on the topmost wale are approximated by the equation

Equation 13-7: $M = \frac{wl^2}{8}$ (Wale at top)

and the wales below that by the equation

Equation 13-8: $M = \frac{wl^2}{10}$ (All other wales)

Where

- M = moment in wale
- w = anchor load in force per unit length of wall. General practice for moment calculation is to reduce the load due to soil pressure only by 20% to account for arching.
- l = distance between struts

The vertical sheeting spans are also continuously (but not necessarily uniformly) loaded beams over multiple supports. This results in a statically indeterminate structure. Three methods can be employed to analyse multiply supported walls:

❖ Area distribution.¹⁴⁴ This involves dividing up the sheet into areas, generally demarcated by the midpoints between the supports. This concept is illustrated in Figure 13-6. The

load in these areas is then concentrated on the respective supports. This method is best used with conventional, multiply supported anchored sheet pile walls with standard Rankine, Coulomb or log-spiral earth pressure theories. It can also be used with water cofferdams. It is the simplest method to use but can create inconsistencies in the computation of the moments.

- ❖ Hinge method. This method reduces the system to a statically determinate system by placing hinges at all of the supports except for the top one. Although a little more difficult to implement, this method does result in more consistent calculation results, especially when Equation 13-13 is used. Strictly speaking, this is the only method that can be used with the Peck earth pressure charts for braced cofferdams as shown in Figure 13-2.
- ❖ Use of a structural analysis program, which can properly handle a statically indeterminate structure. The maximum moment in the sheet piling will depend on the arrangement of struts and wales. A cantilever may exist

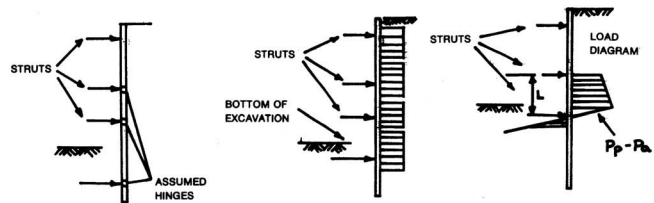


Figure 13-6: Assumptions Used in the Hinge Method

at the top or bottom of the excavation, and simply supported or continuous spans elsewhere. For a uniformly loaded cantilever,

Equation 13-9: $M_{max} = \frac{w(\Delta H)^2}{2}$

where

- w = uniform load
- (ΔH) = Length of cantilever

For simply supported uniformly loaded spans, such are assumed with the hinge method,

Equation 13-10: $M_{max} = \frac{w(\Delta H)^2}{8}$

where (ΔH) = distance between support points (may be governed by construction procedure)

For continuous spans, as appear with the area distribution method,

Equation 13-11: $M_{max} = \frac{w(\Delta H)^2}{10}$

¹⁴⁴Armento, WJ. (1977) "Criteria for Lateral Pressures for Braced Cuts." *Proceedings of the ASCE Specialty Conference on Performance on Earth and Earth Supported Structures*, Vol. 1, Part 2, pp. 1283- 1302.

For flexible walls ($EI/L^4 < 50$ ksf/ft), deflections may be accompanied by soil arching resulting in a reduction of soil pressure near the centre of spans and a concentration at the supports. Hence, the actual bending moments in sheeting and wales may be less than that which would be computed assuming a uniform loading on these members. Based on experience, Armento and Goldberg, et al., recommend using 80 percent of the loading diagram loads in computing moments in sheeting and wales supported by three or more struts. For raker bracing and tiebacks, and for rigid walls ($EI/L^4 > 50$ ksf/ft), the full pressure diagram should be used. For water, full pressure loadings should be used of course.

One other factor that needs to be considered in the design of braced cofferdams is that of penetration of the wall below the bottom of the excavation. Although stopping the sheet piling wall at the excavation bottom is the simplest solution, it has two important shortcomings:

- It may be necessary to extend the sheeting in order to improve base stability; this is discussed elsewhere.
- A “no-toe” design tends to both load the bottom struts and wales and the lower parts of the sheeting to a higher degree than if a toe were present, which would necessitate a more substantial (and thus more expensive) sheet pile profile, along with stronger wales and struts.

Both of these factors must be taken into consideration in determining if—and how much—the sheet pile should penetrate below the excavation line. If the sheet does extend below the excavation line, assuming active pressure behind the part of the wall below the dredge line and passive pressure in front, the maximum moment developed due to base heave loading and/or lateral pressure not assigned to the struts can be computed.

13.3.2. Column Loading of Struts and Wales

Struts are spaced to limit moments in wales and to accommodate excavation and construction inside the walls. No reduction in earth pressure is taken for strut design. AISC or similar specifications are used for reference in designing struts and also wales. Some deep cut and cover excavation specifications have limited $//R$ ratios of 120. Since the struts are the primary support units, general practice has been to be very conservative in sizing these units. Strut loads should be estimated based on simply supported spans rather than continuous.

Struts and corner braces are designed as columns. Wales are also subjected to thrust from loads transferred to the ends by wales on the intersecting wall. This should not be ignored in design. Large bracing frames should be stabilized with posts and cross bracing as appropriate to the conditions.

Figure 13-7 illustrates a typical arrangement of struts and wales in a braced excavation. The struts are designed as compression members, with buckling being the primary consideration. The spacing between struts in both directions must be designed in such a manner that the axial loads and the $//R$

ratios are kept within acceptable limits. Frequent cross strutting is recommended from the design standpoint as it reduces the $//R$ ratios. However, from the construction standpoint, the spacing between struts may be dictated by the required accessibility to the bottom of the excavation. Eight-foot strut spacing is usually considered the minimum acceptable for construction.

Some rebracing or additional sets of bracing should generally be anticipated during construction to meet special conditions. American Institute of Steel Construction specifications are generally used as a reference for designing these frames.

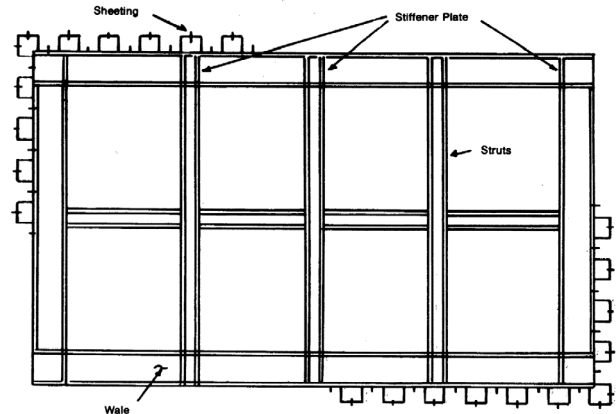


Figure 13-7: Typical Strut Arrangement for a Braced Excavation

Since braced cofferdams are structures with two dimensions in plan as well as elevation, the wales also experience compressive loads from the “ends” as do the struts. These must be analysed together with the beam loading.

13.3.3. Circular Bracing

A ring wale bracing system has been developed for a circular excavation. This design is based upon experience for circular tunnelling using the equation

$$\text{Equation 13-12: } f_s = \frac{T}{A} + \frac{M}{S}$$

Where

- f_s = stress in the ring wale
- T = radius of excavation times the total load per unit length between the ring wales
- A_s = area of steel cross-section
- M = approximate moment at blocking point based upon experience in tunnelling = $0.86Tb$
- B = rise of arc at blocking point = $R - \sqrt{R^2 - \left(\frac{C}{2}\right)^2}$
- R = radius of neutral axis of rib
- C = chord length between neutral axis blocking point
- S = section modulus

To ease construction, a six-inch gap is left between the ring wale and the sheet piling. The gap is then “taken up” at the projection of each sheet pile (blocking point) using two

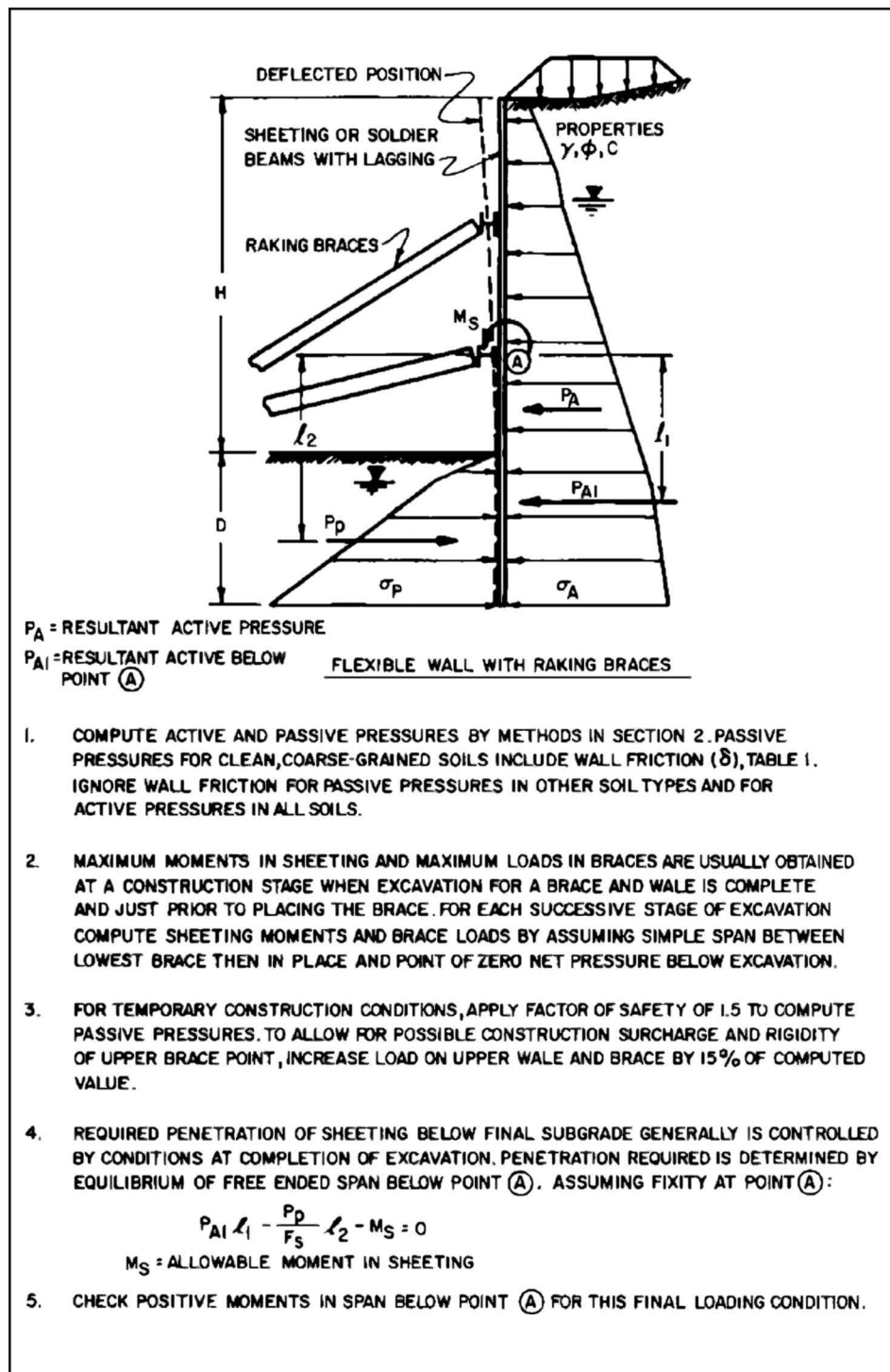


Figure 13-9: Diagram Illustrating the Use of Raking Braces in Construction of a Deep Cut

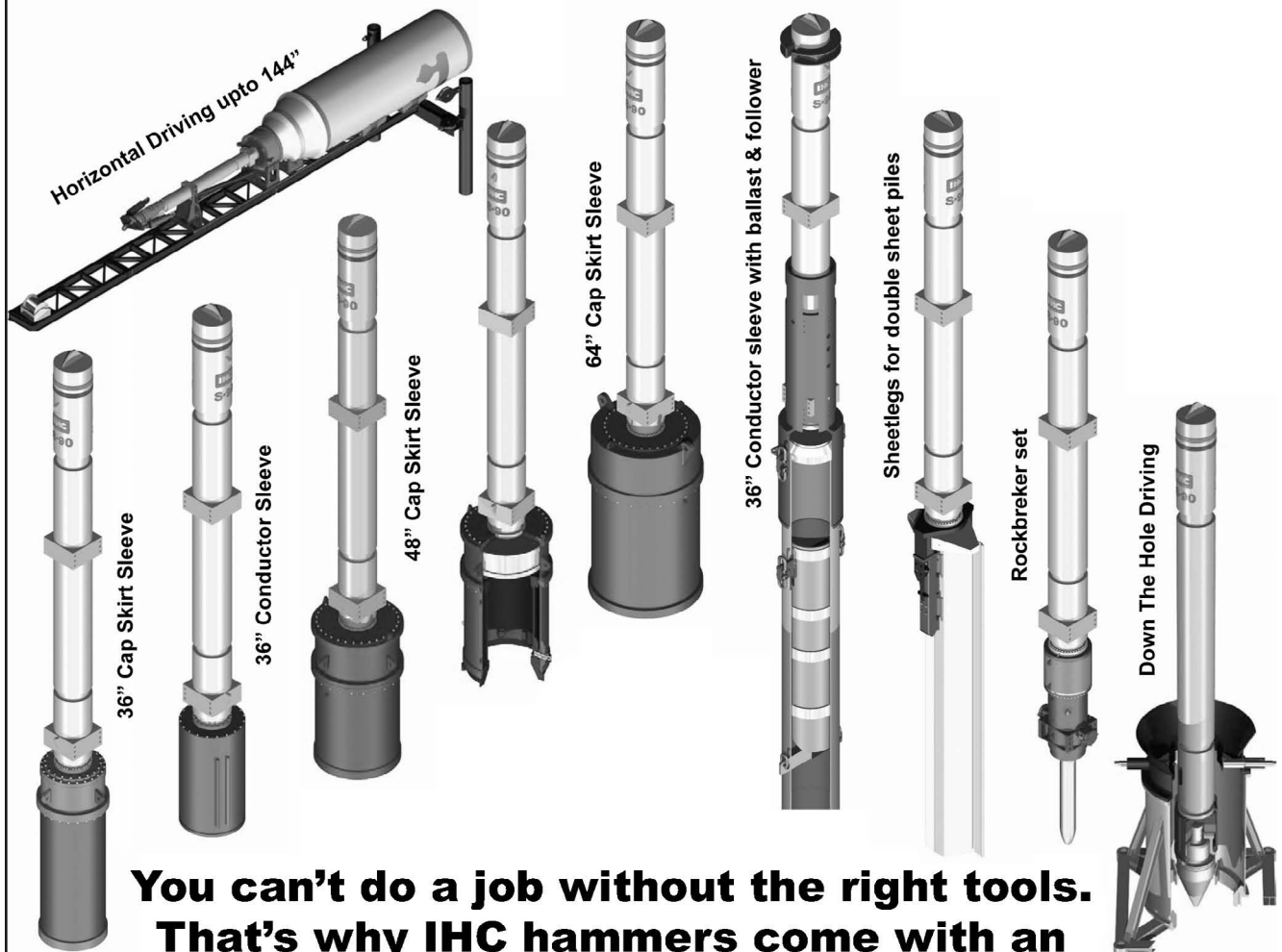
wooden wedges, one driven from above and one from below the ring wale, as shown in Figure 13-8. The ring wales must be checked for buckling¹⁴⁵. Ring wales can also be formed in place, using reinforced concrete formed during various stages of excavation. Design of these is beyond the scope of this manual.

13.3.4. Raking Braces

For large excavations, it is generally not practical to install horizontal braces to extend completely across the excavation. In some instances, the sheeting can be supported by “raking” braces as shown in Figure 13-9.

¹⁴⁵Zagustin, E.A. and Hermann, G. (1967) “Stability of an Elastic Ring in a Rigid Cavity,” *Journal of Applied Mechanics*, April; Hsu, P.T, Elkton, J. and Pian, T.H. (1964) “Note on the Instability of Circular Rings Confined to a Rigid Boundary,” *Journal of Applied Mechanics*, September; Moran, D.F (1966) “Designing Underground Reservoirs,” *Consulting Engineer*, January; Lo, Hsu, Bogandoff, Goldberg and Crawford (1962), “A Bucking Problem of a Circular Ring,” *Proceedings of the Fourth U.S. National Congress of Applied Mechanics*, ASME.

Any Way You Want It



You can't do a job without the right tools. That's why IHC hammers come with an arsenal of accessories for every kind of job. We can only show one size here; we have a wide variety of accessories for every size we make. Call us for details.



**IHC
Hydrohammer®**

PO Box 26
6, Smitweg
2960 AA Kinderdijk, The Netherlands
Phone 011 31 78 6910302
Fax 011 31 78 691 0304
Email sales@ihchh.com
Web site <http://www.ihchh.com>

**North American distributor:
VULCAN FOUNDATION EQUIPMENT**

2501 Riverside Drive
P.O. Box 5413
Chattanooga, TN 37406
Phone (423) 698-1581
Fax (423) 698-1587
Toll Free (800) 742-6637

Email sales@vulcanhammer.com
Web site <http://www.vulcanhammer.com>



Member of the IHC Caland Group

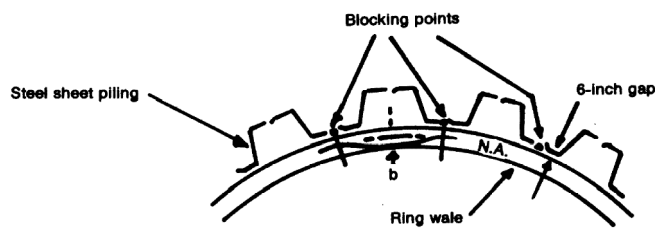


Figure 13-8: Sketch of Circular Ring Wale System

13.4. Examples of Braced Excavations

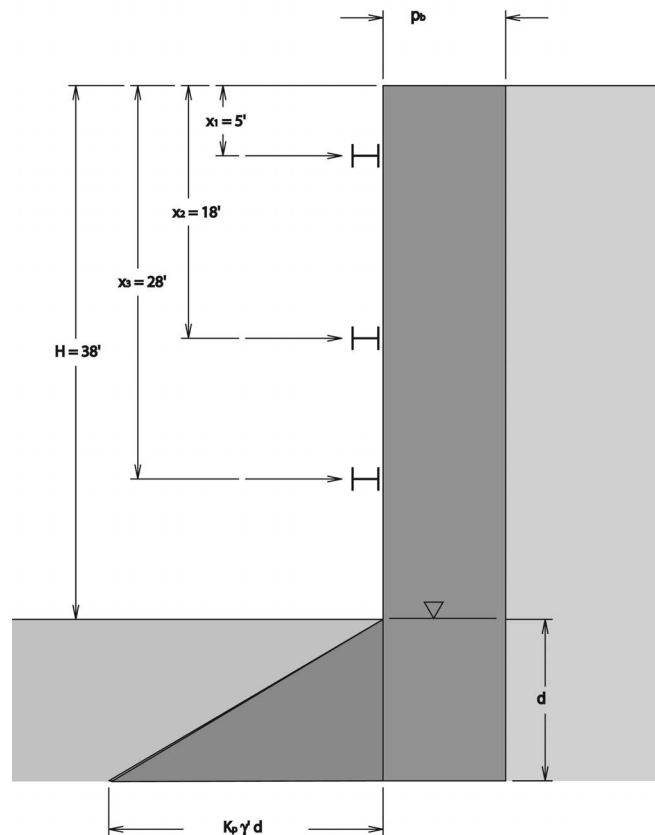
Example 20 Braced Excavation in Granular Soil

❖ Given

➤ Braced excavation as shown in Figure 13-10.

➤ Uniform granular soil

- $\gamma = 115$ pcf
- $\gamma' = 53$ pcf
- $\phi = 32^\circ$
- $\delta = 17^\circ$



- $K_a = \tan^2 (45 - \phi/2) = 0.307$ (Rankine Theory)
- K_p is computed using log-spiral theory (Figure 18-16) and then reduced for the factor of safety by dividing by 2. Thus, $K_p = (0.72)(8)/2 = 2.88$.
- $N\gamma_2 = 27.9$ (see Table 15-2)
- Water table at the bottom of the excavation.
- Struts are spaced 18' apart in plan

❖ Find

- Base Stability of Excavation
- Embedment length
- Required section modulus for sheeting with embedment
- Strut loads
- Design of wales

❖ Solution

➤ Base Stability of Excavation

- An excavation of this kind is considered a “reverse foundation.” The factor of safety for this foundation is computed by Equation 13-2. Substituting the variables, the factor of safety is computed as $FS = (2)(27.9) (53/115)(.307)(\tan 32^\circ) = 4.937 > 1.5$, so this factor of safety is acceptable.
- Since we have base stability with this excavation, it is possible to design the sheeting to extend only to the excavation level. We will consider this later in the example. We will first design the wall with an embedment below the excavation line, which will enable us to reduce the maximum moment in the sheeting and thus use a lighter (if longer) section. In this case, the decision whether to include an embedment is largely an economic one.

➤ Compute the embedment length.

- Compute lateral earth pressures
- For the active pressures, we will assume that the Terzaghi and Peck pressures will extend all along the length of the sheeting. These can be determined using Figure 13-2(a). The active pressure is thus uniform along the length of the sheet, and is computed to be $(0.65)(0.307) (38) = 872.8$ psf.
- For the passive pressure, this increases in the usual way from the excavation line. The passive pressure thus increases linearly from zero at the excavation line to $K_p \gamma' d = (2.88)(53) d = 152.6 d$ at the toe of the sheeting.
- For a multiply supported wall (braced or tied back), to determine the penetration depth of the sheeting, we ignore the wall above the lowest support and sum moments to zero about the lowest support. In this case, the summation of moments is computed by

Equation 13-13:

$$\sum M_{x_3} = 0 = \frac{K_p \gamma' d^2}{2} \left(H - x_3 + \frac{2d}{3} \right) = p_b \frac{(H - x_3 + d)^2}{2}$$

- Substituting the variables into this equation and solving for d yields the equation $76.32 d^2 (10 + 2d/3) = 436.4 (10 + d^2)$. The only positive root for this cubic equation is $d = 12.6'$, which is our embedment depth.
- Determine the maximum bending moment and required section modulus of the sheeting. For this problem, we will use the hinge method of analysis, as we are using the

Peck chart.

- Determination of the support loads.
Support 1: This is the only support that is not hinged. We thus consider a continuous, simply supported beam from the top of the sheeting to Support 2. For a uniformly loaded, simply supported beam with an overhang, the reaction at the support adjacent to the overhang (support 1) is given by the equation¹⁴⁶

$$\text{Equation 13-14: } R_1 = p_b \frac{x_2^2}{2(x_2 - x_1)}$$

Substituting the variables into this equation yields $R_1 = 10,876$ lbs.

Support 2: The reaction at the support is the sum of the reaction generated by the beam above the support with that of the beam below. The reaction from the beam above is given by the equation

$$\text{Equation 13-15: } R_{2a} = p_b \frac{((x_2 - x_1)^2 - x_1^2)}{2(x_2 - x_1)}$$

The reaction from the beam below – which is a simply supported beam with a uniform load – is given by the equation

$$\text{Equation 13-16: } R_{2b} = p_b \frac{x_3 - x_2}{2}$$

Substituting the variables and adding these two partial reactions gives $R_2 = 9,198$ lbs.

Support 3: By symmetry, the reaction at this support from the beam above is the same as the reaction on the other end of the beam, i.e., $R_{3a} = R_{2b}$.

The reaction from the beam below – which includes the embedded section – is given by summing the loads on that portion of the beam, or

$$\text{Equation 13-17: } R_{3b} = p_b(H - x_3 + d) - K_p \gamma' \frac{d^2}{2}$$

Substituting for both partial reactions and summing yields $R_3 = 11,974$ lbs.

- Determine the location of the point of zero shear and maximum moment.

Although there is a point of zero shear between every support, the zero shear point of interest is below Support 3, as we would expect the maximum moment to take place in the vicinity of the excavation level.

The partial reaction R_{3b} is also the shear at Support 3; this computes to 7,611 lbs. The shear then decreases down the beam by the relationship

$$\text{Equation 13-18: } V = R_{3b} - p_b(x_{v0} - x_3)$$

Where x_{v0} is the distance from the top of the wall to the point of zero shear below Support 3. Setting the shear to zero and solving yields $x_{v0} = 36.7'$.

The moment at this point of zero shear is given by the equation

Equation 13-19:

$$M_{\max} = \frac{K_p \gamma' d^2}{2} \left(H - x_{v0} + \frac{2d}{3} \right) - p_b \frac{(H - x_{v0} + d)^2}{2}$$

Substituting yields $M_{\max} = 33,182$ ft-lbs. For a 25 ksi material, the minimum section modulus would thus be $(33.182)(12)/(25) = 15.93$ in³.

- Design using SPW 911

The results using SPW 911 are shown in *Figure 13-11*. We used the passive earth pressure coefficient for analysis. The use of PZ-27 sheeting was arbitrary; as is the case with the direct stiffness methods it is necessary to select a sheeting profile in order to calculate some kind of deflection.

- Design Using Direct Stiffness (Finite Element) Method
We mentioned earlier that the existence of multiple supports makes the system statically indeterminate. The use of a direct stiffness method allows us to take this into consideration without having to make simplifying assumptions. We will now see whether in this case the results are significantly different. As earlier, we will use the CFRAME program.

Keep in mind that, strictly speaking, the Peck charts are only applicable when the hinge method is used. We first consider the “no toe” case, i.e., the sheeting only extends to the bottom of the excavation. We developed a model in CFRAME that is shown in *Figure 13-12*.

The beam is simply supported at all of the supports and continuous. The uniform Peck load is then applied to the sheeting along its entire length with no other loading. The tabulated results are shown in *Table 13-1* and the moment diagram is shown in *Figure 13-13*.

The results show a maximum moment at the lowest support of 523,200 in-lbs = 43,600 ft-lbs. For 25-ksi steel, the minimum section modulus is 20.9 in³ without consideration of a factor of safety.

We now turn to using CFRAME for a configuration with the toe. We will use the toe computed with the hand calculations. We add an element to represent the sheet extension below the excavation line, and include the passive loads there as well. The loading of the model is shown in *Figure 13-14*.

¹⁴⁶All of the beam equations in this example are taken from the *Manual of Steel Construction*, Eighth Edition. Chicago: American Institute of Steel Construction, 1980

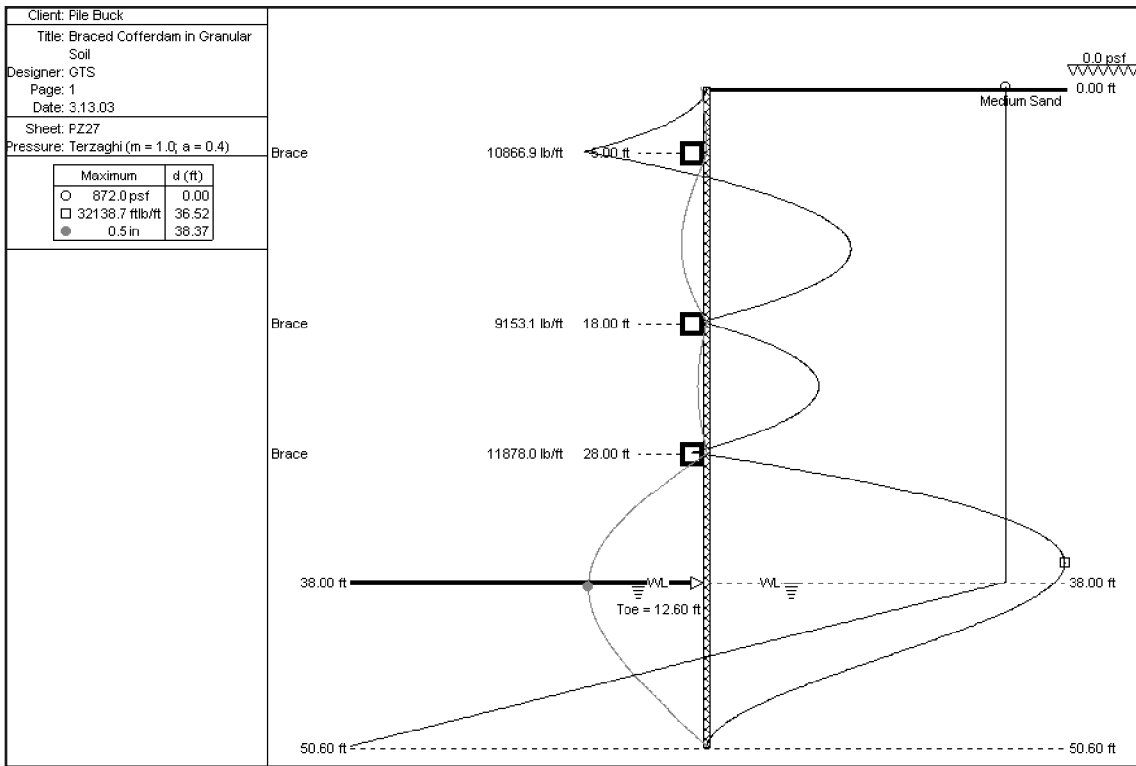


Figure 13-11: SPW 911 Results for Example 20

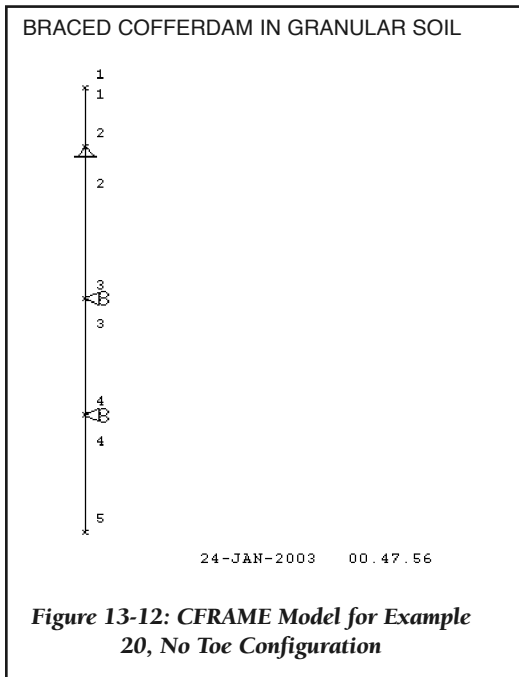


Figure 13-12: CFRAME Model for Example 20, No Toe Configuration

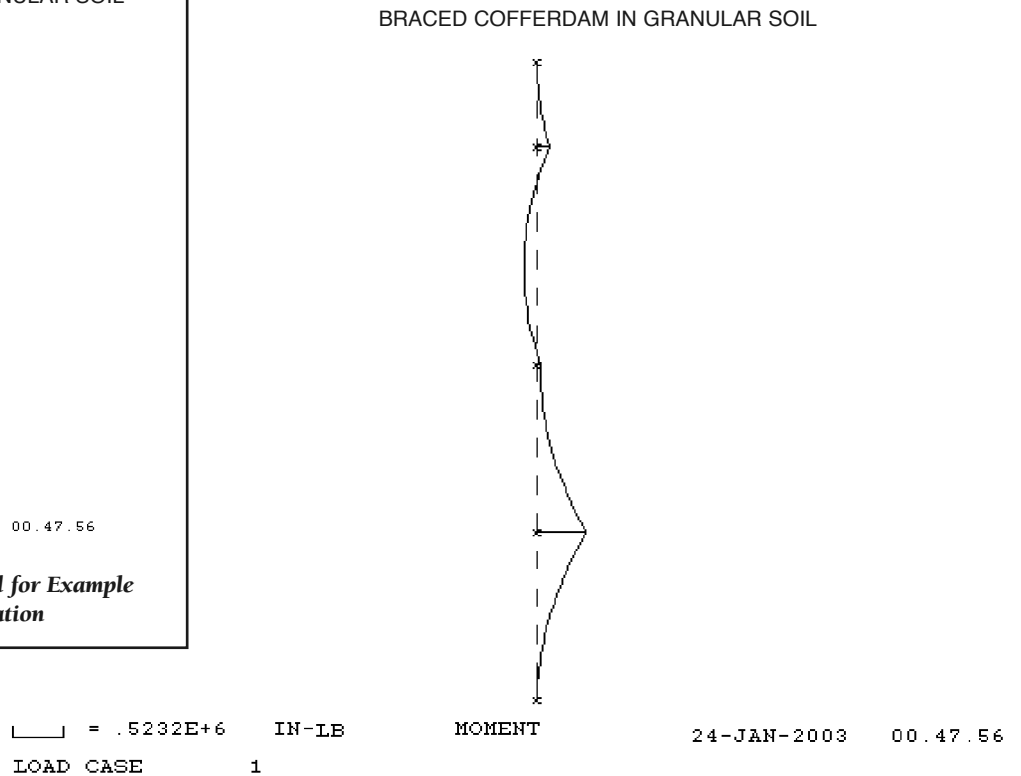


Figure 13-13: CFRAME Moment Diagram for Example 20, No Toe Configuration

Marine Solutions

Solutions for Breakwaters, Shore Protection and Marina Docks

Economy, durability, and versatility

CONTECH® Marine Products provide economical and effective solutions for various marine applications, including shore protection, primary and secondary breakwaters, jetties and marina docks.



For more information, call Toll Free: 800-338-1122.
Or, visit our web site at www.contech-cpi.com

CONTECH
CONSTRUCTION PRODUCTS INC.

INNOVATIVE CIVIL ENGINEERING SITE SOLUTIONS

 American
Owned and Operated

©2003 CONTECH Construction Products Inc. All Rights Reserved

Table 13-1: CFRAME Results for Example 20, No Toe Configuration

RUN DATE = 20-JAN-2003
 RUN TIME = 17.59.19

BRACED COFFERDAM IN GRANULAR SOIL

*** JOINT DATA ***

JOINT	X --- FT ---	Y ---	-----FIXITY-----					
			X	Y	R	KX ---LB / IN---	KY ---	KR IN-LB /RAD
1	.00	.00						
2	.00	-5.00	*	*				
3	.00	-18.00	*					
4	.00	-28.00	*					
5	.00	-38.00						

*** MEMBER DATA ***

MEMBER	END END		LENGTH FT	I IN**4	A IN**2	AS IN**2	E PSI	G PSI
	A	B						
1	1	2	5.00	.1842E+03	.7940E+01	.7940E+01	.2900E+08	.1115E+08
2	2	3	13.00	.1842E+03	.7940E+01	.7940E+01	.2900E+08	.1115E+08
3	3	4	10.00	.1842E+03	.7940E+01	.7940E+01	.2900E+08	.1115E+08
4	4	5	10.00	.1842E+03	.7940E+01	.7940E+01	.2900E+08	.1115E+08

*** LOAD CASE 1

MEMBER	LA	PA	LB	PB	ANGLE DEG
	FT	LB / FT	FT	LB / FT	
1	.00	-.8720E+03	5.00	-.8720E+03	.00
2	.00	-.8720E+03	13.00	-.8720E+03	.00
3	.00	-.8720E+03	10.00	-.8720E+03	.00
4	.00	-.8720E+03	10.00	-.8720E+03	.00

1 LOAD CASE 1

JOINT	JOINT DISPLACEMENTS		
	DX	DY	DR
	IN	IN	RAD
1	-.1880E-01	.0000E+00	.2155E-03
2	.0000E+00	.0000E+00	.7052E-03
3	.0000E+00	.0000E+00	-.1189E-02
4	.0000E+00	.0000E+00	.3112E-02
5	.7320E+00	.0000E+00	.7030E-02

Table 13-1 continued.

MEMBER END FORCES						
MEMBER	JOINT	AXIAL LB	SHEAR LB	MOMENT IN-LB	MOMENT EXTREMA IN-LB	LOCATION IN
1	1	.0000E+00	.0000E+00	.0000E+00	.1308E+06	60.00
	2	.0000E+00	-.4360E+04	.1308E+06	.0000E+00	.00
2	2	.0000E+00	-.6287E+04	.1308E+06	.1308E+06	.00
	3	.0000E+00	-.5049E+04	.3419E+05	-.1412E+06	87.36
3	3	.0000E+00	-.2849E+03	.3419E+05	.5232E+06	120.00
	4	.0000E+00	-.8435E+04	.5232E+06	.3366E+05	4.80
4	4	.0000E+00	-.8720E+04	.5232E+06	.5232E+06	.00
	5	.0000E+00	.0000E+00	.0000E+00	.0000E+00	120.00

STRUCTURE REACTIONS			
JOINT	FORCE X LB	FORCE Y LB	MOMENT IN-LB
2	-.1065E+05	.0000E+00	.0000E+00
3	-.5334E+04	.0000E+00	.0000E+00
4	-.1716E+05	.0000E+00	.0000E+00

TOTAL -.3314E+05 .0000E+00

MEMBER END FORCES							
MEMBER	LOAD CASE	JOINT	AXIAL LB	SHEAR LB	MOMENT IN-LB	MOMENT EXTREMA IN-LB	LOCATION IN
1	1	1	.0000E+00	.0000E+00	.0000E+00	.1308E+06	60.00
		2	.0000E+00	-.4360E+04	.1308E+06	.0000E+00	.00
2	1	2	.0000E+00	-.6287E+04	.1308E+06	.1308E+06	.00
		3	.0000E+00	-.5049E+04	.3419E+05	-.1412E+06	87.36
3	1	3	.0000E+00	-.2849E+03	.3419E+05	.5232E+06	120.00
		4	.0000E+00	-.8435E+04	.5232E+06	.3366E+05	4.80
4	1	4	.0000E+00	-.8720E+04	.5232E+06	.5232E+06	.00
		5	.0000E+00	.0000E+00	.0000E+00	.0000E+00	120.00

BRACED COFFERDAM IN GRANULAR SOIL WITH TOE

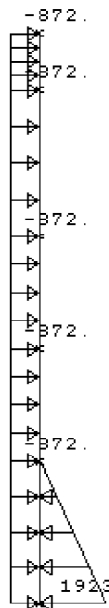


Figure 13-14: Loading of CFRAME Model for Example 20, Configuration with Toe

LOAD CASE 1

21-JAN-2003 00.59.02

Table 13-2: CFRAME Results for Example 20, Configuration with Toe

RUN DATE = 21-JAN-2003
 RUN TIME = 10.23.54

BRACED COFFERDAM IN GRANULAR SOIL WITH TOE

*** JOINT DATA ***

JOINT	X --- FT ---	Y --- FT ---	-----FIXITY-----					
			X	Y	R	KX ---LB / IN---	KY ---LB / IN---	KR IN-LB /RAD
1	.00	.00						
2	.00	-5.00	*	*				
3	.00	-18.00	*					
4	.00	-28.00	*					
5	.00	-38.00						
6	.00	-50.60						

*** MEMBER DATA ***

MEMBER	END END		LENGTH FT	I IN**4	A IN**2	AS IN**2	E PSI	G PSI
	A	B						
1	1	2	5.00	.1842E+03	.1794E+02	.1794E+02	.2900E+08	.1115E+08
2	2	3	13.00	.1842E+03	.1794E+02	.1794E+02	.2900E+08	.1115E+08
3	3	4	10.00	.1842E+03	.1794E+02	.1794E+02	.2900E+08	.1115E+08
4	4	5	10.00	.1842E+03	.1794E+02	.1794E+02	.2900E+08	.1115E+08
5	5	6	12.60	.1842E+03	.1794E+02	.1794E+02	.2900E+08	.1115E+08

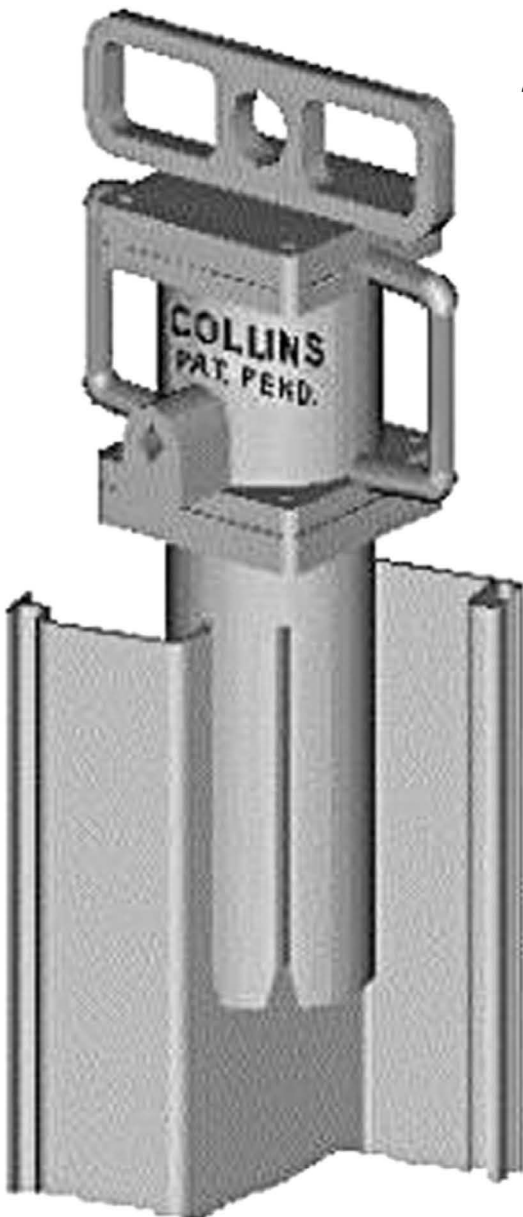
*** LOAD CASE 1

MEMBER	LA	PA	LB	PB	ANGLE DEG
	FT	LB / FT	FT	LB / FT	
1	.00	-.8720E+03	5.00	-.8720E+03	.00
2	.00	-.8720E+03	13.00	-.8720E+03	.00
3	.00	-.8720E+03	10.00	-.8720E+03	.00
4	.00	-.8720E+03	10.00	-.8720E+03	.00
5	.00	-.8720E+03	12.60	-.8720E+03	.00
5	.00	.0000E+00	12.60	.1923E+04	.00

1 LOAD CASE 1

JOINT	JOINT DISPLACEMENTS		
	DX IN	DY IN	DR RAD
1	.1231E-01	.0000E+00	-.3167E-03
2	.0000E+00	.0000E+00	.1730E-03
3	.0000E+00	.0000E+00	-.1028E-03
4	.0000E+00	.0000E+00	-.4626E-03
5	-.3490E+00	.0000E+00	-.6838E-02
6	-.1934E+01	.0000E+00	-.1196E-01

THE COLLINS 150# AIR HAMMER



*New Patent Pending
Design. Out Drives
Heavier Hammers.*

"No Leads" required.

*Drives all brands
of VSP &
CSP+Pin Piles.*

5 day delivery, Cont. U.S.
Visa & MC.

COLLINS COMPANY

Since 1953

Toll Free 888-300-0100

Cell 360-708-5320

www.vinylsheetpiling.com

collins@whidbey.net

Table 13-2 continued.

MEMBER END FORCES						
MEMBER	JOINT	AXIAL LB	SHEAR LB	MOMENT IN-LB	MOMENT EXTREMA IN-LB	LOCATION IN
1	1	.0000E+00	.0000E+00	.0000E+00	.1308E+06	60.00
	2	.0000E+00	-.4360E+04	.1308E+06	.0000E+00	.00
2	2	.0000E+00	-.5577E+04	.1308E+06	.1450E+06	156.00
	3	.0000E+00	-.5759E+04	.1450E+06	-.8313E+05	78.00
3	3	.0000E+00	-.5591E+04	.1450E+06	.1450E+06	.00
	4	.0000E+00	-.3129E+04	-.2673E+04	-.7004E+05	76.80
4	4	.0000E+00	-.7592E+04	-.2673E+04	-.2673E+04	.00
	5	.0000E+00	-.1128E+04	-.3905E+06	-.3993E+06	105.60
5	5	.0000E+00	.1128E+04	-.3905E+06	.0000E+00	151.20
	6	.0000E+00	.0000E+00	.0000E+00	-.3905E+06	.00

STRUCTURE REACTIONS			
JOINT	FORCE X LB	FORCE Y LB	MOMENT IN-LB
2	-.9937E+04	.0000E+00	.0000E+00
3	-.1135E+05	.0000E+00	.0000E+00
4	-.1072E+05	.0000E+00	.0000E+00

TOTAL	-.3201E+05	.0000E+00	

1

MEMBER END FORCES							
MEMBER	LOAD CASE	JOINT	AXIAL LB	SHEAR LB	MOMENT IN-LB	MOMENT EXTREMA IN-LB	LOCATION IN
1	1	1	.0000E+00	.0000E+00	.0000E+00	.1308E+06	60.00
		2	.0000E+00	-.4360E+04	.1308E+06	.0000E+00	.00
2	1	2	.0000E+00	-.5577E+04	.1308E+06	.1450E+06	156.00
		3	.0000E+00	-.5759E+04	.1450E+06	-.8313E+05	78.00
3	1	3	.0000E+00	-.5591E+04	.1450E+06	.1450E+06	.00
		4	.0000E+00	-.3129E+04	-.2673E+04	-.7004E+05	76.80
4	1	4	.0000E+00	-.7592E+04	-.2673E+04	-.2673E+04	.00
		5	.0000E+00	-.1128E+04	-.3905E+06	-.3993E+06	105.60
5	1	5	.0000E+00	.1128E+04	-.3905E+06	.0000E+00	151.20
		6	.0000E+00	.0000E+00	.0000E+00	-.3905E+06	.00

BRACED COFFERDAM IN GRANULAR SOIL WITH TOE

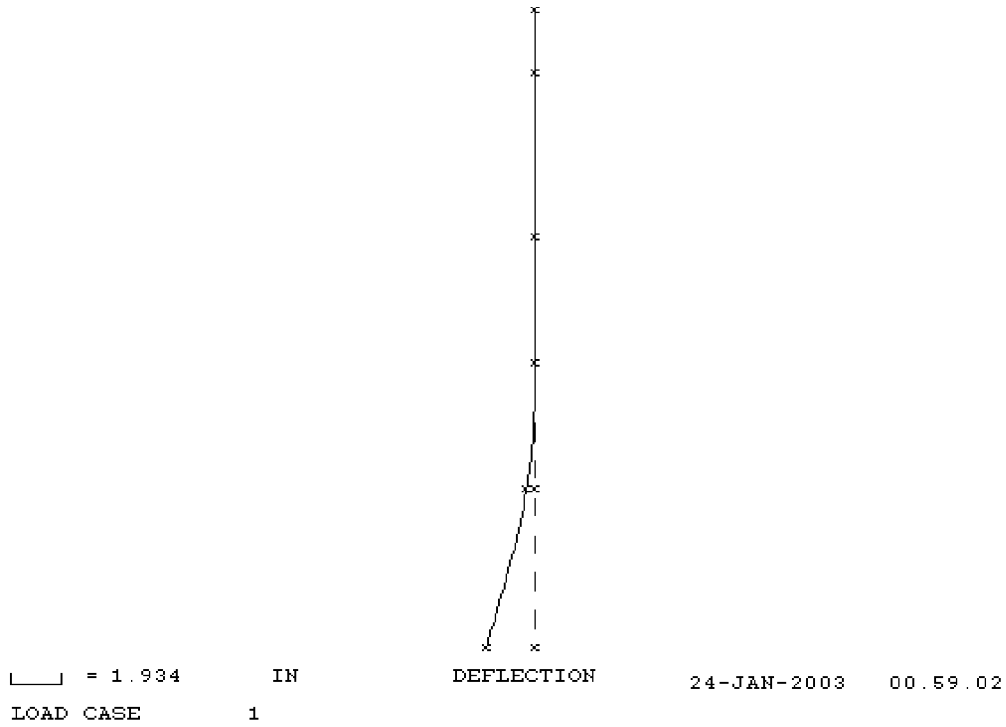


Figure 13-15: CFRAME Deflection Plot for Example 20, Configuration with Toe

BRACED COFFERDAM IN GRANULAR SOIL WITH TOE

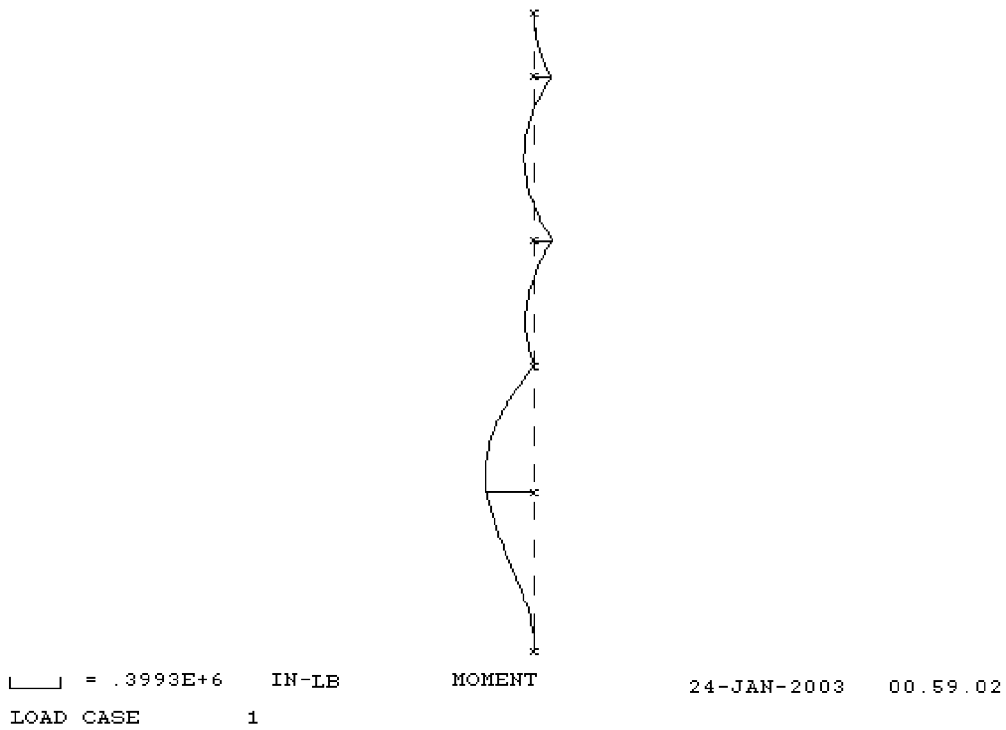


Figure 13-16: CFRAME Moment Diagram for Example 20, Configuration with Toe

The tabulated results from the CFRAME model are shown in *Table 13-2*, the deflection plot is shown in *Figure 13-15*, and the moment diagrams shown in *Figure 13-16*.

The maximum moment for this case is 399,300 in-lbs = 33,275 ft-lbs, which is very close to the results we obtained from hand calculations, as is the location of the moment.

- Comparison and Discussion of Results
 - The results for all of these methods are shown below.

Table 13-3: Summary of Results for Example 20

Method	Reaction 1, kips/ft	Reaction 2, kips/ft	Reaction 3, kips/ft	Maximum Moment kips/ft
Hand Calculations	10.9	9.2	12.0	33.2
SPW 911	10.9	9.11	1.9	32.1
CFRAME (with toe)	9.9	11.4	10.7	33.3
CFRAME (no toe)	10.7	5.3	17.2	43.6

- Discussion of the results

For the three methods used with a toe, the maximum moment for the sheeting is virtually the same for all three methods.

The hand calculations and SPW 911 return virtually the same results for the strut loads; there are some variations with CFRAME. The first two methods are to be preferred since the Peck charts are based on the hinge method. This is the main weakness of using CFRAME.

CFRAME showed that the moment computed without a toe was 31% higher than that for the sheeting with a toe. The sheeting sectional modulus requirements are proportionally higher, but the penetration depth is less. This is an important factor in the economic considerations of the design. CFRAME also showed the maximum moments for the case with no toe to take place at the lowest support, a result unobtainable from the hinge method strictly applied.

The deflections of SPW 911 and CFRAME are very different for the same case. This is because SPW 911, as is the case with classical theory, assumes that the

deflection of the toe is zero. The deflections shown by CFRAME, however, square reasonably well with the concepts of active and passive pressures and the deflections that cause them.

The toe penetration calculations are based on the free earth support method. CFRAME can also be used to determine the penetration for fixed earth support if this is desired.

The accuracy of the CFRAME results is based on the accuracy of the assumption that the sheeting is simply supported. This assumption may be modified based on how the sheet is actually attached to the frame.

- Design of Wales and Struts

Since there are no wales at the top of the excavation, the moments can be computed using **Equation 13-7**:

$$M = \frac{wl^2}{8} \quad \text{(Wale at top)}$$

and the wales below that by the equation

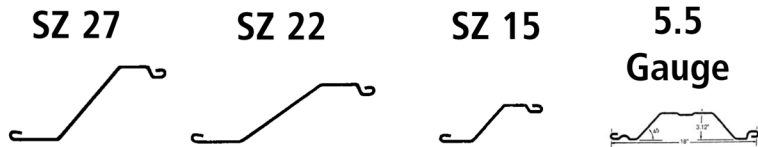
- Equation 13-8. The value for w is actually the same as for the support loads before they are distributed amongst the struts, although these are normally increased by 15% for wale design. For the top supports, the maximum moment in the wales is given by (1.15)(10876)(18 2)/10 = 405.2 ft-kips (using the support load derived in hand calculations.) Using the same equation, the middle and lowest moments in the wales are 342.7 and 388 ft-kips, respectively.
- The load on an individual strut is simply the load per foot of wall for each support multiplied by the spacing of

SHORELINE STEEL, INC.

P.O. Box 480519, 58201 Main Street • New Haven, MI 48048
(800) 522-9550 • (586) 749-9559 • Fax (586) 749-6653

www.shorelinesteel.com

We are a leading producer of domestic cold formed steel sheet piling in sections ranging from 10 gauge to 3/8" thick. For any sheet piling requirement we can satisfy your needs with a top quality product and prompt delivery.



	Thickness (Nominal)	Weight (Sq. ft.)	Weight (Lin. Ft.)	Sec. Mod in ⁴ (Ft. Wall)	Moment of Inertia in ⁴ (Ft. Wall)	Laying Width	Wall Depth
10-10 ga.	.134	7.2	10.8	2.2	3.5	18.00	3.12
8-8 ga.	.164	8.8	13.2	2.62	4.2	18.00	3.12
7-7 ga.	.179	9.6	14.4	2.8	4.4	18.00	3.12
6-6 ga.	.194	10.5	15.8	3.0	4.9	18.00	3.12
5-5 ga.	.209	11.3	16.9	3.4	5.4	18.00	3.12
LZ 8	.164	8.3	17.2	3.6	8.1	25.00	4.50
LZ 7	.179	9.1	18.8	3.9	8.9	25.00	4.50
LZ 5	.209	10.6	21.9	4.6	10.4	25.00	4.50
LZ 3	.239	11.9	24.6	5.2	11.8	25.00	4.50
LZ 250	.250	12.3	25.6	5.4	12.4	25.00	4.50
SZ-10	.164	9.4	17.2	7.3	27.4	22.00	7.50
SZ-11	.179	10.3	18.8	7.9	29.8	22.00	7.50
SZ-12	.209	12.0	21.9	9.2	34.8	22.00	7.50
SZ-14	.239	13.5	24.6	10.4	39.9	22.00	7.50
SZ-15	.250	14.0	25.6	10.9	41.8	22.00	7.50
SZ-14.5	.250	14.5	32.4	13.0	61.49	26.75	9.46
SZ-14.5	.270	15.8	35.1	14.0	86.40	26.75	9.46
SZ-18	.312	18.1	40.4	16.2	76.83	26.75	9.46
SZ-20	.340	19.8	44.1	17.5	83.37	26.75	9.46
SZ-21	.350	20.3	45.3	18.1	86.00	26.75	9.46
SZ-22	.375	21.8	48.6	19.3	91.92	26.75	9.46
SZ-222	.312	22.1	40.4	26.7	163.09	22.00	12.25
SZ-250	.250	15.9	32.4	16.6	89.42	24.46	10.75
SZ-313	.312	19.9	40.4	20.6	111.53	24.46	10.75
SZ-340	.340	21.5	44.1	22.4	121.45	24.46	10.75
SZ-350	.350	22.1	45.3	22.9	124.62	24.46	10.75
SZ-375	.375	23.7	48.6	24.5	133.55	24.46	10.75
SZ-24	.340	24.1	44.1	29.0	177.52	22.00	12.25
SZ-25	.350	24.8	45.3	29.7	181.91	22.00	12.25
SZ-27	.375	26.6	48.6	32.0	195.18	22.00	12.25

DOMESTIC STEEL SHEET PILING

- All sections available in bare or galvanized steel.
- All Zee sections available in doubles.
- All sections produced exactly to customer specified length(s).
- All steel fully melted and manufactured in the USA.



For more information, please call toll free
(800) 522-9550

or visit our website at: www.shorelinesteel.com

Also Available:

- Corners
- Tees and Crosses
- Capping
- Coatings

SHORELINE  STEEL, INC.

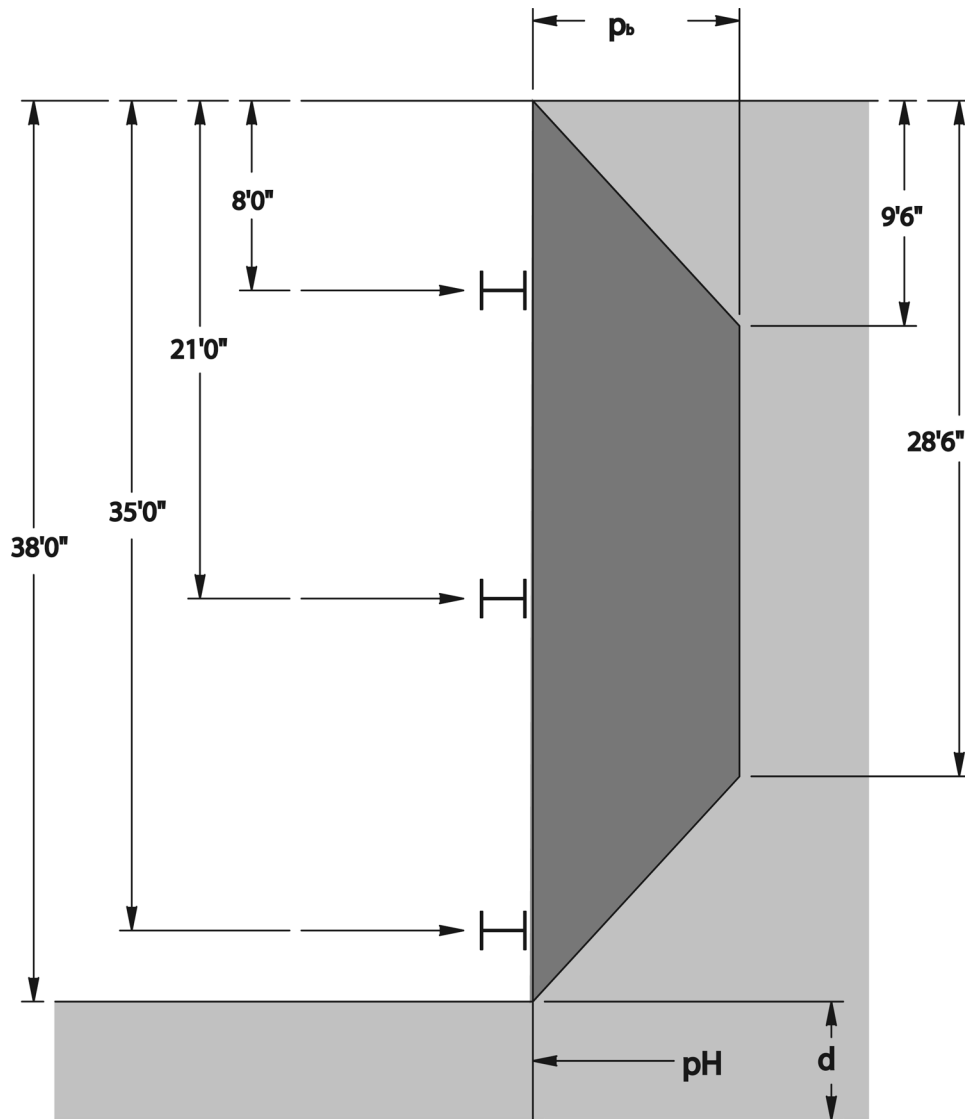


Figure 13-17: Braced Excavation for Example 21

the struts. Thus, for the top support, the strut load is $(10876)(18) = 195.8$ kips. The strut load on the middle and lowest supports are 165.6 and 215.5 kips, respectively. The struts can be designed as columns using calculations such as given in the *AISC Manual of Steel Construction*.

- For a closed excavation, the wales will also be subject to axial loads from the perpendicular faces of the cofferdam. In this case the wales act as both beams and columns simultaneously. As is the case with the struts, design of combined beams and columns can be done using calculations such as given in the AISC manual. Keep in mind that, unlike the struts, the wales can be assumed to be well supported by the sheet piling.

Example 21: Braced Excavation in Cohesive Soil

- ❖ Given
 - Braced excavation as shown in Figure 13-17.
 - Width of excavation same as height (38').
 - “Continuous” excavation ($B/L = 0$).
 - No surcharge load.
 - Struts space 18' apart along the wall.
 - Uniform cohesive soil
 - $\gamma = 115$ pcf
 - $\phi = 0^\circ$
 - $c = 1000$ psf
 - Water table at excavation line
- ❖ Find
 - Depth of sheeting (if any) below the excavation line for

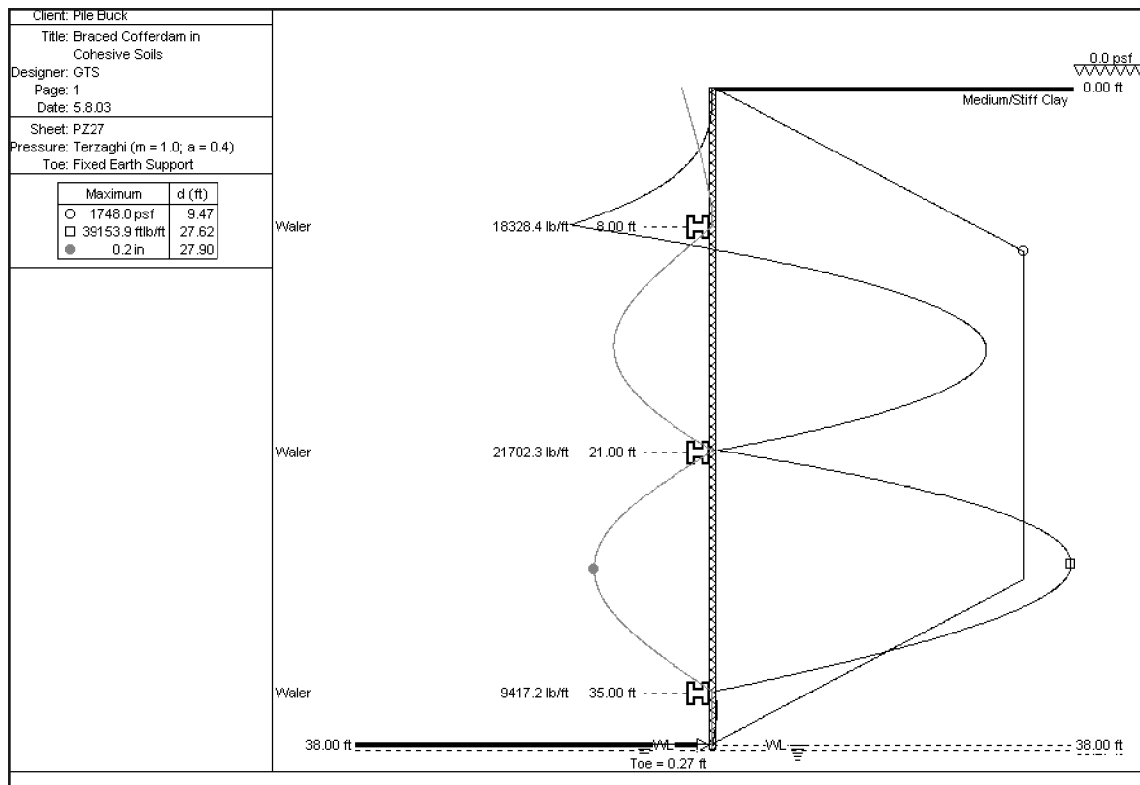


Figure 13-18: SPW Results for Example 21

base stability

- Required section modulus of sheeting
- Loads on struts

❖ Solution

- Determine depth of sheeting “d”
 - We must first determine the stability of the base without additional sheeting depth using Equation 13-5.
 - Using Figure 13-4, $N_c = 6.3$.
 - Using Equation 4-26, $N_o = 4.37$.
 - Using Equation 13-5, $FS = 6.3/4.37 - 0 = 1.44 < 1.5$; thus, we will need to extend the sheeting below the excavation level.
 - The required depth can be computed using Equation 13-6: $d = (38/2)((1.5)(4.37) + 0 - 6.3) = 4.85'$. For the remainder of this problem, we will use $d = 5'$.
- Compute the required section modulus for the sheeting
 - We must first determine the pressure distribution along the sheeting. Since $N_c = 4.37$, we are between the distributions Figure 13-2 (b) and Figure 13-2 (c); thus, we use the distribution with the greater maximum pressure.

Figure 13-2 (b): $p_b = K_a \gamma H$. $K_a = 1 - 4m/N_o = 1 - (4)(1)/4.37 = 0.085$. ($m = 1$ is a reasonable assumption in this case.) Thus $p_b = (0.085)(115)(38) = 370$ psf.

Figure 13-2 (c): $p_b = a \gamma H$. $a = 0.4$ as shown. Thus, $p_b = (0.4)(115)(38) = 1748$ psf. We will use this distribu-

tion. The distribution is illustrated in Figure 13-17.

- We must also determine the load along the sheeting under the excavation line. To use Equation 13-4, we must first determine the value of $\sqrt{2B/3} = 17.9'$. Based on this, we use the lower expression in this equation, and compute $PH = -1350.4$ lbs/ft, which acts 2.5' below the excavation line (we treat this as a line load.)
- We can compute the moments as we did in the previous example; however, the ramped loads complicate the hand solution considerably. We will thus use our two computer programs and compare them. The same comments about the methodology of each from Example 20 apply here.
 - Solution using SPW 911. The solution using SPW 911 is shown in Figure 13-18. SPW 911 does not compute the toe penetration in this case because the program does not consider base stability, but only wall loads. SPW will analyse the sheeting with an extended toe, but this extension must be done manually. The difference in moment due to the extension of the sheeting is not a major factor in this case.
 - Solution using CFRAME
 - The basic model is shown in Figure 13-19. Nodes are placed not only at supports but also at points where loads change or the line load takes place.

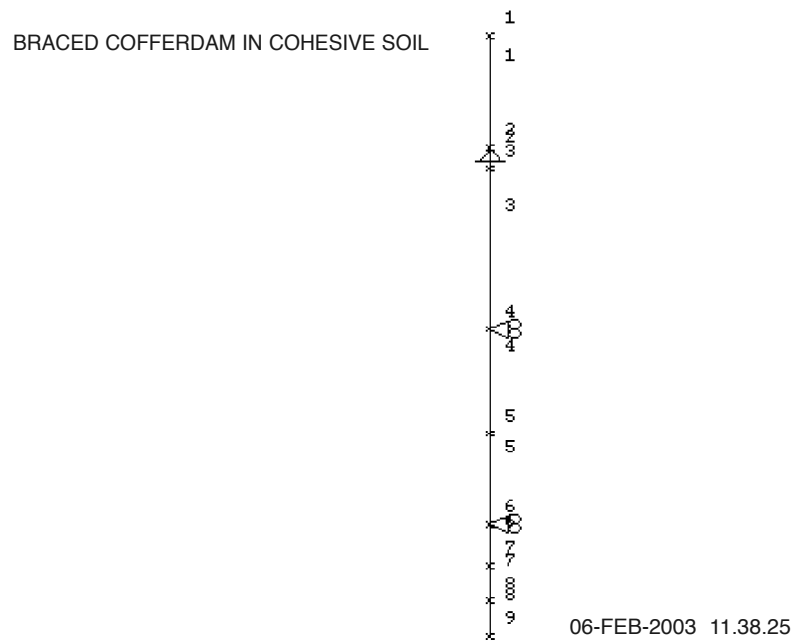


Figure 13-19: CFRAME Model for Example 21

- The loading for the CFRAME model is shown in.

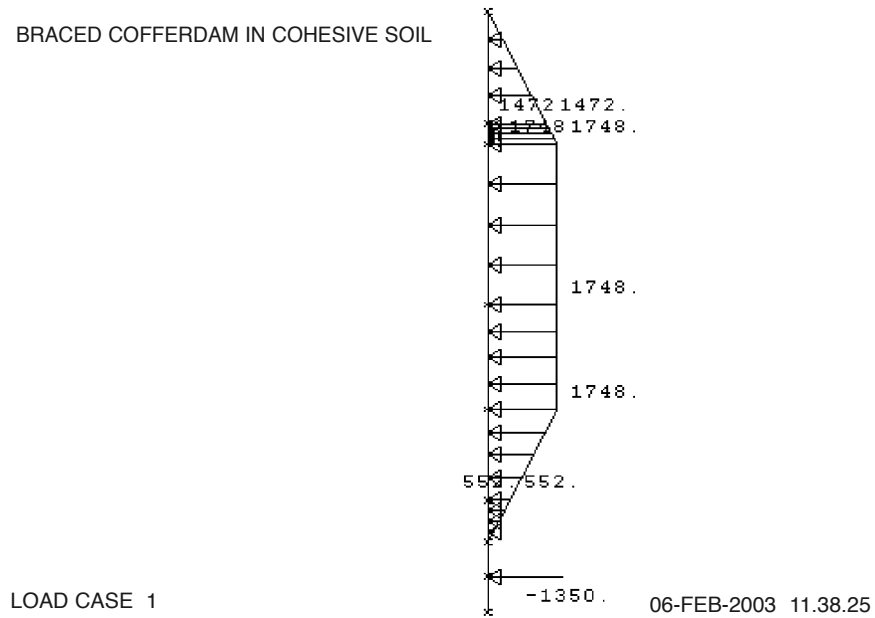
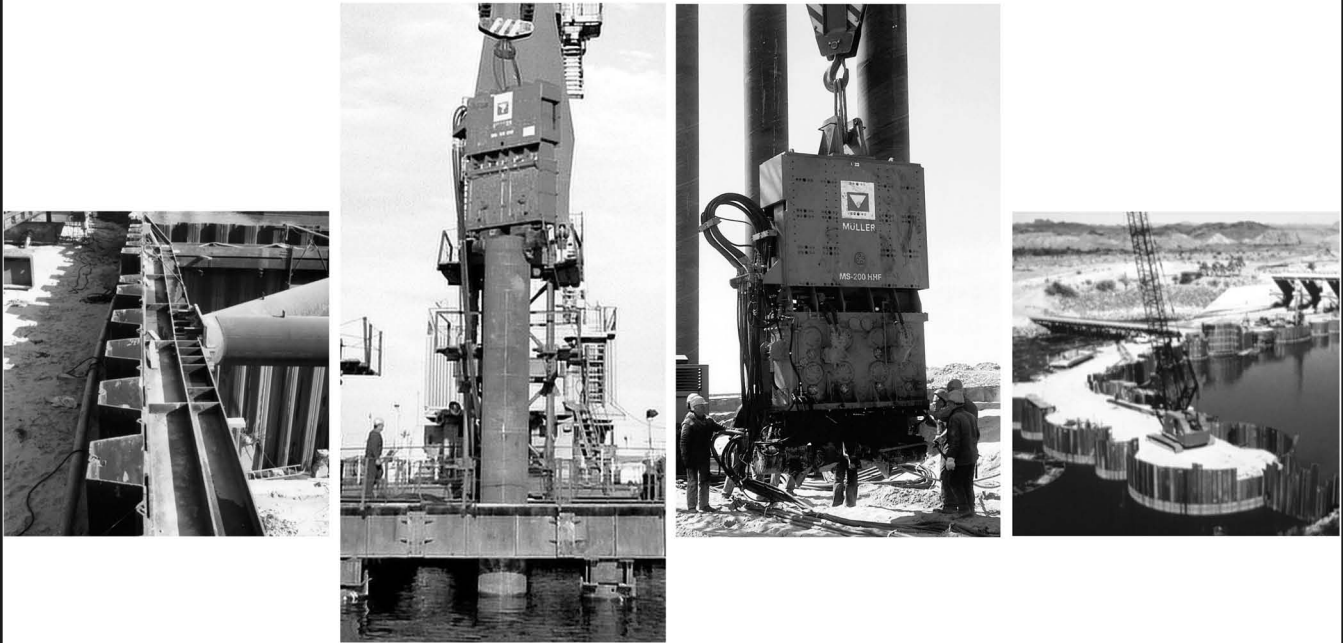


Figure 13-20: CFRAME Loads for Example 21

- The tabular results are shown in Table 13-4.

Leading supplier of systems for port and special construction works.



For individual solutions we present tailor-made system offers for

- **Driven sections**

Steel Sheet Piles System LARSEN and HOESCH, UNION Straight Web Sections, Light Weight Sections, Trench Sheets, Wall-Sections, LARSEN Box-Piles, UNION-Box Piles, Peine Steel Bearing Piles PST, Peine Steel Sheet Piling PSp including special services i.e. Coating, Welding, Interlock Sealing, Water Tightness etc.

- **Driving and extracting technology**

Vibrators, Excavator-mounted Vibrators, Ramming Hammers, Drilling Equipment, Leaders and Carriers, Power-packs

- **Anchor technology**

- **Trenching technology**

- **Flood protection**

ThyssenKrupp GfT Bautechnik GmbH

P.O.Box 10 22 53, D-45022 Essen

Altendorfer Str. 120, D-45143 Essen

Phone: +49 (2 01) 188-39 77

Fax: +49 (2 01) 188-37 72

export-bautechnik@tkx-gft.thyssenkrupp.com

www.tkgftbautechnik.com

ThyssenKrupp GfT Bautechnik

A company of ThyssenKrupp Services



ThyssenKrupp

Table 13-4 Continued

JOINT	FORCE X LB	FORCE Y LB	MOMENT FT-LB
8	-.1350E+04	.0000E+00	.0000E+00

1	LOAD CASE	1
---	-----------	---

JOINT	JOINT DISPLACEMENTS		
	DX IN	DY IN	DR RAD
1	-.7387E-02	.0000E+00	.2374E-03
2	.0000E+00	.0000E+00	-.6091E-03
3	-.1577E-01	.0000E+00	-.9667E-03
4	.0000E+00	.0000E+00	-.3467E-03
5	-.9628E-01	.0000E+00	-.1382E-04
6	.0000E+00	.0000E+00	.1623E-02
7	.4883E-01	.0000E+00	.1170E-02
8	.8145E-01	.0000E+00	.1056E-02
9	.1131E+00	.0000E+00	.1056E-02

MEMBER	JOINT	MEMBER END FORCES				LOCATION IN
		AXIAL LB	SHEAR LB	MOMENT IN-LB	MOMENT EXTREMA IN-LB	
1	1	.0000E+00	.0000E+00	.0000E+00	.0000E+00	.00
	2	.0000E+00	.5888E+04	-.1884E+06	-.1884E+06	96.00
2	2	.0000E+00	.9914E+04	-.1884E+06	-.3108E+05	18.00
	3	.0000E+00	-.7499E+04	-.3108E+05	-.1884E+06	.00
3	3	.0000E+00	.7499E+04	-.3108E+05	.1619E+06	52.44
	4	.0000E+00	.1260E+05	-.3833E+06	-.3833E+06	138.00
4	4	.0000E+00	.1333E+05	-.3833E+06	.2261E+06	90.00
	5	.0000E+00	-.2162E+03	.2261E+06	-.3833E+06	.00
5	5	.0000E+00	.2162E+03	.2261E+06	.2263E+06	1.56
	6	.0000E+00	.7259E+04	-.9906E+05	-.9906E+05	78.00
6	6	.0000E+00	.2178E+04	-.9906E+05	-.4051E+05	36.00
	7	.0000E+00	-.1350E+04	-.4051E+05	-.9906E+05	.00
7	7	.0000E+00	.1350E+04	-.4051E+05	.0000E+00	30.00
	8	.0000E+00	-.1350E+04	.0000E+00	-.4051E+05	.00
8	8	.0000E+00	.0000E+00	.0000E+00	.0000E+00	.00
	9	.0000E+00	.0000E+00	.0000E+00	.0000E+00	.00

JOINT	STRUCTURE REACTIONS		
	FORCE X LB	FORCE Y LB	MOMENT IN-LB
2	.1580E+05	.0000E+00	.0000E+00
4	.2593E+05	.0000E+00	.0000E+00
6	.9437E+04	.0000E+00	.0000E+00

TOTAL	.5117E+05	.0000E+00	

Table 13-4 Continued

1	MEMBER	LOAD CASE	MEMBER END FORCES			MOMENT EXTREMA IN-LB	LOCATION IN	
			JOINT	AXIAL LB	SHEAR LB			MOMENT IN-LB
1	1	1	1	.0000E+00	.0000E+00	.0000E+00	.00	
			2	.0000E+00	.5888E+04	-.1884E+06	-.1884E+06	96.00
2	1	2	2	.0000E+00	.9914E+04	-.1884E+06	-.3108E+05	18.00
			3	.0000E+00	-.7499E+04	-.3108E+05	-.1884E+06	.00
3	1	3	3	.0000E+00	.7499E+04	-.3108E+05	.1619E+06	52.44
			4	.0000E+00	.1260E+05	-.3833E+06	-.3833E+06	138.00
4	1	4	4	.0000E+00	.1333E+05	-.3833E+06	.2261E+06	90.00
			5	.0000E+00	-.2162E+03	.2261E+06	-.3833E+06	.00
5	1	5	5	.0000E+00	.2162E+03	.2261E+06	.2263E+06	1.56
			6	.0000E+00	.7259E+04	-.9906E+05	-.9906E+05	78.00
6	1	6	6	.0000E+00	.2178E+04	-.9906E+05	-.4051E+05	36.00
			7	.0000E+00	-.1350E+04	-.4051E+05	-.9906E+05	.00
7	1	7	7	.0000E+00	.1350E+04	-.4051E+05	.0000E+00	30.00
			8	.0000E+00	-.1350E+04	.0000E+00	-.4051E+05	.00
8	1	8	8	.0000E+00	.0000E+00	.0000E+00	.0000E+00	.00
			9	.0000E+00	.0000E+00	.0000E+00	.0000E+00	.00

- The shear, moment and deflection diagrams are shown in Figure 13-21, Figure 13-22 and Figure 13-23 respectively.

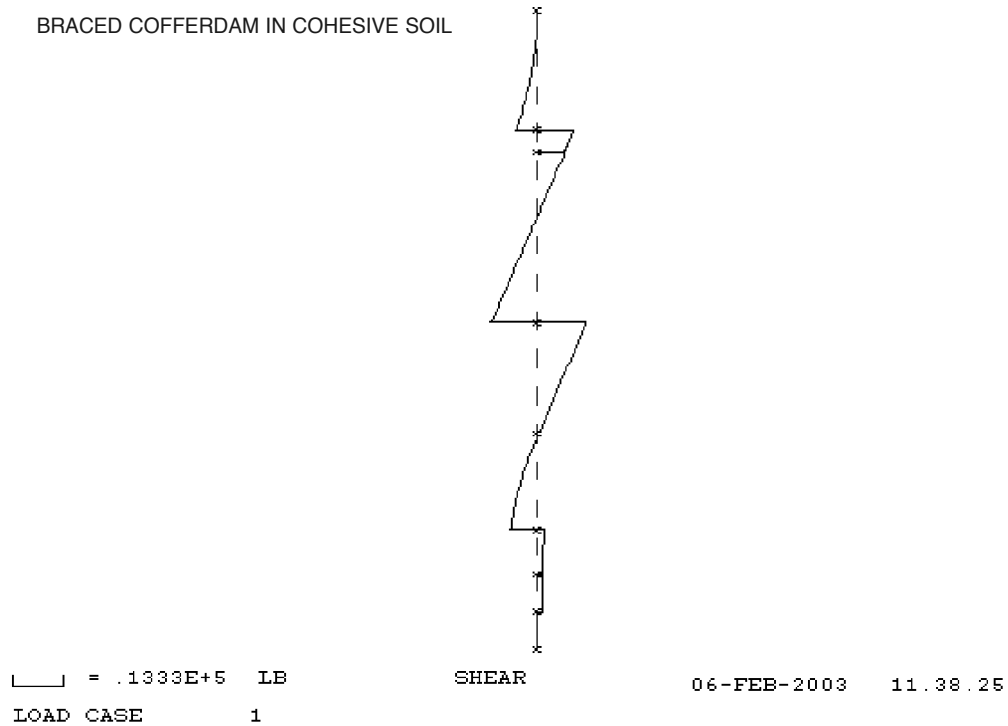


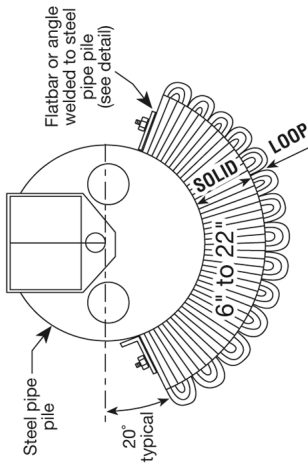
Figure 13-21: CFRAME Shear Diagram for Example 21

MARINE FENDERS OFFSHORE OR DOCKSIDE

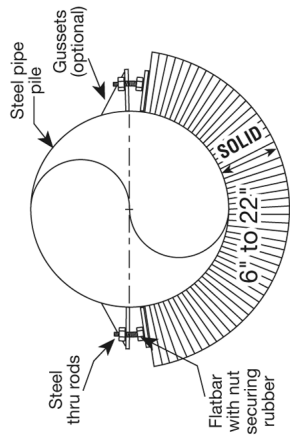
MODEL 153



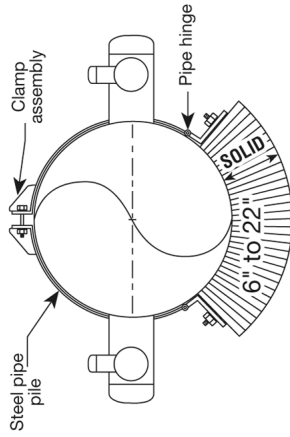
153 TYPE "A" WELD-ON



153 TYPE "B" BOLT-ON



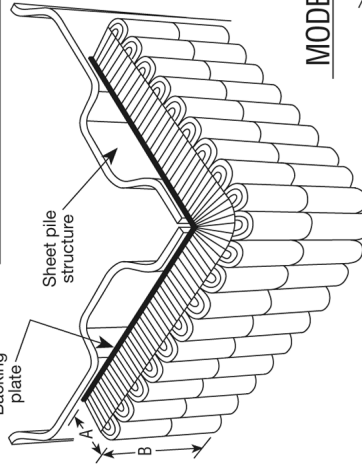
153 TYPE "C" STRAP-ON



MODEL 153 PIPE PILE/DOLPHIN FENDERS

Weld-On, Bolt-On, Strap-On
Applications: Ferry Landings, Barge Facilities,
Mooring Dolphins, Bridge Foundations

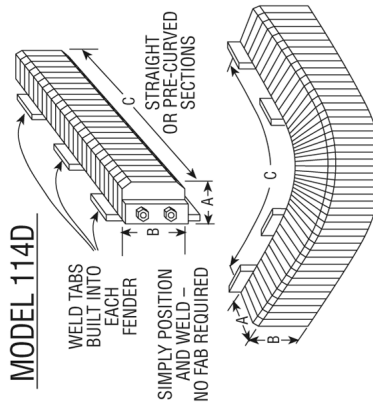
MODEL 114 SHEET PILE FENDERS



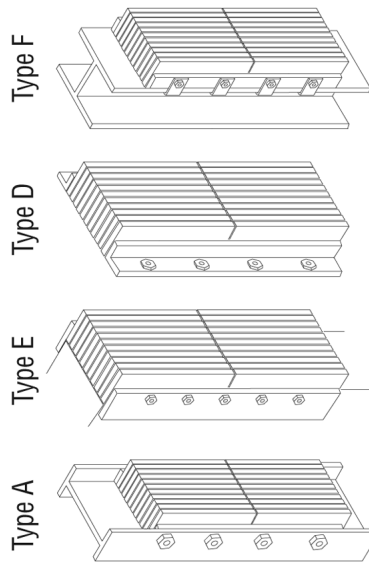
Weld-On or Bolt-On
Applications
Designed and
Engineered to Your
Specifications

WELD-ON D-GUARD FENDERS

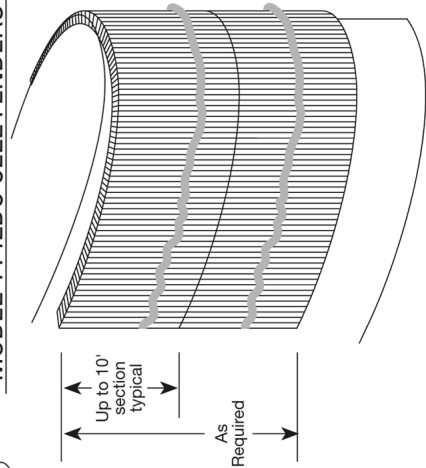
MODEL 114D



MODEL 115 I-BEAM/STRUCTURAL FENDERS



MODEL 114LDC CELL FENDERS



1-800-426-3917

Email: sales@schuylerubber.com
Website: www.schuylerubber.com

16901 Wood-Red Rd.
Woodinville, WA 98072
425-488-2255 Fax: 425-488-2424



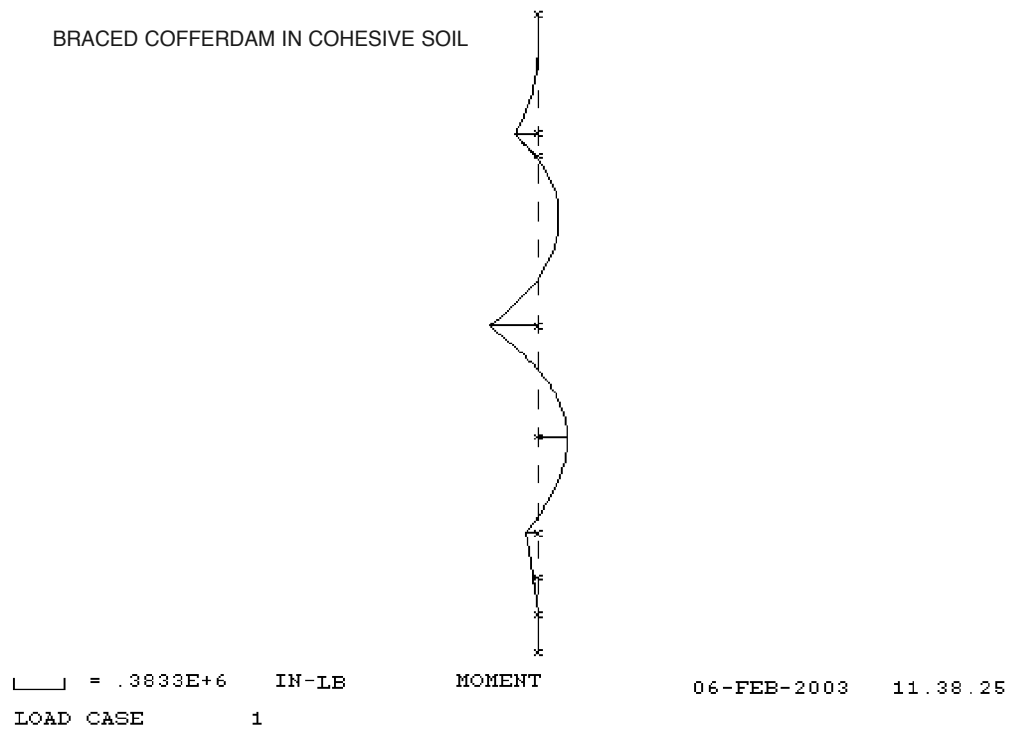


Figure 13-22: CFRAME Moment Diagram for Example 21

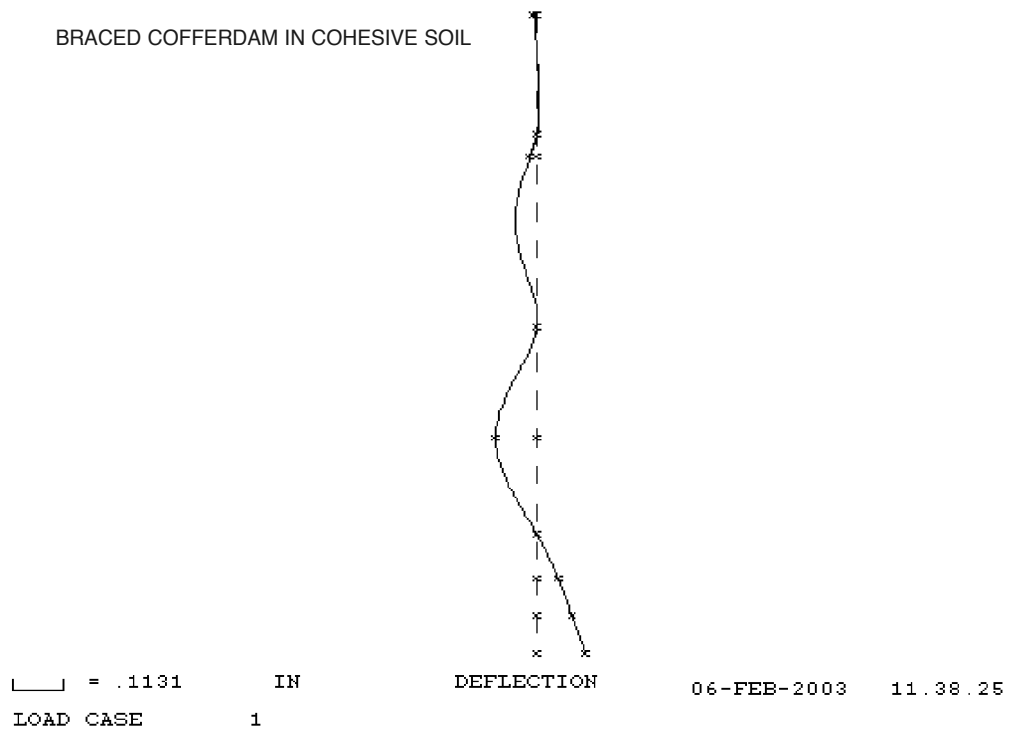


Figure 13-23: CFRAME Deflection Diagram for Example 21

➤ Discussion of the results for both moments and strut loads. These loads are tabulated in the following table.

$$C = 0$$

$$K_a = 0.31$$

Method	Reaction 1, kips/ft	Reaction 2, kips/ft	Reaction 3, kips/ft	Maximum Moment kips/ft
SPW 911	18.3	21.7	9.4	39.1
CFRAME	15.8	25.9	9.4	31.9

As with the cohesionless soil example, the reactions on the struts are differently distributed. SPW 911's result is to be preferred due to the Peck charts.

The moment computed by SPW 911 is considerably higher than CFRAME. This may or may not be realistic; the hinge method is not a particularly accurate modelling method for a continuous beam. SPW 911 would require a PZ 27 section for ASTM A328 steel, while CFRAME would allow a PZ 22 section.

Determine the loads on the struts. For example, CFRAME directly reports these as the reactions at Nodes 2, 4 and 6. These are as follows:

- ◆ Upper struts (Node 2): 15,800 lbs/ft of wall, or $(15.8)(18) = 284.4$ kips for 18' centres.
- ◆ Middle struts (Node 4): 25,930 lbs/ft of wall, or $(25.9)(18) = 466.7$ kips for 18' centres.
- ◆ Lower struts (Node 6): 9,437 lbs/ft of wall, or $(9.4)(18) = 169.9$ kips for 18' centres.
- ◆ The same method can be used with SPW 911 results.

Example 22: Design of Braced Cofferdam for Seepage

◆ Given

➤ Braced excavation

- Depth of excavation = 38'
- Width of excavation = 32'
- Supports at 5', 18', and 30' below the top of the sheeting
- Sheeting penetrates 28' below the bottom of the excavation
- Impervious layer 20' below the toe of the sheeting (66' below the top of the sheeting.)
- Water table at the excavation level on the excavation side and at 6' below the top of the sheeting on the soil side.
- Uniform surcharge load of 200 psf at the surface.
- Soil conditions: Uniform Medium Sand
 - $\gamma_{\text{moist}} = 105$ psf
 - $\gamma_{\text{sat}} = 115$ psf
 - $\gamma' = 53$ psf
 - $\phi = 32^\circ$

$$K_p = 3.25$$

$$\text{Hydraulic conductivity } k = .0003 \text{ ft/sec}$$

◆ Find

- Factor of safety against piping
- Quantity of seepage to the excavation

◆ Solution

- Sheeting configuration. We first analyse the sheeting for structural and geotechnical integrity. We do this with SPW911; the results of the analysis are shown in Figure 13-24; this is also our diagram for the configuration. It shows that the maximum moment is 167.8 ft-kips, this is too high for any of our sample shapes in ASTM A328 and is slightly above PZ40 using ASTM A572. So we will have to use a higher section modulus sheeting in this case.

➤ Checking against piping.

- Chart solution. Since we have an impervious layer, we will use the lower part of Figure 7-6. The three ratios we need are as follows:
 - $W/H_W = 16/32 = 0.5$
 - $D/H_W = 28/32 = 0.88$
 - $H_1/H_W = 20/32 = 0.62$

Apply this to the chart, we learn that, for $H_1/H_W = 1$, the factor of safety is about 2.5 and, for $H_1/H_W = 2$, it is 1.7. By linear "interpolation," the factor of safety from the chart is about 2.8. Since the chart is drawn for $\gamma' = 75$ psf, the actual factor of safety $FS_{\text{actual}} = (53)(2.8)/75 = 2 > 1.5$, so this is acceptable, although going off the chart range is not really the best way to analyse the problem.

- Equation 7-17. Substituting the appropriate variables, the gradient is computed as $i_y = (32)/((3)(28)) = 0.38$. From Equation 7-16, $i_{\text{critical}} = 53/62.4 = 0.85$, and the factor of safety against piping (Equation 7-17) is $0.85/0.38 = 2.23 > 1.5$. This turns out to be the least conservative of the methods shown.
- Finite element analysis. This requires the use of a computer program. In this case we will use the program SEEP-W, which is available from GEO-SLOPE International, Ltd., Calgary, Alberta, Canada. The finite element model we use is shown in Figure 13-25.

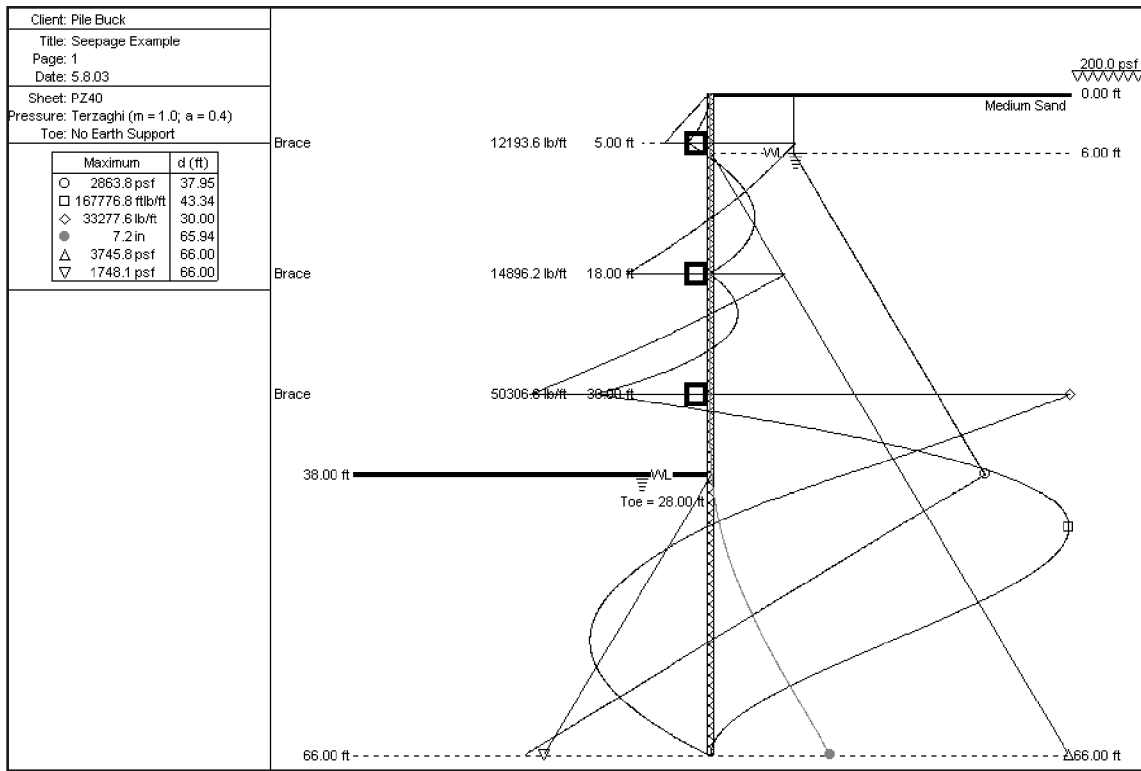


Figure 13-24: SPW 911 Results for Example 22

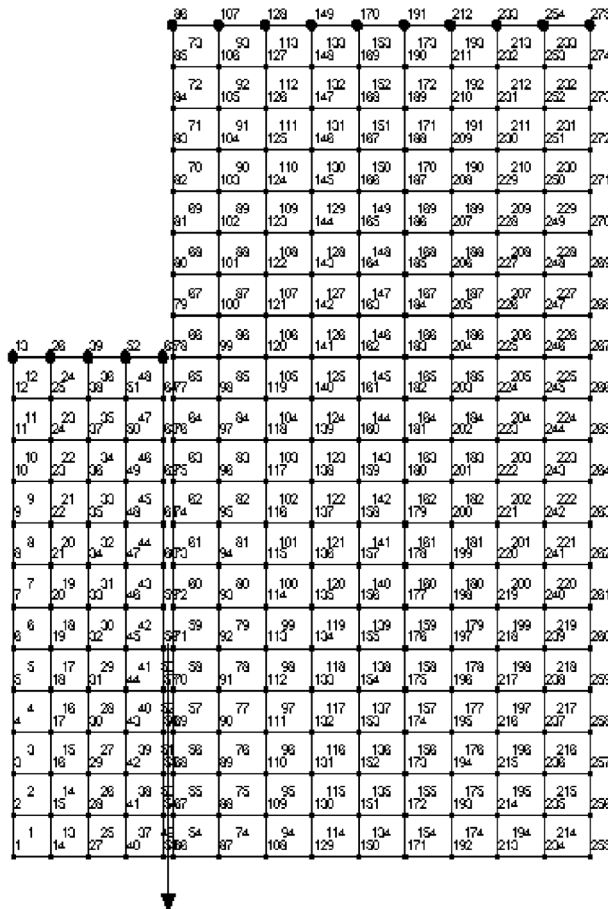


Figure 13-25: SEEP-W Finite Element Model



HOT ROLLED SHEET PILE SECTIONS FROM

CORUS

ONLY AVAILABLE THROUGH

**— JD —
FIELDS
& Company, Inc.**

FRODINGHAM Z-PILING

Section	Centres	Height	Web	Flange	Section Area	Mass		Combined Moment of Inertia	Section Modulus
						lbs/ft	lbs/ft ²		
1N-RU3	19.00	6.72	0.38	0.38	6.35	34.22	21.61	47.28	14.08
1N	19.00	6.69	0.35	0.35	5.98	32.22	20.35	44.46	13.29
1N-RD3	19.00	6.66	0.32	0.32	5.49	29.58	18.67	40.78	12.25
2N-RU3	19.00	9.28	0.36	0.41	7.32	39.42	24.90	106.65	22.98
2N	19.00	9.25	0.33	0.38	6.84	36.84	23.27	99.89	21.60
2N-RD3	19.00	9.22	0.30	0.35	6.36	34.25	21.63	93.11	20.20
3NA	19.00	12.00	0.37	0.38	7.62	42.14	26.61	188.27	31.38
4N-RU3	19.00	13.03	0.44	0.58	10.87	58.58	37.00	306.44	47.04
4N	19.00	13.00	0.41	0.55	10.31	55.57	35.10	291.96	44.92
4N-RD3	19.00	12.97	0.38	0.52	9.76	52.57	33.20	277.50	42.79
5	16.75	12.25	0.47	0.67	14.29	67.88	48.82	381.23	58.88

LARSEN SECTIONS

Section	Driving width per pile	depth	Flat of Pan	Thickness		Weight		Combined Section Modulus per ft of wall	Combined Moment of Inertia per ft of wall
				flange	web	per lin ft of pile	per sq. ft. of wall		
Frodingham	in. (b)	in. (h)	in. (f)	in. (d)	in. (t)	lbs	lbs	in ³ /ft	in ⁴ /ft
6W	20.67	8.35	13.03	0.31	0.25	30.04	17.48	11.35	47.66
LX 8	23.62	12.2	9.84	0.32	0.31	36.66	18.62	15.44	94.19
LX 12	23.62	12.2	15.2	0.38	0.32	42.89	21.79	22.47	137.14
LX 12d	23.62	12.2	15.2	0.39	0.32	43.85	22.28	23.06	140.73
LX 12d10	23.62	12.2	15.2	0.39	0.39	48.91	24.85	23.84	145.48
LX 16	23.62	14.96	14.37	0.41	0.35	49.79	25.28	30.53	228.35
LX 20	23.62	16.93	12.99	0.49	0.35	55.84	28.37	37.62	318.43
LX 20d	23.62	17.72	12.99	0.44	0.39	56.6	28.76	37.36	330.97
20Wd	20.67	15.75	13.11	0.44	0.39	54.18	31.45	37.73	297.12
LX 25	23.62	18.11	13.82	0.53	0.39	63.78	32.4	46.63	422.21
LX 25d	23.62	17.72	12.83	0.61	0.43	67.11	34.09	47.32	419.21
LX 32	23.62	18.11	13.39	0.75	0.43	76.78	39.01	59.68	540.44
LX 32d	23.62	17.72	12.6	0.85	0.51	84.92	43.14	62.27	551.59
LX 38	23.62	18.11	13.27	0.89	0.57	94.28	47.9	70.77	640.83
GSP2	15.75	7.87	10.43	0.41	0.34	33.13	25.24	16.29	64.12
GSP3	15.75	9.84	10.67	0.51	0.34	40.36	30.75	24.28	119.48
GSP4	15.75	13.39	10.2	0.61	0.38	51.13	39.93	42.39	283.7
6-42	19.69	17.72	12.99	0.81	0.55	89.27	54.41	78.33	693.33
6 (122)	16.54	17.32	9.76	0.87	0.55	82.23	59.66	77.88	674.54
6 (131)	16.54	17.32	9.88	1	0.55	87.73	63.65	85.9	743.99
6 (138)	16.54	17.32	9.88	1.13	0.55	92.84	67.36	93.09	806.31

SALES & RENTALS

-ALSO-

- H-BEAMS 8", 10", 12" & 14"
- STEEL PIPE 1/2" - 48" O.D.
- USED SHEET PILING

J.D. FIELDS & CO. INC. CORPORATE HEADQUARTERS
 15995 North Barkers Landing, Suite 230, Houston, TX 77079
 (281) 558-7199 F (281) 558-9918

www.jdfields.com

ADDITIONAL OFFICES THROUGHOUT THE U.S.

- | | | | |
|------------------|----------------|-----------------|----------------|
| Dallas, TX - | (972) 869-3794 | Chicago, IL | (708) 333-5511 |
| New Orleans, LA | (504) 832-7294 | Tulsa, OK | (918) 459-4638 |
| Philadelphia, PA | (610) 317-6308 | Denver, CO | (303) 331-6190 |
| Antioch, CA | (925) 778-9740 | Los Angeles, CA | (714) 257-2005 |

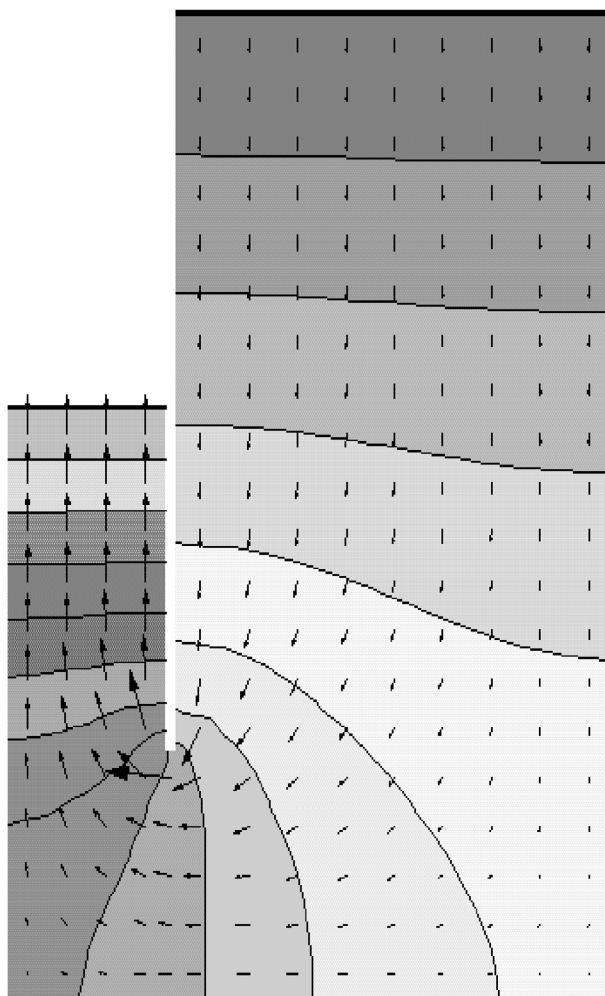


Figure 13-26: SEEP-W Results: Total Head

The head at both the excavation level and the water table is set. A “cut” in the model is included for the sheet piling. We also make provision to analyse the flow of water between the sheeting and the impervious layer, which will give us the flow into the excavation. Keep in mind that this is a “half” model; the other half is assumed the same by symmetry.

If we run and solve the model, the distribution of total head is shown in *Figure 13-26*. As one would expect, the head varies from its maximum value at the water table to its minimum value (32' less) at the excavation level.

The variation of gradient is shown in *Figure 13-27*. The gradient shown here is the total gradient (as opposed to the gradient in just the horizontal or vertical direction.) The maximum gradient takes place (as one would expect) at the toe of the sheeting, and is reported to equal

to 1.03. Although this is interesting, the gradient we are actually looking for from a boiling stand-point is at the base of the excavation. The program reports that the gradient here varies from 0.474 to 0.477, so let us use a value of 0.48. From Equation 7-16, $i_{\text{critical}} = 53/62.4 = 0.85$, and the factor of safety against piping (Equation 7-17) is $0.85/0.48 = 1.77 > 1.5$, so it is acceptable, but considerably lower than we see with the chart solution.

One thing we can do with finite element analysis that we cannot do with the other solutions is to analyze the gradient at all points. If we do this, we should keep in mind for this case that, using a factor of safety of 1.5, the maximum acceptable gradient is $0.85/1.5 = 0.57$.

Finally, the program reports that we have water flow of $0.00228 \text{ ft}^3/\text{sec}/\text{ft}$ of wall between the toe of the sheeting and the impervious layer. Since our analysis is steady state, this is also the flow into the excavation.

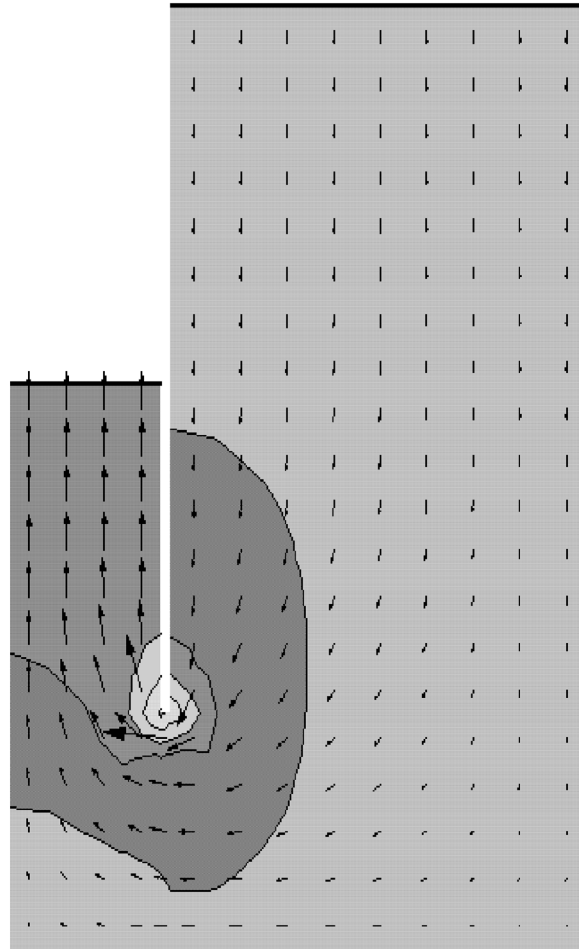


Figure 13-27: SEEP-W Results: Gradient

Translated into gallons per minute, this is $(0.00228)(449) = 1.02$ gpm/ft of wall. Obviously this is only for one side of the wall; for the complete excavation, we will need to double this number.

- Flow net. A flow net for this excavation is shown in Figure 13-28; in fact, this flow net was generated with SEEP-W. We note the following about this:

The flow net has 4 flow tubes and 16 equipotential drops, and is designed so that the “aspect ratio” of the “squares” in the flow net is effectively unity, which is optimal in flow netting.

Directly under the excavation, the squares are 4' x 4'.

With 16 equipotential drops, each drop represents $32/16 = 2'$ of head. The gradient directly under the excavation is thus $\Delta h/\Delta l = 2'/4' = 0.5$. The factor of

safety with this gradient is $0.85/0.5 = 1.7 > 1.5$, which is also acceptable and slightly below that from the finite element analysis.

The total flow using flow netting is given by the equation

$$\text{Equation 13-20: } Q' = k\Delta h \frac{N_F}{N_D} \frac{b}{a}$$

where

- ◆ Q' = water flow, ft³/sec/ft of wall
- ◆ k = hydraulic conductivity, ft/sec
- ◆ Δh = total head drop, ft
- ◆ N_F = number of flow tubes
- ◆ N_D = number of equipotential drops
- ◆ b/a = “aspect ratio” of “squares”

Using this equation, the total flow is $(0.0003)(32)(4/16)(1) = 0.0024$ ft³/sec/ft of wall = 1.08 gpm/ft of wall. This is also close to the actual finite element analysis.

The problem with using a hand-generated flow net to

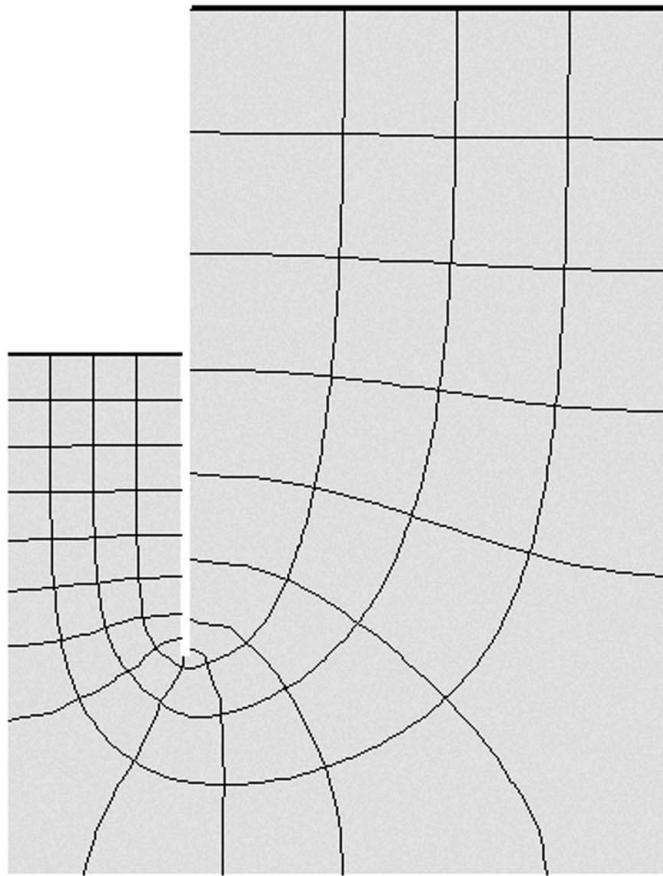


Figure 13-28: Flow Net for Seepage Example

determine piping is that the flow net must be very accurate for piping analysis, whereas it does not need to be so for the total flow.

Example 23: Water Cofferdam with Transverse Bending⁸

The purpose of this problem is to illustrate two aspects of sheet piling design: a) a cofferdam in water, and b) the effects of transverse bending.

- ❖ Given
 - Bridge pier cofferdam as shown in *Figure 13-29*.
- ❖ Find
 - Sheet piling section, using both conventional and transverse bending.
- ❖ Solution
 - Basic solution of earth pressures and moments
 - The problem was solved using SPW 911; the solution is shown in *Figure 13-30*. The maximum moment is obviously at the bottom support; however, there are actually two points of interest when considering trans-

verse bending:

The point at a support with the maximum moment. This is at the fourth support (Elevation 594.5, or 22.5' below the surface.) SPW911 reports the moment to be 29,053 ft-lbs = 349 in-kips. The lateral earth pressure at this point is 2566 psf = 17.83 psi, which we will use in the transverse bending calculations.

The point along a span and below the soil line with the maximum moment. This occurs between the second and third supports (approximate Elevation 606.5, or 10.5' below the surface. SPW911 reports the maximum moment in this span to be approximately 6,940 ft-lbs = 83.3 in-kips. The lateral earth pressure at this point is 1576 psf = 10.94 psi.

Any of our typical sections can be used in this sheet-

HPSI Vibros



from a
"Little Guy"

to a
"BIG Guy"

Whether it's an excavator mounted vibratory for driving lightweight vinyl or aluminum sheet piling on up to a 20,000 in. lb. machine for driving large diameter caisson, we have a vibro suitable for your job.



SALES & RENTALS

(Distributors throughout North America)

From "The Engineers of Pile Driving Equipment"™

HYDRAULIC POWER SYSTEMS, INC.

Kansas City Offices and Plant
1203 Ozark
N. Kansas City, MO 64116
Phone (816) 221-4774
Fax (816) 221-4591
E-mail info@hpsi-worldwide.com
<http://www.hpsi-worldwide.com>



International & Domestic Sales
745 U.S. Hwy 1
N. Palm Beach, FL 33408
Phone (561) 687-5525
Fax (561) 841-3479
E-mail info@hpsi-worldwide.com
<http://www.hpsi-worldwide.com>

*Vibratory Pile Hammers • Hydraulic Augers • Winch Systems
Custom Manufacturing • Hydraulic Impact Hammers • Lead Systems*

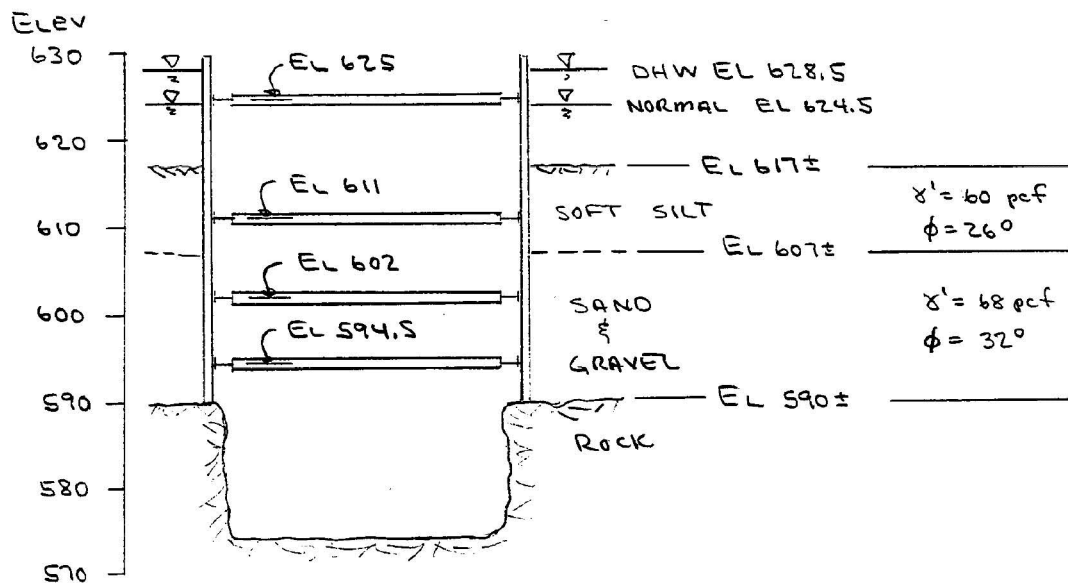


Figure 13-29: Bridge Pier Cofferdam for Example 23

ing wall based purely on conventional bending, including PZ22 and PZ27.

Inspection of Figure 13-30 also shows that most of the lateral force on the wall is due to hydrostatic pressure, not only above the mud line (where it is the only lateral force) but below it as well. The maximum hydrostatic pressure at the pile toe is $(628.5 - 590)(62.4) = 2402.5$ psf.

- To include the effects of transverse sheeting, we need to substitute the necessary parameters into Equation 2-5 in order to evaluate the combined effects of conventional and transverse bending. The parameter λ_t (and to some extent c_t also) are determined either experimentally or by finite element analysis. Complicating matters further is the fact that the stress distribution for transverse bending at the wales and at the centre of spans is different. The simplest way to deal with this is to present the various “versions” of Equation 2-5 for our sample sections. These are as follows:

Equation 13-21: $M_L = 13.30f_y - 25.86p$ (PZ22, Wale Location)

Equation 13-22: $M_L = 12.19f_y - 14.66p$ (PZ22, Span Location)

Equation 13-23: $M_L = 21.29f_y - 34.81p$ (PZ27, Wale Location)

Equation 13-24: $M_L = 19.96f_y - 27.97p$ (PZ27, Span Location)

Equation 13-25: $M_L = 34.27f_y - 25.21p$ (PZ35, Wale Location)

Equation 13-26: $M_L = 31.52f_y - 19.20p$ (PZ35, Span Location)

Equation 13-27: $M_L = 42.83f_y - 29.98p$ (PZ40, Wale Location)

Equation 13-28: $M_L = 39.64f_y - 25.25p$ (PZ40, Span Location)

For all of the sections, let us assume that $f_y = 39$ ksi for

all sections. For the wale location, $p = 17.83$ psi and for the span location, $p = 10.94$ psi. Substituting these values into each of the above equations, the results are then compared with the actual conventional bending moments to determine whether a section is acceptable or not. Table 13-6 shows the results of this process.

We see from these results that the PZ22 and PZ27 sections are no longer acceptable in this alloy. Using a 50 ksi yield strength changes only one case, i.e., the use of PZ27 at the wale.

13.5. Pressurised Tiebacks

External tiebacks, as shown in Figure 13-31, are an acceptable method for supporting retaining walls where conditions are favourable. In general, the economics must be favourable, there must be room to attain required anchorage length without encroachment, and soil conditions must meet certain conditions. The advantage of the system is (1) experienced people generally do installation and design on a sub-contract basis, and (2) the excavation is unencumbered by tiers of internal bracing. Combinations of bracing and tiebacks have been utilized where the advantages of each system could be realized.

Figure 13-32 shows the computation of lateral pressures for tied back walls. Use the same design procedure as shown in Figure 13-2.

A typical tieback system uses high strength alloy steel bars, 1 1/2 to 2 1/2 inches in diameter, with 145 ksi ultimate strength, or seven-wire strands of 250 – 270 ksi nominal ultimate strength.

The tiebacks are installed by augering or driving 4 to 8 inch

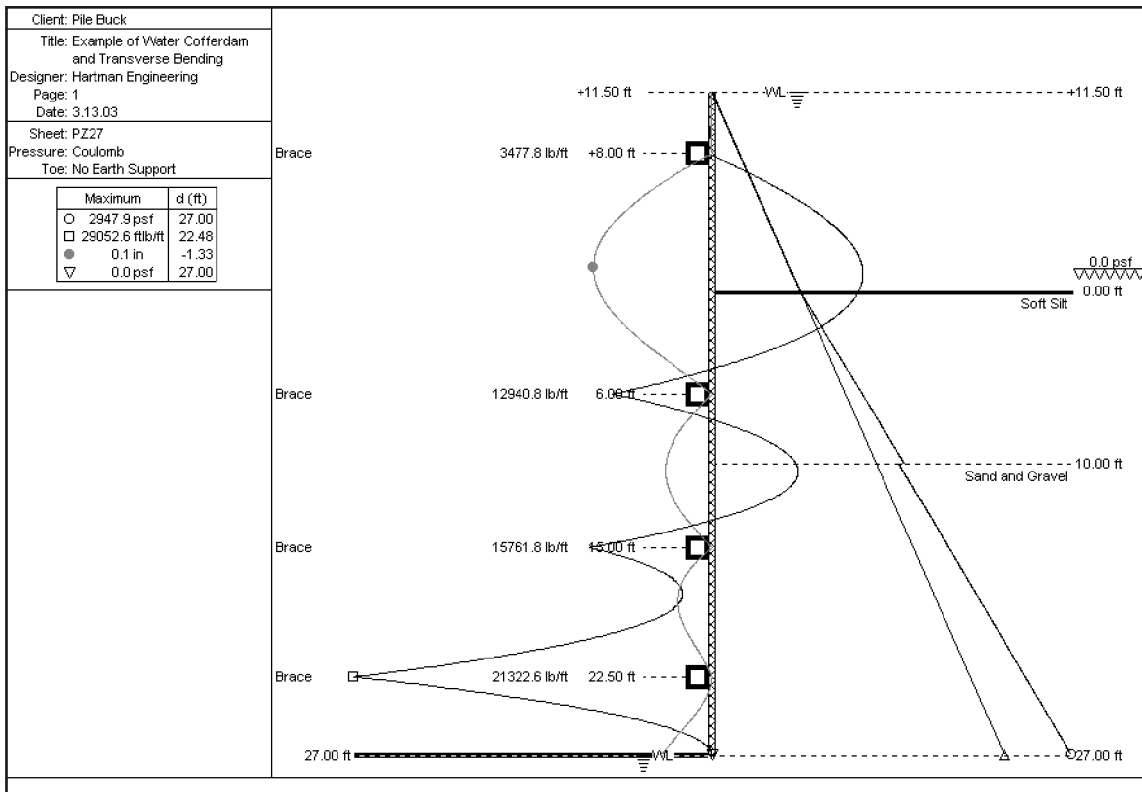


Figure 13-30: SPW 911 Solution for Example 23

Table 13-6: Results of Transverse Bending Analysis

Section	Loading Point	Allowable Moment M_L for ASTM A328, in-kips	Allowable Moment M_L for ASTM A572, in-kips	Actual Bending Moment	Acceptable with ASTM A328?	Acceptable with ASTM A572?
PZ22	Wale	58	204	349	No	No
PZ22	Span	315	449	83.3	Yes	Yes
PZ27	Wale	210	444	349	No	Yes
PZ27	Span	472	692	83.3	Yes	Yes
PZ35	Wale	887	1371	349	Yes	Yes
PZ35	Span	1019	1366	83.3	Yes	Yes
PZ40	Wale	1136	1610	349	Yes	Yes
PZ40	Span	1270	1706	83.3	Yes	Yes

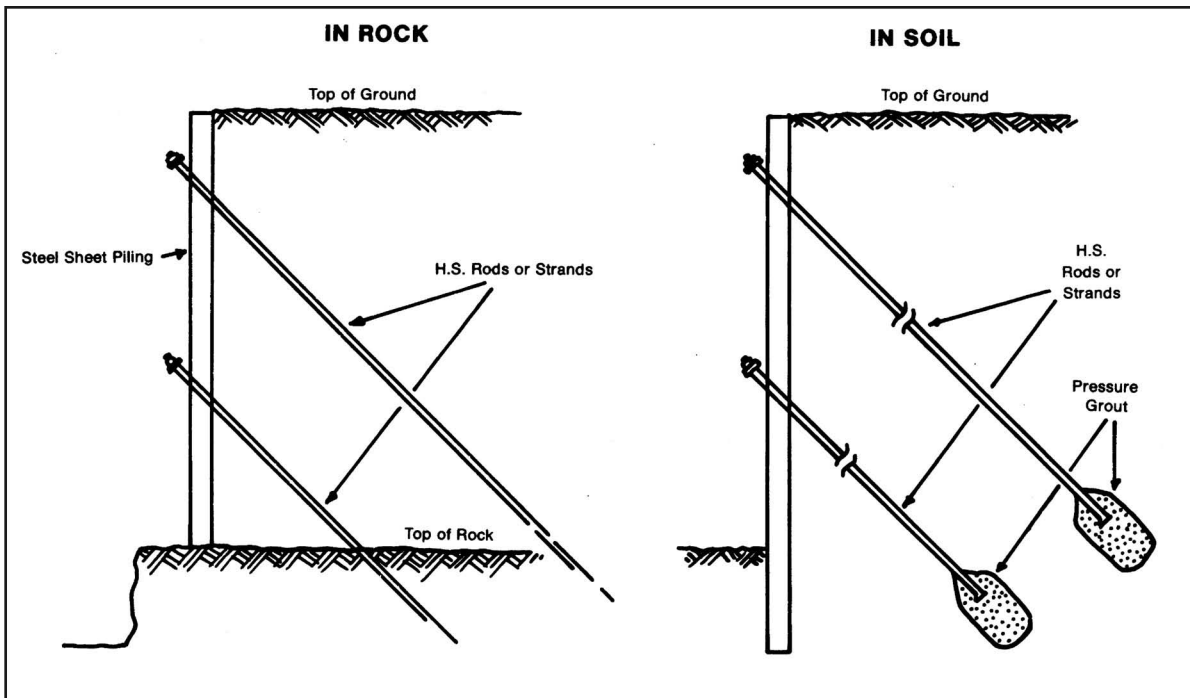
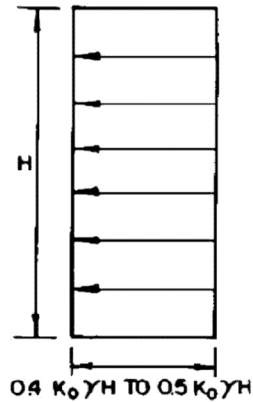


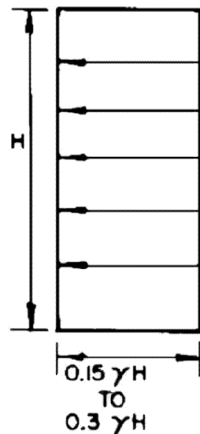
Figure 13-31: Typical Cross-Section of Tieback System

SANDS



Where deformations are critical and tie-backs are prestressed to 100% of design load, compute pressure based on at-rest conditions. Use $K_0 = 0.4$ for dense sand, and $K_0 = 0.5$ for loose sand.

STIFF TO VERY STIFF CLAY



Use pressure ordinate to produce the same force as for braced excavation. 0.3 is applicable for stability number of about 4, and 0.15 is applicable when stability number is less than 4. Use design procedure as in Figure 26.

Figure 13-32: Pressure Distribution for Tied Back Walls

"Skyline is all you need"

SKYLINE

Skyline Steel, LLC

Best of ALL Worlds

"There's one near you"

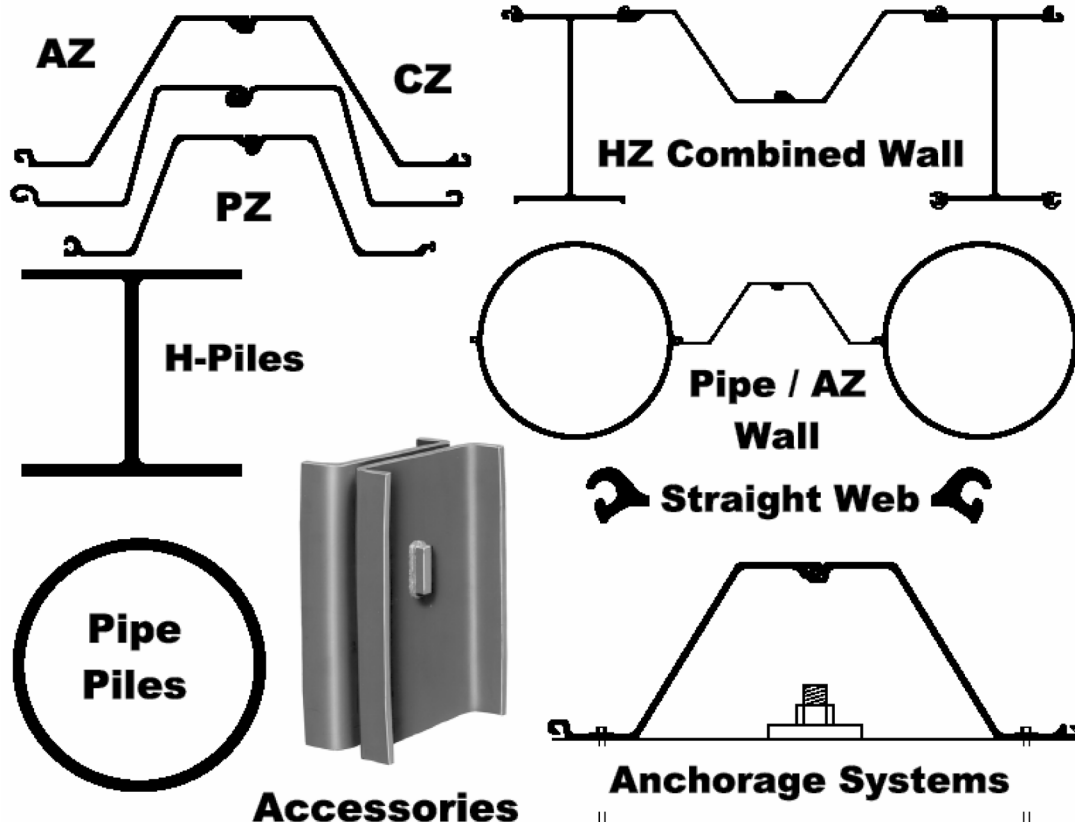
- General Catalog
- HZ Steel Wall System
- Product Datasheets
- Anchorage Systems
- Installation of Steel Sheet Piles
- Impervious Wall: Part 1 Design
- Impervious Wall: Part 2 Practical Aspects
- Impervious Wall: Movie
- Project Planning
- Prosheet Design Software
- Sheet Piling Durability Analysis
- HZ / AZ Stresses
- Autocad Sections
- Contact Us

Technical Hotline
1-866-8Skyline
1-866-878-9546

Corporate
(973) 428-6100

Call for an office near you.

1-866-8Skyline www.skylinesteel.com



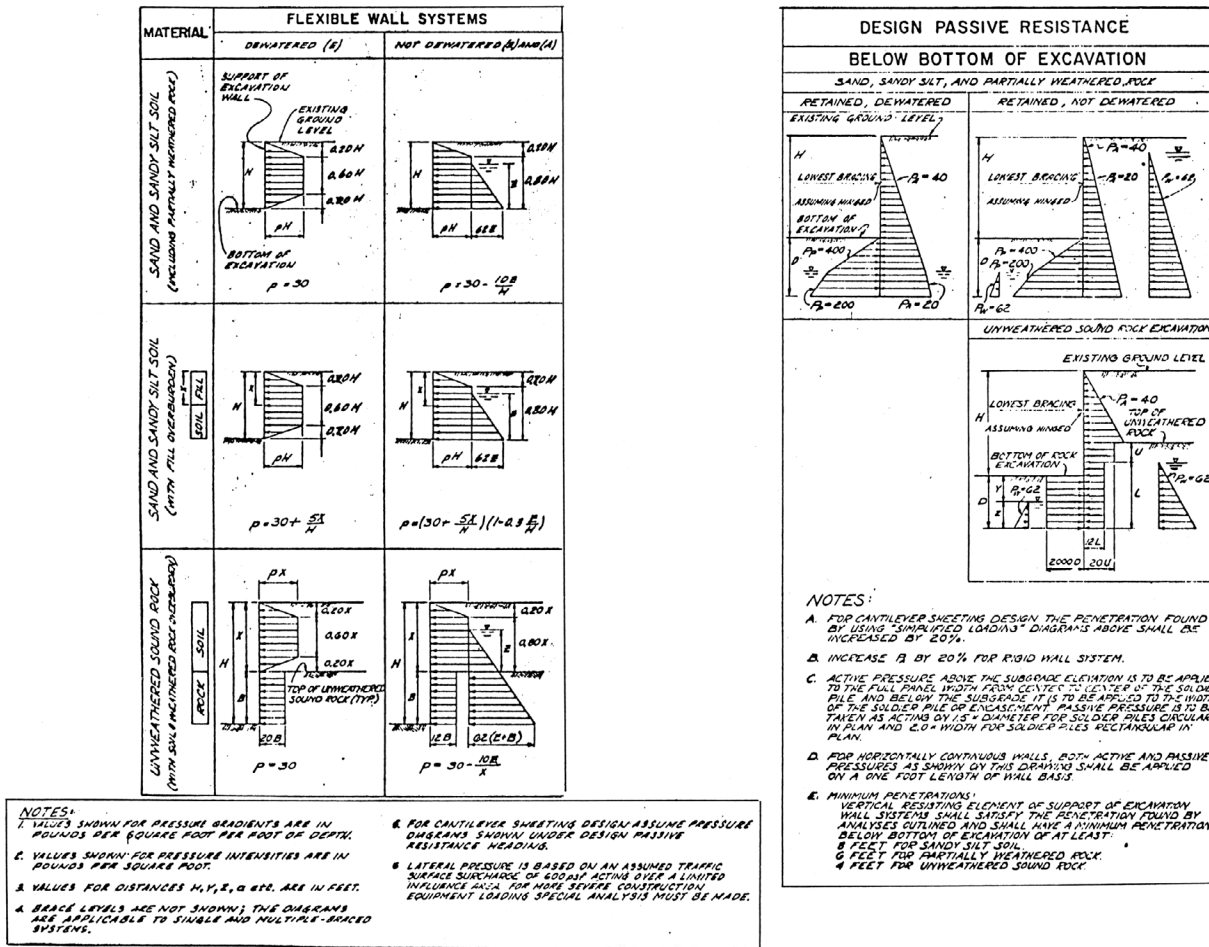


Figure 13-33: Lateral Pressure Distribution for Deep Cut-and-Cover Tunnelling

diameter pipe into the ground at the desired angle. A pneumatic drifter will drill a 3 to 6 inch diameter rock socket approximately 10 to 25 feet deep from the same rig that drove pipe. Prior to installing tendon tiebacks, an air or water jet cleans the holes in rock. Quick drying, nonexpanding grout is installed by gravity flow. The tiebacks are then prestressed with hydraulic jacks to about 25% higher than their working stress. The working stress is equal to about 50% is ultimate strength.

The allowable design load on the prestressed tiebacks can be estimated using the bond strength between the rock or soil and the cement grout. Consideration must be made for the highest possible pore water pressure conditions. Also, the steel sheet piling must be driven to rock or into soil that is able to withstand the downward compressive stress exerted by the tieback system. This may limit distance x in Figure 13-31. A more detailed discussion is provided in 11.3.

13.6. Deep Open Cut Excavations

Since the mid-1960's, a number of large North American cities including Toronto, Washington, Atlanta and San

Francisco have built underground transportation systems utilizing deep open cut or cut and cover construction methods. The design standards established for the required retaining structures evolved from project to project based on prior experience. The standards include pressure diagrams for various soil and groundwater conditions and surcharges. Both rigid and flexible wall systems were utilized as well as internally braced and externally tied support systems. Steel sheet piling is included among the flexible wall systems.

The good experience from these projects provides a useful reference for other proposed projects. A sample design lateral pressure profile (in this case from Atlanta's MARTA system) is shown in Figure 13-33. It is included here for comparison with other methods described in this handbook.¹⁴⁷

Several items are to be noted in the approach to earth pressure calculations utilized by designers of these projects:

A uniform load of 600 psf effective from the edge of the excavation to a distance 12 ft. behind accounts for traffic, routine construction operations, materials storage etc. Concentrated loads from point or line loads are ref-

¹⁴⁷ A more complete review of cut and cover methods and lateral pressure in deep cuts can be found in *Earth Support Systems and Retaining Structures*, available from Pile Buck. The sample distribution shown is also taken from this work.

erenced but not specifically addressed. It should be noted that the uniform surcharge load extends only a limited depth rather than to full depth assumed in bulk head design.

The pressure diagrams are generally assumed to take a trapezoidal shape rather than the rectangular shape proposed by Peck as shown in *Figure 13-2(a)*. Total loads probably exceed Peck's suggested values, however distribution against the top wales may differ only slightly.

Emphasis is placed on the safety of the bracing system rather than the membrane wall in both pressures used for design and allowable stresses. This emphasis is based on experience with measured loads, failures, and the critical elements of these support systems.

13.7. Notes Regarding Braced Cofferdams

Overexcavation below proposed bracing levels should be carefully controlled in that additional load may be imposed on previously installed elements and excessive deflections may result. Bracing removal as the permanent work rises must also be carefully planned, and this procedure may occasionally be a major factor in determination of the support member sizes.

Sheet pile walls have the advantage of reasonably maintaining ground water levels outside the excavation if that is nec-

essary. The development of passive resistance in certain soils exceeds the capacity of soldier piles. Sheet piling may be driven deep enough to prevent boiling of the bottom where an unbalanced ground water head exists.

Sheets should be blocked against the wales where alignment against the complete wall cannot be maintained.

High strength steel is useful in bracing systems. Fabrication is generally best accomplished in a shop rather than the field. While wide flange structural steel is usually used for wales and struts, pipe has some advantage for the type of loads carried by struts and has been used extensively.

Preloading of a completed bracing level helps control inward deformation that will occur following additional excavation. This action also is beneficial for controlling stresses from extreme temperature variations.

In deep open cut or cut and cover subway work, bracing sets are usually placed a few feet above each slab level (base slab, intermediate slabs and roof) with a maximum distance between supports of 16 feet (depending on ground conditions).

When removing bracing, the wall support must be adequate for the worst construction condition: between any last bracing level and the excavated bottom during excavation, or between a slab and the next higher bracing level during concreting.

Chapter Fourteen: High Modulus Walls

There has been an increasing demand for sheet piling with the strength to resist the high bending moments associated with deep-water construction. The introduction of Z-shaped sheet piles during the 1920's was the first step toward meeting those requirements. The largest Z-type piles manufactured today provide section modulus values of about 80 in³/ft of wall. When combined with Grade 50 steel, these sections produce a resisting moment of about 2.6 million inch-pounds/ft of wall, good for about 40 feet of water depth under average circumstances. These Z-piles are about the limit for existing mill facilities without expensive and probably impractical improvements.

There are several ways to handle deep water or heavy surcharge loads when designing sheet pile bulkheads. A relieving platform on piles to carry surcharges and overburden is one possibility. The platform can be designed as a low level structure behind the sheet pile face wall, or as a high level platform with the sheeting acting as a cut-off wall behind the platform

Cellular cofferdam bulkheads are another method of constructing deep-water facilities. This system has been used in many port and dry-dock projects where water depths exceeded the practical limits of anchored sheet piling walls. This solution has some drawbacks in relative material and construction costs, in addition to a problem of curved facing.

A closed-faced, anchored bulkhead wall may still be the desirable type under many circumstances. When the available sheet piling sections are inadequate for the anticipated loads and bending moments, there are several traditional and newer methods for increasing the section modulus of the proposed wall.

14.1. Piles Reinforced with Cover Plates

Welding plates to the flanges can increase the section modulus of rolled structural beams. The same approach can be taken with steel sheet piling. This has been a common method for handling higher bending moments for many years. Reinforcing plates can be long enough where the bending moment exceeds the capacity of the plain sheet. The weight of the wall becomes an average of plain and reinforced section weight. Section modulus can be doubled if necessary with high strength plates adding to the efficiency. Because of extra costs associated with fabrication, it is generally more practical to reinforce the heavier Z-shapes rather than to reinforce the lighter Z-shapes to do a job that a heavier plain shape could do¹⁴⁸. Cover plate dimensions will be governed by the space available to attach them to the piling flanges. Plate thickness should probably range from 1/4" to allow good welding, and a maximum limit based on the thickness of the base material. Plates are normally not available in standard sheet piling grade A-328; therefore, structural grades

ASTM A-36 or A-572 are selected. Fillet welds should be continuous and the plate ends also sealed. Flange plates are best attached in a fabricating shop under controlled conditions. It is important to avoid distortion of the piling section by proper attention to the sequencing of the welding. At some loss in efficiency, cover plates can be installed on the inside of flanges if their presence on the outer face is objectionable. Most manufacturers publish section properties for reinforced sheet piling and most can supply these units fabricated. Field fabrication is possible, however the manufacturer should be consulted regarding procedures.

As with any welded structure, the strength of the structure is dependent upon the strength and quality of the welds. One inferior quality weld can lead to the loss of a cover plate, which in turn reduces the effective section modulus of one part of the wall, and ultimately the entire wall. Fabrication is best performed in a welding shop under controlled conditions to insure proper welding quality and to control warping and shrinkage.

14.2. Master Piles, King Piles And Box Piles

The moment resisting capacity of sheet piling can be increased significantly by the inclusion of heavy structural elements such as wide flange beams or box sections. There are a number of methods for accomplishing this.

14.2.1. Master Piles

A master pile system combines the high moment capacity of wide flange beams with cellular design advantages. Straight web sections or parts are welded to the beams to provide interlocks. Master piles are spaced from about 6 to 10 feet apart depending on the straight(or shallow arch) section used. Soil pressures are transferred from the intermediate arcs to the wide flange beams by hoop tension, loading them as beams. Tension in the interlocks is theoretically based on the radius of the draped arc. When master piles are spaced as close as six feet, soil arching probably transfers load directly to the master piles rather than through the sheet pile arcs. Section modulus of the wall can safely be based on the moment resisting properties of the master pile. Master pile systems are more costly than some other high modulus systems now available and usage has been declining.

14.2.2. Arc Buckstay Walls

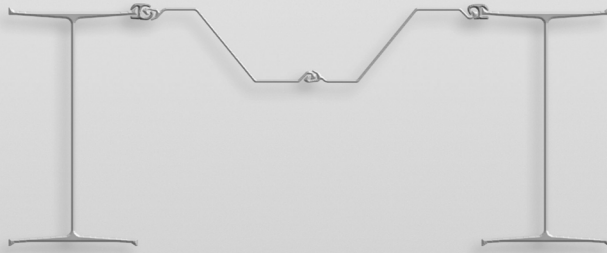
A traditional but infrequently used master pile system utilizes wide flange beams in combination with flat or shallow- arch sheet piling. The regular sheet piling is designed to assume an arc shape under load so that the sheets do not go into bending but transfer loads to the master pile by tension across the interlocks. The radius of the arc is limited by the

¹⁴⁸This may not be true in all circumstances.

800.848.6249 www.fosterpiling.com

COMBI-WALL SYSTEMS HZ or PIPE Z AVAILABLE

- Deep Draft Application
- High Strength
- Appropriate for Difficult Soil Conditions
- Flexible Design Solution
- Interchangeable with Other Designs



 **Foster**
Piling
A Division of L.B. Foster Company



minimum interlock strength of the sheets, similar to cellular design. The wide flange master pile carries all transferred loads from the arcs connecting to it acting as a beam. Both water and land cofferdams and also permanent deep-water marine facilities have been built with this method. It is a relatively expensive design due to the fabrication costs and the potentially more difficult installation procedures.

Individual anchors are generally attached to each master pile by plates and clevis welded to the web returning to an anchor wall or pile A-frame. Average wall section modulus values of up to about 200 in³/foot of wall can be obtained with this method. This system lends itself well to sites where high rock and deep water preclude more conventional methods, since the master piles can be dropped into pre-bored holes in the rock and grouted in. Both water and land cofferdams and also permanent deep-water marine facilities have been built with this system. Fabrication costs and the need for special installation techniques have limited utilization of this method to special situations

14.2.3. Z-type Master or King Pile Walls

Wide flange beams can be fitted with interlocks stripped from Z-type sheet piling and combined in walls using Z-type piles as intermediates. This system depends on soil arching action for its assumptions regarding wall section modulus. By limiting spacing of master piles to about five feet, soil pressures are transferred to the strong point by arching rather than application to each individual foot of wall. With this assumption, the wall strength can be averaged between the wide flange master or king piles and the lighter intermediate Z-piles. General practice is to use heavy wide flange beams that take the majority of the load and lighter-weight Z-type intermediate piles. The wide flange master piles can be reinforced with flange plates in critical areas to provide some saving in weight rather than using a heavier section. Section modulus values of up to 280 in³/foot of wall can be obtained with this method. The section modulus/weight efficiency of this system is about 3 compared to about 1.3 for heavyweight plain Z-type sheet piling. This is helpful when considering

the additional cost of fabrication of the king piles, however this system may not be fully competitive with similar systems that do not require fabrication.

14.2.4. Box Piles

Box piles are an assembly of several sheet pile sections into a box shape with very high section modulus. The box retains the interlocks of some of its parts so that the box pile can be interlocked with similar plain sections to form a continuous wall. Welding and/or bolting plain sections together fabricate the boxes. There are a number of basic designs.

Some producers offer box piles as a standard catalogue item and publish section modulus and other properties for them. Box piles function in combination walls similar to master or king piles. Box piles are also introduced into walls where the wall must also carry vertical loads. Because of the large radius of gyration of boxes, these units make excellent columns or bearing piles. In certain cases, steel box piles may be cleaned-out and filled with concrete for greater vertical bearing capacity. When used to support vertical loads and also as king piles in a wall, combined stresses must be taken into account in design. Box piles have not been used extensively in North America. Generally, steel H-piles or other pile types were used for vertical loads, separate from the wall function

14.2.5. Pipe Sections

Large diameter pipe has been designed for use as sheet piling by some East Asian producers. Interlocks have been “borrowed” from sheet pile sections, welded to the pipes and assembled to make walls with very high section modulus. In another design, smaller diameter pipes are welded to the larger pipes, slit longitudinally, and used to interlock two pipe sections together in a type of interlock. These large pipe piles could be excavated out and filled with concrete to increase strength and also provide some additional service life where severe corrosion might be a factor. The pipe system has not been used in North America.

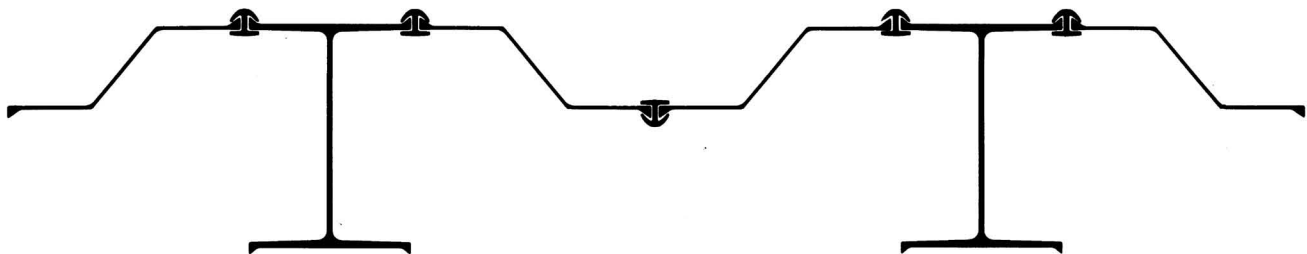


Figure 14-1: HZ Wall System

¹⁴⁰A similar system is also offered by Peine Salzgitter of Germany.

14.3. HZ Wall Systems

ProfilArbed S.A., Luxembourg, introduced the HZ system for high modulus wall construction in the mid-1970s¹⁴⁹. The elements of this system consist of wide flange (HZ) shapes, Z-type (ZH) shapes and H-shaped bar connector sections (RH). The flanges of the HZ and ZH shapes contain bulb shaped enlargements that provide the male portion of an interlock. The special connector (RH) provides two sockets that are the means for joining HZ shapes to each other, or HZ shapes to ZH shapes to form continuous walls. A plan view of this system is shown in Figure 14-1.

The HZ beams are currently available in depths of from 14 – 39 inches, providing a range of section modulus values of from about 130 – 600 in³ /foot of wall when these are interlocked continuously. A more commonly used system consists of a combination of wide flange HZ master piles with intermediate pairs of ZH piles. This arrangement offers section modulus values of from 36 up to about 300 in³ foot of wall. All elements of the HZ Wall System are standard, hot-rolled mill items from the manufacturer. This feature would tend to offer potential economic advantages over fabrication as a means of increasing wall strength.

14.3.1. Design

HZ walls have proven to be advantageous for very deep land or water based cofferdams and deep-water marine bulkheads where standard sheet piling would not meet strength requirements. Procedures similar to those used for conventional sheet pile wall analysis can be utilized. The most rigid wall would consist of a continuously joined series of HZ sections. RH connectors used for joining these sections can contribute to the section modulus of the wall if welded to the HZ pile. The wide flange HZ sections are also efficient columns or bearing piles and are often introduced into a wall to carry vertical loads.

Combination walls using HZ piles as master piles and ZH sections as intermediate sheets are a more common design. This arrangement employs one or two HZ sections alternating with a pair of ZH piles to form a panel section. By limiting the spacing of master piles to about five feet, the light intermediate sections function more as containment or curtain wall and loads attributed to the panel are transferred to the master pile by soil arching¹⁵⁰.

Section Modulus values for various combinations of HZ shapes and intermediate ZH sections are provided in the manufacturer's literature. The moment of inertia of a combined wall is the sum of the moments of inertia of the parts divided by the panel width, or

$$\text{Equation 14-1: } I_{wall} = \frac{I_{HZ} + I_{ZH} + I_{RH}}{B_{panel\ width}}$$

Also, the section modulus of the wall is

$$\text{Equation 14-2: } S_{wall} = \frac{I_{wall}}{v}$$

where v = the distance from the neutral axis of the panel to the outer fibre of the HZ section. Stresses in the intermediate ZH section are proportional to their contribution to the section modulus of the total and are always less than forty percent of stresses in the HZ shape. All passive pressure is transferred to the master pile as if the wall were continuous to the full depth of the master piles. The intermediate ZH piles are generally terminated at some elevation below the zero pressure point after allowing a safety factor for over dredging or seepage.

HZ piles may be reinforced with welded cover plates in critical areas to provide additional section modulus. The cost of fabrication must be weighed against the potential savings in weight.

Where water pressure is the dominant active pressure, particularly with water-based cofferdams, the assumptions regarding proportioning of the load on various elements of the system will not apply. Stresses in intermediate ZH sections could exceed safe values and such sheets might require reinforcement as well as additional penetration to offset head differential considerations. Continuous box walls of interjoined H-sections are generally required.

14.3.2. Anchor Systems for HZ Walls

HZ walls may be anchored by conventional wales and tie rods, or more conveniently by providing each HZ master pile with a tie rod attached to HZ sections by welding plates to the web through slits in the flanges and joining the tie rod using a clevis and pin connection. HZ wall are also supported with earth or rock anchors or battered H-pile anchors where conditions favour those systems. The HZ is particularly well designed to take the downward component from an angled tie-back, when it has been driven to sufficient bearing capacity

14.3.3. Design Procedures for HZ and King Pile Systems

Design of retaining walls and bulkheads can be carried out by conventional methods such as free earth or fixed earth support. The minimum penetration depths required for stability will be applied to the master piles as if the entire wall was to be driven to this depth. The usual safety factors should be applied. If intermediate piles are used between master sections, they need only be driven to the zero pressure point below the dredge line with a safety factor for overdredging.

Bending moments are determined in the usual way and satisfied by reference to the manufacturers tables for section modulus. Moment reduction procedures (such as Rowe's) should not be utilised for king pile systems since these are relatively stiff structural members. Moment reduction is based on pile flexibility. It may be practical to compare both free and fixed earth support methods for the most economical solution.

Cofferdams retaining water should not be proportioned by the same assumptions used for soil (which transfer all horizontal loads to the master pile). These structures should be designed for uniform loading across the width of the wall that

¹⁵⁰This is an old concept similar to soldier beam/timber-lagging type construction for temporary retaining walls.

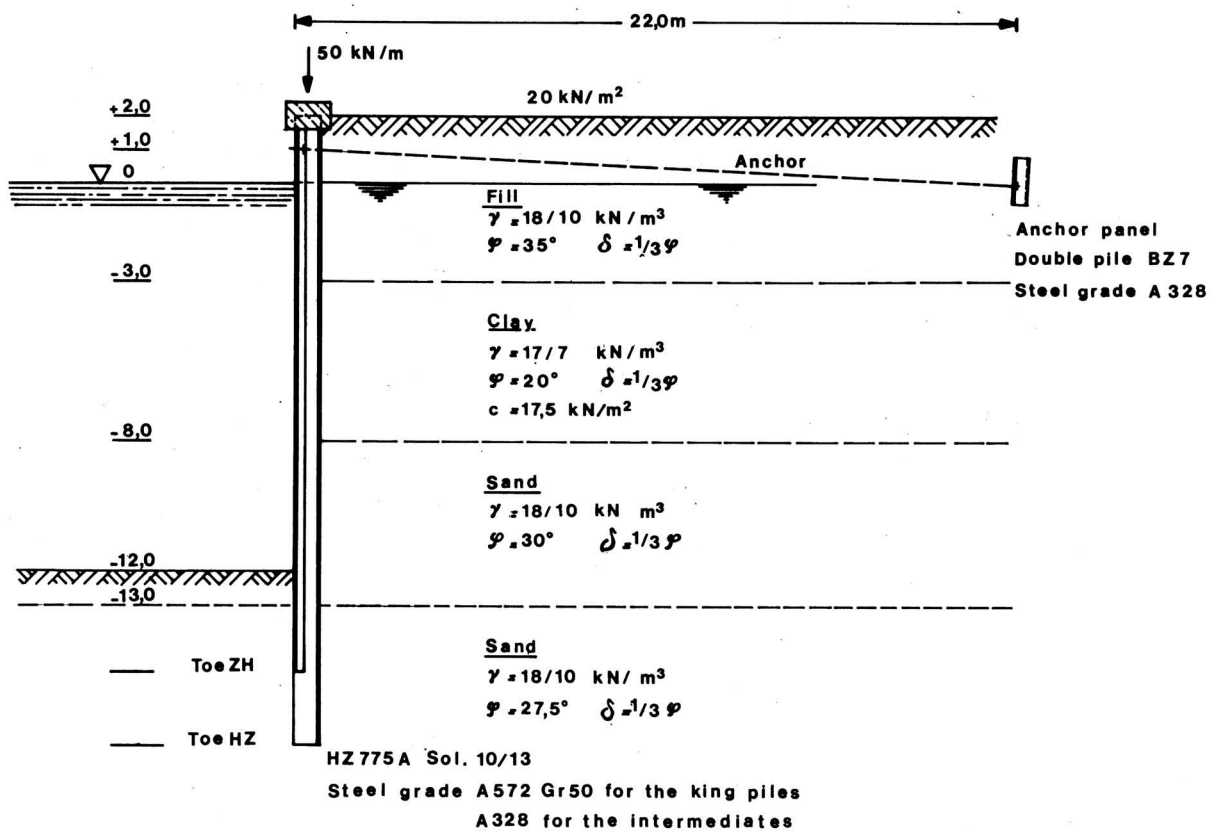


Figure 14-2: HZ Wall For Example 24

negates the use of a master pile system but not the use of the master piles continuously joined if required.

Example 24: HZ Wall Design

This example has two purposes: a) to show the design of an HZ wall, and b) to show the use of mixed cohesive and cohesionless soils.

❖ Given

- o Wall as shown in Figure 14-2
- o Lateral earth pressure coefficients (Coulomb model) are as follows:
 - Fill Layer, 0-5 m: $K_a = 0.246$, $K_p = 5.563$
 - Clay Layer, 5-10 m: $K_a = 0.455$, $K_p = 2.398$
 - Sand Layer, 10-15 m: $K_a = 0.304$, $K_p = 4.080$
 - Sand Layer, > 15 m: $K_a = 0.337$, $K_p = 3.539$
- o HZ 775A system used with AZ 18 sheets. The distance from the centreline of one H pile to another in this case is 1790 mm.

❖ Find

- o Depth of toe HZ
- o Whether the section is suitable for the HZ wall configuration specified
- o Outline of the anchor design

❖ Solution

- o We first analyse this wall with SPW 911, using the free earth support method. The results are shown in Figure 14-3.

There are several important things to note about this result, which are as follows:

- SPW 911 uses the concept of “minimum equivalent fluid pressure” or “minimum fluid density” with cohesive soils. This forces the analysis to consider a minimum load, even when a purely cohesive soil will result in a zero load on the wall. This is most important to consider for permanent works. In this example, we assume it to be 3 kN/m³ (SPW 911 default is 5 kN/m³).
- SPW 911 normally uses bulk density in cohesive soils and assumes the limit of water pressure in cohesive soils is the depth where hydrostatic pressure = soil pressure. Effectively, this means the pressure is the higher value of the hydrostatic pressure and the soil pressure. SPW 911 also treats water above the layer as additional overburden and deducts the buoyancy of the layer when you move into granular material below the layer. Although this assumption can be used, in this case we opted to allow the lateral earth pressure below the mixed layer (at 10m) to remain the effective stress times the Coulomb active lateral earth pressure coefficient. This was done by setting the cohesion in the clay layer to zero but keeping the calculated earth pressure coefficients the same.
- The maximum anchor pull is 196 kN/m.
- The maximum moment is 1012.5 kN-m/m of wall just



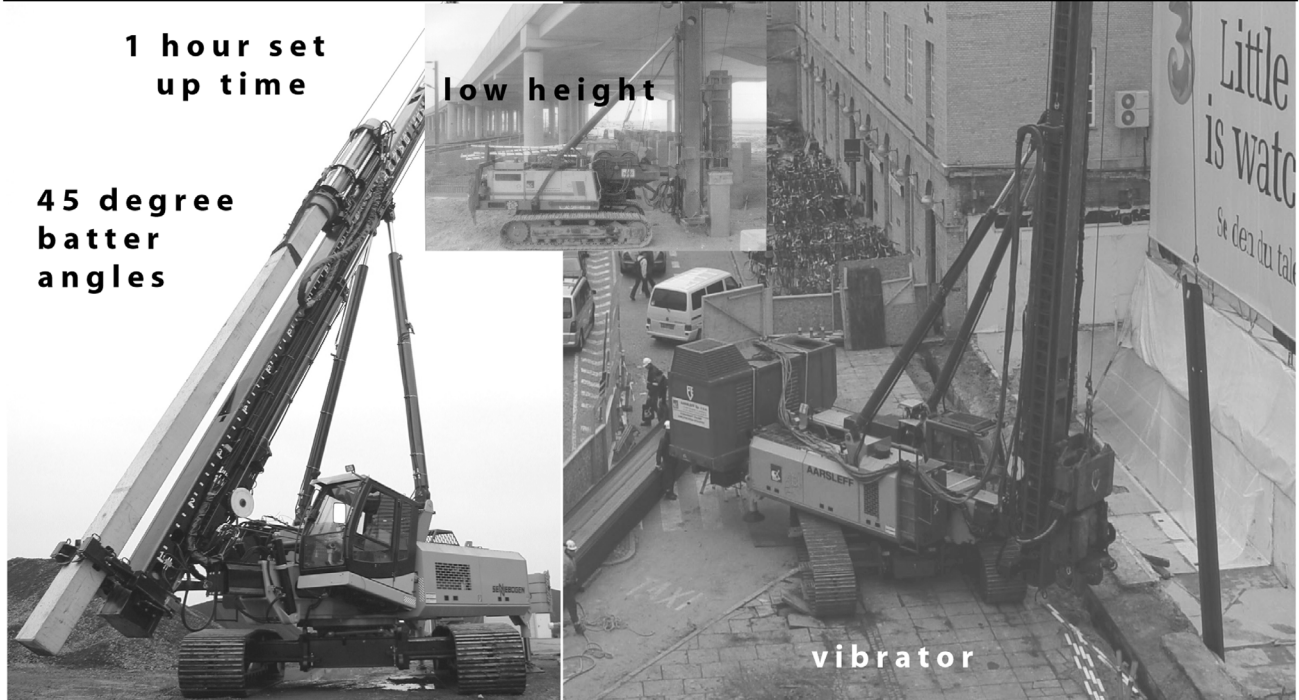
BANUT PILE DRIVING RIGS

large batter angles, 60ft stroke
impact precast piles, beams, casings & more
vibrate beams, casings & more
pre-drill, drill piles, drill out casings & more

CAN YOU DRIVE 80 PILES, 40FT LONG/ DAY ?



OUR CUSTOMERS HAVE, WITH A BANUT RIG!



HAMMER & STEEL, INC
(WEST COAST)
TOLL FREE: 877-224-3356
www.abi-delmag.com

CALL FOR SALES & RENTALS

HAMMER & STEEL, INC
(MID-WEST & EAST COAST)
TOLL FREE: 800-325-7453
www.hammersteel.com

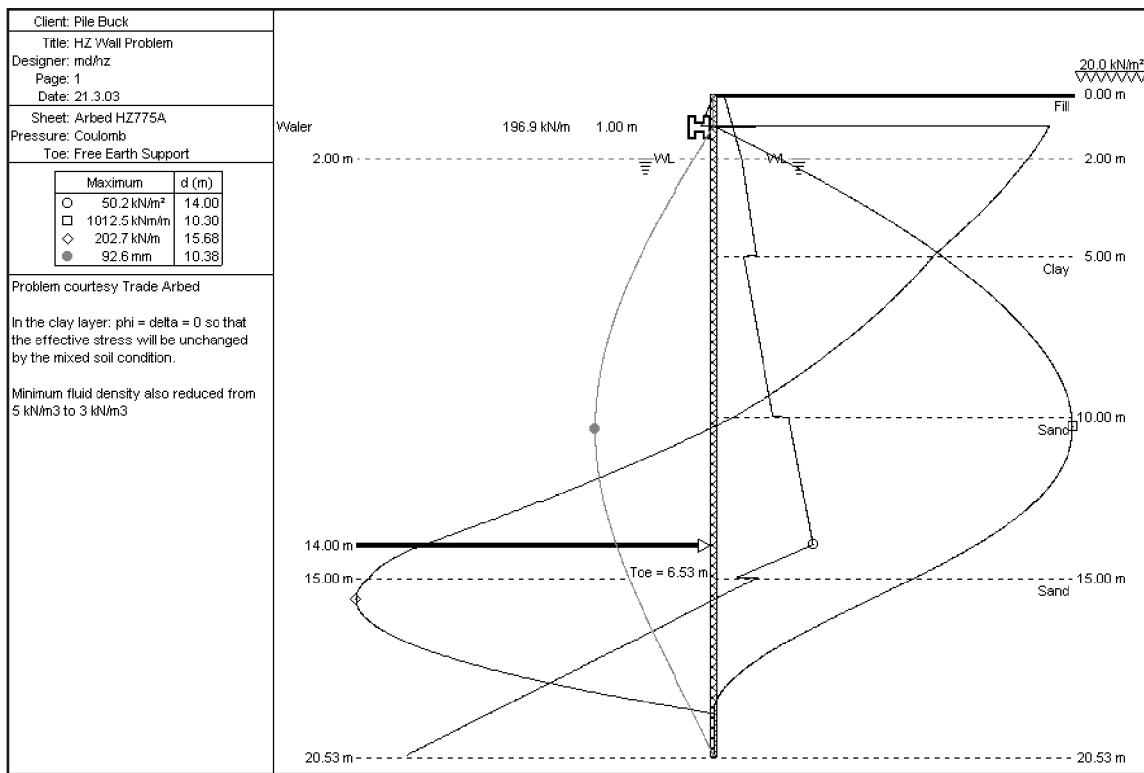


Figure 14-3: SPW 911 Results for Example 24

below the clay layer. However, because of the presence of axial loading of the wall, which SPW 911 does not analyse, we will need to investigate further the stresses. This is where the deflection result of 92.6 mm becomes important to us.

- The toe needs to be 20.53 m below the top of the wall. SPW 911 was run using full passive coefficients and a factor of safety of 2.
- It should be noted that, although SPW 911 usually assumes a uniform cross-section along the length of the sheet, in most cases the AZ sections are shorter than the HZ ones. This is not a problem so long as the foreshortening of the AZ sections does not extend into high moment areas of the sheet.
- o Compute the actual maximum stress in the wall, considering the axial loading.
 - The axial load of 50 kN/m of wall actually is borne only by the H-piles. Thus, the axial load on each pile is $P_{axial} = (50)(1.79) = 89.5 \text{ kN}$.
 - The maximum stress in the wall (considering the axial load) is given by the Equation 2-3. The variables for this are as follows:
 - P_{axial} = axial load on each H pile, kN = 89.5 kN
 - A_{axial} = cross-sectional area of the H pile = .02579 m²
 - δ_{max} = maximum deflection, m = 0.0926 m
 - S_{wall} = total section modulus of the wall, m³ /m of wall = .00477 m³ /m of wall
 - ep = eccentricity of the load = 0

- Substituting these variables into the equation yields $\sigma_{max} = 217.6 \text{ MPa}$, which is below the allowable stress of the steel of 240 MPa. So the design is acceptable.
- o Anchor Design. We have shown elsewhere in detail anchor design procedures; we will simply sketch out the results of the same kinds of calculations we have elsewhere.
 - Tie rod spacing. The nature of HZ walls dictates the spacing of the tie rods, which is the same as the spacing of the H beams, or 1790 mm.
 - Sheet pile anchor. Figure 14-2 shows the anchor 22 m back from the wall. It also shows the anchor not to reach the surface. If we assume that the anchor does in fact reach the surface, if we sum forces, the anchor wall needs to be 3.1 m deep; for a summation of moments, the anchor must be at least 3.2 m deep, which becomes the controlling value. In both cases we have increased the anchor load by the usual factor of 1.3. Even with our assumption that the anchor reaches the surface, we can (as we have done elsewhere) trip the top of the anchor without significant effect on the anchor capacity. The drawing also shows a slight incline of the anchor rod, but since this angle is small we neglected its effect.
 - Concrete slab anchor. Using Ovesen's Method ($K_v = 5$, $\xi = 0.362$), we first assume that the bottom of the anchor is 3 m below the surface and that the anchor is 2.5 m high. From this we determine the following:
 - $P_H = 137 \text{ kN/m}$

- $R_o = 4.73$
- $T_o = 647.9 \text{ kN/m}$
- $G_w = 115 \text{ kN/m}$
- $F_A = -26 \text{ kN/m}$
- We will use 50 cm for our slab thickness. A structural analysis of the anchor slab is recommended. The minimum cover for reinforcement should be 7 cm.
- $MH = 169.7 \text{ kN-m/m}$
- $Z_o = 1.41 \text{ m}$
- $Z = 1.25 \text{ m}$. This means that the optimum place-

ment of the tie rod is 1.25 m above the base of the slab, or 1.75 m below the surface.

Of the four values of L we normally analyse, the one with the factor of safety nearest 2 but not lower than that is 0.5, where $FS_{\text{Ovesen}} = 2.1$.

- Again increasing the computed anchor load by the factor of 1.3, for steel with an allowable strength of 270 MPa, the minimum tie rod area is 0.0017 m^2 , thus the minimum diameter is 46 mm; we should use 50 mm diameter tie rods.

Chapter Fifteen:

Cellular Cofferdams

Cellular cofferdams, in most instances, serve as a high head or moderately high head dam for extended periods of time, protecting personnel, equipment, and completed work and maintaining the navigation pool. Planning, design, and construction of these structures must be accomplished by the same procedures and with the same high level of engineering competency as those required for permanent features of the work. Adequate foundation investigation and laboratory testing must be performed to determine soil and foundation parameters affecting the integrity of the cofferdam. Hydraulic and hydrologic design studies must be conducted to determine the most economical layout.

The analytical design of cellular cofferdams requires close coordination between the structural engineer and the geotechnical engineer. Close coordination is necessary, not only for the soil and for foundation investigations noted above, but also to ensure that design strengths are applied correctly and that assumptions used in the design, such as the saturation level within the cell fill, are realistic. Though cofferdams are often referred to as temporary structures, their importance, as explained above, requires that they be designed for the same factors of safety as those required for permanent structures.

To ensure compliance with all design requirements and conformity with safe construction practices, the cellular cofferdam construction should be subjected to intensive inspection by both construction and design personnel. Periodic and timely visits by design personnel to the construction site are required to ensure that:

- Site conditions throughout the construction period are in conformance with design assumptions, contract plans, and specifications;
- Project personnel are given assistance in adapting the plans and specifications to actual site conditions as they are revealed during construction; and
- Any engineering problems not fully assessed in the original design are observed and evaluated, and appropriate action is taken.

Coordination between construction and design should be sufficient to enable design personnel to respond in a timely manner when changed field conditions require modifications of design.

The design of the dewatering system, generally, will be the responsibility of the contractor so that the contractor can utilize his particular expertise and equipment. However, the dewatering system must be designed to be consistent with the assumptions made in the cofferdam design, including the elevation of the saturation level within the cell fill and the rate of dewatering. To achieve this, the requirements for the dewatering

system must be explicitly stated in the contract specifications, and the contractor's design must be carefully reviewed by the cofferdam designer to ensure that the intent and provisions of the specifications are met.

15.1. Planning, Layout and Elements of Cofferdams

15.1.1. Areas of Consideration

For a construction cofferdam to be functional, it must provide a work area free from frequent flooding and of sufficient size to allow for necessary construction activities. These two objectives are dependent on several factors and are interrelated as described below.

15.1.1.1. Height of Protection

The top of the cofferdam should be established so that a dry working area can be economically maintained. To establish an economical top elevation for cofferdam and flooding frequency, stage occurrence and duration data covering the practical range of cofferdam heights must be evaluated, taking into account the required life of the cofferdam. Factors that affect the practical range of cofferdam heights include:

- Effects on channel width to accommodate stream flow and navigation where required;
- Increased flow velocity during high river stages and the resultant scour; effects on completed adjacent structures to which the cofferdam joins (the "tie-in"), i.e., these structures must be designed to resist pools to top of cofferdam; and
- Practical limitations on the size of cell due to interlock stresses and sliding stability.

By comparing these factors with the effects of lost time and dewatering and cleanup costs resulting from flooding, an economical top elevation of cofferdam can be established.

15.1.1.2. Area of Enclosure

The area enclosed by the cofferdam should be minimized for reasons of economy but should be consistent with construction requirements. The area often will be limited by the need to maintain a minimum channel width and control scour and to minimize those portions of completed structures affected by the tie-in. The minimum area provided must be sufficient to accommodate berms, access roads, an internal drainage system, and a reasonable working area. Minimum functional area requirements should be established in coordination with construction personnel.



“Having three ICE pile driving tools at hand gave us the flexibility to complete this difficult project without any delay”

W. “Junior” Hager, Piledriving Superintendent, Hal Jones Contractor, Inc.

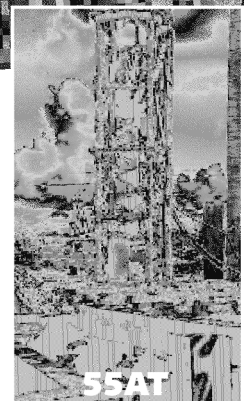
PROJECT: Civil and Marine Ltd.'s new \$30 million ground granulated blast furnace slag (GGBFS) processing facility a Port Canaveral, Florida, the world's first quadramodel (land, sea, air and space) transportation facility.

CONTRACTOR: Hal Jones Contractor, Inc.

JOB REQUIREMENTS: Drive the foundation piling for the facility - a total of 165 24"-square reinforced precast concrete piles. The project called for 50 piles to support each of the two slag silos and 65 piles to support the foundation of the main grinding mill and office.

EQUIPMENT USED: ICE Model 44-50 Vibratory Driver/Extractor; ICE Model 55AT Auger; ICE Model 220 Hydraulic Impact Hammer; two ICE power units; two 80' sets of ICE leads; Linkbelt crawler crane.

JOB STATUS: Completed without delay.



**INTERNATIONAL
CONSTRUCTION
EQUIPMENT, INC.**
www.iceusa.com

301 Warehouse Drive • Matthews, NC 28104
Phones: 888 ICEUSA1
& 704 821-8200
Fax: 704 821-8201 • e-mail: info@iceusa.com

TECHNO DRILL 

Matthews NC • Lakeland FL • Metairie LA • Seattle WA • New Town Square PA • Sayreville NJ • Houston TX
Fort Wayne IN • Virginia Beach VA • Boston MA • Montreal Quebec • Singapore • Kuala Lumpur • Shanghai

15.1.1.3. Staging

When constructing a cofferdam in a river, the flow must continue to be passed and navigation maintained. Therefore, the construction must be accomplished in stages, passing the water temporarily through the completed work, and making provisions for a navigable channel. The number of stages should be limited because of the costs and time delays associated with the removal of the cells in a completed stage and the construction of the cells for the following stage. However, the number of stages must be consistent with the need to minimize stream flow velocities and their associated effects on scour, stream bank erosion, upstream flooding, and navigation. When developing the layout for a multistage cofferdam, special attention should be given to maximizing the number of items common to each stage of the cofferdam.

With proper planning some cells may be used for two subsequent stages. In those cells that will be common to more than one stage, the connecting tees or wyes that are to be utilized in a future stage must be located with care.

15.1.1.4. Hydraulic Model Studies

Hydraulic model studies are often necessary to develop the optimum cofferdam layout, particularly for a multistage cofferdam. From these studies, currents that might adversely affect navigation, the potential for scour and various remedies can be determined.

15.1.2. Elements of Cofferdams

15.1.2.1. Scour Protection

Flowing water can seriously damage a cofferdam cell by undermining and the subsequent loss of cell fill. Still further, scour caused by flowing water can lead to damage by increased underseepage and increased interlock stresses. The potential for this type of damage is dependent upon the velocity of the water, the eddies produced, and the erodibility of the foundation material. Damage can be prevented by protecting the foundation outside of the cell with riprap or by driving the piling to a sufficient depth beneath the anticipated scour. Deflectors designed to streamline flow are effective in minimizing scour along the face of the cofferdam. These deflectors consist of a curved sheet pile wall, with appropriate bracing, extending into the river from the outer upstream and downstream corners of the cofferdam. *Figure 15-1* shows a schematic deflector layout. As noted previously, hydraulic model studies are useful in predicting the potential for scour and in developing the most efficient deflector geometry.

15.1.2.2. Berms

A soil berm may be constructed inside the cells to provide additional sliding and overturning resistance. The berm will also serve to lengthen the seepage path and decrease the upward seepage gradients on the interior of the cells. However, a berm will require a larger cofferdam enclosure and an increase in the overall length of the cofferdam, and will increase construction and maintenance costs. Also, an inside berm inhibits inspection of the inside piling for driving damage and makes cell drainage maintenance more difficult. It is generally advisable, therefore, to increase the diameter of the cells instead of constructing a berm to achieve stability since the amount of piling per lineal foot of cofferdam is, essentially, independent of the diameter of the cells. Any increase in the diameter of the cells must be within the limitations of the maximum allowable interlock stress. In order for a berm to function as designed, the berm must be constantly maintained and protected against erosion and the degree of saturation must be consistent with design assumptions.

15.1.2.3. Flooding Facilities

Flooding of a cofferdam by overtopping can cause serious damage to the cofferdam, perhaps even failure. An overflow can wash fill material from the cells and erode berm material. Before overtopping occurs, the cofferdam should therefore be filled with water in a controlled manner by providing floodgates or sluiceways. The floodgates or sluiceways can also be used to facilitate removal of the cofferdam by flooding. Floodgates are constructed in one or more of the connecting arcs by cutting

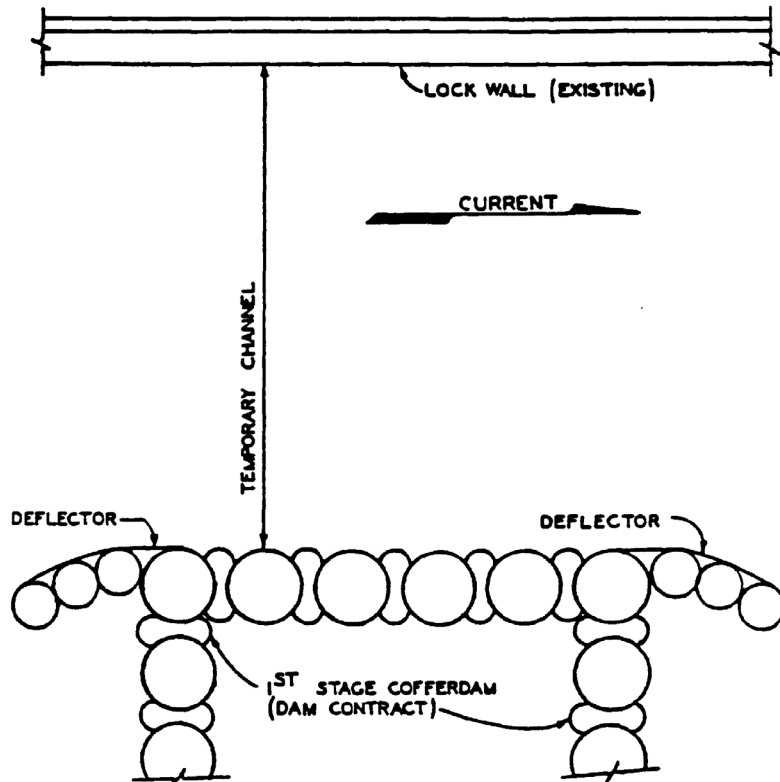


Figure 15-1: Schematic Deflector Layout

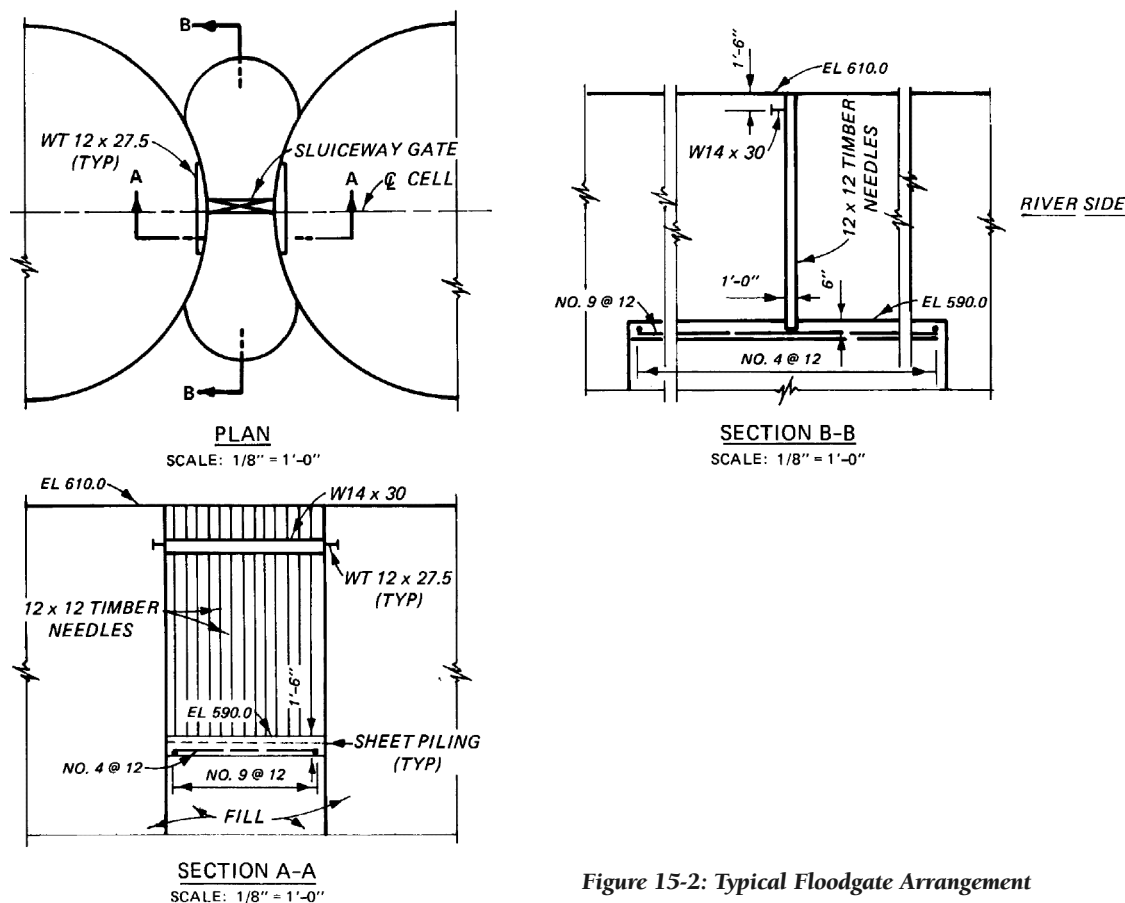


Figure 15-2: Typical Floodgate Arrangement

the piling at the appropriate elevation and capping the arc with concrete to provide a nonerodible surface. Control is maintained by installing timber needle beams that can be removed when flooding is desired. Figure 15-2 shows a typical floodgate arrangement. Sluiceways consist of a steel pipe placed through a hole cut in the piling of a connecting arc. Flow is controlled by means of a slide gate or valve operated from the top of the cell. The size, number, and invert elevations of the flooding facilities are determined by comparing the volume to be filled with the probable rate of rise of the river. These elements must be sized so that it is possible to flood the cofferdam before it is overtopped. For either system, the adjacent berm must be protected against the flows by means of a concrete flume, a splash pad, or heavy stone.

15.1.2.4. Tie-ins

Cofferdams often must be connected to land and to completed portions of the structure.

15.1.2.4.1. Tie-in to Land

Where the cofferdam joins a steep sloping shoreline, the first cell is usually located at a point where the top of the cell intersects the sloping bank. A single wall of steel sheet piling connected to the cell and extending landward to form a cut-off wall is often required to increase the seepage path and reduce the velocity of the water. The length of the cut-off wall

will depend upon the permeability of the overburden. The wall should be driven to rock or to a depth in overburden as required by the permeability of the overburden. The depths of overburden into which the cells and cut-off wall are driven should be limited to 30 feet in order to prevent driving the piling out of interlock. Otherwise, it will be necessary to excavate a portion of the overburden prior to driving the piling. Where the cofferdam abuts a wide floodplain that is lower than the top of the cofferdam cells, protection from floodwaters along the land side can be obtained by constructing an earth dike with a steel sheet pile cut-off wall. The dike may join the upstream and downstream arms of the cofferdam or extend from the end of the cofferdam into the bank, depending upon the type of overburden, location of rock, and extent of the floodplain.

15.1.2.4.2. Tie-in to Existing Structures

Tie-ins to a vertical face of a structure can be accomplished by embedding a section of sheet piling in the structure to which a tee pile in the cell can be connected. Another method of tie-in to a vertical face consists of wedging a shaped-to-fit timber beam between the cell and the vertical face. As the cofferdam enclosure is de-watered, the hydrostatic pressure outside the cofferdam seats the beam, thus creating a seal. Tie-ins to a sloping face are somewhat more complicated, and it is necessary to develop details to fit each individual configura-

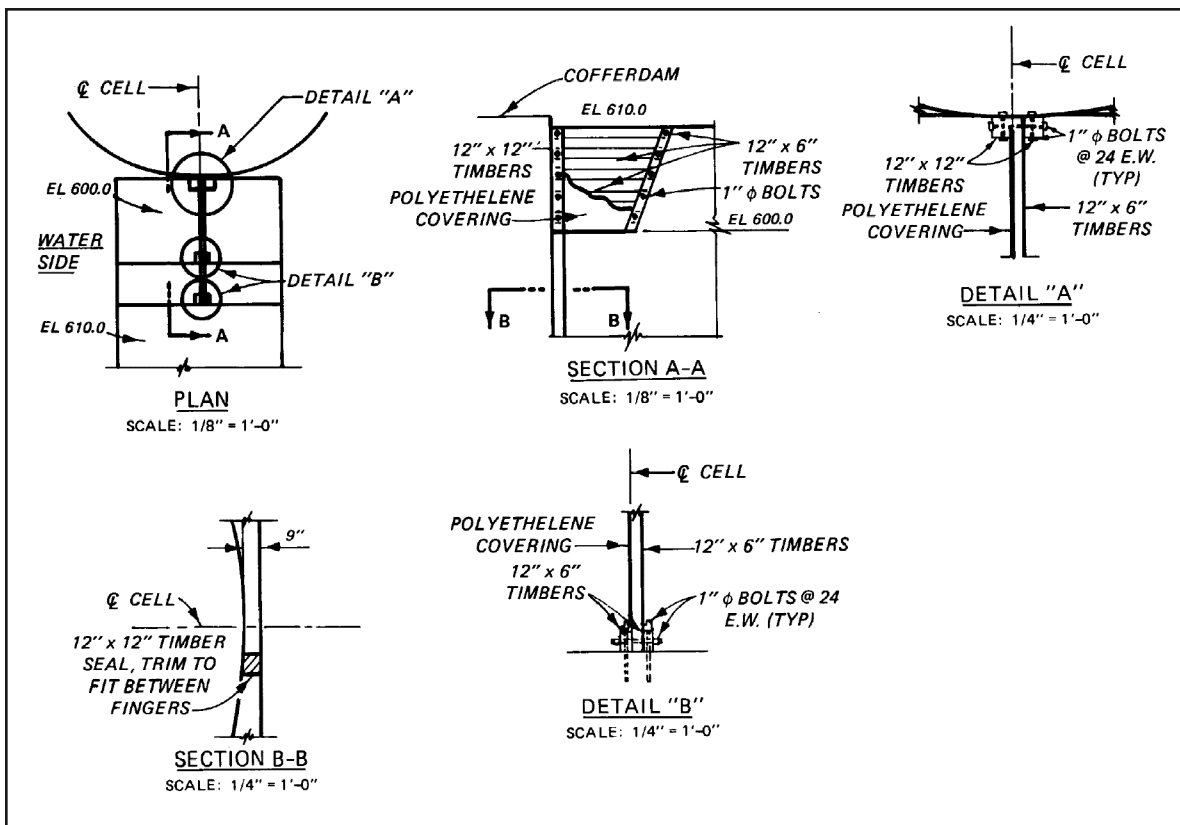


Figure 15-3: Typical Tie-in Details

tion. The most common schemes consist of timber bulkheads or timber cribs tailored to fit the sloping face. See Figure 15-3 for typical tie-in details.

15.1.2.5. Cell Layout and Geometry

The cofferdam layout, generally, should utilize only one cell size that satisfies all design requirements. In some areas, it might be possible to meet all stability requirements with smaller cells; however, the additional costs resulting from the construction and use of more than one size template will usually exceed the additional cost of an increase in the cell diameter. The geometry of the various cell types was discussed in 1.2.1.4.

These suggested arrangements should, however, be modified to require an odd number of piles between the connecting wyes or tees as shown in Figure 15-4. This will allow the use of only one type of fabricated wye or tee rather than two types if an even number of piles are used between connections. Although two additional piles might be required for each cell, this cost would be off-set by the ease of checking shop drawings and simplifying construction, i.e., the tees or wyes could not be placed and driven in the wrong location. In developing details for other configurations, special attention should be given to the location of tees or wyes and the number of piles between connections. Given this type of layout, the number of piles and their exact layout is obviously dependent upon the configuration of the sheeting and the

types of connectors available. Most manufacturers of flat sheeting furnish detailed information on layouts possible with given sections; these should be consulted in detail when designing cellular cofferdams.

15.1.2.6. Protection and Safety Features

Other features that must be considered in the planning and layout of a cofferdam include:

- A rock or concrete cap on the cell to protect the cell fill from erosion and to provide a suitable surface for construction equipment;
- Personnel safety facilities, including sufficient stairways and an alarm system; and navigation warnings, including painting of cells, reflective panels, and navigation lights.

15.2. Design Parameters

Cellular cofferdams consist of two very different materials, steel and soil, resulting in a complex interaction that makes a rational design approach very difficult. Although various theories have been suggested to derive analytical solutions for the stresses in a cell, most designers in this field still rely heavily on past practice and experience. The theoretical considerations presented herein represent one approach to this problem. However, an attempt has also been made to supply the reader with experience to enable him to develop designs consistent with proven sound engineering practices. It must be pointed out that good judgement should always prevail.

American Construction Material Exchange, Inc.

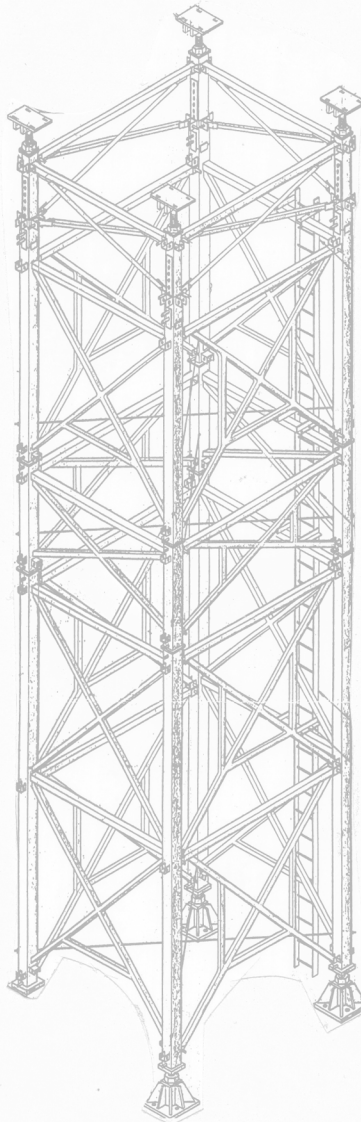
USED PIPE

10-3/4" O.D. X .250
12.75" O.D. X .312
14" O.D. X .500
18" O.D. X .375
18" O.D. X .500
22.75 O.D. X .375
24" O.D. X .375
24" O.D. X .500
36" O.D. X .750 NEW
42" O.D. X 1.000 NEW

USED/SURPLUS STEEL BEAMS

W40x149#
W36x300#, W36x260#, W36x245#
W36x230#, W36x210#, W36x194#
W36x182#, W36x170#, W36x160#
W36x150#, W36x135#
W33x291#, W33x241#, W33x221#
W33x201#
W30x211#, W30x191#, W30x173#, 116#
W27x94#, W27x84#
W24x146#, W24x131#, W24x117#
W24x104#, W24x94#
W21x122#, W21x111#, W21x101#
W18x119#, W18x97#, W18x96#
W18x86#, W18x76#, W18x55#
W16x100#, W16x89#, W16x57#
W14x159#, W14x145#, W14x132#, W14x120#
W14x109#, W14x99#, W14x90#, W14x82#
W14x74#, W14x68#, W14x61#
W12x120#, W12x79#, W12x72#, W12x65#
W12x53#, W12x45#, W12x35#, W12x26#
W10x112#, W10x100#, W10x68#, W10x49#,
W8x48#, W8x40#

MOST STOCK LOCATED ON THE WEST COAST



WANTED:

We are looking for:
**Used Flat Sheet Piles
& AZ18 Sheets**

USED MISC. AVAILABLE

HP12x53#, HP12x74#,
HP12x84#, HP14x89#
HP14x102#, HP14x117#
STEEL PLATES
CHANNELS - 8", 12" & 15"
18" DOUBLE CHANNELS
CREOSOTE TIMBERS
180 Pcs. 14"x14'x23'-28'
120 Pcs. 8"x24'x30'

SHORE TOWER SYSTEM

100 KIP PER LEG
LARGE QUANTITY AVAILABLE
WILL RENT OR SELL

NEW, PRIME W/MTR'S

W14 x 90, W14 x 109
W14 x 120
HP14x89#

E-Mail Address: rogerkadel@comcast.net

"ACME" P.O. Box 2600 TUALATIN, OR. 97062

PHONE: (503) 590-5100 FAX: (503) 590-5200 MOBILE: (503) 705-1190

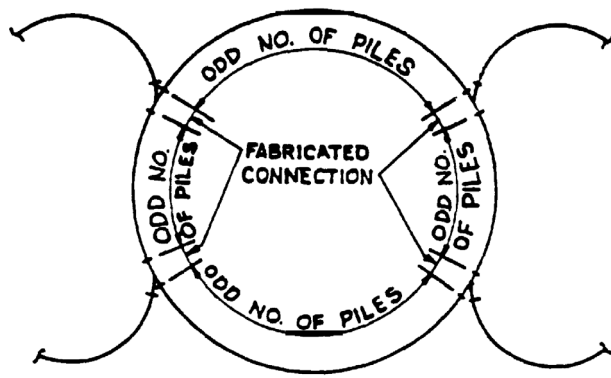


Figure 15-4: Arrangements of Connecting Wyes and Tees

Precise mathematical evaluations can result in misleading and dangerous conclusions in the hands of inexperienced designers. Under these circumstances, any cellular sheet pile structure of importance should have the benefit of the best obtainable professional engineering advice. This is particularly true for cases where difficult foundation conditions exist.

Generally, the design of a cellular cofferdam proceeds much the same as that of an anchored wall. Before a design can be initiated, the necessary controlling dimensions must be set and a site reconnaissance made. The height of the cofferdam must be established from flood records so that its top is at least at the level of the anticipated high water during the life of the cofferdam. For high cofferdams, a berm might also be considered to reduce the relative height above ground.

15.2.1. Forces

15.2.1.1. Applied External Forces

Steel sheet pile cells are subject to external forces resulting from static water head, wave action, lateral earth pressure, and surcharge due to live load, earthquake, etc.

15.2.1.2. Reactive Berm Force

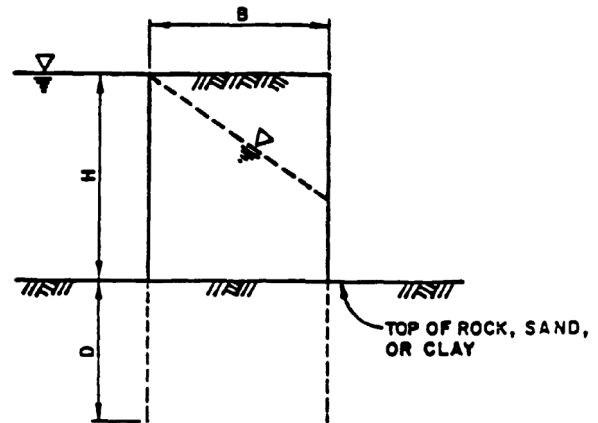
The passive force developed by a berm should be determined by a wedge analysis that accounts for the intersection of the failure wedge with the back slope of the berm. The Coulomb method of analysis or a Culmann graphical solution can be used when appropriate, although graphical methods in general have gone out of fashion. The resistance provided by the berm should be limited to a value consistent with the berm reaction resulting from a sliding analysis.

15.2.2. Saturation Line and Seepage Control

As is the case with any dam, cellular cofferdams generally operate with two different levels of water on either side. As is the case with earthen dams, the saturation level will vary within the cofferdam itself. Before stability of the assumed cell configuration can be checked the degree of saturation within the cell fill must be considered.

15.2.2.1. Seepage through Cell

The location of the free water surface in a cell is usually estimated using empirical relationships based on the type of cell fill. The recommendations in Figure 15-5 serve as a guide and starting point for estimating the location of the seepage line.



SLOPE OF FREE-WATER SURFACE IN CELLS DEPENDS ON PERMEABILITY OF CELL FILL UNLESS SPECIAL DRAINAGE IS PROVIDED AND SLOPE IS CONTROLLED, ASSUME THE FOLLOWING:

- FREE-DRAINING COARSE-GRAINED FILL (GW, GP, SW, SP): SLOPE 1 VERTICAL TO 1 HORIZONTAL
- SILTY COARSE-GRAINED FILL (GM, GC, SM, SC): SLOPE 1 VERTICAL TO 2 HORIZONTAL
- FINE-GRAINED FILL: SLOPE 1 VERTICAL TO 3 HORIZONTAL

Figure 15-5: Estimate of Free Water Location in Fill

In cases where an earth berm is used, the saturation line slopes to the top of the berm. In the berm itself, two locations of saturation line should be considered, as shown in Figure 15-20 to make provision for the more critical location. A horizontal line, at an elevation so chosen as to represent the average expected condition of saturation should serve just as well, at the same time simplifying computations.

These recommendations are conservative for most applications; however, each design should be evaluated for conditions that would tend to raise the seepage line. If both the quality of the cell fill and the assurance of proper inspection cannot be guaranteed during the design of the project, full saturation of the cell should be considered for design purposes. Some conditions that require evaluation are:

- (1) Possible leakage from pipelines crossing the cells.
- (2) Waves overtopping the outboard piles.
- (3) Excessive leakage through the outboard piles.
- (4) Poor drainage through the inboard piles.
- (5) Lower permeability than expected of the cell fill.
- (6) Hydraulic filling of cell fill.

The quantity of seepage through the cell is a function of both the tightness and integrity of the outboard piles and the type of cell fill, the chief barrier being the outboard piling. The tightness of the outboard piling depends on the physical condition of the piling and the piling interlock force. An increase in seepage through the cell can generally be expected when:

- (1) Second-hand piling is used. New piling in good condition should be considered for major structures. For other structures, used piling may be considered when seepage conditions either are slight or pose little threat to the safety to the structure.
- (2) Rough driving is experienced during construction. The foundation exploration program should investigate conditions that lead to rough driving. Contract specifications should restrict hard driving.
- (3) The interlock forces are small. The increase in seepage due to this condition is usually small, and is usually not considered.

15.2.2.2. Foundation Underseepage

Foundation underseepage is generally not a problem for structures built on clay or good quality rock foundations. Problems usually are confined to coarse-grained soil such as gravel and sand and sometimes silty materials. The most treacherous conditions occur where undetected pervious seams exist in the foundation.

Cofferdams on sand are often designed using a trial sheet pile penetration of two thirds of the height of the structure above the dredge line. A flow net is most often used to estimate the seepage forces. If the exit gradient at the toe of the structure is large, a loaded filter or a wide-base berm should be considered.

Depending on the site conditions, up to 50 percent of the passive resistance, even with 2/3H penetration, at the toe can be lost due to seepage forces. This loss increases the possibility of excessive penetration of the inboard piles.

15.2.3. Loading Conditions

Now that we have discussed the variations of water level within the cofferdam itself, we need to note that, not only differ from each other in level but also in time, depending upon the condition of the body of water. Variations in this was level will induce changes in the level of saturation inside of the cofferdam. The following loading conditions and requirements must be investigated:

15.2.3.1. Maximum Pool Condition

The river pool is to top of cell. The cell fill saturation line

is assumed to slope from top outboard face of the cell to the inboard face. The slope is dependent upon the type of fill, the presence of a berm, and any positive measures taken to control the phreatic surface in the cell or the berm, such as weep holes in the cell or drains and pumped wells in the berm, Figure 15-6. It should be emphasized that the saturation level within the cell fill is perhaps the single most important consideration in the design of the cells; therefore, its location must be estimated with extreme care.

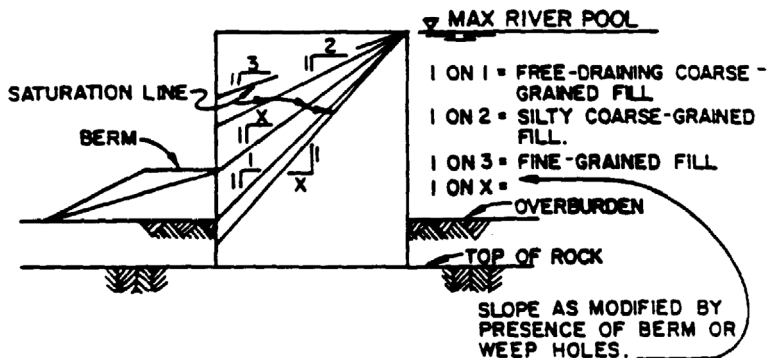


Figure 15-6: Maximum Pool Condition

15.2.3.2. Initial Filling Condition

Balanced pools are on both the inside and outside of the cofferdam; for determination of maximum interlock stress, cell fill is assumed to be completely saturated to top of cell unless positive measures are taken to preclude fill saturation, Figure 15-7.

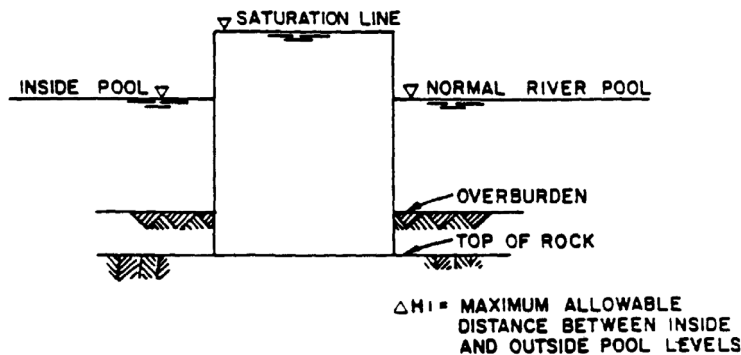


Figure 15-7: Initial Filling Condition

15.2.3.3. Drawdown Condition

Pool level inside cofferdam is some specified distance below pool level outside cofferdam; cell fill saturation level varies uniformly between the outside pool level and some specified distance above the pool level inside the cofferdam, Figure 15-8. This condition is checked to determine the maximum rate of dewatering. This condition can be critical for stability and interlock stress. The designer establishes the maximum rate of dewatering, as influenced by the cell fill saturation level, at which level the allowable interlock stress

should not be exceeded and all factors of safety should be met. Since the cell fill saturation level is critical, the actual saturation level must be monitored in the field during dewatering to verify the assumed conditions. Instructions to this effect and the critical parameters should be included in the contract specifications and/or in "Special Instructions" to the resident engineer. Note that the forces acting upon a cofferdam can change with time. For example, overburden may be present on the inside of a cofferdam when it is initially dewatered; however, the overburden may subsequently be excavated, thus perhaps adversely affecting the stability of the cofferdam. In short, loading conditions not present during construction and initial dewatering must be anticipated and taken into account during design.

15.2.4. Site Conditions

The site reconnaissance should include information on the existing ground surface and the depth of scour, as well as a complete subsurface investigation. Exploratory borings extending to rock should be located to provide a complete

picture of the soil strata and the general configuration of the rock surface. Laboratory tests give the engineer first-hand knowledge of the character and the properties of the materials in design. Care should be exercised, however, in the application of laboratory test results because of the complicated response of the structure to actual field conditions. These conditions are almost impossible to duplicate by ordinary testing procedures. It is advisable to extend several borings into the rock to determine its general character and competency. Also, the depth and extent of soft soils (soft clay, silt and organic deposits, etc.) should be carefully ascertained, since these soils must be removed and replaced by granular soils.

$$\text{Equation 15-1: } B = \frac{A}{2L}$$

Where

B = equivalent or effective width of the cell, ft.

A = area of main cell plus one connecting cell, ft²

2L = centre-to-centre distance between main cells, ft.

The variables are illustrated in *Figure 15-9*.

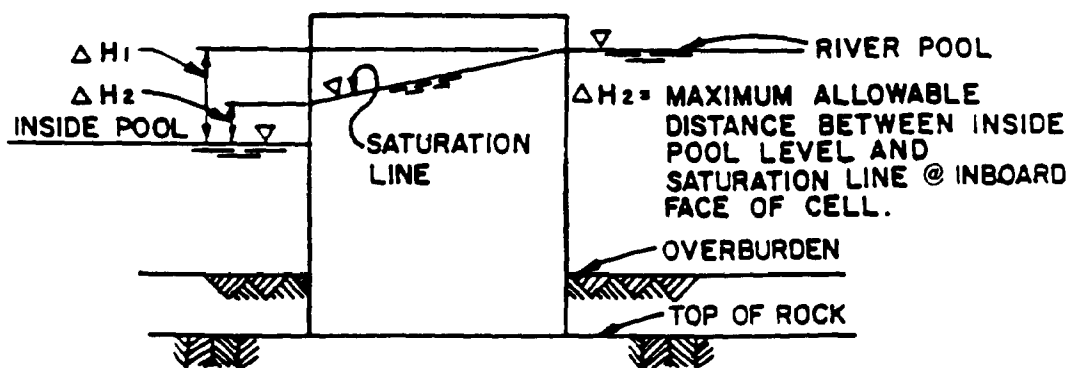


Figure 15-8: Drawdown Condition

picture of the soil strata and the general configuration of the rock surface. Laboratory tests give the engineer first-hand knowledge of the character and the properties of the materials in design. Care should be exercised, however, in the application of laboratory test results because of the complicated response of the structure to actual field conditions. These conditions are almost impossible to duplicate by ordinary testing procedures. It is advisable to extend several borings into the rock to determine its general character and competency. Also, the depth and extent of soft soils (soft clay, silt and organic deposits, etc.) should be carefully ascertained, since these soils must be removed and replaced by granular soils.

15.2.5. Equivalent Width

After the height of the cofferdam is established and the pertinent physical properties of the underlying soils together with the cell fill are determined, a tentative equivalent width, B, is chosen. Cellular cofferdams are, by nature, "lumpy"

structures in that a series of circles is joined together to form a long wall. Analysis of a cellular cofferdam would be considerably simpler if this "lumpiness" could be ignored and the walls be assumed to be two straight, parallel walls with the fill in between, the cells thus becoming rectangles. The use of the *equivalent width* concept is the method by which this simplification is implemented. The equivalent width, B, of the cofferdam is defined as the width of an equivalent rectangular section having a section modulus equal to that of the actual cofferdam. For design purposes this definition may be simplified to equivalent areas, from which

Equation 15-2:

$$B = 0.818D \quad (\theta = 15^\circ, 30^\circ Y)$$

$$B = 0.875D \quad (\theta = 22.5^\circ, 90^\circ T)$$

$$B = 0.785D \quad (\theta = 15^\circ, 90^\circ T, \text{ rarely used})$$

15.2.6. Soil Fill Materials

15.2.6.1. Selection of Cell Fill

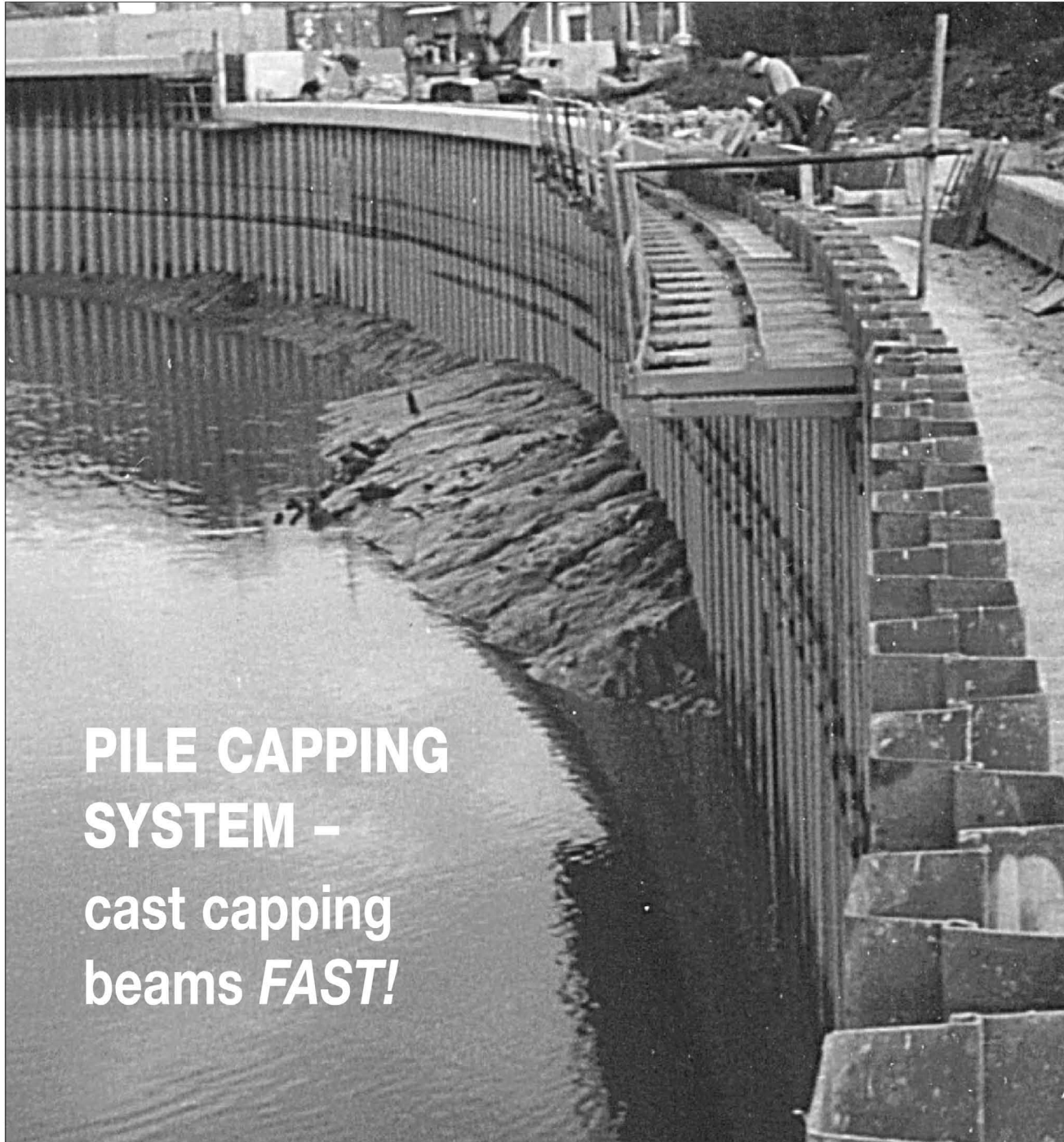
Most modern cellular sheet pile structures are designed based on the assumption that a free-draining granular fill will be available near the construction site. Soils with less than about 5 percent of the particles by weight passing the No. 200 sieve and 15 percent passing the No. 100 sieve are usually termed free draining. Granular fills with many fines and even fine-grained fills have occasionally been used in the



DAWSON

INNOVATIVE PILING EQUIPMENT

DAWSON CONSTRUCTION PLANT LTD
 Chesney Wold, Bleak Hall
 Milton Keynes MK6 1NE, England
 Tel: 011 44 1908 240300
 Fax: 011 44 1908 240222
 Email: mark@dcruk.com
 Website: www.dcruk.com



**PILE CAPPING
 SYSTEM -
 cast capping
 beams *FAST!***

**American Equipment
 & Fabricating Corp.**

100 Water Street
 East Providence
 Rhode Island 02914
 U.S.A.

Contact: John Sheerin
 Tel: 401 438 2626
 or: 1-800-368-7453
 Fax: 401 438 0764

Bay Machinery Corp.

PO Box 70430
 Richmond
 CA 94807
 U.S.A.

Contact: Bob Knop
 Tel: 510 236 9000
 Fax: 510 236 7212

**Equipment Corporation
 of America**

PO Box 387
 Aldan
 PA 19018
 U.S.A.

Contact: Ben Dutton
 Tel: 610 626 2200
 Fax: 610 626 2245

Hammer & Steel Inc.

11912 Missouri Bottom Rd.
 St Louis
 Missouri 63042-2313
 U.S.A.

Contact: Bob Laurence
 Tel: 314 895 4600
 or 1-800-325-7453
 Fax: 314 895 4070

Mabey Bridge & Shore Inc. *

6770 Dorsey Road
 Baltimore
 MD 21227
 U.S.A.

Contact: Joe Atkinson
 Tel: 410 379 2800
 or 1-800-42-MABEY
 Fax: 410 379 2801

*Do not supply HPH Hydraulic Hammers

**Mississippi River
 Equipment Co.**

PO Box 249
 520 Good Hope St.
 Norco, LA 70079
 U.S.A.

Contact: J J Waguespack
 Tel: 985 764 1194
 Fax: 985 764 1196

**Pacific American
 Commercial Co.**

7400 Second Avenue S.
 P.O. Box 3742
 Seattle, WA 98124
 U.S.A.

Contact: Ted Obermeit
 Tel: 206 762 3550
 or 1-800-678-6379
 Fax: 206 763 4232

Pile Equipment Inc.

1058 Roland Avenue
 Green Cove Springs
 Florida 32043-8361
 U.S.A.

Contact: Mike Elliott
 Tel: 904 284 1779
 or 1-800-367-9416
 Fax: 904 284 2588

**Special Construction
 Machines**

166 Bentworth Avenue
 Toronto
 Ontario M6A 1P7
 Canada

Contact: Steve Calow
 Tel: 416 787 4259
 or 1-800-760-0925
 Fax: 416 787 4362

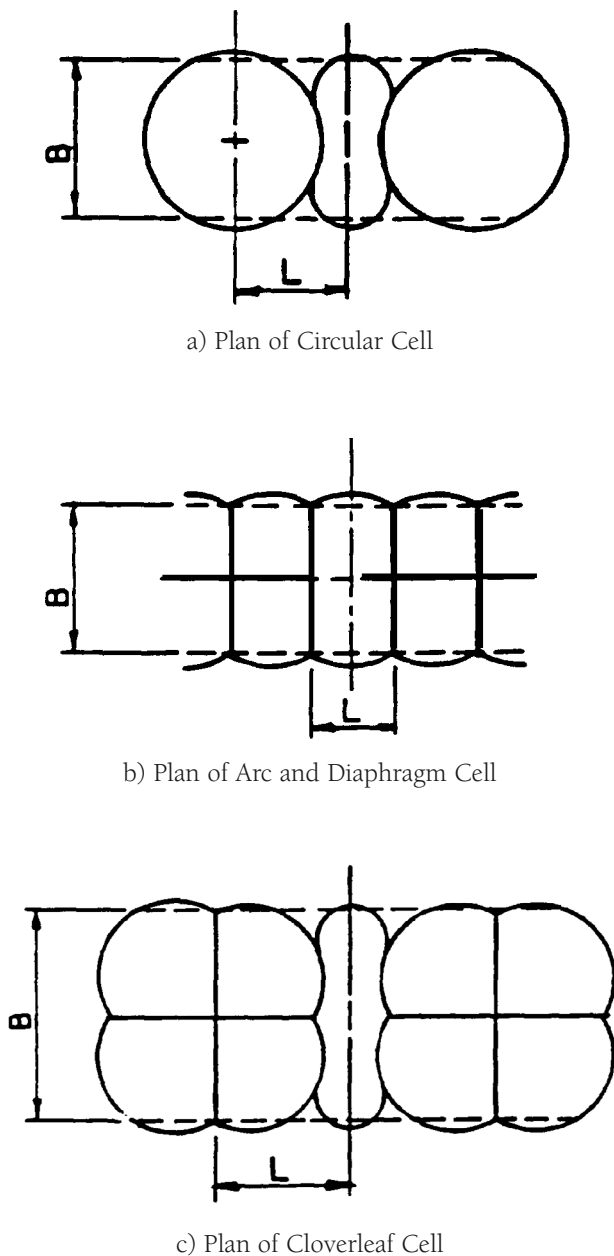


Figure 15-9: Typical Cellular Cofferdam Geometry for Equivalent Width

past; however, the poor performance of these fills usually favours use of better quality fill.

The performance of the sheet pile structure is directly related to the drainage characteristics of the cell fill. Free-draining fill will have a lower seepage line within the fill than less pervious material. The lower seepage line improves the cell performance by:

(1) Reducing the sheet pile interlock force. (Reducing this force is especially beneficial for high cells or where marginal material is used. However, a reduction in the interlock force may reduce the stiffness of the structure, with slightly larger structural movements.)

(2) Increasing the effective stress at the base of the cell, increasing lateral sliding resistance.

(3) Increasing the internal shear resistance.

15.2.6.2. Borrow Area

Borrow-related problems occur frequently in earth-work-related construction, and sometimes result in costly design changes and contract modifications. Special diligence during the exploration and characterization of borrow fill will be beneficial during both the design and construction of the project.

15.2.6.3. Location

Borrow areas are generally located as close to the project site as possible to reduce hauling costs. The final selection of the borrow site, however, is governed by several additional considerations:

1) Cell Fill Properties. When the most desirable cell fill is not locally available, the cost of processing or designing the structure around marginal cell fill should be compared with the increase in cost due to longer haul distances.

2) Land Use. Although cell fill is often dredged from river channels, it is sometimes desirable to locate the borrow areas outside of the river. When this occurs, special consideration and planning should be initiated to provide proper reclamation of the area.

3) Environmental Aspects. Environmental considerations may restrict the use of certain potential borrow sites. Early reviews of the probable borrow sites for any detrimental environmental consequences should be considered. These consequences are sometimes mitigated by placing restrictions on the use of the borrow area and by special reclamation of the site. For example, wildlife habitats or recreational areas can sometimes be created at these sites with a small additional cost.

15.2.7. Factors of Safety

The required FS for the various potential failure modes described below are listed in *Table 15-1*. As previously stated, cofferdams are not classified as temporary structures, nor are the loads imposed upon them generally considered temporary as far as FS's are concerned. However, some loading conditions can be classed as temporary where failure would not result in loss of life, severe property damage, or loss of the navigation pool, e.g., initial dewatering of a cofferdam which does not maintain a navigation pool. *Table 15-1* is also a useful checklist for the various failure modes that may apply to a given situation.

Table 15-1: Design Criteria--Factors of Safety

Failure Mode	Required Factor of Safety ¹⁵¹ Loading Condition		
	Normal	Temporary	Seismic
Sliding	1.5	1.5	1.3
Overturning (gravity block)	<i>Inside Kern</i>	<i>Inside Kern</i>	<i>Inside Base</i>
Rotation (Hansen)	1.5	1.25	1.1
Deep seated sliding	1.5	1.5	1.3
Bearing capacity			
Sand	2.0	2.0	1.3
Clay	3.0	3.0	1.5
Seepage control			
Interlock tension ¹⁵²	2.0	1.5	1.3
Vertical Shear Resistance			
Terzaghi	1.5	1.25	1.1
Schroeder-Maitland	1.5	1.25	1.1
Horizontal Shear Resistance			
Cummings	1.5	1.25	1.1
Pullout of outboard sheets	1.5	1.25	1.1
Penetration of inboard sheets	1.5	1.25	1.1

15.3. Classical Design Methods

15.3.1. Historical Overview

The design of cellular structures has progressed from the use of empirical rules based on gravitational analysis to recent attempts at finite element procedures. The actual way in which these units function in service is still not well understood. However, observation, experience, and technical expertise have been combined to provide some design procedures that are more technically correct than earlier methods.

From 1908 until TVA's investigations in the early 1940's, cellular cofferdams were assumed to function as rigid, gravity walls, and were analysed accordingly. If the resultant fell within the middle third of the base, the cell was considered safe. Sliding on the base and interlock stresses were the other consideration in design. Many successful cofferdams were built utilizing this method. It has been rationalized that success was due to selection of granular fill materials and coinci-

dence that provided whatever safety factors these structures enjoyed.

In reality, the stability of a sheet pile cell results from the composite action of the soil fill and the interlocking steel piling. A cofferdam cell consists of a flexible sheet pile membrane that encloses a soil fill. Rather than acting like a can filled with sand, it resembles more, a shaped, flexible bag filled with sand. The interaction between the two elements of fill and container has been the basis of all progress in failure mode analysis since 1940.

15.3.2. Design Process

An adequate assessment of sliding stability must account for the basic structural behaviour, the mechanism of transmitting compressive and shearing loads to the foundation, the reaction of the foundation to such loads, and the secondary effects of the foundation behaviour on the structure. A fully coordinated team of geotechnical and structural engineers

¹⁵¹These FS's/criteria are for cofferdams only. Design should not be based on modes of failure in italics, but these should be employed as sensitivity checks only.

¹⁵²The FS against interlock tension failure should be applied to the interlock strength value guaranteed by the manufacturer for the particular grade of steel. The guaranteed value for used piling should be reduced as necessary depending upon the condition of the piling.

and geologists should ensure that the results of the sliding analyses are properly integrated into the design. Critical aspects of the design process which require coordination include:

- Preliminary estimates of geotechnical data, subsurface conditions, and type of structure;
- Selection of loading conditions, loading effects, potential failure mechanisms, and other related features of the analytical models;
- Evaluation of the technical and economic feasibility of alternative structures;
- Refinement of the preliminary design to reflect the results of detailed geotechnical site explorations, laboratory testing, and numerical analyses; and
- Modification of the structure during construction due to unexpected variations in the foundation conditions.

15.3.3. External Cell Stability

15.3.3.1. Sliding Analysis by Trial Wedge Method

For design and investigation of sheet pile cellular structures, the procedures outlined in the following paragraphs should be used to assess sliding stability on rock and soil foundations.

15.3.3.1.1. Method of Analysis

The sliding analysis is based on the principles of structural and geotechnical mechanics, which apply a safety factor to the material strength parameters in a manner that places the forces acting on the structure and foundation wedges in sliding equilibrium. The factor of safety (FS) is defined as the ratio of the shear strength and the applied shear stress as follows.

$$\text{Equation 15-3: } FS = \frac{\tau_F}{\tau} = \frac{c + \sigma'_n \tan \phi}{\tau}$$

Where the variables are shown in *Figure 4-1*. A sliding mode of failure will occur along a presumed failure surface when the applied shearing force exceeds the resisting shear forces.

The failure surface can be any combination of plane and curved surfaces, but for simplicity, all failure surfaces are assumed planes that form the bases of wedges. The critical failure surface with the lowest safety factor is determined by an iterative process. Sliding stability of most sheet pile cellular structures can be adequately assessed by using a limit equilibrium approach. Designers must exercise sound judgment in performing these analyses.

Assumptions and simplifications are as follows:

(a) A two-dimensional analysis is presented. These principles should be extended if unique, three-dimensional, geometric features and loads critically affect the sliding stability of a specific structure.

(b) Only force equilibrium is satisfied in this analysis.

Moment equilibrium is not used. The shearing force acting parallel to the interface of any two wedges is assumed negligible. Therefore, the portion of the failure surface at the bottom of each wedge is loaded only by the forces directly above or below it. There is no interaction of vertical effects between the wedges.

(c) Analyses are based on assumed plane failure surfaces. The calculated safety factor will be realistic only if the assumed failure mechanism is kinematically possible.

(d) Considerations regarding displacements are excluded from the limit equilibrium approach. The relative rigidity of different foundation materials and the sheet pile cellular structure may influence the results of the sliding stability analysis. Such complex structure-foundation systems may require a more intensive sliding investigation than a limit equilibrium approach. The effects of strain compatibility along the assumed failure surface may be included by interpreting data from in situ tests, laboratory tests, and finite element analyses.

(e) A linear relationship is assumed between the resisting shearing force and the normal force acting along the failure surface beneath each wedge.

15.3.3.1.2. Multiwedge System Analysis

A general procedure for analysing multiwedge systems includes:

(a) Assuming a potential failure surface that is based on the stratification, location and orientation, frequency and distribution of discontinuities of the foundation material, and the configuration of the structure.

(b) Dividing the assumed slide mass into a number of wedges, including a single structural wedge.

(c) Drawing free body diagrams which show all the forces assumed to be acting on each wedge.

(d) Solving for the safety factor by direct or iterative methods. The equations for sliding stability analysis of a general wedge system are based on the right hand sign convention, which is commonly used in engineering mechanics. The origin of the coordinate system for each wedge is located in the lower left hand corner of the wedge. The x and y axes are horizontal and vertical respectively. Axes that are tangent (t) and normal (n) to the failure plane are oriented at an angle α with respect to the +x and +y axes. A positive value of α is a counter- or anti- clockwise rotation; a negative value of α is a clockwise rotation.

800.848.6249 www.fosterpiling.com

COMBI-WALL SYSTEMS HZ or PIPE Z AVAILABLE

- Deep Draft Application
- High Strength
- Appropriate for Difficult Soil Conditions
- Flexible Design Solution
- Interchangeable with Other Designs



 **Foster**
Piling
A Division of L.B. Foster Company



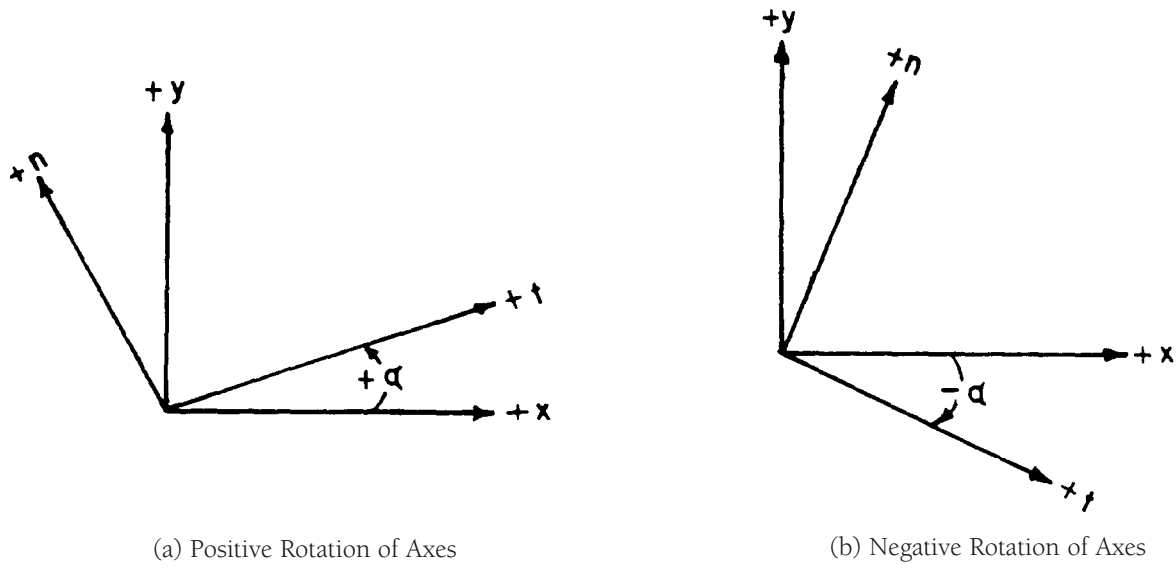


Figure 15-10: Sign convention for geometry

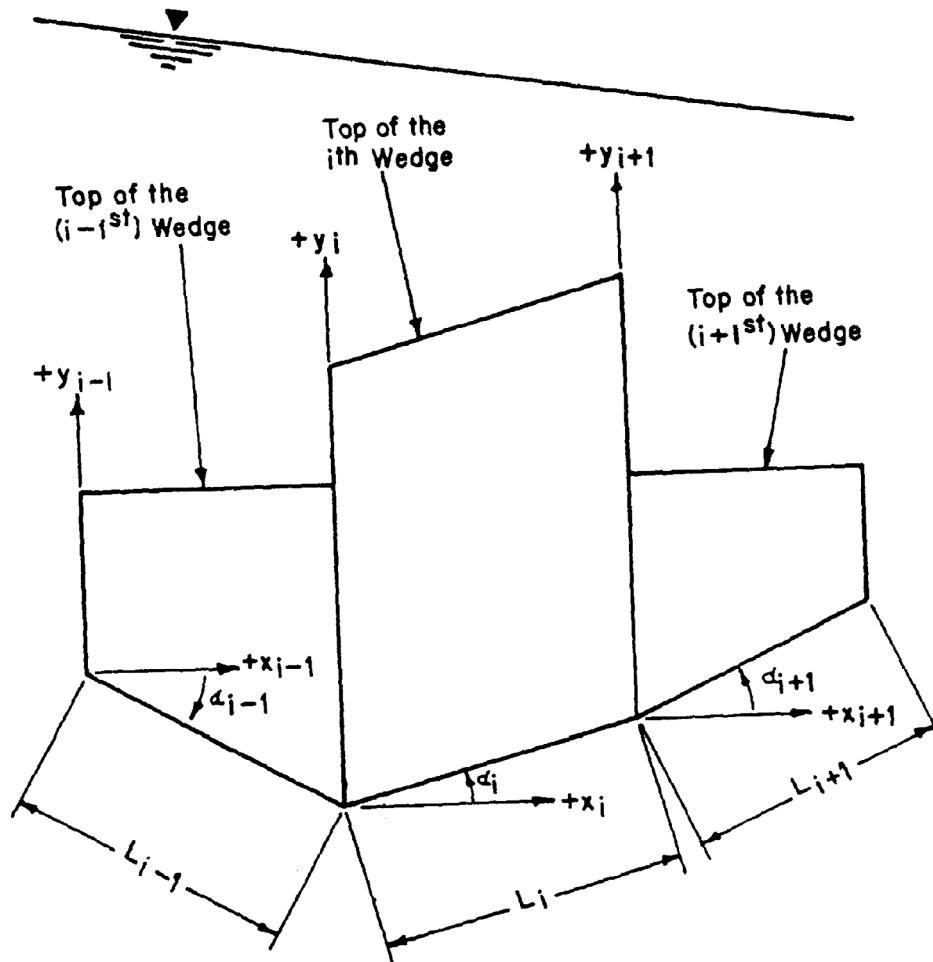


Figure 15-11: Geometry of the Typical i^{th} Wedge and Adjacent Wedges

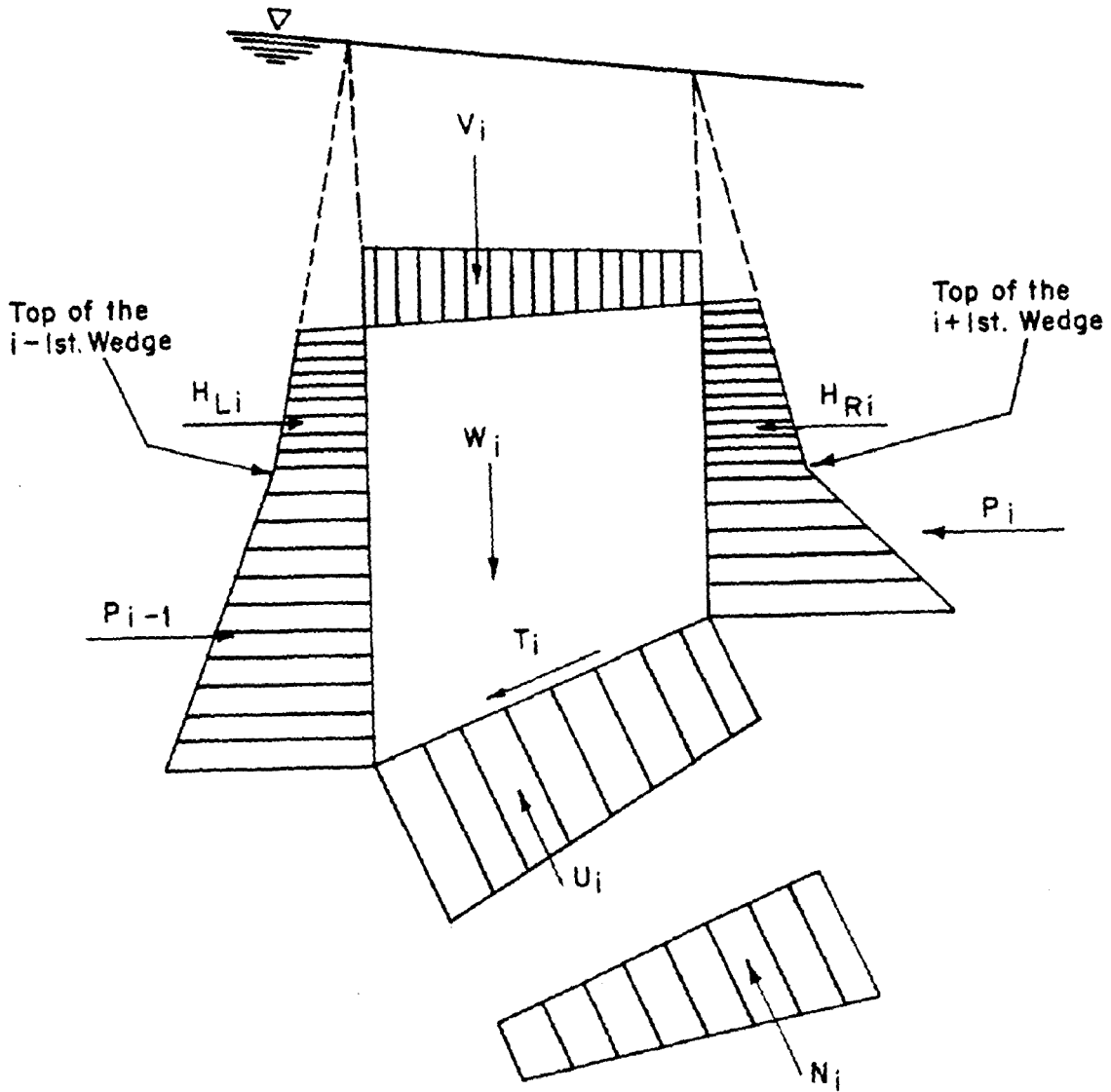


Figure 15-12: Distribution of Pressures and Resultant Forces Acting on a Typical Wedge

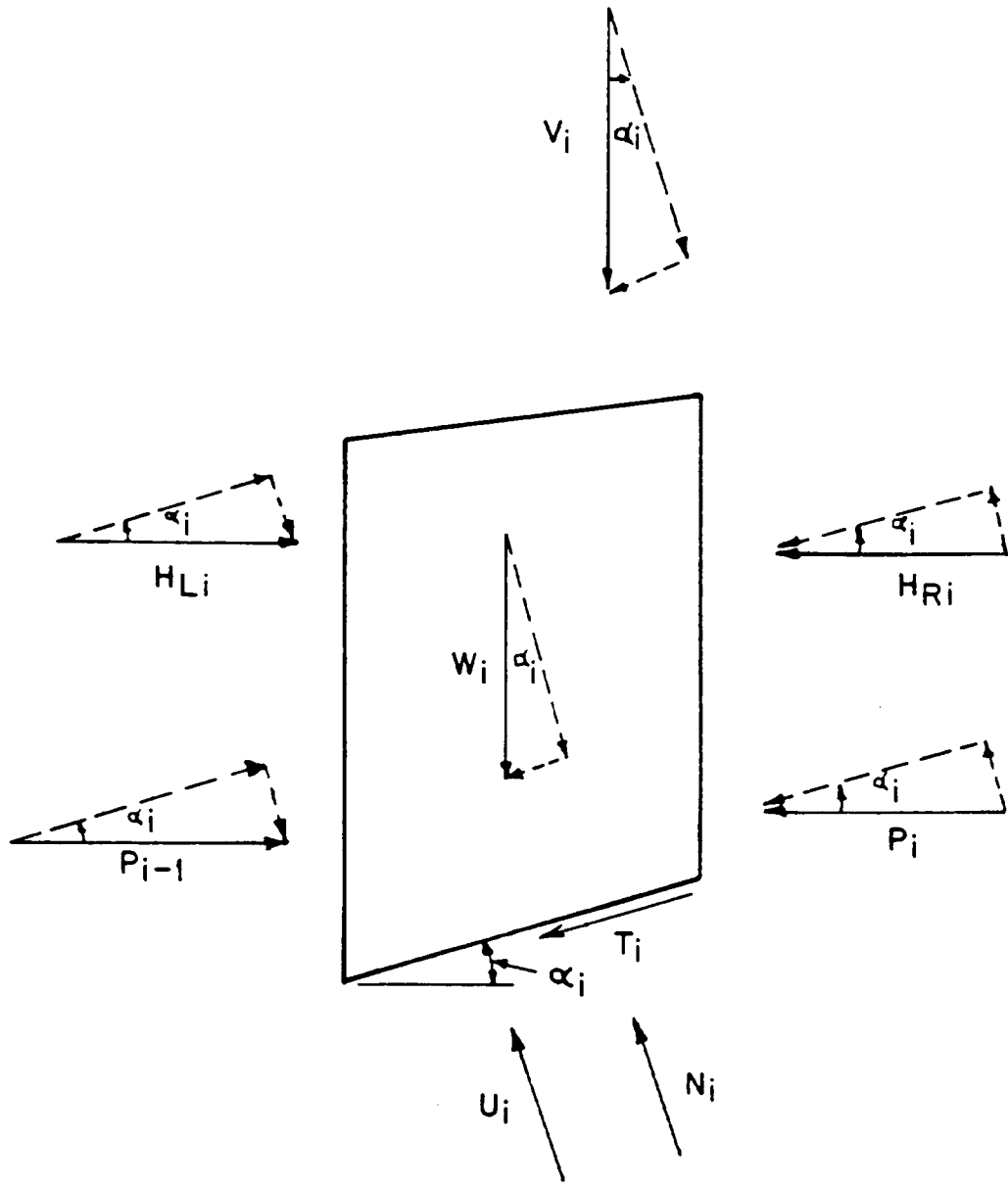
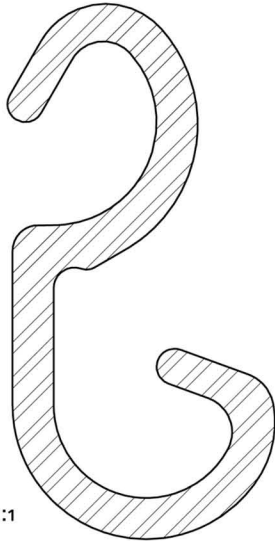


Figure 15-13: Free Body Diagram of the P^{th} Wedge

AZ 90

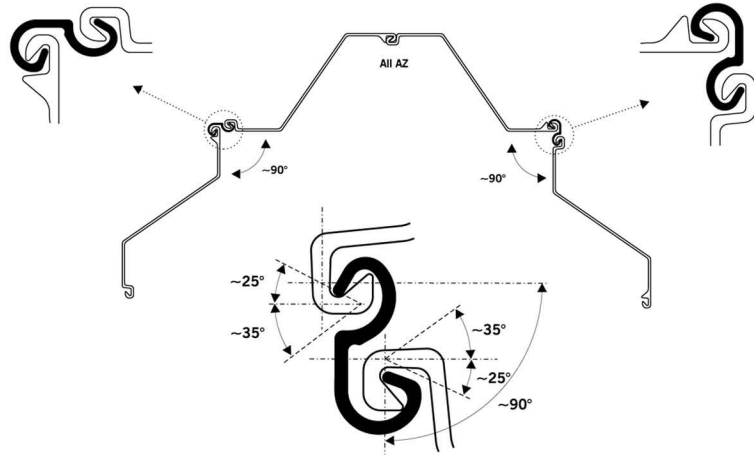
Available for immediate delivery, nation-wide

Applications: 90° corner (~25° to ~155°)



Weight: 8.9 lbs/ft (13.2 kg/m)

Steel grade: Astm A572 Grade 50 (S 355 GP)



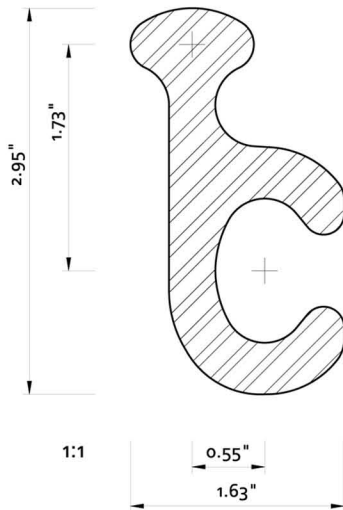
Installation Guidelines:

1. Thread the connector into the interlock while the sheet pile is out of the ground.
2. Adjust the connector to the appropriate position.
3. Tack or spot-weld the connector in place (typically a 10" weld attaching the connector to the sheet pile at the top is sufficient.)
4. Drive/extract the sheet (with the connector attached) as you would normally.

PZ 90

Priced delivered to the job site

Applications: 90° corner (~54° to ~126°)

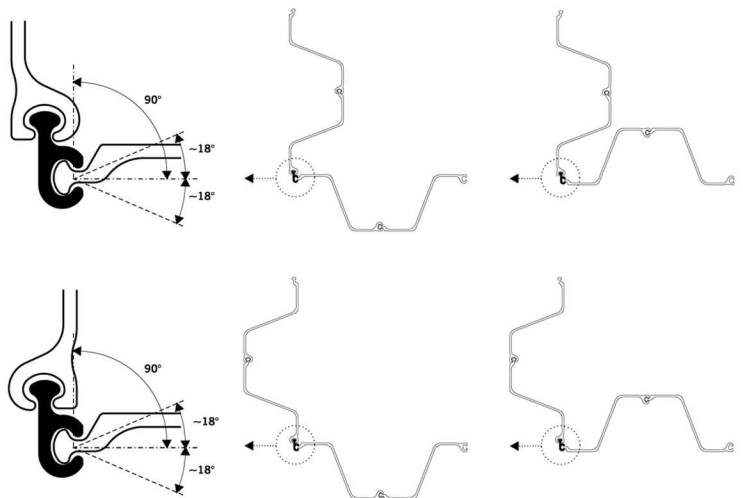


Weight: 7.1 lbs/ft (10.5 kg/m)


Steel grade: Astm A572 Grade 50 (S 355 GP)

Proper Interlocking Examples

Each interlock has a typical degree swing of 18° (+/- 5°) so that the probable swivel range is 36° (+/- 10°) when interlocking two PZ sheets via the connector.



Equilibrium Equations

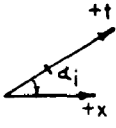


$$\Sigma F_n = 0$$

$$0 = N_i + U_i - W_i \cos \alpha_i - V_i \cos \alpha_i - H_{Li} \sin \alpha_i + H_{Ri} \sin \alpha_i + \dots$$

$$\dots - P_{i-1} \sin \alpha_i + P_i \sin \alpha_i$$

$$N_i = (W_i + V_i) \cos \alpha_i - U_i + (H_{Li} - H_{Ri}) \sin \alpha_i + (P_{i-1} - P_i) \sin \alpha_i$$



$$\Sigma F_t = 0$$

$$0 = -T_i - W_i \sin \alpha_i - V_i \sin \alpha_i + H_{Li} \cos \alpha_i - H_{Ri} \cos \alpha_i + \dots$$

$$\dots + P_{i-1} \cos \alpha_i - P_i \cos \alpha_i$$

$$T_i = (H_{Li} - H_{Ri}) \cos \alpha_i - (W_i + V_i) \sin \alpha_i + (P_{i-1} - P_i) \cos \alpha_i$$

Mohr-Coulomb Failure Criterion

$$T_F = N_i \tan \phi_i + c_i L_i$$

Safety Factor Definition

$$FS = \frac{T_F}{T_i} = \frac{N_i \tan \phi_i + c_i L_i}{T_i}$$

Governing Wedge Equation

$$FS_i = \frac{\{(W_i + V_i) \cos \alpha_i - U_i + [(H_{Li} - H_{Ri}) + (P_{i-1} - P_i)] \sin \alpha_i\} \tan \phi_i + c_i L_i}{[(H_{Li} - H_{Ri}) + (P_{i-1} - P_i)] \cos \alpha_i - (W_i + V_i) \sin \alpha_i}$$

$$(P_{i-1} - P_i) (\cos \alpha_i - \sin \alpha_i \frac{\tan \phi_i}{FS_i}) = [(W_i + V_i) \cos \alpha_i - U_i + (H_{Li} - H_{Ri}) \sin \alpha_i] \frac{\tan \phi_i}{FS_i} + \dots$$

$$\dots + \frac{c_i}{FS_i} L_i - (H_{Li} - H_{Ri}) \cos \alpha_i + (W_i + V_i) \sin \alpha_i$$

$$(P_{i-1} - P_i) = \frac{[(W_i + V_i) \cos \alpha_i - U_i + (H_{Li} - H_{Ri}) \sin \alpha_i] \frac{\tan \phi_i}{FS_i} - (H_{Li} - H_{Ri}) \cos \alpha_i + (W_i + V_i) \sin \alpha_i + \frac{c_i}{FS_i} L_i}{(\cos \alpha_i - \sin \alpha_i \frac{\tan \phi_i}{FS_i})}$$

NOTE: A negative value of the difference $(P_{i-1} - P_i)$ indicates that the applied forces acting on the i^{th} wedge exceed the forces resisting sliding along the base of the wedge. A positive value of the difference $(P_{i-1} - P_i)$ indicates that the applied forces acting on the i^{th} wedge are less than the forces resisting sliding along the base of that wedge.

Figure 15-14: Derivation of the General Wedge Equation

The governing wedge equation is thus

Equation 15-4:

$$(P_{i-1} - P_i) = \frac{[(W_i + V_i) \cos \alpha_i - U_i + (H_{Li} - H_{Ri}) \sin \alpha_i] \frac{\tan \phi_i}{FS_i}}{\cos \alpha_i - \sin \alpha_i \frac{\tan \phi_i}{FS_i}}$$

$$\frac{(H_{Li} - H_{Ri}) \cos \alpha_i + (W_i + V_i) \sin \alpha_i + \frac{c_i}{FS_i} L_i}{\cos \alpha_i - \sin \alpha_i \frac{\tan \phi_i}{FS_i}}$$

Where

- i = number of wedges
- $(P_{i-1} - P_i)$ = summation of applied forces acting horizontally on the i^{th} wedge.
- W_i = total weight of water, soil, rock, etc., in the i^{th} wedge
- V_i = any vertical force applied above top of the i^{th} wedge
- α_i = angle between the inclined plane of the potential failure surface of the i^{th} wedge and the horizontal (positive is counter- or anti-clockwise)
- U_i = uplift force exerted along the failure surface of the i^{th} wedge
- H_{Li} = any horizontal force applied above the top or below the bottom of the left-side adjacent wedge
- H_{Ri} = any horizontal force applied above the top or below the bottom of the right-side adjacent wedge
- f_i = angle of shearing resistance or internal friction of the i^{th} wedge
- c_i = cohesion or adhesion, whichever is the smaller on the potential failure surface of the i^{th} wedge. (Cohesion should not exceed the adhesion at the structure-foundation interface.)
- L_i = length along the failure surface of the i^{th} wedge

The governing equation applies to the individual wedges. For a system of wedges to act as an integral failure mechanism, the factors of safety (FS) for all wedges must be identical, therefore

Equation 15-5:

$$FS_1 = FS_2 = \dots FS_{i-1} = FS_i = FS_{i+1} = \dots FS_N$$

Where N = number of wedges in the failure mechanism. The actual FS for sliding equilibrium is determined by satisfying overall horizontal equilibrium ($\Sigma F_H = 0$) for the entire system of wedges; therefore

Equation 15-6:

$$\sum_{i=1} (P_{i-1} - P_i) = 0$$

and $P_0 = P_N = 0$. Usually an iterative solution process is used to determine the actual FS for sliding equilibrium. The analysis proceeds by assuming trial values of the safety factor and unknown inclinations of the slip path until the governing equilibrium conditions, failure criterion, and definition of FS are satisfied. An analytical or a graphical procedure may be used for this iterative solution.

15.3.3.1.3. Design Considerations

Some special considerations for applying the general wedge equation to specific site conditions are discussed below.

(a) The interface between the group of active wedges and the structural wedge is assumed a vertical plane located at the heel of and extending to the base of the structural wedge. The magnitudes of the active forces depend on the actual values of the FS and the inclination angles, a of the slip path. The inclination angles, corresponding to the maximum active forces for each potential failure surface, can be determined by independently analysing the group of active wedges for a trial FS. In rock, the inclination may be predetermined by discontinuities in the foundation. The general equation only applies directly to active wedges with assumed horizontal active forces.

(b) The governing wedge equation is based on the assumption that shearing forces do not act on the vertical wedge boundaries; hence there can only be one structural wedge because the structure transmits significant shearing forces across vertical internal planes. Discontinuities in the slip path beneath the structural wedge should be modelled by assuming an average slip plane along the base of the structural wedge.

(c) The interface between the group of passive wedges and the structural wedge is assumed to be a vertical plane located at the toe of the structural wedge and extending to the base of the structural wedge. The magnitudes of the passive forces depend on the actual values of the safety factor and the inclination angles of the slip path. The inclination angles, corre-

sponding to the minimum passive forces for each potential failure mechanism, can be determined by independently analysing the group of passive wedges for a trial safety factor. The general equation only applies directly to passive wedges with assumed horizontal passive forces.

(d) Sliding analyses should consider the effects of cracks on the active side of the structural wedge in the foundation material due to differential settlement, shrinkage, or joints in a rock mass. The depth of cracking in cohesive foundation material can be estimated in accordance with the following:

Equation 15-7:
$$d_c = \frac{2c_d}{\gamma} \tan \left(45^\circ - \frac{\phi_d}{2} \right)$$

Where

d_c = depth of crack in cohesive foundation material

$$c_d = \frac{c}{FS}$$

$$\phi_d = \tan^{-1} \left(\frac{\tan \phi}{FS} \right)$$

The value d_c in a cohesive foundation cannot exceed the embedment of the structural wedge. Cracking depth in massive strong rock foundations should be assumed to extend to the base of the structural wedge. Shearing resistance along the crack should be ignored, and full hydrostatic pressure should be assumed to act at the bottom of the crack. The hydraulic gradient across the base of the structural wedge should reflect the presence of a crack at the heel of the structural wedge.

(e) The effects of seepage forces should be included in the sliding analysis. Analyses should be based on conservative estimates of uplift pressures. For the estimation of uplift pressures on the wedges, it can be assumed that the uplift pressure acts over the entire area of the base of the wedge and if seepage from headwater to tailwater can occur across a cell, the pressure head at any point should reflect the head loss due to water flowing through the medium. The approximate pressure head at any point can be determined by the line-of-seepage method, which assumes that the head loss is directly proportional to the length of the seepage path. The seepage path for the structural wedge extends from the upper surface of the untracked material adjacent to the heel of the cell, along the embedded perimeter of the structural wedge, to the upper surface adjacent to the toe of the cell. Referring to *Figure 15-15*, the seepage distance is defined by points "a" and "b." The pressure head at any point is equal to the elevation head minus the produce of the hydraulic gradient times the distance along the seepage path to the point in question. Estimates of pressure heads for the active and passive wedges should be consistent with those of the heel and toe of the structural wedge.

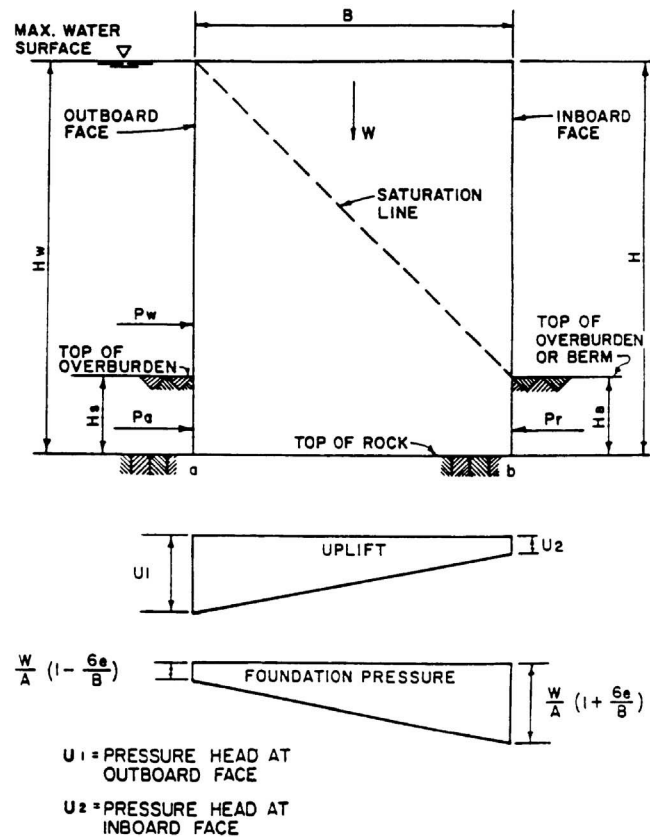


Figure 15-15: Overturning Stability, Typical Loading and Nomenclature

Uplift pressures can be reduced by pressure relief systems. The pressure heads acting on the wedges developed from the line-of-seepage analysis should be modified to reflect the effects of pressure relief systems. For the majority of structural stability computations, the line-of-seepage method is considered sufficiently accurate. However, there may be special situations where the flow net method is required to evaluate seepage forces.

15.3.3.1.4. Seismic Sliding Stability

The sliding stability of a sheet pile cellular structure for an earthquake-induced base motion should be checked by assuming the specified horizontal earthquake acceleration, and the vertical earthquake acceleration if in the analysis, will act in the most unfavourable direction. The earthquake-induced forces on the structure and foundation wedges can then be determined by a rigid body analysis. The horizontal earthquake acceleration can be obtained from seismic zone maps or, in the case where a design earthquake has been specified for the structure, an acceleration developed from analysis of the design earthquake. The vertical earthquake acceleration is normally neglected but can be taken as two-thirds of the horizontal acceleration, if included in the analysis. The added mass of the retained pool and soil can be approximated by Westergaard's parabola, and the Mononobe-Okabe method, respectively. The structure should be

Marine Solutions

Solutions for Breakwaters, Shore Protection and Marina Docks

Economy, durability, and versatility

CONTECH® Marine Products provide economical and effective solutions for various marine applications, including shore protection, primary and secondary breakwaters, jetties and marina docks.



For more information, call Toll Free: 800-338-1122.
Or, visit our web site at www.contech-cpi.com

CONTECH
CONSTRUCTION PRODUCTS INC.

INNOVATIVE CIVIL ENGINEERING SITE SOLUTIONS

 American
Owned and Operated

©2003 CONTECH Construction Products Inc. All Rights Reserved

designed for a simultaneous increase in force on one side and decrease on the opposite side of the cell when such can occur.

15.3.3.2. Overturning

A soil-filled cellular structure is not a rigid gravity structure that could fail by overturning about the toe of the inboard side. Before overturning could occur, the structure must have failed from causes such as pullout of the sheet piles at the heel and subsequent loss of cell fill. Nevertheless, a gravity-block analysis may serve as a starting point for determining the required cell diameter. Considering that the cell fill cannot resist tension, the cell should be proportioned so that the resultant of all forces falls within the middle one third of the equivalent rectangular base. This type of analysis will also serve to determine foundation pressures with

Equation 15-8:
$$FP = \frac{W}{A} \left(1 \pm \frac{6e}{B} \right), e \leq \frac{B}{6}$$

Where

- FP = computed foundation pressure
- W = effective weight of cell fill
- A = area of base = B x 1.0 for 1-foot strip
- e = eccentricity of resultant of all forces from centre of cell

See Figure 15-15. Again, it must be emphasized that overturning computations based on the gravity block concept do not give a true indication of cell stability.

15.3.3.3. Rotation (Hansen's Method ¹⁵³)

This method considers cellular structures to act as rigid bodies. For cells founded on rock, failure occurs along a circular sliding surface in the cell fill intercepting the toe of the sheet piles; however, for ease of calculation it is convenient to assume a logarithmic spiral of radius

Equation 15-9:
$$r = r_0 e^{\theta \tan \phi}$$

where

- r and θ = variables in the polar coordinate system
- r_0 = radius to the beginning of the spiral
- ϕ = angle of internal friction

As shown in Figure 15-16, the resultant of the unknown internal forces on the spiral will pass through the pole of the spiral and thus not enter into the equation of moments about the pole.

The FS against failure is defined as the ratio of moments about the pole, that is, the ratio of the effective weight of the cell fill above the failure surface to the net overturning force.

Thus

Equation 15-10:
$$FS = \frac{M_B}{M_\omega}$$

- M_B = moment about pole due to ΣR
- ΣR = resultant of W'_s , Pe_a , Pe_R , and U
- W'_s = total weight of cell fill above failure surface
- Pe_a and Pe_R = active and passive forces on embedded portion of cell, respectively
- M_ω and ΣP = as previously defined

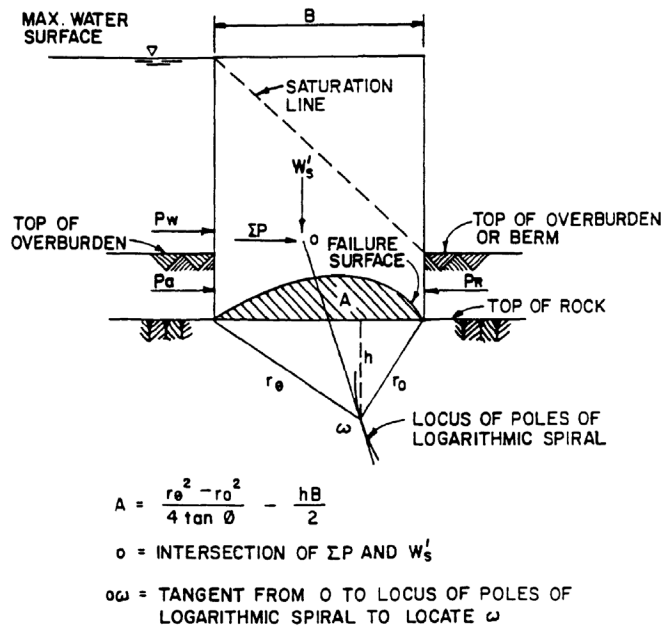


Figure 15-16: Rotation -- Hansen's method, cell founded on rock

where

- M_B = moment about pole of $W'B$
- W'_B = effective weight of cell fill above failure surface
- M_ω = moment about pole due to resultant overturning force ΣP
- $\Sigma P = (P_w + P_a - P_r)$ as shown in Figure 15-16.

The pole of the logarithmic spiral may be found by trial until the minimum factor of safety is determined. However, since the pole of the failure spiral is on the locus of poles of the logarithmic spirals that pass through the toes of the sheet piles, the failure plane pole can be found by drawing the tangent to this locus from the intersection.

Hansen's method, as applied to cells founded on rock, is applicable only where the rock is not influenced by discontinuities in the foundation to at least a depth h (Figure 15-16).

The Hansen method of analysis for cells founded on soil is similar to that of cells founded on rock, except that the failure surface can be convex or concave, i.e., the surface of rupture can be in the cell fill or in the foundation. Both possibilities must be investigated to determine the minimum FS. The FS is defined using Equation 15-10 but the variables are defined in the following manner:

¹⁵³Brinch Hansen, J. (1953). *Earth Pressure Calculations*, The Danish Technical Press, The Institution of Danish Civil Engineers, Copenhagen.

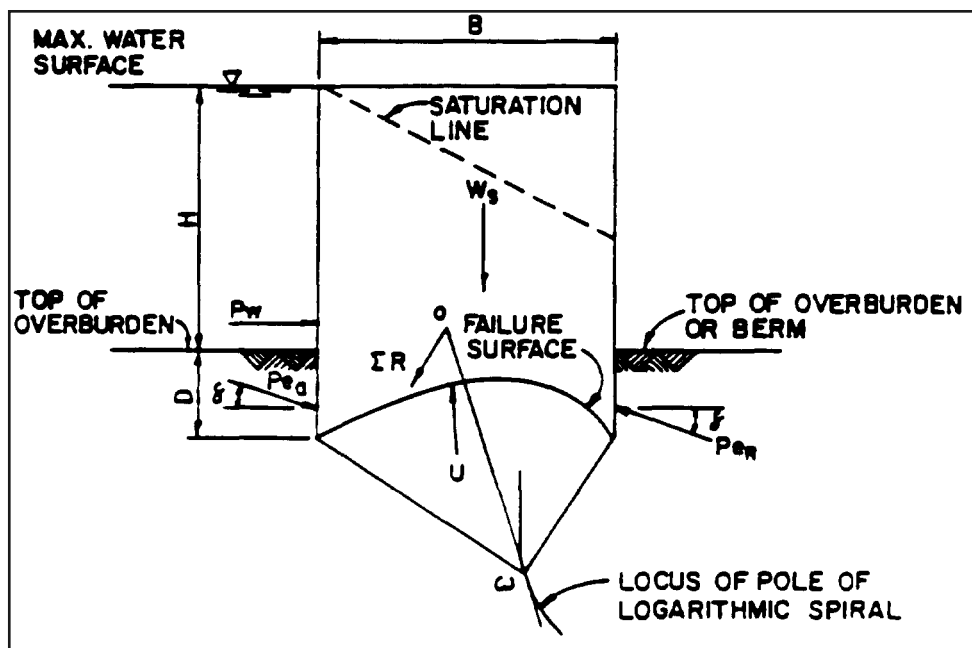


Figure 15-17: Rotation – Hansen's Method, Cell Founded on Soil, Rupture Surface into the Cell Fill

See Figure 15-17 and Figure 15-18.

Stability, as determined by the Hansen method, is directly related to the engineering properties of the cell fill and the foundation and properly considers the saturation level within the cell as well as seepage forces beneath the cell. This method of analysis is particularly appropriate for cells founded in overburden. A more detailed explanation of this method can be found in discussions by Hansen¹⁵³ and Ovesen¹⁵⁴.

15.3.4. Deep-Seated Sliding Analysis

15.3.4.1. Introduction

Sliding stability has been discussed earlier. In general, a cell on rock will very rarely fail on its base, probably because of friction of the fill and anchoring of the sheet pile penetrated to some distance into the rock¹⁵⁵. Analysis and tests on sheet pile cells driven into sand indicated that failure by tilting due to overturning moment should occur long before the maximum sliding resistance is reached¹⁵⁴. Failure by sliding would

occur if the resultant lateral force acts near the base of the cell, which is an unlikely event¹⁵⁶.

However, sedimentary rock formations frequently contain clay seams between competent rock strata¹⁵⁷. Slickensides or a plane of weakness in a rock shelf may exist beneath the cell. Seams of pervious sand within the clay deposit, which may permit the development of excess hydrostatic pressure below the base of the cell, may also exist. Excess hydrostatic pressure reduces the effective stress and, subsequently, reduces shearing resistance to a very small value. This is a very common occurrence in alluvial soils¹⁵⁸.

Drop of shear strength of clay shale to its residual strength due to removal of overburden pressure after Bjerrum observed excavation¹⁵⁹. Fetzner¹⁶⁰ reported a progressive failure of clay shale below Cannelton cofferdam.

Hence, the possibility of a deep-seated failure along any weak seam below a cellular structure always exists before any other type of failure could occur. A detailed study of the sub-

¹⁵⁴Ovesen, N. K. (1962). "Cellular Cofferdams Calculation Method and Model Tests," Bulletin 14, Danish Geotechnical Institute, Copenhagen.

¹⁵³Belz, C. A. 1970. "Cellular Structure Design Methods," Design and Installation of Pile Foundations and Cellular Structures, Enviro Publishing Co., Inc., Lehigh Valley, Pennsylvania; Cummings, E. M. 1957 (Sep). "Cellular Cofferdams and Docks," Journal of the Waterways and Harbors Division, American Society of Civil Engineers, New York, New York.; Swatek, E. P., Jr. 1967 (Aug). "Cellular Cofferdam Design and Practice," Journal, Waterways and Harbors Division, American Society of Civil Engineers, New York, New York, WW 3; Swatek, E. P., Jr. 1970. "Summary - Cellular Structure Design and Installation," Design and Installation of Pile Foundations and Cellular Structures," Enviro Publishing Co., Inc., Lehigh Valley, Pennsylvania; TVA Division of Engineering and Construction. 1966 (Nov). "Steel Sheet Piling Cellular Cofferdams on Rock," Tennessee Valley Authority, Office of Chief of Engineers, Technical Monograph No. 75, Vol 1, Knoxville, Tennessee.

¹⁵⁶Maitland, J. K. and Schroeder, W. L. 1979 (Jul). "Model Study of Circular Sheet Pile Cells," American Society of Civil Engineers, GT 7, New York, New York.

¹⁵⁷Gaddie, T. and Gray, H. 1976 (Aug). "Cellular Sheet Pile Structures," Corps-Wide Conference on Computer-Aided Design in Structural Engineering, U. S. Army Engineer Waterways Experiment Station, Vicksburg, Mississippi.

¹⁵⁸Lacroix, Y., Esrig, M. I., and Luscher, U. 1970 (Jun). "Design, Construction, and Performance of Cellular Cofferdams," "Lateral Stresses in the Ground and Earth Retaining Structures," Journal, Soil Mechanics and Foundation Division, American Society of Civil Engineers, Specialty Conference, Cornell University, Ithaca, New York, pp 271-328; Wu, T. H. 1966. "Problems of Stability," Soil Mechanics, Section 10.9, Allyn and Bacon, Inc., Boston, Massachusetts.

¹⁵⁹Bjerrum, L. 1967 (Sep). "The Third Terzaghi Lecture: Progressive Failure in Slopes of Overconsolidated Plastic Clay and Clay Shales," Journal, Soil Mechanics and Foundation Division, New York, New York, American Society of Civil Engineers, Vol 98, No. SM 5, Part 1.

¹⁶⁰Fetzner, C. A. 1975. "Progressive Failure in Shale (Cannelton Dam Stage I, Cofferdam Failure)," Ohio River Valley Seminar VI, Ft. Mitchell, Kentucky.

¹⁶¹Broms, B. B. 1975. "Landslides," Foundation Engineering Handbook, Chapter 11, Van Nostrand Reinhold Co., New York, New York.

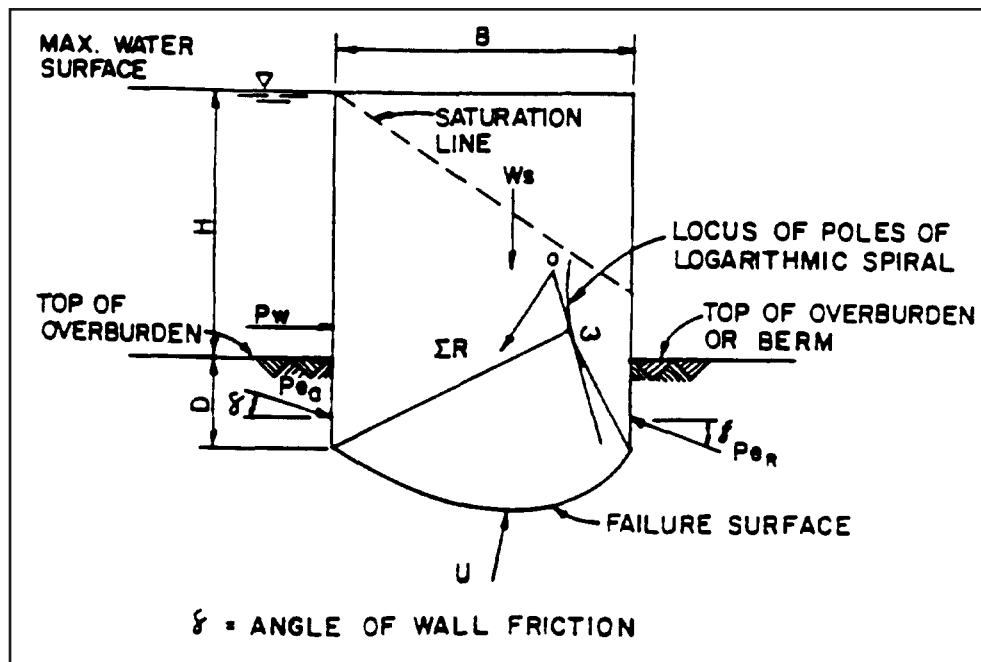


Figure 15-18: Rotation – Hansen’s Method, Cell Founded on Soil, Rupture Surface into the Foundation

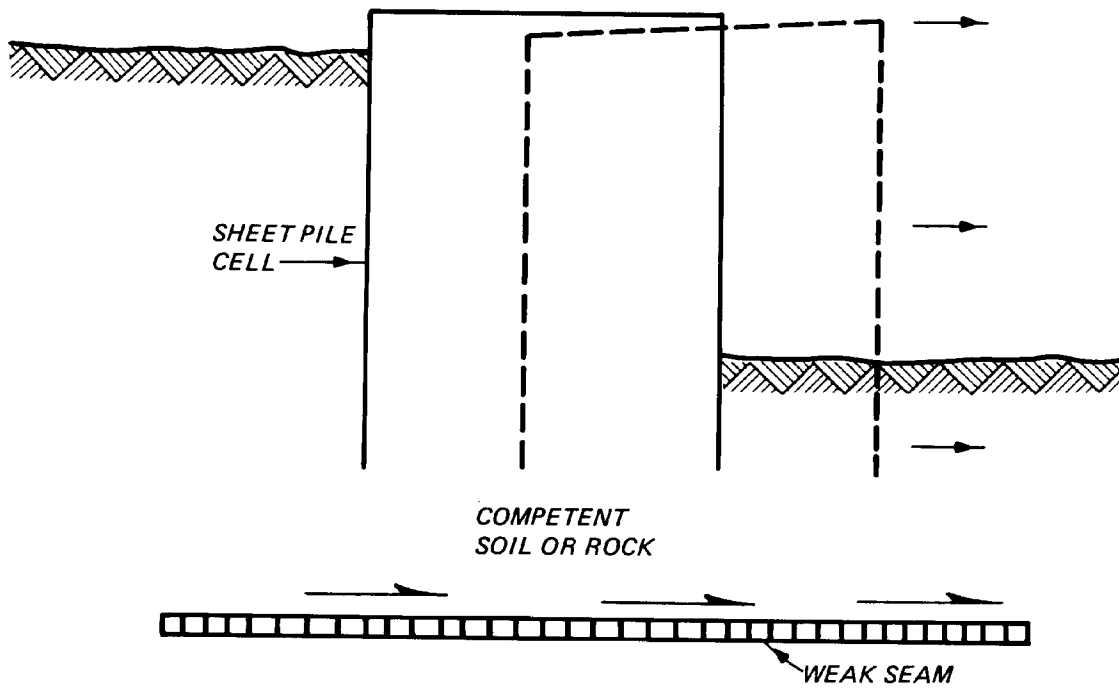


Figure 15-19: Deep-seated sliding failure ¹⁶¹

surface below the design bottom of the cell and an adequate sliding analysis should, therefore, be conducted at the time of a cellular cofferdam design. If any potential for a sliding failure exists, adequate measures to prevent such failure should be incorporated in the cell design. Details of such investigation and preventive measures are discussed in subsequent paragraphs. Figure 15-19 illustrates how a deep-seated sliding failure may occur below a cell.

15.3.4.2. Study of Subsurface Conditions

The subsurface investigation should be extended to at least 15 to 20 feet below the design base level of the cell. Continuous sampling of soils or coring of rock should be performed in the presence of experienced geotechnical personnel to identify and locate any weak seam below the base. The presence of any cracks or joint pattern in the apparently competent rock mass below the base should be carefully investi-

PTC 50HD Vibrodriever

JOB REPORT

A 50HD installing moorings in Buzzards Bay in New England, U.S.A.

1.2 m (48") diameter casings have to be driven in 12 m (40') deep water near Buzzards bridge. Casings are vertical and also 20° raked.

Average length of the casings 24 m (80'). Max length 40 m (130').

Wall thickness : 11 mm (7/16").

To drive these casings customer has chosen a **PTC 50HD** Vibrodriever of 4,400 in-lbs eccentric moment.

A Linkbelt 100 t crawler crane is utilized mounted on a pontoon.

Soil : silty sand.with S.P.T ≤ 20

TECHNICAL DATA AND EQUIPMENT:

One **PTC** Vibrodriever **50HD** with 2x 85 t Duplex caissons clamps.

PTC Hydraulic Power pack Type **450**



Casing guide

20° Raked Piles



- 20 °C



International Headquarters

158, rue Diderot, F-93698 PANTIN CEDEX - FRANCE
 Tel: + 33 1 49 42 72 95 Fax: + 33 1 48 44 00 02
 website: www.ptc.fr E-Mail Vibrofonneur@ptc.fr

PTC branch in the US
 P.O.BOX 396
 Marylhurst , OR, USA 97096
 Andy Schroeder
 Phone: (503) 656-0422
 fax : (503) 656-2652
 e-mail andrew.schroeder@comcast.net

U.S. Distributors:
American Equipment & Fabricating Co.
 100 Water Street
 E. Providence, RI, USA 02914
 Phone: (401) 438-2626
 Fax: (401) 438-0764
 e-mail: WIN@AMERICAN-EQUIPMENT.COM

Foundation Equipment & Supply, Inc.
 PO Box 1226
 Newberg, OR, USA 97132
 Phone: (503) 537-9994
 Fax: (503) 554-9322
 Mobile: (503) 860-2207
 e-mail : mcolby@teleport.com

Conmaco Inc.
 1602 Engineers Road
 Belle Chasse, LA, USA 70037-3137
 Phone: (504) 394-7330
 Fax: (504) 393-8715
 e-mail: mfavaloro@comaco.com

Conmaco Inc.
 3036 Yadkin Road
 Chesapeake, VA, USA 23323
 Phone: (757) 485-5010
 Fax: (757) 485-0856

gated. If soft seams or presheared surfaces due to faulting are found, extremely low shear strengths approaching the residual strengths should be used in the analysis. Unless 100 percent core recovery is achieved, the presence of a soft or presheared seam should be assumed where the core is missing. Investigation of any weak seam below the cell should be extended to some distance beyond the inboard and the outboard sides of the cofferdam. This information will be useful in conducting sliding stability analyses.

15.3.4.3. Methods of Sliding Stability Analysis

15.3.4.3.1. Wedge Method

The FS against sliding failure along a weak seam below the cell can be determined by using the method of wedge analysis described earlier. For deep-seated sliding, a major portion of the failure mass slides along the weak seam. Hence, for each trial analysis, a large part of the failure surface should pass through the weak seam. The structural wedge is formed by the boundary of the cell section extended downward to the assumed failure surface. This wedge acts as the central block between the active and the passive wedge systems. Other assumptions including some simplifications made in the sliding analysis are the same as those discussed earlier.

The effects of cracks in the active wedge system and of seepage within the sliding mass including the uplift pressure beneath the structural wedge should be considered in the manner described earlier. For each trial failure surface system, the minimum FS should be determined. The lowest value from all of these trials is likely to be the actual FS against sliding failure. A FS of 1.5 is adequate against a deep-seated sliding failure.

15.3.4.3.2. Approximate Method

The approximate method may be used when the weak

seam is located near the bottom of the sheet pile. The cofferdam is subjected to the lateral driving pressures on the outboard face, the frictional resistance along the bottom of the cofferdam and berm (if one is used) and the passive resistance of the soil on the inboard face, as shown in *Figure 15-20*.

Notation for *Figure 15-20*:

- B = equivalent width of cell
- H_W = head of water on the outboard side
- H_S = height of overburden on the outboard side
- H_B = height of berm or overburden on the inboard side
- W = weight of cell fill above the weak seam
- P_W = hydrostatic pressure due to head, H_W
- P_a = active earth pressure due to overburden of height, H_S
- P_R = resultant of passive earth pressure due to buoyant weight of the berm + hydrostatic pressure due to height, H_B
- R_S = lateral resistance along weak seam

The safety factor for horizontal sliding of the cofferdam is obtained by considering the driving forces and the potential resisting forces acting per unit length. The driving forces are

Equation 15-11: $P_W = 1/2 \gamma_w H_W^2$

And

Equation 15-12: $P_a = 1/2 K_a \gamma' H_S^2$

where

- K_a = active earth pressure coefficient of overburden materials
- γ' = submerged unit weight of soil on the outboard side of the cofferdam
- γ_w = unit weight of water = 62.4 pounds per cubic foot or 9.81 kN/m³

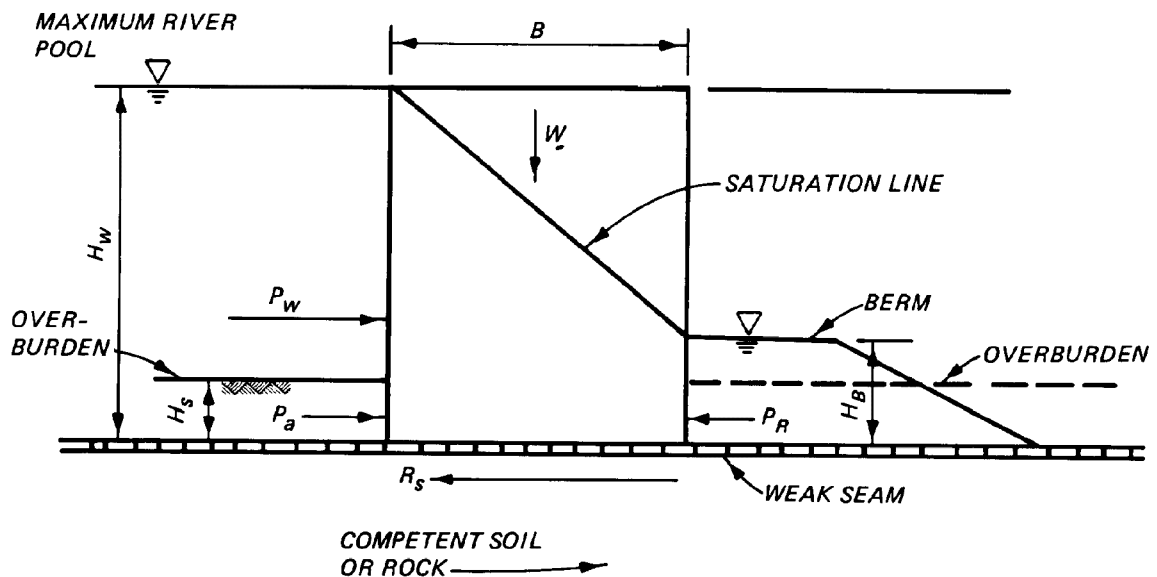


Figure 15-20: Sliding along Weak Seam Near Bottom Of Cell (approximate method)

The resisting forces are

(1) Passive resistance of soil and berm on inboard face of cofferdams:

$$\text{Equation 15-13: } P_R = P_P = \frac{1}{2} \gamma' K_p H_B^2$$

Values of K_p should be determined by Rankine or Coulomb¹⁶² theory modified to account for any intersection of the failure wedge with the back slope of the berm. These theories should be used because the presence of the rock will not permit a log-spiral failure to develop.

(2) Friction force along bottom of the cell:

$$\text{Equation 15-14: } R_S = W \tan \phi + Bc$$

$$W = \frac{1}{2} (\gamma_c + \gamma'_c) B (H_W - H_B) + \gamma'_c B H_B$$

where

- W = effective weight of cell fill =
- γ_c = unit weight of the cell fill
- γ'_c = submerged unit weight of the cell fill
- ϕ = internal friction angle of the soil
 - o $\tan \phi = 0.5$ for a cell resting on smooth rock
 - o For clay, $\phi = 0$ and $c = c$
 - o For sand, $\phi = \phi$ and $c = 0$

The resulting safety factor against sliding is:

$$\text{Equation 15-15: } FS = \frac{R_s + P_R}{P_W + P_A}$$

15.3.4.3.3. Culmann's Method

For a berm with combined horizontal and inclined surfaces, passive pressure should be calculated using Culmann's graphical method or any other suitable method. The lateral resistance at the interface of the berm and the weak seam should also be calculated. The smaller of the lateral resistance and the passive pressure should be considered in calculating the FS against sliding¹⁶³. For overburden with the horizontal surface to a great distance on the inboard side, the passive pressure can be calculated, using the passive earth pressure coefficient K_p . Since no effect of the weak seam is considered in the passive pressure calculation, the FS based on this passive pressure may be approximate.

For a more precise analysis, the wedge method described previously should be adopted.

15.3.4.4. Prevention of Sliding Failure

The potential for sliding stability failure can be considerably reduced by adopting the following measures.

(1) Seepage Control below Cell. The extension of the sheet piles to considerably deeper levels below the cell will develop longer drainage paths and reduce the flow rate through the foundation materials, thereby decreasing the uplift pressure below the structural and the passive wedge systems and increasing the FS against sliding failure.

(2) Dissipation of Excess Hydrostatic Pressure. Excess hydrostatic pressure within a sand seam between clay strata below the cell will be dissipated quickly if adequate relief wells are installed within the seam. The shear strength of the sand seam will be increased and the potential for sliding failure along the seam will be reduced.

(3) Berm Construction on the Inboard Side. An inside berm will increase the passive resistance and will also aid in lengthening the seepage path discussed above only if impermeable berm is used. The berm should be constructed of free-draining sand and gravel to act as an inverted filter maintaining the free flow of pore water from the cell fill and the foundation materials.

The increase in the passive resistance due to berm construction will improve the FS against sliding failure.

15.3.5. Bearing Capacity Analysis

The cells of a cofferdam must rest on a base of firm material that possesses the bearing capacity to sustain the weight of the filled cells. Presence of weak soil beneath the cell may cause a bearing capacity failure of the entire structure inducing the cell to sink or rotate excessively¹⁶⁴. Figure 15-21 shows graphically bearing capacity failure of a cell supported on weak soil.

The bearing capacity of rock is usually controlled by the defects in the rock structure rather than the strength alone. Defective and weak rock, such as some chalks, clay shales, friable sandstones, very porous limestones, and weathered, cavernous, or highly fractured rock may cause very large settlements under a relatively small load and reduce the load bearing capacity. Interbedding of hard (such as cemented sandstone) and very soft (such as claystone) layers may also cause bearing capacity problems¹⁶⁵. A cofferdam on rock may not function properly due to shear failure of soil on the base of the rock or by deep-seated sliding along any weak seam within the rock. This aspect of the design has been discussed. The methods of determining bearing capacity of soils and rock to support a sheet pile cellular structure are discussed below.

¹⁶²In some cases excessively high values of K_p are obtained from Coulomb theory. These should be avoided. See 5.3.

¹⁶³Dismuke, T. D. 1975. "Cellular Structures and Braced Excavations," *Foundation Engineering Handbook*, Van Nostrand Reinhold, Co., New York, New York.

¹⁶⁴Maitland, J. K. 1977. "Behavior of Cellular Bulkheads in Deep Sands," Ph. D. Thesis submitted at Oregon State University, Corvallis, Oregon.

¹⁶⁵Goodman, R. E. 1980. "Applications of Rock Mechanics to Foundation Engineering," *Introduction to Rock Mechanics*, John Wiley and Sons, New York, New York, and Sowers, G. F. 1962. "Shallow Foundations," *Foundation Engineering*, McGraw-Hill Book Co., Inc., New York, New York.

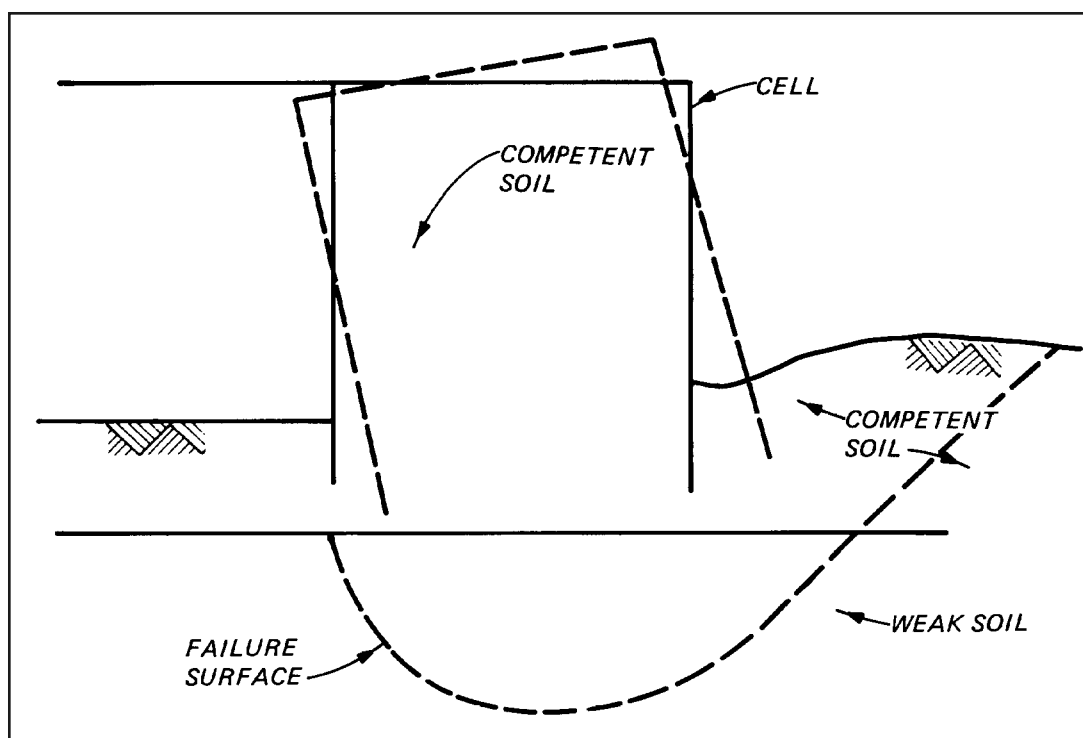


Figure 15-21: Bearing capacity failure

15.3.5.1. Bearing Capacity of Soil

The bearing capacity of granular soils is generally good if the penetration of the sheet piles into the overburden is adequate and seepage of water underneath the cell base is controlled. Using an adequate berm on the inboard side can control the seepage that reduces the shear strength of the soil on the inboard side of the cofferdam and thus reduces the bearing capacity. Cellular structures on clay are not very common. The bearing capacity of clay depends on the consistency of the soils; the stiffer or harder the clay, the better the bearing capacity. For a good bearing capacity, the clay should be stiff to hard. However, even on relatively soft soils, cellular structures have been successfully constructed using heavy sand or rockfill berms¹⁶⁶. The bearing capacity of both cohesive and granular soils supporting cellular structures can be determined by Terzaghi's method of analysis¹⁶⁷. However, the failure planes assumed for the development of the Terzaghi bearing capacity factors¹⁶⁸ do not appear to be as realistic as those developed specifically for cellular structures by Brinch Hansen¹⁶⁹. Hence, for bearing capacity investigation, the Hansen method of analysis should also be used¹⁷⁰. The investigation of failure along any weak stratum below the cell can

be conducted by using the limit equilibrium analysis, as discussed previously. Methods of determining bearing capacity of soils are given below.

15.3.5.1.1. Terzaghi Method

Since we have already assumed the cofferdam be modelled as a continuous wall, for bearing capacity failure we can also assume that the dam can be modelled as a continuous footing. The ultimate bearing capacity is given by for a continuous, strip-loaded area is defined by the equation

$$\text{Equation 15-16: } q_f = cN_c + \gamma D_f N_q + \frac{\gamma B N_\gamma}{2}$$

and for a circular loaded area

$$\text{Equation 15-17: } q_f = 1.3cN_c + \gamma D_f N_q + \frac{3\gamma B N_\gamma}{10}$$

Where

- γ = unit weight of soil around cell (can be wet for submerged)
- B = equivalent cell width
- N_c , N_q and N_γ = Terzaghi bearing capacity factors (see

¹⁶⁶Cummings, E. M. 1957 (Sep). "Cellular Cofferdams and Docks," *Journal of the Waterways and Harbors Division*, American Society of Civil Engineers, New York, New York.

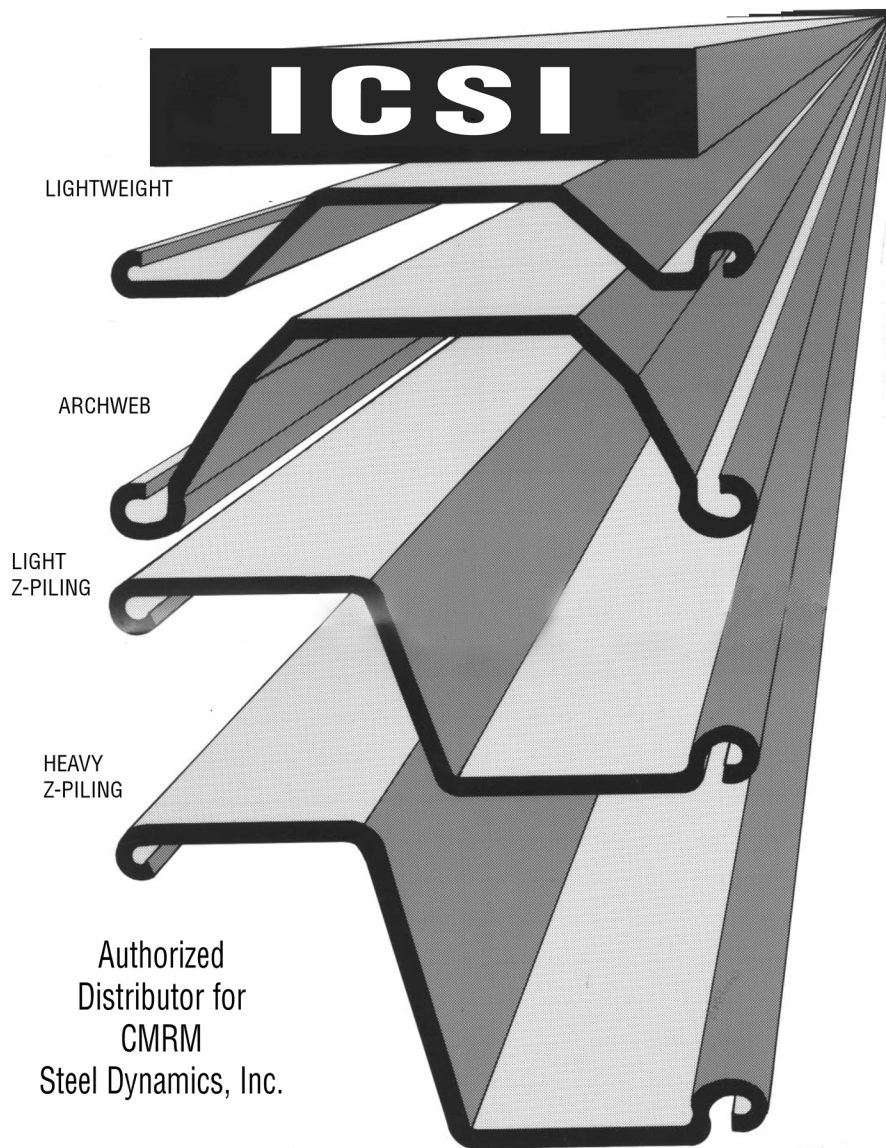
¹⁶⁷An excellent overview of the Terzaghi method can be found in Coduto, D.P. (2001) *Foundation Design: Principles and Practices*. Upper Saddle River, NJ: Prentice-Hall. Coduto also details Vesic's method, which is more inclusive of a wide variety of variables, and can be used for this type of analysis. Other references include Dismuke, T. D. 1975. "Cellular Structures and Braced Excavations," *Foundation Engineering Handbook*, Van Nostrand Reinhold, Co., New York, New York, and United States Steel Corporation. 1972. "Cellular Cofferdams," *US Steel Sheet Piling Design Manual*, Pittsburgh, Pennsylvania.

¹⁶⁸Terzaghi, K. 1943. "Bearing Capacity," *Theoretical Soil Mechanics*, John Wiley and Sons, Inc., New York, New York.

¹⁶⁹Brinch Hansen, J. 1961. "Stability and Foundation Problems," *Pressure Calculation*, The Danish Technical Press, The Institution of Danish Civil Engineers, Second Edition, Copenhagen.

¹⁷⁰Gaddie, T. and Gray, H. 1976 (Aug). "Cellular Sheet Pile Structures," *Corps-Wide Conference on Computer-Aided Design in Structural Engineering*, U. S. Army Engineer Waterways Experiment Station, Vicksburg, Mississippi.

INTERNATIONAL CONSTRUCTION SERVICES, INC.



Authorized
Distributor for
CMRM
Steel Dynamics, Inc.

**We have
PZ-22,
PZ-27,
PZ-35
and
PZ-40
Equivalents!!**

**NEW AND USED
FOR SALE
FOR RENT**

ALSO
Lightweight Piling
Waterloo Sheet Piling
H-bearing Pile
Structural Sections
Piling Accessories
Coatings

Call Now!

**International Construction Services, Inc.
Corporate Headquarters
P.O. Box 15598
Pittsburgh, PA 15244-0598
Ph: (888) 593-1600 or (412) 788-6430
Fax: (412) 788-9180 • E-mail: icsi@nb.net**

**New York Area
888-593-1600**

**Chicago, IL
815-609-9527**

**Sacramento, CA
916-989-6720**

Table 15-2); these are functions of the internal angle of friction of the soil ϕ

- c = cohesion of soil
- D_f = distance from the ground surface to the toe of the cell.

Table 15-2: Terzaghi Bearing Capacity Factors (after EM 1110-1-1905)

ϕ^* , Degrees	N_q	N_c	N_γ
0	1.00	5.70	0.0
2	1.22	6.30	0.2
4	1.49	6.97	0.4
6	1.81	7.73	0.6
8	2.21	8.60	0.9
10	2.69	9.60	1.2
12	3.29	10.76	1.7
14	4.02	12.11	2.3
16	4.92	13.68	3.0
18	6.04	15.52	3.9
20	7.44	17.69	4.9
22	9.19	20.27	5.8
24	11.40	23.36	7.8
26	14.21	27.09	11.7
28	17.81	31.61	15.7
30	22.46	37.16	19.7
32	28.52	44.04	27.9
34	36.50	52.64	36.0
35	41.44	57.75	42.4
36	47.16	63.53	52.0
38	61.55	77.50	80.0
40	81.27	95.66	100.4
42	108.75	119.67	180.0
44	147.74	151.95	257.0
45	173.29	172.29	297.5
46	204.19	196.22	420.0
48	287.85	258.29	780.1
50	415.15	347.51	1153.2

The FS against bearing capacity failure should be determined by the maximum pressure at the base of the cellular structures. Figure 15-22 shows the section of cofferdam of equivalent width, B , and subjected to a hydrostatic pressure of P_w , and active and passive pressures of P_a and P_R , respectively.

The net overturning moment due to these lateral pressures is given by

$$\text{Equation 15-18: } M = 1/3(P_w H_w + P_a H_s - P_R H_B)$$

where H_w , H_s , and H_B are as shown in Figure 15-22. The bearing soil is subjected to a uniform vertical compressive stress of W/B , where W is the weight of the cell fill. In addition, the soil is also subjected to a compressive stress developed due to the net overturning moment, M . This stress is equal to $6M/B^2$. Hence, the FS against bearing capacity failure is

$$\text{Equation 15-19: } FS = \frac{q_f}{\left(\frac{6M}{B^2}\right) + \frac{W}{B}}$$

where q_f can be determined from Equation 15-16.¹⁷¹ The FS for sand should not be less than 2 and for clay not less than 3, as given in Table 15-1.

15.3.5.1.2. Hansen Method

In the Hansen method of analysis, cells supported on soils are assumed to have surface of rupture within the cell fill (convex failure surface) or in the foundation soils below the cell (concave failure surface). Both possibilities must be investigated to determine the minimum FS. Details of this method of analysis have been discussed in 15.3.3.3.

15.3.5.1.3. Limit-equilibrium Method

This analysis is based on assumed plane failure surfaces that form the bases of the failure wedges. A FS is applied to the material strength parameters such that the failure wedges are in limiting equilibrium. The critical failure surface with the lowest safety factor is determined by trial wedge method. Details of this method of analysis have been discussed earlier. For the preliminary design of a cofferdam on soils, bearing capacity can be determined by the Terzaghi method. However, more rigorous analysis by the limit-equilibrium method should be applied for the final design. Hansen's method of analysis should be used to determine FS against a rotational failure of the cellular structure.

15.3.5.2. Bearing Capacity of Rock

The bearing capacity of rock is not readily determined by laboratory tests on specimens and mathematical analysis, since it is greatly dependent on the influence of nonhomogeneity and microscopic geologic defects on the behaviour of rock under load¹⁷². The bearing capacity of homogeneous rock having a constant angle of internal friction and unconfined compressive strength q_u can be given as

¹⁷¹This equation is valid in this format for continuous foundations only (such as a cellular cofferdam wall.) For a single circular foundation, see Example 28.

¹⁷²D'Appolonia, E., D'Appolonia, D. J., and Ellison, R. D. 1975. "Drilled Piers," *Foundation Engineering Handbook*, Van Nostrand Reinhold, Co., New York, New York; Goodman, R. E. 1980. "Applications of Rock Mechanics to Foundation Engineering," *Introduction to Rock Mechanics*, John Wiley and Sons, New York, New York; Sowers, G. F. 1962. "Shallow Foundations," *Foundation Engineering*, McGraw-Hill Book Co., Inc., New York, New York.

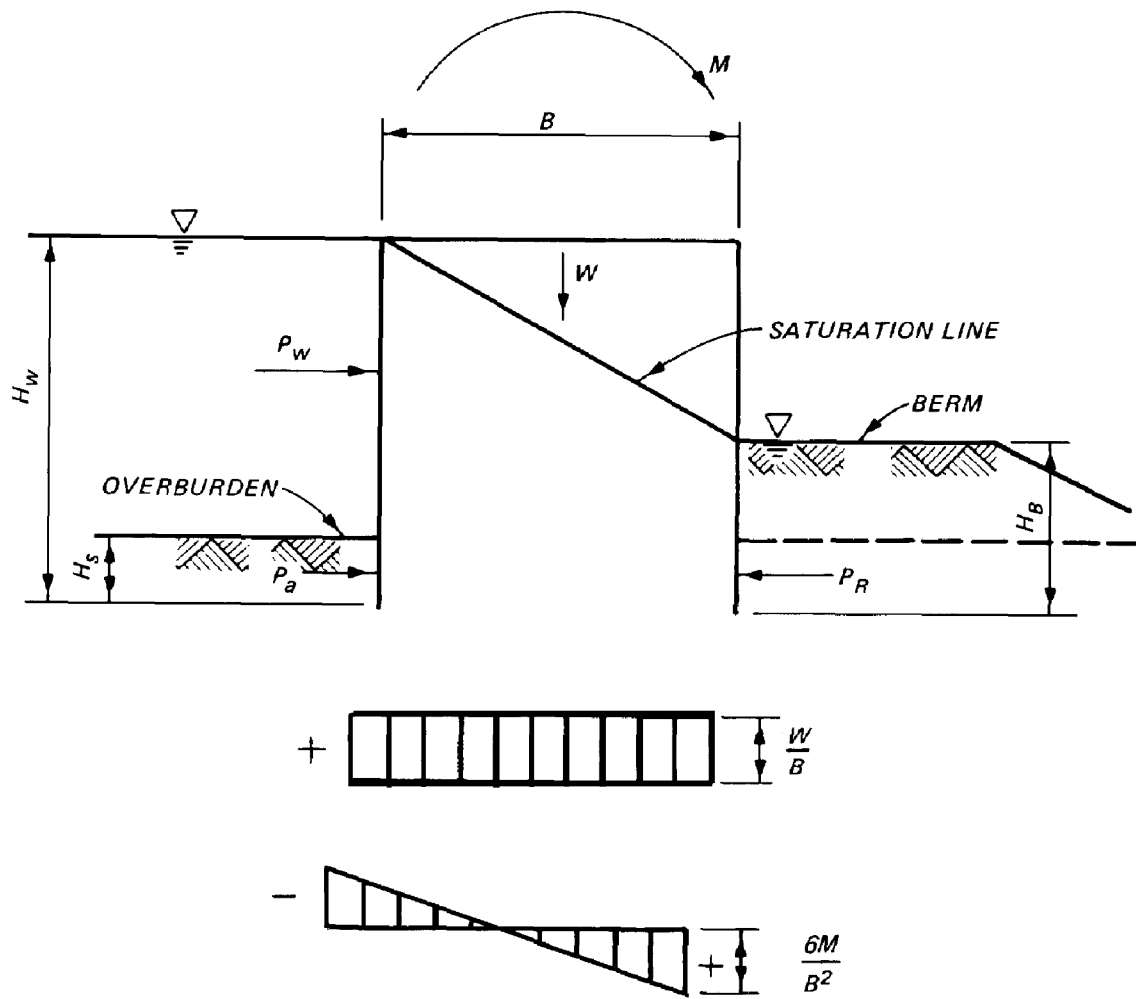


Figure 15-22: Base soil pressure diagram

Equation 15-20: $q_f = q_u (N_\phi + 1)$

Where $N_\phi = \tan^2 \left(45^\circ + \frac{\phi}{2} \right)$

To allow for the possibility of unsound rock, a high value of the FS is generally adopted to determine allowable bearing pressure. A FS of 5 may be used to obtain this allowable pressure from Equation 15-20. Even with this FS, the allowable loads tend to be higher than the code values sampled in Table 15-3. In the absence of test data on rock samples, the somewhat conservative values in Table 15-3 may be used for preliminary design.

When the rock is not homogeneous, the bearing capacity is controlled by the weakest condition and the defects present in the rock. For a rock mass having weak planes or fractures, direct shear tests conducted on presawn shear surfaces give lower bound residual shear strengths¹⁷³. A minimum of three specimens should be tested under different normal stresses to determine cohesion *c* and angle of internal friction. The ultimate bearing capacity can then be determined from Equation 15-16 and Equation 15-17 (Terzaghi method) by using the *c* and values obtained as described above.

¹⁷³Clough, G. W. and Hansen, L. A. 1977. "A Finite Element Study of the Behavior of the Willow Island Cofferdam," Technical Report CE-218, Department of Civil Engineering, Stanford University.

Table 15-3: Allowable Bearing Pressures for Fresh Rock of Various Types¹⁷⁴

Rock Type	Age	Location	Allowable Bearing Pressure (MPa) (1 MPa=10.4 tsf)
Massively bedded limestone ¹⁷⁵		United Kingdom ¹⁷⁶	3.8
Dolomite	Late Palaeozoic	Chicago	4.8
Dolomite	Upper Palaeozoic	Detroit	1.0-9.6
Limestone	Late Palaeozoic	Kansas City	0.5-5.8
Limestone	Upper Palaeozoic	St. Louis	2.4-4.8
Mica schist	Precambrian	Washington	0.5-1.9
Mica schist	Precambrian	Philadelphia	2.9-3.8
Manhattan schist ¹⁷⁷	Precambrian	New York	5.8
Fordham gneiss ¹⁷⁷	Precambrian	New York	5.8
Schist and slate	Precambrian	United Kingdom ¹⁷⁶	0.5-1.2
Argillite		Cambridge, MA	0.5-1.2
Newark shale	Triassic	Philadelphia	0.5-1.2
Hard, cemented shale	Cretaceous	United Kingdom ¹⁷⁶	1.9
Eagleford shale		Dallas	0.6-1.9
Clay shale		United Kingdom ¹⁷⁶	1.0
Pierre shale	Cretaceous	Denver	1.0-2.9
Fox Hills sandstone	Tertiary	Denver	1.0-2.9
Solid chalk	Cretaceous	United Kingdom ¹⁷⁶	0.6
Austin chalk	Cretaceous	Dallas	1.4-4.8
Friable sandstone and claystone	Tertiary	Oakland	0.4-1.0
Friable sandstone (Pica formation)	Quaternary	Los Angeles	0.5-1.0

15.3.6. Settlement of Sheet Pile Cofferdam

A cellular cofferdam underlain by compressible soils below its base will undergo settlement due to the weights of the cell and berm fills. As observed by Terzaghi¹⁷⁸, if the compressible soils below the cofferdam continue to consolidate after the

overturning moment has been applied, a relatively small moment suffices to produce a very unequal distribution of pressure at the base of the cell. This reduces the capacity of the cofferdam to carry overturning moment. Large postconstruction settlements of cellular wharf structure might dam-

¹⁷⁴Thorburn, S. H. 1966. "Large Diameter Piles Founded in Bedrock," *Proceedings of Symposium on Large Bored Piles*, Institute of Civil Engineers, London; Woodward, R. J., Gardner, W. S., and Greer, D. M. 1972. *Drilled Pier Foundations*, McGraw-Hill Book Co., Inc., New York, New York. When a range is given, it relates to usual rock conditions. According to typical building codes, reduce values accordingly to account for weathering or unrepresentative fracturing.

¹⁷⁵Thickness of beds greater than 1 m, joint spacing greater than 2 m; unconfined compressive greater than 7.7 MPa (for a 4" cube).

¹⁷⁶Institution of Civil Engineers Code of Practice 4.

¹⁷⁷Sound rock such that it rings when struck and does not disintegrate. Cracks are unweathered and open lines less than 1 cm.

¹⁷⁸Terzaghi, K. 1945. "Stability and Stiffness of Cellular Cofferdams," *American Society of Civil Engineers, Transactions*, Vol 110, Paper No. 2253, pp 1083-1202.

COMPOSITE Z™



Composite Z sheet profile

FEATURES

- Corrosion resistant
- High strength reinforced composite
- No coating required
- Lightweight for easy installation
- Non-conductive
- Easy to cut
- Easy to thread
- Domestic "Ball & Socket" interlock

Products

- Z-100 sheet pile
- Z-200 sheet pile
- Z-90 Corner
- Z-100 Cap system
- Z-200 Cap system
- Z-Beam wale system
- EZ-Deck composite decking

Equipment

- Vibratory Hammers
- Model 10
- Model 20



"the sheet pile of tomorrow available today"

Contact us:

Voice: 561-848-2050
 Fax: 561-842-7209
 Z@compositeZ.com

Composite Components, Inc.

P.O. Box 14295
 North Palm Beach, FL 33408
 www.CompositeZ.com

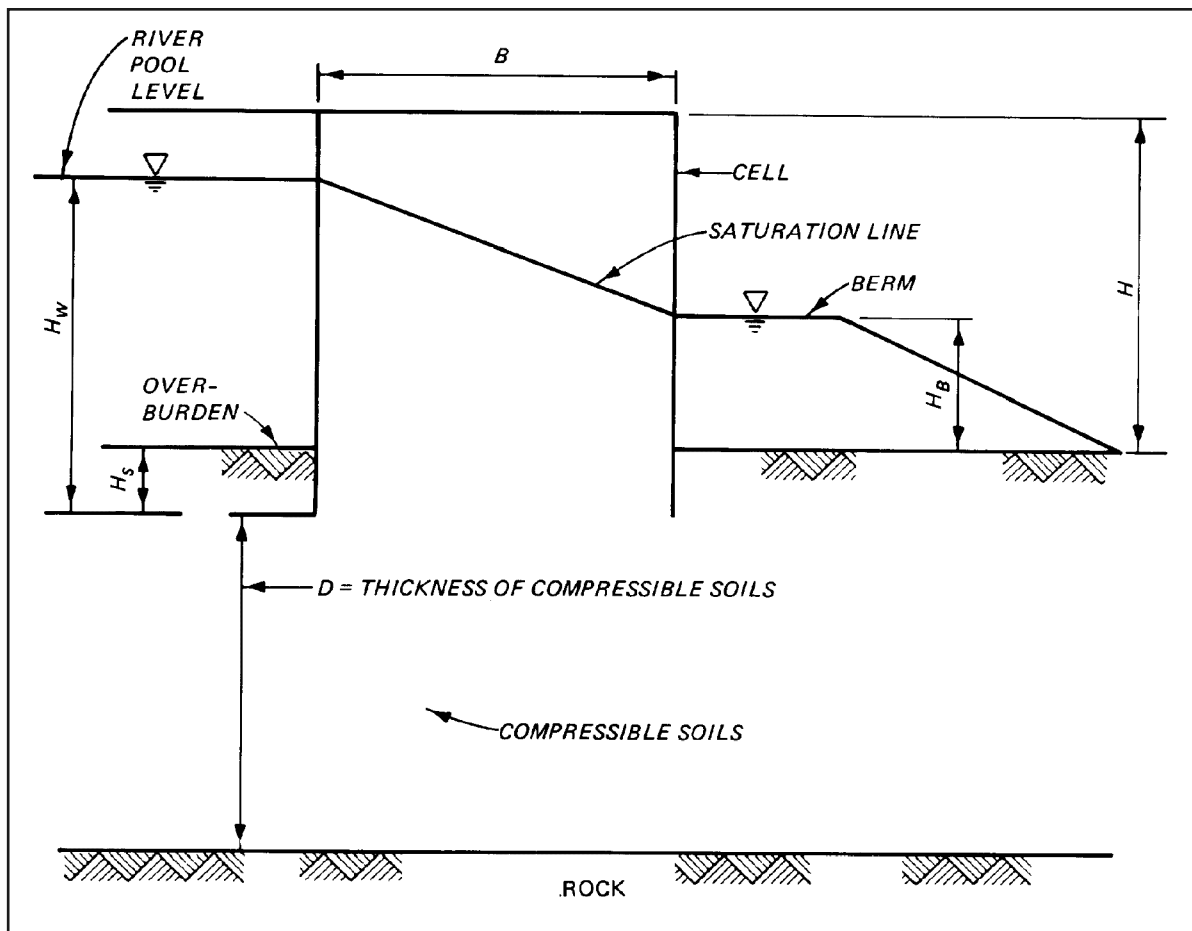


Figure 15-23: Cellular cofferdam on compressible soils

age the deck slab and interfere with all normal operations from the deck. A study of settlement behaviour of a cellular structure is an essential part of the design. This settlement can be computed by classical consolidation theory if the cell is underlain by clay, and by methods such as the Schmertmann method if underlain by granular soils.

15.3.6.1. Settlement of Cofferdam on Clay

In a clay layer beneath the cofferdam, more settlement will occur below the centre than will occur below the edges of the cofferdam because of larger stresses below the centre than the edges under the uniform flexible load of the cell fill at the base of the cells. Additional unequal settlements will occur below the cells if berm or backfill is present on one side of the cofferdam. Figure 15-23 is a sketch of a cell on compressible soils underlain by rock.

Stresses at various levels below the centre and the sides of the cellular cofferdam can be determined using Boussinesq's theory of stress distribution. The load due to cell fill in the

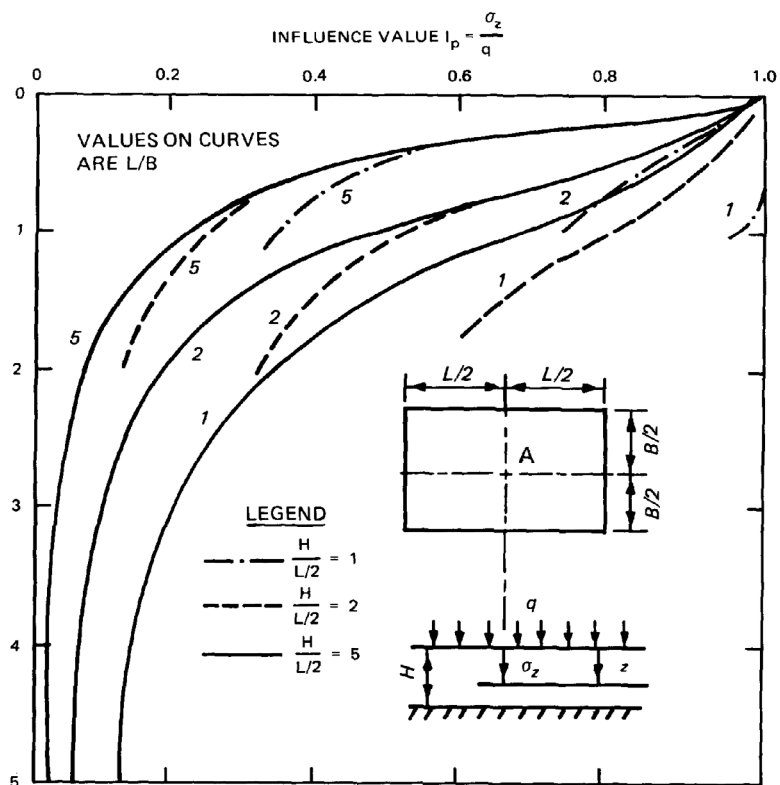
cofferdam may be assumed a uniformly distributed contact pressure of a continuous footing of equivalent width B . For preliminary calculation, B may be taken as 0.85 times the cell diameter. If no rock is encountered at a relatively shallow depth, the Boussinesq or Westergaard charts as shown in most soil mechanics textbooks may be used to compute stresses in the compressible soil below any point in the cofferdam.

If rock is encountered at a relatively shallow depth, stresses may be computed from the influence values given in the Sovinc¹⁷⁹ chart that includes correction for the finite thickness of the stressed medium (Figure 15-24). The trapezoidal section of the berm fill may be approximated to a rectangular section and the stresses may then be computed as described before. Alternately, the berm section may be divided into a rectangular and a triangular section. The stresses below the cell, due to these rectangular and triangular surface loadings, may then be calculated using vertical stress tables by Jumikis¹⁸⁰ or from appropriate charts given in textbooks.

¹⁷⁹Sovinc, I. 1961. "Stresses and Displacements in a Limited Layer of Uniform Thickness, Resting on a Rigid Base, and Subjected to a Uniformly Distributed Flexible Load of Rectangular Shape," *Proceedings, Fifth International Conference on Soil Mechanics and Foundation Engineering*, Vol 1, p 823, Paris, France.

¹⁸⁰Jumikis, A. R. 1971. "Vertical Stress Tables for Uniformly Distributed Loads on Soil," Engineering Research Publication No. 52, Rutgers University, New Brunswick, New Jersey.

Figure 15-24: Influence value I for vertical stress P at depth z below the centre of a rectangular loaded area on a uniformly thick layer resting on a rigid base.



15.3.6.2. Settlement of Cofferdam on Sand

The settlement of a foundation on sand occurs at a very rapid rate following application of the load. For a cellular cofferdam on sand, a large part of the settlement of the foundation soils would occur during placement of fill inside the cells. As discussed before, the estimate of the total and differential settlements of a cellular structure is very important to examine any possibility of damage due to such settlements. The settlement of a structure on granular soils can be calculated by Schmertmann's or other methods.

15.3.6.2.1. Settlement Due to Dewatering of Cofferdam Area

Dewatering may cause drawdown of water levels within soil layers below existing structures or utility lines near the cofferdam area. This drawdown increases the effective weight of the soil layers previously submerged. Drawdown of water levels below the dredge level increases the effective stress in soils below the base of the cell. This increase in effective stress causes settlements of compressible soils underneath the structures within the drawdown zone¹⁸¹. An estimate of these settlements is possible by using the methods discussed earlier utilizing the drawdown depths to be determined by procedures below.

15.3.7. Seepage Analysis

Generally, two types of seepage are to be considered for

designing a cellular cofferdam: seepage through the cell fill and foundation underseepage.

15.3.7.1. Seepage through Cell Fill

The free water surface within the cell fill is to be estimated in order to check the stability of the assumed cell configuration. In general, the slope of the free water surface or saturation line may be assumed to be as shown in Figure 15-6, Figure 15-7 or Figure 15-8. The effects on the saturation line during maximum pool, initial filling, and drawdown conditions have been discussed in 15.2.3. For simplifying seepage computations, a horizontal line may be chosen at an elevation representative of the average expected condition of saturation of the cell fill¹⁸². However, adequate measures (e.g., providing weep holes and keeping free-draining quality of cell fill) should always be adopted to assure a reasonable low elevation of saturation.

The zone of saturation within the cell fill is influenced by the following factors:

- Leakage of water into the cell through the outboard piles.
- Drainage of water from the cell through the inboard piles.
- Lower permeability than expected of the cell fill.
- Flood overtopping the outboard piles or wave splash.
- Possible leakage of water into the cell fill from any pipeline crossing the cells.

¹⁸¹Lincoln, Frank L. 1963 (Oct). "Reconstruction of Dry Dock No. 3 at the Portsmouth Naval Shipyard (Part Two)," Journal of the Boston Society of Civil Engineers, Boston, MA, Vol 50, No. 4.

¹⁸²United States Steel Corporation. 1975. "Cellular Cofferdams," US Steel Sheet Piling Design Manual, Pittsburgh, Pennsylvania.

HPSI Vibros



from a
"Little Guy"

to a
"BIG Guy"



Whether it's an excavator mounted vibratory for driving lightweight vinyl or aluminum sheet piling on up to a 20,000 in. lb. machine for driving large diameter caisson, we have a vibro suitable for your job.

SALES & RENTALS

(Distributors throughout North America)

From "The Engineers of Pile Driving Equipment"™

HYDRAULIC POWER SYSTEMS, INC.

Kansas City Offices and Plant
1203 Ozark
N. Kansas City, MO 64116
Phone (816) 221-4774
Fax (816) 221-4591
E-mail info@hpsi-worldwide.com
<http://www.hpsi-worldwide.com>



International & Domestic Sales
745 U.S. Hwy 1
N. Palm Beach, FL 33408
Phone (561) 687-5525
Fax (561) 841-3479
E-mail info@hpsi-worldwide.com
<http://www.hpsi-worldwide.com>

*Vibratory Pile Hammers • Hydraulic Augers • Winch Systems
Custom Manufacturing • Hydraulic Impact Hammers • Lead Systems*

ting is shown in *Figure 15-25*. The width of the foundation of cellular cofferdams makes the problem of flow netting similar in some ways to that with earth or concrete dams. Finite element analysis can also be used. Some items that should be kept in mind with this kind of analysis are as follows:

1) As with braced cofferdams, the critical area of analysis for piping or boiling is on the “excavation” side of the sheet pile wall, i.e., the area “abcd” shown in *Figure 15-25*.

2) The gradient factor of safety against piping or boiling should be at least 1.5. For clean sand, exit gradients between 0.5 and 0.75 will cause unstable conditions for men and equipment. To provide security against piping failures, exit gradients should not exceed 0.30 to 0.40. High values of the hydraulic gradient near the toe of the cell greatly reduce the effective weight of the sand near the toe and decrease the passive resistance of the soils. This will increase the possibility of sliding failures of cofferdams.

3) The total flow under the cofferdam can be determined from the flow net in addition to the critical gradient.

15.3.7.3. Control of Seepage

The following methods may be adopted to prevent seepage problems:

15.3.7.3.1. Penetration of Sheet Piles to Deeper Levels

The penetration of sheet piles deep into the sand stratum below the dredge line will increase the length of the percolation path that the water must travel to flow from the upper to the lower pool under the cofferdam¹⁸⁶. The exit gradient to be determined from the new flow net can be lowered to an acceptable value of 0.3 to 0.4, as discussed before, by adequately increasing the penetration depth of the sheet piles. The excess hydrostatic force U acting on prism abcd (*Figure 15-25*) will also be reduced to yield a higher value of the factor of safety. Terzaghi recommends a penetration depth equal to $2H/3$ to reduce hydraulic gradients at critical locations, where H is the upstream head of water. If the water level is lowered to at least $H/6$ below the inboard ground surface, the penetration may be reduced about one-half the height. However, critical hydraulic gradients should always be checked by actual flow net analysis.

15.3.7.3.2. Providing Berm on the Downstream Surface

Deeper penetration of sheet piles in some cases may be uneconomical and impractical. A pervious berm can then be used on the downstream side to increase the FS against piping failures. The berm being more permeable than the protected soil will not have any influence on the flow net, but will counteract the vertical component of the seepage force.

The factor of safety will then be

$$\text{Equation 15-21: } FS = \frac{W + W'}{U}$$

Where

- U = the excess hydrostatic force acting per unit length of the prism “abcd”
- W' = submerged weight of the prism of unit length
- W = added weight of this berm acting as inverted filter

The effect of the berm can be enhanced by covering the danger zone with a loaded, inverted filter under the berm. The filter material must satisfy two independent conditions. It should be coarse enough to permit free discharge of the seepage water and its largest voids must be small enough to prevent clogging from the finer soil particles of the underlying soil.

15.3.7.3.3. Increasing the Width of Cofferdam

The equivalent width of the cofferdam can be increased by using larger diameter cells. This will increase the percolation path of water under the cell from the outboard to the inboard sides. Adequate design may eliminate the necessity of berm on the downstream side. This may be very convenient for construction but is very expensive.

15.3.7.3.4. Installation of Pressure Relief Systems

The exit gradient can also be reduced using adequate pressure relief systems that will lower the artesian head below the bottom of excavation to control upward seepage force¹⁸⁷. The relief wells act as controlled artificial springs that prevent boiling of soil. If the discharge required to produce head reduction is not excessive, better drainage and, therefore, increased stability can often be realized by installation of well points and deep wells underneath the cells near the inboard side. These serve to pick up the flow of water into the cofferdam area under the sheet pile perimeter. The well can be pumped individually by turbine pumps or connected to a collector pipe with a centrifugal well point pump system.

15.3.8. Internal Cell Stability

15.3.8.1. Basic Concepts

Internal cell stability refers to prevention of both failure due to failure of the interlocks and failure due to inadequate horizontal or vertical shear resistance. Before we get to the methods of computing internal cell stability, we need to highlight two important concepts: maximum internal cell pressure and the point of fixity for the inboard sheets.

15.3.8.1.1. Maximum Internal Cell Pressure

Basic soil mechanics indicate that the pressure inside of the cofferdam cell will increase with depth. How this pressure

¹⁸⁶White, R. E. 1962. “Caissons and Cofferdams,” *Foundation Engineering*, McGraw-Hill Book Co., New York, New York.

¹⁸⁷Mansur, C. I. and Kaufman, R. I. 1962. “Dewatering,” *Foundation Engineering*, G. A. Leonards, McGraw-Hill Book Co., Inc., New York, New York.

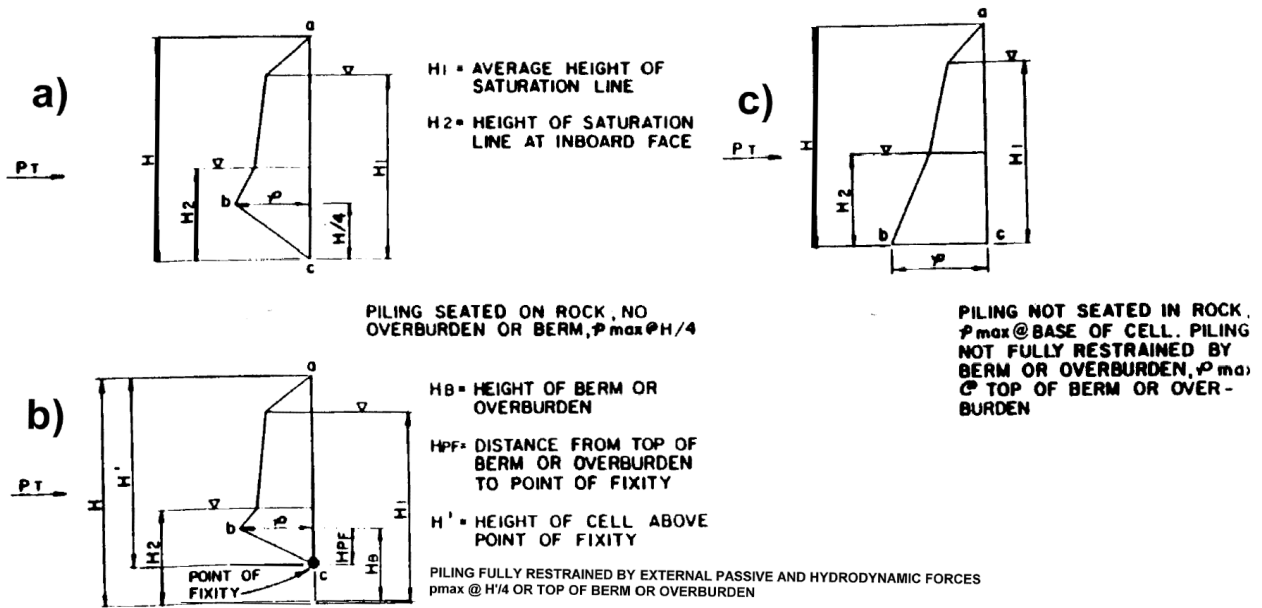


Figure 15-26: Resultant Interlock Pressure and Point of Maximum Horizontal Pressure

increases, and what affect it has on various aspects of internal cell stability, depends upon the type of fill, the location of the saturation line, the type of foundation (rock or soil), the interaction of the cell fill at the inboard sheeting with the overburden or berm, and other factors.

At the centreline of the cell, the computation is straightforward. If the saturation line is assumed straight, (which it usually is) the location of the phreatic surface at the centreline is the average of the height of the saturation line at the outboard face and the inboard face. The lateral pressure at the centreline is the effective stress multiplied by a lateral earth pressure coefficient. The value of that lateral earth pressure coefficient is not a conventional active earth pressure coefficient and its value has been a source of controversy since rational cellular cofferdam design began with TVA's work in the 1930's.

With the inboard face, (which is the most likely point of interlock failure) the maximum internal cell pressure acting on the inboard sheets takes place at a point other than the bottom of the cofferdam, as is the case at the centreline, because of interaction with the berm, overburden, foundation, or a combination of these. The location of this point varies with the type of foundation and berm being used; various lateral earth pressure charts for the inboard sheets are shown in Figure 15-26.

These pressures project themselves on the inboard sheeting. To illustrate how these charts can be used, consider the case of Figure 15-26(a). This is the classic TVA "cofferdam in rock" case; here, their engineers generally assumed that the maximum pressure occurs at a point one-fourth of the total cell height from the bottom. The interlock tension thus developed in a cellular cofferdam on rock is a function of the vari-

ation of the internal cell pressure. From this pressure diagram, the following equation for the maximum cell pressure at point "b" can be computed as follows:

Equation 15-22

$$p = K \left(\gamma(H - H_1) + \gamma' \left(H_1 - \frac{H}{4} \right) \right) + \gamma_w \left(H_2 - \frac{H}{4} \right)$$

(Figure 15-26(a))

Where

- p = maximum inboard sheeting pressure, psf
- K = coefficient of internal pressure for cellular cofferdam fill, depending upon the type of cell fill material and the method of placement (see Table 15-4). For hydraulic fill, TVA used the Coulomb active coefficient together with full water pressure.
- H, H_1, H_2 as shown in Figure 15-26 In a similar way, for the case shown in Figure 15-26(a), lateral pressures at the other points can be computed as

$$\text{Equation 15-23: } p_{H_1} = \gamma K (H - H_1)$$

$$\text{Equation 15-24: } p_{H_2} = K \left(\gamma(H - H_1) + \gamma'(H_1 - H_2) \right)$$

Where p_{H_1}, p_{H_2} are the pressures at the heights H_1 and H_2 , respectively.

These pressures known, the net force P_T can be computed using the equation

Table 15-4: Coefficients of Internal Pressure

Method of Placement	Type of Material				
	Crushed Stone	Coarse Sand and Gravel	Fine Sand	Silty Sand and Gravel	Clayey Sand and Gravel
Hydraulic dredge	1.4K _a		1.5K _a		1.6K _a
Placed dry and sluiced		1.4K _a		1.5K _a	
Wet clammed	1.3K _a		1.4K _a		1.5K _a
Dry material placed in dry		1.3K _a		1.4K _a	
Dumped through water	1.2K _a		1.3K _a		1.4K _a

Equation 15-25:

$$P_T = \frac{p_{H_1}}{2}(H - H_1) + \frac{p_{H_1} + p_{H_2}}{2}(H_1 - H_2) + \frac{p_{H_2} + p}{2}\left(H_2 - \frac{H}{4}\right)$$

(Figure 15-26(a))

where P_T = net force on the inboard sheets. Values for p and P_T for the other two cases can be computed in a similar manner from the lateral earth pressure profiles.

15.3.8.1.2. Point of Fixity

Figure 15-26(b) illustrates yet another important concept that concerns the inboard sheeting and thus the internal cell stability: the location of the point of fixity. If the berm or overburden is higher than the H/4 point of maximum pressure in Figure 15-26(a), the point of maximum pressure will shift from the H/4 point to the level of the berm or overburden. In this condition, the inboard sheets act like a cantilever sheet pile wall, and since the passive pressures are greater than the active ones, the slope of the lateral pressure line will reverse itself below the top of the berm or overburden and eventually the net pressure will equal zero. This point is referred to as the point of fixity, and is shown in Figure 15-26(b). Although the value of p for this case can be computed without knowing the point of fixity, to arrive at a value of P_T does require establishing the point of fixity.

15.3.8.2. Pile Interlock Tension

A cell must be stable against bursting pressure, i.e., the pressure exerted against the sheets by the fill inside the cell must not exceed the allowable interlock tension.

The FS against excessive interlock tension is defined as the ratio of the interlock strength as guaranteed by the manufacturer to the maximum computed interlock tension. The interlock tension developed in a cell is a function of both the internal cell pressure and the radius of the cell. The maximum interlock tension in the main cell is given by

Equation 15-26: $t = p R$

Where

- t = interlock tension, lbs.
- R = radius of cellular cofferdam, feet (see Figure 15-27)

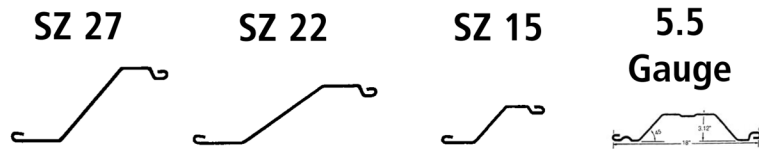
Since the radii of connecting arcs are so much smaller than the main cells and the action within approximates bin action, there is generally no need to check interlock stresses in these elements. However, the pull generated by the connecting arcs is transferred to the main cells through the connector tees or wyes. It is assumed that the maximum stress in the cell interlocks occurs in the cross wall sheets adjacent to the connector pile. The interlock stress at the connections as shown in Figure 15-27, and may be approximated by

SHORELINE STEEL, INC.

P.O. Box 480519, 58201 Main Street • New Haven, MI 48048
(800) 522-9550 • (586) 749-9559 • Fax (586) 749-6653

www.shorelinesteel.com

We are a leading producer of domestic cold formed steel sheet piling in sections ranging from 10 gauge to 3/8" thick. For any sheet piling requirement we can satisfy your needs with a top quality product and prompt delivery.



	Thickness (Nominal)	Weight (Sq. ft.)	Weight (Lin. Ft.)	Sec. Mod in ⁴ (Ft. Wall)	Moment of Inertia in ⁴ (Ft. Wall)	Laying Width	Wall Depth
10-10 ga.	.134	7.2	10.8	2.2	3.5	18.00	3.12
8-8 ga.	.164	8.8	13.2	2.62	4.2	18.00	3.12
7-7 ga.	.179	9.6	14.4	2.8	4.4	18.00	3.12
6-6 ga.	.194	10.5	15.8	3.0	4.9	18.00	3.12
5-5 ga.	.209	11.3	16.9	3.4	5.4	18.00	3.12
LZ 8	.164	8.3	17.2	3.6	8.1	25.00	4.50
LZ 7	.179	9.1	18.8	3.9	8.9	25.00	4.50
LZ 5	.209	10.6	21.9	4.6	10.4	25.00	4.50
LZ 3	.239	11.9	24.6	5.2	11.8	25.00	4.50
LZ 250	.250	12.3	25.6	5.4	12.4	25.00	4.50
SZ-10	.164	9.4	17.2	7.3	27.4	22.00	7.50
SZ-11	.179	10.3	18.8	7.9	29.8	22.00	7.50
SZ-12	.209	12.0	21.9	9.2	34.8	22.00	7.50
SZ-14	.239	13.5	24.6	10.4	39.9	22.00	7.50
SZ-15	.250	14.0	25.6	10.9	41.8	22.00	7.50
SZ-14.5	.250	14.5	32.4	13.0	61.49	26.75	9.46
SZ-14.5	.270	15.8	35.1	14.0	86.40	26.75	9.46
SZ-18	.312	18.1	40.4	16.2	76.83	26.75	9.46
SZ-20	.340	19.8	44.1	17.5	83.37	26.75	9.46
SZ-21	.350	20.3	45.3	18.1	86.00	26.75	9.46
SZ-22	.375	21.8	48.6	19.3	91.92	26.75	9.46
SZ-222	.312	22.1	40.4	26.7	163.09	22.00	12.25
SZ-250	.250	15.9	32.4	16.6	89.42	24.46	10.75
SZ-313	.312	19.9	40.4	20.6	111.53	24.46	10.75
SZ-340	.340	21.5	44.1	22.4	121.45	24.46	10.75
SZ-350	.350	22.1	45.3	22.9	124.62	24.46	10.75
SZ-375	.375	23.7	48.6	24.5	133.55	24.46	10.75
SZ-24	.340	24.1	44.1	29.0	177.52	22.00	12.25
SZ-25	.350	24.8	45.3	29.7	181.91	22.00	12.25
SZ-27	.375	26.6	48.6	32.0	195.18	22.00	12.25

DOMESTIC STEEL SHEET PILING

- All sections available in bare or galvanized steel.
- All Zee sections available in doubles.
- All sections produced exactly to customer specified length(s).
- All steel fully melted and manufactured in the USA.



For more information, please call toll free
(800) 522-9550

or visit our website at: www.shorelinesteel.com

Also Available:

- Corners
- Tees and Crosses
- Capping
- Coatings

$$\text{Equation 15-27: } t_{\max} = p L \sec(\theta)$$

Where

- t_{\max} = interlock tension at connection
- p = as previously defined
- L = as shown in Figure 15-27

This value of t_{\max} is smaller than when computed by the "exact" analysis of combining the ring tension of the small and large cells into a force polygon.¹⁸⁸

It must be emphasized, however, that the above equation is an approximation since it does not take into account the bending stresses in the connection sheet pile produced by the tensile force in the sheet piles of the adjacent cell. Consequently, for critical structures, special analyses such as finite element should be used to determine interlock tension at the connections. In computing the maximum interlock tension, the location of the maximum unit horizontal pressure p should be assumed to occur at a point one fourth of the height of the cell above the level at which cell expansion is fully restrained. Full restraint can be assumed where the external passive forces, due to overburden or a berm, and hydrostatic forces equal the internal cell pressures. In this case, it is generally sufficiently accurate and conservative to assume the point of maximum pressure to be at the top of the overburden or berm.

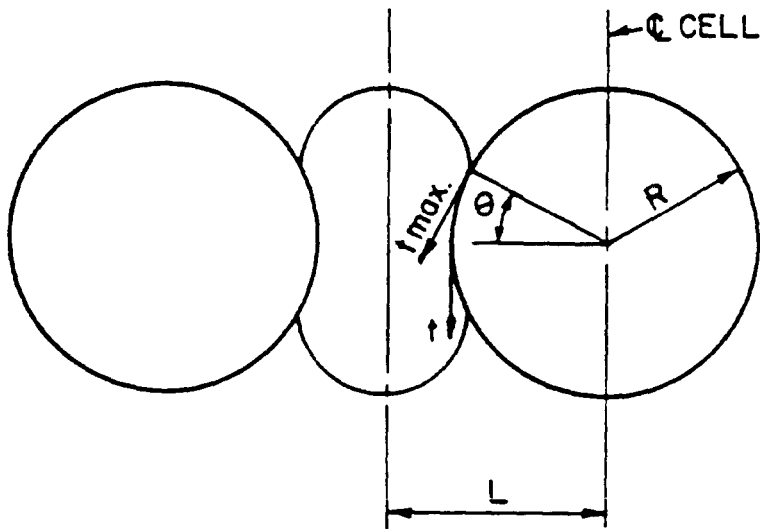


Figure 15-27: Interlock Stress at Connection

When there is no overburden or berm, full restraint can be assumed to be at top of rock if the piling is seated on and bites into the rock. Maximum pressure should be assumed to occur at the base of cells that are neither seated in rock nor fully restrained by overburden or berm. See Figure 15-26 for typical pressure distributions. As stated previously, future changes in the depth of overburden, removal of berms, changes in saturation level in the cell fill, rate of dewatering, etc., must be anticipated when determining the maximum interlock tension.

15.3.8.2.1. Dealing with Interlock Tension

In order to minimize interlock tension, the following details should be considered:

(1) Adequate weep holes should be provided on the interior sides of the cells in cofferdams to reduce the degree of saturation of the cell fill. The weep holes should be adequately maintained during the life of the cofferdam.

(2) Hydraulic filling of cells at low water conditions will produce the maximum stress in the interlocks and is a good test for the integrity of the cell. Some failures that did not affect the safety of the completed cofferdam have appeared during filling where the consequences are much less serious. One example of a failure that takes place during hydraulic filling is driving the sheets out of interlock. This results from driving through excessive overburden or striking boulders in the overburden. Overburden through which the piling must be driven should be limited to 30 feet. If the overburden exceeds this depth, consideration should be given to removing the excess prior to pile driving. The degree to which boulders may interfere with watertightness and driving of the cells can be estimated after a complete foundation exploration program.

(3) In an effort to reduce the effect of the connecting arc pull on the main cells, wye connectors are preferable to tees since the radial component of the pull on the outstanding leg is less for arcs of equal radius. Manufacturers in the United States provided suggested layouts plans with geometrical dimensions which fit piling for circular cofferdams based on fitting piles to geometrics. When 90° tees were utilized, cells were purposely held as closely together as possible to obtain a small radius and activate bin action to avoid excessive pull from the arcs. The use of 30° wye connectors was an improvement in that it reduced the radii of arcs and allowed the main cells to be placed further apart.

(4) Pull on the outstanding leg of connector piles can be reduced by keeping the radius of the connecting arc as small as practicable. The arc radius should not exceed one half of the radius of the main cell.

(5) Since tees and wyes are subjected to high local bending stresses at the connection, strong ductile connections are essential. Welded connections do not always meet this requirement because neither the steel nor the fabrication procedure is controlled for weldability. Therefore, all fabricated tees, wyes, and crosspieces shall utilize riveted connections. In addition, the piling section from which such connections are fabricated shall have a minimum web thickness of one-half inch.

(6) Only straight web pile sections shall be used for cells, as the hoop-tension forces would tend to straighten arch webs, thus creating high bending stresses.

(7) Used piling is often utilized with little regard to the manufacturer. Because of small differences in interlock configuration and dimensional tolerances, sheets from different manufacturers may not be compatible and may not develop the assumed interlock strength. Splices have been made without considering the dimensions of the sheets joined. Splicing two sheets that do not have exactly the same width can cause a stress concentration in the narrower sheet. Where previously used piling is employed, care should be taken to ensure both that the sheets are gauged and will interlock, and that the sheets are compatible for splicing.

**15.3.8.3. Shear Failure within the Cell
(Resistance to Tilting)**

Both the mechanism and the method of calculation of the shear failure within the cell have been the subject of controversy since the beginning of rational cellular cofferdam design.

One of the lasting triumphs of the TVA effort was the determination by TVA engineers that resistance of the fill to vertical shearing along the centreline of the cofferdam was the actual basis for stability, with assistance from interlock frictional forces. Using this approach TVA successfully designed a number of large cofferdams. They were able to come to this conclusion in advance of Karl Terzaghi¹⁸⁹, who arrived at this same decision independently and unaware of TVA's work. The method of Schroeder and Maitland¹⁹⁰ is an advance on both TVA and Terzaghi theory, although the basic premise is the same.

Based on his own experiments and other considerations, Cummings¹⁹¹ concluded that the primary shear resistance takes place by resisting sliding on horizontal planes, as opposed to vertical ones. Cummings' theory has been controversial from its publication, in part because no experimental evidence has shown a failure mode similar to the one upon which his theory is based.¹⁹²

However, in view of the seriousness of the consequences of failure in cellular cofferdams, both vertical and horizontal shear should be checked to determine the adequacy of the cell to resist tilting. For vertical shear, this would include the Terzaghi-TVA and the Schroeder-Maitland Methods; for horizontal shear, this includes Cummings' Method.

15.3.8.4. Vertical Shear Resistance

15.3.8.4.1. Terzaghi's Method

Excessive shear on a vertical plane through the centre line of the cell is a possible mode of failure by tilting. For stability, the shearing resistance along this plane, together with the frictional resistance in the interlocks, must be equal to or greater than the shear due to the overturning forces. The frictional resistance in the interlocks must be included since shear failure cannot occur without simultaneous slippage in the interlocks. Figure 15-28a shows the assumed stress distribution on the base due to the net overturning moment. The total shearing force on the neutral plane at the centre line of the cell is equal to the area of the triangle.

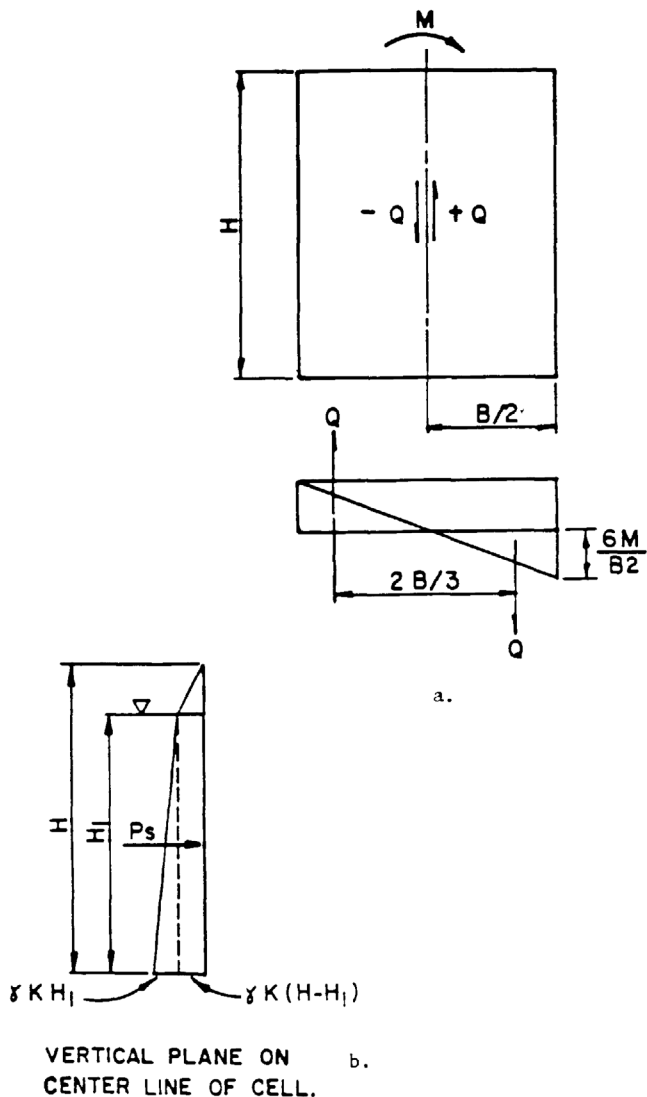


Figure 15-28: Vertical shear resistance, Terzaghi method

¹⁸⁹Terzaghi, K. 1945. "Stability and Stiffness of Cellular Cofferdams," American Society of Civil Engineers, Transactions, Volume 110, Paper No. 2253, pp 1083-1202. Considering Terzaghi's prodigious achievements in soil mechanics and foundation design, this was no mean feat.
¹⁹⁰Schroeder, W. L. and Maitland, J. K. 1979 (Jul). "Cellular Bulkheads and Cofferdams," Journal, Geotechnical Engineering Division, American Society of Civil Engineers, New York, New York, Vol 105, GT 7, Paper 14713, pp 823-837.
¹⁹¹Cummings, E. M. 1957 (Sep). "Cellular Cofferdams and Docks," Journal of the Waterways and Harbors Division, American Society of Civil Engineers, New York, New York.
¹⁹²Rosow, M., Demsky, E., and Mosher, R. (1987) Theoretical Model for Design of Cellular Sheet Pile Structures (Cofferdams and Retaining Structures) ITL-87-5. Vicksburg, MS: U.S. Army Corps of Engineers, Waterways Experiment Station.

$$\text{Equation 15-28: } Q = \left(\frac{1}{2}\right)\left(\frac{B}{2}\right)\left(\frac{6M}{B^2}\right) = \frac{3M}{2B}$$

where Q = total shearing force per unit length of cofferdam, and the net overturning moment M is given by Equation 15-18.

To prevent rupture, the shear resistance on the neutral plane must be equal to the shearing force Q on this plane. The shear resistance on the neutral plane is due to the lateral pressure of the cell fill and is equal to this pressure times the coefficient of internal friction of the cell fill. Thus, as illustrated in Figure 15-28(b),

Equation 15-29:

$$P_s = K\left(\frac{1}{2}\gamma(H - H_1)^2 + \gamma(H - H_1)H_1 + \frac{1}{2}\gamma H_1^2\right)$$

Where

- P_s = total lateral force per unit length of cofferdam due to cell fill
- γ = unit weight of cell fill above saturation line
- γ' = submerged unit weight of cell fill
- K = empirical coefficient of earth pressure. D.P. Krynine¹⁹³ has suggested obtaining K from Mohr's Circle projections, in which case

$$\text{Equation 15-30: } K = \frac{\cos^2 \phi}{2 - \cos^2 \phi} \quad (\text{Krynine})$$

The vertical resisting shear within the cell fill along the centreline of the cofferdam is equal to

$$\text{Equation 15-31: } S_s = P_s \tan \phi$$

The frictional resistance in the sheet pile interlock is equal to the interlock tension times the coefficient of friction of steel on steel. The resistance against slippage per unit length is therefore

$$\text{Equation 15-32: } S_f = fP_T$$

Where

- S_f = frictional resistance against slippage
- f = coefficient of friction of steel on steel at the interlock = 0.3

The lateral pressure is assumed to reduce to zero at a point c because the lower end of the piling bites into the rock, reducing the ring tension. The total shearing resistance along

the centreline of the cell per unit length is therefore

$$\text{Equation 15-33: } S_T = S_s + S_f = P_s \tan \phi + f P_T$$

The safety factor against failure is

$$\text{Equation 15-34: } FS = \frac{S_T}{Q} = \frac{(P_s \tan \phi + f P_T) \frac{2B}{3M}}{3M}$$

The foregoing is applicable to cells founded on rock, sand, or stiff clay. The determination of P_T is dependent upon whether the piling is seated on rock, the presence of a berm or overburden, and the degree of restraint provided thereby, as discussed previously. In the case of cells on soft to medium clay, a relatively small overturning moment will produce an unequal distribution of pressure on the base of the fill in the cell causing it to tilt. The stability of the cell is virtually independent of the strength of the cell fill since the shear resistance through vertical sections offered by the cell fill cannot be mobilized without overstressing the interlocks. Therefore, for cells on compressible soils, the shear resistance of the fill in the cells is neglected, and the factor of safety against a vertical shear failure is based on the moment resistance mobilized by interlock friction as follows:

$$\text{Equation 15-35: } FS = \frac{\text{Prf} \left(\frac{B}{L}\right) \left(\frac{L + 0.25B}{L + 0.50B}\right)}{M}$$

Where

- P = pressure difference on the inboard sheeting
- R = radius

15.3.8.4.2. Schroeder-Maitland Method¹⁹⁴

This design approach is a variation of the Terzaghi method of vertical shear resistance. It is particularly applicable to cells founded on sand or stiff to hard clay. The main premises, as determined from field and laboratory studies, are:

- The coefficient of lateral earth pressure K should be taken as 1 as a result of the compression the cell fill undergoes during the application of the overturning force; and
- The height of the cell over which vertical shear resistance is applied should extend from the top of the sheet piles on the cell centre line to the point of fixity for the embedded portion of the sheets.

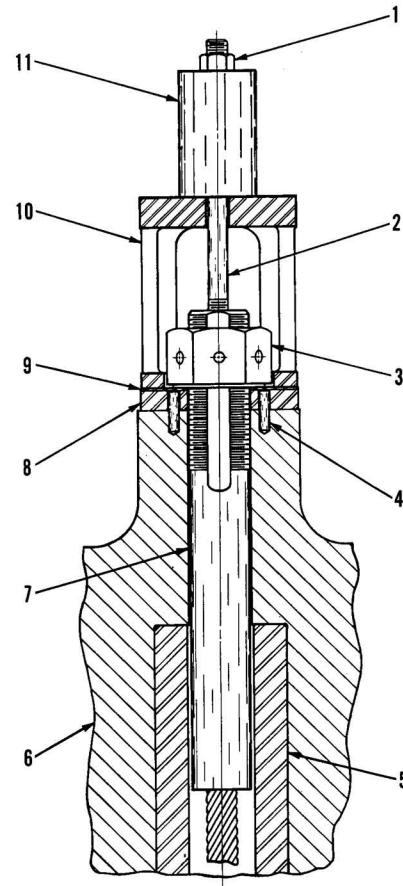
Thus, as illustrated in Figure 15-29:

$$\text{Equation 15-36: } S_T = \frac{1}{2} \gamma K (H')^2 (\tan \phi + f)$$

¹⁹³Krynine, D.P. (1945) "Discussion on Stability and Stiffness of Cellular Cofferdams." *Transactions of the American Society of Civil Engineers*, Vol. 110. Krynine detonated yet another controversial point in cellular cofferdam design, because, according to his formula, the higher the ϕ angle and the better the soil, the value of K decreases. Terzaghi recommended that the Rankine K_a be multiplied by 1.2 to 1.6 for K . As an example of the difference between the two theories, for sand having a ϕ value of 30°, the Rankine K_a is 0.33. Terzaghi's recommendation for a 20 to 60 percent increase would result in K values of .40 to .53. Krynine's value from Equation 15-30 would set K at about .60. For the purposes of this manual, the K for Equation 15-29 will be computed using Equation 15-30, and that for Equation 15-22 (and related equations and problems) will be computed using the values given in Table 15-4.

¹⁹⁴Schroeder, W. L. and Maitland, J. K. 1979 (Jul). "Cellular Bulkheads and Cofferdams," *Journal, Geotechnical Engineering Division, American Society of Civil Engineers*, New York, New York, Vol 105, GT 7, Paper 14713, pp 823-837. It is interesting to note that W.L. Schroeder's best-known work is his book *Soils in Construction* (Prentice-Hall); as of this writing, one of the authors of this book (Warrington) is preparing the Fifth Edition of this work.

Tying it All Together



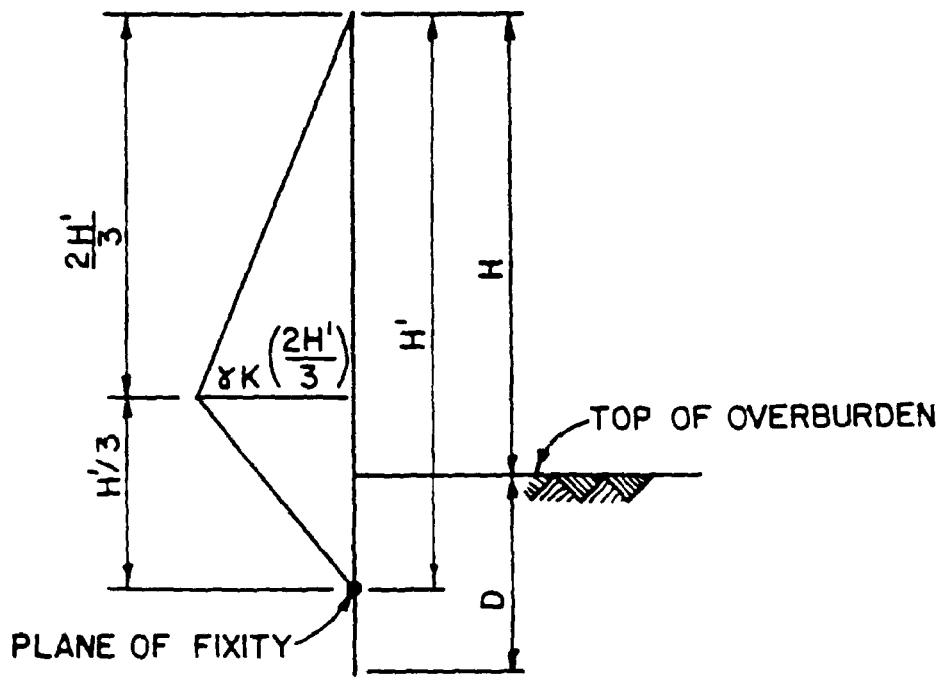
Sometimes it's hard to make sense out of some of the jobs we get, let alone a profit. That's where Vulcan Cable-tied Hammers can help. By eliminating the column keys, your downtime can be reduced and your profit can be enhanced. All new hammers are cable tied and many older ones can be converted. Call your nearest Vulcan representative and let us help you make sense of your job--and a profit from it.

- ✍ **Vulcan Air/Steam Pile Hammers**
- ✍ **IHC Hydrohammers**
- ✍ **IHC Fundex Equipment**
- ✍ **Genuine Factory Parts**
- ✍ **Service and Technical Support**
- ✍ **Extensive Dealer Network**

VULCAN FOUNDATION EQUIPMENT

111 Berry Road
 P.O. Box 16099
 Houston, TX 77222
 Phone (713) 691 3000
 Fax (713) 691 0089
 Toll Free (800) 742-6637
 Email sales@vulcanhammer.com
 Web site <http://www.vulcanhammer.com>

Member of the IHC Caland Group



VERTICAL PLANE ON CENTER LINE OF CELL

Figure 15-29: Vertical Shear Resistance, Schroeder-Maitland Method

Where

- S_T = total shearing resistance along the centre line of the cell
- K = coefficient of lateral earth pressure = 1.0
- H' = height of cell over which vertical shear resistance is applied
- γ , ϕ and f = as previously defined

The point of fixity and the required depth of embedment, as determined by Matlock and Reese¹⁹⁵ for laterally loaded embedded piles, is $3.1T$ and $>5T$, respectively, where

Equation 15-37:
$$T = \sqrt[5]{\frac{EI}{n_h}}$$

Where

- E = modulus of elasticity of the pile
- I = moment of inertia of the pile
- n_h = constant of horizontal subgrade reaction

Application of this method has the effect of satisfying the FS requirement against vertical shear failure with a smaller diameter cell than that required by the Terzaghi method. In installations where seepage resulting from an unbalanced head is not a critical consideration, i.e., a bulkhead installation as opposed to a cofferdam, the depth of embedment of

the piling should be that required to provide passive resistance to translational failure rather than $D = 2H/3$ as recommended by Terzaghi. Sheet pile cells are flexible structures with a plane of fixity only a short distance below the dredge line. In determining the depth of embedment, the plane of fixity should be determined by the analytical methods noted previously and the passive resistance available be calculated above this plane.

15.3.8.5. Horizontal Shear Resistance

Cummings has proposed a theory of cellular cofferdam failure known as the interior sliding theory, where the resistance of a cell to failure by tilting is gained largely through horizontal shear in the cell fill and on the resisting moment due to the frictional resistance of the pile interlock.

This theory is based on the pre-

mise that the cell fill will resist lateral distortion of the cell through the build-up of soil resistance to sliding on horizontal planes. Based on model tests, Cummings concluded that the shear resistance is developed only in a triangle forming an angle to the horizontal as shown in *Figure 15(b)*

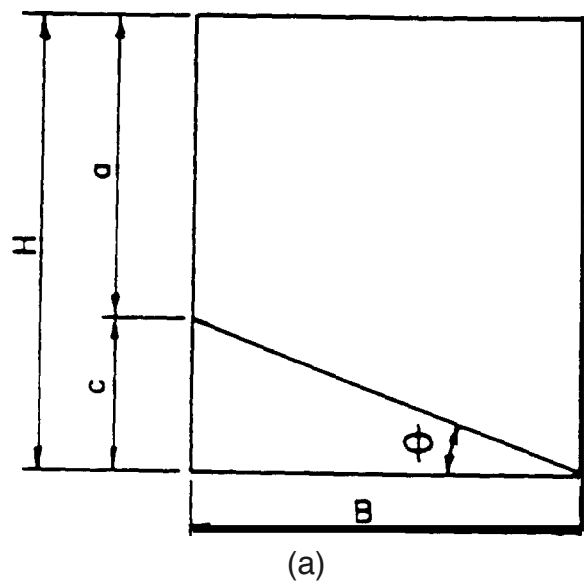
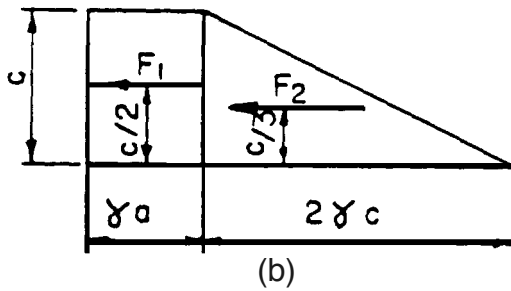


Figure 15-30: Horizontal Shear Resistance, Cummings Method

¹⁹⁵Matlock, H. and Reese, L. C. 1960. "Generalized Solutions for Laterally Loaded Piles," Journal, Soil Mechanics and Foundations Division, American Society of Civil Engineers, Vol 86, No. SM5, pp 63-91.



The soil below this slanted line fails by sliding on horizontal planes as shown and thereby produces a resisting pressure on the outboard sheeting. The following equations derived by Cummings summarize his method of computing the resisting moment due to this pressure. The ultimate lateral shear resistance of the cell – which is the resisting force – is given by:

$$\text{Equation 15-38: } F = \gamma BH \tan \phi$$

Substituting

$$\text{Equation 15-39: } H = a + c$$

And

$$\text{Equation 15-40: } B = \frac{c}{\tan \phi}$$

we have

$$\text{Equation 15-41: } F = \gamma c(a + c)$$

The lateral force is represented graphically by the diagram shown in Figure 15-30(b), the area of which is equal to the total resistance F . This diagram is treated similar to a pressure diagram, from which the resisting moment about the base can be computed.

The total moment of resistance per foot of wall about the base of the cofferdam is

$$\text{Equation 15-42: } M_r = F_1 \frac{c}{2} + F_2 \frac{c}{3}$$

Since

$$\text{Equation 15-43: } F_1 = \alpha c \gamma$$

And

$$\text{Equation 15-44: } F_2 = c^2 \gamma$$

Equation 15-42 then becomes

$$\text{Equation 15-45: } M_r = \frac{\alpha c^2 \gamma}{2} + \frac{c^3 \gamma}{3}$$

In addition, the interlock friction also provides shear resistance. It is computed as the tension caused by the pressure of the cell fill acting on a vertical one foot slice times the coefficient of interlock friction, f .

$$\text{Equation 15-46: } F_i = P_T r f$$

Where

- F_i = interlock friction force

- P_T = area abc as shown in Figure 15-26
- r is as shown in Figure 1-10, Figure 1-11 and Figure 1-12.
- f is as previously defined

The friction force F_i is assumed to act equally on all interlocks; therefore, an individual pile will have equal but opposite friction forces at each end. The resisting moment, M_i , against tilting due to the interlock tension results from the summation of the individual couples caused by the opposite friction force on each pile. Therefore, resisting moment per foot width is

$$\text{Equation 15-47: } M_i = \frac{F_i B}{r} = P_T f B$$

Excessive tilting results from the use of weak cell fill; therefore, the fill should be well graded and free draining to the maximum extent possible. Further, since the shear resistance of the cell is derived from the material in the lower portion of the cell, it may be necessary to excavate any weak material encountered in the overburden. Should the shear resistance of the cell fill material be inadequate to withstand the external forces, consideration should be given to the use of a berm to assist in stabilization of the cell. If a berm is used, the resisting moment due to the effective passive pressure of the berm should be included. Thus, the safety factor against tilting is

$$FS = \frac{\text{Resisting Moment}}{\text{Driving Moment}}$$

Equation 15-48:

$$FS = \frac{M_r + M_f + P_p \frac{H_B}{3}}{P_w H + P_a H_s} \cdot 3$$

15.3.8.6. Pullout of Outboard Sheets

The penetration of sheet piling in granular soils is controlled by the need to extend the length of the flow paths of the water percolating beneath the cell. However, the penetration must also be adequate to insure stability with respect to pullout of the outboard sheeting due to tilting. The calculated overturning moments are applied to the sheet piles that are assumed to act as a rigid shell. Resistance to pullout is computed as the frictional or cohesive forces acting on the embedded length of piling.

The average pile reaction due to the overturning moment on the outboard piling is given by

$$\text{Equation 15-49: } Q_p = \frac{P_w H_w + P_a H_s - P_p H_B}{3B \left(1 + \frac{B}{4L} \right)}$$

Where the variables are as defined previously.

The ultimate pile pullout capacity per linear foot of wall, Q_u , depends on the material into which the pile is driven. For

clay

Equation 15-50: $Q_u = c$ (perimeter) (embedded length)

For granular soils

Equation 15-51: $Q_u = 0.5 K_a \gamma D^2 \tan \delta$ (perimeter)

where

- D = embedded length
- $\tan \delta$ = coefficient of friction for steel against underlying soil. See Table 15-5 for recommended values

Table 15-5: Wall Friction

Steel Sheet Piles Against the Following Soils	$\tan \delta$
Clean gravel, gravel-sand mixtures, well graded rock fill with spalls	0.40
Clean sand, silty sand-gravel mixture, single size hard rock	0.30
Silty sand, gravel or sand mixed with silt or clay	0.25
Fine sandy silt, nonplastic silt	0.20

The factor of safety is thus computed by

15.3.8.7. Penetration of Inboard Sheets

For cellular cofferdams on sand, the inboard sheet piles should be driven to a sufficient depth to counteract the vertical downward friction force F_1 caused by the interaction of the cell fill and the inner face. This friction force is given by

Equation 15-53: $F_1 = P_T \tan \delta$ (Force per unit length)

Where

- F_1 = vertical downward friction force, force/unit length

The FS against sheet pile penetration is defined as the ratio

of the shear resistance on both sides of the embedded portion of the piles on the unloaded side to the internal downward shear force on the unloaded side. This is expressed as M

Where

- M = net overturning moment
- D = embedded length

15.3.8.8. Slipping Between Sheet piling and Cell Fill

When a cellular cofferdam on rock is subject to large overturning forces, failure can occur by lifting the outboard piling and losing the cell fill as it runs out the heel of the cell. In such cases, slippage occurs between the sheet piles on the outboard face and the cell fill. In order to compute the safety factor against such a failure, moments are summed about the inboard toe. The resisting moment is due to the frictional forces on the inner and outer face of the outboard sheeting, plus the effective passive resistance of the soil and berm on the inboard face. The weight of the cell does not provide resisting moment, since it is assumed that the cell fill does not lift up with the piling. The resulting expression is

Equation 15-55:

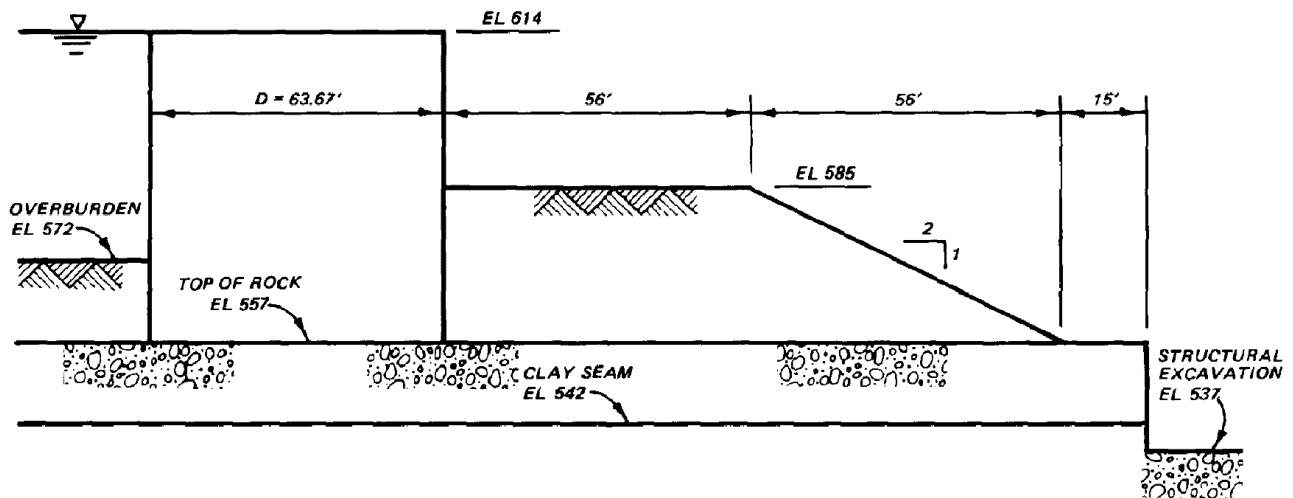
Resisting Moment Due to Friction on Outboard Piling and Passive Soil Pressure

$$FS = \frac{\text{Resisting Moment Due to Friction on Outboard Piling and Passive Soil Pressure}}{\text{Driving Moment Due to Water and Active Soil Pressures}}$$

$$FS = \frac{B(P_w + P_a)\tan \delta + P_p \frac{H_B}{3}}{\frac{P_w H_w + P_a H_s}{3}}$$

15.3.9. Examples of Cellular Cofferdam Design Using Classical Methods

Example 25: Cellular Cofferdam on Rock



Leading supplier of systems for port and special construction works.



For individual solutions we present tailor-made system offers for

- **Driven sections**

Steel Sheet Piles System LARSEN and HOESCH, UNION Straight Web Sections, Light Weight Sections, Trench Sheets, Wall-Sections, LARSEN Box-Piles, UNION-Box Piles, Peine Steel Bearing Piles PSt, Peine Steel Sheet Piling PSp including special services i.e. Coating, Welding, Interlock Sealing, Water Tightness etc.

- **Driving and extracting technology**

Vibrators, Excavator-mounted Vibrators, Ramming Hammers, Drilling Equipment, Leaders and Carriers, Power-packs

- **Anchor technology**

- **Trenching technology**

- **Flood protection**

ThyssenKrupp GfT Bautechnik GmbH

P.O.Box 10 22 53, D-45022 Essen
 Altendorfer Str. 120, D-45143 Essen
 Phone: +49 (2 01) 188-39 77
 Fax: +49 (2 01) 188-37 72
 export-bautechnik@tkx-gft.thyssenkrupp.com
 www.tkgftbautechnik.com

ThyssenKrupp GfT Bautechnik

A company of ThyssenKrupp Services



ThyssenKrupp

DESIGN DATA:

o Piling Configuration:

- Diameter of cell, $D = 63.67'$
- Effective width, $B = 53.06'$
- Guaranteed piling interlock strength, $t_g = 16,000$ pounds per linear inch of interlock

o Cell Fill, Overburden and Berm Properties:

- $\phi = 30^\circ$, $\tan \phi = 0.577$
- $\gamma = 110$ pcf (moist)
- $\gamma' = 72.5$ pcf (submerged)

$$K_a = \frac{1 - \sin \phi}{1 + \sin \phi} = \frac{1 - 0.50}{1 + 0.50} = 0.33; \quad K_p = \frac{1 + \sin \phi}{1 - \sin \phi} = \frac{1 + 0.50}{1 - 0.50} = 3.00$$

$$p_a = \gamma K_a = 110(0.33) = 36.7 \text{ psf/ft}$$

$$p'_a = \gamma' K_a = 72.5(0.33) = 24.2 \text{ psf/ft}; \quad p'_p = \gamma' K_p = 72.5(3.00) = 217.5 \text{ psf/ft}$$

o Rock and Clay Seam Properties:

$$\gamma = 155 \text{ pcf}$$

- $\phi^{\text{rock}} = 20^\circ, \quad \tan \phi = 0$

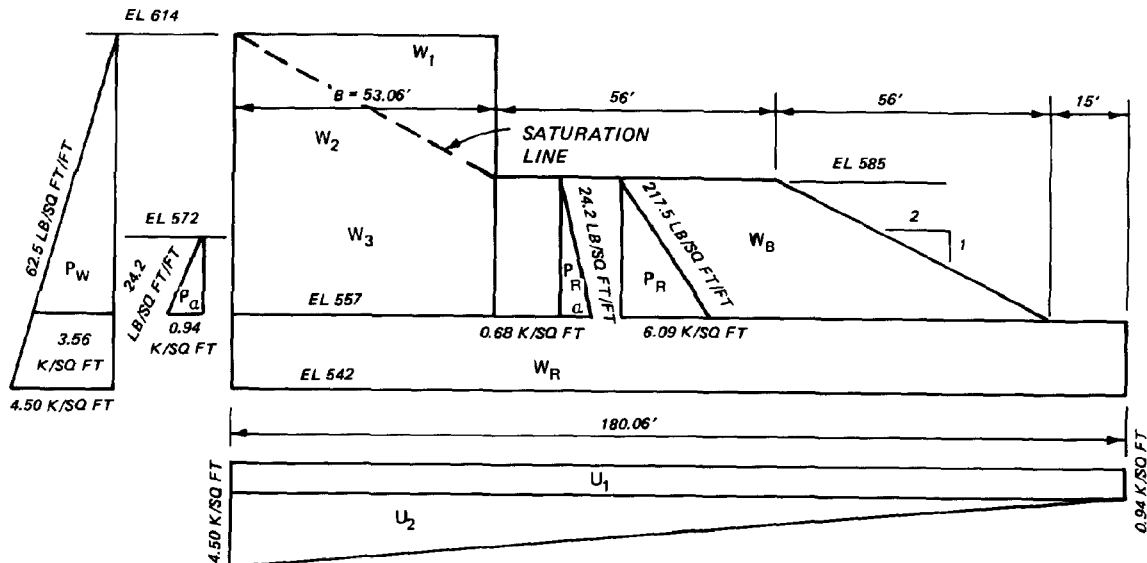
- $c = 750$ psf

o Coefficient of Friction:

- Soil on rock, $\tan \phi = 0.50$
- Steel on steel at interlocks, $f = 0.30$

LOADING

o Service Condition - Water to top of cell; cell fill saturated to top of berm; berm saturated



SLIDING STABILITY:**El 557 w/o Berm**

W_1	$1/2 \times 53.06 \times 29 \times 0.110$	84.6	
W_2	$1/2 \times 53.06 \times 28 \times 0.0725$	55.8	
W_3	$53.06 \times 28 \times 0.0725$	107.7	
P_a	$1/2 \times 0.36 \times 15$		→ 2.7
P_w	$1/2 \times 3.56 \times 57$		→ 101.5
		<hr/> 248.1 ^k	<hr/> 104.2 ^k

$$(P_{i-1} - P_i) = \frac{\left[(W_i + V_i) \cos \alpha_i - U_i + (H_{L_i} - H_{R_i}) \sin \alpha_i \right] \frac{\tan \phi_i}{FS_i}}{\cos \alpha_i - \sin \alpha_i \left(\frac{\tan \phi_i}{FS_i} \right)}$$

$$- \frac{\left(H_{L_i} - H_{R_i} \right) \cos \alpha_i + (W_i + V_i) \sin \alpha_i + \frac{C_i}{FS_i} (L_i)}{\cos \alpha_i - \sin \alpha_i \left(\frac{\tan \phi_i}{FS_i} \right)}$$

Solve for FS when $i = 1$, $H_{R_i} = 0$, $V_1 = 0$, $\alpha_1 = 0$ and $c = 0$

$$FS = \frac{W \tan \phi}{H_{L_i}} = \frac{248.1(0.50)}{104.2} = 1.19 < 1.50 \quad \text{berm required.}$$

El 557 w/Berm

$$W_B = \left(\frac{56 + 112}{2} \right) (28)(0.0725) = 170.5^k$$

Sliding resistance of berm on rock = $170.5(0.50) = 85.3^k$

Passive resistance of berm, $P_R = 1/2(6.09)(28) = 85.3^k$

Passive failure of berm will occur concurrent w/sliding of entire berm on rock.

$$FS = \frac{(W + W_B) \tan \phi}{H_{L1}} = \frac{(248.1 + 170.5)(0.50)}{104.2} = 2.01 > 1.50 \quad \text{ok}$$

EI 542

		W	H
W ₁	See Above	84.6	
W ₂	See Above	55.8	
W ₃	See Above	107.7	
W _B	See Above	170.5	
W _R	180.06 x 15 x 0.155	417.6	
V ₁	0.94 x 180.06	-169.3	
V ₂	1/2 x 3.56 x 180.06	-320.5	
P _a	See Above		→ 2.7
P _w	1/2 x 4.50 x 72		161.0
		347.4 kips	→ 164.7 kips

$$FS = \frac{W \tan \phi + cL}{H_{L1}} = \frac{347.4(0.364) + 0.75(180.06)}{164.7} = 1.59 > 1.50 \quad \text{ok}$$

OVERTURNING STABILITY
EI 557

		<u>W</u>	<u>H</u>	<u>Arm</u>	<u>+ M</u>
W ₁	See Page 2	84.6		17.69	1,497
W ₂	"	55.8		35.37	1,974
W ₃	"	107.7		26.53	2,857
P _a	"		→ 2.7	5.00	-14
P _w	"		→ 101.5	19.00	-1,929
P _{Ra}	1/2 x 0.68 x 28		← 9.5	9.33	89
		248.1 ^k	→ 94.7 ^k		4,474 ^{ft-k}

$$M/W = 18.03$$

$$B/3 = \frac{17.69}{0.34'} \text{ inside kern} \quad \text{ok}$$

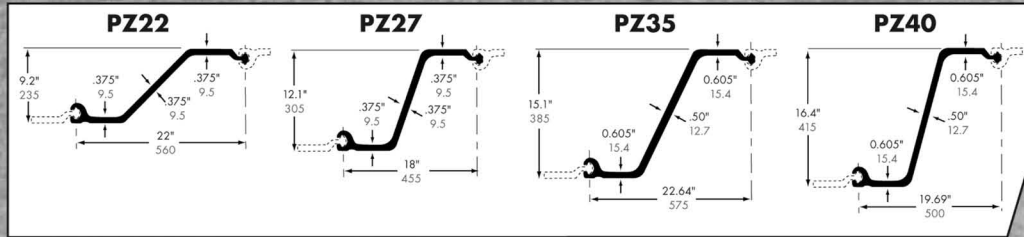
SHEET PILING

DIMENSIONS AND PROPERTIES

GRADES:
 ASTM A328
 ASTM A572 Gr. 50 & 60
 ASTM A588
 ASTM A690

U.S. Standard
 Metric (mm)

Z-PILING

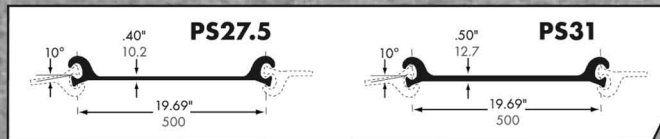


U.S. STANDARD									
Section Designation	Area in. ²	Nominal Width, in.	Weight In Pounds		Moment of Inertia in. ⁴	Section Modulus, in. ³		Surface Area sq ft per lin. ft of bar	
			Per lin. ft of bar	Per ft ² of Wall		Single Section	Per lin. ft of wall	Total Area	Nominal Coating Area *
PZ22	11.9	22	40.3	22.0	155.3	33.8	18.4	4.94	4.48
PZ27	11.9	18	40.5	27.0	281.2	46.5	31.0	4.94	4.48
PZ35	19.4	22.64	66.0	35.0	697.0	92.3	48.9	5.83	5.37
PZ40	19.3	19.69	65.6	40.0	824.8	100.6	61.3	5.83	5.37

METRIC									
Section Designation	Area cm ²	Nominal Width, mm	Weight In Kilograms		Moment of Inertia cm ⁴	Section Modulus, cm ³		Surface Area sq m per lin. m of bar	
			Per lin. m of bar	Per m ² of wall		Single Section	Per lin. m of wall	Total Area	Nominal Coating Area *
PZ22	76.5	560	60.0	107.3	6,460	552	988	1.51	1.37
PZ27	76.8	455	60.3	131.9	11,700	760	1,663	1.51	1.37
PZ35	125.2	575	98.2	170.9	29,010	1,510	2,628	1.78	1.64
PZ40	124.4	500	97.6	195.3	34,330	1,650	3,301	1.78	1.64

PRODUCED BY TXI CHAPARRAL STEEL

FLAT SHEET PILING



U.S. STANDARD									
Section Designation	Area in. ²	Nominal Width, in.	Weight in Pounds		Moment of Inertia in. ⁴	Section Modulus, in. ³		Surface Area sq ft per lin. ft of bar	
			Per lin. ft of bar	Per ft ² of wall		Single Section	Per lin. ft of wall	Total Area	Nominal Coating Area *
PS27.5	13.27	19.69	45.1	27.5	5.3	3.3	2.0	4.48	3.65
PS31	14.96	19.69	50.9	31.0	5.3	3.3	2.0	4.48	3.65

METRIC									
Section Designation	Area cm ²	Nominal Width, mm	Weight in Kilograms		Moment of Inertia cm ⁴	Section Modulus, cm ³		Surface Area sq m per lin. m of bar	
			Per lin. m of bar	Per m ² of wall		Single Section	Per lin. m of wall	Total Area	Nominal Coating Area *
PS27.5	85.6	500	67.1	134.3	221	54	108	1.37	1.11
PS31	96.5	500	75.7	151.4	221	54	108	1.37	1.11

PRODUCED BY TXI CHAPARRAL STEEL

Notes:

All dimensions given are nominal.
 PS27.5 and PS31 interlock only with each other.
 All Z-sections interlock with one another.
 * Excludes socket interior and ball of interlock.

Interlock Strength:

PS27.5 and PS31, when properly interlocked, develop a minimum ultimate interlock strength of 16 kips/in (2800KN/m). Higher interlock strengths are available upon inquiry.

Version 3.0 • January 2003



CHAPARRAL STEEL
 teamed with



1-800-255-4500 • www.fosterpiling.com

VERTICAL SHEAR RESISTANCE

$$K_{C_{cell}} = \frac{\cos^2 \phi}{2 - \cos^2 \phi} = \frac{0.75}{2 - 0.75} = 0.60$$

$\phi = 30^\circ$

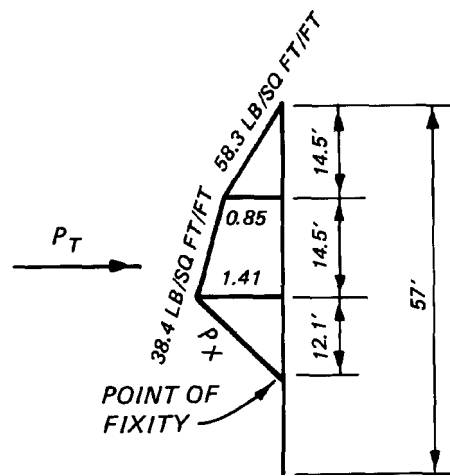
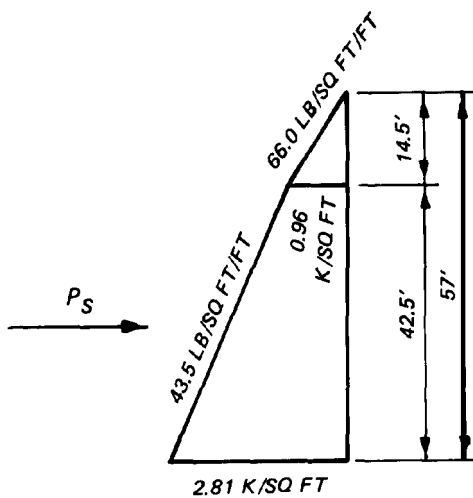
$p = \gamma K = 110(0.60) = 66.0 \text{ psf/ft}$

$p' = \gamma' K = 72.5(0.60) = 43.5 \text{ psf/ft}$

$K_{inboard \text{ sheeting}} = 1.6K_a = 1.6(0.33) = 0.53$

$p = \gamma K = 110(0.53) = 58.3 \text{ psf/ft}$

$p' = \gamma' K = 72.5(0.53) = 38.4 \text{ psf/ft}$



VERTICAL PLANE ON CENTER LINE OF CELL

INBOARD SHEETING

Point of Fixity:

$p_x = p'_p - (p' + p_w) = 217.5 - (38.4 + 62.5) = 116.6 \text{ psf/ft}$

$h = \frac{1.41}{0.1166} = 12.1'$

$H' = 14.5 + 14.5 + 12.1 = 41.1'$, $H'/4 = 10.3'$

use 12.1'

$P_s = 1/2(0.96)(14.5) + 1/2(0.96 + 2.81)(42.5) = 87.1 \text{ k/ft}$

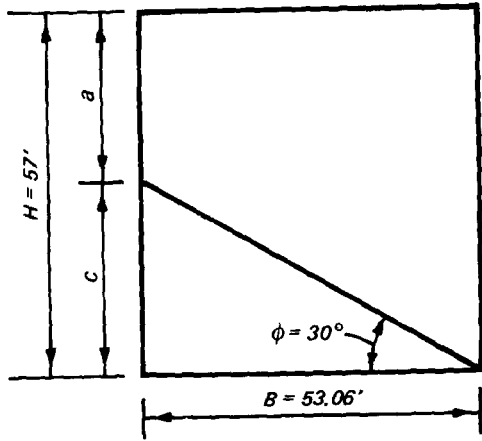
$P_T = 1/2(0.85)(14.5) + 1/2(0.85 + 1.41)(14.5) + 1/2(1.41)(12.1) = 31.1 \text{ k/ft}$

$Q = \frac{3M}{2B} = \frac{3[P_w(H_w/3) + P_a(H_s/3) - P_R(H_B/3)]}{2B}$

$$= \frac{3[101.5(19.00) + 2.7(5.00) - 85.3(9.33)]}{2(53.06)} = 32.4 \text{ k/ft}$$

$$FS = \frac{P_s \tan \phi + fP_T}{Q} = \frac{87.1(0.577) + 0.3(31.1)}{32.4} = 1.84 > 1.50 \quad \text{ok}$$

HORIZONTAL SHEAR RESISTANCE



- $C = B \tan \phi = 30.5'$
- $a = H - c = 26.5'$
- Assume entire cell saturated.

$$M_R = \frac{\gamma' a c^2}{2} + \frac{\gamma' c^3}{3} = \frac{0.0725(26.5)(30.5)^2}{2} + \frac{0.0725(30.5)^3}{3}$$

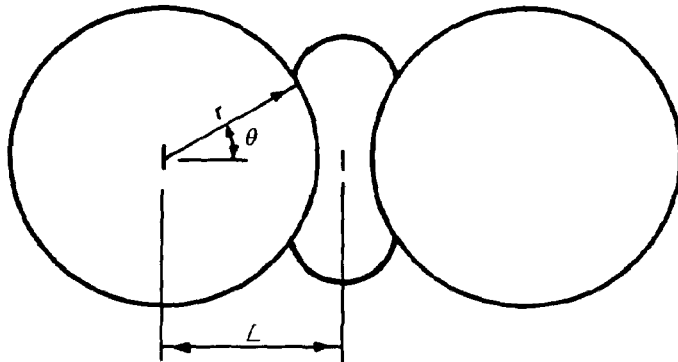
$$= 1,579 \text{ ft-k}$$

$$M_f = P_T f B = 31.1(0.30)(53.06) = 495 \text{ ft-k}$$

$$M_o = P_w (H_w/3) + P_a (H_s/3) = 101.5(19.00) + 2.7(5.00) = 1,943 \text{ ft-k}$$

$$FS = \frac{M_R + M_f + P_R (H_B/3)}{M_o} = \frac{1,579 + 495 + 85.3(9.33)}{1,943} = 1.48 \approx 1.50 \quad \text{ok}$$

INTERLOCK TENSION



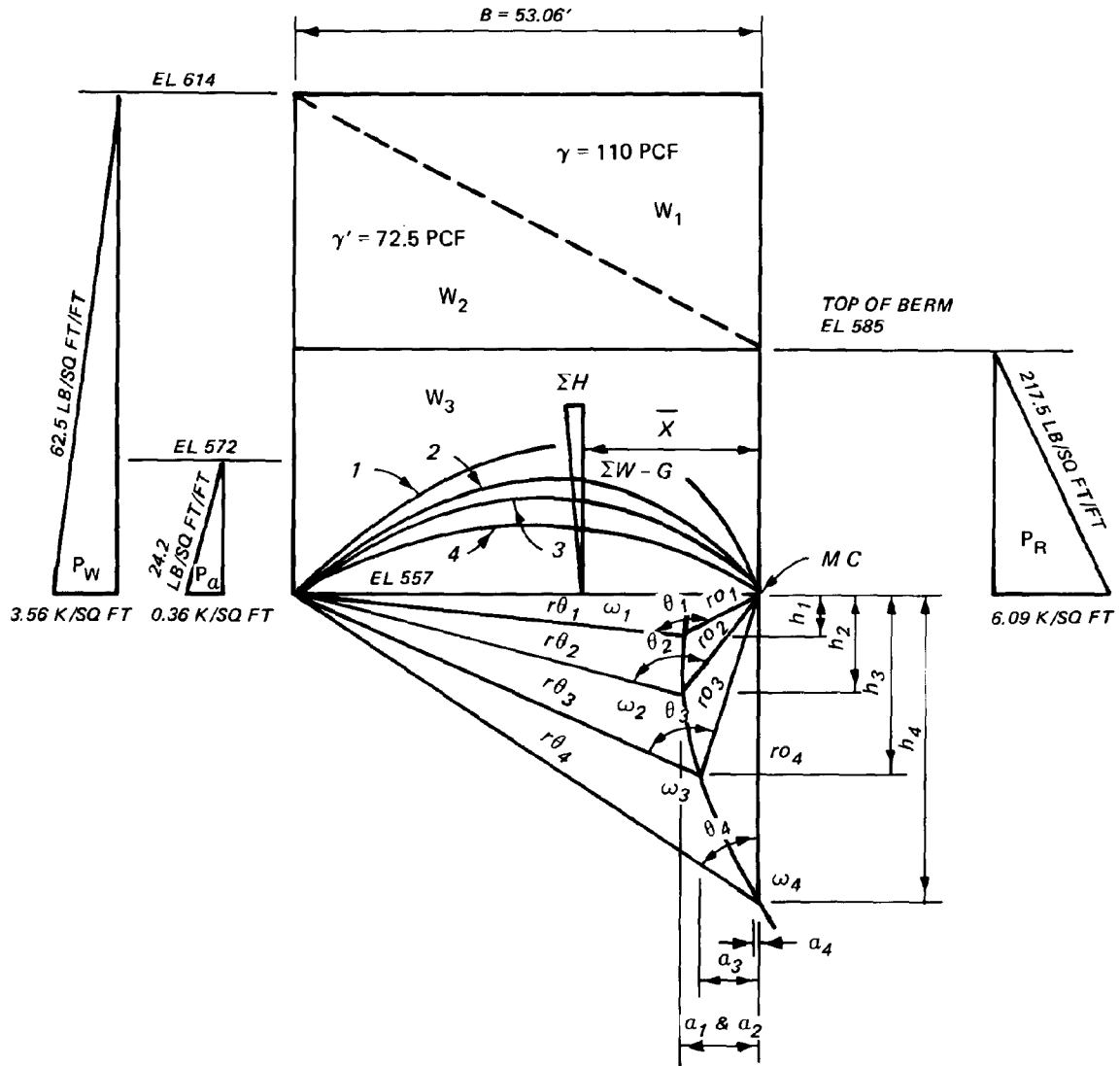
- $r = 31.83'$
- $\theta = 30^\circ$
- $L = 37.76'$

$$t_{\max} = pL$$

$$= \frac{1.41}{12} (37.76) = 4.44 \text{ k/Lin. in.}$$

$$FS = \frac{tg}{t_{\max}} = \frac{16.0}{4.44} = 3.6 > 2.0 \quad \text{ok}$$

HANSEN'S METHOD



Try $\theta_3 = 1.5 \text{ rad.}$, $\phi = 30^\circ$

$$\frac{r_{\theta_3}}{r_{\theta_3}} = e^{\theta_3 \tan \phi} = 2.37$$

$r_{\theta_3} = 52'$, $r_{\theta_3} = 22'$, $h_3 = 20.5'$, $a_3 = 7.0'$



LARGE DIAMETER DRILL SHAFT EQUIPMENT



SALES / RENTALS / ENGINEERING

Crane Mounted Drills, Pile Top Drills, Circulation Drill Strings, Kelly Bars, Circulation Swivels, Flat Bottom DC/RC Bits, Dual Wall Core Barrels, Core Breaker/Retrievers, Drill Pipe, Augers, Drill Buckets, Core Barrels, Cleanout Buckets, Belling Tools, Drop Chisels, Special Tooling

713 E. WALNUT STREET GARLAND, TEXAS 75040

U.S.A. TOLL FREE 1-800-527-1315

PHONE (972) 272-6461 FAX (972) 272-9194

WWW.SMHAINCO.COM

$$G = \gamma A = \gamma' \left(\frac{r_{\theta 3}^2 - r_{o 3}^2}{4 \tan \phi} - \frac{Bh_3}{2} \right)$$

$$= 0.0725 \left[\frac{(52)^2 - (22)^2}{4(0.577)} - \frac{53.06(20.5)}{2} \right] = 30^k$$

		<u>W</u>	<u>H</u>	<u>Arm</u>	<u>M</u>
W_1	See Page 3	84.9		17.69	1,497
W_2	"	55.8		35.37	1,974
W_3	"	107.7		26.53	2,857
G		-30.0		26.53 ⁽¹⁾	-786
P_a	See Page 3		→ 2.7	5.00	-14
P_w	"		→ 101.5	19.00	-1,929
P_R	$1/2 \times 6.09 \times 28$		← 85.3	9.33	796
		<u>218.4^k</u>	→ 18.9 ^k		<u>4,385^{ft-k}</u>

$$\bar{x} = 20.0'$$

(1) Approximate.

$$M_R = 84.9(17.69 - 7.0) + 55.8(35.37 - 7.0) + 107.7(26.53 - 7.0)$$

$$-30.0(26.53 - 7.0) + 85.3(9.33 + 20.5) = 6,553^{\text{ft-k}}$$

$$M_o = 2.7(5.00 + 20.5) + 101.5(19.00 + 20.5) = 4,078^{\text{ft-k}}$$

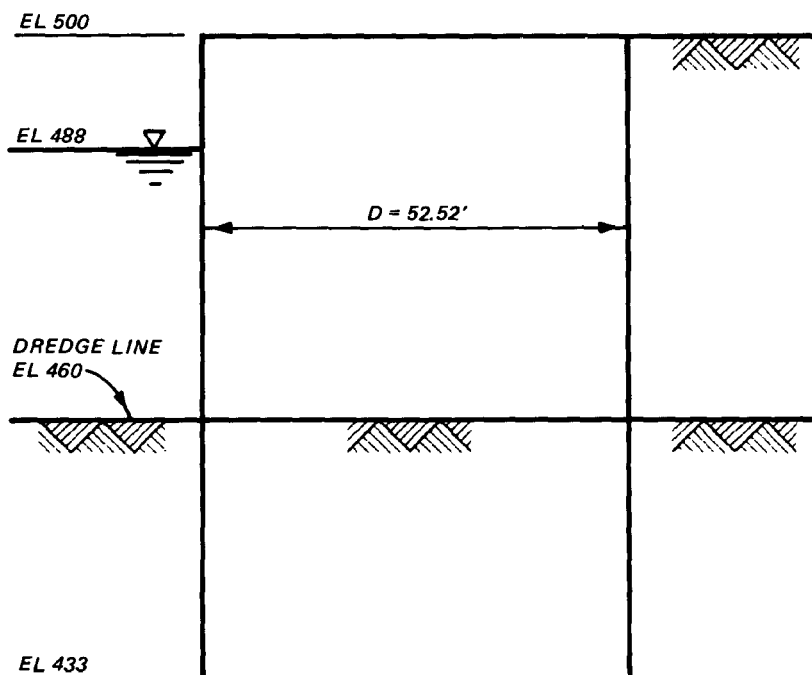
$$FS = \frac{M_R}{M_o} = \frac{6,553}{4,078} = 1.61 > 1.5 \quad \text{ok}$$

Summary

	θ	r_o	r_{θ}	h	a	G	x	M_R	M_o	FS
1	2.5	10	42	5.0	10.0	43	19.7	4,575	2,463	1.86
2	2.0	14	44	11.5	10.0	33	20.0	5,130	3,141	1.63
3	1.5	22	52	20.5	7.0	30	20.0	6,553	4,078	1.61
4	1.0	36	64	35.0	0.5	20	20.4	9,208	5,589	1.65

Values in *italics* are scaled values.

Example 26: Cellular Retaining Wall on Sand



DESIGN DATA

- Diameter of cell, $D = 52.52'$
 - Effective width, $B = 43.99'$
 - Guaranteed piling interlock strength, $t_g = 16,000$ pounds per linear inch of interlock
- o Cell Fill, Backfill, and Overburden Properties:

$$\phi = 30^\circ, \quad \tan \phi = 0.577$$

$$\gamma = 110 \text{ pcf (moist)}$$

$$\gamma' = 70 \text{ pcf (submerged)}$$

$$K_a = \frac{1 - \sin \phi}{1 + \sin \phi} = \frac{1 - 0.50}{1 + 0.50} = 0.33 ; \quad K_p = \frac{1 + \sin \phi}{1 - \sin \phi} = \frac{1 + 0.50}{1 - 0.50} = 3.00$$

$$P_a = \gamma K_a = 110(0.33) = 36.7 \text{ psf/ft}$$

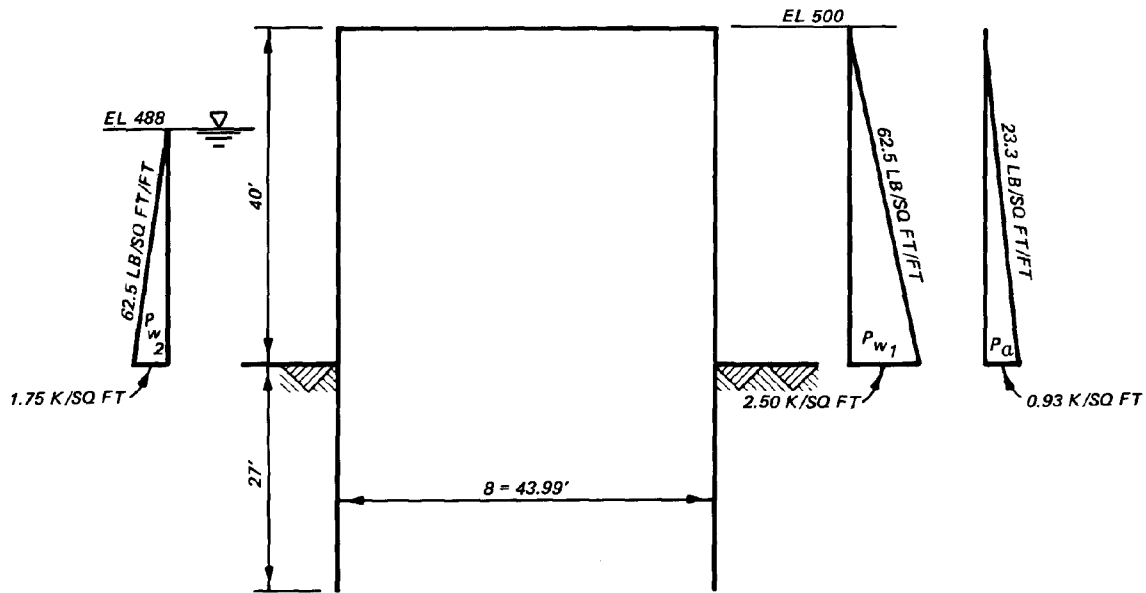
$$P'_a = \gamma' K_a = 70(0.33) = 23.3 \text{ psf/ft} ; \quad P'_p = \gamma' K_p = 70(3.00) = 210.0 \text{ psf/ft}$$

o Coefficient of Friction:

- Soil on steel, $\tan \delta = 0.40$
- Steel on steel at interlocks, $f = 0.30$

o LOADING

- Service Condition - Cell fill and backfill both saturated to $el\ 500$. Pool at $el\ 480$.



VERTICAL SHEAR RESISTANCE

$$K_{C_{cell}} = \frac{\cos^2 \phi}{2 - \cos^2 \phi} = \frac{0.75}{2 - 0.75} = 0.60$$

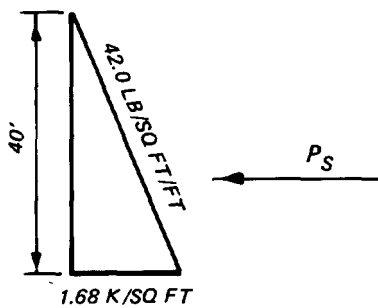
$$\phi = 30^\circ$$

$$p' = \gamma'K = 70(0.60) = 42.0 \text{ psf/ft}$$

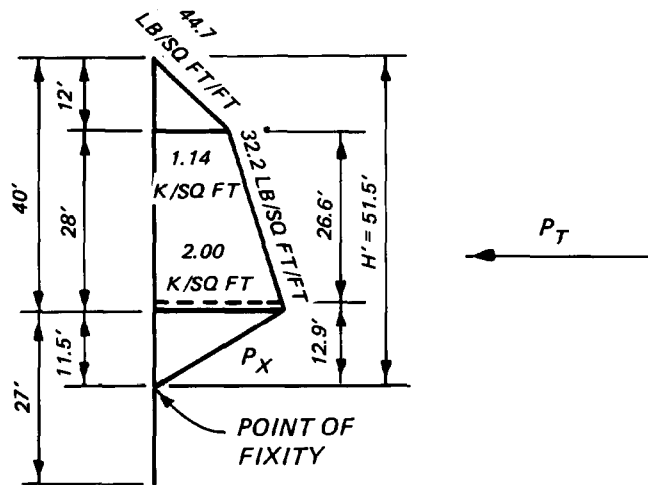
$$K_{\text{outboard sheeting}} = 1.4K_a = 1.4(0.33) = 0.46$$

$$p = \gamma'K + \gamma_w = 70(0.46) + 62.5 = 94.7 \text{ psf/ft}$$

$$p' = \gamma'K = 70(0.46) = 32.2 \text{ psf/ft}$$

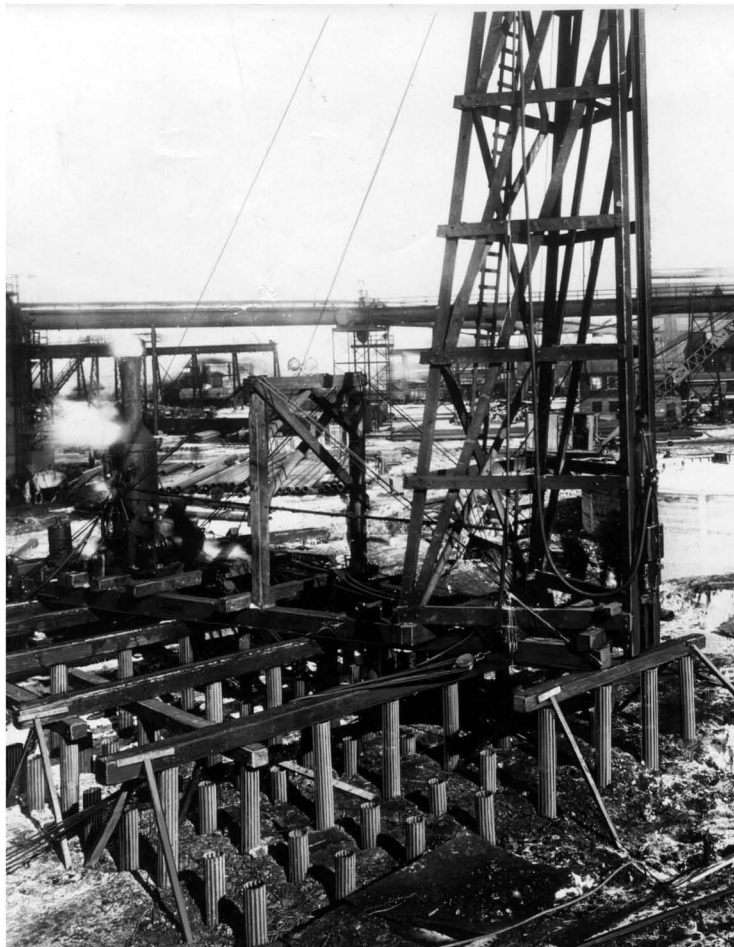


VERTICAL PLAN ON CENTER LINE OF CELL



OUTBOARD SHEETING

Working for You... Then and Now



- ✦ **Vulcan Air/Steam Pile Hammers**
- ✦ **IHC Hydrohammers**
- ✦ **IHC Fundex Equipment**
- ✦ **Genuine Factory Parts**
- ✦ **Service and Technical Support**
- ✦ **Extensive Dealer Network**

VULCAN FOUNDATION EQUIPMENT

111 Berry Road
 P.O. Box 16099
 Houston, TX 77222
 Phone (713) 691 3000
 Fax (713) 691 0089
 Toll Free (800) 742-6637
 Email sales@vulcanhammer.com
 Web site <http://www.vulcanhammer.com>

Member of the IHC Caland Group

Point of Fixity:

$$P_x = p'_p - p' = 210.0 - 32.2 = 177.8 \text{ psf/ft}$$

$$h = \frac{2.04}{0.1778} = 11.5'$$

$$H' = 11 + 28 + 11.5 = 51.5' , \quad H'/4 = 12.9'$$

$$P_s = 1/2(1.68)(40) = 33.6 \text{ k/ft}$$

$$P_T = 1/2(1.14)(12) + 1/2(1.14 + 2.00)(26.6) + 1/2(2.00)(12.9) = 61.5 \text{ k/ft}$$

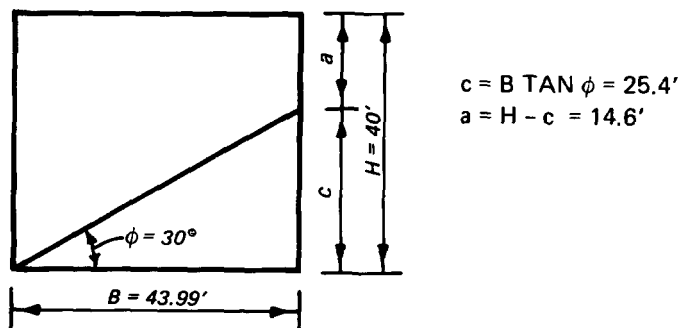
$$Q = \frac{3M}{2B} = \frac{3 \left[P_{w1} \left(\frac{H_{w1}}{3} \right) + P_a \left(\frac{H_s}{3} \right) - P_{w2} \left(\frac{H_{w2}}{3} \right) \right]}{2B}$$

$$= \frac{3 \left[1/2(2.50)(40)(13.33) + 1/2(0.93)(40)(13.33) - 1/2(1.75)(28)(9.33) \right]}{2(43.99)}$$

$$= 23.4 \text{ k/ft}$$

$$FS = \frac{P_s \tan \phi + fP_T}{Q} = \frac{33.6(0.577) + 0.30(61.5)}{32.4} = 1.62 > 1.50 \quad \text{ok}$$

HORIZONTAL SHEAR RESISTANCE



$$M_r = \frac{\gamma' a c^2}{2} + \frac{\gamma' c^3}{3} = \frac{0.070(14.6)(25.4)^2}{2} + \frac{0.070(25.4)^3}{3} = 712 \text{ ft-k}$$

$$M_f = P_T f B = 61.5(0.30)(43.99) = 812 \text{ ft-k}$$

$$M_o = P_{w1} \left(\frac{H_{w1}}{3} \right) + P_a \left(\frac{H_s}{3} \right) = 50(13.33) + 18.6(13.33) = 914 \text{ ft-k}$$

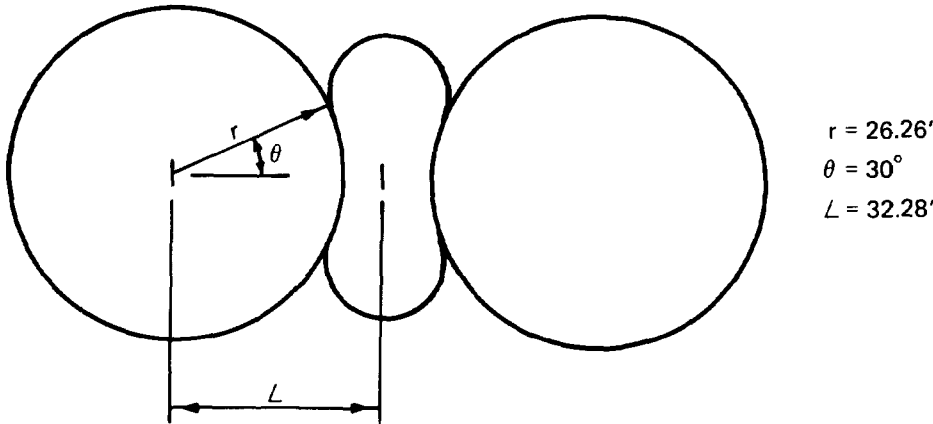
$$M_r = \frac{\gamma' a c^2}{2} + \frac{\gamma' c^3}{3} = \frac{0.070(14.6)(25.4)^2}{2} + \frac{0.070(25.4)^3}{3} = 712 \text{ ft-k}$$

$$M_f = P_T f B = 61.5(0.30)(43.99) = 812 \text{ ft-k}$$

$$M_o = P_{w1} \left(\frac{H_{w1}}{3} \right) + P_a \left(\frac{H_s}{3} \right) = 50(13.33) + 18.6(13.33) = 914 \text{ ft-k}$$

$$FS = \frac{M_r + M_f + P_{w2} \left(\frac{H_{w2}}{3} \right)}{M_o} = \frac{712 + 812 + 24.5(9.33)}{914} = 1.92 > 1.50 \quad \text{ok}$$

INTERLOCK TENSION



$$\begin{aligned} r &= 26.26' \\ \theta &= 30^\circ \\ L &= 32.28' \end{aligned}$$

$$t_{\max} = pL$$

$$= \frac{2.00}{12} (32.28) = 5.38 \text{ k/Lin. in.}$$

$$FS = \frac{tg}{t_{\max}} = \frac{16.0}{5.38} = 2.97 > 2.0 \quad \text{ok}$$

PULLOUT RESISTANCE OF LAND FACE SHEETS

$$Q_u = 1/2 \gamma K a D^2 \tan \delta (\text{perimeter})$$

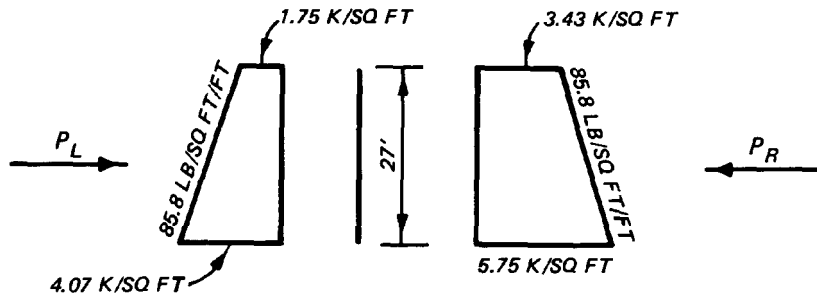
$$= 1/2(0.070)(0.33)(27)^2(0.40)(2 \times 1) = 6.7^k$$

$$Q_p = \frac{P_{w1} \left(\frac{H_{w1}}{3} \right) + P_a \left(\frac{H_s}{3} \right) - P_{w2} \left(\frac{H_{w2}}{3} \right)}{3B(1 + B/4L)}$$

$$= \frac{50(13.33) + 18.6(13.33) - 24.5(9.33)}{3(43.99) + \frac{43.99}{4(32.28)}} = 3.9^k$$

$$FS = \frac{Q_u}{Q_p} = \frac{6.7}{3.9} = 1.72 > 1.50 \quad \text{ok}$$

PENETRATION RESISTANCE OF OUTBOARD SHEETS



$$F_R = (P_L + P_R) \tan \delta = \left(\frac{1.75 + 4.07}{2} + \frac{3.43 + 5.75}{2} \right) (27) (0.40) = 81.0^k/ft$$

$$F_I = P_T \tan \delta = 51.4(0.40) = 20.6^k/ft$$

$$FS = \frac{F_R}{F_I} = \frac{81.0}{20.6} = 3.93 > 1.50 \quad \text{ok}$$

BEARING CAPACITY @ TOE

$$q_f = 1/2\gamma B N_\gamma + C N_c + \gamma D_f N_q = 1/2(0.070)(43.99)(20) + 0.070(27)(22) = 72.4 \text{ ksf}$$

$$W = \gamma B H = 0.070(43.99)(40) = 123.2^k$$

$$M = P_{w1} (H_1/3) + P_a (H_s/3) - P_{w2} (H_w/3) = 50(13.33) + 18.6(13.33) - 24.5(9.33) = 686^{\text{ft-k}}$$

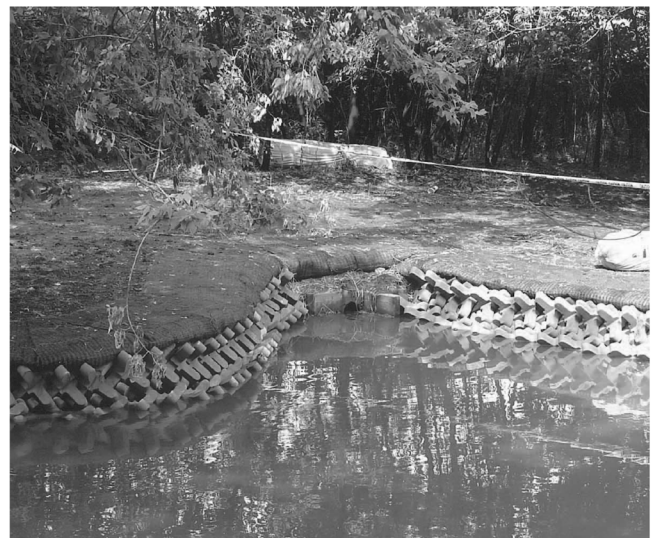
$$FS = \frac{q_f}{\frac{W}{B} + \frac{6M}{B^2}} = \frac{72.4}{\frac{123.2}{43.99} + \frac{6(686)}{(43.99)^2}} = 24.6 > 2.0 \quad \text{ok}$$

Marine Solutions

Solutions for Breakwaters, Shore Protection and Marina Docks

Economy, durability, and versatility

CONTECH® Marine Products provide economical and effective solutions for various marine applications, including shore protection, primary and secondary breakwaters, jetties and marina docks.



For more information, call Toll Free: 800-338-1122.
Or, visit our web site at www.contech-cpi.com

CONTECH
CONSTRUCTION PRODUCTS INC.

INNOVATIVE CIVIL ENGINEERING SITE SOLUTIONS

 American
Owned and Operated

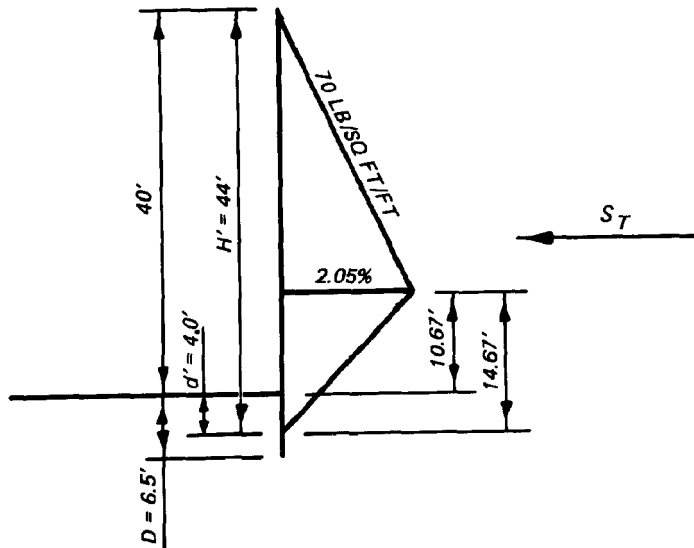
©2003 CONTECH Construction Products Inc. All Rights Reserved

VERTICAL SHEAR RESISTANCE (Schroeder-Maitland)

PS28 sheet piling: $E = 29,000,000 \text{ p/in.}^2$, $I = 2.8 \text{ in.}^4$

$n_h = 160,000 \text{ pcf}$ (medium dense sand)

$\gamma' = 70 \text{ pcf}$, $K = 10$



$$T = 5 \sqrt{\frac{EI}{n_h}} = 5 \sqrt{\frac{29,000,000(2.8)}{\frac{160,000}{1,728}}} = 15.44 \text{ in.} = 1.3 \text{ ft}$$

$$d' = 3.1T = 3.1(1.3) = 4.0'$$

$$D = 5T = 5(1.3) = 6.5'$$

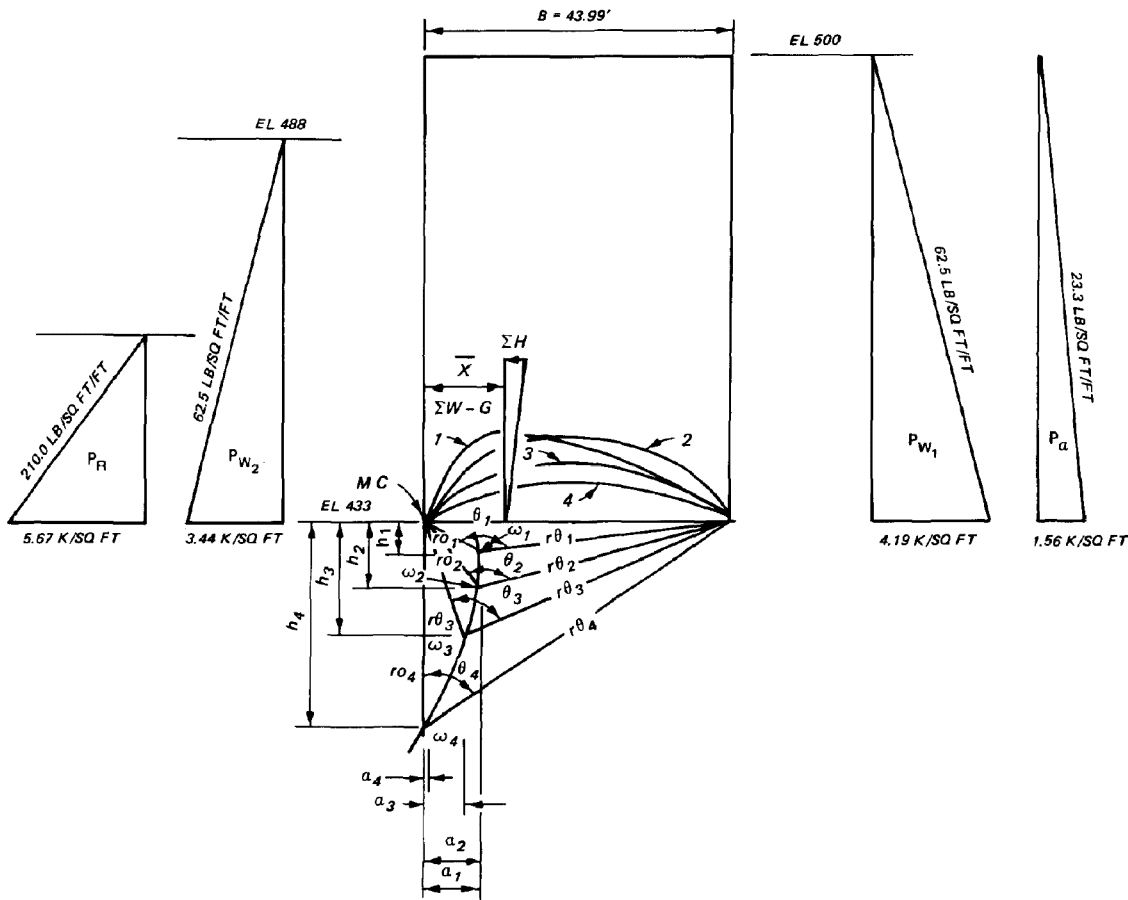
$$H' = 40 + 4.0 = 4.4'$$

$$S_T = 1/2 \gamma' K (H')^2 (\tan \phi + f) = 1/2 (0.070) (1.0) (44)^2 (0.577 + 0.30) \\ = 59.4 \text{ k/l}$$

$$Q = 23.4 \text{ k/l} \text{ - See Page 3}$$

$$\text{F.S.} = \frac{S_T}{Q} = \frac{59.4}{23.4} = 2.54 > 1.5 \quad \text{ok}$$

HANSEN'S METHOD



Try $\theta_2 = 2.0 \text{ rad.}$, $\phi = 30^\circ$ Neglect wall friction

$$\frac{r_{\theta_2}}{r_{o_2}} = e^{\theta_2 \tan \phi} = 3.15$$

$$r_{\theta_2} = 39.5' , r_{o_2} = 12.5' , h_2 = 9.5' , a_2 = 8.0'$$

$$G = \gamma A = \gamma' \left(\frac{r_{\theta}^2 - r_o^2}{4 \tan \phi} - \frac{B h_2}{2} \right)$$

$$= 0.07 \left[\frac{(39.5)^2 - (12.5)^2}{4(0.577)} - \frac{43.99(9.5)}{2} \right] = 28^k$$

		W	H	Arm	M
					+
W	$43.99 \times 67 \times 0.070$	206.3		22.00	4,539
G		-28.0		22.00 ⁽¹⁾	-616

P_{W_1}	$1/2 \times 4.19 \times 67$		←	138.7	22.67	-3,144
P_a	$1/2 \times 1.56 \times 67$		←	52.3	22.67	-1,186
P_{W_2}	$1/2 \times 3.44 \times 55$		→	94.6	18.33	1,734
P_R	$1/2 \times 5.67 \times 27$		→	76.5	9.00	689
		178.3	←	19.9 ^k		2,016 ^{ft-k}
						$\bar{x} = 11.31'$

(1) Approximate.

$$M_R = 206.3(22 - 8.0) - 28(22 - 8.0) + 94.6(18.33 + 9.5) + 76.5(9.00 + 9.5) = 6,544 \text{ ft-k}$$

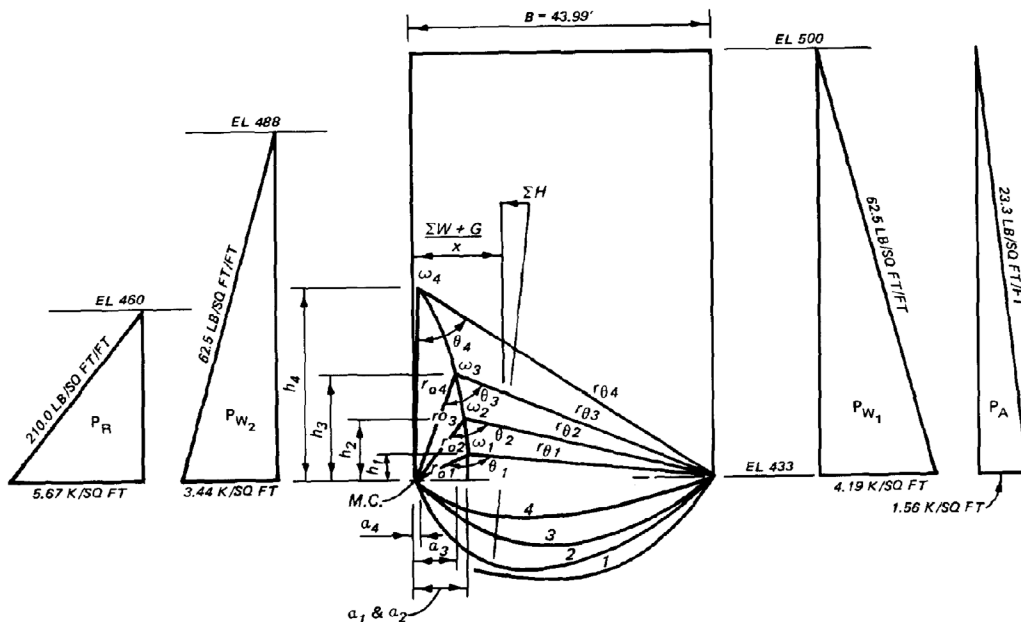
$$M_O = 138.7(22.67 + 9.5) + 52.3(22.67 + 9.5) = 6,144 \text{ ft-k}$$

$$FS = \frac{M_R}{M_O} = \frac{6,544}{6,144} = 1.07 < 1.5 \quad \text{cell diameter should be increased}$$

Summary

	θ	r_o	r_θ	h	a	G	x	M_R	M_o	FS
1	2.5	9.0	35.5	4.5	8.0	29	11.12	5,675	5,194	1.09
2	2.0	12.5	39.5	9.5	8.0	28	11.31	6,544	6,144	1.06
3	1.5	18.0	42.5	16.0	6.0	20	11.71	8,141	7,386	1.10
4	1.0	29.5	52.5	29.5	1.0	12	12.19	11,550	9,964	1.16

Values in *italics* are scaled values.





BANUT PILE DRIVING RIGS

large batter angles, 60ft stroke
impact precast piles, beams, casings & wood
vibrate sheets, beams, casings & more
pre-drill, drill piles, drill out casings & more

CAN 1 RIG DRILL & DRIVE WITHOUT SWAPPING ?



Fully hydraulic

2 high speed winches

hydraulic hammers up to 26,400 lbs pistons (132,000 ft.lbs)

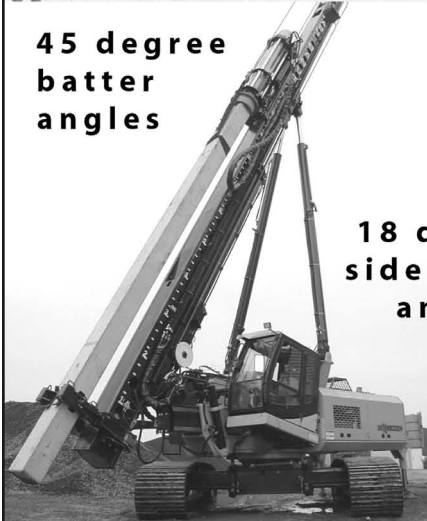
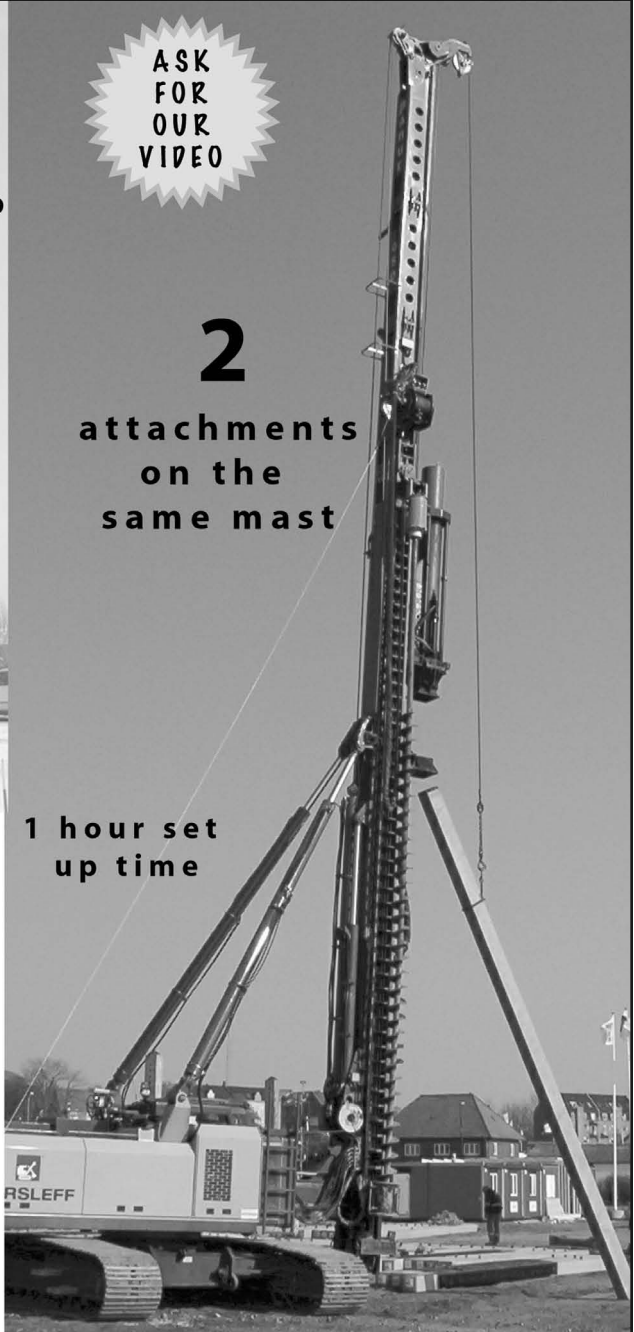
0-100 blows/min

ASK FOR OUR VIDEO

2

attachments on the same mast

1 hour set up time



45 degree batter angles

18 degree side batter angles

HAMMER & STEEL, INC (WEST COAST)
TOLL FREE: 877-224-3356
www.abi-delmag.com

CALL FOR SALES & RENTALS

HAMMER & STEEL, INC (MID-WEST & EAST COAST)
TOLL FREE: 800-325-7453
www.hammersteel.com

Try $\theta_3 = 1.5 \text{ rad.}$, $\phi = 30^\circ$ - neglect wall friction

$$\frac{r_{\theta_3}}{r_{o_3}} = e^{\theta_3 \tan \phi} = 2.36$$

$$r_{\theta_3} = 42.5' , \quad r_{o_3} = 18' , \quad h_3 = 16' , \quad a_3 = 6.0'$$

$$G = \gamma A = \gamma' \left(\frac{r_{\theta}^2 - r_o^2}{4 \tan \phi} - \frac{Bh_3}{2} \right)$$

$$= 0.07 \left[\frac{(42.5)^2 - (18)^2}{4(0.577)} - \frac{43.99(16)}{2} \right] = 20^k$$

		<u>W</u>	<u>H</u>	<u>Arm</u>	<u>\bar{M}</u>
W	See Page 9	206.3			4,539
G		20.0		22.00 ⁽¹⁾	440
P_{w_1}	See Page 9		←		-3,144
P_a	d_o		←		-1,186
P_{w_2}	d_o		→		1,734
P_R	d_o		→		689
		<u>226.3^k</u>	<u>19.9^k</u>		<u>3,072^{ft-k}</u>

$$\bar{x} = 13.57'$$

(1) Approximate.

$$M_R = 206.3(22 - 6.0) + 20(22 - 6.0) + 94.6(18.33 - 16) = 3,841^{\text{ft-k}}$$

$$M_o = 138.7(22.67 - 16) + 52.3(22.67 - 16) - 76.5(9.00 - 16) = 1,810^{\text{ft-k}}$$

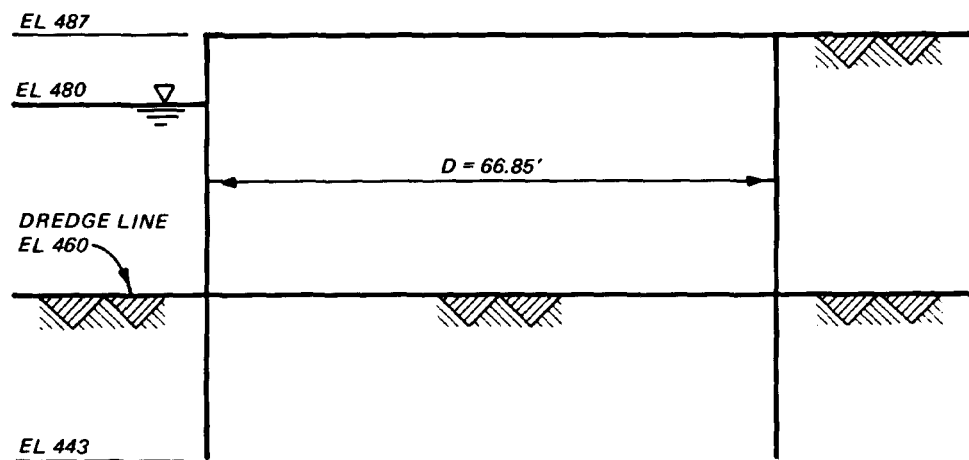
$$FS = \frac{M_R}{M_o} = \frac{3,841}{1,810} = 2.12 > 1.5 \quad \text{ok}$$

Summary

	θ	r_o	r_θ	h	a	G	x	M_R	M_o	FS
1	2.5	9.0	35.5	4.5	8.0	29	13.90	4,946	3,470	1.42
2	2.0	12.5	39.5	9.5	8.0	28	13.86	4,115	2,553	1.61
3	1.5	18.0	42.5	16.0	6.0	20	13.57	3,841	1,810	2.12
4	1.0	29.5	52.5	29.5	1.0	12	13.27	5,889	2,625	2.24

Values in *italics* are scaled values.

Example 27: Cellular Retaining Wall on Clay



DESIGN DATA

- Diameter of cell, $D = 66.85'$
- Effective width, $B = 58.57'$
- Guaranteed piling interlock strength, $t_g = 16,000$ pounds per linear inch
- o Cell Fill and Backfill Properties (sand and gravel)

$$\phi = 30^\circ, \quad \tan \phi = 0.577$$

$$\gamma = 110 \text{ pcf (moist)}$$

$$\gamma' = 70 \text{ pcf (saturated)}$$

$$K_a = \frac{1 - \sin \phi}{1 + \sin \phi} = \frac{1 - 0.50}{1 + 0.50} = 0.33$$

$$p_a = \gamma K_a = 110(0.33) = 36.7 \text{ psf/ft}$$

$$p'_a = \gamma' K_a = 70(0.33) = 23.3 \text{ psf/ft}$$

o Overburden Properties (medium stiff clay)

$$n_h = 150,000 \text{ pcf}, \quad C_a = 1,000 \text{ psf}, \quad \gamma = 120 \text{ pcf}, \quad \gamma' = 65 \text{ pcf}$$

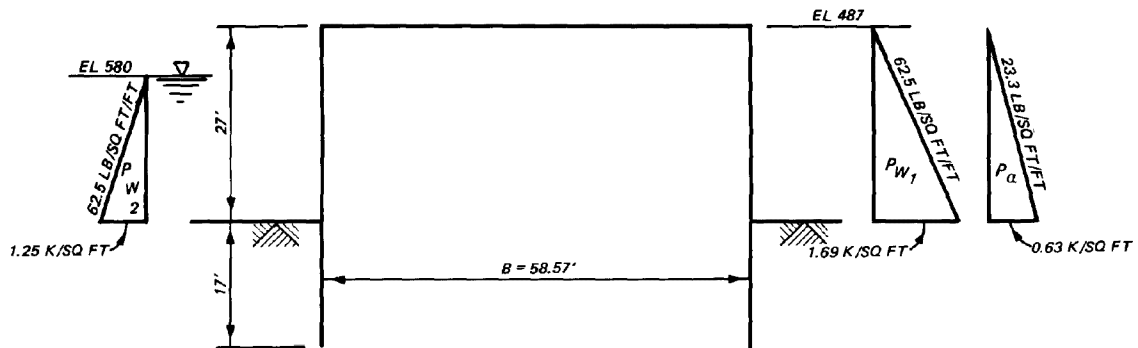
o Coefficient of Friction:

- Soil on steel, $\tan \delta = 0.40$
- Steel on steel at interlocks, $f = 0.30$

LOADING

o Service Condition

- Cell fill and backfill both saturated to el 487. Pool at el 480.

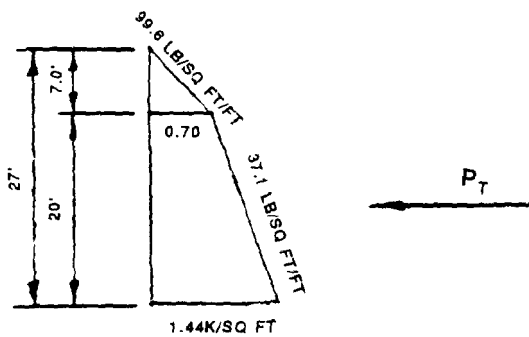


VERTICAL SHEAR RESISTANCE

$$K_{\text{outboard sheeting}} = 1.6K_a = 1.6(0.33) = 0.53$$

$$p = \gamma'K + \gamma_w = 70(0.53) + 62.5 = 99.6 \text{ psf/ft}$$

$$p' = \gamma'K = 70(0.53) = 37.1 \text{ psf/ft}$$



$$\Delta P = P_T - P_p$$

$$P_T = 1/2(0.70)(7.0) + \frac{0.70 + 1.44}{2} (20) = 23.9 \text{ k/ft}$$

$$FS = \frac{\Delta P R f \left(\frac{B}{L}\right) \left(\frac{L + 0.25B}{L + 0.50B}\right)}{M}$$

#1 in Marine Dock Products...

Dock Fenders ♦ Dock Boxes ♦ Line Hangers
Power Pedestals ♦ Fish Tables ♦ Piling Caps
Cleats ♦ Hose Holders ♦ Trash Receptacles
Vertical Lift Ladders ♦ Standard Ladders
Floating Docks, Hardware & Floats

Manufacturer & Distributor for:

**FEND-ALL® Family
of Dock Fenders**
(Patent #6,289,836)

**FEND-OFF® Family
of Dock Fenders**

PerfectLine® Dock Boxes

The Leader in Quality and Service

Service is the #1 priority at Marina & Dock Equipment, as you, our customer, are our best and most important salespeople. Regardless of the size of your needs, you will receive the benefit of our twenty plus years of experience, expertise and integrity in the marine industry.

...Because Our Products are the Best!

PerfectLine® Dock Boxes



- ♦ All Resins and Gelcoats are Pure, Marine Grade Isophtalics
- ♦ UV Gelcoat for Long-lasting Protection
- ♦ Molded Non-skid Surface on Lids
- ♦ Lids have Foam Core for added Strength
- ♦ Continuous Heavy Duty Hinge and Fasteners
- ♦ Locking Hasp and Lid Retainer Cable

FEND-ALL® Dock Fenders



- ♦ Only Continuously Supported, Double-wall Fender Available
- ♦ 300% Elongation Before Breakage
- ♦ Internal Highenergy Absorption Web
- ♦ Life Expectancy of Fender Material is 10+ Years
- ♦ Contains UV and Mildew Inhibitors
- ♦ Available in Black, White or Gray

**New Style
Trash Receptacle &
Dock Boxes
Available Now!**



Marina & Dock Equipment

*A division of Alltel Industries
of South Florida, Inc.*

**1 (877) ALL-DOCK
(255-3625)**

(561) 540-2520

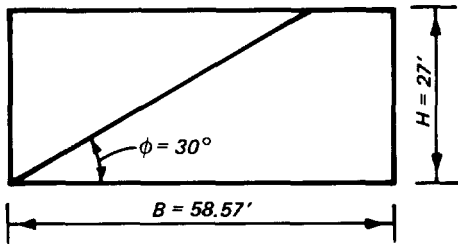
Fax (561) 540-2522

www.dockequipment.com or
www.marina-dock.com
e-mail: info@marina-dock.com

425 Industrial Street ♦ #4 ♦ Lake Worth, FL 33461

$$= \frac{23.9(33.43)(0.3) \left(\frac{58.57}{36.04} \right) \left[\frac{36.04 + 0.25(58.57)}{36.04 + 0.50(58.57)} \right]}{\frac{1}{2} (1.69 + 0.63) \frac{(27)^2}{3} - \frac{1}{2} (1.25) \frac{(20)^2}{3}} = 1.52 > 1.50$$

HORIZONTAL SHEAR RESISTANCE



$c = B \tan \phi = 33.82' - \text{USE } 27'$
 $a = H - c = 0$

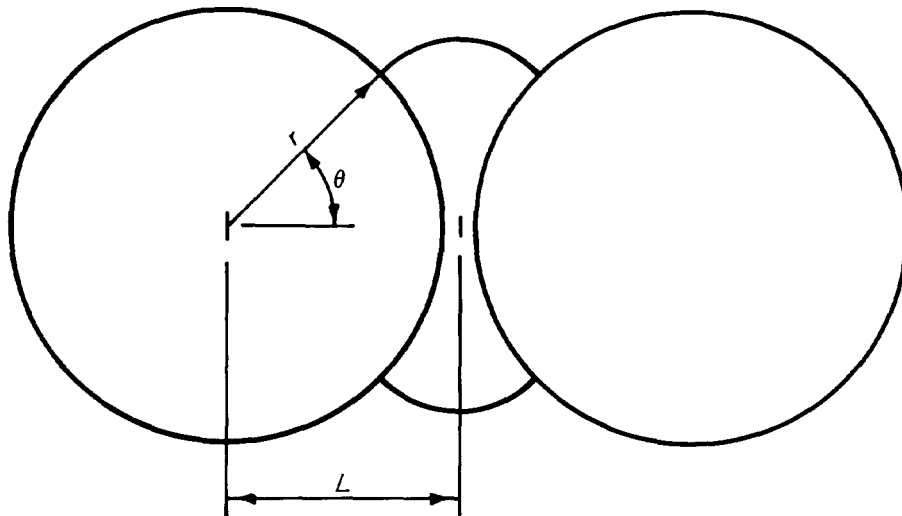
$$M_r = \frac{\gamma' a c^2}{2} + \frac{\gamma' c^3}{3} = 0 + \frac{0.070(27)^3}{3} = 459 \text{ ft-k}$$

$$M_f = P_T f B = 23.9(0.30)(58.57) = 420 \text{ ft-k}$$

$$M_o = P_{w1} \left(\frac{H_{w1}}{3} \right) + P_a \left(\frac{H_s}{3} \right) = 22.8(9.0) + 8.5(9.0) = 282 \text{ ft-k}$$

$$FS = \frac{M_r + M_f + P_{w2} \left(\frac{H_{w2}}{3} \right)}{M_o} = \frac{459 + 420 + 12(6.67)}{282} = 3.40 > 1.50 \quad \text{ok}$$

INTERLOCK TENSION



$r = 33.43'$
 $\theta = 45^\circ$
 $L = 36.04'$

$$t_{\max} = pL$$

$$= \frac{1.44}{12} (36.04) = 4.32 \text{ k/Lin. in.}$$

$$FS = \frac{tg}{t_{\max}} = \frac{16.0}{4.32} = 3.7 > 2.0 \quad \text{ok}$$

PULLOUT RESISTANCE OF LAND FACE SHEETS

$$Q_u = C_a D(\text{perimeter}) = 1.50(17)(2 \times 1) = 51^k$$

$$Q_p = \frac{M}{3B(1 + B/4L)} = \frac{282 - 12(6.67)}{3(58.57) \left[1 + \frac{58.57}{4(36.04)} \right]} = 0.8^k$$

$$FS = \frac{Q_u}{Q_p} = \frac{51}{0.8} = 64 > 1.5 \quad \text{ok}$$

BEARING CAPACITY

$$q_f = 1/2 \gamma' B N_{\gamma} + c N_c + \gamma D_f N_q = 1.00(5.70) + 0.070(17)(1.0)$$

$$= 6.9 \text{ ksf}$$

$$W = \gamma' B H = 0.070(58.57)(27) = 110.7^k$$

$$M = 282 - 12(6.67) = 199^{\text{ft-k}}$$

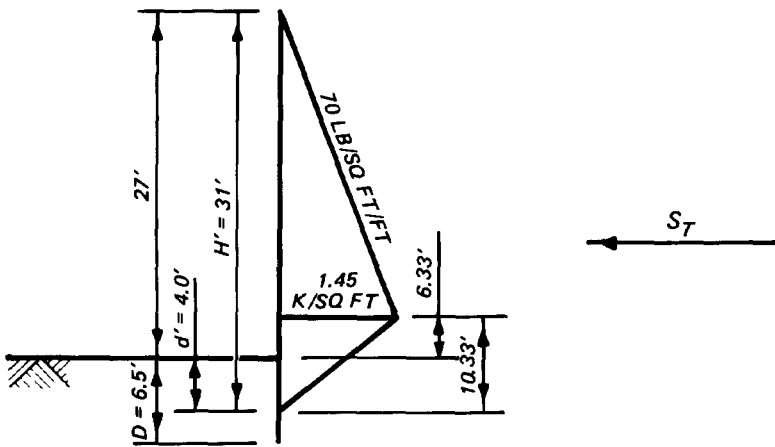
$$FS = \frac{q_f}{\frac{W}{B} + \frac{6M}{B^2}} = \frac{6.9}{\frac{110.7}{58.57} + \frac{6(199)}{(58.57)^2}} = 3.1 > 3.0 \quad \text{ok}$$

VERTICAL SHEAR RESISTANCE (Schroeder-Maitland)

$$\text{PS28 sheet piling: } E = 29,000,000 \text{ p/in.}^2, \quad I = 2.8 \text{ in.}^4$$

$$n_h = 150,000 \text{ pcf (medium dense sand) - cell fill}$$

$$\gamma' = 70 \text{ pcf}, \quad K = 1.0$$



$$T = 5 \sqrt{\frac{EI}{n_h}} = 5 \sqrt{\frac{29,000,000(2.8)}{\frac{150,000}{1,728}}} = 15.64 \text{ in.} = 1.3 \text{ ft}$$

$$d' = 3.1T = 3.1(1.3) = 4.0'$$

$$D = 5T = 5(1.3) = 6.5'$$

$$H' = 27 + 4.0 = 31.0'$$

$$S_T = 1/2 \gamma' K (H')^2 (\tan \phi + f) = 1/2 (0.070) (1.0) (31)^2 (0.577 + 0.30) = 19.4 \text{ k/1}$$

$$Q = \frac{3M}{2B} = \frac{3(199)}{2(58.57)} = 5.1 \text{ k/ft}$$

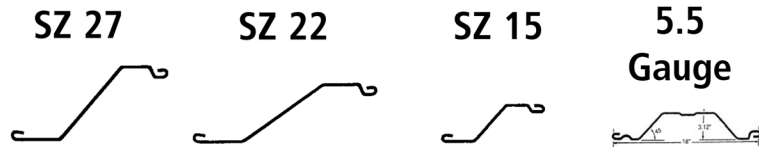
$$FS = \frac{S_T}{Q} = \frac{19.4}{5.1} = 3.80 > 1.50 \quad \text{ok}$$

SHORELINE STEEL, INC.

P.O. Box 480519, 58201 Main Street • New Haven, MI 48048
(800) 522-9550 • (586) 749-9559 • Fax (586) 749-6653

www.shorelinesteel.com

We are a leading producer of domestic cold formed steel sheet piling in sections ranging from 10 gauge to 3/8" thick. For any sheet piling requirement we can satisfy your needs with a top quality product and prompt delivery.



	Thickness (Nominal)	Weight (Sq. ft.)	Weight (Lin. Ft.)	Sec. Mod in ³ (Ft. Wall)	Moment of Inertia in ⁴ (Ft. Wall)	Laying Width	Wall Depth
10-10 ga.	.134	7.2	10.8	2.2	3.5	18.00	3.12
8-8 ga.	.164	8.8	13.2	2.62	4.2	18.00	3.12
7-7 ga.	.179	9.6	14.4	2.8	4.4	18.00	3.12
6-6 ga.	.194	10.5	15.8	3.0	4.9	18.00	3.12
5-5 ga.	.209	11.3	16.9	3.4	5.4	18.00	3.12
LZ 7	.164	8.3	17.2	3.6	8.1	25.00	4.50
LZ 8	.179	9.1	18.8	3.9	8.9	25.00	4.50
LZ 5	.209	10.6	21.9	4.6	10.4	25.00	4.50
LZ 3	.239	11.9	24.6	5.2	11.8	25.00	4.50
LZ 250	.250	12.3	25.6	5.4	12.4	25.00	4.50
SZ-10	.164	9.4	17.2	7.3	27.4	22.00	7.50
SZ-11	.179	10.3	18.8	7.9	29.8	22.00	7.50
SZ-12	.209	12.0	21.9	9.2	34.8	22.00	7.50
SZ-14	.239	13.5	24.6	10.4	39.9	22.00	7.50
SZ-15	.250	14.0	25.6	10.9	41.8	22.00	7.50
SZ-14.5	.250	14.5	32.4	13.0	61.49	26.75	9.46
SZ-14.5	.270	15.8	35.1	14.0	86.40	26.75	9.46
SZ-18	.312	18.1	40.4	16.2	76.83	26.75	9.46
SZ-20	.340	19.8	44.1	17.5	83.37	26.75	9.46
SZ-21	.350	20.3	45.3	18.1	86.00	26.75	9.46
SZ-22	.375	21.8	48.6	19.3	91.92	26.75	9.46
SZ-222	.312	22.1	40.4	26.7	163.09	22.00	12.25
SZ-250	.250	15.9	32.4	16.6	89.42	24.46	10.75
SZ-313	.312	19.9	40.4	20.6	111.53	24.46	10.75
SZ-340	.340	21.5	44.1	22.4	121.45	24.46	10.75
SZ-350	.350	22.1	45.3	22.9	124.62	24.46	10.75
SZ-375	.375	23.7	48.6	24.5	133.55	24.46	10.75
SZ-24	.340	24.1	44.1	29.0	177.52	22.00	12.25
SZ-25	.350	24.8	45.3	29.7	181.91	22.00	12.25
SZ-27	.375	26.6	48.6	32.0	195.18	22.00	12.25

DOMESTIC STEEL SHEET PILING

- All sections available in bare or galvanized steel.
- All Zee sections available in doubles.
- All sections produced exactly to customer specified length(s).
- All steel fully melted and manufactured in the USA.



For more information, please call toll free
(800) 522-9550

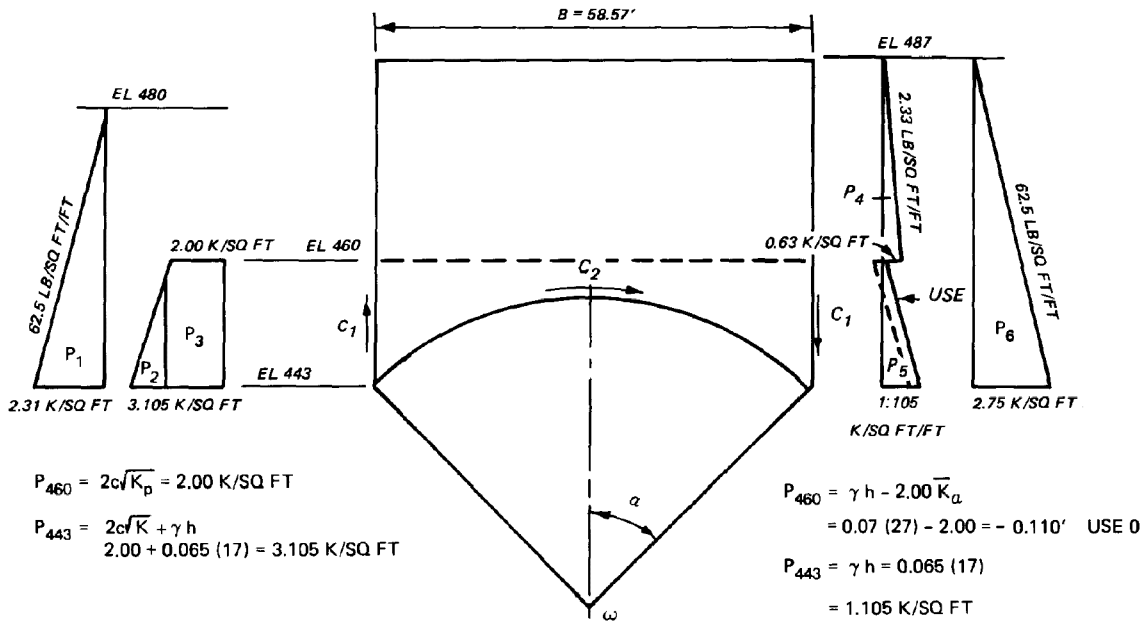
or visit our website at: www.shorelinesteel.com

Also Available:

- Corners
- Tees and Crosses
- Capping
- Coatings

SHORELINE STEEL, INC.

HANSEN'S METHOD



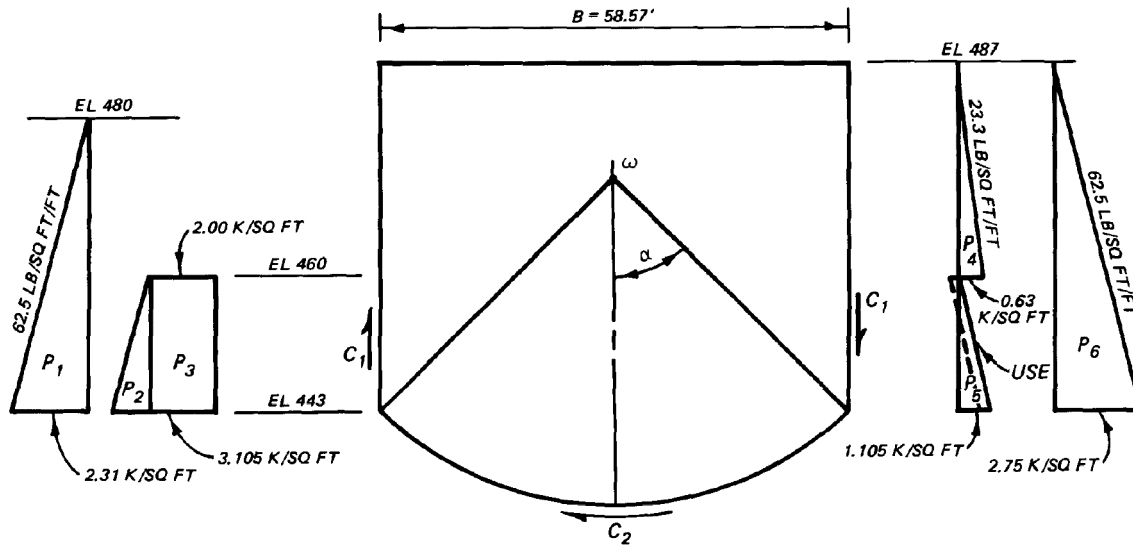
Try $\alpha = 45^\circ$, $C = 1,000 \text{ psf}$

		<u>F</u>	<u>Arm</u>	<u>M_R</u>	<u>M_O</u>
P ₁	$1/2 \times 2.31 \times 37$	42.7	41.62	1,777	
P ₂	$1/2 \times 1.105 \times 17$	9.4	34.96	329	
P ₃	2.00×17	34.0	37.79	1,285	
P ₄	$1/2 \times 0.63 \times 27$	8.5	55.29		470
P ₅	$1/2 \times 1.105 \times 17$	9.4	34.96		329
P ₆	$1/2 \times 2.75 \times 44$	60.5	43.96		2,660
C ₁	$2 \times 1.00 \times 17$	34.0	29.29	996	
C ₂	$1.00 \times \frac{29.29}{0.707} \times \frac{\pi}{2}$	65.1	41.43	<u>2,697</u>	
				7,084	3,459

$FS = \frac{M_R}{M_O} = \frac{7,084}{3,459} = 2.05 > 1.5 \quad \text{ok}$

Summary

α	M_R	M_O	FS
45	7,084	3,459	2.05
60	3,920	2,488	1.58
70	2,985	1,992	1.50
75	2,645	1,777	1.49
80	2,352	1,567	1.50
85	2,095	1,362	1.54



Try $\alpha = 45^\circ$, $C = 1,000$ psf

		<u>F</u>	<u>Arm</u>	<u>M_R</u>	<u>M_O</u>
P ₁	See Page 6	42.7	-16.96		724
P ₂	d _o	9.4	-23.62		222
P ₃	d _o	34.0	-20.79		707
P ₄	d _o	8.5	-3.29	28	
P ₅	d _o	9.4	-23.62	222	
P ₆	d _o	60.5	-14.62	885	
C ₁	d _o	34.0	29.29	996	
C ₂	d _o	65.1	41.43	<u>2,697</u>	
				4,828	1,653

$$FS = \frac{M_R}{M_O} = \frac{4,828}{1,653} = 2.92 > 1.5 \quad \text{ok}$$

Summary

α	M _R	M _O	FS
45	4,828	1,653	2.92
70	1,316	493	2.67
85	1,431	757	1.89

15.3.10. Recommended Practices for Design and Installation of Cellular Cofferdams

The following recommendations regarding design, construction, and maintenance of cellular sheet pile cofferdams have already been discussed elsewhere. However, their importance should again be stressed.

a. Analyses should evaluate the effect of full saturation of the cell fill unless positive measures are taken to control the saturation level throughout the life of the cofferdam.

b. Welded connector piles have not proven satisfactory in the past and shall no longer be used. Riveted or bolted connections with minimum 1/2-inch thick webs shall be required.

c. Wye connectors are preferable to tees. The tension in the outstanding leg of the connector is less for a wye since the load is applied more nearly at a tangent, rather than at right angles, as is the case with a tee.

d. Pull on the outstanding leg of connector piles should be limited by keeping the radius of the connecting arc as small as possible. The arc radius should not exceed one half of the radius of the main cell.

e. Where there is used piling in a cofferdam, care should be taken to make sure the sheets are gauged and will interlock properly. Special care should be taken in splicing used sheets to make sure the spliced sheets are compatible.

f. All handling holes in the sheet piling on the loaded side of the cofferdam should be plugged. This is necessary to prevent an objectionable amount of water from entering the cell or loss of cell fill.

g. Sheet piling should not be driven through overburden containing boulders. Extremely dense overburden should be excavated to a depth such that it can be penetrated without damaging the piling. Although dependent on the nature of the overburden, 30 feet is generally accepted as a maximum depth to drive through overburden.

h. When driving is difficult, jetting may be used to facilitate driving. However, this technique should be used with caution since there is a danger that the sheet piles will follow the jetted hole and will split out the interlock.

i. If it is neither possible nor practical to fully penetrate the overburden with the sheet piles and if scour by river flow is a possibility, the overburden should be protected against scour.

j. Setting sheet piling on bare rock should be avoided wher-

ever possible since support from the overburden is beneficial in helping maintain the desired cell configuration.

k. Each run of piling shall be driven to grade progressively from the start, so that the bottom end of any pile shall not lead the adjacent pile by more than 5 feet. This requirement will reduce the chances of splitting the interlocks.

l. The direction of the pile hammer advance should be reversed after each pass in order to ensure that the piles are driven plumb.

m. Connecting arcs should be driven and filled after the adjacent main cells have been driven and filled. However, at least the first two sheets of the connecting arc adjacent to the main cells should be driven prior to filling the main cells; otherwise, barrelling of the main cells would make driving of the arcs extremely difficult.

n. Diver inspection of the interlocks, after filling of the cells, should be required.

o. Wherever cells and fill are placed against sloped or stepped faces of existing concrete, care should be taken to seal the contact between the sheet piles and concrete to prevent infiltration of water which could saturate the fill or cause piping.

p. The cofferdam cells should be located a sufficient distance from open excavations to protect them from any instability of the excavated faces.

15.4. Finite Element Methods

15.4.1. Background

The application of FEM analysis to date has been to develop its state of the art to the point where it can be used to refine existing design techniques and to analyse potential failure modes that cannot be checked by other methods. All studies so far have been made by researchers or engineers who are extremely familiar with the FEM techniques using specialized FEM programs for soil and structure modelling. The FEM analysis does not yet lend itself to application by typical design engineers working with currently available general-use programs. Due to FEM techniques currently being used for research applications, the information provided by this section will be limited to a review of available literature and methods used for analysis.

Relatively little has been published concerning finite element analyses of cellular cofferdam structures. Kittisatra¹⁹⁶ was one of the first to apply FEM to cellular cofferdams by using a linear elastic axisymmetric model.

Clough and Hansen¹⁹⁷ were the first to utilize FEM soil-structure interaction techniques in the analyses of cellular

¹⁹⁶Kittisatra, L. 1976 (Jun). "Finite Element Analysis of Circular Cell Bulkheads," Ph. D. Thesis, Oregon State University, Corvallis, Oregon.

¹⁹⁷Clough, G. W. and Hansen, L. A. 1977. "A Finite Element Study of the Behavior of the Willow Island Cofferdam," Technical Report CE-218, Department of Civil Engineering, Stanford University.

Horsepower specs are one thing.

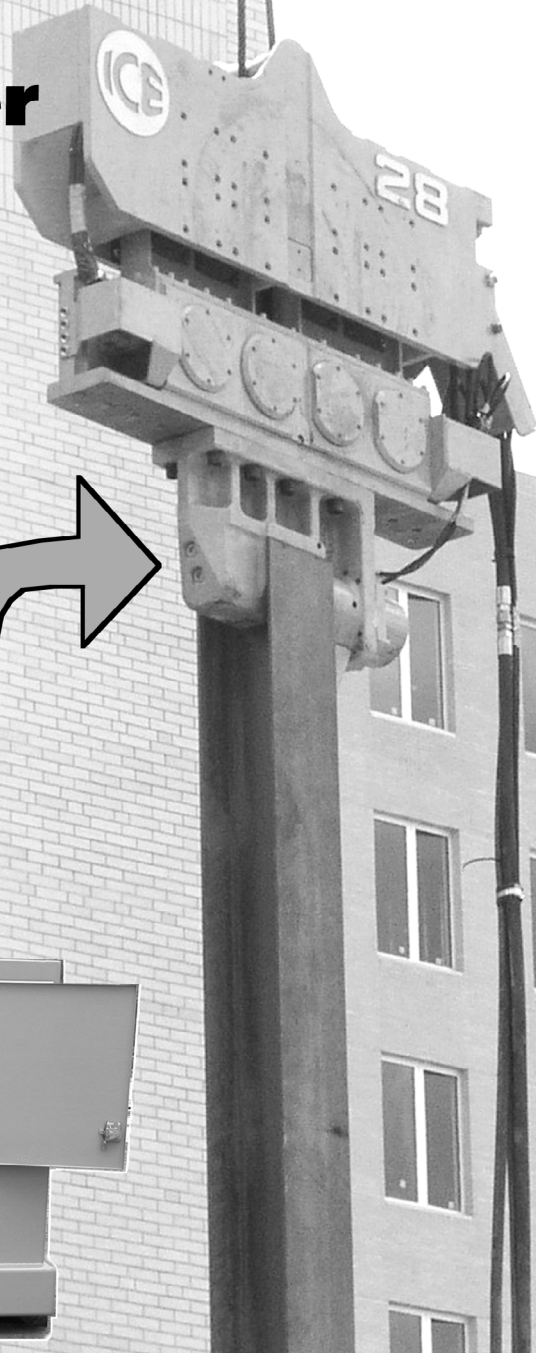
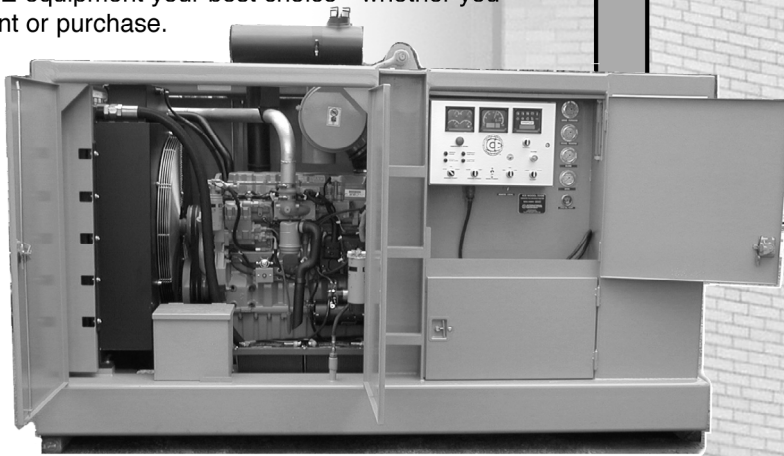
Net Horsepower at the tip of the pile is another.

ICE uses state-of-the-art hydraulic manifolds and highly-efficient piston equipment to transfer power to the piles. The other guys don't.

The difference is, ICE vibratory driver/extractors transfer 90%+ of available horsepower to the tip of the piles. The other guys average about 60%.

Clearly, this difference in power transfer efficiency directly affects job profitability. ICE vibros deliver more horsepower right where it matters most - at the tip of the piles.

Compare ICE vibros to the other guys' and you'll discover many engineering differences that make ICE equipment your best choice - whether you rent or purchase.



**INTERNATIONAL
CONSTRUCTION
EQUIPMENT, INC.**
www.iceusa.com

301 Warehouse Drive • Matthews, NC 28104

Phones: 888 ICEUSA1

& 704 821-8200

Fax: 704 821-8201 • e-mail: info@iceusa.com

TECHNO DRILL

Matthews NC • Lakeland FL • Metairie LA • Seattle WA • New Town Square PA • Sayreville NJ • Houston TX
Fort Wayne IN • Virginia Beach VA • Boston MA • Montreal Quebec • Singapore • Kuala Lumpur • Shanghai

cofferdams. They developed a vertical slice model that was used to analyse the US Army Corps of Engineers Willow Island Cofferdam. Later, Dr. Clough used this model along with two others, axisymmetric and horizontal slice models, to analyse the US Army 4-55 Corps of Engineers Lock and Dam No. 26 (Replacement) for Shannon and Wilson, Inc.¹⁹⁸.

15.4.2. Finite Element Cofferdam Models

Due to the difficulty of early investigations to define exactly the forces involved with interaction between sheet piles, soils, and the foundation, empirical methods for design of cellular cofferdams have been adopted over the years. Recent studies of the finite element method have shown that two-dimensional models of a circular cell cofferdam can, with a few basic assumptions, accurately determine interactive forces between cell elements. A finite element program must contain four special capabilities:

- Non-linear stress-strain material behaviour,
- Slip elements,
- Construction simulation, and
- Orthotropic shell response.

Soils are known to have a complex stress-strain response. The stress-strain behaviour of a sand is characterized by a family of non-linear curves in loading and a second family of essentially linear responses in unloading-reloading that depends upon the confining stress level. Three types of finite element models have been performed on cellular cofferdams as described below:

15.4.2.1. Vertical Slice Analysis

The first and most common model is a "Vertical Slice" analysis through the centre of a circular cell from upstream to downstream side. This model has been used with good results by Dr. Clough for Shannon and Wilson, Inc. to simulate analysis of all stages and construction for cells resting on soil. A vertical slice model was also used in the report on Willow Island Cofferdam by Clough and Hansen¹⁹⁷, in which cells founded on rock with an underlying soft clay seam are analysed. *Figure 15-31* and *Figure 15-32* show this particular finite element model.

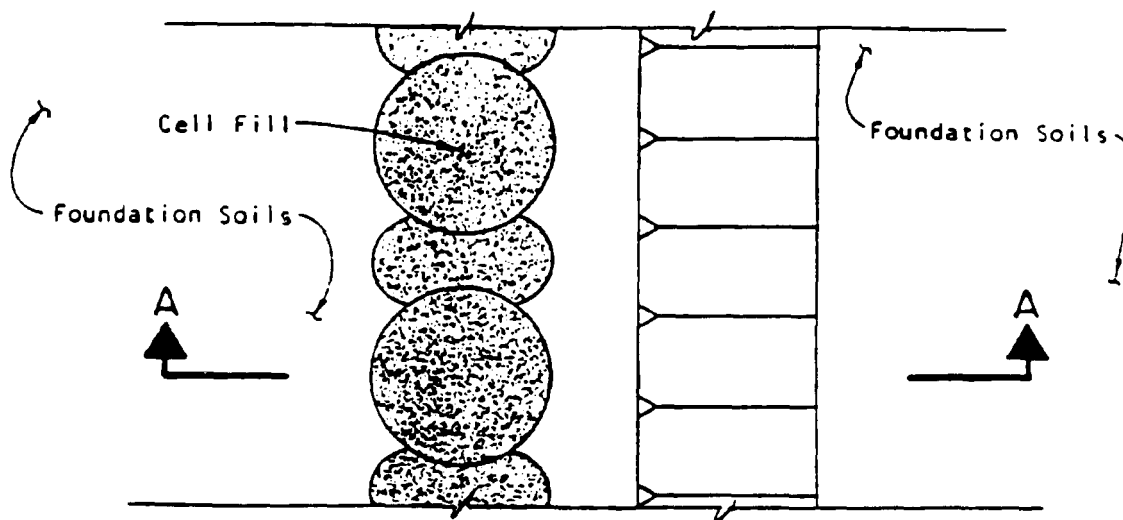


Figure 15-31: Schematic drawing, vertical slice model

¹⁹⁸Shannon and Wilson, Inc. 1982 (Sep). "Final Report, Tasks 3.2, 3.3, and 3.4, Finite Element Models," Report on Lock and Dam No. 26 (Replacement) for U. S. Army Engineer District, St. Louis. This report also describes the one set of variations of the finite element program "Soil-Struct," developed by Dr. Wayne Clough, which contains all of the special capabilities needed for soil-cofferdam interaction modelling.

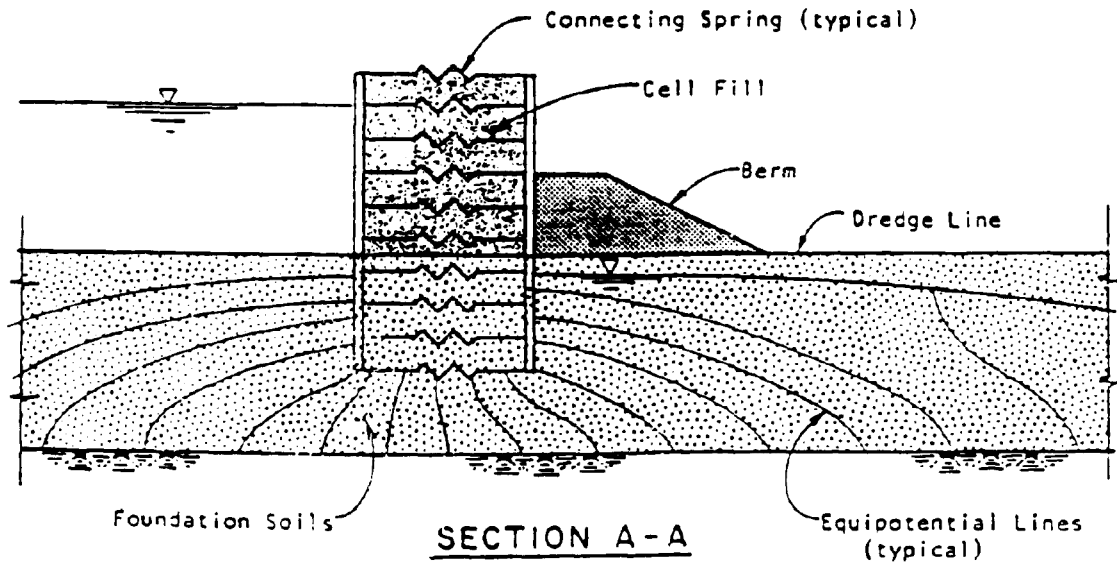


Figure 15-31: Schematic drawing, vertical slice model

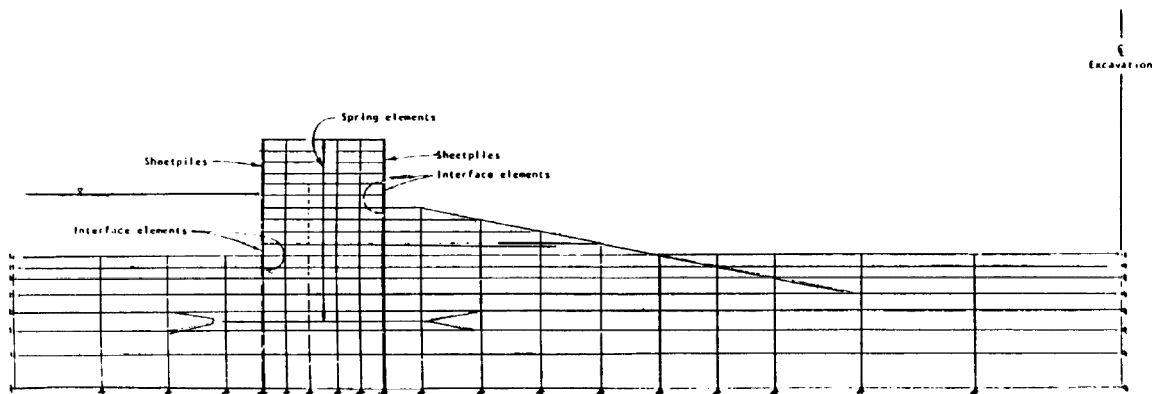


Figure 15-32: Vertical Slice Analysis, Finite Element Method

15.4.2.2. Axisymmetric Cell Analysis

The second model type is a vertical slice cut through the cell from centre line out called an "Axisymmetric Model," shown in Figure 15-33 and Figure 15-34. This analysis technique computes stresses and deflections of the sheet piling, cell fill, and foundation during cell filling. This model is not useful for other construction steps due to the assumption of axisymmetric loading. Axisymmetric Model Analysis was used by Dr. Clough for Shannon and Wilson, Inc. in their analysis of the Lock and Dam 26 (Replacement). Both this and the vertical slice types of models are analysed with interface slip elements between sheets and cell fill, and on any planes in the foundation where slippage could occur.

15.4.2.3. Horizontal Slice Analysis

The third analysis model, Figure 15-35 and Figure 15-36, is a "Horizontal Slice" including from centre-line main cell to centre line of arc cell and from outermost edge to centre line of cofferdam. This horizontal slice model may be used at many different elevations in the cell to obtain a better analysis of interlock tension and sheet pile stresses. Since a symmetrical loading is assumed on the structure, this analysis technique can only be used for analysing forces due to cell filling.

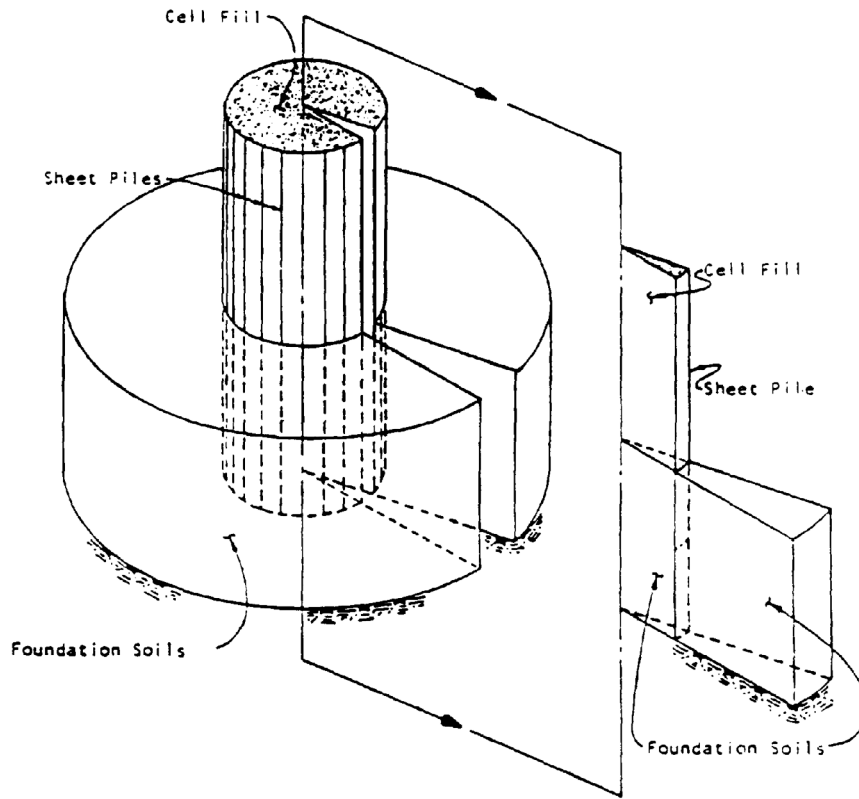


Figure 15-33: Schematic drawing, axisymmetric model

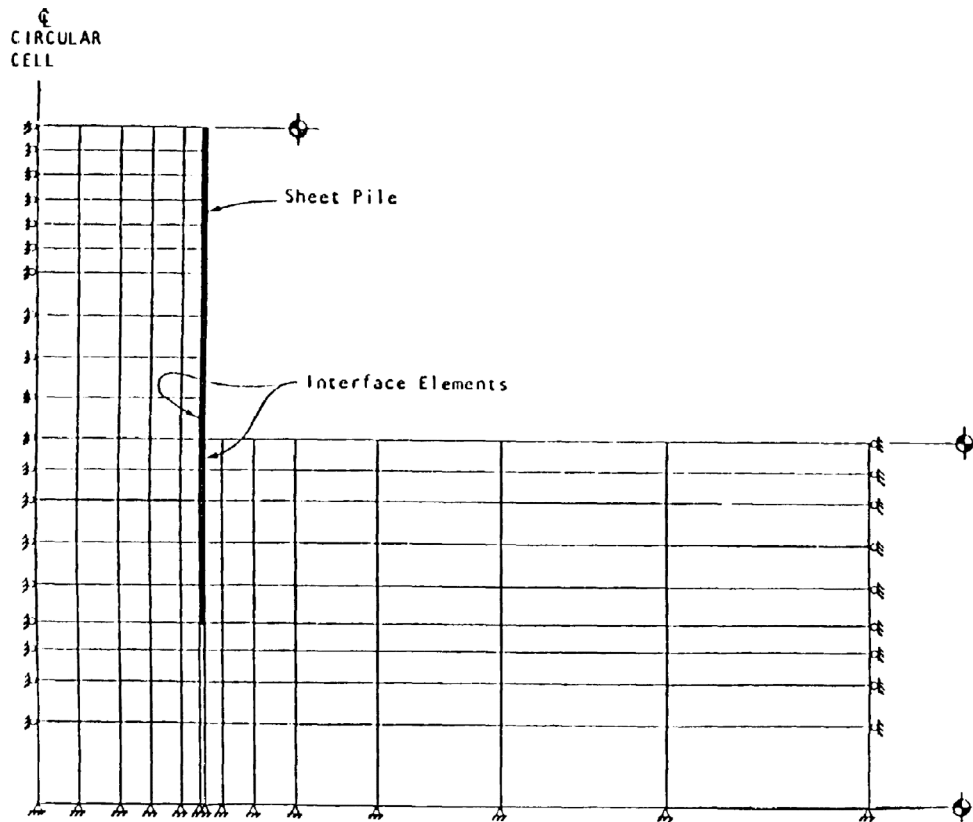


Figure 15-34: Finite Element Mesh for Axisymmetric Analyses of Main Cell Filling

ADVERTISE YOUR BUSINESS IN PILE BUCK® NEWSPAPER!



Pile Buck® is the #1 Newspaper targeted specifically for the Pile Driving, Foundation, Marine Contractor and Engineer throughout the world.

For 20 years, Pile Buck® Newspaper has been the leading source for information on Pile Driving, Foundation, Marine Construction and related news, equipment and material.

OUR ADVERTISING RATES ARE STILL SO LOW, IN MOST CASES, YOU CAN ADVERTISE IN PILE BUCK® NEWSPAPER ALL YEAR FOR WHAT IT COSTS TO RUN IN OTHER PUBLICATIONS ONE TIME.

How Do We Do It?

- 1) We offer no fancy media kit.
- 2) We publish in black and white. No color.
- 3) We publish a tabloid on bright white newsprint.
- 4) We offer no ad agency discounts.
- 5) We do all ad copy in house, own our own equipment, at no cost to you..the customer... **and most importantly...**
- 6) We don't have five girls with charming "southern accents" hounding you on a weekly basis to advertise in their magazine or newspaper.

CONSIDERING A 1/2 PG. OR FULL PG. AD IN PILE BUCK® NEWSPAPER?

For those of you who do not presently advertise in Pile Buck® Newspaper and are considering a 1/2 or full page ad, you should read the following...

THIS IS OUR ONE-TIME CHARGE "ADVANCE PAY" DISCOUNTED RATE SHEET.

At the time of this printing, every 1/2 and Full page advertiser in **Pile Buck® Newspaper** (except for one), takes advantage of our "Pre-Paid / Discounted" rates for 1/2 page and Full Page. This offer is extended only to 1/2 and full page ads, no smaller ad sizes.

- All rates are the total cost for insertion in One Full Year of **Pile Buck® Newspaper** (12 months).
- A Full Page Ad measures 10" wide x 13-1/2" high. Half page is 10" wide x 7" high.
- As always, we do all ad copy at no cost to you the advertiser.
- Ad copy may change at any time. Some advertisers have us maintain 2-6 different ads at all times, which we rotate every month. We encourage all yearly advertisers to take advantage of this.

***WE OFFER MAJOR DISCOUNTS FOR THOSE WHO CHOOSE TO RUN MORE THAN 1 PAGE.**

Number of pages	Total Cost For Year If Billed Every 2 Months at "Non-Yearly" Rate	Your Total Cost for our One Time "Prepaid" Discounted Yearly Rate	YEARLY SAVINGS!
q 1/2	\$7,800	\$5,200	\$2,600
q 1	\$13,200	\$7,800	\$5,400
q 2	\$26,400	\$10,500*	\$16,900*
q 3	\$39,600	\$12,500*	\$27,100*
q 4	\$52,800	\$14,000*	\$38,800*

This offer has been available for the past ten years and is only extended to 1/2 page and full page advertisers in **Pile Buck® Newspaper**. If you have any interest, please check the appropriate box, fill out your company information below, and **FAX THIS FORM** to our office. **Remember!! Our Annual "Prepaid / Discounted" rates are available at any time. "Your 12 consecutive months" can begin at any time during the year.**

SIMPLY FAX THIS PAGE TO: 772-231-8400

Company: _____ Contact: _____
 Phone: _____ Fax: _____



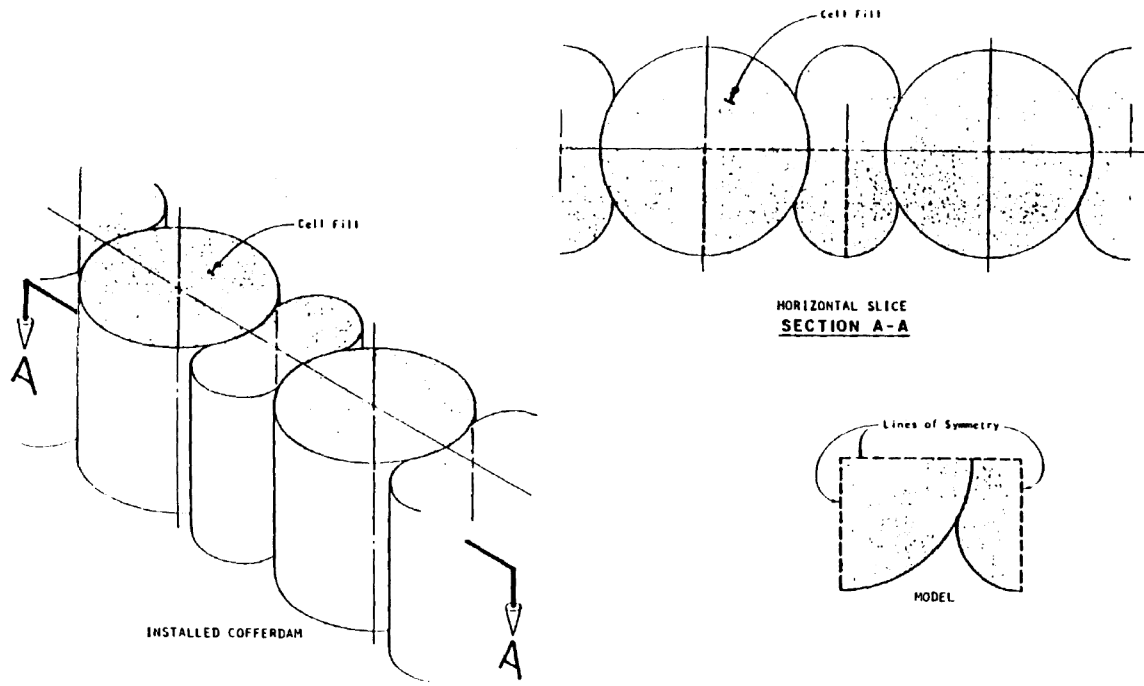


Figure 15-35: Schematic Drawing, Horizontal Slice Analysis

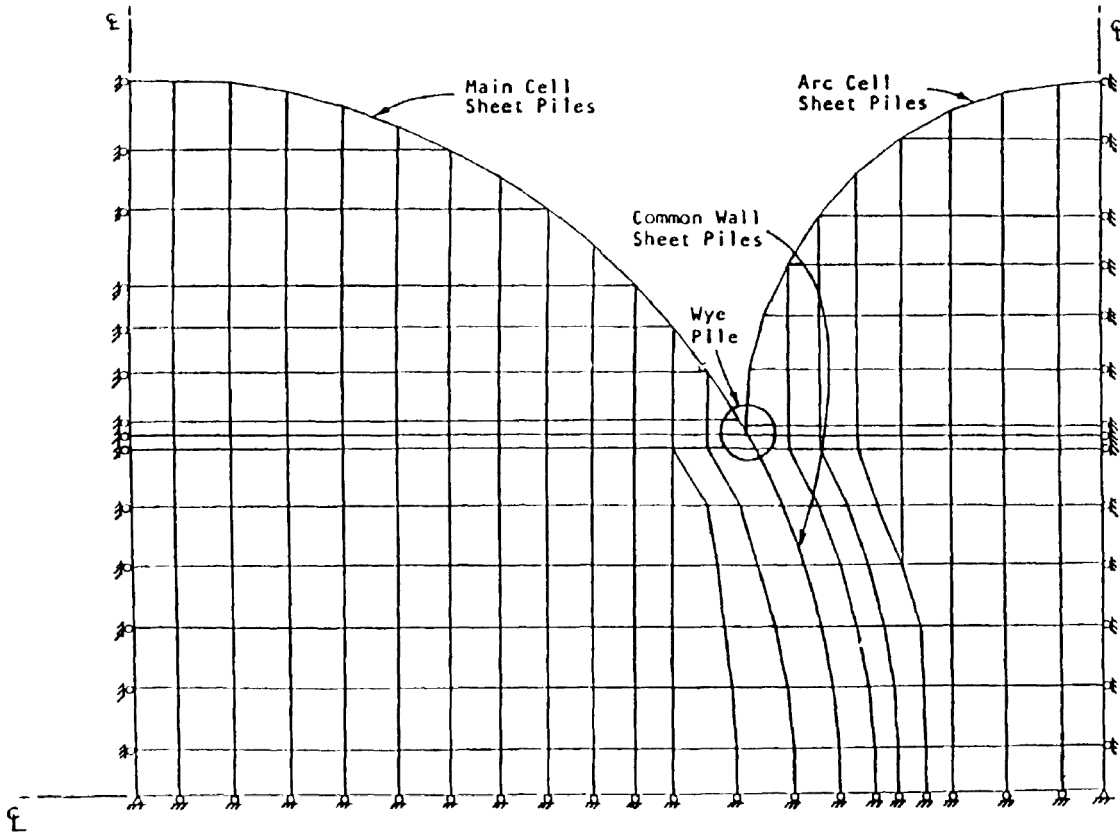


Figure 15-36: Finite Element Mesh for Horizontal Slice Analysis of Cell Filling

15.4.2.4. General Modelling Techniques

Best results have been achieved on the three models by assuming the cell acts as an orthotropic shell by reducing the stiffness of sheet piles in the radial and circular directions during cell filling and acts as an isotropic material for all future construction steps. This is accomplished by reducing the modulus of elasticity in these directions. It is important for the analysis technique to breakdown the analysis into a series of incremental construction steps to allow deflections, settlement, and stresses to uniformly increase in the cell and foundation. Simulation of the actual sequence of loading is important because the stress-strain response of soil is nonlinear and stress-path dependent.

15.4.3. Estimates of Cell Deformations

15.4.3.1. Cell Bulging during Filling

During filling, the cell walls deflect outward as the fill pressures increase. This deflection in the radial direction, resisted by the sheet pile structure and foundation, causes the cell to form an area of maximum deflection and maximum interlock tension in the lower one third of the height above dredge line. This process of radial deflection transforms the cellular structure from a loosely pinned set of sheets into a structure more closely resembling a rigid cylinder. Because the cell is not a rigid cylinder, the finite element model assumes that the sheet piles act orthotropically with less stiffness in the radial and circumferential directions than in the vertical. Three factors, other than stress-strain deflections, in the sheet piles support this assumption and contribute to higher deformations. First, interlocks are not perfect pins and gaps form in connections. The slack produced by gaps is taken up when pressure is applied to the inside of the cell by filling. Second, the interlocks provide a very small bearing area to transmit radial and circumferential forces from sheet pile to sheet pile. This allows for a small amount of rotation and local yielding in the interlocks. Third, due to the slack in the interlock it is possible for misalignment to occur during driving and, consequently, the cells have an irregular shape. The cells will tend to realign to a perfect cylindrical shape during filling. To account for these deformations, the assumption of the cell's acting as an orthotropic cylinder is made by reducing the modulus of elasticity, horizontally and not vertically. In the Shannon and Wilson studies at Lock and Dam 26 (Replacement), three different ratios of horizontal-to-vertical modulus were used in FEM solutions. These ratios were 1.0, 0.1, and 0.03. The E-ratio of 0.03 yielded results very close to actual field instrumentation. Vertical slice and axisymmetric models should be used for analysing deflections during cell filling.

15.4.3.2. Deflections Produced by Berm Placement

Deflections of the filled cell during berm placement are normally small. Analysis of deformations for this stage can only be done using the vertical slice model and should be

analysed using uniform stages of berm construction. Previous FEM solutions in Lock and Dam 26(R) showed slight deflections toward the outboard side of the cell of approximately 1 inch at the top. Soil stresses also increase on both sides of the sheet pile at the berm location and in the foundation soils under berm. Foundation pressure increases on the outside of the outboard side of the cofferdam indicate the filled cell is now acting as a unit and transferring inboard pressures through the circular cell to the outboard foundation.

15.4.3.3. Cofferdam Unwatering and Exterior Flood

Deflections and soil pressures resulting from cofferdam unwatering and exterior flood conditions are similar and, thus, are discussed together. Modelling of both conditions should be done by using a vertical slice model analysis and incremental load steps as the water level changes to allow non-linear soil deformations to take effect. Loads caused by seepage under the cofferdam should also be included using a flow net or uplift type analysis. From FEM modelling it can be seen that the cofferdam deforms by rotating and causing sliding forces toward the inboard side. These deformations increase the soil pressures in the cell fill and foundation directly under cell. Noted are higher soil pressures in the exterior foundation of the inboard side and in the berm due to passive soil resistance. Deflections of top of cell and high soil pressures in berm during exterior flooding indicate from previous analysis that the cell is moving as a unit with a tendency toward rotation for high exterior water levels. These model techniques were used in Lock and Dam 26(R) and Willow Island Cofferdam where, in addition to flood conditions, it was necessary to analyse an extra filling and unwatering of the cofferdam.

15.4.3.4. Construction Excavation

From previous analysis models, construction excavation has not been shown to cause significant cofferdam deformations except in the case of a cofferdam over a potential slip plane where excavation would reduce passive resistance to planar sliding. The potential slip plane should be modelled using frictional slip elements as shown by Clough and Hansen on the Willow Island Cofferdam study.

15.4.4. Structural Continuity between Cells and Arcs

Cell and arc interaction can be analysed by using a horizontal slice model and plane strain fill elements due to the perpendicular fill loading. A separate model analysis must be made at each elevation for which results are needed to obtain loads. Bar elements are used to represent sheet pile walls, with orthotropic material properties discussed earlier as bar properties. The Y-sheet pile connection between cell and arc should be modelled using exact piling widths as lengths of bar elements with pins at ends and at the Y-connection to more correctly simulate forces in the Y-connection. The simulation of construction steps for the horizontal model is

loaded using results of the axisymmetric model.

This is due to the two-dimensional model's inability to account for arching in the cell and support provided by foundation passive resistance. Also, because of the model's inability to account for cell arching, fill stresses for each construction step must be obtained from the axisymmetric analysis. Results for interlock tension and horizontal deflection that show close correlation to field instrumentation have come from this type of analysis. The horizontal model can only be used to analyse the symmetrical condition of cell filling.

15.4.5. Structure—Foundation Interaction

15.4.5.1. Foundation Stress at Cofferdam Base

Interaction between structure and foundation is modelled using a vertical slice analysis with a model cut wide enough and deep enough for foundation stresses to distribute evenly into foundation. The model should also include any planes of weakness in the foundation near the cofferdam. FEM analysis to date has shown foundation stresses are caused by two types of cofferdam action. First, due to filling of the cell, the sheet piles deflect outward and cause a build-up of passive resistance pressure in the foundation outside of the sheet piling. Vertical pressures in the foundation under the cell fill increase because of fill height above foundation. Second, after filling of the cell is completed, the cofferdam acts against horizontal forces as a monolithic cylinder resisting sliding by shear and passive pressures in the soil and overturning by the masses' resistance to tipping moment. The cell gains additional resistance to both sliding and overturning by the sheet pile's depth and, thus, interaction with the foundation.

15.4.5.2. Investigation of Foundation Problems

Investigation of foundation problems is one important advantage of FEM analysis. In cofferdam modelling, an element known as a planar frictional slip element can be used between elements to model a natural slippage plane between materials. These elements allow a build-up of shear stresses on the plane, and at an ultimate stress the two sides of the slip plane are allowed to slide in relation to each other.

This action allows the adjacent element nodes to separate at the plane under a constant frictional resistance. These elements also have properties that will allow the two sides of the slip plane to pull apart, transverse to the plane, when placed in tension. Possible causes of foundation problems such as cofferdam dewatering, exterior flood, and interior excavation are failure load cases that should be investigated.

15.4.6. Fill Interaction between Cells and Arc

Interaction of the main cell fill and arc cell fill has not currently been modelled due to cylindrical structure assumptions used in the vertical slice and axisymmetric models. In the horizontal slice model the fill was assumed to be placed simultaneously in the main cell and arc that does not model the true sequence of construction. More research is needed in

this area, and would be more applicable for modelling with a three-dimensional soil-structure FEM analysis.

15.4.7. Special Cofferdam Configurations

15.4.7.1. Cloverleaf Cells

Cloverleaf cofferdam cells at Willow Island were modelled in the Clough and Hansen study. The results of this analysis showed inconsistent patterns of deflection and indicated more research is needed. Part of the problem with modelling cloverleaf cells in two dimensions is accurately accessing the stiffness provided to the cell by centre cross-walls.

15.4.7.2. Diaphragm Cells

Past literature shows no attempts to analyse diaphragm cells or other cell configurations by the FEM analysis. Development of a three-dimensional soil-structure finite element program with all of the necessary capabilities will enable modellers to more accurately analyse forces present in any special configuration of cell.

15.5. Foundation Treatment

15.5.1. Problem Foundations and Treatment.

Foundation treatment is sometimes considered for foundations with insufficient bearing capacity or problem seepage conditions. Problem seepage conditions can be the result of excessive seepage quantities or high seepage forces.

The following foundation treatment methods can be used to improve a deficient foundation.

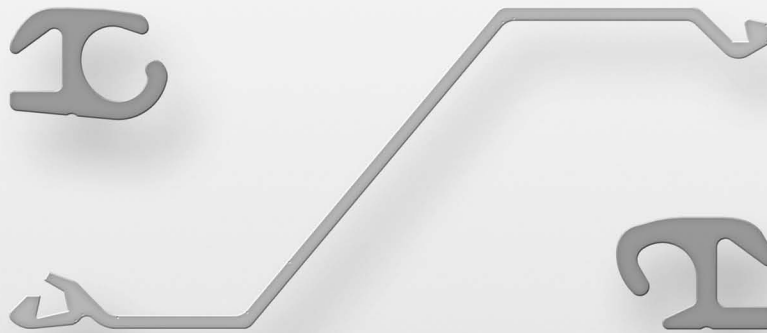
- (1) Removal of objectionable material. Removal may be before or after the piles are driven to form the cell.
- (2) In situ compaction. Several methods are available and include vibroflotation, compaction piles, surcharge loads, and dynamic surface loads.
- (3) Deep penetration of sheet piling. For design purposes, a trial penetration of two thirds of the cell height is usually considered when the cell is sited on a pervious foundation. An adjustment of this length should be based on a careful analysis of the seepage forces at the toe of the structure.
- (4) Berms and blankets. Impervious blankets may be located on the outside of the cells to reduce seepage quantities and pressures. Interior berms reduce the likelihood of boiling at the toe of the structure.
- (5) Consolidation. The strength of foundation material, especially fine-grained material, may be increased by consolidation. Surface preloading of the foundation and the use of sand drains are two of the methods used to accelerate consolidation of the foundation.

800.848.6249 www.fosterpiling.com

Z SHEET PILING

- Preferred Sheet Pile Shape
- High Strength to Weight Ratio
- Cost Effective Walls
- Wide Range of Connectors Available

 **Foster**
Piling
A Division of L.B. Foster Company



15.5.2. Grouting

15.5.2.1. Correctional Methods

As for all such structures, foundation treatment should be carefully considered for cellular cofferdams. In many cases, removal of the unfavourable foundation material may be impracticable, if not impossible, and other methods of treatment must be selected. Grouting is one such method that should be considered, especially in instances where the piling of a cellular cofferdam will be driven to rock. During the evaluation of the data developed during the subsurface investigations, special note should be made of any unfavourable foundation condition that would justify at least some consideration of grouting. Such unfavourable foundation conditions might be noted as a result of evidences of solution activity such as soluble rock or drill rods dropping during drilling, open joints or bedding planes, joints or bedding planes filled with easily erodible material, faults, loss of drill fluid circulation, or unusual ground-water conditions. Generally, the problems related to such unfavourable foundation conditions can be grouped into two categories: problems related to the strength of the foundation material and problems related to the permeability of the foundation material.

15.5.2.2. Problems Related to Strength

Among the problems related to strength that should be anticipated are:

- (1) Insufficient bearing capacity;
- (2) Insufficient resistance to sliding failure; and
- (3) General structural weaknesses due to under-ground caverns or solution channels, or due to voids that develop during or following construction.

Problem 3 is closely related to Problems 1 and 2 and should be considered jointly. In developing parameters for allowable bearing capacity, deficiencies noted in Problem 3 must be carefully considered. All too often, rock strength parameters are used in stability analyses that are based on rock sample strengths rather than mass rock strengths. The various discontinuities that reduce the foundation rock strengths may result in consequential reductions in the ultimate bearing capacity. As mentioned above, the bedrock may contain bedding plane cavities and solution channels that can extend to considerable depth (low crossbed shear strength). In recognizing the presence of such discontinuities, the possibility must also be recognized that an unfavourable combination of these discontinuities could exist under the cellular cofferdam, thus adversely affecting the sliding stability of the structure. The presence of these weak planes must be carefully considered when doing a sliding stability analysis.

15.5.2.3. Problems Related to Permeability

Among the problems related to permeability that should be

anticipated are: reduction in the strength of the foundation materials due to high seepage forces, high uplift forces at the base of the structure, and inability to economically maintain the coffered area in an unwatered state. In many cases, the piling of a cellular cofferdam will be driven to rock. The presumption should be that some seepage would occur not only at the piling/bedrock contact, but also through openings in the bedrock. This seepage may result in piping of materials through the bedrock openings below the cofferdam, greatly reducing the strength of the foundation. These openings along bedding planes can also result in high uplift pressures.

Quite often, the vertical permeability of the rock above the open bedding plane is only a small fraction of the permeability along the plane. If such a situation exists, it is possible that the high uplift pressures will jack the foundation. The size and continuity of solution channels acting as water passageways may have a serious economic impact on the dewatering of the work area within the cofferdam. Unfortunately, there is no way to accurately estimate the dewatering problems and costs that might result from such solution channels in the foundation.

15.5.2.4. Selection of Treatment

Treatment of the cofferdam foundation by grouting may be used to lessen, if not eliminate, defects in the foundation, resulting in a strengthened foundation with reduced seepage. Grouting should be selected as a method of foundation treatment only after a careful and thorough evaluation of all pertinent factors. Primary factors that must be necessarily considered before selection of grouting as the method of treatment are the engineering design requirements, the subsurface conditions, and the economic aspects.

Although cost is just one factor to consider, in many circumstances, cost may be the controlling factor. The cost of grouting must be weighed against such other costs as that of pumping, delays, claims, and/or failure. It may be that there is no benefit in reducing minor leakage by costly grouting.

(1) General. Information obtained and evaluated during the subsurface investigations for design of the structure should be adequate to plan the grouting program. If the grouting program is properly designed and conducted, it becomes an integral part of the ongoing subsurface investigations. A comprehensive program must necessarily take into account the type of structure, the purpose of the structure, and the intent of the grout program. As an example, foundation grouting for a cellular cofferdam is not intended to be permanent nor 100 percent effective. The program should be designed to provide the desired results as economically as possible. The program should be flexible enough to be revised during construction and performed only where there is a known need.

(2) To Strengthen. Grouting has been used on occasion to strengthen the foundation by area or consolidation grouting

under the cells to increase the load-bearing capacity of the rock. This may be a viable option if the grouting is intended to increase the already acceptable factor of safety. However, if it appears that the factor of safety falls appreciably below the allowable factor of safety, total reliance should not be placed on grouting. The effectiveness of such grouting is impossible to predict or to evaluate. Certainly complete grouting is impossible because of the irregularity of the openings as well as the amount and character of any filling material.

(3) To Reduce Seepage. The principal purpose of grouting for cellular cofferdams has been in conjunction with seepage control and drainage. Curtain grouting is one method used to reduce uplift pressures and leakage under the cofferdam and thus reduce total dewatering costs. Although a single line curtain will suffice in most cases, the rock conditions may be such that it will be necessary to install a multiline curtain or a curtain with multiline segments. The exact location of the grout curtain will be influenced by a number of factors including the type of structure, the foundation conditions peculiar to the site, and the time the curtain is installed. For most cellular cofferdams, the grout curtain is located on or near the axis of the structure. However, if the curtain is not installed until the cofferdam has been constructed, it may be impracticable to drill holes through the cell fill. In this case the grout line should be moved off and just outside the cells. When installing the grout curtain, the flow of grout must be carefully controlled to prevent the grout from flowing too far, resulting in grout waste. To prevent such waste, it may be necessary to limit the quantity of grout injected, or to add a "stopper" line grouted at low pressure. The orientation and inclination of the holes should be adjusted to intercept the principal water passageways. Occasionally, however, conditions may render this impracticable and it may be that vertical holes on closer centres are more feasible.

(4) Development of Program. Following an evaluation of the foundation conditions and the selection of grouting as a method of foundation treatment, the evaluations, conclusions, and recommendations should be included in the report of the subsurface investigations. Using data developed from the investigations, the pertinent reference manuals, and especially past experience, plans and specifications should be prepared for the grouting program. After having reviewed all available and pertinent data and having decided on the particular grouting program to be implemented, a number of basic factors must be decided: the area selected for grouting, the selection of the grout, the selection of the type of grouting, and the need for special instructions, provisions, or restrictions.

15.5.2.5. Selection of Location

The area indicated for grouting should be a zone large enough to include any anticipated treatment. This is especial-

ly important in installing a grout curtain for a cellular cofferdam. This should be coincidental with provisions to provide for grouting anytime within the contract period without additional mobilization and demobilization costs. The drawings rightfully should show a grout curtain to be installed beneath the cofferdam along an approximate alignment and to definite limits. However, because of the numerous unknowns inherent in a grouting program, the plans and specifications should provide that the area of grouting extend some distance beyond the limits shown.

15.5.2.6. Selection of Grout

The selection of the grout should be made only after a careful evaluation of the foundation conditions or materials being tested. The type of grout used in reducing or stopping high velocity flows would be different from that used for slow seeps, or the grout used to fill large cavities might be different from that used to fill small voids. A factor to be considered in sealing high velocity flow would be the time of set; the large quantities and costs would necessarily be considered in filling large cavities; while in filling small voids, the size of the void and the particle size of the grout are necessary considerations.

15.5.2.7. Selection of Type of Grouting

Grouting may be done before, during, and/or after installation of the cofferdam or other construction activities in any given area. In the installation of a grout curtain, all or portions of the curtain may be constructed from the original ground surface and/or from floating plant in the river. If done from floating plant, in general, stop-grouting methods should be used because it is not practical to stage drill and grout from floating plant. Drilling and grouting from floating plant by the stop-grouting method should be considerably less costly than stage grouting, the holes being drilled and grouted to the bottom of the curtain in one set-up.

15.5.2.8. Special Instructions

In drilling from floating plant, it should be expressly understood that the depth of water penetrated would not be credited to the drilling footage for payment. If drilling and grouting are performed from the cofferdam, only drilling that is required below the original ground surface should be paid for. To effectively grout water-bearing openings associated with cavernous rock, the following general procedure should be followed:

- The grout holes should be drilled through the overburden and the casing should be seated a minimum of 1 foot in rock;
- The hole should be drilled at least 5 feet into rock, if the top of rock is lower than anticipated;
- If stop-grouting methods are used, grouting of the rock should be performed through a packer set just below the bottom of the casing;
- Should a special feature be encountered in the hole, the

packer setting may be varied to isolate and treat this feature. Grouting of the overburden, if necessary, can then be done immediately following the rock grouting. The specifications should provide that if, as the work progresses, supplemental grouting is required at any area within specified limits at any time, such additional grouting will be at the established contract unit prices for the items of work involved. Although pressure testing should be provided for in the specifications, the condition of the foundation may be such that all grout holes should be grouted, in which case, pressure testing would not be necessary. If possible, the initial dewatering of the cofferdam should be performed at the lowest possible river stage or other measures should be taken to ensure a stable cofferdam capable of being unwatered until the foundation and the adequacy of the foundation treatment can be checked.

15.6. Dewatering and Pressure Relief

15.6.1. Purpose of Design

A cellular cofferdam is a temporary structure constructed in a river, lake, etc., to exclude water from an enclosed area. This allows the interior of the cofferdam to be dewatered and the permanent structure to be constructed in the dry. Usually cofferdams must withstand large differential heads of water; therefore, it is imperative that surface water and seepage be controlled, artesian pressure is relieved, and emergency facilities to prevent overtopping be made a part of the cofferdam to ensure a stable and competent structure.

15.6.2. Dewatering and Pressure Relief

Dewatering of a cofferdam can be accomplished in two phases. The first phase is initial dewatering (or pump down) to remove water from the interior of the cofferdam. The second phase is foundation dewatering to lower (or draw down) the ground water, to ensure a dry and stable construction area. The size and type of the dewatering system depends on the size of the cofferdammed area to be dewatered, total quantity of water to be pumped, geological conditions, and soil characteristics. A properly designed, installed, and operated dewatering and pressure relief system can greatly facilitate construction in the cofferdammed area by: intercepting seepage that would otherwise emerge from the slopes or bottom of the excavation; increasing the stability of the slopes and preventing the loss of material from the slopes or bottom of the excavation; reducing lateral loads on cofferdams; and improving the excavation and backfill characteristics of sandy soils.

15.6.2.1. Initial Dewatering

The maximum rate of dewatering is controlled by the stabili-

ty of the inside land bank, by cell drainage, and by cell interlock stresses. Generally, the first 15 feet are dewatered without restrictions so that differential pressure can be developed quickly to close the interlocks tightly. Thereafter, the rate for dewatering is 5 feet per day, which is normal for large cofferdams¹⁹⁹. Drainage of the cells and connecting arcs must closely follow the dewatering of the cofferdammed area, and should cell drainage lag, the dewatering rate should be slowed down. For "clean" cell fill, weep holes should be burned in the inboard sheet pile of all cell and connecting arcs during dewatering. Current practice is to burn 1-inch-diameter weep holes at about 5- to 6-1/2-foot centres vertically on every third to sixth sheet pile down to the top of the berm or to the inside ground surface if no berm is used. Throughout dewatering operations, the weep holes should be systematically rodded to maintain cell drainage.

For marginal or "dirty" cell fill, weep holes by themselves may be insufficient to drain the cells; therefore, well points or deep wells should be installed in the cells to ensure adequate drainage and to increase cell rigidity. Occasionally, cell drainage is impeded by tremendous inflows through the interlocks on the outboard side of the cofferdam. Dropping clay, slag, cinders, or coal dust around the outside of the cofferdam to plug openings in the interlocks will rectify this condition²⁰⁰. The need to keep the cells and connecting arcs free-draining cannot be overstated. As the cofferdammed area is dewatered the sheet pile should be examined for damage. If split sheets or separated interlocks are revealed, dewatering must be stopped, according to Patterson²⁰¹. Should the damage extend for some distance, it may be necessary to reflood the cofferdam, excavate the fill from the questionable cell, and replace the damaged piling. If the damage is not extensive, straps should be welded across the split a short distance above the top of the split. Strapping should be carried closely along as the dewatering is continued. Dewatering of the cofferdammed area dictates that maximum pumping capacity be provided.

Plenty of reserve pumping capacity should also be available in case of mechanical breakdowns. The pumps should be placed as near the water level as possible because the pumps will push water more efficiently than they will pull it.

15.6.2.2. Foundation Dewatering

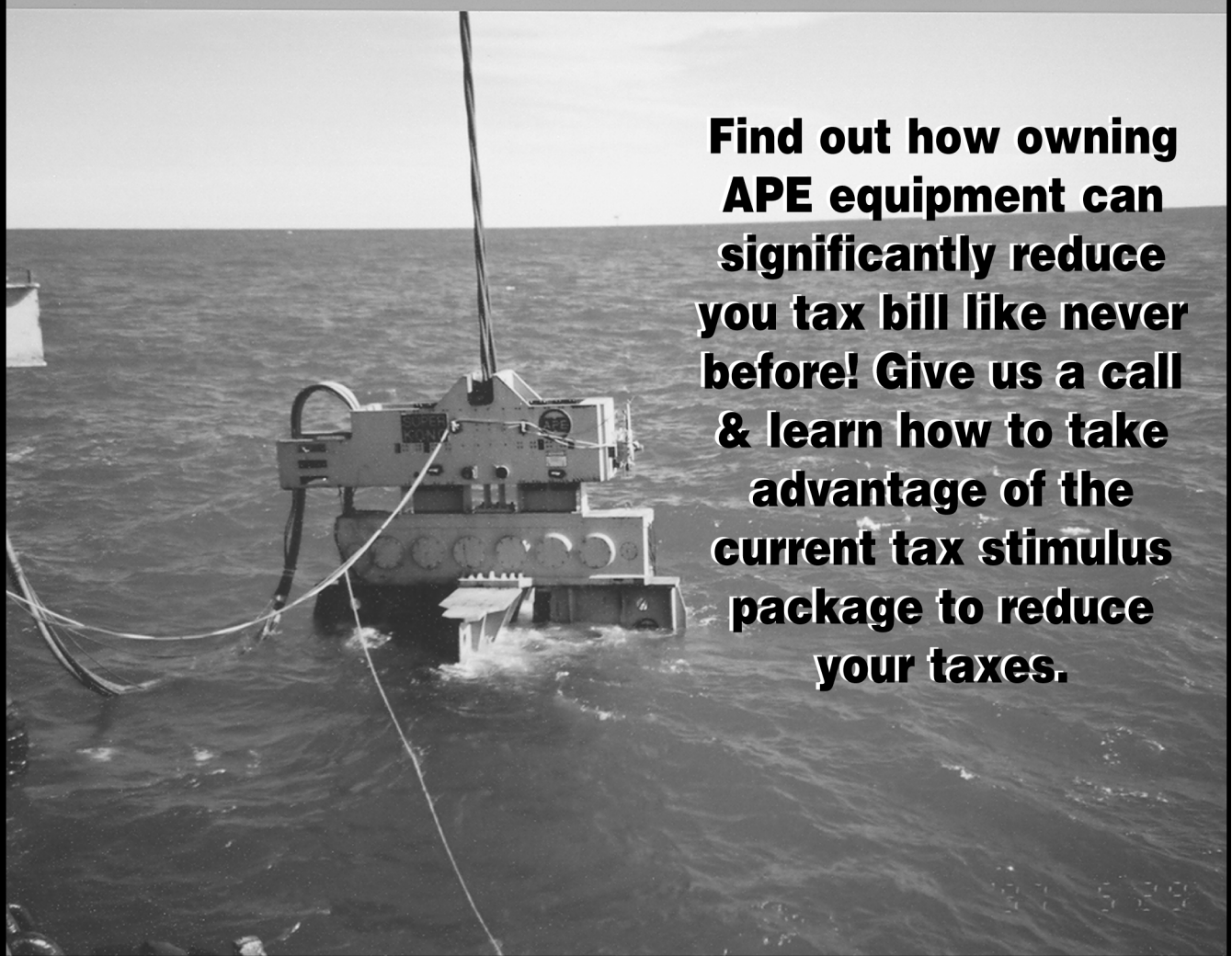
After completion of the initial dewatering phase, the ground water in the foundation must be controlled throughout construction of the permanent structure. The ground water must be drawn down so that a dry and stable construction area is provided. The primary sources of ground water are seepage through and underneath the cells and surface water that percolates into the ground before it can be collect-

¹⁹⁹Ovesen, N. K. 1962. Cellular Cofferdams Calculation Method and Model Tests, Bulletin 14, Danish Geotechnical Institute, Copenhagen; Swatek, E. P., Jr. 1967 (Aug). "Cellular Cofferdam Design and Practice," Journal, Waterways and Harbors Division, American Society of Civil Engineers, New York, New York, WW 3.

²⁰⁰How Contractors Brace Steel Sheet-Pile Cofferdams," Construction Methods and Equipment, McGraw Hill, New York, New York (1962).

²⁰¹Patterson, John H. 1970. "Installation Techniques for Cellular Structures," Design and Installation of Pile Foundations and Cellular Structures, Envo Publishing Co., Inc., Lehigh Valley, Pennsylvania.

Are taxes sending your cash flow under water? Don't just get mad, GO APE!



Find out how owning APE equipment can significantly reduce your tax bill like never before! Give us a call & learn how to take advantage of the current tax stimulus package to reduce your taxes.

When a pile driver talks... we listen™. Please call or write:



APE Corporate Offices
7032 South 196th
Kent, Washington 98032
800-248-8498 or
253-872-0141
Fax: 253-872-8710

APE CANADA
1965 Ramey Road
Port Colburn, ON
LZG 7MG
905-328-0850
Fax: 905-834-8486

APE Mid-Atlantic Regional Ofc.
500 Newton Rd. Suite 200
Virginia Beach, VA 23462
866-399-7500
Fax: 757-518-9741
Cell: 757-373-9328

APE Northeast Regional Ofc.
Route 15 North & Taylor Rd.
Wharton, NJ 07885
973-989-1909
Fax: 973-989-1923
888-217-7524

APE Southeast Regional Ofc.
1023 Snively Avenue
Winter Haven, FL 33880
863-324-0378
Fax: 863-318-9409

APE S. Central Regional Ofc.
11128 FM Hwy. 1488
Conroe, TX 77384
936-271-1044
Fax: 936-271-1046
800-596-2877

APE Western Regional Office
160 River Road
Rio Vista, CA 94571
707-374-3266
Fax: 707-374-3270
888-245-4401

Alessi Equipment, Inc.
35 Rosslyn Place
Mt. Vernon, NY 10550
914-699-6300
Fax: 914-699-5300

Imeco-Austria
431-368-2513
Fax: 431-369-8104

ed and pumped out. The most commonly used dewatering method for soils that can be drained by gravity flow is the conventional well point system. It is limited to about 15 feet of drawdown per stage; however, multiple stages may be used. This system is most practical for large excavations in the cofferdam basin where the depth of excavation does not exceed 30 to 40 feet. For large excavations deeper than 40 feet or where artesian pressure in a deep aquifer must be relieved, deep wells with turbine or submersible pumps should be used. Deep wells can be installed around the periphery of the excavation, thus leaving the construction area free of dewatering equipment.

15.6.2.3. Pressure Relief

Artesian pressures from underlying aquifers that endanger the stability of the cofferdam and berms or excavation in the interior of the cofferdam must be relieved. Depending on the piezometric level, pressure reduction in the aquifer may be required before dewatering of the cofferdam²⁰². Complete relief of artesian pressures to a level below the bottom of the excavation is not always required depending on the thickness, uniformity, and permeability of the materials. Artesian pressure can be relieved by deep wells or well points. The penetration of the wells or well points should be no more than that required to achieve the drawdown required to minimize artesian flows. Because of the critical nature of pressure relief and the rapid rate at which an aquifer would recover if pumping were interrupted, backup systems should be provided. The system should be designed for a capacity approximately 50 percent greater than that expected to be required.

15.6.3. Surface Water Control

A well-designed dewatering and pressure relief system must include provisions for collecting and pumping surface water so that dewatering pumps cannot be flooded. Surface water, which includes rainwater, inflow through the interlocks, drainage through the weep holes, and seepage that emerges from the surfaces of berm and excavation slopes, may be controlled with ditches, French drains, or sumps. The area enclosed by the cofferdam should be sloped to drain toward one or more centrally located sumps where the surface water is collected and pumped out. In addition, ditches or French drains should ring the perimeter of the cofferdammed area to divert inflow through the interlocks and drainage through the weep holes to the sumps. The number and size of the ditches, French drains, and sumps depend on the size of the cofferdammed area, characteristic of the soil, rainfall frequency and intensity, and the estimated inflow and

drainage through the interlocks and weep holes, respectively. The estimated inflow through the interlock should be assumed to equal at least 0.025 gallons per minute per square foot of wall per foot of net head across the wall for installations in moderately to highly permeable soil²⁰³.

15.6.4. Emergency Flooding

Large cellular cofferdams in areas where they may be overtopped should be constructed with sluiceways, floodgates, or both to control floodwaters²⁰⁴. Flooding of the interior of the cofferdam by allowing uncontrolled floodwaters to overtop the cells may cause serious damage to the cofferdam by washing material from the cells or by eroding the berm, not to mention the damage to the permanent structure under construction.

Frequently the cells are capped with 6 to 12 inches of lean concrete to prevent the washing out and saturation of cell fill. Enough floodgates should be provided so that, the cofferdammed area can be flooded at least two-thirds full within 4 to 6 hours, or before any cell is overtopped, if the cofferdam is in imminent danger of being overtopped²⁰⁵. The size and number of floodgates depend on the size of the cofferdammed area to be flooded and the anticipated rate of rise of the river.

a. Construction of a floodgate is best done by using a connecting arc area between two circular cells at the downstream end of the cofferdam. The connecting arc sheet piles should be burned off near normal pool, and the area should be capped with 18 to 24 inches of reinforced concrete. A recess should be formed in the concrete cap to support the bottom of a timber or steel bulkhead. The area adjacent to the connecting arc should be sloped and protected with stone to prevent scouring as floodwaters enter the interior of the cofferdam.

b. Flood-stage predictions must be carefully monitored as a basis for determining when equipment should be evacuated from the cofferdammed area, and the floodgates should be opened to prevent overtopping. If serious inflows through the interlocks occur due to the flood stage, it may become necessary to flood the cofferdammed area to equalize pressures and prevent serious damage to the cofferdam, even though predictions do not anticipate that the cofferdam will be overtopped by floodwaters. Floodgates and sluiceways are also used for flooding the interior of the cofferdam upon completion of the construction and just prior to the removal of the cofferdam.

²⁰²Slope Indicator Company. 1984. Brochure, Seattle, Washington.

²⁰³United States Steel Corporation. 1975. "Cellular Cofferdams," US Steel Sheet Piling Design Manual, Pittsburgh, Pennsylvania.

²⁰⁴TVA Division of Engineering and Construction. 1966 (Nov). "Steel Sheet Piling Cellular Cofferdams on Rock," Tennessee Valley Authority, Office of Chief of Engineers, Technical Monograph No. 75, Vol 1, Knoxville, Tennessee.

²⁰⁵Swatek, E. P., Jr. 1970. "Summary - Cellular Structure Design and Installation," Design and Installation of Pile Foundations and Cellular Structures," Envo Publishing Co., Inc., Lehigh Valley, Pennsylvania.

15.7. Instrumentation of Cellular Cofferdams

15.7.1. Systematic Monitoring

Planning the monitoring program should be approached systematically. Ideally, the planning process begins with a definition of objectives and ends with actions dictated by an evaluation of the data. A hasty and unplanned approach is likely to omit consideration of many pertinent factors. The planning process should include appropriate steps as outlined below. Omission or inadequate consideration of these key-planning steps will guarantee a high probability of failure and vice versa.

15.7.2. Proper Planning

A checklist for planning will include the following steps ²⁰⁶ (item 28):

a. Definition of Project Conditions. This will entail an understanding of the type, function, and duration of the structures, subsurface stratigraphy and engineering properties, ground-water conditions, status of nearby structures or other facilities, environmental conditions, construction methods, scheduling, and funding.

b. Purpose of Instrumentation. Details are discussed below.

c. Selecting Variables to Monitor. The variables selected for monitoring will depend on the project conditions and the purpose of the instrumentation. These may include water levels in the fill and stabilizing berm, pore pressure in the foundation, earth pressure in the soil mass and at the soil-structure contact, surface and subsurface horizontal deformation within the foundation, the fill, and along a sheet pile member, strain in the sheet pile, and load in anchors and tiebacks.

d. Predicting Behaviour. This step helps to establish the range and accuracy or precision of the instruments. It also helps to determine where instruments should be located, Prediction of behaviour also establishes a numerical value of deviation from anticipated performance at which some action must be taken to prevent failure, protect property and human life, or alter construction procedures.

e. Responsibility. It must be decided who will be responsible for procurement, calibration, installation, monitoring, and maintenance of the instrumentation system. The data must be promptly processed and evaluated by responsible individuals. It must also be decided who will react to the data and who has overall responsibility.

f. Selection of Instruments. The most desirable feature to be considered in selecting an instrument is reliability. It should be the simplest instrument that will get the job done, be durable to withstand the ambient environment, and not be

very sensitive to climatic and other extraneous conditions. Other factors to be considered are cost, skills required to process the data, interference to construction, instrument calibration, special access while monitoring, accuracy, and the range of predicted responses compared with the range of the instrument.

g. Instrument Layout. A few selected critical zones should be instrumented fully; whereas, other locations may be equipped with fewer and less expensive instruments. The layout should facilitate obtaining appropriate information during each critical stage and be flexible enough such that changes can be made should there be malfunctions and as new information becomes available.

h. Preparation of Plans and Specifications. A general plan and appropriate sections and details should be developed which clearly show the locations, quantity, and installation details of each instrument. The specifications should specify who has responsibility for each activity (e.g., procurement, installation, calibration, maintenance, data collection, and evaluation) and give special instructions pertaining to each. The method of payment should be spelled out, overall responsibility designated, and authority to make changes specified. These two documents must be consistent and complete to avoid ambiguity and subsequent claims by the contractor.

i. Processing and Evaluating Data. This step includes preparing data sheets; establishing monitoring schedules; setting requirements for collecting and transmitting data; data reduction, analysis, and interpretation; and data evaluation.

j. Other Considerations. Determining factors that may influence measured data, planning to ensure reading correctness, listing specific purpose for each instrument, and acquainting new personnel with the system must be studied.

15.7.3. Purpose of Instrumentation

a. The purpose of the monitoring program must be known, understood, and accepted by all pertinent parties to ensure success. Much time, energy, and money can be saved if the purpose is derived early in the process. Understanding the purpose helps to direct available resources toward specific activities, and extraneous efforts are essentially eliminated.

b. The purpose of the monitoring program may be singular or pluralistic, including one or more of the following:

- (1) Verifying design assumptions and methods.
- (2) Verifying contractor's compliance with the specifications.

²⁰⁶Dismuke, T. D. 1975. "Cellular Structures and Braced Excavations," Foundation Engineering Handbook, Van Nostrand Reinhold, Co., New York, New York.

- (3) Verifying long-term satisfactory performance.
- (4) Safety.
- (5) Legal reasons.
- (6) Advancing the state of the art.
- (7) Verifying adequacy of a new construction technique.
- (8) Controlling the rate of progress of construction.
- (9) Accessing impact on environmental conditions.

c. The purpose will be influenced significantly by such project conditions as the type, function, and duration of the structure, the subsurface conditions, the nature and extent of the ground-water conditions, the proposed construction methods and procedures, environmental conditions, confidence in the design approach, potentials for litigation, etc. Most of this information is developed in the design stages, with new data and changes provided as the project progresses. The designer of the monitoring program should assume the responsibility of acquiring, understanding, and keeping abreast of all factors that may impact upon the monitoring program.

15.7.4. Types of Instruments

The kinds of instruments selected will depend on the purpose, project conditions, and the variables that will be monitored.

Each variable monitored will require a specific kind of instrument, e.g., pore pressure will be monitored with some type of piezometer. A variety of instruments varying in the degree of sophistication are available from both U.S. and non-U.S. manufacturers and suppliers. The following is a brief description of the more common instruments used in a program to monitor steel sheet pile structures.

15.7.4.1. Observation Wells

The observation well consists of a riser pipe connected to a perforated or porous tip at the lower end and is installed in a borehole to some specified depth or attached to the sheet pile before driving. The annular space of the borehole is backfilled with sand or fine gravel and sealed at the ground surface with grout or other suitable impervious material to prevent entrance of surface water. Observation wells are mainly used to measure unconfined ground-water levels and are monitored directly by a probe or tape. If observation wells penetrate more than one aquifer or penetrate a perched water table and an underlying aquifer, the resulting water levels are average ground-water levels and are generally not very meaningful. This is a decisive disadvantage of observation wells, but if the subsurface conditions and the nature of the ground-water

regime are well defined, observation wells can be installed to provide very meaningful data. Observation wells may be installed to monitor ground-water levels in the cell fill, back-fill materials, and stabilizing berms. Installation can be made during sheet pile driving by attaching the casing and slotted or perforated tip (an inexpensive well point can be used) to the sheet pile. Provisions should be made to protect the tip and casing during driving if damage is likely to occur.

15.7.4.2. Piezometers

The term piezometer is used to denote an instrument for monitoring pore pressures in a sealed-off zone of a borehole or fill. Piezometers can be classified into five types, depending on the principle used to activate the device and transmit the data to the point of observation. The five types of piezometers include the open standpipe piezometer, the closed hydraulic piezometer, the diaphragm piezometer, the vibrating wire strain gage piezometer, and the semiconductor strain gage piezometer. A variety of each type of piezometer is available from U.S. and non-U.S. manufacturers and suppliers. Piezometers are used to monitor pore pressures in the cell fill and foundation, in the stabilizing berms, and in the back-fill material. The type of piezometer selected should be based on such things as reliability, ruggedness, suitability, simplicity, cost, interference to construction, etc.

The open standpipe piezometer has the advantage of simplicity and its use is widespread. In those cases where minimum time lag is a significant factor and when high artesian pressures must be monitored, a pneumatic or a vibrating wire strain-type gage piezometer would be more suitable. Installation can be made during pile driving by securely attaching the piezometer to the sheet pile and protecting the tip and riser pipe or tubes from damage. Installation after fill placement is complete can be done by any appropriate conventional method.

15.7.4.3. Inclometers

Inclometers can be used to monitor horizontal deformation within the cell fill, along the length of a sheet pile section, in the cell foundation, and within the stabilizing berm. The inclinometer system consists of a pipe installed in a vertical borehole or securely attached to the surface of a sheet pile in the cell. Normally, the lower end of the casing is anchored in rock and serves as a reference point. Casing attached to sheet pile is normally not anchored in rock. The top of the casing is referenced to monuments outside the construction area. A sensor, which measures the inclination of the casing at depths determined by the observer, is used to monitor the full length of the casing. The sensor is connected to a graduated electrical cable that is used to lower and raise the sensor in the casing. The upper end of the cable is attached to a readout device that records the inclination of the casing from the vertical. Tilt readings and depth measurements are compared with initial data to determine move-

ADVERTISING RATES

Reach **PILEDIVING**
FOUNDATION, MARINE CONSTRUCTION AND RELATED
CONTRACTORS, ENGINEERS AND MORE!

THE FOLLOWING RATES ARE THE TOTAL PRICE FOR INSERTION IN 2 CONSECUTIVE MONTHS.

DISPLAY ADVERTISEMENTS: (Ad appears in 2 consecutive months)

Size W" x H"	Cost Rate(\$)	Size W" x H"	Cost Rate(\$)	Size W" x H"	Cost Rate(\$)
2-1/2" x 2"	190	7-1/2" x 5"	890	Full Pg. (10" x 14")	2,200
2-1/2" x 3"	260	5" x 8"	985	Double Pg.	3,400
5" x 2"	360	5" x 9"	1,100	Front Pg.*	1,800
5" x 3"	450	5" x 10"	1,200	Inside Front	2,300
5" x 4"	540	1/2 Page	1,300	Inside Back	2,275
5" x 5"	630	(10" x 7") or (5" x 13-3/4")		Page 3	2,300
5" x 6"	750	7-1/2" x 10"	1,400	Center Spread	3,600
1/4 Pg. (5" x 7")	850	10" x 10"	1,700	Back Page	2,500

*Available for 1 issue only. Ad will run for 2 issues, but will appear elsewhere for the additional issue.

DISPLAY ADVERTISEMENTS: (Yearly Rates - Billed every 2 months)

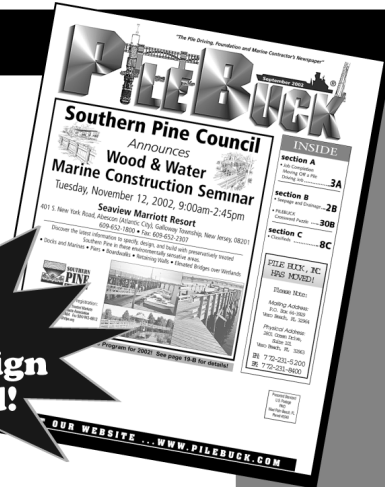
The following rates are for our customers who run in Pile Buck® all year. They receive 6 bills throughout the year, one every 2 months. Ad copy may change at anytime at no additional cost to the advertiser.

Size W" x H"	Cost Rate(\$)	Size W" x H"	Cost Rate(\$)	Size W" x H"	Cost Rate(\$)
2-1/2" x 2"	175	7-1/2" x 5"	700	Full Pg. (10" x 14")	1,600
2-1/2" x 3"	220	5" x 8"	800	Double Pg.	2,400
5" x 2"	275	5" x 9"	900	Front Pg.* (1 issue only)	
5" x 3"	350	5" x 10"	1,000	Inside Front	1,700
5" x 4"	410	1/2 Page	1,100	Inside Back	1,700
5" x 5"	500	(10" x 7") or (5" x 13-3/4")		Page 3	1,700
5" x 6"	580	7-1/2" x 10"	1,200	Center Spread	2,500
1/4 Pg. (5" x 7")	650	10" x 10"	1,300	Back Page	1,800

MAIL, FAX OR E-MAIL ALL ADVERTISEMENTS TO:

REGULAR MAIL:
 Pile Buck, Inc.,
 Advertising Dept.
 P.O. Box 64-3929
 Vero Beach, FL USA 32964

PH: (772) 231-5200 Fax: (772) 231-8400
 E-Mail: pilebuck@pilebuck.com • Website: pilebuck.com



PRESS DATES

ISSUE	ISSUE DATE	COPY DEADLINE
JANUARY	1-1	
FEBRUARY	2-1	10 DAYS
MARCH	3-1	PRIOR TO
APRIL	4-1	ACTUAL
MAY	5-1	ISSUE DATE.
JUNE	6-1	
JULY	7-1	CAMERA READY
AUGUST	8-1	ADS ACCEPTED
SEPTEMBER	9-1	5 DAYS PRIOR
OCTOBER	10-1	TO ISSUE DATE.
NOVEMBER	11-1	
DECEMBER	12-1	

MISC. INFORMATION:

Number of Issues per Year: 12 (published monthly)
Rates: All rates are the **total price for insertion in two consecutive issues** (one 2-month running). There is no discount for a one month running.
Display ads: The preparation and typesetting of your display ad is included in the cost of the ad. Any artwork, photograph, logo, etc. to be included in the ad must be supplied to Pile Buck®.
Camera Ready Discounts and Agency Commissions: Not available
Terms: Please enclose payment with initial order. **Credit may be extended only after a proven payment record has been established.**
Credit Cards Accepted: Visa, Mastercard and American Express

DIGITAL REQUIREMENTS

AD FILE TYPES

For the highest quality it is best that files be submitted in their true form - if a file is created in QuarkXpress it should be submitted as a QuarkXpress 5.0 OR LESS file and not be converted to another file type. With each conversion, the file loses quality. All of the final layout is done in QuarkXpress and we are Macintosh-based.

- Mechanical Specifications:** Printing - web press • Line screen - 85
 • Columns - 4 • Column width - 2-3/8"
 • Live matter area - 10" wide x 13-3/4" high.

Remember the following . . .

FOR QUARK USERS:

All art must be collected with the file - along with the fonts.

WE DO NOT ACCEPT ADS CREATED IN PAGEMAKER or WORD

FOR FREEHAND OR ILLUSTRATOR USERS

EPS images - make sure that all your fonts are made to paths - otherwise - please include the fonts as well.

FOR PHOTOSHOP USERS

Ads should be created to size and should be no less than 288 dpi.

EPS and TIFF files ONLY are acceptable.

IMAGES - SCANNED

For optimum quality - all scans should be no less than 288 dpi.

Save all art as Grayscale or bitmap (for line art) at 800 dpi.

Files below this dpi can be used but the quality of the pictures will be compromised. Once a file has been submitted it, it is difficult to manipulate scanned images, so if you have any questions before scanning your images please feel free to call.

SUBMISSION:

Files may be submitted on Zip 100, CD Rom, or stuffed and emailed to: pilebuck@pilebuck.com .

PDF FILES:

If you are emailing a PDF file of an ad, make sure all the dpi's and contrast are done correctly before distilling the ad. Pile Buck will NOT be responsible for any ads that didn't come out correctly after printing process. A PDF file cannot be manipulated on our end. Try not to use .eps files within the document, they have been known to print out as gray boxes.

Mail: Pile Buck® Inc., PO Box 64-3929, Vero Beach, FL, USA 32964
 Phone: 772-231-5200 • Fax: 772-231-8400 • E-mail: pilebuck@pilebuck.com
 Website: www.pilebuck.com

ments that have occurred. Plastic, aluminium, and steel casing of various sizes and shapes have been successfully used with sheet pile cellular structures. Circular casing with guide grooves and square casing are available from US manufacturers. Casing within the cell fill and in the stabilizing berm are installed in boreholes.

Casing connected to sheet pile sections must be attached so that the casing remains undamaged and securely fastened to the sheet pile after the pile has been completely driven to the design depth. In-place inclinometers may be installed to provide continuous or automatic monitoring with alarm capability. In-place inclinometers can be monitored manually or automatically. The manual system consists of one or more sensors, a readout station, and a portable indicator. The automatic system consists of one or more sensors, a junction box, power supply, and data logger. For safety, the alarm option automatically generates an alarm when movement of one of the sensors exceeds a preset threshold.

15.7.4.4. Earth Pressure Measuring Devices

Earth pressure measuring devices fall into two categories. One is designed to measure the total stress at a point in an earth mass and the other is designed to measure the total stress or contact stress against the face of a structural element. Devices in the latter category are relatively accurate and reliable, provided the device is designed to behave similarly to the structure. In addition, the earth pressures on a structure may be reasonably uniform for the structure as a whole, but are usually nonuniform over an area the size of a pressure cell. This condition results in a wide scatter of data that is difficult to interpret.

Earth pressure measuring devices designed to measure stress at a point in a soil mass are not considered as accurate and as reliable as devices to measure stress against a structure. The main problem centres on the measuring device and the difference in the elastic properties of the surrounding backfill and the mass fill. Devices in this category are still in the development stages. A more complete discussion on earth measuring devices is presented by Sellers and Dunnicliff²⁰⁷. Earth pressure cells must be inspected and tested for leaks in a water bath prior to installation. The cell should be calibrated while undergoing the leak test and rechecked immediately before and after installation to ensure that the cell is still responsive to pressure change. The earth pressure cell may be installed by bonding the cell to a thin steel plate that is bolted or welded to the sheet pile member. This type of installation will cause the face of the cell to protrude beyond the face of the sheet pile. Attaching the cell such that the face of the cell is flush with the surface of the sheet pile is a more desirable installation. Measures should be taken to protect the leads and transducer from damage during driving.

15.7.4.5. Strain Gages

Several types of strain gages are in common use today. They may be grouped according to the principles by which they operate. Three principles of operations are used: mechanical, electrical resistance, and vibrating wire. The latter two are more common in gages used to monitor sheet pile structures. Each is designed to measure very small changes in length of the structural member at the point of installation. The change in length is converted into stress, load, or bending moment. In cellular structures, strain gages have been used principally to observe interlock tension within sheet pile members. The gages are made such that they can be attached to a surface by means of an epoxy adhesive or by welding. Two types of electrical resistance strain gages are available, including the bonded types and the weldable types. Bonded types are designed to be bonded to the surface of a structural member by means of an adhesive epoxy. The success of this type of gage depends on the surface preparation of the structural members, which should be perfectly clean and dry, the gage bonding, waterproofing of the gage, which is absolutely essential, and the physical housing provided to protect the gage and lead wires. The weldable-type gages are spot welded to the structural surface with a portable welder. The resistance element is bonded or welded to a very thin stainless steel shim stock, which is spot welded to the clean smooth surface of the structural member. The success of this gage depends very much on the same factors as those affecting the success of the bonded-type gage. Vibrating wire strain gages are usually arc welded or spot welded to the surface of the structural member. Gages that are arc welded are bolted into fixed end blocks under the correct tension. The end blocks are arc welded to the structural member at the proper spacing. In gages that are spot welded to the surface, the wire is pretensioned and welded to a shim stock, and the shim stock is spot welded to the surface of the structural member. Vibrating wire strain gages are equipped with a plucking and cable assembly. This assembly is detachable with most models and can be used with more than one gage if they are in proximity. The vibrating wire strain gage operates on the principle that the natural frequency of a vibrating wire, constrained at both ends, varies with the square root of the tension in the wire. Any change in strain in the member to which the gage is attached is indicated by a change in tension in the wire. The frequency of the wire is determined by plucking the wire and measuring its frequency. Zero drift in vibrating wire strain gages, caused by stretching or creep in the wire or by slippage at the wire grips, has been reduced by heat treating the wire during manufacturing, by keeping the tension in the wire to less than 25 percent of the yield stress, and by using no load gages. Gages with thermistors for temperature measurements are available if temperature measurements are desired. *Table 15-6* lists advantages, limitations, and other pertinent information for

²⁰⁷Sellers, Barrie and Dunnicliff, John. 1982 (Apr). "Measurement of Load and Strain in Structural Members," 6th Annual Short Course on Field Instrumentation of Soil and Rock, University of Missouri-Rolla, Rolla, Missouri.

various types of strain gages used to monitor steel sheet pile structures.

Gage Type	Advantage	Limitations	Gage Length in.	Range in.	Sensitivity in./in.	System Accuracy in./in.	Reliability	Cost
Bonded electrical resistance strain gage	Small size Low cost Remote reading Can be temperature compensated	Needs great skill to install Needs great skill to waterproof Lead wire effects Cable lengths limited to 1,000 feet	0.008 to 6	±20,000	1	5 to 100	Poor to excellent	Low material; high labor
Weldable electrical resistance strain gage	Remote reading Factory waterproofing Easy installation Temperature compensation	Lead wire effects Less accurate than good bonded types	1 to 5	20,000	1	15	Good	Medium
Vibrating wire strain gage (arc welded or bolted to surface)	Remote reading Lead wire effects minimal Factory waterproofing Long history of use Robust, reusable	Small range Large size Cannot measure dynamic strain Sensitive to temperature	5 to 10	± 2,500	1	5	Very good	High
Vibrating wire strain gage (spot weldable to surface)	Remote reading Lead wire effects minimal Factory waterproofing Small size Very easy installation	Small range Cannot measure dynamic strains Sensitive to temperature Weld points need waterproofing	2 to 3	± 2,500	1	5	Good	High

Table 15-6: Advantages and Disadvantages of Various Types of Surface-Mounted Strain Gages

15.7.4.6. Precise Measurement Systems

Horizontal and vertical surface displacement can be detected by making precise measurements of lengths, angles, and alignments between reference monuments and selected points on the structure. These measurements can be grouped into three categories: precise alignment measurement, precise distance and elevation measurements, and triangulation and trilateration surveys. The instruments commonly used to make these measurements include laser transmitters and receivers, precision theodolites and levels, electronic distance measurement instruments, alignment targets and reflectors, and auxiliary equipment. The reference monuments should be set in rock or stable soil, located outside the influence of the construction area, and protected from incidental disturbances. At least two reference monuments, each with a clear line-of-sight to the other and the selected points on the structure, should be installed. The selected points on the structure should be permanently marked such that the exact same points are used during each survey. In addition to the foregoing measurement systems, plumb lines can be used to measure bending, tilting, or deflections of sheet pile structures from external loading, sliding, and deformation of the foundation.

15.7.5. Accuracy of Required Measurements

Accuracy indicates the degree of agreement between the measured value and the true value. It signifies the range the measured value will deviate from the true value. Accuracy is not to be confused with precision or sensitivity. Precision indicates the degree of agreement between repeated measurements of the same quantity and sensitivity represents the smallest quantity observable as a measurement is made. Several factors influence the accuracy of field measurements. Among these factors are the physical features of the device, installation procedures, environmental conditions, conformance of the instrument to the actual changing conditions, data reduction procedures, and observer errors. Accuracy should be verified.

This can be done by monitoring two or more systems independently or by using instruments that can be removed, checked and/or recalibrated periodically, and reinstalled. The last will be virtually impossible with many instruments and installations. The required accuracy is related to several factors, including: the sensitivity of the structure to the required measurements, the magnitude of the measurements during the observational period, the length of the observational period, and the purpose of the monitoring program. These factors

should be carefully considered in connection with the type of sheet pile structure being monitored and the field measurements desired. Generally, the accuracy of most readily available instruments will meet the accuracy requirements for performance evaluation of most monitoring programs, provided the instrument is installed, operated, and maintained in accordance with the manufacturer's recommendations. The accuracy of most instruments can be obtained from the manufacturer's literature. Gould and Dunicliff²⁰⁸ and Wilson and Mikkelsen²⁰⁹ presented tabular data on the accuracy of various measurement methods and instruments common to measuring deformation and pore pressure.

15.7.6. Collection, Processing, and Evaluation of Data

Data must be collected, processed, and evaluated as expeditiously as possible if the monitoring program is to have any chance of success. Careful attention must be given to whoever will collect the data. This can be the responsibility of the contractor or the owner. In any event, the person collecting the data must have experience or be trained to collect the data. This person must be aware of what constitutes abnormal data, malfunctioning monitoring equipment, and instruments that have been damaged. If the data are to be collected by the contractor, the specifications must be definite regarding who will collect the data, when and how it will be collected, transmitting the data to the owner, processing and evaluating the data, reporting malfunctions, repairing and replacing damaged equipment and instruments, and other factors unique to the monitoring program. A monitoring schedule should be established to provide data that are needed to eval-

uate the structure under all conditions of concern.

The schedule should include special monitoring during critical load phases of the structure. Input by the design engineers will be very helpful in establishing a meaningful monitoring schedule. Initial observations should be made on all instruments immediately after installation. This is base data, and most subsequent data will be compared with this initial data. Collected data should be promptly processed for easy review and evaluation. This can be done manually or by computer technology, if computer facilities and suitable software are readily available. The choice of processing the data by computer or manually should be weighed against the volume of data to be processed, the cost of the computer systems, the personnel available, and the convenience of each method to the people evaluating the data. Regardless of the method chosen, the data should be presented in some graphic form that is readily updated as new data are acquired. Graphic presentation of data helps to establish trends, pinpoint variations, and guards against overlooking important data. Data that have been collected and processed should be promptly evaluated by design engineers and others involved in the design and construction process. The evaluation should include an assessment of the validity of the data, a determination of the existence of any adverse situation that calls for immediate attention, a correlation of the data with other activities, and a comparison of the data with predicted behaviour. Care must be taken not to reject what seems to be abnormal data without due consideration of the factors likely to produce the data.

²⁰⁸Gould, James P., and Dunicliff, John C. 1982 (Apr). "Accuracy of Field Deformation Measurement," 6th Annual Short Course on Field Instrumentation of Soil & Rock, University of Missouri-Rolla, Rolla, Missouri.

²⁰⁹Wilson, Stanley D., and Mikkelsen, Erik P. 1978. "Field Instrumentation," Transportation Research Board Special Report 176, Landslides: Analysis and Control, National Academy of Science.

²¹⁰Department of the Army, Corps of Engineers, St. Louis District. 1983 (Nov) . Lock & Dam 26 (Replacement) Mississippi River, Alton, Illinois, Summary Report, Instrumentation Data Analysis and Finite Element Studies for First Stage Cofferdam, Shannon & Wilson, Inc.

Marine Solutions

Solutions for Breakwaters, Shore Protection and Marina Docks

Economy, durability, and versatility

CONTECH® Marine Products provide economical and effective solutions for various marine applications, including shore protection, primary and secondary breakwaters, jetties and marina docks.



For more information, call Toll Free: 800-338-1122.
Or, visit our web site at www.contech-cpi.com

CONTECH
CONSTRUCTION PRODUCTS INC.

INNOVATIVE CIVIL ENGINEERING SITE SOLUTIONS

 American
Owned and Operated

©2003 CONTECH Construction Products Inc. All Rights Reserved

Chapter Sixteen: Cellular Sheet Piling Structures, Mooring Cells and Dolphins

16.1. General

Dolphin-marine structures for mooring vessels²¹¹ are commonly used in combination with piers and wharves to shorten the length of these structures and are also a principal part of the fixed mooring berth type of installation used extensively in bulk cargo handling. They are also used for typing up ships or barges and for transferring cargo from one ship to another when moored along both sides of the dolphins. Dolphins are of two types: breasting and mooring.

Breasting dolphins are designed to take the impact of the vessel when docking and to hold it against a broad-side wind. They usually also have bollards (mooring posts) to take ship lines, particularly springing lines for moving the vessel along the dock or holding it against the current. These lines are not very effective in a direction normal to the dock, particularly if the vessel is light. Therefore, to hold the vessel against a broad-side wind blowing in a direction away from the dock, additional dolphins called "mooring dolphins" must be provided off the bow and stern, located some distance in back of the face of the dock. These mooring dolphins are located in back of the face line of the dock where they will not be hit, and therefore, are not designed for the impact of the ship. Mooring dolphins are provided with bollard posts for routine loads and with capstans (winches) when heavy lines are to be handled. The maximum pull on a single line will usually not exceed 50 tons; however, two lines may sometimes be attached to a single bollard resulting in a pull of 100 tons.

If bottom soil conditions are suitable, sheet pile cells make excellent dolphins and if provided with adequate fenders can be designed to withstand the forces associated with large ships.

Cells, because of their circular shape, are well suited for turning or warping the ship around at the end of the dock. A cellular sheet-pile dolphin with a fender system is shown in Figure 16-1. This dolphin was designed to accommodate a 35,000 DWT ship. Cellular dolphins are usually capped with a heavy concrete slab to which the mooring post is anchored.

Dolphins are designed principally for the horizontal loads of impact and/or wind and current forces from a vessel when it is docking and during the time it is moored.

16.2. Loads

16.2.1. Lateral Loads

Lateral loads from mooring lines pull the ship along the dolphin or hold it against the force of wind or current. The average wind pressure in psf on the exposed broadside of a

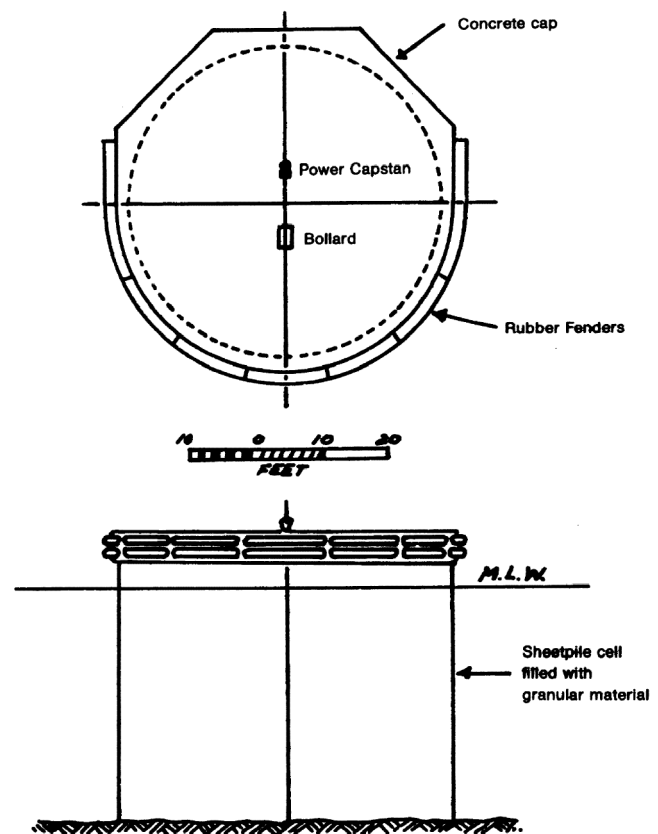


Figure 16-1: Cellular Sheet-Pile Dolphin (Isolated Single Cell)

ship in a light condition can be computed from the wind pressure formula, assuming a shape factor of 1.3 and an average air density, as

$$\text{Equation 16-1: } P = V_{\text{wind}}^2 / 300$$

Where

- P = wind pressure on the exposed broadside of a ship, psf
- V_{wind} = wind velocity, miles per hour.

The shape factor 1.3 is a combined factor taking into consideration the shape of common ships and the decrease in air pressure on the leeward side of the ship. The design wind pressure is usually assumed to be not less than 10 or more than 20 psf corresponding to wind velocities of about 55 to 78 miles per hour.

The average pressure due to the water current (in pounds per square foot) is determined from the following expression:

²¹¹Quinn, A.deF. (1972) Design and Construction of Ports and Marine Structures. New York: McGraw-Hill.

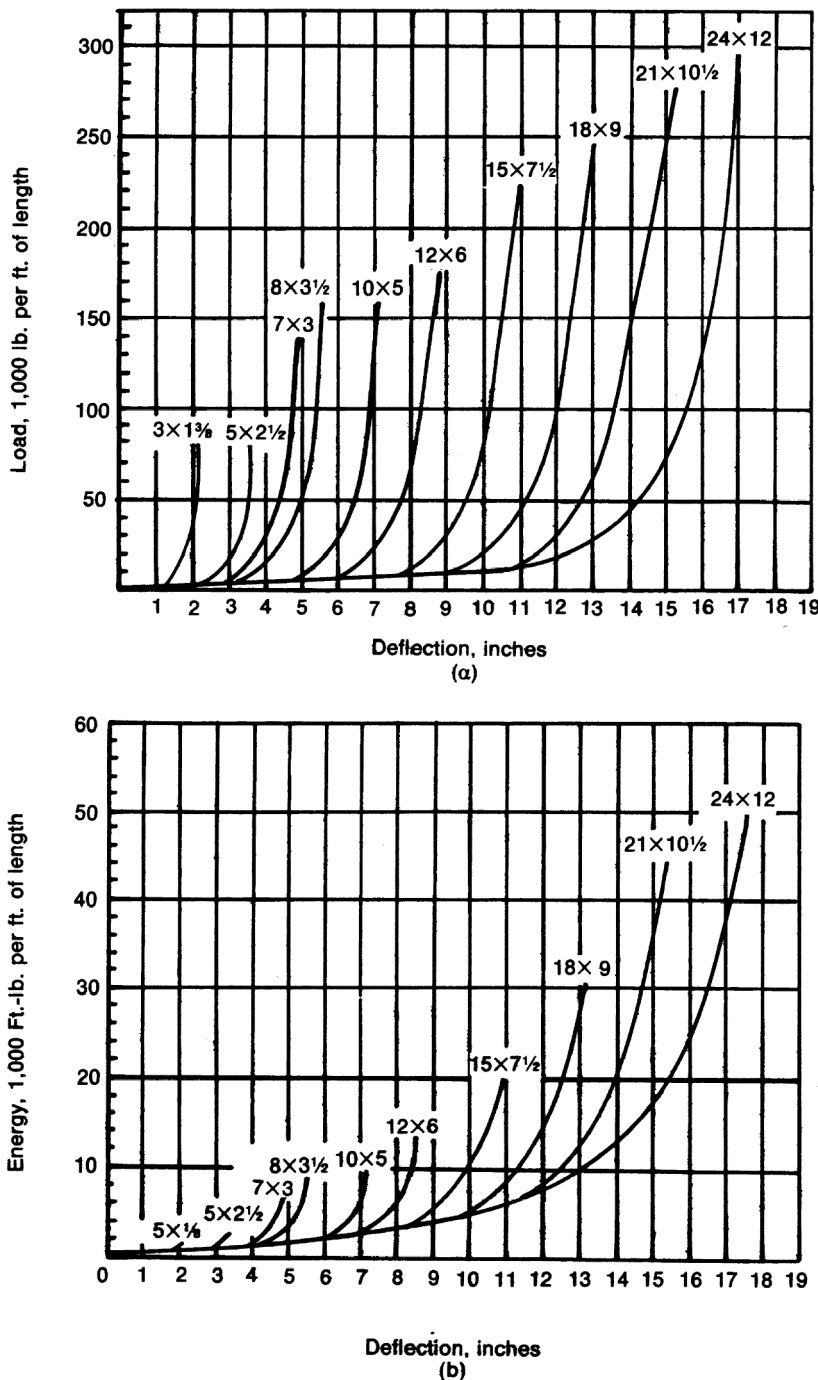


Figure 16-2: Load and Energy-Deflection Curves for Cylindrical Rubber Fenders, Side Loaded²¹²

- (a) Approximate Load-Deflection Curves
- (b) Approximate Energy-Deflection Curves

Equation 16-2:
$$p = \frac{wV_{water}^2}{2g}$$

Where

- p = pressure due to the water current, psf
- w = unit weight in pounds per cubic foot
- $\gamma = 32.2 \text{ ft/sec}^2$
- V_{water} = velocity of current in ft/sec.

For salt water this results in a pressure per square foot equal to approximately V^2 . The velocity of current will usually vary between one and four feet per second. The pressure due to current will be applied to the area of the ship below the water line when the ship is fully loaded. Since the ship is generally berthed parallel to the current, this force is seldom a controlling factor.

16.2.2. Impact

The ship striking the dolphin when berthing causes docking impact. For the purpose of design the assumption is usually made that the maximum impact to be considered is that produced by a ship fully loaded (displacement tonnage) striking the dolphin at an angle of 10 degrees with the face of the dolphin with a velocity normal to the dolphin of 0.25 to 0.5 feet per second. Fender systems are designed to absorb the docking energy of impact and the resulting force to be resisted by the dolphin will depend upon the type and construction of the fender.

In its simplest form, the fender may be a horizontal wood member or a number of vertical wood members or rubbing strips fastened to the deck. However, rubber has come into extensive use for fender systems. Cylindrical rubber fenders come in sizes ranging from 5" O.D. by 2-1/2" I.D. to 18" O.D. by 9" I.D. Figure 16-2 gives (a) the force developed and (b) the corresponding energy absorbed for a given deflection for cylindrical rubber fenders in the range of sizes given above. Figure 16-3 gives similar information for rectangular rubber fenders.

The kinetic energy of impact is

Equation 16-3:
$$E = \frac{MV_{ship}^2}{2}$$

and substituting W/g for the mass M ,

Equation 16-4:
$$E = \frac{WV_{ship}^2}{2g}$$

Where

- E = the energy in ft-tons
- W = the total weight of the ship and cargo in tons

²¹²Fender Dimensions: 10" O.D. and 5" I.D. Courtesy of Goodyear Tire & Rubber Company.

- V_{ship} = the velocity of the ship normal to the dock in ft/sec
- g = the acceleration due to gravity (32.2 ft/sec^2).

The energy assumed to be absorbed by the fender system and dock is $1/2E$, as the remaining one half is assumed to be absorbed by the ship and water. This energy, $1/2E$ must be absorbed by the fender system and dolphin in bringing the ship to rest.

16.2.3. Wave Action

The lateral force transmitted to a structure hit by a wave is much greater when the wave breaks as it approaches (shallow water) than when it does not break (deep water). Deep water in this sense means a water depth at the structure greater than about 1.5 times the maximum expected wave height. A discussion of lateral force due to wave action is beyond the scope of this design manual. The length, height, breaking point, and other essential characteristics of waves depend on many factors such as wind velocity, wind direction and frequency of occurrence, shore line configuration, and depth and slope of beach near the structure. Therefore, specialists in this branch of oceanography should do the determination of wave characteristics and the wave pressure diagram against a structure. Once a lateral pressure diagram has been developed, it can be used in computing the lateral force on the structure.

16.2.4. Earthquake Force

Earthquake forces will have to be considered in areas of seismic activity. The horizontal forces acting on a dolphin due to an earthquake will include the force to accelerate the dolphin and any increased mooring forces. Forces on a given mass will equal acceleration developed times the mass, applied at the centre of gravity. The weights to be used in computing horizontal forces are total dead loads plus one-half of any live loads.

16.2.5. Vertical Loads

Vertical loads consist of: dead load (weight of the structure), and live load (uniform loads or wheel loads from trucks or mobile cargo handling cranes, and loads from other equip-

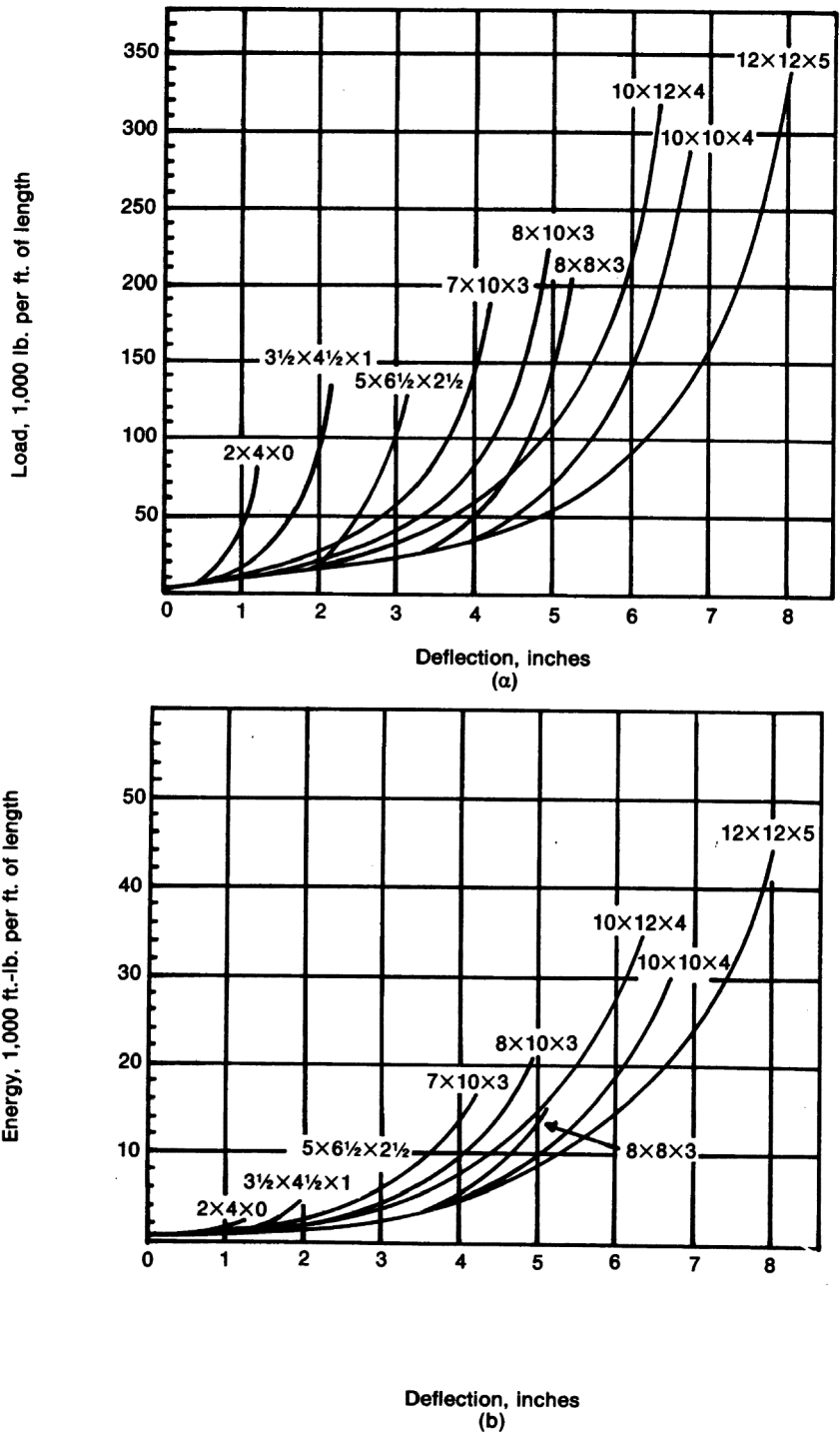


Figure 16-3: Load and Energy-Deflection Curves for Rectangular Rubber Fenders, Side Loaded 213
 (a) Approximate Load-Deflection Curves
 (b) Approximate Energy-Deflection Curves

ment in the case of breasting dolphins).

16.3. Stability of Dolphins

Preliminary concepts will be developed by considering a

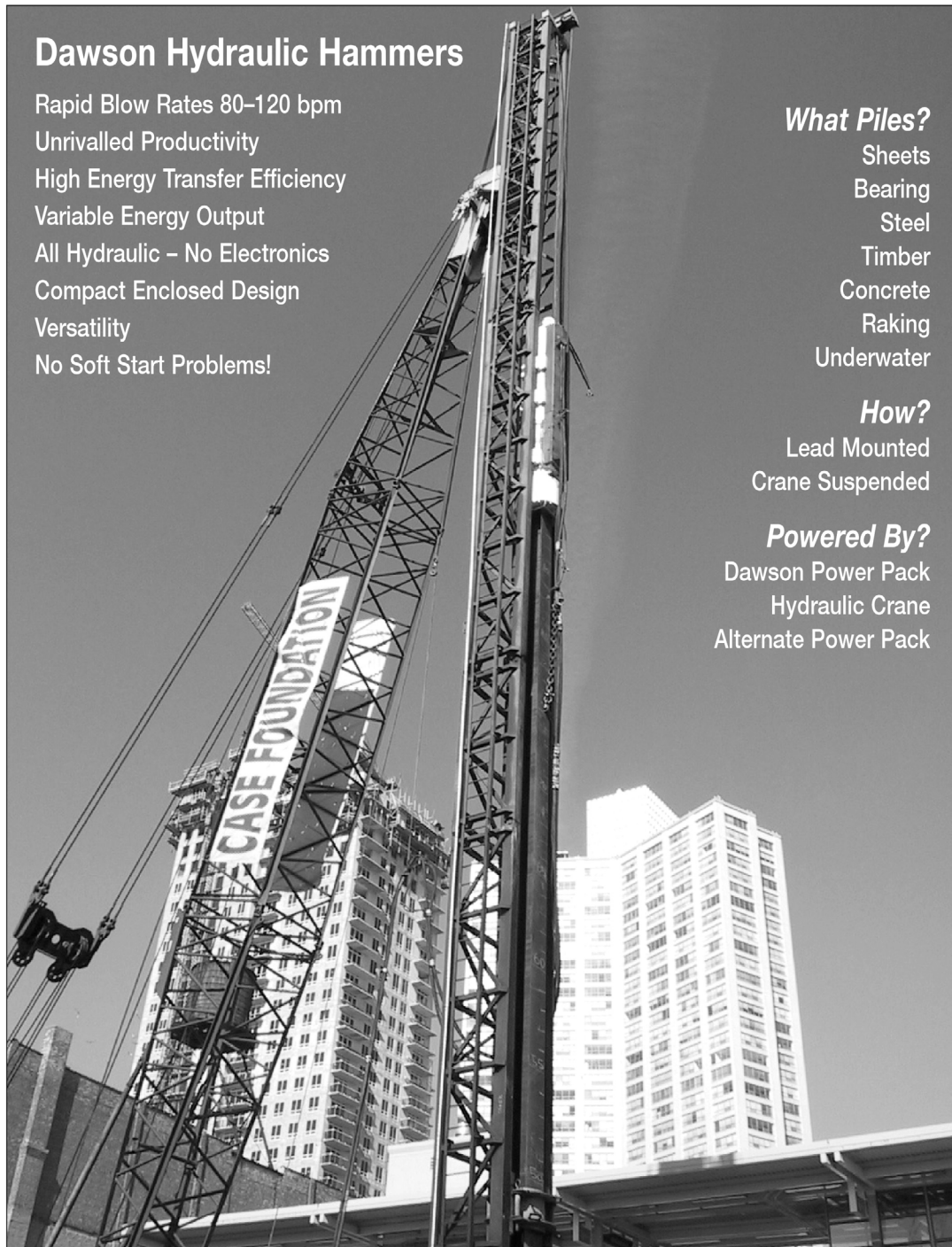
²¹³Fender Dimensions: 7" x 10" x 3".



DAWSON

INNOVATIVE PILING EQUIPMENT

DAWSON CONSTRUCTION PLANT LTD
 Chesney Wold, Bleak Hall
 Milton Keynes MK6 1NE, England
 Tel: 011 44 1908 240300
 Fax: 011 44 1908 240222
 Email: mark@dcpuk.com
 Website: www.dcpuk.com



Dawson Hydraulic Hammers

Rapid Blow Rates 80–120 bpm
 Unrivalled Productivity
 High Energy Transfer Efficiency
 Variable Energy Output
 All Hydraulic – No Electronics
 Compact Enclosed Design
 Versatility
 No Soft Start Problems!

What Piles?

Sheets
 Bearing
 Steel
 Timber
 Concrete
 Raking
 Underwater

How?

Lead Mounted
 Crane Suspended

Powered By?

Dawson Power Pack
 Hydraulic Crane
 Alternate Power Pack

American Equipment & Fabricating Corp.
 100 Water Street
 East Providence
 Rhode Island 02914
 U.S.A.

Contact: John Sheerin
 Tel: 401 438 2626
 or: 1-800-368-7453
 Fax: 401 438 0764

Bay Machinery Corp.
 PO Box 70430
 Richmond
 CA 94807
 U.S.A.

Contact: Bob Knop
 Tel: 510 236 9000
 Fax: 510 236 7212

Equipment Corporation of America
 PO Box 387
 Aldan
 PA 19018
 U.S.A.

Contact: Ben Dutton
 Tel: 610 626 2200
 Fax: 610 626 2245

Hammer & Steel Inc.
 11912 Missouri Bottom Rd.
 St Louis
 Missouri 63042-2313
 U.S.A.

Contact: Bob Laurence
 Tel: 314 895 4600
 or: 1-800-325-7453
 Fax: 314 895 4070

Mabey Bridge & Shore Inc. *
 6770 Dorsey Road
 Baltimore
 MD 21227
 U.S.A.

Contact: Joe Atkinson
 Tel: 410 379 2800
 or: 1-800-42-MABEY
 Fax: 410 379 2801

Mississippi River Equipment Co.
 PO Box 249
 520 Good Hope St.
 Norco, LA 70079
 U.S.A.

Contact: J J Waguespack
 Tel: 985 764 1194
 Fax: 985 764 1196

Pacific American Commercial Co.
 7400 Second Avenue S.
 P.O. Box 3742
 Seattle, WA 98124
 U.S.A.

Contact: Ted Obermeit
 Tel: 206 762 3550
 or: 1-800-678-6379
 Fax: 206 763 4232

Pile Equipment Inc.
 1058 Roland Avenue
 Green Cove Springs
 Florida 32043-8361
 U.S.A.

Contact: Mike Elliott
 Tel: 904 284 1779
 or: 1-800-367-9416
 Fax: 904 284 2588

Special Construction Machines
 166 Bentworth Avenue
 Toronto
 Ontario M6A 1P7
 Canada

Contact: Steve Calow
 Tel: 416 787 4259
 or: 1-800-760-0925
 Fax: 416 787 4362

*Do not supply HPH Hydraulic Hammers

small diameter vertical shaft embedded in soil below the dredge line and designed to resist a horizontal force P transmitted to it by mooring line from a vessel. Tschebotarioff²¹⁴ describes procedures for the estimation of the depth of embedment D required for safe stability of a small diameter shaft.

16.3.1. In Sand

The lateral resistance in sand for the determination of embedment depth is shown in Figure 16-4.

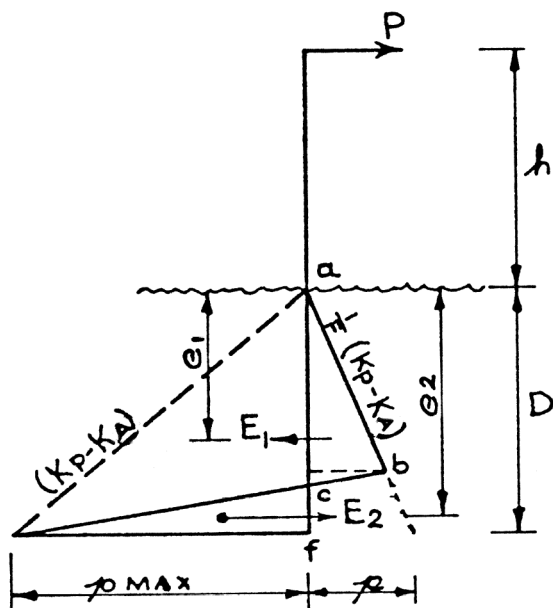


Figure 16-4: Determination of Embedment Depth D for Vertical Shaft Subject to a Horizontal Force in Sand

The maximum possible passive resistance of the sand at a depth D is

$$\text{Equation 16-5: } p = \gamma D (K_p - K_a)$$

Equilibrium requires that

$$\text{Equation 16-6: } P = E_1 - E_2$$

$$\text{Equation 16-7: } P_h = E_2 e_2 - E_1 e_1$$

The value of E_1 is governed by $p = p_{max}/F$, where the factor of safety, F should be ≥ 2.5 . The force E_1 is taken to equal the area abc multiplied by $2d$, where d is the shaft diameter. The force E_2 is taken to equal the area cdf multiplied by $2d$. [The K_p value can be computed assuming the angle of wall friction, $\delta = 0$ or if the force P has a downward component, the K_p value may be increased to correspond to δ values up to $2/3\phi$. Similarly, if P is likely to have an upward component, the K_p value should be decreased to correspond to δ values as low as $2/3\delta$]. The simplest way to estimate D is by trial and error. After drawing a diagram of the type shown in Figure 4a, select a Point c so that the force E_1 will be somewhat larger than P .

The pick a point f so that the force E_2 will satisfy Equation 16-6 and check to see if Equation 16-7 is satisfied. If not, repeat this procedure for a different distance ac .

The bending moments and shears in the shaft can then be determined by simple statics from the force P and the earth pressure diagram $abcdf$. The result will be on the safe side compared with the probable actual pressure distribution indicated by dotted lines.

16.3.2. In Clay

Figure 16-5 refers to the stability of a vertical shaft embedded in clay.

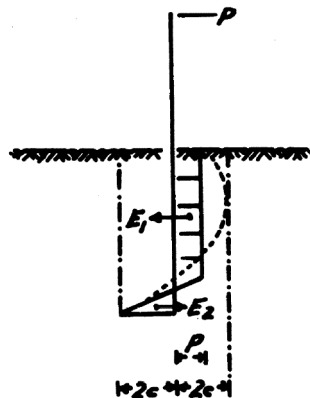


Figure 16-5: Determination of Embedment Depth D for Vertical Shaft Subject to a Horizontal Force in Clay

The procedure is the same as that for sand except that special caution is required when selecting the c value of sensitive clays susceptible to remoulding and $p = 2c/F$, where F = factor of safety.

16.3.3. Frictional Forces

Large diameter dolphins formed by driving steel sheet piles, forming an isolated, cylindrical, sand-filled cell of 5- to 15-foot diameter have similar stability considerations as that of a small diameter shaft except that cell weight and friction along the cell walls will provide additional resistance to overturning as shown in Figure 16-6.

Forces accounting for the friction can be estimated as follows:

$$\text{Equation 16-8: } \begin{aligned} F_1 &= E_1 \tan \delta = \text{wall friction} \\ F_2 &= E_2 \tan \delta \end{aligned}$$

Both forces F_1 and F_2 shown in Figure 16-6 will be applied in plan at the centre of gravity of the half ring along the outer periphery of which they will be acting, so that their resisting moment with respect to the centreline of the cylinder will be d/p . Taking moments about the centre of the circular base will give

²¹⁴ Tschebotarioff, G.P. (1951) Soil Mechanics, Foundations and Earth Structures. New York: McGraw-Hill, Inc.

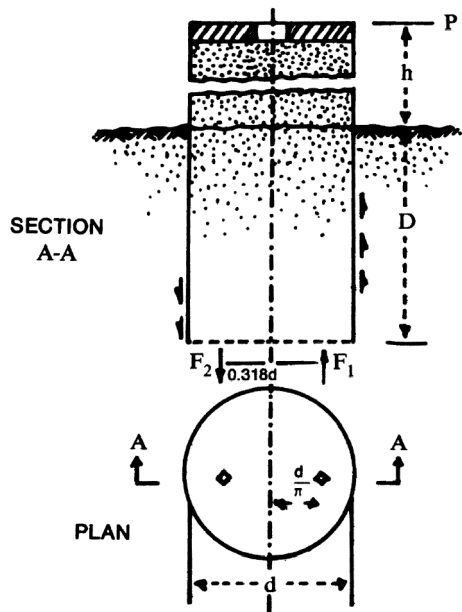


Figure 16-6: Frictional Forces Contributing to Stability of Sheet-Pile Dolphin in Sand

Equation 16-9:

$$P h = \frac{d(E_1 + E_2) \tan \delta}{\pi} + E_2 e_2 - E_1 e_1$$

A concrete stiffening slab at the top of the sheet pile caisson is advisable, with an opening to permit addition of sand in case the fill within the cell settles.

16.4. Bearing Capacity

Sheet pile dolphins on sand or clay foundations involve a surcharge loading imposed upon the supporting stratum at the inboard toe. An estimate of the factor of safety against a bearing capacity failure of the supporting stratum should be made and is illustrated in the example problems.

Sliding Stability. The factor of safety of the cell against sliding along its base should be estimated as described in

the chapter on cellular cofferdams, and in the example problems.

Shear Failure on Centreline of Cell. The factor of safety against failure due to vertical shear can be investigated as described in the cellular cofferdam chapter and in the example problems.

Selection of Sheet Pile Section. The selection of the sheet pile section should be based on the interlock tension. Maximum interlock tension occurs at a depth where the earth pressure on the sheet pile wall is a maximum. This design procedure is illustrated in the chapter on cellular cofferdams and example problems.

16.5. Skeletal Sheet Pile Cell Docks

Sheet pile cells have also been widely used for “skeletal” type docks particularly along inland rivers for mooring bulk cargo barge strings.²¹⁵ The isolated single cells vary in diameter from about 10 ft. to 30 ft. and in height up to 60 ft. above the river bottom if necessary. They are particularly useful where extreme fluctuations in water depths preclude the use of continuous bulkheads. The cells are built parallel to shore and separated from each other at distances based on the barge lengths and other design considerations. Some docks built thusly have extended 2500 ft. or more along the shoreline having as many as 25 individual cells comprising the docking facility. Barges from the fleet move from mooring sites along the upstream cells to the unloading or loading facility in the centre, then to downstream fleeting areas along with other empties. The economies in such a dock have resulted in many such facilities being built to date. Horstman provides a detailed review of the history application, design and construction of the docks. Design principals employed in the design of mooring cells would also be effective in the design problem and the reader is directed to the previous section on mooring cells along with information supplied by Horstman and others regarding practical application.

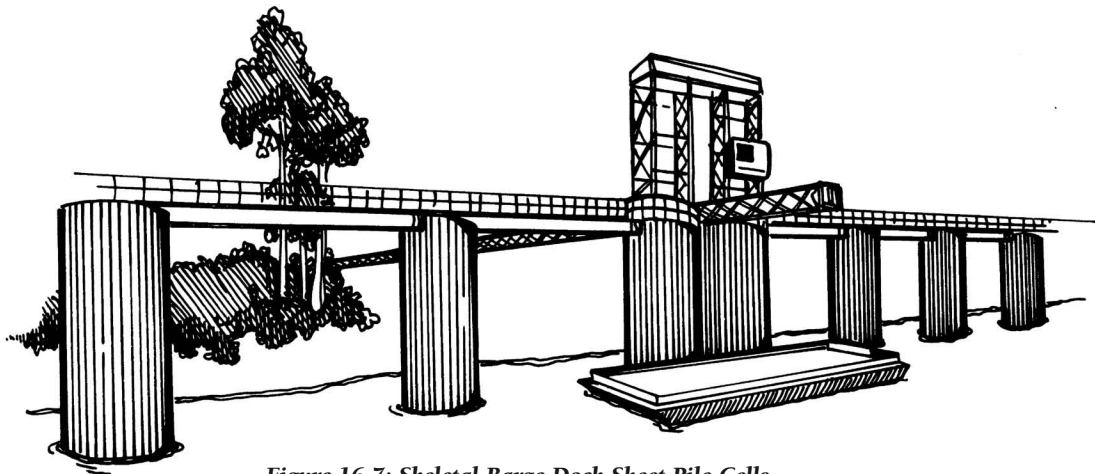


Figure 16-7: Skeletal Barge Dock Sheet Pile Cells

²¹⁵ Horstman, W. (1964) “Barge Dock for Inland Waterways.” *ASCE Proceedings*, Vol. 90, No. WW4, November.

Example 28: Design of a Mooring Dolphin – Granular Soil

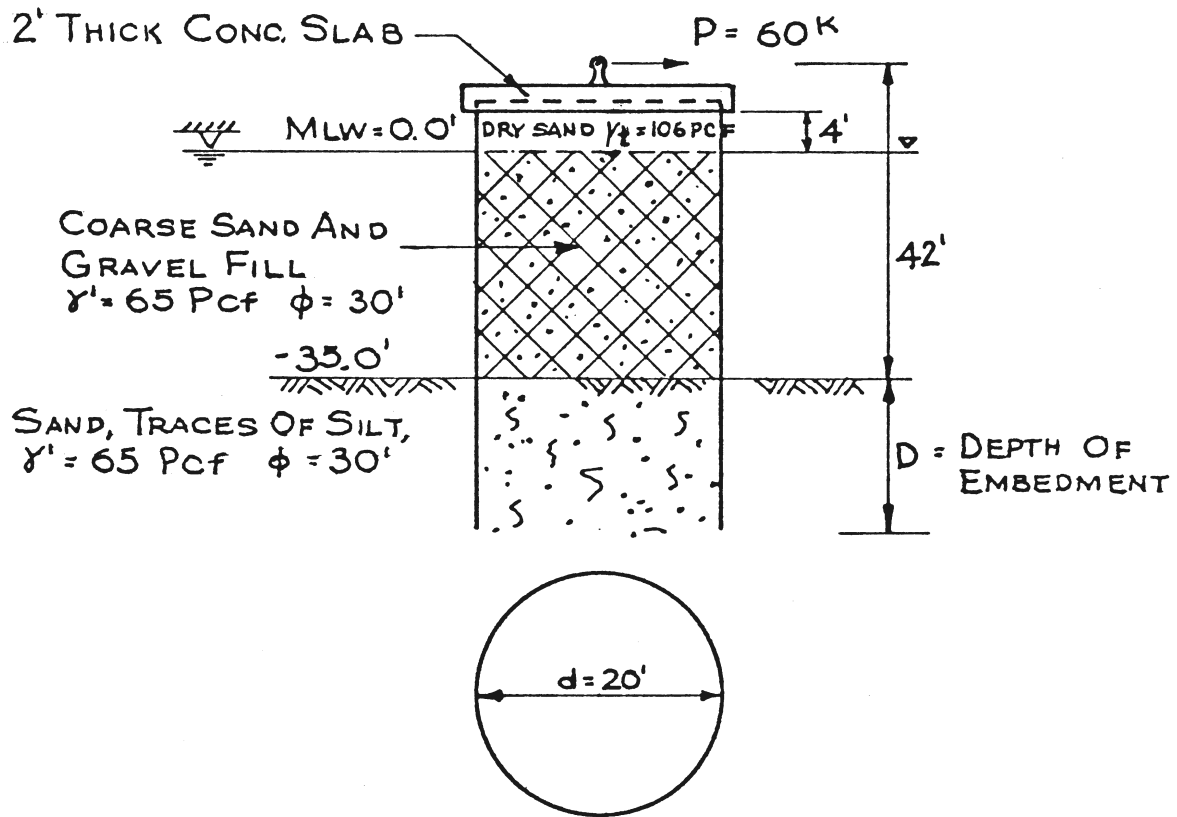


Figure 16-8: Elevation View for Example 28

- ❖ Given
 - Problem as shown in Figure 16-8.
 - Additional downward live load $p_{live} = 250$ psf
 - Wall friction angle δ of 20°
 - Neglect wave loads.
 - Use factor of safety for earth pressure coefficients of 2.5.

- ❖ Find
 - Depth of penetration D .
 - Check against overturning and bearing failure.
 - Compute interlock forces and specify sheet piling.
- ❖ Solution

➤ Determine earth pressure profile for depth of embedment. See Figure 16-4. The solution of the problem is similar to a cantilever wall solved by the conventional method. The equations of equilibrium to be used are Equation 16-6 for the forces and Equation 16-9 for the moment.

- The forces E_1 and E_2 are

$$\text{Equation 16-10: } E_1 = \frac{\gamma' c^2 d (K_p - K_a)}{FS}$$

$$\text{Equation 16-11: } E_2 = \gamma' D (D - c) d (K_p - K_a)$$

These are based on the triangle area shown in the diagram for each force.

- For determination of the depth, we take moments about point a. The two moment arms are thus

$$\text{Equation 16-12: } e_1 = \frac{2c}{3}$$

$$\text{Equation 16-13: } e_2 = \frac{2D + c}{3}$$

- If we substitute Equation 16-10, Equation 16-11, Equation 16-12 and Equation 16-13 into Equation 16-6 and Equation 16-9, along with all of the other known variables, we obtain

$$60000 = 1386.7c^2 - 3466.7D(D - c)$$

$$2520000 = 3213c^2 + 8032.6D(D - c) + 3466.7D(D - c)(0.667D + 0.333c) - 924.44c^3$$

We thus have two equations in two unknowns, c and D . The problem is that the first (force) equation is quadratic in both variables and the second (moment) cubic. To simplify the solution, we plot both of these equations, computing D (y -axis) for various values of c (x -axis). The results of this are shown in Figure 16-9.

The two lines intersect when c is approximately 15'; this corresponds to a value of D of about 19'. To be conservative, we will use an embedment depth of $D = 20'$, which corre-

COMPOSITE Z™



FEATURES

Corrosion resistant
 High strength reinforced composite
 No coating required
 Lightweight for easy installation
 Non-conductive
 Easy to cut
 Easy to thread
 Domestic "Ball & Socket" interlock

Products

Z-100 sheet pile
 Z-200 sheet pile
 Z-90 Corner
 Z-100 Cap system
 Z-200 Cap system
 Z-Beam wale system
 EZ-Deck composite decking



Composite Z sheet profile

Equipment

Vibratory Hammers
 Model 10
 Model 20



"the sheet pile of tomorrow available today"

Contact us:

Voice: 561-848-2050
 Fax: 561-842-7209
 Z@compositeZ.com

Composite Components, Inc.

P.O. Box 14295
 North Palm Beach, FL 33408
 www.CompositeZ.com

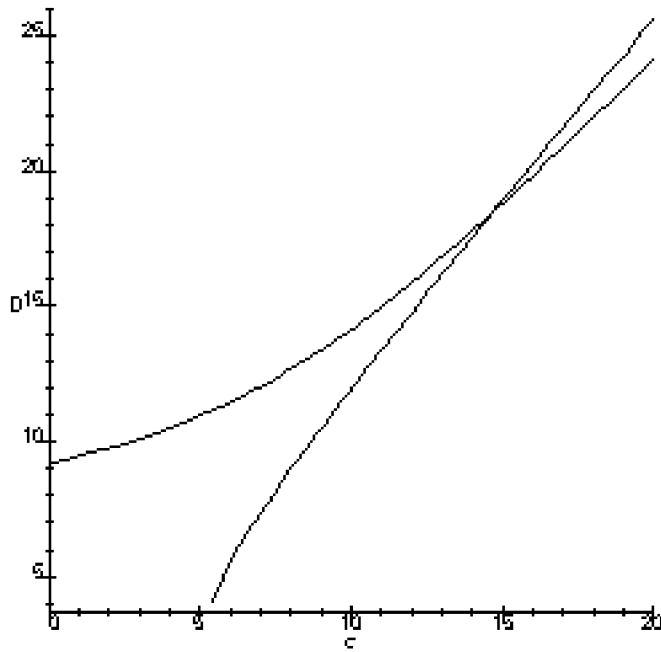


Figure 16-9: Plot of D vs. c for Example 28

sponds to a value of $c = 16'$. We can thus compute the values of the forces and moment arms, which are as follows:

- $D = 20'$
- $c = 16'$
- $E_1 = 354986.7$ lbs.
- $e_1 = 10.67'$
- $E_2 = 277333.3$ lbs.
- $e_2 = 18.67'$

➤ Check overturning moment. We will sum moments about point A to check this value. A force diagram is shown in Figure 16-10. We will neglect the effect of the live load in this case (but will consider it for bearing capacity and interlock tension.)

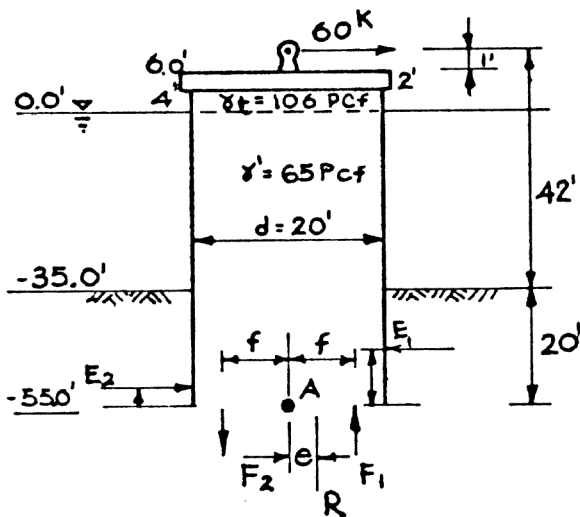


Figure 16-10: Force Diagram for Overturning Moment

- The summation of moments about point A is given by the equation

Equation 16-14:

$$\sum M_A = R e + (F_1 + F_2) f - P (h + D) - E_2 (D - e_2) + E_1 (D - e_1)$$

The value of the reaction R is given as

Equation 16-15: $R = W_{cell} + F_2 - F_1$

The weight of the cell W_{cell} is given as

Equation 16-16:

$$W_{cell} = A_{cell} (L_{con} \gamma_{con} + L_{dry} \gamma + L_{sub} \gamma) = \frac{\pi}{4} d^2 (L_{con} \gamma_{con} + L_{dry} \gamma + L_{sub} \gamma)$$

The values $L_{con} \gamma_{con}$ refer to the thickness (2') and specific weight (150 pcf), respectively, of the concrete cap.

The value $L_{dry} \gamma$ refer to the thickness of the cell fill (4') and its dry unit weight (106 pcf), respectively, above the water line.

The value L_{sub} is the thickness of the cell fill below the water line to the base of the mooring dolphin. $L_{sub} = 35' + 20' = 55'$.

The frictional forces F_1 and F_2 are given by Equation 16-8.

Substituting the variables leads to the following values for these variables:

- ♦ $A_{cell} = 314.2$ ft²
- ♦ $W_{cell} = 1,350,571$ lbs.
- ♦ $F_1 = 129,205$ lbs.
- ♦ $F_2 = 100,941$ lbs.
- ♦ $R = 1,322,307$ lbs.

Substituting these values into Equation 16-14, setting the sum to zero and solving for the eccentricity yields $e = -.52'$. To be in the middle third, $|e| < 3.33'$, which it certainly is.

➤ Check for bearing capacity failure.

- The bearing capacity formula for circular foundations is given in Equation 15-17. For $\phi = 30^\circ$, $N_q = 22.46$ and $N_\gamma = 19.7$ (Table 15-2.) The depth of penetration D corresponds to the variable D_f ; the diameter d corresponds to the variable B. Submerged unit weights are used throughout the formula. Substituting all of the values (along with a cohesion $c = 0$) yields $q_f = 36,881$ psf.
- For a trapezoidal load with the resultant in the middle third, the maximum and minimum bearing stresses on the foundation are given by the equation

Equation 16-17:
$$q_{\max,\min} = \frac{R}{A_{\text{cell}}} \left(1 \pm \frac{6e}{d} \right) + p_{\text{live}}$$

The live load is only now included because it should not be considered in overturning calculations, as it would act against overturning and cannot be counted on to be present in all cases. Substituting for all of the variables, the maximum foundation pressure $q_{\max} = 5117$ psf.

The factor of safety against bearing failure is $36881/5117 = 7.2$, which is more than satisfactory.

- Compute interlock force and select sheet piling.
 - The interlock force reaches its maximum at the sea bottom. To compute the lateral earth pressure, we use the at-rest condition. The lateral earth pressure coeffi-

cient is thus computed by Equation 4-13, or $K_o = 0.5$ for $\phi = 30^\circ$. The internal pressure at the ground line is given by the equation

Equation 16-18:
$$p_a = K_o (L_{\text{con}} \gamma_{\text{con}} + L_{\text{dry}} \gamma + h \gamma') + p_{\text{live}}$$

In this case, $p_a = 1625$ psf.

- The interlock tension is given by Equation 15-26. The radius $R = d/2 = 10'$. The interlock tension is thus $(1625)(10) = 16,250$ lb/ft = 1354 lb/in. A PSA 23 sheet pile can withstand this interlock tension; 46 pieces of this are required for a 19' 6-1/4" diameter cell.

Chapter Seventeen:

Corrosion and Protection

Anyone who works in a marine environment is aware that corrosion is one of the most important factors to consider in the long-term life of a structure. Corrosion is a factor for virtually any metal structure, or structure that contains metal (such as precast or prestressed concrete.) With sheet piling, corrosion concerns steel and aluminium sheet piling. Corrosion of aluminium sheet piling is discussed in *Pile Driving by Pile Buck*, available from Pile Buck; this chapter will discuss corrosion as it pertains to steel sheet piling.

17.1. Overview of Corrosion

The life expectancy of sheet pile structures will be strongly influenced by environmental factors. Among the natural influences that might affect the useful service life of steel sheet piling structures are damage from impact, overloading, storms, earthquake, abrasion and corrosion. In hostile surroundings when unprotected, metals lose thickness to corrosion, timber is attacked by biological organisms and rot, and concrete is vulnerable to weather and chemical damage. An understanding of these circumstances will allow the designer to make provisions for protection of his selected materials if necessary.

Corrosion is a natural electro-chemical action that affects all metals to one degree or another. The conditions necessary to initiate the process are moisture (the electrolyte), a conductor (the metal) and a difference in potential between areas of the metal. This last element could be something as simple as minute chemical or physical differences present in the metal or the environment but could also be caused by scratches, abrasions, galvanic couples, bacteria and other factors. The corrosion process has been compared to a battery in which there are two electrodes, an anode and a cathode. When connected, electrons flow from anode to cathode. The anode loses some of itself (corrodes) during the time the current is flowing and the cathode gains. It is in this same manner that anodic areas of metals corrode when these miniature batteries are in operation on their surfaces

Metals begin as ores in which they are combined with oxygen, silicates, sulphur and other elements. Iron, for example, is found in a number of minerals, the most important of which are magnetite and hematite. Magnetite (Fe_3O_4) is composed of 72% iron and 28% oxygen. Oxygen is removed during the refining process. As steel, the metal seeks to revert to its more stable form of ferrous oxide or rust. Rust is a product of the corrosion process. While rust may not be attractive, it is actually beneficial in that the deterioration slows considerably and sometimes ceases after the formation of a tight

coating of rust. The alloy “weathering steels” take advantage of this fact in achieving their exceptional performance in atmospheric applications. Even construction grade steels will develop a tight, uniform coating of rust in the atmosphere under the right set of conditions.

All metals are subject to corrosion activity unless otherwise protected by methods that will be discussed later. It must be understood therefore, that the important consideration is not whether steel will corrode, but in what form and at what rate. If the rate is low and cosmetic appearance is not a consideration, it is generally desirable to utilize sheet piling in its least expensive form that is bare and unprotected. If the environment is aggressive and the rate expected to be high, protective measures for some or all portions of the structure may be necessary.

Many factors influence the type and rate of corrosion. The presence of moisture is the most important element since it increases the electrical conductivity of the environment in contact with the metal surface. This will permit the flow of larger electrical currents and result in higher corrosion rates. Most steels if exposed to air with a relative humidity of less than 30% would show no signs of corrosion.

Oxygen is the other important element in the corrosion process. Free oxygen and oxidizing compounds stimulate the cathodic reaction by depolarisation in the presence of moisture. Variations in oxygen concentration on the metal at various depths form differential aeration cells and promote galvanic activity. Areas of low oxygen concentrations become anodic to areas of higher concentration.

Chlorides found in marine environments are the principal reason for the more aggressive attack on steel and other metals in seawater. They increase the electrical conductivity and thus the corrosion currents. They may form complexes with the metal products of corrosion, increasing the solubility of the metal ion and further stimulating corrosion.

There are many other potentially influential elements in the corrosion of metals that lie beyond the scope of this chapter. Our purpose is to outline the causes of corrosion, the situations where steel may need protection due to excessive rates, and the current methods of providing such protection²¹⁶.

17.2. Types of Corrosion in Steel Sheet Piling

17.2.1. Pitting Corrosion

Pitting corrosion is defined as a localised attack of a metal where the corrosion rate is substantially higher at some exposed areas than at others. Pitting corrosion may result in attack ranging from broad, shallow craters to deep holes.

²¹⁶A more detailed discussion of corrosion can be found in the *Handbook of Corrosion Protection for Steel Pile Structures in Marine Environments* from the American Iron and Steel Institute, Washington D.C.

vulcanhammer.net

Your complete
online
resource for
information on
geotechnical
engineering
and deep
foundations:

The Wave
Equation Page for
Piling

Geotechnical
Courses

Online books on
all aspects of soil
mechanics and
foundations

Free general
engineering and
geotechnical
software

And much more...

<http://www.vulcanhammer.net>

<http://www.vulcanhammer.org>
email me@vulcanhammer.net

<http://www.chet-aero.com>

Pitting is a localized attack and is generally associated with immersed piling in salt water. Pitting is serious in buried pipelines or tanks since a perforation will cause loss of the contents. Perforations of sheet pile structures are readily repaired and the loss of some fill is not serious.

Prestressing steel for tendons and tiebacks must be inspected for pitting, as heavy pitting in tendons can lead to a reduction in cross-sectional area and ultimately failure. Metal centralisers should be avoided, especially if the metal is anodic to the tendon.

17.2.2. Uniform Corrosion

Uniform corrosion is defined as corrosion that occurs at substantially the same rate over the entire exposed surface of a metal. When uniform corrosion occurs, very small electrochemical cells are established on the surface of the metal due to small differences in metal composition or the nonuniform nature of corrosion product layers that form on the surfaces. Corrosion of sheet piling takes the form of both uniform roughening of the surfaces and pitting. However, general, distributed loss of metal is of more interest, since this contributes to a reduction in the strength of the section and potential failure by overstressing. Corrosion resulting from exposure to the atmosphere and fresh water immersion is usually of the uniform type.

This form of attack can be evaluated in terms of loss of thickness, usually expressed in mils (0.001") per year. This value is often determined experimentally by measuring the weight loss of exposed specimens and calculating an equivalent uniform loss of thickness.

With tiebacks and tendons, uniform corrosion is commonly observed during storage on the construction site. It is generally not harmful to tendon performance if the heavy rust is removed prior to installation. Complete tendon derusting is not advised or necessary as overzealous scraping or abrasion may cause pitting.

17.2.3. Galvanic Action

Galvanic corrosion is defined as the accelerated corrosion of a metal due to electrical contact with a more passive metal. This is a classical example of the electrochemical cell in action. The anode is the corroding metal, while the cathode is a more passive metal. Current flows through an external circuit due to the difference in potential between the two metals. Coupling of dissimilar metals in a seawater structure will cause galvanic corrosion to occur on the anodic member while the cathodic member is rendered essentially inactive.

The potential difference between the two metals is best given by a listing of the metals in order of their activity in a common environment such as seawater. Since the actual measured potentials will vary with the actual conditions, a series, called the galvanic series is a relative listing and is usually given without actual potential values. The galvanic series for seawater is shown in *Table 17-1*.

Table 17-1: Galvanic Series for Seawater

ACTIVE END (Anode)	
Magnesium	
Zinc	
Galvanized Steel	
Aluminium Alloys	
Cadmium Coated Steel	
Mild Steel	
Alloy Steel	
Cast Iron	
Monel (Active)	
400 Series Stainless Steel (Active)	
Solder	
300 Series Stainless Steel (Active)	
Lead	
Tin	
Muntz Metal	
Manganese Bronze	
Naval Brass	
Yellow Brass	
Admiralty Brass	
Aluminium Bronze	
Red Brass	
Copper	
Silicon Bronze	
Copper-Nickel 90-10	
Copper-Nickel 70-30	
G-Bronze	
M-Bronze	
Silver Solder	
Monel (Passive)	
400 Series Stainless Steel (Passive)	
300 Series Stainless Steel (Passive)	
Silver	
Inconel 625	
Titanium	
Graphite	
Gold	
Platinum	
PASSIVE END (Cathode)	

The metals at the active end of the series will act as an anode when coupled to a metal below them in the series or towards the passive end. Corrosion of the more passive metal in the couple is usually reduced.

In marine pile construction, fasteners, welds, splash zone sheathing and fittings are sometimes fabricated from metals other than plain carbon steel. In such cases, if these metals are cathodic to the pile and are of small area relative to the pile surface area, little acceleration of corrosion will occur on the adjacent anodic pile surface and the cathodic metals would

be unaffected. If the reverse situation existed, where a small anodic fitting is attached to the cathodic pile, rapid destruction of the fitting would occur.

One special form of galvanic action that is important with sheet piling takes place with mill scale. Mill scale is the tightly adherent scale that forms on hot-rolled structural members. Upon cooling, numerous small cracks develop exposing the base steel. Exposure in seawater results in an active galvanic cell in which the vulnerable small exposed steel assumes the anodic role and corrodes by forming pits. The surrounding intact mill scale assumes the cathodic role in this galvanic cell. Over the short-term, pit depth exceeds the normal corrosion rate; however, over the long term stabilization develops.

17.2.4. Stray Current Corrosion

Direct current from external sources around marine construction can cause accelerated damage to piles if such current is collected by the structure and leaves to enter the electrolyte. Direct current from improperly grounded welding generators, ship service systems, nearby cathodic protection systems and electric railway systems can cause stray current corrosion damage to ungrounded structures in a harbour area. One ampere of direct current passing from a structure to the seawater will remove approximately 20 pounds of steel in one year. Alternating stray currents are of little or no consequence.

It is essential that stray direct currents be eliminated at their source or that the structure be properly grounded to the negative return leg of the stray current source. With tendons and tiebacks, the designer should review plans to determine the special areas of possible stray currents. In areas where this is a problem, the tendons should be encapsulated with a corrugated grout-filled plastic tube.

17.2.5. Fatigue Corrosion

Fatigue corrosion is the accelerated failure of metal under the combined effects of corrosion and repeated or cyclical stress. Another way of defining fatigue corrosion is the reduction of the air fatigue resistance of a metal by a corrosive environment. Various factors related to stress such as mode, magnitude, duration and frequency, in addition to the environmental factors affecting corrosion, tend to complicate the process. The effect of corrosion on fatigue is essentially to eliminate the characteristic air fatigue limit. In the design of marine structures, the designer must anticipate fatigue loading so that preventive measures can be taken to avoid future difficulties.

Static stresses, whether applied or residual internal stresses, in combination with corrosion culminate in cracking known as stress-corrosion cracking. Stress-corrosion cracking is not a serious problem for typical steel used in piling applications.

17.2.6. Bacteria and Fouling

Anaerobic bacteria are potential, though unlikely source of accelerated corrosion at or near the mud line. The origin of this pollution is usually a broken sewer or illegal discharge. Certain oxygen deficient soils containing sulphates can harbour bacteria which convert and sulphates to sulphides. Combined with hydrogen generated at the cathode, they accelerate the corrosion proceeding at the anodic surface.

In marshy land containing acidic soils, the designer should consider the possibility of accelerated corrosion of the tendons and tiebacks. As with stray current corrosion, a tendon or tieback should be encapsulated with a corrugated, grout-filled plastic tube.

Fouling is the result of a variety of plants and animals that attach themselves to marine structures. While dense, uninterrupted growth can protect steel structures by restricting the oxygen reaching the surface, severe but localized corrosion can occur from the presence of biological organisms such as barnacles and worms.

17.3. Corrosion Environments

The sheet pile designer is usually concerned with one of two separate environmental situations: Coastal Marine Environments and Non-Marine Environments. On the other hand, coastal marine environments can be quite hostile to many types of materials utilized for piling and this possibility should be examined and allowances made. Moreover corrosion in each of these environments takes place in three different zones: atmospheric zone, immersed and semi-immersed zone, and buried zone.

A great volume of data has been collected from both controlled testing and in service measurements in many varied locations and environments. Reference to some of this will give the designer insight regarding the life expectancy of his or her structure. Test data is strongly influenced by local conditions, sample sizes and shape, and evaluation methods. The data should be clear as to whether it is based on weight loss or pitting measurements (weight loss is more meaningful). Many test panels have two sides exposed, while sheet piling bulkheads are exposed one side. Such data should be halved. Designers should use published average rates or actual data as a guide rather than as an indication of what actual rates might be. Local experience provides the most meaningful data.

17.3.1. Non-Marine Environments

Land-sited sheet pile structures and those exposed to fresh water generally enjoy very low corrosion rates that insure their longevity in service. Steel sheet piling structures well over sixty years old are common in the Great Lakes and along fresh water inland rivers²¹⁷. Most texts do not dwell on this subject but proceed on to the more serious question of corrosion in salt-water marine environments.

²¹⁷There may be a few exceptions to this general statement that will be explained subsequently.

17.3.2. Coastal and Marine Environments

Saltwater marine environments are potentially hostile to most construction materials including steel. The presence of chloride ions in the water greatly stimulates the corrosion process. Wind and waves combine to provide oxygen and moisture for an electro-chemical reaction and abrasion may remove any protection rust film. Not all salt-water environments are dangerously aggressive to steel, and not all areas of the piling are attacked at the same rate. There are five distinct areas of corrosion activity on steel piles in seawater:

- Atmospheric Zone
- Splash Zone
- Tidal Zone
- Continuously Submerged Zone
- Soil (Buried) Zone

17.3.2.1. Corrosion Rates by Zone

The corrosion rates on steel piling surfaces normally vary considerably by zone. The corrosion rate profile for steel sheet piling, averaged for several harbour installations, is shown in Figure 17-1. The varying corrosion loss indicated in each zone is the average of eight harbour installations after 19 years' exposure. In general, the maximum reduction in metal

thickness occurs in the splash zone immediately above mean high water level. A significant loss usually occurs a short way below mean low water in the continuously submerged zone.

With the exception of those few cases where scour is a factor, the least affected zone is usually found below the mud line, with higher losses at the water-mud line interface. Another low loss area exists in the tidal zone about halfway between mean high water and mean low water levels.

Where steel sheet piling is exposed to water on one side, the average corrosion rate varies from 1 to 4.5 mils per year (mpy), reaching maximums of 3 to 14 mpy. Where steel sheet piling is exposed to water on both sides, the total rate of corrosion of the member is doubled. Pitting will cause localized corrosion attack at 1.5 to 3 times the average rates over an extended exposure period.

17.3.2.2. pH Value

The pH (degree of acidity or alkalinity) of seawater is almost a constant, ranging narrowly from 7.2 to 8.2. A pH value below 7 is acidic, and above 7 is alkaline. In harbour waters containing pollutants, the pH may vary somewhat, but over the mid-range, the corrosion rate of steel is almost constant.

17.3.2.3. Salinity

Water in the open sea has a salt content of about 3.5 percent. In unpolluted harbours and other seacoast locations dilution occurs with fresh water runoff, but the proportions of the various salts relative to each other remain virtually the same. Of the various ions in seawater resulting from dissolved salts, the chloride ion is the most significant because of its large concentration. The chloride ion is able to penetrate protective films formed by corrosion products to cause localized corrosion. Its presence also influences the solubility of oxygen in the water. From Figure 17-2, which is a plot of corrosion rate and dissolved oxygen versus salinity, it can be seen that the corrosion rate increases with increasing salinity until it reaches a peak of about 1% NaCl and then decreases with increasing salinity. Corrosion increases with increasing salinity until it reaches a peak at about one percent sodium chloride and then decreases with increasing salinity. Significantly, the amount of dissolved oxygen is constant up to the one percent sodium chloride concentration and then begins to drop off markedly with increasing salinities.

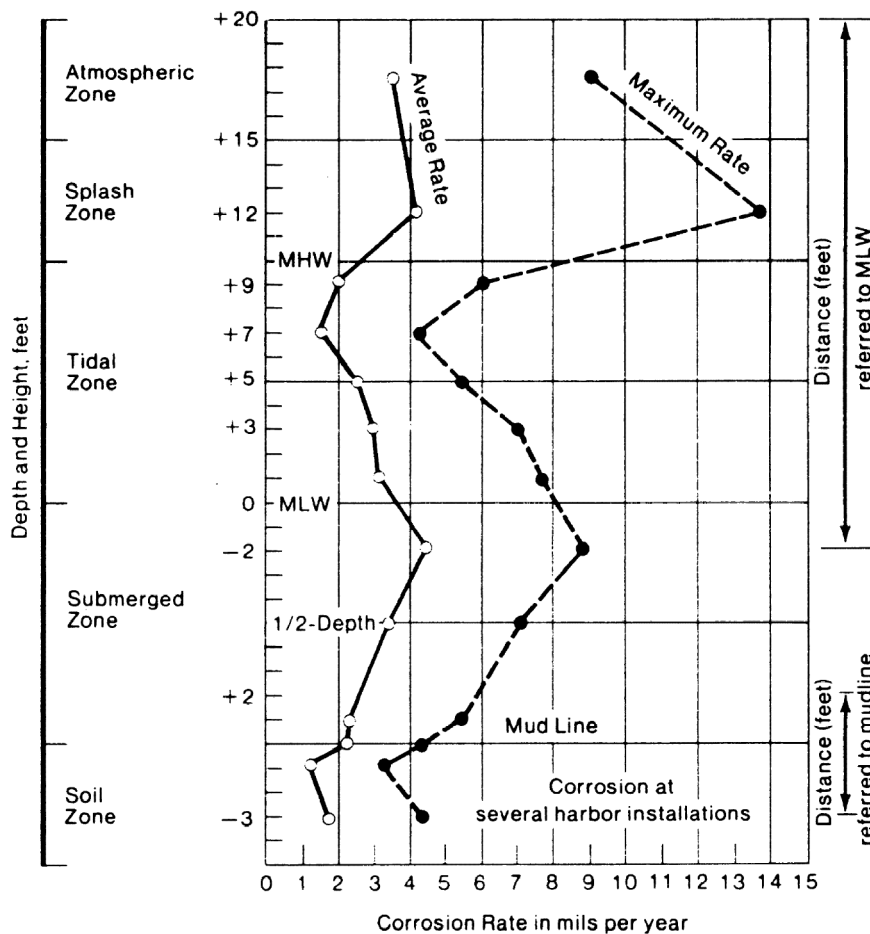


Figure 17-1: Corrosion Rate Profile of Steel Sheet Piling 218

²¹⁸Edwards, WE. (1963) "Marine Corrosion: Its Cause and Care." *Proceedings of the Eighth Annual Appalachian Underground Corrosion Short Course*, Technical Bulletin No. 69, p. 486.

HPSI Vibros



from a
"Little Guy"

to a
"BIG Guy"



Whether it's an excavator mounted vibratory for driving lightweight vinyl or aluminum sheet piling on up to a 20,000 in. lb. machine for driving large diameter caisson, we have a vibro suitable for your job.

SALES & RENTALS

(Distributors throughout North America)

From "The Engineers of Pile Driving Equipment"™

HYDRAULIC POWER SYSTEMS, INC.

Kansas City Offices and Plant
1203 Ozark
N. Kansas City, MO 64116
Phone (816) 221-4774
Fax (816) 221-4591
E-mail info@hpsi-worldwide.com
<http://www.hpsi-worldwide.com>



International & Domestic Sales
745 U.S. Hwy 1
N. Palm Beach, FL 33408
Phone (561) 687-5525
Fax (561) 841-3479
E-mail info@hpsi-worldwide.com
<http://www.hpsi-worldwide.com>

*Vibratory Pile Hammers • Hydraulic Augers • Winch Systems
Custom Manufacturing • Hydraulic Impact Hammers • Lead Systems*

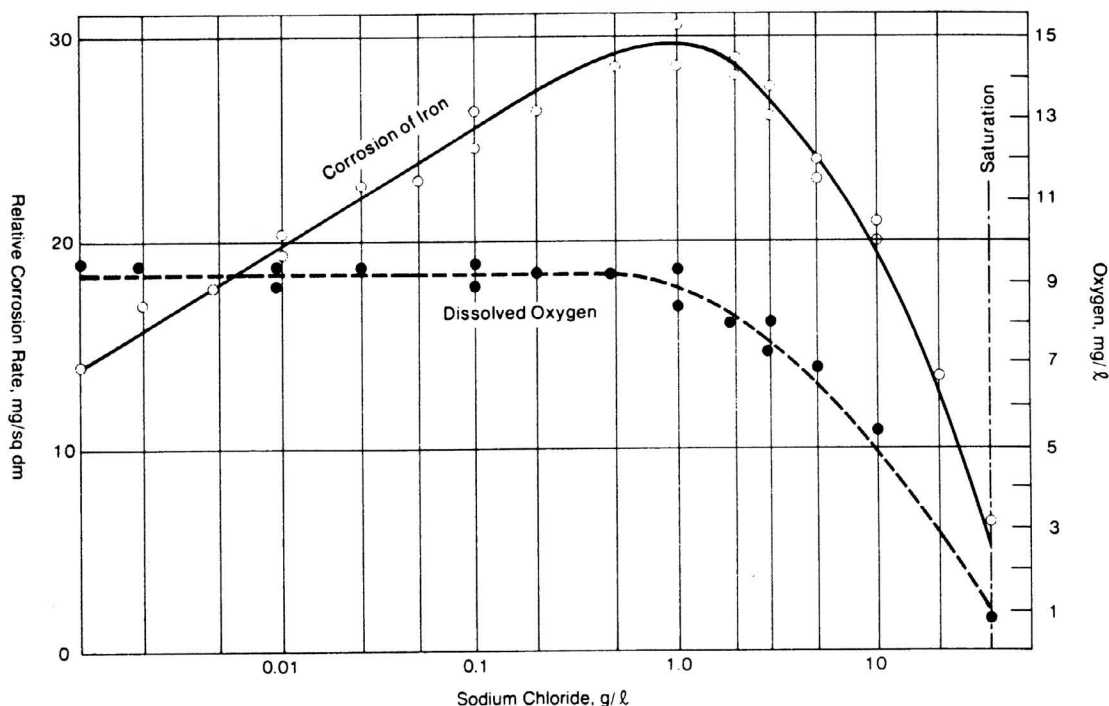


Figure 17-2: Variation in Corrosion of Iron as a Function of Salinity²¹⁹

This graph also illustrates that fresh water and seawater are not as aggressive as brackish waters containing 0.1 percent chloride ion concentration.

17.3.2.4. Pollution

Pollution in harbours may include anything from domestic sewage to complex industrial waste, oil well brines and spilled oil. Pollution generally causes harm to biological species by its toxic effect or by depletion of the dissolved oxygen. The destruction of the oxygen-dependent fouling organisms in seawater may alter corrosion rates unfavourably by permitting the survival of anaerobic bacteria. Contaminants that reduce pH or introduce sulphides locally at the site of the piles increase the corrosion rate of steel. Oil contamination, although hazardous to marine animals, can provide partial corrosion protection by coating the metal structure in the splash and tidal zones.

17.3.2.5. Wind

Wind can whip up wave action and carry salt-laden mist to deposit on the structure. The residue of dried salt, being hygroscopic, can attract moisture and continue the corrosion action.

17.3.2.6. Rain

Rain exerts a washing action; however, where it is retained in crevices, it can stimulate corrosion by maintaining damp conditions.

17.3.3. Atmospheric Zone

The rate of corrosion of bare structural steel in an urban or rural atmosphere depends on the length of time moisture is in contact with the surface, the extent of contamination in the air, and the chemical composition of the steel. *Table 17-2* illustrates the influence of local environmental conditions on relative corrosion rates.

It will be seen that the rate for a rural location is many times that of the arid location, and that the rate increases for the industrial sites and as we near the ocean. *Figure 17-3* compares the uniform loss rate in an industrial environment to those in a marine environment for a variety of alloys.

This shows the influence of alloy additions to carbon steel. Designers contemplating a sheet pile wall where appearance is important may wish to discuss the application of alloy steel with their supplier.

17.3.3.1. Fresh Water

In fresh water, the rates of loss in the atmospheric area are very low. However, designers should be aware of special situations, such as where the steel is continually moist, where it would be exposed to chlorides, sulphurous compounds, or a combination of these situations. In these cases, some protection in the form of paint or coating might be beneficial.

17.3.3.2. Salt Water

Marine corrosion rates can be influenced significantly by distance from the ocean, rainfall, sunshine, and fog. At Kure

²¹⁹Fink, FW. (1960) "Corrosion of Metals in Seawater," U.S. Department of Interior, Office of Saline Water, Report No. 46.

Table 17-2: Relative Corrodibility of Atmospheres at 20 Locations throughout the World

Location	Type of Environment	Relative Corrodibility
<i>Khartoum, Sudan</i>	Dry inland	1
<i>Abisco, North Sweden</i>	Unpolluted	3
<i>Aro, Nigeria</i>	Tropical inland	8
<i>Singapore</i>	Tropical marine	9
<i>Basrah, Iran</i>	Dry inland	9
<i>Apapa, Nigeria</i>	Tropical marine	15
<i>State College, PA</i>	Rural	25
<i>South Bend, IN</i>	Semi-rural	29
<i>Berlin, Germany</i>	Semi-industrial	32
<i>Llanwrtyd Wells, U.K.</i>	Semi-marine	35
<i>Kure Beach, NC</i>	Marine	38
<i>Calshot, U.K.</i>	Marine	41
<i>Sandy Hook, NJ</i>	Marine, semi-industrial	50
<i>Congella, S. Africa</i>	Marine	50
<i>Kearny, NJ</i>	Industrial-marine	52
<i>Motherwell, U.K.</i>	Industrial	55
<i>Vandergrift, PA</i>	Industrial	56
<i>Pittsburgh, PA</i>	Industrial	65
<i>Sheffield, U.K.</i>	Industrial	78
<i>Frodingham, U.K.</i>	Industrial	100

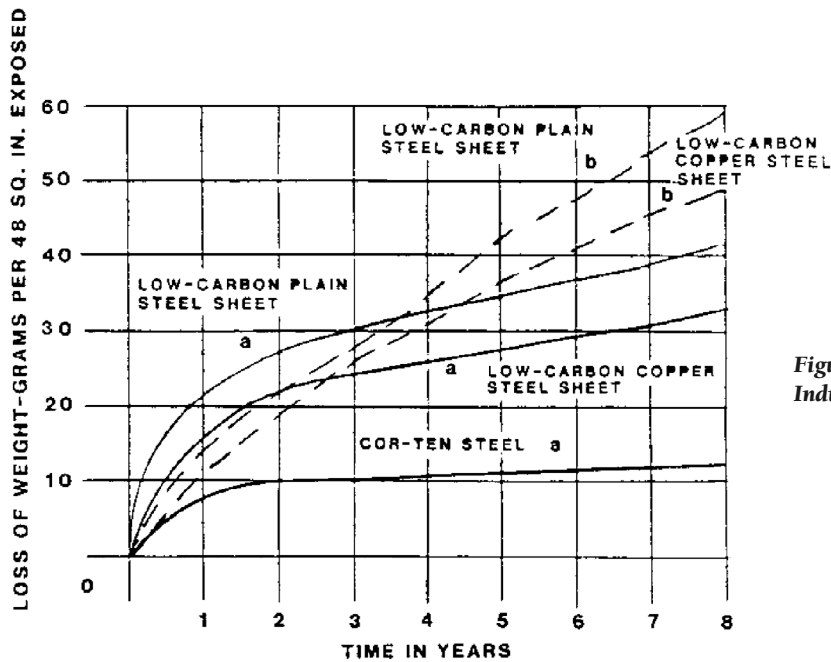


Figure 17-3: Time-corrosion Curves for Industrial and Marine Atmospheres

(a) INDUSTRIAL ATMOSPHERE
 (KEARNY, N.J.-2 MILES FROM JERSEY CITY)
 (b) MARINE ATMOSPHERE
 (KURE BEACH, N.C.-250 YARDS FROM OCEAN)

Beach, North Carolina, there is a tenfold difference in corrosivity at the beach compared to a location 800 ft. landward²²⁰. At Pt. Reyes, California the test specimens were elevated some distance above the ocean, where there is daily fog but little rainfall. The time of wetting of the surface and the amount of chlorides in the atmosphere are the most important factors in marine atmospheric corrosion.

As Table 17-2 illustrates, structures built in the ocean or along the beach will experience very high rates of corrosion in the atmospheric zone, whereas bulkheads built some distance from the beach enjoy rates that are more favourable.

17.3.4. Immersed and Semi-Immersed Zone

17.3.4.1. Fresh Water

Steel has enjoyed many years of successful application in sheet piling structures in relatively clean fresh water. Unless extremely thin sections are proposed, or an extended long life span is required, steel piling needs no further protection. Lacroix et. al. suggest average corrosion rates of 2.5 mils per year to consider in design²²¹. Others describe rates of from 2 to 5 mils per year for the first several years, after which the rate decreases to an insignificant amount.

Fresh water generally has a chloride count of less than 1000 ppm and a pH close to neutral. As time passes, a thin, natural protective coating builds on immersed steel that serves to virtually stop further deterioration after the first few years. Fresh water that carries granular materials at high velocities might provoke higher corrosion rates since the natural coating could be affected. Localized pollution from sewage or chemicals would also be a source of concern if the situation were long standing. Alloying additions have no effect on the corrosion rates of immersed steel, the rate being approximately the same for all grades (except stainless steel).

17.3.4.2. Salt Water

17.3.4.2.1. Splash Zone

Numerous tests and surveys have been reported which show the area of steel piling at and immediately above the high tide line and subject to frequent wetting from splashing water to be the zone of most serious corrosion activity. Rayner and Ross²²² reported rates as high as 63 mils per year for steel groins subjected to two-sided attack. The *AISI Handbook of Corrosion Protection for Steel Piles in Marine Environments*²²³ suggests a rate of 10 mils per year. The U.S. Navy²²⁴ took coupons from existing structures in both northern and semi-tropical locations as shown in Table 17-3. Some of these installations had received a protective coating and some others were cathodically protected. However, the general Navy

Table 17-3: Corrosion Rate of Sheet Piling at Various Locations

Piling Location	(mils per year)							
	Boston	Norfolk	Key West	Coco Solo	Puget Sound	Alameda*	San Diego*	Pearl Harbor
Splash Zone Above Mean High Water	2	3	10	10	5	3	7	4
Tidal Zone	1-2	1	1-2	1	2	2-5	8	1
Two Feet Below Mean Low Water	6	8	4	5	5	—	—	5
Below Mud Line	4	2	3	2	2	0.5	10	2

conclusions agreed with that of previous researchers regarding the splash zone.

Figure 17-4 is a nine-year comparative test of two sheet-piling steels at Wrightsville Beach, North Carolina. The test strips were exposed to attack on two sides but illustrate the usual pattern of attack in the various zones including the splash zone.

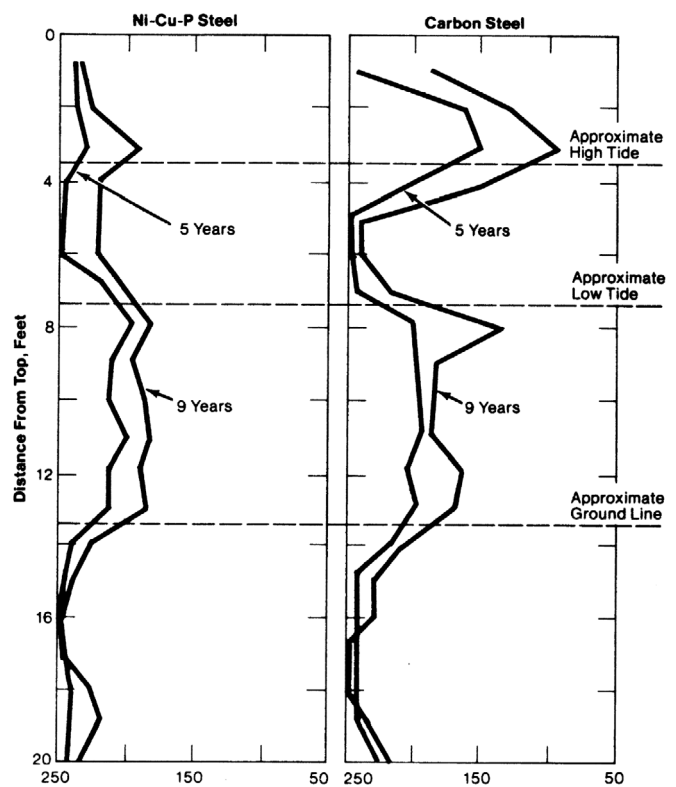


Figure 17-4: Comparative Corrosion of Two Types of Steel in a Marine Environment

²²¹Lacroix, Y., Esrig, M. I., and Luscher, U. 1970 (Jun). "Design, Construction, and Performance of Cellular Cofferdams," "Lateral Stresses in the Ground and Earth Retaining Structures," Journal, Soil Mechanics and Foundation Division, American Society of Civil Engineers, Specialty Conference, Cornell University, Ithaca, New York, pp 271-328.

²²²Raynor, A.C., and Ross, C.W. (1952) "Durability of Steel Sheet Piling in Shore Structures." Technical Memorandum No. 12, Beach Erosion Board, U.S. Army Corps of Engineers, February.

²²³Handbook of Corrosion Protection for Steel Piles in Marine Environments. (1981) First Edition. Edited by T. Dismuke, S.K. Coburn and C.M. Hirsch. Washington, DC: American Iron and Steel Institute.

²²⁴Ayers, J.R. and Stokes, R.C. (1961) "Corrosion of Steel Piles in Salt Water" Proceedings of the American Society of Civil Engineers, Journal of Waterways and Harbors, 87, No. 3, 95.



INTERNATIONAL

**More Locations.
More Equipment.
More Support.**

Same Local Service.

Our expanding, easy-to-work with network of servicing dealers and exceptional parts and service support keeps your drilling job right on schedule. You've got the power to take your operation to the next level of productivity and profit. For unstoppable support on a local level, get the IMT advantage.



**For Product Support Coast to Coast
Call (561) 683-2015 ext. 179**



KELLY TRACTOR



**ATLANTIC &
SOUTHERN**
EQUIPMENT, LLC

Ayers and Stokes describe the high rate in this area as due to thin films of electrolyte in the form of salt water and saturated with oxygen collects on the surface of the piling throughout the tidal zone. Between this wetted area and the immersed area, corrosion cells are produced by the differing oxygen concentrations. The metal underwater is anodic to the exposed area, and the corrosion rates are intense because of the short electrical paths. This high rate continues because of the constantly changing anodic and cathodic areas during the tide changes.

17.3.4.2.2. Tidal Zone

Surprisingly, tests indicate relatively low corrosion rates in the tidal area, generally in line with rates found in the immersed zone. The explanation for this is that this area is also immersed at least part of the time, furthermore the metal in this zone benefits from being cathodic to the metal just below low tide where a secondary high corrosion rate is generally found.

17.3.4.2.3. Continuously Submerged Zone

A corrosion rate of 5 mils per year is commonly used as a guide for carbon steel in seawater. However, Schmitt and Phelps²²⁵ point out that this rate was arrived at from short-term tests, and that longer term testing indicates the rate drops considerably with time, to values below 5 mpy. The rates are generally found to be initially high but after a few years level off to a long-term average of 1 to 3 mpy. In Ayers and Stokes, corrosion rates in the immersed sections of the marine structures were among the lowest rates recorded. For example at the Naval Station, Coco Solo Canal Zone, 77% of the metal at half-depth remained after 24 years exposure. At Norfolk, Virginia about 84% remained at half-depth. However, the rate in the splash zone reached 17 mpy. Actually, the exposure at the eight locations checked ranged from 13 to 27 years and the only location where less than 80% of the metal remained at half-depth was the Coco Solo installation. Obviously, it is the shortage of dissolved oxygen at the water metal interface that is responsible for the low corrosion rate in the immersed zones of both salt and fresh water and not the salinity of the solution.

17.3.5. Buried Zone

Structures built of steel sheet piling obtain a good part of their stability from embedment into sound, natural soil. Some walls are driven into pre-existing soil, and then excavated on one side to create the final structure. Others are driven, and then backfilled with dredged or trucked-in fill soil. There are therefore two separate situations to be considered (1) that of steel embedded in natural undisturbed soil, and (2) that of steel in contact with backfill.

At one time, it was assumed that embedded steel piling was vulnerable to the same potential corrosion as a buried pipeline. In this instance, soil resistivity and pH are measured and if found to be low, pipelines are coated and provided with cathodic protection. Corrosion on pipelines tends to be a pitting type rather than uniform and pitting is generally not a problem with sheet piling. Typical corrosion rates for various types of soil are shown in *Figure 17-5*.

The National Bureau of Standards had participated in studies of pipeline corrosion and they transferred this information to all buried steel. When extractions of driven steel piling seemed to indicate strongly differing information, the Bureau launched an investigation into the reasons²²⁶. The Bureau conclusions were based on data from 19 different sites where samples from existing piling could be obtained. The piles had been in service from 7 to 40 years. While no specific average rate was found for these undisturbed zones, corrosion was described as insignificant and of no importance, regardless of the composition of the soil. Their conclusions differentiate between steel piles driven into "undisturbed", natural soils and pipelines backfilled with "disturbed" soil. The Bureau's investigator attributes the difference in performance to the oxygen content of disturbed soils and the lack of oxygen in undisturbed soil.

17.3.5.1. Disturbed Soil

The question of disturbed soils in non-marine environments was addressed by the Bureau of Standards in their 1962 report and a subsequent supplemental report. Corrosion rates in filled ground range from negligible to a 40 percent reduction in thickness after 37 years exposure. Those samples that lost some section did so just above and in the shallow zone affected by water table fluctuations. Most of the corrosion rates measured were insignificant and it is well known that the rate of corrosion slows as soon as the steel takes on its film of corrosion products. Sand fill is particularly protective as it forms a coat of ferrosilicate with the steel that is an impervious, insoluble film.

Fill soils that contain new deposits of cinders or soils contaminated with salts are to be avoided or the steel protected in these exposed areas.

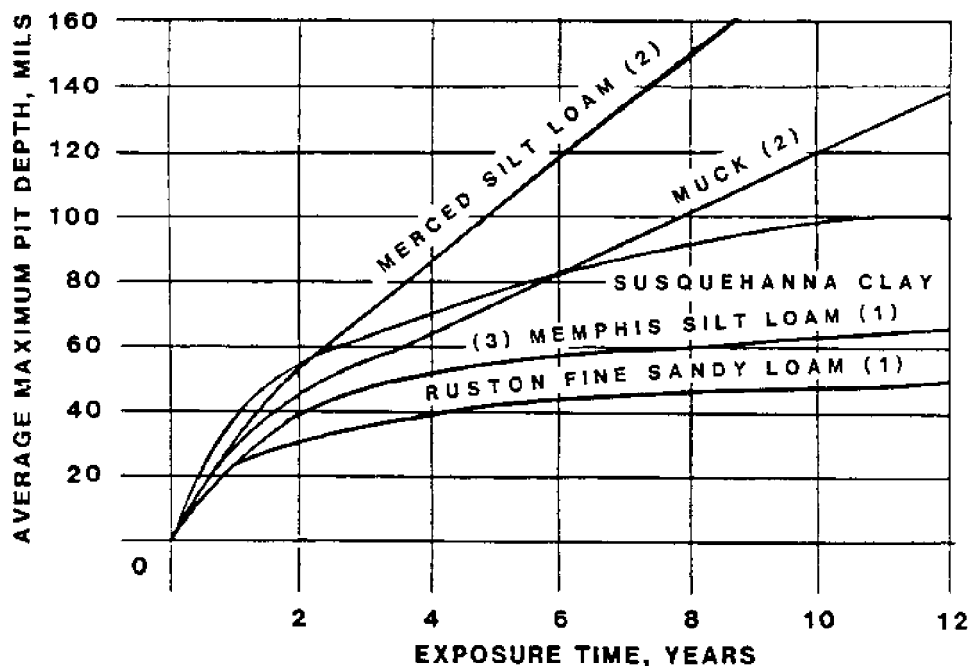
17.3.5.2. Salt Water

Corrosion rates of steel piles embedded in natural soils are insignificant averaging in the range of zero to 3 or 4 mils per year. This is in line with the findings described by the Bureau of Standards and others for these exposures.

A differential aeration cell occurs at the mud line because of the relatively lower oxygen content below this elevation. Some higher rates are found in this area, as the steel is anodic to the steel above. However, these rates are generally less

²²⁵Schmitt, R.J., and Phelps, E.H. (1969) "Corrosion Performance of Constructional Steel in Marine Applications." *Proceedings of the Offshore Technology Conference, Houston, Texas*. Dallas, Texas: Offshore Technology Conference.

²²⁶Romanoff, M. (1962) "Corrosion of Steel Pilings in Soil." *Journal of Research, National Bureau of Standards*, 66C, July-September.

**NOTE:**

- (1) WELL DRAINED SOILS
- (2) POORLY DRAINED SOIL OF LOW RESISTIVITY
- (3) MATERIALS USED IN TEST WERE CARBON STEEL, WROUGHT IRON AND CAST IRON

Figure 17-5: Time-Corrosion Curves for Soils

than will be found in the tidal zone.

The question of aerated dredged or dumped backfill and a fluctuating water table behind steel bulkheads needs to be addressed. The quality of backfill placed behind an engineered bulkhead is an important consideration in the design. Invariably a clean sandy fill is specified with final density approaching that of natural, in place soils. The sand itself forms a protective deposit on the back of the steel over a period. The restriction of free oxygen in the fill in turn limits the potential attack which can take place in this zone. The exception to this might be where porous fill such as coral is used as fill, or in the exceptional case of polluted or organic materials placed as part of a mixed group of fill material.

17.4. Design for Protection of Steel Piling In Marine Environments

17.4.1. Methods for Protecting Steel Piling

The necessity of providing protection for sheet piling depends on the combined factors of environment, desired life, and material selection.

Temporary structures as a class can generally be installed without further regard for protection. Installations on land and in fresh water enjoy relatively low rates of corrosion and

it would be unusual to find cases where protective measures would be required. The exception might be the case of light-weight sheet piling, some sections of which provide only about 100 mils of thickness. At a uniform rate of 2 mils per year these sections could reach half-section in 25 years. Most manufacturers of "gauge piling" also offer them with a hot-dipped galvanized coating. Based on the discussion in previous paragraphs, there are areas of steel piling destined for marine environments that may require some protection from one or a combination of methods.

17.4.2. Sacrificial Metal

The case either in favour or against utilizing thicker piling as a hedge against anticipated corrosion losses is not clear since it involves so many unrelated factors. These include the present and replacement cost of steel, coatings, cathodic protection, the extent and type of attack, the accuracy of corrosion data, the reliability of the protective systems and the desired service life of the structure.

In general, the sacrificial metal method has been considered uneconomical and less positive than coatings and/or cathodic protection that can reduce losses to zero, at least for the term they are in operation. In other cases protection is

required only for a relatively small area in the lower tidal and splash zones while the extra weight extends over the entire wall.

In some cases where extra material has been designed into the sheeting, it has been one to obtain 75 to 100 years life on civil works projects, often in combination with coatings and cathodic protection.

The U.S. Navy will specify 1/2" material for the exposed areas and regular 3/8" thickness for the interiors of cellular bulkheads. When interlocks are stressed a maximum of 8000 lbs./in., webs are stressed at 21,300 psi and 16,000 psi respectively, providing a large initial factor of safety against tension failure. The added cost for the heavier material is only about 14% for a 33% increase in thickness (the interlocks of both foot-weights are identical). The added cost overall is only increased about 4%. The 125 mils of metal could be a relatively good buy under these circumstances, even if combined with supplemental protective measures.

Sheet pile beam walls seem to offer a variable opportunity for utilizing heavier sections against corrosion losses. Historically, supplemental protection has been selected almost without exception. In seawater, doubling the weight and the cost to gain a few years extra life of a lightweight section and utilizing the added metal to protect a few feet of splash zone is not practical. However, if a problem exists in the immersed zone where bending moments are highest, there may be some situations where metal will be more economical than coatings.

Example 29: Sacrificial Metal Requirements

An anchored sheet pile bulkhead wall is to be built in an aggressive marine environment.

The maximum bending moment is 725,000 inch-pounds, which is exactly satisfied by a PZ 27 section.

- o $t_{flanges} = .375$
- o $t_{web} = .375$
- o $S = 30.2 \text{ in}^3$
- o ASTM A-328 Grade steel ($F_s = 39,000 \text{ psi}$ $F_y = 24,000 \text{ psi}$)
- o Steel is estimated to cost 35 cents per pound delivered.

- The sheets will be 50' long with 15' embedment.
- Corrosion rates are estimated as follows:
 - o 5 mpy in the atmospheric and immersed zones
 - o 10 mpy in the splash and lower tidal zones
 - o 2 mpy in the tidal and embedded zones.
- A reliable coating with estimated useful life of 20 years is available at \$2.00 per square foot. It is proposed to coat from the top of wall to the mud line, one side or 35'.

Compare coated PZ 27 with an alternate of a heavier section without coating.

- First Cost per 100 linear foot of wall PZ-27, Section o $50' \times 100' = 5000 \text{ sq. ft.} \times 27\#/\text{sq. ft.} = 135,000\# \times .35 = \$47,250$ o 100' divided by 1.5' = 67 pcs. $\times 35' = 2345 \text{ lf}$

$\times 2.25 \text{ sq. ft./ft.} = 5276 \text{ sq. ft. coated one side} \times \$2.00 = \$10,550$ for coating.

o Total cost coated PZ 27/100 ft. wall = \$57,800.

There are a number of Z-type sections available with flange thickness of .500" or more. For the purpose of this comparison, we will only consider PZ 35 having the following properties:

- PZ 35
 - o Wt. = 5 psf
 - o $t_{flanges} = 0.600"$ (600 mils)
 - o $t_{web} = 0.500"$ (500 mils)
 - o $S = 48.5 \text{ in.}^3/\text{ft. wall.}$
- First Cost per 100 lf of Wall PZ 35 Section
 - o $50' \times 100' = 5000 \text{ sq. ft.} \times 35 \text{ psf} = 175,000\# \times .35 = \$61,250.$

At this stage, the coated PZ 27 is cheaper by about 6%.

A Z-type bulkhead theoretically loses metal at a uniform rate from the outside of one flange, the inside of the opposite flange and one side of the web. The change in section modulus due to the loss of area is almost directly proportionally to the percentage of loss. Therefore, a rough approximation of the new section modulus can be made from percentage losses.

After twenty years, the coating is no longer effective but the steel has maintained its full section (assuming no losses on the back side). The coating has cost \$10,550 over twenty years \$10,550 divided by 5000 sq. ft. divided by 20 years or .105 cents per sq. ft. per year. The PZ 35 losing section uniformly at the rate of 10 mils per year would reduce to the PZ 27 section modulus of 30.2 in.³/ft. after a period of $48.5/30.2 = 140\% - 100\% = 40\%$ reduction in flange thickness. The original thickness was .600" (600 mils) so at the rate of 10 mpy, this would occur in $.40 \times 600$ divided by 10 = 24 years. The sacrificial metal has cost \$61,250 - 47,250 = \$14,000 divided by 5000 = \$2.80 divided by 24 years = .116 cents per sq. ft. At this stage, the sacrificial metal approach is about 10% higher than the coating method for the first twenty years. However, it is at this time that the superior original section modulus of the PZ 35 becomes an important factor.

The underwater deterioration that will result in stresses reaching the yield point of the steel (39000 psi) will occur when the section modulus declines to 725,000 divided by 39,000 = 18.6 in.³/ft. This would occur when the now bare PZ 27 flanges thin by about 18.6 divided by 30.2 = 40%. The original flanges are .375" thick (375 mils) so at the rate of 10 mpy this would occur in $375 \times .40$ divided by 10 = 15 years. The total life of the PZ 27 with coating in $20 + 15 = 35$ years.

The total period for the PZ 35 to reduce to an equivalent section modulus of 18.8 is calculated from 18.8 divided by 48.5 = 62% loss. $.62 \times 600 = 372 \text{ mils}$ divided by 10 mpy = 37.2 years total.

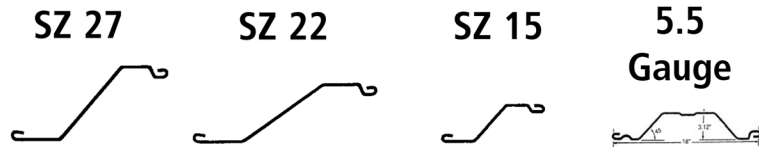
The total annual cost for the coated piling is 57,800 divided by 5000 divided by 35 years = .328 cents per sq. ft.; for the PZ 35 61,250 divided by 5000 divided by 37 years = .331 cents per sq. ft.

SHORELINE STEEL, INC.

P.O. Box 480519, 58201 Main Street • New Haven, MI 48048
(800) 522-9550 • (586) 749-9559 • Fax (586) 749-6653

www.shorelinesteel.com

We are a leading producer of domestic cold formed steel sheet piling in sections ranging from 10 gauge to 3/8" thick. For any sheet piling requirement we can satisfy your needs with a top quality product and prompt delivery.



	Thickness (Nominal)	Weight (Sq. ft.)	Weight (Lin. Ft.)	Sec. Mod in ³ (Ft. Wall)	Moment of Inertia in ⁴ (Ft. Wall)	Laying Width	Wall Depth
10-10 ga.	.134	7.2	10.8	2.2	3.5	18.00	3.12
8-8 ga.	.164	8.8	13.2	2.62	4.2	18.00	3.12
7-7 ga.	.179	9.6	14.4	2.8	4.4	18.00	3.12
6-6 ga.	.194	10.5	15.8	3.0	4.9	18.00	3.12
5-5 ga.	.209	11.3	16.9	3.4	5.4	18.00	3.12
LZ 8	.164	8.3	17.2	3.6	8.1	25.00	4.50
LZ 7	.179	9.1	18.8	3.9	8.9	25.00	4.50
LZ 5	.209	10.6	21.9	4.6	10.4	25.00	4.50
LZ 3	.239	11.9	24.6	5.2	11.8	25.00	4.50
LZ 250	.250	12.3	25.6	5.4	12.4	25.00	4.50
SZ-10	.164	9.4	17.2	7.3	27.4	22.00	7.50
SZ-11	.179	10.3	18.8	7.9	29.8	22.00	7.50
SZ-12	.209	12.0	21.9	9.2	34.8	22.00	7.50
SZ-14	.239	13.5	24.6	10.4	39.9	22.00	7.50
SZ-15	.250	14.0	25.6	10.9	41.8	22.00	7.50
SZ-14.5	.250	14.5	32.4	13.0	61.49	26.75	9.46
SZ-14.5	.270	15.8	35.1	14.0	86.40	26.75	9.46
SZ-18	.312	18.1	40.4	16.2	76.83	26.75	9.46
SZ-20	.340	19.8	44.1	17.5	83.37	26.75	9.46
SZ-21	.350	20.3	45.3	18.1	86.00	26.75	9.46
SZ-22	.375	21.8	48.6	19.3	91.92	26.75	9.46
SZ-222	.312	22.1	40.4	26.7	163.09	22.00	12.25
SZ-250	.250	15.9	32.4	16.6	89.42	24.46	10.75
SZ-313	.312	19.9	40.4	20.6	111.53	24.46	10.75
SZ-340	.340	21.5	44.1	22.4	121.45	24.46	10.75
SZ-350	.350	22.1	45.3	22.9	124.62	24.46	10.75
SZ-375	.375	23.7	48.6	24.5	133.55	24.46	10.75
SZ-24	.340	24.1	44.1	29.0	177.52	22.00	12.25
SZ-25	.350	24.8	45.3	29.7	181.91	22.00	12.25
SZ-27	.375	26.6	48.6	32.0	195.18	22.00	12.25

DOMESTIC STEEL SHEET PILING

- All sections available in bare or galvanized steel.
- All Zee sections available in doubles.
- All sections produced exactly to customer specified length(s).
- All steel fully melted and manufactured in the USA.



For more information, please call toll free
(800) 522-9550

or visit our website at: www.shorelinesteel.com

Also Available:

- Corners
- Tees and Crosses
- Capping
- Coatings

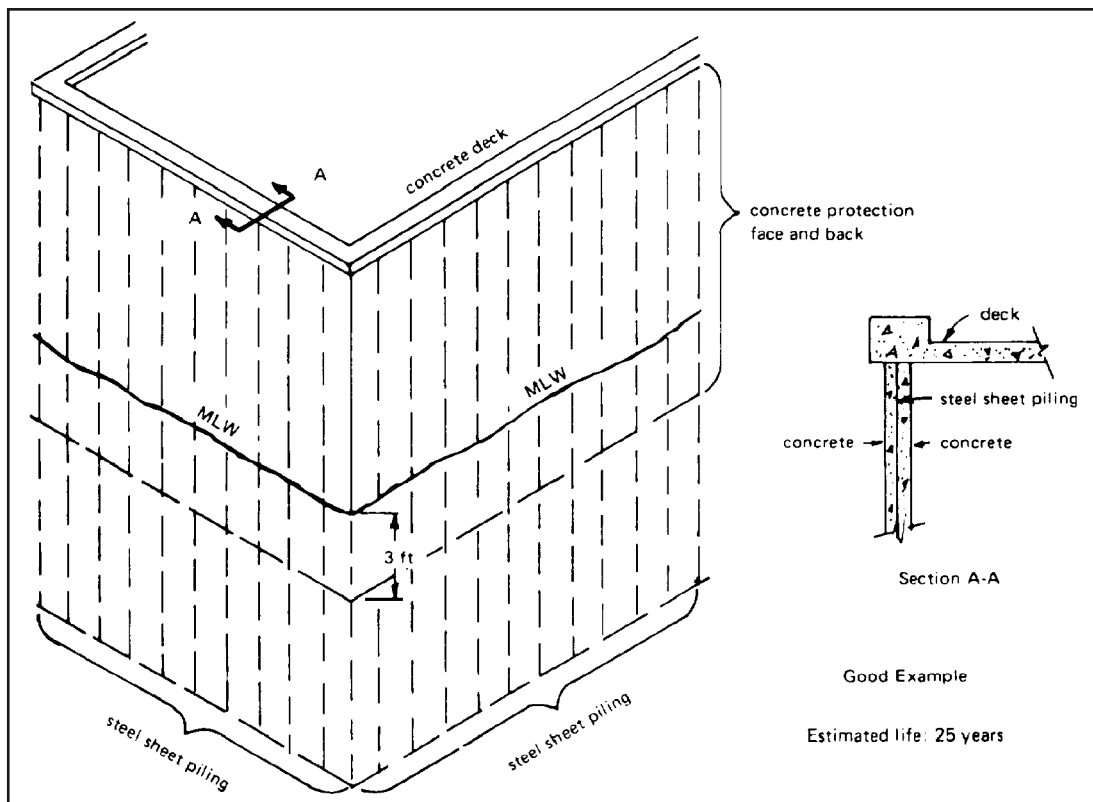


Figure 17-6: Encased Sheet Pile Wall

The situation in the splash zone has not been addressed. The rate is quite high and the PZ 27 would perforate in 375 divided by 15 = 25 years after the coating is exhausted. The PZ 35 will perforate in 600 divided by 15 = 40 years. Therefore, in this instance the coated PZ 27 slightly better as a choice.

17.4.3. Encasement

Encasement of steel piling in concrete is a method for providing protection in the area from grade mean low water. This system, if properly accomplished, can provide complete protection for the atmospheric, splash and tidal zones for many years. If there is a need for protection in the immersed zone, cathodic protection is utilized or alternately a coating. The reinforced encasement also provides a smooth face for the working portion of the bulkhead. An example of an encased wall is shown in Figure 17-6.

Encasement provides protection to both faces of the sheet piling in this area that might be particularly advantageous in the case of porous backfills such as coral. The U.S. Navy as a standard generally requires its new steel bulkheads to be encased when installed in warm, tropical water. Their standard design allows alternate pairs of piles to be staggered in the encased area saving some steel. As the section drawing indicates, the jacket on the backside also encases the wales of the anchor system.

The Navy's jacket design for a cellular structure takes the form of a cladding in that it is applied only to the front face.

The Navy has generally used diaphragm type cells in their deep steel pier design where they have used cells and the encasement is for protection, not structural application.

Concrete jackets are not without some potential problems however. It has been found that the steel just outside the concrete becomes strongly cathodic to the steel within, the corrosion rates in excess of what would be anticipated in the immersed zone are the area immediately below are higher than normal immersed zone rates. This problem can be handled by insulating the steel with a coating for several feet into and below the concrete jacket.

17.4.4. Special Steels

The addition of certain alloys to carbon steel has been found to enhance its performance in some environments. As early as 1913, experimental work by the steel industry indicated that small amounts of copper would enhance the atmospheric corrosion resistance of carbon steel. By 1933, proprietary steel had been developed which offered increased yield strength (50,000 psi vs. 36,000 psi) and 3 times the atmospheric corrosion resistance over regular construction grade steel. This was one of the weathering steels that are now described by ASTM A-242 and A-588 specifications.

All steels need to react with oxygen in order to obtain the protective oxide film that is the key to the performance.

Tests confirm this need and these grades show no improvement over regular grades of steel when buried or immersed in soil or water.

The application of any of the weathering steels to sheet piling projects has not been practical because of the limited benefits compared to the additional cost.

Copper can be added to carbon steel upon order at a small cost. This selection may have some merit for permanent land walls where appearances might be improved somewhat by the tighter rusting.

17.4.4.1. ASTM A-690 Grade

Recognizing that in many cases, corrosion in the splash zone was the main problem encountered by many marine (salt water) facilities constructed of steel, one steel company developed a formulation which seemed to offer an improvement over carbon steel at a reasonable cost. Tests indicated a superiority of up to three times, however in some cases the advantage was negligible. This formulation was adopted by ASTM and specification A-690 now describes steel for conversion into sheet or H-pile shapes.

This grade has a number of possible applications.

(1) As a superior grade for enhanced atmospheric corrosion resistance somewhat like ASTM A-588 (which is not available as hot rolled sheet piling).

(2) As a high strength steel which would allow a lighter section to be substituted or which would provide a higher reserve against yield strength against yield after corrosion losses. All improvement over carbon steel in the splash zone would be a bonus.

(3) As a high strength steel and superior base for a coating. It has been found that the weathering type steels hold paint and coatings better than carbon steel, scratches and gouges apparently do not undercut so severely and they heal with less undercutting.

Any economic evaluation of this grade should take into account the 28% increase in strength rather than a straight section-for-section comparison with carbon steel.

17.4.5. Coatings

Protective coatings for metals can be classified by the means in which they prevent corrosion as anodic, cathodic, inert, and inhibitive.

Anodic coatings prevent corrosion by sending electric current to areas of the base metal. In a sense, they are sacrificial in nature. Aluminium and zinc, both of which are “less noble” in the galvanic Series than iron are metals sometimes used as a coating to protect steel.

Inert coatings simply insulate areas of the base metal from others so that electro-chemical action will not begin or will be retarded. Organic and synthetic paints fall into this category.

Inhibitive coatings contain agents that are designed to inhibit both the start and the spread of corrosion. Paints containing zinc or aluminium in several forms are typical.

17.4.5.1. Metallic Coatings

17.4.5.1.1. Galvanizing

Galvanizing is the process whereby a thin coat of molten zinc is bonded to the steel base metal. In the case of structural shapes including sheet piling, this is accomplished by hot-dipping the item in a tank of molten zinc. Galvanizing has not been an important method of protecting steel sheet piling in the United States probably because of cost factors. Most producers of light-gauge cold-finished sheet piling products offer both bare steel and galvanized finish. It is well accepted that thin gauge steel must be protected against corrosion of all types.

Galvanized steel has performed well in corrosion tests. A hot-dipped H-pile was included in the samples tested in the Bureau of Standards/AISI tests at Dams Neck, VA²²⁷. This sample showed an overall corrosion rate of 0.14 mils per year over a six-year period compared to 6 mils per year for bare steel. (See *Table 17-4*). ASTM Specification A 123 is the standard generally used for hot-dipped galvanizing procedures.

Table 17-4: Description of Coating Systems on Steel Piles Exposed to the Atlantic Ocean at Dam Neck, VA

Piling System Number	Coating Designation	Number of Coats	Coating Thickness on Each Pile (mils)²²⁸	Remarks²²⁹
1	Bare Carbon Steel	-	-	
2	Bare Carbon Steel With Zinc Anodes	-	-	Protected beneath waterline with two Zinc anodes

²²⁷Romanoff, M., Gerhold, W.F., and Schwerdfegger, W.F., Iverson, W.P., Sanderson, B.T., and Escalante, E. (1972) “Protection of Steel Piles in a Natural Seawater Environment – Part I” Proceedings of the Third International Conference on Marine Corrosion and Fouling, October; and Escalante, E., Iverson, W.P., Gerhold, W.F., Sanderson, B.T., and Alumbaugh, R.L. (1976) “Protection of Steel Piles in a Natural Seawater Environment – Part II.” NBSIR 76-1104. Prepared for the American Iron and Steel Institute, Washington, DC.

²²⁸Piles in each system were coated as follows:

²²⁹All piles were carbon steel “H” piles unless noted otherwise.

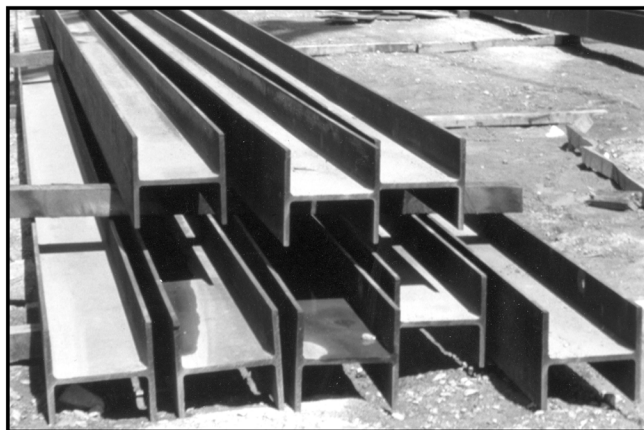
Table 17-4: Continued

Piling System Number	Coating Designation	Number of Coats	Coating Thickness on Each Pile (mils)²²⁸	Remarks²²⁹
3	Bare Carbon Steel With Aluminium Anodes	-	-	Protected beneath waterline with two Aluminium anodes
4	Polyamide Cured Coal-Tar Epoxy	2	A-16 B-16 C-15	
5	Polyamide Cured Coal-Tar Epoxy	2	A-20 B-20 C-19	Protected beneath waterline with two Zinc anodes
6	Polyamine Cured Coal-Tar Epoxy	2	A-15 B-15 C-13	
7	Polyamide Cured Coal-Tar Epoxy Coal-Tar Epoxy And Aluminium Oxide	2 1	A-15 (33) B-23 (38) C-21 (36)	Third coat and Aluminium Oxide applied between 16' and 22' from bottom of piles only.
8	Aluminium Pigmented Coal-Tar Epoxy Amine Cured, Red-Lead Pigmented, Coal-Tar Epoxy Primer Amine Cured Coal-Tar Epoxy Intermediate Amine Cured, Aluminium Pigmented, Coal-Tar Epoxy Finish	1 1 1	A-27 B-25 C-28	
9	Aluminium Pigmented Coal-Tar Epoxy Epoxy Primer Amine Cured Coal-Tar Epoxy Intermediate Amine Cured, Aluminium Pigmented, Coal-Tar Epoxy Finish	1 1 1	A-19 B-18 C 18	
10	Hot Dipped Zinc (Galvanized)	1	A-9 B-8 C-8	

STEELANNEX.COM

**WE BUY ALL
STEEL IN 72 HOURS!**

- Beams • Bridge Rail • Channel • Caisson • Rebar
- Pipe • Plate • Wide Flange • Sheet Piling • H-Beams
- Surplus • Scrap and More!



Simply go on-line to www.steelannex.com, complete your “inventory listing” and we will contact you with an offer to purchase your *ENTIRE INVENTORY* of surplus steel in 72 hours!

STEEL ANNEX, L.L.C.

P.O. Box 2170, Palm City, Florida, USA 34991

Phone: 866-3STEEL3 (866-378-3353) • Local: 772-232-0661

Faxes: Toll Free 866- 535-0659 • Local 772-232-0659

Email: steelannex@steelannex.com • www.steelannex.com

Table 17-4: Continued

Piling System Number	Coating Designation	Number of Coats	Coating Thickness on Each Pile (mils)²²⁸	Remarks²²⁹
11	Hot Dipped Zinc (Galvanized)	1	A-7 B-9 C-7	Protected beneath waterline with two Zinc anodes
12	Polyvinylidene Chloride Formula 113/54, Mil-L-18389 (Alternate Orange And White Coats)	7	A-7 B-5 C-7	
13	Flame sprayed Aluminium Wire	1	A-9 B-9 C-9	Aluminium preceded with a flame sprayed steel wire flash bonding coat one mil thick
14	Sealed Flame sprayed Aluminium Flame sprayed Aluminium Wire Wash Prime, Formula 117, Mil- P-153288 Clear Vinyl Seal coat	1 1 2	A-10 B-9 C-9	Aluminium preceded with flame sprayed steel wire flash bonding coat one mil thick
15	Coated Flame sprayed Zinc Flame sprayed Zinc Wire Polyvinylidene Chloride, Formula 113/54, Mil-L-18389(Alternate Orange And White Coats)	1 7	A-12 B-12 C-13	
16	Coated Flame sprayed Zinc Flame sprayed Zinc Wire Vinyl Red Lead Primer, Formula A119 Mil-P-15929	1 5	A-8 B-6 C-6	

Table 17-4: Continued

Piling System Number	Coating Designation	Number of Coats	Coating Thickness on Each Pile (mils)²²⁸	Remarks²²⁹
17	Phenolic Mastic Amine Cured, Red Lead Pigmented, Phenolic Mastic Primer (With Mica Filler)	1	A-13 B-18 C-14	
	Amine Cured Phenolic Mastic Finish	1		
18	Coated Zinc Rich Epoxy Zinc Rich Epoxy Primer	1	A-19 B-21 C-22	
	Polyamide Cured Coal- Tar Epoxy Finish	2		
19	Coated Zinc Inorganic Silicate Zinc Inorganic Silicate Primer	1	A-12 B-10 C-12	
	High Build Vinyl Finish	1		
20	Coated Zinc Inorganic Silicate Zinc Inorganic Silicate Primer (Self Cured)	1	A-10 B-14 C-12	
	Polyamide Cured High Build Epoxy Finish	2		
21	Coated Zinc Inorganic Silicate Zinc Inorganic Silicate Primer (Self Cured)	1	A-21 B-22 C- 19	
	Amine Cured Coal-Tar Epoxy Finish	1		
22	Coated Zinc Inorganic Silicate Zinc Inorganic Silicate Primer (Post Cured)	1	A-10 B-8 C-13	
	Strontium-Chromate, Iron-Oxide, Vinyl Phenolic Primer Vinyl Mastic Finish 1	1		
23	Bare A-690 Steel	-	-	Low Alloy Steel H-piles

Table 17-4: Continued

Piling System Number	Coating Designation	Number of Coats	Coating Thickness on Each Pile (mils)²²⁸	Remarks²²⁹
24	Bare A-690 Steel With Zinc Anodes	-	-	Protected beneath waterline with two Zinc anodes
25	Polyamide Cured Coal-Tar Epoxy	2	A-17 B-16 C-17	Low Alloy Steel H-piles
26	Bare Carbon Steel	-	-	Carbon Steel Pipe Piles
27	Polyamide Cured Coal-Tar Epoxy	2	A-20 B-17 C-24	Carbon Steel Pipe Piles
28	Polyamide Cured Coal-Tar Epoxy Coal-Tar Epoxy And Aluminium Oxide	2 1	A-21 (36) B-21 (32) C-16 (34)	Carbon Steel Pipe Piles Third coat and aluminium oxide applied between 16' and 22' from bottom of piles only
29	Flakeglass Filled Polyester	1	A-32 B-30 C-34	
30	Bare Carbon Steel	-	-	
31	Bare Carbon Steel	-	-	

17.4.5.1.2. Flame Spraying

Flame spraying is an old, established procedure whereby metal wire is fed into a hand gun, melted and blown by compressed air onto the surface to be protected. The molten particles, of aluminium or zinc, alloy into the surface layers of the steel forming a tight bond.

The results of an 18-year test of flame sprayed samples

sponsored by the American Welding Society were discussed by Coburn²³⁰. Samples were exposed to various environmental conditions at seven locations including immersed and tidal exposure at a coastal site. Film thicknesses of both aluminium and zinc ranged from 3 to 18 mils for the test purpose. The films were both sealed and unsealed. The principal findings of interest are shown in Table 17-5.

²³⁰Coburn, S.K. (1988) "Corrosion Factors to be considered in the Use of Steel Piling in Marine Structures." *Pile Buck Annual* pp. 319-357.

When you look down on a job...you need to see productivity



And that's exactly what you will see with the new IHC S-150 Hydrohammer. At land, at sea, or on the waterfront, IHC Hydrohammers give you reliability and efficiency for the toughest jobs. Contact us to learn more.



IHC
IHC Hydrohammer®
PO Box 26
6, Smitweg
2960 AA Kinderdijk, The Netherlands
Phone 011 31 78 6910302
Fax 011 31 78 691 0304
Email sales@ihchh.com
Web site <http://www.ihchh.com>

North American distributor:
VULCAN FOUNDATION EQUIPMENT
111 Berry Road
P.O. Box 16099
Houston, TX 77222
Phone (713) 691 3000
Fax (713) 691 0089
Toll Free (800) 742-6637
Email sales@vulcanhammer.com
Web site <http://www.vulcanhammer.com>



Member of the IHC Caland Group

Table 17-5: Aluminium vs. Zinc Flame Sprayed Coatings

Aluminium	Zinc
<p>Films 3 mils and 6 mils, unsealed, give complete protection in seawater and in severe marine and industrial atmospheres.</p> <p>Thin coat films offer better protection than thick films.</p>	<p>Films 12 mils and higher, unsealed and sealed, give complete protection in seawater. Films 9 mils thick unsealed, and 3 mils to 6 mils sealed are required to give complete protection in severe marine and industrial atmospheric zones.</p> <p>Films 9 mils unsealed, and 3 mils and 6 mils sealed required to give complete protection in severe marine and industrial atmospheres.</p>

Coburn also discussed the U.S. Navy's ten-year test program at Port Hueneme, CA. The test site simulated the various zones of corrosion in a marine environment. Sprayed zinc and aluminium, both with and without sealing coats were included in the test. The conclusions:

- (1) The organic coatings enhanced the performance of metalised zinc. In every case, their performance was better than when they were over metalised aluminium or over wash-primed steel.
- (2) Excellent protection can be expected for 10 years from Saran, red-lead Navy vinyl, vinyl, and epoxy polyamide over metalised zinc.
- (3) Excellent protection can be expected for 10 years from metalised aluminium without primer or sealer protection.
- (4) Unsealed and otherwise unprotected metalised zinc has a limited service life.

Steel H-piles, flame-sprayed only and flame-sprayed and sealed, were included in the tests conducted in the ocean at Dam Neck, VA by the Bureau of Standards over a six year period from 1967 to 1972²²⁷. This process provided very satisfactory results and was among the best of the large number of systems tested. (See *Table 17-4*) It would appear that a metallic coating applied by flame spray and sealed with an appropriate supplemental agent offers a superior protective system which should be considered if initial costs are not a consideration.

17.4.5.2. Non-Metallic Coatings

Non-metallic coatings are by far the leading method for

protecting steel in hostile environments. They are usually cheaper on a first cost basis than metalising or sacrificial thickness and more reliable than cathodic protection alone. Cathodic protection functions only in the fully immersed zone and may be difficult to maintain, over an extended length of time.

Prior to 1950, coatings were generally made up of coal-tar pitch solutions that were field applied in thin coats with a brush. When applied over a poorly prepared surface, their service-life and ultimate value were minimal, often less than five years.

Modification of coal tar pitch with various synthetic resins led to the coal tar epoxies. These can produce thicker and harder surfaces. Since the quality and performance is highly dependent on the surface preparation of the steel prior to coating, this operation is best conducted under roof, with specialized equipment under controlled atmospheric conditions. Sheet piling that has been factory coated can still be transported long distances to the job site. Any damage to the coating is generally repairable prior to installation.

Since the introduction of the coal tar epoxies, a great number of organic and synthetic coatings and systems have been developed and tested. Coburn²³⁰ reported on such systems that were tested at Dam Neck. Coal tar epoxy over a zinc-rich inorganic primer did exceedingly well in all zones again proving the worth of the coal tar formulations. Vinyls performed well in combination with various base coats. An aluminium pigmented coal tar epoxy did well as did glass flake polyester.

Similar findings were made in a U.S. Army Corps of Engineers test²²⁷. The best coatings were coal tar epoxy over zinc-rich primer, polyester-glass flake and vinyl seal over metalised aluminium.

The U.S. Navy's guide publication²³¹ recommends the following coatings to its design engineers.

²³¹Naval Facilities Engineering Command (1969). *Paints and protective coatings*. NAVFAC MO-110. Washington, D. C. (Joint Service; Army TM5-618; Air Force AFM85-3).

- o Epoxy polyamide (3 coats of MIL-P-24441) or coal tar epoxy polyamide (2 coats of SSPC Paint No. 16 or Corps of Engineers C-200) are recommended for piling and other steel structures which are to be immersed in seawater. Coal tar epoxies become brittle from prolonged exposure in direct sunlight, and are not recommended for this exposure. Epoxies perform well in direct sunlight except for chalking. If chalking is objectionable, substitute a coat of aliphatic polyurethane (MIL-C-83286) for the third coat of epoxy polyamide to obtain excellent weathering in direct sunlight.
- o For milder atmospheric exposure, an alkyd system (1 coat of TT-P-645 primer and 2 topcoats of TT-E-490) will provide adequate protection.
- o Coal tar coatings (MIL-C-18480) are occasionally used for temporary protection over marginally prepared surfaces. They provide good temporary protection until a more permanent coating system can be applied. They may also be used as a dip coating for components such as chain that are difficult to coat otherwise.

All of the above coatings can be applied by brush, roller, or spray, but brushing of the prime coats onto the steel will achieve surface penetration. Adjacent coats should be applied on successive days²³².

Coatings may be specified for one side, both sides or selected parts of the pile. The interior of the interlocks is normally not coated since it could interfere with interlocking. The products of corrosion generally protect the heavy interlocks and these are the last parts of the pile to disappear under lengthy attack.

Since handling of the steel is a significant part of the coating cost, coating small portions of the surface will be disproportionately higher on a unit cost basis than a large area.

Coatings can be used in conjunction with cathodic protection 1) to reduce the amount of current required for protection 2) to protect the portions of the pile not covered by the cathodic system i.e. the splash and atmospheric areas.

The importance of surface preparation cannot be overemphasized. The Steel Structures Painting Council defines various levels of cleanliness of steel prior to painting for various coatings and class of service. SSPC SP 5 is often applied to coal tar epoxy coatings for marine service and calls for a "near white" steel condition prior to coating.

17.4.5.3. Cathodic Protection

Cathodic protection is the use of the galvanic series (see 17.2.3) to prevent corrosion of the sheet pile wall rather than to promote it. Such a structure collects current from a sacrificial anode system that is readily replaced. Due to a normal and inherent difference in electrical potential between iron and such metals as zinc, magnesium and aluminium, the latter serve as sacrificial anodes and supply the necessary protective current to cancel out the need for the steel to corrode (see *Figure 17-7*, left panel.) Alternatively, a direct current from an external power source (referred to as an impressed current system) can supply the same protective current to the steel structure (see *Figure 17-7*, right panel.)

Thus, galvanic anodes and impressed currents may be used to protect a steel structure in seawater. Usually the cost of a galvanic anode system exceeds that of an impressed current system. However, the galvanic anodes, once installed, require no addition to requiring an available source of power. Zinc anodes do not overprotect a coated system and, therefore, are not likely to damage a coating as would an impressed system. The protective current requirements on a bare steel structure are directly related to the corrosion rate in the submerged zone. It requires a current flow of about two milliamperes per square foot flowing continuously to corrode a steel surface at the rate of one mil per year. Therefore, if it is determined that the average corrosion rate in the submerged zone is 5 mils per year it means an average corrosion current of 10 milliamperes per year is flowing continuously. Hence, an equivalent current of 10 milliamperes per square foot will be necessary to stop the corrosion by means of cathodic protection. One mul-

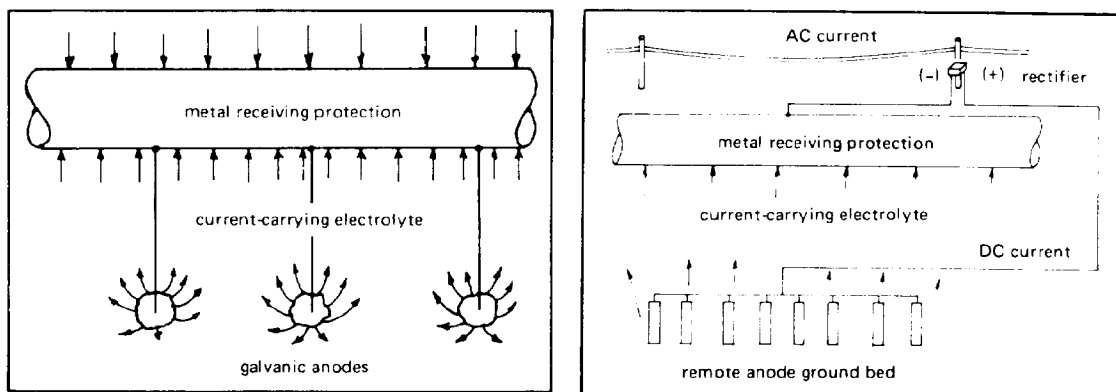


Figure 17-7: Cathodic Protection Systems

²³²Instructions for application of MIL-P-24441 can be found in Chapter 631 of Naval Ships' Technical Manual NAVSEA S9086-VD-STM-000. Instructions for applying SSPC Paint No. 16 can be found in Steel Structures Painting Manual Vol. 2, Systems and Specifications.

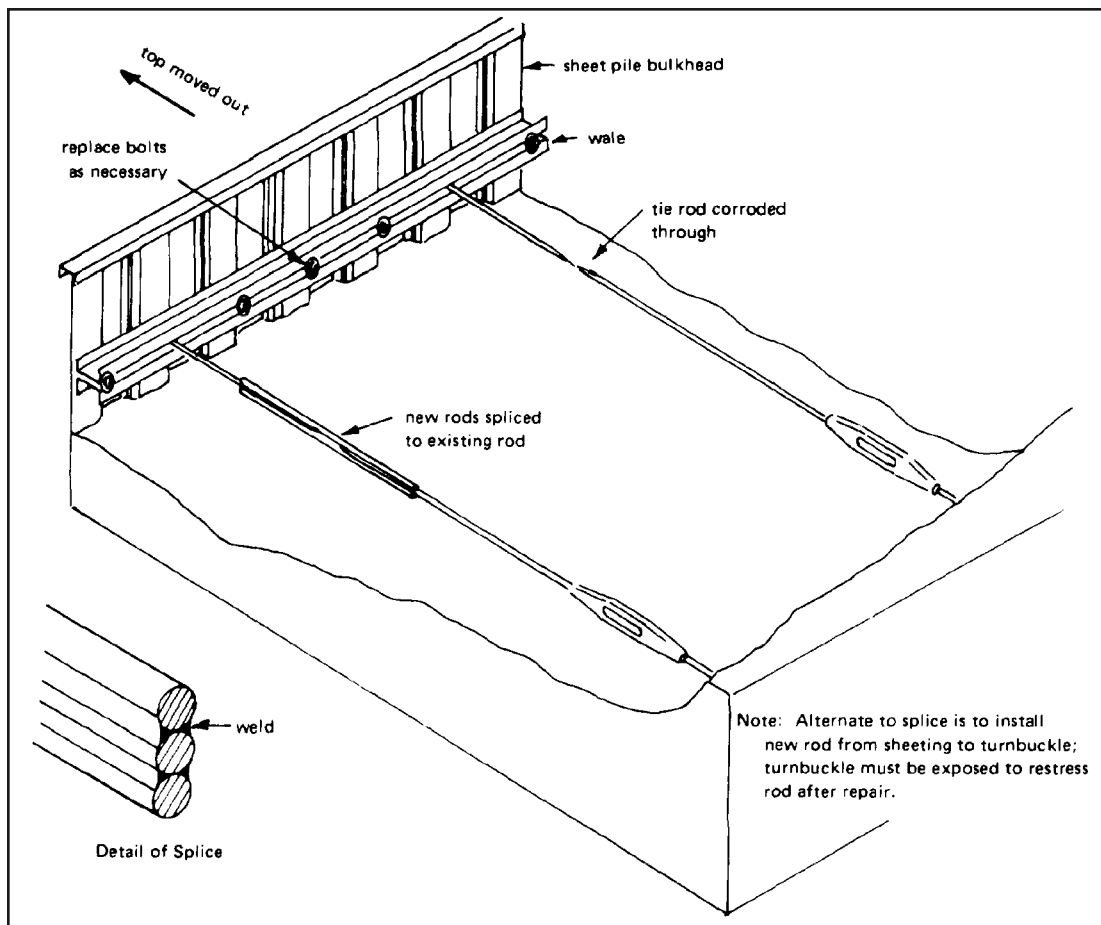


Figure 17-8: Repairing Tie Rods

multiplies the total area in square feet by the required protective current to get the total protective current necessary for protection of the immersed zone. About 20 percent of this figure is added on so the coating is capable of protecting the steel in the embedded area. A small margin is added to this calculation to give the required amount of protective current.

In anticipation on an early or potential need for the imposition of cathodic protection to an entire marine structure, it is necessary that all piles be bonded together metallurgically to insure electrical continuity. Each bent of a pier is tied together electrically by means of welded cross bracing. When a concrete cap is used as a pier deck, it is necessary to weld the reinforcing bars to each bent and to each other to ground the whole structure before casting the cap. If the encasement is to be in contact with water, it is best to paint the encased steel with a heavy bituminous coating prior to encasement to effectively isolate the steel from the concrete.

Sheet piling bulkheads and cellular wharves need to have individual elements bonded together, either by welding a flat bar horizontally across the piles, or by welding the interlock for a suitable length, depending on structure size. A separate cathodic protection system is required to protect sheet piling on the landside in addition to the system used for protection of the piling on the seaside.

Tie rods on sheet piling bulkheads and similar structures

located below the water level frequently suffer accelerated corrosion immediately behind the bulkhead on the earth side due to the formation of a differential environment cell. Corrosion cells of this type are readily eliminated by means of cathodic protection.

The bonding of the ground return circuit from the negative terminal of the rectifier to the structure is extremely important and critical and, therefore, great care must be exercised to insure that a secure electrical and mechanical connection is made that will not deteriorate in service.

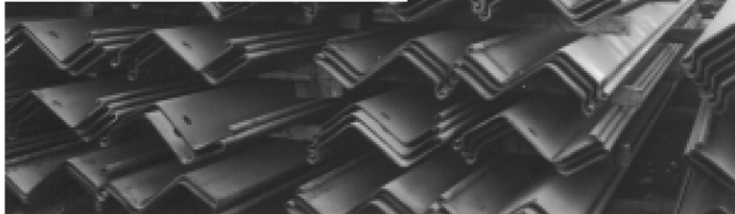
17.5. Protection of Wales, Tie Rods, and Accessories

Wales and tie rods are an important part of the structural system that is a sheet pile bulkhead. Wales are generally located above the low tide line where they can be replaced or repaired if necessary. Inside wales are located on the embedded rear face of the wall and are subject to the same corrosion rates as the sheet piling in that area.

Tie rods, like pipelines are embedded in disturbed soil, and subject to a similar pitting type attack along with uniform corrosion. Tie rods cannot be readily inspected and the unsuspected failure of one rod could throw additional load on other rods that may fail the wall. It is important that these elements survive.

**PITTSBURGH
COATINGS**

**APPLICATORS OF
PROTECTIVE COATINGS**



**Complete Coating Services
for over 40 Years.**

**BLAST
PAINT
METALLIZE
FABRICATE**

**Barge facility with 120 ton lifting capacity
Rail siding into plant • 120,000 sq. ft. of enclosed space
Capability of processing sheets in pairs**

**Conveniently located on the Ohio River in Pittsburgh at Milepost 16.5
103 Port Ambridge Drive • Ambridge, PA 15003
412-366-5159 • Fax 412-366-6019
www.pittcoat.com**

H&M VIBRO, INC.

P.O. Box 224, Grandville, MI 49468

Toll Free: (800) 648-3403

(616) 538-4150

www.hmvibro.com

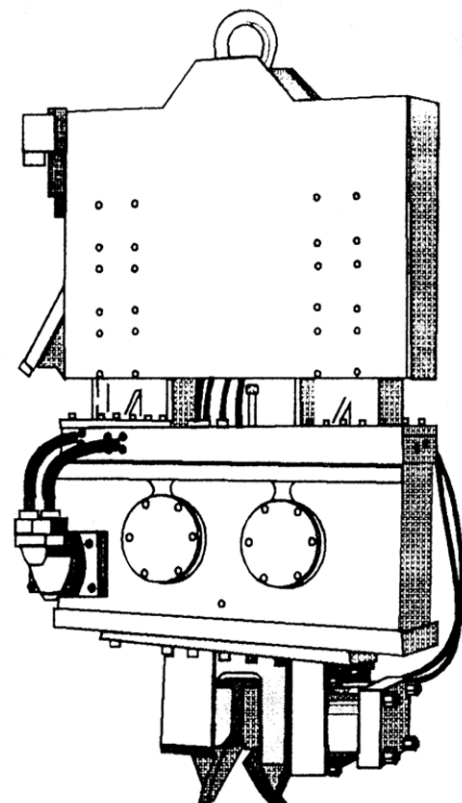
Model H-1700

Vibratory Driver/Extractor

Features:

- 75 Ton Pile Clamping Force
- 30 Ton Extraction Line Pull
- Weight: 7,000 Pounds
- Optional Counterweight: 3,600 Pounds
- CAT 3126 Power Pack

SALES AND RENTALS



Systems similar to those used for protecting pipelines are effective such as coating and wrapping, providing for metal loss by oversizing, or both. If it is deemed necessary to protect the embedded rear of the sheeting, the wales should also be protected. This can be accomplished by coatings or galvanizing, which is done occasionally. Holding hardware such as bolts and plates are galvanized. The U.S. Navy for example²³³ sets minimum diameters for bolts and thickness for sometimes galvanized straps and fittings.

Bolts and other hardware can be oversized to account for corrosion losses. It is important not to mix metals for example using stainless steel or aluminium bolts with carbon steel without insulating them from each other. Galvanized steel does not produce this potential problem. Cathodic protection is another means of protecting these elements, but is not commonly used because of the sometimes difficulty of servicing the installations.

If it is necessary to replace deteriorated tie rods, a trench is dug from the sheet piling to the deadman, and the new rods with new turnbuckles are installed one at a time. They should be covered with a bituminous coating, a fabric tape, and a final bituminous coating. The deadman should be inspected, and necessary repairs made before the trench is backfilled. An example of this is shown in *Figure 17-8*.

Very few tests of coatings are carried through to complete breakdown and loss of protective ability on the part of the coatings. At the same time, results from actual applications are difficult to assess because of differing environmental conditions. The designer who needs information of this type should obtain current information from the manufacturers of the product.

17.6. Corrosion Considerations In Design of Tiebacks

17.6.1. Corrosion of Prestressing Steel

While corrosion is generally not a consideration in the selection and design of tiebacks for short term or temporary applications, the continued performance of permanent ground anchors depends on their ability to withstand corrosive attacks from the environment. Underground corrosion of steel begins and continues when a difference in potential exists between two points that are electrically connected and immersed in an electrolyte, or due to direct chemical attack in an aggressive environment such as sanitary landfills or organic deposits. However, an innocent item, air, generates the most trouble. Composed principally of nitrogen, oxygen, and gases of a corrosive nature (such as sulphur, chlorides, and oxides in areas of industrial fumes), air reacts with moisture to produce a solution of corrosive character. Hence, in documented failures, the overwhelming percentage of failure occurred within 6 feet of the anchor head in the zone of aeration.

Electrochemical cells may develop between the tendon and

an exterior dissimilar metal object of between tiny areas on the same tendon that have differing concentrations of the elements composing the steel. In either case, this galvanic type corrosion occurs as metal loss from the exposed steel tendon through the ground water to a nearby metal element that is of lower potential.

There are two requirements for galvanic corrosion to occur; first, a good electrical connection must exist between the two metals; and second, the solution immersing the metals must be an electrical conductor. If these conditions are met, the degree of corrosion will depend on other characteristics of the soil-anchor system. Major variables affecting corrosion are presented below:

1. Ground Water – extremely acid, alkaline, or salt solutions are good conductors.
2. Temperature – high temperatures increase corrosion, low temperatures retard corrosion; embedded portions of anchors are at relatively low ground temperatures normally.
3. Velocity of flow of Ground Water – high flow rates increase corrosion, low flow rates retard corrosion; in low permeability clays the chance of corrosion is remote because chemical protective films develop.
4. Stress Condition in the Tendon – high stresses or cyclic stresses may increase the rate of corrosion; in anchor design the former is usually present, but not the latter.

When corrosion does occur, the results are manifested in various forms. The type of corrosion and the degree of corrosion can have widely varying effects on a tendon. The most prevalent types, the mechanisms and effect on the tendon are listed in 17.2.

The foregoing brief explanation of the corrosion mechanism is presented to give the designer an appreciation of the importance of considering corrosion in the design phase. Recent research in anchor corrosion has determined that many environments where anchors are installed are relatively nonaggressive. Various degrees of corrosion protection can be applied to the anchor depending on the relative degree of the potential for corrosion. In past years, anchors have been placed with two basic degrees of protection; a lot or none. The former was used when corrosion was considered by the designer and the latter when the designer was unaware of the ramifications. Interestingly, of those many installations, relatively few failures have occurred and, as expected, all failures were in the “unprotected” or improperly installed anchors. As previously mentioned, most corrosion related failures occurred within 6 feet of the anchor head. Such data indicates some basic guidelines to be followed:

²³³MIL HDBK 1025/6, General Criteria for Waterfront Construction.

1. All anchors used for permanent application require corrosion protection in the free stressing length and at the anchor head.
2. For routine applications, only a single degree of corrosion protection (grease and sheath) will be required in the free stressing length with only grout used to protect the bond zone; i.e., minimum grout cover 0.5 inches in thickness.

5. One-time treatment for protection as installed systems cannot be maintained or replaced.
6. Flexible enough to resist failure during stressing, especially at junctions with other components.
7. Tough enough to withstand handling damage during manufacture, transport, storage, and installation.

17.6.2. Anchor Protection Against Corrosion

The British Code of Practice for Ground Anchorages (1981) lists the following requirements for an anchor corrosion protection system.

1. Effective of the tendon is at least equal to that required of the facility.
2. No adverse effects on the environment or the efficiency of the protected anchor.
3. Unrestricted tendon movement in the unbonded zone.
4. Comprised of mutually compatible materials with respect to deformability, permanence, and corrosion.

With these basic criteria in mind, the designer should consider basic methods of anchor protection to suit the application for a particular project. The guideline methods listed below are only the basic systems now in general use for anchor protection. Schematic sections are shown in *Figure 17-9* and *Figure 17-10*. Many additional proprietary methods exist which will accomplish equal degrees of corrosion protection. At this time, it is suggested the designer specify the basic systems on the plans, but clearly state that proprietary systems which are equivalent, in the opinion of the engineer, to the system shown will be accepted.

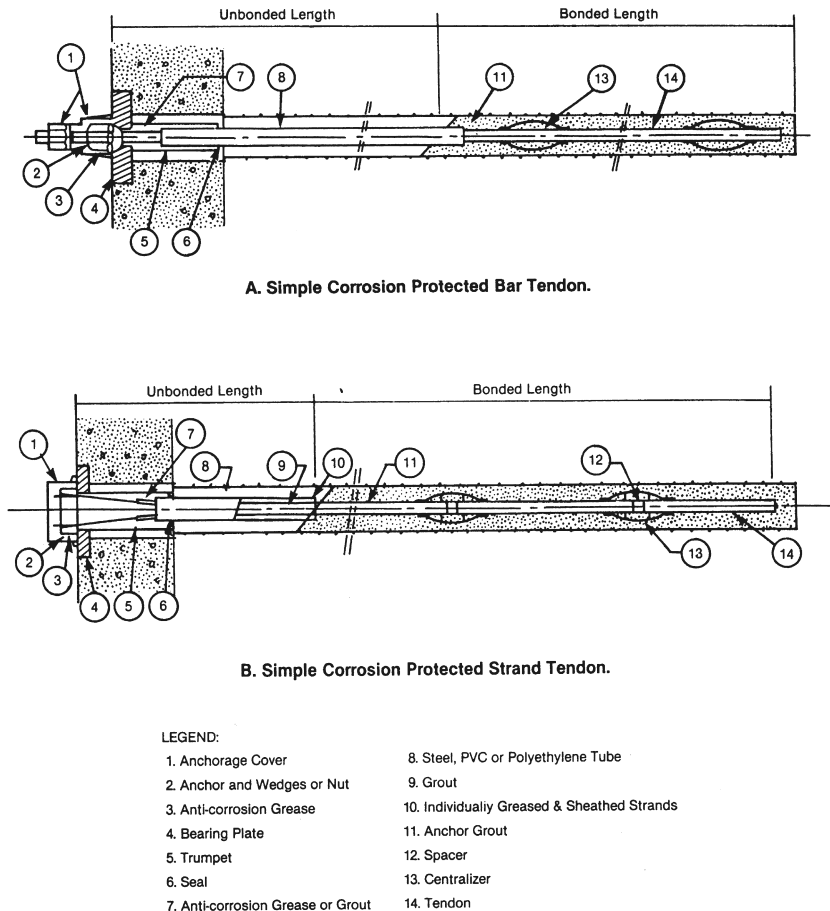
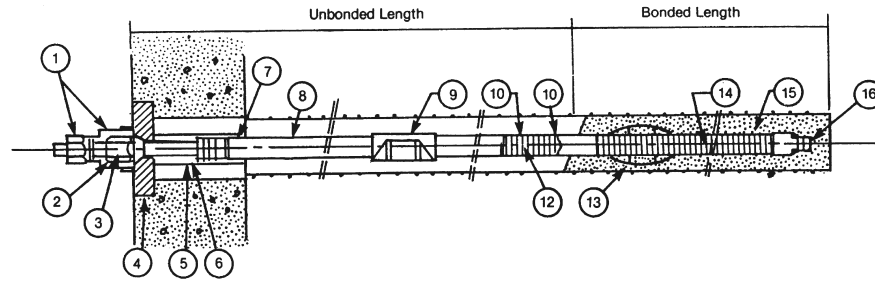
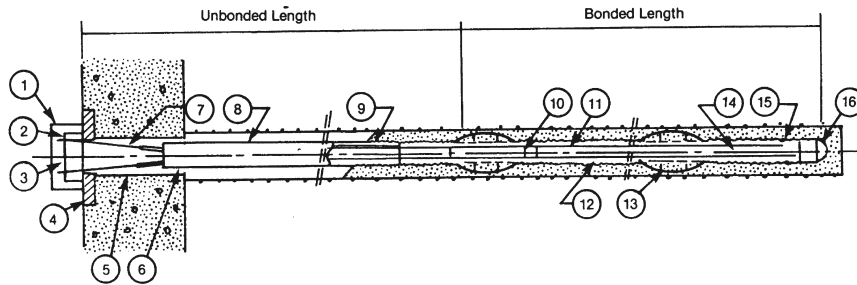


Figure 17-9: Simple Corrosion Protected Tendon



A. Encapsulated Bar Tendon



B. Encapsulated Strand Tendon

LEGEND:

- | | |
|--|------------------------------------|
| 1. Anchorage Cover | 10. Spacer or Internal Centralizer |
| 2. Anchor Head or Nut | 11. Strand Tendon |
| 3. Anti-corrosion Grease | 12. Corrugated Polyethylene or PVC |
| 4. Bearing Plate | 13. Centralizer |
| 5. Trumpet | 14. Internal Grout |
| 6. Seal | 15. External Grout |
| 7. Anti-corrosion Grease or Grout | 16. End Cap |
| 8. PVC or Polyethylene Tube | |
| 9. Individually Greased & Sheathed Strands | |

Figure 17-10: Encapsulated Double Corrosion Protected Tendons

17.6.2.1. Protection of the Bond Zone

a) Simple Protection: The use of simple protection relies on Portland cement grout to protect the tendon, bar or strand, in the bond zone. Steel will not corrode in a high pH environment such as Portland cement that possesses pH values up to 12.6. When Portland cement is used for protection, it is assumed that the pH will not be lowered with time. When the simple protection is used, care should be taken that the tendon has at least 0.5 inches of the free length sheathing.

b) Double Protection: A corrugated PVC, high-density polyethylene, or steel tube accomplishes complete encapsulation of the anchor tendon. The tube must be capable of with-

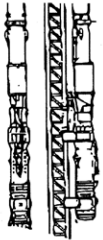
standing the deformation associated with transportation, installation, stressing and testing of the anchor, and transferring load applied to the tendon. Regardless of the encapsulating medium, the annular space between the corrugated tube and tendon is usually filled with neat cement grout containing admixtures to control bleed of water from the grout. Shorter tendons are grouted before insertion in the drilled hole.

17.6.2.2. Protection of Unbonded Length

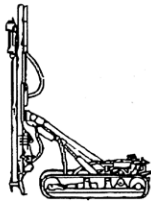
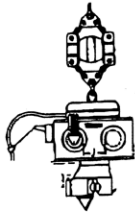
The unbonded length is protected by a variety of means since the protection is not required to transfer stresses from the tendon to the ground. The protection must:

PACIFIC AMERICAN COMMERCIAL COMPANY

45 YEARS OF SERVICE TO THE PILE DRIVING INDUSTRY



**AIR, DIESEL,
VIBES &
HYDRAULIC
IMPACT**



**QUARRY
DRILLS**

BUCKETS



**PORTABLE
PONTOON
BARGES**



**DIESEL AIR
COMPRESSORS**

FAST QUOTATIONS - ALL YOUR FOUNDATION EQUIP. NEEDS - COMPLETE PACKAGES

HAMMERS, VIBRATORYS, LEADS, SPOTTERS
TOP HEADS, CROSS HEADS, FOLLOWER BLOCKS, DRILLS and AUGERS

RENTALS-SALES-REPAIR PARTS AVAILABLE

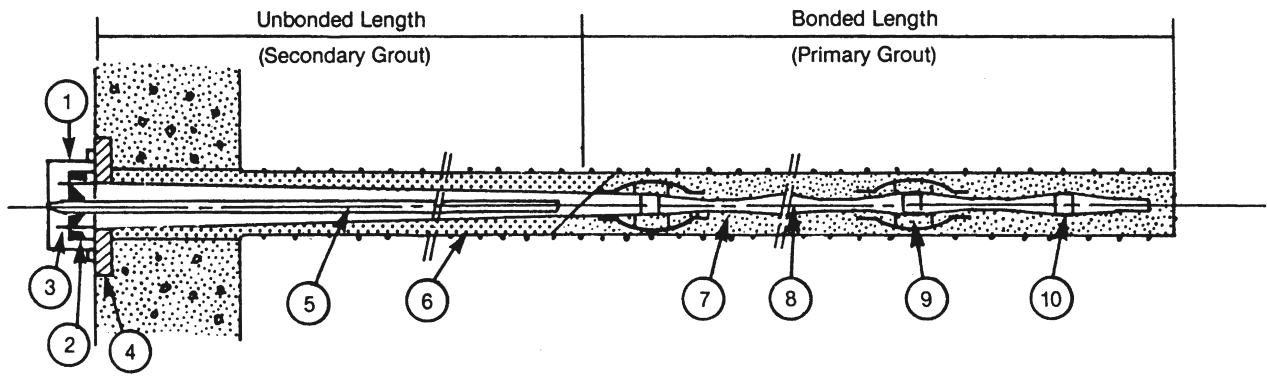
CALL: 1-800-678-6379 or FAX 1-206-763-4232



MERCO, INC.

TUNNEL & BRIDGE CONTRACTORS

**1117 Route 31 South
Lebanon, NJ 08833
Tel: 908-730-8622
Fax: 908-730-6472**



LEGEND:

- | | |
|--------------------------|--------------------|
| 1. Anchorage Cover | 6. Secondary Grout |
| 2. Anchor Head | 7. Primary Grout |
| 3. Anti-corrosion Grease | 8. Tendon |
| 4. Bear Plate | 9. Centralizer |
| 5. Grout Tube | 10. Spacer |

Figure 17-11: Bonded Tendon

- a. Accommodate elastic movements during testing and stressing.
- b. Withstand potential damage during storage, handling, and construction.
- c. Resist attack in aggressive environments.
- d. Allow elastic movements after lock-off if unbonded.

The most common methods of protecting the unbonded length are sheaths filled with anti-corrosion grease, heat shrink sleeves, and secondary grouting after stressing. Except for secondary grouting, the protection is usually in place prior to inserting the tendon in the hole.

Most frequently when “secondary grout” is mentioned, the procedure referred to involves filling the annular space between the ground and the smooth sheath in the free length. Secondary grouting should be done by gravity of low methods to prevent damage to the sheath and load transfer to the ground in the unbonded length. In addition, the grout should terminate before the bearing plate area to prevent load transfer up the grout column to the structure. Such secondary grouting, when done properly, provides an extra insurance against corrosion and is recommended for most installations.

Secondary grout, in the true sense, refers to grout placement after stressing and lock-off around a tendon with an unshathed free length. After set, the grout surrounding the free length becomes bonded to the ground and the tendon over the initially unbonded length. *Figure 17-11* illustrates such an anchor. These anchors are only normally recommended for semi-permanent, low risk applications. When secondary grouting is used for these anchors, extreme care must be taken to insure no void in the grout exists beneath

the anchor bearing plate. Such areas are unprotected against corrosion in the most critical zone.

17.6.2.3. Protection at the Anchor Head

The most critical area to protect from corrosion is in the vicinity of the anchor head connection. Below the bearing plate, the corrosion protection over the unbonded length is usually terminated to expose the bare tendon. Above the bearing plate, the bare tendon is gripped by either wedges, nuts, or deformed in the case of wires. Regardless of the type of tendon, the gripping mechanism creates stress concentrations at the connection. In addition, a very aggressive corrosion environment may exist at the anchor head since oxygen is readily available. The vulnerability of this area is demonstrated by the fact that most anchor failures occur within a short distance of the anchor head.

Figure 17-12 shows a typical protection system for the anchor head. A “trumpet” which is usually steel or strong, durable plastic, is used as a transition from the anchorage to the unbonded length corrosion protection. One end of the trumpet is fastened and sealed to the bearing plate and the other fitted with a deformable seal such as an O ring which fits tightly around the protective tube but allows the tendon to move within the trumpet. The annular space between the trumpet and the tendon is filled with anti-corrosion grease. The anchor head is protected by an anti-corrosion grease filled cap or left embedded in concrete. Covering the head with a grease filled cap permits future lift off testing or load adjustment. When filling the trumpet and cap, care is required to insure that the grease or grout fills the entire space.

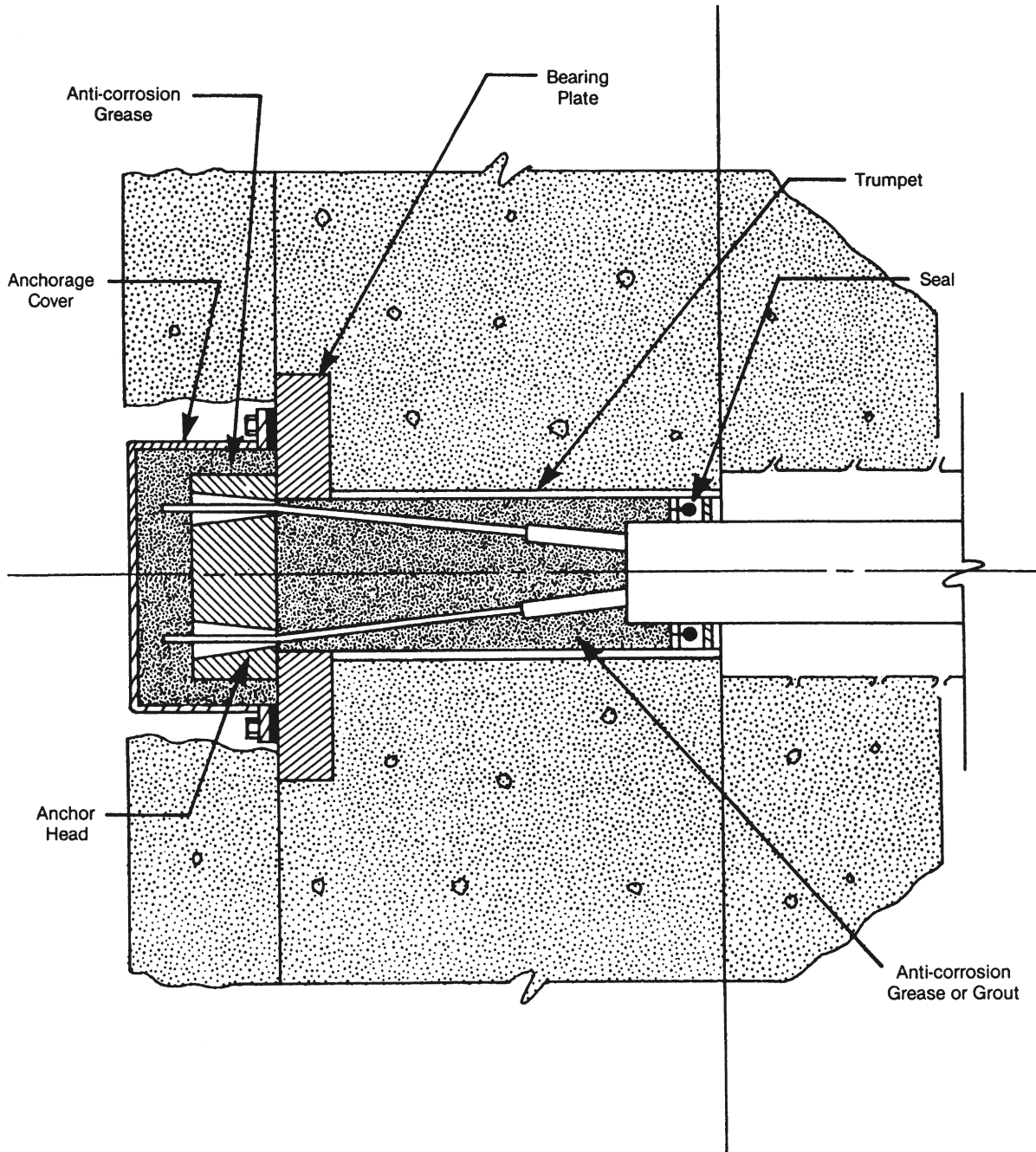


Figure 17-12: Anchor Head Details

Chapter Eighteen: Lateral Earth Pressure Tables and Charts

18.1. Rankine Theory

Friction Angle ϕ , Degrees	Backfill Angle β , Degrees						
	0	5	10	15	20	25	30
26	0.3905	0.3959	0.4134	0.4480	0.5152	0.6999	
28	0.3610	0.3656	0.3802	0.4086	0.4605	0.5727	
30	0.3333	0.3372	0.3495	0.3729	0.4142	0.4936	0.8660
32	0.3073	0.3105	0.3210	0.3405	0.3739	0.4336	0.5741
34	0.2827	0.2855	0.2944	0.3108	0.3381	0.3847	0.4776
36	0.2596	0.2620	0.2696	0.2834	0.3060	0.3431	0.4105
38	0.2379	0.2399	0.2464	0.2581	0.2769	0.3070	0.3582
40	0.2174	0.2192	0.2247	0.2346	0.2504	0.2750	0.3151
42	0.1982	0.1997	0.2044	0.2129	0.2262	0.2465	0.2784

Figure 18-1: Rankine Active Earth Pressure Coefficients K_a

Friction Angle ϕ , Degrees	Backfill Angle β , Degrees						
	0	5	10	15	20	25	30
26	2.5611	2.5070	2.3463	2.0826	1.7141	1.1736	
28	2.7698	2.7145	2.5507	2.2836	1.9176	1.4343	
30	3.0000	2.9431	2.7748	2.5017	2.1318	1.6641	0.8660
32	3.2546	3.1957	3.0216	2.7401	2.3618	1.8942	1.3064
34	3.5371	3.4757	3.2946	3.0024	2.6116	2.1352	1.5705
36	3.8518	3.7875	3.5980	3.2926	2.8857	2.3938	1.8269
38	4.2037	4.1360	3.9365	3.6154	3.1888	2.6758	2.0937
40	4.5989	4.5272	4.3161	3.9766	3.5262	2.9867	2.3802
42	5.0447	4.9684	4.7437	4.3827	3.9044	3.3328	2.6940

Figure 18-2: Rankine Passive Earth Pressure Coefficients K_p

QUICK RESPONSE**Quality Assessment
of Piles and Shafts****Services Include:**

- Pile Driving Monitoring
- Dynamic Load Testing (PDA+CAPWAP, APPLE)
- Wave Equation Analysis (GRLWEAP)
- SPT and Becker Drill Energy Measurements
- Integrity Testing (pulse echo and cross hole)



GRL
engineers, inc.

4535 Renaissance Pkwy.
Cleveland, OH 44128 USA

www.pile.com
info@pile.com

- Professional, Experienced Field Engineers
- State-of-the-Art Methods and Equipment

OFFICES:

GRL Central
Ph: 216-831-6131

California
Ph: 661-259-2977

Colorado
Ph: 303-666-6127

Florida
Ph: 407-826-9539

Illinois
Ph: 847-670-7720

North Carolina
Ph: 704-593-0992

Ohio
Ph: 216-292-3076

Pennsylvania
Ph: 610-459-0278

H&M VIBRO, INC.

P.O. Box 224, Grandville, MI 49468

Toll Free: (800) 648-3403

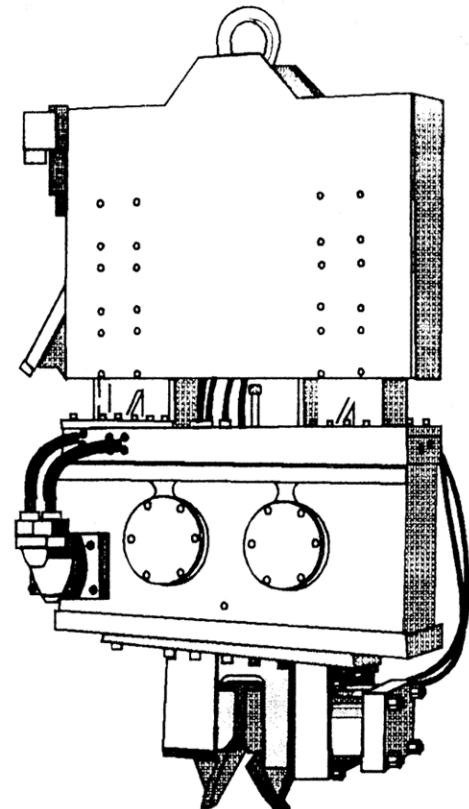
(616) 538-4150

www.hmvibro.com

Model H-1700**Vibratory Driver/Extractor****Features:**

- 75 Ton Pile Clamping Force
- 30 Ton Extraction Line Pull
- Weight: 7,000 Pounds
- Optional Counterweight: 3,600 Pounds
- CAT 3126 Power Pack

SALES AND RENTALS



18.2. Coulomb Theory

Friction Angle ϕ , Degrees	Backfill Angle β , Degrees						
	0	5	10	15	20	25	30
26	0.3905	0.4139	0.4431	0.4822	0.5420	0.6776	
28	0.3610	0.3817	0.4071	0.4403	0.4882	0.5747	
30	0.3333	0.3516	0.3737	0.4019	0.4411	0.5045	0.7500
32	0.3073	0.3233	0.3425	0.3667	0.3991	0.4481	0.5475
34	0.2827	0.2968	0.3135	0.3342	0.3612	0.4001	0.4677
36	0.2596	0.2720	0.2865	0.3041	0.3268	0.3582	0.4081
38	0.2379	0.2487	0.2612	0.2763	0.2954	0.3210	0.3593
40	0.2174	0.2269	0.2377	0.2506	0.2666	0.2876	0.3177
42	0.1982	0.2064	0.2157	0.2267	0.2401	0.2575	0.2814

Figure 18-3: Coulomb Active Earth Pressure Coefficients K_a , $\delta = 0^\circ$

Friction Angle ϕ , Degrees	Backfill Angle β , Degrees						
	0	5	10	15	20	25	30
26	0.3722	0.3959	0.4256	0.4657	0.5276	0.6704	
28	0.3448	0.3656	0.3913	0.4251	0.4743	0.5642	
30	0.3189	0.3372	0.3595	0.3881	0.4281	0.4934	0.7529
32	0.2945	0.3105	0.3299	0.3542	0.3871	0.4372	0.5402
34	0.2714	0.2855	0.3023	0.3230	0.3504	0.3899	0.4593
36	0.2497	0.2620	0.2765	0.2942	0.3171	0.3488	0.3998
38	0.2292	0.2399	0.2525	0.2676	0.2867	0.3125	0.3515
40	0.2098	0.2192	0.2300	0.2429	0.2589	0.2801	0.3106
42	0.1916	0.1997	0.2090	0.2200	0.2335	0.2508	0.2750

Figure 18-4: Coulomb Active Earth Pressure Coefficients K_a , $\delta = 5^\circ$

		Backfill Angle β, Degrees						
Friction Angle ϕ, Degrees								
	0	5	10	15	20	25	30	
26	0.3590	0.3831	0.4134	0.4545	0.5186	0.6691		
28	0.3330	0.3541	0.3802	0.4147	0.4653	0.5590		
30	0.3085	0.3269	0.3495	0.3786	0.4195	0.4870	0.7616	
32	0.2852	0.3015	0.3210	0.3457	0.3792	0.4306	0.5376	
34	0.2633	0.2775	0.2944	0.3154	0.3431	0.3835	0.4551	
36	0.2426	0.2550	0.2696	0.2874	0.3106	0.3429	0.3951	
38	0.2230	0.2338	0.2464	0.2616	0.2809	0.3072	0.3469	
40	0.2045	0.2139	0.2247	0.2377	0.2539	0.2753	0.3062	
42	0.1870	0.1951	0.2044	0.2155	0.2290	0.2466	0.2711	

Figure 18-5: Coulomb Active Earth Pressure Coefficients K_a , $\delta = 10^\circ$

		Backfill Angle β, Degrees						
Friction Angle ϕ, Degrees								
	0	5	10	15	20	25	30	
26	0.3501	0.3745	0.4056	0.4480	0.5146	0.6735		
28	0.3251	0.3465	0.3732	0.4086	0.4609	0.5587		
30	0.3014	0.3202	0.3432	0.3729	0.4150	0.4850	0.7765	
32	0.2791	0.2955	0.3153	0.3405	0.3749	0.4279	0.5396	
34	0.2579	0.2723	0.2894	0.3108	0.3391	0.3806	0.4548	
36	0.2379	0.2504	0.2652	0.2834	0.3069	0.3401	0.3939	
38	0.2190	0.2299	0.2426	0.2581	0.2777	0.3045	0.3453	
40	0.2011	0.2105	0.2215	0.2346	0.2511	0.2729	0.3046	
42	0.1841	0.1923	0.2017	0.2129	0.2266	0.2445	0.2695	

Figure 18-6: Coulomb Active Earth Pressure Coefficients K_a , $\delta = 15^\circ$

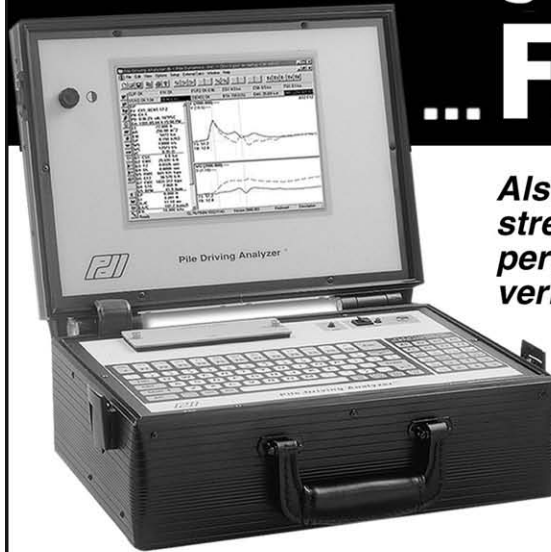
		Backfill Angle β, Degrees					
Friction Angle ϕ, Degrees							
	0	5	10	15	20	25	
26	0.3447	0.3698	0.4017	0.4457	0.5152	0.6836	
28	0.3203	0.3422	0.3696	0.4062	0.4605	0.5632	
30	0.2973	0.3165	0.3400	0.3707	0.4142	0.4871	
32	0.2755	0.2923	0.3126	0.3384	0.3739	0.4289	
34	0.2549	0.2695	0.2870	0.3089	0.3381	0.3810	
36	0.2354	0.2481	0.2632	0.2818	0.3060	0.3401	
38	0.2169	0.2280	0.2410	0.2568	0.2769	0.3044	
40	0.1994	0.2090	0.2202	0.2336	0.2504	0.2728	
42	0.1828	0.1912	0.2007	0.2121	0.2262	0.2444	

Figure 18-7: Coulomb Active Earth Pressure Coefficients K_a , $\delta = 20^\circ$

		Backfill Angle β, Degrees					
Friction Angle ϕ, Degrees							
	0	5	10	15	20	25	
26	0.3425	0.3684	0.4015	0.4473	0.5203	0.6999	
28	0.3186	0.3412	0.3695	0.4074	0.4642	0.5727	
30	0.2959	0.3156	0.3399	0.3717	0.4170	0.4936	
32	0.2745	0.2917	0.3126	0.3393	0.3761	0.4336	
34	0.2542	0.2692	0.2872	0.3098	0.3400	0.3847	
36	0.2350	0.2480	0.2635	0.2827	0.3077	0.3431	
38	0.2167	0.2281	0.2414	0.2577	0.2785	0.3070	
40	0.1995	0.2093	0.2208	0.2346	0.2519	0.2750	
42	0.1831	0.1916	0.2014	0.2131	0.2276	0.2465	

Figure 18-8: Coulomb Active Earth Pressure Coefficients K_a , $\delta = 25^\circ$

Assess Bearing Capacity ...FAST!



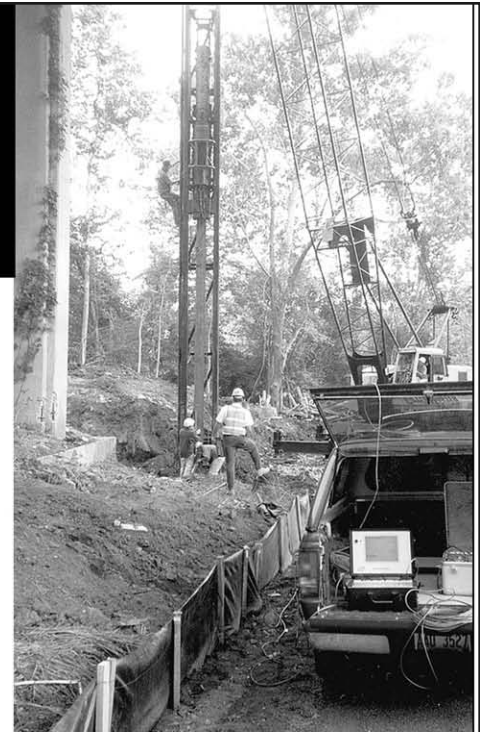
Also monitor driving stresses & hammer performance and verify pile integrity.

Pile Driving Analyzer®



Pile Dynamics, Inc.
Quality Assurance for
Deep Foundations

4535 Renaissance Pkwy.
Cleveland, OH 44128 USA
Tel: +1 216-831-6131
Fax: +1 216-831-0916



www.pile.com

e-mail: info@pile.com

Kahn Steel Co., Inc.

Supplying the Piling industry!

**We carry Large OD Pipe and
many sizes of WF Beams**

Call 800-828-5246 or 800-684-5246

Fax Fred at 913-642-7512 or
email him at kahn@kahnsteel.com
for a current stock list

Or contact us via the internet:

Please visit:
www.kahnsteel.com

Sign up to receive email offers at
www.kahnsteel.com



		Backfill Angle β, Degrees					
Friction Angle ϕ, Degrees							
	0	5	10	15	20	25	
26	0.3435	0.3704	0.4050	0.4531	0.5303	0.7231	
28	0.3197	0.3431	0.3726	0.4123	0.4721	0.5875	
30	0.2972	0.3176	0.3429	0.3760	0.4236	0.5046	
32	0.2759	0.2937	0.3154	0.3432	0.3817	0.4423	
34	0.2557	0.2712	0.2899	0.3134	0.3449	0.3918	
36	0.2366	0.2501	0.2661	0.2860	0.3120	0.3491	
38	0.2184	0.2301	0.2440	0.2608	0.2824	0.3122	
40	0.2012	0.2114	0.2232	0.2375	0.2555	0.2796	
42	0.1849	0.1937	0.2038	0.2159	0.2310	0.2506	

Figure 18-9: Coulomb Active Earth Pressure Coefficients K_a , $\delta = 30^\circ$

		Backfill Angle β, Degrees					
Friction Angle ϕ, Degrees							
	0	5	10	15	20	25	
26	0.3477	0.3759	0.4123	0.4631	0.5454	0.7543	
28	0.3237	0.3482	0.3792	0.4211	0.4846	0.6085	
30	0.3011	0.3224	0.3489	0.3838	0.4342	0.5206	
32	0.2797	0.2983	0.3210	0.3503	0.3909	0.4552	
34	0.2594	0.2756	0.2951	0.3198	0.3530	0.4027	
36	0.2402	0.2543	0.2711	0.2919	0.3193	0.3585	
38	0.2220	0.2343	0.2487	0.2663	0.2890	0.3203	
40	0.2047	0.2153	0.2277	0.2426	0.2615	0.2869	
42	0.1883	0.1975	0.2081	0.2207	0.2364	0.2571	

Figure 18-10: Coulomb Active Earth Pressure Coefficients K_a , $\delta = 35^\circ$

		Backfill Angle β, Degrees						
Friction Angle ϕ, Degrees								
	0	5	10	15	20	25	30	
26	2.5611	2.9429	3.3854	3.9134	4.5641	5.3968	6.5125	
28	2.7698	3.2027	3.7125	4.3311	5.1078	6.1235	7.5204	
30	3.0000	3.4918	4.0804	4.8069	5.7372	6.9818	8.7426	
32	3.2546	3.8147	4.4959	5.3521	6.4708	8.0051	10.2437	
34	3.5371	4.1769	4.9678	5.9805	7.3331	9.2380	12.1142	
36	3.8518	4.5848	5.5066	6.7101	8.3554	10.7411	14.4841	
38	4.2037	5.0465	6.1253	7.5633	9.5795	12.5984	17.5455	
40	4.5989	5.5717	6.8405	8.5697	11.0616	14.9293	21.5923	
42	5.0447	6.1727	7.6732	9.7676	12.8788	17.9072	27.0909	

Figure 18-11: Coulomb Passive Earth Pressure Coefficients K_p , $\delta = 0^\circ$

		Backfill Angle β, Degrees						
Friction Angle ϕ, Degrees								
	0	5	10	15	20	25	30	
26	2.9541	3.4761	4.1042	4.8853	5.8948	7.2616	9.2247	
28	3.2149	3.8088	4.5357	5.4568	6.6730	8.3628	10.8706	
30	3.5052	4.1832	5.0276	6.1187	7.5925	9.6987	12.9401	
32	3.8293	4.6063	5.5915	6.8907	8.6893	11.3397	15.5895	
34	4.1928	5.0870	6.2418	7.7983	10.0110	13.3848	19.0530	
36	4.6023	5.6358	6.9970	8.8747	11.6226	15.9759	23.6961	
38	5.0658	6.2662	7.8804	10.1638	13.6144	19.3230	30.1127	
40	5.5930	6.9951	8.9225	11.7248	16.1139	23.7469	39.3206	
42	6.1962	7.8437	10.1632	13.6390	19.3074	29.7573	53.1836	

Figure 18-12: Coulomb Passive Earth Pressure Coefficients K_p , $\delta = 5^\circ$

Backfill Angle β, Degrees							
Friction Angle ϕ, Degrees	0	5	10	15	20	25	30
26	3.4376	4.1516	5.0471	6.2149	7.8112	10.1272	13.7651
28	3.7698	4.5882	5.6341	7.0278	8.9826	11.9128	16.7218
30	4.1433	5.0857	6.3141	7.9885	10.4039	14.1582	20.6376
32	4.5653	5.6561	7.1073	9.1346	12.1500	17.0324	25.9683
34	5.0445	6.3140	8.0400	10.5159	14.3262	20.7897	33.4741
36	5.5915	7.0779	9.1462	12.2004	17.0833	25.8260	44.4997
38	6.2198	7.9715	10.4712	14.2822	20.6448	32.7849	61.6067
40	6.9460	9.0257	12.0756	16.8948	25.3517	42.7694	90.1761
42	7.7915	10.2807	14.0430	20.2326	31.7460	57.7989	143.1343

Figure 18-13: Coulomb Passive Earth Pressure Coefficients K_p , $\delta = 10^\circ$

Backfill Angle β, Degrees							
Friction Angle ϕ, Degrees	0	5	10	15	20	25	30
30	4.9765	6.3104	8.1447	10.8147	15.0036	22.3043	37.2376
32	5.5409	7.1066	9.3132	12.6250	18.0374	28.0395	50.5243
34	6.1915	8.0426	10.7215	14.8812	22.0030	36.1138	71.8691
36	6.9468	9.1528	12.4389	17.7398	27.3181	47.9726	109.2722
38	7.8301	10.4823	14.5614	21.4322	34.6617	66.3693	183.7383
40	8.8720	12.0923	17.2251	26.3121	45.1974	97.0873	366.0992
42	10.1122	14.0664	20.6281	32.9412	61.0551	154.0184	1033.2083

Figure 18-14: Coulomb Passive Earth Pressure Coefficients K_p , $\delta = 15^\circ$

Backfill Angle β, Degrees						
Friction Angle ϕ, Degrees	0	5	10	15	20	25
40	11.7715	17.0828	26.5688	46.4592	101.6121	390.3539
42	13.7053	20.4683	33.2702	62.7596	161.1674	1101.3008

Figure 18-15: Coulomb Passive Earth Pressure Coefficients K_p , $\delta = 20^\circ$

H&M VIBRO, INC.

P.O. Box 224, Grandville, MI 49468

Toll Free: (800) 648-3403

(616) 538-4150

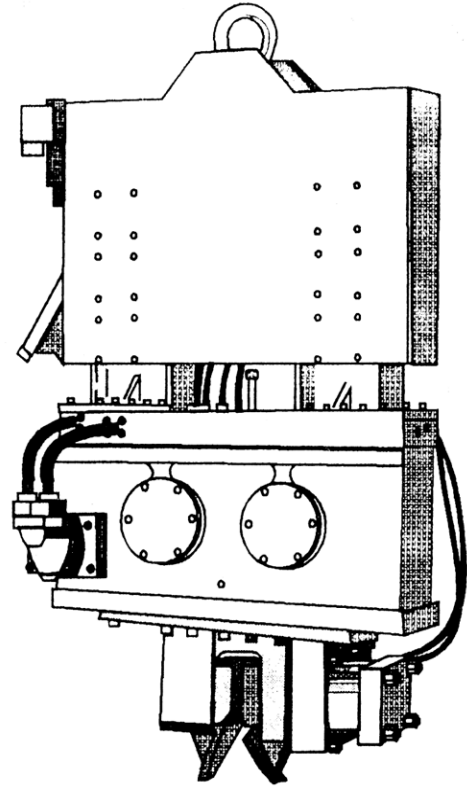
www.hmvibro.com

Model H-1700

Vibratory Driver/Extractor

Features:

- 75 Ton Pile Clamping Force
- 30 Ton Extraction Line Pull
- Weight: 7,000 Pounds
- Optional Counterweight: 3,600 Pounds
- CAT 3126 Power Pack



SALES AND RENTALS

Used / New Beams, Plate, Sheeting, Pipe HP Sections & Channels Now Available

WIDE FLANGE BEAMS: RHODE ISLAND

36" WF 328# 8pcs 32.83 thru 50'
36" WF 359# 4pcs 41.17 thru 47.58
36" WF 393# 37pcs 39.75 thru 54.33
* List Upon Request

PLATE: IN STOCK 1 1/8" x 1

8' x 20' & 10' x 30'



The only good thing about new steel is it becomes used . . . and we have it!

MILL ROLLING:

DOMESTIC W.F
Chaparral Steel/upon request
F.O.B. Petersburg, VA.

STEEL SHEET PILING:

XZ - 85 - 90 - 95
NEW & USED

WIDE FLANGE:

USED
14" x 193# 730# JUMBO
24" x 62# 76# 131# 146#
27" x 84# 94# 102#
33" x 118# 141# 172#
36" x 150# to 359#
36" x 300# DECK BEAMS W/C.P.

RHODE ISLAND: PIPE 42" X 1.008 WALL X 70

1 pc 16'
1 pc 19'8"
5 pcs 20' thru 29'
5 pcs 30' 10" thru 39'5"
13 pcs 40'3" thru 49'6"
8 pcs 50' thru 58'4"

PIPE: 16" X .188 WALL R.I.

16 pcs 35' thru 45'

IN STOCK DOMESTIC 36/GD.50:\ NEW

8" WF 35#
10" WF 49# 54#
12" WF 65# 72# 79#
14" WF 74# 84# 90# 109# 120# 132#
21" WF 83#

Call NESTOR or LAURIE • 516-546-7900 • FAX: 516-546-7992

NESTOR/MERRICK MATERIALS, INC.

Nestor Palahnuik, 1745 Merrick Avenue, Suite #8 • Merrick, New York 11566

18.3. Log-Spiral Theory

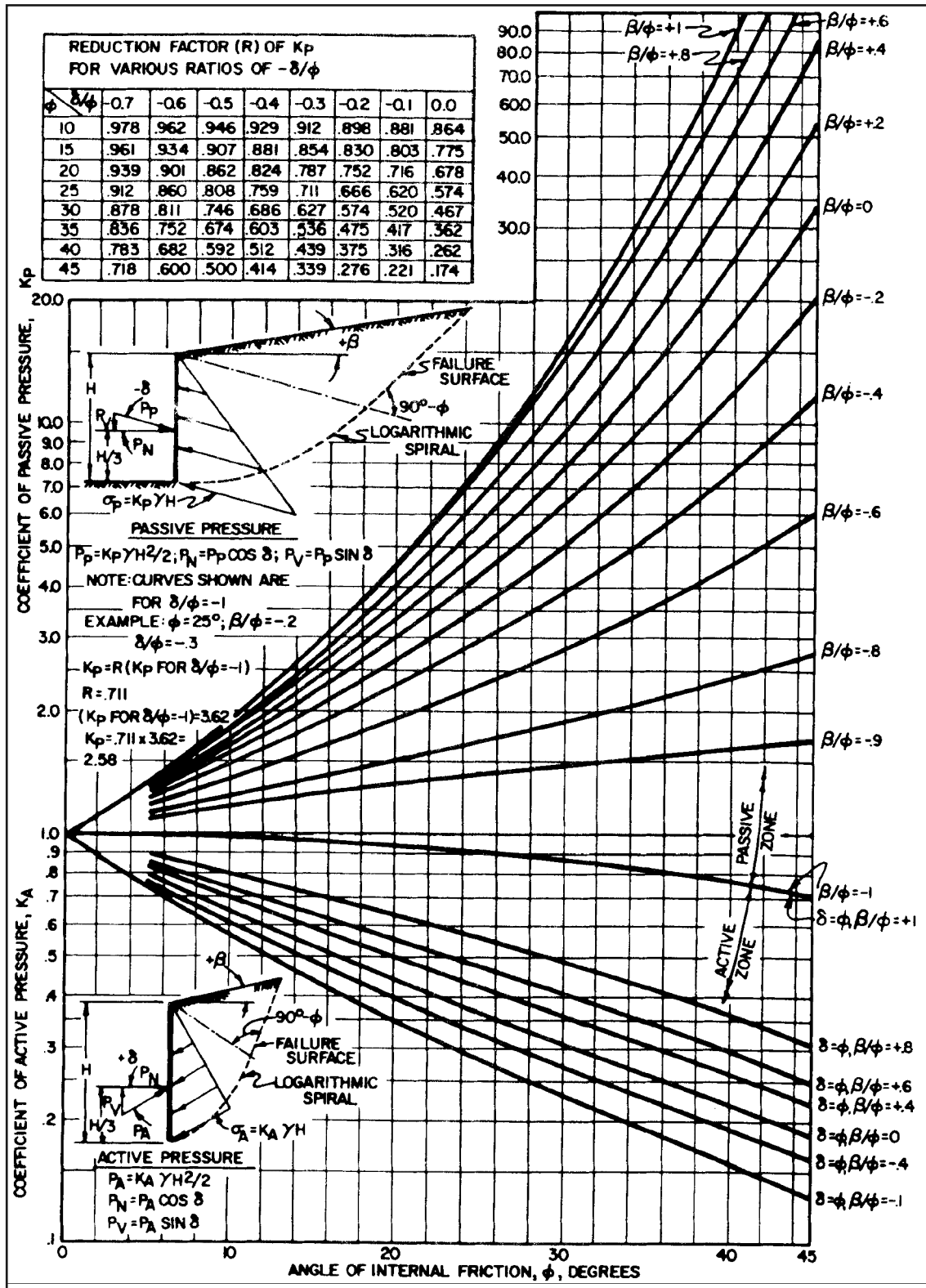


Figure 18-16: Active and passive earth pressure coefficients with wall friction-sloping backfill

Chapter Nineteen: References, Notation and Glossary

19.1. References and Bibliography

References which were copied directly in this manual are in **bold**.

- Agbabian Associates. 1980. "Seismic Response of Port and Harbor Facilities," Report P80-109- 499, El Segundo, CA.
- Al Homound, A. 1990. "Evaluating Tilt of Gravity Retaining Wall During Earthquakes," ScD Thesis, Department of Civil Engineering, Massachusetts Institute of Technology, Cambridge, MA.
- Ambraseys, N. N., and Menu, J. M. 1988. Earthquake-Induced Ground Displacements, Earthquake Engineering and Structural Dynamics, Vol. 16, pp. 985-1006.
- American Association of State Highway and Transportation Officials. 1983. "Guide Specifications for Seismic Design of Highway Bridges," AASHTO, Washington, DC.
- American Institute of Steel Construction – *Manual of Steel Construction*, 8 th Edition, AISC Chicago, IL
- Amono, R., Azuma, H., and Ishii, Y. 1956. "A Seismic Design of Walls in Japan," Proceedings 1st World Conference on Earthquake Engineering, pp. 32-1 to 32-17.
- Anderson, C., Whitman, R., and Germaine, J. 1987. "Tilting Response of Centrifuge-Modeled Gravity Retaining Wall to Seismic Shaking: Description of Tests and Initial Analysis of Results," Report No. R87-14, Department of Civil Engineering, Massachusetts Institute of Technology, Cambridge, MA.
- Anderson, P. 1956. *Substructure Analysis and Design*, Ronald Press, New York, New York.
- Armento, W. J., Criteria for Lateral Pressures for Braced Cuts, ASCE Specialty Conference on Performance on Earth and Earth Support Structures, (Proceedings), 1977, Vol. I, Part 2, pp. 1283-1302.
- Applied Technology Council. 1978 (Jun). "Tentative Provisions for the Development of Seismic Regulation for Buildings," ATC Publication 3-06, Palo Alto, California.
- Ayers, J. A. and R. C. Stokes, *The Design of Flexible Bulkheads*, Transactions, ASCE, Vol. 119, 1954.
- Bakeer, R., Bhatia, S., and Ishibashi, S. 1990. "Dynamic Earth Pressure with Various Gravity Wall Movements," Proceedings of ASCE Specialty Conference on Design and Performance of Earth Retaining Structures, Geotechnical Special Publication No. 25., pp. 887-899.
- Bjerrum, L. 1967 (Sep). "The Third Terzaghi Lecture: Progressive Failure in Slopes of Overconsolidated Plastic Clay and Clay Shales," Journal, Soil Mechanics and Foundation Division, New York, New York, American Society of Civil Engineers, Vol 98, No. SM 5, Part 1.
- Bjerrum, L. and O. Eide, *Stability of Structured Excavations in Clay*, Geotechnique, Vol. 6, No. 1, 1956.
- Bjerrum, L. 1972 (Jun). "Embankments on Soft Ground," State-of-the-Art Paper, Proceedings, Specialty Conference on Performance of Earth and Earth-Supported Structures, American Society of Civil Engineers, Purdue University, Lafayette, Ind., Vol II, pp 1-54. Published by American Society of Civil Engineers, New York, New York.
- Booker, J., Rahman, M., and Seed, H. B. 1976 (Oct). "GAD-FLEA - A Computer Program for the Analysis of Pore Pressure Generation and Dissipation During Cyclic or Earthquake Loading," Report No. EERC 76-24, Earthquake Engineering Research Center, University of California- Berkeley, Berkeley, CA.
- Bowles, J. E., *Foundation Analysis and Design*, McGraw-Hill, Inc. New York, 1977.
- Brinch Hansen, J., *Earth Pressure Calculation*, The Danish Technical Press, The Institution of Danish Civil Engineers, Copenhagen, 1953.
- Brinch Hansen, J., *Resistance of a Rectangular Anchor Slab*, The Danish Geotechnical Institute, Bulletin No. 21, Copenhagen, 1966.
- Broms, B. B. 1975. "Landslides," *Foundation Engineering Handbook*, Chapter 11, Van Nostrand Reinhold Co., New York, New York.
- Burwell, E. B., Jr., and Moneymaker, B. C. 1967. "Geology in Dam Construction," *Application of Geology to Engineering Practice*, Geological Society of America, New York, New York, Berkeley Vol, pp 11-43.

Burwell, E. B., Jr., and Roberts, G. D. 1967. "The Geologist in the Engineering Organization," Application of Geology to Engineering Practice, Geological Society of America, New York, New York, Berkeley Vol, pp 1-9.

California, State of (1990) Trenching and Shoring Manual. Division of Structure Construction. Revision 12, January 2000.

Caquot, A. and J. Kerisel, *Tables for the Calculation of Passive Pressure, Active Pressure, and Bearing Capacity of Foundations*, Gauthier-Villars, Paris, 1948.

Cedergren, H. R. 1977. "Seepage Principles" and "Structural Drainage," *Seepage, Drainage, and Flow Nets*, John Wiley and Sons, Inc., New York, New York.

Chakrabarti, S.; Husak, A.; Christiano, P.; and Troxel, D., *Seismic Design of Retaining Walls and Cellular Cofferdams*, ASCE Conference on Earthquake Engineering and Soil Dynamics, Pasadena, June 1, 1978, pp. 325-341.

Chapman, K. R.; Cording, E. J.; and Achnabel, H. Jr.; *Performance of a Braced Excavation in Granular and Cohesive Soils*, ASCE Specialty Conference on Performance of Earth and Earth Supported Structures, (Proceedings), 1972, Vol. III, pp. 271-293.

Chellis, Robert, *Pile Foundations*, McGraw-Hill, Inc., New York, 1961.

Cheney, R.S., *Permanent Ground Anchors*, U.S. Department of Transportation, Federal Highway Administration Report, FHWA-DP-68-1, pp. 13-53, January 1984.

Chang, M., and Chen, W. 1982. "Lateral Earth Pressures on Rigid Retaining Walls Subjected to Earthquake Forces," *Solid Mechanics Archives*, Vol. 7, No. 4, pp. 315-362.

Chang, C., Power, M., Mok, C., Tang, Y., and Tang, H. 1990 (May). "Analysis of Dynamic Lateral Earth Pressures Recorded on Lotung Reactor Containment Model Structure," *Proceedings 4th US National Conference on Earthquake Engineering*, EERI, Vol. 3, Palm Springs, CA.

Chopra, A. K. 1967 (Dec). "Hydrodynamic Pressures on Dams During Earthquakes," *ASCE, Journal of Engineering Mechanics Division*, Vol. 93, No. EM6, pp 205-223.

Christian, J. T., and Swiger, W. F. 1975 (Nov). "Statistic of Liquefaction and SPT Results," *Journal, Geotechnical Engineering Division, American Society of Civil Engineers*, New York, New York, Vol 101, GT11, pp 1135-1150.

Clough, G. W. and Hansen, L. A. 1977. "A Finite Element Study of the Behavior of the Willow Island Cofferdam," *Technical Report CE-218*, Department of Civil Engineering, Stanford University.

Clough, G. W. and Duncan, J. M. 1991. Chapter 6: Earth Pressures, in *Foundation Engineering Handbook*, Second Edition, edited by H. Y. Fang, Van Nostrand Reinhold, NY, pp. 223-235.

Committee on Earthquake Engineering, Commission on Engineering and Technical Systems, National Research Council. 1985. *Liquefaction of Soils During Earthquakes*, National Academy Press, WA.

Coulomb, C. A. 1776. "Essai sur une application des règles des maximis et mininis à quelques problèmes de statique relatifs à l'architecture", *Mèm. acad. roy. près divers savants*, Vol. 7, Paris.

Cummings, E. M. 1957 (Sep). "Cellular Cofferdams and Docks," *Journal of the Waterways and Harbors Division*, American Society of Civil Engineers, New York, New York.

D'Appolonia, E., D'Appolonia, D. J., and Ellison, R. D. 1975. "Drilled Piers," *Foundation Engineering Handbook*, Van Nostrand Reinhold, Co., New York, New York.

Davisson, M. T. and Salley, J. R. 1972. "Settlement Histories of Four Large Tanks on Sand," *Proceedings of the Specialty Conference on Performance of Earth and Earth-Supported Structures*, Purdue University, Lafayette, Indiana.

Dawkins, W. P. 1991 (Mar). "User's Guide: Computer Program for Design and Analysis of Sheet-Pile Walls by Classical Methods (CWALSHT) with Rowe's Moment Reduction," *Instruction Report ITL 91-1*, Information Technology Laboratory, US Army Engineer Waterways Experiment Station, Vicksburg, MS.

Dawkins, W.P. (2001) Investigation of Wall Friction, Surcharge Loads, and Moment Reduction Curves for Anchored Sheet Pile Walls. ERDC/ITL TR-01-04. Vicksburg, MS: U.S. Army Corps of Engineers, Waterways Experiment Station, Engineer Research and Development Centre, Information Technology Laboratory.

Deere, D.U. 1974. "Geological Considerations," *Rock Mechanics in Engineering Practice*, John Wiley and Sons, Inc., New York, New York, pp 1-20.

Department of the Army, U.S. Army Corps of Engineers. Design Of Sheet Pile Cellular Structures Cofferdams And

**JINNINGS EQUIPMENT LLC OFFERING BSP'S NEW ASSISTED
& DOUBLE ACTING HYDRAULIC IMPACT HAMMERS.**

THEY ARE RELIABLE, VERSATILE, ECONOMICAL AND HAVE PROVEN TECHNOLOGY

INTRODUCING THE NEW BSP MODEL SCV-60 ... OUT DRIVING THE COMPETITION IN COST!

MIDWEST DISTRIBUTOR FOR FULL LINE OF INTERNATIONAL CONSTRUCTION EQUIPMENT



JINNINGS EQUIPMENT, LLC.

PH) 260-447-4343

FAX) 260-447-4363

MERCO, INC.
TUNNEL & BRIDGE
CONTRACTORS

1117 Route 31 South
Lebanon, NJ 08833
Tel: 908-730-8622
Fax: 908-730-6472

Retaining Structures. EM 1110-2-2503. Washington, DC, 1989.

Department of the Army, Corps of Engineers. 1973. *An Analysis of Cellular Sheet Pile Cofferdam Failures*, Ohio River Division, Cincinnati, Ohio.

Department of the Army, Corps of Engineers, St. Louis District. 1983 (Nov). *Lock & Dam 26 (Replacement) Mississippi River, Alton, Illinois, Summary Report, Instrumentation Data Analysis and Finite Element Studies for First Stage Cofferdam*, Shannon & Wilson, Inc.

Department of the Army, U.S. Army Corps of Engineers. Design Of Sheet Pile Walls. EM 1110-2-2504. Washington, DC, 1994.

Department of the Army, U.S. Army Corps of Engineers. Retaining and Flood Walls. EM 1110-2-2502. Washington, DC, 1989.

Department of Defense. Maintenance of Waterfront Facilities. TM 5-622. Washington, DC: Department of Defense, 1978.

Department of Defence. Soil Dynamics and Special Design Aspects. MIL-HDBK-1007/ 3. Norfolk, VA: Naval Facilities Engineering Command, 1997.

Department of the Interior, Bureau of Reclamation. 1965. *Design of Small Dams*.

Department of the Navy. 1983 (Apr). "NAVFAC DM-7.3, Soil Dynamics, Deep Stabilization, and Special Geotechnical Construction, Design Manual 7.3," Department of the Navy, Naval Facilities Engineering Command, 200 Stovall Street, Alexandria, VA.

Department of Transportation, Federal Highway Administration. 1977.

Dismuke, T. D. 1975. "Cellular Structures and Braced Excavations," *Foundation Engineering Handbook*, Van Nostrand Reinhold, Co., New York, New York.

Dismuke, T. 1991. Chapter 12: Retaining Structures And Excavations, *Foundation Engineering Handbook*, Second Edition, edited by H. Y. Fang, Van Nostrand Reinhold, NY, pp. 447-510.

Driscoll, D.D. Retaining Wall Design Guide. Portland, OR: U.S.D.A. Forest Service Region 6, 1979.

Duncan, J. M. 1985. *Lecture Notes Regarding the Design of Anchored Bulkheads*.

Duncan, J. M., Clough, G. W., and Ebeling, R. M. 1990. "Behavior and Design of Gravity Earth Retaining Structures," ASCE Specialty Conference on Design and Performance of Earth Retaining Structures, Geotechnical Special Publication 25, pp. 251- 277.

Dunham, C. W., *Foundations of Structures*, McGraw-Hill, Inc. New York, 1962.

Dunncliff, John. 1982 (Apr). "Systematic Approach to Planning Monitoring Programs," 6th Annual Short Course on Field Instrumentation of Soil & Rock, University of Missouri-Rolla, Rolla, Missouri.

Earthquake Engineering Technology, Inc. 1983. "Super FLUSH - Computer Response Analysis Of Soil-Structure Systems Under Various Input Environments."

Ebeling, R. 1990 (Dec). "Review Of Finite Element Procedures for Earth Retaining Structures," Miscellaneous Paper ITL-90-5, Information Technology Laboratory, US Army Engineer Waterways Experiment Station, Vicksburg, MS.

Ebeling, R. M., Duncan, J. M., and Clough, G. W. 1990 (Oct). "Methods of Evaluating the Stability and Safety of Gravity Earth - Retaining Structures Founded on Rock, Phase 2 Study," Technical Report ITL-90-7, Information Technology Laboratory, US Army Engineer Waterways Experiment Station, Vicksburg, MS.

Ebeling, R. M., Clough, G. W., Duncan, J. M., and Brandon, T. L. 1992 (May). "Methods of Evaluating the Stability and Safety of Gravity Earth Retaining Structures Founded on Rock," Technical Report REMR-CS-29, Information Technology Laboratory, US Army Engineer Waterways Experiment Station, Vicksburg, MS.

Ebeling, R.M., and Morrison, E.E. The Seismic Design Of Waterfront Retaining Structures. NCEL Technical Report R-939. Port Hueneme, California: Naval Civil Engineering Laboratory, 1993.

Edris, E. V., and Wright, S. C. 1987 (Aug). "User's Guide: UTEXAS2 Slope-Stability Package, Volume 1: User's Manual," Instruction Report GL-87-1, Geotechnical Laboratory, US Army Engineer Waterways Experiment Station, Vicksburg, MS.

Elms, D., and Richards, R. 1990. "Seismic Design of Retaining Walls," Proceeding of ASCE Specialty Conference on Design and Performance of Earth Retaining Structures, Geotechnical Special Publication No. 25., pp. 854-871.

- Esrig, M. I. 1970. "Stability of Cellular Cofferdams Against Vertical Shear," Soil Mechanics and Foundation Division, American Society of Civil Engineers, New York, New York, Vol 96, No. SM 6, pp 1853-1862.
- Fetzer, C. A. 1975. "Progressive Failure in Shale (Cannelton Dam Stage I, Cofferdam Failure)," Ohio River Valley Seminar VI, Ft. Mitchell, Kentucky.
- Finn, W., Liam, D., Yogendrakumar, M., Yoshida, N., and Yoshida, H. 1986. "TARA-3: A Program for Non-Linear Static and Dynamic Effective Stress Analysis," Soil Dynamics Group, University of British Columbia, Vancouver, B.C.
- Florida Department of Transportation. Soils and Foundation Handbook 2000. Gainesville, FL: Florida Department of Transportation, State Materials Office, 2000.**
- Franklin, C. and Chang, F. 1977 (Nov). "Earthquake Resistance of Earth and Rockfill Dams: Report 5: Permanent Displacement of Earth Embankments by Newmark Sliding Block Analysis," Miscellaneous Paper 5-71-17, Soils And Pavements Laboratory, US Army Engineer Waterways Experiment Station, Vicksburg, MS.
- Gaddie, T. and Gray, H. 1976 (Aug). "Cellular Sheet Pile Structures," Corps-Wide Conference on Computer-Aided Design in Structural Engineering, U. S. Army Engineer Waterways Experiment Station, Vicksburg, Mississippi.
- Gazetas, C., Dakoulas, P., and Dennehy, K. 1990. "Empirical Seismic Design Method for Waterfront Anchored Sheetpile Walls," Proceedings of ASCE Specialty Conference on Design and Performance of Earth Retaining Structures, Geotechnical Special Publication No. 25., pp. 232- 250.
- Geokon, Inc. 1983. Brochure, West Lebanon, New Hampshire.
- Goldberg, D. T.; Jaworski, W. E.; and Gordon M. D.; *Lateral Support Systems and Underpinning, Volume II, Design Fundamentals*, Federal Highway Administration Report No. FHWA-RO-75-129, Washington, D.C., April, 1976.
- Guidelines for Cone Penetration Tests: Performance and Design, FHWA Report TS-78-209 and Appendix II.
- Goodman, R. E. 1980. "Applications of Rock Mechanics to Foundation Engineering," Introduction to Rock Mechanics, John Wiley and Sons, New York, New York.
- Gould, James P., and Dunnclif, John C. 1982 (Apr). "Accuracy of Field Deformation Measurement," 6th Annual Short Course on Field Instrumentation of Soil & Rock, University of Missouri-Rolla, Rolla, Missouri.
- Gray, H. and K. Nair, *Stability of Soil Subject to Seepage Forces Adjacent to Sheet Pile*, Geotechnique, Vol. 17, No. 2, 1967.
- Green, R. 1992. "Selection of Ground Motions for the Seismic Evaluation of Embankments," ASCE Specialty Conference on Stability and Performance of Slopes and Embankments II, A 25- Year Perspective, Geotechnical Special Publication No. 31, Vol. I, pp. 593-607.
- Hallquist, J. 1982. "User's Manual for DYNA2D - An Explicit Two-Dimensional Hydrodynamic Finite Element Code With Interactive Rezoning," University of California, Lawrence Livermore National Laboratory, Report UCID-18756, Rev. 1.
- Hansen, J. B. 1953. Earth Pressure Calculations, The Danish Technical Press, The Institution of Danish Civil Engineers, Copenhagen.
- Hansen, J. B. 1961. "Stability and Foundation Problems," Pressure Calculation, The Danish Technical Press, The Institution of Danish Civil Engineers, Second Edition, Copenhagen.
- Hansen, L. A. and Clough, G. W. 1982. "Finite Element Analyses of Cofferdam Behavior," Proceedings, 4th International Conference on Numerical Methods in Geomechanics, Vol 2, pp 899-906, Edmonton, Canada.
- Hartman, R.J, and Neal, J.A. "Report of Investigation of the Effect of the Behavior of Z-Shape Steel Sheet Piling." Prepared for the L.B. Foster Company and Bethlehem Steel Corporation. Project No. 94-419. 1997.**
- Horstman, Wil. *Barge Dock for Inland Waterways*, ASCE Proceedings Vol. 90, No. WW4, Nov. 1964.
- Hsu, P. T.; Elkon, J.; and Pian, T. H. H.; *Note on the Instability of Circular Rings Confined to a Rigid Boundary*, Journal of Applied Mechanics, September, 1964.
- Hung, S., and Werner, S. 1982. "An Assessment of Earthquake Response Characteristics and Design Procedures for Port and Harbor Facilities," Proceeding 3rd International Earthquake Microzonation Conference, Report No. SF/CEE-82070 Seattle, WA, pp. 15.
- Hvorslev, M. J. 1948 (Nov). "Subsurface Exploration and Sampling of Soils for Civil Engineering Purposes," U. S. Army Engineer Waterways Experiment Station, Vicksburg, Mississippi.

- Hynes-Griffin, M. E., and Franklin, A. C. 1984. "Rationalizing the Seismic Coefficient Method," Miscellaneous Paper S-84-13, US Army Engineer Waterways Experiment Station, Vicksburg, MS.
- Iai, S., and Kameoka, T. 1991. "Effective Stress Analysis of a Sheet Pile Quaywall," Proceeding of Second International Conference on Recent Advances in Geotechnical Earthquake Engineering and Soil Dynamics, Paper No. 4.14, Vol. I, St. Louis, MO, pp. 649-656.
- Ichihara, M., and Matsuzawa, H. 1973 (Dec). "Earth Pressure During Earthquake," Soils and Foundations, Vol. 13, No. 4, pp. 75-86.
- Idriss, I. M. 1985. Evaluating Seismic Risk in Engineering Practice, Proceeding 11th International Conference on Soil Mechanics and Foundation Engineering, Vol. 1, pp. 255-320.
- Irad Goge. 1983. Brochure, A Division of Crear Products, Inc., Lebanon, New Hampshire.
- Ishibashi, I., and Fang, Y. 1987 (Dec). "Dynamic Earth Pressures with Different Wall Modes," Soils and Foundations, Vol. 27, No. 4, pp. 11-22.
- Ishibashi, I., and Madi, L. 1990 (May). "Case Studies On Quaywall's Stability With Liquefied Backfills," Proceeding of 4th U.S. Conference on Earthquake Engineering, EERI, Vol. 3, Palm Springs, CA, pp. 725-734.
- Ishibashi, I., Matsuzawa, H., and Kawamura, M. 1985. "Generalized Apparent Seismic Coefficient for Dynamic Lateral Earth Pressure Determination," Proceeding of 2nd International Conference on Soil Dynamics and Earthquake Engineering, edited by C. Brebbia, A. Cakmak, and A. Chaffer, QE2, pp. 6-33 to 6-42.
- Johnson, E. 1953 (Apr). "The Effects of Restraining Boundries on the Passive Resistance of Sand, Results of a Series of Tests with a Medium-Scale Testing Apparatus," Masters of Science Thesis In Engineering, Princeton University.
- Joyner, W. B., and Boore, D. M. 1988. "Measurement, Characterization and Prediction of Strong Ground Motion," Earthquake Engineering and Soil Dynamics II - Recent Advances in Ground Motion Evaluation, ASCE Geotechnical Special Publication No. 20, pp. 43-102.
- Jumkis, Alfreds R., *Mechanics of Soils*, D. Van Nostrand and Company, Inc., Princeton, New Jersey, 1964.
- Jumikis, A. R. 1971. "Vertical Stress Tables for Uniformly Distributed Loads on Soil," Engineering Research Publication No. 52, Rutgers University, New Brunswick, New Jersey.
- Kerisel, J. , and Absi, E. 1990 (May). Active and Passive Earth Pressure Tables ,” A. A. Balkema International Publishers, pp. 234.
- Kirkman, R., *Discussion*, Proceedings, Brussels Conference 58 on Earth Pressure Problems, Brussels, 1958.
- Kittisatra, L. 1976 (Jun). "Finite Element Analysis of Circular Cell Bulkheads," Ph. D. Thesis, Oregon State University, Corvallis, Oregon.
- Kitajima, S., and Uwabe, T. 1979 (Mar). "Analysis on Seismic Damage in Anchored Sheet- Piling Bulkheads," Report of the Japanese Port and Harbor Research Institute, Vol. 18, No. 1, pp. 67-130. (in Japanese).
- Krynine, D. P., *Discussion on Stability and Stiffness of Cellular Cofferdams*, Transactions, ASCE, Vol. 110, 1945.
- Krynine, D. P and Judd, W. R., *Principles of Engineering Geology and Geotechnics*, McGraw-Hill, Inc., New York, 1957.
- Kurata, S., Arai, H. and Yokoi, T. (1965). "On the Earthquake Resistance of Anchored Sheet Pile Bulkheads," Proceedings, 3rd World Conference On Earthquake Engineering, New Zealand.
- Lacroix, Y., Esrig, M. I., and Luscher, U. 1970 (Jun). "Design, Construction, and Performance of Cellular Cofferdams," "Lateral Stresses in the Ground and Earth Retaining Structures," Journal, Soil Mechanics and Foundation Division, American Society of Civil Engineers, Specialty Conference, Cornell University, Ithaca, New York, pp 271-328.
- Ladd, C. 1991 (Apr). "Stability Evaluation During Staged Construction," ASCE, Journal of Geotechnical Engineering, Vol. 117, No. 4, pp. 540-615.
- Lambe, T. W. and Whitman, R. V., *Soil Mechanics*, John Wiley and Sons, Inc., New York, 1969.
- Lee, Donovan H., *Deep Foundations and Sheet Piling*, Concrete Publications Limited, London, 1961.
- Lee, M., and Finn, W. D. Liam. 1975. "DESRA-1: Program for the Dynamic Effective Stress Response Analysis of Soil Deposits including Liquefaction Evaluation," Report No. 36, Soil Mechanic Service, Department of Civil Engineering, University of British Columbia, Vancouver, B.C.
- Lee, M., and Finn, W. D. Liam. 1978. "DESRA-2: Dynamic Effective Stress Response Analysis of Soil Deposits with Energy Transmitting Boundary Including Assessment of Liquefaction Potential," Report No, 38,

Engineering Services for Contractors

Pile Load Testing • Dynamic Pile Testing
 Underpinning • Sheeting/Shoring Design
 Deep Foundations • Geotechnical Instrumentation
 Temporary Structures • Demolition/Erection Plans
 Pre-Construction Surveys • Vibration Monitoring
 Subsurface Explorations • Site Characterization
 Value Engineering • Contaminated Soils Management



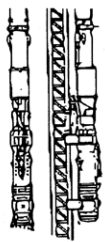
984 SOUTHFORD ROAD
MIDDLEBURY CT. 06762

GEODESIGN
INCORPORATED

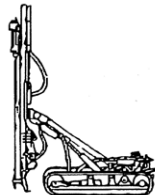
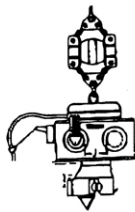
TELEPHONE: (203)758-8836
FACSIMILE: (203)758-8842
WEBSITE: www.geodesign.net

PACIFIC AMERICAN COMMERCIAL COMPANY

45 YEARS OF SERVICE TO THE PILE DRIVING INDUSTRY



**AIR, DIESEL,
VIBES &
HYDRAULIC
IMPACT**



**QUARRY
DRILLS**

BUCKETS



**PORTABLE
PONTOON
BARGES**



**DIESEL AIR
COMPRESSORS**

FAST QUOTATIONS - ALL YOUR FOUNDATION EQUIP. NEEDS - COMPLETE PACKAGES

HAMMERS, VIBRATORYS, LEADS, SPOTTERS
TOP HEADS, CROSS HEADS, FOLLOWER BLOCKS, DRILLS and AUGERS

RENTALS-SALES-REPAIR PARTS AVAILABLE

CALL: 1-800-678-6379 or FAX 1-206-763-4232



Soil Mechanic Service, Department Of Civil Engineering, University of British Columbia, Vancouver, B.C.

Leonards, G. A. 1962. "Engineering Properties of Soils," *Foundation Engineering*, McGraw-Hill Book Co., Inc., New York, New York.

Li, X. 1990. "Free-Field Soil Response under Multi-Directional Earthquake Loading, Ph.D. Thesis, Department of Civil Engineering, University of California, Davis, CA.

Lincoln, Frank L. 1963 (Oct). "Reconstruction of Dry Dock No. 3 at the Portsmouth Naval Shipyard (Part Two)," *Journal of the Boston Society of Civil Engineers*, Boston, MA, Vol 50, No. 4.

Lindahl, H.A., editor. *Pile Buck Steel Sheet Piling Design Manual*. Jupiter, FL: Pile Buck, 1986.

Lo, Hsu, Bogdanoff, Goldberg and Crawford, *A Buckling Problem of a Circular Ring*, Proceedings of the Fourth U.S. National Congress of Applied Mechanics, ASME, 1962.

Lysmer, J., Udaka, T., Tsai, C., and Seed, H. B. 1975. "FLUSH: A Computer Program For Approximate 3-D Analysis of Soil-Structure Interaction Programs," Report No. EERC 75-30, Earthquake Engineering Research Center, University of California, Berkeley, CA.

Mackenzie, Thomas R., *Strength of Deadman Anchors in Clay*, Master's Thesis, Princeton University, Princeton, New Jersey, 1955.

McMahon, D. 1986. Tiebacks for Bulkheads, Collection of Five Papers, Proceeding of a Session Sponsored by the Geotechnical Engineering Division of the ASCE in Conjunction with the ASCE Convention in Seattle, WA., Geotechnical Special Publication No. 4., 90 p.

Maitland, J. K. 1977. "Behavior of Cellular Bulkheads in Deep Sands," Ph. D. Thesis submitted at Oregon State University, Corvallis, Oregon.

Maitland, J. K. and Schroeder, W. L. 1979 (Jul). "Model Study of Circular Sheet Pile Cells," *American Society of Civil Engineers*, GT 7, New York, New York.

Makdisi, F. I., and Seed, H. B. 1979. "Simplified Procedure for Estimating Dam and Embankment Earthquake-Induced Deformations," *ASCE, Journal of the Geotechnical Engineering Division*, Vol. 104, No. GT7, pp. 849-867.

Mansur, C. I. and Kaufman, R. I. 1962. "Dewatering,"

Foundation Engineering, G. A. Leonards, McGraw-Hill Book Co., Inc., New York, New York.

Marcuson, W., Hynes, M., and Franklin, A. 1990 (Aug). "Evaluation and Use of Residual Strength in Seismic Safety Analysis of Embankments," *Earthquake Spectra*, pp. 529-572.

Marsland, A., *Model Experiments to Study the Influence of Seepage on the Stability of a Sheeted Excavation in Sand*, *Geotechnique*, Vol. 3, 1953.

Matlock, H. and Reese, L. C. 1960. "Generalized Solutions for Laterally Loaded Piles," *Journal, Soil Mechanics and Foundations Division, American Society of Civil Engineers*, Vol 86, No. SM5, pp 63-91.

Matsuo, H., and Ohara, S. 1965. "Dynamic Pore Water Pressure Acting on Quay Walls During Earthquakes," *Proceedings of the Third World Conference on Earthquake Engineering*, Vol 1, New Zealand, pp. 130-140.

Matsuzawa, H., Ishibashi, I., and Kawamura, M. 1985 (Oct). "Dynamic Soil and Water Pressures of Submerged Soils," *ASCE, Journal of Geotechnical Engineering*, Vol. 111, No. 10, pp. 1161-1176.

Meyerhof, G.G. 1953. "The Bearing Capacity of Foundation Under Inclined and Eccentric Loads," *3rd International Conference Of Soil Mechanics And Foundation Engineering*, Vol. 1, pp 440-445.

Mononobe, N., and Matsuo, H. 1929. "On the Determination of Earth Pressures During Earthquakes," *Proceedings, World Engineering Congress*, 9.

Moran, D. F., *Designing Underground Reservoirs*, Consulting Engineering, January, 1966.

Nadiem, F., and Whitman, R. 1983 (May). "Seismically Induced Movement of Retaining Walls," *ASCE, Journal of Geotechnical Engineering*, Vol. 109, No. 7, pp. 915-931.

National Earthquake Hazards Reduction Program (NEHRP). 1988. *Recommended Provisions for the Development of Seismic Regulations for New Buildings: Building Seismic Safety Council*.

National Research Council. 1988. *Probabilistic Seismic Hazard Analysis: National Academy Press, Washington, DC*, 97 p.

National Research Council. 1985. *Liquefaction of Soils During Earthquakes: National Academy Press, Washington, DC*, 240 p.

Naval Civil Engineering Laboratory. *Corrosion Control*. Techdata Sheet Series. Port Hueneme, CA: Naval Civil Engineering Laboratory. Includes the following Techdata Sheets:

- *Corrosion Control Ashore*, 85-01, January 1985
- *Forms of Corrosion I: Uniform Corrosion/No Attack*, 85-02, January 1985
- *Forms of Corrosion II: Galvanic Corrosion*, 85-03, February 1985
- *Forms of Corrosion III: Pitting*, 85-04, February 1985
- *Forms of Corrosion IV: Crevice Corrosion*, 85-05, February 1985
- *Forms of Corrosion V: Dealloying and Intergranular Corrosion*, 85-06, February 1985
- *Forms of Corrosion VI: Stress Corrosion Cracking and Hydrogen Embrittlement*, 85-07, March 1985
- *Forms of Corrosion VII: Erosion Corrosion and Cavitation Corrosion*, 85-08, March 1985
- *Forms of Corrosion VIII: Corrosion Fatigue and Fretting Corrosion*, 85-09, March 1985
- *Corrosion Control I: Introduction to Corrosion Control/Protective Coatings*, 85-10, March 1985
- *Corrosion Control II: Materials Selection*, 85-11, March 1985
- *Corrosion Control III: Cathodic Protection*, 85-12, March 1985
- *Corrosion Control IV: Control of Environment/Corrosion Allowance*, 85-13, March 1985
- *Corrosion Control V: Design Factors for Corrosion Control*, 85-14, March 1985.
- *Cathodic Protection: No Longer a Mystery!* 93-03, May 1993
- *Cathodic Protection System: Inspection I*, 93-04, June 1993
- *Cathodic Protection System: Inspection II*, 93-05, July 1993
- *Cathodic Protection System: Inspection III*, 93-06, August 1993
- *Cathodic Protection System: Inspection IV*, 93-07, September 1993
- *Cathodic Protection System: Inspection V*, 2002-SHR, February 1994
- *Cathodic Protection System: Inspection VI*, 2003-SHR, February 1994
- *Cathodic Protection System: Design I – The Pre-Design Field Survey*, TDS-2020- SHR, June 1995
- *Cathodic Protection System, Design II – Electrolyte Resistivity Measurement*, TDS-2021-SHR, June 1996
- *Cathodic Protection System, Design III – Sacrificial Anode System Design Principles for Underground Structures*, TDS 2022-SHR, June 1995

NAVFAC DM 7.01, *Soil Mechanics*. Norfolk, VA: Naval Facilities Engineering Command, 1986.

NAVFAC DM 7.02, *Foundations and Earth Structures*. Norfolk, VA: Naval Facilities Engineering Command, 1986.

Naval Facilities Engineering Command. Structural Engineering: Steel Structures. MIL-HDBK- 1002/3. Norfolk, VA: Naval Facilities Engineering Command, 1987.

Neghabat, Farrokh. 1970 (Jun). "Optimization in Cofferdam Design," Ph. D. Dissertation in Applied Science submitted to the University of Delaware, Newark, Delaware.

Newmark, N. N., and Hall, W. J. 1983. Earthquake Spectra and Design, Earthquake Engineering Research Institute, 499 14th Street, Oakland, CA, 103 p.

Office of Emergency Preparedness, Executive Office of the President. 1972. "Disaster Preparedness, A Report to the Congress by the Office of Emergency Preparedness," Washington, DC.

Okabe, S. 1926. "General Theory of Earth Pressures," Journal Japan Society of Civil Engineering, Vol. 12, No. 1.

Okamoto, S. 1984. "Introduction to Earthquake Engineering," second edition, University of Tokyo Press, 629 p.

Ovesen, N. K. 1962. Cellular Cofferdams Calculation Method and Model Tests, Bulletin 14, Danish Geotechnical Institute, Copenhagen.

Ovesen, N. Krebs, Anchor Slabs Calculation Methods and Model Tests, The Danish Geotechnical Institute, Bulletin No. 16, Copenhagen, 1964.

Patterson, John H. 1970. "Installation Techniques for Cellular Structures," Design and Installation of Pile Foundations and Cellular Structures, Envo Publishing Co., Inc., Lehigh Valley, Pennsylvania.

Peck, R. B., Earth Pressure Measurements in Open Cuts, Chicago (Ill.) Subway, Transactions, ASCE, Vol. 108, 1943.

Peck, R. B., Deep Excavations and Tunneling Soft Ground, Seventh International Conference on Soil Mechanics and Foundation Engineering, State-of-the-Art Volume, Mexico, 1969, pp. 225-290.

Peck, R. B., Hanson, W. E., and Thornburn, T. H. 1974. "Techniques of Subsurface Investigation," Foundation Engineering, John Wiley & Sons, Inc., New York, New York.

Peterson, M. S., Kulhawy, F. H., Nucci, L. R., and Wasil, B. A. 1976. "Stress-Deformation Behavior of Soil-Concrete

Interfaces," Contract Report B-49, Department of Civil Engineering, Syracuse University, Syracuse, NY.

Pile Buck Annual. Vero Beach, FL: Pile Buck, Inc., 1988.

Potyondy, J. C. 1961 (Dec). "Skin Friction Between Various Soils and Construction Materials," *Geotechnique*, Vol II, No. 4, pp 339-353.

Poulos, S. J., Castro, G., and France, W. (1985). "Liquefaction Evaluation Procedure." *ASCE Journal of Geotechnical Engineering Division*, Vol. 111, No. 6, pp. 772-792.

Prakash, S., and Basavanna, B. 1969. "Earth Pressure Distribution Behind Retaining Wall During Earthquake," *Proceeding, 4th World Conference on Earthquake Engineering*, Santiago, Chile.

Proctor, R. V., and T. L. White, *Rock Tunneling with Steel Supports*, Youngstown Printing Company, Youngstown, Ohio, 1964.

Prakash, S., and Basavanna, B. 1969. "Earth Pressure Distribution Behind Retaining Wall During Earthquake," *Proceeding, 4th World Conference on Earthquake Engineering*, Santiago, Chile.

Provost, J. 1981 (Jan). "DYNAFLOW - A Nonlinear Transient Finite Element Analysis Program, Report No. 81-SM-1, Princeton University, Princeton, NJ.

Provost, J. 1989. "DYNAID - A Computer Program For Nonlinear Seismic Site Response Analysis, Technical Report NCEER-89-0025, National Center for Earthquake Engineering Research, University of Buffalo.

Quinn, Alonzo DeF., *Design and Construction of Ports and Marine Structures*, McGraw-Hill, Inc., New York, 1972.

Rankine, W. (1857). *On the Stability of Loose Earth*, *Phil. Trans. Roy. Soc. London*, Vol. 147.

Richards, R., and Elms, D. 1979 (April). "Seismic Behavior of Gravity Retaining Walls," *ASCE, Journal of the Geotechnical Engineering Division*, Vol. 105, No. CT4, pp. 449-464.

Richards, R., and Elms, D. 1990. "Seismic Design of Retaining Walls," *Proceedings of ASCE Specialty Conference on Design and Performance of Earth Retaining Structures*, *Geotechnical Special Publication No. 25.*, pp. 854-871.

Roberts, G. D. 1964. "Investigation Versus Exploration," *Engineering Geology, Bulletin of the Association of Engineering Geologists*, Vol 1, No. 2, pp 37-53.

Roberts, G. D. 1970. "Soil Formation and Engineering Applications," *Engineering Geology, Bulletin of the Association of Engineering Geologists*, Vol 7, Nos. 1 & 2, pp 87-105.

Rossow, M. P. 1980 (Apr). "Finite Elements for Generalized Plane Strain," *American Institute of Aeronautics and Astronautics Journal*, Vol 19, No. 4.

Rossow, M. P. "Notes on Finite Element Modeling of a Cellular Cofferdam," U. S. Army Engineer District, St. Louis, Structural Section, Sep 1981 (Revised Jan 1982).

Roth, W. H., Scott, F. F., and Cundall, P. A. 1986. "Nonlinear Dynamic Analysis of a Centrifuge Model Embankment," *Proceedings of the Third US National Conference on Earthquake Engineering*, Vol. I, Charleston, SC, pp. 505-516.

Rowe, P. W. 1952. "Anchored Sheet Pile Walls," *Proceedings of Institution of Civil Engineers*, Vol 1, Part 1, pp 27-70.

Rowe, P. W., *A Theoretical and Experimental Analysis of Sheet Pile Walls*, *Proceedings, Institution of Civil Engineers, Part I, Vol. 1, London, England, 1955.*

Rowe, P. W., *Sheet Pile Walls Encastre at Anchorage*, *Proceedings, Institution of Civil Engineers, Part I, Vol. 1, London England, 1955.*

Rowe, P. W. 1956. "Sheet Pile Walls at Failure," *Proceedings Instruction Civil Engineers London*, Vol. 5, Part I, pp. 276-315.

Rowe, P. W., *Sheet Pile Walls in Clay*, *Proceedings, Institution of Civil Engineers, Part I, Vol. 1, London, England, 1957.*

Rowe, P. W. 1957 (Feb). "Limit Design of Flexible Walls," *Proceedings Midland Soil Mechanic and Foundation Engineering Society*, Vol. 1, pp. 29-40.

Sadigh, K. 1983. "Considerations in the development of site-specific spectra," in *proceedings of Conference XXII, site-specific effects of soil and rock on ground motion and the implications for earthquake resistant design: U.S. Geological Survey Open File Report 83-845.*

Sanglerat, G. 1972. *Penetrometer and Soil Exploration*, Elsevier Publishing Company, Amsterdam, The Netherlands.

Sarma, S. K. 1979. "Response and Stability of Earth Dams During Strong Earthquakes," *Miscellaneous Paper GL-79-13, US Army Engineer Waterways Experiment Station, Vicksburg, MS.*

H&M VIBRO, INC.

P.O. Box 224, Grandville, MI 49468

Toll Free: (800) 648-3403

(616) 538-4150

www.hmvibro.com

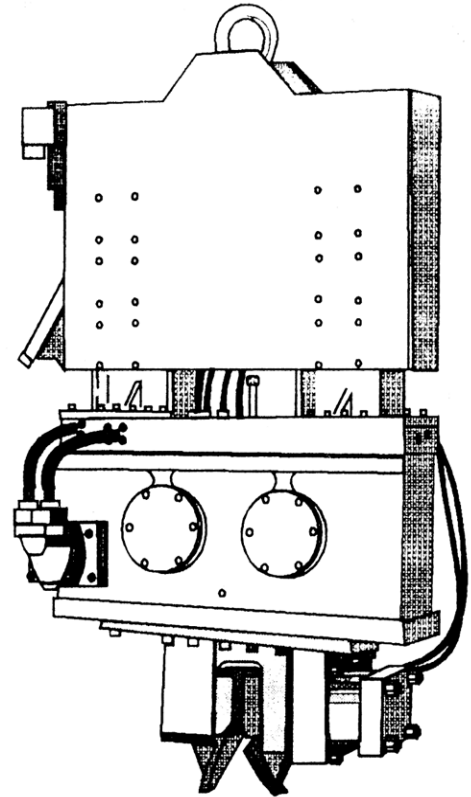
Model H-1700

Vibratory Driver/Extractor

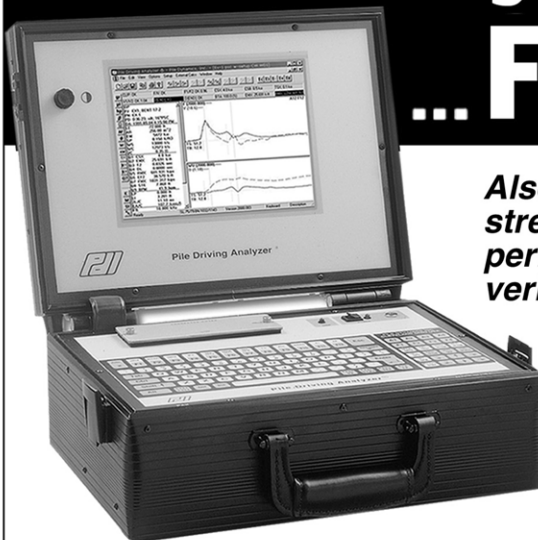
Features:

- 75 Ton Pile Clamping Force
- 30 Ton Extraction Line Pull
- Weight: 7,000 Pounds
- Optional Counterweight: 3,600 Pounds
- CAT 3126 Power Pack

SALES AND RENTALS



Assess Bearing Capacity ... FAST!



Also monitor driving stresses & hammer performance and verify pile integrity.

Pile Driving Analyzer®



Pile Dynamics, Inc.
Quality Assurance for
Deep Foundations

4535 Renaissance Pkwy.
Cleveland, OH 44128 USA
Tel: +1 216-831-6131
Fax: +1 216-831-0916



www.pile.com
e-mail: info@pile.com

- Schmertmann, J. H. 1970 (May). "Static Cone to Compute Static Settlement Over Sand," Journal, Soil Mechanics and Foundation Division, American Society of Civil Engineers, New York, New York.
- Schmertmann, J. H., Hartman, J. P., and Brown, P. R. 1978 (Aug). "Improved Strain Influence Factor Diagrams," Technical Note, Geotechnical Engineering Division, American Society of Civil Engineers, New York, New York.
- Schnabel, P., Lysmer, J., and Seed, H. B. 1972 (Dec). "SHAKE: A Computer Program for Earthquake Response Analysis of Horizontally Layered Sites," Report No. EERC 72-12, Earthquake Engineering Research Center, University Of California, Berkeley, CA.
- Schroeder, W. L., Marker, Dennis K., and Khuayjarernpanishk, Thanasorn. 1977 (Mar). "Performance of a Cellular Wharf," Journal of Geotechnical Engineering Division, American Society of Civil Engineers, Vol 103, GT 3, pp 153-168.
- Schroeder, W. L. and Maitland, J. K. 1979 (Jul). "Cellular Bulkheads and Cofferdams," Journal, Geotechnical Engineering Division, American Society of Civil Engineers, New York, New York, Vol 105, GT 7, Paper 14713, pp 823-837.
- Seed, H. B., Soil Liquefaction and Cyclic Mobility Evaluation for Level Ground During Earthquakes, ASCE Vol. 105, No. GT2, February, 1979, pp. 201-255.
- Seed, H. B. and Idriss, I. M. 1971 (Sep). "Simplified Procedure for Evaluating Soil Liquefaction Potential," Journal, Soil Mechanics and Foundation Division, American Society of Civil Engineers, New York, New York, Vol 97, SM 9, pp 1249-1273.
- Seed, H. B. 1987 (Aug). "Design Problems in Soil Liquefaction," ASCE, Journal of the Geotechnical Engineering Division, Vol. 113, No. 8, pp. 827-845.
- _____. 1971. "Simplified Procedure for Evaluating Soil Liquefaction Potential," ASCE, Journal of the Soil Mechanics and Foundations Division, Vol. 97, No. SM9, pp. 1249-1273.
- Seed, H. B. and Idriss, I. M. 1982. Ground Motions and Soil Liquefaction During Earthquakes , Earthquake Engineering Research Institute, 499 14th Street, Oakland, CA, pp 134.
- Seed, H. B., Idriss, I. M., Arango, I. 1983. "Evaluation of Liquefaction Potential Using Field Performance Data," ASCE, Journal of the Geotechnical Engineering Division, Vol. 109, No. GT3, pp 458-482.
- Seed, H. B., Tokimatsu, K. Harder, L. F., and Chung, R. M. 1985 (Dec). "Influence of SPT Procedures in Soil Liquefaction Resistance Evaluations," ASCE, Journal of the Geotechnical Engineering Division, Vol. 111, No. 12, pp. 1425-1445.
- Seed, H. B., and Whitman, R. 1970. "Design of Earth Retaining Structures for Dynamic Loads," ASCE Specialty Conference on Lateral Stresses in the Ground and Design of Earth Retaining Structures, pp. 103-147.
- Seed, R. B. and Harder, L. F. (1990). "SPT-Based Analysis of Cyclic Pore Pressure Generation and Undrained Strength," Proceedings of the H. B. Seed Memorial Symposium, Bi Tech Publishing, Vol. II, pp. 351-376.
- Sellers, Barrie and Dunnycliff, John. 1982 (Apr). "Measurement of Load and Strain in Structural Members," 6th Annual Short Course on Field Instrumentation of Soil and Rock, University of Missouri-Rolla, Rolla, Missouri.
- Shannon and Wilson, Inc. 1982 (Sep). "Final Report, Tasks 3.2, 3.3, and 3.4, Finite Element Models," Report on Lock and Dam No. 26 (Replacement) for U. S. Army Engineer District, St. Louis.
- Sharma, N. (1989). "Refinement of Newmark Sliding Block Model and Application to New Zealand Conditions," Master Thesis, Department of Civil Engineering, University of Canterbury, NZ, 237p.
- Sherif, M. , Ishibashi, I., and Lee, C. 1982. "Earth Pressure Against Rigid Retaining Walls," ASCE, Journal of the Geotechnical Engineering Division, Vol. 108, No. GT5, pp. 679-695.
- Sherif, M., and Fang, Y. 1983 (Nov). " Dynamic Earth Pressures Against Rotating and Non- Yielding Retaining Walls ," Soil Engineering Research Report No. 23, Department of Civil Engineering, University of Washington, Seattle, WA, pp. 45-47.
- Sherif, M., and Fang, Y. 1984a. "Dynamic Earth Pressures on Rigid Walls Rotating About the Base," Proceedings, Eighth World Conference on Earthquake Engineering, Vol. 6, San Francisco, CA, pp. 993-100.
- Sherif, M., and Fang, Y. 1984b. "Dynamic Earth Pressures on Walls Rotating About the Top," Soils and Foundations, Vol. 24, No. 4, pp. 109-117.
- Skempton, A. W., The Bearing Capacity of Clays, Building Research Congress, London, 1951, Div. 1, pp. 180-189.
- Slope Indicator Company. 1984. Brochure, Seattle, Washington.

- Spangler, M. 1938. "Lateral Earth Pressures on Retaining Walls Caused by Superimposed Loads," Proceedings of the 18th Annual Meeting of the Highway Research Board, Part II, pp. 57- 65.
- Sorota, Max D., and Kinner, Edward B. 1981 (Dec). "Cellular Cofferdams for Trident Drydock: Design," American Society of Civil Engineers, New York, New York, GT 12.
- Sorota, Max D., Kinner, Edward B., and Haley, Mark, X. 1981 (Dec). "Cellular Cofferdam for Trident Drydock: Performance," Journal, Geotechnical Engineering Division, American Society of Civil Engineers, New York, New York, Vol 107, No. GT 12, pp 1657-1676.
- Sovinc, I. 1961. "Stresses and Displacements in a Limited Layer of Uniform Thickness, Resting on a Rigid Base, and Subjected to a Uniformly Distributed Flexible Load of Rectangular Shape," Proceedings, Fifth International Conference on Soil Mechanics and Foundation Engineering, Vol 1, p 823, Paris, France.
- Sowers, G. F. 1962. "Shallow Foundations," Foundation Engineering, McGraw-Hill Book Co., Inc., New York, New York.
- Sowers, G. F. and Royster, D. L. 1978. "Field Investigation," Landslides: Analysis and Control, Transportation Research Board, Special Report 176, National Academy of Science, Washington, DC, pp 81-111.
- Stark, T. D., and Mesri, C. 1992 (Nov). "Undrained Shear Strength of Liquefied Sands for Stability Analysis," ASCE, Journal of the Geotechnical Engineering Division, Vol. 118, No. 11.
- Steedman, R., and Zeng, X. 1988. "Flexible Anchored Walls Subject to Base Shaking," Report CUED/D-soils TR 217, Engineering Department Cambridge University, UK.
- Steedman, R., and Zeng, X. 1990. "The Influence of Phase on the Calculation of Pseudo-Static Earth Pressure on a Retaining Wall," Geotechnique, Vol. 40, No. 1, pp. 103-112.
- Steedman, R., and Zeng, X. 1990. "Hydrodynamic Pressures on a Flexible Quay Wall," Report CUED/D-soils TR 233, Engineering Department, Cambridge University, UK.
- Steedman, R., and Zeng, X. 1990. "The Response of Waterfront Retaining Walls," Proceedings of ASCE Specialty Conference on Design and Performance of Earth Retaining Structures, Geotechnical Special Publication No. 25., pp. 872-886.
- Streeter, V., Wylie, and Richart, F. 1974. "Soil Motion Computations by Characteristics Method," Journal of the Geotechnical Engineering Division, ASCE, Vol. 100, No. GT3, pp. 247- 263.
- Swatek, E. P., Jr. 1967 (Aug). "Cellular Cofferdam Design and Practice," Journal, Waterways and Harbors Division, American Society of Civil Engineers, New York, New York, WW 3.
- Swatek, E. P., Jr. 1970. "Summary - Cellular Structure Design and Installation," Design and Installation of Pile Foundations and Cellular Structures," Envo Publishing Co., Inc., Lehigh Valley, Pennsylvania.
- Taylor, D. W., *Fundamentals of Soil Mechanics*, John Wiley and Sons, Inc., New York, 1948.
- Teng, Wayne C., *Foundation Design*, Prentice Hall, Inc., Englewood Cliffs, New Jersey, 1962.
- Tennessee Valley Authority, Division of Engineering and Construction. 1966 (Nov). "Steel Sheet Piling Cellular Cofferdams on Rock," Tennessee Valley Authority, Office of Chief of Engineers, Technical Monograph No. 75, Vol 1, Knoxville, Tennessee.
- Taylor, D. W. 1948. "Permeability" and "Seepage," *Fundamentals of Soil Mechanics*, John Wiley and Sons, Inc., New York, New York.
- Terzaghi, K. 1934 (Feb). "Large Retaining Wall Tests. I. Pressure of Dry Sand," *Engineering News Record*, Vol. III, pp. 136-140.
- Terzaghi, K. 1936 (Apr). "A Fundamental Fallacy in Earth Pressure Calculations," *Boston Society of Civil Engineers*, pp. 71-88.
- Terzaghi, K., *General Wedge Theory of Earth Pressure*, Transactions, ASCE, Vol. 106, 1941.
- Terzaghi, K. 1943. "Bearing Capacity," *Theoretical Soil Mechanics*, John Wiley and Sons, Inc., New York, New York.
- Terzaghi, K. 1945. "Stability and Stiffness of Cellular Cofferdams," *American Society of Civil Engineers, Transactions*, Vol 110, Paper No. 2253, pp 1083-1202.
- Terzaghi, K. 1954. "Anchored Bulkheads," *Transactions of the American Society of Civil Engineers*, Vol. 119, pp. 1243-1324.
- Terzaghi, K. and Peck, R. B. 1967. *Soils Mechanics in Engineering Practice*, Second Edition, John Wiley and Sons, Inc., New York, New York.

- Tokimatsu, A. M., and Seed, H. B. 1987 (Aug). "Evaluation of Settlements In Sands Due to Earthquake Shaking," ASCE, Journal of the Geotechnical Division, Vol. 113, No. 8, pp. 861- 878.
- Tokimatsu, K., and Yoshimi, Y. 1983. "Empirical Correlation of Soil Liquefaction Based on SPT N-Value and Fines Content," Soils and Foundations, Vol. 23, No. 4, pp 56-74.
- Towhata, I., and Islam, S. 1987 (Dec.). "Prediction of Lateral Movement of Anchored Bulkheads Induced by Seismic Liquefaction," Soils and Foundations, Vol. 27, No. 4, pp. 137- 147.
- Tschebotarioff, G. P. et. al., Lateral Earth Pressures on Flexible Retaining Walls, Transactions, ASCE, Vol. 114, 1949.
- Tschebotarioff, G. P., Design and Construction of Flexible Retaining Structures, Presented at the Chicago Soil Mechanics Lecture Series, Chicago, Illinois, 1964.
- Tschebotarioff, G. P., Soil Mechanics, Foundations and Earth Structures, McGraw-Hill, Inc., New York, 1951 and 1973.
- Thorburn, S. H. 1966. "Large Diameter Piles Founded in Bedrock," Proceedings of Symposium on Large Bored Piles, Institute of Civil Engineers, London.
- Underwood, L. B. 1972. "The Role of the Engineering Geologist in the Instrumentation Program," Engineering Geology, Bulletin of the Association of Engineering Geologists, Vol 9, No. 3.
- U. S. Army Corps of Engineers, Design of Pile Structures and Foundations, Manual, U.S. Government Printing Office, Washington, D.C., 1958.
- U.S. Army Corps of Engineers, Shore Protection Planning and Design (TR No. 4), U.S. Government Printing Office, Washington, D.C.
- U. S. Army Engineer Waterways Experiment Station, CE. 1953 (Mar). Unified Soil Classification System, Technical Memorandum 3-357, Vol 1, Vicksburg, Mississippi.
- U. S. Army Engineer Waterways Experiment Station, CE. Rock Testing Handbook, RTH 203-80, Vicksburg, Mississippi.
- U. S. Army Engineer Waterways Experiment Station, CE. Rock Testing Handbook, RTH 381-80, Vicksburg, Mississippi.
- U.S. Department of the Navy, Facilities Engineer Command (NAVFAC), Design Manual DM-7, U.S. Government Printing Office, Washington, D.C., 1971.
- Weatherby, D.E., Tiebacks, Office of Research and Development, U.S. Department of Transportation, Federal highway Administration Report, FHWA/RD-82/047, pp. 2-42 and pp. 139-160, July, 1982.
- Vasquez-Herrera, A., and Dobry, R. 1988. "The Behavior of Undrained Contractive Sand and Its Effect on Seismic Liquefaction Flow Failures of Earth Structures," Rensselaer Polytechnic Institute, Troy, NY.
- Westergaard, H. 1931. "Water Pressure on Dams During Earthquakes," Transactions of ASCE, Paper No. 1835, pp. 418-433.
- Whitman, R. 1979 (Dec). "Dynamic Behavior of Soils and Its Application to Civil Engineering Projects," State of the Art Reports and Special Lectures, 6th Panamerican Conference on Soil Mechanics and Foundation Engineering, Lima, Peru, pp. 59-105.
- Whitman, R. 1985. "On Liquefaction," Proceedings , 11th International Conference on Soil Mechanism and Foundation Engineering, Vol. 7, San Francisco, CA. pp. 1923-1926.
- Whitman, R. 1990. "Seismic Design Behavior of Gravity Retaining Walls," Proceedings of ASCE Specialty Conference on Design and Performance of Earth Retaining Structures, Geotechnical Special Publication No. 25. , pp. 817-842.
- Whitman, R. V. 1992 (Jul). Predicting Earthquake - Caused Permanent Deformations of Earth Structures, Proceedings Wroth Memorial Symposium on Predictive Soil Mechanics, Oxford University (in press).
- Whitman, J., and Christian, J. 1990. "Seismic Response of Retaining Structures," Symposium Seismic Design for World Port 2020, Port of Los Angeles, Los Angeles, CA.
- Whitman, R., and Liao, S. 1985. "Seismic Design of Retaining Walls," Miscellaneous Paper CL-85-1, US Army Engineer Waterways Experiment Station, Vicksburg, MS.
- White, Ardis, Cheney, James A., and Duke, C. Marlin. 1961 (Aug). "Field Study of a Cellular Bulkhead," Journal, Soil Mechanics and Foundation Division, American Society of Civil Engineers, New York, New York, Vol 87, SM 4.
- White, E.D., Design and Construction of Braced Cuts, presented at the Chicago Soil Mechanics Lecture Series, Illinois Section, ASCE, Chicago, 1964.

**JINNINGS EQUIPMENT LLC OFFERING BSP'S NEW ASSISTED
& DOUBLE ACTING HYDRAULIC IMPACT HAMMERS.**

THEY ARE RELIABLE, VERSATILE, ECONOMICAL AND HAVE PROVEN TECHNOLOGY
INTRODUCING THE NEW BSP MODEL SCV-60 ... OUT DRIVING THE COMPETITION IN COST!
MIDWEST DISTRIBUTOR FOR FULL LINE OF INTERNATIONAL CONSTRUCTION EQUIPMENT



JINNINGS EQUIPMENT, LLC.

PH) 260-447-4343 FAX) 260-447-4363

**NEW BEAMS WITH PAPERS...
ALL BEAMS ARE A992/572 except as noted**

**WIDE FLANGE
BEAMS:**

10" x 60#	35', 40', 50', 60'	14" x 82#	45'	27" x 114#	35', 40'
10" x 77#	35', 40', 50', 60'	14" x 109#	30', 35', 50'	27" x 161#	40', 50'
10" x 88#	35', 40', 45', 50', 55'	16" x 77#	40', 45', 50'	27" x 178#	50'
10" x 100#	35', 40', 45', 50', 60'	16" x 89#	40', 60'	30" x 116#	35', 50', 55', 60'
10" x 112#	30', 35', 40', 50'	16" x 100#	35', 40', 50', 60'	33" x 118#	35', 40', 60'
12" x 72#	40', 55'	18" x 71#	40', 50'	33" x 130#	40', 50'
12" x 79#	40', 50', 55', 60'	18" x 76#	50', 60'	33" x 141#	35', 40', 50', 60', 65'
12" x 87#	35', 40', 50', 55', 60'	18" x 86#	35', 50', 60'	33" x 152#	40', 50', 60'
12" x 96#	35', 40', 45', 50'	18" x 106#	35', 40', 50'	33" x 221#	51' 4" thru 54' 8" Randoms
12" x 106#	45'	21" x 73#	40', 50', 60'	36" x 135#	40', 50', 60'
12" x 120#	35'	21" x 83#	40', 45', 50', 60'	36" x 150#	35', 40', 50', 60', 65'
12" x 136#	35', 40', 60'	21" x 93#	30', 40', 45', 50', 60'	36" x 170#	35', 40', 50', 60', 65'
*12" x 170#	40' (A-36)	21" x 101#	35', 40', 50'	36" x 182#	40'
		21" x 111#	40'	36" x 194#	35', 40', 50'
		24" x 104#	40', 50'	36" x 230#	50'
		24" x 131#	35'	36" x 245#	40'
		27" x 102#	40', 45'	36" x 280#	40' 36" x 300#
					35', 50'



*The only good thing
about new steel is it
becomes used . . .
and we have it!*

**Ready for
Shipping
Stored N.Y.-N.J.
Area**

**Quantities in
Most Sizes and
Lengths**

Call NESTOR or LAURIE • 516-546-7900 • FAX: 516-546-7992

NESTOR/MERRICK MATERIALS, INC.

Nestor Palahnuk, 1745 Merrick Avenue, Suite #8 • Merrick, New York 11566

- White, L., and Prentis, E. A. 1950. *Cofferdams*, Columbia University Press, New York, New York.
- White, R. E. 1962. "Caissons and Cofferdams," *Foundation Engineering*, McGraw-Hill Book Co., New York, New York.
- Wilson, Stanley D., and Mikkelsen, Erik P. 1978. "Field Instrumentation," *Transportation Research Board Special Report 176, Landslides: Analysis and Control*, National Academy of Science.
- Woodward, R. J., Gardner, W. S., and Greer, D. M. 1972. *Drilled Pier Foundations*, McGraw-Hill Book Co., Inc., New York, New York.
- Wong, C. 1982. "Seismic Analysis and Improved Seismic Design Procedure for Gravity Retaining Walls," *Research Report 82-32*, Department Of Civil Engineering, Massachusetts Institute of Technology, Cambridge, MA.
- Wood, J. 1973. *Earthquake-Induced Soil Pressures on Structures*, Report No. EERL 73-05, California Institute of Technology, Pasadena, CA, pp. 311.
- Wu, T. H. 1966. "Problems of Stability," *Soil Mechanics*, Section 10.9, Allyn and Bacon, Inc., Boston, Massachusetts.
- Yong, P. M. F. 1985. "Dynamic Earth Pressures Against A Rigid Earth Retaining Wall, Central Laboratories Report 5-8515, Ministry of Works and Development, Lower Hutt, New Zealand.
- Zagustin, E.A. and Herrmann, G., *Stability of an Elastic Ring in a Rigid Cavity*, *Journal of Applied Mechanics*, June 1967.
- Zarrabi, K. 1973. "Sliding of Gravity Retaining Wall During Earthquakes Considering Vertical Acceleration and Changing Inclination of Failure Surface, SM Thesis, Department of Civil Engineering, MIT, Cambridge, MA, pp. 140.
- Zienkiewicz, O. C., and Xie, Y. M. 1991 (Nov.) "Analysis of the Lower San Fernando Dam Failure Under Earthquake," *Dam Engineering*, Vol. II, Issue 4, pp. 307-322.

19.2. Notation

The notation list below shows the various variables used in the book. The list does not include variables that are very specific to one part of the book or another, such as those used with Ovesen's Anchor Slab Method or single cell mooring dolphins, or variables that are used "transitionally" in solved examples. In the case of cellular cofferdams, there are variables that are used differently for these structures than they are with other types of sheet piling; we have a notation list below that applies only to cellular cofferdams.

19.2.1. Greek Letter Symbols

Δh (delta)	Change in total head
ΔK_{AE} (delta)	Incremental dynamic active earth pressure coefficient
ΔK_{PE} (delta)	Incremental dynamic passive earth pressure coefficient with $\delta=0$
Δl (delta)	The length of flow path over which Δh occurs
ΔP_{AE} (delta)	Incremental dynamic active earth pressure force
ΔP_{PE} (delta)	Incremental dynamic passive earth pressure force with $\delta = 0$
Δu (delta)	Excess pore water pressure due to earthquake shaking
Δu (delta)	Resultant excess pore water pressure force along the base of a wall
Ψ_e (psi)	Seismic inertia angle
Ψ_{e1} (psi)	Equivalent seismic inertia angle for the restrained water case with $r_u = 0$
Ψ_{e2} (psi)	Equivalent seismic inertia angle for the free water case with $r_u = 0$
Ψ_{e3} (psi)	Equivalent seismic inertia angle for the restrained water case with $r_u > 0$
Ψ_{e4} (psi)	Equivalent seismic inertia angle for the free water case with $r_u > 0$
Ψ (psi)	Seismic inertia angle
α_A (alpha)	Inclination from horizontal of a planar slip surface extending upward through the backfill, static active case
α_{AE} (alpha)	Inclination from horizontal of a planar slip surface extending upward through the backfill, dynamic active case
α_P (alpha)	Inclination from horizontal of a planar slip surface extending upward through the backfill, static passive case
α_{PE} (alpha)	Inclination from horizontal of a planar slip surface extending upward through the backfill, dynamic passive case through the backfill, dynamic passive case
α (alpha)	Inclination from horizontal of a planar slip surface extending upward through the backfill
α_{tie}	Inclination of tie rod with the horizontal, degrees
β^* (beta)	Inclination of backfill from horizontal, used in the equivalent static procedure for computing K_{AE} and K_{PE}
β (beta)	Inclination of backfill from horizontal
δ_b (delta)	Effective angle of interface friction between the base of the wall and its foundation
δ (delta)	Effective angle of interface friction between the soil and the structure
δ_{max}	Maximum Deflection of the sheeting
ϕ'_{eq} (phi)	Equivalent angle of internal friction for soil with $r_u > 0$
ϕ (phi)	Effective angle of internal friction for soil
γ (gamma)	Effective unit weight of soil
γ_b (gamma)	Buoyant unit weight of soil
γ_d (gamma)	Dry unit weight of soil
γ_e (gamma)	Effective unit weight of a partially submerged backfill for the restrained water case
γ_{e3} (gamma)	Effective unit weight of soil for the restrained water case with $r_u > 0$
γ_l (gamma)	Effective unit weight of soil
γ_w (gamma)	Unit weight of water
γ_{w3} (gamma)	Effective unit weight of water for the restrained water case with $r_u > 0$
λ_t	Ratio of transverse bending stresses to the lateral pressure on the sheeting, dimensionless
ν	Poisson's Ratio
θ^* (theta)	Inclination of the back of the wall to soil interface from vertical, used in the equivalent static procedure for computing K_{AE} and K_{PE}
θ (theta)	Inclination of the back of wall to soil interface from vertical
ρ	Rowe's Moment Reduction variable
σ' (sigma)	Effective normal stress
$\sigma' v$ (sigma)	Vertical effective stress
$\sigma'_{v-initial}$	Pre-earthquake vertical effective stress

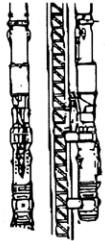
σ'_{wt} (sigma)	Effective weight of backfill, excluding surcharge
σ_a (sigma)	Active earth pressure (effective stress)
σ_p (sigma)	Passive earth pressure (effective stress)
σ (sigma)	Total normal stress
σ_1, σ_3	Principal stresses on soil
σ_{allow}	Allowable stress of structural member
σ_n	Effective normal stress
σ_y	Yield stress of structural member
τ_f (tau)	Shear stress at failure
τ (tau)	Shear stress
τ_{allow}	Maximum allowable shear stress

19.2.2. Roman Letter Symbols

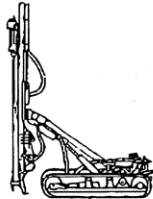
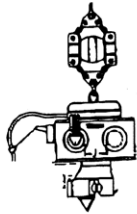
A	Maximum ground acceleration as a fraction of g (dimensionless)
A_{axial}	Cross-sectional area of wall beneath axial load
a_h	Maximum horizontal ground acceleration, equal to $k_h \cdot g$
a_{max}	Maximum ground acceleration, equal to $A \cdot g$
A_{tie}	Cross-sectional area of the tie rod
a_v	Maximum vertical ground acceleration, equal to $k_v \cdot g$
$A_{v,min}$	Minimum shear area
B	Width of wall base
B_e	Effective base width of the wall in contact with the foundation
c	Effective cohesion
c_1	Constant used to compute α_A
c_{1AE}	Constant used to compute α_{AE}
c_2	Constant used to compute α_A
c_{2AE}	Constant used to compute α_{AE}
c_3	Constant used to compute α_p
c_{3PE}	Constant used to compute α_{PE}
c_4	Constant used to compute α_p
c_{4PE}	Constant used to compute α_{PE}
c_t	Distance from neutral axis to the point of maximum transverse stress in sheeting, in or m
D	Distance from excavation line to toe
d_r	Maximum displacement
E4	
e_p	Eccentricity of the load from the centreline of the sheeting
E_{tie}	Young's Modulus of tie rod
F_{AE}	Factor used in the equivalent static procedure to compute K_{AE}
F_b	Factor of safety against bearing capacity failure of a wall
F_{PE}	Factor used in the equivalent static procedure to compute K_{PE}
$F_{reduction}$	Reduction factor of safety for structural member
F_s	Factor of safety against sliding along the base of a wall
FS_p	Factor of safety applied to both the shear strength of the soil and the effective angle of friction along the interface when computing P_{PE} for a sheet pile wall and the anchorage.
FS_{piping}	Factor of safety against piping
F_{sr}	Lateral seismic force component by Woods procedure
F_{tr}	Factor to account for variations in the loading
g	Acceleration of gravity
h	Total head h_e Elevation head h_p Pressure head
h	Height of the sheeting
H	Height of wall
H_c	Critical Height for cohesive soils
$HF_{inertia}$	Inertial component of heavy fluid force behind a wall retaining liquefied backfill during shaking i Seepage gradient, equal to $\Delta h/\Delta l$

PACIFIC AMERICAN COMMERCIAL COMPANY

45 YEARS OF SERVICE TO THE PILE DRIVING INDUSTRY



**AIR, DIESEL,
VIBES &
HYDRAULIC
IMPACT**



**QUARRY
DRILLS**

BUCKETS



**PORTABLE
PONTOON
BARGES**



**DIESEL AIR
COMPRESSORS**

FAST QUOTATIONS - ALL YOUR FOUNDATION EQUIP. NEEDS - COMPLETE PACKAGES

HAMMERS, VIBRATORYS, LEADS, SPOTTERS
TOP HEADS, CROSS HEADS, FOLLOWER BLOCKS, DRILLS and AUGERS

RENTALS-SALES-REPAIR PARTS AVAILABLE

CALL: 1-800-678-6379 or FAX 1-206-763-4232



Engineering Services for Contractors

Pile Load Testing • Dynamic Pile Testing
Underpinning • Sheeting/Shoring Design
Deep Foundations • Geotechnical Instrumentation
Temporary Structures • Demolition/Erection Plans
Pre-Construction Surveys • Vibration Monitoring
Subsurface Explorations • Site Characterization
Value Engineering • Contaminated Soils Management



984 SOUTHFORD ROAD
MIDDLEBURY CT. 06762

G E O D E S I G N
I N C O R P O R A T E D

TELEPHONE: (203)758-8836
FACSIMILE: (203)758-8842
WEBSITE: www.geodesign.net

$H_{F_{static}}$	Static component of heavy fluid force behind a wall retaining liquefied backfill
H_t	Depth of the tie rod anchor from surface
H_w	Depth of the water table
$i_{critical}$	Critical hydraulic gradient
i_{max}	Maximum hydraulic gradient
k	Hydraulic conductivity
K	Lateral earth pressure coefficient
K_A	Static active earth pressure coefficient
K_{AE}	Dynamic active earth pressure coefficient
k_h	Horizontal seismic coefficient as a fraction of g (dimensionless)
K_h	Horizontal earth pressure coefficient
k_h^*	Limiting value for the horizontal seismic coefficient as a fraction of g (dimensionless)
k_{he}	Equivalent horizontal seismic coefficient as a fraction of g (dimensionless)
k_{he1}	Equivalent horizontal seismic coefficient as a fraction of g (dimensionless) for the restrained water case with $r_u = 0$
k_{he2}	Equivalent horizontal seismic coefficient as a fraction of g (dimensionless) for the free water case with $r_u = 0$
k_{he3}	Equivalent horizontal seismic coefficient as a fraction of g (dimensionless) for the restrained water case with $r_u > 0$
k_{he4}	Equivalent horizontal seismic coefficient as a fraction of g (dimensionless) for the free water case with $r_u > 0$
K_o	At-rest horizontal earth pressure coefficient
K_p	Static passive earth pressure coefficient
K_{pE}	Dynamic passive earth pressure coefficient
k_v	Vertical seismic coefficient as a fraction of g (dimensionless)
l	Length of deadman or anchor slab
L	Distance between tie rods or tiebacks
L_{tie}	Length of the tie rod
M_{allow}	Allowable bending moment
$M_{allow-t}$	Allowable bending moment with transverse bending
M_{design}	Design moment for a sheet pile wall
M_{FES}	Maximum moment computed using the Free Earth Support method for a sheet pile wall
M_{max}	Maximum bending moment of sheeting
N	Total normal force between the wall and the foundation
N'	Effective normal force between the wall and the foundation
N^*	Maximum transmissible acceleration coefficient, as a fraction of g (dimensionless)
N_D	Number of hydraulic head drops
N_F	Number of flow channels
OCR	Overconsolidation ratio
p	Lateral pressure on the sheeting
P	Resultant earth pressure force acting on a wall
P_A	Active earth pressure force acting on a wall for static loading
P_{AE}	Active earth pressure force acting on a wall for pseudo-static loading
P_{axial}	Axial load on sheeting
P_o	At-rest earth pressure force acting on a wall
P_p	Passive earth pressure force acting on a wall for static loading
P_{pE}	Passive earth pressure force acting on a wall for pseudo-static loading
P_{wd}	Westergaard hydrodynamic water pressure force q Vertical surcharge stress q_{all} allowable bearing pressure of rock
Q'	Total flow
q_{max}	maximum bearing pressure below toe of wall
q_u	Unconfined compression strength
q_{ult}	ultimate bearing capacity or unconfined compressive strength of concrete
r_d	Moment reduction factor due to Rowe
r_u	Excess pore water pressure ratio, equal to $\Delta u / \sigma'_{v-initial}$
s_a	Active soil stiffness
S_{min}	Minimum Section Modulus
s_p	Passive soil stiffness

S_u	Undrained shear strength of soil
S_{wall}	Section modulus of wall
T	Horizontal shear force along the base of the wall required for equilibrium
T_{design}	Design tie rod force for a sheet pile wall
T_{FES}	Tie rod force computed using the Free Earth Support method for a sheet pile wall
T_{ult}	Ultimate horizontal shear force along the base of the wall
T_{ult-a}	Ultimate force for which the sheet pile wall anchorage is to be designed
t_w	Thickness of the sheet web and flange
u	Hydrostatic water pressure
U_b	Resultant steady state pore water pressure force normal to the base of the wall
$U_{inertia}$	Hydrodynamic water pressure force for the pool, directed away from the wall
U_{pool}	Resultant hydrostatic water pressure force for the pool
U_{shear}	Resultant excess pore water pressure force due to earthquake shaking acting normal to the backfill to wall interface
$U_{shear-b}$	Resultant excess pore water pressure force due to earthquake shaking acting normal to the backfill to sheet pile wall interface
$U_{shear-t}$	Resultant excess pore water pressure force due to earthquake shaking acting normal to the dredge level soil to sheet pile wall interface
$U_{shear-\alpha}$	Resultant excess pore water pressure force due to earthquake shaking acting normal to planar slip surface inclined at a from vertical
U_{static}	Resultant steady state pore water pressure force acting normal to the backfill to wall interface
$U_{static-b}$	Resultant steady state pore water pressure force acting normal to the backfill to sheet pile wall interface
$U_{static-t}$	Resultant steady state pore water pressure force acting normal to the dredge level soil to sheet pile wall interface
$U_{static-\alpha}$	Resultant steady state pore water pressure force acting normal to planar slip surface inclined at a from vertical
v	Maximum ground velocity
v_{max}	Maximum shear on sheeting
w	Water content of soil
w	Width of the sheeting
W	Weight of rigid body (e.g. wall or soil wedge)
X_N	Point of action of normal force N
y	Distance from excavation line to active-passive reversal point
z	Distance from the soil surface

19.2.3. Variables for Cellular Cofferdams

γ	Unit weight of soil around cell (can be wet or submerged)
$\bar{\gamma}$	Submerged unit weight of cell fill
$\bar{\gamma}_c$	Submerged unit weight of the cell fill
γ_c	Unit weight of the cell fill
α_i	Angle between the inclined plane of the potential failure surface of the i^{th} wedge and the horizontal (positive is counter- or anti-clockwise)
ϕ_i	Angle of shearing resistance or internal friction of the i^{th} wedge
$(P_{i-1} - P_i)$	Summation of applied forces acting horizontally on the i^{th} wedge.
$2L$	Centre-to-centre distance between main cells, ft.
A	Area of main cell plus one connecting cell, ft ²
A	Area of base $B \times 1.0$ for 1-foot strip
B	Equivalent or effective width, ft.
c	Cohesion of soil
c_i	Cohesion or adhesion, whichever is the smaller on the potential failure surface of the i^{th} wedge. (Cohesion should not exceed the adhesion at the structure-foundation interface.)
D	Embedded length
d_c	Depth of crack in cohesive foundation material
D_f	Distance from the ground surface to the toe of the cell.
e	Eccentricity of resultant of all forces from centre of cell

E	Modulus of elasticity of the pile
f	Coefficient of friction of steel on steel at the interlock
F_1	Vertical downward friction force, force/unit length
F_i	Interlock friction force
FP	Computed foundation pressure
H'	Height of cell over which vertical shear resistance is applied
H, H_1 ,	As shown in Figure 15-26
H_2	
H_B	Height of berm or overburden on the inboard side
H_{Li}	Any horizontal force applied above the top or below the bottom of the left-side adjacent wedge
H_{Ri}	Any horizontal force applied above the top or below the bottom of the right-side adjacent wedge
H_S	Height of overburden on the outboard side
H_W	Head of water on the outboard side
i	Number of wedges
I	Moment of inertia of the pile
K	Coefficient of internal pressure for cellular cofferdam fill, depending upon the type of cell fill material and the method of placement (see Table 15-4)
K	Empirical coefficient of earth pressure.
K	Coefficient of lateral earth pressure
L	As shown in Figure 15-27
L_i	Length along the failure surface of the i^{th} wedge
M	Net overturning moment
M_B	Moment about pole of W'_B
M_ω	Moment about pole due to resultant overturning force ΣP
N	Number of wedges in the failure mechanism
N_c, N_q and $N\gamma$	Terzaghi bearing capacity factors (see Table 15-2)
n_h	Constant of horizontal subgrade reaction
p	Maximum inboard sheeting pressure, psf
P	Pressure difference on the inboard sheeting
P_a	Active earth pressure due to overburden of height, H_S
P_R	Resultant of passive earth pressure due to buoyant weight of the berm + hydrostatic pressure due to height, H_B
P_s	Total lateral force per unit length of cofferdam due to cell fill
P_T	Net force on the inboard sheets.
P_T	Area abc as shown in Figure 15-26
P_W	Hydrostatic pressure due to head, H_W
Q	Total shearing force per unit length of cofferdam
R	Radius of cellular cofferdam, feet (see Figure 15-27)
R	Radius
r and θ	Variables in the polar coordinate system
r_o	Radius to the beginning of the spiral
R_S	Lateral resistance along weak seam
S_F	Frictional resistance against slippage
S_T	Total shearing resistance along the centre line of the cell
t	Interlock tension, lbs.
t_{max}	Interlock tension at connection
U_i	Uplift force exerted along the failure surface of the i^{th} wedge
V_i	Any vertical force applied above top of the i^{th} wedge
w	Effective weight of cell fill
W	Weight of cell fill above the weak seam
W	Effective weight of cell fill
W'_B	Effective weight of cell fill above failure surface
W_i	Total weight of water, soil, rock, etc., in the i^{th} wedge
ΣP	$(P_w + P_a - P_r)$ as shown in Figure 15-16.
ϕ	Angle of internal friction

19.3. Glossary

Active pressure: The limiting pressure between the wall and soil produced when the relative wall/soil motion tends to allow the soil to expand horizontally.

Anchor force: The reaction force (usually expressed per foot of wall) that the anchor must provide to the wall.

Anchor: A device or structure that, by interacting with the soil or rock, generates the required anchor force.

Anchorage: A mechanical assemblage consisting of wales, tie rods, and anchors that supplement soil support for an anchored wall.

Anchored wall: A sheet pile wall which derives its support from a combination of interaction with the surrounding soil and one (or more) mechanical devices which inhibit motion at an isolated point(s). The design procedures described in this manual are limited to a single level of anchorage.

At-rest pressure: The horizontal in situ earth pressure when no horizontal deformation of the soil occurs.

Backfill: A generic term applied to the material on the retained side of the wall.

Cantilever wall: A sheet pile wall that derives its support solely through interaction with the surrounding soil.

Classical design procedures: A process for evaluating the soil pressures, required penetration, and design forces for cantilever or single anchored walls assuming limiting states in the wall/soil system.

Dredge line: A generic term applied to the soil surface on the dredge side of a retaining or floodwall.

Dredge side: A generic term referring to the side of a retaining wall with the lower soil surface elevation or to the side of a floodwall with the lower water elevation.

Factor of safety:

- Factor of safety for rotational failure of the entire wall/soil system (mass overturning) is the ratio of available resisting effort to driving effort.
- Factor of safety (strength reduction factor) applied to soil strength parameters for assessing limiting soil pressures in Classical Design Procedures.
- Structural material factor of safety is the ratio of limiting stress (usually yield stress) for the material to the calculated stress.

Floodwall: A cantilevered sheet pile wall whose primary function is to sustain a difference in water elevation from one side to the other. In concept, a floodwall is the same as a cantilevered retaining wall. A sheet pile wall may be a floodwall in one loading condition and a retaining wall in another.

Foundation: A generic term applied to the soil on either side of the wall below the elevation of the dredge line.

I-wall: A special case of a cantilevered wall consisting of sheet piling in the embedded depth and a monolithic concrete wall in the exposed height.

Multiple anchored wall: Anchors are attached to the wall at more than one elevation.

Passive pressure: The limiting pressure between the wall and soil produced when the relative wall/soil motion tends to compress the soil horizontally.

Penetration: The depth to which the sheet piling is driven below the dredge line.

Retained side: A generic term referring to the side of a retaining wall with the higher soil surface elevation or to the side of a floodwall with the higher water elevation.

Retaining wall: A sheet pile wall (cantilever or anchored) that sustains a difference in soil surface elevation from one side to the other. Excavation, dredging, backfilling, or a combination may produce the change in soil surface elevations.

Sheet pile wall: A row of interlocking, vertical pile segments driven to form an essentially straight wall whose plan dimension is sufficiently large that its behaviour may be based on a typical unit (usually 1 foot) vertical slice.

Single anchored wall: Anchors are attached to the wall at only one elevation.

Soil-structure interaction: A process for analysing wall/soil systems in which compatibility of soil pressures and structural displacements are enforced.

Tie rods: Parallel bars or tendons that transfer the anchor force from the anchor to the wales.

Wales: Horizontal beam(s) attached to the wall to transfer the anchor force from the tie rods to the sheet piling.

Wall height: The length of the sheet piling above the dredge line.

Sheet Pile Design by Pile Buck

Sheet Pile Design by Pile Buck



Harry A. Lindahl, P.E.

Don C. Warrington, P.E.